

# **HEAT EXCHANGERS**

**Selection, design & construction**

## **Designing for Heat Transfer**

---

**Series editor: David Browning**

*Other titles in the series:*

**Vaporisers—selection, design & operation**

**Condensation and condenser design (*under preparation*)**

517

# HEAT EXCHANGERS

---

SELECTION, DESIGN & CONSTRUCTION

E. A. D. Saunders, B.Sc., C.Eng., M.I.Mech.E.



Copublished in the United States with  
John Wiley & Sons, Inc., New York

**Longman Scientific & Technical**  
Longman Group UK Limited  
Longman House, Burnt Mill, Harlow  
Essex CM20 2JE, England  
*and Associated Companies throughout the world*

*Copublished in the United States with*  
*John Wiley & Sons, Inc., 605 Third Avenue, New York, NY 10158*

© Longman Group UK Limited 1988

All rights reserved; no part of this publication  
may be reproduced, stored in a retrieval system,  
or transmitted in any form or by any means, electronic,  
mechanical, photocopying, recording, or otherwise,  
without the prior written permission of the Publishers,  
or a licence permitting restricted copying in the United  
Kingdom issued by the Copyright Licensing Agency Ltd,  
33-34 Alfred Place, London, WC1E 7DP.

*First published 1988*

**British Library Cataloguing in Publication Data**

Saunders, E. A. D.

Heat exchangers: selection, design &  
construction. — (Designing for heat  
transfer).

1. Heat exchangers

I. Title II. Series

621.402'5 TJ263

ISBN 0-582-49491-5

**Library of Congress Cataloging in Publication Data**

Saunders, E. A. D., 1924-

Heat exchangers.

(Designing for heat transfer)

Bibliography: p.

Includes index.

1. Heat exchangers. I. Title. II. Series.

TJ263.S28 1988 621.402'5 87026171

ISBN 0-470-20870-8 (USA only)

Set in 10/12 pt Linotron 202 Times Roman

Printed in Great Britain at The Bath Press, Avon



---

# Contents

<i>Preface</i>	<i>xiii</i>
<i>Service organisations</i>	<i>xvi</i>

## Part 1 HEAT EXCHANGER TYPES

<b>Chapter 1</b>	<b>Shell-and-tube heat exchangers: construction and thermal features</b>	<b>3</b>
1.1	Introduction	3
1.2	Tubular Exchanger Manufacturers Association Inc. (TEMA)	4
1.3	Types of shell-and-tube heat exchangers	5
1.4	Head types	19
1.5	Thermal design features	21
	References	46
<b>Chapter 2</b>	<b>Shell-and-tube heat exchangers: mechanical design features and fabrication</b>	<b>47</b>
	<i>Mechanical design features</i>	
2.1	Design codes	47
2.2	Flange systems	48
2.3	Stationary head-shell joints	50
2.4	Bolted high-pressure closures	52
2.5	Non-bolted high-pressure closures (TEMA D)	53
2.6	Fixed tubesheet exchangers	54
	<i>Fabrication</i>	
2.7	Barrels	55
2.8	Bonnet-type channels	56
2.9	Nozzles	57
2.10	Flanges	59
2.11	Bolting and bolt tightening	60
2.12	Gaskets	61
2.13	Tubesheets	62
2.14	Expansion joints	64
2.15	Expanded tube-tubesheet joints	66

2.16	Fusion-welded tube-tubesheet joints	71
2.17	Explosively formed tube-end joints	77
2.18	Testing	80
	Acknowledgements	83
	References	83
<b>Chapter 3</b>	<b>Air-cooled heat exchangers</b>	<b>85</b>
3.1	Background	85
3.2	Air versus water cooling	87
3.3	Orientation of bundle	87
3.4	Forced versus induced draught	88
3.5	American Petroleum Institute Standard 661	88
3.6	Construction	88
3.7	Temperature control	101
	Acknowledgements	103
	References	103
<b>Chapter 4</b>	<b>Gasketed-plate heat exchangers</b>	<b>104</b>
4.1	Background	104
4.2	Construction	105
4.3	Inspection and maintenance	111
4.4	Flow arrangements	111
4.5	Features of gasketed-plate heat exchangers	113
4.6	Application	115
	Acknowledgements	115
	References	115
<b>Chapter 5</b>	<b>Other types of heat exchanger</b>	<b>117</b>
5.1	Double-pipe heat exchangers	117
5.2	Heat pipes	122
5.3	Gasketless-plate heat exchangers	126
5.4	Lamella heat exchangers	128
5.5	Spiral heat exchangers	131
5.6	Plate-fin heat exchangers	135
5.7	Embossed-panel heat exchangers	140
5.8	Graphite heat exchangers	142
5.9	Glass heat exchangers	146
5.10	Teflon™ heat exchangers	147
5.11	Rotary regenerative heat exchangers	150
5.12	Electrically heated exchangers	152
	Acknowledgements	156
	References	156
<b>Appendix</b>	<b>Exchanger type selection</b>	<b>157</b>
A1.1	Operating pressure and temperature	157
A1.2	Nature of fluids	157
A1.3	Size range	160
A1.4	Cost	160

**Part 2 HEAT TRANSFER AND FLUID FLOW**

<b>Chapter 6</b>	<b>Heat transfer and pressure loss</b>	<b>163</b>
6.1	Mechanisms of heat flow	163
6.2	Laminar and turbulent flow	163
6.3	'Film' heat transfer coefficient	164
6.4	Determination of heat transfer coefficients	165
6.5	Overall heat transfer coefficient	165
6.6	Surface area	168
6.7	Controlling heat transfer coefficient	168
6.8	Surface temperature	169
6.9	Cooperative research organisations	173
6.10	Heat transfer and pressure loss correlations (single phase)	175
	References	185
	Nomenclature	185
<b>Chapter 7</b>	<b>Mean temperature difference</b>	<b>188</b>
7.1	Countercurrent and cocurrent flow	188
7.2	Temperature approach, meet and cross	188
7.3	Mean temperature difference for countercurrent and cocurrent flow	189
7.4	$U$ varies linearly between inlet and outlet	191
7.5	$U$ varies non-linearly between inlet and outlet	191
7.6	Mean temperature difference for non-countercurrent and non-cocurrent flow	192
7.7	Application to design	197
7.8	Number of transfer units	201
7.9	Theta method	205
	Acknowledgement	205
	References	205
	Nomenclature	206
<b>Chapter 8</b>	<b>Fouling</b>	<b>208</b>
8.1	Fouling mechanisms	208
8.2	Fouling growth	209
8.3	Cost of fouling	210
8.4	Design considerations	210
8.5	Fouling research	215
8.6	Design to minimise fouling	216
	References	218
<b>Chapter 9</b>	<b>Extended surfaces</b>	<b>220</b>
9.1	Fin efficiency	220
9.2	Heat transfer calculations	222
9.3	Pressure loss calculations	227
9.4	Space saving	227
9.5	Surface temperature: longitudinally finned tubes	228
	References	230
	Nomenclature	231

<b>Chapter 10</b>	<b>Internal heat transfer augmentation techniques</b>	<b>232</b>
10.1	Background	232
10.2	Effect on boundary layer	233
10.3	Evaluation of techniques	233
10.4	Roughened surfaces	234
10.5	Twisted tape inserts	235
10.6	Heatex™ tube inserts	235
10.7	Additional techniques	239
10.8	Axial cores	240
	Acknowledgement	241
	References	241
<b>Chapter 11</b>	<b>Shell-side flow-induced tube vibration</b>	<b>245</b>
11.1	Background	245
11.2	Tube failures	246
11.3	Reasons for increase in failures	247
11.4	Excitation mechanisms	247
11.5	Predictive methods	250
11.6	Application to design	264
11.7	Phillips RODbaffle™ exchanger	267
11.8	NESTS™ concept	269
	Acknowledgements	270
	References	271
	Nomenclature	271
<b>Part 3</b>	<b>THERMAL DESIGN</b>	
<b>Chapter 12</b>	<b>Thermal design: shell-and-tube exchangers (plain tubes)</b>	<b>275</b>
12.1	The need for manual design methods	275
12.2	Shell-side flow problem	276
12.3	Thermal design procedure	279
12.4	Tube-side calculations	279
12.5	Shell-side calculation	280
	Acknowledgements	322
	References	322
	Nomenclature	323
<b>Chapter 13</b>	<b>Thermal design: shell-and-tube exchangers (low-fin tubes)</b>	<b>325</b>
13.1	Description	325
13.2	Cost comparison: plain versus low-fin tubes	326
13.3	Design considerations	327
13.4	Thermal design	329
	Acknowledgement	337
	References	337
	Nomenclature	337
<b>Chapter 14</b>	<b>Thermal design: air-cooled exchangers</b>	<b>339</b>
14.1	Design variables	339
14.2	Inlet air temperature	340

14.3	Preliminary sizing	341
14.4	Outlet air temperature	341
14.5	Air velocity	341
14.6	Tube-side heat transfer and pressure loss calculations	342
14.7	Air-side heat transfer and pressure loss calculations	342
14.8	Overall heat transfer coefficient	342
14.9	Surface area and number of rows deep	343
14.10	Mean temperature difference	343
14.11	Air-side pressure loss, fan power consumption and noise	344
14.12	Fan laws	347
14.13	Example of air-side calculations	347
14.14	Design curve for air-side heat transfer coefficients	350
	References	352
	Nomenclature	352
<b>Chapter 15</b>	<b>Thermal design: double-pipe exchangers</b>	<b>354</b>
15.1	Tube-side heat transfer and pressure loss calculations	354
15.2	Annulus heat transfer calculations	354
15.3	Annulus pressure loss calculations	357
15.4	Effect of cut-and-twist	358
15.5	Example of annulus calculations	358
15.6	Design curve for annulus heat transfer coefficients	360
	References	361
	Nomenclature	362
<b>Chapter 16</b>	<b>Thermal appraisal: gasketed-plate heat exchangers</b>	<b>364</b>
16.1	Plate exchanger thermal data	364
16.2	Plate geometry	365
16.3	Heat transfer and pressure loss calculations	367
16.4	Effective temperature difference	368
16.5	Overall heat transfer coefficient	368
16.6	Surface area	369
16.7	Exchanger arrangement	370
	Acknowledgements	372
	References	372
	Nomenclature	372
<b>Chapter 17</b>	<b>Worked examples for thermal design</b>	<b>374</b>
17.1	Thermal design process	374
17.2	Shell-and-tube heat exchangers: plain tubes	383
17.3	Shell-and-tube heat exchangers: low-fin tubes	432
17.4	Air-cooled heat exchangers	440
17.5	Finned-tube double-pipe heat exchangers	445
17.6	Gasketed-plate heat exchangers	454
17.7	Shell-and-tube heat exchangers: comparison of manual and proprietary computer methods	458
17.8	Shell-side pressure loss due to blockage	459
	References	459

<b>Appendix</b>	<b>Tube counts</b>	<b>460</b>
	A3.1 Tube count tables	460
	A3.2 Tube count reduction for untubed areas—procedure	460
	A3.3 Tube count reduction for untubed areas—examples	470
	A3.4 Pull-through floating-head exchangers	471
	Acknowledgement	472
<b>Part 4</b>	<b>MATERIALS AND COST</b>	
<b>Chapter 18</b>	<b>Materials of construction</b>	<b>475</b>
	18.1 Corrosion data and material selection	475
	18.2 Forms of corrosion	476
	18.3 Materials and numbering system	483
	18.4 Carbon and low-alloy steels	484
	18.5 Aluminium and aluminium alloys	488
	18.6 Copper and copper alloys	493
	18.7 Stainless steels	496
	18.8 Nickel and high-nickel alloys	506
	18.9 Titanium and titanium alloys	512
	18.10 Bi-metal construction	515
	18.11 Non-metallic coatings	521
	18.12 National Association of Corrosion Engineers (NACE)	523
	Acknowledgements	523
	References	524
<b>Chapter 19</b>	<b>Size and cost estimation</b>	<b>525</b>
	19.1 Cost data	525
	19.2 Surface area estimation	525
	19.3 Shell-and-tube heat exchangers	527
	19.4 Double-pipe heat exchangers	542
	19.5 Air-cooled heat exchangers	545
	19.6 Gasketed-plate heat exchangers	551
	19.7 Spiral and lamella heat exchangers	552
	19.8 Rotary regenerative heat exchangers	553
	Acknowledgements	554
	References	554
	<i>Index</i>	555

---

## Preface

This book is one of a series on Designing for Heat Transfer. Its chief purpose is to describe the construction and application of many of the unfired heat exchanger types used in the process industries, together with their materials of construction and cost. Most of this information is common to heat transfer equipment generally, whatever its particular function (i.e. heater, cooler, vaporiser, condenser, etc.). Excluded are cooling towers, and exchangers associated with the power industries, such as surface condensers and feed-water heaters.

Other books in the series deal with the design of vaporisers and condensers in which there must be two-phase flow. However, the newcomer will achieve a better understanding of two-phase flow applications if he is conversant with single-phase flow. For this reason, the book also includes heat transfer and pressure loss data, plus thermal design methods and examples, for exchangers involving single-phase flow duties. The methods must, of necessity, be straightforward manual ones. In practice, most thermal design is performed today by computer and the reader should be aware of the activities of the cooperative research organisations: Heat Transfer Research Inc. (HTRI) and the Heat Transfer and Fluid Flow Service (HTFS). Their impact on heat transfer, fluid flow and thermal design methods, coupled with the emergence of computers, during the past twenty five years, has been considerable.

The book has been written for the newcomers to the industrial heat transfer field, and the mechanical and chemical engineering students, who require a broad introduction to the subject of practical heat transfer and heat exchangers generally. It will also be of benefit to designers in the heat transfer field, or process engineers, who wish to broaden their knowledge of the subject.

Much of the text is devoted to shell-and-tube heat exchangers, but this is not surprising since they account for over 50% of all the heat exchangers installed. However, every effort has been made to present the merits of other heat exchanger types, in order to remind the reader that in many cases there are more attractive alternatives to the shell-and-tube type.

The book is divided into four parts. Part 1, entitled 'Heat exchanger types', deals mainly with shell-and-tube, air-cooled, and gasketed-plate



types and describes their construction and design features. These are the principal types used in industry, but some other, mainly specialised, types are described. These include double pipe, heat pipe, spiral, lamella, welded (gasketless) plate, plate-fin, embossed plate, glass, graphite, Teflon™, rotary and electrically heated. An appendix provides a guide to type selection and summarises their merits and limitations.

Part 2 is entitled 'Heat transfer and fluid flow'. The first three chapters introduce thermal design factors which are common to all heat exchangers, whatever their function. These relate to heat transfer, pressure loss, mean temperature difference, and fouling, which is justly regarded as 'the major unresolved problem in heat transfer'. As vaporisation and condensation are presented in other books in the series, heat transfer and pressure loss data have been confined to single-phase flow applications. However, the basic principles need to be fully understood by the newcomer as they form the basis of two-phase flow correlations.

It is not surprising that in recent years interest in techniques for augmenting heat transfer has grown rapidly, in order to conserve energy, although many of the techniques have not reached the stage of full-scale industrial application. Two additional chapters are devoted to this subject—one dealing with the well-established externally finned tubes, and the other with internal augmentation devices, such as cores, tapes and coils. This chapter also contains references and brief descriptions of some of the other augmentation techniques available.

The last chapter deals with flow-induced tube vibration, a phenomenon which is encountered chiefly on the shell-side of shell-and-tube exchangers. It has been the subject of considerable investigation since the late 1960s, and has arisen due to a combination of increased exchanger size and increased shell-side velocity. Before then, it is unlikely that a thermal design engineer considered a vibration check; today an exchanger design is unacceptable unless it has been checked for vibration damage. Thermal design engineers adopted new terminology: Strouhal number, fluid-elastic whirling, no-tube-in-window designs, log decrement, and so on.

Part 3, entitled 'Thermal design', provides manual thermal design methods for shell-and-tube (plain and low-fin), air-cooled, double-pipe, and gasketed-plate types for single-phase applications. The use of computer programs is essential for the thermal design of these exchanger types as they enable the thermal design engineer to investigate rapidly all parameters to arrive at the optimum solution. Hence, there would appear to be little need for manual methods, but in the author's experience, this is not the case and there is a need for them in the initial training period of a thermal design engineer. However sophisticated the program, it is the skill, judgement and experience of the thermal design engineer which finalises the design. The designer is better equipped to do this if, in early training, the interaction and magnitude of the various design parameters by manual methods has been fully understood.

The methods deal with single-phase applications, but will assist the newcomer in the design of vaporisers and condensers.

Part 4, entitled 'Materials and cost', contains two chapters. The first



chapter initially describes some of the corrosion mechanisms encountered in heat transfer equipment. It is then followed by the merits and limitations of some of the materials used in their construction, namely, carbon and low-alloy steels, copper and copper alloys, aluminium and aluminium alloys, stainless steels, high-nickel alloys, titanium and non-metallic linings.

The relative cost of these materials, in relation to steel, is presented in the second chapter. The chief purpose of this chapter is to provide data from which an approximate size and cost of some of the exchanger types described in Part 1 may be determined rapidly.

The author wishes to thank the Managing Director of Whessoe Heavy Engineering Ltd for permission to write this book, Dave Heaviside for preparing some of the drawings and Elizabeth Westhorp for her impeccable typing.

E. A. D. Saunders  
Darlington  
December 1986

However, within their pressure and temperature limitations, the non-tubular equipment, particularly the plate types, provide excellent features and should always be considered as an alternative to the shell-and-tube type, for instance.



## Service organisations

- American Petroleum Institute (API)**, 1220 L Street, Northwest  
Washington, DC 200 05, USA.
- American Society of Mechanical Engineers (ASME)**, United Engineering  
Centre, 345 East 47th Street, New York, NY 10017, USA.
- American Society for Testing and Materials (ASTM)**, 1916 Race Street,  
Philadelphia, Pennsylvania 19103, USA.
- British Standards Institution (BSI)**, 2 Park Street, London W1A 2BS,  
UK.
- Engineering Sciences Data Unit International Ltd (ESDU)**, 251/9 Regent  
Street, London W1R 8ES, UK.
- Heat Transfer and Fluid Flow Service (HTFS)**, Building 392.7, AERE  
Harwell, Oxfordshire, OX11 0RA, UK.
- Heat Transfer Research Inc. (HTRI)**, Research Facilities, 1000 South  
Fremont Avenue, Alhambra, California 91802, USA.
- National Association of Corrosion Engineers (NACE)**, 2400 West Loop  
South, Houston, Texas 77027, USA.
- National Corrosion Service (NCS)**, National Physical Laboratory,  
Teddington, UK.
- Oil Companies Materials Association (OCMA)**, 14 Belgrave Square,  
London SW1 8PS, UK.
- Physical Properties Data Service (PPDS)**, Institution of Chemical  
Engineers, 165-171 Railway Terrace, Rugby, CV21 3HQ, UK.
- Tubular Exchanger Manufacturers Association Inc. (TEMA)**, 25 North  
Broadway, Tarrytown, New York, NY 10591, USA.

E. A. D. Saunders  
Darlington  
December 1986



## PART 1

### CHAPTER 1 Heat exchanger types

#### Shell-and-tube heat exchangers: Construction and thermal features

Part 1 describes the construction and application of some of the unfired heat exchangers used in industry. These exchangers may be divided into four categories, namely:

*tubular:* shell-and-tube, air cooled, double pipe, heat pipe.  
*plate:* gasketed, gasketless, spiral, lamella, plate-fin, embossed.  
*high corrosion-resistant material:* graphite, glass, Teflon™.  
*special:* rotary regenerator, electrically heated.

Excluded are surface condensers, feed-water heaters, cooling towers and waste heat boilers.

Chapters 1 and 2 describe the 'work-horse' of heat transfer equipment, namely, the shell-and-tube exchanger. Chapter 3 describes air-cooled exchangers and Chapter 4 describes gasketed-plate exchangers. Chapter 5 describes the more specialised heat transfer equipment, such as double pipe, heat pipe, gasketless plate, spiral, lamella, plate-fin, embossed panel, graphite, glass, Teflon™, rotary, and electrically heated.

Although two chapters are devoted to the shell-and-tube type, it accounts for about 64% of the European market and is expected to dominate at least until the end of the century, despite increasing competition from the plate types. Considering only the types described in Part 1, analysis of the value of heat exchangers purchased in Europe shows that tubular equipment accounts for 80% of the total, plate types 16%, and the remainder 4%.

Part 1 is completed by an appendix which summarises the features of the various heat exchanger types to assist in type selection. It will be seen that the construction of non-tubular equipment restricts selection to services when either the fluid pressure, or the pressure differences between the fluid streams, is less than about 30 bar. In many cases, the material of construction of either the heat transfer surface or the gaskets limits the fluid temperature to levels well below those handled by tubular equipment.

However, within their pressure and temperature limitations, the non-tubular equipment, particularly the plate types, provide excellent features and should always be considered as an alternative to the shell-and-tube type, for instance.



## CHAPTER 1

# Shell-and-tube heat exchangers: Construction and thermal features

### 1.1 Introduction

The shell-and-tube heat exchanger is the most common of the various types of unfired heat transfer equipment used in industry. Although it is not especially compact, it is robust and its shape makes it well suited to pressure operation. It is also versatile and it can be designed to suit almost any application. Except for the special purpose air-cooled heat exchanger, it is usually the only type which can be considered for large surface areas having pressures greater than 30 bar and temperatures greater than 260 °C.

The basic construction of a shell-and-tube heat exchanger is illustrated by Fig. 1.1, in which the chief components, discussed below, are numbered. As the name implies, a shell-and-tube heat exchanger consists of a shell(1), invariably cylindrical, containing a nest of tubes(21), plain or finned, which run parallel to the longitudinal axis of the shell, and are attached to perforated flat plates, termed tubesheets(22), at each end. The tubes pass through a number of flat plates, termed baffles(25), along their length, which serve to support them and to direct the fluid flow in the shell. The assembly of tubes and baffles, termed the tube bundle, is held together by a system of tie rods and spacer tubes(24). The fluid which flows inside the tubes is directed by means of special ducts, known as stationary and rear heads or channels(10)(11).

The construction of the various shell-and-tube exchanger types is shown in Figs. 1.1–1.15 and Fig. 1.30 shows a typical tube bundle

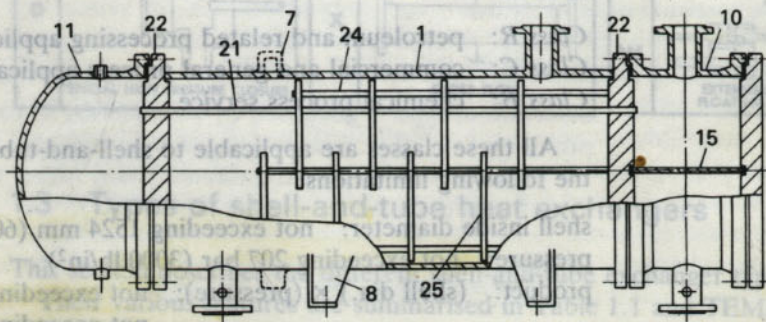


Figure 1.1 Fixed tubesheet exchanger (AEM). (Refer to Table 1.2 for nomenclature of components.)



#### 4 Shell-and-tube heat exchangers: construction and thermal features

assembly including tie rods and spacer tubes. The shell-and-tube heat exchangers discussed in this chapter are generally suitable for, but not restricted to, pressures up to 250 bar and temperatures up to 650 °C.

Section 1.2 introduces the Standards of Tubular Exchanger Manufacturers Association which relate to the types of shell-and-tube heat exchangers described in section 1.3. The advantages and disadvantages of the various head types are discussed in section 1.4, while section 1.5 describes features which relate to thermal design.

Although the pressure components of a shell-and-tube heat exchanger are designed in accordance with a pressure vessel design code, such as the American Society of Mechanical Engineers (ASME), Section VIII, Division 1, or British Standards Specification (BSS) 5500, it is not the function of a pressure vessel code to deal with the special features of shell-and-tube heat exchangers. In order to give guidance and protection to purchasers, designers and fabricators, it is essential to have a supplementary code which deals with these features and, in addition, provides minimum standards relating to design, materials, thicknesses, fabrication, tolerances, testing, inspection, installation, operation, maintenance and guarantees.

Typical supplementary codes are TEMA, described in section 1.2, API Standard 660, published by the American Petroleum Institute and HEI (Heat Exchanger Institute).

### 1.2 Tubular Exchanger Manufacturers Association Inc. (TEMA)

A widely accepted standard is that published by the Tubular Exchanger Manufacturers Association, known as TEMA, which is intended to supplement the ASME Boiler and Pressure Vessel Code, Section VIII, Division 1, although most of the information may be used to supplement other pressure vessel codes if required. The TEMA standard was prepared by a committee comprising representatives of 27 USA manufacturing companies and their combined expertise and experience provide exchangers of high integrity at reasonable cost.

TEMA presents three mechanical standards which specify design, fabrication and materials of unfired shell-and-tube heat exchangers as follows:

- Class R:** petroleum and related processing applications.
- Class C:** commercial and general process applications.
- Class B:** chemical process service.

All these classes are applicable to shell-and-tube heat exchangers with the following limitations:

- shell inside diameter: not exceeding 1524 mm (60 in)
- pressure: not exceeding 207 bar (3000 lb/in<sup>2</sup>)
- product: (shell dia.) × (pressure): not exceeding 105 000 (mm × bar)  
not exceeding 60 000 (in × lb/in<sup>2</sup>)

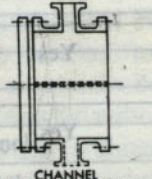
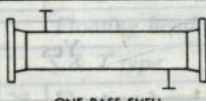
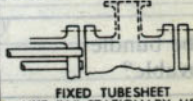
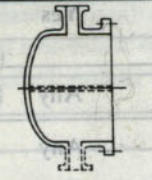
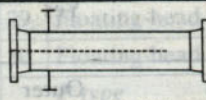
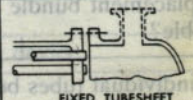
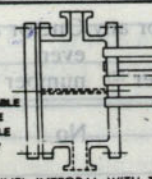
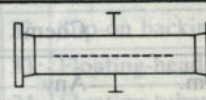
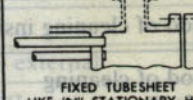
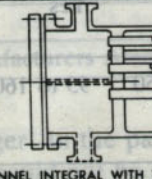
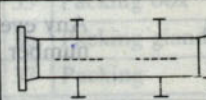
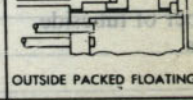
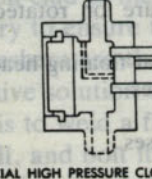
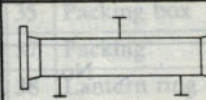

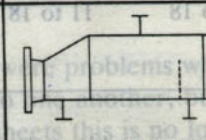
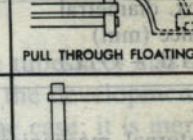
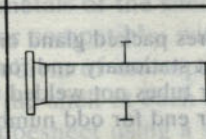
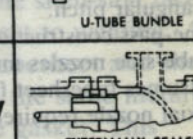
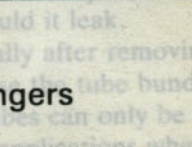




The intent of these parameters is to limit shell barrel thicknesses to about 50.8 mm (2 in) and bolt diameters relating to external flanges to about 76.2 mm (3 in). However, a special section entitled 'Recommended good practice' provides the designer with additional information for diameters up to 2540 mm (100 in), provided design temperatures and materials of construction result in reasonable thicknesses for pressure components.

TEMA also provides a standard type designation system as shown in Fig. 1.2.

Figure 1.2 TEMA type designation (© Tubular Exchanger Manufacturers Association, Section N-1, 1978)

FRONT END STATIONARY HEAD TYPES	SHELL TYPES	REAR END HEAD TYPES
<b>A</b>  CHANNEL AND REMOVABLE COVER	<b>E</b>  ONE PASS SHELL	<b>L</b>  FIXED TUBESHEET LIKE "A" STATIONARY HEAD
<b>B</b>  BONNET (INTEGRAL COVER)	<b>F</b>  TWO PASS SHELL WITH LONGITUDINAL BAFFLE	<b>M</b>  FIXED TUBESHEET LIKE "B" STATIONARY HEAD
<b>C</b>  REMOVABLE TUBE BUNDLE ONLY CHANNEL INTEGRAL WITH TUBE- SHEET AND REMOVABLE COVER	<b>G</b>  SPLIT FLOW	<b>N</b>  FIXED TUBESHEET LIKE "N" STATIONARY HEAD
<b>N</b>  CHANNEL INTEGRAL WITH TUBE- SHEET AND REMOVABLE COVER	<b>H</b>  DOUBLE SPLIT FLOW	<b>P</b>  OUTSIDE PACKED FLOATING HEAD
<b>D</b>  SPECIAL HIGH PRESSURE CLOSURE	<b>J</b>  DIVIDED FLOW	<b>S</b>  FLOATING HEAD WITH BACKING DEVICE
	<b>K</b>  KETTLE TYPE REBOILER	<b>T</b>  PULL THROUGH FLOATING HEAD
	<b>X</b>  CROSS FLOW	<b>U</b>  U-TUBE BUNDLE
		<b>W</b>  EXTERNALLY SEALED FLOATING TUBESHEET

### 1.3 Types of shell-and-tube heat exchangers

This section describes the different shell-and-tube exchanger types.

Their various features are summarised in Table 1.1 and TEMA nomenclature for the individual components is given in Table 1.2.

## 6 Shell-and-tube heat exchangers: construction and thermal features

**Table 1.1** Types of shell-and-tube heat exchangers – summary of features.

Exchanger type	Fixed tubesheet	U-tube	Floating head types				
			Split backing ring	Pull through	Lantern ring	Outside packed	Bayonet tube
TEMA rear-head type	Type L,M,N	Type U	Type S	Type T	Type W	Type P	–
Does it provide for differential movement between shell and tubes?	Yes – with bellows in shell	Yes	Yes	Yes	Yes	Yes	Yes
Is tube bundle removable?	No	Yes	Yes	Yes	Yes	Yes	Yes <sup>(4)</sup>
Is replacement bundle possible?	No	Yes	Yes	Yes	Yes	Yes	Yes <sup>(4)</sup>
Can individual tubes be removed and replaced?	Yes	Outer tubes only	Yes	Yes	Yes	Yes	Yes
Method of cleaning inside	Any	Chem.	Any	Any	Any	Any	Any
Method of cleaning outside <sup>(1)</sup>	Chem.	Any	Any	Any	Any	Any	Any <sup>(4)</sup>
Number of tubeside passes	Any	Any even number	One or any even number <sup>(2)</sup>	One or any even number <sup>(2)</sup>	One or two only <sup>(3)</sup>	Any <sup>(5)</sup>	One (special)
Is double tubesheet construction permissible?	Yes	Yes	No	No	No	Yes	Yes
Are there internal gaskets?	No	No	Yes	Yes	No	No	No
Approx. diametral clearance (mm) (Shell i.d. – OTL)	11 to 18	11 to 18	35 to 50	95 to 160	15 to 35	25 to 50	11 to 18

**Notes:**

- (1) External mechanical cleaning possible only with square or rotated square pitch, or unusually wide triangular pitch.
- (2) One-pass construction requires packed gland or bellows at floating head.
- (3) Tube-side nozzles must be at stationary end for two passes.
- (4) Assumes tubesheet for outer tubes not welded to shell.
- (5) Axial nozzle required at rear end for odd number of passes.

Selection of type is governed by such factors as ease of cleaning, provision for differential expansion between tube bundle and shell and the presence of an internal gasketed joint, rather than the function which it performs (i.e. condenser, vaporiser, etc.).

### 1.3.1 Fixed tubesheet (TEMA L, M, N)

In this type, shown in Fig. 1.1, both tubesheets are welded to the shell to form a box, and for this reason it is sometimes referred to as a box-type

**Table 1.2** TEMA nomenclature for heat exchanger components

No.	Component	No.	Component
<i>Shell</i>		<i>Tube bundle</i>	
1	Shell	21	Tubes
2	Shell cover	22	Stationary tubesheet
3	Shell flange – stationary head end	23	Floating tubesheet
4	Shell flange – rear head end	24	Tie rods and spacers
5	Shell nozzle	25	Baffles
6	Shell cover flange	26	Impingement plate
7	Expansion joint	27	Longitudinal baffle [see Figs 1.28 and 1.29]
8	Saddle	<i>Floating head assembly</i>	
9	Weir	<i>S &amp; T type</i>	
<i>Stationary/rear heads</i>		28	Floating-head cover
10	Stationary (or rear) head – channel	29	Floating-head flange
11	Stationary (or rear) head – bonnet	30	Floating-head backing device
12	Stationary (or rear) head flange	<i>P type</i>	
13	Channel cover (stat. or rear end)	31	Split shear ring
14	Stationary (or rear) head nozzle	32	Slip-on backing flange
15	Pass partition	33	Floating-head cover – external
<i>Miscellaneous parts</i>		34	Floating tubesheet skirt
16	Vent	35	Packing box
17	Drain	36	Packing gland
18	Instrument connection	37	Packing
19	Lifting lug	<i>W type</i>	
20	Liquid level connection	35	Packing box
Numbers relate to Figs 1.1, 1.3, 1.5, 1.6, 1.8, 1.9 and 1.11		37	Packing
		38	Lantern ring

©1978 by Tubular Exchanger Manufacturers Association Inc. Table N-2.

exchanger. In the past there were problems when the tubesheet and shell metals could not be welded to one another, but with the development of explosion-clad bi-metal tubesheets this is no longer the case; it is merely necessary to ensure that the metals of the shell and the shell-side face of the tubesheet are the same, or compatible, with respect to welding. An alternative solution to the problem of incompatible tubesheet and shell metals is to weld a flange to the shell at each end, in the same metal as the shell, and bolt it to the tubesheet using a suitable gasket. This construction is not recommended as the gasket cannot be replaced and the joint has insufficient flexibility for tightening should it leak.

The inside of the tubes may be cleaned mechanically after removing the channel covers, or complete channels, but because the tube bundle cannot be removed, cleaning of the outside of the tubes can only be achieved by chemical means. This type is limited to applications where the shell-side fluid is virtually non-fouling; fouling fluids must be routed through the tubes.

The combination of temperatures and thermal expansion coefficients



of the shell and tubes during service may cause a differential expansion between them, which, if excessive, might loosen the tube – tubesheet joints. The tubesheet must be designed against all differential movements likely to occur in service, not only during steady operation, but also at start-up, shutdown, cleaning out, etc. A fixed tubesheet exchanger can absorb a limited differential movement, but when this causes overstressing of any component an expansion joint (shown dotted in Fig. 1.1) must be fitted in the shell barrel.

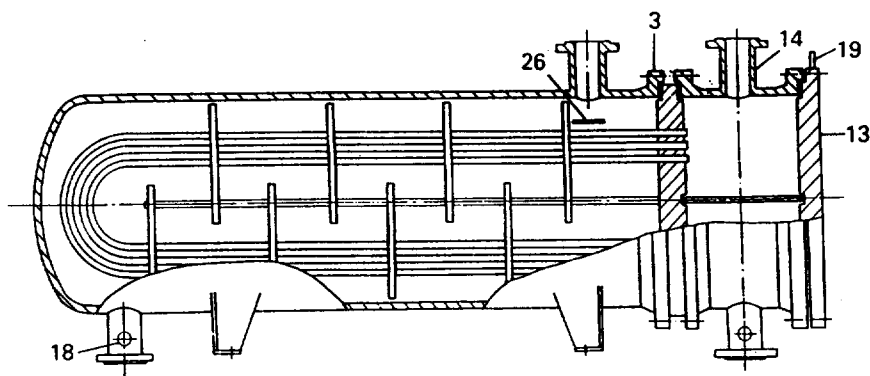
The tube bundle cannot be removed without cutting the shell, but by using special tube cutters and extractors individual tubes may be withdrawn and replaced by new ones. Should a tube lodge or break inside the shell the appropriate tube hole is plugged in each tubesheet.

An important advantage of the fixed tubesheet exchanger is that there are no internal joints, thus eliminating a potential source of leakage of one fluid into the other. Another advantage is that the peripheral tubes may be placed close to the inside of the shell, due to the absence of an internal joint, so that more tubes can be accommodated in a shell of given inside diameter for the fixed tubesheet type than for any other type. In addition the fact that there are no flanges on the shell-side makes it desirable for high-pressure and/or lethal services.

### 1.3.2 U-tube (TEMA U)

The U-tube exchanger, shown in Fig. 1.3, has only one tubesheet, and as each tube is free to move relative to the shell, the problem of differential movement is eliminated. The tube bundle can be withdrawn to enable the outside of the tubes to be cleaned mechanically, but the inside of the tubes is usually cleaned by chemical methods. This type is limited to applications where the tube-side fluid is virtually non-fouling; fouling fluids should be routed through the shell.

Figure 1.3 U-tube exchanger (AEU). (Refer to Table 1.2 for nomenclature of components.)



In most cases U-tubes of varying bend radii are used, with the result that once the bundle has been made only peripheral tubes are readily accessible for renewal and damaged tubes in the inner rows are usually plugged. Some U-tube exchangers are made in which all U-tubes are identical, which is advantageous with regard to standardisation and the stocking of spares, but considerably less tubes can be accommodated.

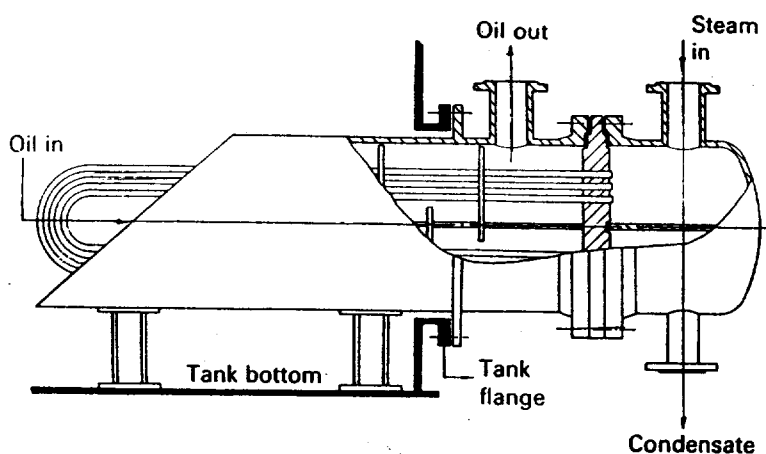
In common with the fixed tubesheet type, the U-tube type has no

internal joints, which means that peripheral tubes may be placed close to the inside of the shell. However, as there is a practical limit to the bend radius of the innermost tubes, the number of tubes accommodated within a given shell diameter is slightly less than that for the fixed tubesheet type. In some cases the stationary tubesheet is welded to the shell, thus eliminating the shell/tubesheet flange. (Component 3, Fig. 1.3). Although the tube bundle cannot be readily removed in these circumstances, this construction may be preferred to the fixed tubesheet type for high-pressure/lethal services if the latter presents differential movement problems.

The tank suction heater shown in Fig. 1.4 is a special application of the U-tube exchanger. The function of this heater is to heat viscous liquids, particularly heavy fuel oils, during pumping from a storage tank to reduce the viscosity of the liquid and assist pumping. In addition, there is no need to maintain the entire tank contents at the required pumping temperature. The heating medium, usually steam, flows inside the tubes which may be plain or, more usually, longitudinally finned.

Another application for U-tubes is the bundle-in-column reboiler ('stab-in' bundle) shown in Fig. 1.11 (inset), as an alternative to the external type.

**Figure 1.4** Tank suction heater (BEU)



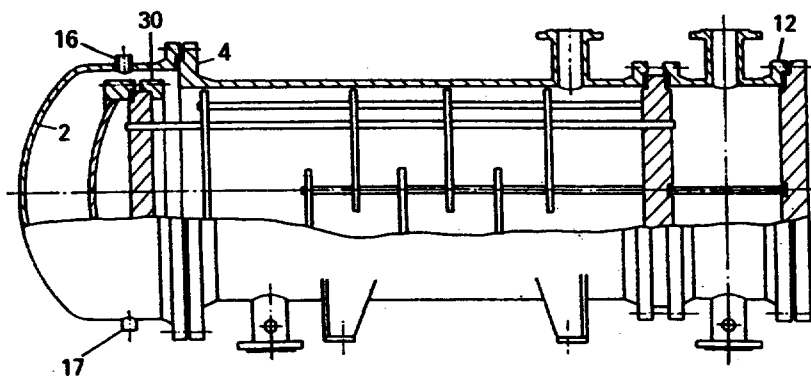
### 1.3.3 Floating-head types

Floating-head exchangers are so called because one tubesheet is fixed relative to the shell, while the other is free to 'float', thus permitting differential movement between shell and tubes, and also complete tube bundle withdrawal. There are four floating-head types, namely, split backing ring (TEMA S), pull through (TEMA T), externally sealed (lantern ring) (TEMA W), and outside packed (TEMA P). They differ only in the design of the floating head.

#### Split backing ring (TEMA S)

This type is shown in Fig. 1.5. To separate the shell- and tube-side fluids at the floating-head end, the tube-side of the floating tubesheet is fitted with a flanged, gasketed cover at its periphery which is held in position by bolting it to a split backing ring on the other side of the tubesheet.

**Figure 1.5** Split backing ring floating-head exchanger (AES). (Refer to Table 1.2 for nomenclature of components.)



The complete floating-head assembly (flange, cover, tubesheet and backing ring) is located beyond the main shell in a shell cover of larger diameter.

Access to the tube ends at the stationary tubesheet is readily obtained by removing the channel cover or complete channel. Access to the tube ends at the floating tubesheet is more involved because the shell cover must first be removed before the split backing ring and floating-head cover can be dismantled. After these operations have been completed the inside of the tubes may be cleaned *in situ*, or the complete bundle removed from the shell for cleaning the outside of the tubes or repair.

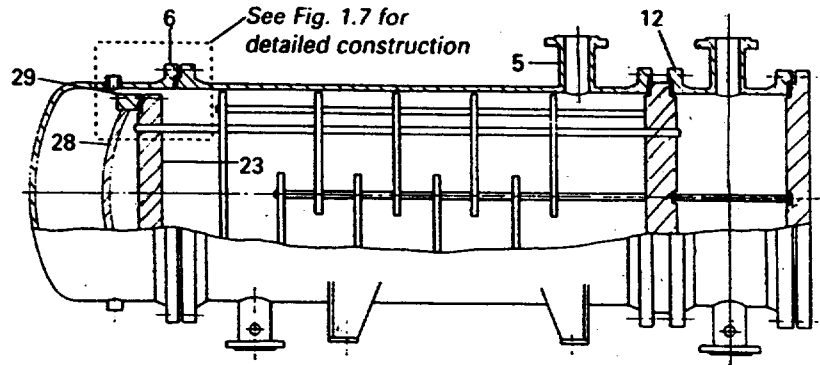
Although this type of floating-head exchanger is widely used it does have an internal joint at the floating head and careful design is essential to avoid leakage of one fluid into another. The nature of the floating-head construction limits it to an internal design pressure of the order of 50 bar (750 lb/in<sup>2</sup>). Peripheral tubes cannot encroach beyond the inside diameter of the floating-head gasket so that this design accommodates a smaller number of tubes than the fixed tubesheet and U-tube types having the same shell inside diameter.

#### **Pull through (TEMA T)**

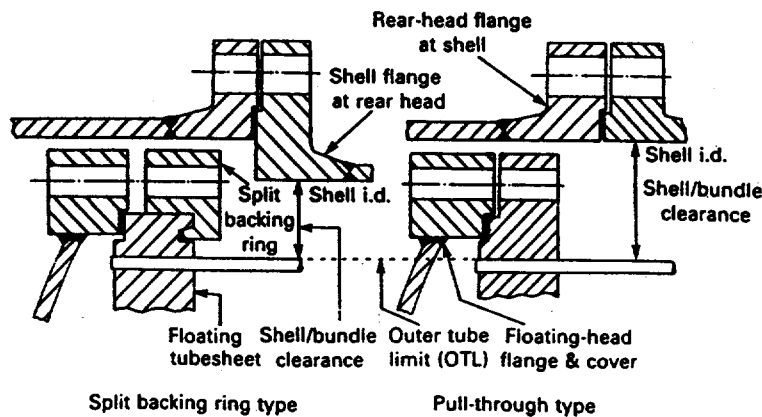
It will be seen from Figs. 1.6 and 1.7 that this type is similar in construction to the split backing ring type except that the floating-head cover flange is bolted directly to the floating tubesheet. The split backing ring is not required and the floating tubesheet diameter must be increased to match the outside diameter of the floating-head flange. As a result, the shell diameter becomes approximately the same as the enlarged shell cover of the split backing ring type to contain the same number of tubes. The pull-through type accommodates a smaller number of tubes in a given shell diameter than any other types. Internal pressure has a significant effect; the flange diameter increases as the pressure increases so that the area available for tubes in a given shell diameter is reduced.

The important advantage of the pull-through type over the split backing ring type lies in reduced maintenance time, because the bundle can be withdrawn from the shell without first removing either shell or floating-head covers. Should it prove difficult to remove a bundle from the shell, the flanged rear head may be removed to gain access to it. A significant cost reduction can be made by omitting the two rear-head flanges (component 6, Fig. 1.6), but the tubes can no longer be inspected or cleaned *in situ* and the bundle must be withdrawn and inserted 'blind'.

**Figure 1.6** Pull-through floating-head exchanger (AET). (Refer to Table 1.2 for nomenclature of components.)



**Figure 1.7** Typical floating-head assembly: split backing ring and pull through. (Outer tube limit the same for both floating-head types.)



Because of this, omission of the rear-head flanges is usually permitted only when fouling on both sides is expected to be small – typically a fouling factor less than  $0.00035 \text{ m}^2 \text{ K/W}$  ( $0.002 \text{ hr}^\circ\text{F ft}^2/\text{Btu}$ ) on both sides (see Chapter 8). This type of construction also allows the substitution of bundles having shortened tube lengths.

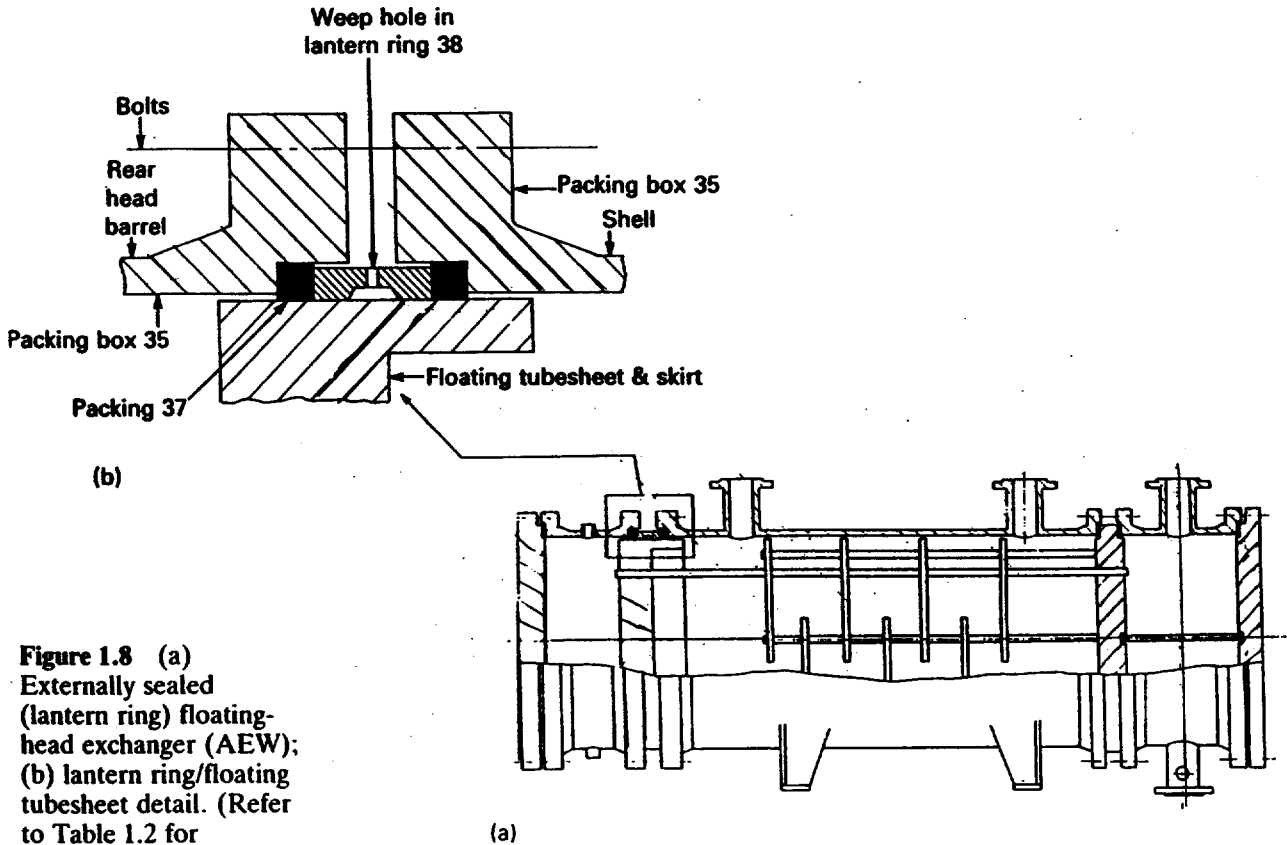
The floating head provides an internal joint and therefore careful design is essential to avoid leakage problems. The pull-through type is usually satisfactory up to internal design pressures of the order of 70 bar ( $1000 \text{ lb/in}^2$ ).

#### Externally sealed (TEMA W)

The feature of this type, which is shown in Fig. 1.8 and is also known as the lantern-ring type, is that separation of the shell- and tube-side fluids at the floating head is obtained by means of packing rings installed between the outside of the floating tubesheet and recesses in the rear-head flanges. The shell- and tube-side fluids each have their own packing rings, which are separated by a lantern ring provided with weep holes for leak detection. Leakage at the packing will not cause mixing of the shell- and tube-side fluids within the exchanger itself.

The width of the machined bearing surface at the floating tubesheet periphery must accommodate the two packing rings, the lantern ring and thermal movements of the bundle. In some cases the pressure thickness of the floating tubesheet is sufficient, but if not the extra bearing width is obtained by providing a machined skirt at the tubesheet periphery. The skirt may be an integral part of the sheet or attached by welding.

This simple type of exchanger provides all the advantages of the split



**Figure 1.8** (a) Externally sealed (lantern ring) floating-head exchanger (AEW); (b) lantern ring/floating tubesheet detail. (Refer to Table 1.2 for nomenclature of components.)

backing ring and pull-through type exchangers, but without the disadvantage of an internal joint. However, it is limited to one or two tube-side passes, which are discussed in section 1.5.6, while the glanded construction on both sides limits its use to low-pressure, non-lethal services. Maximum operating pressure is related to shell diameter, typical examples being 5 bar at 1524 mm diameter and 20 bar at 600 mm diameter. Maximum operating temperature is about 200 °C.

If a skirt is provided at the floating tubesheet the clearance between the inside of the shell and peripheral tubes is similar to that of the split backing type within the above pressure limitations. If there is no skirt this clearance may be reduced slightly, but adequate peripheral metal must remain to eliminate tube-hole distortion arising from expansion or welding of the tube ends.

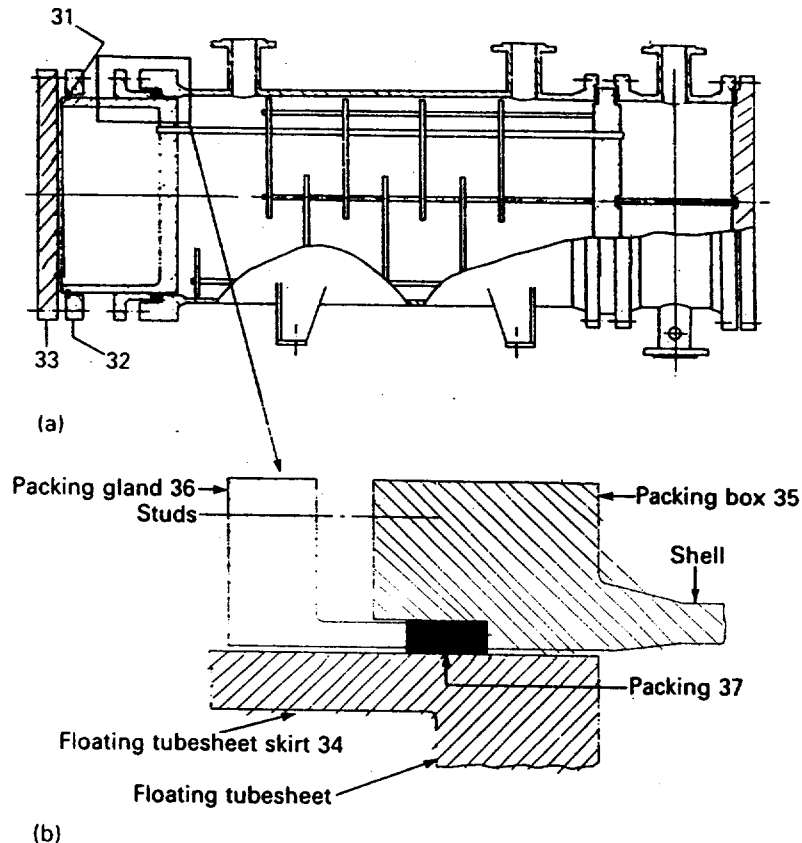
#### Outside-packed (TEMA P)

The outside-packed floating-head exchanger is shown in Fig. 1.9. One end of a cylindrical barrel, or skirt, is welded to the periphery of the floating tubesheet, while the other is fitted with a flat cover, bolted to a slip-on backing flange. The backing flange is held in place by a split shear ring inserted into a groove in the skirt wall. The skirt must slide inside the whole length of the shell during bundle insertion or withdrawal, and the clearance between shell inside diameter and skirt outside diameter is made as small as practicable. The shell-side fluid is contained by packing rings installed between the outside of the skirt, which has a machined finish, and recesses within the rear-head flange. The packing follower ring

(or packing gland) is designed to slide off the skirt. To prepare the bundle for withdrawal, the flat cover, split shear ring, backing flange, packing follower ring and packing are removed in that order. After this, bundle removal is exactly as for the other floating-head types.

This floating-head type provides all the features of the lantern-ring type with the added advantages that there are no restrictions on the choice of tube-side fluid, its temperature and pressure, or the number of tube-side passes. Because of the glanded construction the shell-side is limited to low-pressure, non-lethal fluids.

**Figure 1.9** (a) Outside-packed floating-head exchanger (AEP): (b) outside-packed floating tubesheet detail. (Refer to Table 1.2 for nomenclature of components.)



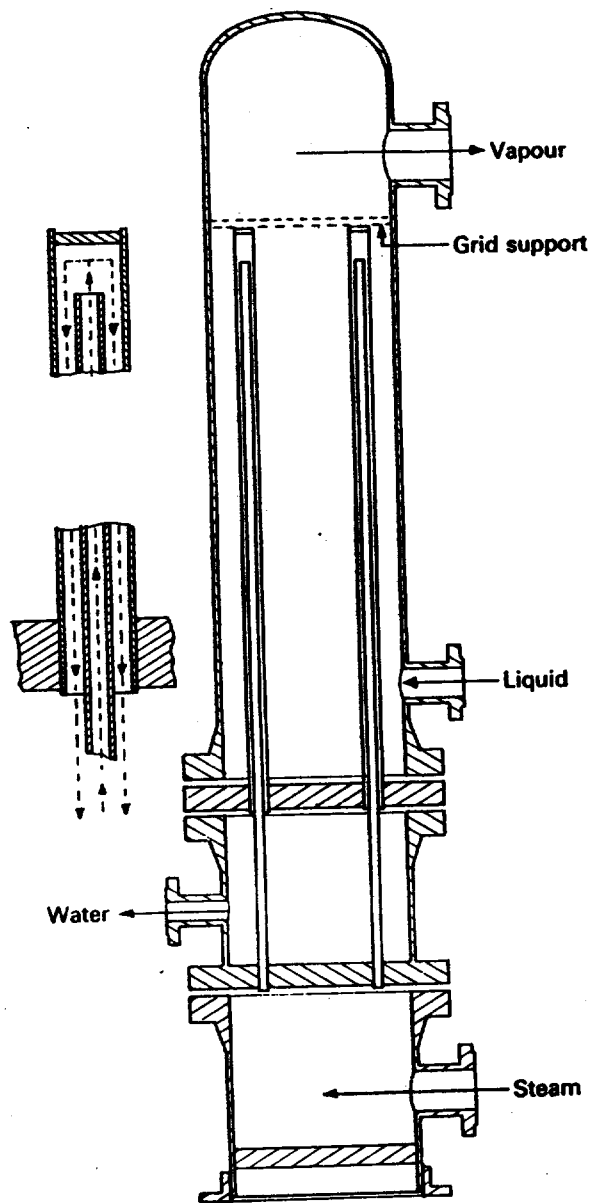
The clearance between the shell inside diameter and peripheral tubes is governed by the thickness of the skirt wall, which is related to the tube-side pressure. The skirt wall thickness is greater than the pressure thickness due to the groove required for the split shear ring. In addition, there must be adequate space between the peripheral tubes and skirt inside diameter to accommodate the tools required for tube-end attachment, tube withdrawal and cleaning. As a result the clearance between the shell inside diameter and peripheral tubes is similar to that of the split-backing type for the same tube-side design pressure.

### 1.3.4 Special designs

#### Bayonet tube

The feature of the bayonet tube, shown in Fig. 1.10, is that the inner tubes, outer tubes and shell are completely free to move independently of one another and it is therefore particularly suited to extremely large

Figure 1.10 Bayonet-tube exchanger



temperature differentials between the two fluids. The free end of the other tube must be sealed with a cover, thus providing an internal joint, but as the cover can be welded to the tube it does not present the same leakage risk as a gasketed joint. The heat transfer surface is that of the outer tube.

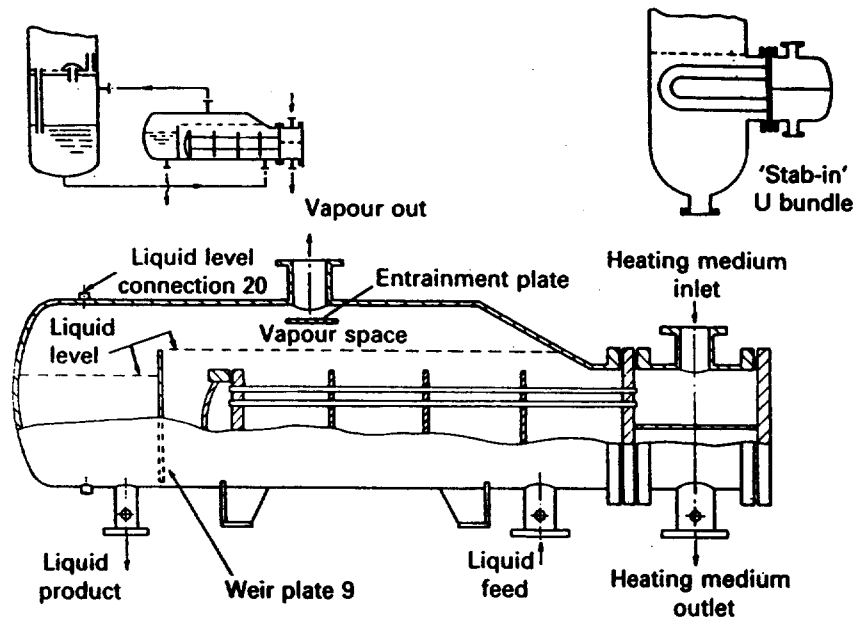
The shell-side may be provided with conventional baffles, but short vertical units are sometimes unbaffled and are suited particularly to certain shell-side condensing and vaporising duties requiring a low pressure loss. Figure 1.10 shows a short vertical tube unit for vaporising liquids at low temperatures in the shell using steam as the heating medium. The presence of steam in the inlet head and inner tubes prevents condensate freezing.

Depending on the shell- and tube-side pressures the outer tubes may be welded or expanded to their tubesheet. As the tubesheet for the inner tubes has to withstand only the pressure loss of the tube-side fluid, there is less incentive to weld the tube ends.

**Kettle reboiler (TEMA shell tube K)**

A special application of the U-tube and pull-through floating-head exchanger is the kettle reboiler shown in Fig. 1.11. Its function is to vaporise the shell-side fluid, and also to disengage any entrained liquid droplets from the exit vapour within the reboiler itself. To achieve this the shell diameter is made greater than the bundle diameter to provide a segmentally shaped disengagement area. The vapour space depth is a function of the number of exit vapour nozzles, the vapour exit flow rate, vapour density and quantity of entrained liquid permitted, but typically it is about one-third of the shell diameter, with a minimum depth of about 225 mm (9 in). For economy the transition from the enlarged shell diameter to the smaller stationary-head diameter is achieved with a conical section to give the kettle reboiler its characteristic shape. Any suitable tube-side heating medium, often steam, may be used.

**Figure 1.11** Kettle reboiler (AKT)



An impingement-type baffle is often placed below each vapour exit nozzle to assist in disengagement, but when a low level of liquid entrainment is required, a 'dry pipe' or woven metallic mesh demister pad, which is particularly effective, is installed at each nozzle. A 'dry pipe' consists of a horizontal length of pipe, closed at both ends and perforated with small holes along its length. A central vapour offtake from the pipe is sealed into the vapour exit nozzle. The vapour/liquid mixture enters the dry pipe via the small holes which 'knock-out' the entrained droplets.

If only a proportion of the shell-side fluid is to be vaporised the liquid level in the reboiler is maintained by a weir plate, as shown in Fig. 1.11, to ensure that the upper tube surfaces are not exposed. Vaporisation is usually limited to about 80% of the inlet liquid feed and the space between the end of the shell and weir plate is sized to provide adequate surge capacity. If 100% vaporisation occurs the liquid level is maintained by level gauges.

The inset of Fig. 1.11 shows a bundle-in-column reboiler ('stab-in' bundle) as an alternative to the external reboilers shown in this figure and



Fig. 1.12. Either pull-through or U-tube bundles may be used, but if the heating medium is clean the latter is preferred. Although a stab-in bundle avoids the cost of a shell, this saving must be compared with the extra cost due to (a) internal supports for the bundle, (b) the flanged connection on the column and (c) the extra column height at the bottom which is required to provide the same hold-up volume.

A 'double-ended' kettle may be provided for U-tube and floating-head construction, which is equivalent to two complete kettles in parallel. A bundle is inserted in each end of the shell, which is coned at both ends, as shown in Fig. 1.12.

### Chiller

The function of a chiller is to cool a fluid to a temperature lower than that which could be achieved with water as the coolant. The fluid to be cooled flows inside the tubes and a refrigerant, such as ammonia, methanol, fluorocarbon, etc., vaporises on the outside. Fixed tubesheet construction is often used because of the absence of fouling and the moderate temperature difference between fluids. See Fig. 1.13.

### Double-bundle exchanger

The double-bundle, or intermediate fluid, exchanger shown in Fig. 1.14 is particularly suited to the vaporisation of low-temperature liquids, using steam as the heating medium. A single-bundle unit, unless carefully designed, is always prone to condensate freezing. An intermediate, or buffer fluid, such as ammonia, methanol or propane, for example, is used on the shell-side, where the steam-heated lower bundle acts as a kettle to vaporise the buffer fluid. The vaporised buffer fluid condenses on the outside of the upper bundle to preheat and vaporise the low-temperature liquid inside the tubes, the buffer fluid condensate falling into the boiling pool around the lower bundle.

This type of unit responds well to rapid changes in demand.

### Coiled tube

The coiled tube heat exchanger was developed at the beginning of the 20th century by Von Linde in Germany, followed by Hampson in England. Although developed initially for the commercial liquefaction of air, it is used widely for liquefaction and vaporising applications in the petrochemical, low-temperature and nuclear industries.

The tubes are wound along the outside of a cylindrical core in the form of coils which are contained within a cylindrical shell. Successive coil layers are wound in opposite directions, separated by spacers, and the core provides strength during manufacture and operation. The ends of the coils are attached to tubesheets, as shown in Fig. 1.15.

One fluid stream flows through the shell, while one or more independent fluid streams flow inside the coils. Design flexibility is provided in that the tube length, tube diameter, coil diameter and coil pitch may be varied as required. The coil construction readily absorbs differential expansion between shell and tubes.

In addition to these features, the coiled tube heat exchanger provides a high thermal effectiveness resulting from a long tube length in

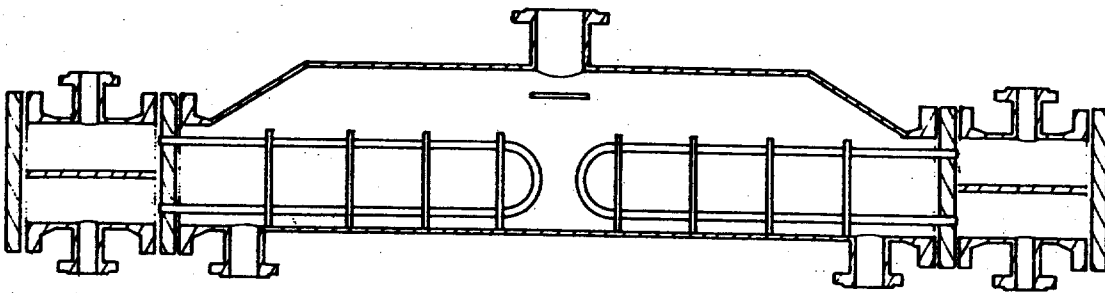


Figure 1.12 Double-ended kettle reboiler

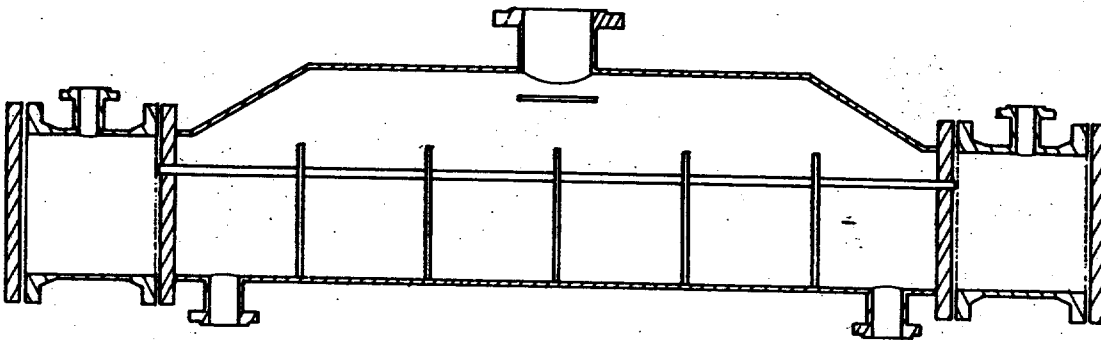


Figure 1.13 Fixed tubesheet kettle reboiler (AKL)

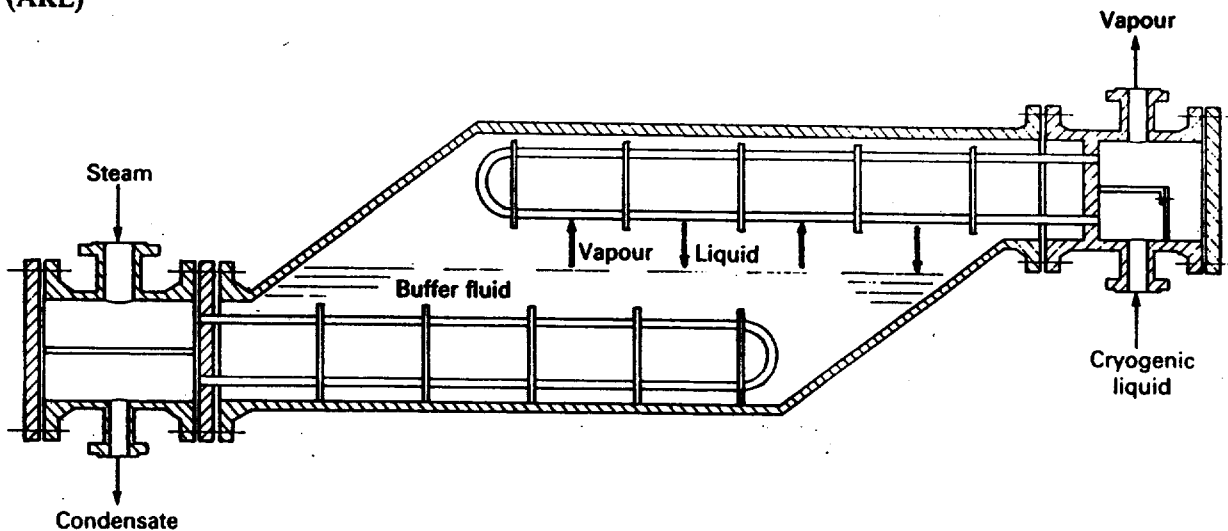


Figure 1.14 Double-bundle vaporiser

countercurrent flow (see Chapter 7). The exchangers have been built with five tube-side streams and a total surface area up to 20 000 m<sup>2</sup>.

#### Double-tubesheet designs

The tube-end joints provide the most likely source of leakage of one fluid into the other and in some services this leakage, however small, could contaminate the process completely. One solution to the problem is to adopt double-tubesheet construction as shown in Figs. 1.16 and 1.17. Any leakage of the tube-end joints in either tubesheet flows into the space between them, from which it may be vented or drained away. No mixing

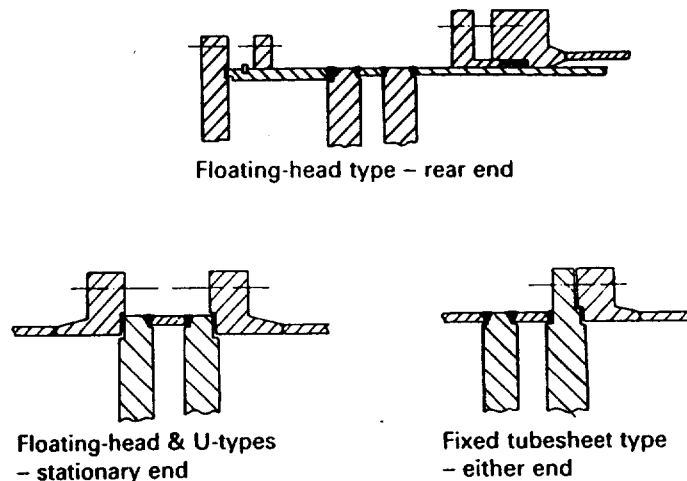


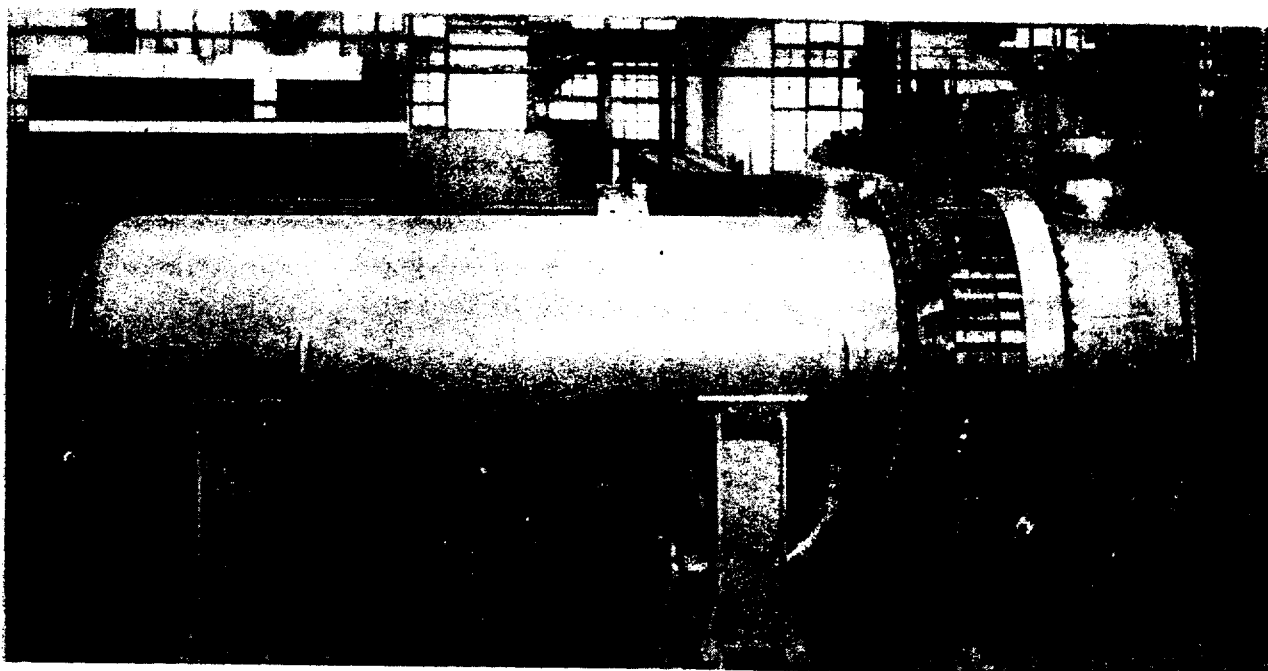
**Figure 1.15** Coiled-tube heat exchanger (courtesy of Linde AG, Werksgruppe TVT, München)

occurs in the shell or heads. Tube-end joints in the outer tubesheet may be welded or expanded, but only expanded joints are possible in the inner tubesheet.

Double tubesheets may be used in all exchanger types, although an outside-packed construction (as shown in Fig. 1.9) with its inherent limitations, is required if a floating-head exchanger is employed.

**Figure 1.16** Double-tubesheet construction





**Figure 1.17** U-tube double-tubesheet exchanger (courtesy of Whessoe Heavy Engineering Ltd, Darlington, UK)

## 1.4 Head types

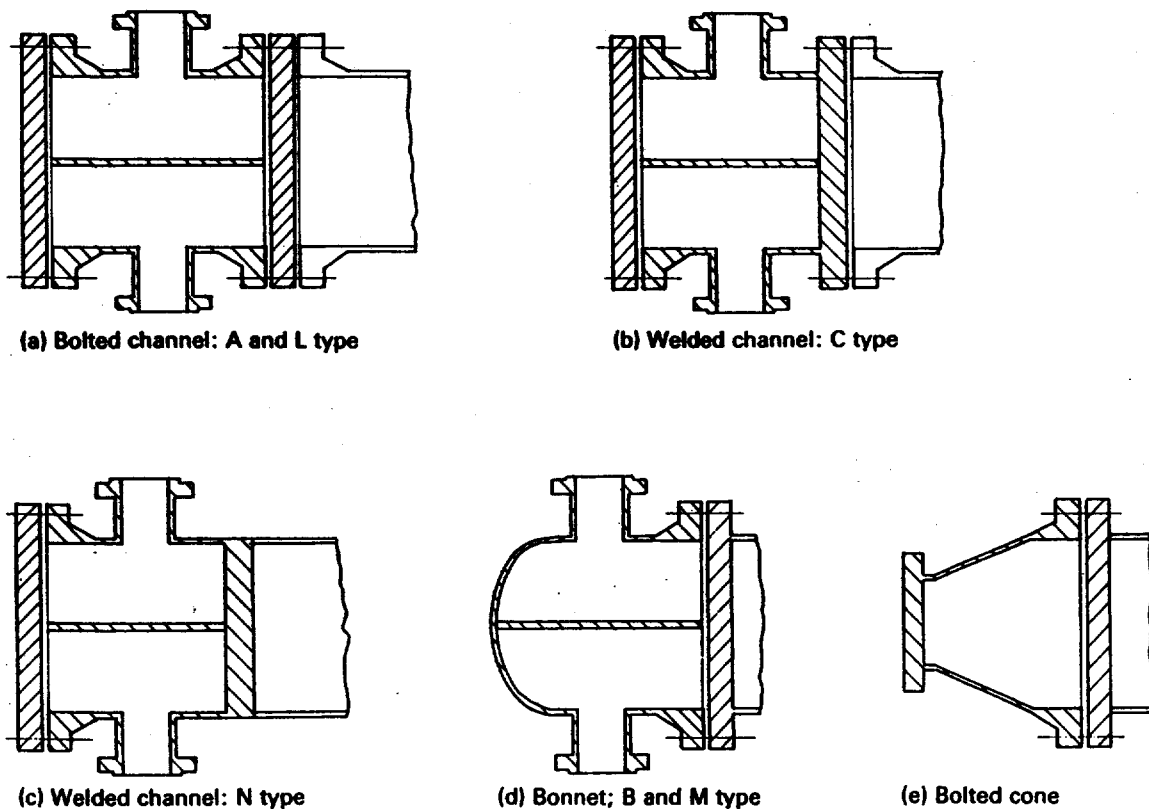
The head types used in shell-and-tube heat exchanger construction are described in the following section. The TEMA stationary and rear-head designations are shown against each head type where applicable.

### 1.4.1 Bolted channel (TEMA A and L)

The bolted channel, shown in Fig. 1.18(a), consists of a cylindrical barrel, or channel, which has a flange at both ends. One flange is bolted to a flat cover, while the other is bolted to the stationary tubesheet or a flange at the end of the shell. Removal of the flat cover provides access to the tube ends *in situ*, without having to unbolt the flanges connecting the external piping to the channel nozzles. After unbolting the nozzle-pipe flanges the complete channel may be removed, either to provide unrestricted access to the tube ends *in situ*, or as an essential stage in the withdrawal of floating-head and U-tube bundles.

Both stationary and rear ends of a fixed tubesheet exchanger may be fitted with bolted channels if required, but it is only worthwhile at the rear end if a nozzle is fitted there.

This type of head is desirable if cleaning of the inside of the tubes is expected to be frequent.



**Figure 1.18** Header types

#### 1.4.2 Welded channel (TEMA C and N)

The welded channel, shown in Figs. 1.18(b) and 1.18(c), is similar to the bolted type and the cylindrical barrel, or channel, has a flange at one end, which is bolted to a flat cover, but the other end is welded to the stationary tubesheet. Again, removal of the flat cover provides access to the tube ends, *in situ*, without having to unbolt the flanges connecting the external piping to the channel nozzles. Because the tubesheet and barrel form an integral unit, unrestricted access to the tube ends is not possible and it is essential to ensure that there is adequate space between the peripheral tubes and the inside of the barrel to accommodate the tools required for tube-end attachment, tube withdrawal and internal cleaning.

Both stationary and rear ends of a fixed tubesheet exchanger may be fitted with welded channels if required, but again it is only worthwhile at the rear end if a nozzle is fitted there.

The welded channel is cheaper than the bolted channel because there is only one flange instead of two, and this type is often selected for high-pressure/lethal services where it is desirable to minimise the number of external joints.

#### 1.4.3 Bonnet (TEMA B and M)

The bonnet-type channel, shown in Fig. 1.18(d), consists of a cylindrical barrel with a bonnet welded-on at one end and a flange at the other. The

flange is bolted to the stationary tubesheet or a flange at the end of the shell. Bonnet-type heads are cheaper than the bolted or welded types and, after removal, provide unrestricted access to the tube ends. However this is achieved only after unbolting the flanges connecting the external piping to the channel nozzles.

Bonnet-type channels are usually fitted at the rear end of fixed tubesheet exchangers when there are no nozzles there.

This type of head is generally used if cleaning of the inside of the tubes is expected to be infrequent.

#### 1.4.4 Bolted cone

When a floating-head or fixed tubesheet exchanger has a single tube-side pass, an axial cone-shaped head, flanged at both ends, as shown in Fig. 1.18(e), may be used as an alternative to bolted, welded and bonnet-type channels. One flange is bolted to the external piping, while the other is bolted to the stationary tubesheet or a flange at the end of the shell. Although the bolted cone provides a neat 'through' layout, access to the tube ends can only be achieved by removing the complete head.

Both ends of a fixed tubesheet exchanger may be fitted with bolted cones. Conical heads usually provide a lower tube-side pressure loss than the other types. Mal-distribution of the tube-side fluid may occur with axial coned heads and the design should be checked for this. If necessary a distributor plate may be installed ahead of the tubesheet.

### 1.5 Thermal design features

#### 1.5.1 Tube diameter

Compact, economical, units are obtained by using small-diameter, closely spaced tubes but the surfaces may foul up quickly and be difficult to clean by mechanical means. The problems of fouling and cleaning may be overcome by using large-diameter, widely spaced tubes, but the units will be less compact and more costly. The selection of tube diameter is therefore a compromise taking into account the fouling nature of the fluids, the space available and the cost. Tubes of 19.05 and 25.4 mm ( $\frac{3}{4}$ -1 in) outside diameter are the most widely used, but small units with clean fluids may use tubes as small as 6.35 mm ( $\frac{1}{4}$  in) outside diameter, and units handling heavy tars may use tubes 50.8 mm (2 in) outside diameter. Large reactors may use tubes 76.2 mm (3 in) outside diameter.

#### 1.5.2 Tube thickness

The tube-wall thickness must be checked against the internal and external pressure separately, or the maximum pressure differential across the wall.

**Table 1.3** Typical diameters, thicknesses and pitch arrangement of tubes

Tube outside diameter		mm	15.88	19.05	25.40	31.75
		in	$\frac{5}{8}$	$\frac{3}{4}$	1	$1\frac{1}{4}$
Tube thickness	Carbon and low-alloy steels	mm	1.65	2.11	2.77	3.40
		in	0.065	0.083	0.109	0.134
		b.w.g.	16	14	12	10
	Stainless steels, aluminium, copper and nickel alloys	mm	1.24	1.65	2.11	2.77
		in	0.049	0.065	0.083	0.109
		b.w.g.	18	16	14	12
Minimum tube pitch	Clean service (30° or 60°)	mm	19.84	23.81	31.75	39.69
		in	$\frac{5}{8}$	$\frac{15}{16}$	$1\frac{1}{4}$	$1\frac{5}{16}$
	Fouling service (45° or 90°)	mm	22.22	25.40	31.75	39.69
		in	$\frac{7}{8}$	1	$1\frac{1}{4}$	$1\frac{5}{16}$

However, in many cases the pressure is not the governing factor in determining the wall thickness. For example, a steel tube, 19.05 mm outside diameter, 2.11 mm thick, at 350 °C, is suitable for internal and external design pressures of 200 bar and 115 bar, respectively, within code rules, which is adequate for many applications. Except when pressure governs, tube-wall thickness is selected on the basis of (a) providing an adequate margin against corrosion, (b) resistance to flow-induced vibration (see Chapter 11), (c) axial strength, particularly in fixed tubesheet exchangers, (d) standardisation for the stocking of spares and (e) cost. Table 1.3 shows typical wall thicknesses for various tube diameters and metals.

Heat exchanger tubes are usually based on specifications related to outside diameter and nominal wall thickness rather than nominal bore because the permitted manufacturing tolerances are smaller. Tubes are available as minimum and average wall thicknesses. The wall thickness of minimum wall tubes must not be less than the nominal thickness, but may exceed it up to a specified maximum, typically 18–20%. The wall thickness of average wall tubes may be larger or smaller than the nominal thickness, typically  $\pm 10\%$ . Because minimum wall tubes cost more than average wall tubes, the pressure and corrosion characteristics of each case must be treated on its merits to decide whether the extra cost is justified. The inside diameter of minimum wall tubes is likely to be less than nominal and should be allowed for in tube-side pressure loss calculations.

Thinning of the tube wall occurs during bending, particularly in the smaller radius bends of U-tube exchangers. If pressure and corrosion requirements are not critical, and if the tube metal is not susceptible to work-hardening, some thinning can be tolerated. For instance, some users

specify that this should not exceed 15–18% of the wall thickness before bending. If thinning cannot be tolerated due to pressure and/or corrosion requirements, it is usual to bend the innermost two rows from straight tubes 15–30% thicker than the remainder. Ovality also occurs in the bends and this should not exceed 9–12% of the tube outside diameter.

### 1.5.3 Tube length

For a given surface area the cheapest exchanger is one which has a small shell diameter and a long tube length, consistent with the space and handling facilities at site and in the fabricator's shop. The incentive, therefore, is to make exchangers as long as possible, limited only by the tube length available from tube suppliers, but practical limitations usually control. Irrespective of the exchanger type, there must be available at site an unrestricted length of about twice the tube length in order that a tube bundle or tube may be withdrawn and replaced. In addition long, thin, removable bundles may present handling difficulties during withdrawal or insertion. The maximum tube length for removable bundle exchangers may be restricted to about 9 m, with a maximum bundle weight of about 20 tonnes. The maximum tube length for fixed tubesheet exchangers is less important but may be limited to about 15 m. However, in order to meet the demands of increased process plant capacities fixed tubesheet exchangers with tube lengths in the region of 22 m are not uncommon.

Tube lengths of 2438, 3658, 4877, 6096 and 7315 mm (8, 12, 16, 20 and 24 ft) are often regarded as standard for both straight and U-tubes, but other lengths may be used.

### 1.5.4 Tube pitch

It is customary practice to arrange the tube pitch (centre – centre distance) such that it is not less than 1.25 times the outside diameter of the tubes. In certain applications involving clean fluids and small tubes, say 12.7 mm ( $\frac{1}{2}$  in) outside diameter and less, the pitch/diameter ratio is sometimes reduced to 1.20. Table 1.3 lists typical tube pitches for various tube diameters and the pitch arrangements are shown in Fig. 1.19.

Selection of pitch angle is as follows:

<i>Pitch pattern</i>	<i>Pitch angle</i>	<i>Nature of shell-side fluid</i>	<i>Flow regime</i>
triangular	30°	clean	all
rotated triangular	60°	clean	rarely used – 30° better
square	90°	fouling	turbulent
rotated square	45°	fouling	laminar

For a given pitch/diameter ratio and shell inside diameter, about 15% more tubes can be accommodated for 30° and 60° pitch angle compared with 45° and 90°. To achieve compactness the incentive is to use 30° and 60° pitch angles, which are satisfactory for clean services, but these patterns are not permitted when external mechanical cleaning is required. To provide adequate mechanical cleaning lanes 45° and 90° pitch angles



## 24 Shell-and-tube heat exchangers: construction and thermal features

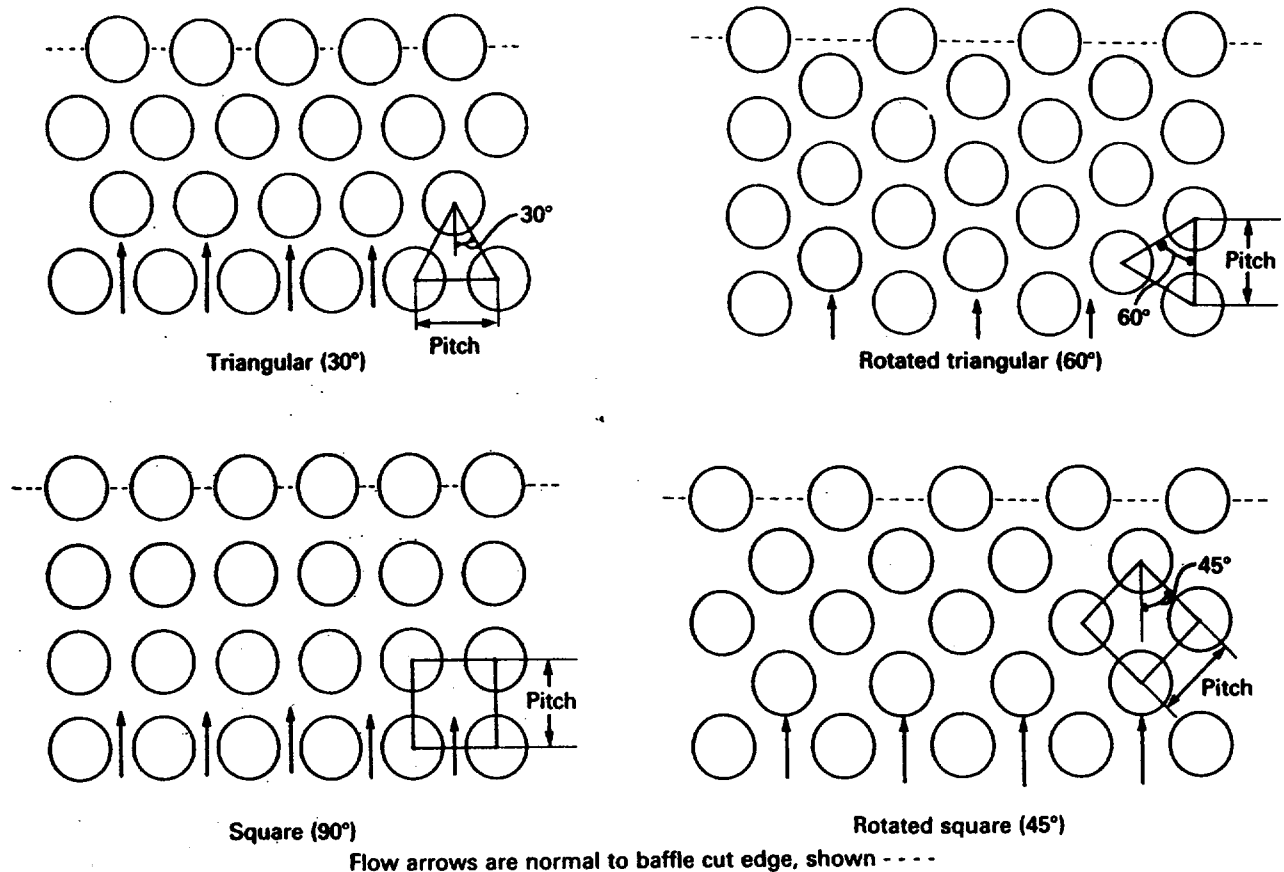


Figure 1.19 Tube pitch arrangements

must be used with a minimum gap between tubes of 6.35 mm ( $\frac{1}{4}$  in). In turbulent flow the  $90^\circ$  pitch angle has superior heat transfer and pressure loss characteristics to the  $45^\circ$  pitch angle; in laminar flow the  $45^\circ$  pitch angle is superior.

A further requirement for the tube layout of  $45^\circ$  and  $90^\circ$  pitch is that the cleaning lanes should be continuous throughout the bundle, or, if this is not possible in practice, every tube must be reached from one side or another.

Tube-end welding, described in sections 2.16 and 2.17, may require a wider tube pitch than normal depending on the tube diameter, thickness and material, and the welding technique employed.

### 1.5.5 Special tubes

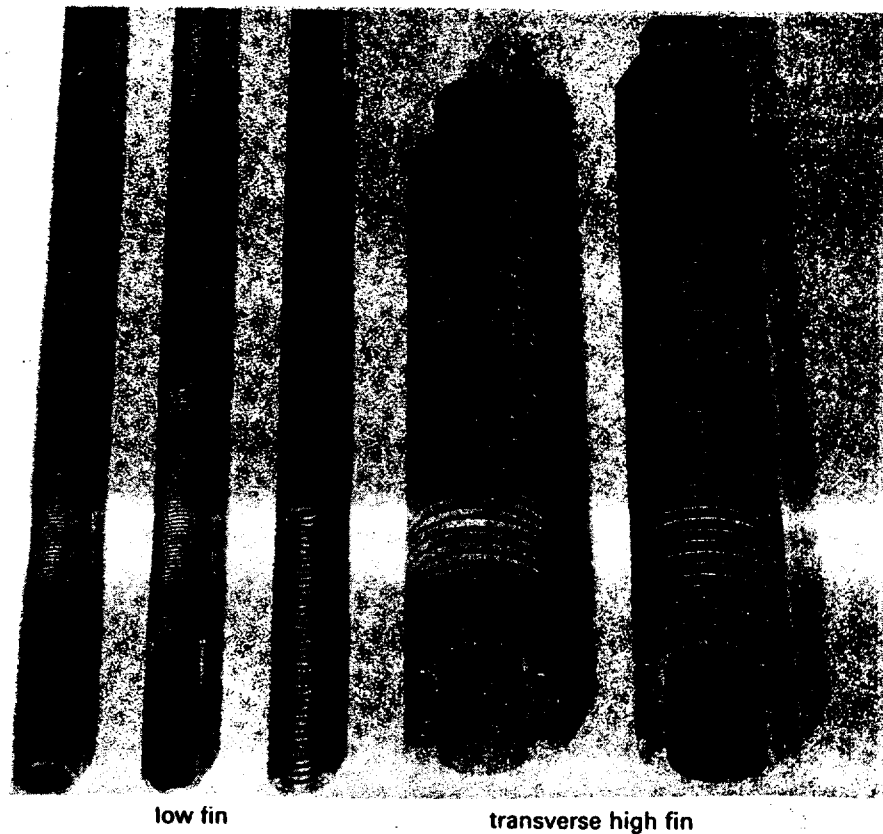
#### Bi-metal

In certain applications it may be difficult or expensive to obtain a single metal tube which will resist the corrosive action of both shell- and tube-side fluids and in this case a bi-metal tube should be considered. Almost any pair of metals may be drawn together to form a mechanically bonded bi-metal tube. If the combined wall thickness is not great the thickness of each tube is made roughly the same, but for a large combined wall thickness it is usual to limit the thickness of the more expensive metal as far as practicable in order to reduce cost.

**Low fin**

Low-fin tubes, in which the fins are extruded from the parent tube, are designed specifically to fit into shell-and-tube heat exchangers in exactly the same manner as plain tubes. (See Fig. 1.20 and also Chapter 9 for discussion of fins generally.) These integrally finned tubes may provide a cheaper design than plain tubes, particularly when the external heat transfer coefficient is lower than the internal coefficient, and an expensive tube material is required. Alternatively, the performance of an existing plain tube exchanger may be increased by retubing with low-fin tubes. (See section 13.1.)

**Figure 1.20** Integrally finned tubes (courtesy of Yorkshire Imperial Alloys, Leeds, UK)

**Transverse high fin**

These are also shown in Fig. 1.20, but are rarely used in shell-and-tube exchangers. Their greatest usage is in air-cooled heat exchangers which are described in Chapter 3. The various types of transverse high-fin tubes are described in section 3.6.2.

**Longitudinal high fin**

These are used in double-pipe exchangers and shell-and-tube exchangers, particularly tank suction heaters (Fig. 1.4) and line heaters handling fuel oil. They are described in section 5.1 which deals with double-pipe heat exchangers.

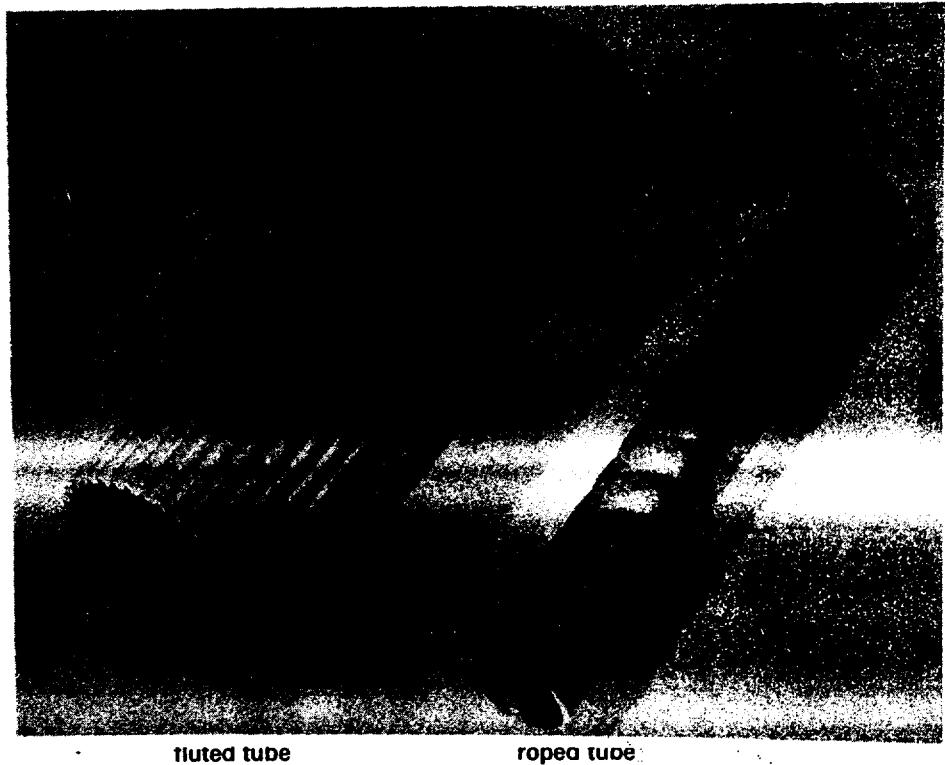
**Roped and fluted**

Both roped and fluted tubes, shown in Fig. 1.21, are used primarily in sea water distillation plants. Roped tubes are used in multi-stage flash preheaters, in which the tubes are horizontal with condensing steam on

the outside and salt water inside. Fluted tubes are used in vertical tube sea water evaporators with condensing steam on the outside and salt water evaporating inside.

The groove depth, pitch and helix angle of roped tubes can be varied widely to suit a diversity of applications. In the case of condensing steam a suitable profile can avoid problems associated with high surface tension in the condensate film by promoting good drainage to achieve a higher condensing coefficient than the corresponding plain tube. As the internal surface is not plain, increased internal coefficients, at increased pressure loss, are obtained and roped tubes may provide an attractive solution to single-phase applications by judicious selection of tube diameter and profile.

**Figure 1.21** Roped and fluted tubes (courtesy of Yorkshire Imperial Alloys, Leeds, UK)



Fluted tubes take advantage of high surface tension in the condensate film, which causes the condensate to flow from the 'peaks' to the 'troughs' of the profile, giving extremely high film coefficients in the region of the peaks.

#### **Tube inserts**

In order to improve the internal heat transfer coefficients, tubes may be fitted with devices such as twisted tapes, coiled wires, etc., inside them. These are known as tube inserts and are described in Chapter 10.

#### **1.5.6 Tube-side passes**

Each traverse of the tube-side fluid from one end of the exchanger to the other is termed a pass. Tube-side passes have thermal significance in that by changing the number of passes, the thermal designer is able to change

**Table 1.4** Typical tube pass numbers

Exchanger type		More common	Permissible but less common
Fixed tubesheet		1, 2, 4, 6, 8	3, 5, 10, 12, 14, etc.
U-tube		2, 4	6, 8
Floating head	Lantern ring	1, 2 <sup>(1)</sup>	–
	Outside packed	2, 4, 6, 8	1, 3, 10, etc. <sup>(2)</sup>
	Split backing ring & pull through	1, 2, 4, 6, 8 <sup>(3)</sup>	10, 12, 14, etc.

**Notes:**

- (1) Tubeside nozzles must be at stationary end for two passes.  
(2) Means to accommodate rear-end nozzle movement with odd number of passes.  
(3) Bellows or gland required at floating-head end for one pass.

the fluid velocity. Depending on process conditions, the number of passes required may be only one or as many as sixteen – typical numbers being given in Table 1.4.

To provide passes the head is fitted with flat metal plates, known as partition plates, which divide it into separate compartments. The pressure differential across each plate normally corresponds to the pressure loss of two passes, and the plate thickness, in the corroded condition, must be designed to suit. Typical partition plate thicknesses are 6.35–15.9 mm ( $\frac{1}{4}$ – $\frac{5}{8}$  in), depending on exchanger size. These are adequate for most applications, but cases arise where the plates must be thickened or stiffened to suit a high-pressure differential. Partition plates usually have a drainage hole.

Except for D-type and other special heads, partition plates for all other TEMA heads are always welded to the head barrel and to any integral tubesheet or cover. Where the tubesheet or cover is not integral with the head barrel, the tubesheet and cover are grooved and the edges of the partition plates sealed by a gasket embedded in the grooves. Typical tube pass layouts are shown in Fig. 1.22, which also shows the pattern of the partition plates, head gasket and grooves in the tubesheets and covers. The gasket is of one-piece construction in most cases. Figure 1.22 also shows the pass arrangements and the bend planes required for U-tube exchangers. The most effective tube packing arrangement for U-tubes with four tube-side passes is to divide the head into four equal quadrants. It should be noted, however, that the inlet and outlet passes are adjacent to one another and careful design is necessary to prevent inter-pass leakage.

In the case of small-diameter exchangers it will become increasingly difficult to weld-in the pass partition plates in the heads if there are a large number of passes.

### 1.5.7 Single tube-side pass floating head

In split backing ring and pull-through floating-head exchangers, having a single tube-side pass, special construction is required at the floating-head

28 Shell-and-tube heat exchangers: construction and thermal features

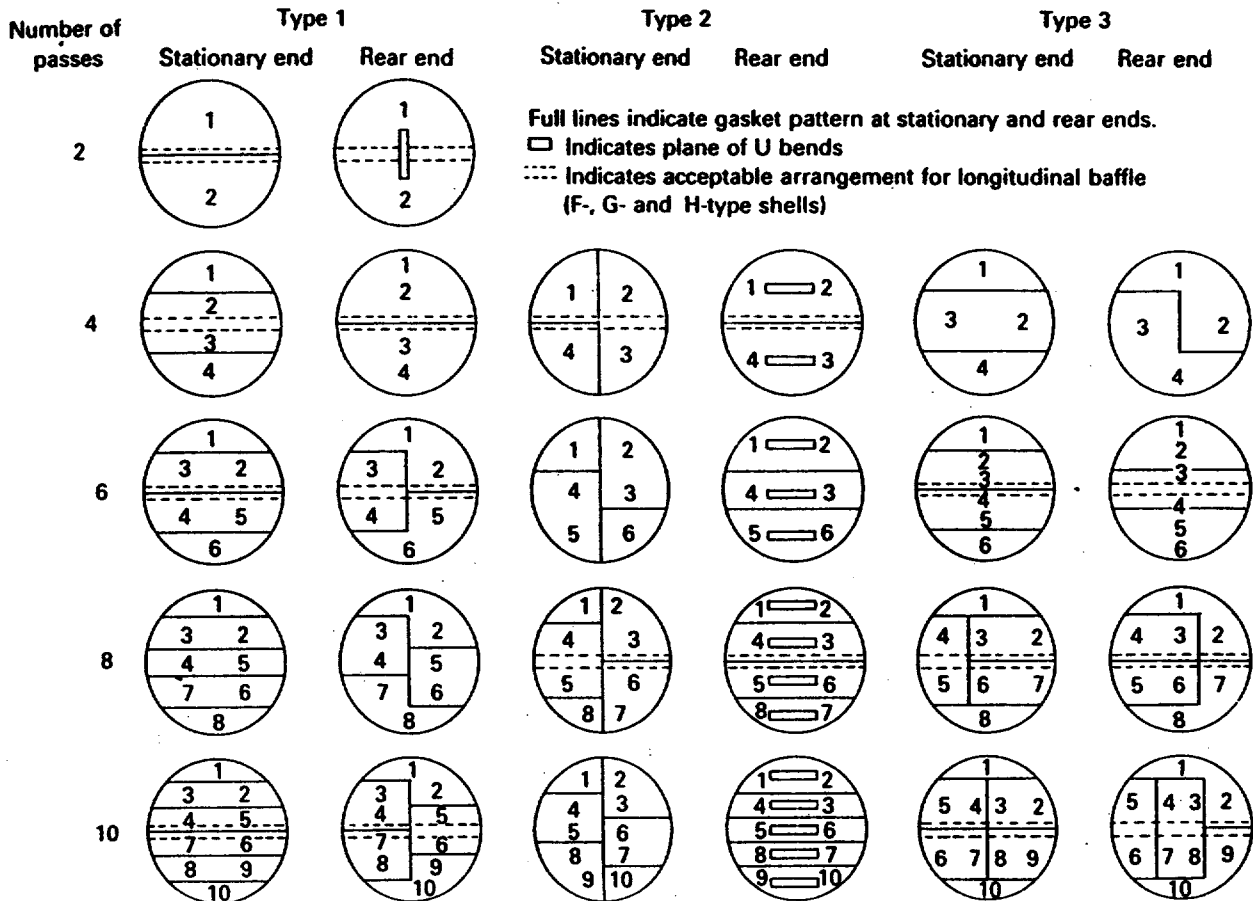


Figure 1.22 Typical tube pass layouts

end to accommodate the tube-side nozzle, which may be an inlet or an outlet. The nozzle must be free to move to accommodate the axial movement of the bundle, and also leak-tight where it passes through the rear head. The typical glanded construction shown in Fig. 1.23(a) is the simplest but is limited to moderate pressure, non-lethal, shell-side fluids such as steam and water. When glanded construction is not acceptable, the typical bellows construction shown in Figs. 1.23(b) and 1.24 is used.

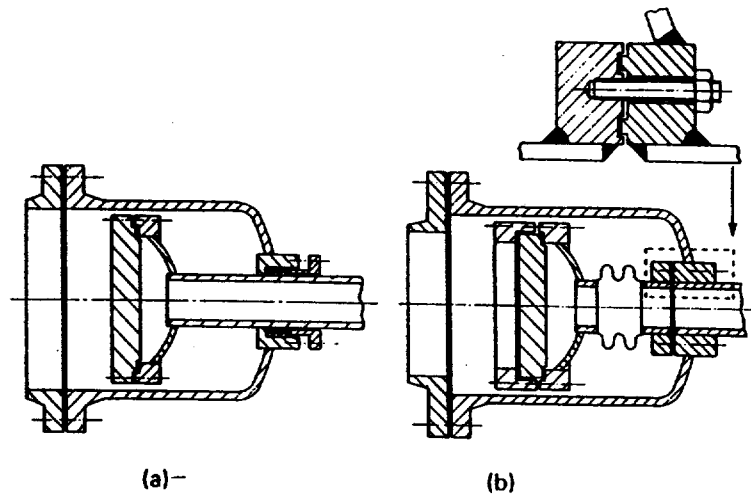
Because of the inherent limitations of packed glands and the fact that the bellows (usually thin-wall type) cannot be readily inspected and maintained, some users will not permit single tube pass floating-head construction.

1.5.8 Cross-type baffles

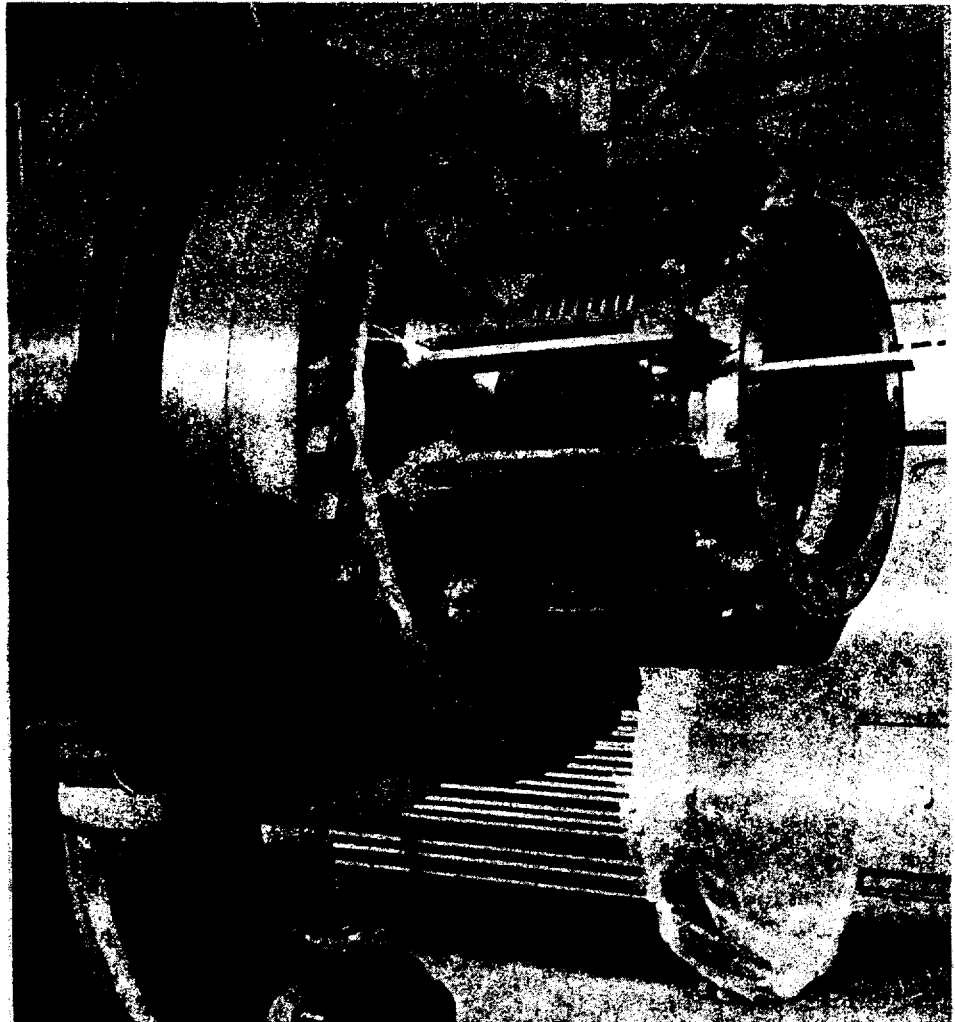
Cross-type baffles have thermal significance in that the shell-side fluid is made to flow to and fro across the bundle from one end of the exchanger to the other. By increasing or decreasing the distance between adjacent baffles, the thermal designer is able, within limits, to change the fluid velocity. Equally important, the baffles are spaced to support the tubes adequately to prevent sag and flow-induced vibration.

Figure 1.25 shows three common cross-type baffles: segmental, double

**Figure 1.23** Floating-head exchangers with one tube-side pass (a) glanded construction (b) bellows construction



**Figure 1.24** Single tube pass split backing ring floating-head exchanger with bellows (restraining bars in position prior to tube-side hydraulic test) (courtesy of Whessoe Heavy Engineering Ltd, Darlington, UK)



segmental, and triple segmental. Segmental baffles are the most common, but where a design is governed by shell-side pressure loss, it may be reduced appreciably by resorting to double- or triple-segmental baffles. In all cases the opening in the baffle through which the shell-side fluid flows from one baffle space to the next is termed the 'baffle window'. The

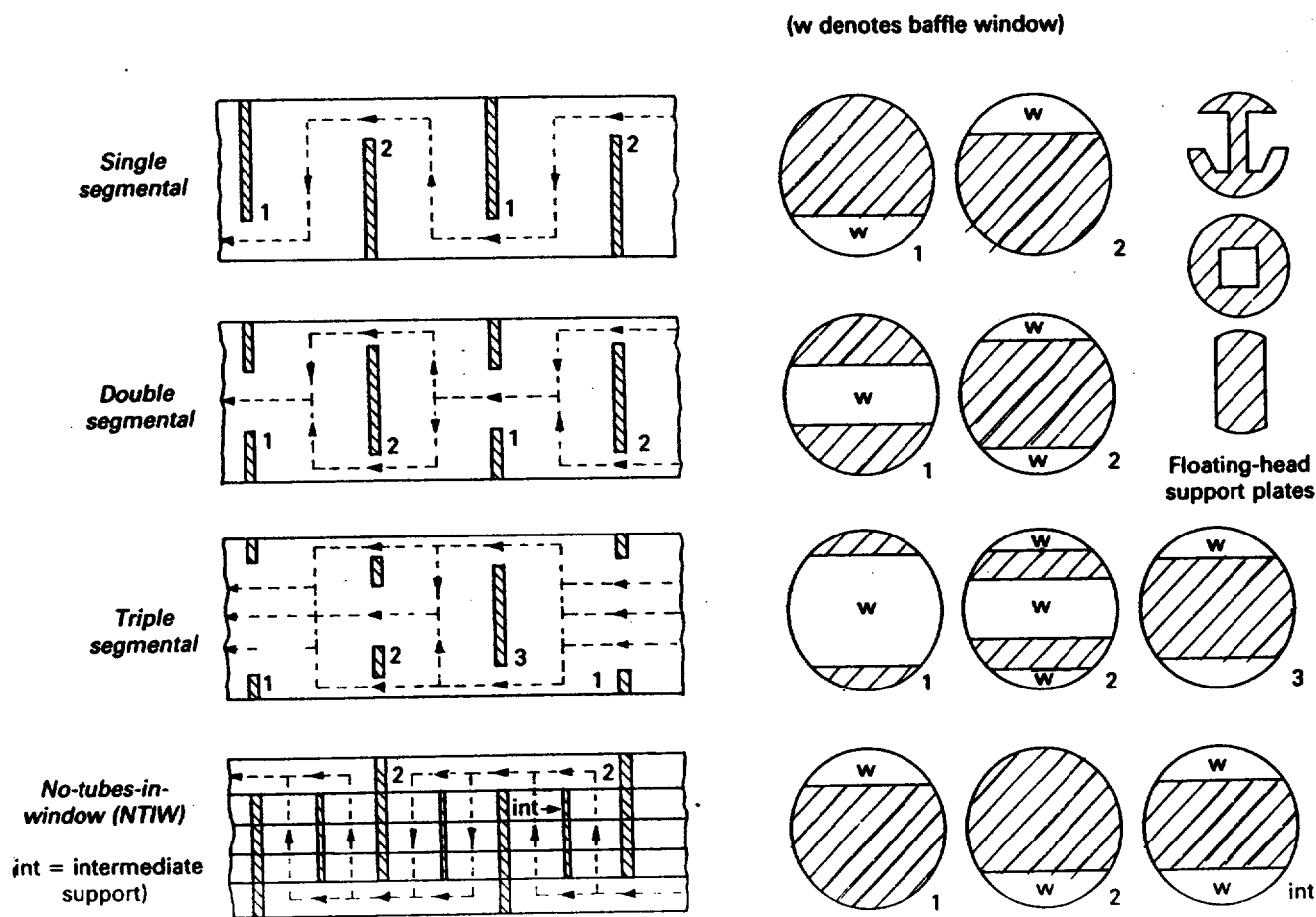


Figure 1.25 Cross-baffle arrangements

window opening segment height, expressed as a percentage of the shell diameter, is termed the 'baffle cut'. Typical baffle cuts are 15–40% for segmental baffles and 20–30% for double-segmental baffles. Adjacent baffles must have overlap at the edges, which ensures that tubes within the overlap are supported by every baffle. Tubes passing through the baffle windows are unsupported over a length of two baffle spaces for the single- and double-segmental type and three baffle spaces for the triple-segmental type.

In a horizontal exchanger the straight edge of the baffle at the window may be in the horizontal position (horizontal cut baffles, up-and-down flow) or vertical position (vertical cut baffles, side-by-side flow). The choice of edge orientation is usually made in accordance with Table 1.5.

Figure 1.25 also shows an arrangement in which there are no tubes in the baffle window (NTIW) and therefore each baffle supports all tubes. This construction was especially developed to overcome vibration problems which are described in Chapter 11. Additional intermediate support baffles may be introduced, which give added tube support and increase the natural frequency of the tubes without affecting heat transfer and pressure loss.

**Table 1.5** Baffle edge orientation

Service	Baffle edge	Notes
Single phase – clean	Either – horizontal more common	–
Single phase – fouling	Vertical	Prevents dirt settlement
Condensing	Vertical	Enables condensate to flow freely
Vaporising	Either	Horizontal prevents stratification

### 1.5.9 Support-type baffles

In shells of TEMA types G, H, K and X the shell-side fluid need not flow to and fro across the bundle, in which case cross-type baffles are not required. 'Full-circle' baffles, or support plates, which are not cut away at all, are used and every tube is supported at every baffle.

Split backing ring and pull-through floating-head exchangers have a special support-type baffle adjacent to the floating head to take the weight of the complete floating-head assembly. Full- or half-circle supports may be used, but the surface between floating tubesheet and support becomes ineffective. In order to increase the effectiveness of this surface it is usual to cut slots of various shapes in the baffle, as shown in Fig. 1.25. It is also usual to ensure that at least half the number of tubes in the bundle are supported by the baffle.

### 1.5.10 Baffle thickness

Thicknesses for cross- and support-type baffles depend on shell diameter and unsupported tube length, but usually range from 3.2 to 19 mm ( $\frac{1}{8}$  to  $\frac{3}{4}$  in). (See TEMA for further information.)

### 1.5.11 Baffle clearance

In order to assemble the bundle there must be a reasonable clearance between the baffle and the tube, but if the clearance is too large it may have an adverse effect on heat transfer and promote flow-induced vibration problems. Customary practice is to drill the hole 0.4–1.0 mm greater than the tube outside diameter, depending on service, tube size and baffle pitch. However, despite a possible increase in fabrication costs, it is sometimes necessary to reduce the clearance still further in order to minimise flow-induced vibration problems.

Irrespective of exchanger type, there must be a reasonable clearance between shell and baffles in order to insert the bundle into the shell, but if the clearance is too large it may have an adverse effect on



performance. The diametral clearance depends on bundle diameter but is usually 3–12 mm. However, greater clearances are permitted when they have no effect on shell-side heat transfer coefficient or mean temperature difference between fluids. (See TEMA for further information.)

### 1.5.12 Maximum unsupported tube length

The maximum unsupported tube lengths specified by TEMA are given in Table 1.6. Table 1.7 provides the maximum distance between adjacent baffles, of various types, taking a 19.05 mm ( $\frac{3}{4}$  in) outside diameter steel tube as an example.

**Table 1.6** TEMA maximum unsupported tube length

Tube outside diameter		Tube materials and temperature limits (°C (°F))			
		Carbon & high-alloy steel: 400 (750) Low-alloy steel & nickel: 454 (850) Nickel-copper: 316 (600) Nickel-chromium-iron: 538 (1000)		Aluminium & alloys Copper & alloys Titanium & zirconium at code maximum temp.	
mm	in	mm	in	mm	in
19.05	$\frac{3}{4}$	1524	60	1321	52
25.40	1	1880	74	1626	64
31.75	$1\frac{1}{4}$	2235	88	1930	76
38.10	$1\frac{1}{2}$	2540	100	2210	87
50.80	2	3175	125	2794	110

© 1978 by Tubular Exchanger Manufacturers Association Inc. Table R-4.52.

**Table 1.7** Maximum spacing between adjacent baffles  
19.05 mm ( $\frac{3}{4}$  in) i.d. steel tube

Baffle type	Maximum spacing (based on Table 1.6)	
	mm	in
Segmental	762	30
Double segmental	762	30
Triple segmental	508	20
Full circle	1524	60

In some cases the end baffle spacing must be made greater than the regular spacing in the remainder of the exchanger to accommodate the required nozzle, with possibly a reinforcing pad (see section 2.9). The longest unsupported tube length is usually that which exists in the baffle window nearest the tubesheets, i.e. between the inner face of the tubesheet and the second baffle from it, for segmental and double-segmental baffles. The unsupported length must not exceed the TEMA maximum as this region is particularly susceptible to flow-induced vibration.

### 1.5.13 Minimum baffle spacing

Segmental baffles should not be spaced closer than about one-fifth of the shell diameter or 50.8 mm (2 in), whichever is the greater. The insertion of tubes, particularly the retubing of a fixed tubesheet exchanger, becomes more demanding with closely spaced baffles in a long bundle. In addition, closely spaced baffles may not be justified thermally. As baffle spacing is reduced in order to increase the shell-side heat transfer coefficient, the increase becomes progressively smaller due to leakage effects described in section 12.2.

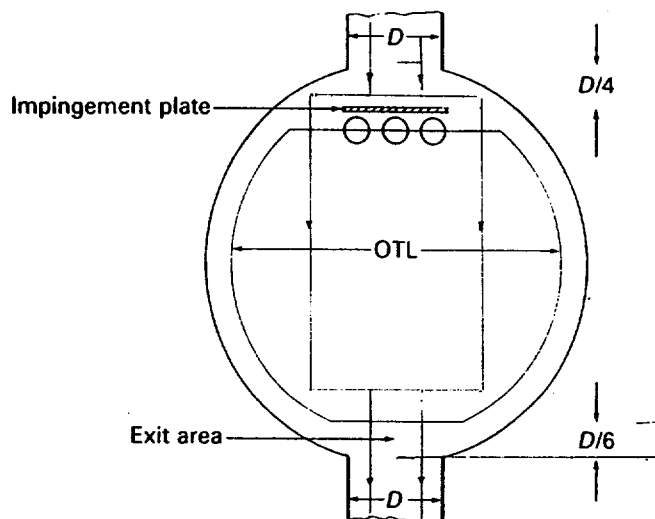
However, it is recognised that special design considerations may dictate a closer baffle spacing. Although there are no mandatory rules, some designers adopt a minimum baffle spacing of one-tenth of the shell diameter for diameters greater than 1524 mm (60 in).

### 1.5.14 Impingement plates

To protect the tubes below the shell-side inlet nozzle from damage due to solid particles or liquid droplets entrained in the shell-side fluid, an impingement plate may be required. This plate is about 6 mm thick, flat or curved, with dimensions slightly greater than the nozzle bore. It is usual to position the plate such that the annular escape area is at least equal to the nozzle cross-sectional area. Hence, if the nozzle bore is  $D$ , the distance between the plate edge and nozzle wall/shell junction is  $D/4$ , as shown in Fig. 1.26. The shell cannot be filled completely with tubes when an internally mounted impingement plate is used and as the nozzle diameter/shell diameter ratio increases, an increasing number of tubes have to be omitted.

At large nozzle diameter/shell diameter ratios other means of impingement protection are used. The impingement plate may be fitted externally in an enlarged nozzle, conical or domed, as shown in Fig. 1.27. Alternatively, an annular distributor (as shown) may be used. An annular distributor has the advantage that any nozzle 'sinkage' (as described in

Figure 1.26 Impingement plate



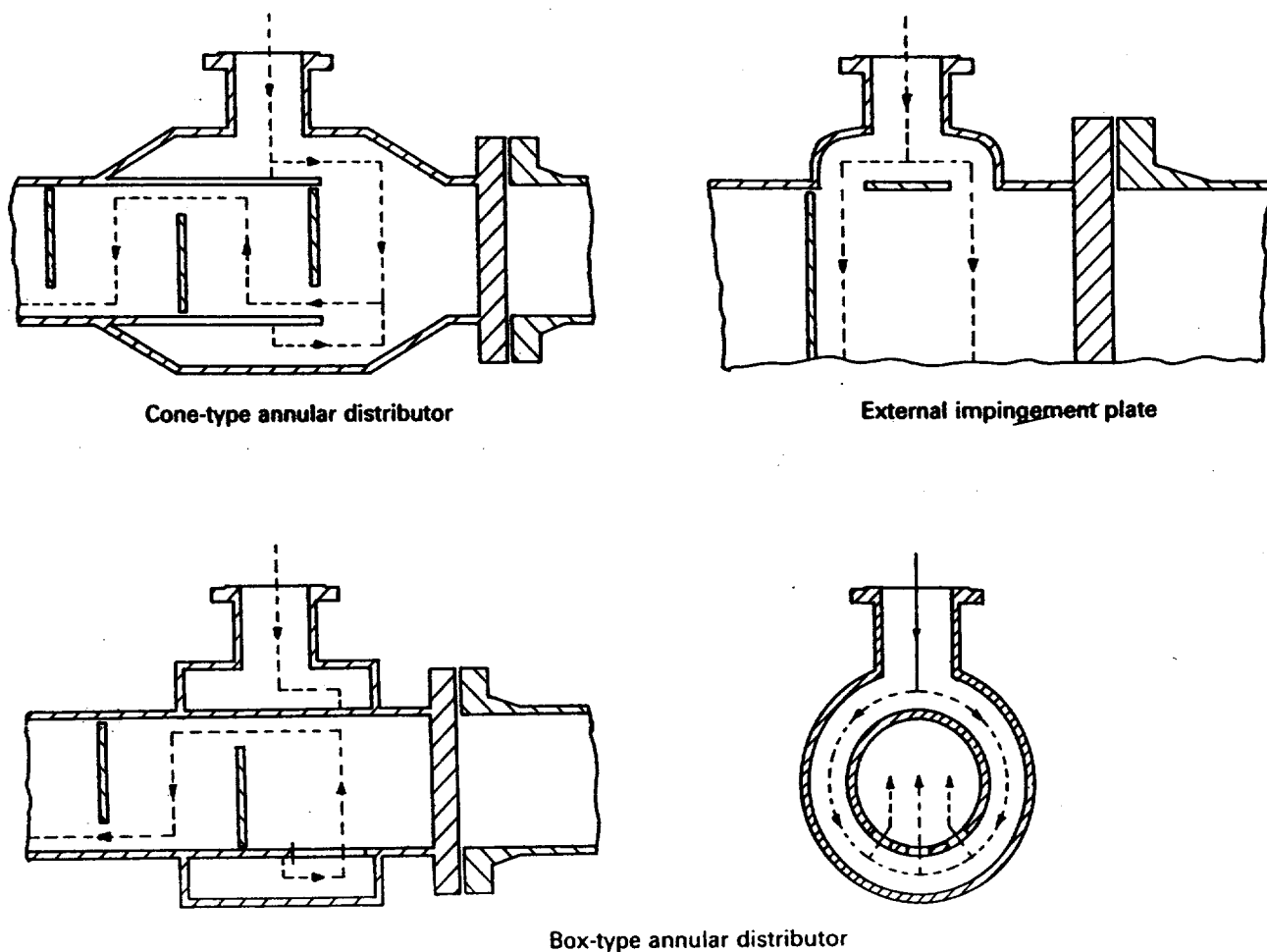


Figure 1.27 Shell-side flow inlet distributors

section 2.7) occurs in the vapour belt barrel where it cannot influence shell/baffle clearance.

TEMA specifies that impingement protection is required when  $\rho V^2$  in the inlet nozzle exceeds the values given in Table 1.8.

Adequate escape area must also be allowed at the outlet nozzle and it is usual to position the closest row of tubes at least  $D/6$  from the outlet nozzle wall/shell junction. If the inlet nozzle requires neither an impingement plate nor a distributor it is usual to position the closest row of tubes at a similar distance from the inlet nozzle wall/shell junction.

Some removable bundles are designed so that they can be rotated through  $180^\circ$  at regular intervals to even out wear at the shell inlet. Hence, if internally fitted impingement plates are used, two plates are required, positioned  $180^\circ$  apart on the bundle periphery.

#### 1.5.15 Longitudinal-type baffle

Most exchangers have a single shell-side pass, but two passes may be provided by installing a flat metal plate, 6–13 mm thick, which runs axially along the shell at the diameter to divide the tube bundle into two semicircular portions. The plate is termed a 'longitudinal baffle' and an

**Table 1.8** TEMA Impingement protection criteria. Impingement baffle required when  $\rho V^2$  exceeds values shown

Type of fluid	$\rho = \text{kg/m}^3$ $V = \text{m/s}$	$\rho = \text{lb/ft}^3$ $V = \text{ft/s}$
Non-corrosive, non-abrasive single phase	2230	1500
All other liquids, including liquid at its boiling point	744	500
All other gases, vapours, saturated vapours and liquid-vapour mixtures	0	0

$\rho$  = Mass density of fluid  
 $V$  = Velocity of fluid

© 1978 by Tubular Exchanger Manufacturers Association Inc. Para. R-4.6.

exchanger with two shell-side and two or more tube-side passes has thermal significance, which is discussed in detail in Chapter 7. The TEMA shell-type designation is F. The longitudinal baffle is usually welded, or otherwise sealed, to the stationary tubesheet, but does not extend the full tube length because space is required at the rear end to permit the shell-side fluid to cross over the bundle from the first pass to the second. The acceptable positions (for thermal reasons) of a longitudinal baffle is shown in Fig. 1.22.

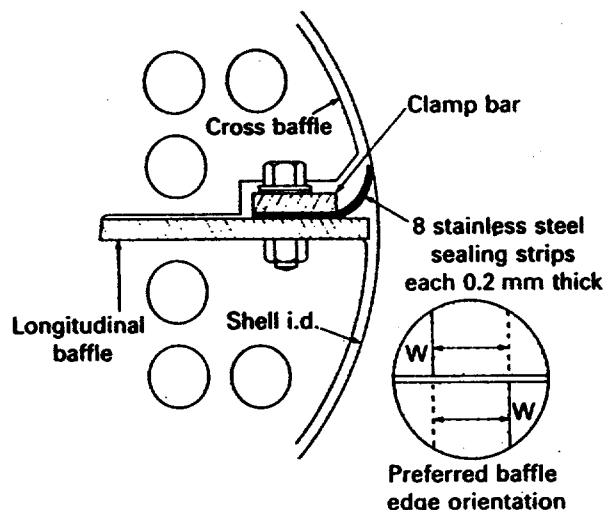
Means must be provided to prevent leakage of the shell-side fluid from the first to the second pass between the edges of the longitudinal baffle and shell. The worst leakage point for loss of both fluid and heat is adjacent to the stationary tubesheet where the inlet and outlet nozzles are diametrically opposed and pressure and temperature differentials are greatest. In a fixed tubesheet exchanger the longitudinal baffle may be welded to the shell, but this is not possible with removable bundle exchangers as the baffle must be removed with the bundle.

Although horizontal cut baffles, which provide up-and-down flow, are sometimes used, vertical cut baffles, which provide side-to-side flow are preferred, as shown in Fig. 1.28 (inset).

The pressure differential across non-welded longitudinal baffles is usually limited to about 0.7 bar (10 lb/in<sup>2</sup>) by some users. If greater pressure differentials are permitted for non-welded baffles, the design must not only be leak-proof, but the structural ability of the baffle to resist the pressure differential should be checked. Because of the sealing problems and the fact that there is always a risk of damaging the sealing devices during insertion or withdrawal, some users will not permit longitudinal baffles to be used.

In the case of removable bundles the gap between longitudinal baffles and shell is sealed by packing devices or flexible strips, and a typical flexible strip design is shown in Fig. 1.28. The flexible strips are placed on

**Figure 1.28** Longitudinal baffle with flexible edge sealing strips



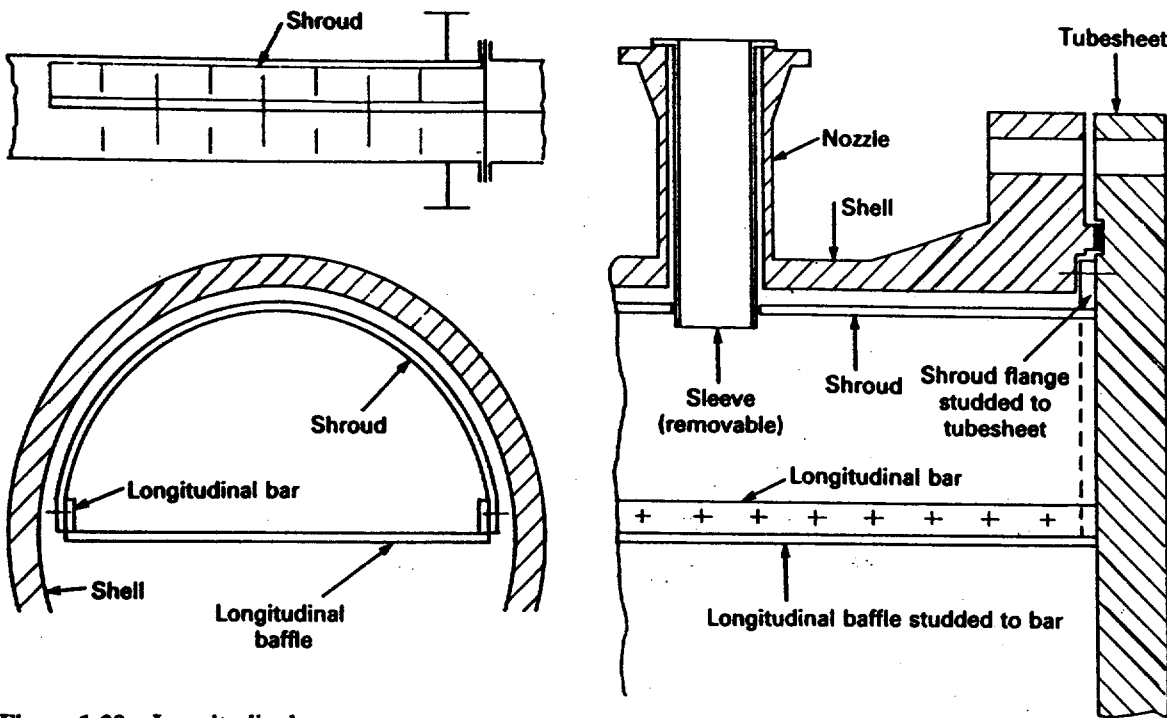
the shell inlet side of the longitudinal baffle so that the higher pressure assists the strips to maintain close contact with the shell. To restrict heat loss from the inlet to the outlet pass two longitudinal baffles, separated by an insulating air gap, may be used.

As an alternative approach, one half of the bundle may be encased by a semicircular lightweight shroud, as shown in Fig. 1.29. The shroud, being studded to the longitudinal baffle and tubesheet, must be removed with the bundle. After this the shroud may be removed from the bundle to expose the tubes. The shell nozzle must be detached from the shroud before the bundle is removed. Figure 1.29 shows a tightly fitting removable sleeve. In order to accommodate the shroud, the outer tube limit for a U-tube exchanger is of the order of 20–25 mm smaller than a normal shell.

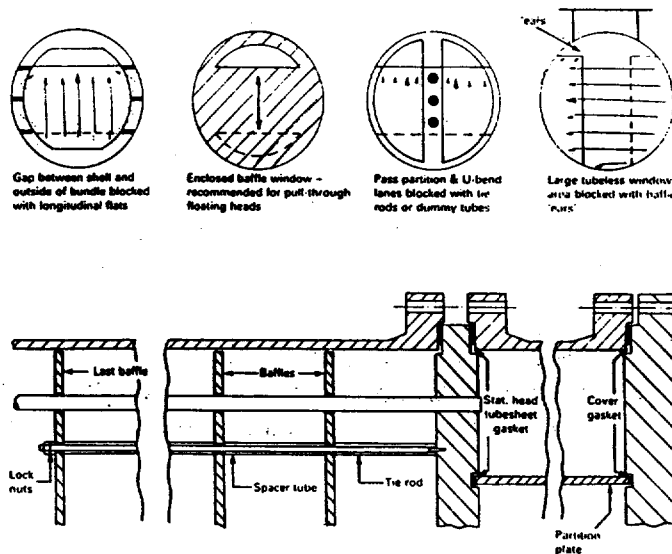
#### 1.5.16 Tie rods, spacers and sealing devices

A number of tie rods and spacers hold the bundle together and locate the baffles in their correct positions. Tie rods are circular metal rods, usually 9.5–15.9 mm diameter, which are screwed into the stationary tubesheet and extend the length of the bundle up to the last baffle, where they are secured by lock nuts. All the rods have spacer tubes fitted over them, each spacer being tube or pipe with an inside diameter slightly greater than that of the tie-rod diameter, and a length equal to the required baffle spacing. Figure 1.30 shows the general arrangement and Figs. 1.31(a)–(d) show typical tie rod positioning. (See TEMA for further information.)

Undesirable shell-side leakage paths, such as the gaps due to pass partitions (pass partition lanes) or gaps between bundle and shell, may be blocked partially by the strategic placing of tie rods and spacers. Dummy tubes, which do not pass through the tubesheets, round bars or flat longitudinal strips inserted into slots in the periphery of the baffles may also be used as sealing devices, as shown in Fig. 1.30. In some cases the largest gap between bundle and shell is that created by an internally fitted impingement plate and if this creates a leakage path it must be sealed



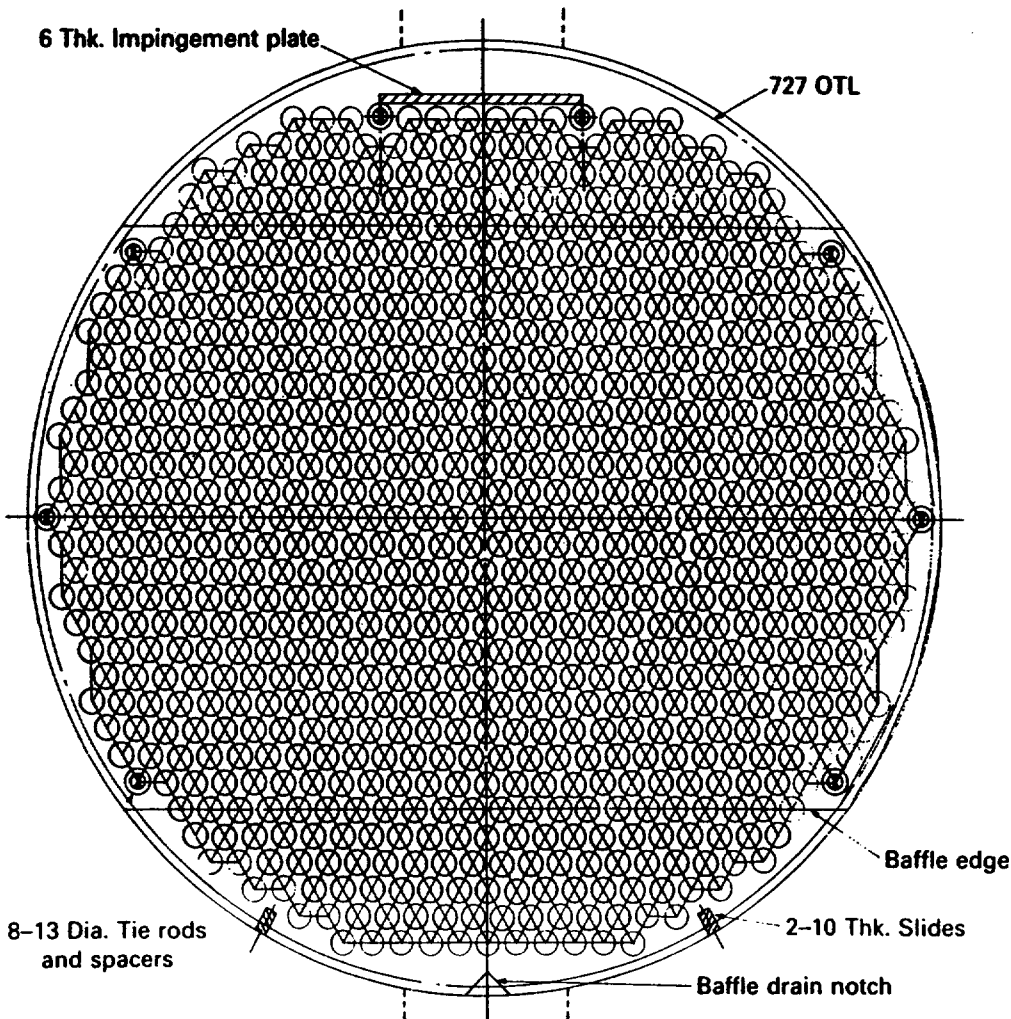
**Figure 1.29** Longitudinal baffle with bolted-on shroud



**Figure 1.30** Tie rods, spacers, and sealing devices

with longitudinal strips or other devices. However, these must not be placed in the inlet baffle space as this considerably reduces the escape area around the impingement plate. The outlet baffle space must be examined on a similar basis.

Figure 1.30 also shows the extensions to a segmental baffle which are required to prevent the shell-side fluid from by-passing the bundle at a



(a) Typical tube layout for a fixed tubesheet exchanger  
740 i/Dia. shell, single pass 780-tubes, 19.05 o/Dia. on  
23.8125 pitch, 30° angle.

**Figure 1.31** Typical tube layouts (a) fixed tubesheet (b) U-tube (c) split backing floating heat (d) pull-through floating heat (all dimensions in mm)

tubeless area in the baffle window created by a large inlet escape area. The extensions are termed 'baffle ears'.

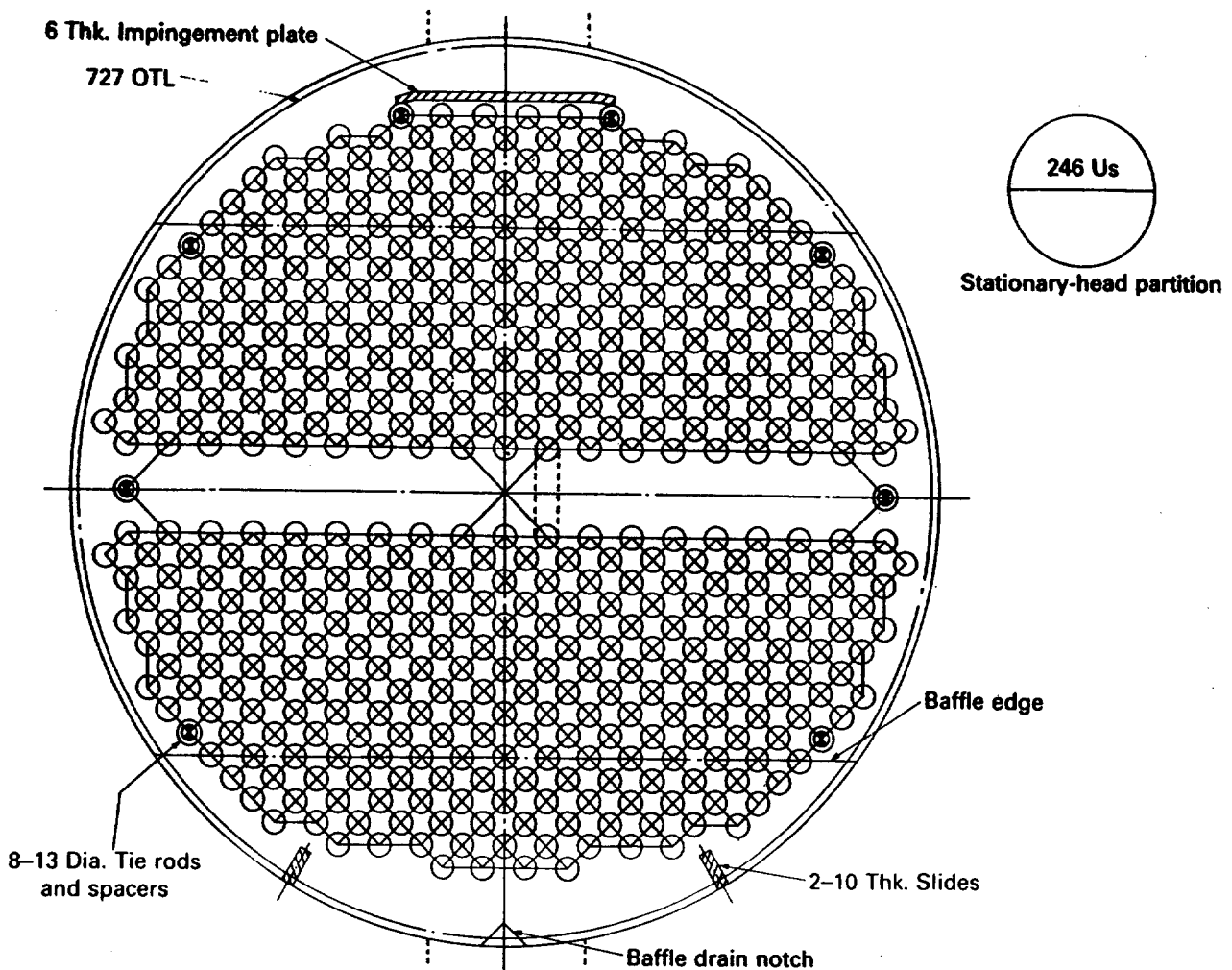
Figure 1.32 shows a tube bundle during construction. The edge notches in the baffles, into which longitudinal sealing strips will be fitted, are shown.

### 1.5.17 Outer tube limit (OTL)

The outer tube limit (OTL) is the diameter of the largest circle drawn about the tubesheet centre, beyond which no tube must encroach.

It is dependent on the type of exchanger and in the case of floating-head exchangers it may be influenced by the design pressures, both shell- and tube-sides, and also whether the tubes are expanded or welded to the tubesheets. The latter method of tube-end attachment may produce a slightly smaller OTL.

Typical values of the diametral clearance between shell inside diameter and outer tube limit are given in Table 1.9.



(b) Typical tube layout for a U-tube exchanger  
740 i/Dia. shell, 2-pass, 246 U-tubes, 19.05 o/Dia. on  
25.4 pitch, 45° angle.

### 1.5.18 Tube count

The number of tubes which can be accommodated within a given shell inside diameter is termed the tube count. For a given shell inside diameter, tube outside diameter, pitch and pitch angle, tube count depends on the factors listed below:

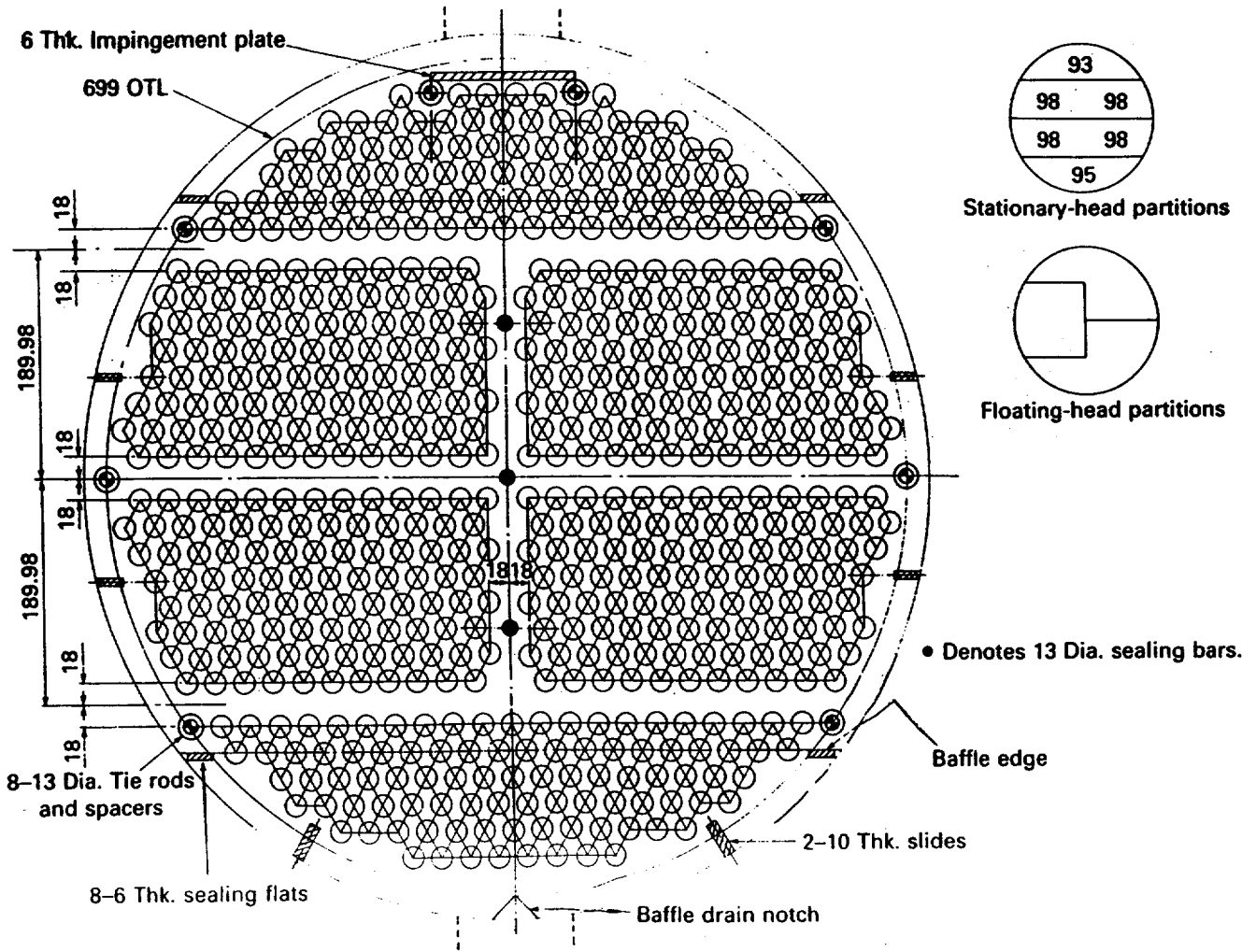
*Type of exchanger.* This determines the OTL.

*Design pressure.* This may reduce the OTL for floating-head type exchangers, as shown in Table 1.9.

*Nozzle diameter.* Adequate escape area around an internally fitted impingement baffle at the inlet nozzles must be provided which cannot be filled with tubes. The greater the nozzle diameter the smaller the tube count. Similar considerations apply at the outlet nozzle. The tube count is independent of nozzle diameter if an externally fitted impingement plate or distributor is used.

*Number of tube-side passes.* As the number of passes increases, tube





(c) Typical tube layout for a split backing ring floating-head exchanger.  
 740 i/Dia. shell, 6-pass, 580 tubes, 19.05 o/Dia. on 25.4 pitch, 30° angle.

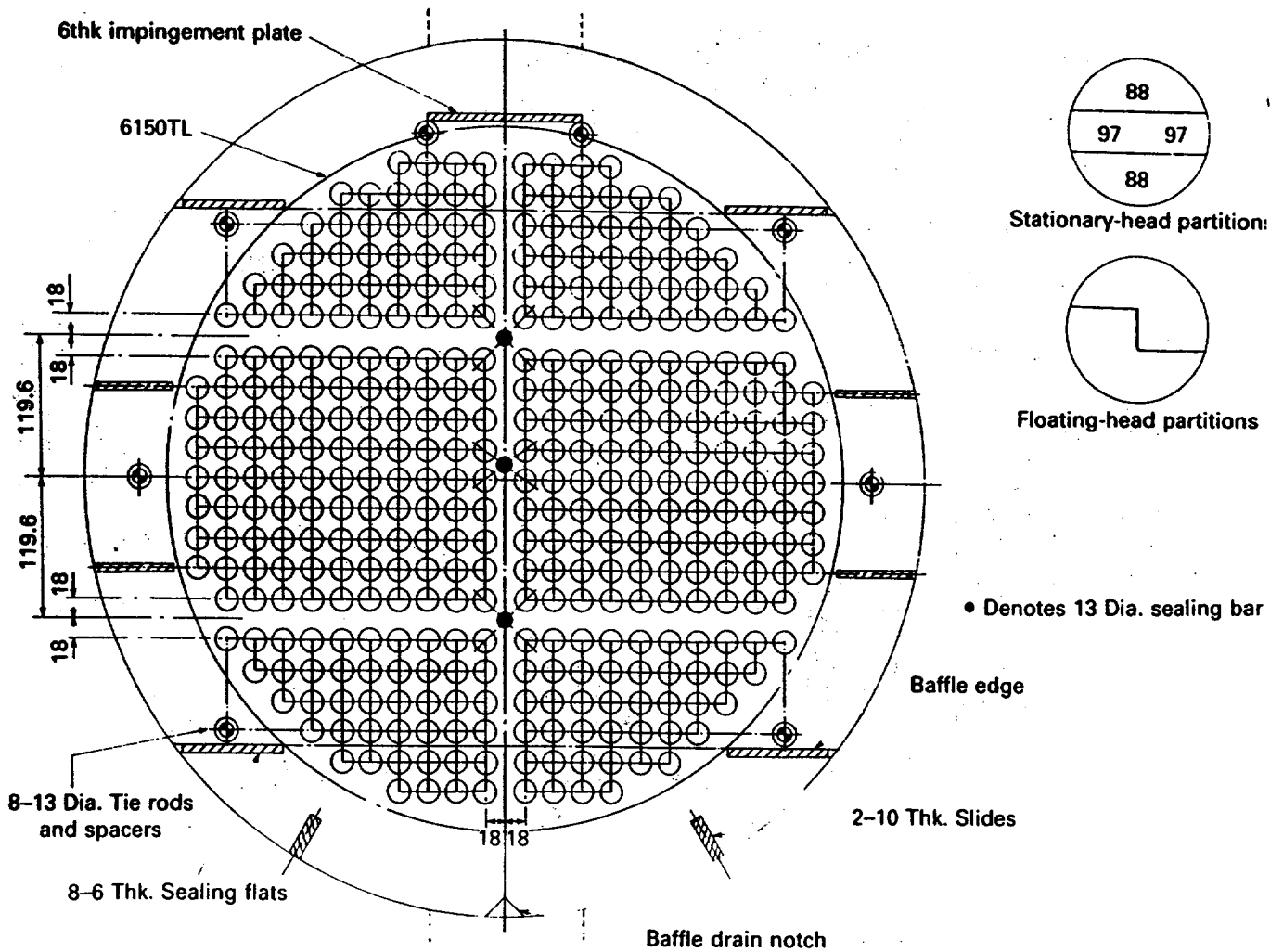
count decreases, as the area occupied by pass partitions cannot be filled with tubes.

**Tube-end attachment.** Welded tube ends may reduce the OTL, and hence tube count, for floating-head exchangers, as mentioned in section 1.5.17. Welded tube ends may also reduce the tube count in multi-pass exchangers of all types because tubes closest to the pass partitions may have to be pitched at a greater distance than normal to accommodate the weld.

**Tie rods, spacers and sealing devices.** The tube count may be reduced to accommodate these items.

**Radiussed tubesheets.** In some cases the tubesheets may have radiussed hubs at the periphery for welding to the shell or head barrel, as shown in Figs. 2.15(e), (f) and (g). The OTL may be reduced as tubes should not encroach into the radii.

**Rotatable bundles.** Rotatable bundles with internally fitted impingement plates require two escape areas on opposite sides of the bundle, resulting in a reduction in tube count.



(d) Typical tube layout for a pull-through floating-head exchanger.  
740 i/Dia. shell, 4-pass, 370 tubes 19.05 o/Dia. on 25.4 pitch, 90° angle.

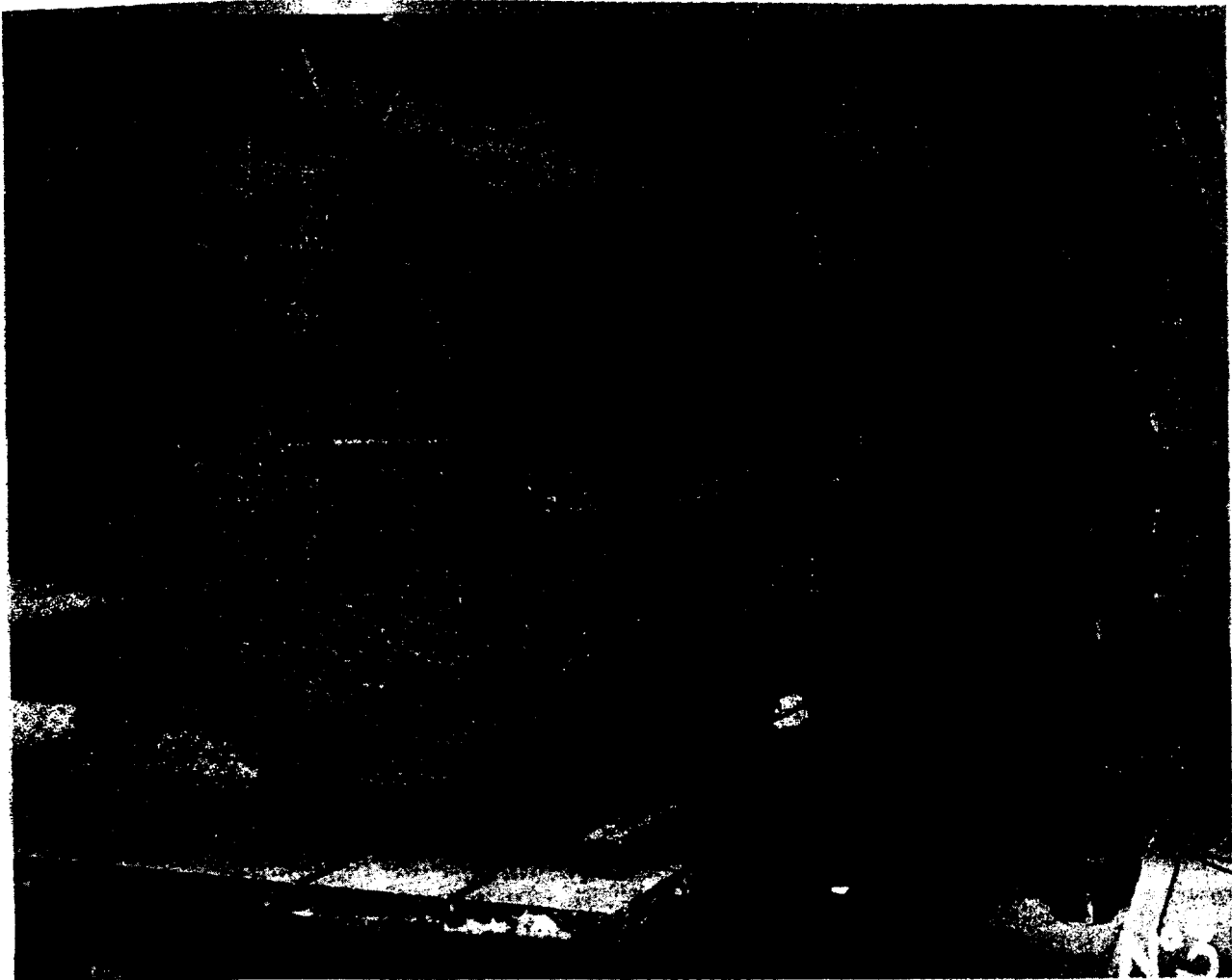
It is not possible to provide exact tube count tables because of the large number of variables. The tube counts given in Part 3, Appendix 1, Tables A3.1–A3.3, are adequate for initial sizing purposes, but the exact count should be obtained from a drawing, such as those shown in Figs. 1.31(a)–(d), or a computer program.

### 1.5.19 Shell-side nozzle arrangements

There are six TEMA standard shell-side nozzle arrangements, namely, types E, F, G, H, J and X, which are applicable to any type of exchanger (see Fig. 1.2).

A seventh TEMA designation, type K, relates to the kettle unit and has been described in section 1.3.4. The thermal significance and disadvantages of the F-type shell have been discussed in section 1.5.15.

The most common arrangement is the E-type shell but when a design is governed by shell-side pressure loss, it may be advantageous to use a divided flow shell type J in which the pressure loss will be reduced considerably. Compared with an E-type shell, having the same shell



**Figure 1.32** Tube bundle during construction (horizontal cut, single segmental baffles, showing edge notches for longitudinal sealing flats) (courtesy of Whessoe Heavy Engineering Ltd, Darlington, UK)

diameter and baffle pitch, half of the total shell-side fluid flows through the same cross-flow area, but for only half the exchanger length. There is a choice of two inlets/one outlet or one inlet/two outlets and in order to minimise nozzle diameters it is usual to provide two inlets/one outlet for single-phase and condensing services and one inlet/two outlets for vaporising services.

In the cross-flow shell type X there are no segmental-type baffles and the shell-side fluid makes only one pass across the bundle, instead of many, as in the baffled E type. As it has lower pressure loss characteristics than the J shell, it should be considered also when a design is governed by shell-side pressure loss. The bundle usually has a flat top and bottom to provide adequate entry and exit flow areas, but in some cases it may be necessary to provide a full-length perforated distributor plate at the bundle inlet to aid flow distribution. Except for short units, the bundle has full circle supports, while in order to eliminate flow-induced vibration any number of intermediate full circle supports may be added, through which all tubes pass, without affecting heat transfer and pressure loss. A typical design may require up to four inlets and outlets, spaced evenly along the shell, to reduce nozzle diameter and obtain a practical nozzle diameter/shell diameter ratio.

**Table 1.9** Typical diametral clearance: (Shell inside diameter)-(OTL)<sup>(1, 2, 3)</sup>

Exchanger inside diameter		Fixed tubesheet & U-tube		Split backing ring floating head				Pull-through floating head							
								Up to 30 bar (450 lb/in <sup>2</sup> )		40 bar (600 lb/in <sup>2</sup> )		10 bar (150 lb/in <sup>2</sup> )		20 bar (300 lb/in <sup>2</sup> )	
mm	in	mm	in	mm	in	mm	in	mm	in	mm	in	mm	in	mm	in
254	10	13	$\frac{1}{2}$	35	$1\frac{3}{8}$	35	$1\frac{3}{8}$	102	4	102	4	102	4	102	4
483	19	13	$\frac{1}{2}$	35	$1\frac{3}{8}$	35	$1\frac{3}{8}$	102	4	102	4	102	4	124	$4\frac{1}{2}$
737	29	13	$\frac{1}{2}$	41	$1\frac{5}{8}$	41	$1\frac{5}{8}$	102	4	102	4	111	$4\frac{3}{8}$	127	5
991	39	13	$\frac{1}{2}$	43	$1\frac{11}{16}$	43	$1\frac{11}{16}$	105	$4\frac{1}{8}$	114	$4\frac{1}{2}$	124	$4\frac{7}{8}$	133	$5\frac{1}{4}$
1219	48	16	$\frac{5}{8}$	43	$1\frac{11}{16}$	48	$1\frac{7}{8}$	111	$4\frac{3}{8}$	124	$4\frac{7}{8}$	140	$5\frac{1}{2}$	159	$6\frac{1}{4}$
1524	60	19	$\frac{3}{4}$	43	$1\frac{11}{16}$	51	2	124	$4\frac{7}{8}$	137	$5\frac{3}{8}$	159	$6\frac{1}{4}$	184	$7\frac{1}{4}$
1829	72	22	$\frac{7}{8}$												
2134	84	22	$\frac{7}{8}$												

**Notes:**

- (1) Roller expanded tube ends.
- (2) Tube-side design pressure shown.
- (3) Subject to considerable variation between fabricators.

The G shell provides greater mean temperature differences for the same terminal temperatures than the E shell, but if fitted with cross baffles at the same spacing, heat transfer and pressure loss characteristics will be similar. In certain condensing and vaporising services, where heat transfer is not dependent on shell-side velocity, one central full circle support is fitted and the cross baffles are omitted entirely. As the shell-side flow is largely parallel to the tubes, the pressure loss will be low.

The H shell is equivalent to two G shells in parallel but joined together end-to-end.

The maximum tube lengths for G and H shells, with only full circle supports, based on the TEMA maximum unsupported lengths for steel tubes, are given in Table 1.10.

The tube-side passes in F-type shells must be arranged symmetrically about the longitudinal baffle in order to provide the correct flow arrangement.

**1.5.20 TEMA type and size designation system**

Sections 1.3 and 1.4 describe five stationary-head types and eight rear-head types, while section 1.5.19 describes seven shell types. The complete TEMA standard lettering code provides a single three-letter type designation system which completely defines an exchanger. The first letter defines the type of stationary head, the middle letter defines the shell type and the last letter defines the type of rear head. Hence the exchangers shown in Figs. 1.1, 1.3, 1.5 and 1.6 are designated AEM,

**Table 1.10** G & H shells with full circle supports approximate maximum tube length (based on Table 1.6)<sup>(1, 2)</sup>

Tube o.d.		G shell		H shell	
mm	in	mm	in	mm	in
15.88	$\frac{5}{8}$	2642	104	5284	208
19.05	$\frac{3}{4}$	3048	120	6096	240
25.40	1	3760	148	7520	296
31.75	$1\frac{1}{4}$	4470	176	8940	352

**Notes:**

- (1) A completely unbaffled shell has an approx. maximum tube length of half that shown for G shell.  
 (2) Lengths based on distance between inner faces of tube sheets.

AEU, AES and AET respectively. If the bolted channel (TEMA type A) is replaced by a bonnet type, the exchangers become BEM, BEU, BES and BET respectively.

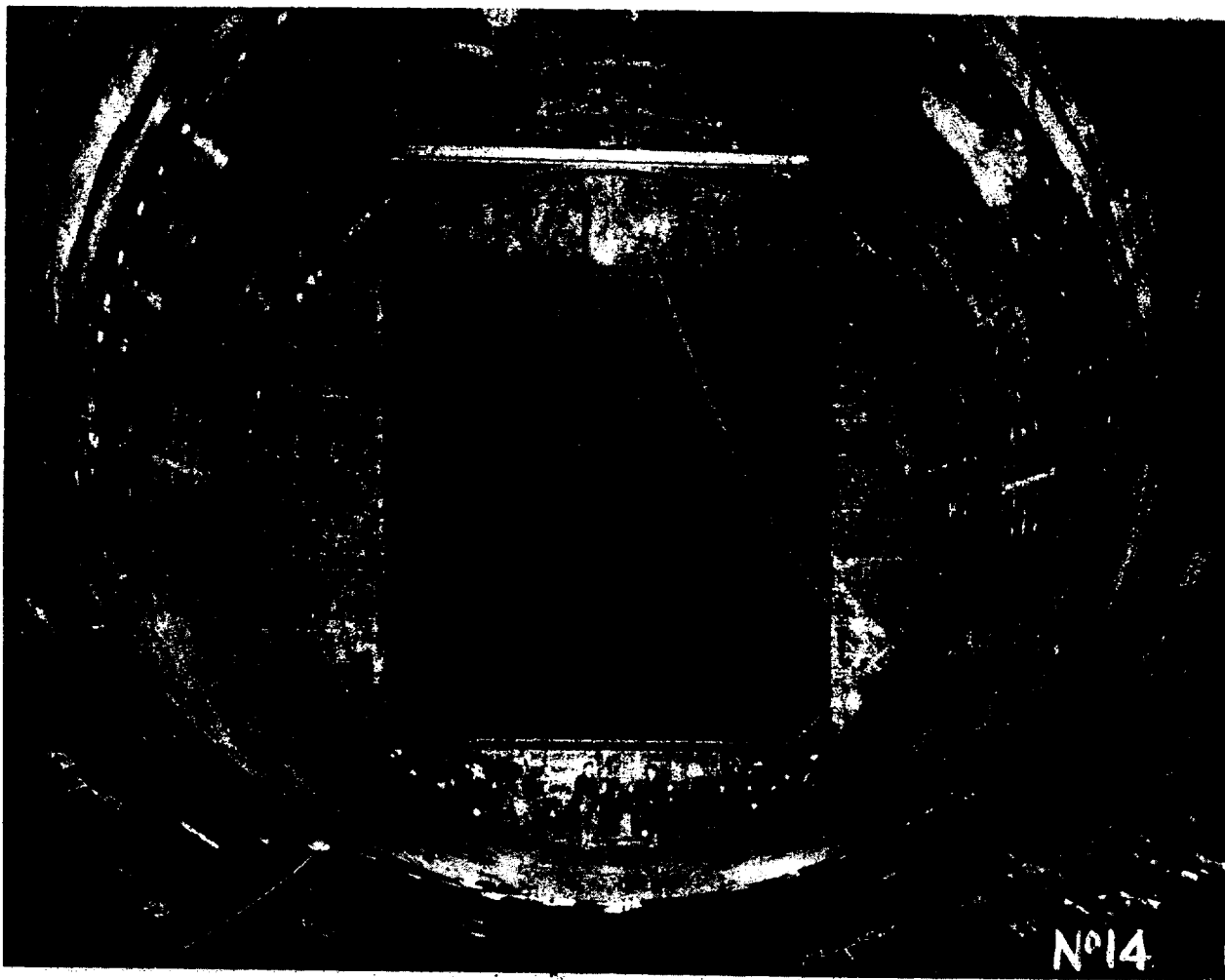
A purchaser who specifies 'a fixed tubesheet exchanger', for instance, without specifying the head types which he requires is open to receive bids for nine alternative designs. This represents the number of stationary- and rear-head combinations which could be provided (cone and D heads omitted). The benefit of the type designation system to purchasers, designers and fabricators is considerable.

TEMA also provide a size designation system in terms of the shell inside diameter in mm, rounded off to the nearest integer, and the straight tube length in mm. The length for straight tubes is the overall tube length, while for U-tubes it is the length from one end to bend tangent. For example, if the split backing ring floating-head exchanger shown in Fig. 1.5 has an inside shell diameter of 1270 mm (50 in) and an overall tube length of 6096 mm (240 in), its size designation would be 1270/6096 (50/240). Its full description would be 1270/6096 AES. If the pull-through kettle shown in Fig. 1.11 has a port diameter of 889 mm (35 in), a shell diameter of 1397 mm (55 in) and a tube length of 4877 mm (192 in), its size designation would be 889/1397/4877 (35/55/192). Its full description would be 889/1397/4877 AKT. © 1978 by Tubular Exchanger Manufacturers Association Inc. Section N-1.

### 1.5.21 Shell diameter

Fabricators have their own standard shell diameters, but in the size range where standard pipe is available, usually up to 457–610 mm (18–24 in) outside diameter, most will design in accordance with standard pipe dimensions. As these are based on outside diameter, the barrel thickness, rounded off to the nearest higher standard pipe thickness, must first be determined before the OTL and tube count can be established.

When the shell is either rolled or forged, modern computerised methods for thermal and mechanical design readily enable the fabricator to design a purpose-built exchanger having any specified shell diameter,



**Figure 1.33** Wind tunnel cooler, approx. 15 m diameter, containing 58 000 tubes, 5.2 m long (courtesy of Whessoe Heavy Engineering Ltd, Darlington, UK)

**Table 1.11** Typical inside diameters for rolled or forged shells

Shell diameter range		Diameter increment	
mm	in	mm	in
489–591 inc.	19 $\frac{1}{4}$ –23 $\frac{1}{4}$	50.8	2
635–991 inc.	25–39	50.8	2
1067–1829 inc.	42–72	76.2	3
1981–3048 inc.	78–120	152.4	6

the only limitation being the availability of matching bonnet-type heads. Except for standard units such as tank suction heaters, engine oil and jacket water coolers, etc., design parameters are too numerous to justify the stocking of standard girth flanges, tubesheets and bonnets.

Typical values for rolled or forged shells are given in Table 1.11. The maximum diameter of 3048 mm (120 in) covers a wide range of applications but some services require even larger diameters. Figure 1.33, for instance, shows a site-built wind tunnel cooler of fixed tubesheet construction which is 14.33 m (47 ft) in diameter.

Although there are no mandatory rules, typical maximum shell diameters for general applications are 1524 mm (60 in) for removable bundle exchangers and 2032 mm (80 in) for fixed tubesheet exchangers.

## References

A list of addresses for the service organisations is provided on p. (xvi).

**American Petroleum Institute**, API Standard 660, *Heat Exchangers for General Refinery Services* (3rd ed), 1976. API, Washington, USA.

**American Society of Mechanical Engineers**, Section VIII, Division 1, *Rules for Construction of Pressure Vessels* (1986 ed). ASME, New York, USA.

**British Standards Institution**, *Specification for Unfired Fusion Welded Pressure Vessels*, BS 5500 : 1985. BSI, London, UK.

**Tubular Exchanger Manufacturers Association Inc.**, *Standards of Tubular Exchanger Manufacturers Association* (6th edn), 1978, and Addenda, 1982. TEMA, New York, USA.

# Shell-and-tube heat exchangers: mechanical design features and fabrication

## MECHANICAL DESIGN FEATURES

### 2.1 Design codes

The mechanical design of a shell-and-tube heat exchanger is carried out using a pressure vessel code. British Standards Institution (1980) provides data for codes covering sixty-five countries. In certain countries a national code is legally enforced and all items supplied to that country, whether built there or imported, must comply with it. In the United Kingdom, for instance, the appropriate national code is BSS 5500 : 1982, but other codes which meet legal requirements, such as that produced by the American Society of Mechanical Engineers (ASME) in Section VIII, Divisions 1 or 2, are acceptable. On the other hand, any pressure vessel installed in the Netherlands, for example, must comply with their national code (Grondslagen), despite the fact that it may have been designed to ASME specification, which has wide acceptance.

Such codes provide rules for design, acceptable materials and fabrication where experience has shown that safe construction is achieved. It is not the intention of codes to stifle originality, and alternative design features – or methods of calculation – may be adopted provided that the designer can satisfy the purchaser and inspecting authority, by test, analysis or experience, that his proposals are sound. Similar considerations apply for components which are not covered by the code. The basic design principles for most components of a shell-and-tube heat exchanger are presented by Ruiz (1983). Morris (1983) provides a comparison of British, American and West German codes, together with a guide to the national practice of seven countries.

Code rules relating to component thickness calculations are usually straightforward, although tedious, and as expected computer programs have been developed by computer bureaux, design houses, contractors and fabricators to carry out these calculations. Despite this, sound engineering judgement must be exercised by the designer at all times. Harris (1983) presents sample manual calculations for a floating-head exchanger. The most comprehensive treatment of heat exchanger mechanical design to date is the book by Singh and Soler (1984). Heat



transfer has been well covered in the literature, but mechanical design has not received the same attention. A publication such as this is long overdue and will be welcomed by industry.

Sections 2.2–2.6 are concerned with those features which may not be covered adequately by code rules and relate specifically to shell-and-tube heat exchangers.

## 2.2 Flange systems

Strict compliance with code rules regarding the calculation of thickness and proportions of a flange does not guarantee a tight joint. In addition to the flange, the design of the whole assembly – flanges, tubesheet if appropriate, bolts and gaskets – must be treated as an integral system, particularly at temperatures above 300 °C or below –50 °C (see Bergman 1966).

Despite the fact that codes may list the permissible design stress for a bolt at a particular temperature, it must not be assumed that the bolt is suitable for the intended service at that temperature. This applies particularly to bolt temperatures above 300 °C, where bolt stress reduces with time (bolt relaxation), as shown by Table 2.1. In addition to the material compositions of the bolts and nuts, bolt relaxation depends on the temperature, duration of service and initial tightening load. These factors must be considered before bolt selection is made.

The expansion or contraction of all components must be calculated, particularly if they have different thermal expansion coefficients, to determine whether the bolts will loosen or tighten. Excessive loosening of the bolts will cause the joint to leak soon after start-up. Excessive tightening of the bolts may cause them to yield, or crush the gasket, or both, resulting in leakage later. The component temperatures need to be established at steady operating conditions and also soon after start-up when the bolt temperature will lag behind those of the other components. To maintain tight joints the use of bolt extension sleeves or spring washers should be considered as shown in Figs. 2.1(a) and (b) (compensation devices). Alternatively, the choice of another bolt material having a different thermal expansion coefficient should also be examined.

The compression and recovery required of the gasket must also be established and the choice of gasket discussed with the maker if necessary. In multi-pass construction, the gaskets required at the stationary tubesheet and channel cover flanges have pass partition bars (see section 1.5.6) and both peripheral and inter-pass leakage must be considered. Multi-pass construction gives rise to circumferential temperature gradients in all components of flange systems at the stationary tubesheet and channel cover. Unless designed carefully the flanges at the stationary tubesheet are especially prone to leakage, particularly at high or sub-zero temperatures. In some cases it may be preferable to redesign the flanges using the constructions described in section 2.3.

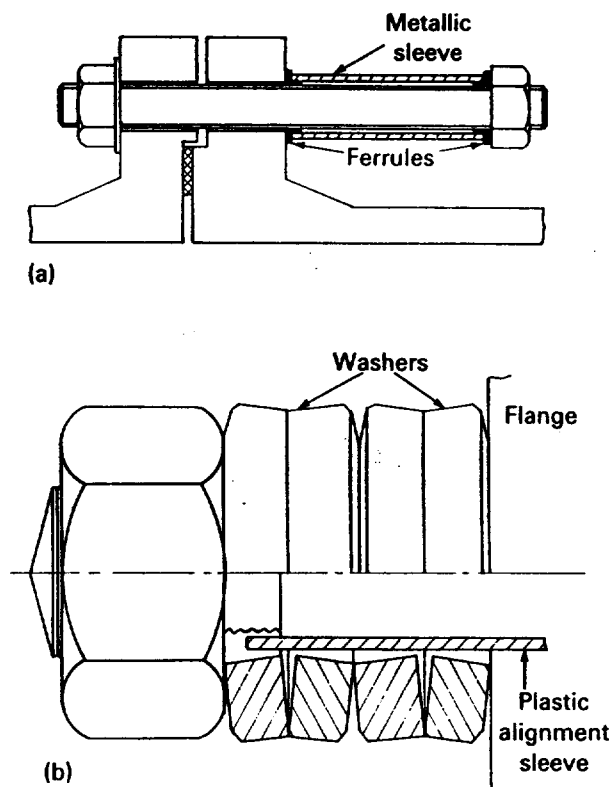
**Table 2.1** Stress relaxation of BS 4882 bolts: % of initial stress retained after 1000 hours over a temperature range 200–600 °C.

Alloy	Grade	Temperatures (°C)					Recommended max. temp (°C)
		200	300	400	500	600	
1% Cr–Mo alloy steel	B7	84	77	56	3	–	400
1% Cr–Mo–V alloy steel	B16	85	77	66	33	–	520
Austenitic stainless steel (18 Cr–8 Ni)	B8	90	90	85	70	56	575
Austenitic stainless steel (18 Cr–10 Ni–3 Mo)	B8M	90	90	83	70	44	600
Austenitic (Ni–Cr–Mo–Ti) precipitation hardening alloy	B17B	–	–	–	82 (at 550)	56	650

Based on Table 3 and Fig. 9 of BS 4882:1973.

Reproduced by permission of British Standards Institution, 2 Park Street, London W1A 2BS, from whom complete copies of the document may be obtained.

**Figure 2.1** Bolt compensation devices (a) extension sleeve (b) spring washers (adapted from the author's contribution to *Heat Exchanger Design Handbook*, Vol. 4, 1983; reproduced by permission of Hemisphere Publishing Corp.)



Although not within the full control of the designer, the tightness of the joint will depend on surface finish and fit-up of the components, and the tightening sequence and tightening equipment used by the fabricator. Bolt tensioners which provide uniform bolt loads around the flange are described in section 2.11.

## 2.3 Stationary head-shell joints

In the case of floating-head and U-tube exchangers having A-, B- or cone-type stationary heads (channels), in which the stationary tubesheet is 'sandwiched' between the shell and channel flanges, it is usual for economic reasons to limit the stationary tubesheet diameter to the gasket outside diameter.

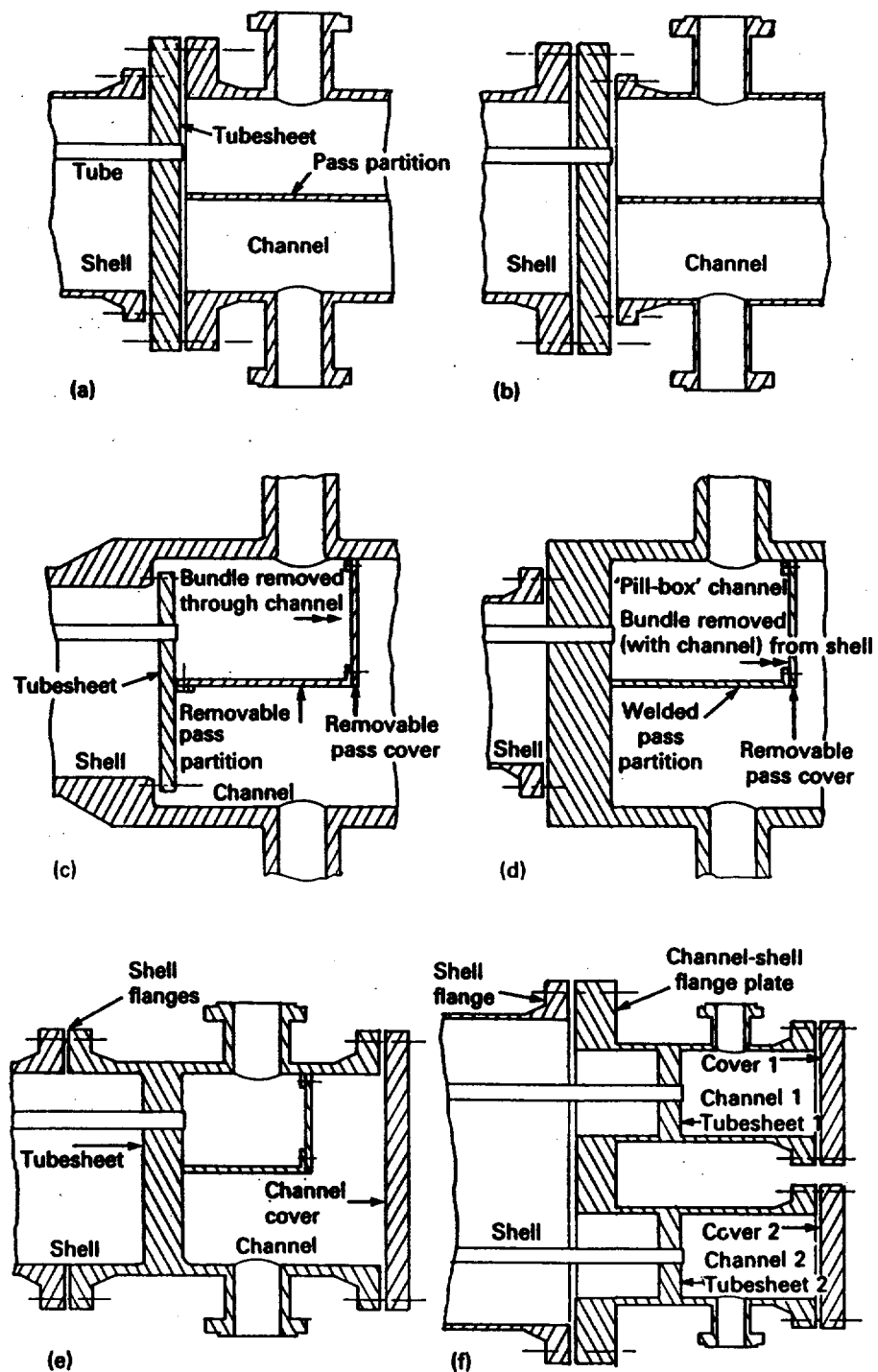
The conventional construction is shown in Figs. 1.3, 1.5, 1.6, 1.8 and 1.9. However, when collar bolts are used to maintain a tight seal between shell flange and tubesheet after the channel has been removed, the diameter of the tubesheet must be increased to match the diameter of the adjacent flanges, as shown in Figs. 1.4, 1.11 and 1.12.

As the shell and channel flanges have common bolting, they must be designed as a pair, and not individually, to their respective design pressures. Irrespective of the pressure difference between the shell-side and the tube-side, the flanges become similar in size. However, if the tube-side pressure greatly exceeds the shell-side pressure, for instance, the smaller shell flange may be studded directly into the stationary tube-sheet, or if the shell-side pressure greatly exceeds the tube-side pressure, the smaller channel flange may be studded directly into the tubesheet. In both cases the tubesheet diameter is increased to match that of the larger flange (channel flange or shell flange, respectively) and the conventional construction is not employed. It will be evident that the periphery of the smaller flange must be clear of the nuts of the larger flange-tubesheet bolting (see Figs. 2.2(a) and (b)).

In high-pressure exchanger design, where it is desirable to minimise the number of external joints, it is usually not practical to have channel/shell joints of the types shown in Figs. 2.2(a) and (b). Typical channel/shell construction for high-pressure exchangers having removable bundles is shown in Figs. 2.2(c) and (d). Because the high-pressure head closure which is described later in sections 2.4 and 2.5, is non-standard, a different design of pass partitions and covers is necessary. In both cases the pass cover is studded to an internal frame so that it is removable. In the design shown in Fig. 2.2(c) it is necessary to have a removable pass partition plate, which is studded to an internal frame, so that the bundle may be withdrawn through the channel. The pass partition plate for the design shown in Fig. 2.2(d) may be welded-in, but is often made removable to give unrestricted access to the tubesheet face. The partition plates, covers, gaskets and studs have only to withstand the tubeside pressure loss and are therefore of light construction.

In exchangers having more than one tubeside pass in A- and B-type channels (see Fig. 1.2), the temperature of the shell and channel flange at the stationary tubesheet will not be uniform around their peripheries, but will correspond roughly to the fluid temperatures in the passes. A similar situation will prevail in the head cover flange in A-, C- and N-type channels (see Fig. 1.2). If the peripheral temperature gradients are large there may be difficulty in maintaining an even bolt tightness around the flange resulting in leakage. The sealing of the pass partition gaskets depends on the pressure exerted by the peripheral bolting and if this is uneven, inter-pass leakage may occur. The problems may be overcome by

**Figure 2.2** Stationary head-shell joints  
 (a) studded-on shell  
 (b) studded-on channel  
 (c) high pressure both sides  
 (d) high pressure on tube-side  
 (e) modified C type  
 (f) multi-head construction



adopting the modified C-type channel, with 'boxed-in' passes, as shown in Fig. 2.2(e) in which the flanges at the stationary tubesheet and head cover will operate at nearly uniform peripheral temperatures. As the pass partition plates are either bolted or welded to the tubesheet, inter-pass leakage cannot occur.

The modified C-type construction is also used in the upper bundle of the double-bundle exchanger of Fig. 1.14 and is particularly suited to low-temperature operation. As a further precaution against flange and pass partition leakage, the U-tube multi-head construction of Fig. 2.2(f)

may be used. Each pass has its own channel, all flanges operate at uniform peripheral temperatures, and there are no pass partitions.

An all-welded exchanger with no girth and nozzle flanges may be employed in order to eliminate leakage to the atmosphere. However, inspection of the tube ends is then no longer possible and usually the channel is provided with a flanged opening and bolted flat cover. For channel diameters less than about 600 mm, a full-diameter opening is provided, identical to the C type (Fig. 1.18(b)). For channel diameters greater than 600 mm, a flanged opening and bolted flat cover (manway), usually 440–610 mm inside diameter, is provided, as shown in Fig. 2.3 for a U-tube exchanger.

In order to remove the bundle, it is necessary to cut the shell barrel adjacent to the tubesheet and also the channel nozzle piping.

## 2.4 Bolted high-pressure closures

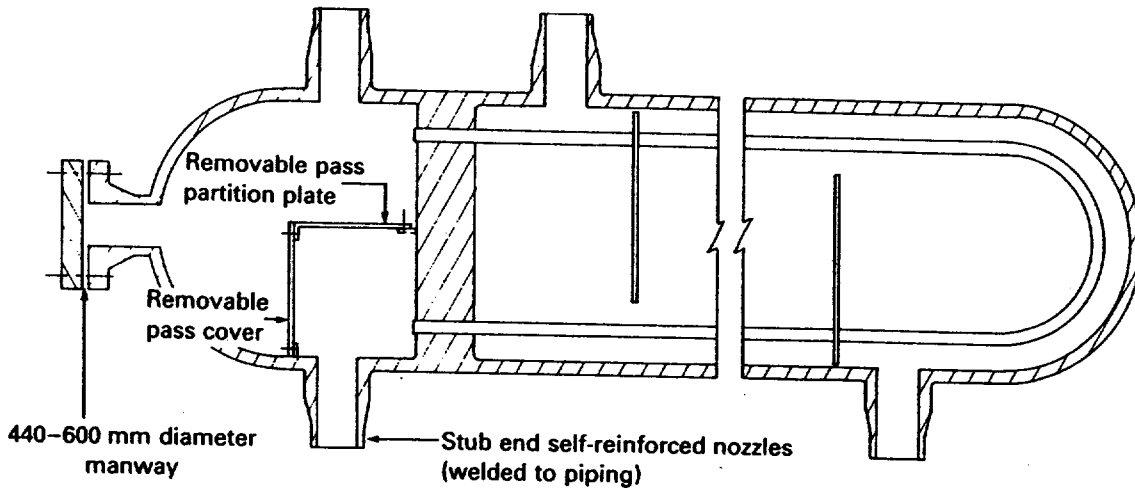
The conventional bolted-on flat cover for A-, C-, L- and N-type channels provides a full-diameter closure which is satisfactory over a wide range of diameter/pressure combinations. There are no mandatory rules, but the following gives an indication of the upper limit for a conventional bolted closure:

$$\text{product of (shell diameter)} \times (\text{pressure}) = \begin{matrix} 150\,000 \text{ (mm} \times \text{bar)} \\ 86\,000 \text{ (in} \times \text{lb/in}^2\text{)} \end{matrix}$$

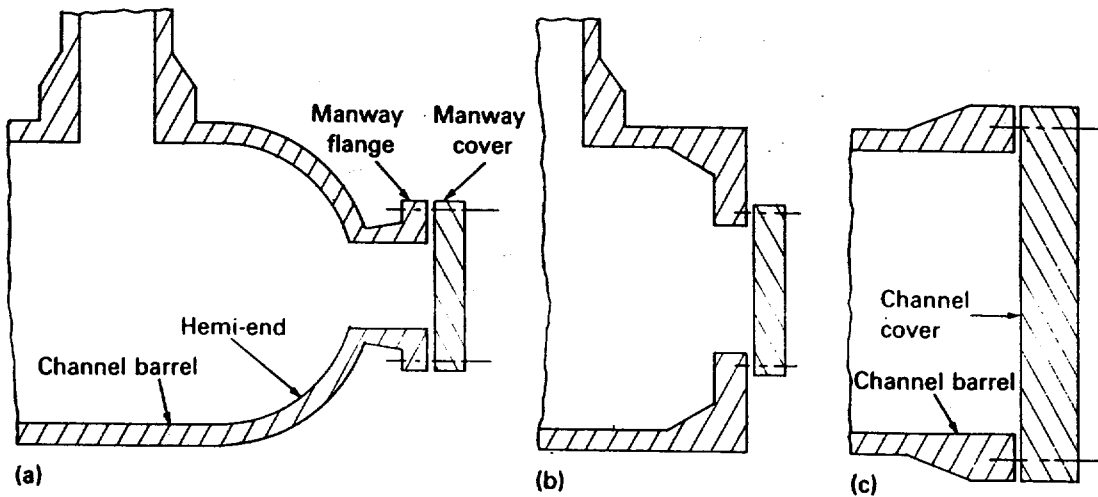
In many cases the conventional closure is adequate for a channel diameter of 600 mm and less, but as diameter and pressure increase it becomes increasingly difficult to provide a conventional closure which provides strength, leak-tightness and serviceability without large-diameter bolts. As an example, a conventional closure, 600 mm diameter, is suitable for a pressure of 250 bar, but at this modest channel size bolts of 75–80 mm diameter will be required, which should be tightened with special bolt-tensioning equipment.

In order to avoid large full-diameter closures, as shown in Fig. 2.4(c), access to the inside of the channel may be provided by a 600 mm diameter conventional manway as shown in Figs. 2.4(a) and (b). As access to the channel is restricted, it may be necessary to increase the channel length to ensure that workmen, probably in bulky protective clothing, can move around freely inside, with equipment, during shutdown for maintenance.

When a high-pressure closure must be supplied, the conventional flange-cover gasket may be replaced with a special type which utilises the contained pressure itself to force it to follow the dilation of the gasket seating surface. Typical examples are shown in Figs. 2.5(a), (b) and (c). An alternative system which does not use a gasket is the welded diaphragm, as shown in Fig. 2.5(d). Although this provides a positive means of containing the pressure, the seal weld at the diaphragm periphery must be machined away each time access to the inside of the



**Figure 2.3** All-welded U-tube exchanger



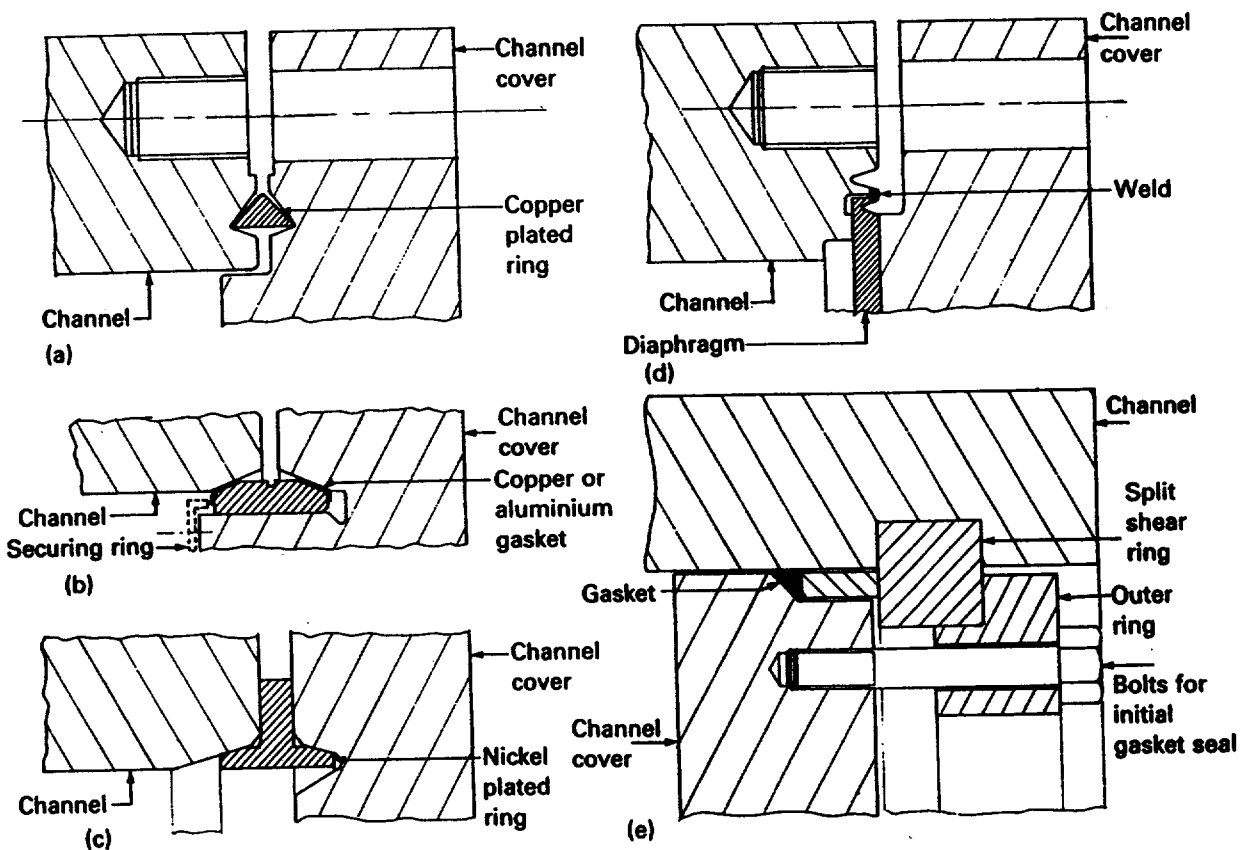
**Figure 2.4** High-pressure channels (a) reduced diameter (hemi-end) (b) reduced diameter (inward-facing flange) (c) full diameter

channel is required. This weld must be re-made before the unit is put into service again and its design is such that the operation can be repeated many times.

## 2.5 Non-bolted high-pressure closures (TEMA D)

Although the closures with special gaskets, or welded diaphragm, minimise the risk of leakage, the bolting must be large enough to withstand at least the hydrostatic end load in all cases. When the bolting becomes too large, a 'non-bolted' closure is used in which the hydrostatic end load is held by pins or rings. There are many designs of this type and Fig. 2.5(e) serves to illustrate the principle involved. After assembly, the small bolts are tightened in order to compress the gasket via the outer and shear rings. When the pressure is applied, the hydrostatic load on the channel cover is resisted by the split shear ring.





**Figure 2.5** High-pressure closures  
 (a) delta ring (b) double cone (c) 'Grayloc'  
 (d) welded diaphragm  
 (e) shear ring

## 2.6 Fixed tubesheet exchangers

The design of tubesheets for floating-head and U-tube exchangers usually presents no problems as they are designed for the higher of the shell- and tube-side pressures, with the other side at zero pressure, except when a differential pressure is specified. Fixed tubesheet exchangers, on the other hand, must cater for the shell-side pressure, tube-side pressure and temperature differential between shell barrel and tubes. Unless a differential pressure is specified, it is customary to consider the three factors individually, and in all combinations, in both the corroded and uncorroded condition, and take the greatest tubesheet thickness. It is important that all temperature conditions experienced by the exchanger are considered, not only those at steady design conditions, but those which arise at start-up, shut-down, chemical cleaning and steaming out, etc. One or more of these conditions may require a shell expansion joint to avoid overstressing the components.

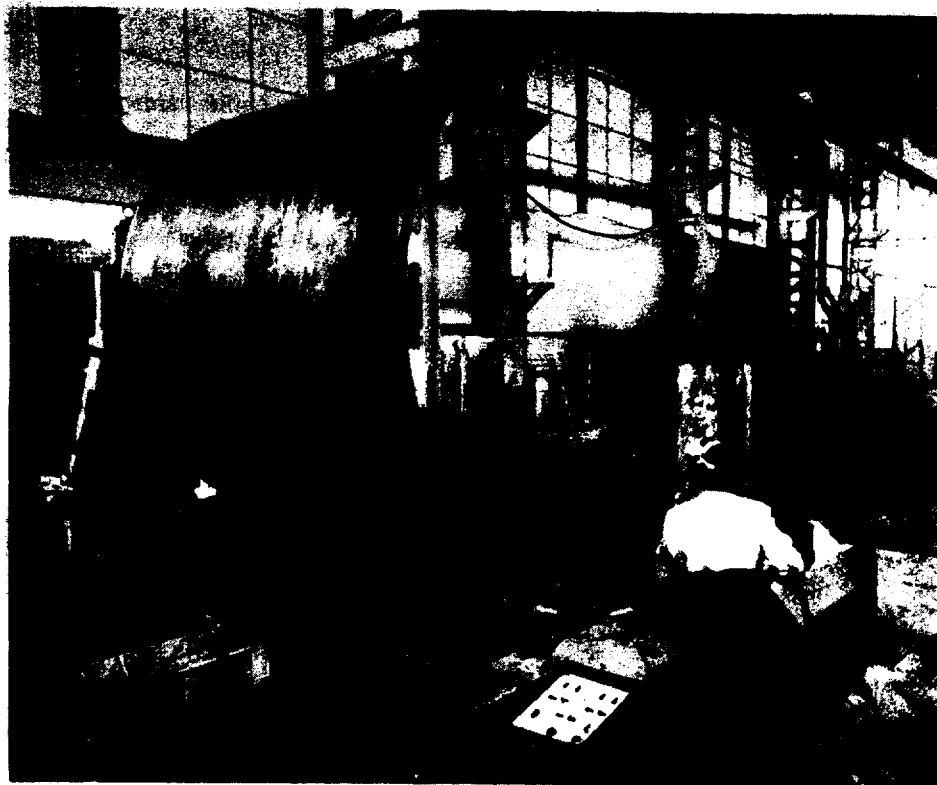
The tube wall temperature at steady design conditions requires a knowledge of the heat transfer coefficients of the shell and tubeside fluids (see Chapter 6) and the fouling factors (see Chapter 8). The method for calculating wall temperatures, once these factors are known, is given in section 6.8.

## FABRICATION

### 2.7 Barrels

When standard pipe is available, the fabricator will prefer to use this for the shell barrel as no rolling is required and welding is greatly reduced. However, pipe is usually only available up to a diameter of about 600 mm (24 in) and most larger shells are 'rolled'. A flat plate is formed into a cylinder by using plate rolls as shown in Fig. 2.6 and the abutting edges welded together to form a longitudinal seam. One such cylinder is termed a strake and a complete shell barrel may comprise several strakes welded together end to end, the welded junction between adjacent strakes being a circumferential seam. Depending on plate-roll capacity and available plate size, it may not be possible to form a strake for a large-diameter barrel from a single piece of plate, in which case two or more plates are each rolled to form part of the cylinder and are welded together with longitudinal seams. Longitudinal seams of adjacent strakes must be staggered.

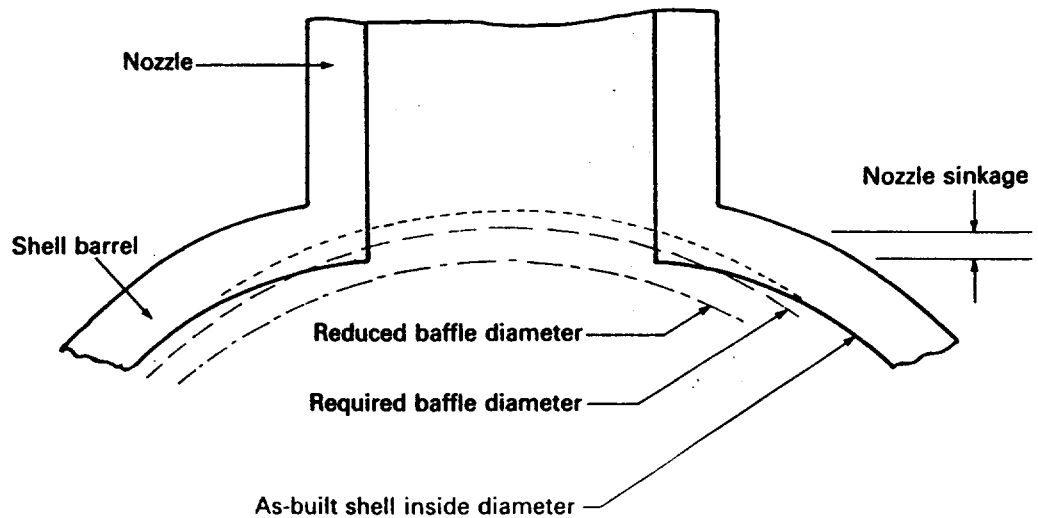
**Figure 2.6** Rolling a shell barrel (courtesy of Whessoe Heavy Engineering Ltd, Darlington, UK)



As a tightly fitting tube bundle has to be inserted into the completed shell barrel, it must be straight, have no out-of-roundness and its diameter must be within the permitted tolerance. The inside diameter of a rolled shell barrel must not be smaller than the design inside diameter, or exceed it by 3.2 mm ( $\frac{1}{8}$  in), as determined by circumferential measurement. Individual strakes may be re-rolled after completing the longitudinal seam to reduce out-of-roundness. All internal welds must be

flush. When large-diameter nozzles are welded into the shell, the fabricator must take special measures, such as the use of temporary stiffeners, to avoid local distortion of the shell. This is known as 'nozzle sinkage'. The exaggerated effect of nozzle sinkage is shown in Fig. 2.7, from which it will be seen that the shell diameter is reduced locally at the nozzle, which in turn reduces the baffle diameter. The increased clearance between shell and baffles provides a greater flow rate in this undesirable leakage path, which will result in a lower shell-side heat transfer coefficient and a distortion of the temperature profiles of the fluids such that the effective temperature difference is greatly reduced. (See Chapters 6, 7 and 12.) Similar distortion may occur when support saddles are welded to thin barrels.

**Figure 2.7** Effect of nozzle sinkage (exaggerated)

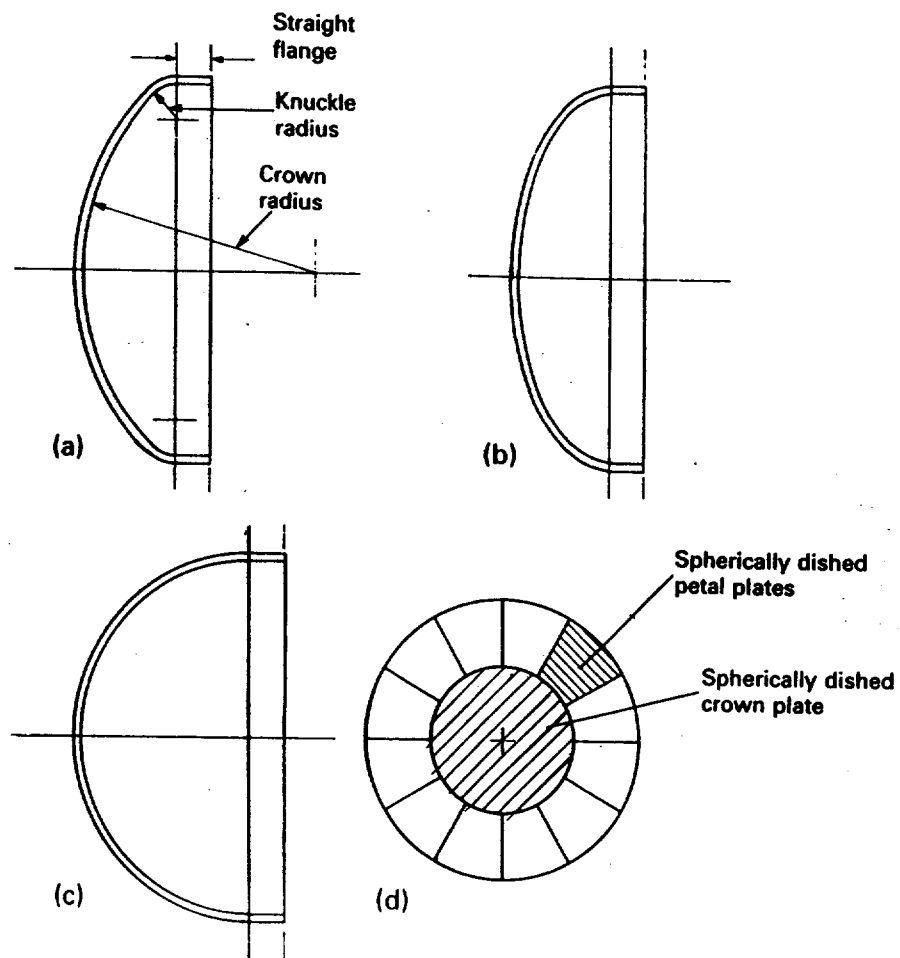


## 2.8 Bonnet-type channels

Bonnet-type, or dished, channels are available as semi-ellipsoidal, torispherical and hemispherical heads, as shown in Fig. 2.8. Semi-ellipsoidal heads usually have '2 : 1 proportions' in which the complete ellipse has a major axis twice that of the minor axis; the inside head depth along the minor axis is therefore one-quarter of the inside head diameter. These are usually available as a standard pipe-cap to match standard pipe diameters and wall thicknesses up to diameters of about 600 mm (24 in). Above this diameter their availability becomes less and *torispherical* heads, comprising spherical crown and peripheral knuckle radii, are used. The thickness of a torispherical head depends on the crown radius and ratio of the crown and knuckle radii and is usually thicker than a semi-ellipsoidal head for the same design conditions. A special form of torispherical head is the Korboggen in which the internal crown radius is 0.8 of the head outside diameter and the internal knuckle radius is 0.154 of the head outside diameter; these proportions yield a head having similar characteristics to the 2 : 1 semi-ellipsoidal head.

Because the thickness of a hemispherical head ('hemi-end') is about half that of a cylinder of the same diameter, it is often used to reduce

**Figure 2.8** Typical bonnet-type channels  
 (a) torispherical (b) semi-ellipsoidal  
 (c) hemispherical  
 (d) crown-and-petal construction



head thickness in high-pressure applications. Their availability decreases as diameter and thickness increases and in many cases they are purpose-made by the fabricator as a welded 'crown and petal' unit. The periphery of the head comprises a number of spherically dished panels (the petals) welded to one other along their radial edges and to a central spherically dished plate (the crown) around its periphery.

The cover of a floating-head assembly is invariably a pressed spherical dish.

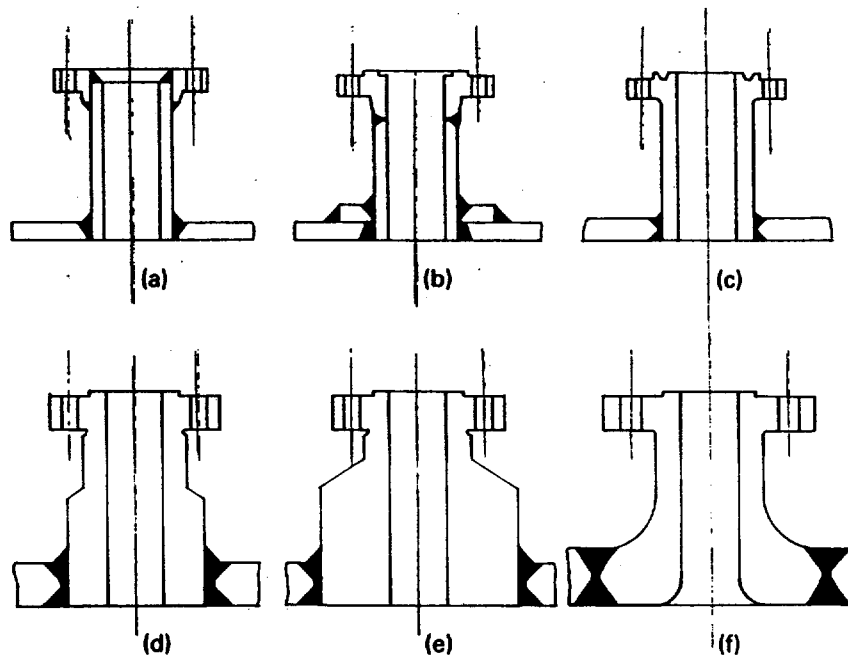
Although most bonnet-type heads are fabricated from plate, cast heads in iron, carbon steel and aluminium bronze are sometimes used, these being restricted to low-pressure, non-lethal applications such as cooling water service.

## 2.9 Nozzles

Typical heat exchanger nozzles are shown in Fig. 2.9. The weld neck and slip-on flanges are widely used with the former being preferred for larger diameters and higher pressures. The forged long weld neck is used for high-integrity services where it is desirable to minimise the amount of

welding. A cylindrical shell, or channel, barrel is weakened by the circular opening which is cut from it to accommodate the nozzle barrel and must be reinforced according to Code rules. This is achieved by local thickening of the shell barrel, or the nozzle barrel, or both, but a common method is the use of a reinforcing pad as shown in Fig. 2.9(b). Code rules dictate the maximum and minimum pad diameter and thickness, but a pad having a diameter twice that of the corroded nozzle bore and a thickness equal to that of the barrel is typical. As only a small quantity of plate is required to fabricate a channel, some fabricators may elect to thicken the whole of the channel barrel rather than use reinforcing pads.

**Figure 2.9** Typical heat exchanger nozzles  
 (a) pipe and slip-on flange  
 (b) pipe, weld-neck flange and reinforcing pad  
 (c) forged long weld neck  
 (d) and (e) forged long weld necks with integral reinforcement  
 (f) as (d) and (e) with contoured base for butt-welding into barrel



Any of the nozzle reinforcement methods described above may be required to meet loads imposed on the nozzle resulting from pipework stresses. In many cases nozzle loads, rather than Code reinforcement rules, dictate nozzle design.

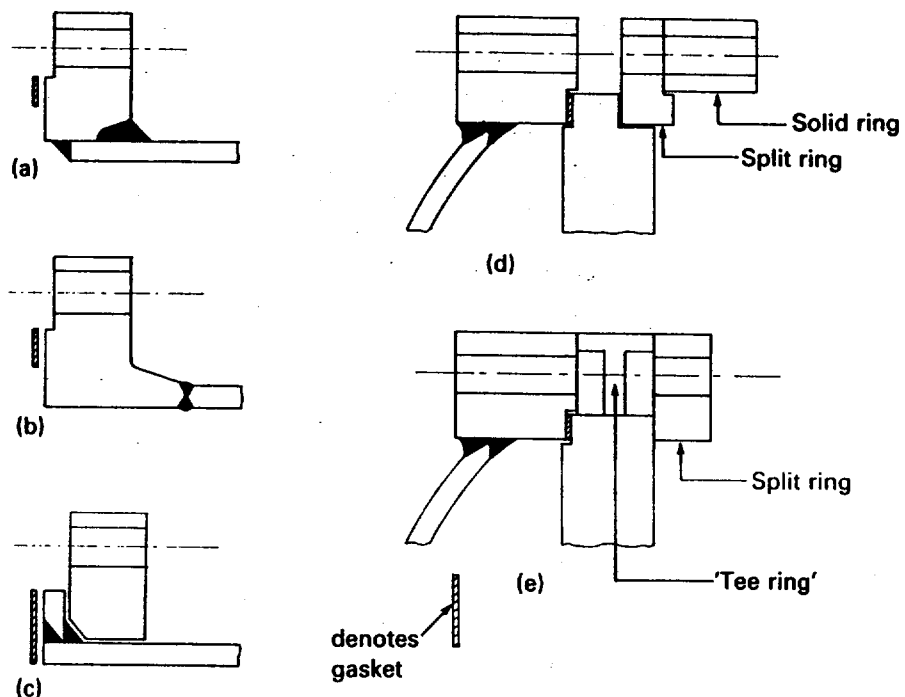
In certain applications, such as hydrogen or low-temperature services, reinforcing pads are not permitted, and where nozzles require reinforcement, forged long weld necks, as shown in Figs. 2.9(c)–(f), are used. The nozzle base is thickened and shaped, as dictated by the Code rules, to provide the amount of reinforcement required. The nozzle shown in Fig. 2.9(f) is contour-forged to provide a base suitable for welding, edge-to-edge, to the barrel (butt-welding), thus permitting all forms of non-destructive testing.

All nozzles are shown as flanged, but in order to eliminate possible leakage from a gasketed joint, a stub-end nozzle may be used. Here the flange is omitted and the nozzle barrel welded at site directly to the line pipe. In this event channels can only be removed after first cutting through the weld seam of the nozzle barrel and line-pipe junction.

## 2.10 Flanges

Figure 2.10(a)–(c) show typical external (or girth) flanges used in heat exchangers. The ring type flange may be cut from plate or purchased as a rolled or forged ring. It is suitable for moderate services, but the weld-neck flange is preferred as diameter, pressure and temperature increase. Its fit-up is simpler and requires less welding, which is especially suited to automatic processes. Although it may be cut from plate under stringent Code rules, it is invariably purchased as a rolled or forged ring, either profiled to the required shape or as a rectangular-section ring which is machined to the required shape.

**Figure 2.10** Typical heat exchanger flanges  
(a) ring (b) weld neck  
(c) lap (d) floating-head assembly – double-ring construction (e) floating-head assembly – tee-ring construction



When an expensive metal is used for the shell barrel, the flange may be a ring or weld-neck type, in either the same metal, or carbon steel; in the latter case it is welded to the outside of the barrel, with the expensive metal weld-deposited to the gasket face to provide a complete corrosion-resistant surface (see Fig. 18.3). However titanium or aluminium, for instance, cannot be weld-deposited to carbon steel and the use of a lap flange as shown in Fig. 2.10(c) should be investigated. The barrel and lap are made in the expensive metal, but the loose backing flange need only be made in cheaper carbon or low-alloy steel. Because the backing flange will have bi-metal contact with the bolts, lap and barrel, the complete system should be checked for possible galvanic corrosion.

The floating-head cover flange and backing ring are also purchased as rolled or forged rings, and Figs. 2.10(d) and (e) show alternative assemblies to that shown in Fig. 1.7. The object of the various assemblies is to prevent rotation, or 'cocking', of the backing flange during bolt tightening.

The floating-head covers shown in Figs. 1.7 and 2.10 comprise a spherical dish welded to the inside of a ring. At diameters below about 450 mm (18 in) it is usually cheaper to provide a 'hogged-out' head in which an integral flange and flat cover are machined out of a circular plate or disc.

## 2.11 Bolting and bolt tightening

Shell-and-tube exchangers invariably use studs and studbolts but for convenience they are referred to below as bolts. Careful tightening of small-diameter bolts is essential to avoid overstressing both bolts and flange. Briscoe (1976) showed that a craftsman using a spanner and hammer to tighten twenty 31.75 mm (1¼ in) diameter alloy steel bolts achieved stresses ranging between 290–827 N/mm<sup>2</sup> (42 000–120 000 lb/in<sup>2</sup>), with an average value of 565 N/mm<sup>2</sup> (82 000 lb/in<sup>2</sup>). He also showed that tightening with a torque wrench achieved more consistent results in that all bolts of an identical set, except two, were tightened to a stress within 138–207 N/mm<sup>2</sup> (20 000–30 000 lb/in<sup>2</sup>). The torque wrench tests were repeated using washers and generous lubrication; neither had any effect in reducing the variation in bolt stress, although the lubrication of the nut faces allowed higher bolt stresses to be achieved. However, torque values are unreliable as they are influenced greatly by the thread forms and also the coefficients of friction and the materials of the bolts, nuts and flanges. Impact wrenching, which may damage the bolts and nuts, produces similar results, and both methods of wrenching introduce undesirable torsional stresses.

Consistent bolt stress values may be achieved by calculating the extension in each bolt, which will produce the required stress, and measuring the actual bolt extension during tightening by an extensometer. The ends of the bolts need special preparation to enable accurate results to be obtained and the tightening process is time-consuming. This may be satisfactory for small-diameter bolts, but for bolt diameters greater than about 50 mm it becomes increasingly difficult to achieve the required bolt stress by manual devices and other methods, such as electrical heating or bolt tensioners, should be employed. Both methods extend the bolt by a predetermined amount, after which the nut is screwed down to its seating by manual means, and the tension released. Torsional stresses and frictional effects are eliminated. Briscoe considered that all bolts greater than 25 mm should be tightened by hydraulic bolt tensioners.

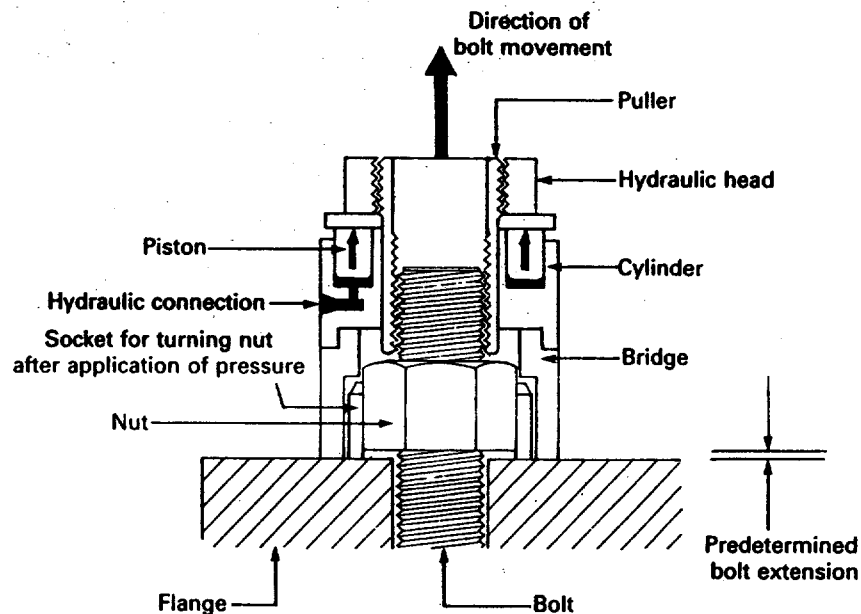
In electrical heating a central hole is drilled axially through the entire length of the bolt to accommodate an electrical heating element. Depending on bolt size the hole diameter may be up to 20 mm, and to compensate for the loss of metal the bolt diameter must be increased to provide the required cross-sectional area. Heating expands the bolt and upon reaching a predetermined extension, corresponding to the required stress, the nut is run down to its seating manually. The bolt is then allowed to cool. This method of tightening is not fast due to the lengthy heating-up and cooling-down periods required.



A bolt tensioner comprises a hydraulic cylinder which is mounted over the bolt to be tightened. The bolt is made about one bolt diameter longer than normal so that a puller bar may be attached to its end above the nut. Application of pressure to a predetermined level, corresponding to the required stress, lifts the puller bar and extends the bolt. The nut is then run down to its seating manually and the pressure released. Although the bolts may be tightened one at a time with a tensioner, it is better practice to provide simultaneous tightening of opposing bolts around the flange by using multiple tensioners in groups of, say, four or eight. If necessary all bolts on the flange may be fitted with tensioners and tightened simultaneously.

Figure 2.11 shows the principle of the hydraulic bolt tensioner and Fig. 2.12 shows multiple bolt tensioning of a heat exchanger flange. Ultrasonic equipment is available for the measurement of bolt stress.

Figure 2.11 Principle of hydraulic bolt tensioner

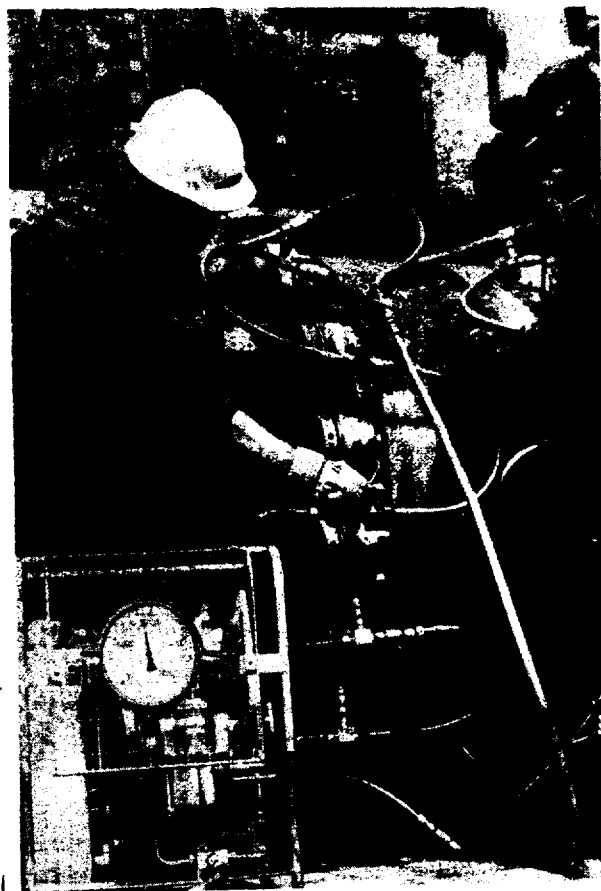


## 2.12 Gaskets

Compressed asbestos fibre gaskets (CAF) consist of asbestos fibres bonded together with suitable binders such as rubber compounds, or fine mesh steel wire gauze, for extra strength. They are widely used for external flanges at pressures of 20 bar and below, but solid metal or metal-jacketed asbestos gaskets are preferred for internal flanges, such as those in floating-head covers. Rubber gaskets are usually confined to low-pressure cooling water services.

Metal-jacketed asbestos gaskets (MJA) are widely used in the petroleum and petrochemical industries. TEMA class R, for instance, specifies that they must be used for all internal floating-head joints, all joints for pressures greater than 20 bar, and all joints in contact with hydrocarbons. They comprise an asbestos millboard filler totally enclosed in a metal jacket of soft iron, 4–6% chrome–molybdenum alloy, copper, aluminium, monel or stainless steel. Also widely used is the spiral wound

**Figure 2.12** Simultaneous tightening of all bolts around a heat exchanger flange using a hydraulic bolt tensioner (a Shell photograph courtesy of Hydra-Tight Ltd, Walsall, UK)



gasket in which a continuous metal strip, preformed into a specially designed V-shaped profile, is wound with a special filler in a spiral formation. Under compression the V-shape provides spring action to achieve a positive seal. The metal of the windings may be stainless steel, monel, titanium or nickel and the filler may be compressed asbestos fibre, PTFE, lead or ceramic.

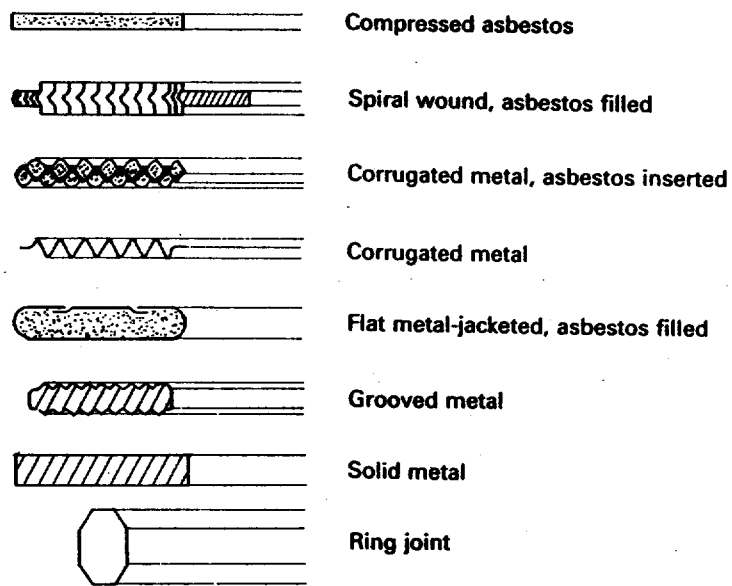
Solid metal gaskets are cut from sheet metal and are used for high-pressure and temperature applications. The surface quality must be good to achieve a sound joint and if made in more than one piece, the welded joints must be smooth, heat treated and the hardness checked in order to avoid damage to the flange. TEMA class R rules for the use of solid metal gaskets are the same as those for MJA gaskets.

Typical gaskets are shown in Fig. 2.13.

### 2.13 Tubesheets

Tubesheets less than 100 mm thick are usually made from plate which has been ultrasonically tested. At greater thicknesses, or for high integrity services, they are made from forged discs. TEMA specifies tolerances for (a) tube-hole diameter, both 'standard fit' and 'special close fit', (b) ligament width (i.e. gap between adjacent tubes) and (c) drill drift and minimum thickness. Drill drift is measured at the face of the tubesheet opposite the drill entry and is the difference between the centre of the

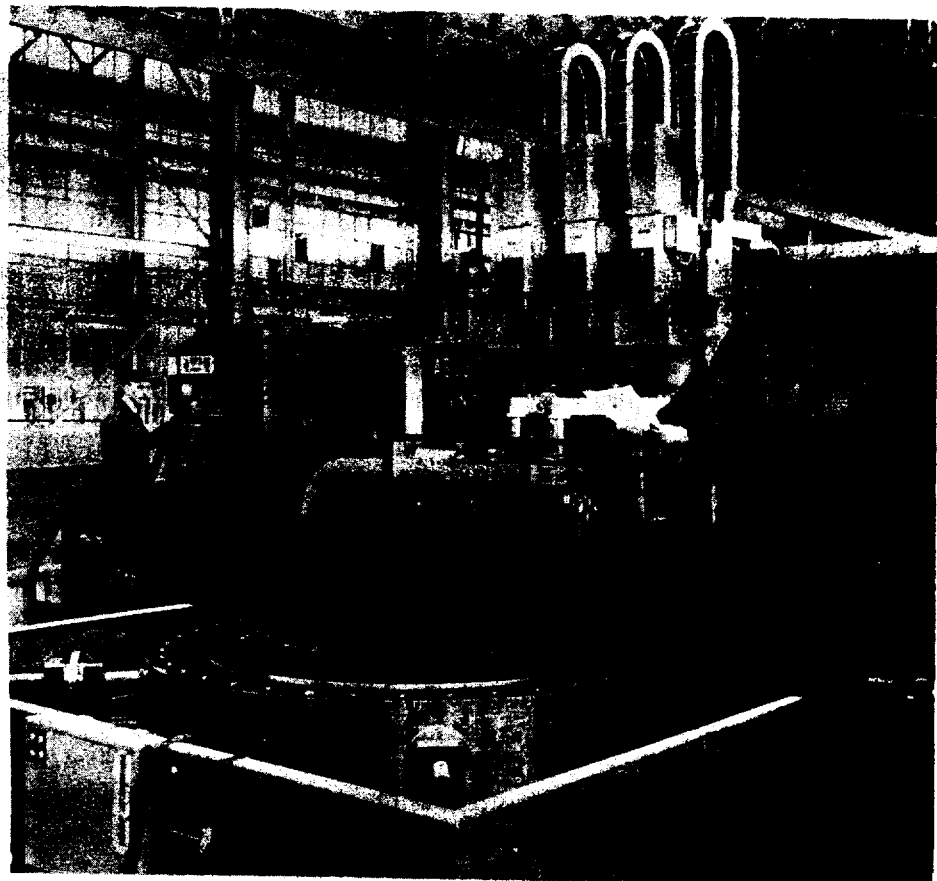
**Figure 2.13** Typical heat exchanger gaskets



hole actually drilled and the true centre of the hole. 'Special close fit' is recommended for tubes which are prone to work-hardening due to expansion. Many fabricators may standardise on greater minimum thicknesses in order to reduce distortion due to tube-end attachment but a typical minimum thickness is the greater of the tube outside diameter and 19 mm. Further details of tubesheet and hole preparation is given in section 2.15.

Figure 2.14 shows a tubesheet, 2.9 m diameter and 320 mm thick,

**Figure 2.14** Tubesheet, 2.9 m diameter and 320 mm thick, being drilled on a three-spindle gantry miller (courtesy of Whessoe Heavy Engineering Ltd, Darlington, UK)

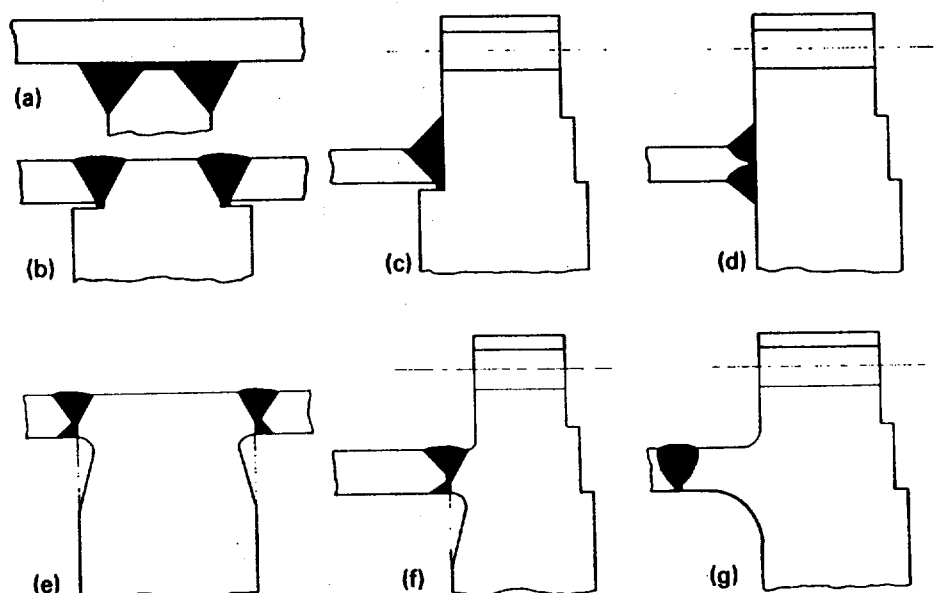


being drilled on a three-spindle gantry miller.

When manufacturing double-tubesheet exchangers it is essential for the holes in each pair of tubesheets to be in exact alignment. If out of alignment, such that force is required to insert the tube through the outer tubesheet into the inner, it may be extremely difficult to make a tight joint in the inner tubesheet where only expansion can be carried out. The tubesheets should be drilled together or jig drilled; once drilled the pair should be fastened together as a matching pair through fabrication.

Figure 2.15 shows typical shell-tubesheet connections for fixed tubesheet exchangers. Types (a), (b), (c) and (d), which do not have integral hubs, are widely used for moderate services and types (b) and (c) are the most common. However, types (b) and (c) have an internal crevice between shell and tubesheet. For high-integrity services types (e), (f) and (g), having integral hubs, are used.

**Figure 2.15** Fixed tubesheet exchangers: typical shell-tubesheet connections

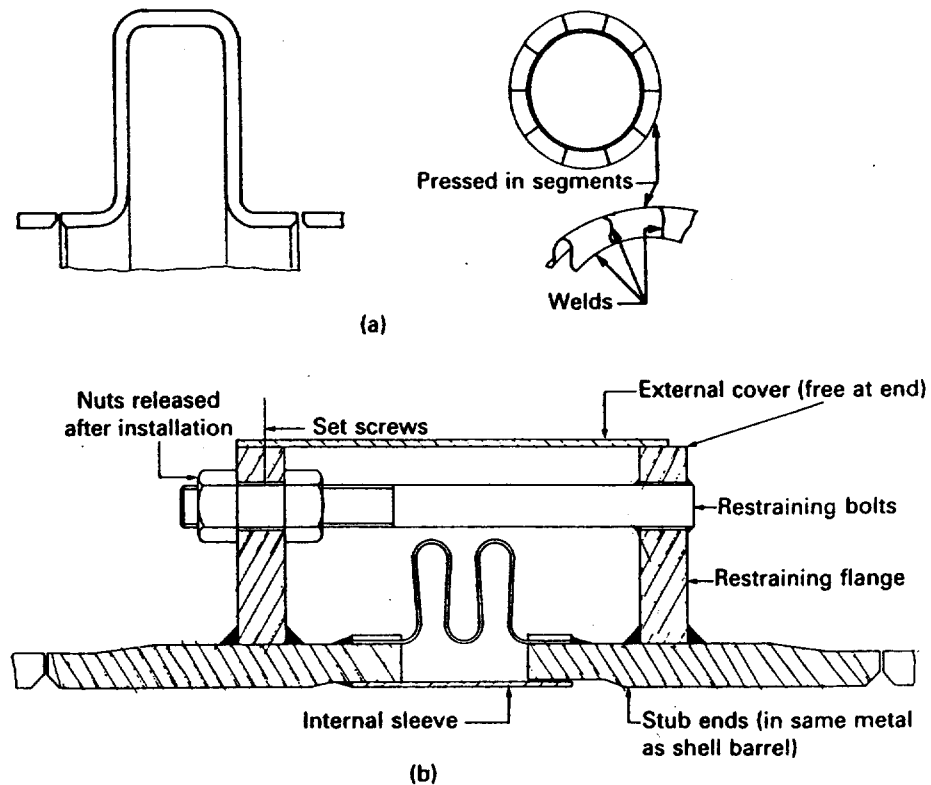


## 2.14 Expansion joints

The shell of a fixed tubesheet exchanger, or the floating-head end of split backing ring and pull-through type exchangers, having a single tube-side pass, may require an expansion joint. There are numerous expansion devices, but three common types produced by specialist manufacturers are the 'thick'-wall, 'thin'-wall and 'medium'-wall types.

The thick-wall joints are rarely used in floating-head exchangers but are commonly used in the shell of fixed tubesheet exchangers. As shown in Fig. 2.16(a), a single convolution is formed from a number of pressed plate segments welded together so that there is no circumferential welding in the convolution itself. The joint is invariably fabricated in the same metal and thickness as the shell barrel. Joint thickness is in the range 4–13 mm, with a convolution depth of 100–150 mm, but because of its inherent stiffness the movement provided by a single convolution is limited to about 2–5 mm. More convolutions may be added to provide

**Figure 2.16** Expansion joints (a) thick-wall type (b) thin-wall type (adapted from the author's contribution to *Heat Exchanger Design Handbook*, Vol. 4, 1983; reproduced by permission of Hemisphere Publishing Corp.)



greater movements, but the cost will become greater than the thin-wall type. The rugged construction permits the complete exchanger to be handled without the need for special protection and each convolution may be vented and drained.

The thin-wall joints are widely used in both fixed tubesheet and floating-head exchangers and a typical joint is shown in Fig. 2.16(b). The convolutions are cold-formed, either by rolling or hydraulic forming, to a depth of 24–75 mm. Standard material is austenitic stainless steel, but Incoloy™ and Monel™ are also used, especially if the environment is likely to produce stress corrosion cracking. Single ply thickness is 0.5–2 mm, but multi-ply construction is used for higher pressures. The number of convolutions depend on the movement required, but movements of  $\pm 40$  mm are readily accommodated. The convolutions are welded to short cylindrical barrels (stub ends) which are welded into the shell barrel, or to the floating-head and shell covers, as appropriate.

Although versatile with regard to pressure, temperature and movement, the joint requires careful handling and in many cases it is provided with internal and external protective liners and external restraining bolts to keep the complete assembly rigid during handling. In a floating-head exchanger one stub end is welded to the floating-head cover and for the purpose of a tube-side pressure test the other stub end is blanked off. One end of each restraining bolt is usually welded to the cover, instead of a restraining flange, and this protects the joint from being overstretched when the tube-side pressure is applied. As shown, the joint cannot be vented or drained, but externally pressurised joints are available which permit this. (See Fig. 1.24.)

The medium-wall joint is hot-formed and offers a compromise between

the thick-wall and thin-wall types. It is more flexible than the thick wall, but its construction is more rugged than the thin wall. Materials are usually chrome-molybdenum alloy and stainless steel, 2–4.5 mm thick with a convolution height of 50–63 mm.

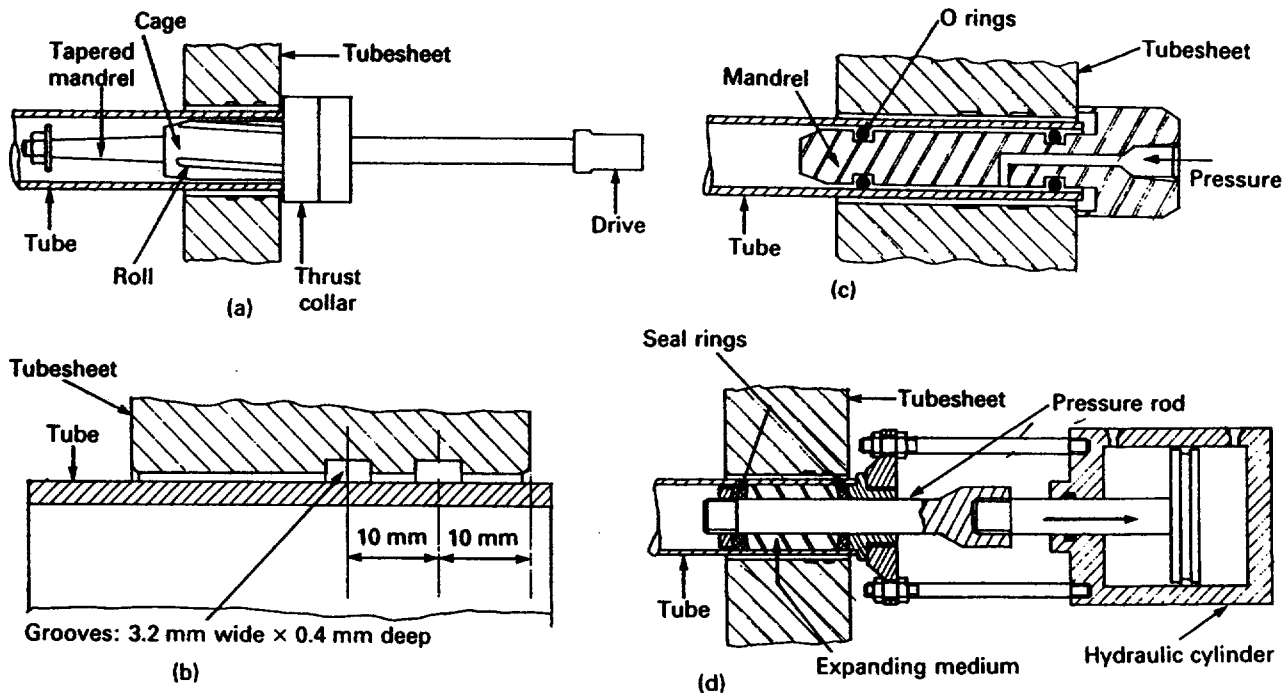
## 2.15 Expanded tube–tubesheet joints

The practice of expanding the end of a tube into a hole in a tubesheet in order to make a tight mechanical joint has been carried out for over a hundred years. In the early days the joint was made by 'drifting', in which a hardened tapered pin was hammered into the end of the tube. Today the expanded tube-end joint is achieved by several methods, namely roller expansion, hydraulic expansion, rubber expansion and explosive expansion. In all cases the object is to enlarge the tube so that its final diameter is greater than that of the original hole, the ideal joint being one in which the tube is stressed beyond its yield point, but not to its ultimate strength, while the tubesheet is not stressed beyond its yield point. Once the expanding process has been completed the tube and tubesheet hole exert forces on one another, as they attempt to recover to their original diameters, the resulting contact pressure being related to the deformation of the tube and tubesheet achieved during expansion and their mechanical properties. In a correctly expanded joint, the hole should return to its original size after removing the tube.

### 2.15.1 Roller expansion

The most common method of expanding a tube into a tubesheet is by roller expansion. A special tool, known as a tube expander, roller expander or tube roller, is inserted in the end of the tube and applies radial force to the tube, which is expanded until a mechanical joint is made between the tube and hole within the tubesheet. The initial expansion of the tube merely closes the annular space between tube and hole, but once metal-to-metal contact is made further cold-working provides the seal. Once the yield point of the tube is exceeded additional expansion causes it to extrude longitudinally in both directions. It has been estimated that 60–75% of the extrusion is in the direction of the bundle and the remaining 25–40% of the extrusion proceeds away from the bundle towards the operator.

A typical tube expander is shown in Fig. 2.17(a) and consists of a cylindrical cage with three to seven equally spaced longitudinal slots, each containing a hardened steel roller which is free to rotate. The cage body at the drive end is threaded and fitted with a thrust collar which can be moved along the cage to achieve the required expansion depth, after which it is locked into position with a set screw. A tapered mandrel, fitted between the rolls, is driven by electric, air or hydraulic motors. In the roller expansion process the forward movement of the mandrel causes the rollers to move outwards to press against the tube; subsequent friction



**Figure 2.17** Tube expansion methods (a) roller expansion (b) typical tube-hole grooving (c) hydraulic expansion (Haskel Hydroswage™) (d) rubber expansion (Hitachi Ltd, Tokyo, Japan)

between the rollers and rotating mandrel induces the rollers to turn and squeeze the tube against the hole.

A roughened tube hole provides a tube-tubesheet joint having strength and stability, but it is not as leak-tight as a smooth hole. A glass-smooth hole, for instance, provides better leak-tightness but it has less strength and stability. In practice a drilled and reamed finish provides the optimum hole surface condition in many applications. In order to achieve roller expanded joints of high integrity the tubes and holes must be free of scale, dust, dirt and scratches or toolmarks. As the tubes are fed through holes in the baffles and tubesheets the holes must be free from burrs in order to avoid scratching of the tubes. The expander itself must be cleaned regularly and discarded once there are signs of wear.

Underexpansion produces a joint which will leak on test and the obvious remedy is to expand again. Overexpansion is more serious as it cold-works the tube excessively, leaving it prone to corrosion, and if excessive, distortion of both tube hole and ligament between adjacent tubes may occur. The optimum amount of expansion (i.e. tube-wall thinning) depends on many factors such as the surface finish of the tube and hole, initial annular clearance between the tube and hole, mechanical properties of the tube and tubesheet, including hardness, width of ligament between adjacent tubes, diameter and wall thickness of tubes, length of expanded joint and type of expander and torque control method used. Because of the large numbers of variables each case must be treated on its merits, but experience shows that a tube-wall thinning of 5–8% covers many industrial applications, with specific values of 8–10% for copper and cupro-nickel, 7–8% for carbon steel and admiralty brass and 4–5% for stainless steel and titanium.

In practice the expander torque value, which provides the required amount of expansion, and at which the expander will automatically cut



out, must be determined from experience and tests. The percentage tube-wall thinning is calculated from the following formula:

$$\% \text{ wall thinning} = \left( 1 - \frac{d_h - d'_i}{d_o - d_i} \right) \times 100$$

where  $d_h$  = measured tube-hole diameter before expansion  
 $d_o$  = measured tube outside diameter before expansion  
 $d_i$  = measured tube inside diameter before expansion  
 $d'_i$  = measured tube inside diameter after expansion.

The measured tube inside diameter after expansion includes the enlargement of the hole itself and the above formula provides the *apparent* percentage wall thinning. Although it is possible to achieve a uniform close fit of the tube within the tube hole, it should be noted that customary tolerances for tube-hole drilling and tube outside diameter are such that the theoretical diametral clearances between hole and tube outside diameter, based on a tube 19.05 mm outside diameter, 2.11 mm nominal thickness, for example, may be:

Largest hole/smallest tube: 0.35 mm

Smallest hole/largest tube: 0.05 mm

The customary tolerances for a minimum wall tube of this size are such that its theoretical inside diameter may range from 13.9 to 14.9 mm. The variation in these dimensions, together with other factors listed earlier, serve to show that the subject of normal tube expansion is not one which can be treated readily on a highly scientific basis, but is best left to the skill and experience of the fabricator.

Figure 2.17(b) shows details of typical expansion grooves which are cut into the tube hole. The grooves provide additional strength and also break and seal off tool marks. It is customary to expand the tube into the tubesheet for a minimum length of 50 mm, or tubesheet thickness less 3 mm, whichever is the smaller. In order to close the annular space between hole and tube, the tube may be expanded for the full thickness of the tubesheet, but expansion beyond the inner face of the tubesheet is prohibited. Full depth expansion is also desirable as the extra stiffening effect enables the tubesheet thickness to be reduced.

When unusual tube and tubesheet combinations are encountered, or when extreme care must be taken to avoid overexpansion, a test block is prepared well before production expanding occurs. The tube material, tube size, tubesheet material and tube-hole drilling must be identical to those in the production exchanger. The tubesheet thickness for the test block should be the same as the tubesheet thickness in the exchanger, but if the latter is more than, say, 75 mm thick, this thickness will suffice in most cases for the test block. A typical test block may contain 30 short tubes, arranged in five rows at six tubes per row, and before expansion each tube-hole diameter, and the outside and inside diameters of each tube, are measured. Hardness readings are also taken on the internal surfaces of the tubes.

A different expander torque value is selected for each of the five rows and after expansion the inside diameter of each tube is measured, from which the percentage wall thinning is determined from the formula given

earlier. The test block is sectioned along the centre of each row of tubes. Tube-bore hardness checks are then made, after which the amount of tube which has been forced into the grooves and its surface condition are noted. These data enable an experienced fabricator to decide on the optimum torque value to be used in the exchanger. Sometimes another test block, capable of being pressurised to the required test pressure, and containing about ten tubes, is made. The tubes are expanded to the selected torque value and pressure-tested; if any leaks occur a higher torque value based on the test block data is selected and the process is repeated. If strength tests are carried out the tube should be removed through the back of the tubesheet. Pushing the tube out of the hole at the front face by applying compressive load at the back face is not recommended. Additional frictional forces may be set up due to the expansion of the tube within the tubesheet thickness and the tube may be bulged at the junction between the tube and hole at the back of the tubesheet; in both cases a false, high-strength value will be obtained. During production frequent random checks are made to ensure that the procedure established by the test blocks is being followed. Torque checks are made, particularly at the beginning of a shift or operator change.

### 2.15.2 Uniform tube-end expansion

Although roller expansion has been the standard method of making a mechanical joint between tube and tubesheet over many years, it has the following disadvantages: (a) the axially orientated grain structure of the tube is changed by the action of the rollers to a circumferential structure giving concentrated stress areas, (b) great care is required to avoid work-hardening certain materials, which leaves them prone to corrosion, (c) the rollers impose high unit forces which cause the tube to extrude axially, (d) the 'cyclic' action of the rollers can produce tube-end fatigue, (e) expanders may not be robust enough to expand small-diameter, thick-wall tubes, (f) the maximum length of tube which can be expanded in one operation, or step, is about 50 mm – hence the full depth expansion of thick tubesheets requires several overlapping steps (step-rolling) which is time-consuming, (g) after expansion into the first tubesheet care must be taken to avoid a twisted bundle when expanding the tubes into the second tubesheet, as roller friction causes the tubes to twist unless they are locked into position and (h) the predetermined expander torque is subject to the condition of the rollers, mandrel, lubrication and the skill and fatigue of the operator – some tubes may be under- or overexpanded and reproducibility is difficult to achieve.

The disadvantages of the roller expansion process are overcome when the tube is expanded uniformly over the required length without the internal surface being contacted by a metallic tool. Uniform expansion, as it is termed, is achieved by either rubber expansion, hydraulic expansion or explosive expansion. (Explosive expansion is described later under explosively formed tube-end joints.) The concept is not new, but technical problems has delayed development of a suitable expander which offers economy, lightweight, unskilled, safe, fast and repeatable

operation, combined with robustness and long life. The roller expander may be approaching obsolescence.

#### **Hydraulic expansion**

The uniform expansion method developed by Haskel Inc. is termed 'Hydroswaging<sup>TM</sup>', in which the uniform radial force is applied to the tube by hydraulic pressure. The complete system comprises six components: power unit, intensifier assembly, control gun and flexible high-pressure capillary tubing, the mandrel and adaptor, the tube-lock tool, and the leak-test tool.

The compressed air operated hydraulic pump of the power unit supplies the intensifier, which increases the water pressure by a fixed ratio to the value required to expand the tube. This is regulated by adjusting the inlet pressure to the intensifier and currently the equipment will produce a maximum expansion pressure of about 4830 bar. The operation of a button on the handle of the lightweight control gun automatically feeds water from the intensifier into the mandrel, via the flexible high-pressure capillary tubing, and then to the sealed annular space between mandrel and inside of the tube, in which the tube expansion occurs. A system of warning lights enables the operator to monitor the process; an amber light signifies the start of the process, a green light signifies the successful completion of the expansion process, but a red light signifies that the required expansion pressure has not been achieved. Because permanent deformation of the tube during expansion is not instantaneous, a time delay during expansion is necessary and the power unit can be preset to provide a dwell time of 1–30 seconds. On completion of the expansion process the water pressure is relieved automatically by returning the water to a reservoir in the power unit. Distilled water is used.

The mandrel is attached to the control gun by a special adaptor designed to provide rapid snap-action connection and release. The mandrel shown in Fig. 2.17(c) has two rubber 'O' rings, with back-up rings to prevent extrusion during expansion, which seal off the annular space between mandrel and tube at each end to contain the pressure. The distance between the 'O' rings can be set exactly to suit the required expansion length within the tubesheet, and the design of the mandrel permits an increase of 1 mm in tube inside diameter during expansion. As the system will expand a tube to any hole configuration, out-of-round holes present no problems. Mandrels are available to suit tube diameters of 5–51 mm and there is no upper limit to tubesheet thickness, although the minimum is 19 mm.

The function of the tube-lock tool is to position the tube axially in the tubesheet and fasten it so that it cannot move when the mandrel is inserted. It also enables each tube to have exactly the same protrusion from the tubesheet face. The tube-lock tool is a hydraulic cylinder, operated from the low-pressure side of the power unit, in which the application of pressure causes polyurethane segment rings to bulge radially and in turn bulges the tube wall until it makes firm contact with the hole. The expansion is not carried out over the full depth of the tubesheet, neither is the joint pressure-tight.

Although the theoretical expansion pressure can be calculated for each tube and tubesheet combination, this cannot cater for (a) the surface condition, or irregularity in shape, of the tube and hole, (b) the condition of the grooves in the tubesheet or (c) irregularities of tube and tubesheet materials. A test block, similar in principle to that used for roller expansion, may be required to determine the correct expansion pressure. There are several methods for pressure-testing the tube-tubesheet joints and the proprietary leak test tool is one device which may be used. It has general application, however, and its use is not restricted to the Hydroswege™ system. Test water is supplied to the tool from the low-pressure side of the power unit at a pressure up to about 193 bar. The tube samples are tested one at a time and any leakage is observed at the back tubesheet face.

#### **Rubber expansion**

The uniform expansion method developed by Hitachi is termed 'rubber expansion' in which the uniform radial force is applied to the tube by the expansion of a cylinder of elastomer inside the tube. The arrangement is shown in Fig. 2.17(d) in which pressure in a hydraulic cylinder pulls the pressure rod in the direction of the arrow shown on the shaft to compress the elastomer, or expanding medium, inside the tube. Seal rings, spaced to suit the required expansion length within the tubesheet, constrain the expanding medium such that it bulges radially to exert uniform expansion pressure on the inside of the tube.

The previous comments concerning hydraulic expansion apply also to rubber expansion—only the expanding medium differs.

## **2.16 Fusion-welded tube-tubesheet joints**

An expanded tube-tubesheet joint cannot be guaranteed to provide leak-free service over a long period. Under test in the fabrication shops, most joints can be made to withstand a pressure differential of 200 bar without difficulty. In service, however, even small expansions and contractions of the tubes, which may occur during the course of normal plant operation, are often sufficient to relax the joint. Thermal cycling and vibratory conditions, both flow-induced and from external sources, will hasten joint relaxation.

Each case must be considered individually, but the decision to weld the tube ends, rather than expand them, is based on any of the following factors:

- (a) if leakage between fluids, however small, must be avoided;
- (b) when there is a high-pressure differential across the tubesheet – firm rules cannot be given as the limiting pressure differential depends on many factors, but consideration should be given to welding at a differential of 50 bar;
- (c) if thermal shock, thermal cycling or vibratory movement is likely to occur;

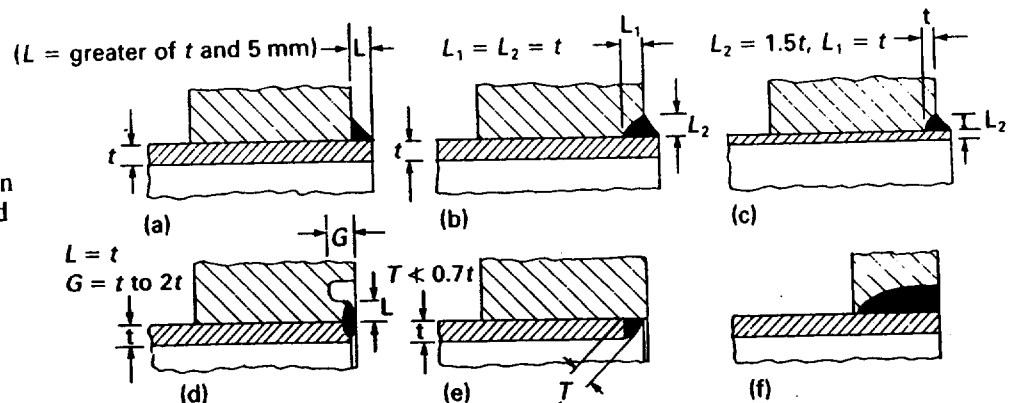
- (d) when the combination of tube and tubesheet metal properties and dimensions do not permit sound expansion:
- (e) when the tube ends and tubesheets have a non-metallic lining which may be difficult to repair if leakage occurs;
- (f) when the tubes and tubesheet have different thermal expansion coefficients which would cause loosening of the joint at low or high temperatures.

The technology of fusion-welded tube-end joints is highly advanced and the subject of continual research by fabricators, suppliers of welding equipment and technical bodies. The most common fusion-welded processes are shielded metal-arc (or the familiar 'stick' method), gas tungsten arc (or TIG – tungsten inert gas) and gas metal arc (or MIG – metal inert gas). Welding may be carried out by manual methods, but like the roller expansion process repeatability is difficult to achieve, being related particularly to the skill and fatigue of the operator. As expected, research is orientated towards fully automatic methods including the application of robotics. In most applications the weld between tube and tubesheet is made at the front, or outer, tubesheet face, but in some applications the weld is made at the back, or inner, tubesheet face.

### 2.16.1 Front tubesheet face welding

There are numerous tube–tubesheet weld configurations for front tubesheet face welding and Fig. 2.18(a)–(f) provides representative samples. The plain fillet shown in Fig. 2.18(a) is used for the welding of tubes having a wall thickness greater than about 2.5 mm. However, the preferred configurations for tubes having a wall thickness greater than about 2.0 mm are the groove and fillet types shown in Fig. 2.18(b) and (c). The use of a groove enables a weld of adequate throat thickness to be achieved without having fillets of excessive size. The groove and fillet configuration may be used for thinner tubes if the welder has the skill to avoid burning through the tube wall, but the preferred method is the castellated configuration of Fig. 2.18(d). The pitch of the tubes must be sufficiently great to provide the castellation around each hole, and the tubesheet thickness calculation must allow for the weakening effect of the grooves. Intersection of the grooves is of no consequence. The castellation also acts as a heat barrier, which assists in minimising distortion and welding stresses.

**Figure 2.18** Typical tube-end welds (front tubesheet face) (a) fillet (b) groove and fillet (thick tube wall) (c) groove and fillet (thin tube wall) (d) castellated (e) recessed (f) waste heat boiler



The advantages of the recessed configuration of Fig. 2.18(e) are (i) no machined preparations are required for tube and tubesheet, (ii) the replacement of a tube is relatively simple with no reduction in corrosion allowance and (iii) an exceptionally good weld profile is achieved, suitable for non-metallic lining, with well maintained fully automatic TIG equipment. Certain materials and welding processes permit the tube end to be flush with the tubesheet face.

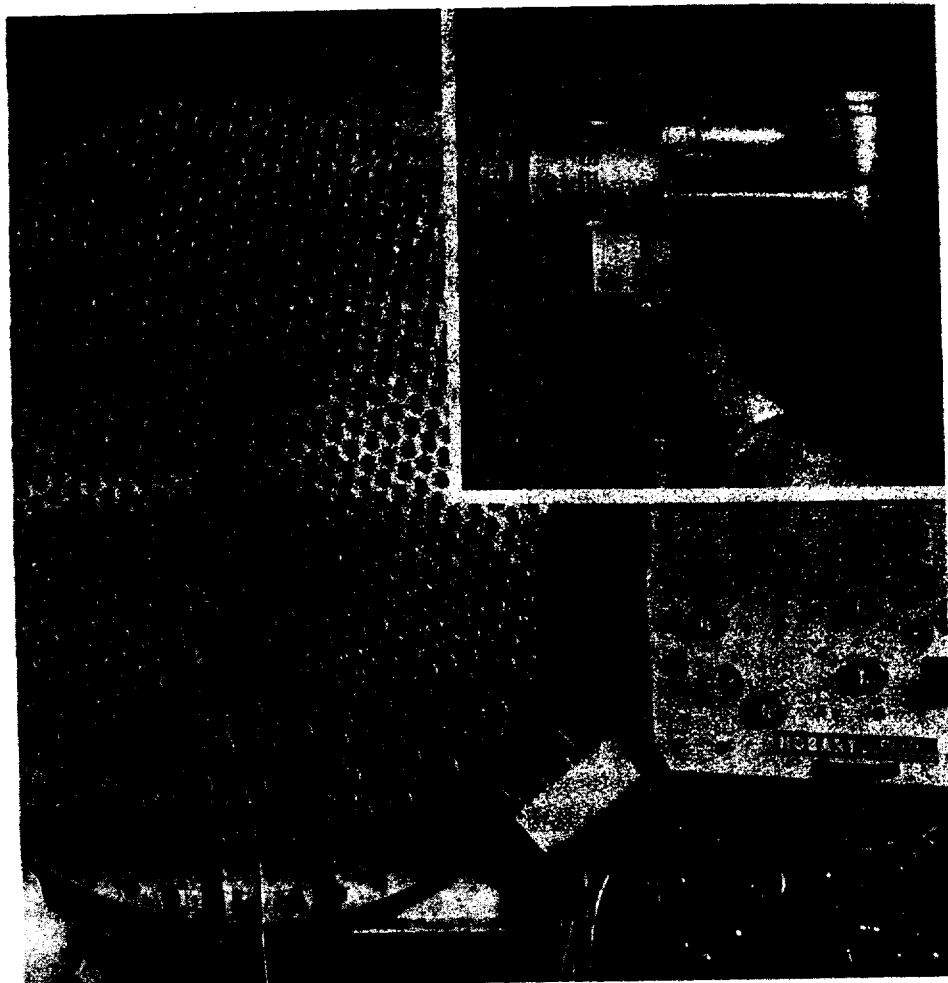
The configuration shown in Fig. 2.18(f) is designed especially for the hot tubesheet of transfer line exchangers and waste heat boilers. As the loads on the tubesheet are taken by stays, the tubesheet is relatively thin. In addition to providing strength, the through-thickness weld eliminates the gap between tube and tubesheet at the back face of the tubesheet where crevice corrosion might occur.

The most widely used process is TIG in which the weld is shielded from the atmosphere by a continuous purge of inert gas, such as argon, helium or carbon dioxide, which flows through the welding nozzle in the annular space between a non-consumable thoriated tungsten electrode and the nozzle wall. (A non-consumable electrode conveys electrical current but is not fused into the weld.) The weld may be made solely by fusion, or wire (filler metal) which may be fed to the weld continuously through the nozzle. The process is extremely sensitive to the cleanliness of the hole and tube, both inside and outside, and even minute traces of dirt, grease, scale, rust and moisture may ruin the weld, and the defect may not be visible on the surface. Thorough degreasing and cleaning prior to welding is essential, and this includes the baffle holes through which the tubes are passed. The outside of the tube is usually finished to bright metal for about 13 mm at each end. TIG is suitable for all weldable metals and may be used for all configurations shown in Fig. 2.18 except (f). When used for steel tube-tubesheet joints, the steel must be silicon killed with a composition range of carbon 0.15% maximum, silicon 0.20% minimum, manganese 1.0% minimum, sulphur 0.035% maximum and phosphorus 0.035% maximum.

The TIG process lends itself to automation and a variety of systems are available, and Fig. 2.19 shows the welding head of the Hobart CYBER-TIG™ automatic tube-tubesheet welding system. Compared with manual methods it is much less dependent on the skill and fatigue of the operator and is therefore capable of providing repeatability. It is claimed to be 30–60% faster than manual methods. The complete welding cycle covering electrical demand and sequence, filler wire flow and speed, welding head rotational speed and shielding gas flow is automatic. Welds may be made with the tubesheet in any position.

In the shielded metal-arc process, the weld is shielded from the atmosphere by a flux which encases the consumable electrode ('stick') operated manually by the welder. It is widely used for ferritic steel tube-tubesheet joints where the tube diameter is usually not less than 19 mm, the wall thickness not less than 2 mm and the ligament between tubes not less than 6 mm or twice the wall thickness, whichever is the greater. Although the importance of cleanliness cannot be overemphasised, the metal-arc process is less sensitive than the TIG process to minor discrepancies in cleanliness and metal composition. Although it may be used for configurations (b), (c) and (e) of Fig. 2.18, it

**Figure 2.19** Hobart  
**CYBER-TIG™**  
automatic tube-end  
welding system



is used chiefly for configurations (a) and (f). In the case of the latter the weld is built up in several passes.

Another process is MIG in which the weld is shielded by inert gases flowing through the nozzle, as in the TIG process, but the consumable electrode is a fine wire which is fed continuously through the nozzle. Compared with the TIG process, it is less sensitive to minor discrepancies in cleanliness and metal composition. It is used with configurations (a), (b) and (c) of Fig. 2.18 and is particularly suited to small ligaments between tubes of about 4.8 mm.

It is customary to give the welds a low-pressure air test or a more searching halogen test on the shell-side at about 0.7 bar before the hydrostatic tests. A halogen test involves the mixing of 1–10% by volume of an organic halide vapour, such as Freon, methylene dichloride or carbon tetrachloride with the air used for the test. A halogen-sensitive probe is then passed over each tube-end weld. Because most halides contain chlorides it is not recommended for austenitic stainless steels. Trichlorethylene or carbon tetrachloride should not be used for degreasing as the detector will respond to minute residues of these solvents and give false readings. The object is to identify and repair leaking tube ends before they come into contact with water as it is more difficult to make sound tube-end repairs afterwards. If the tube ends have



to be welded in more than one run (or pass), then the welds are given a low-pressure test after each pass before proceeding to the next.

During the period 1966–69, a British committee consisting of representatives from end-user companies, contractors, fabricators and the Heat Transfer Society, under the auspices of the Welding Panel of the Oil Companies Materials Association (OCMA), agreed to pool their knowledge and experience in order to produce a recommended practice covering tube-end welding. It was considered that there was no national or international standard which covered the subject adequately. OCMA Specification TEW 1, published in 1969, provided recommendations for the tube-end welding of ferrous materials including welding processes, details of joints, cleaning and preparation, qualification of procedures and operators, preheat, post-weld heat treatment, quality control, tube expansion, testing, leak detection, repairs and materials for electrodes and fillers.

The OCMA specification has become a basis for specifying requirements for the oil, chemical, gas and many other industries in the United Kingdom. Although many of the recommendations appear commonplace today, this was by no means the case prior to 1969. The specification highlighted four factors:

- (a) Previously there had been too much emphasis on joint strength, rather than joint tightness. OCMA considers that a properly welded joint is not only leak-tight, but has a strength approaching that of the tube itself.
- (b) Tube-end expansion before welding is not recommended. Experience showed that expansion before welding causes root defects and porosity in the welds as the gases cannot escape. The tube should be located in position prior to welding either by tack welds, or by a three-point drift which forces three small slugs of tubesheet metal against the tube wall, 120° apart.
- (c) Heavy expansion after welding is not recommended. Instead of adding strength, experience showed that heavy expansion may damage a sound weld. Light expansion is usually desirable to close the gap between tube and hole and is recommended if the joint is likely to experience thermal cycling or vibratory movement. Expansion grooves serve little purpose and are usually omitted. However some designers elect to include them for expansion after welding but locate them well away from the weld.
- (d) Post-weld heat treatment of tube bundles with welded tube ends should be avoided if possible. The use of austenitic stainless steel electrodes, instead of ferritic ones, for example, may change the joint metallurgical structure such that post-weld heat treatment is not required. If post-weld heat treatment is essential, great care must be exercised to avoid weld fracture and distortion; the heating and cooling rates must be carefully controlled and the tubes well supported.

When unusual tube-tubesheet metals are encountered, trial welding is carried out using a test block, similar to that described for roller expanded samples. After welding the block is sectioned by sawing, then

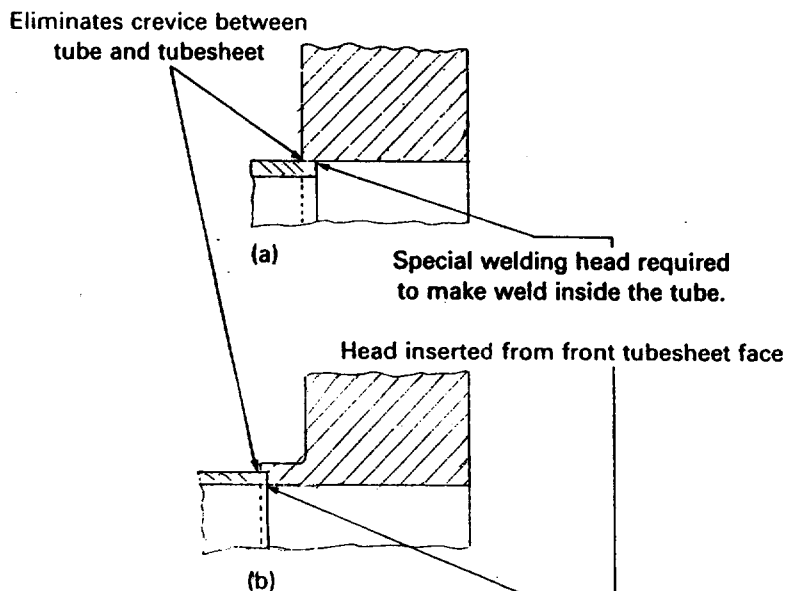
polished and etched. Some welds are examined visually to check for defects, contour, throat thickness and intrusion into the tube bore. Other welds may be subject to X-ray, or metal removed from the welds by repeated skimming parallel to the tubesheet surface, to confirm freedom from porosity and cracks. A tear test may be specified in which part of the tube is bent away from the hole to expose the underside of the weld for inspection. Strength and pressure tests may also be required.

### 2.16.2 Back tubesheet face welding

Whether a tube is expanded only, or welded and then lightly expanded, there is always a length of about 3 mm which is not in contact with the tubesheet at its inner face. Crevice-type corrosion may occur in this gap, but if an attempt is made to close it by expansion of the tube, there is always the danger of bulging the tube just beyond the tubesheet. The crevice is eliminated if the tube is welded to the back face of the tubesheet and this special form of welding is also known as 'internal bore' or 'back-bore' welding.

Figure 2.20 shows two preparations for this type of welding and in both cases a special welding nozzle is inserted down the bore of the tube from the front tubesheet face to make the weld as physical access to the back face is not possible. The back of the tubesheet face adjacent to the weld must be shielded by inert gas during welding. Both types have the advantage of permitting X-ray examination, although special techniques are required for type (a).

Figure 2.20 Typical tube-end welds (back tubesheet face)  
(a) recessed (b) spigot



Although an expensive procedure, there is some bonus because the tube length in a U-tube exchanger, for instance, is shorter than normal by the thickness of the tubesheet. This may be significant if the tubesheet thickness is of the order of 300 mm or more. The tubehole diameter is smaller than normal for the preparation shown in Fig. 2.20(b) because it is the same as the tube bore.

## 2.17 Explosively formed tube-end joints

The expansion and welding of tube-tubesheet joints by explosive means, as an alternative to mechanical expansion and fusion welding, has been the subject of continuous research and development since the late 1950s.

### 2.17.1 Explosive expansion

Explosives provide an alternative to water and rubber as an expanding medium in the uniform expansion process, but their development has perhaps been more concerned with the object of achieving a tighter joint than that provided by other expansion methods. Figure 2.21(a) shows the arrangement prior to the explosion. A predetermined length of plastic tube, containing an explosive charge is inserted into the end of the tube, the explosive charge being sized according to the tube size and mechanical properties of the tube and tubesheet metals. The objective is identical to that described earlier for all expanded tube-tubesheet joints; the tube is expanded beyond its elastic limit but the tube hole is expanded within its elastic limit such that on recovery a tight fit between the two is obtained. On detonation the explosive force is transmitted radially via the plastic tube to bring the metallic tube into intimate contact with the hole. A number of tubes can be expanded in one firing.

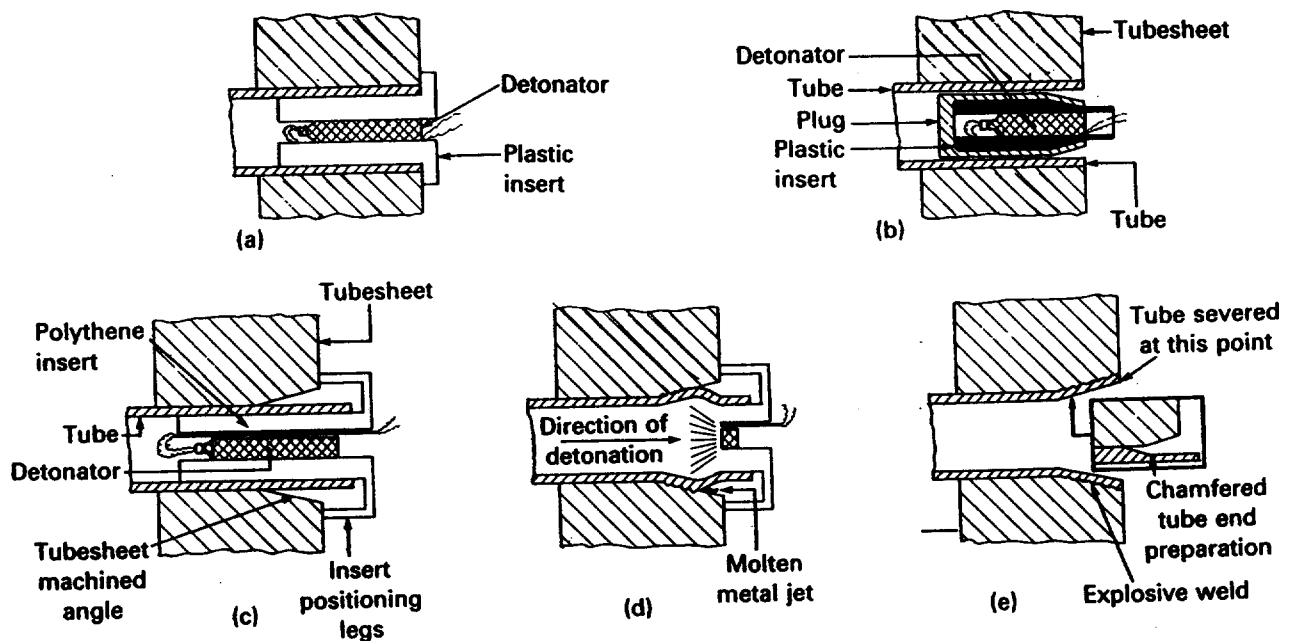
Explosive expansion has all the advantages of uniform expansion technology previously described and it is not sensitive to the hole quality. Because oversize, non-circular, corroded, pitted and dirty holes present no problems, the process is used widely for the re-tubing of leaking bundles where roller expansion is unlikely to provide leak-proof joints. It is also used widely for repairing leaking joints, whether expanded or fusion welded, where roller expansion is incapable of curing the leaks. The process is safe and usually repair work is carried out *in situ*, whereas repairs by welding may be prohibited for safety reasons. Should leaks occur the contaminated joint may be difficult to re-weld in any case.

The minimum ligament between tubes is about 4.8 mm and the smallest tube bore about 13 mm.

### 2.17.2 Explosive plugging

Although a leaking tube-tubesheet joint may be repaired by expansion or welding, the cure for a split tube is either to replace it, which is not always possible, or to plug it at each end. If the decision is made to plug, a welded-in plug may not be feasible because *in-situ* welding may be prohibited for safety reasons, or the tube may be in an inaccessible position for sound welding, or the condition of the tube-end and tubesheet face may prevent sound welds being made. As an alternative a tapered metallic plug may be driven into the bore of the tube. Experience has shown that neither method is entirely satisfactory, particularly under cyclic operation, and explosive plugging is a proven solution.

Figure 2.21(b) shows the explosive plugging arrangement prior to



**Figure 2.21** Explosively formed tube-end joints (a) explosive expansion (b) explosive plugging (c), (d) and (e) explosive welding – before explosion, during explosion, completed weld (Courtesy of Yorkshire Imperial Alloys, YIMPACT Dept).

explosion. The plug consists of a hollow cylinder, closed at one end, into which a plastic tube/explosive charge composite assembly, similar to that required for explosive expansion, is inserted. On detonation the explosive force is transmitted radially via the plastic tube and plug wall, to bring the plug into intimate contact with the tube wall.

Unlike fusion welding, where the plug and tube material must be compatible with one another, the plug material need only provide corrosion resistance to the fluids. The process is also not sensitive to dimensional variations. The stocking of standard plugs is therefore simplified because a large number of different sizes, in a variety of metals, is not required. When the tube-tubesheet joint is by internal bore welding the plug is sized to fit inside the tube hole instead of the tube. This is also done when a leaking joint is to be plugged, instead of repaired, in which case the tube must be drilled out.

In one design of plug its outer wall has machined rings which become embedded in the tube inner wall after the explosion to provide increased strength and leak-tightness. However, in the process shown in Fig. 2.21(b) the open end of the plug is tapered inwards and, as a result, the explosion causes the plug and tube to be *welded* together over the tapered portion and not expanded. The principle of explosive welding is described in the next section.

### 2.17.3 Explosive welding

The sequence of events during explosive welding is shown in Fig. 2.21(c), (d) and (e). The system is similar to the explosive expansion process except that the tube hole is tapered at the other tubesheet face. The total included angle of the taper is about 10–20° over a length of about 12–16 mm. The fundamental requirements for successful welding are (a) the surfaces to be joined must be brought together with sufficient force to

create an interfacial pressure many times greater than the yield strengths of the metals to achieve interfacial melting and (b) the surfaces must collide progressively, with the collision point traversing the surfaces at a velocity not exceeding the velocity of sound within the metals. Under these conditions the molten metal is squeezed out forward of the collision point, including any surface contaminants, to provide clinically clean surfaces. The result is a true metallurgical bond.

The integrity of an explosively welded tube-tubesheet joint is much greater than the expanded and fusion-welded joints on all counts, i.e. axial and tear strength, resistance to fatigue due to pressure and thermal cycling, and operating pressure. The weld may be examined ultrasonically. In addition to its exceptional joint integrity, tube and tubesheet metals which cannot be welded together by conventional means (e.g. admiralty brass-steel, copper-steel, titanium-stainless steel) are readily welded by the explosive process.

As expected, the cost of the explosive-welding process is greater than fusion welding, but this must be weighed against the greatly increased service life. Exchangers using the process may have to be designed with increased ligaments between tubes in order to prevent ligament distortion during the explosion. Minimum ligament is related to tube-wall thickness, rather than tube diameter, as shown in Table 2.2.

Table 2.2 Ligament sizes

Tube-wall thickness			Minimum ligament	
s.w.g.	mm	in	mm	in
22	0.71	0.028	7.94	$\frac{5}{16}$
20	0.91	0.036	7.94	$\frac{5}{16}$
18	1.22	0.048	9.53	$\frac{3}{8}$
16	1.63	0.064	11.11	$\frac{7}{16}$
14	2.03	0.080	12.70	$\frac{1}{2}$
12	2.64	0.104	15.88	$\frac{5}{8}$

The minimum ligament may be reduced by 1.59 mm ( $\frac{1}{16}$  in) if adjacent tubesheet holes are fitted with tapered support plugs. Alternatively the minimum ligament may be reduced by thinning the tube wall locally as shown in the inset of Fig. 2.21(e).

#### 2.17.4 Tube-end inserts

The tube ends of inlet tube-side passes often experience considerable erosion due to high turbulence and the presence of entrained solid particles during service. Instead of replacing the eroded tubes, the eroded areas may be drilled out to a predetermined depth and length and replaced by a metallic sleeve. The sleeve, or tube-end insert, is explosively welded and/or expanded to the thinned tube wall. As a tight bond between tube-end insert and tube can be achieved irrespective of their metals, the insert material may be chosen to provide a long service life. Galvanic corrosion should be checked before a decision is made.

## 2.18 Testing

### 2.18.1 Hydraulic testing

After completion the exchanger is usually pressure tested with water to check the soundness of all welds, the tube-tubesheet attachments and the gasketed joints of the flanges. Sometimes a light oil is used to prevent corrosion. Unless the exchanger has been designed for a differential pressure, the shell-side and tube-side are tested independently to their respective Code test pressures. When the exchanger has been designed for a differential pressure, the shell-side and tube-side are pressurised together, but care must be taken to ensure that the test differential pressure is not exceeded.

Fabricators prefer to test the tube-tubesheet joints by pressurising the shell-side. This enables each joint to be inspected from the outer faces of the tubesheets so that all leaking joints can be positively identified. This is acceptable when the shell-side test pressure is equal to, or greater than, the tube-side test pressure. If the tube-side test pressure is the greater, then the tube-side must be pressurised, but positive identification of leaking tube-tubesheet joints is more difficult. In the case of a removable bundle exchanger, the bundle is tested by itself outside the shell so that leakage is detected initially as drips from the bottom of the bundle. Although the interior of the bundle is then inspected visually with the aid of a lamp, positive identification of the leaking joints is sometimes difficult, particularly with tubes on a close triangular pitch. In the case of a fixed tubesheet exchanger, where the bundle cannot be removed from the shell, leakage from a tube-side test is more difficult to detect due to limited physical and visual access. Every effort is made to minimise unnecessary re-rolling of tube ends but some may be unavoidable.

Split straight and U-tubes are removed and replaced, if practicable, but otherwise they are plugged. Explosive plugging may be used for high-integrity services. TEMA provides guidance on the number of defective tubes which may be plugged by the fabricator in new exchangers without prior agreement with the purchaser.

Testing of fixed tubesheet exchangers normally involves only two tests. The shell-side is pressurised, with the heads or head covers removed, so that the shell welding, tubes and tube-tubesheet joints can be checked. After draining the shell-side, the head and head covers are fitted and the tube-side pressurised to check the welds in the heads and any gasketed head joints.

In order to test the bundles of split backing ring and pull-through floating-head exchangers inside the shell, with the shell-side pressurised, a special test flange and gland is required at the floating head. This enables the tube joints to be inspected from the outer faces of the tubesheets and a typical test flange and gland is shown in Fig. 2.22. The construction of lantern-ring and outside-packed floating-head exchangers is such that a test flange and gland is not required for a shell-side pressure test. Bolt holes in the floating tubesheet of a pull-through exchanger must be plugged temporarily for this type of test. In the case of pull-through floating-head exchangers with no rear-head flanges, including pull-through

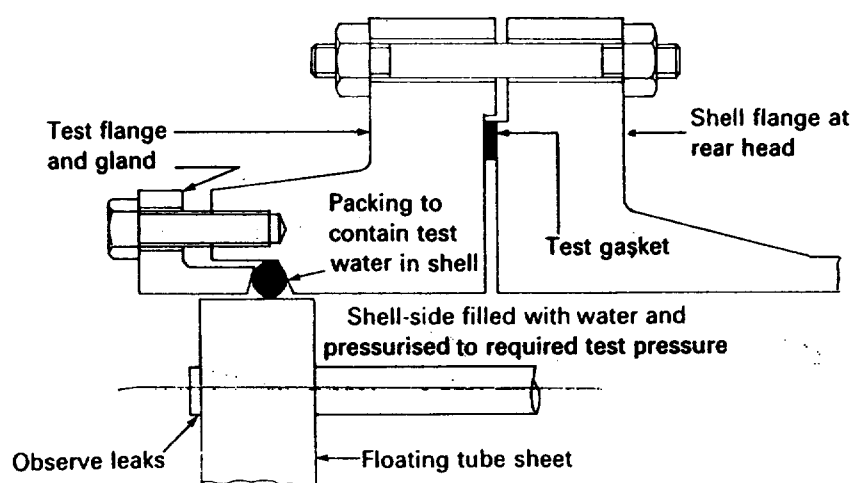
type kettles, the test flange and gland cannot be used. In order to pressurise this type of bundle from the outside, a special test shell is sometimes made, into which the bundle is inserted.

Figure 2.23 shows the testing sequence for a split backing ring floating-head exchanger and Fig. 2.23(a) shows the test flange and gland in position.

When testing a removable bundle inside its shell, with the shell-side pressurised, a joint is required between the shell and stationary tubesheet to contain the shell-side pressure. In addition, access to the outer face of the stationary tubesheet is essential in order to inspect the tube ends. There is no problem in meeting these requirements where the stationary tubesheet is increased in diameter to act as a flange, or if the channel is of the bolted or welded type (A and C). However, a bonnet-type channel (B) cannot be fitted for the test, as there would be no access to the tube ends, and if the tubesheet is not flanged, a temporary backing ring, or test ring, is required on the tube-side of the stationary tubesheet to hold the shell-tubesheet joint.

When testing a removable bundle outside the shell, a joint is required between channel and tubesheet to contain the tube-side pressure. Unless the tubesheet is flanged, or integral with the channel (C-type), a temporary test ring is required on the shell-side of the stationary tubesheet to hold the channel-tubesheet joint. Figure 2.23(b) shows a test ring in position for a bundle test outside the shell.

Figure 2.22 Typical test flange and gland



### 2.18.2 Helium and steam/helium testing

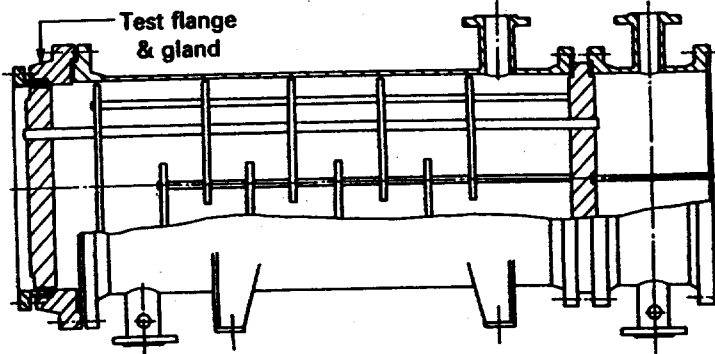
A more costly, but particularly rigorous, method of testing welded tube-tubesheet joints after hydrostatic testing involves the use of helium which is an ideal medium because it has a low relative molecular mass and is safe to use. Leak detection at each joint is achieved by using a mass spectrometer, an instrument which is highly sensitive to extremely minute traces of helium and is capable of detecting a leakage rate of  $10^{-7}$  atm.cm<sup>3</sup>/s.

An even more rigorous test is to heat up the shell-side of the



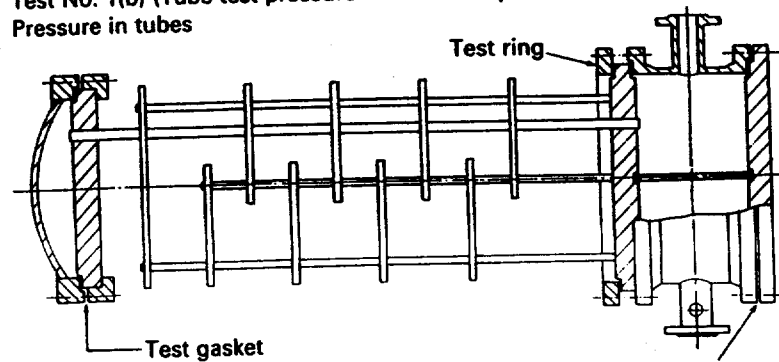
**Figure 2.23** Hydraulic testing of split backing ring floating-head exchanger: tests 1(a), 1(b), 2 and 3

**Test No. 1(a)** (Shell test pressure > Tube test pressure)  
Pressure in shell (test gaskets fitted)



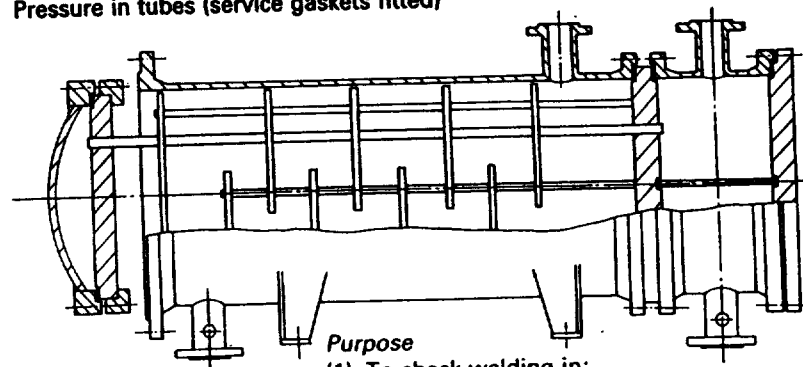
*Purpose*  
To check tube-tubesheet joints and split tubes

**Test No. 1(b)** (Tube test pressure > Shell test pressure)  
Pressure in tubes



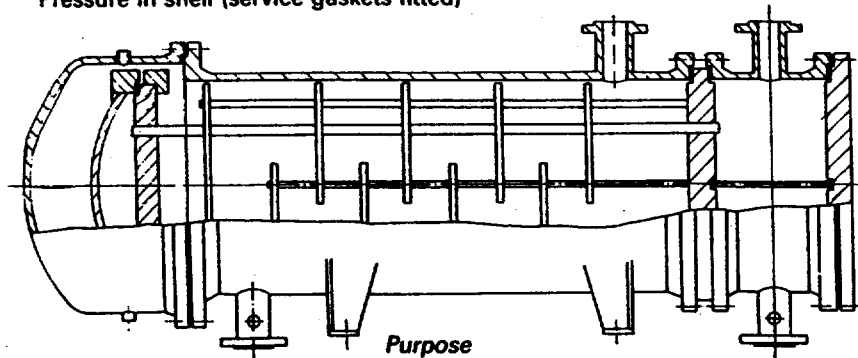
*Purpose*  
To check tube-tubesheet joints and split tubes

**Test No. 2**  
Pressure in tubes (service gaskets fitted)



*Purpose*  
(1) To check welding in:  
floating-head cover  
channel  
(2) To check joints at:  
floating head  
channel-tubesheet  
channel-cover

Test No. 3  
Pressure in shell (service gaskets fitted)



- Purpose**
- (1) To check welding in:
    - shell
    - shell cover
  - (2) To check joints at:
    - shell-shell cover
    - shell-tubesheet

exchanger with steam to about 135 °C, or the design temperature, whichever is the lower value, and allow the exchanger to cool. This cycle is then repeated several times. While the exchanger is still hot, the steam is released and rubber bungs are fitted into all tube ends. Helium at about 3.5 bar gauge is admitted and leak checks carried out using the mass spectrometer. The bungs ensure that only tube-tubesheet joint leaks are detected, and not faulty tubes. The exchanger is then allowed to cool and leak checks repeated at atmospheric temperature. The bungs are removed, one at a time, to check for faulty tubes, each open tube being checked for leaks before removing the bung from the next.

## Acknowledgements

The author is grateful to the following companies for the provision of technical data and illustrations: Haskel Energy Systems Ltd, Sunderland, UK, relating to their hydraulic expansion system. HYDROSWAGE is the registered trade mark of Haskel Inc., Burbank, USA. Hitachi Ltd, Tokyo, Japan, relating to their rubber expander technology, which is covered by UK patents 1594764 and 1598586, US patents 4068372 and 4142581, and West Germany patent 2706400. Hobart Bros (Great Britain Ltd), Letchworth, UK, relating to their CYBER TIG™ automatic tube-end welding system. Hydra-Tight Ltd, Walsall, UK, relating to their hydraulic bolt tensioners. Hydra-Tight is the registered trade mark of Hydra-Tight Ltd. Yorkshire Imperial Alloys, 'YIMPACT' Dept, Leeds, UK, relating to their explosive tube-end welding, plugging and expansion systems. Ormonde Ashton Ltd, Union Works, Ormonde Street, Ashton-under-Lyne, Lancs OL6 8JJ, UK, relating to their tube roller-expanding equipment.

## References

A list of addresses for the service organisations is provided on p. xvi. **American Society of Mechanical Engineers, Section VIII, Division 1, Rules for Construction of Pressure Vessels (1986 edn).** ASME, New York, USA.

- Bergman, D. J.** (1966) 'How to deal with high temperature heat exchanger problems', *Oil & Gas Journal* (3 Oct.), pp. 144-7.
- Briscoe, W. G.** (1976) 'Stud tension reduces heat exchanger joint leakage', *Oil & Gas Journal* (13 Sept.).
- British Standards Institution**, BSS 5500 : 1985, *Specification for Unfired Fusion Welded Pressure Vessels*. BSI, London, UK.
- Harris, D.** (1983) *Heat Exchanger Design Handbook*, Vol. 4, Ch. 4.3. Hemisphere Publishing Corp.
- Morris, M.** (1983) *Heat Exchanger Design Handbook*, Vol. 4, Ch. 4.3. Hemisphere Publishing Corp.
- Oil Companies Materials Association**, (1969) Specification No. TEW 1, *Recommendations for Tube End Welding: Tubular Heat Transfer Equipment*, Part 1-'Ferrous materials'. OCMA, London, UK.
- Ruiz, C.** (1983) *Heat Exchanger Design Handbook*, Vol. 4, Ch. 4.1. Hemisphere Publishing Corp.
- Singh, K. P. and Soler, A. I.** (1984) *Mechanical Design of Heat Exchangers and Pressure Vessel Components*. Arcturus Publishers Inc., Cherry Hill, NJ, USA.
- Tubular Exchanger Manufacturers Association Inc.** (1978) *Standards of Tubular Exchanger Manufacturers Association* (6th edn), and Addenda, 1982. TEMA, New York, USA.

# Air-cooled heat exchangers

### 3.1 Background

The air-cooled heat exchangers described in this chapter are tubular heat transfer equipment in which ambient air, passing over the outside of tubes, acts as the cooling medium to condense and/or cool a fluid inside the tubes. Air-cooled heat exchangers are often referred to as 'air coolers'. This chapter describes the background and construction of air-cooled heat exchangers; thermal design is discussed in Chapter 14.

Air would seem the obvious choice for a coolant, instead of water, in view of the fact that it is around us in unlimited quantities. It has been used by automotive engineers for many years. Unfortunately air is a poor heat transfer medium compared with water, which has a thermal conductivity about 23 times greater at 35 °C. The specific heat of water is four times greater than air, and its density, compared with air at atmospheric temperature and pressure, about 800 times greater. Hence, for given heat load and coolant temperature rise, a greater quantity of air than water would be required, being 4 times by mass and 3200 times by volume.

The concept of air cooling on a large scale in the petroleum industry may be traced back to the late 1920s in the oil and gas fields of the South-Western states in the USA. They consisted of vertically mounted bundles exposed to the wind and were used because little cooling water was available in arid areas. In the mid-1930s, the design changed to horizontally mounted units in which fans were used to pass the coolant air over the bundles, instead of depending on the uncertainty of natural draught cooling. Over a similar period air-cooled exchangers were being developed by the chemical industry in Germany.

The successful performance of the air-cooled units encouraged engineers to consider the use of air as coolant, even when water was not scarce. The first air-cooled refinery was commissioned in 1948 at Corpus Christi, Texas, USA, while the first European air-cooled refinery was commissioned at Whitegate, Eire, in 1958. The first air-cooled refinery in the United Kingdom was not commissioned until 1960 at Milford Haven.

**Table 3.1** Air versus water cooling

Item	Comment
Availability of coolant	Air is always available in unlimited quantities.
Choice of plant location	Choice is unrestricted if air is the coolant, but plant must be adjacent to the source if water is used.
Choice of cooler location	Air coolers cannot be close to large obstructions such as buildings and trees if air recirculation is to be avoided. Shell-and-tube exchanger location is much less restricted.
Space – for cooler only	Air coolers occupy considerably more space, although space underneath may be used for other equipment and storage.
Space – for complete cooling system	If a water-cooled system requires a cooling tower, space requirements are similar. (See ancillary plant required under 'Capital cost'.)
Effect of weather	Air temperature is subject to greater and more rapid fluctuations than water, particularly as a result of sun and showers, making temperature control and performance testing more difficult. Exposed fins may be damaged by hail. In areas subject to low winter air temperatures, careful design is required to prevent freezing of process fluid.
Environmental factors	Noise is a factor which must be considered in air cooler fan design. Air cooling eliminates heating up of lakes, rivers, etc., associated with once-through cooling water systems.
Material of construction	As air is usually non-corrosive, choice of material is governed only by process fluid, whereas both process fluid and cooling water must be considered for water-cooled systems.
Pressure	Mechanical design problems are eased with air coolers as the process fluid is always inside the tubes and there are no large-diameter closures. Wider tube spacing in air coolers results in thinner tubesheets.
Process fluid outlet temperature	Water cooling enables process fluid to be cooled to an outlet temperature 3–6 °C lower than air cooling.
Power failure	Water-cooled systems are shut down completely, whereas natural draught in air coolers provides some cooling capacity.
Contamination	Danger of process fluid contamination is much greater with water-cooled systems. Contamination of cooling water, possibly by toxic process fluid, is always likely in water-cooled systems.
Fouling	Air-side fouling is usually negligible, whereas water-side fouling is frequently a problem.
Cleaning	Air-side cleaning is not usually required, but if necessary air or steam lancing can be carried out during operation. Water-cooled systems may require frequent cleaning on the water side. As the process fluid is always inside the tubes of air coolers, cleaning is easier compared with a shell-and-tube exchanger, where the process fluid is invariably routed through the shell-side. Cleaning the shell-side of shell-and-tube exchangers usually necessitates complete bundle removal.
Maintenance	Maintenance costs for air coolers are considered to be about 25% of those for water-cooled systems.
Capital cost	The capital cost of the air cooler itself may be 2–4 times greater than the corresponding shell-and-tube unit. Air-cooled systems do not require cooling tower, pumps, pump-house, pipes, valves, filters, water treatment plant, etc.

Table 3.1 (cont.)

Item	Comment
Total running cost	The systems must be compared on the basis of depreciation, maintenance and power costs.

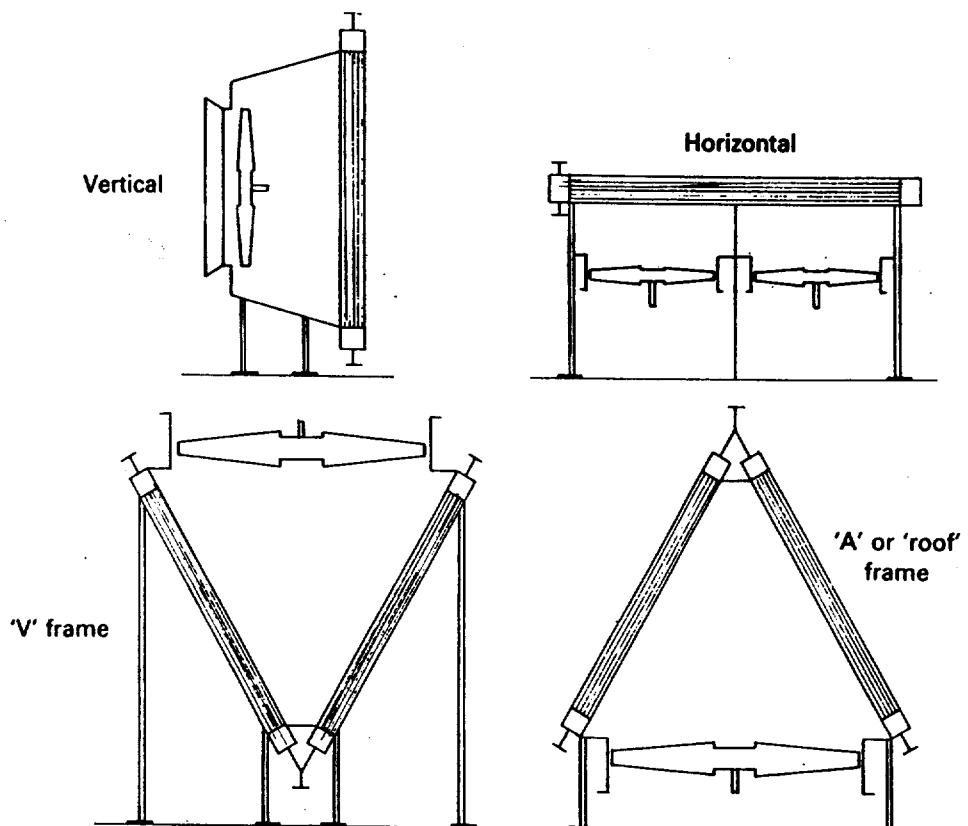
### 3.2 Air versus water cooling

Unless water is unavailable, the choice between air or water as coolant depends on many factors and must be assessed carefully before a decision is made. It may be found that air cooling provides the best solution despite the fact that a plentiful supply of good quality cooling water is available. Table 3.1 lists the factors which have to be considered when assessing air versus water cooling.

### 3.3 Orientation of bundle

Figure 3.1 shows various air-cooled exchanger bundle orientations. The most common orientation of the air-cooled exchanger bundle is in the horizontal plane. A considerable reduction in ground area can be made if the bundle is mounted in the vertical plane, but the performance of the unit is greatly influenced by the direction of the prevailing wind.

Figure 3.1 Air-cooled exchanger bundle orientations



Protective screens are sometimes required to maintain design performance. In general, the use of vertically mounted bundles is confined to small, packaged units. A compromise, which requires about half the ground area of the horizontal unit, is the 'A' or 'V' frame unit. In this type two bundles, sloped at 30–45° from the vertical, are joined by their headers at top or bottom, to form the sloping side of an 'A' or 'V' respectively. The 'A' or 'roof' type is the more common and is used in steam condensing applications.

### 3.4 Forced versus induced draught

Irrespective of the bundle orientation there is a choice between forced- and induced-draught air flow. In forced-draught units the air is drawn through the fan and then forced through the tube bundle. In induced-draught units the air is first sucked through the tube bundle and then the fan.

Table 3.2 lists the advantages and disadvantages of the forced- and induced-draught systems when used with horizontal bundles. Figure 3.2 illustrates the forced- and induced-draught types and their chief components, which are described in section 3.6.

### 3.5 American Petroleum Institute Standard 661

American Petroleum Institute (API) Standard 661 has wide acceptance and is entitled *Air-Cooled Heat Exchangers for General Refinery Service*. The scope states: 'This standard covers the minimum requirements for design, materials, fabrication, inspection, testing and preparation for shipment of refinery process air-cooled heat exchangers.' The standard specifies that the design of pressure parts should be in accordance with Section VIII, Division 1, of the American Society of Mechanical Engineers (ASME) Boiler and Pressure Vessel Code.

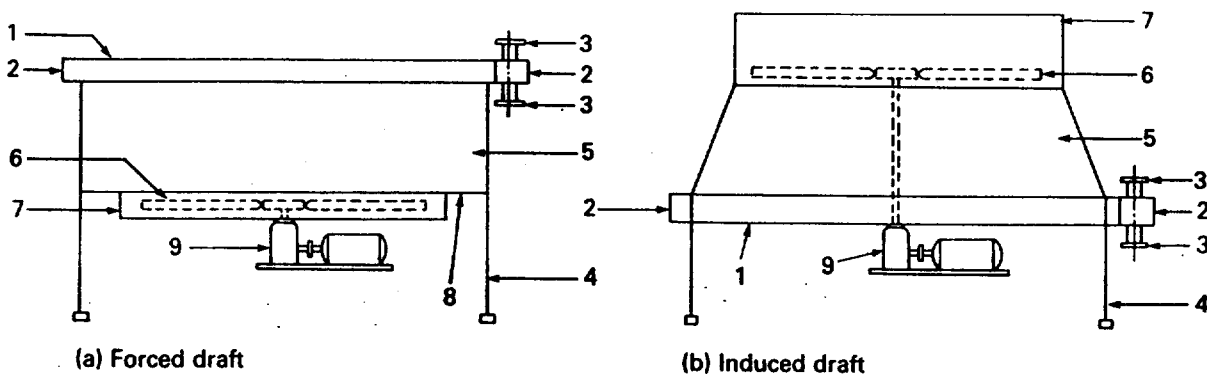
The purpose of API Standard 661 is therefore similar to that of the Tubular Exchanger Manufacturers Association (TEMA), in relation to shell-and-tube heat exchangers. (See section 1.2.)

### 3.6 Construction

An air-cooled heat exchanger comprises three basic parts: the tube bundle, the structure (see Section 3.6.5) and the mechanical drive equipment. The description of the tube bundle has been divided into four parts: bundle size and shape, tubes, headers, and bundle framework. The description of the mechanical drive equipment has been divided into three parts: fan, transmission and drivers.

Table 3.2 Forced versus induced draught

Item	Comment
Position of fan, drive and motor	They are more accessible in the forced-draught type as they may be mounted on ground, or plinth, or suspended from framework. Induced-draught type may require long drive shafts and extra bearings.
Choice of cooler location	The induced-draught type is better for mounting over pipe racks.
Equipment operating temperature	The fan, drive and motor for the forced-draught type operate at a colder temperature than in an induced-draught type.
Exit air circulation	It is less likely with the induced-draught type as air issues vertically from the fan at high velocity so that proximity of buildings and trees have less influence.
Effect of weather	The induced-draught type provides better protection against weather. The performance of the forced-draught type is influenced by rain and sun, making control more difficult, while exposed fins may be damaged by hail.
Environment	The induced-draught type is less noisy.
Air flow rate	The forced-draught type handles colder air resulting in lower volume and power consumption. The induced-draught type provides more uniform air flow.
Air-side heat transfer	The forced-draught type provides higher heat transfer coefficients (for 10 rows and less) due to inlet turbulence.
Power failure	The stack effect of the induced-draught type provides some cooling.



(a) Forced draft

(b) Induced draft

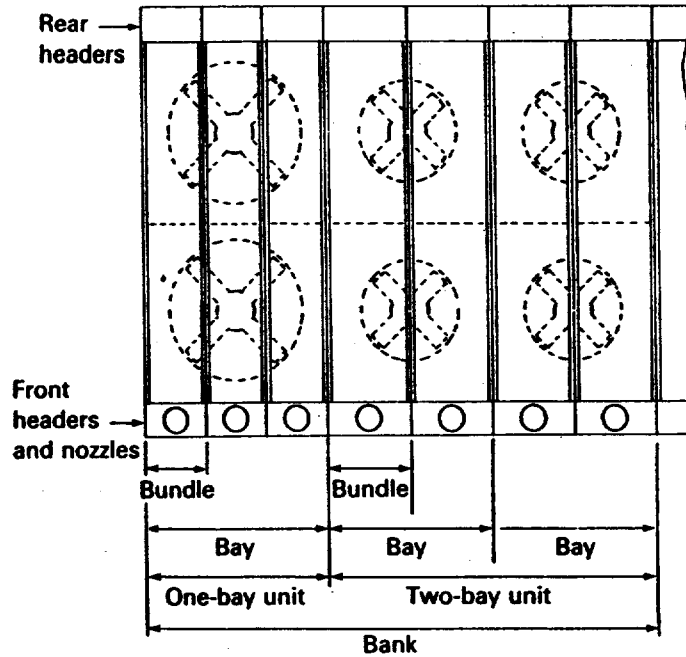
1. Tube bundle (section 3.6.1)
2. Header (section 3.6.3)
3. Nozzle
4. Supporting column
5. Plenum (section 3.6.5)
6. Fan (section 3.6.6)
7. Fan ring (section 3.6.6)
8. Fan deck
9. Drive assembly (section 3.6.7)

Figure 3.2 Forced- and induced-draught air-cooled exchangers and chief components (courtesy of American Petroleum Institute, API 661)

A bay is defined as one or more tube bundles, served by two or more fans, complete with structure, and other attendant equipment. A unit is defined as one or more tube bundles, in one or more bays, for an *individual service*. A bank is defined as one or more bays, including one or more units, arranged in a continuous structure. Figure 3.3 illustrates these definitions.



**Figure 3.3** Definition of bundle, bay, unit and bank



### 3.6.1 Bundle size and shape

Individual tube bundles for air-cooled exchangers are invariably rectangular in plan view, with the longer side corresponding to the tube length and the shorter side corresponding to the header width. It is also of shallow rectangular section in end view, the shorter side corresponding to the header depth, which is related to the number of tube rows in the direction of air flow. The tube bundle accounts for roughly 70% of the total cost of a typical installation and comprises tubes, front and rear headers, side walls and tube support.

Compared with shell-and-tube exchangers, tube bundles for air-cooled heat exchangers can be standardised to a much greater extent. Each manufacturer has his own range of standards, but typical tube lengths range from 1.2 to 15 m (4 to 50 ft), in increments of 0.6 m, (2 ft) up to 4.9 m (16 ft) and 1.2 m (4 ft) thereafter. Typical bundle widths range from 1.2 to 6 m (4 to 20 ft), although widths greater than about 3.7 m (12 ft) are site-built. Bundle depths correspond to 3–8 tube rows giving a nominal bundle depth of 150–457 mm (6–18 in). Greater bundle depths are achieved by stacking two or more bundles on top of each other.

### 3.6.2 Tubes

Because air is a poor heat transfer medium the tubes are invariably finned to increase the external rate of heat transfer. However, when the heat transfer coefficient of the fluid inside the tubes is low, and of similar magnitude to the un-finned air-side heat transfer coefficient, the effectiveness of the finning is greatly reduced. (Fin-efficiency is described in section 9.1.) The use of plain tubes then merits investigation.

### Fin material and geometry

Aluminium is the preferred fin material because it provides high thermal conductivity, low weight and formability. (Of the metals, only silver and copper have greater thermal conductivities.) As the base tube is usually carbon or low-alloy steel, galvanic corrosion might be expected at the fin/tube junction. However, experience has shown that corrosion in service is not as serious as expected, probably because the fin tubes operate under warm, dry conditions.

Typical fin geometry is as follows:

base tube o.d.	= 19.05–50.8 mm (0.75–2 in)
fin thickness	= 0.3–0.5 mm (0.012–0.02 in)
fin height	= 6.35–19.05 mm (0.25–0.75 in)
no. of fins	= 276–433 per m (7–11 per in)

$$\text{approx. surface ratio} \left\{ \frac{\text{total external surface/unit length}}{\text{bare external surface/unit length}} \right\} = 17\text{--}24.$$

One of the most common aluminium-finned tubes used in air coolers has a base tube outside diameter of 25.4 mm (1 in), a fin thickness of 0.4 mm (0.016 in), a fin height of 15.875 mm (0.625 in), a fin outside diameter of 57.15 mm (2.25 in), such that with 433 fins per metre (11 per inch), the surface area ratio is 23.3.

### Fin-tube attachment

The method of attaching the fin to the tube is of vital importance, as any loosening of the bond between them may create an additional resistance to heat flow (bond resistance). If the fin and tube have different thermal coefficients of expansion, the bond may loosen due to a differential movement between them. The loosening effect will increase as the bond temperature increases and consideration must be given to the bond temperature which will be attained should the fan fail. The bond may loosen due to the weakening effect of thermal and pressure cycling and also because of corrosion at the fin-base tube junction. Operating temperature limits for the various fin-tube attachments are given in Table 3.3.

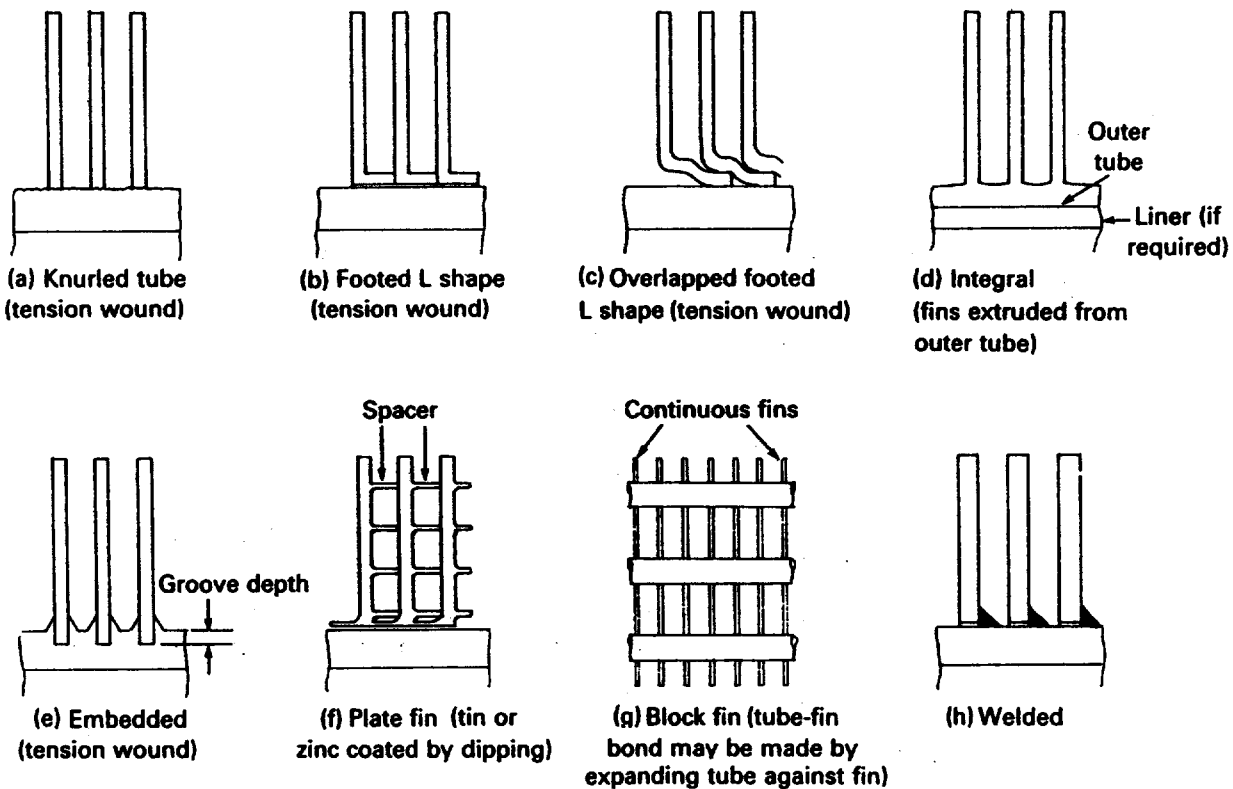
**Table 3.3** Approximate temperature limits for finned tubes

Fin-tube attachment	Fig. no.	Upper temp limit (°C)
Knurled tube	3.3(a)	100
L foot	3.3(b)	150
Integral	3.3(d)	250
Embedded	3.3(e)	350
Plate fin	3.3(f)	See note (1)
Welded	3.3(h)	See note (2)

*Notes:*

(1) Limited by melting point of dipping medium.

(2) Limited only by metallurgical factors at high temperatures.



**Figure 3.4** Types of finned tubing (transverse high fins)

The various fin-tube attachments are illustrated in Fig. 3.4 and described below:

*Knurled base tube (Fig. 3.4(a))*

The aluminium fin is wound mechanically under tension on to the base tube, the surface being knurled to increase fin-tube contact. This simple construction is only used for modest temperatures and has the disadvantage that the base-tube metal, and not aluminium, is exposed to the atmosphere throughout.

*Footed L shape (Fig. 3.4(b))*

The L-shaped aluminium fin is wound mechanically under tension on to the base tube. The short horizontal limb of each L is in contact with the base-tube surface to cover it completely. This construction provides greatly improved fin-tube contact over the knurled base tube. It has been demonstrated by tests that a greatly superior fin-tube contact is achieved by knurling the outside of the base tube and foot of the L-shaped fin. In both designs the whole of the exposed external surface is aluminium.

*Overlapped footed L shape (Fig. 3.4(c))*

This is similar to the footed L shape except that the base of every fin is partially overlapped by the adjacent fin, thus providing greater protection of the base tube from the atmosphere.

*Integral (Fig. 3.4(d))*

The aluminium fins are extruded from an aluminium outer tube, but in air-cooled heat exchangers a different metal is required for the tubeside

fluid. During the finning process a tight mechanical bond is made between the finned aluminium outer tube and an inner base tube of the required metal, which is usually steel. The exposed external surface is aluminium and there are no minute gaps between adjacent fins where moisture can penetrate. As the outer tube and fins are integral with one another there can be no fin-tube bond resistance. However, depending on the temperature, lack of contact between outer and inner tubes can occur to create an additional resistance to heat transfer.

*Embedded (Fig. 3.4(e))*

A helical groove 0.2–0.3 mm (0.008–0.012 in) is ploughed into the outside of the base-tube wall such that metal is only displaced, not removed. The aluminium fin is wound mechanically into the groove under tension, after which the displaced metal is rolled back on each side of the fin to hold it in place. The effective thickness of the base-tube wall is the thickness beneath the groove. This type provides excellent contact, both thermal and mechanical, between fin and groove. Although the base-tube metal is exposed to the atmosphere, tests under severe conditions showed that corrosion over a long period is required before any bond weakness occurs.

*Plate fin (Fig. 3.4(f))*

A finned tube comprising a base tube, elliptical instead of circular in cross-section, having rectangular fins was developed in Germany. Each fin is punched out from sheet and slid on to an elliptical base tube, the correct fin spacing being achieved by protruding tabs of metal. Each fin is provided with a collar in contact with the base tube to increase the surface available for the bond at the point of maximum heat flux. When all fins are in position on the tube, the complete tube is dipped into a bath of molten zinc or tin. This provides a zinc or tin covering for all fin and tube surfaces and a fused metallic bond between fin and tube.

This type of construction allows considerable flexibility in the shape and size of the fins and also the base-tube cross-section.

*Block fin (Fig. 3.4(g))*

Another type of plate fin is the block or radiator-type construction. Instead of being attached to a single tube, each fin extends over a nest of tubes. The circular or elliptical cross-section base tubes of the nest are pushed into the holes in the fins, after which the bond is achieved either by a dipping process, or by expansion. In the latter method each tube is expanded against the fins by drawing a tightly fitting, bullet shaped, bar of metal through it.

*Welded fin (Fig. 3.4(h))*

The fin is welded to the base tube to provide a bond with negligible resistance. These tubes are used at temperatures of the order of 400 °C and above, where the tubes described earlier cannot be used. The fins are usually of a ferrous material having a thermal conductivity about one-fifth of that of aluminium. To increase the fin efficiency (see section 9.1), and to permit sound welding, thicker fins are usually required.

**Base-tube diameter and support**

Although the base-tube diameter range is 19.05–50.8 mm (0.75–2 in), the most common diameter is 25.4 mm (1 in). The base-tube metal, which in many cases is carbon or low-alloy steel, is selected to suit the process fluid. Common practice is to have a minimum tube wall thickness as follows:

	<i>mm</i>	<i>in</i>	<i>b.w.g</i>
Carbon and low-alloy steel	2.74	0.109	12
Austenitic and ferritic steel	1.65	0.065	16
Copper, aluminium	2.11	0.083	14
Titanium	1.24	0.049	18

Except for high-pressure applications, where U-tubes are used, the tubes are straight. They are normally arranged on a triangular pitch, usually equilateral, although isosceles is sometimes adopted. The usual pitch for the most common finned tube referred to above is 60.3 mm (2.375 in), and the gap between fins in adjacent rows is about 3.2 mm (0.125 in). They may be minimum or average wall (see section 1.5.2).

As in a shell-and-tube heat exchanger, the tubes must be supported at intervals along their length to prevent sagging. It is usual to position supports across the bundle at the bottom at intervals such that the unsupported tube length does not exceed 1.8 m (6 ft). In addition, intermeshing of the fins of adjacent tubes must be prevented and suitable devices to prevent this are provided at each bundle support. One method is to wrap an aluminium band, 12.7–19.05 mm (0.5–0.75 in) wide, around each tube, so that the fins are kept apart by two band thicknesses. This simple method has the disadvantage that the weight of the tubes is carried by the fins. One improved method is to cast a zinc alloy ring on to the tube, to encompass both tube and fin, such that the rings of adjacent tubes rest on one another and transmit the load instead of the fins. These rings have a diameter equal to the tube pitch and a width of 12.7–19.05 mm (0.5–0.75 in). Another method, similar in principle to the cast ring, is to encompass both tube and fin by a hollow square box, made in two halves. The length of the sides of the box would be equal to the tube pitch and its depth about 19.05–25.4 mm (0.75–1 in).

**Tube-tubesheet attachment**

Tubes are attached to the tubesheet by expansion or welding, as described in Chapter 2 for shell-and-tube exchangers.

**3.6.3 Headers**

Most applications involve straight tubes attached to front and rear box-shaped headers. The front header is akin to the stationary end of a shell-and-tube exchanger to which the inlet nozzles, and outlet nozzles if there are two or more even number of passes, are attached. The rear header is akin to the floating head of a shell-and-tube exchanger and nozzles will only be attached to it if there are one or more odd number of passes. Similar to a shell-and-tube exchanger, pass partition plates, welded-in, divide the headers into passes.

The wide tube pitch, and ligament between adjacent tubes, used in air-cooled heat exchanger design provides thinner tubesheets than those in shell-and-tube exchangers. In an air-cooled heat exchanger using 25.4 mm (1 in) diameter base tubes, for example, the gap between adjacent tubes is about 35 mm (1.375 in), compared with 6.35 mm (0.25 in) in a shell-and-tube exchanger. Minimum thicknesses of ferrous parts are usually 19.05 mm (0.75 in) for tubesheets and plug sheets, 25 mm (1 in) for cover plates and 13 mm (0.5 in) for other plates.

All box-type headers comprise tubesheet, top and bottom plates to which the nozzles are attached, and end plates. As in a shell-and-tube exchanger, pass partition plates are installed if there are two or more tube-side passes. The four sides of the box may be constructed from four plates, or two U-shapes, welded together. Opposite the tubesheet is a removable cover, removable bonnet or a plug sheet, the functions of which are described below and illustrated in Fig. 3.5.

#### **Removable cover plate header**

This is similar to an N-type stationary head, or channel, of a shell-and-tube exchanger, shown in Figs. 1.2 and 1.18(c), in which the header is welded to the tubesheet at one end and flanged and bolted to a flat cover at the other end. Removal of the flat cover provides access to the exposed tube ends for cleaning and repair, without breaking the nozzle/external pipe joints. This type of construction is used if cleaning is expected to be frequent, but flanged rectangular shaped openings are prone to leakage at the corners.

#### **Removable bonnet header**

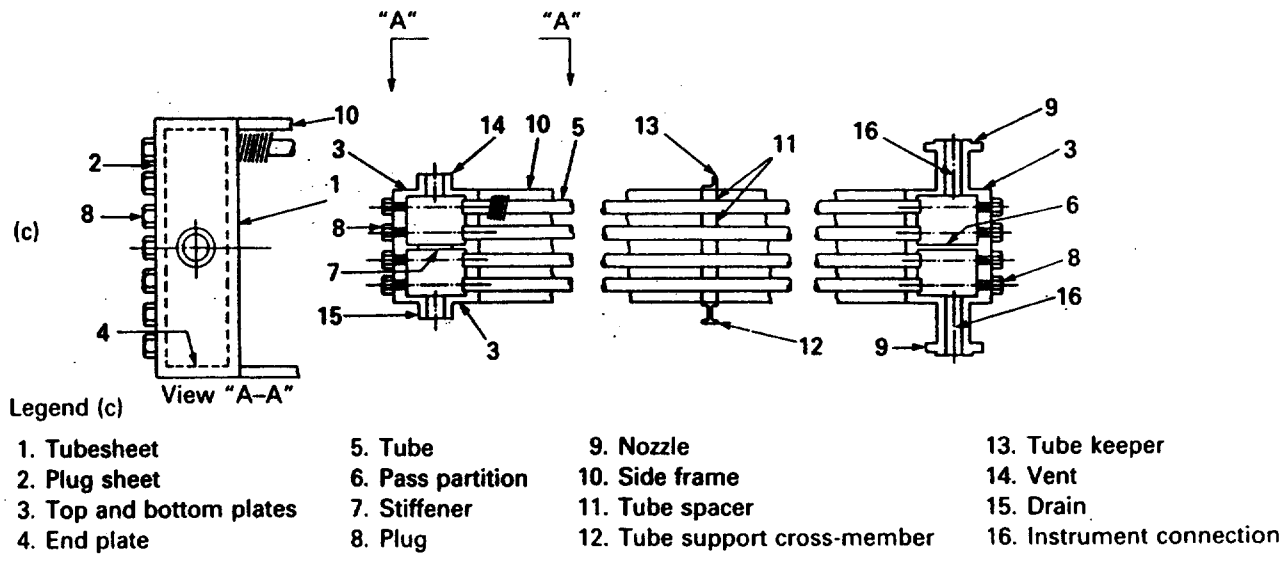
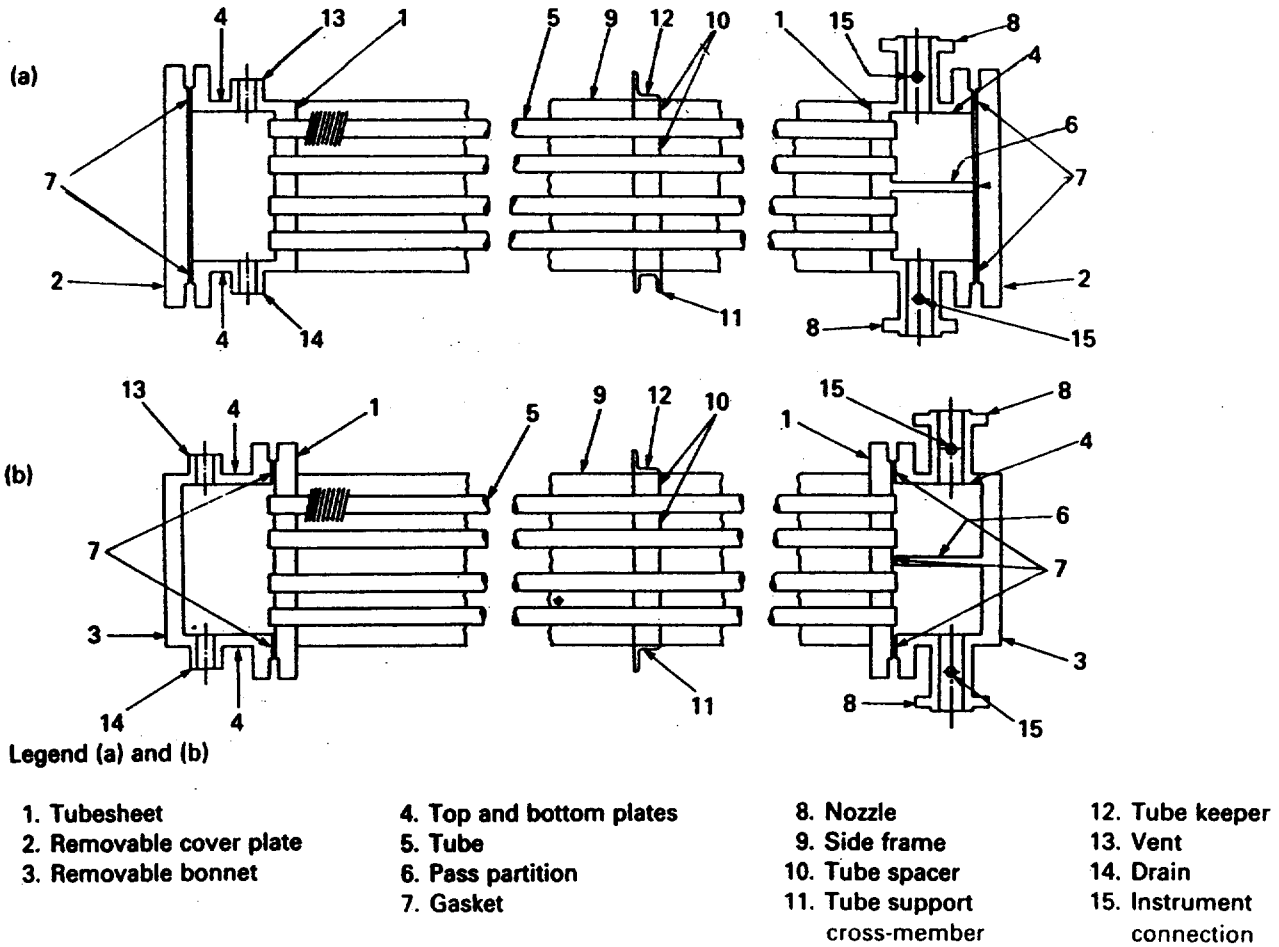
This is similar to a B-type stationary head, or channel, of a shell-and-tube exchanger, shown in Figs. 1.2 and 1.18(d), in which the complete bonnet header is bolted to the tubesheet. Removal of the complete bonnet provides access to the exposed tube ends for cleaning and repair, but nozzle/external pipe joints must be broken first. Although cheaper than the removable cover plate header, the flange is similarly prone to leakage at the corners.

#### **Plug header**

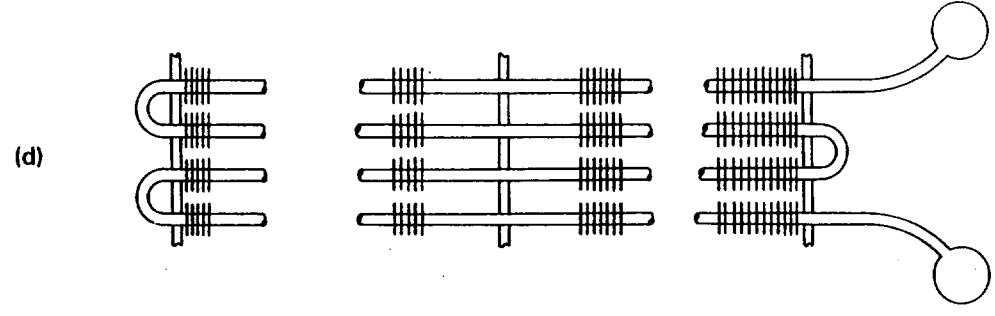
The side opposite the tubesheet is fitted with screwed shoulder plugs which coincide with each tube end. The diameter of the plug hole is about 0.8 mm (0.031 in) greater than the tube outside diameter and all operations involving the tube ends, such as cleaning and tube-tubesheet attachment, must be carried out through the plug hole. The plugs have hexagonal heads and the seal between plug shoulder and plug sheet achieved by a solid metal, or metal-jacketed, gasket. Despite the fact that the tube ends cannot be exposed, the plug header is the most common and used for pressures up to at least 300 bar.

#### **Manifold header**

At high pressures, where the plug header is unsuitable, manifold headers are used, in which the base tubes are welded into cylindrical headers at the inlet and outlet. Welded-on U-bends are used to connect one pass



**Figure 3.5** Typical headers (a) removable cover (b) removable bonnet (c) plug (d) manifold (courtesy of American Petroleum Institute, API 661)



with the next. Such headers have been used for pressures up to 700 bar. Cleaning can be achieved only by chemical means.

#### 3.6.4 Bundle framework

The bundle has stout longitudinal side plates, or channels, one on each side, to contain the tubes. In addition they give the complete bundle sufficient rigidity to enable it to be lifted and transported without damage. Bolted to the top of the side frames, at the same intervals as the bottom tube supports, are cross-members termed tube keepers, whose function is to hold down the tubes within the bundle. As the finned tube bundle is similar to a floating-head or U-tube bundle of a shell-and-tube exchanger, the tubes must be free to expand independently of the framework and supporting structure. To achieve this the front header is 'fixed' and the rear header allowed to 'float'. Should large temperature differences between passes arise the full header must be split into two or more separate headers to prevent loosening of the tube-tubesheet attachment.

In order to prevent the air from by-passing the bundle, leading to a loss in performance, gaps are sealed off with thin metal strips. API 661 considers any gap greater than 10 mm (0.375 in) to be excessive.

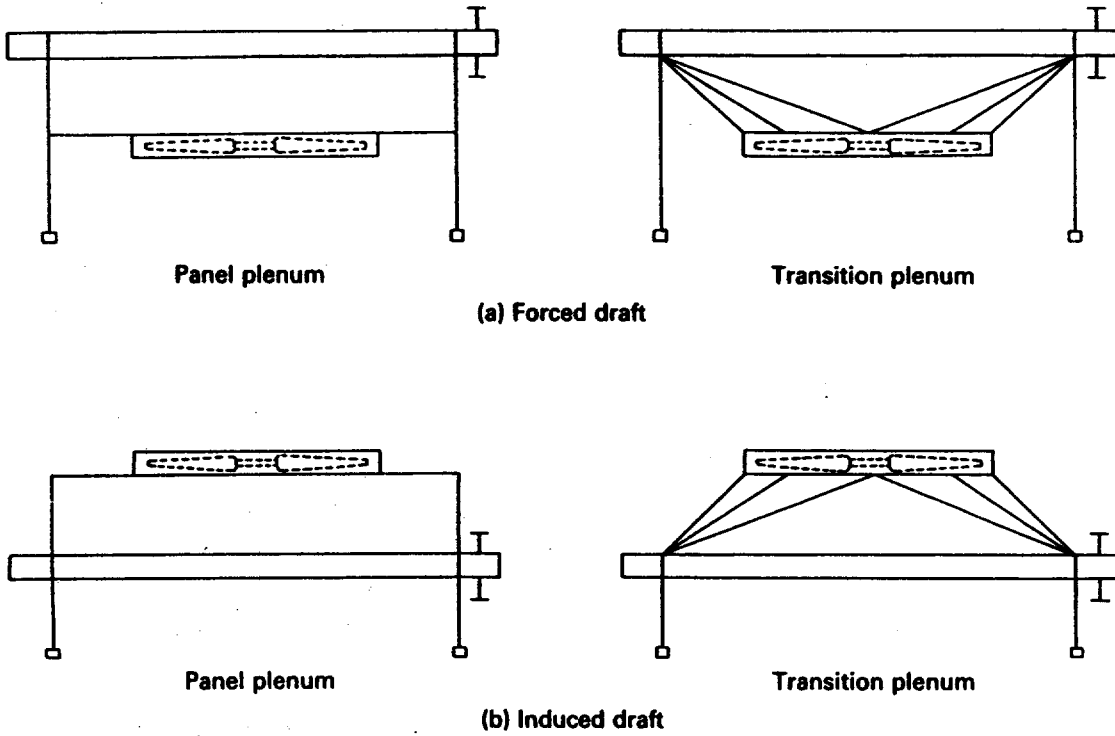
#### 3.6.5 Structure

The structure usually represents about 15% of the total and comprises platform, ladder, fan ring and plenum chamber which ducts the air into the fans (see Fig. 3.2). The weight of these components, plus the finned tube bundle, is taken by supporting columns. If the fans, transmission or drivers are suspended from the structure, the design of the columns must allow for this.

The plenum chamber is constructed of steel sheet with minimum thicknesses of 2 mm (0.075 in) if flat, or 1.6 mm (0.06 in) if ribbed. As shown in Fig. 3.6, panel plenums are box-shaped, which provides a sharp change of section between the plenum entry or exit and the fan ring. As the name implies, transition plenums shown in Fig. 3.6 provide a gradual instead of a sharp change in cross-section between entry or exit and the fan ring.

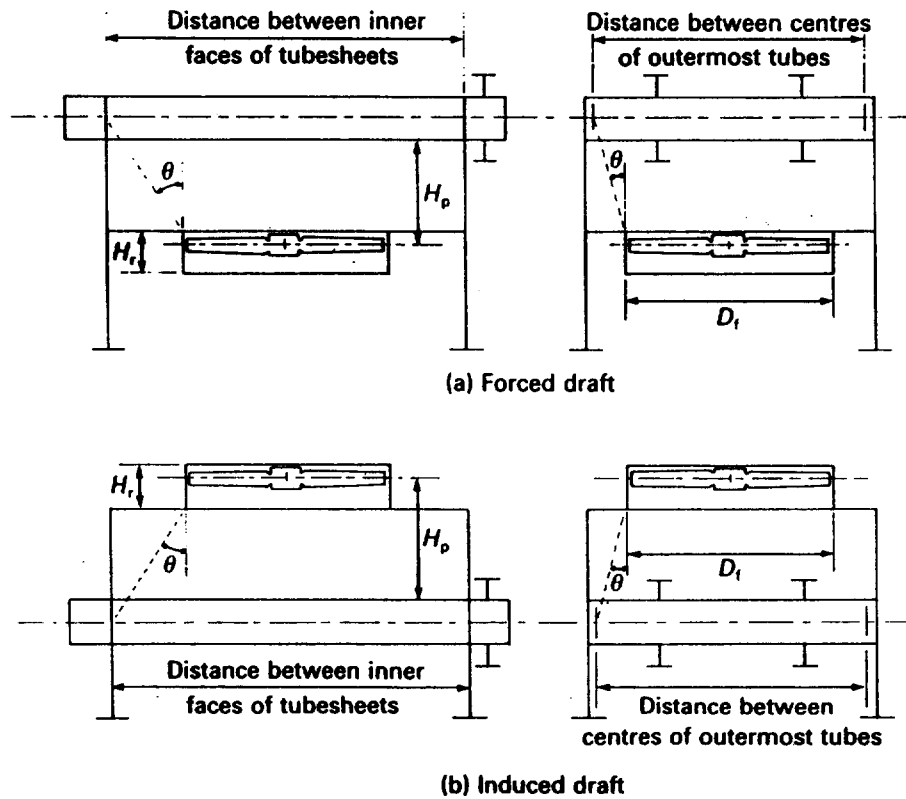
Although simple in appearance, the design of plenum chambers has been the subject of considerable research. The objective has been to produce a uniform air flow across the bundle to achieve maximum fan efficiency and pressure recovery at minimum fan power requirements. Although there are no standard proportions, typical plenum proportions are given below, where  $A_b$  = bundle exposed cross-sectional area normal to air flow (i.e. face area),  $A_f$  = fan ring cross-sectional area,  $D_f$  = nominal fan diameter,  $H_p$  = distance between the plane of the fan and the bundle,  $H_r$  = fan ring height, and  $\theta$  = maximum air dispersion angle (from API 661), defined in Fig. 3.7.





**Figure 3.6** Typical plenum arrangements (courtesy of American Petroleum Institute, API 661)

**Figure 3.7** Plenum dimensions



	<i>Forced draught</i>	<i>Induced draught</i>
$A_f/A_b$ (min)	0.4	0.3
$H_p/D_f$ (min)	0.5	0.3
$H_f/D_f$ (min)	0.16	0.16
$\theta$ (max)	45°	45°

As expected, better performance is achieved if the air discharges into a plenum of square, rather than rectangular, cross-section. A further improvement is obtained if the plenum corners are rounded off by curved plates.

### 3.6.6 Fans

The mechanical drive equipment covering fans, transmission and drivers accounts for about 15% of the total cost of a typical installation.

Axial flow fans are used, and except for small units employing one fan, there will be at least two fans serving each bay such that if one fan fails the remaining fan(s) still provide some cooling capacity. The most common fan-blade material is aluminium which may be in the form of sheet, casting or extrusion. Other materials include fibreglass reinforced plastic, steel, stainless steel and monel. Fan diameters range from 1 to 5 m (3 to 16 ft) and are fitted with 4–10 blades with 4 and 6 blades being the most common. Direct motor drive is used for fans up to about 1.5 m (5 ft) in diameter.

The optimum air-side pressure loss for typical air-cooled heat exchangers is the range 6–16 mm water gauge (0.245–0.63 in w.g.) and fans are designed to suit this. Because of noise API 661 limits the fan-blade tip speed to 61 m/s (12 000 ft/min) for indirect-driven fans and 81 m/s (16 000 ft/min) for direct-driven fans. However, to meet more stringent environmental conditions, some fan-blade tip speeds have been limited to about 50 m/s (9843 ft/min). (See section 14.11.4.) The clearance between fan ring and blade tip has considerable influence on fan efficiency. API 661 specifies that this radial clearance must not exceed 0.5% of the fan diameter or 19 mm (0.75 in), whichever is the smaller, but must not be less than 9 mm (0.375 in).

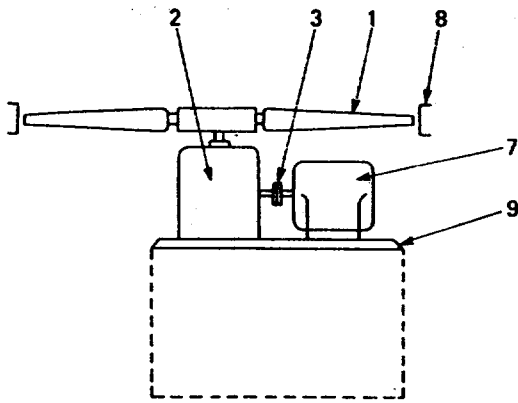
Except for direct-driven fans, individual fan blades are designed to permit manual adjustment for varying the blade pitch. In many cases control of the unit is achieved by the use of automatic variable-pitch blades.

Each fan must be separated from its neighbour by a division plate.

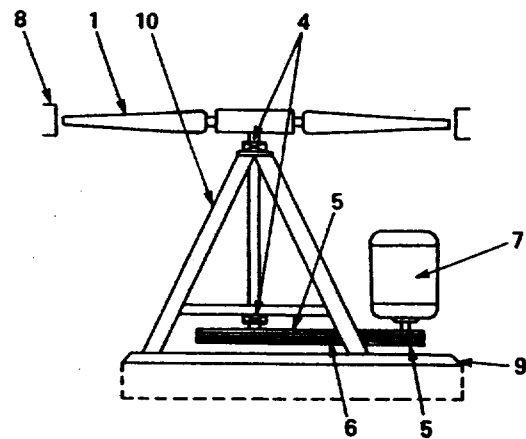
### 3.6.7 Transmission

The transmission relates to the means of transmitting power from the driver to the fan and Fig. 3.8 shows typical arrangements.

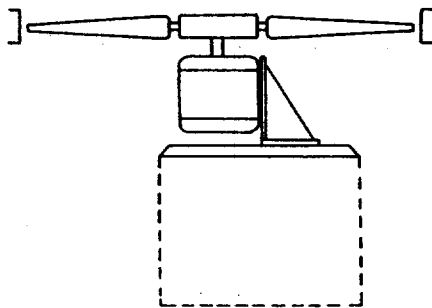
The most common form of transmission is the V-belt drive which is used up to 22 kW (30 h.p.) drive rating. V-belts have a low initial cost, a good operational record if properly installed and maintained, and in some refineries their use is permitted up to 30 kW (40 h.p.). However, API 661



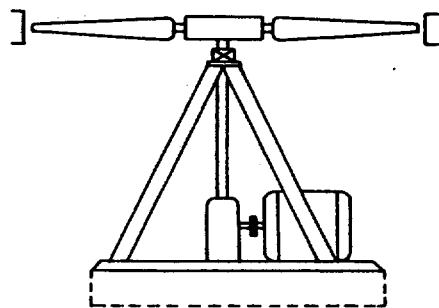
(a) Direct right-angle gear drive



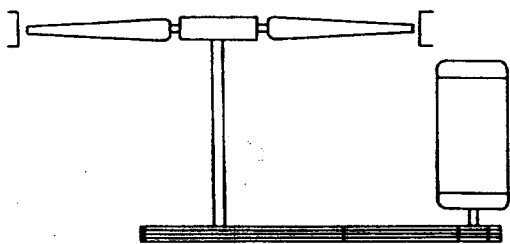
(b) V-belt drive



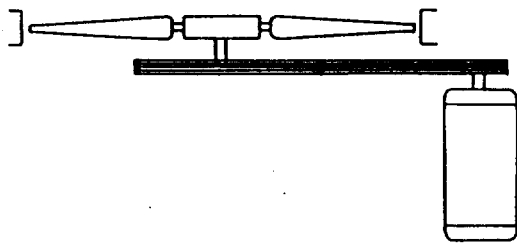
(c) Direct motor drive



(d) Right-angle gear drive with fan support



(e) Suspended V-belt drive, motor shaft down



(f) Suspended V-belt drive, motor shaft up

Legend

1. Fan

2. Gear

3. Coupling

4. Bearing

5. Sheave

6. V-belts

7. Motor

8. Fan ring

9. Base plate

10. Fan support

Figure 3.8 Typical drive arrangements (courtesy of American Petroleum Institute, API 661)

specifies that right-angle gear drives must be used for electric motor rates at 22 kW (30 h.p.) and above, and all steam turbine drives.

3.6.8 Drivers

Over 90% of the drivers are electric motors, but steam turbines, hydraulic motors, gasoline engines, etc., have been used. Another non-electrical form of driver may be useful as standby in the event of

power failure. If the fan blades are not of the automatic variable-pitch type, the motor rating needs careful assessment. In winter, for instance, the low air temperature and corresponding air density increase means that increased power is required because the fan supplies a constant volume. The increase in power may be of the order of 25%.

### 3.7 Temperature control

Several methods are used to control the performance of air-cooled heat exchangers to meet variations in weather and process requirements. Air-cooled heat exchangers operating in extremely cold climates require particular attention. Each case must be considered on its merits to decide on the best method of control. Rubin (1982) and Monroe (1983) state the case for variable pitch fan blades to achieve significant fan power reduction.

#### 3.7.1 By-pass

Control devices are installed which enable part of the process fluid to by-pass the unit. This method has the advantages of low initial cost and close, continuous, control but does not reduce fan power consumption.

#### 3.7.2 Louvres

Instead of diverting some of the process fluid, a system of louvres is fitted above the bundle to reduce the air flow. The positioning of the louvre blades to suit the prevailing operating conditions can be achieved by manual or automatic means. Manual movement has the advantage of low cost and simplicity, but close, continuous, control is achieved with automatic movement. Neither method reduces fan power consumption.

#### 3.7.3 Motor control

In a large unit containing many fans, control is achieved by switching off some of the fans. At no additional capital cost, fan power reduction is achieved, but the control is of a coarse, stepwise nature.

As alternatives, two-speed or variable-speed motors may be used. The latter provides close, continuous, control with fan power reduction.

Motor control is usually restricted to fans having a fixed blade pitch.

#### 3.7.4 Variable-pitch fans

The pitch of each fan blade may be altered manually to suit the prevailing operating conditions, which will reduce fan power consumption. Although fan design permits the alteration of fan-blade pitch to be carried out

rapidly, the control is of a coarse, stepwise nature.

Automatic variable-pitch blades provide close, continuous, control but at greater capital cost.

### 3.7.5 Control for low air temperature

In extremely cold environments, overcooling of the process fluid may cause it to freeze. This may lead to tube rupture, which in turn may necessitate an expensive shutdown for repair. Air-cooled heat exchangers have operated at temperatures of  $-50\text{ }^{\circ}\text{C}$  and several methods are used to prevent overcooling of the process stream.

#### Steam coils

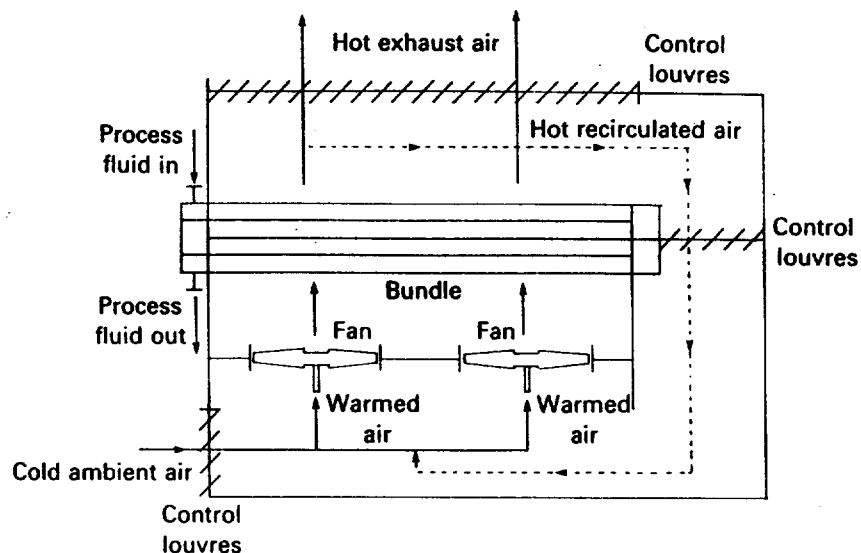
These may be mounted at the cooler base to warm up the inlet air, but must be a separate unit and not part of the process tube bundle. Steam coils are usually employed at start-up to reduce the viscosity of highly viscous fluids.

#### Air recirculation

In this method, which is used with forced-draft units, some of the hot exhaust air is ducted back to warm up the incoming cold air. The principle of this method is shown in Fig. 3.9.

As an alternative, one fan in a bay is arranged to supply air in the opposite direction to the remainder. It draws in hot exhaust air to mix with the inlet cold air.

Figure 3.9 Air recirculation system



#### Cocurrent flow

This method, applicable to multi-pass units, involves the rearrangement of the air flow, or process fluid flow, so that the system is in cocurrent, instead of countercurrent, flow (see section 7.1). By this method the cold inlet air contacts the hot inlet process fluid.

## Acknowledgements

The author is grateful to the following: APV Spiro-Gills Ltd, Pulborough, West Sussex, UK, for the provision of technical data relating to their air-cooled exchangers. American Petroleum Institute, Washington, USA, for permission to publish Figs. 3.2, 3.5, 3.6 and 3.8 and related notes, from API Standard 661, *Air-Cooled Heat Exchangers for General Refinery Service* (2nd edn), Jan. 1978.

## References

A list of addresses for the service organisations is provided on p. xvi.

**American Society of Mechanical Engineers**, Section VIII, Division 1, *Rules for Construction of Pressure Vessels* (6 edn.) 1983. ASME, New York, USA.

**Monroe, R. C.** (1983) 'Energy-saving fans', *Chemical Engineering Progress* (Dec.) pp. 28-32.

**Rubin, F. L.** (1982) 'Power requirements are lower for air-cooled heat exchangers with variable-pitch fan blades', *Oil & Gas Journal* (11 Oct.), pp. 165-7.

**Tubular Exchanger Manufacturers Association Inc** (1978), *Standards of Tubular Exchanger Manufacturers Association* (6th edn), TEMA, New York, USA.

# Gasketed-plate heat exchangers

## 4.1 Background

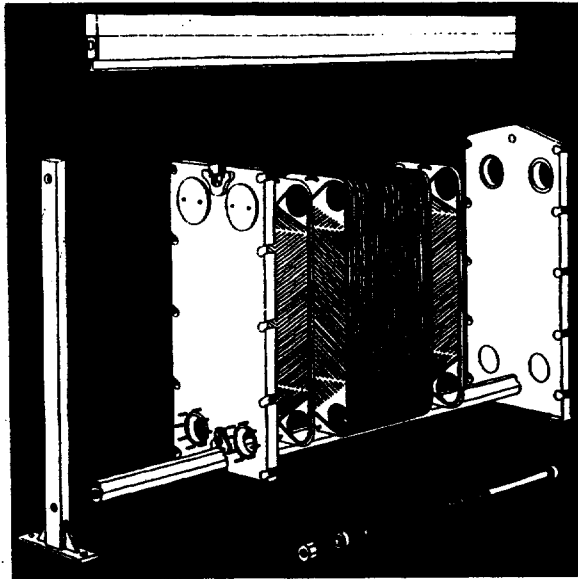
The basic plate consists of a thin, rectangular, metal sheet into which a corrugated pattern has been formed by precision-pressing. One side of each plate has a full peripheral gasket. The complete unit comprises a number of such plates, mounted in a frame, and clamped together, face to face, by a bolting system. The space between adjacent plates forms a flow channel and the system is arranged so that the hot and cold fluids flow through alternate flow channels, parallel to the long side. Openings (ports) in the four corners of each plate direct the two fluids into their flow channels.

Figure (4.1) shows an exploded view of a typical unit and Fig. 4.2 shows the general flow pattern.

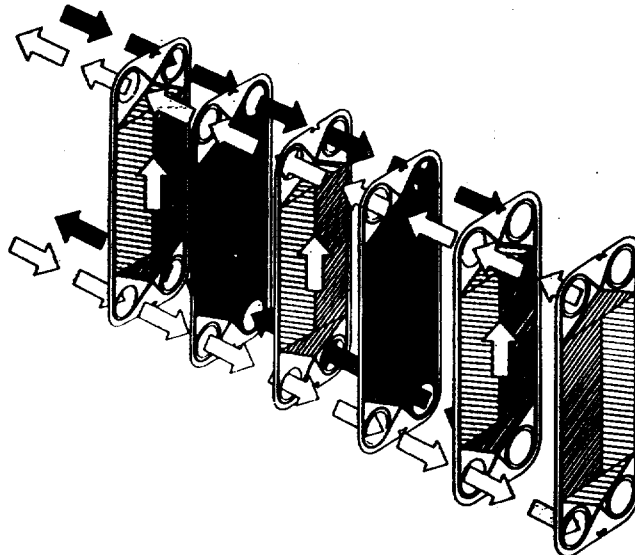
It is surprising to learn from Clark (1974) that patents exist from the late 1870s, and that a German patent was published in 1890 relating to 'improvements in plate heat exchangers'. The concept was not fully exploited until Dr Richard Seligman, the founder of APV, introduced the first commercially successful design in 1923. The original plates were cast gunmetal, but in the early 1930s plates pressed from thin stainless steel sheet were produced. The operating conditions of the early gasketed-plate heat exchangers were limited by the plate seals to a pressure of about 2 bar and a temperature of about 60 °C.

Although the basic design remains almost unchanged, continual developments over the past sixty years have increased the operating pressures and temperatures to 30 bar and 180 °C, respectively, together with larger plate and unit sizes, in a variety of metals. (Compressed asbestos fibre gaskets can operate up to 260 °C – refer to section 4.2.3 for limitations.) In its early days, the gasketed-plate heat exchanger was used in food and drink processing and, in particular, the hygienic requirements of the dairy industry. Although retaining its use in the foodstuff industries, there has been increasing recognition of the unique features of the gasketed-plate heat exchanger and today it is used in a wide range of industrial applications. In many cases it has replaced the shell-and-tube exchanger, which will always be faced with intense competition from the gasketed-plate heat exchanger for services within the latter's operational limits.

**Figure 4.1** Exploded view of a typical gasketed-plate heat exchanger



**Figure 4.2** Flow pattern in a gasketed-plate heat exchanger



## 4.2 Construction

### 4.2.1 Plate metals and sizes

Any metal which is sufficiently ductile to be formed into a pressing may be used in a gasketed-plate heat exchanger but the most common metals are listed in Table 4.1. Stainless steel (type 316) is the most widely used metal, but other plate metals available as standard are titanium, titanium-palladium alloy, Incoloy 825<sup>TM</sup> and Hastelloy C-276<sup>TM</sup>. Chapter 19 shows that heat transfer coefficients in gasketed-plate heat exchangers may be extremely high and therefore the resistance of the plate may be significant. Unfortunately some of the more exotic alloys have low thermal conductivities, as shown by Table 4.1.

A notable absentee is carbon steel, which is rarely used because thin plates are required for pressing, which would have little corrosion resistance.



**Table 4.1** Approx. thermal conductivity for various plate materials at 100 °C (W/m K)

Copper	389	Monel 400™	26
Aluminium	208	Titanium	20
Aluminium brass	100	Stainless steel (316)	17
Nickel 200	66	Inconel 600™	16
90/10 cupro-nickel	52	Incoloy 825™	12
70/30 cupro-nickel	35	Hastelloy C-276™	11

The corrugations in an individual plate are precision-pressed in the cold state in a single operation. Cut-outs for ports, guide bars, etc., are normally made in separate operations following pressing. The largest single plate is of the order of 4.3 m high  $\times$  1.1 m wide. The effective surface area for a single plate lies in the range 0.01–3.6 m<sup>2</sup>. A single unit may contain up to 700 plates, the largest unit providing an effective surface area of 2500 m<sup>2</sup>. In order to avoid poor distribution of the fluid across the plate width, the minimum (length/width) ratio is of the order of 1.8.

Plate thicknesses range between 0.5 and 1.2 mm (approx. 0.02–0.05 in) and are spaced with nominal gaps of 2–5 mm (0.08–0.2 in), yielding equivalent diameters for the flow channels (see section 6.10.3) of 4–10 mm (0.15–0.4 in).

The plates are mass-produced but the design of each plate pattern requires considerable research and investment, plus sound technical and commercial judgement, to ensure market success.

#### 4.2.2 Plate corrugation types

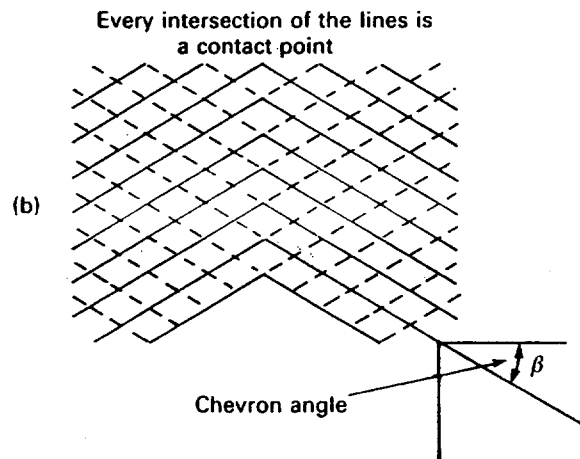
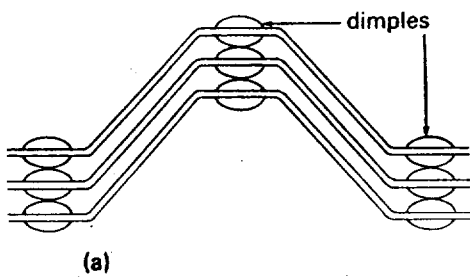
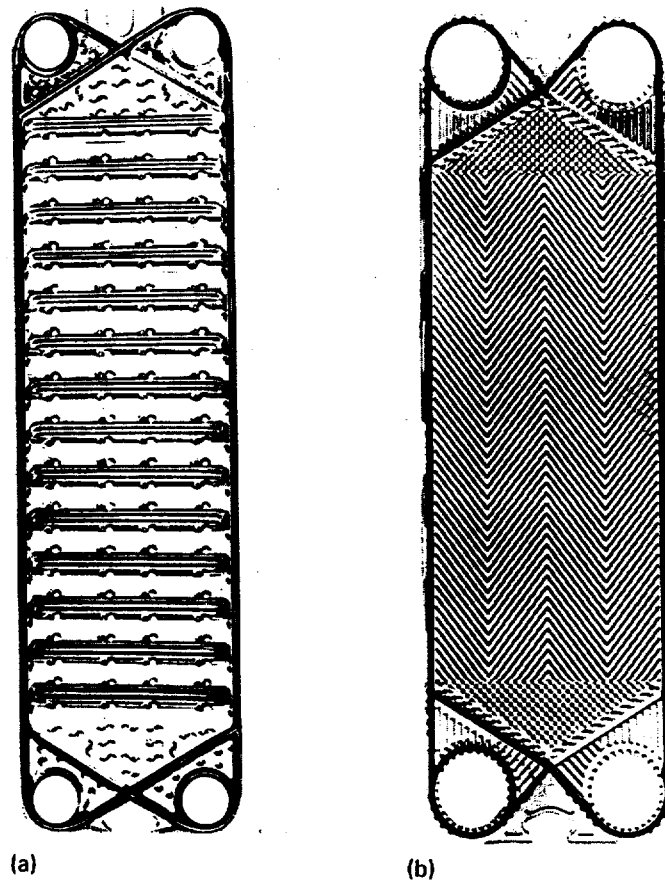
A wide range of corrugation types are available and the pattern and geometry are proprietary. The most widely used corrugation types are the interlocking or 'washboard', and the chevron or 'herringbone'. Figure 4.3 shows both types.

Corrugations increase the effective surface area of the plate and promote turbulence. In the washboard type, turbulence is promoted by a continuously changing flow direction and velocity of the fluid. In the herringbone type adjacent plates are assembled such that the flow channel imparts a swirling motion to the fluid. To enable such thin plates to withstand differential pressures up to at least 10 bar, and in special cases up to 25 bar, the corrugations are essential for strengthening and mutual support of the plates.

In the washboard type, the transverse corrugations may be deeper than the plate spacing and align with those on the adjacent plate. The plate spacing is maintained by dimples which are pressed into the crests and troughs and contact one another on adjacent plates. The washboard type has less contact points, and a greater corrugation depth, than the herringbone type. As a result, it operates at lower pressures but requires heavier plate.

In the herringbone type, the corrugations are pressed to the same depth as the plate spacing. The chevron angle is reversed on adjacent plates so that when the plates are clamped together the corrugations cross

**Figure 4.3** Typical plates (a) intermating type (b) chevron type



**Figure 4.4** Contact points of adjacent plates (a) intermating type (b) chevron type

one another to provide numerous contact points. The herringbone type therefore has greater strength than the washboard type and enables it to withstand greater pressures with smaller plate thicknesses. Its corrugations are also less deep, which assists the pressing operation, and as a result the herringbone type is ideally suited for plate production in expensive metals. It is the most common type in use today.

The contact arrangement of the plates is shown in Fig. 4.4.

### 4.2.3 Gaskets

The periphery of each plate is grooved to house a moulded gasket, which may have a peaked profile. Some gaskets are cemented in, but snap-on gaskets are available which do not require cement. The gasket is designed to compress roughly 25% of its original thickness in order to provide a tight joint without local distortion of the thin plate. The integrity of the complete unit depends greatly on gasket performance, particularly as there may be up to 700 gaskets to keep leak-tight. The gasket material, the gasket shape, the groove geometry and groove support has been the subject of continuous investigation.

Typical gasket materials, together with their maximum operating temperatures and applications are given in Table 4.2. Although compressed asbestos fibre gaskets are listed, these are not widely used. Their elastic properties are inferior to the rubberised types listed in Table 4.2 and stronger frames are required to resist the higher bolting loads required. However, they find use in services involving organic solvents which would attack the other materials. Materials, such as Teflon™ are unsuitable because of their viscoelastic properties.

Figure 4.5 shows a typical gasket arrangement from which it will be seen that there is a double seal between liquid streams so that inter-mixing cannot occur. The interspace between seals is vented to the atmosphere through suitable vents moulded into the gasket. Leakage from either stream occurs only to the atmosphere.

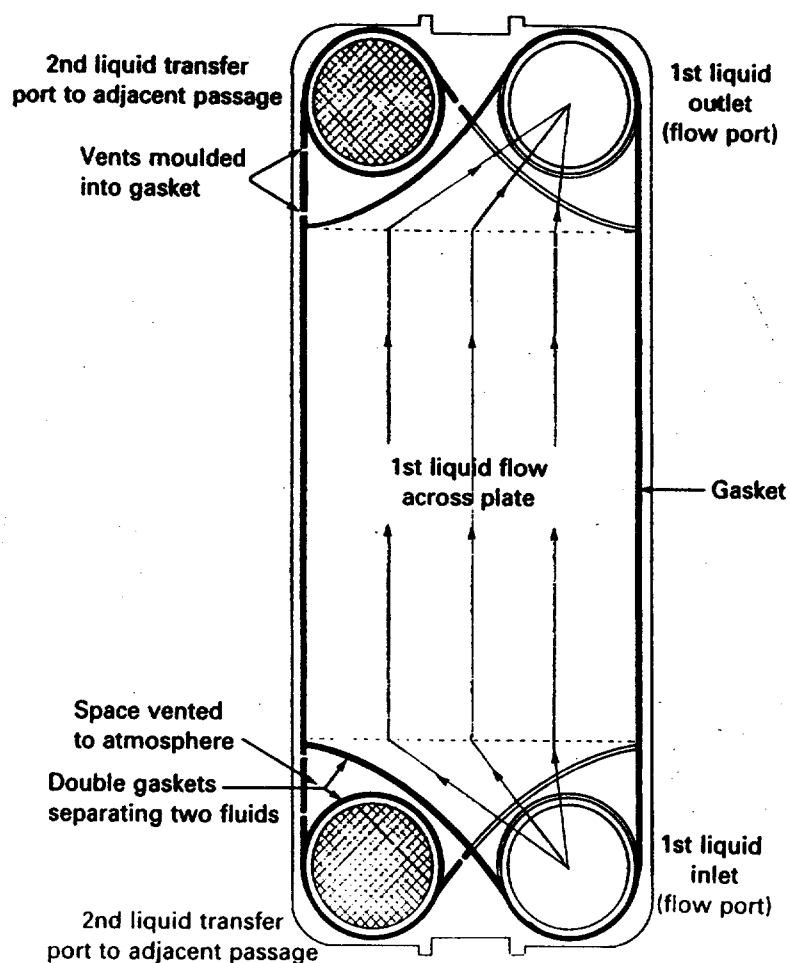
Table 4.2 Typical gasket materials, operating temperatures and applications

Gasket material	Approx. maximum operating temp. (°C)	Application
Acrylonitrile-butadiene (medium nitrile rubber)	135	Fatty materials
Isobutylene-isoprene (resin cured butyl rubber)	150	Aldehydes, ketones, some esters
Ethylene-propylene rubber (EPDM)	150	High-temperature resistance for a wide range of chemicals
Fluorocarbon rubber base (Viton)™	175	Mineral, vegetable and animal oils, fuels
Compressed asbestos fibre	260	Organic solvents such as chlorinated hydrocarbons

### 4.2.4 Frame

Figure 4.1 shows that the frame consists of a fixed head or fixed frame at one end, and a movable head or pressure plate at the other. The vertical sides of both the fixed frame and pressure plates are notched at intervals to engage tie bolts which join the two heads together. The pack of plates are compressed together as the tie bolts are tightened at the movable head end. A horizontal carrier bar at the top of the frame, and a horizontal guide bar at the bottom, are attached to the fixed head plate at

**Figure 4.5** Gasket arrangement

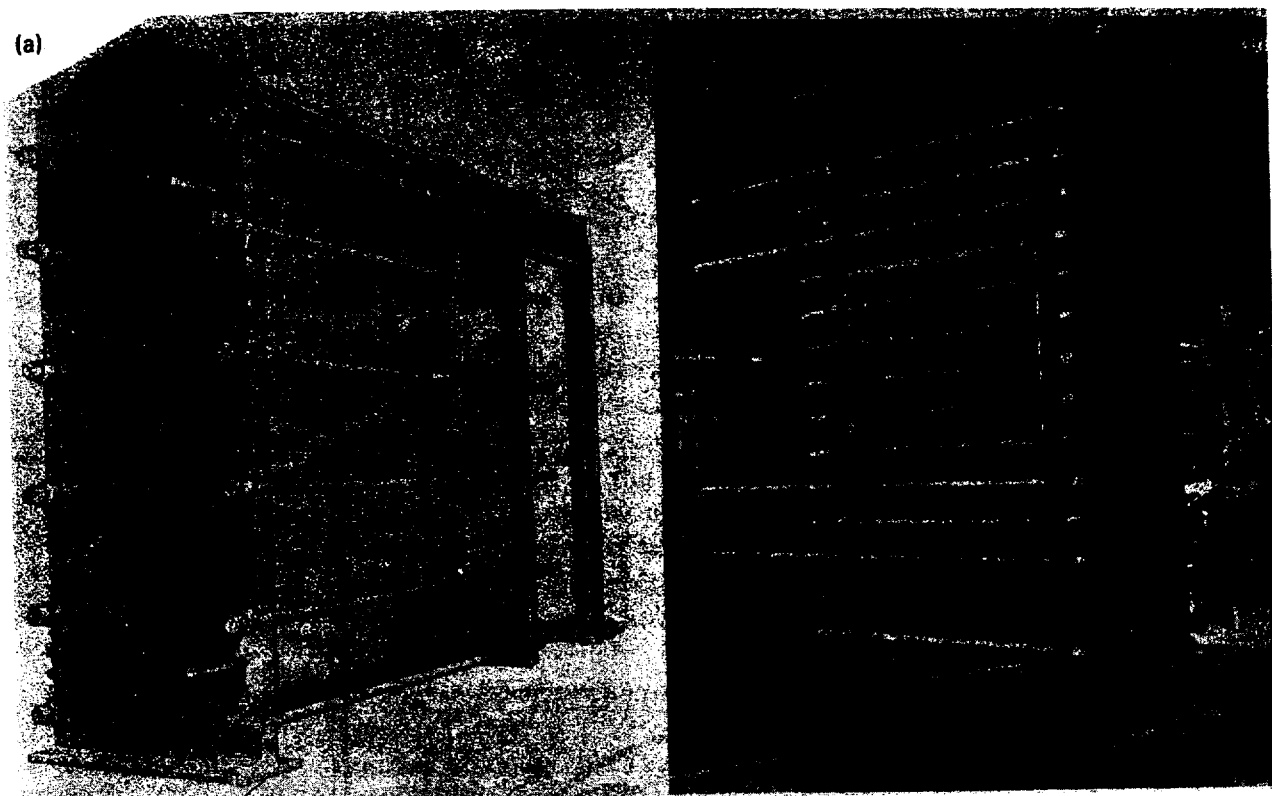


one end and an end support column at the other. Every heat transfer plate is notched at the centre of its top and bottom edges so that it may be suspended from the top carrier bar and guided by the bottom guide bar. Every plate is free to slide along both bars. The movable head plate is similarly notched and free to slide along both bars.

The frame is normally constructed in carbon steel and painted to suit its operating environment. Where stringent cleanliness requirements apply, such as in pharmaceutical or antibiotic production, and the dairy, food and drinks industries, the frame may be supplied in polished stainless steel. The units are normally floor-mounted but small units may be wall-mounted. Figure 4.6 shows two large units.

#### 4.2.5 Ports

The fluids enter the unit via ports (nozzles) located in one or both end plates. If both inlet and outlet ports for both fluids are located in the fixed-head end, then the unit may be opened up without disturbing the external piping. This applies to single-pass arrangements, but with multi-pass arrangements the ports must always be located on both heads. This means that the unit cannot be opened up without disturbing the external piping at the movable-head end.



**Figure 4.6** Two large gasketed-plate heat exchangers (a) APV (SR235), (b) Alfa-Laval (AL35-HA)

Ports may be arranged to provide diagonal flow, in which the fluid enters and leaves at opposite corners, or vertical flow, in which the fluid enters and leaves on the same side. If diagonal flow is used, two different plate designs are required, one being a mirror image of the other, which involves additional expense. Vertical flow avoids this because the inversion of alternate plates reverses the flow and ports, and provides the required flow arrangement. Vertical flow is therefore the most widely used as it is less costly and provides standardisation.

The port entrance area is the weakest part of the plate because, unlike the peripheral gasket, the gasket in an adjacent plate is not supported by a corresponding one. Plate-to-plate contact is achieved by the provision of additional corrugations, or on older designs, welded-on castellated strips, care being taken to avoid restricting the flow.

The port internal surfaces are usually in the same metal as the plates to avoid galvanic effects, but are sometimes rubber-lined. The largest port diameter is nominally 450 mm (18 in). The largest flow rate is 1–1.5 m<sup>3</sup>/s of aqueous fluid depending on the available pressure loss.

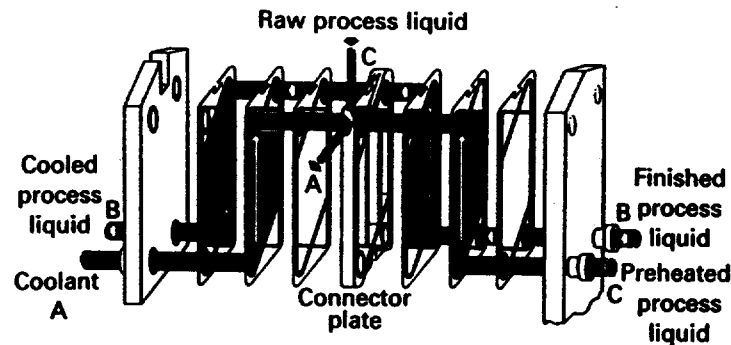
#### 4.2.6 Tie bolts

The tie bolts are usually of 1% chrome–0.5% molybdenum low-alloy steel similar to that used for the stud bolts of most shell-and-tube exchangers. The pack of large units may be compressed by hydraulic, pneumatic or electric pack-tightening mechanisms.

### 4.2.7 Connector plates

It is possible to process three or more fluids in a single gasketed-plate type heat exchanger. This is achieved by means of connector plates, as shown in Fig. 4.7. This practice is widely used in food processing and permits heating, cooling and recuperation of the fluids in a single unit.

**Figure 4.7.** Connector plates to permit three or more fluids to be processed in one unit



## 4.3 Inspection and maintenance

A feature of the gasketed-plate exchanger is the ease with which the pack is opened and closed. Once open, all plates may be inspected on *both* sides and the whole pack hosed down *in situ* if required. Any plate may be removed by detaching first from the guide bar at the bottom, and then from the carrier bar at the top. Replacement of the same, or a new, plate is simply the reverse procedure. If necessary, the duty of the unit may be altered rapidly by adding or removing heat transfer plates, adding connector plates, or by altering pass arrangements.

The gaskets are designed to withstand several opening and closing operations. However, gasket replacement has been eased by the introduction of gaskets attached by tabs projecting through holes in the plate periphery, instead of being glued. When renewal is required it may be necessary to return the complete plate(s) to the makers for re-gasketing, particularly with glued-on gaskets.

Although maintenance is a rapid, simple operation, the heat transfer plates must be handled with care at all times.

## 4.4 Flow arrangements

### 4.4.1 Passes

Each traverse of either fluid from top to bottom of the pack, or vice-versa, is termed a pass. Usually, all passes have the same number of flow channels in each pass, but this is not always the case. Single- or multi-pass flow is possible.

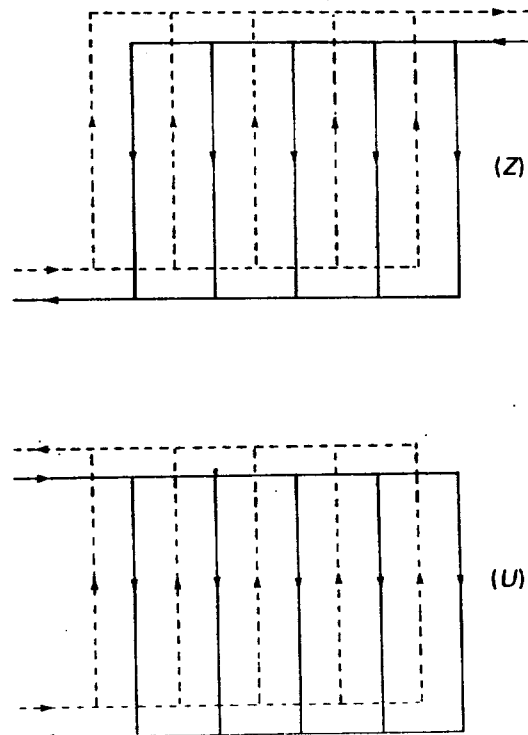
#### 4.4.2 Number of plates

It will be noted that in the outermost channels heat is transferred through one plate only. The end plates are not heat transfer plates so that the effective number of heat transfer plates in a pack is the total number of plates less two. If the number of plates in the pack is large, the effect of the end plates in design is negligible.

#### 4.4.3 Looped flow (1/1 arrangement)

A single pass by both fluids provides countercurrent or cocurrent flow (see Chapter 7) and two arrangements, termed loop flow, are possible as shown in Fig. 4.8. In the Z arrangement, two ports will be on both fixed-head and movable-head plates, which means that the external piping must be disturbed at the movable-head plate before the pack can be opened. In the U arrangement, all four ports will be on the fixed-head plate, with the advantage that the pack can be opened without disturbing any external piping. The U is therefore the preferred arrangement, but consideration must be given to the flow distribution between channels comprising one pass. (See section 4.4.6.)

Figure 4.8 Countercurrent single-pass flow – Z and U arrangements



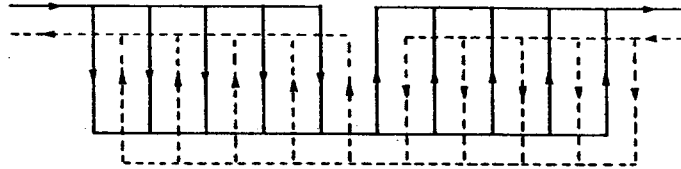
#### 4.4.4 Two-pass/two-pass flow (2/2 arrangement)

Multi-pass arrangements consist of passes connected in series and Fig. 4.9 shows an arrangement in which both fluids flow through two passes in series, with the same number of flow channels in all passes. The system is

in strict countercurrent flow, except for the end effects, described in section 4.4.2, and the centre plate. At this plate, where both fluids change directions, cocurrent flow prevails.

Such a flow arrangement would be considered for services involving a long temperature range and small temperature difference between fluids.

Figure 4.9 Two-pass/  
two-pass flow

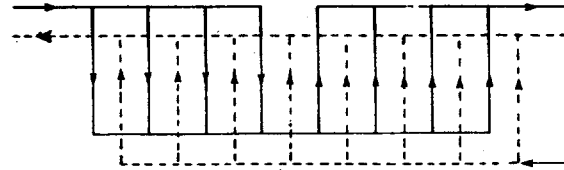


#### 4.4.5 Two-pass/one-pass flow (2/1 arrangement)

Figure 4.10 shows an arrangement in which one fluid flows in a single pass, while the other fluid flows in two passes in series. In this arrangement one half of the unit is in countercurrent flow and the other half is in cocurrent flow.

Such a flow arrangement would be considered when one of the fluids has a much greater flow rate, or a lower permissible pressure loss, than the other.

Figure 4.10 Two-pass/  
one-pass flow



#### 4.4.6 Flow distribution

Obtaining uniform flow distribution between parallel flow channels is often a problem in the design of heat transfer equipment, and must be considered carefully in the design of gasketed-plate heat exchangers. According to Usher (1969) and Wilkinson (1974), the preferred U arrangement of the looped flow system gives a less uniform flow distribution than the Z arrangement. Edwards *et al* (1984) examine flow distribution in greater detail and conclude that neither provides uniform distribution, but the U arrangement provides a flatter distribution.

### 4.5 Features of gasketed-plate heat exchangers

Inevitably when discussing the unique features of gasketed-plate heat exchangers comparisons are made with shell-and-tube exchangers. It should be emphasised that consideration of the plate unit can only be made when (1) the design pressure is less than 30 bar, (2) the design temperature is less than 180 °C (260 °C for compressed asbestos fibre



gaskets, but at lower design pressures), (3) vacuum is not high and (4) volumes of gases and vapours, with or without phase change at low pressure are moderate. Such design conditions are trivial to a shell-and-tube exchanger.

However, *within these design limitations*, Part I Appendix states that the gasketed-plate heat exchanger is likely to be the first choice of exchanger type. Chapter 19, dealing with size estimation and cost, regards a *carbon steel* shell-and-tube unit as no match for a plate unit having stainless-steel plates, with regard to initial cost.

The features of gasketed-plate heat exchangers may be summarised as follows:

- (a) Low initial cost, due to its basic design, which combines high thermal efficiency with relatively straightforward mass-production.
- (b) High heat transfer coefficients of *both* fluids are achieved. Chapter 19 shows that the film heat transfer coefficients may be up to three times those achieved in a shell-and-tube unit. This is due to the turbulence created by the corrugated plates, the small equivalent diameter of the flow channel, and the absence of leakage streams (see Chapter 12) which prevail in shell-and-tube units. Countercurrent flow is readily achieved.

Turbulence inside a tube begins to develop at a Reynolds Number of 2100 (see Chapter 6), whereas turbulence may be induced in plate units at Reynolds Numbers of 10–400, depending on the flow channel geometry.

- (c) Coupled with high film heat transfer coefficients, plate units exhibit low fouling characteristics in many services. This is due to high turbulence, low residence times, and non-stagnant regions in the flow channels. Chapter 19 shows that fouling resistances for plate units are lower than those for shell-and-tube units.
- (d) More than two fluids may be processed in a single unit.
- (e) Corrosion-resistant metals are required only for the heat transfer plates and ports. Stainless steel (type 316) and titanium, with their excellent corrosion-resistant properties, are standard plate materials.
- (f) Compared with shell-and-tube units, plate units are especially compact, with respect to volume, weight and liquid hold-up. This is of vital importance, for example, in off-shore services. Despite their compactness, 2500 m<sup>2</sup> of surface is available in a single unit.
- (g) Plate units are extremely flexible and have a variety of plate designs to suit different applications. They may be altered rapidly to suit other services by adding or removing plates, or modifying pass arrangements.
- (h) Only the plate edges are exposed to the atmosphere. The heat losses are negligible and no insulation is required.
- (i) Inter-mixing of the two fluids cannot occur under gasket failure.
- (j) Small liquid hold-up provides rapid start-up and response to control function changes.
- (k) Plate units withstand thermal shocks and are vibration-free. Flow-induced vibration has become an important factor in the design of shell-and-tube heat exchangers in recent years (see Chapter 11).

- (l) The low fouling characteristics of the plate unit means that less opening-up is required for cleaning. When opening-up is required, however, the operation is rapid and straightforward, and there is full accessibility to *both* sides of the plates for inspection and cleaning. Any plate may be removed without removing other than the adjacent plate. Individual plates may be replaced readily.

## 4.6 Application

Although used primarily for liquid-liquid services, Gray (1984) describes the range of conditions under which gasketed-plate heat exchangers perform well in boiling and condensing applications. Included in the condensing application is, of course, steam as a heating medium. Single-phase gases may be handled, provided the absolute pressure is above about 0.5–1.0 bar, depending on the molecular weight, and that the volume is not too great. Liquids having viscosities up to 10 N s/m<sup>2</sup> (10 000 centipoise) have been processed.

Gasketed-plate heat exchangers find wide industrial application today, but their largest single application has been that of central cooling in large petrochemical, metallurgical and power plants. In central cooling, a closed circuit of high-quality water, which is used to cool a process, is passed through gasketed-plate heat exchangers, in which heat is removed from the closed circuit water by water of a lower quality, such as sea or polluted river water. Its low weight and size, together with the corrosion-resistant plates, makes it ideal for off-shore, and on-ship, applications. In the latter case the plate unit has the ability to withstand the loads imposed by wave action. Hammond (1982) describes how six cupro-nickel shell-and-tube exchangers failed on a North Sea platform in one year. They were replaced by four smaller plate units and no failure has occurred in seven years' service.

## Acknowledgements

The author is grateful to the following companies for the provision of technical data and illustrations: APV International Ltd, Crawley, West Sussex, UK. Alfa-Laval Co. Ltd, Great West Road, Brentford, Middlesex, UK.

## References

A list of addresses for the service organisations is provided on p. xvi.

- Clark, D. F. (1974) 'Plate heat exchanger design and recent development', *The Chemical Engineer* (May).
- Edwards, D. F. *et al.* (1984) 'The flow distribution in plate heat exchangers', presented at 1st UK National Conference on Heat Transfer, University of Leeds,

3-5 July. Inst. Chem. Eng. Symp. Series No. 86, p. 1289.

**Gray, R. M. (1984)** 'The design and use of plate heat exchangers in boiling and condensing applications', presented at 1st UK National Conference on Heat Transfer, University of Leeds, 3-5 July. Inst. Chem. Eng. Symp. Series No. 86, p. 685.

**Hammond, R. H. (1982)** 'Plate heat exchangers save on offshore platforms', *Oil & Gas Journal* (17 May), p. 78.

**Usher, J. D. (1969)** 'The plate heat exchanger', presented at meeting on Compact Heat Exchangers, NEL, Oct. Nat. Eng. Lab. UK Report No. 482, p. 33.

**Wilkinson, W. L. (1974)** 'Flow distribution in plate heat exchangers', *The Chemical Engineer* (May).

# Other types of heat exchanger

## 5.1 Double-pipe heat exchangers

### 5.1.1 Application

The basic double-pipe construction consists of a single pipe or tube, which may be plain or longitudinally finned, placed concentrically inside a larger pipe or tube. In another type there is a bundle of inner tubes instead of a single tube. These units are sometimes referred to as 'hairpin', 'concentric pipe', 'jacketed pipe' and 'jacketed U-tube' exchangers.

Double-pipe exchangers inherently provide countercurrent flow and should be considered as an alternative to shell-and-tube exchangers, particularly when there are low flow rates, a large temperature cross, the duty is less than 500 kW, the number of tubes per pass required is less than about 30 (19.05 mm o.d. tubes), and the diameter of the shell-and-tube exchanger is 200 mm or less. Under these conditions a shell-and-tube exchanger is usually uneconomic because a large number of small-diameter shells in series is required to provide adequate velocities and near-countercurrent flow.

Finned inner tubes are likely to be justified when one of the heat transfer coefficients (see section 9.1) is about one-half, or less, of the other, typical examples being high-viscosity liquid, or a gas, with water or condensing steam as the other fluid. The fluid with the lower coefficient is routed through the annulus when the fin geometry may be sized to provide optimum conditions.

As the dimensions of the components tend to be small, double-pipe units are readily designed for high-pressure services, and units are available for pressures well in excess of those normally encountered in shell-and-tube exchanger design. The closures are such that the double-pipe sections may be stripped down completely for inspection and maintenance. Double-pipe units provide the advantages of standardisation and modular construction.

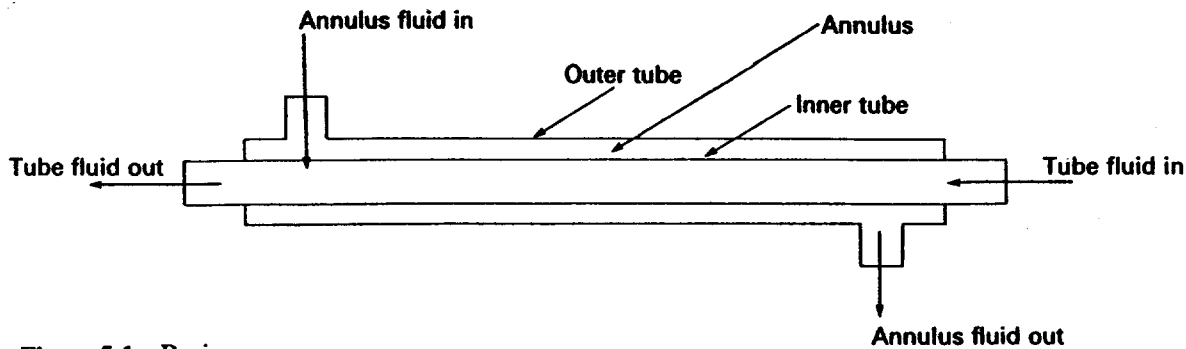


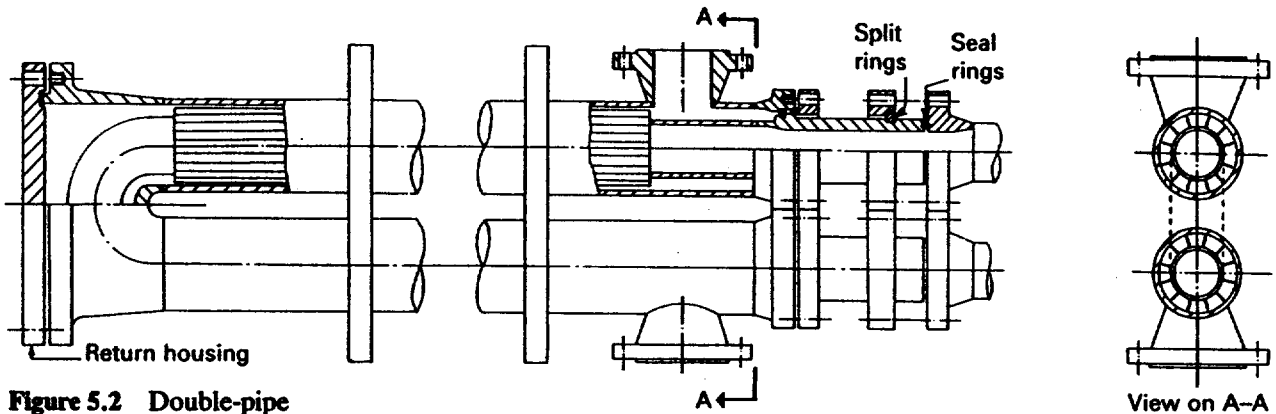
Figure 5.1 Basic double-pipe element

### 5.1.2 Construction

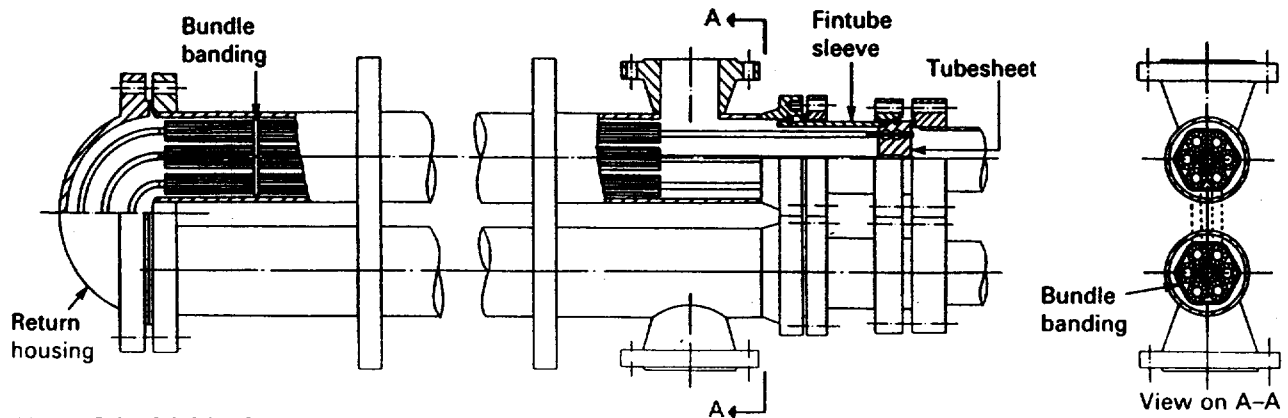
If flat plates are welded to the inner and outer tubes at each end to seal the annulus, a simple, but rugged unit is obtained (see Fig. 5.1). Additional lengths may be welded together to provide the required surface and for many small applications this simple construction will suffice. However, there is no provision for differential expansion between inner and outer tubes and no access to the annulus for maintenance.

A typical industrial double-pipe element, designed to overcome these problems, comprises two such lengths. At one end the two inner tubes are joined together by a welded-on U-bend, while the two outer tubes, or shells, are joined together by a header, fitted with a bolted flat cover, which encases the bend as shown in Fig. 5.2. The header, or return bend housing, is sized to allow free axial thermal movement of the inner tubes and bend within the shells. At the other end, a specially designed closure arrangement, as shown in Fig. 5.2, permits the tube-side connections to be removed. This enables the two inner tubes and bend to be removed as a unit from the shells, from the return housing end, after first removing the flat cover. The closure is designed to prevent the leakage of one fluid into the other. The seal ring between inner tube and shell is usually soft iron, but the tube-side joint may be metal-jacketed asbestos or spiral-wound asbestos. The author is designating this type as a '1/1 double-pipe unit' to distinguish it from the multi-tube, double-pipe units described later.

Multi-tube units, known as 'multis', are similar to the 1/1 double-pipe unit except that there is a bundle of U-tubes, plain or finned, instead of a single inner tube. Each leg of the U-bundle has its own tubesheet and the design permits free thermal movement of the bundle and its withdrawal from the shells, as shown in Fig. 5.3. The return bend housing which joins the two shells may be fitted with a flat cover or bonnet. The other end may be fitted with a unihead or a separated head depending on the pressures and nature of the fluids. In the unihead (not shown) the tubesheet outer edge is fitted with a common sealing ring, but this limits the application of the multi-tube unit to low-pressure, non-hazardous fluids. The separated head, shown in Fig. 5.3, has a peripheral sleeve welded to the back face of the tubesheet and the seal between it and the outer shell is similar to the inner tube/shell seal of the 1/1 double-pipe unit. The tubesheet/tubeside seal comprises a system of split flanges and shear rings such that leakage between fluids cannot occur.



**Figure 5.2** Double-pipe exchanger with single inner tube (1/1 double-pipe unit)



**Figure 5.3** Multi-tube double-pipe exchanger

Longitudinal fins need no supports as the tubes are inherently self-supporting, but intermeshing of the fins is prevented by wrapping metal strips, usually stainless steel, at intervals around the fins. The whole bundle is held together by further metallic strips wound at intervals around its periphery. Plain tubes are supported by spider-type supports in shell diameters less than 150 mm, and segmental baffles at greater shell diameters. To ensure axial flow, both plain and longitudinally finned units require specially shaped peripheral baffles to block the area between bundle and shell.

### 5.1.3 Longitudinally finned tubes

Metal strip is formed into a U-shaped channel to provide two fins, each pair being electric resistance welded to the outside of the inner tube. The

**Table 5.1** Double-pipe heat exchangers. Standard sizes and nomenclature.

Section type	No. tubes	Shell o.d.	Tube o.d.	Shell nozzle (2) Ansi. WN.R.F.	Tube nozzle (1) (2)	Bracket				Overall length add to nominal fin length	Type of baffle or support
						Height		Width			
						Low press.	High press.	Low press.	High press.		
51	1	3.5 in	1.9 in	2 in	1½ in B.W.	13½ in	14½ in	8 in	9 in	1 ft 6 in	-
53	1	4.5 in	1.9 in	3 in	1½ in B.W.	16 in	18 in	10 in	10 in	1 ft 6 in	-
54	1	4.5 in	2.875 in	3 in	2½ in B.W.	16 in	18 in	10 in	10 in	1 ft 6 in	-
55	7	4.5 in	0.75 in	3 in	2½ in S.W.	16 in(4)	16 in(4)	10 in	10 in	1 ft 8 in	Peripheral
56	7	4.5 in	0.875 in	3 in	2½ in S.W.	16 in	-	10 in	-	1 ft 8 in	-
57	7(3)	4.5 in	0.875 in	3 in	2½ in S.W.	16 in(4)	16 in(4)	10 in	10 in	1 ft 8 in	Spider
58	7(3)	4.5 in	1.0 in	3 in	2½ in S.W.	16 in	-	10 in	-	1 ft 8 in	Spider
61	19	8.625 in	0.75 in	6 in	4 in S.W.	30 in	(5)	14 in	(5)	2 ft 4 in	Peripheral
62	19	8.625 in	0.875 in	6 in	4 in S.W.	30 in	(5)	14 in	(5)	2 ft 4 in	Peripheral
64	7	6.625 in	1.0 in	4 in	3 in S.W.	24½ in	(5)	14 in	(5)	1 ft 11 in	-
65	14	6.625 in	0.75 in	4 in	3 in S.W.	24½ in	(5)	14 in	(5)	1 ft 11 in	Peripheral
66	22(3)	6.625 in	0.75 in	4 in	3 in S.W.	24½ in	(5)	14 in	(5)	1 ft 11 in	Segmental
67	22(3)	6.625 in	0.75 in	4 in	3 in S.W.	24½ in	(5)	14 in	(5)	1 ft 11 in	Support
70	55(3)	8.625 in	0.625 in	6 in	4 in S.W.	30 in	(5)	14 in	(5)	2 ft 4 in	Segmental
71	37(3)	8.625 in	0.75 in	6 in	4 in S.W.	30 in	(5)	14 in	(5)	2 ft 4 in	Segmental
72	31(3)	8.625 in	0.875 in	6 in	4 in S.W.	30 in	(5)	14 in	(5)	2 ft 4 in	Segmental
73	55(3)	8.625 in	0.625 in	6 in	4 in S.W.	30 in	(5)	14 in	(5)	2 ft 4 in	Support
74	37(3)	8.625 in	0.75 in	6 in	4 in S.W.	30 in	(5)	14 in	(5)	2 ft 4 in	Support
75	31(3)	8.625 in	0.875 in	6 in	4 in S.W.	30 in	(5)	14 in	(5)	2 ft 4 in	Support
80	1	2.375 in	1.0 in	1½ in	¾ in B.W.	12 in	(5)	7 in	(5)	1 ft 6 in	-
81	1	3.5 in	1.0 in	2 in	¾ in B.W.	13½ in	14½ in	8 in	9 in	1 ft 6 in	-

B.W. = Bevelled for welding S.W. = Socket weld

(3) Available with bare tubes only.

(1) Flanged spool pieces can be supplied on request.

(4) When tubeside design pressure over 1800 lb/in<sup>2</sup> add 2½ in.

(2) Flange rating to suit design conditions.

(5) Available on application.

be soldered to base tubes of copper and copper alloys, but this limits the maximum operating temperature to 205 °C.

The number of fins around the circumference of the base tube is a multiple of 4 being 16 and 20 in the multi-tube units and ranging from 20 to 48 in the double-pipe units. Weldable fins are 0.889 mm thick with heights of 5.33–25.4 mm, whereas soldered fins are 0.5 mm thick up to 12.7 mm high and 0.8 mm thick for greater heights. These combinations produce a total external surface area for a single weldable finned tube of 0.23–1.98 m<sup>2</sup>/m length, which represents 4.7–16.5 times that of the internal surface area of the base tube.

To enhance heat transfer in the laminar or transitional flow regimes the fins are given a 'cut and twist'. At intervals of the order of 300–1000 mm, the fins are cut radially from outside edge to the root, after which the leading edge is twisted until the flow is guided into the adjacent fin channel.

EXAMPLE:  
53-1A018-420

Type	Shell Thk	Tube Thk	Shell Mat'l.	Tube Mat'l.	Fin Mat'l.	No. Fins	20 Nom. fin length in feet																																																																																																																					
53	1	A	0	1	8	4																																																																																																																						
	<table border="1"> <thead> <tr> <th>Digit</th> <th>Tube wall thickness</th> </tr> </thead> <tbody> <tr><td>A</td><td>0.065 in</td></tr> <tr><td>B</td><td>0.083 in</td></tr> <tr><td>C</td><td>0.109 in</td></tr> <tr><td>D</td><td>0.134 in</td></tr> <tr><td>E</td><td>Sch.40</td></tr> <tr><td>F</td><td>Sch.80</td></tr> </tbody> </table>		Digit	Tube wall thickness	A	0.065 in	B	0.083 in	C	0.109 in	D	0.134 in	E	Sch.40	F	Sch.80																																																																																																												
Digit	Tube wall thickness																																																																																																																											
A	0.065 in																																																																																																																											
B	0.083 in																																																																																																																											
C	0.109 in																																																																																																																											
D	0.134 in																																																																																																																											
E	Sch.40																																																																																																																											
F	Sch.80																																																																																																																											
	<table border="1"> <thead> <tr> <th>Digit</th> <th>Shell thk. (Sch. No.)</th> </tr> </thead> <tbody> <tr><td>0</td><td>10 Low press. both</td></tr> <tr><td>1</td><td>40 Low press. both</td></tr> <tr><td>2</td><td>40 High press. tube</td></tr> <tr><td>3</td><td>40 High press. shell</td></tr> <tr><td>4</td><td>40 High press. both</td></tr> <tr><td>5</td><td>80 Low press. both</td></tr> <tr><td>6</td><td>80 High press. tube</td></tr> <tr><td>7</td><td>80 High press. shell</td></tr> <tr><td>8</td><td>80 High press. both</td></tr> <tr><td>9</td><td>Special</td></tr> </tbody> </table>		Digit	Shell thk. (Sch. No.)	0	10 Low press. both	1	40 Low press. both	2	40 High press. tube	3	40 High press. shell	4	40 High press. both	5	80 Low press. both	6	80 High press. tube	7	80 High press. shell	8	80 High press. both	9	Special	<table border="1"> <thead> <tr> <th>Digit</th> <th>Shell Material</th> </tr> </thead> <tbody> <tr><td>0</td><td>Carbon steel</td></tr> <tr><td>1</td><td>--</td></tr> <tr><td>2</td><td>Chrome-moly.</td></tr> <tr><td>3</td><td>Carbon-moly.</td></tr> <tr><td>4</td><td>Stainless</td></tr> <tr><td>5</td><td>Nickel &amp; Ni. alloy</td></tr> <tr><td>6</td><td>Aluminium</td></tr> <tr><td>7</td><td>--</td></tr> <tr><td>8</td><td>--</td></tr> <tr><td>9</td><td>Special</td></tr> </tbody> </table>		Digit	Shell Material	0	Carbon steel	1	--	2	Chrome-moly.	3	Carbon-moly.	4	Stainless	5	Nickel & Ni. alloy	6	Aluminium	7	--	8	--	9	Special	<table border="1"> <thead> <tr> <th>Digit</th> <th>Tube Material</th> </tr> </thead> <tbody> <tr><td>0</td><td>Carbon steel</td></tr> <tr><td>1</td><td>Admiralty</td></tr> <tr><td>2</td><td>Chrome-moly.</td></tr> <tr><td>3</td><td>Carbon-moly.</td></tr> <tr><td>4</td><td>Stainless</td></tr> <tr><td>5</td><td>Nickel &amp; Ni. Alloy</td></tr> <tr><td>6</td><td>Aluminium</td></tr> <tr><td>7</td><td>Cupro-nickel</td></tr> <tr><td>8</td><td>Aluminium brass</td></tr> <tr><td>9</td><td>Special</td></tr> </tbody> </table>		Digit	Tube Material	0	Carbon steel	1	Admiralty	2	Chrome-moly.	3	Carbon-moly.	4	Stainless	5	Nickel & Ni. Alloy	6	Aluminium	7	Cupro-nickel	8	Aluminium brass	9	Special	<table border="1"> <thead> <tr> <th>Digit</th> <th>Fin Material</th> </tr> </thead> <tbody> <tr><td>0</td><td>Carbon steel</td></tr> <tr><td>1</td><td>Admiralty</td></tr> <tr><td>2</td><td>Chrome-moly.</td></tr> <tr><td>3</td><td>Nickel</td></tr> <tr><td>4</td><td>Stainless</td></tr> <tr><td>5</td><td>Nickel alloy</td></tr> <tr><td>6</td><td>Aluminium</td></tr> <tr><td>7</td><td>Cupro-nickel</td></tr> <tr><td>8</td><td>Yellow brass</td></tr> <tr><td>9</td><td>Special</td></tr> </tbody> </table>		Digit	Fin Material	0	Carbon steel	1	Admiralty	2	Chrome-moly.	3	Nickel	4	Stainless	5	Nickel alloy	6	Aluminium	7	Cupro-nickel	8	Yellow brass	9	Special	<table border="1"> <thead> <tr> <th>Digit</th> <th>No. Ext fins</th> </tr> </thead> <tbody> <tr><td>0</td><td>00</td></tr> <tr><td>1</td><td>12</td></tr> <tr><td>2</td><td>16</td></tr> <tr><td>3</td><td>20</td></tr> <tr><td>4</td><td>24</td></tr> <tr><td>5</td><td>28</td></tr> <tr><td>6</td><td>30</td></tr> <tr><td>7</td><td>32</td></tr> <tr><td>8</td><td>36</td></tr> <tr><td>9</td><td>Spec.</td></tr> <tr><td>A</td><td>40</td></tr> <tr><td>B</td><td>48</td></tr> </tbody> </table>		Digit	No. Ext fins	0	00	1	12	2	16	3	20	4	24	5	28	6	30	7	32	8	36	9	Spec.	A	40	B	48
Digit	Shell thk. (Sch. No.)																																																																																																																											
0	10 Low press. both																																																																																																																											
1	40 Low press. both																																																																																																																											
2	40 High press. tube																																																																																																																											
3	40 High press. shell																																																																																																																											
4	40 High press. both																																																																																																																											
5	80 Low press. both																																																																																																																											
6	80 High press. tube																																																																																																																											
7	80 High press. shell																																																																																																																											
8	80 High press. both																																																																																																																											
9	Special																																																																																																																											
Digit	Shell Material																																																																																																																											
0	Carbon steel																																																																																																																											
1	--																																																																																																																											
2	Chrome-moly.																																																																																																																											
3	Carbon-moly.																																																																																																																											
4	Stainless																																																																																																																											
5	Nickel & Ni. alloy																																																																																																																											
6	Aluminium																																																																																																																											
7	--																																																																																																																											
8	--																																																																																																																											
9	Special																																																																																																																											
Digit	Tube Material																																																																																																																											
0	Carbon steel																																																																																																																											
1	Admiralty																																																																																																																											
2	Chrome-moly.																																																																																																																											
3	Carbon-moly.																																																																																																																											
4	Stainless																																																																																																																											
5	Nickel & Ni. Alloy																																																																																																																											
6	Aluminium																																																																																																																											
7	Cupro-nickel																																																																																																																											
8	Aluminium brass																																																																																																																											
9	Special																																																																																																																											
Digit	Fin Material																																																																																																																											
0	Carbon steel																																																																																																																											
1	Admiralty																																																																																																																											
2	Chrome-moly.																																																																																																																											
3	Nickel																																																																																																																											
4	Stainless																																																																																																																											
5	Nickel alloy																																																																																																																											
6	Aluminium																																																																																																																											
7	Cupro-nickel																																																																																																																											
8	Yellow brass																																																																																																																											
9	Special																																																																																																																											
Digit	No. Ext fins																																																																																																																											
0	00																																																																																																																											
1	12																																																																																																																											
2	16																																																																																																																											
3	20																																																																																																																											
4	24																																																																																																																											
5	28																																																																																																																											
6	30																																																																																																																											
7	32																																																																																																																											
8	36																																																																																																																											
9	Spec.																																																																																																																											
A	40																																																																																																																											
B	48																																																																																																																											

Courtesy: Filtration & Transfer Ltd.

5.1.4 Details of standard units

1/1 double-pipe and multi-tube units readily permit standardisation and details of standard models are given in Tables 19.7 and 19.8. It will be seen that 1/1 double-pipe units use shells of 50.8–101.6 mm (2–4 in) nominal diameter, and tubes of 25.4–73 mm (1–2<sup>7</sup>/<sub>8</sub> in) outside diameter; multi-tube units use shells of 101.6–203.2 mm (4–8 in) nominal diameter and tubes of 19.05–25.4 mm (¾–1 in) outside diameter. Shell diameters greater than 203.2 mm (8 in) nominal are available as special designs, if required.

Standard pressure class is 34.5 bar (500 lb/in<sup>2</sup>) for both shell and tubes except for the 203.2 mm (8 in) multi-tube model for which it is 20.7 bar (300 lb/in<sup>2</sup>). Units having higher pressures are available and components such as shell nozzles, tube nozzles, shell/tube closures and return bend housings are designed in a range of standard pressure classes up to



165.5 bar (2400 lb/in<sup>2</sup>) on the shell-side and 345 bar (5000 lb/in<sup>2</sup>) on the tube-side. In the case of 1/1 double-pipe units tube-side components are available up to 1034 bar (15 000 lb/in<sup>2</sup>). The system is designed to simplify maintenance and the stocking of spares.

The units are available in lengths of 1.52–7.62 m, in intervals of 1.52 m, and the maximum surface areas of the various 1/1 double-pipe models, based on a single-two-leg unit, are 7–30 m<sup>2</sup> for finned tubes and 1.2–3.5 m<sup>2</sup> for plain tubes. The corresponding maximum surface areas for the multi-tube models are 25–100 m<sup>2</sup> for finned tubes and 6.4–8.5 m<sup>2</sup> for plain tubes.

The smallest unit may comprise only a single two-leg section, but greater capacities may be achieved by stacking additional sections in parallel, or in series, or a combination of the two. If both fluids flow from one section to the next throughout a series bank, then full countercurrent flow is achieved. In some cases, however, a better design solution may be obtained by routing the shell-side fluid in series throughout the series bank, but splitting the tube-side fluid such that it flows through two or more sections in parallel. In this event full countercurrent flow is not obtained and the temperature difference must be corrected accordingly. (See section 7.6.)

### 5.1.5 Nomenclature

Although there is no international standard for double-pipe exchangers, a system developed by Brown Fintube has achieved some recognition.

A typical designation is 53-1A018-420 which is explained in Table 5.1.

## 5.2 Heat pipes

### 5.2.1 Background

Although a patent application in 1942 described the heat pipe concept, it was not until Grover's patent application in 1963 that the term 'heat pipe' was used. The heat pipe is a device which provides exceptionally high heat transport characteristics and is a relatively new and challenging technology. It was developed originally for the gravity-free environment of space, but is now finding increasing usage in many industrial applications.

The heat pipe is a simple, inexpensive device, without moving parts, which will provide silent, continuous operation over a long period and independent of moderate gravitational and centrifugal forces. It is able to transfer up to 500 times as much heat per unit mass as a solid thermal conductor having the same cross-section.

### 5.2.2 Principle of operation

A heat pipe consists of a closed container, a working fluid and, in the majority of cases, a porous capillary wick, which must make a tight and continuous bond with the inside surface of the container. Because of its ease of manufacture and strength, the container is invariably a tube of circular cross-section. The quantity of working fluid stored in the heat pipe is sufficient to wet the entire wick.

One end of the heat pipe functions as an evaporator, in which heat provided by an external heating medium (heat source) vaporises some of the working fluid within the wick. The vapour is driven through the central core of the heat pipe to the other end, which functions as a condenser (heat sink), in which the vapour condenses to release its latent heat to an external cooling medium. The condensate then returns to the evaporator through the wick by capillary action. The latent heat of vaporisation is therefore transported from one end of the heat pipe to the other, with a negligible temperature gradient, while surface tension forces in the wick return the condensate from the condenser to the evaporator. No external mechanical power is applied. The pressure within the heat pipe is the saturation vapour pressure of the working fluid at its operating temperature.

The heat pipe is flexible in that it may be used with many heat sources including open flames, electrical heaters, solar radiation and nuclear plant. Heat interchange between the source and heat pipe may occur by radiation, convection or conduction.

### 5.2.3 Types

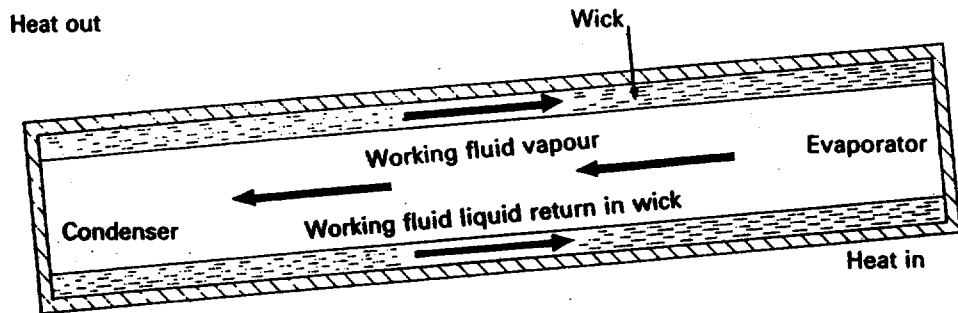
The capillary-driven heat pipe shown in Fig. 5.4 is the most frequently used type. Although shown at an angle to the horizontal, with the evaporator uppermost, in principle there is no restriction on its orientation. Each case must be treated individually, but for some applications it may be more convenient to have the heat pipe vertical, or inclined, with the condenser uppermost. As the condensate is then able to return to the evaporator by gravitational force, the wick may be eliminated and the unit is described as a two-phase closed thermosyphon. Even liquid distribution over the container wall is essential and in the case of inclined thermosyphons it may be necessary to provide a simple wick, wires or spiral grooves in the wall to achieve it.

If the evaporator is at the top of a vertical heat pipe, heat travels downwards, but the condensate must return against the influence of gravity by the capillary action of the wick. According to Chisholm (1983), existing wicks, operating against gravity, limit the vertical heat-pipe height to 400 mm. Heat pipes function well in outer space for which they were originally designed. The wick ensures that the condensate returns on the heat-pipe wall.

Another form of capillary-driven heat pipe is the flat-plate type, of which there are several kinds. Another form of the 'wickless' unit is the

rotating heat pipe in which the liquid is centrifuged back to the evaporator along the tapered inner wall of the container. Electrostatically driven and osmotically driven types are in the early stages of development.

Figure 5.4 Heat pipe



#### 5.2.4 Container

The container material must be suitable for the operating temperature of the heat pipe and have no chemical or metallurgical reaction with the working fluid and wick. Containers have been made of metal, glass and ceramics. In order to improve the rate of heat transfer, the external surfaces of the evaporator, or condenser, or both, may be provided with fins or other types of extended surface.

#### 5.2.5 Working fluid

The working fluid is selected according to the operating temperature of the heat pipe. In addition to being stable at this temperature it must be compatible with the container and wick. Some of the desirable characteristics of the working fluid are (1) a moderate vapour pressure in order to minimise the thickness of the container, (2) a steep vapour-pressure curve such that large pressure differences provide small temperature differences between evaporator and condenser, (3) a high latent heat which will provide a high rate of heat transfer with minimum fluid flow, (4) a high liquid thermal conductivity, (5) a low liquid and vapour viscosity in order to reduce resistance to flow and (6) a high surface tension to assist capillary action in the wick.

Working fluids include acetone, alcohol, ammonia, bismuth, caesium, ethane, glycerin, hydrogen, lithium, mercury, methane, methanol, molten salts, nitrogen, potassium, proprietary refrigerants 12 and 21, silver, sodium, toluene and water.

#### 5.2.6 Wicks

Homogeneous wicks include multiple wire mesh screens, packed spherical particles, felted metal fibres and woven or felted ceramic fibres. Grooved wicks consist of narrow longitudinal grooves, usually rectangular in shape,

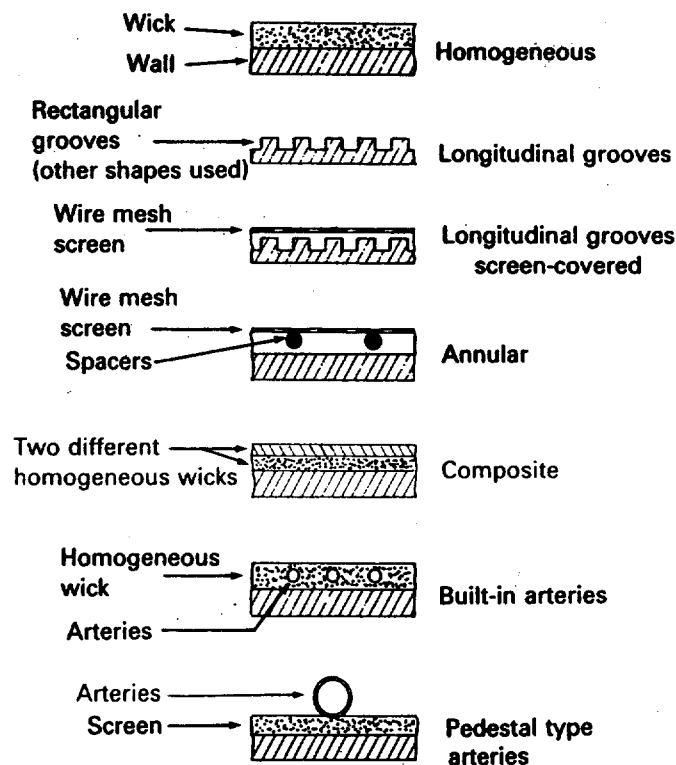
cut into the wall of the container, which provides a simple design, although prone to liquid entrainment. As an alternative the grooved wick may be screen-covered.

Arterial wicks contain passages, known as arteries, which provide a low-resistance path for the liquid flowing from condenser to evaporator. A homogeneous wick, for instance, may be provided with built-in arteries. Another design comprises a central insert having screen-covered arteries and screened container wall.

There are many heat-pipe wicks in use, but most of these are composites or modifications of the homogeneous, grooved and arterial types.

The wick must be compatible with the container and working fluid. Typical heat-pipe wicks are shown in Fig. 5.5.

**Figure 5.5** Typical heat pipe wicks (condensate flow normal to page in all cases)



### 5.2.7 Applications

Heat pipes have been built with diameters of 3 mm to 1 m, aspect ratios of 0.1 to 450, operating temperatures from cryogenic to 2000 °C and surface areas up to 1000 m<sup>2</sup>. The numerous applications include the removal of heat from electronic components, electrical motors, circuit breakers and transformers; non-icing units for bridges, roads and navigation buoys; permafrost layer protection from hot pipelines; cryosurgical probes and solar collectors. Heat exchangers include units for heating, ventilation, air-conditioning, drying and heat recovery systems.

Heat-pipe units are especially suited to applications involving large volumes of low-pressure gas, possibly at high temperature, which are encountered in heat recovery systems. A particular application occurs in

power stations where flue gas, which has been desulphurised to eliminate acid-mist, must be reheated before discharge from a stack to prevent an unsightly discharge. As an alternative to steam heating, heat interchange between the treated and untreated flue gas may be carried out using either rotary exchangers (Ljungstrom type, described in section 5.11, or a heat-pipe unit.

### 5.3 Gasketless-plate heat exchangers

#### 5.3.1 Welded construction

The excellent characteristics of the gasketed-plate type heat exchanger have been described in Chapter 4. The chief limitation at present is its inability to withstand pressures greater than 30 bar, and temperatures greater than 260 °C, although manufacturers are continually seeking gaskets which will enable the maximum pressure and temperature to be increased. If the plates are welded together at the periphery then leakage to the atmosphere is prevented and hazardous fluids may be handled. An exchanger constructed in this way has the disadvantage that it cannot be opened up for maintenance, and cleaning must be carried out by chemical means. This is of little importance for clean services and all the other advantages of plate-type construction remain.

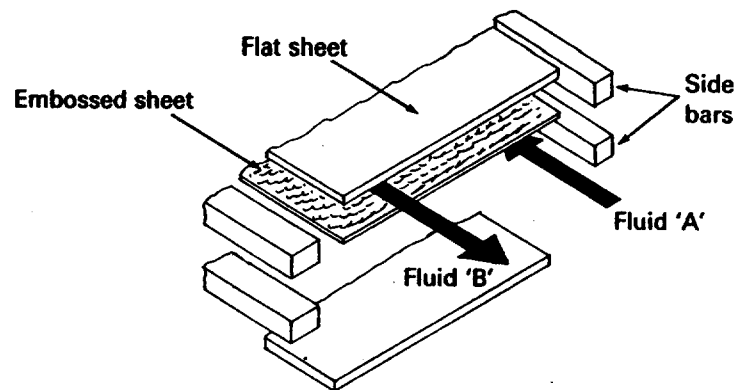
#### 5.3.2 Packinox exchanger

The Packinox is an all-welded, gasketless-plate heat exchanger invented in 1980 by Nouvelles Applications Technologiques (NAT). It comprises a heat exchanger bundle mounted in a pressure vessel, or a conventional plate exchanger support. The bundle is made of explosion-formed sheets stacked on top of each other and welded longitudinally. Spacer pieces ensure the correct distance between the sheets around the edges. It will be seen from Fig. 5.6 that the bundle is formed from alternate flat and embossed sheets, but it may also be formed with all sheets corrugated. At the inlets and outlets the sheets are welded in pairs where separate headers collect the fluid streams. Differential expansion between vessel and bundle is accommodated by expansion bellows (section 2.14). Figure 5.7 shows the bundle and pressure vessel.

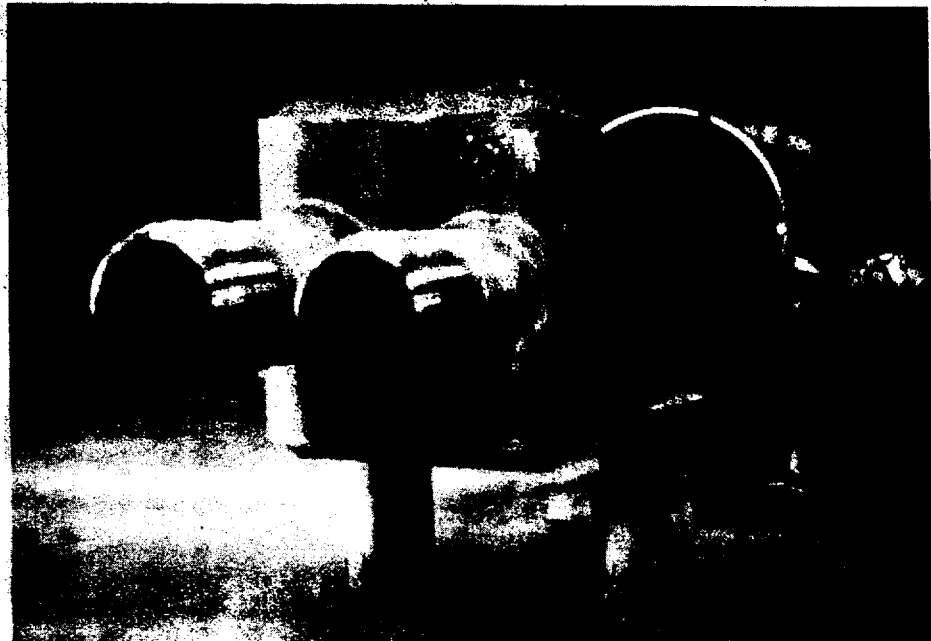
The pressure vessel, flanged at both ends, absorbs the loads. This plate-type construction permits the pressure to be increased to that achieved in conventional tubular equipment such as shell-and-tube, air-cooler and double-pipe types. At present there is, however, a design limitation in that the pressure difference between fluids must not exceed 40 bar.

Compact, lightweight Packinox exchangers are available in various metal alloys and in sizes which provide surface areas of 1000–10 000 m<sup>2</sup>. This enables them to provide a viable alternative to shell-and-tube exchangers for duties which previously could only be accomplished by the

**Figure 5.6** Packinox heat exchanger core



**Figure 5.7** Packinox heat exchanger – bundle and pressure vessel (courtesy of Nouvelles Applications Technologiques)



latter type. One such application is feed/effluent exchangers required for catalytic reforming plant in which the feed to the reactor is heated by the hot effluent from the process. The duty involves two fluids, at similar high pressures and temperatures, exchanging a large quantity of heat over a long temperature range. To achieve a mean temperature difference approaching that of countercurrent flow (see section 7.7), several multi-tube pass shell-and-tube exchangers in series are required. Alternatively, countercurrent flow is achieved by employing one or more 1/1 floating-head exchangers in series (see section 7.7), each having a long tube length, and known as 'Texas towers'.

The merits of the Packinox exchanger were shown at a refinery in Donges, France, in 1982, where four shell-and-tube exchangers for such a duty were replaced by a single Packinox exchanger. The Packinox exchanger contained 330 type-321 stainless-steel sheets, 8 m long, 1.1 m wide, to provide a surface area of 300 m<sup>2</sup> in a pressure vessel 13 m long and 1.8 m diameter. The whole unit weighed 45 tonnes. Design pressures and temperatures on both sides were 44 bar abs and 535 °C, respectively, with a pressure differential of 15.5 bar. It is claimed that the Packinox exchanger saves enough energy to pay for itself in two years.

### 5.3.3 Bavex exchanger

Invented in the early 1970s in West Germany for use in air separation plants, the Bavex exchanger is another all-welded, gasketless-plate heat exchanger and over 100 units are operating successfully in Europe. The heat transfer core is constructed from metal sheets 350 mm wide, up to 16 m long, and 0.2–1 mm thick. The plates are stamped and formed and then resistance welded at the edges on opposite sides in pairs. The corrugated pattern impressed in the plates provide an undulating flow path up to 16 m long and is termed the 'plate-side'. The double sheets are then assembled in banks and plasma-welded at the other edges to form another flow path at right angles to the plate-side. The shape of the second flow path, 350 mm long, is in effect a parallel row of tubes and is termed the 'tube-side'.

Because the exchanger combines both plate and tubular features it is known as the hybrid heat exchanger. The degree of plate pressing may be varied to provide indentations of 2.75–5.75 mm, giving tube diameters of 6–11.1 mm. The spacing between plates may also be varied to suit the nature of the plate-side fluid and ease steam jet or chemical cleaning. Headers are attached to the inlets and outlets of the plate- and tube-sides. Figure 5.8 shows the basic core of the Bavex exchanger.

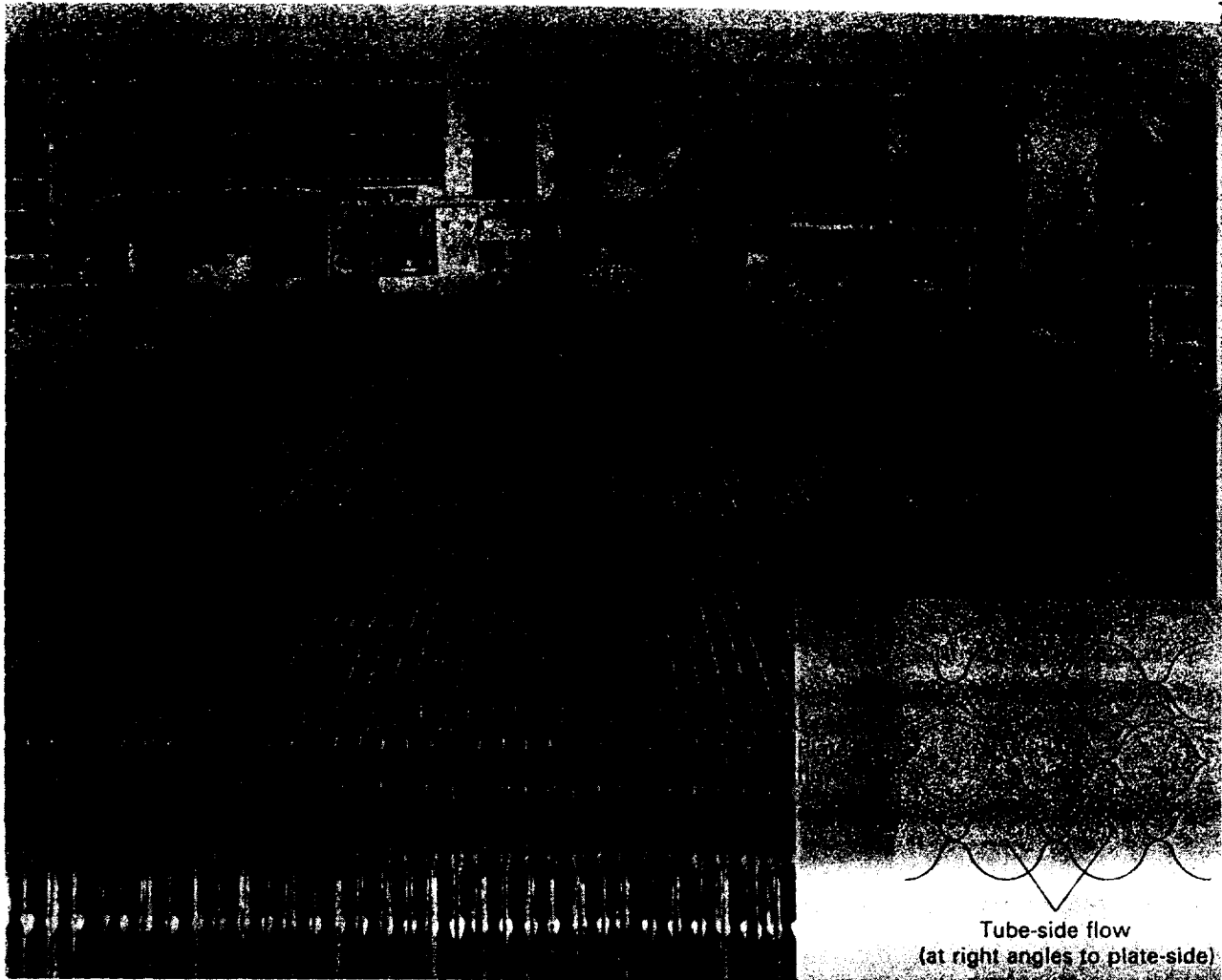
Compact, lightweight Bavex exchangers are available in sizes having 1500 plates in a single block, and surface areas up to 7500 m<sup>2</sup>. Design temperature range is –200 to +980 °C and the maximum pressure differential between the plate- and tube-sides is 80 bar. Although the basic flow pattern is unmixed, single pass, cross-flow on both sides, division plates and headers may be fitted on the tube-side to provide tube-side passes. The flow then becomes similar to that in a baffled shell-and-tube exchanger with the flow pattern approaching countercurrent (see section 7.7). The core may be constructed in a variety of metals including stainless steels, copper and its alloys, nickel and its alloys, titanium, Inconel™, etc.

## 5.4 Lamella heat exchangers

### 5.4.1 Application

The lamella heat exchanger is a modification of the floating-head shell-and-tube type and uses narrow rectangular-shaped flow channels, formed from strip instead of cylindrical tubes. The 'tube-side' fluid flows longitudinally inside the channels, or lamellae, while the 'shell-side' fluid flows longitudinally in the spaces between the channels. Unlike a shell-and-tube exchanger there are no shell-side baffles and therefore lamella exchangers provide true countercurrent flow. The single longitudinal pass on both sides reduces fouling and permits maximum pressure loss utilisation. Suspensions, slurries and fibrous liquids may be handled with ease.

This type of exchanger provides a lightweight, compact design with low liquid hold-up.



**Figure 5.8** Bavex heat exchanger core (courtesy of Bavaria Anlagenbau GmbH)

#### 5.4.2 Construction

The basic element consists of two thin metal strips which are plasma-welded together at the edges to form a long, narrow flow channel or lamella. The metal strips have a pattern of indentations along their length and the strips are spot-welded together at the indentations. The indentations serve the dual function of increasing turbulence and strengthening the lamella to permit higher operating pressures.

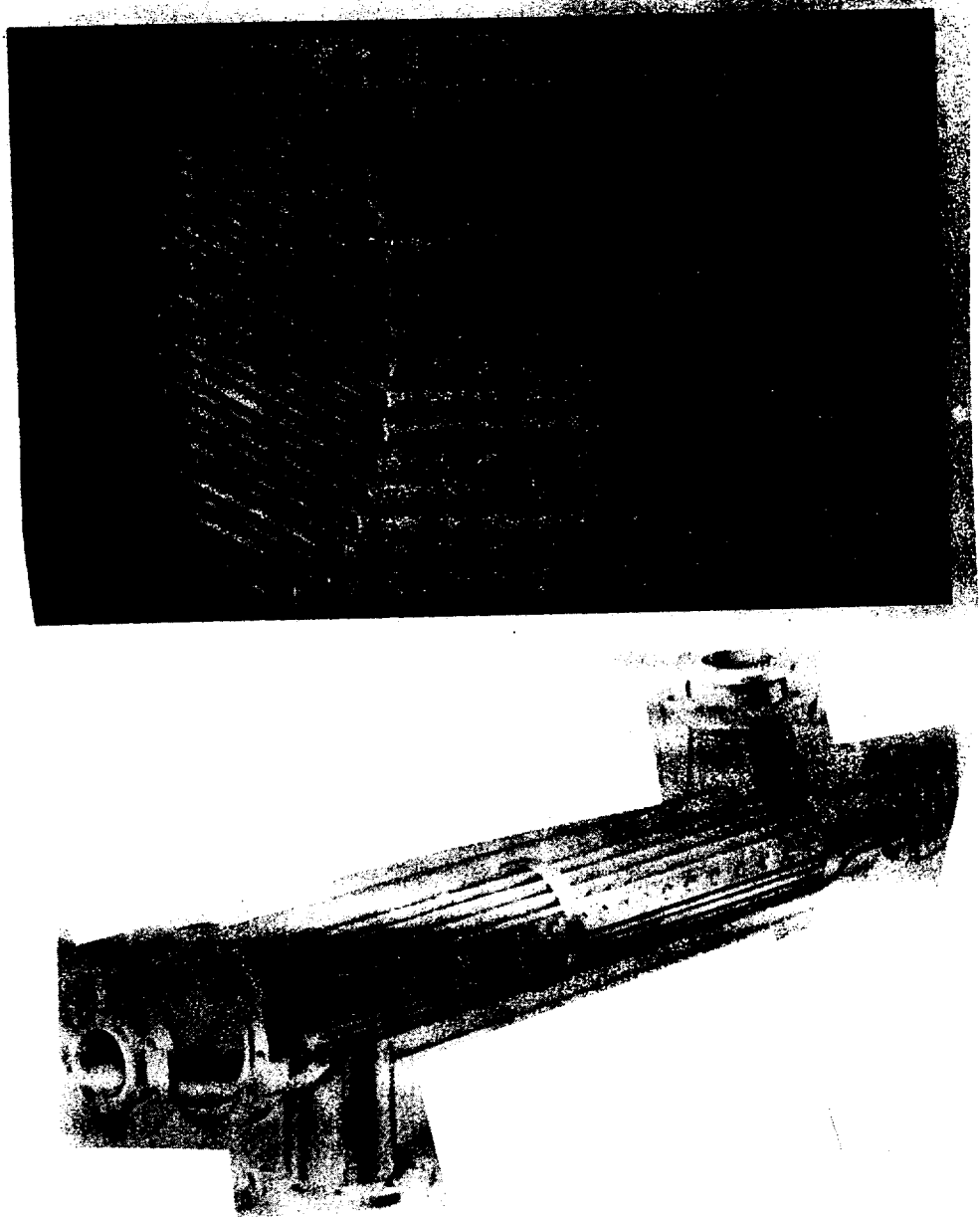
The elements are stacked together and welded at the ends to form a circular bundle which is inserted into a cylindrical shell. The distance between elements is maintained by studs welded to their outer surfaces. At both ends the bundles are welded at the periphery to conical headers, each header having an axial nozzle. At the 'stationary' end the conical header has a girth flange which is bolted to a flange attached to the end of the shell. A different construction is employed at the 'rear' end, however, which permits the bundle to 'float' within the shell, thus eliminating stresses between shell and bundle due to thermal movement. In order to contain the shell-side fluid, but permit bundle movement, it is necessary to use either a stuffing box or expansion bellow, similar to the methods used in shell-and-tube floating-head construction. The rear-end



nozzle flange must be removed before the bundle can be withdrawn, but otherwise bundle withdrawal and insertion follows shell-and-tube practice. The lamella heat exchanger is illustrated in Fig. 5.9.

As the fluid inside the lamella is contained entirely by welds, and not by gasketed joints, there is little likelihood of leakage of one fluid into the other, or to the atmosphere. Gasket selection is related solely to the shell-side fluid.

Figure 5.9 Lamella heat exchanger (courtesy of Alfa-Laval)



#### 5.4.3 Details of standard units

The lamella exchanger is available in a range of shell diameters and lamella lengths. Maximum lamella length is 6 m and there are twelve standard diameters between 125 and 1000 mm giving surface areas of 1–1000 m<sup>2</sup>. Maximum operating temperatures depend primarily on the

gasket material, being 220 °C for PTFE gaskets and 500 °C for asbestos gaskets (with a stainless-steel shell). Maximum operating pressures depend on shell diameters and range from 35 bar at 300 mm diameter to 10 bar at 1000 mm diameter.

Lamella materials may be type 304, 316 and 317 stainless steels, Incoloy 825™, Hastelloy C-276™, titanium and other weldable metals. Shell materials are similar with the addition of carbon steel. The strip thickness forming the lamella is 1.5–2 mm using a gap of 3–10 mm.

The distances between strips and the pattern of the indentations may be altered according to the application to provide optimum conditions. The same flow areas for the shell-side and tube-side fluids can be achieved if necessary. The combination of small hydraulic diameter, and enhancement provided by the indentations, results in high heat transfer coefficients, typical examples being given in Chapter 19. Lamella exchangers are not restricted to single-phase fluids and may be used for condensing and vaporising applications. Lamella bundles only, without shells, may be supplied if required.

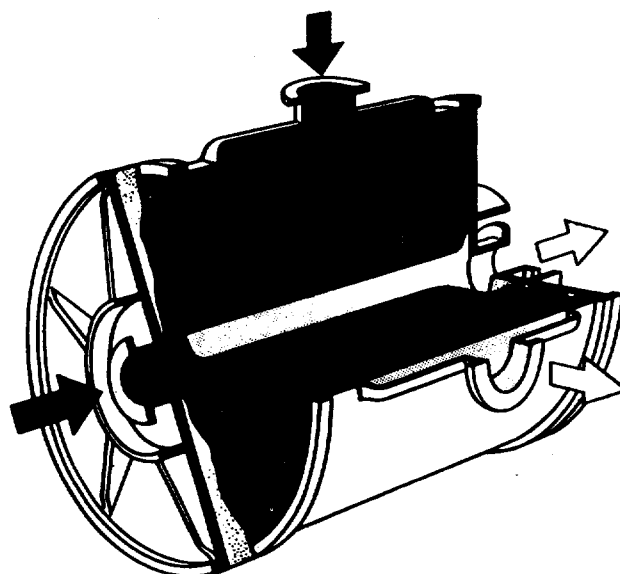
The surfaces inside the lamellae can only be cleaned by chemical means and therefore fouling fluids should be routed through the shell-side. Once the bundle has been withdrawn the external surfaces are readily cleaned by mechanical means.

## 5.5 Spiral heat exchangers

### 5.5.1 Application

The spiral heat exchanger is another 'plate type' unit in which the heat transfer surfaces are formed from plates and not cylindrical tubes. It consists of two sheet metal strips which have been wound from the centre around a roller to form two spiral, parallel channels, one for each fluid. The principle of the spiral heat exchanger is shown in Fig. 5.10.

**Figure 5.10** Principle of the spiral heat exchanger (courtesy of APV Co. Ltd)



The continuously curving single passages on both sides permit countercurrent flow and induce turbulence which enhances heat transfer and reduces fouling. The spiral heat exchanger is particularly effective in handling viscous liquids, sludges and liquids with solids in suspension, including slurries. As the coolant always enters the outer spiral turn of the unit, insulation is seldom required. Because identical passages can be provided for each fluid, it may be used for services in which the switching of fluids enables one fluid to remove scale deposited by the other. A spiral exchanger usually requires less than 60% of the volume, and less than 70% of the flooded weight, of a comparable shell-and-tube exchanger. It is not limited to single-phase fluids and may be used for condensing and vaporising duties.

The spiral heat exchanger is not a new concept and was introduced about fifty years ago for the paper and pulp industry. Although limited to a pressure of about 20 bar gauge its use in other industries may not have been exploited fully. For example, tests have shown that under certain conditions its performance as a vertical thermosyphon is better than the traditional shell-and-tube exchanger.

### 5.5.2 Construction

The distance between sheets in both spiral channels is maintained by spacer studs welded to both sheets prior to rolling. After the spiral pack has been rolled, alternate top and bottom edges of the passages are normally welded together and each end closed by a gasketed flat or conical cover bolted on to the spiral body. Thus any leakage across the gasket occurs either from the periphery of the cover to the atmosphere, or from one passage to the next containing the same fluid. Mixing of the two fluids cannot occur. When dealing with a fluid which must not leak to the atmosphere – for example, sulphuric acid – its flow channels are completely sealed off by welding both top and bottom edges together. Removal of the covers enables the entire length of the passages to be inspected and mechanically cleaned. The single passage on each side permits chemical cleaning without opening the unit if required.

The hot fluid enters the unit at the top or bottom cover via a central axial nozzle and flows from inside to outside, where it leaves via a header welded to the periphery. The cold fluid enters via a similar peripheral header and flows towards the centre where it leaves at the top or bottom cover via a central axial nozzle. Several flow configurations are possible.

### 5.5.3 Details of standard units

The spiral exchanger is available in diameters of 600–1800 mm and heights (i.e. sheet widths) of 200–1800 mm, giving surface areas up to 350 m<sup>2</sup>. Maximum operating temperature is 400 °C and maximum operating pressure 20 bar gauge. The exchanger may be fabricated in any metal which can be cold-formed and welded, such as carbon steel,

stainless steels, high-nickel alloys, titanium, etc. The sheet thickness is normally 1.8–4 mm.

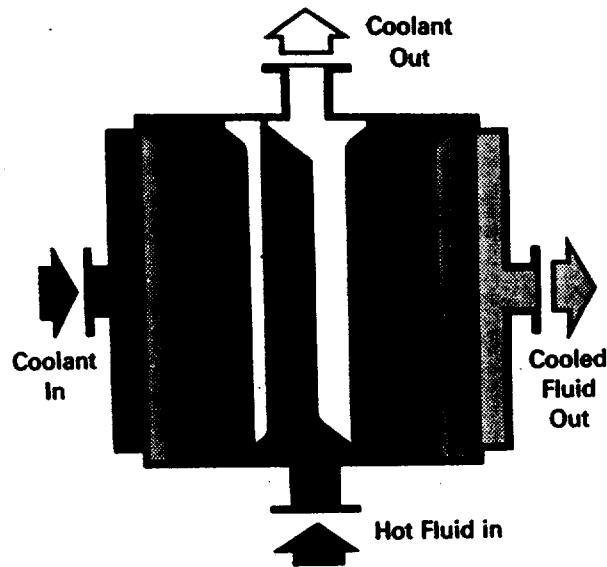
The distance between sheets is in the range 4–20 mm and may be selected for each application to provide optimum conditions. The combination of small hydraulic diameter, and enhancement induced by the curvilinear geometry of the spirals, results in high heat transfer coefficients, typical examples being given in Chapter 19. Overall heat transfer coefficients up to 50% greater than those for conventional tubular exchangers, for the same pressure losses, may be achieved. Sometimes the spacer studs are omitted in order to handle liquids with a high fibre content.

#### 5.5.4 Flow arrangements

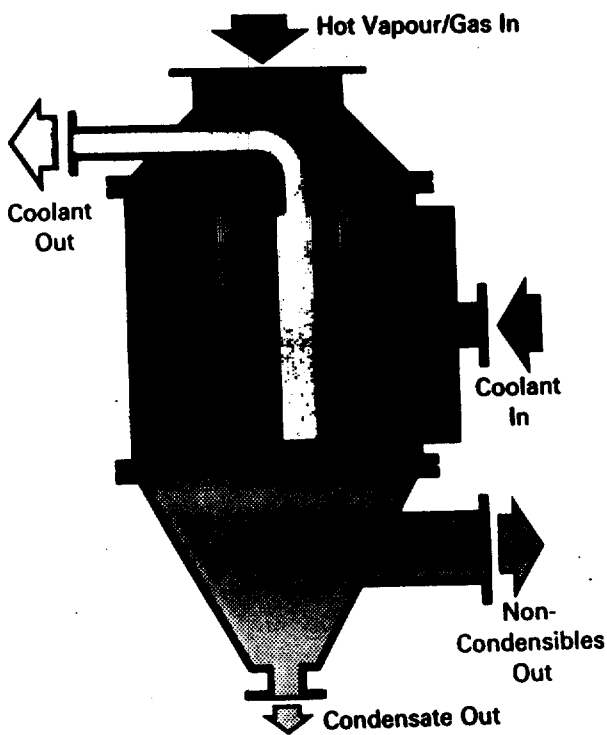
In type 1 flow arrangement (Fig. 5.11(a)) both fluids flow spirally in countercurrent flow and may be used for liquid–liquid, condensing and gas-cooling applications. The unit is usually mounted vertically, particularly when one fluid is a condensing vapour, in which case an additional bottom nozzle for condensate removal is fitted. Horizontal mounting is normal for handling high concentrations of solids which will tend to fall to the invert of each spiral when settling out during periods of low flow rates or standby. Upon resumption of normal flow, the restriction formed by the deposited solids causes proportionate increase in local velocity which re-entrains the solids and carries them out of the unit.

Type 2 flow arrangement (Fig. 5.11(b)) is termed spiral flow/cross flow, one fluid being in spiral flow and the other in cross flow. To achieve this, the spiral-flow passages are welded at each side, but the cross-flow passages are open at each end. This type is particularly suited to handling low-density vapour or gas, which is routed through the straight passage to achieve a low-pressure loss. It may be used for liquid–liquid applications when the flow rate of one fluid is considerably greater than the other. The headers are different to type 1 and comprise either cones, bonnets or extensions with flat covers. The units are mounted vertically for condensing and vaporising applications, but otherwise may be mounted horizontally or vertically.

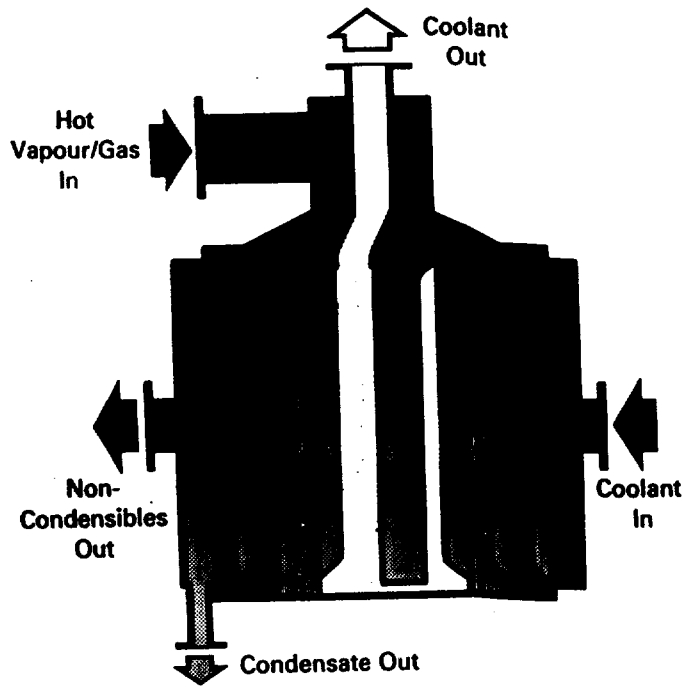
Type 3 is a condenser which is usually mounted vertically (Fig. 5.11(c)). It is designed to cater for the sub-cooling of both condensate and non-condensables and is particularly effective under vacuum. The coolant enters the periphery and flows in a spiral path to the centre where it leaves at the top via a pipe which passes through the vapour inlet dome. Removal of the bottom cover exposes the coolant passages. The removable vapour dome is shaped to distribute vapour uniformly into the central part of the open annuli, which comprises the condensing zone. Several of the outermost turns of the vapour passage are shielded such that non-condensables flow into these relatively small passages, to flow in a spiral path outward and countercurrent to the coolant. The non-condensables are removed via a nozzle towards the top



(a) Type 1: fully countercurrent



(b) Type 2: spiral flow/cross flow



(c) Type 3: distributed vapour, spiral flow

Figure 5.11 Spiral heat exchangers – types 1, 2 and 3

of a peripheral header, at a temperature close to that of the coolant inlet. Condensate in the central condensing zone falls to the bottom to flow outwards in a spiral path countercurrent to the coolant to achieve sub-cooling. The condensate is removed via a nozzle at the bottom of the peripheral header containing the non-condensable exit nozzle.

## 5.6 Plate-fin heat exchangers

### 5.6.1 Application

The use of aluminium plate-and-fin heat exchangers has been established for nearly thirty years. The advantages of compactness, low mass, low heat capacity, good ductility and increasing strength at low temperatures of the alloys involved give particular advantages in cryogenic service.

The plate-and-fin form of heat exchanger construction and the aluminium dip-brazing techniques were first combined for aircraft applications in which a high performance/weight ratio is essential. By extension of the technology and of the manufacturing facilities it has been possible to maintain the high performance of this type of construction for the much larger assemblies required for industrial plants.

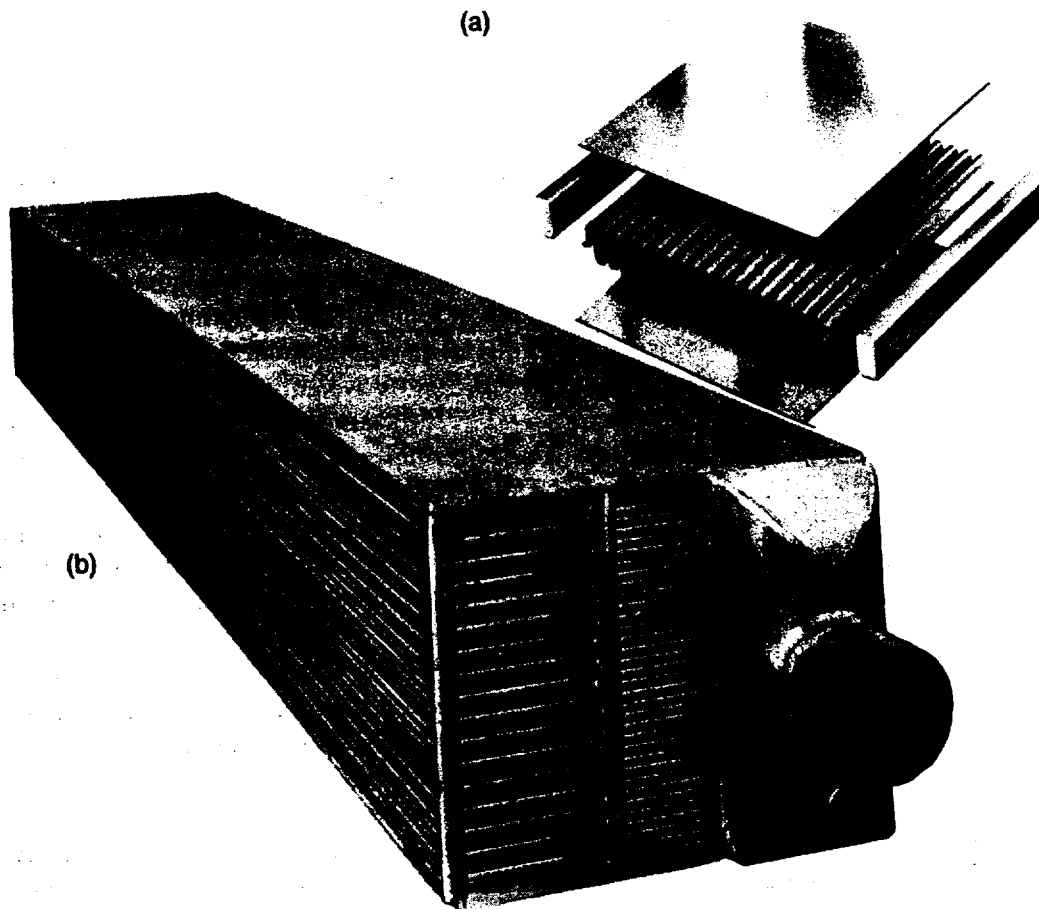
Efficient heat exchanger designs can be provided for any combination of gas, liquid and two-phase streams. A particularly useful feature is the ability to process several streams in a single matrix, and this is of great use in cryogenic applications.

Plate-and-fin heat exchangers have been established for use in air-separation plants and helium liquefaction plants since the early 1950s. The use of ethylene plant dates from 1958, and the early 1960s saw an expansion into 'nitrogen wash' ammonia plants, hydrogen purification plants and natural gas plants. Many other uses have been found in the chemical industry and still further uses are being explored. In some cases filtering of the inlet streams is necessary to overcome possible tendencies to blockage of particular matrix constructions, while other precautions such as cleansing of process fluids are necessary where certain impurities could be harmful to aluminium. The use is not limited to pure heat exchange, and purification by deposition of solids and some fractionation are both possible in this form of construction.

### 5.6.2 Construction

The basic element consists of two flat plates, a strip of corrugated sheet and two edge-sealing bars as shown in Fig. 5.12(a), the corrugated sheet and edge bars being brazed to the flat plates. A number of such elements are stacked together to form a block, which may be designed to incorporate a variety of flow patterns. The flat plates are termed 'primary surface' and the corrugations as 'secondary surface'.

Each block is assembled in a prescribed sequence into specially designed jigs for dip-brazing. The brazing medium is incorporated in the build-up to provide uniform bonds throughout the assembly. Extreme care is taken to ensure high bond integrity as the bonds provide not only the thermal contact between primary and secondary surfaces, but also the mechanical ties to withstand internal pressure loadings. After dip-brazing each block is subjected to extensive washing and cleaning procedures before passing to the final manufacturing stages. Here header tanks and ancillary fittings are attached by argon-arc welding and blocks



**Figure 5.12**  
 (a) Exploded view of a single plate-fin element;  
 (b) complete block in course of manufacture  
 (courtesy of Marston-Palmer Ltd)

incorporated into multi-block batteries or cold-box installations.

Final inspection includes hydraulic pressure tests and also leak tests on each individual stream in each block and pneumatic tests on multiple assemblies. Flow-balancing tests to fine limits may be required. Where the highest standards of tightness against inter-stream and external leakage are required, vacuum tests using helium gas and mass spectrometer detection equipment are made. A complete block is shown in Fig. 5.12(b).

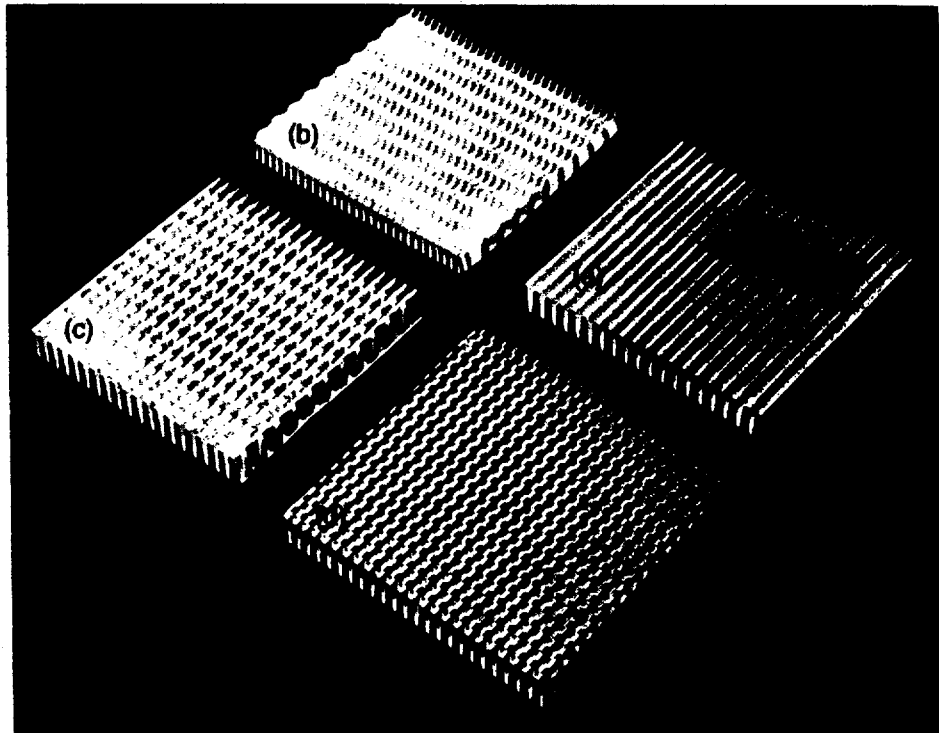
### 5.6.3 Corrugation types

Four corrugation types – namely plain, plain perforated, herringbone and serrated – are shown in Fig. 5.13. The plain type has straight through passages while the plain perforated type is similar, except that holes are punched in the corrugated sheet. The corrugations of the herringbone type are formed into continuous waves. In the serrated, or multi-entry type, the corrugated sheet is cut such that the fins are in staggered formation.

Typical corrugations have thicknesses of 0.203–0.61 mm, corrugation heights of 3.81, 6.35, 8.89 and 11.79 mm, fin densities of 236–708 fins/m yielding a high surface area to matrix volume ratio of 1230 m<sup>2</sup>/m<sup>3</sup>.

The serrated and herringbone corrugations give substantially increased

**Figure 5.13** Corrugation types of plate-fins  
 (a) plain (b) plain perforated  
 (c) herringbone  
 (d) serrated (courtesy of Marston-Palmer Ltd)



heat transfer coefficients compared with straight tubes or plain corrugations, the serrated corrugation, for instance, giving an increase of about four times the straight tube value. The friction factors for the serrated and herringbone types are also increased, so that a greater cross-section is required to maintain the same total pressure drop for a given thermal duty; nevertheless, there is a significant reduction in surface area and, consequently, in matrix volume.

While these characteristics lead to an attractive design of heat exchanger, the advantages of this construction are further enhanced by its inherent versatility. Corrugation heights may be chosen differently in the various streams as, for instance, in liquid-to-gas heat exchangers where low-height corrugation may be used for the liquid stream and tall corrugation for the gas stream, thus matching the product of heat transfer coefficient times area in the liquid stream to that in the gas stream. It is also possible to use two layers on the gas stream for every single layer on the liquid stream. The type of corrugation (plain, serrated, etc.) may also be chosen differently in each stream to attain the same purpose. Optimum use of pressure drops may be achieved in the same way.

The corrugation type is often selected for reasons other than heat exchange. For instance, in the standard air separation plant reversing exchanger, the corrugations are selected chiefly in relation to their suitability for the deposition and subsequent sublimation of solids.

#### 5.6.4 Matrix sizes and pressure limitations

Matrices of the counter-flow type can be brazed up to a size of 1200 mm wide, 1230 mm stacked height and 6200 mm long. This size is suitable for



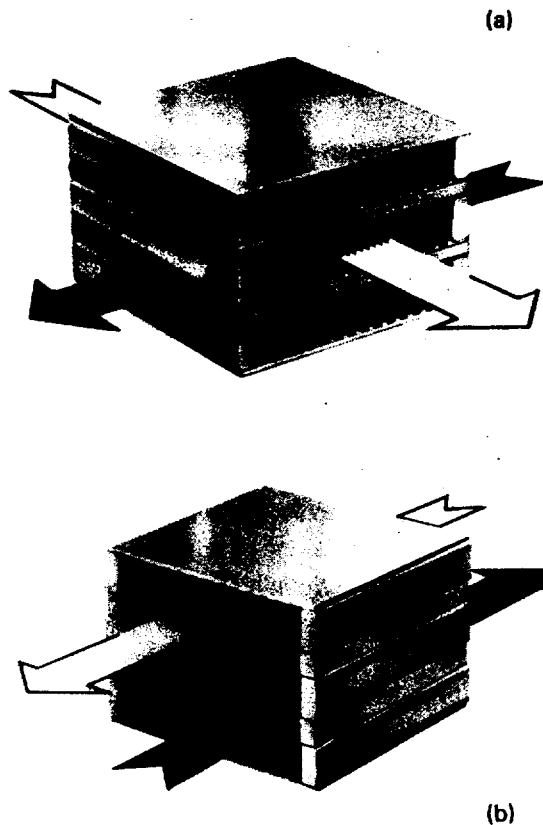
steady pressures of up to 25 bar but when used in the reversing service of air separation plants, the arduous duty imposed by approximately one million pressure reversals over a life of some twenty years reduces the maximum allowable pressure to 11 bar.

The major determinants for operating pressures are the stresses within corrugations and their brazed joints and the junctions of header tanks to the matrix. At present, design pressures up to 80 bar are available, depending upon the overall cross-section.

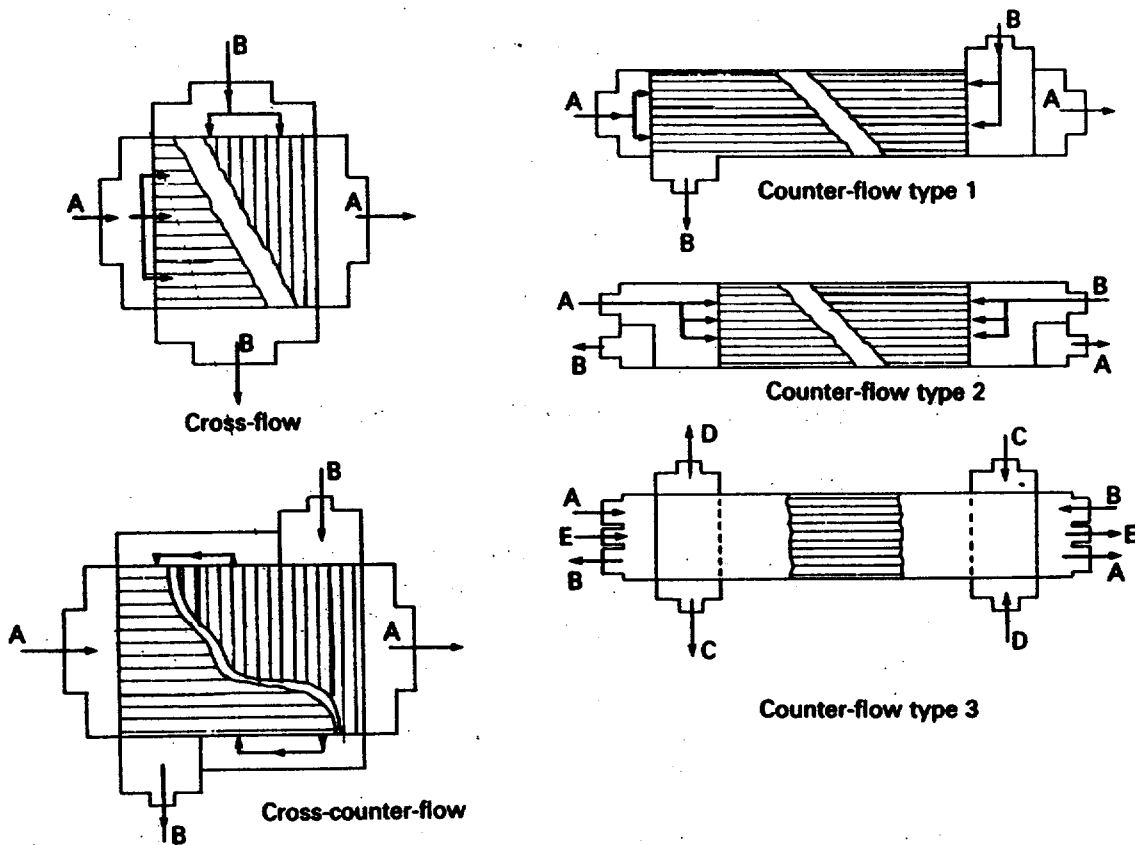
### 5.6.5 Flow patterns

The basic flow patterns are cross-flow and counter-flow as shown in Fig 5.14. However, by the inclusion of suitable internal seals, distributors and external headers various multi-pass and multi-stream patterns may be provided (Fig. 5.15). Counter-flow units are usually required when there is a close terminal temperature approach in relation to the overall temperature range. Type 1 is suitable for handling a moderate pressure stream A; type 2, a symmetrical arrangement, is suitable for reversing duty and for higher steady operating pressures; and type 3 may be used for 3-5 streams.

**Figure 5.14** Basic flow arrangements of plate-fin exchangers (a) cross-flow (b) counter-flow (courtesy of Marston-Palmer Ltd)



The cross-flow unit is suitable when the temperature approach is not especially close, but in some applications the cross-counter-flow unit may provide a better solution.



**Figure 5.15** Multi-pass and multi-stream patterns of plate-fin exchangers (based on data supplied by Marston-Palmer Ltd)

### 5.6.6 Multi-stream units

The versatility of the construction is also demonstrated by its ability to process several streams. Each stream is allocated a suitable number of passages and the header system at the ends of the matrix permits five separate streams to be accommodated with ease. This is of particular advantage in the field of cryogenic processes. Owing to the thermal bonds linking plates and corrugations throughout the matrix, there is a continuity of metal temperature in each direction. Provided that each individual stream is evenly distributed across the whole matrix cross-section the separation plate temperature will also be reasonably constant over the whole cross-section. The local metal temperature controls the heat transfer rate for each separate stream. If several cold streams enter the heat exchanger at different temperatures the coldest streams will heat up more rapidly due to the greater temperature difference between that stream and the metal.

It is quite feasible in these circumstances to include a 'cold' stream in the heat exchanger which has an inlet temperature higher than that of the warm-stream outlet. This return stream would be slightly cooled at inlet, before starting to warm up. The basic requirement is that the weighted mean of all cold-stream inlets must be below the required warm-stream outlets. Where widely differing conditions are specified, often including two-phase operation a step-by-step analysis may be required.

A further variety of multi-stream unit can be obtained by placing bars across the width of the block thus enabling one stream to be taken out part way down the length of the matrix and permitting another stream to be inserted at the other side of the bars in the same passages. This enables several 'hot' streams at different temperature levels to be cooled by the same group of 'cold' streams in one matrix, with consequent savings in pipework and pressure drop.

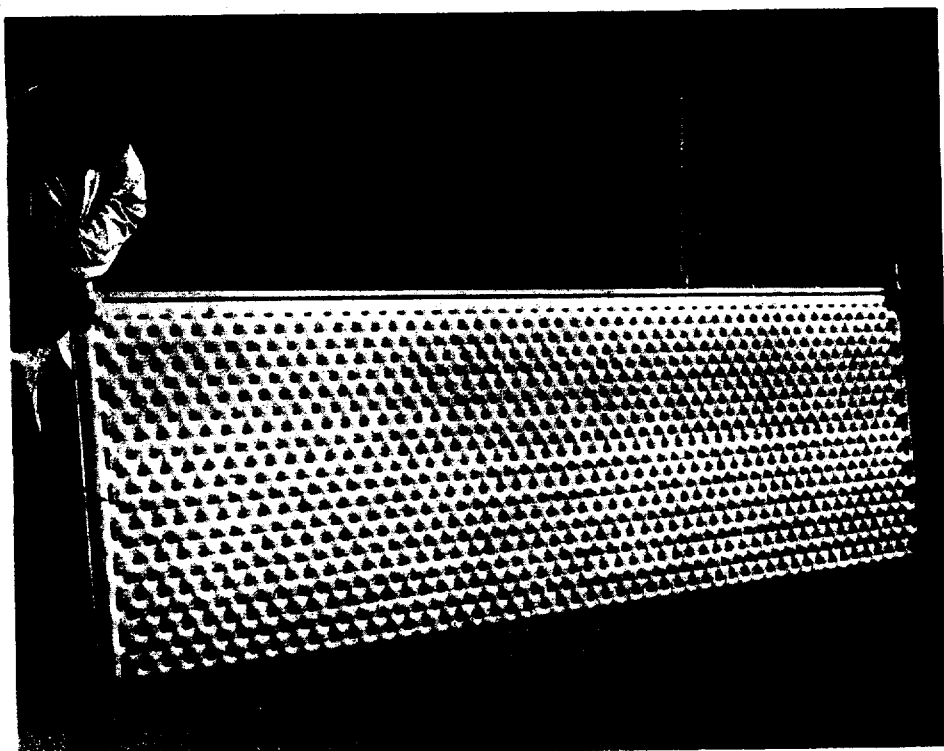
## 5.7 Embossed-panel heat exchangers

### 5.7.1 Application

Although formed from plates, embossed-panel heat exchangers bear no relation to the gasketed and other plate-type exchangers previously described. For numerous applications the embossed-panel heat exchanger can offer thermal, space-saving and other economic advantages over conventional tubular equipment.

The lightweight, compact, panels may be supplied in a variety of sizes and shapes, flat or curved, and are used in many industrial and process applications. The panels may be designed as direct immersion units; integral and clamped-on vessel jackets; falling film, cascade and fluidised bed exchangers; heat shields and cooling trays; and banks for installation associated with heat recovery systems, etc. A typical panel is shown in Fig. 5.16.

**Figure 5.16** Typical embossed panel (courtesy of Senior Platecoil Ltd)



### 5.7.2 Construction

The basic unit comprises two flat metal sheets which are welded together at the perimeter and at spots, in a predetermined pattern, over the core of the plate. By a patented method the interspace of one product is expanded under hydraulic pressure to provide internal flow passages and an embossed external surface of which there are two forms. A double-embossed unit on both sides, whereas a single-embossed unit is embossed on one side only with a flat surface on the other side.

An electric resistance welding technique is employed for standard units and the welding pattern is computer controlled. As the hydraulic pressure required to form the unit can be 4–5 times greater than the recommended maximum operating pressure for service, the expansion process ensures weld integrity. More sophisticated leak tests may be applied if warranted by the service, but a standard air-under-water pressure test is always a mandatory procedure on completion of manufacture.

Although the standard shape of a unit is rectangular, it is not restricted to this and other shapes, dependent on flow pattern, may be provided. An important feature is that both single- and double-embossed units may be supplied as curved, instead of a flat section, and provided with cut-outs if necessary.

### 5.7.3 Details of standard units

A large number of standard panel sizes are available with depth  $\times$  length ranging from 300  $\times$  600 mm to 1200  $\times$  3600 mm. Internal flow is not restricted to a single pass, and two or four passes are provided on certain styles.

Such a construction is achieved by welding the sheets together with continuous weld divisions to provide 'zones'. There is also considerable flexibility by style selection with regard to the positioning of the connection pipes, both on the panel and in relation to another, and the required configuration is achieved by providing similar 'zones' to direct the flow.

The materials include carbon steel, stainless steel, titanium, monel<sup>TM</sup>, nickel and the high-nickel alloys. Standard double-embossed units in carbon steel and stainless steel have sheet thicknesses of 1.5 and 2.0 mm, standard single-embossed units have dissimilar sheet thicknesses varying between 1.5 mm on 2.5 mm and 2.0 mm on 3.0 mm. Maximum operating pressures for carbon steel, stainless steel and monel panels are 18 bar gauge for standard double-embossed units and 12 bar gauge for standard single-embossed units. Standard titanium panels are normally available as double-embossed units only, suitable for an operating pressure of 7 bar gauge up to 165 °C.

### 5.7.4 Installation

A complete installation may comprise one or more units stacked together side by side to form a 'bundle', which may be installed in a duct or

vessel, or used as an immersion-type heater or cooler in a still or agitated tank. In the latter case the units require to be suitably braced to resist the forces set up by the agitator. Immersion-type units may be suspended in the bulk of the tank contents, or hung against the sides of the tank. Both methods permit rapid replacement.

The curved single-embossed units are ideal for clamping to the external curved surfaces of tanks and vessels, or as integral vessel sections to provide a heating or cooling jacket, which, in the case of vessels, can include the dished ends. The attachment for clamping is either by banding, if welding to the container is not permitted, or by bolting to lugs welded to the container. Spring-loaded bolts are used if there is appreciable thermal expansion or contraction and the application of a non-hardening heat transfer mastic is recommended between the panels and vessel to seal air gaps and improve heat transfer. Clamp-on panels are normally limited to holding operations or moderate temperature gradients on heating and cooling.

## 5.8 Graphite heat exchangers

### 5.8.1 Properties of impregnated graphite

'Carbon' and 'graphite' are frequently used synonymously, but in heat exchangers these terms mean different things. Carbon is difficult to machine but is a good thermal insulator, its thermal conductivity being only 5 W/m K, which is about one-tenth of that of steel. Graphite is easy to machine and is a good thermal conductor, its thermal conductivity being 147 W/m K, which is almost three times as high as steel. Graphite therefore has the desirable properties for heat transfer equipment.

Graphite itself has inherent porosity, but it is made impervious by impregnating it under pressure with chemically resistant resins, such as furanic or phenolic, and polymerising with heat. The resultant impregnated graphite is impervious to solutions under pressure, while its desirable properties are unchanged. Although the impregnation process doubles the coefficient of thermal expansion it is still only  $4.6 \times 10^{-6}/K$  compared with steel at  $11.5 \times 10^{-6}/K$ . The combination of high thermal conductivity and low coefficient of thermal expansion gives impregnated graphite excellent resistance to thermal shock and it will not spall or flake. The graphite has a density of 1750 kg/m<sup>3</sup> which is about one-quarter of that of steel.

Although the unimpregnated graphite is not affected by extremely high temperatures, the resin used in the impregnation process restricts the maximum operating temperature of the impregnated material to about 220 °C. Other characteristics reflect its highly anisotropic nature. It is strong in compression but weak in tension, its thermal conductivity is directionally based, it cannot be welded or cast, and it is not ductile or malleable. The manufacture of graphite equipment therefore requires a different technique to that employed with metals. The design of

equipment should exploit its ability to absorb compressive stresses while minimising tensile stresses, and heat transfer surfaces should be orientated to provide heat flow in the direction of highest thermal conductivity.

Impregnated graphite is one of the most chemically inert materials available and is resistant to a wide range of fluids. Unlike metals, its resistance to deterioration does not depend on the formation of a protective surface film and is not affected by aeration or fluid velocity.

In the galvanic series, graphite is always found at the most noble end. Depending on the type of impregnant, it can be used with most concentrations of hydrochloric, phosphoric, sulphuric and hydrofluoric acids at low and high temperatures. Organic acids and their salts, and alkalis and their salts, have little effect. It will withstand neutral and reducing environments, but oxidising conditions require careful consideration. In all cases, consult the manufacturer.

Because of its unique properties there is an incentive to use graphite as a material of construction for heat transfer equipment. Heat exchangers of the shell-and-tube type have been available since the mid-1930s but as these do not exploit the full potential of graphite, this led to the development of the familiar block type.

### 5.8.2 Shell-and-tube type

Graphite shell-and-tube exchangers are generally available as outside-packed floating-head designs and are similar in construction to the metallic types, but the longest graphite tube in a single piece is 3.8 m. Longer lengths are provided by joining two tubes together using a cemented lap-over or scarf joint. Standard tube outside diameters are 31.75, 37 and 50.8 mm, with wall thicknesses of 5.58, 6.5 and 7.9 mm respectively. Radial tube wall thermal conductivity is about 50 W/m K, but despite the need to use thick tubes, the wall conductance is similar to that of a stainless-steel tube having commonly used thicknesses of 1.8–2.4 mm. The ends are cemented to solid graphite tubesheets, 75–785 mm thick. The headers, baffles and spacers are usually graphite and the corrosive fluid is normally routed through the tubes.

The shell is normally carbon steel, but it may be stainless steel, copper, aluminium, or carbon steel lined with lead, rubber or glass, depending on the corrosive nature of the shell-side fluid. The pass arrangements on both sides follow conventional shell-and-tube practice. When a tube has to be replaced, the new tube is cemented into the tube-hole using a sleeve. The joint is compressed by bulk loading and then exposed to moderate heat for 24 hours.

Graphite shell-and-tube exchangers are available in various lengths, shell diameters of 203–1880 mm and surface areas of 1.6–1650 m<sup>2</sup>, and are recommended for surface areas greater than 240 m<sup>2</sup>. The design pressures depend on the model and fluid temperatures; 6 bar gauge can be readily achieved and higher in many cases.

### 5.8.3 Block type

#### Cubic and rectangular type

These exchangers consist of a graphite block perforated longitudinally by horizontal parallel rows of holes, each alternate row being for the process fluid and service fluid respectively.

The holes for the process fluid run at right angles to those for the service fluid. The block is permanently compressed between metallic clamping plates by means of tie bars passing through lugs. The lugs are provided at the corners for the cubic model, and along the side and corners for the rectangular model.

Headers are bolted to the four faces of the block which convey the two fluids and may be graphite, cast iron, carbon steel or lined with rubber or resin, according to the corrosive nature of the fluids. Suitable gaskets are used between the header and block so that failure of any gasket results in leakage to the atmosphere, and not from one fluid to the other. Single- or multi-pass arrangements may be provided. Hole diameters are 9.5 and 12.7 mm for clean services and 19 mm for fouling and vaporising services. In the case of clean process fluids, slots instead of holes may be provided on the process side, which doubles the heat transfer surface area.

Figure 5.17 shows a typical example.

**Figure 5.17** Rectangular block-type graphite exchanger (courtesy of Robert Jenkins Systems Ltd)



This type of exchanger is available in a range of standard sizes, having surface areas of 0.65–153 m<sup>2</sup>, with a design pressure of 5.2 bar gauge, and

higher in many cases. These units are particularly suited for applications where the corrosive nature of both fluids necessitates the use of graphite.

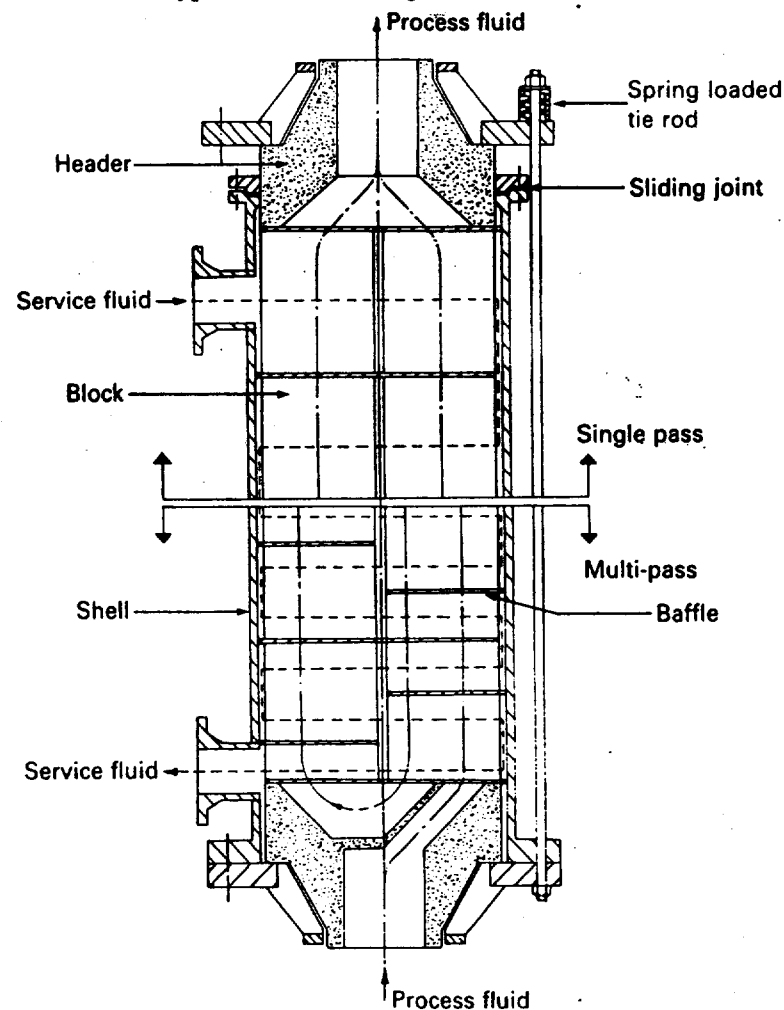
A special range of small block-type exchangers, having surface areas of 0.17–5.6 m<sup>2</sup>, is available for installation into glass process piping without alteration to the glass fittings.

#### Multi-block type

The basic graphite block is a cylindrical billet having axial holes for the process fluid and transverse holes for the service fluid. The blocks are placed one against the other inside a cylindrical shell which may be horizontal or vertical. Polytetrafluoroethylene (PTFE) gaskets are used between adjacent blocks which avoids the use of potentially weak cemented joints. Depending on the model there may be 2–25 blocks, 110–482 mm in depth with hole diameters of 8, 10, 13, 16 and 18 mm on the process side and 8, 10 and 13 mm on the service side. The blocks are maintained in compression by external spring-loading devices while the ends of the shell have gland fittings.

The service fluid makes a series of cross-flow passes through the graphite core, the crossover from one pass to the next occurring in an annular space between core and shell. The shell is usually carbon steel, but may be lined if the service fluid is aggressive. The process fluid may be routed axially through the core with single- or multi-pass flow. The multi-block type is shown in Fig. 5.18.

**Figure 5.18** Multi-block-type graphite exchanger (courtesy of Robert Jenkins Systems Ltd)





They are available in a standard range having surface areas of 0.22–240 m<sup>2</sup> with a design pressure of about 6 bar gauge and higher in many cases. The units are flexible in that they may be enlarged or reduced by the addition or removal of blocks, and are easily stripped down for maintenance.

#### **Cartridge type**

This is similar to the multi-block type, but has a laminated graphite cartridge, with axial holes for the process fluid and transverse slots for the service fluid. Surface areas of 0.16–18.6 m<sup>2</sup> are available.

## **5.9 Glass heat exchangers**

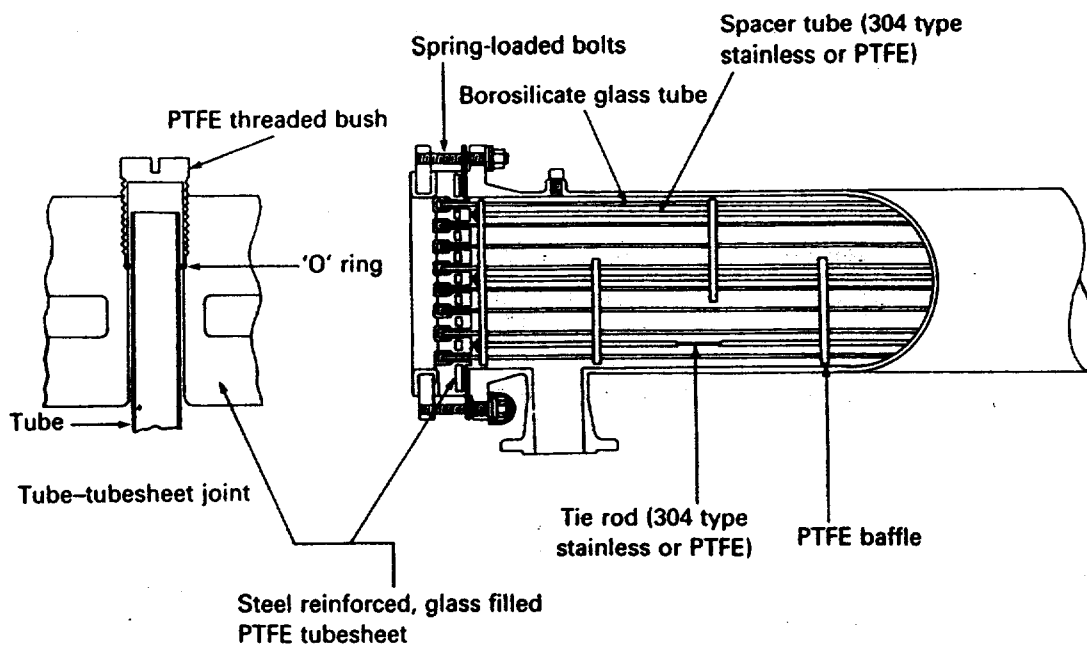
### **5.9.1 Properties of borosilicate glass**

Although glass is attacked by all concentrations of hydrofluoric acid, hot concentrated phosphoric acid and alkaline solutions above pH 11 and 40 °C, its resistance to chemical attack by many other fluids is excellent and only certain precious metals and plastics are superior. The exceptionally smooth surface of glass prevents the formation of deposits and enables it to be cleaned and sterilised readily. Fluids processed in glass equipment are free from contamination. Its undesirable properties for heat transfer equipment are low thermal conductivity, low resistance to thermal shock and low strength, particularly in tension.

Various glasses with improved properties have been developed for specific purposes, among them being borosilicate glass which is widely used in the chemical process industries. Borosilicate glass contains about 80% silica, 13% boric oxide plus soda and alumina. Its thermal conductivity is 1.14 W/m K, which is about six times the value for PTFE but only one-fiftieth of the value of steel. Nevertheless, shell-and-tube heat exchangers fitted with borosilicate glass tubes are made, a typical tube size being 14 mm outside diameter and 1 mm thick. The conductance of the tube wall is therefore 1100 W/m<sup>2</sup> K and only in a small number of applications will it be the controlling resistance. However, operating conditions are limited to 5 bar gauge pressure at 175 °C.

### **5.9.2 Construction**

Typical exchangers for operation up to 5 bar gauge have diameters of 229 and 305 mm, with tube lengths of 2015–4015 mm, giving surface areas of 6.3–26 m<sup>2</sup>. Standard materials for other parts are carbon steel shells, PTFE baffles, steel reinforced PTFE tubesheets and PTFE-lined end flanges, but other materials may be used for the shell, depending on the corrosive nature of the shell-side fluid. Each tube–tubesheet joint consists of an external ‘O’ ring, made of fluorinated ethylene propylene (FEP), or similar, compressed by a PTFE threaded bush. Hence tubes are readily removed and replaced (Fig. 5.19).



**Figure 5.19** Glass heat exchanger (courtesy of Corning Process Systems)

Shell-and-tube exchangers of similar construction, but having glass shells, are also available for applications where the corrosive nature of both fluids warrants the use of glass. Standard diameters are 75, 152, 229 and 305 mm which provide maximum operating pressures of 3.45, 1.38, 1.03 and 0.76 bar gauge respectively. These exchangers provide the additional advantage of transparency.

## 5.10 Teflon™ heat exchangers

### 5.10.1 Properties of Teflon™

Fluorinated ethylene propylene (FEP) provides an unusually high resistance to chemical attack, elimination of product contamination and good electrical insulation compared with conventional plastic. Unfortunately these desirable properties are accompanied by low strength and a low thermal conductivity, being 0.19 W/m K compared with 16 W/m K for stainless steel, which is regarded as a poor metallic conductor. On this evidence, FEP would not appear to be an attractive tube material for typical heat transfer equipment.

However, in 1965 Du Pont introduced a range of shell-and-tube heat exchangers and immersion coils containing thin, small-bore, closely packed tubes made of Teflon™ FEP fluorocarbon resin. These units use tubes having outside diameters of 6.35, 3.175 and 2.5 mm, according to the service, with wall thicknesses of 0.635, 0.3175 and 0.25 mm respectively. The non-stick properties of FEP ensures that fouling is kept to a minimum, which tends to compensate for the relatively low thermal conductivity of the wall compared with metallic tubing.

Published operating limits for the Teflon™ tubing are as follows:

Operating temp. (°C)	Maximum operating pressure (bar)		3.175 and 2.5 mm dia. Internal
	6.35 mm dia. Internal	External	
20	10.0	4.8	10.5
50	6.6	3.2	7.6
100	3.8	1.6	4.7
150	2.2	1.0	2.9

Typical overall heat transfer coefficients are 140–330 W/m<sup>2</sup> K, depending on tube diameter, of which the wall conductances for the 6.35, 3.175 and 2.5 mm diameter tubes are 300, 600 and 760 W/m<sup>2</sup> K respectively.

### 5.10.2 Shell-and-tube exchangers

The shell-and-tube exchangers are of single-pass, countercurrent-flow design, having removable tube bundles. The standard exchanger has a carbon steel shell and carbon steel headers, lined with Teflon™, and the corrosive fluid is routed through the tubes. If both fluids are corrosive the shell may be carbon steel, lined with Teflon™, but solid fibreglass or stainless steel may be used.

The special feature of the shell-and-tube exchangers is the joining together of all the tubes at each end into an integral honeycomb tubesheet. The close packing provides a surface area per unit shell volume up to four times greater than conventional units.

The exchangers are supplied in various lengths, with diameters of 101.6–254 mm. Model 525, for instance, contains 525 tubes, 6.35 mm outside diameter, and may be supplied with effective tube lengths of 0.91–4.88 m, giving heat transfer surface areas of 9.3–50 m<sup>2</sup>. Figures 5.20 and 5.21 show constructional details.

### 5.10.3 Immersion coils

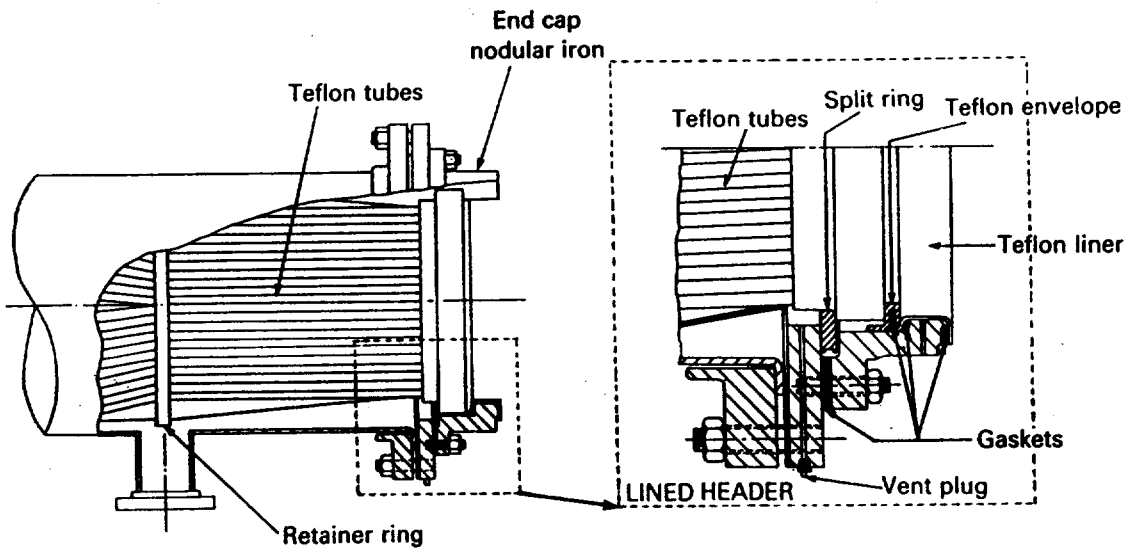
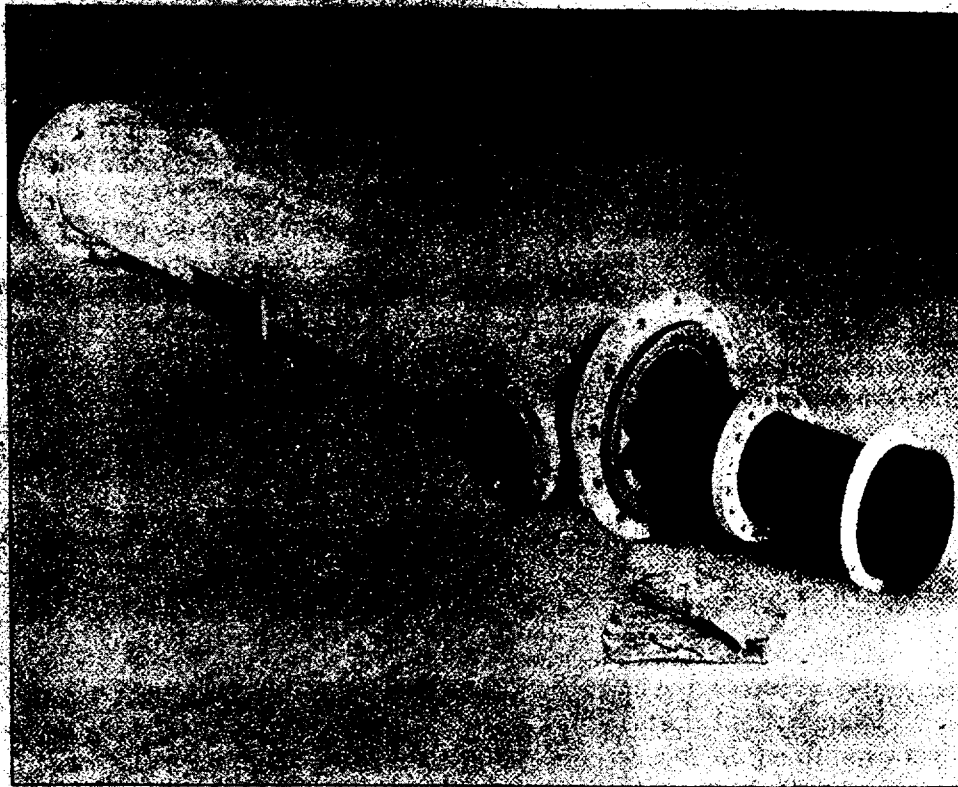
These exposed coils are designed for heating or cooling corrosive baths such as those for chrome plating and pickling applications. There are several models available including Supercoils, Slimline coils and Tank coils.

#### Supercoils

Supercoils are braided coils in which the individual braided layers of tubing are flattened and held apart by spacers of lead wire encapsulated with Teflon™ and polyvinylidene chloride (PVDC) tubes. In the case of electroless nickel applications, the lead weights are replaced by polypropylene bolts, tubing and nuts. The spacers provide the weight needed to submerge the coil and to form it into a rough U-shape, while the relatively open spacing serves to increase the rate of heat transfer.

Tube size is 2.5 mm outside diameter with a wall thickness of 0.25 mm and a nominal length of 1.22–4.88 m. There are two models, one

**Figure 5.20** Teflon™ shell-and-tube heat exchanger (courtesy of Du Pont International)



**Figure 5.21** Header construction for Teflon™ shell-and-tube heat exchanger (courtesy of Du Pont International)

comprising 160 tubes, in 3 braid layers, giving a heat transfer area of 1.4–6.3 m<sup>2</sup>; the other comprising 280 tubes, in 5 braid layers, giving a heat transfer surface area of 2.3–10.5 m<sup>2</sup>.

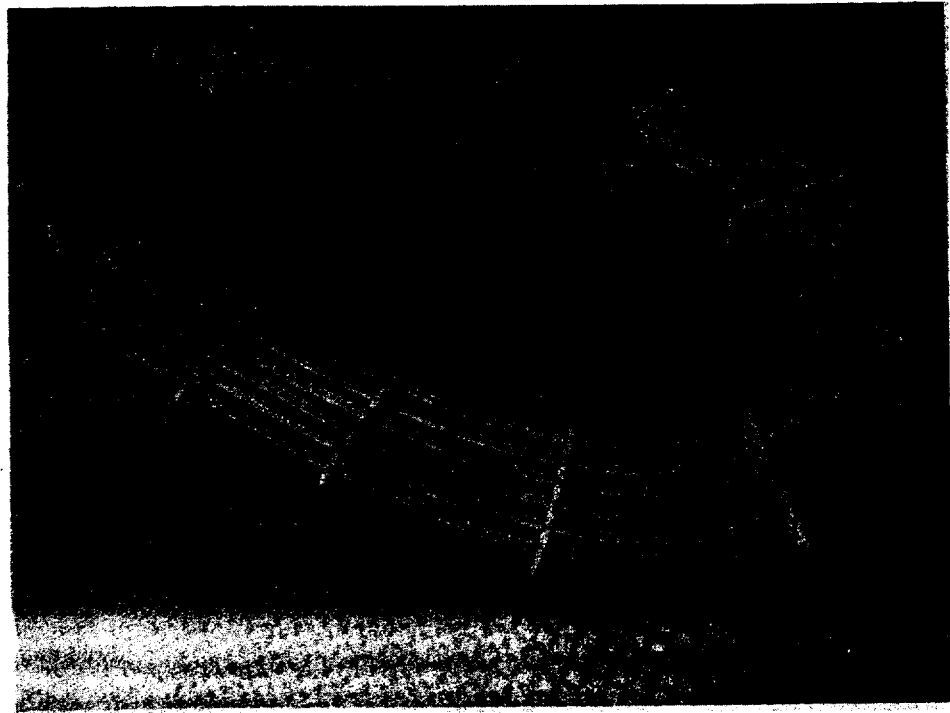
**Slimline coils**

The Slimline coil is similar in principle to the Supercoil, but is designed to provide a rigid U-shaped unit, having closely controlled dimensions, thus enabling it to be positioned accurately in its operating location. This is achieved by the use of perforated Teflon™ spacer plates at 300 mm intervals along the bundle which has a rectangular cross-section. Being

designed for immersion into shallow tanks, the U has a wide base and short vertical limbs.

The standard units contain 650 tubes, 2.5 mm outside diameter, 1.8–4.8 m long, giving a maximum heat transfer surface area of 23.7 m<sup>2</sup>, but similar units with 105 tubes, 6.35 mm outside diameter, are available. (See Fig. 5.22).

**Figure 5.22** Teflon™ immersion coil (105 tubes, 6.35 mm diameter) (courtesy of Du Pont International)



### **Tank coils**

The Tank coil is similar in cross-sectional shape and construction to the Slimline, but larger in size. It is designed for insertion into deep tanks or channels and has small U-bend radii similar to a conventional fuel oil tank suction heater. Longitudinal stainless-steel rods provide additional rigidity.

The units contain 2500 tubes, 3.175 mm outside diameter, 0.3175 mm thick, 3.35–7.01 m long, giving a heat transfer surface area of 56.9–148.2 m<sup>2</sup>.

## **5.11 Rotary regenerative heat exchangers**

### **5.11.1 Application**

Waste heat recovery systems usually involve large volumes of gas or air at a pressure around atmospheric and a temperature which may be as high as 950 °C. Heat transfer coefficients (see Chapter 6) for such gases are low and therefore tubular heat transfer equipment becomes large with

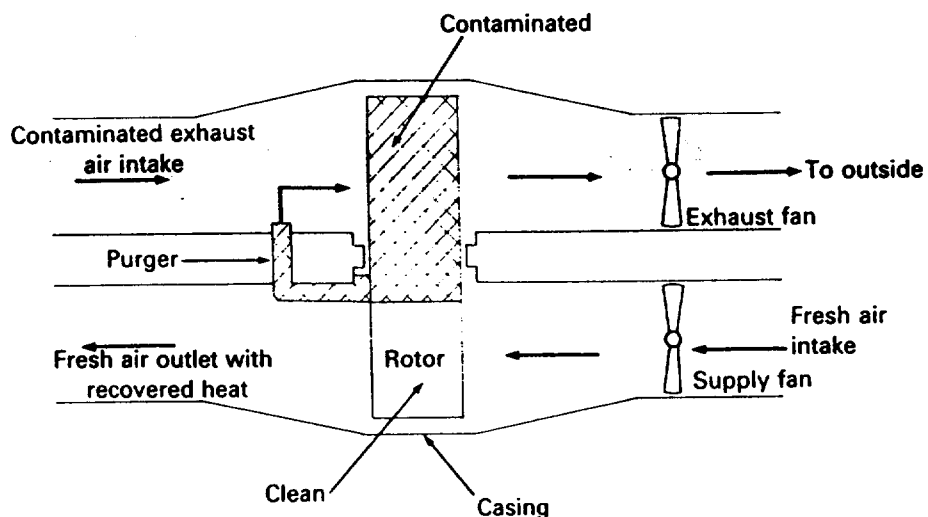
regard to surface area, space and weight. As the heat transfer coefficients of the two fluids are of similar magnitude, both internal and external surfaces must be extended (see Chapter 9) to reduce the size, which is usually impracticable. Compact, lightweight heat transfer equipment for such applications are the heat pipe, which is described in section 5.2, and the rotary regenerative heat exchanger, or 'heat wheel', described below.

The rotary regenerative heat exchanger was invented by Ljungstrom, a Swedish engineer, nearly eighty years ago. It was developed primarily to recover heat from the flue gas of large boiler plant, but has since been used in many other applications including gas turbines and heating and ventilating. Provided the pressure difference between the two fluids is not large, and a small quantity of inter-stream leakage can be tolerated, the rotary regenerative heat exchanger is ideally suited to heat interchange between two gases at a pressure around atmospheric.

### 5.11.2 Construction

A typical rotary unit is shown in Fig. 5.23. It consists of a slowly revolving cylindrical drum which is divided into a number of sector-shaped sections each packed with a matrix of coarsely knitted metal mesh. One gas stream passes axially through one side of the drum, while the other gas stream passes axially through the drum on the other side but in the opposite direction. The flow arrangement is therefore countercurrent (see section 7.7). As the drum rotates, heat picked up by the matrix from the hot stream on one side is delivered to the cold stream on the other side. Electrical power required to drive the rotor is usually negligible compared with the saving in energy recovered. Costs and power consumption are given in Table 19.16.

**Figure 5.23** Rotary regenerative heat exchanger (courtesy of Thermal Technology Ltd)



Materials of construction depend on the temperature and corrosion characteristics of the gas streams involved. Rotor materials may be aluminium up to temperatures of around 200 °C, steel up to about 425 °C and stainless steel, or Incoloy™, up to about 980 °C. Rotors of plastic material are used for highly corrosive applications at modest

temperatures. Rotary heaters are available with rotors up to 6 m in diameter and up to 1 m in depth. Rotor velocity is in the range 5–20 rev/min.

Aluminium, stainless steel and ceramic are among the materials used for the matrix. Depending on the temperature and corrosion characteristics of the gas stream the matrix may comprise layers of different materials. The matrix occupies roughly 3% of the total drum volume, thus providing a low gas pressure loss of the order of 13–25 mm (0.5–1 in) water gauge.

In rotary regenerative heat exchangers contamination of one stream by the other can occur due to (a) leakage around the rotor periphery via the annular space between drum and casing, (b) leakage of radial seals and (c) entrainment in the rotor flow passages. To reduce contamination to a low level (less than 1% by volume) special attention is given to the design of sealing devices, including the provision of peripheral double-labyrinth air seals. To minimise entrainment a purging system is employed, in which each section is flushed out with clean gas as it enters the clean stream.

## 5.12 Electrically heated exchangers

### 5.12.1 Advantages

The various heat exchangers described in sections 5.1–5.11 involve the indirect exchange of heat between two fluids. When these exchangers function as heaters, typical heating mediums are likely to be steam, hot water, proprietary heat transfer fluids, hot air, hot exhaust gas, etc. Despite the higher cost of electrical power, direct electrical heating should also be investigated, and when all factors are considered it may provide the best method of supplying heat. This is likely to be the case if a suitable heating medium is not already available as part of the process. The supply of the heating medium may prove difficult and costly, as it may be necessary to install boilers or heating plants, accompanied by tanks, receivers, ducts, pipework, valves, instrumentation, foundations, etc.

In addition to its compactness and cleanliness, direct electrical heating provides the following additional advantages:

*High efficiency.* Electrically heated exchangers apply heat directly to the fluid to be heated with near 100% efficiency and maximum energy utilisation, producing a rapid response to any temperature changes.

*Control and safety.* Close, continuous, safe control of operating times and temperatures (particularly high temperatures) is readily achieved.

*Versatility.* Electrically heated exchangers may be used for virtually any process, particularly batch operations. They are suitable for heat transfer by conduction, convection and radiation for heating solids, liquids and gases.

### 5.12.2 Construction

The basic heating element consists of resistance wires, embedded in a refractory material, which is enclosed by a cylindrical metal sheath. In most units the tubular elements are formed into a hairpin shape to resemble a U-bundle, in which both legs of each U are attached to a terminal plate (tubesheet) (see Fig. 1.3). The attachment to the terminal plate may be by mechanical coupling, brazing or welding. In small units the tubular elements are formed into coils of circular or rectangular shape, which are attached to the terminal plate in a similar manner. Other coil shapes can be provided.

The sheath metal is selected according to its operating temperature and the corrosive nature of the fluid to which it is exposed. Typical metals are carbon, low-alloy and stainless steels, Incoloy™ 800 and 825, Inconel™ 625, monel™, nickel and titanium. The sheath may be plain or finned if the fluid to be heated has poor heat transfer characteristics.

The terminal plate is connected to the electrical power supply and all electrical equipment enclosed in a terminal box, weatherproofed if required. For installation in hazardous locations, the terminal box can be supplied flameproof/explosion proof to international code standards. The heater head (terminal plate and box) may be supplied with a screwed or flanged connection for mounting to a vessel.

Tubular hairpin elements are supported by 25% cut segmental baffles, as used in shell-and-tube exchanger practice and described in section 1.5.8. When used in circulation-type heaters, described later, they are spaced in accordance with heat transfer and pressure loss requirements.

### 5.12.3 Heater types and applications

#### Immersion heaters

As the name implies, this type of heater is used for the heating of liquids, viscous material, and low melting temperature solids in a tank or vat. If the tank wall is sufficiently thick, small heaters having screwed heads may be used. Larger heaters employ flanged heads. Instead of immersing the heater directly into the fluid, it may be installed in a sealed pocket immersed in the fluid. This enables the heater to be serviced without draining the tank.

Another method is 'over the side', in which the heater head is specially shaped in order that it may be clamped to the tank edge. 'Over the side' heaters have coiled elements with extended non-heated vertical legs, to ensure that the heated coils are below the normal liquid level.

The capacity range of standard units is:

<i>Function</i>	<i>Mounting</i>	<i>Immersed length (mm)</i>	<i>Flange bore (mm)</i>	<i>Rating (kW)</i>
Water heating	Screwed	165–1450	–	0.5–24
Water heating	Flanged	375–2025	65–350	3–600
Oil heating	Screwed	175–2260	–	0.25–9
Water heating	Flanged	870–3200	65–350	3–172



These heaters are used in many industrial applications, particularly electroplating and metal-finishing industries.

#### **Circulation heaters**

These heaters serve a similar function to the U-tube fuel oil line heater described in section 1.3.2. The construction is similar, except that the U-tubes are replaced by electrically heated hairpin elements. The shell, through which the heated fluid flows, is designed and manufactured to international pressure vessel codes exactly as a shell-and-tube exchanger. The channel of the U-tube exchanger is replaced by the flanged head of the electrically heated exchanger described above.

The capacity range of standard units is:

<i>Function</i>	<i>Heater bore (mm)</i>	<i>Heater length (mm)</i>	<i>Rating (kW)</i>
Water heating	100–350	2030–2540	12–450
Oil heating	100–350	2030–2540	12–162

These heaters provide efficient, compact, sources of heat for storage tanks, solar heating, air conditioning, kettles and jacketed vessels and water-bath vaporisers. Oil heaters are used for applications involving fuel oils, asphalts, diesel engines, large gearboxes, heat transfer fluids, etc.

The heaters may be incorporated into a packaged, skid-mounted, heating and pumping set, by the addition of pump, filter, valves and expansion tank.

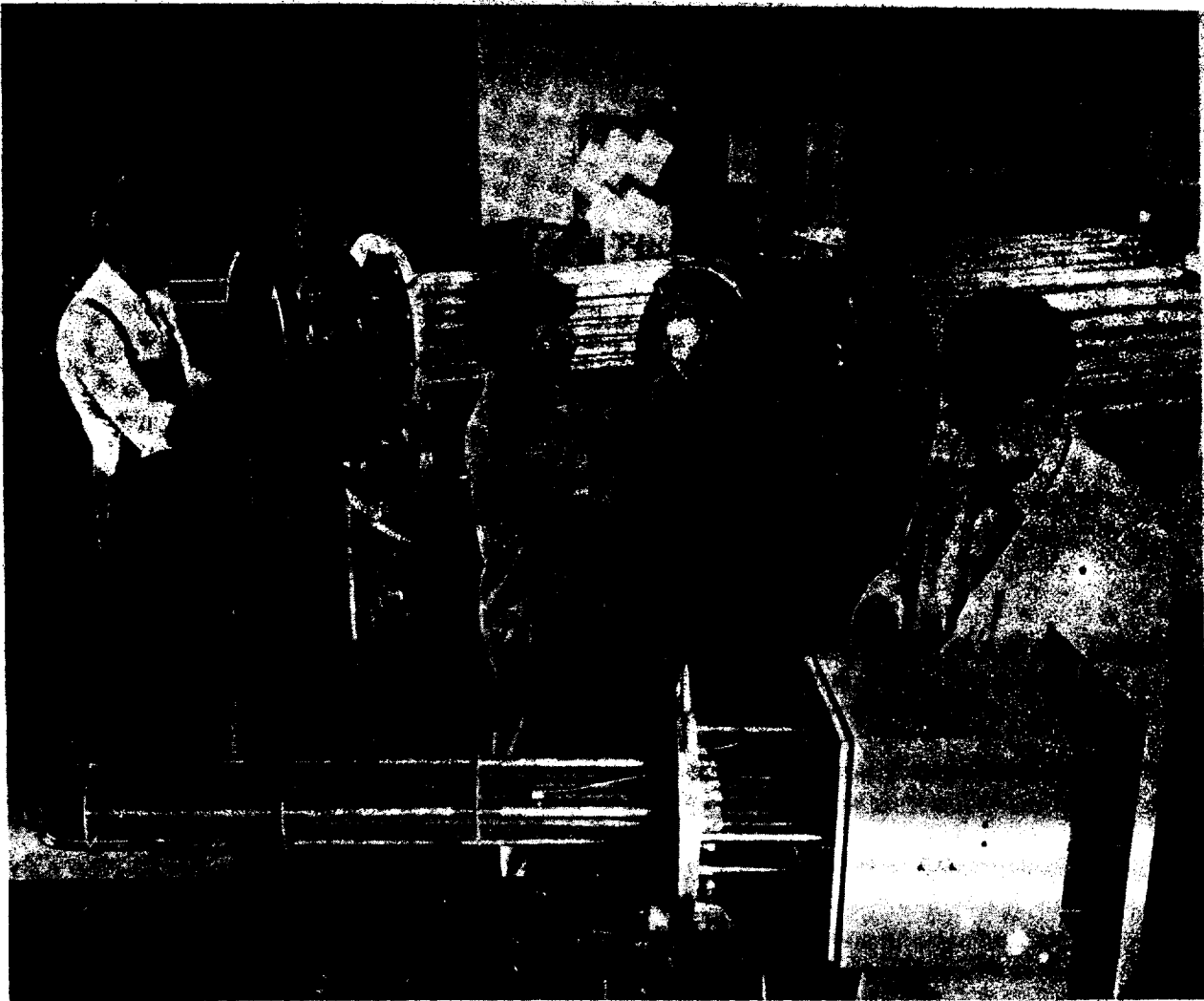
#### **Gas heaters**

These heaters are similar in construction to the circulation heaters described above. They are used to heat a wide variety of industrial gases such as propane, butane, carbon dioxide, nitrogen, etc., in an operating range of  $-272^{\circ}\text{C}$  to  $+850^{\circ}\text{C}$  and full vacuum to 240 bar. Applications include defrosting, catalyst heating, molecular-sieve regeneration and steam superheating.

Of particular importance is the heating of natural gas. It issues from the well-head at a pressure of the order of 130–200 bar, but before entering the turbine the pressure is reduced to about 7–12 bar. If the gas is not heated prior to the pressure reduction, the temperature fall (Joule–Thomson effect) may be such that subsequent valves, pipework and associated equipment must be designed for low temperatures. The reduction in both temperature and pressure may also promote hydrate formation. Crystalline hydrates are formed when natural gas under pressure unites with water. Such deposits foul heat transfer surfaces, while loose deposits cause valve seats to stick and also cause damage to turbine rotor blades.

One method of heating the gas is by water-bath. The high-pressure gas is passed through a bank of heating coils immersed in a bath of water, which is heated up by gas- or oil-fired burners. If neither gas nor oil is available, electrical immersion heaters may be used. Even if electrical heating is used, the water-bath has the disadvantages of large thermal mass, slow response to changes in demand, high weight, large space and high capital cost. Direct electrical heating, using the circulation type heater described above, eliminates these disadvantages.

Similar considerations apply when natural gas, stored under pressure, is released to the distribution system.



**Figure 5.24** Electrically heated exchangers in the course of manufacture (courtesy of Eltron (London) Ltd)

#### **Air-duct heaters**

These heaters serve a similar function and are similar in construction to conventional box-shaped air-conditioning and ventilating units. The plain or finned tubes of the conventional tubular unit are replaced by plain or finned electrically heater hairpin elements.

The casing of the standard units is flanged at both open ends for bolting to matching flanges of the ductwork. Stab-in units are designed for insertion into the side of the ductwork. Stand-off units are similar to the standard unit, except that there is an air gap between the terminal box and duct, with an unheated length of elements.

A wide range of standard and custom-built air-duct heaters is available.

#### **5.12.4 Control**

Thermostats are used where control accuracy is not critical. Up to 3 kW, the thermostat switches the load direct; above this, the load is switched by contactor, the coil of which is wired to the thermostat. Modern sophisticated control systems for direct electrically heated exchangers use

the solid-state thyristor. It is a fast-acting switch with electronic actuation to provide virtually instantaneous response.

Figure 5.24 shows electrically heated exchangers in the course of manufacture.

## Acknowledgements

The author is grateful to the following companies for the provision of technical data and illustrations: Filtration & Transfer Ltd, Poole, UK, a licensee of The Brown Fintube Co., Houston, USA (Double-pipe heat exchangers). Nouvelles Applications Technologiques, 370 Avenue Napoleon-Bonaparte, 92500 Rueil-Malmaison, France (Packinox heat exchanger). Bavaria Anlagenbau GmbH, Hasenheide 7, D-8080 Furstenfeldbruck, W. Germany (Bavex heat exchanger). Alfa-Laval Co. Ltd, Brentford, UK (Lamella and spiral heat exchangers). APV International Ltd, Crawley, UK (Spiral heat exchangers). Marston-Palmer Ltd, Wolverhampton, UK (Plate - fin heat exchangers). Senior Platecoil Ltd, Watford, UK (Plate coil products (embossed panel heat exchangers)). Robert Jenkins Systems Ltd, Rotherham, UK (Graphite heat exchangers). Corning Process Systems, Corning, USA (Glass heat exchangers). Du Pont International, Geneva, Switzerland (Teflon™ heat exchangers - Teflon is the registered trade mark of Du Pont). Thermal Technology Ltd, Trowbridge, UK (Rotary regenerative heat exchangers). Eltron (London) Ltd, Croydon, UK (Electrically heated exchangers).

## References

A list of addresses for the service organisations is provided on p. xvi.

**Chisholm, D.** (1983) *Heat Exchanger Design Handbook*, Vol. 3, Section 3.10. Hemisphere Publishing Corp. Inc. In this presentation Dr Chisholm lists 219 references including his own book: *The Heat Pipe*, Mills & Boon, London, UK.

Also recommended for study are:

**Data Items 79012, 79013, 80013, 80017, 81038** published by Engineering Sciences Data Unit International Ltd (ESDU), London, UK.

## Exchanger type selection

---

Experience of a similar unit operating under similar process conditions is the best guide to exchanger type selection and should always be investigated thoroughly. However, if previous operational experience is not available, the following factors must always be considered before type selection is made.

### A1.1 Operating pressure and temperature

If the operating pressure is below 30 bar and the operating temperature is below 200 °C, then the plate-type exchangers must always be given serious consideration and in particular, the gasketed-plate type. At higher pressures and temperatures, the choice will be between a shell-and-tube exchanger, a gasketless plate exchanger, and a double-pipe exchanger, the latter being particularly competitive for small-capacity, high-pressure applications. If there is a cooling application an air-cooled exchanger may be considered instead of a shell-and-tube exchanger using water as coolant. For all heating duties, an electrically heated exchanger should be considered, particularly if the proposed heating medium is fouling or a suitable medium is not available.

### A1.2 Nature of fluids

If the corrosion characteristics of the fluids are especially aggressive, the high corrosion-resistant exchangers such as graphite, glass or Teflon™ should be considered, provided pressure, temperature and capacity are not great. If suitable plate and gasket materials are available, the gasketed-plate type should also be considered.

The lamella and spiral exchangers minimise the possibility of inter-stream leakage and for fluids which are highly fouling, or suspensions, slurries or fibrous liquids, these types merit consideration if the pressure, temperature and size are within their range. If the fluids are also

Table A1.1 Unfired heat exchanger types – summary of features

Exchanger type	Maximum operating conditions		Typical surface area range for a single unit (m <sup>2</sup> )	Comments <sup>(9)</sup>
	Temperature (°C)	Pressure (bar)		
Shell and tube	-200 to 700	350 <sup>(1)</sup>	5–1000	Versatile and suitable for almost all applications, irrespective of duty, pressure and temperature (which is limited by metallurgical considerations).
Double pipe	-200 to 700	350 <sup>(2)</sup>	0.25–200	Especially suited to small capacities, countercurrent operation and high pressures. Standard sections available.
Air cooler	700	350 <sup>(2)</sup>	5–400 <sup>(3)</sup>	Standardised bundles available. Suitable for almost all cooling duties above atmospheric temperature, irrespective of pressure and temperature (which is limited by metallurgical considerations).
Heat pipe	-100 to 400 <sup>(5)</sup>	40 <sup>(6)</sup>	100–1000	Ideally suited to heat exchange between large volumes of gas at low pressure. Extended surfaces may be employed on both gas sides.
Gasketed plate	-40 to 180 <sup>(7)</sup>	30	1–1200	High thermal efficiency, flexible, low fouling tendency, compact, low weight, no inter-stream mixing or vibration, ease of maintenance. Usually cheapest exchanger type if suitable for operating conditions. Gasket material may inhibit use for certain fluids.
Gasketless plate	-200 to 980 according to type	As S & T type. max. $\Delta P$ between fluids = 40–80 bar according to type	Up to 10 000	Alternative to shell-and-tube and gasketed-plate types provided chemical cleaning is acceptable. Application may be limited by pressure difference between fluids.
Spiral	400	20	0.5–350	
Lamella	PTFE gasket	220	35 (dia. = 300 mm)	High thermal efficiency, low fouling tendency, ease of maintenance. Handles suspensions, slurries and fibrous liquids.
	Asbestos gasket	500	10 (dia. = 1000 mm)	
Plate fin	-260 to 650	25 <sup>(4)</sup>	Up to 1230 m <sup>2</sup> per m <sup>3</sup> volume	Compact, low weight, excellent for cryogenic applications. Multiple streams may be handled.

Table A1.1 (cont.)

Exchanger type		Maximum operating conditions		Typical surface area range for a single unit (m <sup>2</sup> )	Comments <sup>(9)</sup>
		Temperature (°C)	Pressure (bar)		
Embossed plate		350	18 <sup>(8)</sup>	Standard panels up to 1200 × 3600 mm	Compact and low weight. Curved units available. Especially suited to vessel jackets and immersion heaters
Graphite	Shell and tube	180	6	1.6–1650	Exceptional corrosion resistance, low fouling tendency, but limited with regard to temperature and pressure. Limited in capacity except for graphite shell-and-tube and multi-block types.
	Cubic and rectangular	180	5.2	0.65–153	
	Multi-block	180	6	0.22–240	
	Cartridge	180	6	0.16–18.6	
Glass	Shell and tube	175	5	6.3–26	
Teflon™	Shell and tube	20	10	9.3–50	
	Supercoils	50	6.6	2.3–10.5	
	Slimline coils	100	3.8	up to 23.7	
	Tank coils	150	2.2	56.9–148	
Rotary regenerators	Aluminium rotor	200	Near atmospheric	Rotor dia. = 6 m	Compact, but limited to heat exchange between low-pressure gases, even at high temperature. Subject to some inter-stream leakage.
	Steel rotor	425			
	Stainless or Incoloy™ rotor	980			

## Notes:

- (1) Typical upper limit, but higher pressures possible depending on diameters and closures required.
- (2) Typical upper limit, but designs for higher pressures available.
- (3) Shop-built bundle – larger sizes available if site built.
- (4) Pressure reversals may reduce this value to 11 bar. Up to 80 bar available depending on cross-section.
- (5) Higher temperatures possible with special working fluids.
- (6) Typical only for working fluid, i.e. steam at approx. 250 °C.
- (7) 260 °C for compressed asbestos fibre gaskets.
- (8) 7 bar at 165 °C for titanium.
- (9) For all heating duties, consider electrically heated exchangers, particularly if proposed heating medium is fouling, or suitable medium not readily available.

corrosive the graphite, glass or Teflon™ types should be considered.

When dealing with lethal fluids, particular care must be exercised to ensure that the external joints, if any, of the selected exchanger type are of the highest integrity.

### **A1.3 Size range**

The size range of the selected type may be too small to meet the required duty without having a large number of parallel units, leading to expensive pipework and valves, with the possibility of flow distribution problems.

### **A1.4 Cost**

This is obviously an important factor but the exchanger type having the lowest capital cost may provide serious problems in service and become expensive to operate. Each case must be treated individually and it may be necessary to design and cost several alternatives before a decision is made.

Table A1.1 summarises the features of the various exchanger types described in Chapter 5.

## Heat transfer and fluid flow

Part 2 deals with the thermal design of heat transfer equipment in which both fluids are either single phase, or one of them is single phase and the other is steam, condensing isothermally, the steam being used as a heating medium. In the latter case the steam-side heat transfer coefficient, defined in section 6.3, is usually assumed to be  $8500 \text{ W/m}^2 \text{ K}$  ( $1500 \text{ Btu/hr ft}^2 \text{ }^\circ\text{F}$ ). The single-phase data may also be applied to single-phase cooling and heating mediums in tubular vaporisers and condensers, for which Smith (1987) and the forthcoming title on condensers should be consulted, respectively.

Although the general approach to thermal design is similar for all heat transfer equipment, it is not possible to provide detailed design methods for every heat exchanger type described in Part 1. This applies particularly to non-tubular equipment, for which design methods tend to be proprietary.

Chapter 6 provides the single-phase heat transfer and pressure loss correlations for flow inside and outside tubes. Chapter 7 deals with mean temperature difference and the values to be used for a variety of flow configurations. Fouling is discussed in Chapter 8, from which it will be seen that it justifies the description of 'the major unresolved problem in heat transfer'. Considerable savings in cost, space and weight may sometimes be made by using extended surfaces or internal augmentation techniques and these are described in Chapters 9 and 10. Flow-induced tube vibration, relevant chiefly to shell-and-tube exchangers, is the subject of Chapter 11.



# THE HISTORY OF THE UNITED STATES

The history of the United States is a complex and multifaceted story that spans centuries. It begins with the early Native American civilizations, such as the Mayans, Aztecs, and Incas, who built sophisticated societies in the Americas. The arrival of European explorers in the late 15th and early 16th centuries marked the beginning of a new era of discovery and conquest. The Spanish, French, and British established colonies across the continent, each with its own unique culture and traditions. The struggle for independence from British rule culminated in the American Revolution, which led to the formation of the United States as a sovereign nation. The early years of the republic were marked by challenges and growth, as the young nation sought to establish a stable government and economy. The Civil War, fought between 1861 and 1865, was a pivotal moment in American history, as it resolved the issue of slavery and preserved the Union. The Reconstruction period that followed was a time of significant change and progress, as the nation worked to rebuild and integrate the newly freed African American population. The late 19th and early 20th centuries saw rapid industrialization and westward expansion, leading to the rise of a powerful American economy and the emergence of the United States as a global superpower. The 20th century was a period of great turmoil and achievement, with the United States playing a central role in World War II and the subsequent Cold War. The civil rights movement of the 1950s and 1960s led to significant social and political reforms, while the Vietnam War and the Watergate scandal tested the nation's resolve and integrity. Today, the United States continues to evolve and shape the world, facing new challenges and opportunities in the 21st century.

## Heat transfer and pressure loss

### 6.1 Mechanisms of heat flow

The mechanisms of heat flow are conduction, convection and radiation.

#### Conduction

This refers to the flow of heat through a body by the transference of the momentum of individual molecules without mixing; for example, heat flow through the wall of a tube. Because of convection effects, described below, pure conduction through a fluid in bulk is difficult to achieve.

#### Convection

When heat flows by physical mixing or turbulence it is referred to as convection and occurs only in fluids; for example, the flow of a fluid past a tubular surface, which is the subject of this chapter. If the flow is caused by an external source, such as a pump or fan, it is known as forced convection, whereas if the flow is caused by density differences within the fluid, it is known as natural convection.

#### Radiation

This relates to the transfer of energy through space by means of electromagnetic waves, and is outside the scope of this book.

### 6.2 Laminar and turbulent flow

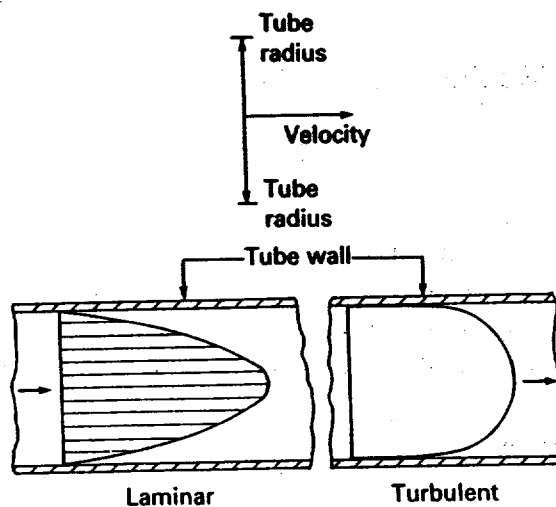
In laminar flow fluid particles pass through a circular tube in distinct parallel lines being characterised by a parabolic velocity profile with a maximum at the centre and approaching zero at the surface. The flow is considered to be akin to thin concentric cylinders of fluid sliding one within the other – ‘telescope fashion’. Laminar flow is sometimes known as streamline, viscous, and rod-like flow.

For flow inside a tube, the Reynolds number ( $Re$ ) is defined as  $Re = (ud\rho/\eta)$  – (dimensionless), where  $u$  = fluid velocity,  $d$  = tube inside diameter,  $\rho$  = fluid density and  $\eta$  = fluid viscosity. Laminar flow in a

circular tube occurs when the Reynolds number is less than about 2100.

As the Reynolds number increases, as a result of increased velocity for instance, the fluid flow is no longer orderly but flows in a random, eddying motion such that mixing occurs. This is termed 'turbulent flow' in which fluid particles pass through the tube in a random pattern. In the case of turbulent flow inside a tube, the velocity profile is no longer parabolic but nearly constant, as shown in Fig. 6.1. Fully developed turbulent flow occurs when the Reynolds number exceeds 10 000, the intermediate Reynolds number range of 2100–10 000 being termed 'the transition region'.

Figure 6.1 Velocity profile for laminar and turbulent flow inside a tube

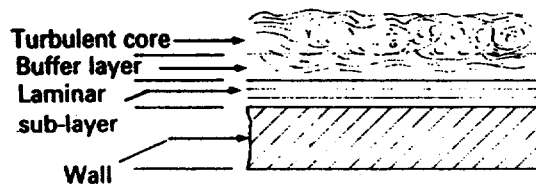


### 6.3 'Film' heat transfer coefficient

Heat transfer occurs when there is a temperature difference between a solid surface and a fluid flowing past it. In the following notes, it is assumed that the surface is hotter than the fluid, but the comments are equally applicable if the surface is colder than the fluid. If the flow is laminar, then heat is regarded as being transferred largely by conduction. Figure 6.2 illustrates the flow pattern which is assumed to exist near a surface for turbulent flow. Despite the fact that the flow is turbulent, immediately adjacent to the surface is a thin layer of fluid known as the laminar sub-layer. No fluid mixing occurs in the laminar sub-layer and heat transfer occurs by pure conduction. From the turbulent core, where particles have an eddying motion, the eddies sweep the edge of the laminar sub-layer. In doing so, particles of hot fluid are carried away through the buffer layer, where heat transfer occurs by conduction and convection into the colder turbulent core where rapid mixing occurs.

As the laminar sub-layer presents a much greater resistance to heat transfer than the buffer layer or turbulent core, most of the temperature difference between surface and fluid occurs in it. In practice the entire resistance to heat transfer is regarded as being in the laminar sub-layer. Despite the fact that heat flows across this layer by conduction, the mechanism is customarily regarded as convective heat transfer.

**Figure 6.2** Flow pattern adjacent to a solid surface



By Newton's law of cooling, heat transfer can be expressed by

$$Q = \alpha A(\Delta T_f) = \alpha A(T_s - T_b) \quad [6.1]$$

where  $Q$  = heat transferred (W)

$A$  = surface area normal to heat flow ( $m^2$ )

$\Delta T_f$  = temperature difference between surface  $T_s$   
and fluid bulk  $T_b (= T_s - T_b)$  (K)

$\alpha$  = heat transfer coefficient ( $W/m^2 K$ )

$$\text{from which } \alpha = Q/(A \Delta T_f) \quad [6.2]$$

Because the entire resistance to heat transfer is assumed to be in the thin laminar sub-layer or 'film',  $\alpha$  is often referred to as the 'film' heat transfer coefficient.  $\alpha$  is also termed the conductance and  $1/\alpha$  the resistance to heat transfer.

## 6.4 Determination of heat transfer coefficients

Consider conduction through a slab of metal, having a cross-sectional area normal to heat flow of  $A(m^2)$ , a thickness in the direction of heat flow of  $t(m)$  and a thermal conductivity of  $\lambda(W/m K)$ . If one face of the slab is at temperature  $T_1$  (K), and the other at  $T_2$  (K), then heat flow through the slab can be expressed as

$$Q = \left(\frac{\lambda}{t}\right) A(T_1 - T_2) \quad [6.3]$$

This is similar to equation [6.1] where  $\alpha = (\lambda/t)$ . In the case of fluids flowing past a surface  $\alpha$  cannot be calculated from this relationship because of the impracticability of measuring layer thickness ( $t$ ). Hence  $\alpha$  must be determined directly from experimental data and it will be seen later that  $\alpha$  is correlated in terms of dimensionless numbers. Some of the dimensionless numbers relevant to single-phase flow, and which are used in subsequent chapters, are given in Table 6.1.

$\alpha$  depends on the flow velocity, the type of heat transfer surface and its diameter or characteristic dimension, together with physical properties such as specific heat, thermal conductivity, dynamic viscosity, density and coefficient of thermal expansion.

## 6.5 Overall heat transfer coefficient

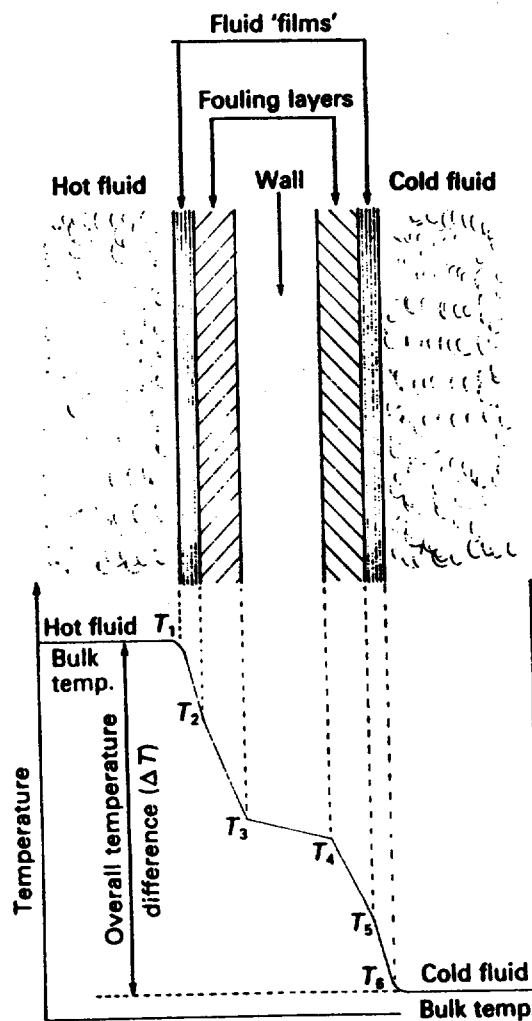
Section 6.3 described how the resistance to heat transfer for a fluid flowing past a surface is assumed to be due to the resistance of a thin film

**Table 6.1** Some dimensionless numbers for heat transfer and pressure loss in single phase flows

Name	Symbol and definition
Euler number	$Eu = \Delta P / (\rho u^2 / 2)$
Grashof number	$Gr = gd^3 \Delta \rho / \nu^2 \rho = gd^3 \rho \Delta \rho / \eta^2$
Graetz number	$Gz = Re Pr d / L = u d^2 \rho c_p / \lambda L = u d^2 / \kappa L$
Nusselt number	$Nu = \alpha d / \lambda$
Peclet number	$Pe = u d / \kappa = \mu d \rho c_p / \lambda = Re Pr = \dot{m} c_p / \lambda$
Prandtl number	$Pr = \nu / \kappa = \eta c_p / \lambda$
Rayleigh number	$Ra = Gr Pr$
Reynolds number	$Re = u d / \nu = u d \rho / \eta = \dot{m} d / \eta$
Stanton number	$St = \alpha / \rho u c_p = Nu / Re Pr = \alpha / \dot{m} c_p$

of fluid adjacent to the heat transfer surface. If dirt is present, it is assumed to be as a uniform layer on the heat transfer surface and the fluid film is assumed to be immediately adjacent to the outer surface of the dirt layer. Figure 6.3 shows the assumed arrangement for heat transfer calculations. Fouling is discussed in greater detail in Chapter 8.

**Figure 6.3** Temperature profile between hot and cold fluids



From Fig. 6.3, using  $\Delta T_i = Q / \alpha A$  from equation [6.1], it will be seen that:

$$T_1 - T_2 = Q/\alpha_i A_i \quad [6.4a]$$

$$T_2 - T_3 = Q/\alpha_{fi} A_i \quad [6.4b]$$

$$T_3 - T_4 = Q/\alpha_w A_w \quad [6.4c]$$

$$T_4 - T_5 = Q/\alpha_{fo} A_o \quad [6.4d]$$

$$T_5 - T_6 = Q/\alpha_o A_o \quad [6.4e]$$

where  $\alpha_i, \alpha_o$  = film heat transfer coefficients

$\alpha_{fi}, \alpha_{fo}$  = conductances of fouling layers

$\alpha_w$  = conductance of wall of heat transfer surface

$A_i, A_o$  = heat transfer surface areas on each side of the wall

$A_w$  = mean surface area of wall.

Adding the five equations above:

$$(T_1 - T_6) = \Delta T = Q \left\{ \frac{1}{\alpha_i A_i} + \frac{1}{\alpha_{fi} A_i} + \frac{1}{\alpha_w A_w} + \frac{1}{\alpha_{fo} A_o} + \frac{1}{\alpha_o A_o} \right\} \quad [6.5]$$

It is convenient to relate all coefficients to a chosen reference surface area ( $A_{ref}$ ). In heat transfer equipment design it is immaterial which surface area is chosen, provided all coefficients in the system are related to it.

Multiplying both sides of equation [6.5], by  $A_{ref}$ :

$$A_{ref} \Delta T = Q \left\{ \frac{1}{\alpha_i (A_i/A_{ref})} + \frac{1}{\alpha_{fi} (A_i/A_{ref})} + \frac{1}{\alpha_w (A_w/A_{ref})} + \frac{1}{\alpha_{fo} (A_o/A_{ref})} + \frac{1}{\alpha_o (A_o/A_{ref})} \right\} \quad [6.6]$$

$$\text{or } A_{ref} \Delta T = \frac{Q}{U_{ref}} \quad [6.7a]$$

$$\text{where } \frac{1}{U_{ref}} = \left\{ \frac{1}{\alpha_i (A_i/A_{ref})} + \frac{1}{\alpha_{fi} (A_i/A_{ref})} + \frac{1}{\alpha_w (A_w/A_{ref})} + \frac{1}{\alpha_{fo} (A_o/A_{ref})} + \frac{1}{\alpha_o (A_o/A_{ref})} \right\} \quad [6.7b]$$

$1/U_{ref}$  is the overall resistance to heat transfer, and is the sum of the individual resistances in the system, all being related to an arbitrary reference surface ( $A_{ref}$ ).

In the case of a cylindrical tube, for example, the chosen reference surface is often its external surface. Chapter 8 shows that  $1/\alpha_{fi}$  and  $1/\alpha_{fo}$  are the internal and external fouling resistances, or fouling factors,  $r_i$  and  $r_o$ , respectively. It can be shown that:

$$U_o = \frac{1}{\left\{ (1/\alpha_i)(A_o/A_i) + r_i(A_o/A_i) + r_w + r_o + (1/\alpha_o) \right\}} \quad [6.7c]$$

$$\text{where } r_w = \frac{d_o \ln(d_o/d_i)}{2\lambda_w} = \text{tube-wall resistance}$$

The derivation of  $r_w$  is given in most heat transfer text books – Kern (1950), for instance.

In general, equation [6.7a] may be expressed as

$$Q = UA \Delta T_m \quad [6.8]$$

where  $U$  must be related to  $A$  as shown above.

If fouling does not occur on one or both sides, then  $r_i$  and  $r_o$  are omitted from equation [6.7c]. In many cases the resistance of the tube wall is negligible in relation to the other resistances in the system, but it is good practice to include it always. For example, a copper tube 0.89 mm (0.035 in, 20 b.w.g.) thick has a conductance of 438 000 W/m<sup>2</sup> K, which will be much greater than other conductances in the system. However, a 25% chrome/20% nickel alloy tube 2.11 mm (0.083 in, 14 b.w.g.) thick has a conductance of 6400 W/m<sup>2</sup> K, which is likely to be of similar magnitude to other conductances in the system.

## 6.6 Surface area

The task of the thermal design engineer is to determine the size, and other pertinent design features, of his heat transfer equipment, using the basic relationship of equation [6.8]  $Q = UA \Delta T_m$  or  $A = QU \Delta T_m$ . In a design problem  $Q$ , the heat load, is always known, and the calculation of  $\Delta T_m$ , the effective temperature difference, is described in Chapter 7. Section 6.5 shows that the calculation of the overall heat transfer equipment ( $U$ ) involves the summation of the individual resistances in the system, in which the tube wall and fouling resistances are known in advance. The resistances of the two fluid films are not known and must be calculated on a trial-and-error basis from the correlations given in section 6.10 consistent with the permissible pressure loss and any other design restraints.

In most single-phase problems, involving low-viscosity fluids,  $A$  may be determined from single representative values of  $U$  and  $\Delta T_m$ . In single-phase problems, involving high-viscosity fluids, however, there may be a considerable change in  $U$  through the equipment and a single representative value is no longer applicable. In these cases the equipment is divided into zones and  $Q$ ,  $U$ ,  $\Delta T_m$  and  $A$  are then calculated for each zone. The zonal surfaces are then summed to give the total surface area for the equipment. A similar approach is required for vaporising and condensing applications and reference should be made to Smith (1987) and the forthcoming condenser title.

In the case of shell-and-tube exchangers, the thermal design engineer will seek a solution which usually has the minimum number of shells, each having the maximum acceptable tube length.

## 6.7 Controlling heat transfer coefficient

In order to reduce size and cost of the heat transfer equipment, the thermal design engineer will endeavour to achieve the highest value of  $U$ ,

Table 6.2 Controlling heat transfer coefficient

Item	Case 1 Basic case – $h_i$ is controlling coefficient		Case 2 Double $h_o$ and compare with basic case		Case 3 Double $h_i$ and compare with basic case	
	Coefficient	Resistance	Coefficient	Resistance	Coefficient	Resistance
$h_c$	5000	0.0002	5000	0.0002	5000	0.0002
$h_i$	500	0.0020	500	0.0020	1000	0.0010
$h_o$	5000	0.0002	10000	0.0001	5000	0.0002
$U$	417	$\Sigma = 0.0024$	435	$\Sigma = 0.0023$	714	$\Sigma = 0.0014$
Comment	—		$U$ increased 1.04 times		$U$ increased 1.71 times	

All values in ( $\text{W}/\text{m}^2 \text{K}$ ) units, assumed to relate to same surface  
 $h_c$  = combined conductance of fouling layers and tube wall  
 $h_i, h_o$  = film heat transfer coefficients

consistent with the permissible pressure loss and other design restraints. Of the five conductances from which  $U$  is obtained, the conductances of the fouling layers and wall are fixed, leaving the conductances of the two fluid films,  $\alpha_i$  and  $\alpha_o$ . The thermal design engineer will endeavour to obtain the highest values of  $\alpha_i$  and  $\alpha_o$  in order to increase  $U$ . In many applications  $\alpha_i$  and  $\alpha_o$  may be of different magnitude and the lower of the two coefficients is termed the controlling heat transfer coefficient. It is the controlling coefficient which must be increased if a significant increase in  $U$  is to be obtained, and this is shown by the example in Table 6.2.

## 6.8 Surface temperature

In the design of heat transfer equipment for high or sub-zero temperatures, it is sometimes necessary to calculate the temperature of the heat transfer surface to check that the chosen metal is suitable for the operating conditions. In the case of heat-sensitive fluids, it may be necessary to calculate the temperature of the adjacent fouling layer or heat transfer surface to check that the safe operating temperature for the fluid is not exceeded.

A knowledge of the surface temperature may also be required for thermal design. Some of the correlations presented for heat transfer and pressure loss involve a factor  $\phi$ , which is termed the viscosity, or physical property, correction factor. If  $\eta_b$  and  $\eta_s$  are the dynamic viscosities at the bulk fluid and adjacent surface temperatures respectively, and  $a$  is a fractional power determined from tests, the viscosity correction factor  $\phi = (\eta_b/\eta_s)^a$ . This represents the viscosity gradient  $\eta_b/\eta_s$  raised to the power  $a$ . In some correlations the physical property correction factor is used. Here  $\phi = (\text{Pr}_b/\text{Pr}_s)^b$  where  $\text{Pr}_b$  and  $\text{Pr}_s$  are the Prandtl numbers at the bulk fluid and adjacent surface temperatures respectively, and  $b$  is a fractional power determined from tests.

A large temperature difference between the heat transfer surface and the bulk of the fluid means that there may be a large physical property



difference between them, the most significant factor being the difference in viscosity, particularly for liquids. Depending on whether the fluid is being heated or cooled, the fluid velocity adjacent to the surface will be increased or decreased, and the velocity profile (Fig. 6.1) will be distorted. Heat transfer coefficients (and pressure losses) will differ from those predicted by the correlations for small surface-bulk temperature differences and it is necessary to correct the results by the introduction of  $\phi$ .

In the case of liquids, where viscosity decreases as the temperature increases,  $\phi$  will be greater than unity when the fluid is being heated, because  $\eta_b$  is greater than  $\eta_s$ . Heat transfer will be increased and pressure loss will be reduced.  $\phi$  will be less than unity when the fluid is being cooled, and heat transfer will be decreased and pressure loss increased. The reverse applies to gases being heated and  $\phi$  is less than unity. For gases being cooled,  $\phi$  is assumed to be unity.

In the case of gases and non-viscous liquids,  $\phi$  is often assumed to be unity, in which case the fouling layer or metal-wall surface temperature may be calculated directly from the heat transfer coefficients in the system. Referring to Fig. 6.3 and equation [6.4], with  $(T_1 - T_6) = \Delta T_o$ , the temperature  $T_x$  at any point  $x$  is given by:

$$T_x = T_1 - (U \Delta T_o) \sum r_{1-x} = T_6 + (U \Delta T_o) \sum r_{x-6} \dots \dots \dots [6.9]$$

where  $U$  = overall heat transfer coefficient

$\sum r_{1-x}$  = sum of all resistances between  $T_1$  and  $T_x$

$\sum r_{x-6}$  = sum of all resistances between  $T_x$  and  $T_6$

*U and all resistances must be related to the chosen reference surface*

Equation [6.9] relates only to plain surfaces. The calculation for the surface temperature of finned tubes is given in section 9.5.

**6.8.1 Example: overall coefficient and surface temperatures (viscosity correction factor = 1)**

This example demonstrates the calculation of the overall heat transfer coefficient from equation [6.7c] and the subsequent calculation of surface temperatures from equation [6.9] when  $\phi = 1$ .

Consider a shell-and-tube heat exchanger having temperatures and heat transfer coefficients at a particular section as follows:

$$A_i = 0.0471 \text{ m}^2/\text{m}, A_o = 0.0597 \text{ m}^2/\text{m}, T_1 = 300 \text{ }^\circ\text{C}, T_6 = 100 \text{ }^\circ\text{C},$$

$$\alpha_i = 500 \text{ W/m}^2 \text{ K}, r_i = 0.00025 \text{ (W/m}^2 \text{ K)}^{-1}, r_w = 0.00004 \text{ (W/m}^2 \text{ K)}^{-1},$$

$$r_o = 0.00035 \text{ (W/m}^2 \text{ K)}^{-1}, \alpha_o = 1000 \text{ W/m}^2 \text{ K}$$

If  $A_o$  is the reference surface, then by substitution into equation [6.7c]:

$$(1.2) \alpha_i \text{ related to ref. surface} \\ = (500 \times 0.0471)/0.0597 = 394.47 \quad \text{resist} = 0.002535$$

$$(2.3) r_i \text{ related to ref. surface} \\ = (0.00025 \times 0.0597)/0.0471 = \quad \text{resist} = 0.000317$$

$$\begin{aligned}
 (3\cdot4)r_w \text{ related to ref.surface} &= 0.00004 & \text{resist} &= 0.000040 \\
 (4\cdot5)r_o \text{ related to ref.surface} &= 0.00035 & \text{resist} &= 0.000350 \\
 (5\cdot6)\alpha_o \text{ related to ref.surface} &= 1000 & \text{resist} &= \underline{0.001000} \\
 & & \Sigma r_{1\cdot6} &= 0.004242 \\
 & & U &= 235.74 \\
 & & \underline{U\Delta T_o} &= \underline{47147.57}
 \end{aligned}$$

The above illustrates typical manual calculations for determining the overall heat transfer coefficient from the individual coefficients in the system.

To obtain the temperatures at various points between the hot and cold bulk fluid temperatures, equation [6.9] is used as follows:

$$\begin{aligned}
 \Sigma r_{1\cdot2} &= 0.002535, \Sigma r_{1\cdot3} = 0.002852, \Sigma r_{1\cdot4} = 0.002892, \Sigma r_{1\cdot5} \\
 &= 0.003242,
 \end{aligned}$$

$$\Sigma r_{5\cdot6} = 0.001, \Sigma r_{4\cdot6} = 0.00135, \Sigma r_{3\cdot6} = 0.00139, \Sigma r_{2\cdot6} = 0.001707$$

$$\begin{aligned}
 T_2 &= 300 - (47147.57 \times 0.002535) \\
 &\text{or } 100 + (47147.57 \times 0.001707) = 180.5^\circ\text{C}
 \end{aligned}$$

$$\begin{aligned}
 T_3 &= 300 - (47147.57 \times 0.002852) \\
 &\text{or } 100 + (47147.57 \times 0.00139) = 165.5^\circ\text{C}
 \end{aligned}$$

$$\begin{aligned}
 T_4 &= 300 - (47147.57 \times 0.002892) \\
 &\text{or } 100 + (47147.57 \times 0.00135) = 163.7^\circ\text{C}
 \end{aligned}$$

$$\begin{aligned}
 T_5 &= 300 - (47147.57 \times 0.003242) \\
 &\text{or } 100 + (47147.57 \times 0.001) = 147.2^\circ\text{C}
 \end{aligned}$$

### 6.8.2 Significant viscosity correction factor

When there is a significant viscosity gradient,  $\phi$  is no longer unity and the heat transfer coefficient,  $\alpha$ , is given by  $\alpha'\phi$ , where  $\alpha'$  is the heat transfer coefficient calculated for  $\phi = 1$ .  $\phi$  cannot be calculated directly because it is related to the surface temperature, which in turn depends on  $\alpha$ . Trial and error is therefore involved.

As an illustration suppose that, on the cold side of Fig. 6.3,  $\phi$  is significantly greater than unity (fluid being heated) and the heat transfer coefficient is  $\alpha_o$ , referred to the external surface. The adjacent surface temperature is  $T_5$ .

$$\alpha_o = \alpha'_o \phi_o = \alpha'_o \left( \frac{\eta_b}{\eta_s} \right)^a$$

by heat balance

$$\alpha'_o \left( \frac{\eta_b}{\eta_s} \right)^a (T_5 - T_6) = \frac{T_1 - T_5}{\Sigma r_{1.5}} \dots \dots \quad [6.10a]$$

Equation [6.10a] must be solved by trial and error, the interrelated unknown factors being  $\eta_s$  and  $T_5$ . The solution involves: (a) assume a value for  $T_5$ , (b) from a viscosity-temperature curve determine  $\eta_s$  at temperature  $T_5$ , (c) substitute into equation [6.10a] and (d) if equation [6.10a] does not balance, assume new values for  $T_5$  and repeat until balance is achieved.

If the hot side of Fig. 6.3 has a value of  $\phi$  significantly less than unity (fluid being cooled) and the heat transfer coefficient referred to the external surface is  $\alpha'_{io}$ ,  $T_2$  must be found by trial and error from:

$$\alpha'_{io} = \alpha'_{io} \phi_i = \alpha'_{io} \left( \frac{\eta_b}{\eta_s} \right)^a$$

and

$$\alpha'_{io} \left( \frac{\eta_b}{\eta_s} \right)^a (T_1 - T_2) = \frac{T_2 - T_6}{\Sigma r_{2.6}} \dots \dots \quad [6.10b]$$

### 6.8.3 Example – coefficient and surface temperature (viscosity correction factor not unity)

In the example given in section 6.8.2, the cold fluid is viscous and, as it is being heated,  $\phi$  will be greater than unity. What are the values of  $\phi_o$ ,  $\alpha_o$ ,  $T_5$  and  $U$ ? Assume  $a = 0.26$ . Cold fluid viscosities are:

Temperature (°C)	100	130	140	150
Viscosity (N s/m <sup>2</sup> )	0.01110	0.00520	0.00427	0.00357

From the previous example,  $\Sigma r_{1.5} = 0.003242 (\text{W/m}^2 \text{K})^{-1}$ ,  $T_1 = 300^\circ \text{C}$ ,  $T_6 = 100^\circ \text{C}$ ,  $\alpha'_o = 1000 \text{ W/m}^2 \text{K}$

Substituting into equation [6.10a]:

$$1000 \times (0.0111/\eta_s)^{0.26} (T_5 - 100) = (300 - T_5)/0.003242$$

By trial and error:  $T_5 = 139^\circ \text{C}$  ( $\eta_s = 0.00438$ )

$$\phi_o = (0.0111/0.00438)^{0.26} = 1.274$$

$$\alpha_o = 1274 \text{ W/m}^2 \text{K} \text{ (27.4\% increase)}$$

$$U = 248.3 \text{ W/m}^2 \text{K} \text{ (5\% increase)}$$

It will be noted that the viscosity ratio is raised to a small power such that a small error in calculating  $T_5$  has a small effect on  $\alpha_o$ . In the previous example with  $\phi_o = 1$ ,  $T_5$  was calculated as  $147.2^\circ \text{C}$ . If this value is used  $\phi_o = 1.325$ ,  $\alpha_o = 1325 \text{ W/m}^2 \text{K}$  and  $U = 250.2 \text{ W/m}^2 \text{K}$ . To avoid tedious trial and error, the surface temperature is sometimes calculated directly from equation [6.9] and this value used to calculate  $\phi$  and  $\alpha$ . The use of equation [6.9] always provides a helpful guide to the likely value of the surface temperature.

If  $\phi$  is not unity for both fluids, then equation [6.10c] must be solved to determine  $T_2$  and  $T_5$ :

$$\alpha'_o \phi_o (T_5 - T_6) = \alpha'_i \phi_i (T_1 - T_2) = \frac{T_2 - T_5}{\Sigma r_{2,5}} \quad [6.10c]$$

## 6.9 Cooperative research organisations

Section 6.4 states that film heat transfer coefficients must be determined from experimental data. The same applies to pressure loss calculations because heat transfer equipment cannot be designed properly unless both heat transfer and pressure loss data are available. Although the rapid development and application of computers in the early 1960s enabled the design of heat transfer equipment to be established on a more sophisticated basis, sound test data are essential to investigate areas of uncertainty and to check and modify proposed design methods.

Site-testing involves the uncertainties of plant-loading, fouling and weather. It must also be conducted at many sites for adequate investigation of the numerous design parameters. Over the years valuable work has been (and still is) carried out by universities and other research organisations. In many cases carefully planned tests on an element of heat transfer equipment, such as a single tube for instance, has yielded valuable results, without the expense of large-scale equipment. As laboratory testing is normally conducted on small-scale equipment, the results may not be applicable to full-size equipment. Testing of any kind involves considerable expenditure which is beyond the resources of many companies.

In order to overcome these problems, Heat Transfer Research Inc. (HTRI) was established in the USA in 1962 and the Heat Transfer and Fluid Flow Service (HTFS) was established in the UK in 1967. Nearly 300 sponsors throughout the world now subscribe to one or both organisations and thus provide them with the large financial resources necessary to conduct heat transfer and fluid flow tests in large-scale equipment with design parameters investigated over wide ranges. The results of their heat transfer and fluid flow research, reports, design methods and supporting computer programs, proprietary equipment testing, and consultancy, has considerably changed the thermal design approach of many sponsors.

One of the early tasks for both organisations was to investigate and develop improved methods for calculating single-phase heat transfer and pressure loss on the shell-side of a baffled shell-and-tube exchanger. This was achieved and comprehensive computer programs were developed independently by both organisations to solve the complex shell-side flow problem. It should be emphasized that the activities of the cooperative research organisations are not confined to shell-and-tube heat exchangers or single-phase flow. Research and design involve other types of heat transfer equipment and related heat transfer and fluid flow problems. As expected, two-phase flow is high in priority.

The computer programs and design data are available to all sponsors, but non-members may obtain heat transfer equipment designed in accordance with HTRI and HTFS proprietary data from design service companies, or from sponsor manufacturers.

## 6.10 Heat transfer and pressure loss correlations (single phase)

In presenting heat transfer data, correlations for heat transfer coefficients may be expressed by two methods. One method involves the Nusselt number in which:

$$\text{Nusselt number} = \text{Nu} = \frac{\alpha d}{\lambda} = \sigma \text{Re}^m \text{Pr}^n \quad [6.11]$$

In equation [6.11],  $\sigma$  is a constant determined from experiments. From this equation a heat transfer factor  $J_h$  may be expressed as:

$$J_h = \text{Nu} \text{Pr}^{-n} = \sigma \text{Re}^m \quad [6.12]$$

Equation [6.11] shows that an increase in  $\text{Re}$ , which arises from an increase in velocity, increases  $\text{Nu}$ , and hence  $\alpha$ . This logical approach generally suits the thermal design engineer and is the method presented in this section. For graphical presentation,  $J_h$  is plotted against  $\text{Re}$  and it will be seen from equation [6.12] that an increase in  $\text{Re}$  increases  $J_h$  and hence increases  $\text{Nu}$  and  $\alpha$ . (Exponents  $m$  and  $n$  are less than 1.)

The second method involves the Stanton number in which:

$$\text{Stanton number} = \text{St} = \frac{\alpha}{c_p \dot{m}} = \frac{\text{Nu}}{\text{Re} \text{Pr}} \quad [6.13]$$

Combining [6.11] and [6.13]

$$\text{St} \text{Pr}^{1-n} = \sigma \text{Re}^{m-1} = j \quad [6.14]$$

For graphical representation  $j$  is plotted against  $\text{Re}$  and it will be seen that  $j$  decreases as  $\text{Re}$  increases,  $m$  being less than 1. However, the advantage of this method is that  $j$  may be compared directly with the friction factor, which follows a similar trend when plotted against  $\text{Re}$ . It will be seen from equations [6.12] and [6.14] that

$$J_h = j \text{Re} \quad [6.15]$$

The friction factor may also be presented in several ways and a check should always be made to ensure that the friction factor applies to the pressure loss equation being used. In this section, pressure loss is based on the Fanning relationship given by equation [6.22].

An ideal tube bank is one in which the gross cross-section of the enclosing duct normal to the flow of the external fluid is square or rectangular, and the tube configuration is constant. Unlike a shell-and-tube exchanger, there is no leakage of the external fluid from the duct.

### 6.10.1 Basis for physical property and Reynolds number determination

In heat transfer and pressure loss correlations, physical properties are determined at various temperatures, such as mean bulk, wall and 'film', which is between the two. In the following correlations, physical properties are always determined at the mean bulk temperature, except when a subscript is shown.

Various flow areas and characteristic dimensions are used to define Reynolds number, and these are clearly stated.

In all cases,  $a$  is the exponent for the viscosity correction factor  $\phi = (\eta/\eta_s)^a$  or  $\phi_1 = (\text{Pr}/\text{Pr}_s)^{a_1}$

### 6.10.2 Inside cylindrical tubes

Heat transfer coefficients and pressure loss for flow inside straight cylindrical tubes may be calculated from equations [6.16] to [6.23].

#### Reynolds number

In all cases

$$\text{Re} = \frac{\dot{m}d_i}{\eta} = \frac{ud_i\rho}{\eta}$$

#### Source

Heat transfer coefficients: ESDU (1967) and (1968)

Pressure loss: see text

#### Heat transfer coefficient

Heat transfer coefficient equations cover turbulent flow ( $\text{Re} > 10\,000$ ), transitional flow ( $2000 \leq \text{Re} \leq 10\,000$ ) and laminar flow ( $\text{Re} < 2000$ ). In laminar flow the forced convection coefficient is corrected for free-convection effects. These depend on whether the tube is horizontal or vertical, and in the latter case, whether the flow is 'assisted' or 'opposed' by free-convection effects, as defined below.

#### Turbulent flow ( $\text{Re} > 10\,000$ )

When  $\alpha_i$  is critical to the design, equation [6.16a] should be used. Usually equation [6.16b] is sufficiently reliable, being least accurate at coincident low Reynolds number and high Prandtl number.

$$\alpha_i = 0.0225 \left(\frac{\lambda}{d_i}\right) \text{Pr}^{0.495} \text{Re}^{0.795} [\exp\{-0.0225(\ln \text{Pr})^2\}] \phi \quad [6.16a]$$

$$\alpha_i = 0.0204 \left(\frac{\lambda}{d_i}\right) \text{Pr}^{0.415} \text{Re}^{0.805} \phi \quad [6.16b]$$

$a = 0.18$  fluid heated,  $0.3$  fluid cooled

#### Transition flow ( $2000 \leq \text{Re} \leq 10\,000$ )

$$\alpha_i = 0.1 \left(\frac{\lambda}{d_i}\right) (\text{Re}^{2/3} - 125) \text{Pr}^{0.495} [\exp\{-0.0225(\ln \text{Pr})^2\}] \left\{1 + \left(\frac{d_i}{L}\right)\right\}^{2/3} \phi \quad [6.17]$$

$a = 0.14$

#### Laminar flow ( $\text{Re} < 2000$ , $Gz > 9$ )

Horizontal tubes

$$\alpha_i = 1.75 \left(\frac{\lambda}{d_i}\right) [Gz + 0.0083(\text{Gr Pr})^{0.75}]^{1/3} \phi \quad [6.18]$$

Vertical tubes – ‘assisted’ flow (heated upflow or cooled downflow)

$$\alpha_i = 1.75 \left( \frac{\lambda}{d_i} \right) \left[ Gz + 0.0722E \left\{ Gr, Pr, \left( \frac{d_i}{L} \right) \right\}^{0.84} \right]^{1/3} \quad [6.19]$$

Vertical tubes – ‘opposed’ flow (cooled upflow or heated downflow)

$$\alpha_i = 1.75 \left( \frac{\lambda}{d_i} \right) \left[ Gz - 0.0722E \left\{ Gr, Pr, \left( \frac{d_i}{L} \right) \right\}^{0.75} \right]^{1/3} \quad [6.20]$$

Note:  $\{Gr, Pr, (d_i/L)\} < 16.84 Gz^{4/3}$

Obtain  $E$  for equations [6.19] and [6.20] from Table 6.3.

Table 6.3 Value of  $E$  for use in equations [6.19] and [6.20]

$\frac{\pi a d_i}{Gz \lambda}$	$E$	$\frac{\pi a d_i}{Gz \lambda}$	$E$	$\frac{\pi a d_i}{Gz \lambda}$	$E$
0.0	1.00	1.2	0.57	2.8	0.29
0.1	0.95	1.3	0.54	3.0	0.27
0.2	0.91	1.4	0.51	3.2	0.25
0.3	0.87	1.5	0.49	3.4	0.23
0.4	0.83	1.6	0.47	3.6	0.22
0.5	0.79	1.7	0.45	3.8	0.20
0.6	0.75	1.8	0.43	4.0	0.19
0.7	0.72	1.9	0.41	4.5	0.16
0.8	0.68	2.0	0.39	5.0	0.13
0.9	0.65	2.2	0.36	5.5	0.11
1.0	0.62	2.4	0.34	6.0	0.09
1.1	0.59	2.6	0.31	$\infty$	0

Laminar flow ( $Re < 2000, Gz \leq 9$ )

Horizontal and vertical tubes

$$\alpha_i = 3.66 \left( \frac{\lambda}{d_i} \right) \quad [6.21]$$

Pressure loss

The frictional pressure loss in straight cylindrical tubes is given by the Fanning equation below:

$$\Delta P_i = \left\{ \frac{4f_i L \dot{m}^2}{2\rho d_i \phi} \right\} \quad [6.22]$$

$$a = 0.14 \text{ for } Re \geq 2100$$

$$= 0.25 \text{ for } Re < 2100$$

The friction factor ( $f_i$ ) is obtained from the curves given by Fig. 6.4 based on the work of Moody (1944). The friction factor depends on the Reynolds number over its complete range, and in the turbulent region it also depends on the relative roughness. Roughness ( $e$ ) is the distance from peak to valley of the tube or pipe surface and relative roughness is ( $e/d_i$ ). Values of  $e$  for various surfaces is given in Table 6.4 but for the design of tubular heat transfer equipment equations [6.23c] and [6.23d] are widely used. These equations are superimposed on the curves of Fig. 6.4 and their relationship to relative roughness will be seen.

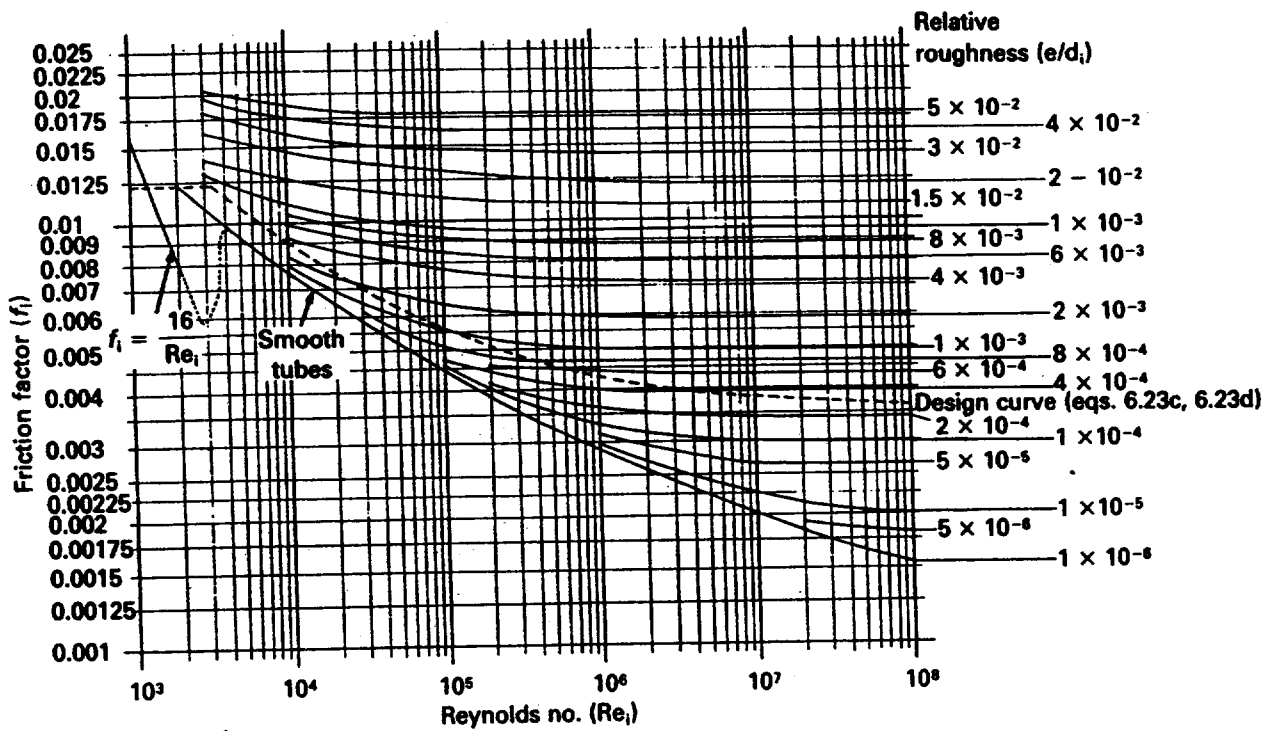


Figure 6.4 Fanning friction factor for flow inside straight circular pipes (based on Moody 1944)

Table 6.4 Surface roughness ( $e$ ) for various materials

Material	Surface roughness (m)
Drawn tubing	$1.5 \times 10^{-6}$
Commercial steel or wrought iron	$46 \times 10^{-6}$
Asphalted cast iron	$122 \times 10^{-6}$
Galvanised iron	$152 \times 10^{-6}$
Cast iron	$254 \times 10^{-6}$
Concrete	$305 \times 10^{-6}$ (min)

*Laminar flow ( $Re \leq 1311$ )*

All tubes

$$f_i = \frac{16}{Re} \quad [6.23a]$$

*Turbulent region ( $Re \geq 2100$  – smooth tubes;  $\geq 3380$  – commercial pipe or slightly corroded tubes)*

Smooth tubes

$$f_i = 0.0014 + \frac{0.125}{Re^{0.32}} \quad [6.23b]$$

Commercial pipe or slightly corroded tubes

$$f_i = 0.0035 + \frac{0.264}{Re^{0.42}} \quad [6.23c]$$



*Transition region (1311 < Re < 2100 – smooth tubes, 1311 < Re < 3380 – commercial pipe or slightly corroded tubes)*

$$f_i = 0.0122 \quad [6.23d]$$

### 6.10.3 Inside uniform channels

Heat transfer and pressure loss in uniform channels, other than tubes, may be calculated from equations [6.16]–[6.23], if the inside diameter ( $d_i$ ) is substituted by ( $d_e$ ), the equivalent diameter, where:

$$d_e = \frac{4A_x}{P_w} = 4 \left\{ \frac{\text{cross-sectional area for flow}}{\text{wetted perimeter}} \right\} \quad [6.24]$$

Hence, for a uniform channel of rectangular cross-section, with sides measuring  $y$  and  $z$ ,  $A_x = yz$ ,  $P_w = 2(y + z)$  and hence  $d_e = 2yz/(y + z)$ . If  $z$  is large in relation to  $y$ , as provided by closely spaced plates,  $d_e \approx 2y$ . In the case of a concentric annulus having an outer tube of inside diameter  $D_i$  and annulus tube of outside diameter  $D_o$ ,

$$A_x = (\pi/4) (D_i^2 - D_o^2), P_w = \pi(D_i + D_o)$$

and hence  $d_e = (D_i - D_o)$ . The use of  $d_e$  for calculating heat transfer in an annulus is an approximation. A more rigorous treatment is given by ESDU (1981).

### 6.10.4 Outside ideal plain tube banks

Heat transfer coefficients and pressure loss for cross-flow outside ideal plain tube banks may be calculated from equations [6.25] and [6.26]. These equations provide the basis for shell-side calculations in baffled shell-and-tube heat exchangers. However, the tube banks are not 'ideal' and reference should be made to Chapter 12 for the design of shell-and-tube exchangers.

#### *Reynolds number*

In all cases, this is based on the minimum cross-flow area between tubes as given by Fig. 12.3. The cross-flow area may be calculated from  $S_m$  given in Table 12.1, with  $D_s$  and  $l_s$  as the dimensions of the enclosing duct normal to flow.

$$Re = \frac{\dot{m}_m d_o}{\eta}$$

#### *Source*

Heat transfer coefficients: ESDU (1973)  
Pressure loss: ESDU (1974) and (1979)

#### *Heat transfer coefficient*

$$\alpha_o = J_h \left( \frac{\lambda}{d_o} \right) Pr^{0.33} \phi_1 \quad [6.25]$$

Obtain  $J_h$  from Figs 6.5(a)–(c)  
 $a_1 = 0.26$

Pressure loss

$$\Delta P_o = \left\{ \frac{2f_o \dot{m}_m^2 N_r}{\rho \phi} \right\} \quad [6.26]$$

Obtain  $f_o$  from Figs 6.5(a)–(c)  
 $a = 0.38 \text{ Re}^{-0.24}$

### 6.10.5 Outside ideal high-finned tube banks

Because of the large number of factors which influence the performance of high-finned tubes, it is advisable to seek experimental data which relate closely to the type, geometry and configuration of the finned tubes under consideration. Most data have been obtained for *air flowing across smooth, plain, helical fins on cylindrical tubes*, some of which are shown in Fig. 3.4. If experimental data are not available, equations [6.27] and [6.28] may be used to predict heat transfer and pressure loss for air flowing across such tubes, arranged on an *equilateral triangular pitch*.

*Reynolds number, velocity and diameter*

In all cases, Reynolds number and velocity are based on the minimum cross-flow area between tubes in a row, as shown in Table 9.2 for ideal banks. The characteristic diameter for Reynolds number is always the fin root diameter, except where noted, i.e.

$$\text{Re} = \frac{\dot{m}_m d_r}{\eta} = \frac{u_m d_r \rho}{\eta}$$

*Source*

Equations [6.27] and [6.28] are based on the recommendations of Gianolio and Cuti (1981) whose experimental work shows that both heat transfer and pressure loss depend on whether the air flow is forced or induced. In addition, heat transfer is influenced by the number of tube rows in the bank when less than six.

Equation [6.27a] is based on Briggs and Young (1963) and Ward and Young (1959). Equation [6.28c] is that of Jameson (1945). The remaining equations have been derived by Gianolio and Cuti (1981).

*Heat transfer coefficient (induced draught – 6 or more rows)*

$$\alpha_o = 0.134 \left( \frac{\lambda}{d_r} \right) \text{Pr}^{0.33} \text{Re}^{0.681} \left( \frac{s}{l_f} \right)^{0.2} \left( \frac{s}{t_f} \right)^{0.1134} \quad [6.27a]$$

$N_r < 6$ : multiply equation [6.27a] by  $(1 + u_m/N_r^2)^{-0.14}$

*Heat transfer coefficient (forced draught – 6 or more rows)*

$$\alpha_o = 0.271 \left( \frac{\lambda}{d_r} \right) \text{Pr}^{0.33} \text{Re}^{0.685} \left( \frac{A_t}{A_b} \right)^{-0.311} \quad [6.27b]$$

$2 < N_r < 6$ : multiply equation [6.27b] by  $(N_r/6)^{-0.138}$



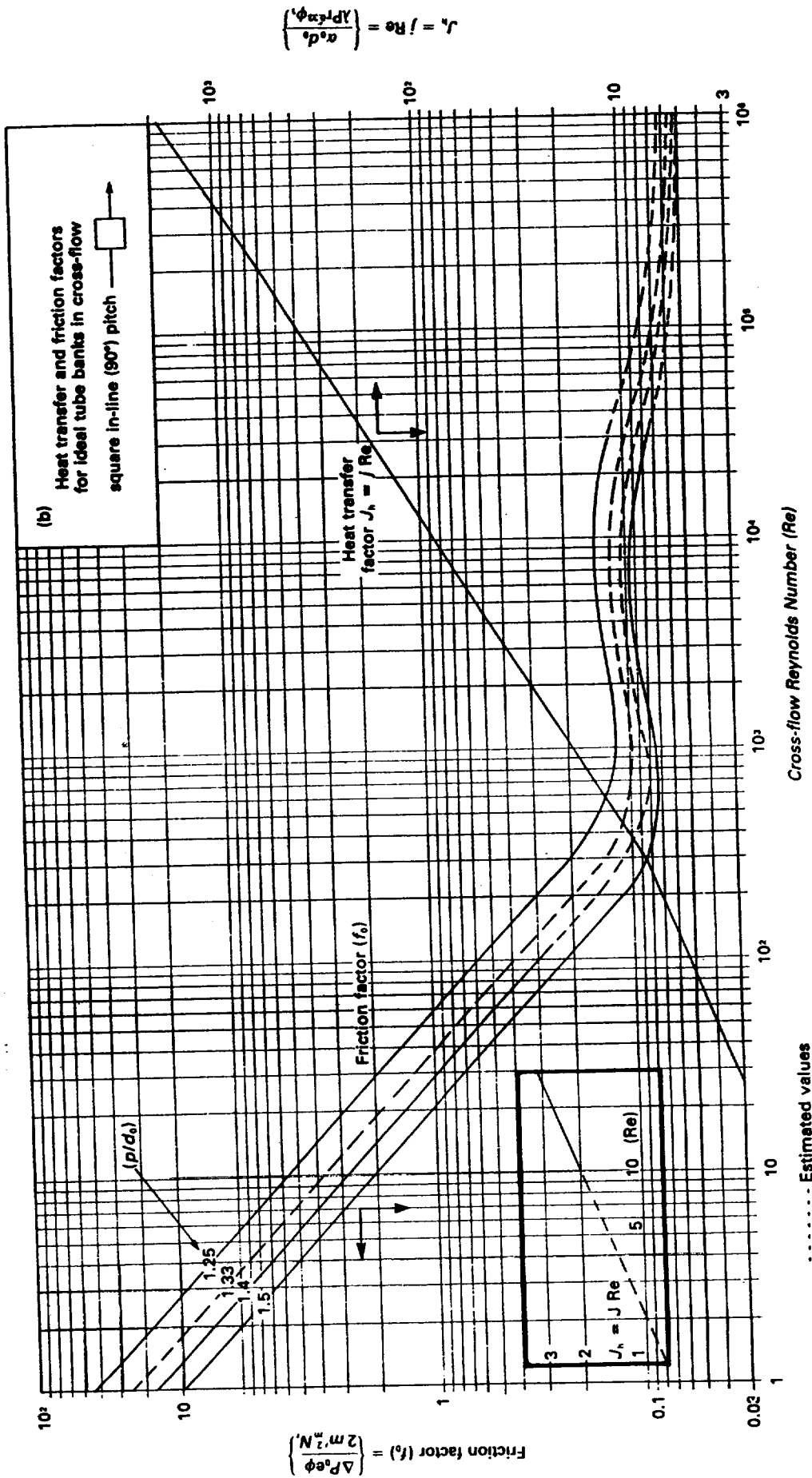


Figure 6.5 (cont.)



**Pressure loss**

$$\Delta P_o = \left\{ \frac{2f_o \dot{m}_m^2 N_r}{\rho} \right\} \quad [6.28a]$$

**Induced draught:**

$$f_o = 16.36 \text{Re}^{-0.412} \left( \frac{p_t}{d_r} \right)^{-1.54} \left( \frac{A_t}{A_b} \right)^{0.3} \quad [6.28b]$$

**Forced draught:**

$$f_o = 1.532 \text{Re}_p^{-0.25} \quad [6.28c]$$

$$\text{Re}_p = \frac{\dot{m}_m d_p}{\eta}$$

$$d_p = \frac{d_h}{[(l_f/2s)^{0.4} \{1/(p_t/d_h - 1)\}^{1/2}]^4}$$

$$d_h = \left\{ \frac{(A_t/A_b) d_r}{2l_f N_f + 1.0} \right\}$$

**6.10.6 Outside ideal low-finned tube banks**

Heat transfer coefficients and pressure loss for cross-flow outside ideal low-finned tube banks, arranged on an equilateral triangular pitch may be calculated from equations [6.29] and [6.30]. *Heat transfer and pressure loss for baffled shell-side flow in shell-and-tube exchangers, using low-finned tubes, are treated differently as described in Chapter 13.*

**Reynolds number**

In all cases this is based on the minimum cross-flow area between tubes in a row, as shown in Table 9.2 for ideal banks, i.e.

$$\text{Re} = \frac{d_r \dot{m}_m}{\eta}$$

**Source**

Rabas *et al* (1980)

**Heat transfer coefficient**

$$J_h = 0.292 \text{Re}^q \left( \frac{s}{d_f} \right)^{1.115} \left( \frac{s}{l_f} \right)^{0.257} \left( \frac{l_f}{s} \right)^{0.666} \left( \frac{d_f}{d_r} \right)^{0.473} \left( \frac{d_f}{l_f} \right)^{0.7717} \quad [6.29]$$

where  $q = \{0.585 + 0.0346 \ln(d_f/s)\}$ .

Use  $J_h$  in equation [6.25] with  $\phi = 1$ .

**Pressure loss**

$$f_o = 3.805 \text{Re}^{-0.2336} \left( \frac{s}{d_f} \right)^{0.2512} \left( \frac{l_f}{s} \right)^{0.7593} \left( \frac{d_r}{d_f} \right)^{0.7292} \left( \frac{d_r}{p_t} \right)^{0.7085} \left( \frac{p_t}{p_l} \right)^{0.3791} \quad [6.30]$$

Use  $f_o$  in equation [6.26] with  $\phi = 1$ .

### 6.10.7 Shell-and-tube exchangers – headers and nozzles

Pressure losses in the headers and nozzles of shell-and-tube exchangers may be calculated from equations [6.31a]–[6.31c]. The losses are expressed in terms of  $K$  (dimensionless) velocity heads.

#### Channel inlet and outlet nozzles

These are based on the fluid mass velocity ( $\dot{m}_n$ ), or fluid velocity ( $u_n$ ), in the nozzle bore.

$$\Delta P_{nt} = K_{nt} \left( \frac{\dot{m}_n^2}{2\rho} \right) = K_{nt} \left( \frac{\rho u_n^2}{2} \right) \quad [6.31a]$$

$$K_{nt} = 1.1 \text{ (inlet nozzle)} \\ = 0.7 \text{ (outlet nozzle)}$$

#### Headers

These are based on the fluid mass velocity ( $\dot{m}_t$ ), or fluid velocity ( $u_t$ ), inside the tubes. The total loss due to one tube-side pass is that due to a contraction loss at entry, expansion loss at exit, plus a  $180^\circ$  turn-around loss if there is more than one tube-side pass.

For  $N_p$  passes,

$$\Delta P_h = K_h \left( \frac{\dot{m}_t^2}{2\rho} \right) N_p = K_h \left( \frac{\rho u_t^2}{2} \right) N_p \quad [6.31b]$$

$$K_h = 0.9 \text{ for one tube-side pass} \\ = 1.6 \text{ for two or more tube-side passes, including U-tubes}$$

#### Shell-side nozzles

These are based on the fluid mass velocity ( $\dot{m}_n$ ) or fluid velocity ( $u_n$ ) in the nozzle bore, based on Smith (1987).

$$\Delta P_{ns} = K_{ns} \left( \frac{\dot{m}_n^2}{2\rho} \right) = K_{ns} \left( \frac{\rho u_n^2}{2} \right) \quad [6.31c]$$

with impingement plate

$$K_{ns} = 1 + \left( \frac{S_n}{S_c} \right)^2$$

without impingement plate

$$K_{ns} = 1 + \frac{1}{(S_c/S_n) + 0.6 (p_t - d_o/p_t)^2}$$

with distributor

$$K_{ns} = 1 + \frac{1}{4} \left\{ \frac{d_n}{D_b - D} \right\}^2 + \left\{ \frac{(\pi/4)d_n^2}{S_v(p_t - d_o/p_t)} \right\}^2$$

## References

A list of addresses for the service organisations is provided on p. xvi.

- Bell, K. J. (1963) 'Final Report of the Cooperative Research Program on Shell and Tube Heat Exchangers', *Univ. of Delaware Eng. Exp. Stat. Bulletin* 5.
- Briggs, D. E. and Young, E. H. (1963) 'Convection heat transfer and pressure drop of air flowing across triangular pitch banks of finned tubes', *Chemical Engineering Progress Symposium*, Series No. 41, Vol. 59, p.1.
- Engineering Sciences Data Unit International Ltd, London, UK: ESDU (1967) and (1968), Data items 67016, 68006, 68007; ESDU (1973), Data item 73031; ESDU (1974) and (1979), Data items 74040, 79034; ESDU (1981), Data item 81045.
- Gianolio, E. and Cuti, F. (1981) Heat transfer coefficients and pressure drops for air coolers with different numbers of rows under induced and forced draft, *Heat Transfer Engineering*, Vol. 3 (No.1, July-Sept.) pp. 38-48.
- Jameson, S. L. (1945) 'Tube spacing in finned tube banks, *Trans. ASME*, Vol. 67, pp. 633-42.
- Moody, L. F. (1944) 'Friction factors for pipe flow', *J. Heat Transfer*, Vol. 66, pp. 671-84.
- Rabas, T. J. *et al.* (1980) 'The effect of fin density on the heat transfer and pressure drop performance of low-finned tube banks', *ASME/AIChE Heat Transfer Conference, Orlando, 27-30 July*.
- Smith, R. A. (1987) *Vaporisers - Selection Design & Operation*. Longman.
- Ward, D. J. and Young, E. H. (1959) 'Heat transfer and pressure drop of air in forced convection across triangular pitch banks of finned tubes', *Chemical Engineering Progress Symposium*, Series 29, Vol. 55, p. 37.

## Nomenclature

Symbol	Description	Units
$a, a_1$	Exponents for viscosity ratio (see $\phi$ and $\phi_1$ )	—
$A$	Surface area (general)	$m^2$
$A_i$	Internal surface area	$m^2$
$A_o$	External surface area	$m^2$
$A_i/A_b$	Ratio of surface area of finned tube to that of base tube without fins	—
$A_{ref}$	Reference surface area (equations [6,6], [6.7a], and [6.7b])	$m^2$
$A_x$	Cross-sectional area for fluid flow for non-circular channels	$m^2$
$A_w$	Mean surface area of heat transfer surface or wall	$m^2$
$c_p$	Specific heat	J/kg K
$d$	Diameter (general)	m
$d_e$	Equivalent diameter for non-circular channels (equation [6.24])	m
$d_f$	Fin outside diameter	m
$d_h, d_p$	Equivalent diameters for high-finned tube banks (equation [6.28c])	m
$d_i$	Inside tube diameter	m
$d_{ip}$	Impingement plate diameter	m
$d_1$	Distance between nozzle and impingement baffle, or closest tubes = $h_i$ or $h_o$ as appropriate, from Fig. A3.1	m
$d_n$	Nozzle inside diameter	m
$d_o$	Outside tube diameter	m
$d_r$	Fin root diameter	m



$D$	Shell outside diameter (equation [6.31c])	m
$D_b$	Shell distributor inside diameter (equation [6.31c])	m
$D_i$	Inside diameter of outer tube of concentric tubes	m
$D_o$	Outside diameter of inner tube of concentric tubes	m
$E$	Factor for calculating heat transfer in laminar flow inside a vertical tube (equations [6.19], [6.20] and Table 6.3)	—
$Eu$	Euler number (defined in Table 6.1)	—
$f_i, f_o$	Friction factors, inside and outside circular tubes	—
$Gr, Gr_s$	Grashof number (defined in Table 6.1), at bulk and wall temperatures, respectively	—
$Gz$	Graetz number (defined in Table 6.1)	—
$j$	Heat transfer factor based on Stanton number (equation [6.14])	—
$J_h$	Heat transfer factor based on Nusselt number (equation [6.12])	—
$K_h, K_{ns}, K_{nt}$	Number of velocity heads lost in headers, shell-side nozzles and tube-side nozzles respectively	—
$l_f$	Fin height	m
$L$	Tube length	m
$m$	Exponent in equation [6.11]	—
$\dot{m}$	Mass velocity	kg/s m <sup>2</sup>
$\dot{m}_m$	Mass velocity based on minimum cross flow area between tubes	kg/s m <sup>2</sup>
$\dot{m}_n, \dot{m}_t$	Mass velocity in nozzle and tubes respectively	kg/s m <sup>2</sup>
$n$	Exponent in equation [6.11]	—
$N_f$	Number of fins in 1 metre length	1/m
$N_p$	Number of tube-side passes	—
$N_r$	Number of tube rows crossed in direction of flow outside tube banks	—
$Nu$	Nusselt number (defined in Table 6.1)	—
$p_l$	Longitudinal tube pitch: distance between centres of adjacent rows parallel to external flow	m
$p_t$	Transverse tube pitch: distance between centres of adjacent tubes in a row normal to external flow	m
$p_w$	Wetted perimeter for non-circular channels (equation [6.24])	m
$Pe$	Peclet number (defined in Table 6.1)	—
$Pr, Pr_s$	Prandtl number (defined in Table 6.1) at bulk and wall temperatures, respectively	—
$q$	Exponent for Reynolds number for use in equation [6.29]	—
$Q$	Heat transferred (general)	W
$r_i, r_o$	Internal and external fouling resistance	(W/m <sup>2</sup> K) <sup>-1</sup>
$r_w$	Resistance of heat transfer surface wall	(W/m <sup>2</sup> K) <sup>-1</sup>
$Ra$	Rayleigh number (defined in Table 6.1)	—
$Re$	Reynolds number (defined in Table 6.1)	—
$s$	Fin spacing	m
$S_c$	Escape area at shell nozzle (= $\pi d_{ip} d_i$ or $\pi d_n d_i$ )	m <sup>2</sup>
$S_n$	Nozzle internal cross-sectional area	m <sup>2</sup>
$S_v$	Cross-sectional area for flow into shell from distributor, either end space (cone type) or slots (box type) – see Fig. 1.27	m <sup>2</sup>
$St$	Stanton number (defined in Table 6.1)	—
$t$	Thickness (general)	m
$t_f$	Fin thickness	m
$T$	Temperature (general)	K
$T_b$	Bulk fluid temperature	K
$T_s$	Heat transfer surface or wall temperature	K
$u$	Fluid velocity (general)	m/s

$u_m$	Fluid velocity based on minimum cross-flow area between tubes	m/s
$u_n$	Fluid velocity in nozzle	m/s
$u_t$	Fluid velocity in tubes	m/s
$U$	Overall heat transfer coefficient (general)	W/m <sup>2</sup> K
$U_o$	Overall heat transfer coefficient related to external surface	W/m <sup>2</sup> K
$U_{ref}$	Overall heat transfer coefficient related to reference surface	W/m <sup>2</sup> K
$\alpha$	Heat transfer coefficient (general)	W/m <sup>2</sup> K
$\alpha_{fi}, \alpha_{fo}$	Conductances of internal and external fouling layers	W/m <sup>2</sup> K
$\alpha_i, \alpha_o$	Internal and external heat transfer coefficients	W/m <sup>2</sup> K
$\alpha_w$	Conductance of heat transfer surface wall	W/m <sup>2</sup> K
$\Delta P$	Pressure loss (general)	Pa
$\Delta P_h$	Pressure loss in headers	Pa
$\Delta P_i$	Pressure loss inside tubes	Pa
$\Delta P_{ns}, \Delta P_{nt}$	Pressure loss in shell-side and tube-side nozzles, respectively	Pa
$\Delta P_o$	Pressure loss outside tubes	Pa
$\Delta T$	Temperature difference (general)	K
$\Delta T_f$	Temperature drop across film (= $T_s - T_b$ )	K
$\eta, \eta_s$	Dynamic viscosity at bulk and wall temperatures, respectively	N s/m <sup>2</sup>
$\kappa$	Thermal diffusivity (used in Table 6.1) (= $\lambda/\rho c_p$ )	m <sup>2</sup> /s
$\lambda$	Fluid thermal conductivity	W/mK
$\lambda_w$	Thermal conductivity of heat transfer surface wall	W/mK
$\nu$	Kinematic viscosity	m <sup>2</sup> /s
$\rho$	Fluid density	kg/m <sup>3</sup>
$\sigma$	Constant in equation [6.11]	—
$\phi$	Viscosity correction factor (= $(\eta/\eta_s)^a$ ) ( $a$ is given in text)	—
$\phi_1$	Viscosity correction factor (= $(Pr/Pr_s)^{a_1}$ ) ( $a_1$ is given in text)	—

---

## Mean temperature difference

In the case of heat flow through a tube wall in which the hot and cold faces are maintained at uniform temperatures of  $T_1$  and  $T_2$  respectively, the driving force, or mean temperature difference (MTD), is simply  $(T_1 - T_2)$ . In a heat exchanger where heat is being transferred between two fluids whose temperatures are usually changing during their passage through the exchanger, the determination of the mean temperature difference (MTD) is more complex.

### 7.1 Countercurrent and cocurrent flow

Consider one length of a double-pipe exchanger, as shown in Fig. 7.1, in which the hot fluid enters the annulus at end A at temperature  $T_1$  and is cooled to leave at end B at temperature  $T_2$ . At end B, the cold fluid enters the inner pipe at  $t_1$  and is heated to  $t_2$ , to leave at end A. Because the fluids flow in strict opposition to one another, the flow system is termed *countercurrent*.

Consider the same length of double-pipe exchanger in which the hot fluid enters the annulus at end B at  $T_1$ , while the cold fluid enters the inner pipe at end B at  $t_1$ . The annulus fluid is cooled to  $T_2$  and leaves at end A, while the inner pipe fluid is heated to  $t_2$  and also leaves at end A. Because the fluids flow strictly in parallel with one another the flow system is termed *cocurrent*.

### 7.2 Temperature approach, meet and cross

The difference between the outlet temperature of the cooled fluid ( $T_2$ ) and the outlet temperature of the heated fluid ( $t_2$ ) has particular thermal significance and introduces the terminology of temperature approach, temperature meet and temperature cross. In the three cases below,  $T_1$  and  $t_1$  are the inlet temperatures of the hot and cold fluids respectively.

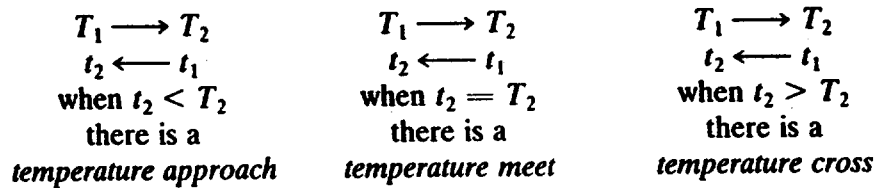


Figure 7.1 shows that with countercurrent flow the outlet temperature of the cold fluid may be appreciably greater than the outlet temperature of the hot fluid and may also approach the hot fluid inlet temperature closely. Hence, a temperature approach, meet and cross are readily achieved. In the case of cocurrent flow, Fig 7.1 shows that a temperature meet and cross can never be achieved. Countercurrent flow is therefore the preferred system and there would appear to be little incentive to use cocurrent flow. However, in certain applications it may be advantageous to provide cocurrent instead of countercurrent flow because (a) it produces a more uniform wall temperature, which minimises thermal stresses and (b) it has a lower maximum tube-wall temperature, which may eliminate problems of fouling, fluid decomposition and tube material selection. Countercurrent shell-and-tube exchangers may have structural limitations as described in section 7.7.1.

When one of the fluids is isothermal it is immaterial whether the flow is countercurrent or cocurrent.

### 7.3 Mean temperature difference for countercurrent and cocurrent flow

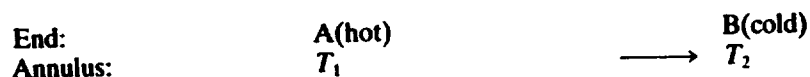
#### 7.3.1 Assumptions

To derive the mean temperature difference for single-phase fluids in countercurrent or cocurrent flow, the following assumptions are made:

- (a) The heat transfer coefficient, flow rates and specific heats of both fluids are constant throughout the unit.
- (b) The temperature of each fluid is constant over any cross-section of its path through the unit, which means complete mixing without stratification or by-passing (see sections 1.5.16 and 12.2.2)
- (c) There is negligible heat loss to the surroundings.
- (d) In the case of shell-and-tube exchangers a further assumption is that within one baffle space the temperature change of the shell-side fluid is small in relation to its total temperature change through the unit; this means that there must be a large number of baffles – a factor which is often overlooked and is discussed further in section 7.7.7.

#### 7.3.2 Logarithmic mean temperature difference

Consider the countercurrent system below:



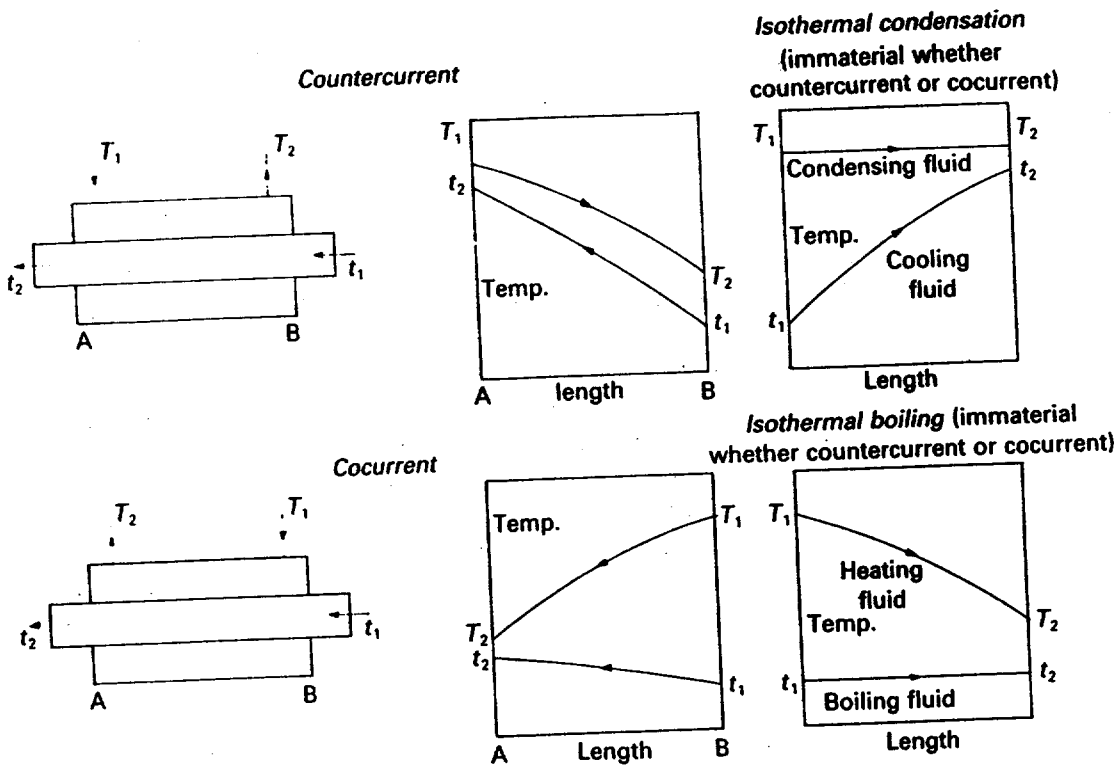


Figure 7.1 Countercurrent and cocurrent flow

Pipe:  $\leftarrow t_1$   
 Terminal difference:  $T_1 - t_2 = \Delta T_h$   $T_2 - t_1 = \Delta T_c$   
 Overall coefficient:  $U_h$   $U_c$

Kern (1950), for instance, showed that the mean temperature difference for such a system is the logarithmic mean of the terminal temperature differences (log MTD or  $\Delta T_{lm}$ ); that is

$$\Delta T_{lm} = \log \text{MTD} = \frac{\{\Delta T_h - \Delta T_c\}}{\ln\{\Delta T_h/\Delta T_c\}} \quad [7.1a]$$

If  $\Delta T_h$  is less than  $\Delta T_c$ , the above expression is merely reversed to give a positive numerator and a natural logarithm greater than unity.

Hence if GTTD = greater terminal temperature difference  
 and LTTD = lesser terminal temperature difference

$$\Delta T_{ln} = \log \text{MTD} = \frac{\text{GTTD} - \text{LTTD}}{\ln(\text{GTTD}/\text{LTTD})} \quad [7.1b]$$

The log MTD is also applicable to the conditions where

- (a) there is cocurrent flow;
- (b) either fluid is isothermal;
- (c) the fluids are switched, i.e. the cold fluid flows inside the annulus and the hot fluid flows inside the pipe.

### 7.3.3 Example of log MTD calculation

The following example demonstrates the application of equation [7.1] for both countercurrent and cocurrent systems.

Flow:	Countercurrent		Cocurrent	
	A (hot)	B (cold)	A (cold)	B (hot)
End:				
Annulus (°C):	500 →	300	300 ←	500
Pipe (°C):	<u>200</u> ←	<u>60</u>	<u>200</u> ←	<u>60</u>
Terminal difference (°C):	<u>300</u>	<u>240</u>	<u>100</u>	<u>440</u>
log MTD:	$\frac{300 - 240}{\ln(300/240)}$ = 269 °C		$\frac{440 - 100}{\ln(440/100)}$ = 229 °C	

For given terminal temperatures the log MTD for countercurrent flow is greater than that for cocurrent flow and hence a smaller surface area is required to perform a given duty. The arithmetic MTD, which in this particular example is 270 °C, has no theoretical basis and should not be used, although when the ratio of the terminal temperature differences is close to unity it provides a reasonable approximation.

#### 7.4 $U$ varies linearly between inlet and outlet

One of the assumptions made in deriving the log MTD is that the overall heat transfer coefficient is constant throughout the exchanger. This is nearly true for gases and non-viscous liquids, but there may be a greater variation with viscous liquids, particularly if viscosity changes considerably throughout the exchanger.

If  $U$  varies linearly with respect to temperature between inlet and outlet, but all other assumptions apply, Kern (1950), for instance, showed that the true product ( $U \Delta T$ ) for use in the equation  $Q = UA \Delta T$  is the logarithmic mean of the crossed products of  $U$  and  $\Delta T$ , that is:

$$\text{true } (U \Delta T) = \log(U \Delta T)_{\text{lm}} = \frac{\{U_h \Delta T_c - U_c \Delta T_h\}}{\ln\{(U_h \Delta T_c)/(U_c \Delta T_h)\}} \quad [7.2]$$

This equation is applicable to countercurrent and cocurrent flow, but has the disadvantage that two values of  $U$  ( $U_h$  and  $U_c$ ) must be calculated instead of one. If  $U_h \Delta T_c$  is less than  $U_c \Delta T_h$  the above expression is merely reversed to give a positive numerator and a natural logarithm greater than unity.

#### 7.5 $U$ varies non-linearly between inlet and outlet

Because of a large change in viscosity, for instance,  $U$  may vary in a non-linear manner between inlet and outlet. Equations [7.1] and [7.2] cannot be applied to the complete exchanger and a stepwise procedure is adopted. The temperature range is divided into suitable increments such that in each increment  $U$  can be regarded as either constant or linear. Either equation [7.1] or equation [7.2] can then be applied to each increment without serious error.

In a design case, the surface area for each increment is calculated from either  $A = Q/(U \Delta T_{\text{lm}})$  or  $A = Q/\log(U \Delta T_{\text{lm}})$  and the incremental areas added together to provide the total surface area.

## 7.6 Mean temperature difference for non-countercurrent or non-cocurrent flow

### 7.6.1 Log MTD correction factor $F$

Many shell-and-tube exchangers have more than one tube-side pass and in an E-type shell with an even number of tube-side passes, for example, half of the passes will be in countercurrent flow and the other half in cocurrent flow. In a cross-flow tubular exchanger, such as an air cooler, for example, the external fluid flows in a single pass across the bundle and there is one or more tube-side passes. Strict countercurrent flow cannot be achieved although the overall direction of flow of one fluid relative to the other may be countercurrent. As a result the true MTD will be less than the log MTD obtained from equation [7.1].

In the ' $F$  correction factor' method,  $F$  is defined as the ratio of the true mean temperature difference for the non-countercurrent flow system under consideration, to the log MTD for countercurrent flow. It is calculated in terms of dimensionless ratios  $R$  and  $P$  as follows:

$$\text{True } \Delta T = \Delta T_m = F \Delta T_{lm} \quad [7.3]$$

( $\Delta T_{lm}$  must be based on countercurrent flow)

$$\text{Heat capacity ratio} = R = \frac{T_1 - T_2}{t_2 - t_1} \quad [7.4]$$

which must be used in conjunction with  $P$  where:

$$\text{Thermal effectiveness} = P = \frac{t_2 - t_1}{T_1 - t_1} \quad [7.5]$$

It should be noted that interchangeability is permissible in *certain* cases and sometimes it is advantageous to use  $R' = (t_2 - t_1)/(T_1 - T_2)$  in conjunction with  $P' = (T_1 - T_2)/(T_1 - t_1)$ , where  $R' = (1/R)$  and  $P' = RP$ .

Also for temperature meet,  $P(R + 1) = 1$ ; for temperature cross,  $P(R + 1) > 1$ ; for temperature approach,  $P(R + 1) < 1$ . It should be noted that  $R$ , as defined by equation [7.4], may be expressed as  $R = (wc)/(WC)$ , where  $W$  and  $w$  are the hot and cold fluid flow rates, and  $C$  and  $c$  are the hot and cold fluid specific heats, respectively.

### 7.6.2 Pass designation system

In shell-and-tube exchangers the pass arrangements on the shell-side and tube-side have particular significance in MTD calculations. Although there is no standard, a typical base designation system is  $m/n$ , where  $m$  and  $n$  are indicative of the number of passes on the shell-side and tube-side respectively.

$m = 1$  for an E-type shell

$= 2$  for an F-type shell

= G, H, J or X, i.e. the TEMA shell type designation for other shells

= number of shell-side passes, three or greater, for non-standard systems

$n$  = 1, 2, 3, 4, 5, 6, etc., for a specified number of tube-side passes

=  $2^+$ , the '+' sign denoting an unspecified even number of tube-side passes

=  $4^+$ ,  $6^+$ ,  $8^+$ , etc., the '+' sign denoting unspecified multiples of 4, 6, 8, etc., tube-side passes.

As examples:  $1/6$  = specific case of an E shell with 6 tube-side passes;  
 $2/4^+$  = general case of an F shell with an unspecified multiple of 4 tube-side passes, i.e. there could be 4, 8, 12, 16, etc., tube-side passes,  
 $J/2^+$  = J shell with an unspecified even number of tube-side passes, i.e. there could be 2, 4, 6, 8, etc., tube-side passes.

It will be noted that  $1/1$  and  $2/2$  exchangers provide countercurrent flow.  $3/3$  and  $4/4$  exchangers, etc., are special designs and seldom used.

### 7.6.3 $F$ curves: general application

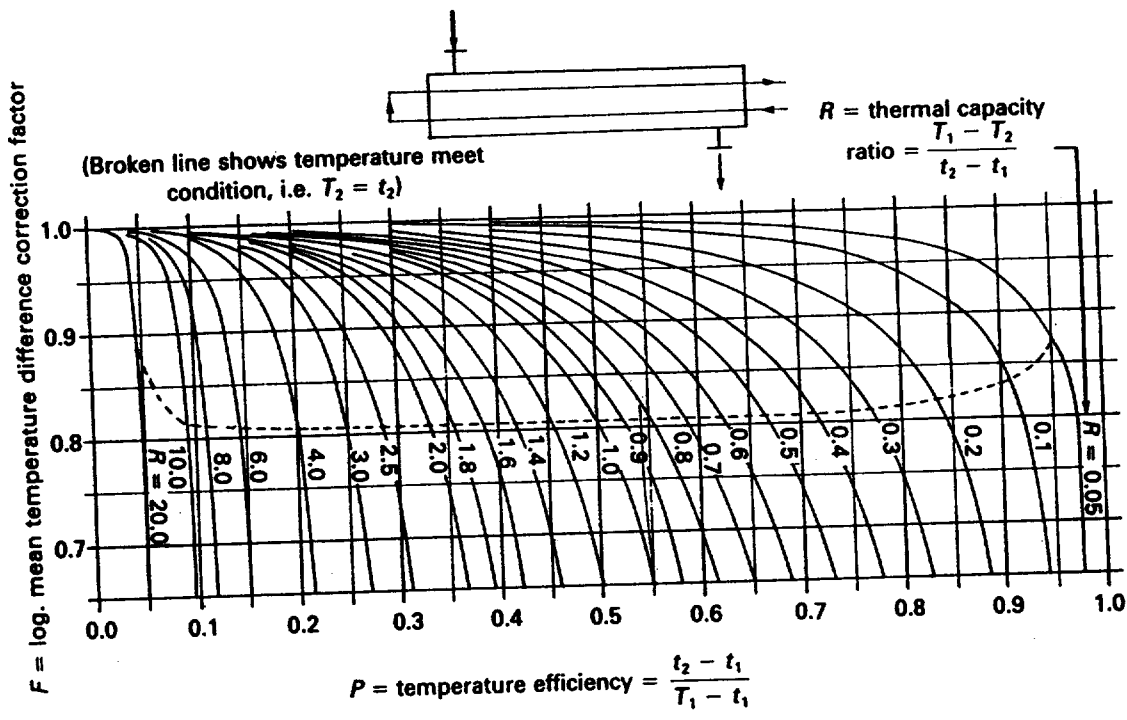
Curves relating  $F$  to  $P$  and  $R$  from equations [7.4] and [7.5] are presented in the literature for a variety of industrially important cases which are applicable to shell-and-tube exchangers, and cross-flow units such as air heaters, economisers and air-cooled exchangers. Sources include TEMA (1978) for shell-and-tube exchangers, and Taborek (1983) for both shell-and-tube and cross-flow exchangers. As examples, Figs 7.2(a) and (b) present  $F$  curves for  $1/2^+$  shell-and-tube exchangers and one common cross-flow configuration respectively. (The formulae relating  $F$ ,  $P$  and  $R$  for  $1/2^+$  shell-and-tube exchangers are given in equations [7.7a] and [7.7b].)

$F$  is indicative of the penalty which is incurred due to the fact that the flow is not strictly countercurrent. For instance, if  $F = 0.8$ , then compared with countercurrent flow, 25% additional surface area will be required for a given  $Q$ ,  $U$  and log MTD. For strict countercurrent flow,  $F = 1$ .

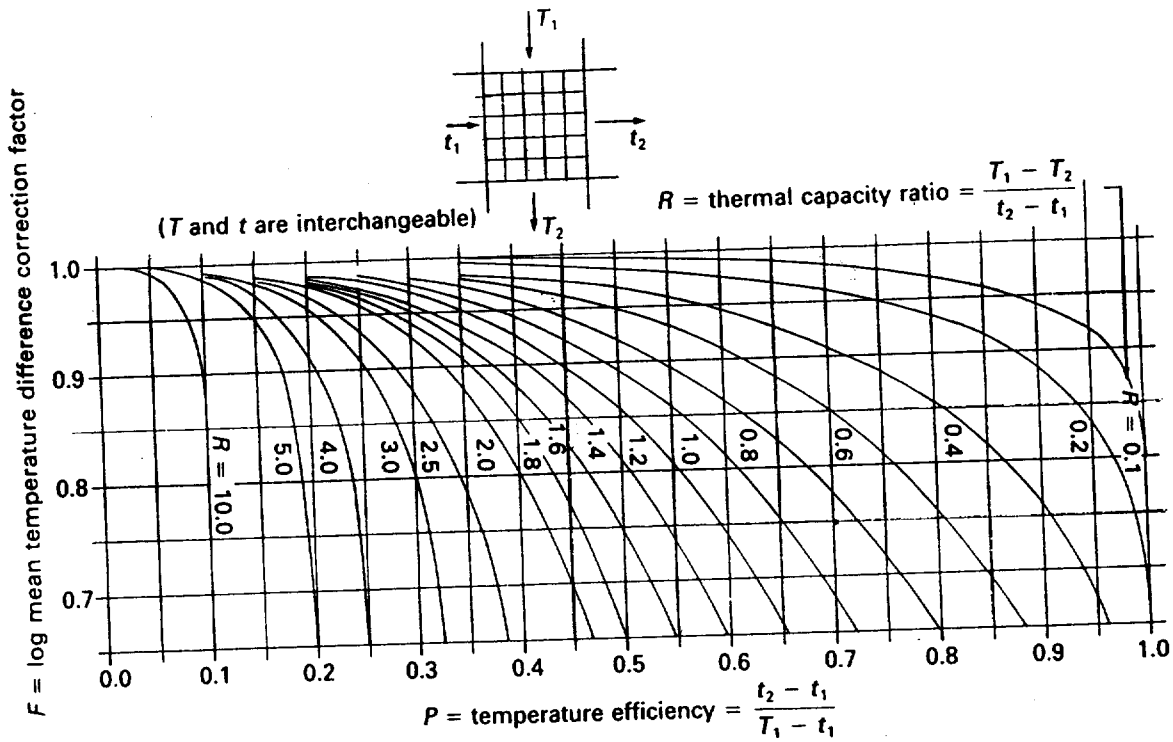
Examination of the curves presented in Figs 7.2(a) and (b) shows that in all cases lines for  $R < 1$  are less steep than those for  $R > 1$ . It is easier and more accurate to derive  $F$  from the portion of the curve where  $R < 1$  and the alternative values of  $P$  and  $R$  given in section 7.6.1, ( $P'$  and  $R'$ ), should be used *where permissible*, to achieve this. All lines become steep at values of  $F$  below about 0.75, which means that performance becomes sensitive to small changes from the given temperatures, and this portion of the curve should be avoided.

The temperature meet condition,  $P(R + 1) = 1$ , has been superimposed on Fig. 7.2(a). This line is sometimes called the 'threshold', and points above the line correspond to a temperature approach, while those below the line correspond to a temperature cross.





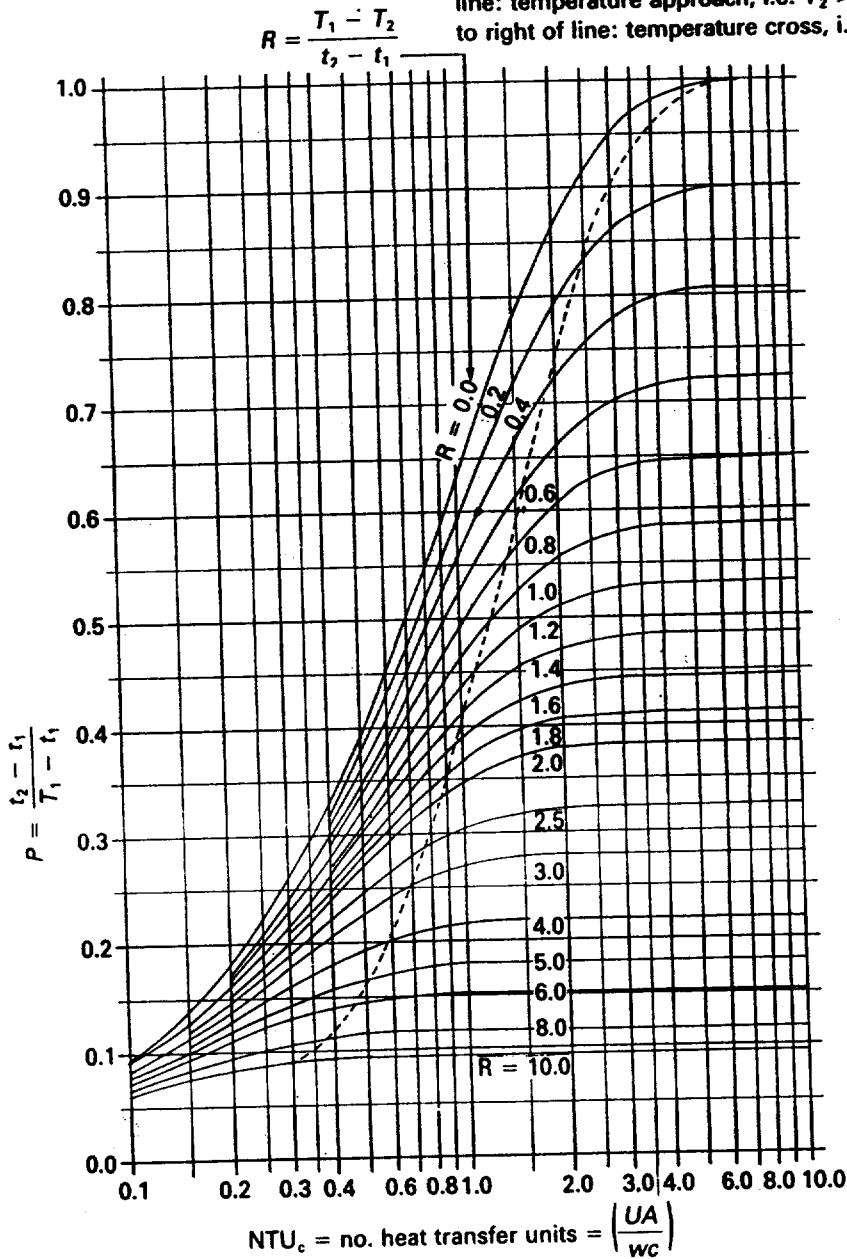
(a) Log mean temperature difference correction factor for one shell pass and an even number of tube passes (1/2+ exchanger)



(b) Log mean temperature difference correction factor for a cross-flow exchanger, single pass for each stream, both streams unmixed.

Figure 7.2 F curves

Broken line shows temperature meet condition, i.e.  $T_2 = t_2$ . Points to left of line: temperature approach, i.e.  $T_2 > t_2$ ; points to right of line: temperature cross, i.e.  $t_2 > T_2$



(c) NTU-P-R curves for one shell pass and an even number of tube passes (1/2+ exchanger)

### 7.6.4 F curves: shell-and-tube exchangers

In the case of shell-and-tube exchangers it will be found that only a limited temperature cross can be achieved in a 1/2+ exchanger, but the ability to accommodate a temperature cross increases rapidly as the number of exchangers in series is increased. Although F curves are available in the literature for 3/6+, 4/8+, 5/10+ and 6/12+ exchangers, only special designs have more than two shell-side passes. In practice the same F values are achieved by using an equivalent number of 1/2+

exchangers in series, or  $2/4^+$  exchangers in series, if longitudinal baffles are permitted, as shown in Table 7.1.

**Table 7.1** Mean temperature difference calculations. Equivalent number of  $1/2^+$  and  $2/4^+$  shell-and-tube exchangers in series on both shell-side and tube-side.

<i>F</i> curve designation (one shell)	$1/2^+$ type	$2/4^+$ type
$2/4^+$	2	1
$3/6^+$	3	—
$4/8^+$	4	2
$5/10^+$	5	—
$6/12^+$	6	3

Strictly the  $1/2$ ,  $1/4$ ,  $1/6$ , . . . ,  $1/n$ , . . . ,  $1/\infty$  arrangements should each have their own *F* curve, but Dodd (1980) has shown that although  $F(1/2) > F(1/4) > \dots > F(1/\infty)$ , the  $F(1/2^+)$  curves may be used for all higher even values of *n* with a maximum error of only +1.66%, if  $F < 0.75$  and +0.83% if  $F < 0.8$ .

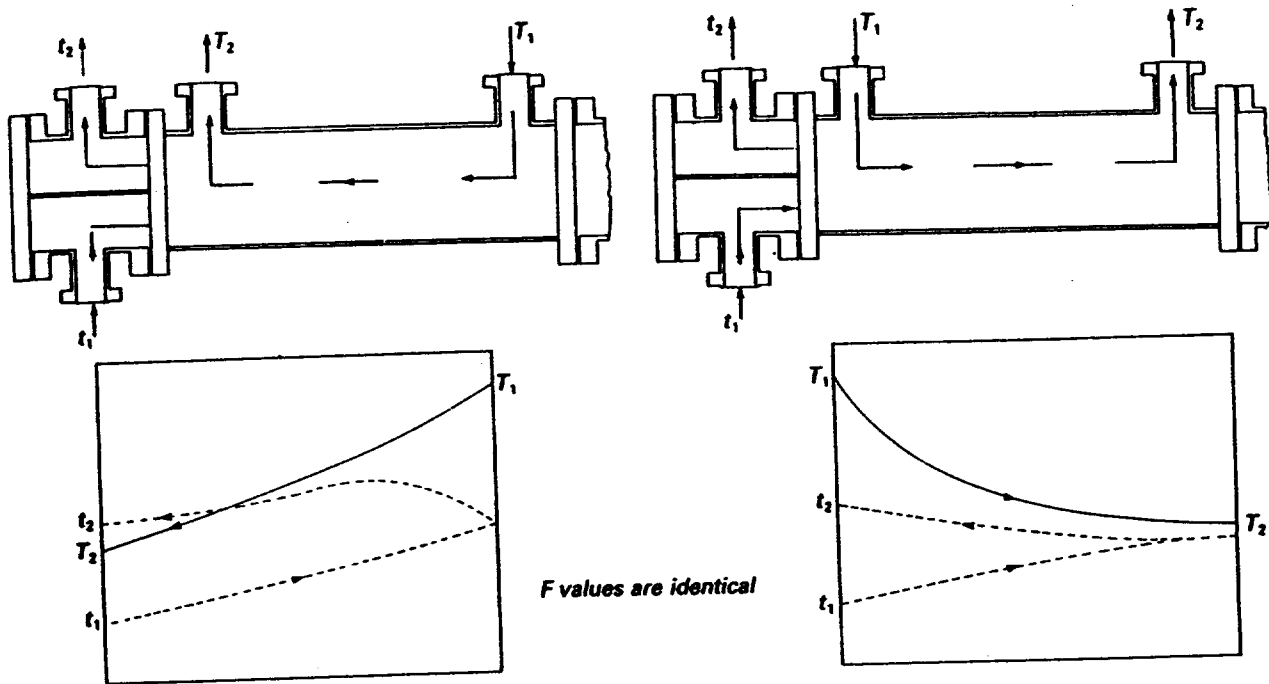
It is interesting to record that the  $F(1/2^+)$  curves give identical results irrespective of whether the shell-side fluid enters at the stationary end and leaves at the rear end, or vice-versa. The temperature profiles are different for the two cases, as shown in Fig. 7.3, but mathematically *F* is the same.

In a  $1/2^+$  exchanger *F* is usually taken as 0.8 for any temperature meet condition and the threshold curve plotted on Fig. 7.2(a) shows that it is substantially true. The exception is at extremely low and high values of *P*, where higher values of *F* are achieved.

### 7.6.5 *F* curves: cross-flow exchangers

In these cases *F* depends not only on *R* and *P*, but also on whether the fluids are mixed or unmixed during their flow through the exchanger. Consider a hot fluid in one pass inside the tubes of a long, horizontal bundle, rectangular in shape in both plan and elevation, comprising several vertical rows of tubes. If cold air is passed vertically upwards through the bundle, a narrow stream of air passing over the tubes near the hot fluid inlet will be heated more than a similar stream of air passing over the tubes near the outlet end. Thus there will be a temperature gradient in the air in any horizontal plane and if there was no sideways mixing of the air, which could be achieved by using a large number of closely spaced vertical baffles, then the air would be termed unmixed. Since the air temperature changes from row to row, the temperature of the tube-side fluid will vary from row to row at any vertical cross-section. If the tube-side flow path is continuous from one end to the other, the tube-side fluid will be unmixed. Single-pass, unmixed, cross-flow of both fluids represents the basic cross-flow case.

In single-pass flow on each side, *F* will depend on whether both fluids are mixed, or both fluids are unmixed, or one fluid mixed and the other



**Figure 7.3** Temperature profiles in shell-and-tube exchanger having one shell-side pass and two tube-side passes (small temperature cross)

unmixed. In multi-pass flow  $F$  also depends on the flow directions of the multi-pass stream and whether a fluid is mixed or unmixed between passes, irrespective of whether it was mixed or unmixed when in contact with the heat transfer surface.

It will be found that  $F$  (both unmixed)  $>$   $F$  (mixed, unmixed)  $>$   $F$  (both mixed) and engineering judgement will be required to decide which is applicable to the problem. Although the use of  $F$ (both mixed) provides the safest design, it has no industrial applications.

## 7.7 Application to design

### 7.7.1 Minimum number of shell-and-tube exchangers in series

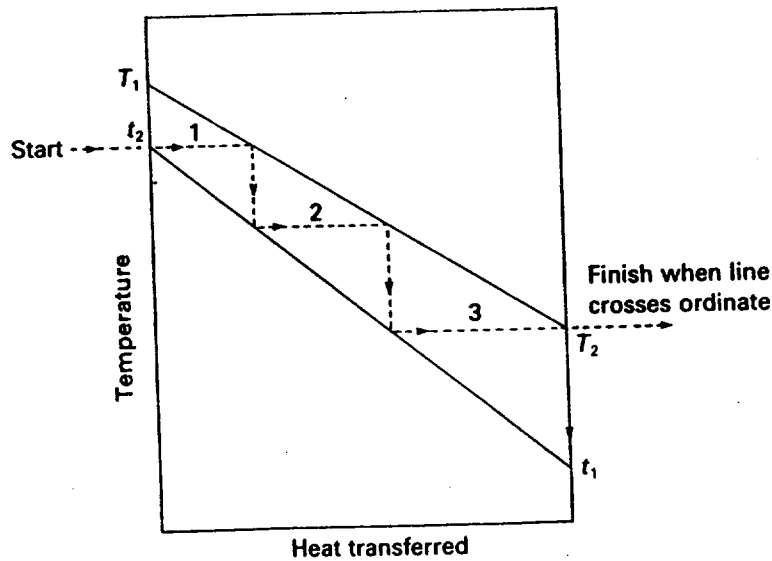
1/1 and 2/2 shell-and-tube exchangers provide countercurrent flow and therefore the highest MTD, but these exchangers will not provide the best solution in many cases. This is because there are only one or two tube-side passes which may yield low tube-side heat transfer coefficients. Despite its thermal significance a 1/1 floating-head exchanger may not be acceptable because a gland or bellows is required at the floating-head end. A 2/2 exchanger of the floating-head or U-tube type may not be acceptable, despite its thermal significance, because a removable longitudinal baffle will be required. (See Chapter 1.)

Despite the ' $F$  penalty', which reduces the MTD, 1/2<sup>+</sup> or 2/4<sup>+</sup> exchangers having a greater number of tube-side passes may provide a better solution. If a single 1/2<sup>+</sup> exchanger provides  $F < 0.75$ , two 1/2<sup>+</sup> exchangers in series, or a single 2/4<sup>+</sup> exchanger must be investigated. If  $F$  is still less than 0.75, then three 1/2<sup>+</sup> exchangers in series, or two 2/4<sup>+</sup>

exchangers, are investigated and the process continued by adding shells in series until  $F \geq 0.75$ . It should be noted that changing from a  $1/2^+$  exchanger to a  $G/2^+$  exchanger or  $X/2^+$  exchanger provides a significant increase in  $F$ , although the shell-side heat transfer coefficient will be reduced with the X shell. Each case must be treated on its merits.

An approximate method for calculating the number of  $1/2^+$  exchangers in series is the stepwise procedure shown in Fig. 7.4 which assumes a temperature meet in each exchanger.

**Figure 7.4** Approximate method for determining the required number of  $1/2^+$  shell-and-tube exchangers in series (three in example shown)



(Dotted line provides temperature meet in each shell - every horizontal line represents one shell)

### 7.7.2 Examples using $F$ curves

(1) A shell-and-tube exchanger is required to cool a hot fluid from  $300^\circ\text{C}$  to  $150^\circ\text{C}$  using a coolant entering at  $125^\circ\text{C}$  and leaving at  $140^\circ\text{C}$ . As there is no temperature cross, a  $1/2^+$  exchanger is satisfactory for the temperature conditions. What is  $F$ ? ( $\Delta T_m = 72.7^\circ\text{C}$ )

Let  $T_1 = 300$ ,  $T_2 = 150$ ,  $t_1 = 125$  and  $t_2 = 140$ .

From equations [7.4] and [7.5]:

$$R = (300 - 150)/(140 - 125) = 10,$$

$$P = (140 - 125)/(300 - 125) = 0.0857$$

From Fig. 7.2(a);  $F = 0.91$  ( $R$  line is steep)

From equation [7.3]:  $\Delta T_m = (0.91)(72.7) = 66.2^\circ\text{C}$

The same result could have been obtained using the alternative values of  $R$  and  $P$ , namely:

$$R' = (140 - 125)/(300 - 150) = 0.1,$$

$$P' = (300 - 150)/(300 - 125) = 0.857$$

From Fig. 7.2(a);  $F = 0.91$  (value easier to read)

[TEMA Fig. T-3.2A gives  $F = 0.907$ ]

(2) Shell-and-tube exchangers are required to cool a hot fluid from 260 °C to 110 °C using a coolant entering at 60 °C and leaving at 210 °C. Despite the fact that there is a temperature cross, and countercurrent flow should be investigated, 1/1, 2/2 and 2/4<sup>+</sup> exchangers are not permitted for the structural limitations given in section 7.7.1. How many 1/2<sup>+</sup> exchangers in series are required? ( $\Delta T_{lm} = 50$  °C)

Let  $T_1 = 260$ ,  $T_2 = 110$ ,  $t_1 = 60$  and  $t_2 = 210$ .

From equations [7.4] and [7.5]:

$$R = (260 - 100)/(210 - 60) = 1,$$

$$P = (210 - 60)/(260 - 60) = 0.75$$

From TEMA Fig. T-3.2B, equivalent to two 1/2<sup>+</sup> exchangers in series:

$$F < 0.75 \text{ (no use)}$$

From TEMA Fig. T-3.2C, equivalent to three 1/2<sup>+</sup> exchangers in series:

$$F = 0.81 \text{ (OK)}$$

At least three 1/2<sup>+</sup> exchangers in series are required with  $F = 0.81$ . From equation [7.3]:  $\Delta T_m = 0.81 \times 50 = 40.5$  °C.

### 7.7.3 Formulae relating $F$ , $P$ and $R$ for any number ( $N$ ) of 1/2<sup>+</sup> shells in series

TEMA (1978) and Tabor (1983) present  $F$  curves for one to six 1/2<sup>+</sup> shell-and-tube exchangers in series, but if curves are not available,  $F$  may be calculated for any number ( $N$ ) of 1/2<sup>+</sup> exchangers in series as shown below.  $P$  and  $R$  are obtained from equations [7.4] and [7.5].

$N = 1$ : Use equations [7.7a] or [7.7b], as appropriate, with  $P = P^*$

$N > 1$ : Use equations [7.6a] or [7.6b], and [7.7a] or [7.7b], as appropriate, as follows: calculate

$$P^* = \frac{\left(\frac{1 - PR}{1 - P}\right)^{1/N} - 1}{\left(\frac{1 - PR}{1 - P}\right)^{1/N} - R} \text{ for } R \neq 1 \quad [7.6a]$$

If  $R = 1$ ,

$$P^* = \frac{P}{P - NP + N} \quad [7.6b]$$

Substitute  $P^*$  and  $R$  into equations [7.7a] or [7.7b], as appropriate. (These equations apply to one 1/2<sup>+</sup> exchanger, with  $P = P^*$ , and presented in Fig. 7.2(a).

If  $R \neq 1$ ,

$$F = \frac{(R^2 + 1)^{1/2} \ln\left(\frac{1 - P^*R}{1 - P^*}\right)}{(1 - R) \ln\left\{\frac{2 - P^*(R + 1 - (R^2 + 1)^{1/2})}{2 - P^*(R + 1 + (R^2 + 1)^{1/2})}\right\}} \text{ for } R \neq 1 \quad [7.7a]$$

If  $R = 1$ ,

$$F = \frac{2^{1/2} P^*}{(1 - P^*) \ln \left\{ \frac{2 - P^* (2 - 2^{1/2})}{2 - P^* (2 + 2^{1/2})} \right\}}$$

$$\approx \frac{1.4142 P^*}{(1 - P^*) \ln \left\{ \frac{2 - 0.5858 P^*}{2 - 3.4142 P^*} \right\}} \quad [7.7b]$$

#### 7.7.4 Example using formulae

(1) If four  $1/2^+$  shells in series are considered instead of the minimum of 3 in example (2) above, what is  $F$ ?

$N = 4$ ,  $P = 0.75$ ,  $R = 1$ , hence use equations [7.6b] and [7.7b].

From equation [7.6b]:

$$P^* = 0.75 / \{0.75 - (4 \times 0.75) + 4\} = 0.4286$$

From equation [7.7b]:

$$F = \frac{1.4142 \times 0.4286}{(1 - 0.4286) \ln \left\{ \frac{2 - (0.5858 \times 0.4286)}{2 - (3.4142 \times 0.4286)} \right\}} = 0.898$$

A change from three to four shells in series increases MTD by  $(0.898) / (0.81) = 1.11$  times.

#### 7.7.5 Divided-flow shells

$F$  values for divided-flow shells, having two or more even numbers of tube-side passes ( $J/2^+$  exchangers) are identical to the mixed-mixed cross-flow case as given by Taborek (1983), but the  $1/2^+$  E shell given in Fig. 7.2(a) may be used with negligible error. It is assumed that the tube-side fluid enters on the same side as the shell outlet nozzles.

For a quick appraisal,  $F$  values of divided-flow shells having one tube-side pass ( $J/1$  exchangers), are greater than those for  $J/2^+$  exchangers, and therefore,  $1/2^+$  exchangers.

#### 7.7.6 Split-flow shells

$F$  values for single and double split-flow shells, having two or more even numbers of tube-side passes ( $G/2^+$ ,  $H/2^+$  exchangers), are about the same. On the assumption that the tube-side fluid enters on the same side as the shell outlet nozzles, split-flow shells have significantly higher  $F$  values than the  $1/2^+$  exchanger.

#### 7.7.7 Effect of a small number of baffles in a shell-and-tube exchanger

The assumptions made for the derivation of the logarithmic mean

temperature difference were given in section 7.3.1. Assumption (d) of the section states that there must be a 'large' number of baffles in the exchanger, and immediately poses the question as to what is meant by 'large'. Despite the fact that in a 1/1 exchanger, where the shell-side and tube-side fluids enter at opposite ends, the system appears countercurrent, significant errors may be made in the log MTD calculation if assumption (d) is violated. Similar considerations apply to 1/2<sup>+</sup> exchangers.

The whole problem has been re-appraised by Gardner and Taborek (1976) and it was concluded that 1/2<sup>+</sup> exchangers may be designed with the customary MTD correction provided that the number of baffle spaces exceeds five. It was considered that the penalty for fewer baffle spaces was non-existent in some circumstances, and never severe in any practical case.

The minimum number of baffle spaces for 1/1 exchangers cannot be expressed as a single figure and the reader should refer to the publication of Gardner and Taborek (1976), or Caglayan and Buthod (1976). The latter present MTD correction factor curves  $F$  for 1/1 exchangers with 2–7 baffle spaces, and typical values are shown in Table 7.2.

## 7.8 Number of transfer units

The log MTD correction factor ( $F$ ) is ideally suited to design cases where the requirement is to determine the surface area from known flow rates and terminal temperatures. The true mean temperature difference is readily determined from the  $F$  curves and makes the designer immediately aware of the extra surface area which will be required for non-countercurrent flow. However, when the performance of a given unit has to be determined under different process conditions, the problem may be solved using the  $F$  curves, but trial and error is necessary because only two of the terminal temperatures will be known. The concept of the number of transfer units (NTU) provides a rapid, direct, solution to the problem. This popular approach also provides a quick solution to design problems, of course, but the designer is less aware of the penalty paid for non-countercurrent flow.

If  $W$  and  $w$  refer to the hot and cold fluid flow rates, respectively, and  $C$  and  $c$  refer to the hot and cold fluid specific heats respectively, the heat load ( $Q$ ) is given by

$$Q = WC(T_1 - T_2) = wc(t_2 - t_1) \quad [7.8]$$

If  $A$  = surface area and  $U$  = overall heat transfer coefficient, then using the definitions of TEMA (1978):

$$NTU_c = \frac{UA}{wc} \text{ or } NTU_h = \frac{UA}{WC} \quad [7.9]$$

From equations [7.4] and [7.8]

$$R = \frac{T_1 - T_2}{t_2 - t_1} = \frac{wc}{WC} \quad [7.10]$$

also  $P = (t_2 - t_1)/(T_1 - t_1)$  from equation [7.5]. The product: (flow



Table 7.2 Shell and tube heat exchangers. One shell pass, one tube pass, countercurrent flow. Approximate values of  $F$  versus  $P$  and  $R$  for 2, 3, 4 and 5 baffle spaces.

$P =$	0.15	0.2	0.3	0.4	0.5	0.6	0.7	0.8	0.9	0.95	0.95	0.95	0.95	0.95	$= P$	
$R$	1 baffle - 2 baffle spaces										2 baffles - 3 baffle spaces					$R$
0.6						0.97	0.94	0.89	0.79	0.66			0.97	0.95	0.88	0.6
0.8					0.97	0.95	0.90	0.81	0.62	(0.935)			0.98	0.96	0.90	0.8
1.0					0.97	0.92	0.83	0.68		(0.875)			0.98	0.96	0.76	1.0
1.2					0.97	0.94	0.87	0.73		(0.780)			0.97	0.94	0.50	1.2
1.5					0.96	0.91	0.74			(0.652)			0.98	0.95	0.84	1.5
2.0					0.97	0.92	0.55			(0.505)			0.96	0.50*		2.0
2.5					0.96	0.65				(0.405)			0.98	0.80		2.5
3.0					0.98	0.91				(0.330)			0.96			3.0
4.0					0.97					(0.240)			0.98			4.0
5.0					0.97	0.80*				(0.200)			0.90*			5.0
$R$	3 baffles - 4 baffle spaces										4 baffles - 5 baffle spaces					$R$
0.6																0.6
0.8																0.8
1.0																1.0
1.2																1.2
1.5																1.5
2.0																2.0
2.5																2.5
3.0																3.0
$P =$	0.15	0.2	0.3	0.4	0.5	0.6	0.7	0.8	0.9	0.95	0.95	0.95	0.95	0.95	$= P$	

Notes: Basis:- Caglayan & Buthod (1976) \*  $P$  value is asymptotic.

rate)  $\times$  (specific heat) is the thermal capacity of the fluid.

Using the above definitions of  $NTU_c$ ,  $P$  and  $R$ , Fig. 7.2(c) shows  $NTU_c$  plotted against  $P$ , with  $R$  as parameter, for a  $1/2^+$  exchanger, as a typical example. This curve will also apply if the alternative values of  $R$  and  $P$  given in section 7.6.1, and  $NTU_h$  from equation [7.9], are used. The 'threshold' line, corresponding to a temperature meet, when  $T_2 = t_2$  and  $P(R + 1) = 1$  is also shown.

NTU curves for a variety of industrial cases are presented by Taborek (1983) and ESDU (1985), which are sometimes known as temperature efficiency curves. When using unfamiliar curves, the definitions of  $NTU$ ,  $P$  and  $R$  should be checked thoroughly. ESDU, for instance, use the following definitions:

$$NTU = UA/(\text{smaller thermal capacity})$$

$$R = (\text{smaller thermal capacity})/(\text{larger thermal capacity})$$

$$\text{and } P = (\text{larger fluid temperature change})/(\text{temp. diff: } \{(\text{hot fluid in}) - (\text{cold fluid in})\})$$

Figure 7.2(c) will show that the performance of a given exchanger may be determined for various operating conditions, without trial and error. In all cases the terminal temperatures are always related to one another by the following relationships:

$$t_2 - t_1 = P(T_1 - t_1) \quad [7.11]$$

$$T_1 - T_2 = R(t_2 - t_1) \quad [7.12]$$

### 7.8.1 Examples using NTU-P-R curves

(1) A  $1/2^+$  shell-and-tube exchanger is designed to cool 15 kg/s of hot fluid from 200 °C to 120 °C using 37.5 kg/s of coolant entering at 80 °C and leaving at 100 °C. The hot and cold fluid specific heats are 2500 and 4000 J/kg K, respectively, the overall heat transfer coefficient is 500 W/m<sup>2</sup>K and the surface area is 98.4 m<sup>2</sup>. What outlet temperatures would be achieved if the hot and cold fluid inlet temperatures are 190 °C and 95 °C respectively, all other conditions being unchanged? Thus  $U = 500$ ,  $A = 98.4$ ,  $W_h = 15$ ,  $C_h = 2500$ ,  $w = 37.5$ ,  $c = 4000$ ,  $T_1 = 190$ ,  $t_1 = 95$   
Design  $Q = 15 \times 2500 \times (200 - 120) = 37.5 \times 4000 \times (100 - 80) = 3 \times 10^6$  W

From equation [7.9]:

$$NTU_c = (500 \times 98.4)/(37.5 \times 4000) = 0.328$$

From equation [7.10]:

$$R = (37.5 \times 4000)/(15 \times 2500) = 4$$

From Fig. 7.2(c):

$$P = 0.167$$

From equation [7.11]:

$$t_2 = 95 + \{0.167 \times (190 - 95)\} = 110.9 \text{ °C}$$

From equation [7.12]:

$$T_2 = 190 - \{4 \times (110.9 - 95)\} = 126.4 \text{ }^\circ\text{C}$$

$$Q = 15 \times 2500 \times 63.6 = 37.5 \times 4000 \times 15.9 = 2.385 \times 10^6 \text{ W}$$

(2) A 1/2+ shell-and-tube exchanger is designed to cool 15 kg/s of hot fluid from 500 to 300 °C, using 10 kg/s of coolant entering at 100 °C and leaving at 200 °C. The hot and cold fluid specific heats are 1333 and 4000 J/kg K, respectively, the overall heat transfer coefficient is 400 W/m<sup>2</sup> K and the surface area is 43.14 m<sup>2</sup>. At start-up, when the unit is clean, the overall heat transfer coefficient is expected to be 480 W/m<sup>2</sup> K. What outlet temperatures will be achieved at start-up, all other conditions being unchanged?

Thus  $U = 480$ ,  $A = 43.14$ ,  $W = 15$ ,  $C = 1333$ ,  $w = 10$ ,  $c = 4000$ ,  
 $T_1 = 500$ ,  $t_1 = 100$

$$\text{Design } Q = 15 \times 1333 \times 200 = 10 \times 4000 \times 100 = 4 \times 10^6 \text{ W}$$

From equation [7.9]:

$$\text{NTU}_c = (480 \times 43.14)/(10 \times 4000) = 0.518$$

From equation [7.10]:

$$R = (10 \times 4000)/(15 \times 1333) = 2$$

From Fig. 7.2(c):

$$P = 0.274$$

From equation [7.11]:

$$t_2 = 100 + \{0.274 \times (500 - 100)\} = 209.6 \text{ }^\circ\text{C}$$

From equation [7.12]:

$$T_2 = 500 - \{2 \times (209.6 - 100)\} = 280.8 \text{ }^\circ\text{C}$$

$$\text{new } Q = 15 \times 1333 \times 219.2 = 10 \times 4000 \times 109.6 = 4.384 \times 10^6 \text{ W}$$

(3) In the exchanger of example (2), only 7.5 kg/s of coolant is available under emergency conditions. Under these conditions the overall heat transfer coefficient is expected to be 380 W/m<sup>2</sup> K. What outlet temperatures will be achieved, if all other conditions remain unchanged?

Thus  $U = 380$ ,  $A = 43.14$ ,  $W = 15$ ,  $C = 1333$ ,  $w = 7.5$ ,  $c = 4000$ ,  
 $T_1 = 500$ ,  $t_1 = 100$

From equation [7.9]:

$$\text{NTU}_c = (380 \times 43.14)/(7.5 \times 4000) = 0.546$$

From equation [7.10]:

$$R = (7.5 \times 4000)/(15 \times 1333) = 1.5$$

From Fig. 7.2(c):

$$P = 0.31$$

From equation [7.11]:

$$t_2 = 100 + \{0.31 \times (500 - 100)\} = 224 \text{ }^\circ\text{C}$$

From equation [7.12]:

$$T_2 = 500 - \{1.5 \times (224 - 100)\} = 314^\circ\text{C}$$

$$\text{new } Q = 15 \times 1333 \times 186 = 7.5 \times 4000 \times 124 = 3.72 \times 10^6 \text{ W}$$

## 7.9 Theta method

Taborek (1983) provides a further method for presenting heat exchanger performance.

By definition

$$\theta = \frac{\Delta T_m}{T_1 - t_1} \quad [7.13a]$$

It can also be shown that

$$\theta = \frac{P}{NTU_c} \quad [7.13b]$$

Two sets of curves are presented, one above the other. The upper curves relate  $\theta$  versus  $P$ , with  $R$  as parameter. This permits  $\Delta T_m$  to be determined from equation [7.13a] when  $P$  and  $R$  are known, the separate calculation of  $F$  and  $\Delta T_{lm}$  being unnecessary. Superimposed on these curves are a series of straight lines, each corresponding to a value of  $NTU_c$ . These emanate from the common origin of  $\theta = 0$ ,  $P = 0$ , and express equation [7.13b]. This provides similar information to the temperature efficiency curves such as Fig. 7.2(c), with the added advantage that  $\Delta T_m$  may be determined without separate calculation of  $F$  and  $\Delta T_{lm}$ . The lower curves are the conventional ones relating  $F$  versus  $P$  with  $R$  as parameter, similar to Fig. 7.2(a).

A schematic arrangement is shown in Fig. 7.5 from which it will be seen that all parameters relating to mean temperature difference calculations are available in a single presentation.

## Acknowledgement

The author is grateful to Dr R. Dodd, Schools of Chemical Engineering, University of Bradford, UK, for the provision of data relating to Fig. 7.2.

## References

A list of addresses for the service organisations is provided on p. xvi.

- Caglayan, A. N. and Buthod, P. (1976) 'Factors correct air-cooler and S & T Exchanger LMTD', *Oil & Gas Journal* (6 Sept.), pp. 91-4.
- Dodd, R. (1980) 'Temperature efficiency of heat exchangers with one shell pass and even number of tube passes', *Proc. 2nd World Congress in Chemical Engineering (Montreal)*, Vol. 4, pp. 463-7.
- Engineering Sciences Data Unit International Ltd, (1985) *Effectiveness - NTU Relationships for the Design and Performance Evaluation of Two-Stream Heat Exchangers*. ESDU Publication No. 85042.
- Gardner, K. and Taborek, J. (1976) *ASME-AIChE 16th National Heat Transfer*

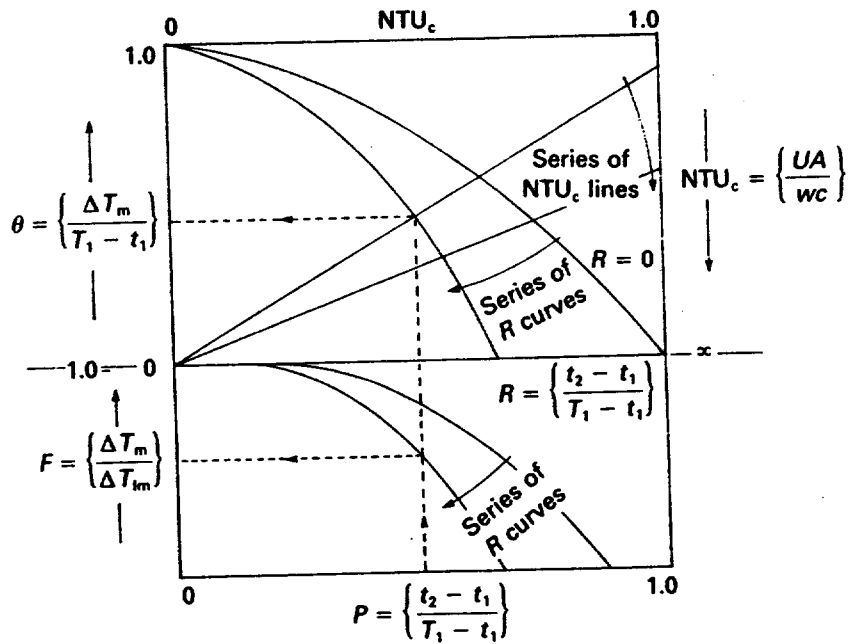


Figure 7.5 Schematic arrangement of  $F$ ,  $NTU_c$ , and  $\theta$  curves

Conference, Session on Process Heat Transfer, St Louis, Missouri.  
 Kern, D. Q. (1950) *Process Heat Transfer*. McGraw-Hill Inc., New York.  
 Taborek, J. (1983) *Heat Exchanger Design Handbook*, Vol. 1, Section 1.5, Hemisphere Publishing Corp.  
 Tubular Exchanger Manufacturers Association, Inc. (1978) *Standards of Tubular Exchanger Manufacturers Association* (6th edn). TEMA, New York, USA.

### Nomenclature

Symbol	Description	Units
$A$	Surface area	$m^2$
$c, C$	Specific heat of cold and hot fluid, respectively	$J/kg\ K$
$F$	Correction factor applied to log MTD (equation [7.3])	—
$m$	Number of shell-side passes	—
$n$	Number of tube-side passes	—
$N$	Number of exchangers in series	—
$NTU$	Number of transfer units (equation [7.9])	—
$P, P^*$	Thermal effectiveness (equations [7.5] and [7.6] respectively)	—
$Q$	Heat load	$W$
$R$	Heat capacity ratio (equations [7.4] and [7.10])	—
$t$	Cold fluid temperature: $t_1$ = inlet, $t_2$ = outlet	$K$
$T$	Hot fluid temperature: $T_1$ = inlet, $T_2$ = outlet	$K$
$w, W$	Mass flow rate: cold and hot fluid, respectively	$kg/s$
$\Delta T$	Temperature difference (between hot and cold fluids): $\Delta T_c$ at cold end, $\Delta T_h$ at hot end, $\Delta T_{lm}$ = logarithmic mean (equation [7.1]), $\Delta T_m$ = true or effective (equation [7.3])	$K$
$U$	Overall heat transfer coefficient, $U_c$ at cold end, $U_h$ at hot end	$W/m^2\ K$
$\theta$	Parameter defined by equation [7.13]	—

## Fouling

### 8.1 Fouling mechanisms

Fouling may be defined as any undesirable deposits on a heat transfer surface which increase resistance to both heat transfer and fluid flow. Somerscales (1980) identifies six categories of thermal fouling, the categories being based on the immediate cause of fouling, i.e. according to the dominant, but not necessarily the rate-controlling, fouling mechanism. He notes that categories (1) and (6) usually involve surface crystallisation (crystallisation fouling). Among categories (1)–(5), which are generally promoted by liquid heating, there are often strong interactions, which usually have mutually reinforcing effects, although occasionally there may be weakening effects. Category (6), alone, is promoted by liquid cooling.

- (1) *Precipitation fouling*. This relates to the precipitation of dissolved substances on the heat transfer surface. Certain dissolved substances, such as calcium sulphate, magnesium silicate and lithium carbonate, for instance, have inverse solubility versus temperature characteristics, and precipitation occurs on superheated rather than sub-cooled surfaces. This process is often referred to as *scaling*.
- (2) *Particulate fouling*. This occurs when finely divided solids (rust, dust, sand, etc.) suspended in the process fluid accumulate on the heat transfer surface. If the solids settle by gravity the process is referred to as *sedimentation* fouling.
- (3) *Chemical reaction fouling*. Deposits formed by chemical reactions at the heat transfer surface, where the surface material itself is not a reactant, describe this category. Polymerisation, cracking and coking of hydrocarbons are typical examples.
- (4) *Corrosion fouling*. As the name implies the heat transfer surface itself reacts to produce adherent corrosion products. These products may in turn promote the attachment of other fouling materials.
- (5) *Biological fouling*. This relates to biological organisms which adhere to the heat transfer surface. Adherent slimes may also be generated.
- (6) *Freezing fouling*. This occurs as a result of the solidification of a liquid, or some of its higher melting components, on a sub-cooled heat transfer surface.

## 8.2 Fouling growth

It is convenient to record the extent of fouling in terms of its resistance to heat transfer (reciprocal of its conductance) rather than the thickness of the fouling layer. Figure 8.1 illustrates various ways in which fouling resistance increases with respect to time. In Fig. 8.1(a) the deposition rate of the foulant is greater than the removal rate such that the fouling resistance increases linearly with time. Regular cleaning of the unit would be required to remove fouling. In Fig. 8.1(b) the fouling resistance increases initially, but eventually assumes a constant value (asymptotic fouling resistance). Evidently some mechanism causes the adhesion characteristics of the foulant to weaken as the thickness of the foulant increases. If the asymptotic fouling resistance could be predicted with confidence, heat transfer equipment could be designed which would operate continuously.

Figure 8.1 Fouling resistance versus time

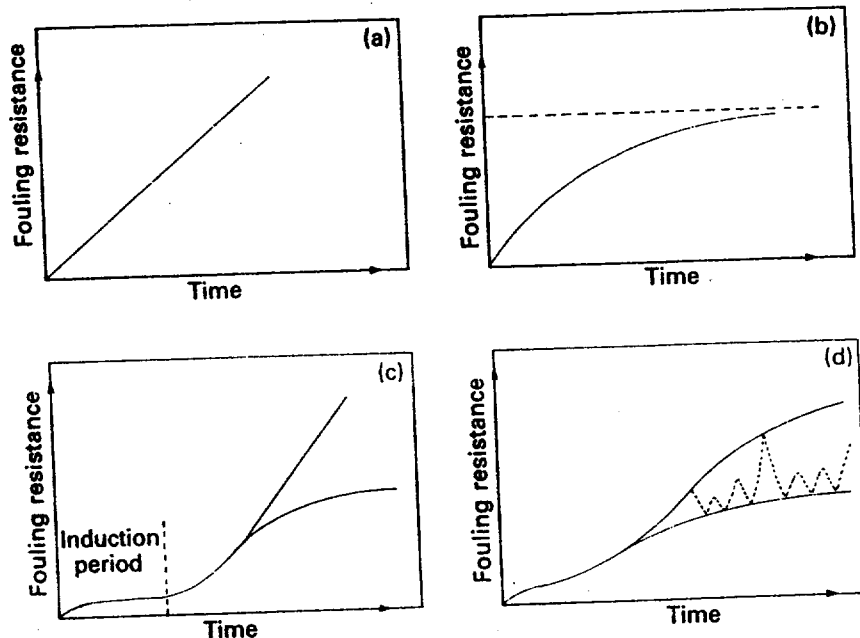


Figure 8.1(c) shows curves similar to Figs 8.1(a) and 8.1(b), except that a rapid growth of the foulant is preceded by an initial induction period during which foulant deposition is low. Figure 8.1(d) also shows curves similar to Figs 8.1(a) and 8.1(b), but after an initial induction period the fouling resistance fluctuates, as shown by the broken lines. The lower line is indicative of a non-removable base foulant on which a removable loose-type deposit forms and then breaks away. The design of an exchanger would probably be based on a mean line between the upper and lower lines.

Watkinson and Epstein (1970) observed that an incompletely cleaned exchanger, after being put into service again, fouled at a faster rate than a thoroughly cleaned one.

### 8.3 Cost of fouling

Von Nostrand *et al.* (1981) estimated the total cost of fouling for petroleum refining in the non-Communist countries as \$4.41 billion per year. Pritchard (1981) estimated the total cost of fouling in the United Kingdom as £300–£500 million per year based on 1978 values. These depressing values are based on additional capital, energy, maintenance and shutdown costs as a result of fouling. A breakdown of Pritchard's costs is given below.

#### Capital costs

These arise from several sources. Heat transfer equipment must be provided with additional surface area to compensate for the reduction in heat transfer due to fouling. The increase in exchanger size generates increased installation costs, while restriction of the flow passages due to fouling causes increased pressure loss, which necessitates larger pumps and motors. Additional capital costs are required for industrial water-treatment plant and the provision of design features to ease dismantling and cleaning during maintenance.

The total annual capital cost in the UK due to fouling is estimated to be £100 million.

#### Energy costs

These are incurred in providing increased pumping power to meet increased pressure loss, while in refrigerators and power condensers the thermal efficiency may be lowered due to fouling.

The total annual energy cost in the UK due to fouling is estimated to be £60 million.

#### Maintenance costs

These arise from dismantling, cleaning and reassembly of heat transfer equipment, together with the operation of water-treatment plant and the cost of chemicals and other additives to reduce fouling.

The total annual maintenance cost in the UK due to fouling is estimated to be £80 million.

#### Shutdown costs

The value of lost production which occurs when heat transfer equipment is shut down due solely to fouling is difficult to assess, but it is estimated that the total shutdown cost in the UK due to fouling is £60 million.

#### Total costs

These total £300 million (1978 values), but Pritchard considers that this value may be low and the true cost may be nearer £500 million.

### 8.4 Design considerations

Having designed the heat transfer equipment for 'clean' conditions, the thermal design engineer must cater for 'fouled' conditions if frequent



cleaning is to be avoided. Depending on the extent of fouling, thermal performance may decrease rapidly below the design duty, and/or the pressure loss may increase rapidly to an unacceptable level, unless suitable provision is made. The thermal design of the equipment for clean conditions may have involved the use of a highly sophisticated computer program (developed by one of the cooperative research organisations), which required considerable research, testing, analysis, etc., at a multi-million pound cost. The thermal designer is unlikely to find the same degree of sophistication when dealing with fouling.

In most cases, neither the composition of the foulant nor its thermal conductivity will be known. Even if thermal conductivity is known, it is unlikely to be of assistance, particularly in the shell-side design of a shell-and-tube exchanger, as the designer will be unable to predict where the foulant will be deposited, or its thickness. In addition, it is unlikely that the designer will know the rate at which the fouling layer thickness increases with time, or how the equipment will be operated with respect to changes in throughput and temperature. As a result it will not be possible to predict the time that will elapse before heat transfer or pressure loss reach unacceptable levels and cleaning becomes necessary – one can only guarantee that the equipment performance at commissioning will not be less than the design duty. Despite the problems associated with fouling some users demand that performance is 'guaranteed under fouled conditions', which implies that it must never fall below the design duty during its lifetime.

#### 8.4.1 Heat transfer calculations

##### Cleanliness and fouling factors

With regard to the heat transfer calculations the thermal design engineer must resort to the use of cleanliness factors, or fouling factors, unless data, based on identical operating conditions, are available. Cleanliness factors are chiefly used in steam surface condenser design and as the services tend to be similar they can be predicted with more reliability than fouling factors. If  $U_D$  = overall heat transfer coefficient under fouled conditions, and  $U_c$  = overall heat transfer coefficient under clean conditions, the cleanliness factor is defined as  $U_D/U_c$ .

The fouling factor concept assumes that the foulant covers the entire heat transfer surface with a uniform thickness and the fouling factor is the anticipated resistance (reciprocal of heat transfer coefficient) to heat transfer of the fouling layer. The assumed temperature profile is shown in Fig. 6.3 and, in the case of a tube, the overall heat transfer coefficient is calculated from:

$$\frac{1}{U_D} = \left\{ \frac{1}{\alpha_o} + \left( \frac{1}{\alpha_i} \right) \left( \frac{d_o}{d_i} \right) + r_w \right\} + \left\{ r_o + r_i \left( \frac{d_o}{d_i} \right) \right\} \quad [8.1a]$$

$$= \left\{ \frac{1}{\alpha_o} + \left( \frac{1}{\alpha_i} \right) \left( \frac{d_o}{d_i} \right) + r_w \right\} + \left\{ \text{sum of fouling factors} \right\} \quad [8.1b]$$

$$= \frac{1}{U_c} + (\text{total resistance due to fouling}) \quad [8.1c]$$

where  $U_D, U_c$  = fouled and clean overall heat transfer coefficients, respectively, referred to outside of tube  
 $\alpha_o, \alpha_i$  = film heat transfer coefficients, outside and inside the tube, respectively, under clean conditions  
 $r_w$  = resistance of tube wall, referred to outer surface  
 $r_o, r_i$  = fouling factor on outer and inner surfaces, respectively  
 $d_o, d_i$  = tube outer and inner diameter, respectively.

A similar treatment is given to non-tubular equipment and in all cases each coefficient must be related to the chosen reference surface. This includes the fouling factors which are assumed to apply to the surface on which they occur. In the case of shell-and-tube exchangers, at least, it is not usual to attempt to alter the clean film heat transfer coefficients arising from velocity changes due to the blockage of the flow passages by the foulants.

#### Source of fouling factors

Typical fouling factors are given in Chapter 19, but the principal published source is TEMA (1978) which provides data for a modest range of industrial applications with particular emphasis on petroleum refining. *Although heavily criticised these have served industry for over forty years and may well continue to do so for many more.* The criticisms are: (a) the continuous operating period which the fouling factors are intended to achieve is not stated, (b) the fouling factors appear to relate to shell-and-tube exchangers, but no distinction is made between shell-sides and tube-sides, (c) no mention is made of tube size and pitch, (d) where fouling factors are related to temperature, the fluid bulk temperature is specified rather than the surface temperature, (e) fouling factors, related to bulk temperature and fluid velocity, are given for water and crude-oil streams, but not for other fluids and (f) the source of the data is not stated.

#### Effect on surface area

The fouling factors provided by TEMA may increase the clean surface area considerably and virtually dominate the design, a typical example being a water/water shell-and-tube exchanger. External and internal heat transfer coefficients of  $5680 \text{ W/m}^2 \text{ K}$  ( $1000 \text{ Btu/hr ft}^2 \text{ }^\circ\text{F}$ ) are readily achieved, giving a clean overall heat transfer coefficient of  $2840 \text{ W/m}^2 \text{ K}$  ( $500 \text{ Btu/hr ft}^2 \text{ }^\circ\text{F}$ ). A total fouling factor of  $0.000528 \text{ (W/m}^2 \text{ K)}^{-1}$  or  $0.003 \text{ (Btu/hr ft}^2 \text{ }^\circ\text{F)}^{-1}$  is typical, giving a fouled overall heat transfer coefficient of  $1136 \text{ W/m}^2 \text{ K}$  ( $200 \text{ Btu/hr ft}^2 \text{ }^\circ\text{F}$ ). In this example the surface area required to account for fouling is 2.5 times that of the clean exchanger.

In some cases the fouling factors provided by TEMA may increase the clean surface area by only a small amount. A typical clean overall heat transfer coefficient for a steam/fuel-oil exchanger is  $114 \text{ W/m}^2 \text{ K}$  ( $20 \text{ Btu/hr ft}^2 \text{ }^\circ\text{F}$ ) and a typical overall fouling factor is  $0.00097 \text{ (W/m}^2 \text{ K)}^{-1}$  or  $0.0055 \text{ (Btu/hr ft}^2 \text{ }^\circ\text{F)}^{-1}$  giving a fouled overall heat transfer coefficient of  $102.6 \text{ W/m}^2 \text{ K}$  ( $18.0 \text{ Btu/hr ft}^2 \text{ }^\circ\text{F}$ ). In this example the surface area required to account for fouling is only 1.11 times that of the clean exchanger.

For simplicity in these examples, tube-wall resistance has been ignored and all coefficients are related to the same reference surface. In order to meet standards imposed by the user, such as tube length, for instance, the designer may have to provide even greater oversurface.

#### Effect on performance

Although greater oversurface may achieve greater on-stream life in many cases, it may achieve the opposite effect. In its early life the duty of the water/water exchanger cited above is easily achieved as it has considerable oversurface. If the cooling water flow is reduced to avoid overcooling the hot stream, the reduced water velocity and the resulting higher wall temperature may produce rapid fouling. Another example is an oversized kettle reboiler, in which the design temperature difference imposed on the unit at start-up, may produce film boiling, with a higher wall temperature, which in turn may produce rapid fouling.

#### 8.4.2 Pressure loss calculations

Despite its deficiencies the fouling factor concept in heat transfer calculations is well established, being defined by equations [8.1a]–[8.1c]. The fouling factors are of little assistance in the case of pressure loss calculations. Modern thermal design programs for shell-and-tube exchangers permit the selection of whatever inherent shell-side constructional clearances are required. This allows the selection of reduced, or zero, clearances for shell/baffle, baffle hole/tube and inter-tube gaps to simulate partial or complete blockage by fouling, assuming uniform foulant deposition over the entire external tube surface. Unfortunately, the fouling layer thickness or its distribution over the surface will not be known.

One approximation used in industry is to assume that the fouling layer thickness in inches is the same as the fouling factor in  $(\text{Btu/hr ft}^2 \text{ }^\circ\text{F})^{-1}$  units, which assumes that the foulant always has a thermal conductivity of  $0.0833 \text{ Btu/ft hr }^\circ\text{F}$ , which is equivalent to that of paper or asbestos at  $0^\circ\text{C}$ .

A more widely used approach for shell-and-tube exchangers, using modern computer programs, is to calculate the pressure loss for fouled conditions assuming that the foulant completely blocks the baffle hole/tube gap. It is assumed that the shell/baffle and inter-tube gaps are completely clear. Table 8.1 provides the *calculated* ratio of fouled/clean pressure loss for various fouling layer thicknesses affecting the baffle hole/tube and inter-tube gaps. The ratios are tabulated for the split backing ring floating-head type only, because exchanger type has little effect on this ratio. The calculated results are considerably influenced by tube configuration and ratio of baffle space/shell diameter for a given degree of fouling. It is questionable whether this approach is realistic; the inference that fouling will have less effect on pressure loss as the baffle space and cut increase, does not accord with practice. (See section 8.6.3 – Stagnant areas.)

The manual method presented in Chapter 12 does not provide data to

enable the user to calculate the shell side pressure loss when only the baffle/tube gap is completely blocked, with no fouling layer on the tube surface. A conservative approach for the manual method is to calculate the cross flow pressure loss for an 'ideal' exchanger, as described in section 12.5.5. In an 'ideal' exchanger, both shell/baffle and baffle/tube gaps are blocked. A comparison between manual and proprietary computer methods is given in Table 8.2, which confirms that the proposed manual approach does over-predict cross flow pressure loss considerably.

In the case of flow outside tubes, the increase in pressure loss due to the presence of a known fouling layer is readily calculated. As an approximation, it may be assumed that the fouled/clean pressure loss ratio, due to a uniform fouling layer, at the same flow rate and baffle spacing, is  $\{G/(G - 2F_L)\}^2$  where  $G$  is the design gap between adjacent tubes and  $F_L$  is the fouling layer thickness.

In the case of flow inside tubes, the increase in pressure loss due to the presence of a known fouling layer is readily calculated. As an approximation, it may be assumed that the fouled/clean frictional pressure loss ratio, due to a uniform fouling layer, at the same flow rate, is  $(d_c/d_f)^5$  where  $d_c$  and  $d_f$  are the clean and fouled tube bores respectively.

## 8.5 Fouling research

The cost of fouling is so high that there would appear little difficulty in justifying extensive research into the problem. Although its importance has always been recognised, it is only in recent years that it has been given considerable attention. Taborek *et al.* (1972), for instance, remind us that (up to 1972) there was not a single representative reference book dealing with the subject, and heat transfer texts rarely acknowledged its existence, despite the fact that in many cases it represents the major resistance to heat transfer.

In the past, fouling factors have been used to provide a margin of safety where thermal design methods were considered unreliable, but as a result of the activities of the cooperative research organisations, discussed in section 6.9, this is seldom the situation facing the thermal design engineer today. There would appear to be little purpose in continuing research to improve heat transfer equipment design unless it is matched by an improved knowledge of fouling.

The lack of attention given to the problem of fouling in the past may be criticised, but it is an extremely complex phenomenon which lacks repeatability, and makes a systematic programme of research difficult to define. Nevertheless, various organisations are now conducting vigorous research into the many aspects of fouling. One aspect is to obtain a better understanding of the complex processes of foulant deposition and breakaway. Another involves the use of both laboratory and field rigs to obtain general fouling data, with water being the most thoroughly

investigated fluid. Although valuable, it may prove difficult to adapt such data to provide reliable full-scale equipment design. The use of anti-foulants in the form of fluid dosing, surface treatment and on-line cleaning form other lines of investigation, although the latter may only be suited to large plants.

At present fouling remains the 'major unresolved problem in heat transfer' (Taborek *et al.* 1972) and the thermal design engineer is 'restricted to the mythology of fouling factors' (Hewitt 1981).

Table 8.1 Typical calculated ratios of fouled:clean pressure loss for shell-side flow

Shell inside diameter = 489 mm (19½ in)												
Tube outside diam. (mm)	Tube pitch (mm)	Pitch angle (deg grees)	Flow rate (kg/s)	BSR	Baffle hole/tube diametral clearance					Pitch angle (deg rees)	Tube pitch (in)	Tube outside diam. (in)
					0.65 mm (0.0256 in)	0.4 mm (0.0156 in)	nil	nil	nil			
					Fouling layer thickness on outside of tubes							
					nil	nil	nil	0.325 mm (0.0128 in)	0.65 mm (0.0256 in)			
15.88	19.84	30	17.6	0.2	1.0	1.52	3.34	3.79	4.56	30	25/32	5/8
19.05	23.81	30		0.2	1.0	1.43	2.71	3.03	3.52	30	15/16	3/4
25.40	31.75	30		0.2	1.0	1.32	2.08	2.27	2.56	30	1¼	1
25.40	31.75	90		0.2	1.0	1.26	1.85	2.03	2.31	90	1¼	1
31.75	39.69	45		0.2	1.0	1.18	1.54	1.67	1.87	45	1⅝	1¼
15.88	19.84	30		1.4*	1.0	1.12	1.21	1.44	1.79	30	25/32	5/8
19.05	23.81	30		1.4	1.0	1.10	1.15	1.35	1.60	30	15/16	3/4
25.40	31.75	30		1.4	1.0	1.06	1.09	1.23	1.40	30	1¼	1
25.40	31.75	90		1.4	1.0	1.03	1.07	1.17	1.31	90	1¼	1
31.75	39.69	45		1.4	1.0	1.01	1.04	1.13	1.21	45	1⅝	1¼

Shell inside diameter = 489 mm (19½ in)												
Tube outside diam. (mm)	Tube pitch (mm)	Pitch angle (deg grees)	Flow rate (kg/s)	BSR	Baffle hole/tube diametral clearance					Pitch angle (deg rees)	Tube pitch (in)	Tube outside diam. (in)
					0.65 mm (0.0256 in)	0.4 mm (0.0156 in)	nil	nil	nil			
					Fouling layer thickness on outside of tubes							
					nil	nil	nil	0.325 mm (0.0128 in)	0.65 mm (0.0256 in)			
15.88	19.84	30	37.8	0.2	1.0	1.84	5.87	7.07	8.94	30	25/32	5/8
19.05	23.81	30		0.2	1.0	1.52	4.46	5.16	6.09	30	15/26	3/4
25.40	31.75	30		0.2	1.0	1.44	3.05	3.41	3.81	30	1¼	1
25.40	31.75	30		0.2	1.0	1.56	2.89	3.24	3.59	90	1¼	1
31.75	39.69	45		0.2	1.0	1.31	2.55	2.86	3.23	45	1⅝	1¼
15.88	19.84	30		0.6	1.0	1.36	1.80	2.40	3.21	30	25/32	5/8
19.05	23.81	30		0.6	1.0	1.28	1.58	2.00	2.47	30	15/26	3/4
25.40	31.75	30		1.0*	1.0	1.11	1.17	1.43	1.66	30	1¼	1
25.40	31.75	30		1.0*	1.0	1.08	1.10	1.38	1.58	90	1¼	1
31.75	39.69	45		1.0	1.0	1.06	1.07	1.28	1.41	45	1⅝	1¼

Table 8.1 (cont.)

Shell inside diameter = 489 mm (19½ in)												
Tube outside diam. (mm)	Tube pitch (mm)	Pitch angle (deg grees)	Flow rate (kg/s)	BSR	Baffle hole/tube diametral clearance					Pitch angle (deg rees)	Tube pitch (in)	Tube outside diam. (in)
					0.65 mm (0.0256 in)	0.4 mm (0.0156 in)	nil	nil	nil			
					Fouling layer thickness on outside of tubes							
nil		nil		nil		0.325 mm (0.0128 in)	0.65 mm (0.0256 in)					
15.88	19.84	30	47.8	0.2	1.0	2.00	6.59	7.74	9.34	30	25/32	5/8
19.05	23.81	30		0.2	1.0	1.86	5.08	5.80	6.69	30	15/16	3/4
25.40	31.75	30		0.2	1.0	1.65	3.80	3.87	4.29	90	1½	1
25.40	31.75	90		0.2	1.0	1.56	2.89	3.24	3.59	90	1½	1
31.75	39.69	45		0.2	1.0	1.40	2.15	2.34	2.57	45	1 3/8	1 1/4
15.88	19.84	30		0.4	1.0	1.67	2.72	3.50	4.50	30	25/32	5/8
19.05	23.81	30		0.6*	1.0	1.32	1.58	2.05	2.53	30	15/16	3/4
25.40	31.75	30		0.6	1.0	1.24	1.41	1.76	2.00	30	1½	1
25.40	31.75	90		0.6	1.0	1.15	1.27	1.53	1.73	90	1½	1
31.75	39.69	45		0.6	1.0	1.18	1.17	1.45	1.64	45	1 3/8	1 1/4

Notes:

- (1) Results based on HTRI proprietary program.
- (2) Shell-side pressure loss ratios are based on central bundle loss, i.e. exclude end space and nozzle losses.
- (3) Pressure losses based on water at average temperature of 70 °C (158 °F).
- (4) Exchanger type = split backing ring floating head (AES).
- (5) Baffles = single segmental type.
- (6) Shell-bundle and shell-baffle clearances are based on Table 12.2.
- (7) Reynolds number range = 4000 – 180 000.
- (8) Fouling layer assumed to be uniform over entire external surface.
- (9) (BSR) = baffle spacing ratio = baffle space/shell diameter.
- (10) Baffle spacing greater than TEMA maxima for steel tubes are denoted by \*

Table 8.2 Shell-side cross flow pressure loss due to blockage – comparison of manual and proprietary computer methods

Example no.	Design no.	'Ideal' exchanger: shell/baffle and baffle/tube gaps blocked	'Real' exchanger: baffle/tube gap only blocked	'Real' exchanger: basic design without blockage
1		2.51	1.70	1.00
2	A	1.64	1.23	1.00
	B	2.01	1.46	1.00
3	A	2.45	1.52	1.00
	B	1.79	1.10	1.00
	C	1.84	1.15	1.00
7		2.05	1.35	1.00

Calculation method	Manual – as chapters 12 and 13	Proprietary computer program (HTRI)

## 8.6 Design to minimise fouling

As it is almost impossible to forecast the fouling tendency of new heat transfer equipment, previous operational experience under similar process conditions should be sought. If such data are not available the most important decisions to be made at the design stage are the choice of exchanger type and its material of construction.

### 8.6.1 Exchanger type

Part 1 describes many types of heat transfer equipment available to the designer and their advantages and disadvantages are summarised in Table A1.1 of Part 1 Appendix. If fouling is expected to be a problem, first considerations would be given to gasketed-plate, spiral, graphite or Teflon™ types. However, all have pressure and temperature limitations and the graphite and Teflon™ types are limited with regard to size. If the heating medium is fouling, electrically heated exchangers should be considered.

If the choice must be a shell-and-tube exchanger, it is important to ensure that its type, routing of the fluids, head type and tube configuration follows the guidelines of Chapter 1 in order to ease cleaning.

### 8.6.2 Materials of construction

Corrosion arising from an incorrect choice of material not only reduces the equipment life, but blockage of the exchanger passages due to deposition of corrosion products may result in frequent, costly shutdowns for cleaning. Materials should therefore be selected on the basis of minimising overall costs within the expected lifespan of the exchanger, rather than initial cost.

Graphite, glass and Teflon™ exchangers provide high corrosion-resistance, while the more expensive metals, such as titanium and high-nickel alloys, can be accommodated more cheaply in the gasketed-plate exchanger than in the shell-and-tube type. If the choice must be a shell-and-tube exchanger, the use of bi-metal barrels, tubesheets and tubes should always be considered to reduce cost. Where dissimilar metals are used, electrical or physical contact between them must be assessed carefully to avoid galvanic corrosion. Non-metallic linings may be a suitable alternative for some applications.

Rough surfaces act as a key for the adhesion of deposits; once the build up of deposits begins the rough fouling layer encourages more growth, and so on. Surface finish is important and exchangers with 'smooth' surfaces are preferred and include those constructed of graphite, glass and Teflon™. The flexibility of the latter's tubes is also claimed to assist in shedding deposits. Chapter 18 describes shell-and-tube exchangers with phenolic resin-lined tubes having 'non-stick' properties.

Chapter 19 provides cost data for various exchanger types and Chapter 18 describes materials of construction.

### 8.6.3 Design features

Whatever type of heat exchanger is chosen, certain common design factors relating to fouling must always be considered.

#### **Velocity**

The exchanger must be designed with fluid velocities which will discourage fouling and they depend on the type of unit, its material and related erosion/corrosion characteristics. Typical tube-side velocities for shell-and-tube exchangers, for various materials, are given in Table 18.2. Although fouling may be avoided at design throughput, the performance of the exchanger should be assessed under turndown conditions. Unless considered at the design stage, reduced velocities at low throughput may result in rapid fouling. The velocities must be checked in nozzles and headers in addition to the flow passages.

In order to achieve the required velocities, the user may have to permit higher pressure losses than normal. Despite the importance of energy saving, increased pressure losses may be justified if this provides greater on-stream life.

#### **Flow distribution**

Having decided on the velocities required to minimise fouling the design of the exchanger should be examined to check that these velocities will be achieved and maldistribution of the fluids will not occur. Low velocities in some of the flow passages due to maldistribution encourage deposits to settle. In addition, any reduction in heat transfer coefficient arising from reduced velocities increases the possibility of producing hot or cold spots on the heat transfer surface. In the case of hot spots, where the temperature of the heated fluid approaches that of the heating medium, the fluid may fuse on to the surface. In the case of cold spots, where the temperature of the cooled fluid approaches that of the coolant, the fluid may solidify on the surface.

Spiral and 1/1 double-pipe exchangers have only one flow passage for each fluid so that maldistribution cannot occur. If fouling does occur in these types, the flow passage areas are decreased, but the velocities are increased, which may assist in minimising fouling.

#### **Stagnant areas**

Low velocities in stagnant areas encourage deposits to settle and the shell-side of shell-and-tube exchangers is particularly prone to this. Deposits tend to build up on both sides of the baffle plates as shown in Fig. 8.2. Gilmour (1965) considered that shell-side fouling occurred chiefly from poor design and most of his advice is accepted today: namely (a) the baffle cut should preferably be 20% and should not exceed 25%, (b) have a small shell-baffle clearance, (c) seal-off the shell-bundle gap



with dummy tubes or rods (d) use a tube layout with pass partitions normal to shell-side flow; if the layout (see Figs 1.30 and 1.31) provides pass partitions parallel to the flow direction they must be sealed off with dummy tubes or rods, (e) use only horizontal cut baffles with single-phase fluids and (f) have no drainage or venting notches in baffles.

Deposits are also likely to form in a stagnant area in the header on the tubesheet face, and opposite the shell-side inlet nozzle.

Spiral- and plate-type exchangers have no baffles and therefore no stagnant areas where deposits could build up. They do have headers, however, where stagnant areas must be avoided.

Vents and drains in shells and headers must be correctly positioned to ensure that gases and liquids do not become entrapped and cause localised corrosion. They must also be of adequate size so that they do not become blocked by solid matter.

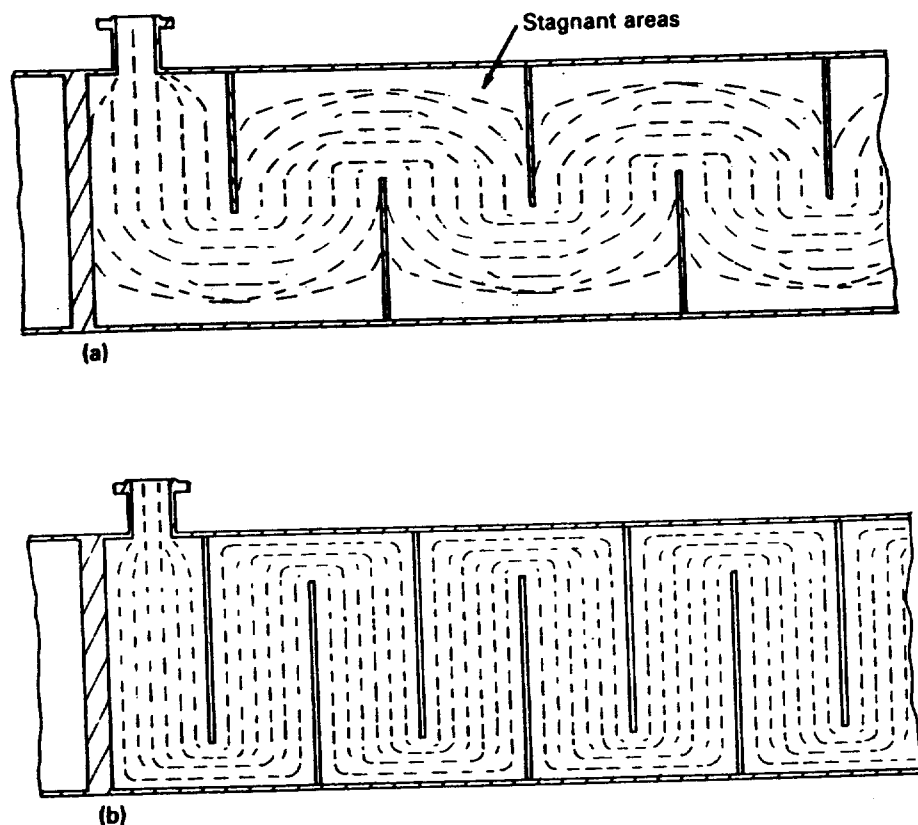
## References

A list of addresses for the service organisations is provided on p. xvi.

Gilmour, C. H. (1965) 'No fooling - no fouling', *Chem. Eng. Progress*, 61 (No. 7), pp. 49-54.

Hewitt, G. F. (1981) 'The potential for development in heat exchanger plant', *Conference on Future Developments in Process Plant Technology*, IMechE Headquarters, 24/25 Feb.

Figure 8.2 Stagnant areas on shell-side of shell-and-tube exchanger (a) poor design resulting from large baffle cut in relation to baffle space : shell diameter ratio (b) improved design resulting from correctly sized baffle cut in relation to baffle space : shell diameter ratio



- Pritchard, A. M.** (1981) *Fouling of Heat Transfer Equipment* (edited by Somerscales, E.F.C. and Knudsen, J. G.). Hemisphere Publishing Corp.
- Somerscales, E. F. C.** (1981) *Fouling of Heat Transfer Equipment* (edited by Somerscales, E.F.C. and Knudsen, J. G.). Hemisphere Publishing Corp.
- Taborek, J. et al.** (1972) 'Fouling: the major unresolved problem in heat transfer', Parts I and II, *Chem. Eng. Progress*, **68** (No. 2), 59-67, and **68** (No. 7), 69-78.
- Tubular Exchanger Manufacturers Association, Inc.** (1978) *Standards of Tubular Exchanger Manufacturers Association* (6th edn). TEMA, New York, USA.
- Von Nostrand, W. L. et al.** (1981) *Fouling of Heat Transfer Equipment* (edited by Somerscales, E.F.C. and Knudsen, J. G.). Hemisphere Publishing Corp.
- Watkinson, A. P. and Epstein, N.** (1970) 'Particulate fouling of sensible heat exchangers', *4th Int. Heat Transfer Conference*, Paris, Versailles, Paper HE 1.6.

## Extended surfaces

When the heat transfer coefficient on the outside of a tube is much lower than that on the inside, as for example, in oil/steam or low-pressure gas/water exchangers, the use of externally extended surface tubes should be considered. Extended surfaces increase the rate of heat transfer per unit tube length and the resulting exchanger may be smaller and cheaper than the corresponding plain tube exchanger.

A tube surface may be 'extended' by attaching pieces of metal to it in various ways in the form of continuous longitudinal or transverse strips (fins), wire coils, or discontinuous solid studs or spines of different shapes (see Fig. 9.1). A tube surface may be extended on its outer surface, inner surface, or both. If the metal used for extending the tube surface was a perfect heat conductor (i.e. infinite thermal conductivity), the extension would be 100% effective in transferring heat between the fin-side fluid and the tube wall. In practice, of course, this cannot be achieved, and it will be seen from below that there is nothing to be gained by extending the surface beyond that necessary to provide an economic solution. The cost of the metal used for the extension, the cost of forming it to the required shape and the cost of attaching it to the tube must be considered.

The most common form of extended surface is fins.

### 9.1 Fin efficiency

Consider a length of externally finned tube which is receiving heat from the external fluid (Fig. 9.2). In order that heat received by the fin may be conducted through it to the base and thence to the tube-side fluid, a temperature gradient must exist in the fin, the tip being hotter than the root. The effect of the temperature gradient in the fin is to reduce the 'driving force' for heat transfer, i.e. the temperature difference between external fluid and fin. In order to allow for the reduced temperature difference between external fluid and fin, a fin efficiency is introduced into the heat transfer calculations, this being defined as the ratio of the heat actually transferred to the base tube to that which could be transferred with an infinitely conducting fin.

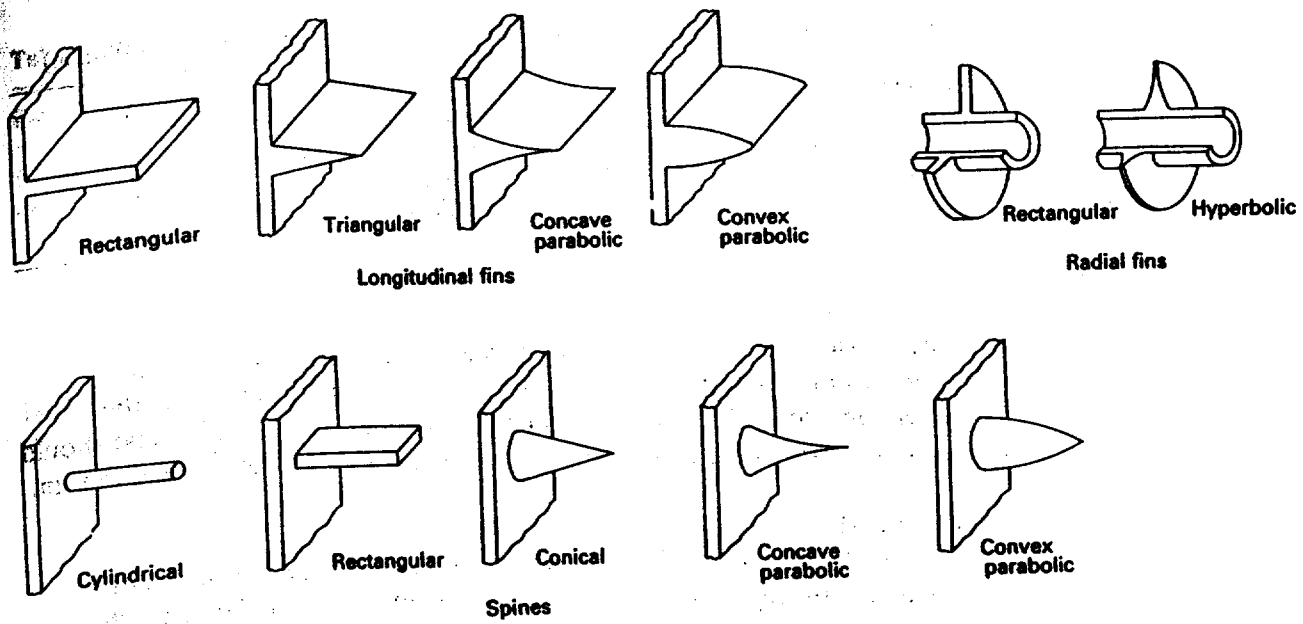


Figure 9.1 Types of extended surface

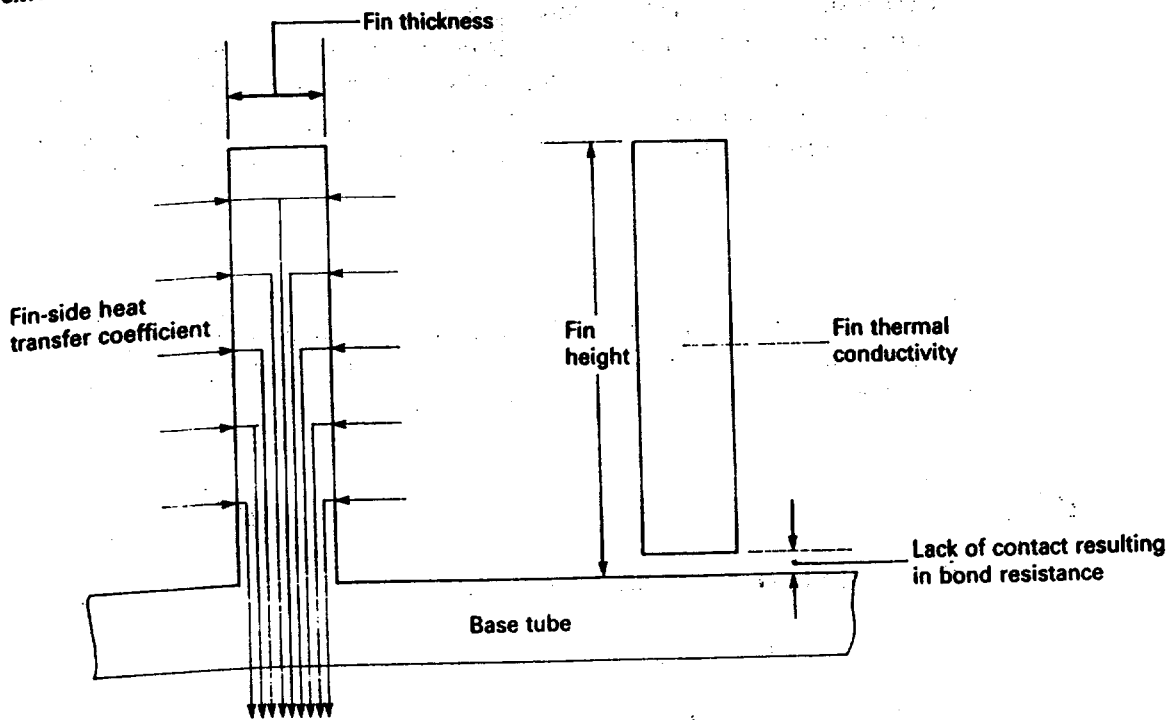


Figure 9.2 Factors affecting fin efficiency

Certain factors affect fin efficiency, and the comments below apply irrespective of whether the tube is finned on the inside or the outside, or whether heat is being transferred to or from the fin.

**Fin thermal conductivity**

The higher its thermal conductivity the higher the fin efficiency, as heat is more readily conducted through the fin. Table 9.1 gives the thermal conductivity for typical fin materials, from which it will be seen that copper has the highest value. Despite this, aluminium or steel is often preferred due to the lower cost. Stainless-steel is a poor fin material because of its high cost and low thermal conductivity.

**Table 9.1** Approx. thermal conductivities of various metals at 100 °C (W/m K)

Copper	389	90/10 Cupro-nickel	52
Aluminium	208	Steel	52
Admiralty brass	121	70/30 Cupro-nickel	35
Aluminium brass	100	Monel	26
Nickel	66	Stainless steel	17

**Fin thickness**

The greater the fin thickness, the higher the fin efficiency, as the cross-sectional area for heat flow is greater. On the other hand, the weight and cost of the fin material are increased. The fin thickness should increase towards the root to match the increasing heat flow down the fin.

**Fin height**

The greater the fin height, the lower the fin efficiency, because heat conducted through the fin has a greater length to travel. On the other hand, the external surface area is increased.

**Heat transfer coefficient to finned surface**

The greater the heat transfer coefficient to the finned surface, the greater the quantity of heat to be conducted through the fin and hence the fin efficiency is lower. The ratio of fin-side to plain base-tube surface areas should be roughly the same as the ratio of plain-side to fin-side heat transfer coefficients.

**Bond resistance**

Although derivations of fin efficiency assume no bond resistance, this is not always the case and depends on the type of finned tube and its fin/tube attachment. Any bond resistance must be included in the heat transfer calculations.

**9.2 Heat transfer calculations****9.2.1 Heat transfer coefficient to finned surface**

The first step is to calculate the heat transfer coefficient to the finned surface ( $\alpha_f$ ), and Chapter 6 provides correlations for longitudinally finned, low-finned and high-finned tubes. Longitudinally finned tubes are used primarily for double-pipe exchangers and fuel-oil heaters. They are described in Chapter 5 and cost data for double-pipe exchangers are given in Chapter 19. Low-fin tubes are used primarily in shell-and-tube exchangers, being described in Chapter 13. The design of shell-and-tube exchangers using low-fin tubes is also given in Chapter 13. High-finned tubes are widely used in air-cooled heat exchangers and the various types are described in Chapter 3.

Certain geometrical factors are required for finned tube calculations and these may be calculated from Table 9.2 and Fig. 9.3.

**Table 9.2** Geometrical factors for finned tubes (based on Fig. 9.3)

Fin type	Item	Formulae	
Longitudinal (welded U-fins)	Surface per metre length of one tube	Unfinned	$\pi d_r - N_f t_f$
		Finned	$2N_f l_f$
	Free area for flow outside tubes	$A_e - \left\{ \frac{\pi d_r^2}{4} + N_f t_f \left( l_f + \frac{r_f}{2} \right) \right\} N_f$	
Longitudinal (extruded fins)	Surface per metre length of one tube	Unfinned	$\pi d_r - N_f t_f$
		Finned	$2N_f l_f + N_f t_f$
	Free area for flow outside tubes	$A_e - \left\{ \frac{\pi d_r^2}{4} + N_f l_f t_f \right\} N_f$	
Radial	Surface per metre length of one tube	Unfinned	$\pi N_f d_r s_f$
		Finned	$(\pi/2)N_f(d_f^2 - d_r^2) + \pi N_f d_f t_f$
	Free area ratio	$1 - \frac{N_f(d_f t_f + d_r s_f)}{P}$ (applicable to $\square$ pitch and $\Delta$ pitch where minimum flow area is in transverse pitch in a row)	

**Notes:**

- (1) Total external surface per metre = unfinned surface per metre + finned surface per metre.
- (2) Longitudinal welded U-fins:  $r_f = 3t_f$  (usually).
- (3)  $A_e$  = total enclosure area containing  $N_f$  longitudinally finned tubes.
- (4)  $P$  = transverse tube pitch for radially finned tubes,  $S_f = (1 - N_f t_f)/N_f$ .
- (5) Free area ratio (FAR) =  $\frac{\text{free area for flow outside tubes}}{\text{gross area for flow as though tubes were absent}}$

**9.2.2 Calculation of fin efficiency (rectangular longitudinal fins)**

If the finned surface has a layer of dirt, the clean fin-side heat transfer coefficient  $\alpha_f$  must be combined with that of the dirt layer, to provide the fouled fin-side heat transfer coefficient  $\alpha'_f$ , as shown by equation [9.1], for use in equations [9.2] and [9.3], i.e.

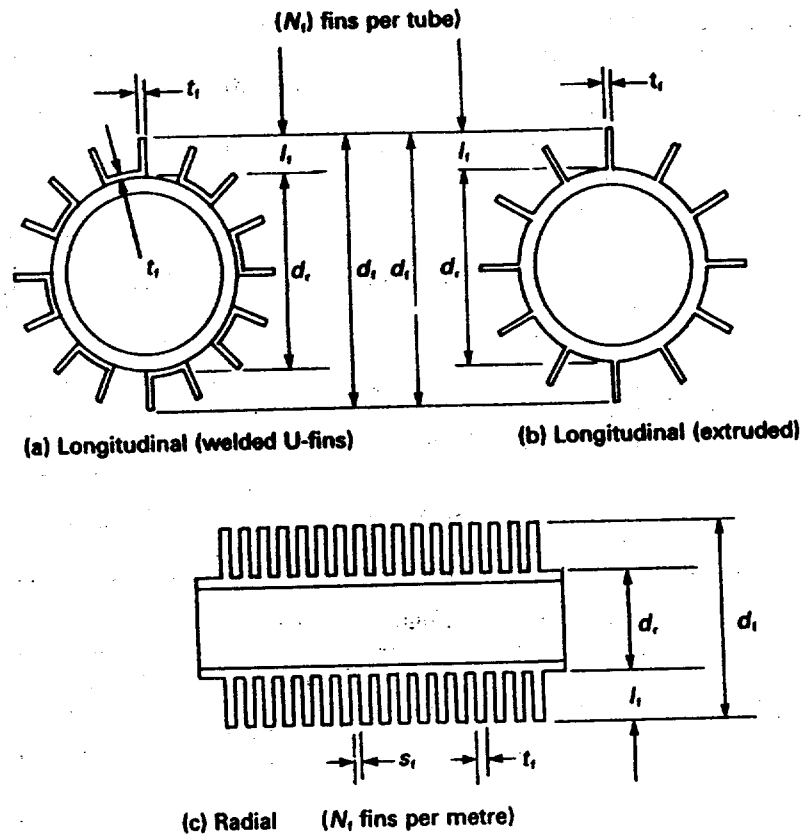
$$\frac{1}{\alpha'_f} = \frac{1}{\alpha_f} + r_o \quad [9.1]$$

where  $r_o$  = fin-side fouling resistance ( $\text{W/m}^2 \text{K}$ )<sup>-1</sup>.

Having calculated  $\alpha'_f$ , the second step is to calculate the fin efficiency,  $\Omega_f$ . Many textbooks, including Kern and Kraus (1972), for example, cater for fin-efficiency data for a variety of finned tubes, but the fin efficiency for longitudinally finned tubes, *having fins of constant cross-section*, is given by:

$$\Omega_f = \frac{\tanh(ml_f)}{ml_f} \quad [9.2]$$

Figure 9.3 Geometry of finned tubes



where  $m = \left\{ \frac{2\alpha_f'}{\lambda_f t_f} \right\}^{1/2}$

$l_f$  = fin height (m)

$t_f$  = fin thickness (m)

$\lambda_f$  = fin thermal conductivity (W/m K)

The derivation of fin efficiency assumes (a) the heat flow is steady, (b) the fin material is homogeneous and of identical composition throughout, (c) there is no heat source within the fin itself, (d) the heat exchange between fin surface and surroundings at any point is proportional to the temperature difference between fin and surroundings at that point, (e) the thermal conductivity of the fin is constant, (f) the fin-side heat transfer coefficient is the same over the entire surface, (g) the temperatures of the surrounding fluid and fin base are uniform, (h) the fin thickness is small in relation to height so that the temperature gradients across fin thickness may be neglected, (i) there is negligible heat flow into the outer fin edge compared with the sides and (k) there is no resistance at the fin-tube junction.

### 9.2.3 Calculation of fin efficiency for other fin types

Longitudinally finned tubes are not restricted to fins having a rectangular profile in which the cross-sectional area is constant. The profile may be triangular or parabolic (concave and convex) and the cross-sectional area is no longer constant. With radially finned tubes the cross-sectional area

**Table 9.3** Equivalent fin thickness and fin height for fin-efficiency calculations

Type of fin	Profile	Actual fin thickness or diameter		Effective fin thickness ( $t_{fe}$ )	Effective fin height ( $l_{fe}$ ) (actual height = $l_f$ )
		At tip	At root		
Longitudinal	Rectangular	$t_f$	$t_f$	$t_f$	$l_f$
Longitudinal	Trapezoidal	$t_{fr}$	$t_{fb}$	$0.75t_{fb} + 0.25t_{fr}$	$l_f$
Radial	Rectangular	$t_f$	$t_f$	$t_f$	} $l_f \left\{ 1 + \frac{t_{fe}}{2l_f} \right\} \left\{ 1 + 0.35 \ln \left( \frac{d_f}{d_r} \right) \right\}$
Radial	Triangular	$t_{fr}$	$t_{fb}$	$0.5(t_{fb} + t_{fr})$	
Spine	Circular	$d_s$	$d_s$	$0.5d_s$	$l_f + 0.25d_s$

Note:  $l_f/t_f > 3$ ,  $d_f/d_r < 3$

**Table 9.4** Fin-efficiency values

$m_c l_{fe}$	$\Omega_f$	$m_c l_{fe}$	$\Omega_f$	$m_c l_{fe}$	$\Omega_f$
0.00	1.000	0.80	0.830	1.55	0.590
0.10	0.997	0.85	0.813	1.60	0.576
0.15	0.993	0.90	0.796	1.65	0.563
0.20	0.987	0.95	0.779	1.70	0.550
0.25	0.980	1.00	0.762	1.75	0.538
0.30	0.971	1.05	0.745	1.80	0.526
0.35	0.961	1.10	0.728	1.85	0.515
0.40	0.950	1.15	0.711	1.90	0.503
0.45	0.938	1.20	0.695	1.95	0.493
0.50	0.924	1.25	0.679	2.00	0.482
0.55	0.910	1.30	0.663	2.05	0.472
0.60	0.895	1.35	0.647	2.10	0.462
0.65	0.880	1.40	0.632	2.15	0.453
0.70	0.863	1.45	0.618	2.20	0.444
0.75	0.847	1.50	0.603	2.25	0.435

Based on equation [9.3] and applicable to fin types listed in Table 9.3

of the fin changes from tip to base, irrespective of whether the profile is rectangular or shaped. The derivation of fin efficiency for these types is more complex and the results are expressed graphically for manual calculations. Kern and Kraus (1972) provide graphical solutions for various shapes of longitudinal fins, radial fins and spines.

Schmidt (1966) showed that within certain limits, equation [9.2] could be used for other fin types, with little error, if the actual fin height ( $l_f$ ) and actual fin thickness ( $t_f$ ) were replaced by an equivalent fin height ( $l_{fe}$ ) and equivalent fin thickness ( $t_{fe}$ ). The general equation is then:

$$\Omega_f = \frac{\tanh(m_c l_{fe})}{m_c l_{fe}} \tag{9.3}$$

$$\text{where } m_c = \left\{ \frac{2\alpha'_f}{\lambda t_{fe}} \right\}^{1/2}$$

Values of  $l_{fe}$  and  $t_{fe}$  are given in Table 9.3 for some industrially important cases. To simplify calculations involving equation [9.3], Table 9.4 provides  $\Omega_f$  for various values of  $m_c l_{fe}$ .



### 9.2.4 Overall heat transfer coefficient

The total extended surface area per unit tube length ( $A_t$ ) is the sum of the area of the finned surface per unit length ( $A_f$ ) and the unfinned, surface area per unit length ( $A_u$ ). The fin-efficiency derivation assumes that the fin-side heat transfer coefficient ( $\alpha'_f$ ) is the same over the entire surface, i.e. applicable to both  $A_f$  and  $A_u$ . The fin-efficiency concept applies only to the finned surface. Hence the effective fin-side heat transfer coefficient ( $\alpha_{fi}$ ), for combining with the other coefficients in the system, is given by

$$\alpha_{fi} A_t = \alpha'_f (\Omega_f A_f + A_u) \quad [9.4]$$

In equation [9.4],  $\alpha_{fi}$  is related to the total external surface, but it may be related to any convenient reference area such as the inside surface of the tube  $A_i$ , or the bare external surface  $A_b$  as though the fins did not exist, for calculating the overall heat transfer coefficient.

Hence the effective fin-side heat transfer coefficient, related to the inside surface  $\alpha_{fi}$ , is given by:

$$\alpha_{fi} = \frac{\alpha'_f (\Omega_f A_f + A_u)}{A_i} \quad [9.5]$$

$$\text{and } \frac{1}{U_i} = \frac{1}{\alpha_{fi}} + r_{ui} + r_i + \frac{1}{\alpha_i} \quad [9.6]^*$$

or, related to the bare external surface, the effective fin-side heat transfer coefficient ( $\alpha_{fo}$ ) is given by:

$$\alpha_{fo} = \frac{\alpha'_f (\Omega_f A_f + A_u)}{A_b} \quad [9.7]$$

$$\text{and } \frac{1}{U_o} = \frac{1}{\alpha_{fo}} + r_{to} + r_{io} + \frac{1}{\alpha_{io}} \quad [9.8]^*$$

where  $r_i, r_{io}$  = internal fouling resistance, referred to inside surface and bare external surface, respectively ( $\text{W/m}^2 \text{K}$ )<sup>-1</sup>

$r_{ui}, r_{to}$  = tube-wall resistance, † referred to inside surface and bare external surface, respectively ( $\text{W/m}^2 \text{K}$ )<sup>-1</sup>

$U_i, U_o$  = overall heat transfer coefficient, referred to inside surface and bare external surface, respectively ( $\text{W/m}^2 \text{K}$ )

$\alpha_i, \alpha_{io}$  = internal fluid heat transfer coefficient, referred to inside surface and bare external surface, respectively ( $\text{W/m}^2 \text{K}$ )

For manual calculations it is of great assistance to plot or tabulate  $\alpha_{fi}$  or  $\alpha_{fo}$  versus  $\alpha'_f$  for finned tubes of known geometries. Examples of this are given for longitudinally finned tubes in Table 15.1 and Fig. 15.2, and for high-finned tubes in Table 14.3.

From equation [9.4], and noting that  $A_u = A_t - A_f$ , it can be shown that

\* Assumes no bond resistance – this must be included if present.

† In the case of L-fins (Figs 3.4(a) and (b)), the resistance of the L foot should be included. In the case of integral fins (Fig. 3.4(d)), the resistances of the outer tube and liner should be included.

$$\frac{\alpha_{ft}}{\alpha'_f} = \frac{\Omega_f A_f + A_u}{A_t} = \left\{ 1 - \left( \frac{A_f}{A_t} \right) (1 - \Omega_f) \right\} = \Omega_w \quad [9.9]$$

$\Omega_w$  is termed the weighted fin efficiency. In the above equations there are  $\Omega_f$  and  $\Omega_w$ , together with  $\alpha_f$ ,  $\alpha'_f$  and  $\alpha_{ft}$  and confusion can arise if these are not clearly defined.  $\alpha_{ft}$  is the coefficient obtained as the result of tests on finned tubes and relates only to the specific tube and fin metal and geometry being tested. It therefore accounts for the effect of fin efficiency, bond resistance and manufacturing features.  $\alpha'_f$  or  $\alpha_f$  can be obtained from equation [9.9] for use with finned tubes of identical geometry but different fin metals. Values of  $\Omega_w$  versus  $\alpha'_f$  are tabulated in Table 13.4 for low-fin tubes in various metals.

### 9.2.5 Heat flow through fin edge (longitudinal fins)

In the derivation of fin efficiency leading to equations [9.2] and [9.3], it was assumed that there was negligible heat flow into the outer fin edge compared with the sides. If the heat flow into the edge is not negligible it can be accounted for by adding half the fin-tip thickness to the fin height and using this corrected fin height  $l_{fe}$ , instead of  $l_f$ , in the equations, viz.:

longitudinal fin, rectangular profile, use  $l_{fe} = l_f + t_f/2$  in equation [9.3]

longitudinal fin, trapezoidal profile, use  $l_{fe} = l_f + t_{ft}/2$  in equation [9.3]

### 9.2.6 Non-uniform heat transfer coefficient

Another assumption made in the derivation of fin efficiency is that the fin-side heat transfer coefficient is the same over the entire surface. The fin efficiency ( $\Omega_f$ ) calculated from equations [9.2] and [9.3], may be corrected for a non-uniform heat transfer coefficient, by multiplying it by  $C_f$  where

$$C_f = \{ 1 - 0.058(ml_f) \} \text{ or } \{ 1 - 0.058(m_e l_{fe}) \}$$

It should be emphasised that this approach is entirely empirical.

## 9.3 Pressure loss calculations

Chapter 6 provides correlations for longitudinally finned, low-finned and high-finned tubes. The required geometrical factors may be calculated from Table 9.2 and Fig. 9.3.

## 9.4 Space saving

The saving in space arising from the use of extended surfaces must not be overlooked. Table 13.1 provides a comparison of shell-and-tube

exchangers having plain and low-fin tubes. It will be seen that the use of low-fin tubes always reduces the number of shells required.

The massive wind tunnel cooler shown in Fig. 1.33 is of the fixed tubesheet type having air inside the tubes and cooling water outside. Its nominal dimensions are 14.3 m square, normal to the air flow, and 5.2 m deep, parallel to the air flow. It was replaced by a radial high-fin exchanger having air outside the tubes and cooling water inside. Again its nominal dimensions normal to the air flow are 14.3 m square, but its nominal depth, parallel to the air flow, is reduced from 5.2 m to 1.4 m. The use of extended surfaces has reduced the cooler volume to nearly one-quarter of its original value.

## 9.5 Surface temperature: longitudinally finned tubes

Section 6.8 provides a method for calculating surface temperatures for plain tubes. In the case of longitudinally finned tubes the fin and base tubes are not at the same temperature, neither is the fin at a uniform temperature. The temperature distribution on the fin-side is therefore complex, but the simple method described below permits an average fin temperature to be determined for the subsequent calculation of  $\phi$ .

Equation [9.5] shows that the fin-side coefficient  $\alpha'_f$  becomes  $\alpha_{fi} = \alpha'_f(\Omega_f A_f + A_u)/A_i$  when related to the base tube internal surface. If the fin is a perfect conductor,  $\alpha'_f$  becomes  $\alpha'_{fi} = \alpha'_f (A_f + A_u)/A_i$  when related to the base tube internal surface. The resistance of the fin metal, related to the base tube internal surface  $r_{fm}$ , is given by:

$$r_{fm} = \frac{1}{\alpha_{fi}} - \frac{1}{\alpha'_{fi}} \quad [9.10]$$

Having established equation [9.10], the procedure for calculating surface temperatures follows that of section 6.8. Referring to Fig. 9.4 and equation [6.9]

$$T_x = T_1 \pm (U \Delta T_o) \sum r_{1-x} = T_7 \mp (U \Delta T_o) \sum r_{x-7} \dots \quad [9.11]$$

where  $U$  = overall heat transfer coefficient

$\sum r_{1-x}$  = sum of all resistances between  $T_1$  and  $T_x$

$\sum r_{x-7}$  = sum of all resistances between  $T_x$  and  $T_7$

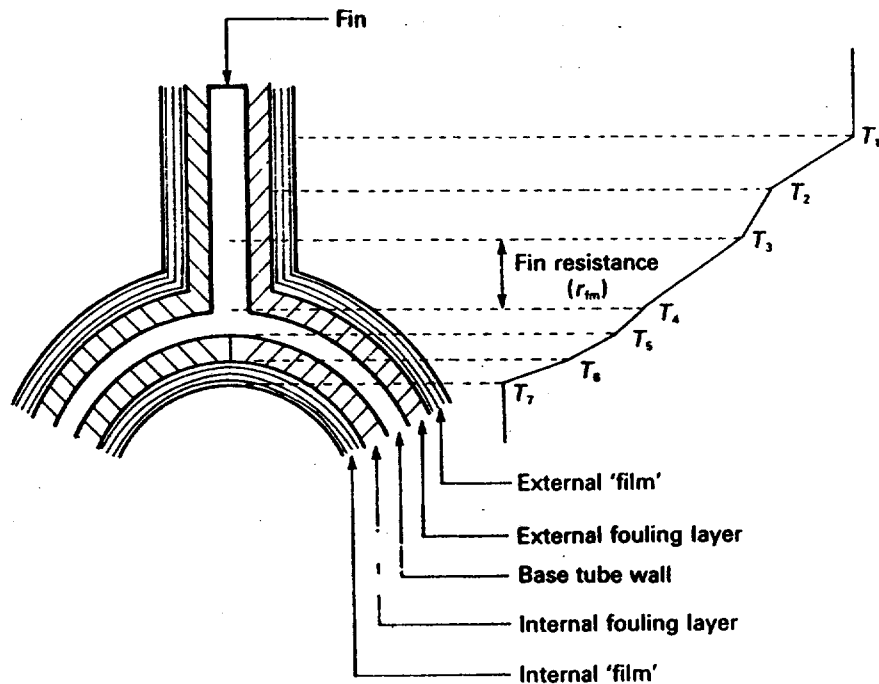
(upper signs when  $T_7 > T_1$ ; lower signs when  $T_7 < T_1$ )

$U$  and all resistances must be related to the chosen reference surface.

### 9.5.1 Example: average fin temperature (Viscosity corrosion factor = 1)

The example demonstrates the calculation of the average fin temperature for a longitudinally finned double-pipe heat exchanger having the

**Figure 9.4** Temperature profile for longitudinally finned tubes



following characteristics:

$$A_i = 0.1286 \text{ m}^2/\text{m}, (A_f + A_u) = 0.7407 \text{ m}^2/\text{m}, T_1 = 106.7 \text{ }^\circ\text{C},$$

$$T_7 = 37.2 \text{ }^\circ\text{C}, \alpha_f = 521.3 \text{ W/m}^2 \text{ K}, r_o = 0.000352 \text{ (W/m}^2 \text{ K)}^{-1},$$

$$r_{fi} = 0.00007 \text{ (W/m}^2 \text{ K)}^{-1}, r_i = 0.000528 \text{ (W/m}^2 \text{ K)}^{-1}, \alpha_i = 4514.2 \text{ W/m}^2 \text{ K}$$

(all conductances and resistances are related to their adjacent surfaces)

$$\alpha'_f = 1/(1/\alpha_f) + r_o = 1/(1/521.3) + 0.000352 = \underline{440.5 \text{ W/m}^2 \text{ K}}$$

From makers' curves for this particular tube:

$$\text{when } \alpha'_f = 440.5, \text{ then } \alpha_{fi} = \underline{1448 \text{ W/m}^2 \text{ K}}$$

$$\text{also } \alpha'_{fi} = (440.5 \times 0.7407)/0.1286 = \underline{2537 \text{ W/m}^2 \text{ K}}$$

From equation [9.10]

$$r_{fm} = (1/1448) - (1/2537) = \underline{0.000296 \text{ (W/m}^2 \text{ K)}^{-1}}$$

If the reference surface is base tube internal surface:

$$\begin{aligned} \alpha_f \text{ related to reference surface} &= (521.3 \times 0.7407)/0.1286 = 3002.5 \quad \text{resist} = 0.000333 \end{aligned}$$

$$\begin{aligned} r_o \text{ related to reference surface} &= (0.000352 \times 0.1286)/0.7407 = \quad \text{resist} = 0.000061 \end{aligned}$$

$$\begin{aligned} r_{fm} \text{ related to reference surface} &= 0.000296 \quad = \quad \text{resist} = 0.000296 \end{aligned}$$

$$\begin{aligned} r_{fi} \text{ related to reference surface} &= 0.00007 \quad = \quad \text{resist} = 0.000070 \end{aligned}$$

$$\begin{aligned} r_i \text{ related to reference surface} &= 0.000528 \quad = \quad \text{resist} = 0.000528 \end{aligned}$$

$$\begin{aligned} \alpha_i \text{ related to reference surface} &= 4514.2 & = & \text{resist} = \underline{0.000222} \\ & & & \Sigma r_{1,7} = 0.001510 \\ & & & U = 662.25 \\ & & & \underline{U \Delta T} = \underline{46026.4} \end{aligned}$$

From equation [9.11], with  $\Sigma r_{1,2} = 0.000333$  and  $\Sigma r_{2,7} = 0.00151 - 0.00033 = 0.001177$

$$\begin{aligned} T_2 &= 106.7 - (46026.4 \times 0.000333) = 37.2 + (46026.4 \times 0.001177) \\ &= \underline{91.4^\circ\text{C}} \end{aligned}$$

### 9.5.2 Average fin temperature – viscosity correction factor not unity

If  $\phi$  is not unity, on the inside, outside, or both, equation [9.11] must be solved by trial and error as for plain tubes. In the case of longitudinally finned tubes, if  $\phi$  is not unity on the fin-side then  $\alpha_f = \alpha'_f \phi_f$ , where  $\alpha'_f$  = fin-side heat transfer coefficient calculated for  $\phi = 1$  and  $\phi_f$  is the appropriate viscosity correction factor as described in section 6.8.

Equation [9.11] may be replaced by equation [9.12a], which must be solved by trial and error for  $T_2$  and  $\phi_f$ . The latter is a function of the fluid viscosity at  $T_1$ , which is known, and at  $T_2$ , which is unknown.

$$\alpha'_f \phi_f (T_1 \sim T_2) = \frac{T_2 - T_7}{\Sigma r_{2,7}} \quad [9.12a]$$

If  $\phi$  is not unity on the inside of the tube, then  $\alpha_i = \alpha'_i \phi_i$ , where  $\alpha'_i$  = inside heat transfer coefficient for  $\phi = 1$  and  $\phi_i$  is the appropriate viscosity correction factor. Equation [9.12b] must be solved by trial and error for  $T_6$  and  $\phi_i$ . The latter is a function of the fluid viscosity at  $T_7$ , which is known, and at  $T_6$ , which is unknown.

$$\frac{T_1 - T_6}{\Sigma r_{1,6}} = \alpha'_i \phi_i (T_6 \sim T_7) \quad [9.12b]$$

If  $\phi$  is not unity for both fluids, then equation [9.12c] must be solved by trial and error to determine  $T_2$  and  $T_6$ :

$$\alpha'_f \phi_f (T_1 \sim T_2) = \alpha'_i \phi_i (T_6 \sim T_7) = \frac{T_2 - T_6}{\Sigma r_{2,6}} \quad [9.12c]$$

An example of these calculations is given in section 17.5.2 for the fin-side of a longitudinally finned double-pipe exchanger.

## References

A list of addresses for the service organisations is provided on p. xvi.

Kern, D. Q. and Kraus, A. D. (1972) *Extended Surface Heat Transfer*. McGraw-Hill Inc., New York.

Schmidt, T. E. (1966) 'Improved methods for calculation of heat transfer on finned surfaces', *Kaeltetechnik-Klimatisierung* 18, Part 4.

## Nomenclature

Symbol	Description	Units
$A_b$	Bare external surface per metre, as though fins did not exist	$m^2/m$
$A_f$	External finned surface per metre	$m^2/m$
$A_i$	Internal plain surface per metre	$m^2/m$
$A_t$	Total external surface per metre = $A_f + A_b$	$m^2/m$
$A_u$	External unfinned surface per metre	$m^2/m$
$C_f$	Correction factor for non-uniform external heat transfer coefficient	—
$d_f$	Fin outside diameter	m
$d_r$	Fin root diameter	m
$d_s$	Diameter of circular spine	m
$l_f$	Fin height	m
$l_{fe}$	Equivalent fin height (Table 9.3)	m
$m$	Fin efficiency parameter (= $(2\alpha'_f/\lambda_f t_f)^{1/2}$ ) (see equation [9.2])	$(m)^{-1}$
$m_e$	Fin efficiency parameter (= $(2\alpha'_f/\lambda_f t_{fe})^{1/2}$ ) (see equation [9.3])	$(m)^{-1}$
$N_f$	Number of longitudinal fins on one tube (dimensionless), or number of radial fins per metre	$(m)^{-1}$
$P$	Transverse tube pitch for radially finned tube	m
$r_i$	Internal fouling resistance, referred to inside surface	$(W/m^2 K)^{-1}$
$r_{io}$	Internal fouling resistance, referred to bare external surface	$(W/m^2 K)^{-1}$
$r_o$	External fouling resistance	$(W/m^2 K)^{-1}$
$r_{ii}$	Tube-wall resistance, referred to inside surface	$(W/m^2 K)^{-1}$
$r_{io}$	Tube-wall resistance, referred to bare external surface	$(W/m^2 K)^{-1}$
$s_f$	Radial fin spacing	m
$t_f$	Mean fin thickness	m
$t_{fb}$	Fin thickness at base	m
$t_{fe}$	Equivalent fin thickness (Table 9.3)	m
$t_{ft}$	Fin thickness at tip	m
$U_i$	Overall heat transfer coefficient referred to inside surface	$W/m^2 K$
$U_o$	Overall heat transfer coefficient referred to bare external surface	$W/m^2 K$
$\alpha_f$	Heat transfer coefficient to external surface	$W/m^2 K$
$\alpha'_f$	$\alpha_f$ combined with external fouling (equation [9.1])	$W/m^2 K$
$\alpha'_{fi}$	$\alpha'_f$ referred to internal surface (equation [9.5])	$W/m^2 K$
$\alpha'_{ft}$	$\alpha'_f$ referred to total external surface (equation [9.4])	$W/m^2 K$
$\alpha'_{fo}$	$\alpha'_f$ referred to bare external surface (equation [9.7])	$W/m^2 K$
$\alpha_i$	Internal heat transfer coefficient	$W/m^2 K$
$\alpha_{io}$	$\alpha_i$ referred to bare external surface	$W/m^2 K$
$\lambda_f$	Fin thermal conductivity	$W/m K$
$\Omega_f$	Fin efficiency	—
$\Omega_w$	Weighted fin efficiency	—
$\phi$	Viscosity correction factor	—

# Internal heat transfer augmentation techniques

## 10.1 Background

The various techniques for achieving improved heat transfer are usually referred to as heat transfer augmentation, or heat transfer enhancement. Less common is heat transfer intensification. The vital present-day need to conserve energy and materials has resulted in a huge growth in research and development to improve heat transfer equipment design. The objective is to reduce as many of the following factors as possible: capital cost, power cost, maintenance cost, space and weight, consistent with safety and reliability.

Bergles (1983) presents a chart which shows that references dealing with heat transfer augmentation have been recorded since the mid-1800s. Up to the late 1950s the number of references per year (excluding patents and manufacturers' data) did not exceed 10, but this figure rose sharply between 1960 and 1978 (the last full year recorded). Between 1970 and 1978, the number never fell below 80 and peaked at 145.

The principal technique of industrial importance for the augmentation of single-phase heat transfer on the *outside* of tubes is by the use of fins. Chapter 9 deals with fins on a general basis and design methods for the three most widely used types are given in Chapter 13 (transverse low fin), Chapter 14 (transverse high fin), and Chapter 15 (longitudinal fin). Other methods for external enhancement are the Phillips RODbaffle™ and NESTS™ exchangers described in Chapter 11. Although designed for anti-vibration purposes, their construction augments axial flow heat transfer by increasing turbulence of the external fluid.

This chapter describes the principal techniques of industrial importance for the augmentation of single-phase heat transfer on the *inside* of tubes, namely roughened surfaces and twisted tape and coiled wire inserts. Other techniques are mentioned but these are of lesser industrial importance at present. Techniques which relate specifically to boiling and condensation applications are excluded as they are not within the scope of this book.

## 10.2 Effect on boundary layer

In the relentless search to improve the design of heat transfer equipment many techniques for augmenting heat transfer have been investigated. Referring to section 6.3 and Fig. 6.2, it will be seen that in order to augment heat transfer, the technique must affect the boundary layer (laminar and buffer layers) by reducing its thickness, or increasing its surface area, or increasing the turbulence.

The boundary layer thickness may be reduced by fitting protruberances to the heat transfer surface. These interrupt the fluid flow so that a thick boundary layer cannot form. Alternatively, the boundary layer thickness may be reduced by imparting a rotational motion to a fluid flowing inside a tube. The boundary layer surface area may be increased by extending the surface with fins, spines, coils and strips, etc., as described in Chapter 9. Turbulence may be increased on the internal and external surfaces by artificial roughening, or using special devices inside tubes known as turbulence promoters.

Augmentation techniques are termed active or passive. Active techniques are those which require external power, the cost of which must be included in the overall evaluation. Passive techniques require no external power and at present appear to be the preferred method for industrial applications.

## 10.3 Evaluation of techniques

The evaluation of heat transfer augmentation techniques is rarely straightforward as numerous factors are involved. This applies whether one technique is being compared with another, or whether it is being compared with the conventional, non-augmented, approach. The heat transfer coefficient and related pressure loss are of obvious importance. Both must be available to the thermal design engineer and the value of some experimental work has been reduced because pressure loss has not been measured or reported. Other factors to be considered are the cost of producing the augmented heat transfer surface or device, the capital cost of the exchanger, its weight and space requirements and its operating cost. This covers both fluid-pumping and maintenance costs. Safety and reliability must not be overlooked.

Maintenance costs include the cost of opening the heat exchanger for inspection and cleaning if the surface is fouled. The adoption of some augmentation techniques has not been considered in certain industries because of fouling. This attitude is understandable when one considers the time involved in removing and replacing, say, 3000 turbulence promoters from fouled tubes. On the other hand, it might be found that certain augmentation techniques reduce, or even eliminate, fouling. The removal of turbulence promoters from the tubes may assist in cleaning the internal surfaces, thus reducing maintenance time. Unless the service is known to be clean, experimental evidence should be obtained before using augmentation techniques inside tubes.



## 10.4 Roughened surfaces

Roughening of the heat transfer surface was one of the earliest techniques to be investigated. An increase in surface roughness increases both the heat transfer coefficient and friction factor, and hence pumping power. Only a careful evaluation will show whether the use of a roughened surface is justified for the proposed application.

In order to provide a fully defined basis for analysis and design, roughened surfaces must be produced by artificial means. Some of the methods for producing roughness include (a) attaching sand grains, or similar material, in a random manner to the tube surface (sand-grain-type roughness), (b) machining threads of square, or 60 °V shape, into the tube wall to produce a regular pattern of grooves and protruberances, (c) providing transverse protruberances by wire coils, and (d) providing axial or spiral fins of low height. In methods (a), (b) and (c), some of the heat transfer augmentation will be contributed by the 'fin effect', but this is difficult to isolate from the total. In method (d), calculations must follow the methods for extended surfaces described in Chapter 9.

Bergles (1983) states that 'in view of the infinite number of possible geometric variations, it is not surprising that even after more than 200 studies [by Bergles *et al.*, 1979], no unified treatment is available'. To deal with roughened surfaces for methods (a), (b) and (c), the reader should study the references, given at the end of the chapter, most closely related to his proposed application. Of particular importance is the publication by ESDU International Ltd (1982).

In the case of internal fins, the following correlation of Carnavos (1979), based on the turbulent flow of air and water, may be used for straight and spiral fins:

$$Nu = 0.023 Pr^{0.4} Re^{0.8} \left(\frac{A_x}{A_{xt}}\right)^{0.1} \left(\frac{A_b}{A_t}\right)^{0.5} (\sec \psi)^3 \quad [10.1]$$

$$f = 0.046 Re^{-0.2} \left(\frac{A_x}{A_{xn}}\right)^{0.5} (\sec \psi)^{0.75} \quad [10.2]$$

where  $Nu$  = Nusselt number ( $= \alpha d_e / \lambda$ )

$Pr$  = Prandtl number ( $= c_p \eta / \lambda$ )

$f$  = friction factor

$\psi$  = helix angle for spiral fin

$A_x$  = free flow area

$A_{xt}$  = free flow area within fin-tip radius

$A_b$  = surface area if fins were absent

$A_t$  = total surface area (fins + bare tube)

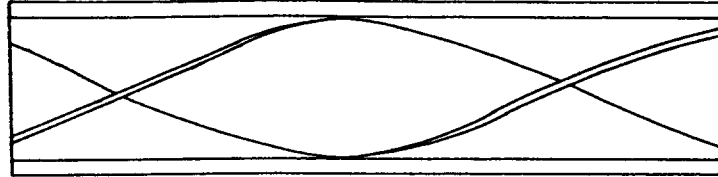
$A_{xn}$  = free-flow area if fins were absent

The appropriate diameter for calculating the Nusselt and Reynolds numbers is the equivalent diameter  $d_e$  defined by equation [6.24] and the fin geometry of Table 9.2.

## 10.5 Twisted tape insert

The twisted metal tape insert shown in Fig. 10.1 is the chief method of inducing swirl or vortex flow to a fluid flowing inside a tube because it can be made easily. Other methods using internal devices are coiled wires, spiral fins, propellers spaced at intervals along the tube and custom-designed vortex generators at the tube inlet. Coiling the tube into a helix is another method of augmenting heat transfer.

**Figure 10.1** Twisted tape insert



Usually the tape is easy to make and fit. However, if the fit is too loose, the fin effect, and some of the swirling action of the fluid, is lost. In addition, damage to the tube may be caused by being hit repeatedly by the tape. If the fit is too tight, there may be difficulty in inserting the tape into the tube, which may be scored along its length and after a period of operation it may be difficult to remove.

In the case of turbulent flow, the correlations of Lopina and Bergles (1969) may be used for twisted tape:

$$\text{Nu} = F \left[ 0.023 \left\{ 1 + \left( \frac{\pi}{2y} \right)^2 \right\}^{0.4} \text{Re}^{0.8} \text{Pr}^{0.4} + 0.193 \left\{ \text{Re}^2(y)^{-1} \left( \frac{d_c}{d_i} \right) \beta \Delta T \text{Pr} \right\}^{1/3} \right] \quad [10.3]$$

$$f = 0.046(y)^{-0.046} \text{Re}^{-0.2} \quad [10.4]$$

where  $\beta$  = thermal expansion coefficient of fluid (1/K)

$\Delta T = T_w - T_b$  = (wall temp.) - (bulk fluid temp.) (K)

$d_i$  = tube inside diameter

$d_c$  = hydraulic diameter

$y = (p_h/2d_i)$

$p_h$  = helical pitch (360° twist)

The appropriate diameter for calculating the Nusselt and Reynolds numbers is  $d_c$ , defined by equation [6.24].

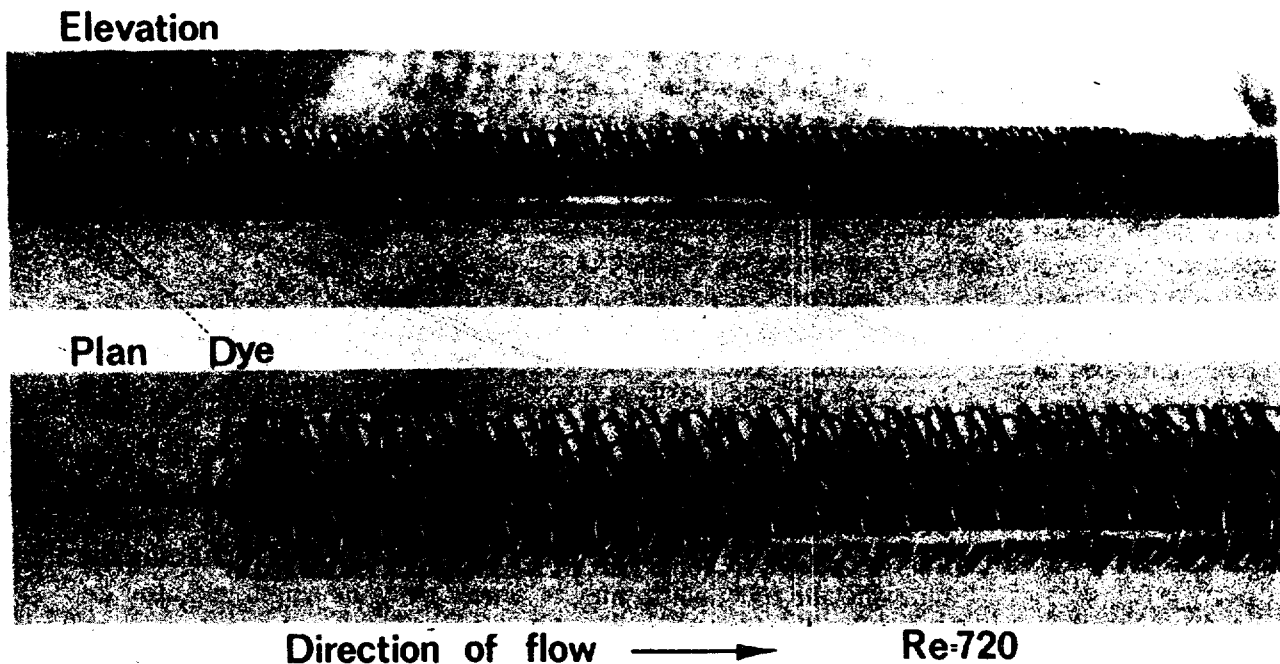
$F$  is a fin factor which represents the ratio of total heat transfer to the heat transferred by the wall alone. If the tape fit is loose  $F = 1.0$ , but  $F$  may be as high as 1.25 for a tight fit.  $F$  is determined from conduction calculations.

## 10.6 Heatex™ tube inserts

The Heatex tube inserts developed by Cal Gavin Ltd is shown in Fig. 10.2. The insert is designed to position a matrix of wire filaments

## Removal of dye stream (boundary layer) from tube wall and subsequent mixing with bulk fluid

CAL GAVIN LTD  
BIRMINGHAM  
ENGLAND  
HEATEX SYSTEM  
U.K. PATENT No. 209710  
14 OVERSEAS PATENTS GRANTED



**Figure 10.2** Heatex tube insert (courtesy of Cal Gavin Ltd)

close to the inside wall of a tube. The filaments are supported by a central spine to form a skeletal structure through which the tube-side fluid flows. In addition to supporting the filaments, the central spine provides the means of pulling the insert into the tubes, which may have diameters from 4 mm to at least 150 mm, and lengths up to 15 m. The insert design enables the filaments to be sprung on to the tube wall to achieve good wire-wall contact. If required the inserts may be metal-bonded to the tube wall, but this is only recommended for clean services. The inserts are supplied in a variety of metals including carbon and stainless steels, aluminium, bronze, copper and titanium. Tubes may be shaped and bent after the installation of the inserts.

The inserts provide maximum performance in the laminar and transition flow regimes, i.e. Reynolds number less than 10 000, when heat transfer can be increased by 6–15 times. They have also been found to provide useful performance over the full range of Reynolds number met in industrial applications. In viscous flow the inserts create turbulence in the boundary layer and mix the bulk fluid with fluid displaced from the wall. A dominant central core of viscous fluid is prevented from forming by the matrix which redistributes and mixes the fluid throughout the cross-section.

The calculation of the heat transfer coefficient inside a tube containing an insert ( $h_i$ ) is similar to that for plain non-augmented tubes. The internal mass velocity ( $m_i$ ) and Reynolds number ( $Re_i$ ) are calculated as though the tube had no insert. Each insert model has its own heat transfer factor ( $J_h$ ) versus Reynolds number curve, correlated to suit the Sieder and Tate (1936) relationship, rather than the ESDU correlations of section 6.10.2.

The calculation of frictional pressure loss inside the tube  $(\Delta P_i)_i$  is similar and equation [6.22] is applicable. Each insert model has its own friction factor  $(f_i)_i$  versus Reynolds number curve for use in this equation.

Using the nomenclature of Chapter 6:

$$(\dot{m}_i)_i = \frac{\dot{M}}{(\pi/4) d_i^2} \quad [10.5]$$

$$(Re_i)_i = \frac{(\dot{m}_i)_i d_i}{\eta_b} \quad [10.6]$$

$$(h_i)_i = (J_h)_i \left( \frac{\lambda}{d_i} \right) \left( \frac{c_p \eta}{\lambda} \right)^{1/3} \phi \quad [10.7]$$

$$(\Delta P_i)_i = \frac{4(f_i)_i L (\dot{m}_i)_i^2}{2\rho d_i \phi} \quad [10.8]$$

where  $\phi = (\eta/\eta_w)^{0.14}$ .

The heat transfer coefficient from equation [10.7] is referred to the inside of the tube. Although  $\phi$  is the same as presented by Sieder and Tate (1936) for plain tubes, this factor may require further investigation.  $(J_h)_i$  and  $(f_i)_i$  are obtained from Fig. 10.3. The makers should be consulted before finalising thermal design. By design changes to the insert geometry they can engineer insert performance to match the required duty for a particular service, with maximum cost-effectiveness. This applies particularly to the exchanger re-rating required for plant debottlenecking.

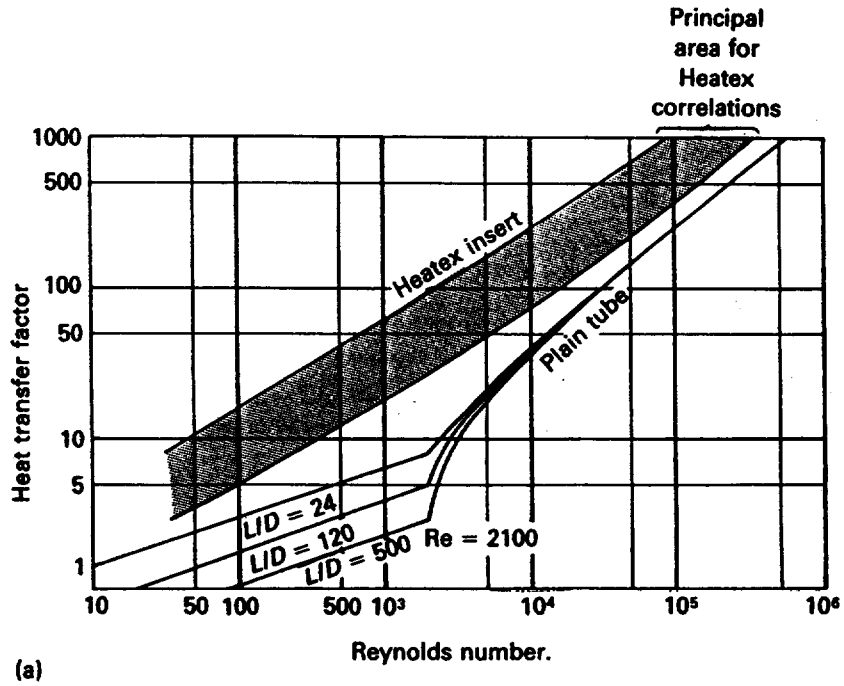
One successful industrial application of the Heatex inserts cited by the makers concerns a residual tar oil heater. Steam was the heating medium and the tar flowed inside 19.05 mm diameter U-tubes. Without augmentation, the tube-side fouled rapidly such that the overall heat transfer coefficient fell from 149.3 W/m<sup>2</sup> K at commissioning to 83.8 W/m<sup>2</sup> K after two months' operation. The overall heat transfer coefficient fell to 76.6 W/m<sup>2</sup> K after a further two months' operation. Cleaning was carried out about every 10 weeks.

Analysis of the foulant showed that it comprised rust flakes, soot, glassy fibres and quartz grains with particle sizes up to 1 mm.

After the installation of inserts the overall heat transfer under clean conditions increased by 53% to 228.7 W/m<sup>2</sup> K, which only fell to 218.9 W/m<sup>2</sup> K after six months' continuous operation. Fouling was found to be negligible after nine months' operation. The inserts enabled the heater to sustain an overall heat transfer coefficient nearly three times as great as the original design. The tar pressure loss was, of course, increased by the inserts, but the makers claim that this was compensated by the reduced pumping losses in downstream pipework resulting from the increased tar exit temperature and corresponding decrease in tar viscosity.

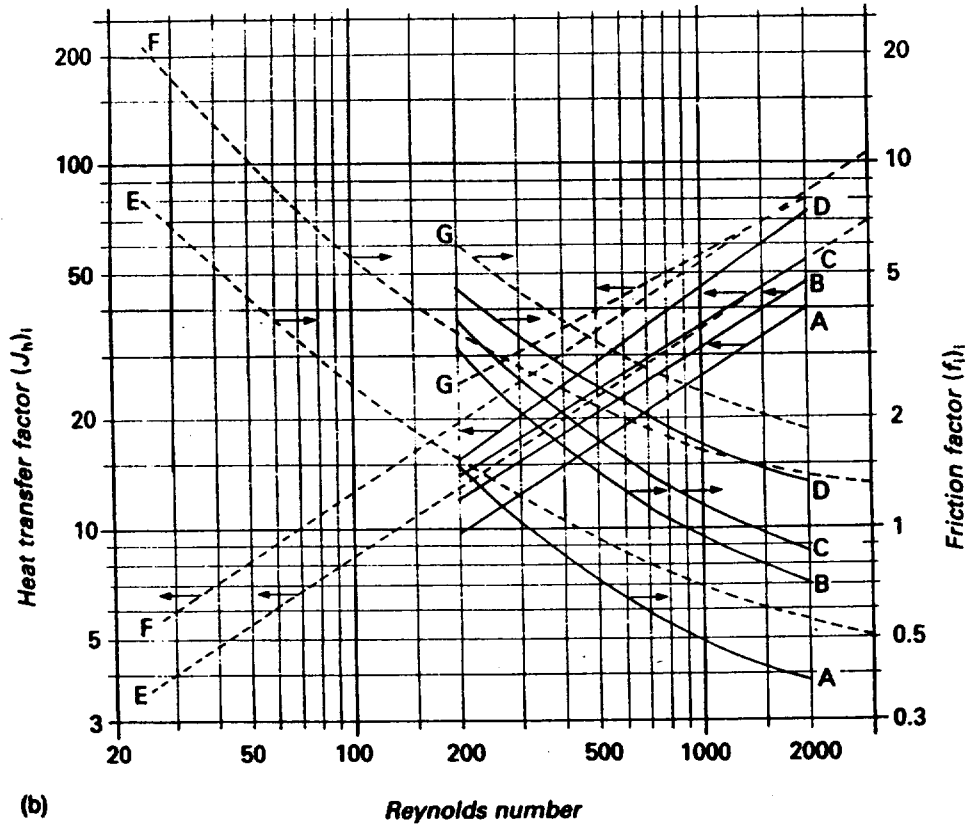
Heatex inserts are suitable for a wide variety of single-phase fluid flow regimes in most types of tubular heat transfer equipment. They have been used successfully in boiling applications and in the near future the makers expect to provide design data for both boiling and condensation. The makers illustrate the use of inserts in an air-cooled heat exchanger cooling

**Figure 10.3** Performance data for Heatex inserts  
 (a) heat transfer comparison between plain tube and tubes containing Heatex inserts  
 (b) heat transfer and friction factors for typical Heatex inserts (courtesy of Cal Gavin Ltd)



(a)

Key — Insert types: A, B, C, D – 25.4 mm tubes  
 - - - - - Insert types: E, F, G – 19 mm tubes



(b)

lube oil – a typical application where both surfaces are augmented. The comparison is as follows:

	<i>No inserts</i>	<i>With inserts</i>
External surface area (m <sup>2</sup> )	3059	563
Fan power (kW)	11.8	5.0
Face area (m <sup>2</sup> )	19.9	6.2
No. of rows deep	6	3
Tube-side pressure loss (Pa)	71430	71154

## 10.7 Additional techniques

### 10.7.1 Vibration

Research has been directed towards two techniques. One technique involves the mechanical vibration of the heat transfer surface using electrodynamic vibrators, or motor-driven eccentrics. The other technique involves the vibration of the fluid itself.

### 10.7.2 Electrostatic fields

The fluid is subjected to an electrostatic field to enhance heat transfer by promoting greater bulk mixing near the heat transfer surface.

### 10.7.3 Gas–solid suspensions

If solid particles in the approximate size range 0.03–1 mm are added to a gas stream, the mixture provides a higher heat capacity and promotes greater bulk mixing near the heat transfer surface. At high temperatures a further increase in heat transfer is achieved due to radiation from the solid particles.

### 10.7.4 Internal scraping

As the name implies, the inside of the tube is scraped mechanically. This is done by revolving blades. Scraped exchangers have been used for many years for handling viscous fluids, particularly those which will solidify on the tube wall unless continuously removed. The technique is applied to lube oil dewaxing, palm oil fractionation and sodium sulphate recovery, for instance.

### 10.7.5 Surface rotation

The heat transfer surface itself is rotated by mechanical means.

### 10.7.6 Injection/suction

Injection involves the injection of gas to a fluid through a porous heat transfer surface. Suction involves the withdrawal of fluid through a porous heated surface. In both cases the boundary layer turbulence is increased.

### 10.8 Axial cores

If power saving is not important, tube-side heat transfer may be augmented by the use of axial cores. The cores are usually tubes, sealed at the inlet end (core tubes) or solid rods of circular or square section, which may be straight or twisted. The cores are positioned along the longitudinal axis of the tubes and maintained in position by legs at intervals. Although axial cores augment heat transfer they are crude in relation to other augmentation devices previously described, and are best suited for boosting performance of an existing unit, if the greatly increased pressure loss can be tolerated.

Although cores restrict the flow area and therefore increase fluid velocity, Kern (1950) states that the Reynolds number for heat transfer is the same as the uncored tube. Increased heat transfer arises from a reduction in equivalent tube diameter. Inspection of equation [6.16] shows that for a given Reynolds number and Prandtl number, the heat transfer coefficient is inversely proportional to the tube diameter. If  $d_i$  = uncored tube diameter and  $(d_e)_h$  = equivalent diameter of the cored tube, the heat transfer coefficient for the cored tube will be  $\{(d_i)/(d_e)_h\}$  times that of the uncored tube, under identical conditions.

$$\text{for a plain tube, } Re_i = \frac{\dot{m}d_i}{\eta} = \frac{\dot{M}d_i}{(\pi/4)d_i^2\eta} = \frac{(4/\pi)\dot{M}}{d_i\eta}$$

When a circular core or rod of diameter  $d_c$  is inside a tube of diameter  $d_i$ , heat transfer occurs at the tube surface only, and the equivalent diameter for heat transfer is based on  $d_i$ ; hence, for heat transfer:

$$\text{wetted perimeter of cored tube} = (P_w)_h = \pi d_i$$

$$\text{internal flow area of cored tube} = A_x = (\pi/4)(d_i^2 - d_c^2)$$

From equation [6.24]:

$$\text{equivalent diameter} = (d_e)_h = \frac{4A_x}{(P_w)_h} = \frac{d_i^2 - d_c^2}{d_i} \quad [10.9]$$

$$(Re_i)_h = \frac{\dot{m}d_e}{\eta} = \frac{\dot{M}d_e}{A_x\eta} = \frac{\dot{M}(d_i^2 - d_c^2)}{(\pi/4)(d_i^2 - d_c^2)(d_i)(\eta)} = \frac{(4/\pi)\dot{M}}{d_i\eta} \quad [10.10]$$

i.e. as for plain tube

For pressure loss

$$(d_e)_p = d_i - d_c \quad (\text{section 6.10.3}) \quad [10.11]$$

and

$$(\text{Re}_i)_p = \frac{\dot{m}d_c}{\eta} = \frac{\dot{M}(d_i - d_c)}{(\pi/4)(d_i^2 - d_c^2)\eta} = \frac{(4/\pi)\dot{M}}{(d_i + d_c)\eta} \quad [10.12]$$

In the case of a square core with a side of  $s$ :

$$(d_c)_h = \frac{4\{(\pi/4)d_i^2 - s^2\}}{\pi d_i} \quad [10.13]$$

$$\text{Re}_h = \frac{4\dot{M}}{\pi d_i \eta} \quad (\text{as for plain tube})$$

$$(d_c)_p = \frac{4\{(\pi/4)d_i^2 - s^2\}}{\pi d_i + 4s} \quad [10.14]$$

$$\text{Re}_p = \frac{4\dot{M}}{(\pi d_i + 4s)\eta} \quad [10.15]$$

(The maximum value of  $s = 0.707d_i$ )

Equations [10.9] – [10.15] are used in the equations for heat transfer and pressure loss inside plain tubes presented in Chapter 6, except that natural convection terms are omitted.

ESDU (1981) provides a comprehensive treatment for heat transfer in annuli.

## Acknowledgement

The author is grateful to Cal Gavin Ltd, Birmingham, UK, for permission to publish technical data relating to 'Heatex' tube inserts. 'Heatex' tube inserts are the subject of patents in the UK and overseas.

## References

A list of addresses for the service organisations is provided on p. xvi.

Bergles, A. E. (1983) *Heat Exchanger Design Handbook*, Section 2.5.11. Hemisphere Publishing Corp.

Bergles, A. E., Webb, R. L., Junkhan, G. H. and Jensen, M. K. (1979) 'Bibliography on augmentation of convective heat and mass transfer' HTL-19, ISU-ERI-Ames-79206. Iowa State University.

Carnavos, T. C. (1979) 'Heat transfer performance of internally finned tubes in turbulent flow', *Advances in Enhanced Heat Transfer*. ASME, pp. 61–7.

Engineering Sciences Data Unit (1982) *Pressure Loss and Heat Transfer for Single-Phase Turbulent Flow in Roughened Channels: Methods of Calculation*. ESDU Publication No. 82021.

Lopina, R. F. and Bergles, A. E. (1969) 'Heat transfer and pressure drop in tape generated swirl flow of single-phase water', *Trans. ASME, J. Heat Transfer* **91**, 434–42.

Sieder, E. N. and Tate, G. E. (1936) 'Heat transfer and pressure drop of liquids in tubes', *Ind. Eng. Chem.* **28**, 1429–35.



## Additional subject references

### General survey

Bergles *et al.* (1979) as above.

### Evaluation

Bergles, A. E., Blumenkrantz, A. R. and Taborek, J. (1974) 'Performance evaluation criteria for enhanced heat transfer surfaces', *Proc. 5th Int. Heat Transfer Conference, Tokyo* (Sept.), Vol. II, Paper FC6.3.

Lahaye, P. G., Neugebauer, F. J. and Sakhuga, R. K. (1974) 'A generalised prediction of heat transfer performance and exchanger optimisation', *Trans. ASME, J. Heat Transfer* (c) **96**, 511-17.

### Roughened surfaces

Bergles, A. E. and Jensen, M. K. (1977) 'Enhanced single-phase heat transfer for OTEC systems', *Proc. 4th Annual Conference on Ocean Thermal Energy Conservation, New Orleans* (March).

Bergles, A. E., Junkhan, G. H. and Webb, R. L. (1979) 'Energy conservation via heat transfer enhancement', COO-4649-5. Iowa State University.

Collinson, B. (1973) 'The effect of graphite surface roughness on fuel element pressure drop', *Proc. Int. Meeting on Reactor Heat Transfer, Karlsruhe* (Oct.), Paper No. 79.

Dipprey, D. F. and Sabersky, R. H. (1963) 'Heat and momentum transfer in smooth and rough tubes at various Prandtl numbers', *Int. J. Heat and Mass Transfer* **6**.

Webb, R. L., Eckert, E. R. G. and Goldstein, R. J. (1971) 'Heat transfer and friction in tubes with repeated rib roughness', *Int. J. Heat and Mass Transfer* **14**, 601-17.

Webb, R. L., Eckert, E. R. G. and Goldstein, R. J. (1972) 'Generalised heat transfer and friction correlations with repeated rib roughness', *Int. J. Heat and Mass Transfer* **15**, 180-4.

Withers, J. G. (1980) 'Tubeside heat transfer and pressure drop for tubes having helical internal ridging with turbulent/transitional flow of single phase fluid'. Part I: 'Single helix ridging', *Heat Transfer Engineering* **2** (No. 1, July-Sept.).

### Twisted tapes, internal fins and curved tubes

Hong, S. W. and Bergles, A. E. (1976) 'Augmentation of laminar flow heat transfer by means of twisted-tape inserts', *Trans. ASME, J. Heat Transfer* **98**, 251-6.

Masliyah, J. H. and Nandkumar, K. (1981) 'Steady laminar flow through twisted pipes - fluid flow', *Trans. ASME, J. Heat Transfer* **103** (Nov.), 785-90.

Masliyah, J. H. and Nandkumar, K. (1981) 'Steady laminar flow through twisted pipes - heat transfer', *Trans. ASME, J. Heat Transfer* **103** (Nov.), 791-6.

Marnier, W. J. and Bergles, A. E. (1978) 'Augmentation of tubeside laminar flow heat transfer by means of twisted-tape inserts, static-mixer inserts and internally finned tubes', *6th Int. Heat Transfer Conference, Toronto* (Aug.), Vol. 2, pp. 583-8.

Patankar, S. V., Ivanovic, M. and Sparrow, E. M. (1979) 'Analysis of turbulent flow and heat transfer in internally finned tubes and annuli', *Trans. ASME, J. Heat Transfer* **101** (Feb.), 29-37.

- Scott, M. J. and Webb, R. L.** (1981) 'Analytic prediction of the friction factor for turbulent flow in internally finned channels', *Trans. ASME, J. Heat Transfer* **103** (Aug.), 423-8.
- Van Rooyen, R. S. and Kroger, D. G.** (1978) 'Laminar flow heat transfer in internally finned tubes with twisted-tape inserts', *6th Int. Heat Transfer Conference, Toronto* (Aug.), Vol. 2, pp. 577-81.
- Watkinson, A. P., Miletti, D. C. and Kupanek, G. R.** (1975) 'Heat transfer and pressure drop of internally finned tubes in laminar oil flow', ASME Paper No. 75-HT-41.

### Vibration

- Kryukov, Y. V. and Boykov, G. P.** (1973) 'Augmentation of heat transfer in an acoustic field', *Heat Transfer - Soviet Research* **5** (No. 1), 26-8.
- Lemlich, R.** (1961) 'Vibration and pulsation boost heat transfer', *Chem. Eng.* **68**, 171-6.

### Electrostatic fields

- Moss, R. A. and Grey, J.** (1966) 'Heat transfer augmentation by steady and alternating electric fields', *Proc. 1966 Heat Transfer and Fluid Mech. Inst. Stanford Univ. Press*, pp 210-35.
- Porter, J. E. and Poulter, R.** (1970) 'Electro-thermal convection effects with laminar flow heat transfer in an annulus', *4th Int. Heat Transfer Conference, Paris*, Paper FC3.7.
- Sadek, S. E., Fax, R. G. and Hurwitz, M.** (1972) 'The influence of electric fields on convective heat and mass transfer from a horizontal surface under forced convection', *Trans. ASME, J. Heat Transfer* (c) **94**, 144-8.

### Gas-solid suspensions

- Depew, C. A. and Kramer, T. J.** (1973) 'Heat transfer to flowing gas-solid mixtures', *Advances in Heat Transfer*, Vol. 9. Academic Press, New York, pp. 113-80.

### Scraping

- Hagge, J. K. and Junkhan, G. H.** (1975) 'Mechanical augmentation of convective heat transfer in air', *Trans. ASME, J. Heat Transfer* **97**, 516-20.

### Surface rotation

- Miyazaki, H.** (1971) 'Combined free and forced convective heat transfer and fluid flow in a rotating curved circular tube', *Int. J. Heat and Mass Transfer* **14**, 1295-309.
- Mori, Y., Fukada, T. and Nakayama, W.** (1971) 'Convective heat transfer in a rotating radial circular pipe (2nd report)', *Int. J. Heat and Mass Transfer* **14**, 1807-24.

### Injection/suction

- Aggarwal, J. K. and Hollingsworth, M. A. (1973)** 'Heat transfer for turbulent flow with suction in a porous tube', *Int. J. Heat and Mass Transfer* **16**, 591-609.
- Tauscher, W. A., Sparrow, E. M. and Lloyd, J. R. (1970)** 'Amplification of heat transfer by local injection of fluid into a turbulent tube flow', *Int. J. Heat and Mass Transfer* **13**, 681-8.

### Axial cores

- Engineering Sciences Data Unit (1981)** *Forced Convective Heat Transfer in Concentric Annuli with Turbulent Flow*. ESDU Publication No. 81045.
- Kern, D. Q. (1950)** *Process Heat Transfer*. McGraw-Hill Inc., New York.

# Shell-side flow-induced tube vibration

## 11.1 Background

Shell-side flow-induced tube vibration became a serious problem by late 1960 and, as a result, thermal design procedures for shell-and-tube heat exchangers were revised to include an analysis of this phenomenon. Numerous companies had been designing exchangers for many years without apparently experiencing tube failures due to vibration, whereas other less fortunate companies suddenly experienced failures which sometimes proved expensive, due partly to the high cost of redesign and repair and partly to loss of production. In extreme cases failures were reported before the exchangers had completed their commissioning period. Failures due to flow-induced vibration had no doubt occurred previously, but they were not widespread, and the real cause may have been misinterpreted and a systematic investigation not carried out. Failures occurred with liquids, gases and vapours.

It should be noted that the phenomenon arises solely from the flow of the shell-side fluid across the tubes and is not associated with other undesirable sources of vibration such as pump pulsations or mechanically transmitted vibrations from rotating equipment. It must also be appreciated that flow-induced vibration calculations are an integral part of thermal design and as essential as the calculations for heat transfer, pressure loss and mean temperature difference.

Flow-induced vibration may reveal itself in the form of either a loud noise, which has been known to reach 150 decibels at 1 m range, or an increase in shell-side pressure loss, which may be nearly double the expected value, but it is usually revealed by leaking tubes and/or tube-tubesheet joints as described in section 11.2.

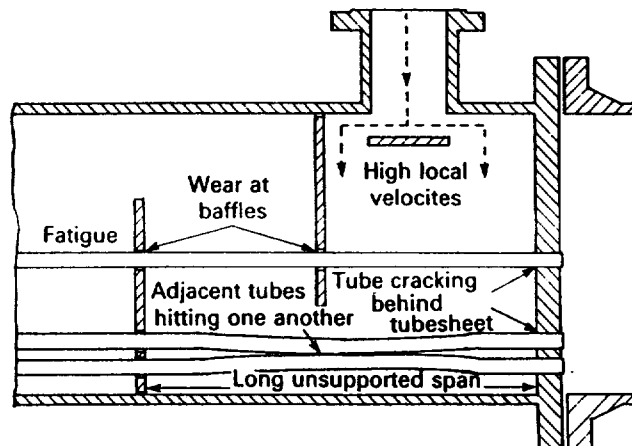
Section 11.3 discusses the reason for the increase in flow-induced vibration failures, and Section 11.4 describes briefly some of the excitation mechanisms which have been observed. Some of the relatively simple predictive methods in current use, and a brief comparison between them, are given in section 11.5, design recommendations being given in section 11.6. Section 11.7 describes the Phillips RODbaffle™ exchanger, which was especially developed to overcome the problem of flow-induced vibration, and section 11.8 describes the NESTS™ concept which provides anti-vibration characteristics.

## 11.2 Tube failures

Flow-induced vibration causes tubes to fail by the mechanisms shown in Fig. 11.1 and described below.

- (a) Fatigue due to repeated bending.
- (b) Repeated impact between adjacent tubes at mid-span; flat spots occur leading to thinning of the tube walls with eventual splitting. This is termed 'collision damage'.
- (c) Cutting at the baffles, particularly if the baffles are thin or harder than the tubes or there is a large baffle-tube clearance due to repeated impact between tube and baffle. The tubes thin and eventually split, or completely sever, in extreme cases. This is termed 'baffle damage'.
- (d) Cutting at the tube-hole edges at the inner tubesheet face due to repeated impact between tube and tubesheet.
- (e) Loosening of roller expanded tube-tubesheet joints, with and without expansion grooves. Failures in welded tube-tubesheet joints have also been recorded.

**Figure 11.1** Tube damage due to flow-induced vibration



Although tube failures have been reported in most parts of an exchanger tube bundle, the majority, as expected, have been found in regions of long unsupported tube spans, such as the inlet baffle space, and high local velocity. In the inlet region the distance between the first baffle and adjacent tubesheet is often greater than the usually regular baffle spacing in the rest of the exchanger, which has been calculated to meet heat transfer and pressure loss requirements. The position of the inlet nozzle, and hence the position of the first baffle, is governed by several factors. These include the nozzle diameter itself, which might be greater than the regular baffle spacing, together with the presence of a shell-tubesheet flange and nozzle reinforcement pad. As the shell-side fluid leaves the first baffle space to enter the second via the baffle window, where the flow pattern is extremely complex, it encounters what is usually the longest unsupported tube span in the exchanger, being the sum of the first and second baffle spaces. Many failures have been reported in the first baffle window, usually in the second or third row beyond the baffle edge.

Most of the tubes in the inlet space are supported by the tubesheet and first baffle, but the escape velocity around the impingement plate, if fitted, or the bundle penetration velocity if no internal impingement baffle is fitted, may be extremely high and a source of failure. High-velocity leakage streams around the bundle periphery are a further source of failure and should be blocked off.

### 11.3 Reasons for increase in failures

The reason why failures due to flow-induced vibration became a serious problem is associated primarily with exchanger size. As plant capacities increased, the exchanger sizes increased accordingly and also the baffle spacings up to, and in some cases, beyond the TEMA recommended limits, to cater for the increased flow rates. Because of the structural limitations in the end zones described in section 11.2, some designers chose to ignore, or may have overlooked, the TEMA recommendations in order to solve their design problems and many failures occurred in these zones. Analysis of failures suggested that had unsupported tube lengths been restricted to about 80% of TEMA values, few failures would have occurred. The effect of reducing the unsupported tube length to 80% of its initial value increases the tube natural frequency by 56%.

In addition to the use of large baffle spacings more reliable predictive methods for heat transfer and pressure loss became available by the late 1960s and, in general, this resulted in the use of much higher shell-side velocities than before. This was desirable both to increase heat transfer and reduce fouling.

### 11.4 Excitation mechanisms

The tubes in most exchangers vibrate to some extent, but in many cases the amplitudes of vibration are not sufficiently large to cause damage, the amplitude of vibration being defined as the displacement of the vibrating tube on either side of its still position. To predict the occurrence of vibration, which may lead to damage, it is necessary to investigate the phenomena which produce the excitation forces and the dynamic response of the tube bundle. The excitation forces fluctuate at characteristic frequencies which increase continuously as the flow rate increases, whereas the tubes vibrate at unique frequencies termed their natural frequencies. If the exciting frequency coincides with the tube natural frequency a resonance condition is established, which may lead to large amplitudes of vibration and subsequent damage.

Although flow inside tubes has produced vibration, this is rare, and flow outside the tubes is the major source. Vortex shedding, turbulent buffeting, fluid-elastic whirling and parallel flow eddy formation are four excitation mechanisms which have been observed, the first three for cross-flow outside tube bundles and the last for parallel or axial flow

along tube bundles. However, most failures in axial flow have occurred in special exchangers which had extremely long unsupported tube spans and high axial fluid velocities. Although axial flow occurs to a limited extent in the window zone of a baffled shell-and-tube exchanger it has not been found to be a source of failure due to eddy formation.

The three cross-flow mechanisms are the chief sources of vibration and they are described briefly in the following sections. The references at the end of the chapter should be consulted for more comprehensive information.

#### 11.4.1 Vortex shedding

When a fluid flows across a tube a series of vortices break away alternatively from opposite sides of the tube in the downstream wake, the phenomenon being known as vortex shedding. The alternate shedding of vortices produces alternating forces on the tube in two directions: (a) the lift direction, which is at right angles to both flow and tube axes, and (b) the drag or flow direction. The frequency of the alternating force in the drag direction is twice that in the lift direction, but of smaller amplitude. If the vortex-shedding frequency coincides with the tube natural frequency, a resonance condition is established.

The vortex-shedding frequency ( $f_v$ ) in the lift direction is given by the following relationships:

Single tube:

$$f_v = Sr \left( \frac{u}{d_o} \right) \quad [11.1]$$

Ideal banks:

$$f_v = Sr \left( \frac{u_r}{d_o} \right) \quad [11.2]$$

where  $u$  = velocity across a single tube (m/s)

$u_r$  = cross-flow velocity based on minimum transverse area between tubes in a row (m/s)

$d_o$  = tube outside diameter (m)

$Sr$  = Strouhal number, characterising vortex shedding as defined by equations [11.1] and [11.2].

It has been found that for single cylinders the Strouhal number ( $Sr$ ) has a constant value of about 0.2 and therefore the vortex-shedding frequency is directly proportional to the cross-flow velocity. Vortex shedding has also been observed for pure cross flow in ideal tube banks, but the Strouhal number is no longer a single value but dependent on the pitch/diameter ratio and pitch angle, as shown by Table 11.1.

Vortex shedding is a fluid-dynamic phenomenon and does not depend on the movement of the tubes for its existence. However, if the tubes vibrate at, or near, the vortex-shedding frequency, the vortices are shed at the tube-vibration frequency and not that given by equations [11.1] and [11.2]. This feature is termed a 'lock-in' effect and there is evidence that

this can prevail at a frequency of about 0.7–1.3 of the tube natural frequency.

**Table 11.1** Approximate Strouhal numbers (Sr)

Pitch angle	Tube pitch/diameter ratio		
	1.25	1.33	1.50
30°	0.18	0.22	0.29
60°	0.80	0.75	0.61
90°	0.42	0.35	0.29
45°	0.58	0.59	0.57

Basis: *Heat Exchanger Design Handbook* (1983)

The presentations of Strouhal numbers for tube banks are largely due to Chen (1968) and Fitz-Hugh (1973), the values in Table 11.1 being based on Chen.

#### 11.4.2 Turbulent buffeting

Turbulent buffeting relates to the fluctuating forces acting on the tubes under extremely turbulent cross-flow conditions for fluids at high Reynolds numbers. It is an extremely complex mechanism. The turbulence buffets the tubes, which extract energy selectively from the turbulence at their natural frequency from the wide spectrum of frequencies present. Owen (1965) presents data for determining the turbulent buffeting frequency.

#### 11.4.3 Fluid-elastic whirling

Fluid-elastic whirling describes a self-excited form of vibration in which the tubes vibrate with a large whirling motion. The momentary displacement of a tube within a bank from its equilibrium position alters the flow pattern. This changes the force balance on adjacent tubes with the result that these tubes alter their positions in a vibratory manner. Once fluid-elastic whirling begins, a 'run-away' condition develops if the energy absorbed by the tube from the fluid exceeds that which can be dissipated by damping. Connors (1970) presents data for determining the critical cross-flow velocity above which fluid-elastic whirling can develop.

#### 11.4.4 Acoustic vibration

When the shell-side fluid is a vapour or gas, acoustic resonance may occur if the standing acoustic waves in the shell coincide with the vortex shedding or turbulent buffeting frequencies. The standing waves are at right angles to both flow direction and the tube axes and the vibration is similar to air-column excitation in an organ pipe. Intense noise may



occur, possibly accompanied by an increase in shell-side pressure loss, but serious mechanical damage has not been reported as a result of acoustic vibration. The velocity of sound in liquids is too high to cause acoustic problems.

Similar to an organ pipe, the acoustic frequency in the shell is related to the velocity of sound in the fluid and a characteristic length as follows:

$$f_a = \frac{nu_a}{2l} \quad [11.3]$$

where  $f_a$  = acoustic frequency (Hz)

$u_a$  = velocity of sound (m/s)

$l$  = characteristic length (m)

$n$  = mode number.

The acoustic frequency is related to the mode number ( $n$ ) and the lowest value is produced when  $n = 1$ , the fundamental tone. First, second and third overtones, where  $n = 2, 3$  and  $4$  respectively, vibrate at  $n$  times the fundamental. The characteristic length ( $l$ ) is determined at right angles to both flow direction and tube axes and is usually the shell diameter.

Barrington (1973) describes acoustic vibration and practical remedies for its prevention.

## 11.5 Predictive methods

As a result of the rapid increase in tube failures due to flow-induced vibration, there was an urgent need to provide designers with methods for predicting either the limiting conditions above which vibration occurs, or the limiting conditions above which damage occurs. Numerous reports, both theoretical and practical, were produced on the subject, while systematic investigations were undertaken by HTRI, HTFS, TEMA and other international organisations.

Experimental work carried out with ideal bundles, in pure cross flow or pure axial flow, although valuable, does not represent conditions prevailing on the shell-side of a baffled shell-and-tube exchanger. The flow pattern is extremely complex and as the shell-side fluid flows through the exchanger it is subjected to repeated acceleration, deceleration and changes in direction, such that it impinges on the tubes at all angles. Testing of production-size exchangers is essential so that the complex flow pattern, the variety of tube and baffle geometries, the effect of impingement plates, high-velocity leakage paths, damping, fatigue and wear can be investigated.

Predictive methods emerged, which gave the designer a relatively simple approach to the problem, and although some methods may be regarded as conservative, this was acceptable, particularly to companies which had experienced vibration failures. It will be appreciated that the prevention of vibration must eliminate damage, but the presence of vibration does not mean that damage is certain to occur. Information relating to damage is the essential requirement of designers.

**Table 11.2** Frequency constant ( $C_n$ ) for straight tubes. Multiple equal spans – 1st, 2nd and 3rd modes

No. of equal spans	Both ends clamped			One end clamped; other end simply supported			Both ends simply supported		
	1	2	3	1	2	3	1	2	3
1	72.36	198.34	388.75	49.59	160.66	335.20	31.73	126.94	285.61
2	49.59	72.36	160.66	37.02	63.99	137.30	31.73	49.59	126.94
3	40.52	59.56	72.36	34.32	49.59	67.65	31.73	40.52	59.56
4	37.02	49.59	63.99	33.02	42.70	56.98	31.73	37.02	49.59
5	34.99	44.19	55.29	33.02	39.10	49.59	31.73	34.99	44.19
6	34.32	40.52	49.59	32.37	37.02	44.94	31.73	34.32	40.52
7	33.67	38.40	45.70	32.37	35.66	41.97	31.73	33.67	38.40
8	33.02	37.02	42.70	32.37	34.99	39.81	31.73	33.02	37.02
9	33.02	35.66	40.52	31.73	34.32	38.40	31.73	33.02	35.66
10	33.02	34.99	39.10	31.73	33.67	37.02	31.73	33.02	34.99
11	32.37	34.32	37.02	31.73	33.67	36.33	31.73	32.37	34.32
12	32.37	34.32	37.02	31.73	33.02	35.66	31.73	32.37	34.32

Basis: McDuff and Felgar (1957)

*Although considerable knowledge has been gained, none of the simple predictive methods described in the following sections can be regarded as accurate and sound engineering judgement must be used in their application.*

11.5.1 Tube natural frequency

Some of the predictive methods require a knowledge of the tube natural frequencies which are given by the following equation:

$$f_n = 0.04944 C_n \left\{ \frac{EI}{m_e L^4} \right\}^{1/2} \tag{11.4}$$

- where  $f_n$  = tube natural frequency (Hz)
- $E$  = modulus of elasticity (N/m<sup>2</sup>)
- $I$  = sectional moment of inertia (m<sup>4</sup>)
- $m_e$  = equivalent mass of tube per unit length (kg/m)
- $L$  = unsupported tube length (m)
- $C_n$  = frequency constant.

Although more rigorous methods are available, the values of  $C_n$  given in Table 11.2, as presented by MacDuff and Felgar (1957), are sufficiently accurate for calculating tube natural frequencies. In all cases it is assumed that the spans are of equal length with simple intermediate supports. It will be noted from Table 11.2 that  $C_n$  depends on the mode number, the number of spans and the end support conditions, as defined below:

End support conditions	In exchanger (refer to Fig. 11.2)
both clamped	tubesheet to tubesheet (i.e. no baffles)
both simply supported	baffle to next supporting baffle (zone 3)
one clamped, one simply supported	tubesheet to baffle (zones 2 and 4)

For safety in design it is usual to consider only the first mode, or

lowest, natural frequency and Table 11.2 shows that  $C_n$  is almost independent of the end support at more than four spans. Experimental results suggest that the clamped-clamped end support condition should be adopted for multi-span straight tubes.

It is also necessary to calculate  $m_e$ , the equivalent mass of tube per unit length, which is the sum of the mass per unit length of the empty tube plus the mass per unit length of the fluid inside the tube plus the mass per unit length of the external fluid displaced by the tube. There is experimental evidence to show that the actual displaced mass is greater than the theoretically displaced mass. The latter is corrected by introducing a multiplier  $M_a$ , termed the 'added mass coefficient', which depends on the tube pitch/diameter ratio. Approximate values of  $M_a$  are given in Table 11.3.

**Table 11.3** Approximate added mass coefficients ( $M_a$ )

Tube pitch : diameter ratio	$M_a$
1.25	3.0
1.33	2.5
1.50	1.9

The natural frequency is also related to the axial load in the tube  $W_a$  (Newtons), being increased due to tension (+ve value), which is the usual objective, and decreased due to compression (-ve value). It has been shown that the natural frequency under stress ( $f_{ns}$ ) is related to that in the unstressed condition ( $f_n$ ) by the relationship:

$$f_{ns} = f_n \left\{ 1 \pm \frac{W_a L^2}{\pi^2 EI} \right\}^{1/2} \quad [11.5]$$

In the case of U-bends the out-of-plane vibration frequency is lower than the in-plane frequency. An approximate method for calculating the out-of-plane vibration frequency of an unsupported U-bend is: (a) calculate the length of the outermost bend, (b) using this length calculate the natural frequency from equation [11.4] as though the tube was straight ( $f_{nb}$ ) and (c) calculate the natural frequency of the U-bend ( $f_{nu}$ ) from:

$$f_{nu} = 0.8 f_{nb} \quad [11.6]$$

Experience has shown that smaller baffle-tube clearances and thicker baffles do not alter the tube natural frequency significantly, although they reduce damage and increase damping. If the hardness of the baffle material is greater than that of the tube, replacing the baffle with a softer material will also reduce damage.

### 11.5.2 Cross-flow areas and velocities

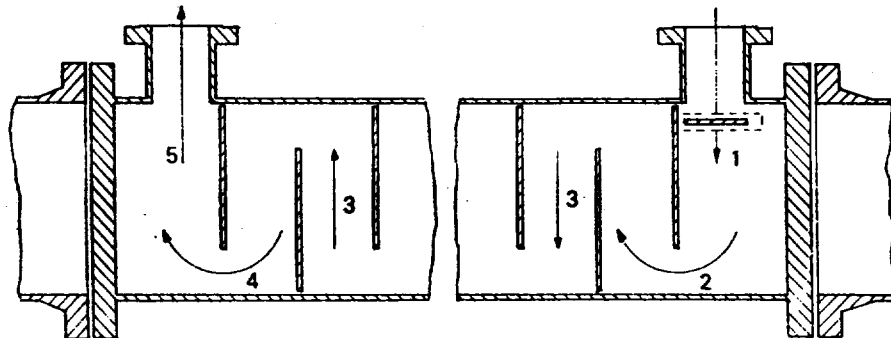
Irrespective of the predictive method used, the cross-flow areas, and hence cross-flow velocities, must be determined at various zones in the

exchanger. Cross-flow areas for heat transfer and pressure loss calculations are based on the minimum free area between tubes ( $u_t$ ), which in the case of 45° and 60° pitch angles, at customary tube pitch diameter ratios, occurs in the diagonal gaps between tubes in successive rows. For certain vibration calculations, however, cross-flow areas are based on the free area between tubes in the same row ( $u_r$ ). The cross-flow areas are therefore identical to those for heat transfer and pressure loss for 30° and 90° pitch angles, but differ for 45° and 60° pitch angles. The relationship between them is as follows, where  $P$  = tube pitch and  $d_o$  = tube outside diameter as shown in Figs 1.19 and 12.3:

Pitch angle	( $u_r/u_t$ )
30	1.0
60	$2\left\{\left(\frac{P}{d_o}\right) - 1\right\} / \left\{1.732\left(\frac{P}{d_o}\right) - 1\right\}$
90	1.0
45	$2\left\{\left(\frac{P}{d_o}\right) - 1\right\} / \left\{1.414\left(\frac{P}{d_o}\right) - 1\right\}$

In the case of economisers and air heaters, etc., the duct cross-section is usually constant between inlet and outlet. The flow is also unidirectional, without leakage, such that the calculation of cross-flow area and velocity is straightforward. The calculations are less straightforward for a shell-and-tube exchanger because of the leakage effects described in section 12.2. The cross-flow area at each zone recommended in section 11.6.1 and Fig. 11.2 is readily calculated, but the true flow rate at each zone is less certain.

Figure 11.2 Zones for vibration check



Irrespective of the thermal design method used the safest approach for a shell-and-tube exchanger is to ignore leakage effects and calculate the cross-flow velocity at every zone (Fig. 11.2) on the basis of total shell-side flow rate. This may not be greatly on the safe side for zones 1 and 5, but may be too conservative for zones 2, 3 and 4. If the thermal design method considers leakage effects and provides a more realistic cross-flow velocity, or flow rate, at each zone, these should be used for the vibration check, but in the fouled condition.

In all cases, temporary increases in flow rate above the design flow rate must not be overlooked.

### 11.5.3 Frequency match – vortex shedding

The objective is to avoid a match between the vortex-shedding frequency ( $f_v$ ), based on equation [11.2] and Table 11.1, and the tube natural frequency ( $f_n$ ), based on equations [11.4]–[11.6] and Table 11.2. Because of the 'lock-in' effect it is usual to provide a design in which:

$$f_v/f_n < 0.5 \quad [11.7]$$

In addition to the uncertainty of Strouhal numbers and tube natural frequency calculations, some investigators question whether vortex shedding is actually established in a shell-and-tube heat exchanger where the closely packed tubes may cause mutual interference between wakes and vortices. It is also suggested that in order to comply with equation [11.7], the exciting forces in many designs become too small to cause damage.

### 11.5.4 Frequency match – turbulent buffeting

Owen (1965) showed that the turbulent buffeting frequency ( $f_{tb}$ ) is given by the relationship

$$f_{tb} = \frac{u_r d_o}{P_l P_t} \left[ 3.05 \left\{ 1 - \left( \frac{d_o}{P_l} \right) \right\}^2 + 0.28 \right] \quad [11.8]$$

where  $P_l$  = longitudinal tube pitch (m)  
 $P_t$  = transverse tube pitch (m)

Again the objective is to avoid a match between the turbulent buffeting frequency ( $f_{tb}$ ), based on equation [11.8], and the lowest tube natural frequency ( $f_n$ ). It is usual to provide a design in which

$$\frac{f_{tb}}{f_n} < 0.5 \quad [11.9]$$

Equation [11.8] has not been adequately tested for liquids and should therefore be restricted to gases. In addition, its derivation is based on the assumption that the transverse pitch is much greater than the tube diameter and caution is recommended at the small transverse pitch/diameter ratios commonly used in shell-and-tube exchangers.

### 11.5.5 Fluid-elastic whirling

Connors (1970) showed that the critical velocity ( $u_{co}$ ) above which vibration occurs due to fluid-elastic whirling is given by the relationship

$$u_{co} = \beta f_n d_o \left\{ \frac{m_e \delta_o}{\rho_o d_o^2} \right\}^{1/2} \quad [11.10]$$

where  $\beta$  = instability constant  
 $\delta_o$  = log decrement of the tube bundle (see below)  
 $\rho_o$  = shell-side fluid density (kg/m<sup>3</sup>).

The objective is to provide a design in which the cross-flow velocity  $u_t$  is less than  $u_{co}$  hence:

$$u_t < u_{co} \quad [11.11]$$

where  $u_t$  = cross-flow velocity based on minimum free area between tubes (m/s).

This promising approach to the problem is handicapped by lack of data for determining  $\delta_o$ . This is the logarithm of the ratio of successive amplitude peaks as the vibration of a bundle dies away in still air. It is a measure of the bundle damping characteristic and is dependent on the tube material, bundle geometry and the viscosity of the shell-side fluid. Values of  $\delta_o$  between 0.001 and 0.1 have been reported, which is of little assistance to a designer who is seeking a safe but economic exchanger. Considerable research is being carried out to determine  $\delta_o$  and at present a typical value for design is 0.03 for gases and 0.1 for liquids.

The instability constant ( $\beta$ ) depends on pitch angle and pitch ratio and is given in Table 11.4.

Table 11.4 Instability constant ( $\beta$ )

Pitch angle	Tube pitch diameter ratio		
	1.25	1.33	1.50
30°	4.6	5.2	6.8
60°	3.8	4.0	4.1
90°	3.9	3.9	4.1
45°	3.9	4.5	5.7

### 11.5.6 Thorngren damage numbers

Thorngren adopted a practical approach by treating the tube as a beam under a uniformly distributed static load proportional to the shell-side fluid dynamic pressure. The shear stress at the baffle is compared with the limiting shear stress in order to derive a non-dimensional baffle damage number  $N_{BD}$  given by:

$$N_{BD} = \frac{\rho_o(u_t)^2 L^2 d_o}{F_B S_f A_m B_t} \quad [11.12]$$

By similar means he derived a non-dimensional collision damage number  $N_{CD}$  such that the mid-span deflection of the tube does not exceed half the distance between adjacent tubes, namely:

$$N_{CD} = \frac{0.625 \rho_o(u_t)^2 L^4 d_o}{F_B^4 A_m (d_o^2 + d_i^2) E C_t} \quad [11.13]$$

where  $u_t$  = cross-flow velocity based on minimum transverse area between tubes in a row (m/s)

$F_B$  = tube-baffle clearance factor

$S_f$  = tube fatigue stress (N/m<sup>2</sup>)

$A_m$  = cross-sectional area of tube metal (m<sup>2</sup>)

- $B_t$  = baffle thickness (m)  
 $d_i$  = inside tube diameter (m)  
 $C_t$  = minimum gap between adjacent tubes (m).

The damage numbers are indicative of the damage which vibration might cause, and Thorngren stated that this would be avoided if both damage numbers are less than unity:

$$N_{BD} \text{ and } N_{CD} < 1 \quad [11.14]$$

However, field experience showed that this approach was reasonable for the heavier liquids, such as water, but considerably unsafe for gases.

### 11.5.7 Erskine and Waddington damage approach

After studying case histories, Erskine and Waddington (1973) decided that the Thorngren damage number approach gave reasonable results if the damage numbers were related to the density and absolute viscosity of the shell-side fluid. Damage would be avoided if:

$$N_{BD} \text{ and } N_{CD} < \left\{ \frac{0.00429 \rho_o^{0.47}}{\eta_o^{0.235}} \right\} \quad [11.15]$$

### 11.5.8 Noise

Equation [11.3] for the acoustic frequency may be transformed into a more useful design equation by expressing the velocity of sound in a gas as:

$$u_a = \left\{ \frac{Z\gamma\tilde{R}T}{\tilde{M}} \right\}^{1/2} \quad [11.16]$$

expressing  $\tilde{M}$  in terms of  $\rho_o$  and substituting into equation [11.3], with  $Z = 1$  and  $\gamma = 1.41$

$$f_a = 0.594 \left( \frac{n}{l} \right) \left( \frac{P}{\rho_o} \right)^{1/2} \quad [11.17]$$

- where  $Z$  = compressibility factor for gas  
 $\gamma$  = ratio of specific heats for gas  
 $\tilde{R}$  = universal gas constant (8314.3 J/kmol K)  
 $\tilde{M}$  = molecular weight of gas (kg/kmol)  
 $T$  = absolute temperature of gas (K)  
 $P$  = pressure of gas (N/m<sup>2</sup>).

The following procedure is necessary only if the shell-side fluid is a gas. In order to prevent intense noise, the objective is to avoid a match between (a) the vortex-shedding frequency (equation [11.2] and Table 11.1) and the acoustic frequency (equation [11.17]), and (b) the turbulent buffeting frequency (equation [11.8]) and (c) the acoustic frequency. Because of the 'lock-in' effect it is usual to provide a design in which

$$0.7 > \frac{f_v}{f_a} > 1.3 \quad [11.18]$$

$$0.7 > \frac{f_{th}}{f_a} > 1.3 \quad [11.19]$$

It is also necessary to ensure that the tube natural frequency (equation [11.4] and Table 11.2) does not coincide with the acoustic frequency, i.e.

$$f_n \neq f_a \quad [11.20]$$

Equation [11.3] shows that the acoustic frequency  $f_a$  is inversely proportional to characteristic length  $l$ , so that an increase in  $f_a$ , which is the usual objective, may be achieved by reducing  $l$ . In practice this means installing one or more flat plates parallel to the direction of flow, which do not affect heat transfer and pressure loss. These are termed detuning plates as shown in Fig. 11.3(d). One detuning plate, dividing the shell in two, doubles  $f_a$ ; two detuning plates, dividing the shell in three, triples  $f_a$ , and so on.

### 11.5.9 Comparison of predictive methods

Table 11.5 gives the maximum permissible cross-flow velocities for four predictive methods, namely, frequency match – vortex shedding, Thorngren collision damage, Erskine and Waddington damage approach and fluid-elastic whirling. The comparison relates to water and a gas. The comparison shows that there is a large difference between the four predictive methods and confirms that considerable research remains to be done. Unless previous experience is available the lowest velocity would be selected for safety in design. Factors for calculating predictive methods are given in Tables 11.6 and 11.7.

**Table 11.5** Shell-side flow-induced vibration. Comparison of some predictive methods. Maximum permissible cross-flow velocities (m/s)

Fluid	Predictive method			
	Frequency match	Thorngren collision damage	'Modified Thorngren' (Erskine)	Connors
Water (15 °C)	1.87	2.61	1.95	0.71
Gas	2.62	14.54	8.32	3.93

Tubes: 19.05 mm o.d. × 2.1 mm thick × 25.4 mm square pitch-steel

Gas: Density = 32 kg/m<sup>3</sup>, viscosity = 0.01 cP

Baffles: 8 spans, 1016 mm each, log decrement = 0.03

### 11.5.10 Calculation of predictive methods – examples

Two examples are given to demonstrate the use of the factors provided by Tables 11.6 and 11.7 for calculating predictive methods. When using the tube natural frequency factors  $K_{nf}$ , 'empty' means that a gas is present, its density being negligible in relation to those of steel and water.

It will be seen that the factors are based on the following values:



**Table 11.6** Factors for calculating flow-induced vibration predictive methods (steel tubes)

Tube size (mm) o.d.×thk.	Natural frequency ( $K_n$ )		Fluid-elastic whirling ( $K_w$ )		Damage numbers		Tube size o.d.(in)× b.w.g.
	Empty both sides	Water both sides	$\delta = 0.03$	$\delta = 0.1$	Baffle damage ( $K_{bd}$ )	Collision damage ( $K_{cd}$ )	
15.875×2.77	37.68	28.89	24.48	44.69	$1.313 \times 10^{-4}$	$1.904 \times 10^{-4}$	×12
15.875×2.11	39.37	28.48	22.82	41.66	$1.648 \times 10^{-4}$	$2.212 \times 10^{-4}$	×14
15.875×1.65	40.31	27.45	21.02	38.38	$2.039 \times 10^{-4}$	$2.587 \times 10^{-4}$	×16
15.875×1.24	41.36	26.08	19.06	34.81	$2.611 \times 10^{-4}$	$3.152 \times 10^{-4}$	×18
15.875×0.89	42.13	23.82	16.58	30.28	$3.576 \times 10^{-4}$	$4.129 \times 10^{-4}$	×20
19.05×3.40	45.21	34.84	35.60	64.99	$1.073 \times 10^{-4}$	$1.089 \times 10^{-4}$	×10
19.05×2.77	46.61	34.44	33.75	61.63	$1.268 \times 10^{-4}$	$1.210 \times 10^{-4}$	×12
19.05×2.11	48.16	33.36	31.03	56.64	$1.603 \times 10^{-4}$	$1.431 \times 10^{-4}$	×14
19.05×1.65	49.42	32.04	28.55	52.13	$1.992 \times 10^{-4}$	$1.697 \times 10^{-4}$	×16
19.05×1.24	50.57	30.09	25.64	46.84	$2.583 \times 10^{-4}$	$2.109 \times 10^{-4}$	×18
19.05×0.89	51.03	27.13	22.16	40.46	$3.530 \times 10^{-4}$	$2.779 \times 10^{-4}$	×20
25.4×3.40	62.96	45.65	58.63	107.05	$1.022 \times 10^{-4}$	$0.537 \times 10^{-4}$	1×10
25.4×2.77	64.40	44.42	54.91	100.26	$1.219 \times 10^{-4}$	$0.610 \times 10^{-4}$	1×12
25.4×2.11	66.03	42.27	49.85	91.01	$1.556 \times 10^{-4}$	$0.740 \times 10^{-4}$	1×14
25.4×1.65	67.33	39.98	45.42	82.92	$1.947 \times 10^{-4}$	$0.894 \times 10^{-4}$	1×16
25.4×1.24	68.47	36.90	40.38	73.72	$2.547 \times 10^{-4}$	$1.133 \times 10^{-4}$	1×18
25.4×0.89	69.46	33.07	34.90	63.72	$3.508 \times 10^{-4}$	$1.518 \times 10^{-4}$	1×20
31.75×3.40	80.60	55.37	85.31	155.76	$0.989 \times 10^{-4}$	$0.316 \times 10^{-4}$	1½×10
31.75×2.77	82.26	53.42	79.41	144.98	$1.189 \times 10^{-4}$	$0.365 \times 10^{-4}$	1½×12
31.75×2.11	84.06	50.24	71.54	130.61	$1.529 \times 10^{-4}$	$0.451 \times 10^{-4}$	1½×14
31.75×1.65	85.15	46.93	64.69	118.10	$1.921 \times 10^{-4}$	$0.550 \times 10^{-4}$	1½×16
31.75×1.24	86.25	42.92	57.28	104.57	$2.513 \times 10^{-4}$	$0.701 \times 10^{-4}$	1½×18
31.75×0.89	87.11	38.06	49.26	89.93	$3.469 \times 10^{-4}$	$0.947 \times 10^{-4}$	1½×20

Natural frequency  $f_n = K_n/L^2$  [11.3a]  
 Fluid-elastic whirling  $u_{co} = K_{fe}/\{(\rho_o)^{1/2}L^2\}$  [11.7]  
 Baffle damage  $N_{BD} = K_{bd}(\rho_o u_i^2 L^2)$  [11.9]  
 Collision damage  $N_{CD} = K_{cd}(\rho_o u_i^2 L^4)$  [11.10]  
 Densities (kg/m<sup>3</sup>): Steel = 7842, water = 998

- Tube metal density (steel):  $\rho_m = 7842 \text{ kg/m}^3$
- Tube modulus of elasticity (steel):  $E = 2 \times 10^{11} \text{ N/m}^2$
- Tube fatigue stress (steel):  $S_f = 8.33 \times 10^7 \text{ N/m}^2$
- Baffle thickness:  $B_t = 0.0127 \text{ m}$
- Tube-baffle hole clearance factor:  $F_B = 1$
- Instability constant:  $\beta = 4$
- Log decrement:  $\delta_o = 0.03 \text{ and } 0.1$
- Minimum gap between adjacent tubes:  $C_t = 0.00635 \text{ m}$
- Frequency constant:  $C_n = 32$
- Added mass coefficient:  $M_a = 2.75$
- Equivalent mass of tube per unit length:  $m_e = \text{steel tube: empty and water both sides } (\rho_o = \rho_i = 998 \text{ kg/m}^3)$

If the exchanger involves different values of  $E$ ,  $S_f$ ,  $B_t$ ,  $\beta$ ,  $\delta_o$ ,  $C_t$  and  $C_n$ , then the factors in Table 11.6 are readily corrected in accordance with the

**Table 11.7** Tube natural frequency calculations: factors for calculating tube equivalent mass ( $m_e$ )

Tube size o.d.×thk.	Tube only (kg/m) <sup>(1)</sup> ; both sides empty	External mass <sup>(2)</sup> ; water outside (kg/m)	Internal mass <sup>(3)</sup> ; water inside (kg/m)	Total equiv. mass <sup>(3)</sup> ; water both sides (kg/m)	Tube size o.d.(in)× b.w.g.
15.875×2.77	0.896	0.543	0.084	1.523	×12
15.875×2.11	0.713	0.543	0.107	1.363	×14
15.875×1.65	0.577	0.543	0.124	1.244	×16
15.875×1.24	0.451	0.543	0.140	1.134	×18
15.875×0.89	0.329	0.543	0.156	1.028	×20
19.05×3.40	1.316	0.782	0.117	2.215	×10
19.05×2.77	1.113	0.782	0.143	2.038	×12
19.05×2.11	0.881	0.782	0.172	1.835	×14
19.05×1.65	0.708	0.782	0.194	1.684	×16
19.05×1.24	0.546	0.782	0.215	1.543	×18
19.05×0.89	0.400	0.782	0.234	1.416	×20
25.4×3.40	1.841	1.391	0.271	3.503	1×10
25.4×2.77	1.543	1.391	0.309	3.243	1×12
25.4×2.11	1.210	1.391	0.352	2.953	1×14
25.4×1.65	0.966	1.391	0.383	2.740	1×16
25.4×1.24	0.738	1.391	0.411	2.540	1×18
25.4×0.89	0.536	1.391	0.437	2.364	1×20
31.75×3.40	2.378	2.173	0.488	5.039	1½×10
31.75×2.77	1.978	2.173	0.539	4.690	1½×12
31.75×2.11	1.537	2.173	0.594	4.304	1½×14
31.75×1.65	1.225	2.173	0.634	4.032	1½×16
31.75×1.24	0.936	2.173	0.671	3.780	1½×18
31.75×0.89	0.679	2.173	0.704	3.556	1½×20

Notes: (1) Steel tube. (2) Added mass coefficient,  $M_a = 2.75$ . (3) Densities (kg/m<sup>3</sup>): steel = 7842, water = 998.

following relationships:

Natural frequency (equation [11.4]):

$$f_n \propto C_n \left( \frac{E}{m_e} \right)^{0.5} \tag{11.21}$$

Fluid-elastic whirling (equation [11.10]):

$$u_{co} \propto \beta C_n (\delta_o E)^{0.5} \tag{11.22}$$

Baffle damage (equation [11.12]):

$$N_{BD} \propto \frac{1}{S_t B_t} \tag{11.23}$$

Collision damage (equation [11.13]):

$$N_{CD} \propto \frac{1}{EC_t} \tag{11.24}$$

Corrections to the factors for different values of the added mass coefficient ( $M_a$ ), and tube and fluid densities, which are required for calculating the equivalent mass of tube per unit length ( $m_e$ ), are not

straightforward, unless the tube is empty. The value of  $K_{nf}$  must be estimated from Table 11.6 or  $m_e$  calculated from Table 11.7. From equation [11.4],  $f_n \propto 1/m_e^{0.5}$ . Because of its empirical nature it is usual to maintain  $F_B = 1$ .

### Example 1

An E-type split backing ring floating-head exchanger, 991 mm inside diameter, has tubes 25.4 mm o.d.  $\times$  2.77 mm thick  $\times$  31.75 mm  $\times$  30° pitch. Single-segmental baffles, 10 mm thick, are spaced at 396 mm. The fluid flowing in shell and tubes is water at 41.58 kg/s, having average properties of  $\eta_o = 9.052 \times 10^{-4}$  Ns/m<sup>2</sup> and  $\rho_o = 998$  kg/m<sup>3</sup>. The tubes are steel such that  $E = 2 \times 10^{11}$  N/m<sup>2</sup> and  $S_f = 8.33 \times 10^7$  N/m<sup>2</sup>.

Is vibration damage likely to occur?

### Solution

Cross-flow area/m baffle pitch (Table 12.3(b)):

$$S_{mu} = 0.2311 \text{ m}^2/\text{m}$$

Cross-flow area:

$$S_m = 0.2311 \times 0.396 = 0.09152 \text{ m}^2$$

Max. cross-flow velocity ( $U_r = U_t$  for 30° pitch):

$$u_r = 41.58 / (998 \times 0.09152) = 0.455 \text{ m/s}$$

Unsupported tube length:

$$L = 2 \times 0.396 = 0.792 \text{ m}$$

Strouhal number (Table 11.1):

$$S_r = 0.18$$

Natural frequency factor (Table 11.6):

$$K_{nf} = 44.42 \text{ (water both sides)}$$

Instability constant (Table 11.4):

$$\beta = 4.6 \text{ (for pitch dia. ratio} = 1.25, 30^\circ)$$

Fluid-elastic whirling factor (Table 11.6):

$$K_{fe} = 100.26 \text{ } (\delta_o = 0.1 \text{ for water)}$$

Baffle damage factor (Table 11.6):

$$K_{bd} = 1.219 \times 10^{-4}$$

Collision damage factor (Table 11.6):

$$K_{cd} = 0.61 \times 10^{-4}$$

Maximum damage number (equation [11.15]):

$$= (0.00429 \times 998^{0.47}) / (9.052 \times 10^{-4})^{0.235} = 0.572$$

### Vortex shedding

Tube natural frequency (Table 11.6):

$$f_n = 44.42/0.792^2 \simeq 70.82 \text{ Hz}$$

Vortex-shedding frequency (equation [11.2]):

$$f_v = (0.18 \times 0.455)/0.0254 = 3.22 \text{ Hz}$$

(equation [11.7]):

$$f_v/f_n = 3.22/70.82 = 0.045 (< 0.5, \text{OK})$$

*Fluid-elastic whirling*

Instability constant correction (equation [11.22]):

$$4.6/4 = 1.15$$

Corrected value of  $K_{fe}$ :

$$100.26 \times 1.15 = 115.3$$

Critical velocity (Table 11.6)

$$u_{co} = 115.3/(998^{0.5} \times 0.792^2) = 5.82 \text{ m/s} (> 0.455, \text{OK})$$

*Baffle damage*

Baffle thickness correction (equation [11.23]):

$$0.0127/0.01 = 1.27$$

Corrected values of  $K_{bd}$ :

$$(1.219 \times 10^{-4}) \times 1.27 = 1.548 \times 10^{-4}$$

Baffle damage number (Table 11.6):

$$N_{BD} = (1.548 \times 10^{-4}) \times 998 \times 0.455^2 \times 0.792^2 = 0.02 (< 0.572, \text{OK})$$

*Collision damage*

Collision damage number (Table 11.6):

$$N_{CD} = (0.61 \times 10^{-4}) \times 998 \times 0.455^2 \times 0.792^4 = 0.005 (< 0.572, \text{OK})$$

*Vibration damage is unlikely to occur in this part of the exchanger.*

### Example 2

An E-type U-tube exchanger, 787 mm inside diameter, has tubes 31.75 mm o.d.  $\times$  2.11 mm thick  $\times$  39.688 mm 45° pitch. Single-segmental baffles, 16 mm thick, are spaced at 787 mm. The fluid flowing in the shell is a gas at 35 kg/s, having average properties of  $\eta_o = 8 \times 10^{-6} \text{ N s/m}^2$  and  $\rho_o = 20 \text{ kg/m}^3$ ; the fluid flowing in the tubes a liquid with  $\rho_i = 930 \text{ kg/m}^3$ . The tubes are 70/30 cupro-nickel such that  $E = 1.27 \times 10^{11} \text{ N/m}^2$ ,  $S_t = 1.27 \times 10^8 \text{ N/m}^2$  and  $\rho_m = 8947 \text{ kg/m}^3$ .

Is vibration damage likely to occur?

### Solution

Cross-flow area/m baffle pitch (Table 12.3a):

$$0.2229 \text{ m}^2/\text{m}$$

Cross-flow area:

$$0.2229 \times 0.787 = 0.1754 \text{ m}^2$$

Max cross-flow velocity:

$$u_t = 35 / (20 \times 0.1754) = 9.98 \text{ m/s}$$

Inter-row velocity ( $P/d_o = 1.25$ )

$$u_r/u_t = \{2 \times (1.25 - 1)\} / \{1.414 \times (1.25) - 1\} = 0.651$$

(section 11.5.2)

$$u_r = 9.98 \times 0.651 = 6.50 \text{ m/s}$$

Unsupported tube length:

$$U = 2 \times 0.787 = 1.574 \text{ m}$$

Strouhal number (Table 11.1):

$$S_r = 0.58$$

Added mass coefficient (Table 11.3):

$$M_a = 3.0$$

Natural frequency factor (Table 11.6):

$$K_{nf} = 50.24 \text{ (water both sides)}$$

Instability constant (Table 11.4):

$$\beta = 3.9 \text{ (for pitch : dia. ratio} = 1.25, 45^\circ)$$

Fluid-elastic whirling factor (Table 11.6):

$$K_{fe} = 71.54 \text{ } (\delta_o = 0.03 \text{ for gas)}$$

Baffle damage factor (Table 11.6):

$$K_{bd} = 1.529 \times 10^{-4}$$

Collision damage factor (Table 11.6):

$$K_{cd} = 0.451 \times 10^{-4}$$

Maximum damage number (equation [11.15]):

$$(0.00429 \times 20^{0.47}) / (8 \times 10^{-6})^{0.235} = 0.277$$

Tube mass (Table 11.7):

$$1.537 \text{ kg/m (for } \rho_m = 7842 \text{ kg/m}^3)$$

External mass (Table 11.7):

$$2.173 \text{ kg/m (for } M_a = 2.75 \text{ and } \rho_o = 998 \text{ kg/m}^3)$$

Internal mass (Table 11.7):

$$0.594 \text{ kg/m (for } \rho_i = 998 \text{ kg/m}^3)$$

Total equivalent mass (Table 11.7):

$$4.304 \text{ kg/m (water both sides)}$$

Corrected tube mass:

$$(1.537 \times 8947) / 7842 = 1.754 \text{ kg/m}$$

Corrected external mass:

$$2.173 \times (3/2.75) \times (20/998) = 0.048 \text{ kg/m}$$

Corrected internal mass:

$$0.594 \times (930/998) = 0.554 \text{ kg/m}$$

Tube equivalent mass:

$$1.754 + 0.048 + 0.554 = 2.356 \text{ kg/m}$$

*Vortex shedding*

Tube natural frequency

Mod. of elasticity correction (equation [11.21]):

$$\{(1.27 \times 10^{-11})/(2 \times 10^{-11})\}^{0.5} = 0.797$$

Equiv. mass correction (equation [11.21]):

$$(4.304/2.356)^{0.5} = 1.352$$

Corrected value of  $K_{nf}$ :

$$50.24 \times 0.797 \times 1.352 = 54.14$$

Tube natural frequency (Table 11.6):

$$f_n = 54.14/1.574^2 = 21.9 \text{ Hz}$$

Vortex-shedding frequency (equation [11.2]):

$$f_v = (0.58 \times 6.5)/0.03175 = 118.7 \text{ Hz}$$

(equation [11.7]):

$$f_v/f_n = 118.7/21.9 = 5.42$$

(> 0.5, possible damage)

*Fluid-elastic whirling*

Instability constant correction (equation [11.22]):

$$3.9/4 = 0.975$$

Mod. of elasticity correction (equation [11.22]):

$$\{(1.27 \times 10^{-11})/(2 \times 10^{-11})\}^{0.5} = 0.797$$

Corrected value of  $K_{fe}$ :

$$71.54 \times 0.975 \times 0.797 = 55.59$$

Critical velocity (Table 11.6):

$$u_{co} = 55.59/(20^{0.5} \times 1.574^2) = 5.02 \text{ m/s}$$

(< 9.98 m/s, possible damage)

*Baffle damage*

Fatigue stress correction (equation [11.23]):

$$= (8.33 \times 10^7)/(1.27 \times 10^8) = 0.656$$

Baffle thickness correction (equation [11.23]):

$$= 0.0127/0.016 = 0.794$$

Corrected value of  $K_{bd}$ :

$$(1.529 \times 10^{-4}) \times 0.656 \times 0.794 = 0.796 \times 10^{-4}$$

Baffle damage number (Table 11.6):

$$N_{BD} = (0.796 \times 10^{-4}) \times 20 \times 6.5^2 \times 1.574^2 = 0.167$$

(< 0.277, OK)

*Collision damage*

Mod. of elasticity correction (equation [11.24]):

$$(2 \times 10^{11})/(1.27 \times 10^{11}) = 1.575$$

Tube gap correction (equation [11.24]):

$$0.00635/0.00794 = 0.8$$

Corrected value of  $K_{cd}$

$$(0.451 \times 10^{-4}) \times 1.575 \times 0.8 = 0.568 \times 10^{-4}$$

Collision damage number (Table 11.6):

$$N_{CD} = (0.568 \times 10^{-4}) \times 20 \times 6.5^2 \times 1.574^4 = 0.295$$

(> 0.277, possible damage)

*Acoustic vibration*

As the shell-side fluid is a gas, a check must be made for acoustic vibration. If the gas pressure is  $2 \times 10^4$  N/m<sup>2</sup> and  $n = 1$  for lowest value of acoustic frequency (section 11.4.4):

Acoustic frequency (equation [11.17]):

$$f_a = 0.594 \times \{1/0.787\} \{(2 \times 10^4)/20\}^{0.5} = 23.9 \text{ Hz}$$

(close to  $f_n$ , possible acoustic vibration)

*Vibration damage and acoustic vibration is likely to occur in this part of the exchanger.*

## 11.6 Application to design

### 11.6.1 Zones for vibration check

In the case of a shell-and-tube exchanger, it is recommended that a vibration check is carried out in five zones, shown in Fig. 11.2, namely:

Zone no.	Position in exchanger
1	First row of tubes at inlet.
2	Baffle edge of first crossover.

<i>Zone no.</i>	<i>Position in exchanger</i>
3	Baffle edge of 'central' crossover where baffle spacing is uniform
4	Baffle edge of last crossover
5	Last row of tubes at outlet.

Shell-side velocities in each zone are calculated on an inter-gap or inter-row basis, as appropriate, except in zones 1 and 5. If there is no impingement baffle in zone 1, the shell-side velocity is assumed to be equal to the nozzle velocity. If an impingement baffle is fitted, the shell-side velocity is based on the inter-row velocity across the first row allowing for the blockage of the impingement baffle. In zone 5, the shell-side velocity is the greater of the exit nozzle velocity and the inter-row velocity across the last row.

### 11.6.2 Design recommendations

Current knowledge suggests that if the designer checks against all the predictive methods described in section 11.5 and uses the most stringent result, the possibility of vibration failure is extremely unlikely. In the case of shell-and-tube exchangers, for instance, a cross-flow shell (X type) or a no-tube-in-window (NTIW) design virtually guarantees freedom from vibration failure. This is achieved by the addition of intermediate support baffles, which may be spaced to suit the most stringent predictive method. Their cost is low and they have little effect on heat transfer and pressure loss. Each case must be considered on its merits, but the X and NTIW types may not be as punitive as they appear and in some cases may provide the best design irrespective of vibration problems.

The recommended procedure for design, if X and NTIW types are not being employed, is as follows:

- (a) At each zone calculate the Thorngren baffle and collision damage numbers  $N_{BD}$  and  $N_{CD}$  from equations [11.12] and [11.13], but use the Erskine and Waddington approach as the criterion for damage from equation [11.15]. Hence:

$$\text{both } N_{BD} \text{ and } N_{CD} \succ \left\{ \frac{0.00429(\rho_o^{0.47})}{\eta_o^{0.235}} \right\}$$

- (b) If damage is predicted for zone 1, and sometimes this is the only danger zone, the problem may be solved by installing a small support plate in the inlet baffle space as shown in Fig. 11.3(a). Similar considerations apply to zone 5. Alternatively shell-side flow distributors may be fitted as shown in Fig. 1.27. Subject to thermal considerations, the velocity in zone 1 may be reduced by cutting away part of the first baffle as shown in Fig. 11.3(a).

If damage is predicted in the other zones, the options listed below must be investigated. A change from an E shell to a J shell halves the shell-side velocities in all zones and this may solve the problem. A change from single-segmental to double- or triple-segmental baffles Fig. 1.25 reduces the velocities in zones 2, 3 and 4, which may solve



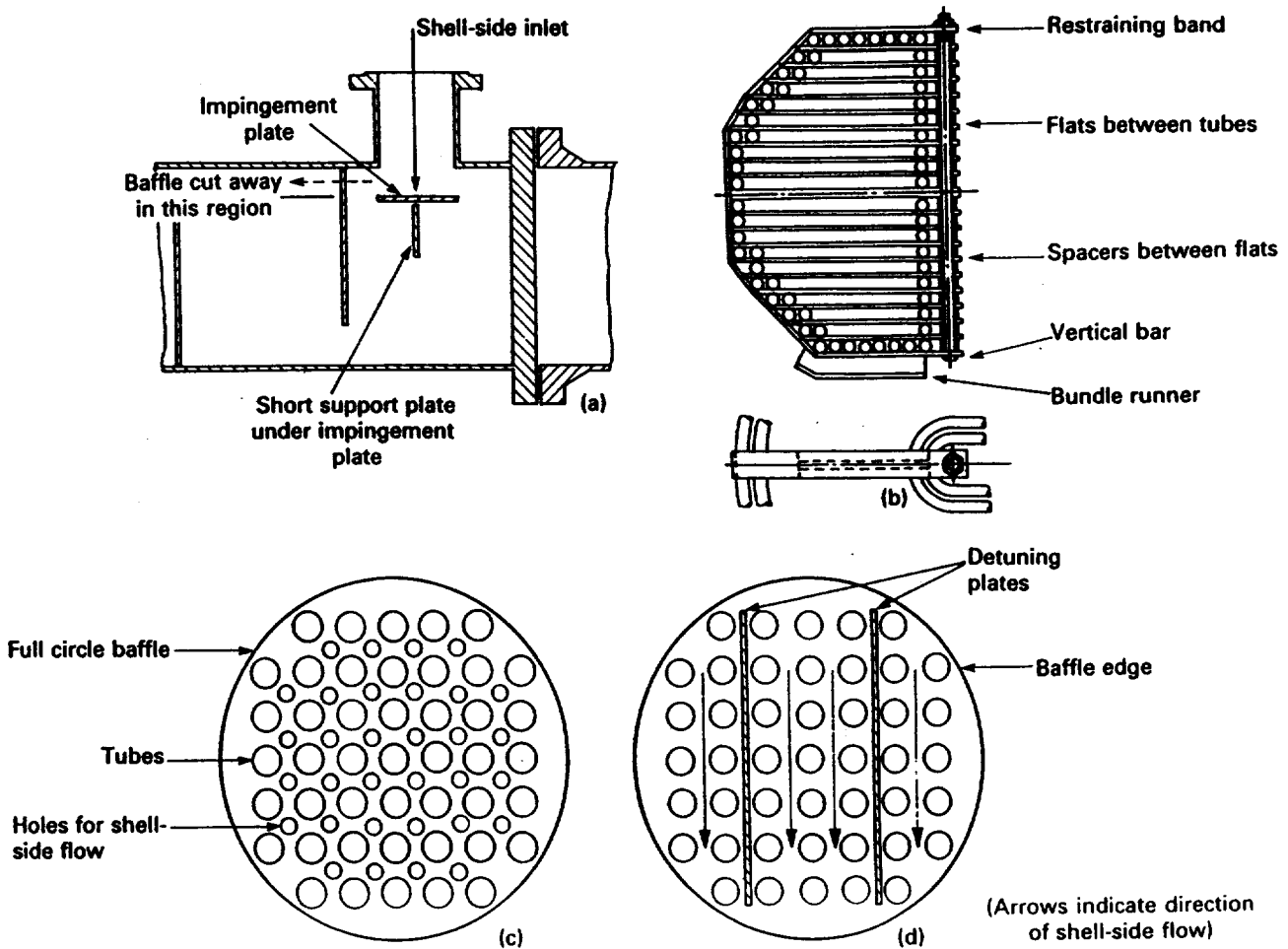


Figure 11.3 Anti-vibration measures (a) inlet support plate (b) U bend support (c) 'holed' baffle (d) detuning plates

the problem in those zones. However, the velocities in zones 1 and 5 will be unchanged and small support plates or distributors may be required.

These options will reduce both heat transfer coefficient and pressure loss, for the same baffle spacing, and revision to the thermal design is likely to be required, particularly if shell-side heat transfer is controlling (section 6.7)

- (c) A divided flow (J-type) shell.
- (d) Double- or triple-segmental baffles.
- (e) A divided flow (J-type) shell with double or triple segmental baffles.
- (f) A complete redesign using a wider tube pitch and/or different pitch angle.
- (g) If the U-bend unsupported span length exceeds TEMA maximum, or there is full shell-side fluid flow through the bends, install an anti-vibration device as shown in Fig. 11.3(b).
- (h) If the shell-side heat transfer coefficient is not controlling, consider full-circle 'holed' supports as shown in Fig. 11.3(c).
- (i) If the shell-side fluid is a gas, and acoustic problems are envisaged, install detuning plates to satisfy equations [11.18], [11.19] and [11.20] (see Fig. 11.3(d)).
- (j) Additional safety may be provided by reducing baffle-tube clearance (skip-finning in the case of low-fin tubes see Fig. 13.1), increasing the

baffle thickness and using a baffle material which is not harder than the tube, but these must not be regarded as major remedies.

The above procedures apply to conventional shell-and-tube exchangers. The designer may also wish to consider the Phillips RODbaffle™ design or the NESTS™ concept described in sections 11.7 and 11.8.

## 11.7 Phillips RODbaffle™ exchanger

### 11.7.1 Development

In 1970, a butadiene plant owned by Phillips Petroleum Co. lost three large shell-and-tube exchanger bundles from failures due to flow-induced tube vibration. Emergency repairs were made to alter the design which eliminated tube failure and also revealed unexpected, but significantly improved, operating characteristics. This merited further investigation which led to the development of the Phillips patented RODbaffle exchanger (RBE) as described in section 11.7.2. The RBE technology is available to fabricators and users on a licence basis and 600 such units are in operation throughout the world at the end of 1982.

The RBE may be used for both single-phase and condensing shell-side fluids, while Gentry *et al.* (1982a) presented a conceptual design study of the RBE for large-scale nuclear steam generation service. Because of its low pressure loss (i.e. energy-saving) characteristics, the RBE may prove more attractive than a conventional baffled shell-and-tube exchanger for applications where vibration is not a problem.

The RODbaffle concept itself is not new and the RBE may initiate an investigation of other energy-saving devices as a substitute for perforated plate baffles in a shell-and-tube exchanger.

In addition to eliminating tube failure due to vibration, Phillips claim other advantages for the RBE over the conventional baffled shell-and-tube exchanger. Fouling rates are lower because there is uniform shell-side flow, which sweeps the tubes clean, and there are no stagnant regions where deposits can accumulate. The interval between cleaning the original butadiene plant bundles has been increased from 6 weeks to 9 months after installing rod baffles. Cleaning takes only half the time because fouling is uniformly distributed and square tube pitch is always used. The RODbaffle construction is inherently stiff and minor damage which sometimes occurs during bundle removal has not been experienced.

A significant bonus is claimed with regard to heat transfer and pressure loss characteristics compared with a shell-and-tube exchanger having double-segmental baffles to minimise pressure loss. After installing rod baffles in the original bundles, the duty has increased by 35%, but despite an increase in throughput of 30%, the pressure loss has reduced by 30%. A comparison was made by Gentry *et al.* (1982b) between the two types, under identical geometrical and flow conditions (water on both sides). This showed that although the overall heat transfer coefficient for the RBE was 20% lower, its bundle pressure loss (i.e. excludes nozzle losses)

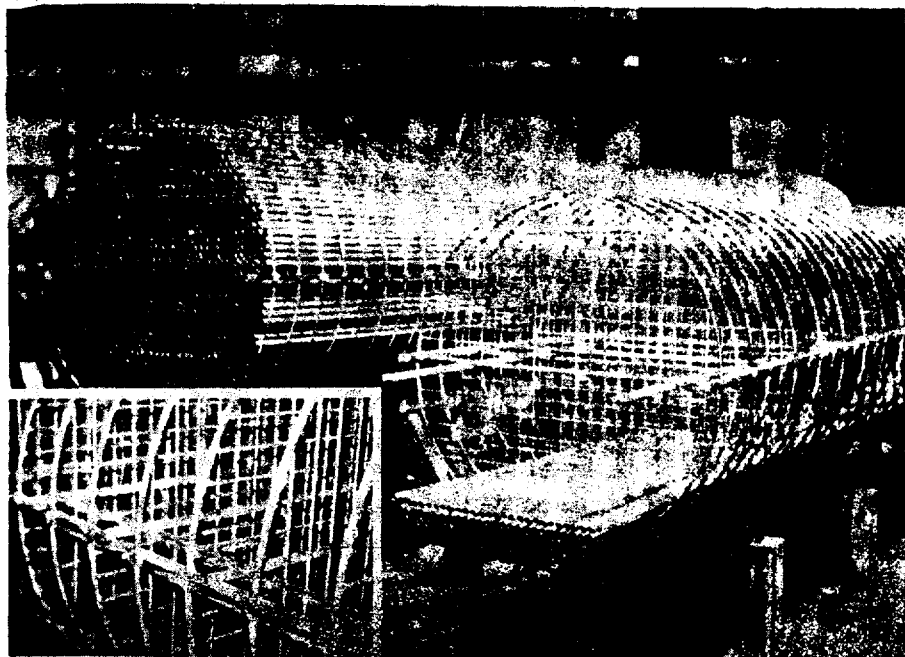
was only one-seventh, and the ratio of heat transfer coefficient: pressure loss was 6.5 times greater. The absence of stagnant regions in the RBE means that the entire heat transfer surface is effective; in addition vortices shed from the flow across the rods develop vortex streets which provide turbulence to enhance heat transfer, but at a low energy-dissipation rate.

### 11.7.2 Construction

As the name implies the supports for the tubes are rods which replace the conventional perforated plate baffles. A baffle set comprises four baffles, spaced 150 mm apart, the first two baffles having vertical rods and the second two baffles having horizontal rods. The vertical rods support rows 1, 3, 5, 7, etc. in the first baffle and rows 2, 4, 6, 8, etc. in the second baffle. The pattern is repeated for the horizontal rods in the third and fourth baffles. The baffle set provides positive 4-point tube support and the exchanger has a number of baffle sets according to the tube length. The system is shown in Fig. 11.4.

The tubes are arranged on a square pitch and the rod diameter is equal to the clearance between tube rows. Each baffle has its own peripheral support ring such that its outside diameter is the shell diameter minus the usual shell to plate baffle clearance, and its inside diameter is the bundle OTL. The peripheral ring may be made from bar, rod, or plate rolled into a cylinder and cut to the required thickness. Each baffle is made on a jig. The bundle cage is formed and held together by welding every baffle support ring to longitudinal bars, diametrically placed at the outside of the bundle. The bars run the whole length of the bundle and are welded to the stationary tubesheet. The bundle is tubed-up in a similar manner to a conventional baffled exchanger. Baffle material is selected to suit the shell-side fluid.

**Figure 11.4** Phillips RODbaffle™ exchanger (courtesy of Phillips Petroleum Co.)



The RBE may be a fixed tubesheet, U-tube or floating-head type. However, because the shell-side flow is longitudinal, annular peripheral gaps between bundle and shell must be sealed off at each rod baffle assembly, which applies particularly to the floating-head types. This is achieved by annular peripheral baffle plates which replace the peripheral support rings. The rods are welded to the peripheral baffles.

The use of annular distributors for the shell-side nozzles, rather than internally fitted impingement plates, also eliminates peripheral gaps. (See Figs 1.26 and 1.27).

## 11.8 NESTS™ concept

### 11.8.1 Development

Although developed in order to provide improved tube supports for steam condensers, and as an energy-saving device, the NESTS™ (Neoteric Endo-Stratiformed Tube Supports) system provides a vibration-free design. The system was devised by Ecolaire-Heat Transfer Co. and at present is available to industry only from their associated fabricators.

### 11.8.2 Construction

Each support is built up from accurately preformed metallic strip to form a rigid honey-comb structure as illustrated in Fig. 11.5. To assist in the assembly of each support, and to maintain each strip in its correct position, a dome and hole interlocking mechanism is used. In all strips each apex has a dome, roughly 3 mm in diameter, which is designed to engage with a hole of slightly larger diameter in each valley of the mating strip. Each tube in the bundle is supported in a precise V-shaped cradle, but as the strips are structural members, independent of the tubes, no load is transmitted to the tubes. The tubes are free to move in an axial direction, but the smooth finish of the strip (about 20 r.m.s.) eliminates scratching and galling. The ends of the strips are welded to a circular

**Figure 11.5** NESTS™ concept (courtesy of Ecolaire Heat Transfer Co.)



metallic band so that the complete assembly is similar to an 'egg-box' type baffle.

The support system, as described, provides axial flow of the shell-side fluid and is therefore ideally suited to low pressure loss applications where conventionally baffled exchangers may not be economical. If required an annular plate may be welded to the periphery of each support to minimise undesirable axial leakage of the shell-side fluid between bundle and shell. As every tube is supported the distance between adjacent supports may be twice that for conventional single- or double-segmental baffles.

A further feature of the NESTS™ concept is the provision of baffle tabs. As shown in Fig. 11.5 triangular tabs may be formed along the centre of each strip and bent through 90° from the plane of the strip such that they block most of the open axial-flow area around the tube. Tabs may be provided as required over the cross-section of the bundle to prevent axial flow through selected areas. A variety of shell-side flow patterns may be achieved including those relating to single-, double- and triple-segmental baffles.

Type 304 stainless steel is the standard strip material, but other stainless-steel grades, monel and titanium may be used. Strip thickness is usually 1.25 mm (0.049 in, 18 b.w.g.) but some applications may require a greater thickness of 1.90 mm (0.075 in, 14 b.w.g.). The strip width is 25–35 mm which is greater than the thickness of conventional baffles.

### 11.8.3 Anti-vibration characteristics

In addition to exhibiting a low shell-side pressure loss, the axial flow of the shell-side fluid provided by the supports, without tabs, in all zones (except inlet and outlet), offers freedom from flow-induced vibration. Unless distributor belts are provided some cross flow will exist in the inlet and outlet zones and additional supports may be required to avoid vibration problems.

It is claimed that the degree of support provided by the NESTS™ concept is superior to that of conventional baffles, partly due to the increased length of support, and partly due to the dampening effect arising from the local flexibility of the edge of the strip. Supports, with tabs, enable a variety of shell-side flow patterns to be achieved, with better anti-vibration characteristics than conventional baffles.

## Acknowledgements

The author is grateful to the following companies for providing technical data and illustrations: Phillips Petroleum Co., relating to their RODbaffle™ design; Ecolaire Heat Transfer Co., relating to their NESTS™ concept.

## References

A list of addresses for the service organisations is provided on p. xvi.

- Barrington, E. A. (1973) 'Acoustic vibrations in tubular exchangers', *Chem. Eng. Progress*, **69** (No. 7) 62-8.
- Chen, Y. N. (1968) 'Flow induced vibration and noise in tube-bank heat exchangers due to von Karman streets', *Trans. ASME, J Engineering for Industry* (B) **90**, 134-46.
- Connors, H. J. (1970) 'Fluidelastic vibration of tube arrays excited by cross-flow', *Proc. of Symposium on Flow-Induced Vibration in Heat Exchangers*. ASME Annual Meeting, New York, pp. 42-56.
- Erskine, J. B. and Waddington, W. (1973) 'A review of some tube vibration failures in shell and tube heat exchangers and failure prediction methods', *Int. Symposium on Vibration Problems in Industry, Keswick, UK* (10/12 April).
- Fitz-Hugh, J. S. (1973) 'Flow-induced vibration problems in heat exchangers', *Int. Symposium on Vibration Problems in Industry, Keswick, UK* (10/12 April).
- Gentry, C. C. et al. (1982a) 'A conceptual RODbaffle nuclear steam generator design', *ASME Joint Power Generation Conference, Nuclear Heat Exchanger Sessions, Denver, Colorado, USA* (17/21 Oct.).
- Gentry, C. C. et al. (1982b) 'RODbaffle Heat Exchanger. Thermal-Hydraulic Predictive Methods', *7th Int. Heat Transfer Conference, Munich, FRG* (6/10 Sept.).
- Heat Exchanger Design Handbook* (1983) Vol. 4, Section 4.6, Hemisphere Publishing Corp.
- MacDuff, J. N. and Felgar, R. P. (1957) 'Vibration design charts', *Trans. ASME* **79**, 1459-74.
- Owen, P. R. (1965) 'Buffeting excitation of boiler tube vibration', *J. Mech. Eng. Science* **7** (No. 4), 431-99.
- Thorngren, J. T. (1970) 'Predict exchanger tube damage', *Hydrocarbon Processing*, pp. 129-31.
- Tubular Exchanger Manufacturers Association* (1978) *Standards of Tubular Exchanger Manufacturers Association* (6th edn). TEMA, New York, USA.

## Nomenclature

Symbol	Description	Units
$A_m$	Cross-section area of tube metal	$m^2$
$B_t$	Baffle thickness	m
$C_n$	Frequency constant (equation [11.4])	—
$C_t$	Minimum gap between adjacent tubes	m
$d_i, d_o$	Inside and outside tube diameters	m
$E$	Modulus of elasticity	$N/m^2$
$f_a$	Acoustic frequency	Hz
$f_v$	Vortex shedding frequency	Hz
$f_n$	Tube natural frequency	Hz
$f_{tb}$	Turbulent buffeting frequency	Hz
$F_B$	Tube-baffle hole clearance factor	—
$I$	Sectional moment of inertia ( $= \pi/64(d_o^4 - d_i^4)$ )	$m^4$
$l$	Characteristic length for acoustic vibration (equation [11.3])	m
$L$	Unsupported tube length	m
$m_e$	Equivalent mass of tube per metre [ $= (\pi/4) d_i^2 \rho_i + (\pi/4) d_o^2 \rho_o M_a + W_i$ ]	kg/m
$\tilde{M}$	Molecular weight	kg/kmol

$M_a$	Added mass coefficient	—
$n$	Mode number	—
$N_{BD}, N_{CD}$	Thorngren baffle and collision damage numbers	—
$p$	Pressure of gas	N/m <sup>2</sup>
$P$	Tube pitch (as defined by Figs 1.19 and 12.3)	m
$P_l$	Longitudinal tube pitch—distance between centres of adjacent rows parallel to shell-side flow	m
$P_t$	Transverse tube pitch—distance between centres of adjacent tubes in a row normal to shell-side flow	m
$\tilde{R}$	Universal gas constant	8314.3 J/ kmol K
$S_f$	Tube fatigue stress	N/m <sup>2</sup>
$S_r$	Strouhal number	—
$T$	Absolute temperature	K
$u_a$	Velocity of sound for shell-side fluid	m/s
$u_{co}$	Critical velocity for fluid-elastic whirling	m/s
$u_r$	Cross-flow velocity based on free area between tubes in the same row	m/s
$u_t$	Cross-flow velocity based on minimum free area between tubes	m/s
$W_a$	Axial load in tube	N
$W_t$	Weight of tube per metre	kg/m
$Z$	Compressibility factor for gas	—
$\beta$	Instability constant	—
$\gamma$	Ratio of specific heats of gas	—
$\delta_o$	Log decrement	—
$\eta_o$	Absolute viscosity of shell-side fluid	Ns/m <sup>2</sup>
$\rho_i, \rho_o$	Tube-side and shell-side fluid density	kg/m <sup>3</sup>

---

## Thermal design

Chapters 12–16 provide thermal design methods for some of the heat exchanger types presented in Part 1: namely, shell-and-tube, both plain and low fin, described in Chapters 1 and 2; air-cooled (Chapter 3); gasketed plate (Chapter 4); and double pipe (Chapter 5). The application of the methods to the thermal design of these heat exchanger types is presented as worked examples in Chapter 17. Where applicable, the heat transfer and pressure loss data presented in Part 2 is used.

The thermal design methods and worked examples are concerned with a single heat exchange unit for which the design conditions, i.e. heat load, flow rates, terminal temperatures and allowable pressure losses, have been determined. However, in an energy-conscious world, the determination of the number of heat exchange units required, and the design conditions for each, for a plant involving several process streams, is increasingly carried out by sophisticated methods, termed heat exchanger network synthesis (HENS).

According to Govind *et al.* (1986), HENS is stated in the following manner. Given  $N_h$  hot-process streams (which must give up heat) and  $N_c$  cold-process streams (which must accept heat), each with specified supply temperature, target temperature, heat capacity and flow rate, synthesise a network of heat exchangers which brings each stream to its target temperature and minimises the annualised sum of operating and investment cost. The investment cost is a function of the number of heat exchangers used and their heat transfer areas; the operating cost is proportional to the utility stream consumption and the annual operating time.

Boland and Hindmarsh (1984) report savings of in the range of 35–60% by the application of HENS to both new and existing plants.

Heat exchanger network synthesis is beyond the scope of this book, but several references are given below.

**Boland, D. and Hindmarsh, E.** (1984) 'Heat exchanger network improvements', *Chem. Eng. Prog.* **80** (7), 47–54.

**Flower, J. R. and Linnhoff, B.** (1980) 'A thermodynamic-combinatorial approach to the design of optimum heat exchanger networks', *AIChE Journal* **26** (1), 1–9.

**Govind, R., Mocsny, D., Cosson, P. and Klei, J.** (1986) 'Exchanger network synthesis on a microcomputer', *Hydrocarbon Processing* (July), pp. 53–7.



- Linnhoff, B., Mason, D. R. and Wardle, I. (1979)** 'Understanding heat exchanger networks', *Proc. of the 12th Symposium on Computer Applications in Chemical Engineering, Montreux, Switzerland.*
- Linnhoff, B. and Hindmarsh, E. (1983)** 'The pinch design method for heat exchanger networks', *Chem. Eng. Sci.* **38** (5), 745-63.
- Linnhoff, B. and Vredeveld, D. R. (1984)** 'Pinch technology has come of age', *Chem. Eng. Prog.* **80** (7), 33-40.
- Mocsny, D. and Govind, R. (1984)** 'Decomposition method for the synthesis of minimum-unit heat exchanger networks', *AIChE Journal* **30** (5), 853-6.
- Nishida, N., Stephanopoulos, G. and Westerberg, A. W. (1981)** 'A review of process synthesis' *AIChE Journal* **27** (3), 321-51.

## Thermal design: shell-and-tube exchangers (plain tubes)

### 12.1 The need for manual design methods

Most shell-and-tube heat exchangers today are designed by computer, the use of which is essential to solve, for example, the complex flow patterns in the shell described in section 12.2.2. Widely used programs are those based on comprehensive large-scale tests by the cooperative research organisations, HTFS and HTRI, whose activities were discussed in Chapter 6. Also widely used are programs developed by computer service companies, such as B-JAC International Ltd, (Richmond, Virginia, USA) who combine expertise and experience of both computing and heat exchanger engineering.

In addition to solving the complex shell-side flow problem, computers enable the large number of design parameters to be investigated rapidly to produce the optimum design. Accordingly there is little interest in manual design methods. However, in the author's experience there remains a need for them, partly for use when only an approximate design is required, but chiefly as an introduction to the subject for the inexperienced thermal design engineer. Manual calculations during training gives the designer a better 'feel' for the magnitude of Reynolds numbers, velocities, heat transfer coefficients, pressure losses, etc. It also provides a sounder appreciation of the effect on heat transfer, pressure loss, temperature difference and flow-induced vibration due to changes in baffle type and spacing, number of passes, shell-side flow arrangement, tube size, pitch, orientation, length, etc.

In the manual design of an exchanger, the thermal design engineer cannot avoid the trial and error routine which will be required to establish the optimum unit, but this is precisely the skill and judgement which is to be developed. Hence the manual method should be suitable for a hand-held calculator, but have a sound basis such that the results are realistic. In addition, tedious geometrical calculations should be minimised.

The Bell (1963) manual method is considered by Taborek (1983) 'to be the best available and the most suitable for general engineering applications'. In view of this recommendation, and with the above objectives in mind, simple design factors are provided which enable the

method proposed by Bell to be used rapidly for a fixed set of geometrical parameters.

Before describing the proposed method, the shell-side flow problem and certain other manual design methods are discussed briefly.

## 12.2 Shell-side flow problem

### 12.2.1 Idealised shell-side flow model

It is possible to manufacture special shell-and-tube heat exchangers in which (a) each segmental baffle is welded around its periphery to the inside of the shell, thereby preventing flow between baffle and shell, (b) the annular space around each tube where it passes through the baffle, is fitted with a tightly fitting plastic sleeve, or similar device, thereby preventing flow between baffle and tubes and (c) the tubes completely fill the shell in a uniform manner, such that there are no gaps due to pass partitions, impingement plates, or between tube bundle and shell, through which the bundle could be by-passed.

In an exchanger of this construction, the shell-side flow would be that of the ideal flow model shown in Fig. 12.1. There is no leakage of the shell-side fluid between adjacent baffle spaces and no by-passing of the tube bundle within a baffle space. Heat transfer and pressure loss could be derived from the ideal tube bank correlations of Chapter 6.

However, because of constructional difficulties, the need to have certain bundles removable, and the cost, the vast majority of shell-and-tube exchangers are constructed as described in Chapters 1 and 2. In practice there are always gaps between baffle/shell and baffle/tubes. According to the type of exchanger there may also be gaps between bundle/shell and, depending on the design, there may be additional gaps due to the presence of pass partitions and impingement baffles.

### 12.2.2 Tinker (1951) shell-side flow model

Because by-passing occurs at the inherent constructional gaps described in section 12.2.1, only a portion of the shell-side fluid passes over the whole bundle in cross-flow. The flow on the shell-side of a baffled shell-and-tube exchanger is complex and Fig. 12.2 shows the widely accepted Tinker (1951) shell-side flow model. The stream designations proposed by Tinker, namely A, B, C, and E, with the later addition of the F stream, have largely become standard in the industry.

The A stream is leakage between tube and baffle, but it still contributes to heat transfer because it is in contact with the tubes. The C stream is leakage between the outer tube limit (OTL) and the shell, the gap depending on the exchanger type as described in Chapter 1. Leakage is reduced by the use of longitudinal sealing strips between OTL and shell, as described in Fig. 1.30 and section 1.5.16. They are not usually required for fixed tubesheet and U-tube exchangers, but essential for

Figure 12.1 Idealised shell-side flow model

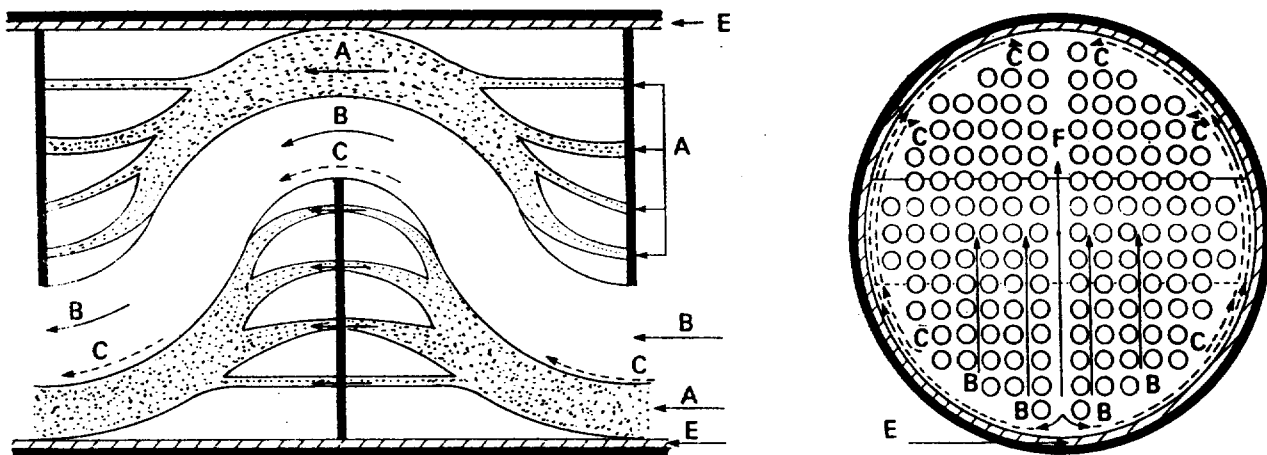
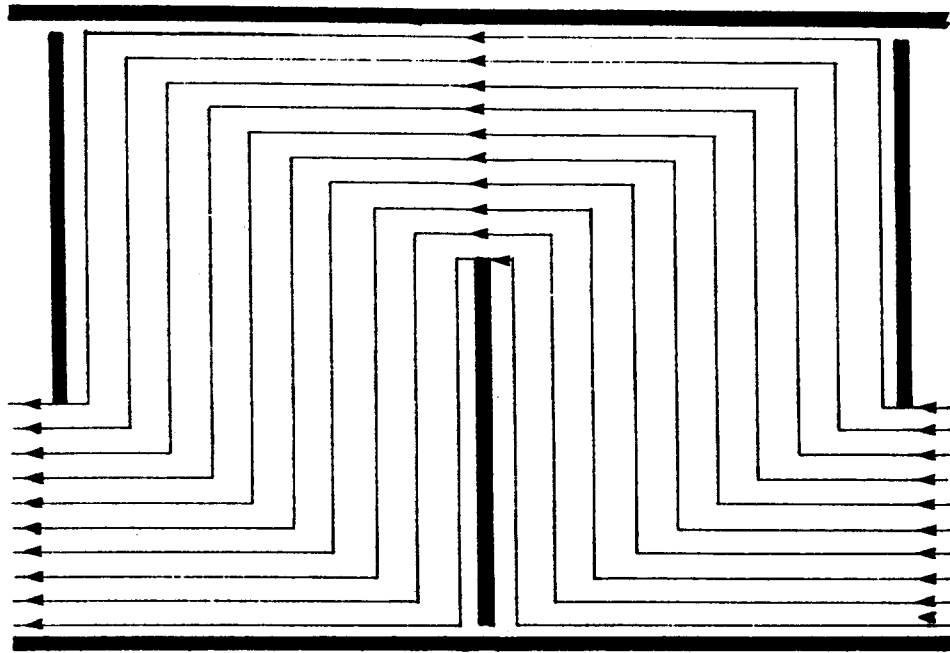


Figure 12.2 Shell-side flow streams (Tinker model)

floating-head exchangers having single-phase shell-side fluids. Because some of the C stream is in contact with peripheral tubes it makes a small contribution to heat transfer.

The E stream is leakage between baffle and shell and is insidious because it not only by-passes the bundle, but also tends to 'distort' the temperature profiles of the two fluids assumed in the log MTD derivation, with a subsequent reduction of effective temperature difference. The manufacturer must ensure that the gap between baffle and shell is within the dimension specified by TEMA or the thermal design engineer. The F stream arises from gaps in the bundle itself due to the presence of pass partitions and impingement plates. The leakage is reduced by the insertion of tie rods or dummy tubes, as described in Fig. 1.30 and section 1.5.16.

The B stream is the fraction of the total shell-side flow which flows across the baffle space, nominally in cross-flow. It is assumed to be unity in the idealised shell-side flow model, but may be as low as 0.1 in a poorly designed exchanger, as seen below.

Palen and Taborek (1969), of HTRI, applied the proprietary 'stream analysis method' developed there to calculate the fraction of the total shell-side flow passing through each leakage stream, using a large data bank from test exchangers, with the following results:

<i>Typical stream flow fractions</i>			
<i>Stream</i>	<i>Usual stream designation</i>	<i>Turbulent</i>	<i>Laminar</i>
Tube-baffle hole	A	0.09–0.23	0.00–0.10
Actual cross-flow	B	0.30–0.65	0.10–0.50
Bundle-shell	C	0.15–0.35	0.30–0.80
Baffle-shell	E	0.06–0.21	0.06–0.48
Pass partition gaps	F	(not in Tinker's model)	

### 12.2.3 Some manual design methods

Using Fig. 12.2 as a basis, Tinker (1951) provided a method for determining individual stream flow fractions, from which the single-phase shell-side heat transfer coefficient and pressure loss could be calculated. Despite the soundness of his approach, the method depended on the calculation of individual stream resistances where experimental data were scarce or unreliable. Above all, the method could not be applied readily by the designer because of the lack of computer facilities, although it was later simplified by Tinker (1958), which provided a basis for further simplification by Devore (1962) and Fraaz and Ozisik (1965).

Until the late 1960s many designers resorted to the straightforward manual methods developed by Donohue (1949), Kern (1950) and Gilmour (1952–54). These methods assume that the shell-side fluid flows across the bundle in pure cross-flow without leakage, as in Fig. 12.1, but an in-built correction factor derates the ideal heat transfer coefficient to account for all leakage streams. Palen and Taborek (1969) compared various shell-side design methods against a large experimental data bank of HTRI and concluded that the Donohue and Kern methods produced 'predominant error ratios of such large magnitude that they could not be considered valid entries for the solution of the shell-side problem'. *Nevertheless these methods served industry well over a long period.*

Using data obtained from extensive research at the University of Delaware, Bell (1963) published a method which not only accounted for the various leakage streams, but involved relatively straightforward calculations. Details of the calculations, step-by-step with supporting curves, are admirably presented by both Bell (1984) and Taborek (1983).

Despite their more realistic approach, the methods of Tinker and Bell were found by Palen and Taborek (1969) to produce significant errors, the ratio (calculated value)/(experimental value) for shell-side Reynolds numbers of  $2.0 \times 10^5$ , in single-phase flow, being as follows:

<i>Method</i>	<i>Heat transfer coefficient</i>	<i>Pressure loss</i>
Tinker	0.5–4.0	0.2–4.0
Bell	0.5–2.0	0.5–4.0
Palen and Taborek (HTRI)	0.7–1.3	0.7–1.4

### 12.3 Thermal design procedure

In a single-phase design problem, the flow rates, heat load ( $Q$ ) and terminal temperatures are known, from which the log MTD ( $\Delta T_{lm}$ ) may be calculated. If the flow is not strictly countercurrent or cocurrent, it will be necessary to multiply  $\Delta T_{lm}$  by  $F$ , the MTD correction factor, as described in Chapter 7, to provide the effective temperature difference ( $\Delta T_m$ ).  $F$  depends on the number of shells in series and the shell-side flow arrangement. Unless experience dictates otherwise, an E-type shell is the usual tentative arrangement.

The design steps are as follows:

- (a) Estimate an overall heat transfer coefficient, ( $U$ ), based on experience, or using values given in Chapter 19. The time taken to establish a firm design will depend on the closeness of the estimated value to the true value.
- (b) Calculate a tentative surface area ( $A$ ) from  $Q/(U \Delta T_m)$ . Using the proposed tube diameter, pitch and a known, or estimated, length, the tentative number of tubes required may be calculated. The tentative shell diameter for the proposed exchanger type is then taken from the tube count tables A3.1–A3.3.
- (c) The heat transfer coefficients ( $\alpha_o$  and  $\alpha_i$ ), and pressure losses ( $\Delta P_s$  and  $\Delta P_T$ ) are calculated as described in this chapter for the shell-and-tube sides, respectively. To do this, it is necessary to assume the baffle spacing and number of tube-side passes (see Chapter 17).
- (d) If heat transfer coefficients are related to the outside surface, then the overall heat transfer coefficient ( $U_o$ ) is determined by equation [6.7c], i.e.

$$U_o = \frac{1}{\{(1/\alpha_i)(d_o/d_i) + r_i(d_o/d_i) + r_w + r_o + (1/\alpha_o)\}} \quad [12.1]$$

All symbols and units are as defined for equation [6.7c].

- (e) The calculated  $U_o$  is compared with the assumed value, and pressure losses compared with the allowable values. Flow-induced vibration must not be overlooked, and this should be checked in accordance with the recommendations of Chapter 11.
- (f) If there is not close agreement, or there is a possibility of flow-induced vibration, it may be necessary to change one or more of the design parameters, i.e. shell diameter, tube length, shell-side flow arrangement, baffle type and spacing, or number of tube-side passes. Considerable skill and judgement is required by the thermal design engineer at this stage to decide how the tentative design should be changed to provide a rapid solution. The experienced thermal design engineer is often able to decide on the final design from the first or second trial designs.

### 12.4 Tube-side calculations

Heat transfer and pressure loss for single-phase flow inside the tubes of shell-and-tube exchangers are well established and the correlations given

in Chapter 6 may be used. Heat transfer and pressure loss inside tubes for vaporising flow is given by Smith (1987) and for condensing flow in the forthcoming condenser title.

## 12.5 Shell-side calculations

Single-phase shell-side heat transfer and pressure loss calculations are carried out in accordance with the method based on Bell (1963) described below. Before using the method, the presentations of Bell (1984) and Taborek (1983) must be studied closely, so that its principles are understood. Figure 12.3 shows the flow areas involved in the calculations and Table 12.1 lists the formulae for calculating them.

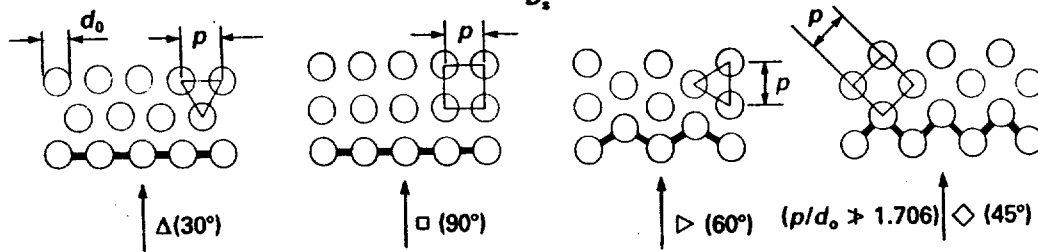
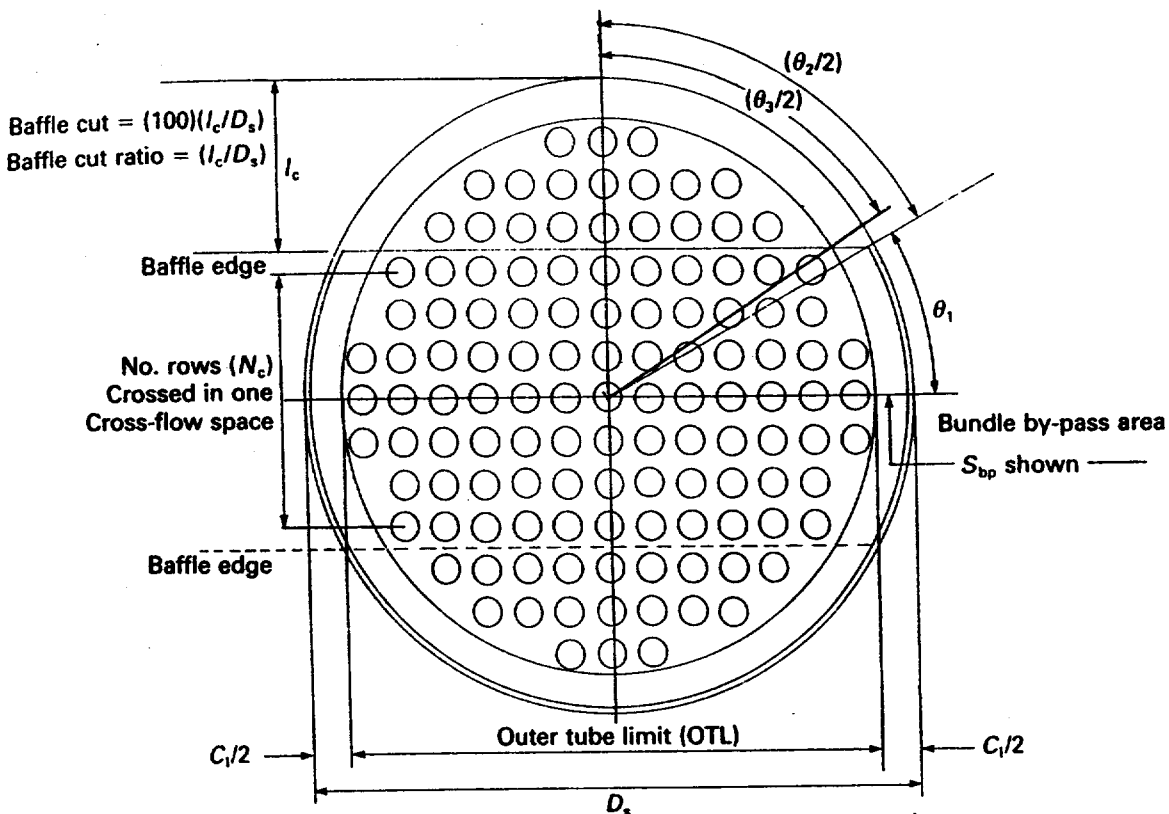
### 12.5.1 Proposed manual method

The basis of the Bell method is to calculate heat transfer coefficient, cross-flow pressure loss and window pressure loss for flow outside an 'ideal' bank of tubes. This is similar to using the ideal model of Fig. 12.1 where no leakage occurs. The coefficient and pressure losses are then multiplied by experimentally determined correction factors to account for leakage due to the A, C and E streams shown in Fig. 12.2, and discussed in section 12.2.2. The correction factors depend on the exchanger geometry and constructional clearances.

The proposed method and data are generally as presented by Bell (1984) except for his factors  $J_1$  and  $R_1$ , where the values recommended by Taborek (1983) have been used. However, over the range of design parameters given in Table 12.2, this change did not affect the results greatly. In addition, heat transfer and pressure loss data for ideal tube banks have been taken from Figs 6.5(a)–(c) and not those presented by Bell or Taborek. To suit the proposed method, the pressure loss curves ( $f_o$  versus Reynolds number) have been replaced by closely fitting straight lines, with the exception of the curves for square ( $90^\circ$ ) pitch in the turbulent region. These curves undulate in this region and a modified procedure is necessary, which is described later. The heat transfer curves ( $J_h$  versus Reynolds number) are straight lines and needed no alteration.

Design factors based on the Bell method, and modifications described above, have been derived for fixed constructional data, representing modern design and manufacturing practice, for 4 exchanger types, 24 shell diameters, 13 common tube configurations, any ratio of baffle space/shell diameter between 0.2 and 1.4, and any tube length. The fixed constructional data are given in Table 12.2, cross-flow areas for calculating shell-side Reynolds number are given in Table 12.3, and design factors are given in Tables 12.4–12.9.

Although derived initially for E-type shells and plain tubes, it will be seen later that the method may be applied to other shell types and low-fin tubes. The method is suitable for both design and rating. Design refers to the determination of the exchanger size and internal geometry from a knowledge of the process data. Rating is the reverse procedure in which



Cross-flow area ( $S_m$ ) shown

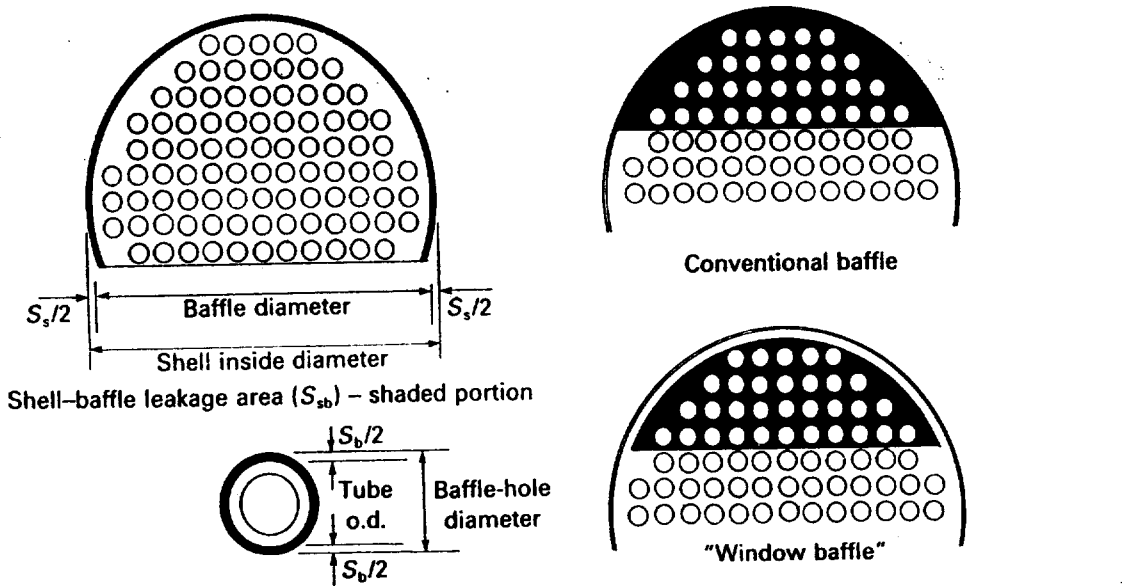


Figure 12.3 Shell-side flow areas



If  $R = 1$ ,

$$F = \frac{2^{1/2} P^*}{(1 - P^*) \ln \left\{ \frac{2 - P^* (2 - 2^{1/2})}{2 - P^* (2 + 2^{1/2})} \right\}}$$

$$\approx \frac{1.4142 P^*}{(1 - P^*) \ln \left\{ \frac{2 - 0.5858 P^*}{2 - 3.4142 P^*} \right\}} \quad [7.7b]$$

#### 7.7.4 Example using formulae

(1) If four  $1/2^+$  shells in series are considered instead of the minimum of 3 in example (2) above, what is  $F$ ?

$N = 4$ ,  $P = 0.75$ ,  $R = 1$ , hence use equations [7.6b] and [7.7b].

From equation [7.6b]:

$$P^* = 0.75 / \{0.75 - (4 \times 0.75) + 4\} = 0.4286$$

From equation [7.7b]:

$$F = \frac{1.4142 \times 0.4286}{(1 - 0.4286) \ln \left\{ \frac{2 - (0.5858 \times 0.4286)}{2 - (3.4142 \times 0.4286)} \right\}} = 0.898$$

A change from three to four shells in series increases MTD by  $(0.898) / (0.81) = 1.11$  times.

#### 7.7.5 Divided-flow shells

$F$  values for divided-flow shells, having two or more even numbers of tube-side passes ( $J/2^+$  exchangers) are identical to the mixed-mixed cross-flow case as given by Taborek (1983), but the  $1/2^+$  E shell given in Fig. 7.2(a) may be used with negligible error. It is assumed that the tube-side fluid enters on the same side as the shell outlet nozzles.

For a quick appraisal,  $F$  values of divided-flow shells having one tube-side pass ( $J/1$  exchangers), are greater than those for  $J/2^+$  exchangers, and therefore,  $1/2^+$  exchangers.

#### 7.7.6 Split-flow shells

$F$  values for single and double split-flow shells, having two or more even numbers of tube-side passes ( $G/2^+$ ,  $H/2^+$  exchangers), are about the same. On the assumption that the tube-side fluid enters on the same side as the shell outlet nozzles, split-flow shells have significantly higher  $F$  values than the  $1/2^+$  exchanger.

#### 7.7.7 Effect of a small number of baffles in a shell-and-tube exchanger

The assumptions made for the derivation of the logarithmic mean

temperature difference were given in section 7.3.1. Assumption (d) of the section states that there must be a 'large' number of baffles in the exchanger, and immediately poses the question as to what is meant by 'large'. Despite the fact that in a 1/1 exchanger, where the shell-side and tube-side fluids enter at opposite ends, the system appears countercurrent, significant errors may be made in the log MTD calculation if assumption (d) is violated. Similar considerations apply to 1/2<sup>+</sup> exchangers.

The whole problem has been re-appraised by Gardner and Taborek (1976) and it was concluded that 1/2<sup>+</sup> exchangers may be designed with the customary MTD correction provided that the number of baffle spaces exceeds five. It was considered that the penalty for fewer baffle spaces was non-existent in some circumstances, and never severe in any practical case.

The minimum number of baffle spaces for 1/1 exchangers cannot be expressed as a single figure and the reader should refer to the publication of Gardner and Taborek (1976), or Caglayan and Buthod (1976). The latter present MTD correction factor curves  $F$  for 1/1 exchangers with 2–7 baffle spaces, and typical values are shown in Table 7.2.

## 7.8 Number of transfer units

The log MTD correction factor ( $F$ ) is ideally suited to design cases where the requirement is to determine the surface area from known flow rates and terminal temperatures. The true mean temperature difference is readily determined from the  $F$  curves and makes the designer immediately aware of the extra surface area which will be required for non-countercurrent flow. However, when the performance of a given unit has to be determined under different process conditions, the problem may be solved using the  $F$  curves, but trial and error is necessary because only two of the terminal temperatures will be known. The concept of the number of transfer units (NTU) provides a rapid, direct, solution to the problem. This popular approach also provides a quick solution to design problems, of course, but the designer is less aware of the penalty paid for non-countercurrent flow.

If  $W$  and  $w$  refer to the hot and cold fluid flow rates, respectively, and  $C$  and  $c$  refer to the hot and cold fluid specific heats respectively, the heat load ( $Q$ ) is given by

$$Q = WC(T_1 - T_2) = wc(t_2 - t_1) \quad [7.8]$$

If  $A$  = surface area and  $U$  = overall heat transfer coefficient, then using the definitions of TEMA (1978):

$$\text{NTU}_c = \frac{UA}{wc} \text{ or } \text{NTU}_h = \frac{UA}{WC} \quad [7.9]$$

From equations [7.4] and [7.8]

$$R = \frac{T_1 - T_2}{t_2 - t_1} = \frac{wc}{WC} \quad [7.10]$$

also  $P = (t_2 - t_1)/(T_1 - t_1)$  from equation [7.5]. The product: (flow

Table 7.2 Shell and tube heat exchangers. One shell pass, countercurrent flow. Approximate values of  $F$  versus  $P$  and  $R$  for 2, 3, 4 and 5 baffle spaces.

$P =$	1 baffle - 2 baffle spaces										2 baffles - 3 baffle spaces										
	0.15	0.2	0.3	0.4	0.5	0.6	0.7	0.8	0.9	0.95	0.15	0.2	0.3	0.4	0.5	0.6	0.7	0.8	0.9	0.95	$= P$
$R$	2 baffles - 3 baffle spaces																				
0.6	$F > 0.98$ in this region										$F < 0.5$ in this region (figures in parenthesis give values of $P$ at which $F = 0.5$ , corresponding to stated values of $R$ )										
0.8	$F > 0.98$ in this region										$F < 0.5$ in this region (figures in parenthesis give values of $P$ at which $F = 0.5$ , corresponding to stated values of $R$ )										
1.0	$F > 0.98$ in this region										$F < 0.5$ in this region (figures in parenthesis give values of $P$ at which $F = 0.5$ , corresponding to stated values of $R$ )										
1.2	$F > 0.98$ in this region										$F < 0.5$ in this region (figures in parenthesis give values of $P$ at which $F = 0.5$ , corresponding to stated values of $R$ )										
1.5	$F > 0.98$ in this region										$F < 0.5$ in this region (figures in parenthesis give values of $P$ at which $F = 0.5$ , corresponding to stated values of $R$ )										
2.0	$F > 0.98$ in this region										$F < 0.5$ in this region (figures in parenthesis give values of $P$ at which $F = 0.5$ , corresponding to stated values of $R$ )										
2.5	$F > 0.98$ in this region										$F < 0.5$ in this region (figures in parenthesis give values of $P$ at which $F = 0.5$ , corresponding to stated values of $R$ )										
3.0	$F > 0.98$ in this region										$F < 0.5$ in this region (figures in parenthesis give values of $P$ at which $F = 0.5$ , corresponding to stated values of $R$ )										
4.0	$F > 0.98$ in this region										$F < 0.5$ in this region (figures in parenthesis give values of $P$ at which $F = 0.5$ , corresponding to stated values of $R$ )										
5.0	$F > 0.98$ in this region										$F < 0.5$ in this region (figures in parenthesis give values of $P$ at which $F = 0.5$ , corresponding to stated values of $R$ )										
$R$	3 baffles - 4 baffle spaces																				
0.6	$F > 0.98$ in this region										$F < 0.5$ in this region (figures in parenthesis give values of $P$ at which $F = 0.5$ , corresponding to stated values of $R$ )										
0.8	$F > 0.98$ in this region										$F < 0.5$ in this region (figures in parenthesis give values of $P$ at which $F = 0.5$ , corresponding to stated values of $R$ )										
1.0	$F > 0.98$ in this region										$F < 0.5$ in this region (figures in parenthesis give values of $P$ at which $F = 0.5$ , corresponding to stated values of $R$ )										
1.2	$F > 0.98$ in this region										$F < 0.5$ in this region (figures in parenthesis give values of $P$ at which $F = 0.5$ , corresponding to stated values of $R$ )										
1.5	$F > 0.98$ in this region										$F < 0.5$ in this region (figures in parenthesis give values of $P$ at which $F = 0.5$ , corresponding to stated values of $R$ )										
2.0	$F > 0.98$ in this region										$F < 0.5$ in this region (figures in parenthesis give values of $P$ at which $F = 0.5$ , corresponding to stated values of $R$ )										
2.5	$F > 0.98$ in this region										$F < 0.5$ in this region (figures in parenthesis give values of $P$ at which $F = 0.5$ , corresponding to stated values of $R$ )										
3.0	$F > 0.98$ in this region										$F < 0.5$ in this region (figures in parenthesis give values of $P$ at which $F = 0.5$ , corresponding to stated values of $R$ )										
$P =$	0.15	0.2	0.3	0.4	0.5	0.6	0.7	0.8	0.9	0.95	0.15	0.2	0.3	0.4	0.5	0.6	0.7	0.8	0.9	0.95	$= P$
$R$	4 baffles - 5 baffle spaces																				
0.6	$F > 0.98$ in this region										$F < 0.5$ in this region (figures in parenthesis give values of $P$ at which $F = 0.5$ , corresponding to stated values of $R$ )										
0.8	$F > 0.98$ in this region										$F < 0.5$ in this region (figures in parenthesis give values of $P$ at which $F = 0.5$ , corresponding to stated values of $R$ )										
1.0	$F > 0.98$ in this region										$F < 0.5$ in this region (figures in parenthesis give values of $P$ at which $F = 0.5$ , corresponding to stated values of $R$ )										
1.2	$F > 0.98$ in this region										$F < 0.5$ in this region (figures in parenthesis give values of $P$ at which $F = 0.5$ , corresponding to stated values of $R$ )										
1.5	$F > 0.98$ in this region										$F < 0.5$ in this region (figures in parenthesis give values of $P$ at which $F = 0.5$ , corresponding to stated values of $R$ )										
2.0	$F > 0.98$ in this region										$F < 0.5$ in this region (figures in parenthesis give values of $P$ at which $F = 0.5$ , corresponding to stated values of $R$ )										
2.5	$F > 0.98$ in this region										$F < 0.5$ in this region (figures in parenthesis give values of $P$ at which $F = 0.5$ , corresponding to stated values of $R$ )										
3.0	$F > 0.98$ in this region										$F < 0.5$ in this region (figures in parenthesis give values of $P$ at which $F = 0.5$ , corresponding to stated values of $R$ )										

Notes: Basis:- Caglayan & Buthod (1976) \*  $P$  value is asymptotic.

rate)  $\times$  (specific heat) is the thermal capacity of the fluid.

Using the above definitions of  $NTU_c$ ,  $P$  and  $R$ , Fig. 7.2(c) shows  $NTU_c$  plotted against  $P$ , with  $R$  as parameter, for a  $1/2^+$  exchanger, as a typical example. This curve will also apply if the alternative values of  $R$  and  $P$  given in section 7.6.1, and  $NTU_h$  from equation [7.9], are used. The 'threshold' line, corresponding to a temperature meet, when  $T_2 = t_2$  and  $P(R + 1) = 1$  is also shown.

NTU curves for a variety of industrial cases are presented by Taborek (1983) and ESDU (1985), which are sometimes known as temperature efficiency curves. When using unfamiliar curves, the definitions of NTU,  $P$  and  $R$  should be checked thoroughly. ESDU, for instance, use the following definitions:

$$\begin{aligned} NTU &= UA/(\text{smaller thermal capacity}) \\ R &= (\text{smaller thermal capacity})/(\text{larger thermal capacity}) \\ \text{and } P &= (\text{larger fluid temperature change})/(\text{temp. diff. } \{(\text{hot fluid in}) - \\ &\quad (\text{cold fluid in})\}) \end{aligned}$$

Figure 7.2(c) will show that the performance of a given exchanger may be determined for various operating conditions, without trial and error. In all cases the terminal temperatures are always related to one another by the following relationships:

$$t_2 - t_1 = P(T_1 - t_1) \quad [7.11]$$

$$T_1 - T_2 = R(t_2 - t_1) \quad [7.12]$$

### 7.8.1 Examples using NTU-P-R curves

(1) A  $1/2^+$  shell-and-tube exchanger is designed to cool 15 kg/s of hot fluid from 200 °C to 120 °C using 37.5 kg/s of coolant entering at 80 °C and leaving at 100 °C. The hot and cold fluid specific heats are 2500 and 4000 J/kg K, respectively, the overall heat transfer coefficient is 500 W/m<sup>2</sup> K and the surface area is 98.4 m<sup>2</sup>. What outlet temperatures would be achieved if the hot and cold fluid inlet temperatures are 190 °C and 95 °C respectively, all other conditions being unchanged? Thus  $U = 500$ ,  $A = 98.4$ ,  $W_h = 15$ ,  $C_h = 2500$ ,  $w = 37.5$ ,  $c = 4000$ ,  $T_1 = 190$ ,  $t_1 = 95$   
Design  $Q = 15 \times 2500 \times (200 - 120) = 37.5 \times 4000 \times (100 - 80) = 3 \times 10^6$  W

From equation [7.9]:

$$NTU_c = (500 \times 98.4)/(37.5 \times 4000) = 0.328$$

From equation [7.10]:

$$R = (37.5 \times 4000)/(15 \times 2500) = 4$$

From Fig. 7.2(c):

$$P = 0.167$$

From equation [7.11]:

$$t_2 = 95 + \{0.167 \times (190 - 95)\} = 110.9 \text{ °C}$$

From equation [7.12]:

$$T_2 = 190 - \{4 \times (110.9 - 95)\} = 126.4 \text{ }^\circ\text{C}$$

$$Q = 15 \times 2500 \times 63.6 = 37.5 \times 4000 \times 15.9 = 2.385 \times 10^6 \text{ W}$$

(2) A  $1/2^+$  shell-and-tube exchanger is designed to cool 15 kg/s of hot fluid from 500 to 300  $^\circ\text{C}$ , using 10 kg/s of coolant entering at 100  $^\circ\text{C}$  and leaving at 200  $^\circ\text{C}$ . The hot and cold fluid specific heats are 1333 and 4000 J/kg K, respectively, the overall heat transfer coefficient is 400 W/m<sup>2</sup>K and the surface area is 43.14 m<sup>2</sup>. At start-up, when the unit is clean, the overall heat transfer coefficient is expected to be 480 W/m<sup>2</sup>K. What outlet temperatures will be achieved at start-up, all other conditions being unchanged?

Thus  $U = 480$ ,  $A = 43.14$ ,  $W = 15$ ,  $C = 1333$ ,  $w = 10$ ,  $c = 4000$ ,  
 $T_1 = 500$ ,  $t_1 = 100$

$$\text{Design } Q = 15 \times 1333 \times 200 = 10 \times 4000 \times 100 = 4 \times 10^6 \text{ W}$$

From equation [7.9]:

$$\text{NTU}_c = (480 \times 43.14)/(10 \times 4000) = 0.518$$

From equation [7.10]:

$$R = (10 \times 4000)/(15 \times 1333) = 2$$

From Fig. 7.2(c):

$$P = 0.274$$

From equation [7.11]:

$$t_2 = 100 + \{0.274 \times (500 - 100)\} = 209.6 \text{ }^\circ\text{C}$$

From equation [7.12]:

$$T_2 = 500 - \{2 \times (209.6 - 100)\} = 280.8 \text{ }^\circ\text{C}$$

$$\text{new } Q = 15 \times 1333 \times 219.2 = 10 \times 4000 \times 109.6 = 4.384 \times 10^6 \text{ W}$$

(3) In the exchanger of example (2), only 7.5 kg/s of coolant is available under emergency conditions. Under these conditions the overall heat transfer coefficient is expected to be 380 W/m<sup>2</sup>K. What outlet temperatures will be achieved, if all other conditions remain unchanged?

Thus  $U = 380$ ,  $A = 43.14$ ,  $W = 15$ ,  $C = 1333$ ,  $w = 7.5$ ,  $c = 4000$ ,

$$T_1 = 500, t_1 = 100$$

From equation [7.9]:

$$\text{NTU}_c = (380 \times 43.14)/(7.5 \times 4000) = 0.546$$

From equation [7.10]:

$$R = (7.5 \times 4000)/(15 \times 1333) = 1.5$$

From Fig. 7.2(c):

$$P = 0.31$$

From equation [7.11]:

$$t_2 = 100 + \{0.31 \times (500 - 100)\} = 224 \text{ }^\circ\text{C}$$

From equation [7.12]:

$$T_2 = 500 - \{1.5 \times (224 - 100)\} = 314^\circ\text{C}$$

$$\text{new } Q = 15 \times 1333 \times 186 = 7.5 \times 4000 \times 124 = 3.72 \times 10^6 \text{ W}$$

## 7.9 Theta method

Taborek (1983) provides a further method for presenting heat exchanger performance.

By definition

$$\theta = \frac{\Delta T_m}{T_1 - t_1} \quad [7.13a]$$

It can also be shown that

$$\theta = \frac{P}{NTU_c} \quad [7.13b]$$

Two sets of curves are presented, one above the other. The upper curves relate  $\theta$  versus  $P$ , with  $R$  as parameter. This permits  $\Delta T_m$  to be determined from equation [7.13a] when  $P$  and  $R$  are known, the separate calculation of  $F$  and  $\Delta T_{lm}$  being unnecessary. Superimposed on these curves are a series of straight lines, each corresponding to a value of  $NTU_c$ . These emanate from the common origin of  $\theta = 0$ ,  $P = 0$ , and express equation [7.13b]. This provides similar information to the temperature efficiency curves such as Fig. 7.2(c), with the added advantage that  $\Delta T_m$  may be determined without separate calculation of  $F$  and  $\Delta T_{lm}$ . The lower curves are the conventional ones relating  $F$  versus  $P$  with  $R$  as parameter, similar to Fig. 7.2(a).

A schematic arrangement is shown in Fig. 7.5 from which it will be seen that all parameters relating to mean temperature difference calculations are available in a single presentation.

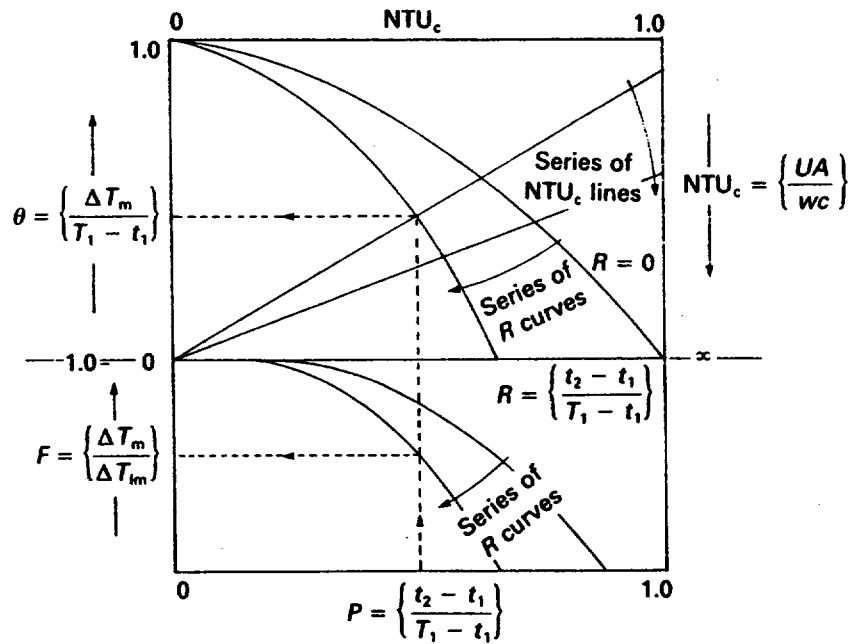
## Acknowledgement

The author is grateful to Dr R. Dodd, Schools of Chemical Engineering, University of Bradford, UK, for the provision of data relating to Fig. 7.2.

## References

A list of addresses for the service organisations is provided on p. xvi.

- Caglayan, A. N. and Buthod, P. (1976) 'Factors correct air-cooler and S & T Exchanger LMTD', *Oil & Gas Journal* (6 Sept.), pp. 91-4.
- Dodd, R. (1980) 'Temperature efficiency of heat exchangers with one shell pass and even number of tube passes', *Proc. 2nd World Congress in Chemical Engineering (Montreal)*, Vol. 4, pp. 463-7.
- Engineering Sciences Data Unit International Ltd, (1985) *Effectiveness - NTU Relationships for the Design and Performance Evaluation of Two-Stream Heat Exchangers*. ESDU Publication No. 85042.
- Gardner, K. and Taborek, J. (1976) *ASME-AIChE 16th National Heat Transfer*



**Figure 7.5** Schematic arrangement of  $F$ ,  $NTU_c$ , and  $\theta$  curves

Conference, *Session on Process Heat Transfer*, St Louis, Missouri.  
 Kern, D. Q. (1950) *Process Heat Transfer*. McGraw-Hill Inc., New York.  
 Taborek, J. (1983) *Heat Exchanger Design Handbook*, Vol. 1, Section 1.5. Hemisphere Publishing Corp.  
 Tubular Exchanger Manufacturers Association, Inc. (1978) *Standards of Tubular Exchanger Manufacturers Association* (6th edn). TEMA, New York, USA.

### Nomenclature

Symbol	Description	Units
$A$	Surface area	$m^2$
$c, C$	Specific heat of cold and hot fluid, respectively	$J/kg\ K$
$F$	Correction factor applied to log MTD (equation [7.3])	—
$m$	Number of shell-side passes	—
$n$	Number of tube-side passes	—
$N$	Number of exchangers in series	—
$NTU$	Number of transfer units (equation [7.9])	—
$P, P^*$	Thermal effectiveness (equations [7.5] and [7.6] respectively)	—
$Q$	Heat load	$W$
$R$	Heat capacity ratio (equations [7.4] and [7.10])	—
$t$	Cold fluid temperature: $t_1 =$ inlet, $t_2 =$ outlet	$K$
$T$	Hot fluid temperature: $T_1 =$ inlet, $T_2 =$ outlet	$K$
$w, W$	Mass flow rate: cold and hot fluid, respectively	$kg/s$
$\Delta T$	Temperature difference (between hot and cold fluids): $\Delta T_c$ at cold end, $\Delta T_h$ at hot end, $\Delta T_{lm}$ = logarithmic mean (equation [7.1]), $\Delta T_m$ = true or effective (equation [7.3])	$K$
$U$	Overall heat transfer coefficient, $U_c$ at cold end, $U_h$ at hot end	$W/m^2\ K$
$\theta$	Parameter defined by equation [7.13]	—

# Fouling

### 8.1 Fouling mechanisms

Fouling may be defined as any undesirable deposits on a heat transfer surface which increase resistance to both heat transfer and fluid flow. Somerscales (1980) identifies six categories of thermal fouling, the categories being based on the immediate cause of fouling, i.e. according to the dominant, but not necessarily the rate-controlling, fouling mechanism. He notes that categories (1) and (6) usually involve surface crystallisation (crystallisation fouling). Among categories (1)–(5), which are generally promoted by liquid heating, there are often strong interactions, which usually have mutually reinforcing effects, although occasionally there may be weakening effects. Category (6), alone, is promoted by liquid cooling.

- (1) *Precipitation fouling*. This relates to the precipitation of dissolved substances on the heat transfer surface. Certain dissolved substances, such as calcium sulphate, magnesium silicate and lithium carbonate, for instance, have inverse solubility versus temperature characteristics, and precipitation occurs on superheated rather than sub-cooled surfaces. This process is often referred to as *scaling*.
- (2) *Particulate fouling*. This occurs when finely divided solids (rust, dust, sand, etc.) suspended in the process fluid accumulate on the heat transfer surface. If the solids settle by gravity the process is referred to as *sedimentation* fouling.
- (3) *Chemical reaction fouling*. Deposits formed by chemical reactions at the heat transfer surface, where the surface material itself is not a reactant, describe this category. Polymerisation, cracking and coking of hydrocarbons are typical examples.
- (4) *Corrosion fouling*. As the name implies the heat transfer surface itself reacts to produce adherent corrosion products. These products may in turn promote the attachment of other fouling materials.
- (5) *Biological fouling*. This relates to biological organisms which adhere to the heat transfer surface. Adherent slimes may also be generated.
- (6) *Freezing fouling*. This occurs as a result of the solidification of a liquid, or some of its higher melting components, on a sub-cooled heat transfer surface.



## 8.2 Fouling growth

It is convenient to record the extent of fouling in terms of its resistance to heat transfer (reciprocal of its conductance) rather than the thickness of the fouling layer. Figure 8.1 illustrates various ways in which fouling resistance increases with respect to time. In Fig. 8.1(a) the deposition rate of the foulant is greater than the removal rate such that the fouling resistance increases linearly with time. Regular cleaning of the unit would be required to remove fouling. In Fig. 8.1(b) the fouling resistance increases initially, but eventually assumes a constant value (asymptotic fouling resistance). Evidently some mechanism causes the adhesion characteristics of the foulant to weaken as the thickness of the foulant increases. If the asymptotic fouling resistance could be predicted with confidence, heat transfer equipment could be designed which would operate continuously.

Figure 8.1 Fouling resistance versus time

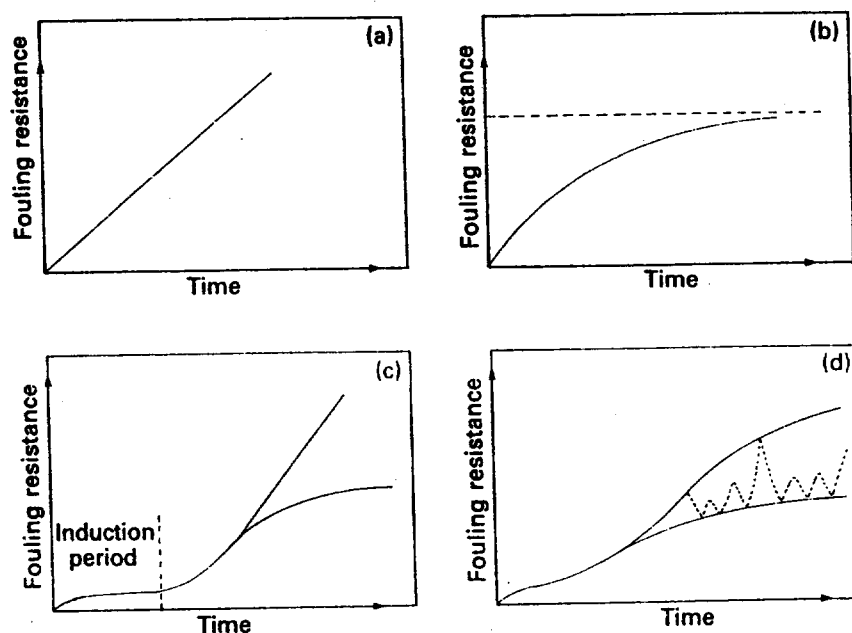


Figure 8.1(c) shows curves similar to Figs 8.1(a) and 8.1(b), except that a rapid growth of the foulant is preceded by an initial induction period during which foulant deposition is low. Figure 8.1(d) also shows curves similar to Figs 8.1(a) and 8.1(b), but after an initial induction period the fouling resistance fluctuates, as shown by the broken lines. The lower line is indicative of a non-removable base foulant on which a removable loose-type deposit forms and then breaks away. The design of an exchanger would probably be based on a mean line between the upper and lower lines.

Watkinson and Epstein (1970) observed that an incompletely cleaned exchanger, after being put into service again, fouled at a faster rate than a thoroughly cleaned one.

### 8.3 Cost of fouling

Von Nostrand *et al.* (1981) estimated the total cost of fouling for petroleum refining in the non-Communist countries as \$4.41 billion per year. Pritchard (1981) estimated the total cost of fouling in the United Kingdom as £300–£500 million per year based on 1978 values. These depressing values are based on additional capital, energy, maintenance and shutdown costs as a result of fouling. A breakdown of Pritchard's costs is given below.

#### Capital costs

These arise from several sources. Heat transfer equipment must be provided with additional surface area to compensate for the reduction in heat transfer due to fouling. The increase in exchanger size generates increased installation costs, while restriction of the flow passages due to fouling causes increased pressure loss, which necessitates larger pumps and motors. Additional capital costs are required for industrial water-treatment plant and the provision of design features to ease dismantling and cleaning during maintenance.

The total annual capital cost in the UK due to fouling is estimated to be £100 million.

#### Energy costs

These are incurred in providing increased pumping power to meet increased pressure loss, while in refrigerators and power condensers the thermal efficiency may be lowered due to fouling.

The total annual energy cost in the UK due to fouling is estimated to be £60 million.

#### Maintenance costs

These arise from dismantling, cleaning and reassembly of heat transfer equipment, together with the operation of water-treatment plant and the cost of chemicals and other additives to reduce fouling.

The total annual maintenance cost in the UK due to fouling is estimated to be £80 million.

#### Shutdown costs

The value of lost production which occurs when heat transfer equipment is shut down due solely to fouling is difficult to assess, but it is estimated that the total shutdown cost in the UK due to fouling is £60 million.

#### Total costs

These total £300 million (1978 values), but Pritchard considers that this value may be low and the true cost may be nearer £500 million.

### 8.4 Design considerations

Having designed the heat transfer equipment for 'clean' conditions, the thermal design engineer must cater for 'fouled' conditions if frequent

cleaning is to be avoided. Depending on the extent of fouling, thermal performance may decrease rapidly below the design duty, and/or the pressure loss may increase rapidly to an unacceptable level, unless suitable provision is made. The thermal design of the equipment for clean conditions may have involved the use of a highly sophisticated computer program (developed by one of the cooperative research organisations), which required considerable research, testing, analysis, etc., at a multi-million pound cost. The thermal designer is unlikely to find the same degree of sophistication when dealing with fouling.

In most cases, neither the composition of the foulant nor its thermal conductivity will be known. Even if thermal conductivity is known, it is unlikely to be of assistance, particularly in the shell-side design of a shell-and-tube exchanger, as the designer will be unable to predict where the foulant will be deposited, or its thickness. In addition, it is unlikely that the designer will know the rate at which the fouling layer thickness increases with time, or how the equipment will be operated with respect to changes in throughput and temperature. As a result it will not be possible to predict the time that will elapse before heat transfer or pressure loss reach unacceptable levels and cleaning becomes necessary – one can only guarantee that the equipment performance at commissioning will not be less than the design duty. Despite the problems associated with fouling some users demand that performance is 'guaranteed under fouled conditions', which implies that it must never fall below the design duty during its lifetime.

#### 8.4.1 Heat transfer calculations

##### Cleanliness and fouling factors

With regard to the heat transfer calculations the thermal design engineer must resort to the use of cleanliness factors, or fouling factors, unless data, based on identical operating conditions, are available. Cleanliness factors are chiefly used in steam surface condenser design and as the services tend to be similar they can be predicted with more reliability than fouling factors. If  $U_D$  = overall heat transfer coefficient under fouled conditions, and  $U_c$  = overall heat transfer coefficient under clean conditions, the cleanliness factor is defined as  $U_D/U_c$ .

The fouling factor concept assumes that the foulant covers the entire heat transfer surface with a uniform thickness and the fouling factor is the anticipated resistance (reciprocal of heat transfer coefficient) to heat transfer of the fouling layer. The assumed temperature profile is shown in Fig. 6.3 and, in the case of a tube, the overall heat transfer coefficient is calculated from:

$$\frac{1}{U_D} = \left\{ \frac{1}{\alpha_o} + \left( \frac{1}{\alpha_i} \right) \left( \frac{d_o}{d_i} \right) + r_w \right\} + \left\{ r_o + r_i \left( \frac{d_o}{d_i} \right) \right\} \quad [8.1a]$$

$$= \left\{ \frac{1}{\alpha_o} + \left( \frac{1}{\alpha_i} \right) \left( \frac{d_o}{d_i} \right) + r_w \right\} + \left\{ \text{sum of fouling factors} \right\} \quad [8.1b]$$

$$= \frac{1}{U_c} + (\text{total resistance due to fouling}) \quad [8.1c]$$

where  $U_D, U_c$  = fouled and clean overall heat transfer coefficients, respectively, referred to outside of tube  
 $\alpha_o, \alpha_i$  = film heat transfer coefficients, outside and inside the tube, respectively, under clean conditions  
 $r_w$  = resistance of tube wall, referred to outer surface  
 $r_o, r_i$  = fouling factor on outer and inner surfaces, respectively  
 $d_o, d_i$  = tube outer and inner diameter, respectively.

A similar treatment is given to non-tubular equipment and in all cases each coefficient must be related to the chosen reference surface. This includes the fouling factors which are assumed to apply to the surface on which they occur. In the case of shell-and-tube exchangers, at least, it is not usual to attempt to alter the clean film heat transfer coefficients arising from velocity changes due to the blockage of the flow passages by the foulants.

#### Source of fouling factors

Typical fouling factors are given in Chapter 19, but the principal published source is TEMA (1978) which provides data for a modest range of industrial applications with particular emphasis on petroleum refining. *Although heavily criticised these have served industry for over forty years and may well continue to do so for many more.* The criticisms are: (a) the continuous operating period which the fouling factors are intended to achieve is not stated, (b) the fouling factors appear to relate to shell-and-tube exchangers, but no distinction is made between shell-sides and tube-sides, (c) no mention is made of tube size and pitch, (d) where fouling factors are related to temperature, the fluid bulk temperature is specified rather than the surface temperature, (e) fouling factors, related to bulk temperature and fluid velocity, are given for water and crude-oil streams, but not for other fluids and (f) the source of the data is not stated.

#### Effect on surface area

The fouling factors provided by TEMA may increase the clean surface area considerably and virtually dominate the design, a typical example being a water/water shell-and-tube exchanger. External and internal heat transfer coefficients of  $5680 \text{ W/m}^2 \text{ K}$  ( $1000 \text{ Btu/hr ft}^2 \text{ }^\circ\text{F}$ ) are readily achieved, giving a clean overall heat transfer coefficient of  $2840 \text{ W/m}^2 \text{ K}$  ( $500 \text{ Btu/hr ft}^2 \text{ }^\circ\text{F}$ ). A total fouling factor of  $0.000528 \text{ (W/m}^2 \text{ K)}^{-1}$  or  $0.003 \text{ (Btu/hr ft}^2 \text{ }^\circ\text{F)}^{-1}$  is typical, giving a fouled overall heat transfer coefficient of  $1136 \text{ W/m}^2 \text{ K}$  ( $200 \text{ Btu/hr ft}^2 \text{ }^\circ\text{F}$ ). In this example the surface area required to account for fouling is 2.5 times that of the clean exchanger.

In some cases the fouling factors provided by TEMA may increase the clean surface area by only a small amount. A typical clean overall heat transfer coefficient for a steam/fuel-oil exchanger is  $114 \text{ W/m}^2 \text{ K}$  ( $20 \text{ Btu/hr ft}^2 \text{ }^\circ\text{F}$ ) and a typical overall fouling factor is  $0.00097 \text{ (W/m}^2 \text{ K)}^{-1}$  or  $0.0055 \text{ (Btu/hr ft}^2 \text{ }^\circ\text{F)}^{-1}$  giving a fouled overall heat transfer coefficient of  $102.6 \text{ W/m}^2 \text{ K}$  ( $18.0 \text{ Btu/hr ft}^2 \text{ }^\circ\text{F}$ ). In this example the surface area required to account for fouling is only 1.11 times that of the clean exchanger.

For simplicity in these examples, tube-wall resistance has been ignored and all coefficients are related to the same reference surface. In order to meet standards imposed by the user, such as tube length, for instance, the designer may have to provide even greater oversurface.

#### Effect on performance

Although greater oversurface may achieve greater on-stream life in many cases, it may achieve the opposite effect. In its early life the duty of the water/water exchanger cited above is easily achieved as it has considerable oversurface. If the cooling water flow is reduced to avoid overcooling the hot stream, the reduced water velocity and the resulting higher wall temperature may produce rapid fouling. Another example is an oversized kettle reboiler, in which the design temperature difference imposed on the unit at start-up, may produce film boiling, with a higher wall temperature, which in turn may produce rapid fouling.

### 8.4.2 Pressure loss calculations

Despite its deficiencies the fouling factor concept in heat transfer calculations is well established, being defined by equations [8.1a]–[8.1c]. The fouling factors are of little assistance in the case of pressure loss calculations. Modern thermal design programs for shell-and-tube exchangers permit the selection of whatever inherent shell-side constructional clearances are required. This allows the selection of reduced, or zero, clearances for shell/baffle, baffle hole/tube and inter-tube gaps to simulate partial or complete blockage by fouling, assuming uniform foulant deposition over the entire external tube surface. Unfortunately, the fouling layer thickness or its distribution over the surface will not be known.

One approximation used in industry is to assume that the fouling layer thickness in inches is the same as the fouling factor in  $(\text{Btu/hr ft}^2 \text{ }^\circ\text{F})^{-1}$  units, which assumes that the foulant always has a thermal conductivity of  $0.0833 \text{ Btu/ft hr } ^\circ\text{F}$ , which is equivalent to that of paper or asbestos at  $0^\circ\text{C}$ .

A more widely used approach for shell-and-tube exchangers, using modern computer programs, is to calculate the pressure loss for fouled conditions assuming that the foulant completely blocks the baffle hole/tube gap. It is assumed that the shell/baffle and inter-tube gaps are completely clear. Table 8.1 provides the *calculated* ratio of fouled/clean pressure loss for various fouling layer thicknesses affecting the baffle hole/tube and inter-tube gaps. The ratios are tabulated for the split backing ring floating-head type only, because exchanger type has little effect on this ratio. The calculated results are considerably influenced by tube configuration and ratio of baffle space/shell diameter for a given degree of fouling. It is questionable whether this approach is realistic; the inference that fouling will have less effect on pressure loss as the baffle space and cut increase, does not accord with practice. (See section 8.6.3 – Stagnant areas.)

The manual method presented in Chapter 12 does not provide data to

enable the user to calculate the shell side pressure loss when only the baffle/tube gap is completely blocked, with no fouling layer on the tube surface. A conservative approach for the manual method is to calculate the cross flow pressure loss for an 'ideal' exchanger, as described in section 12.5.5. In an 'ideal' exchanger, both shell/baffle and baffle/tube gaps are blocked. A comparison between manual and proprietary computer methods is given in Table 8.2, which confirms that the proposed manual approach does over-predict cross flow pressure loss considerably.

In the case of flow outside tubes, the increase in pressure loss due to the presence of a known fouling layer is readily calculated. As an approximation, it may be assumed that the fouled/clean pressure loss ratio, due to a uniform fouling layer, at the same flow rate and baffle spacing, is  $\{G/(G - 2F_L)\}^2$  where  $G$  is the design gap between adjacent tubes and  $F_L$  is the fouling layer thickness.

In the case of flow inside tubes, the increase in pressure loss due to the presence of a known fouling layer is readily calculated. As an approximation, it may be assumed that the fouled/clean frictional pressure loss ratio, due to a uniform fouling layer, at the same flow rate, is  $(d_c/d_f)^5$  where  $d_c$  and  $d_f$  are the clean and fouled tube bores respectively.

## 8.5 Fouling research

The cost of fouling is so high that there would appear little difficulty in justifying extensive research into the problem. Although its importance has always been recognised, it is only in recent years that it has been given considerable attention. Taborek *et al.* (1972), for instance, remind us that (up to 1972) there was not a single representative reference book dealing with the subject, and heat transfer texts rarely acknowledged its existence, despite the fact that in many cases it represents the major resistance to heat transfer.

In the past, fouling factors have been used to provide a margin of safety where thermal design methods were considered unreliable, but as a result of the activities of the cooperative research organisations, discussed in section 6.9, this is seldom the situation facing the thermal design engineer today. There would appear to be little purpose in continuing research to improve heat transfer equipment design unless it is matched by an improved knowledge of fouling.

The lack of attention given to the problem of fouling in the past may be criticised, but it is an extremely complex phenomenon which lacks repeatability, and makes a systematic programme of research difficult to define. Nevertheless, various organisations are now conducting vigorous research into the many aspects of fouling. One aspect is to obtain a better understanding of the complex processes of foulant deposition and breakaway. Another involves the use of both laboratory and field rigs to obtain general fouling data, with water being the most thoroughly

investigated fluid. Although valuable, it may prove difficult to adapt such data to provide reliable full-scale equipment design. The use of anti-foulants in the form of fluid dosing, surface treatment and on-line cleaning form other lines of investigation, although the latter may only be suited to large plants.

At present fouling remains the 'major unresolved problem in heat transfer' (Taborek *et al.* 1972) and the thermal design engineer is 'restricted to the mythology of fouling factors' (Hewitt 1981).

Table 8.1 Typical calculated ratios of fouled:clean pressure loss for shell-side flow

Shell inside diameter = 489 mm (19 1/4 in)												
Tube outside diam. (mm)	Tube pitch (mm)	Pitch angle (deg grees)	Flow rate (kg/s)	BSR	Baffle hole/tube diametral clearance					Pitch angle (deg rees)	Tube pitch (in)	Tube outside diam. (in)
					0.65 mm (0.0256 in)	0.4 mm (0.0156 in)	nil	nil	nil			
					Fouling layer thickness on outside of tubes							
					nil	nil	nil	0.325 mm (0.0128 in)	0.65 mm (0.0256 in)			
15.88	19.84	30	17.6	0.2	1.0	1.52	3.34	3.79	4.56	30	25/32	5/8
19.05	23.81	30		0.2	1.0	1.43	2.71	3.03	3.52	30	15/16	3/4
25.40	31.75	30		0.2	1.0	1.32	2.08	2.27	2.56	30	1 1/4	1
25.40	31.75	90		0.2	1.0	1.26	1.85	2.03	2.31	90	1 1/4	1
31.75	39.69	45		0.2	1.0	1.18	1.54	1.67	1.87	45	1 5/16	1 1/4
15.88	19.84	30		1.4*	1.0	1.12	1.21	1.44	1.79	30	25/32	5/8
19.05	23.81	30		1.4	1.0	1.10	1.15	1.35	1.60	30	15/16	3/4
25.40	31.75	30		1.4	1.0	1.06	1.09	1.23	1.40	30	1 1/4	1
25.40	31.75	90		1.4	1.0	1.03	1.07	1.17	1.31	90	1 1/4	1
31.75	39.69	45		1.4	1.0	1.01	1.04	1.13	1.21	45	1 5/16	1 1/4

Shell inside diameter = 489 mm (19 1/4 in)												
Tube outside diam. (mm)	Tube pitch (mm)	Pitch angle (deg grees)	Flow rate (kg/s)	BSR	Baffle hole/tube diametral clearance					Pitch angle (deg rees)	Tube pitch (in)	Tube outside diam. (in)
					0.65 mm (0.0256 in)	0.4 mm (0.0156 in)	nil	nil	nil			
					Fouling layer thickness on outside of tubes							
					nil	nil	nil	0.325 mm (0.0128 in)	0.65 mm (0.0256 in)			
15.88	19.84	30	37.8	0.2	1.0	1.84	5.87	7.07	8.94	30	25/32	5/8
19.05	23.81	30		0.2	1.0	1.52	4.46	5.16	6.09	30	15/26	3/4
25.40	31.75	30		0.2	1.0	1.44	3.05	3.41	3.81	30	1 1/4	1
25.40	31.75	30		0.2	1.0	1.56	2.89	3.24	3.59	90	1 1/4	1
31.75	39.69	45		0.2	1.0	1.31	2.55	2.86	3.23	45	1 5/16	1 1/4
15.88	19.84	30		0.6	1.0	1.36	1.80	2.40	3.21	30	25/32	5/8
19.05	23.81	30		0.6	1.0	1.28	1.58	2.00	2.47	30	15/26	3/4
25.40	31.75	30		1.0*	1.0	1.11	1.17	1.43	1.66	30	1 1/4	1
25.40	31.75	30		1.0*	1.0	1.08	1.10	1.38	1.58	90	1 1/4	1
31.75	39.69	45		1.0	1.0	1.06	1.07	1.28	1.41	45	1 5/16	1 1/4

Table 8.1 (cont.)

Shell inside diameter = 489 mm (19 1/4 in)												
Tube outside diam. (mm)	Tube pitch (mm)	Pitch angle (deg grees)	Flow rate (kg/s)	BSR	Baffle hole/tube diametral clearance					Pitch angle (deg rees)	Tube pitch (in)	Tube outside diam. (in)
					0.65 mm (0.0256 in)	0.4 mm (0.0156 in)	nil	nil	nil			
					Fouling layer thickness on outside of tubes							
					nil	nil	nil	0.325 mm (0.0128 in)	0.65 mm (0.0256 in)			
15.88	19.84	30	47.8	0.2	1.0	2.00	6.59	7.74	9.34	30	25/32	5 1/4
19.05	23.81	30		0.2	1.0	1.86	5.08	5.80	6.69	30	15/16	5 1/4
25.40	31.75	30		0.2	1.0	1.65	3.80	3.87	4.29	90	1 1/4	1
25.40	31.75	90		0.2	1.0	1.56	2.89	3.24	3.59	90	1 1/4	1
31.75	39.69	45		0.2	1.0	1.40	2.15	2.34	2.57	45	1 3/8	1 1/4
15.88	19.84	30		0.4	1.0	1.67	2.72	3.50	4.50	30	25/32	5 1/4
19.05	23.81	30		0.6*	1.0	1.32	1.58	2.05	2.53	30	15/16	5 1/4
25.40	31.75	30		0.6	1.0	1.24	1.41	1.76	2.00	30	1 1/4	1
25.40	31.75	90		0.6	1.0	1.15	1.27	1.53	1.73	90	1 1/4	1
31.75	39.69	45		0.6	1.0	1.18	1.17	1.45	1.64	45	1 3/8	1 1/4

Notes:

- (1) Results based on HTRI proprietary program.
- (2) Shell-side pressure loss ratios are based on central bundle loss, i.e. exclude end space and nozzle losses.
- (3) Pressure losses based on water at average temperature of 70 °C (158 °F).
- (4) Exchanger type = split backing ring floating head (AES).
- (5) Baffles = single segmental type.
- (6) Shell-bundle and shell-baffle clearances are based on Table 12.2.
- (7) Reynolds number range = 4000 - 180000.
- (8) Fouling layer assumed to be uniform over entire external surface.
- (9) (BSR) = baffle spacing ratio = baffle space/shell diameter.
- (10) Baffle spacing greater than TEMA maxima for steel tubes are denoted by \*

Table 8.2 Shell-side cross flow pressure loss due to blockage – comparison of manual and proprietary computer methods

Example no.	Design no.	'Ideal' exchanger: shell/baffle and baffle/tube gaps blocked	'Real' exchanger: baffle/tube gap only blocked	'Real' exchanger: basic design without blockage
1		2.51	1.70	1.00
2	A	1.64	1.23	1.00
	B	2.01	1.46	1.00
3	A	2.45	1.52	1.00
	B	1.79	1.10	1.00
	C	1.84	1.15	1.00
7		2.05	1.35	1.00
Calculation method		Manual – as chapters 12 and 13	Proprietary computer program (HTRI)	



## 8.6 Design to minimise fouling

As it is almost impossible to forecast the fouling tendency of new heat transfer equipment, previous operational experience under similar process conditions should be sought. If such data are not available the most important decisions to be made at the design stage are the choice of exchanger type and its material of construction.

### 8.6.1 Exchanger type

Part 1 describes many types of heat transfer equipment available to the designer and their advantages and disadvantages are summarised in Table A1.1 of Part 1 Appendix. If fouling is expected to be a problem, first considerations would be given to gasketed-plate, spiral, graphite or Teflon™ types. However, all have pressure and temperature limitations and the graphite and Teflon™ types are limited with regard to size. If the heating medium is fouling, electrically heated exchangers should be considered.

If the choice must be a shell-and-tube exchanger, it is important to ensure that its type, routing of the fluids, head type and tube configuration follows the guidelines of Chapter 1 in order to ease cleaning.

### 8.6.2 Materials of construction

Corrosion arising from an incorrect choice of material not only reduces the equipment life, but blockage of the exchanger passages due to deposition of corrosion products may result in frequent, costly shutdowns for cleaning. Materials should therefore be selected on the basis of minimising overall costs within the expected lifespan of the exchanger, rather than initial cost.

Graphite, glass and Teflon™ exchangers provide high corrosion-resistance, while the more expensive metals, such as titanium and high-nickel alloys, can be accommodated more cheaply in the gasketed-plate exchanger than in the shell-and-tube type. If the choice must be a shell-and-tube exchanger, the use of bi-metal barrels, tubesheets and tubes should always be considered to reduce cost. Where dissimilar metals are used, electrical or physical contact between them must be assessed carefully to avoid galvanic corrosion. Non-metallic linings may be a suitable alternative for some applications.

Rough surfaces act as a key for the adhesion of deposits; once the build up of deposits begins the rough fouling layer encourages more growth, and so on. Surface finish is important and exchangers with 'smooth' surfaces are preferred and include those constructed of graphite, glass and Teflon™. The flexibility of the latter's tubes is also claimed to assist in shedding deposits. Chapter 18 describes shell-and-tube exchangers with phenolic resin-lined tubes having 'non-stick' properties.

Chapter 19 provides cost data for various exchanger types and Chapter 18 describes materials of construction.

### 8.6.3 Design features

Whatever type of heat exchanger is chosen, certain common design factors relating to fouling must always be considered.

#### Velocity

The exchanger must be designed with fluid velocities which will discourage fouling and they depend on the type of unit, its material and related erosion/corrosion characteristics. Typical tube-side velocities for shell-and-tube exchangers, for various materials, are given in Table 18.2. Although fouling may be avoided at design throughput, the performance of the exchanger should be assessed under turndown conditions. Unless considered at the design stage, reduced velocities at low throughput may result in rapid fouling. The velocities must be checked in nozzles and headers in addition to the flow passages.

In order to achieve the required velocities, the user may have to permit higher pressure losses than normal. Despite the importance of energy saving, increased pressure losses may be justified if this provides greater on-stream life.

#### Flow distribution

Having decided on the velocities required to minimise fouling the design of the exchanger should be examined to check that these velocities will be achieved and maldistribution of the fluids will not occur. Low velocities in some of the flow passages due to maldistribution encourage deposits to settle. In addition, any reduction in heat transfer coefficient arising from reduced velocities increases the possibility of producing hot or cold spots on the heat transfer surface. In the case of hot spots, where the temperature of the heated fluid approaches that of the heating medium, the fluid may fuse on to the surface. In the case of cold spots, where the temperature of the cooled fluid approaches that of the coolant, the fluid may solidify on the surface.

Spiral and 1/1 double-pipe exchangers have only one flow passage for each fluid so that maldistribution cannot occur. If fouling does occur in these types, the flow passage areas are decreased, but the velocities are increased, which may assist in minimising fouling.

#### Stagnant areas

Low velocities in stagnant areas encourage deposits to settle and the shell-side of shell-and-tube exchangers is particularly prone to this. Deposits tend to build up on both sides of the baffle plates as shown in Fig. 8.2. Gilmour (1965) considered that shell-side fouling occurred chiefly from poor design and most of his advice is accepted today: namely (a) the baffle cut should preferably be 20% and should not exceed 25%, (b) have a small shell-baffle clearance, (c) seal-off the shell-bundle gap

with dummy tubes or rods (d) use a tube layout with pass partitions normal to shell-side flow; if the layout (see Figs 1.30 and 1.31) provides pass partitions parallel to the flow direction they must be sealed off with dummy tubes or rods, (e) use only horizontal cut baffles with single-phase fluids and (f) have no drainage or venting notches in baffles.

Deposits are also likely to form in a stagnant area in the header on the tubesheet face, and opposite the shell-side inlet nozzle.

Spiral- and plate-type exchangers have no baffles and therefore no stagnant areas where deposits could build up. They do have headers, however, where stagnant areas must be avoided.

Vents and drains in shells and headers must be correctly positioned to ensure that gases and liquids do not become entrapped and cause localised corrosion. They must also be of adequate size so that they do not become blocked by solid matter.

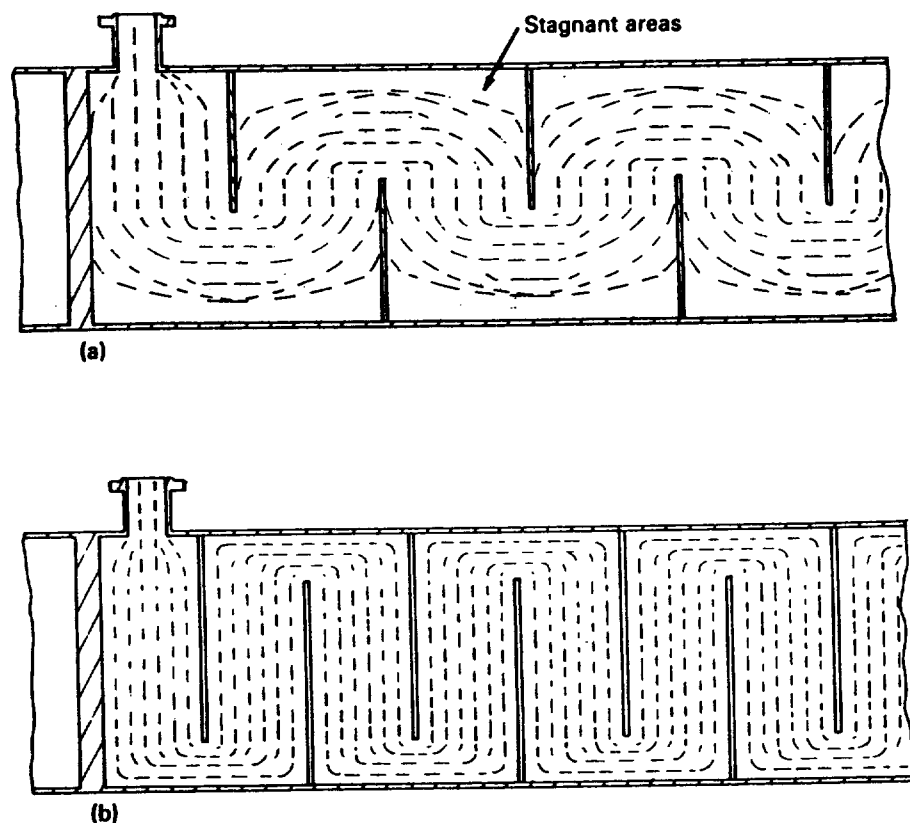
## References

A list of addresses for the service organisations is provided on p. xvi.

Gilmour, C. H. (1965) 'No fooling - no fouling', *Chem. Eng. Progress*, 61 (No. 7), pp. 49-54.

Hewitt, G. F. (1981) 'The potential for development in heat exchanger plant', *Conference on Future Developments in Process Plant Technology*, IMechE Headquarters, 24/25 Feb.

**Figure 8.2** Stagnant areas on shell-side of shell-and-tube exchanger (a) poor design resulting from large baffle cut in relation to baffle space: shell diameter ratio (b) improved design resulting from correctly sized baffle cut in relation to baffle space: shell diameter ratio



- Pritchard, A. M.** (1981) *Fouling of Heat Transfer Equipment* (edited by Somerscales, E.F.C. and Knudsen, J. G.). Hemisphere Publishing Corp.
- Somerscales, E. F. C.** (1981) *Fouling of Heat Transfer Equipment* (edited by Somerscales, E.F.C. and Knudsen, J. G.). Hemisphere Publishing Corp.
- Taborek, J. et al.** (1972) 'Fouling: the major unresolved problem in heat transfer', Parts I and II, *Chem. Eng. Progress*, **68** (No. 2), 59-67, and **68** (No. 7), 69-78.
- Tubular Exchanger Manufacturers Association, Inc.** (1978) *Standards of Tubular Exchanger Manufacturers Association* (6th edn). TEMA, New York, USA.
- Von Nostrand, W. L. et al.** (1981) *Fouling of Heat Transfer Equipment* (edited by Somerscales, E.F.C. and Knudsen, J. G.). Hemisphere Publishing Corp.
- Watkinson, A. P. and Epstein, N.** (1970) 'Particulate fouling of sensible heat exchangers', *4th Int. Heat Transfer Conference*, Paris, Versailles, Paper HE 1.6.

## Extended surfaces

When the heat transfer coefficient on the outside of a tube is much lower than that on the inside, as for example, in oil/steam or low-pressure gas/water exchangers, the use of externally extended surface tubes should be considered. Extended surfaces increase the rate of heat transfer per unit tube length and the resulting exchanger may be smaller and cheaper than the corresponding plain tube exchanger.

A tube surface may be 'extended' by attaching pieces of metal to it in various ways in the form of continuous longitudinal or transverse strips (fins), wire coils, or discontinuous solid studs or spines of different shapes (see Fig. 9.1). A tube surface may be extended on its outer surface, inner surface, or both. If the metal used for extending the tube surface was a perfect heat conductor (i.e. infinite thermal conductivity), the extension would be 100% effective in transferring heat between the fin-side fluid and the tube wall. In practice, of course, this cannot be achieved, and it will be seen from below that there is nothing to be gained by extending the surface beyond that necessary to provide an economic solution. The cost of the metal used for the extension, the cost of forming it to the required shape and the cost of attaching it to the tube must be considered.

The most common form of extended surface is fins.

### 9.1 Fin efficiency

Consider a length of externally finned tube which is receiving heat from the external fluid (Fig. 9.2). In order that heat received by the fin may be conducted through it to the base and thence to the tube-side fluid, a temperature gradient must exist in the fin, the tip being hotter than the root. The effect of the temperature gradient in the fin is to reduce the 'driving force' for heat transfer, i.e. the temperature difference between external fluid and fin. In order to allow for the reduced temperature difference between external fluid and fin, a fin efficiency is introduced into the heat transfer calculations, this being defined as the ratio of the heat actually transferred to the base tube to that which could be transferred with an infinitely conducting fin.

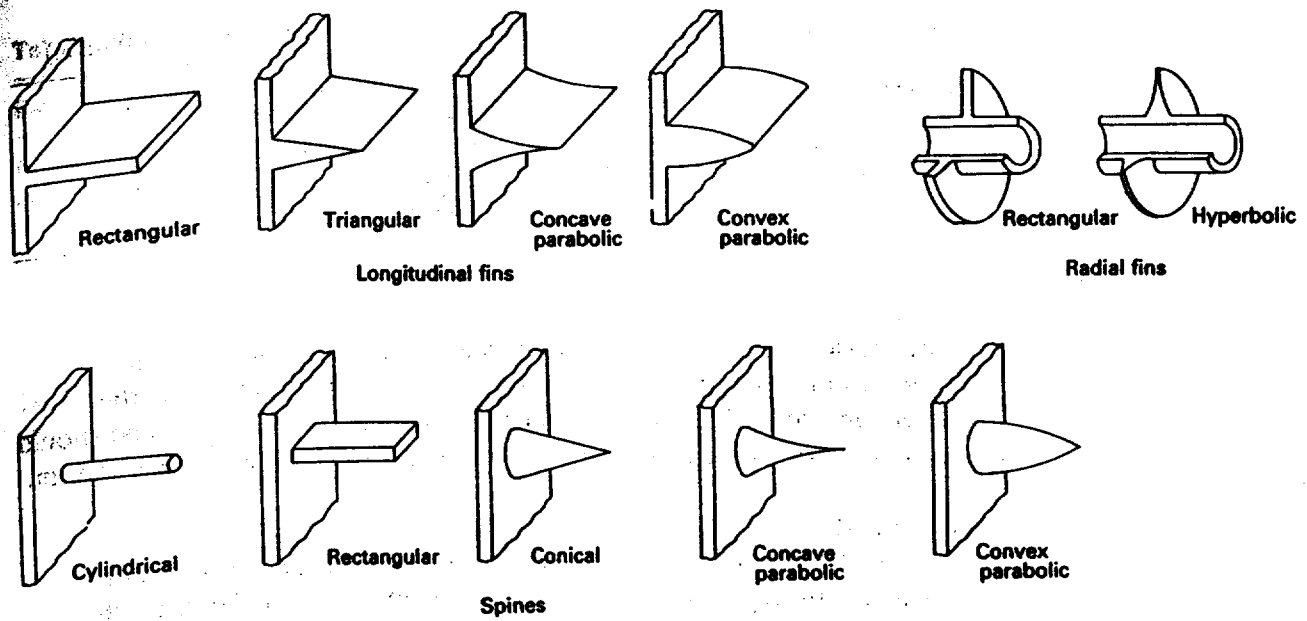


Figure 9.1 Types of extended surface

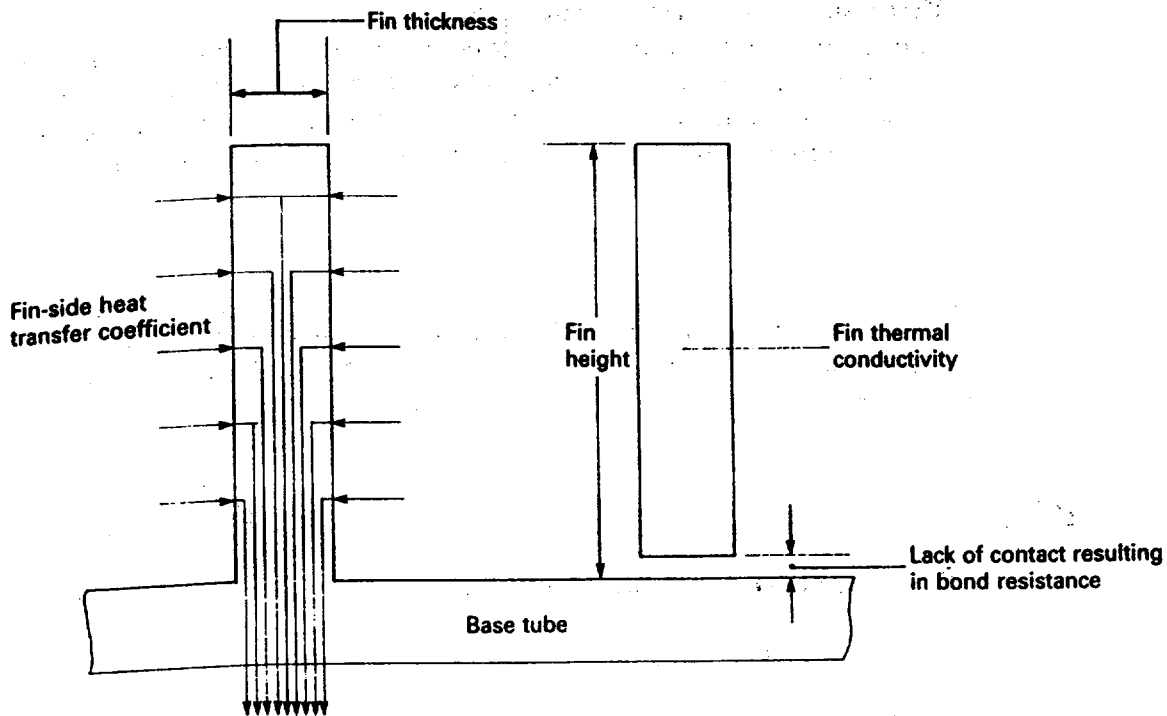


Figure 9.2 Factors affecting fin efficiency

Certain factors affect fin efficiency, and the comments below apply irrespective of whether the tube is finned on the inside or the outside, or whether heat is being transferred to or from the fin.

**Fin thermal conductivity**

The higher its thermal conductivity the higher the fin efficiency, as heat is more readily conducted through the fin. Table 9.1 gives the thermal conductivity for typical fin materials, from which it will be seen that copper has the highest value. Despite this, aluminium or steel is often preferred due to the lower cost. Stainless-steel is a poor fin material because of its high cost and low thermal conductivity.

**Table 9.1** Approx. thermal conductivities of various metals at 100 °C (W/m K)

Copper	389	90/10 Cupro-nickel	52
Aluminium	208	Steel	52
Admiralty brass	121	70/30 Cupro-nickel	35
Aluminium brass	100	Monel	26
Nickel	66	Stainless steel	17

**Fin thickness**

The greater the fin thickness, the higher the fin efficiency, as the cross-sectional area for heat flow is greater. On the other hand, the weight and cost of the fin material are increased. The fin thickness should increase towards the root to match the increasing heat flow down the fin.

**Fin height**

The greater the fin height, the lower the fin efficiency, because heat conducted through the fin has a greater length to travel. On the other hand, the external surface area is increased.

**Heat transfer coefficient to finned surface**

The greater the heat transfer coefficient to the finned surface, the greater the quantity of heat to be conducted through the fin and hence the fin efficiency is lower. The ratio of fin-side to plain base-tube surface areas should be roughly the same as the ratio of plain-side to fin-side heat transfer coefficients.

**Bond resistance**

Although derivations of fin efficiency assume no bond resistance, this is not always the case and depends on the type of finned tube and its fin/tube attachment. Any bond resistance must be included in the heat transfer calculations.

**9.2 Heat transfer calculations****9.2.1 Heat transfer coefficient to finned surface**

The first step is to calculate the heat transfer coefficient to the finned surface ( $\alpha_f$ ), and Chapter 6 provides correlations for longitudinally finned, low-finned and high-finned tubes. Longitudinally finned tubes are used primarily for double-pipe exchangers and fuel-oil heaters. They are described in Chapter 5 and cost data for double-pipe exchangers are given in Chapter 19. Low-fin tubes are used primarily in shell-and-tube exchangers, being described in Chapter 13. The design of shell-and-tube exchangers using low-fin tubes is also given in Chapter 13. High-finned tubes are widely used in air-cooled heat exchangers and the various types are described in Chapter 3.

Certain geometrical factors are required for finned tube calculations and these may be calculated from Table 9.2 and Fig. 9.3.

Table 9.2 Geometrical factors for finned tubes (based on Fig. 9.3)

Fin type	Item		Formulae
Longitudinal (welded U-fins)	Surface per metre length of one tube	Unfinned	$\pi d_r - N_f t_f$
		Finned	$2N_f l_f$
	Free area for flow outside tubes		$A_e - \left\{ \frac{\pi d_r^2}{4} + N_f t_f \left( l_f + \frac{r_f}{2} \right) \right\} N_f$
Longitudinal (extruded fins)	Surface per metre length of one tube	Unfinned	$\pi d_r - N_f t_f$
		Finned	$2N_f l_f + N_f t_f$
	Free area for flow outside tubes		$A_e - \left\{ \frac{\pi d_r^2}{4} + N_f l_f t_f \right\} N_f$
Radial	Surface per metre length of one tube	Unfinned	$\pi N_f d_r s_f$
		Finned	$(\pi/2)N_f(d_f^2 - d_r^2) + \pi N_f d_f t_f$
	Free area ratio		$1 - \left\{ \frac{N_f(d_f t_f + d_r s_f)}{P} \right\}$ (applicable to $\square$ pitch and $\Delta$ pitch where minimum flow area is in transverse pitch in a row)

## Notes:

- (1) Total external surface per metre = unfinned surface per metre + finned surface per metre.
- (2) Longitudinal welded U-fins:  $r_f = 3t_f$  (usually).
- (3)  $A_e$  = total enclosure area containing  $N_f$  longitudinally finned tubes.
- (4)  $P$  = transverse tube pitch for radially finned tubes,  $S_f = (1 - N_f t_f)/N_f$ .
- (5) Free area ratio (FAR) = 
$$\frac{\text{free area for flow outside tubes}}{\text{gross area for flow as though tubes were absent}}$$

## 9.2.2 Calculation of fin efficiency (rectangular longitudinal fins)

If the finned surface has a layer of dirt, the clean fin-side heat transfer coefficient  $\alpha_f$  must be combined with that of the dirt layer, to provide the fouled fin-side heat transfer coefficient  $\alpha'_f$ , as shown by equation [9.1], for use in equations [9.2] and [9.3], i.e.

$$\frac{1}{\alpha'_f} = \frac{1}{\alpha_f} + r_o \quad [9.1]$$

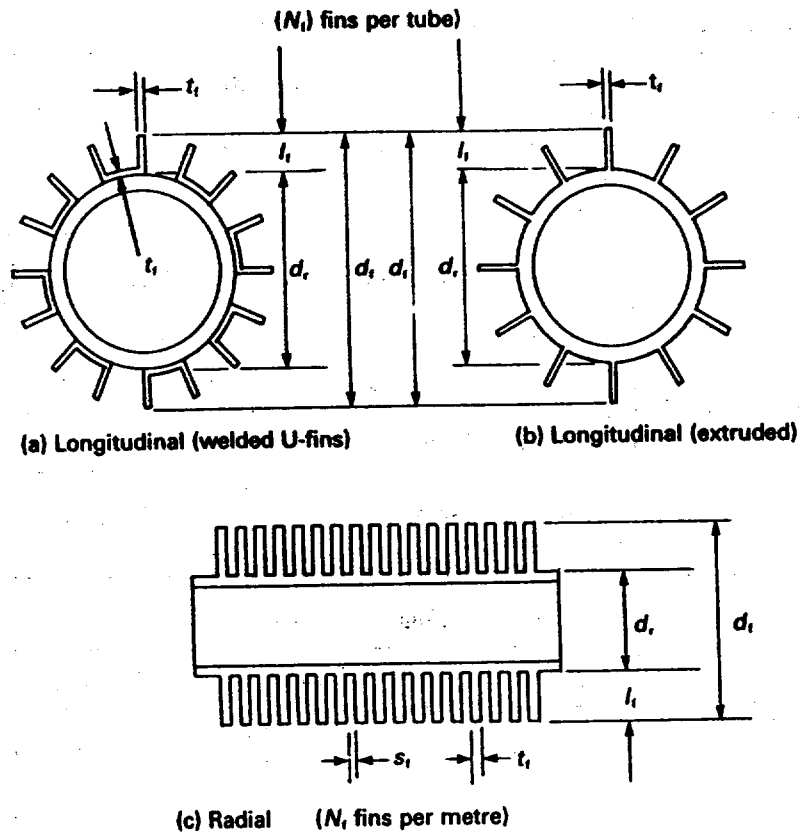
where  $r_o$  = fin-side fouling resistance ( $\text{W/m}^2 \text{K}$ )<sup>-1</sup>.

Having calculated  $\alpha'_f$ , the second step is to calculate the fin efficiency,  $\Omega_f$ . Many textbooks, including Kern and Kraus (1972), for example, cater for fin-efficiency data for a variety of finned tubes, but the fin efficiency for longitudinally finned tubes, *having fins of constant cross-section*, is given by:

$$\Omega_f = \frac{\tanh(ml_f)}{ml_f} \quad [9.2]$$



Figure 9.3 Geometry of finned tubes



where  $m = \left\{ \frac{2\alpha_f}{\lambda_f t_f} \right\}^{1/2}$

$l_f$  = fin height (m)

$t_f$  = fin thickness (m)

$\lambda_f$  = fin thermal conductivity (W/m K)

The derivation of fin efficiency assumes (a) the heat flow is steady, (b) the fin material is homogeneous and of identical composition throughout, (c) there is no heat source within the fin itself, (d) the heat exchange between fin surface and surroundings at any point is proportional to the temperature difference between fin and surroundings at that point, (e) the thermal conductivity of the fin is constant, (f) the fin-side heat transfer coefficient is the same over the entire surface, (g) the temperatures of the surrounding fluid and fin base are uniform, (h) the fin thickness is small in relation to height so that the temperature gradients across fin thickness may be neglected, (j) there is negligible heat flow into the outer fin edge compared with the sides and (k) there is no resistance at the fin-tube junction.

### 9.2.3 Calculation of fin efficiency for other fin types

Longitudinally finned tubes are not restricted to fins having a rectangular profile in which the cross-sectional area is constant. The profile may be triangular or parabolic (concave and convex) and the cross-sectional area is no longer constant. With radially finned tubes the cross-sectional area

**Table 9.3** Equivalent fin thickness and fin height for fin-efficiency calculations

Type of fin	Profile	Actual fin thickness or diameter		Effective fin thickness ( $t_{fe}$ )	Effective fin height ( $l_{fe}$ ) (actual height = $l_f$ )
		At tip	At root		
Longitudinal	Rectangular	$t_f$	$t_f$	$t_f$	$l_f$
Longitudinal	Trapezoidal	$t_{ft}$	$t_{fb}$	$0.75t_{fb} + 0.25t_{ft}$	$l_f$
Radial	Rectangular	$t_f$	$t_f$	$t_f$	} $l_f \left\{ 1 + \frac{t_{fe}}{2l_f} \right\} \left\{ 1 + 0.35 \ln \left( \frac{d_f}{d_r} \right) \right\}$
Radial	Triangular	$t_{ft}$	$t_{fb}$	$0.5(t_{fb} + t_{ft})$	
Spine	Circular	$d_s$	$d_s$	$0.5d_s$	$l_f + 0.25d_s$

Note:  $l_f/t_f > 3$ ,  $d_f/d_r < 3$

**Table 9.4** Fin-efficiency values

$m_e l_{fe}$	$\Omega_f$	$m_e l_{fe}$	$\Omega_f$	$m_e l_{fe}$	$\Omega_f$
0.00	1.000	0.80	0.830	1.55	0.590
0.10	0.997	0.85	0.813	1.60	0.576
0.15	0.993	0.90	0.796	1.65	0.563
0.20	0.987	0.95	0.779	1.70	0.550
0.25	0.980	1.00	0.762	1.75	0.538
0.30	0.971	1.05	0.745	1.80	0.526
0.35	0.961	1.10	0.728	1.85	0.515
0.40	0.950	1.15	0.711	1.90	0.503
0.45	0.938	1.20	0.695	1.95	0.493
0.50	0.924	1.25	0.679	2.00	0.482
0.55	0.910	1.30	0.663	2.05	0.472
0.60	0.895	1.35	0.647	2.10	0.462
0.65	0.880	1.40	0.632	2.15	0.453
0.70	0.863	1.45	0.618	2.20	0.444
0.75	0.847	1.50	0.603	2.25	0.435

Based on equation [9.3] and applicable to fin types listed in Table 9.3

of the fin changes from tip to base, irrespective of whether the profile is rectangular or shaped. The derivation of fin efficiency for these types is more complex and the results are expressed graphically for manual calculations. Kern and Kraus (1972) provide graphical solutions for various shapes of longitudinal fins, radial fins and spines.

Schmidt (1966) showed that within certain limits, equation [9.2] could be used for other fin types, with little error, if the actual fin height ( $l_f$ ) and actual fin thickness ( $t_f$ ) were replaced by an equivalent fin height ( $l_{fe}$ ) and equivalent fin thickness ( $t_{fe}$ ). The general equation is then:

$$\Omega_f = \frac{\tanh(m_e l_{fe})}{m_e l_{fe}} \quad [9.3]$$

$$\text{where } m_e = \left\{ \frac{2\alpha'_f}{\lambda t_{fe}} \right\}^{1/2}$$

Values of  $l_{fe}$  and  $t_{fe}$  are given in Table 9.3 for some industrially important cases. To simplify calculations involving equation [9.3], Table 9.4 provides  $\Omega_f$  for various values of  $m_e l_{fe}$ .

### 9.2.4 Overall heat transfer coefficient

The total extended surface area per unit tube length ( $A_t$ ) is the sum of the area of the finned surface per unit length ( $A_f$ ) and the unfinned, surface area per unit length ( $A_u$ ). The fin-efficiency derivation assumes that the fin-side heat transfer coefficient ( $\alpha'_f$ ) is the same over the entire surface, i.e. applicable to both  $A_f$  and  $A_u$ . The fin-efficiency concept applies only to the finned surface. Hence the effective fin-side heat transfer coefficient ( $\alpha_{fi}$ ), for combining with the other coefficients in the system, is given by

$$\alpha_{fi} A_t = \alpha'_f (\Omega_f A_f + A_u) \quad [9.4]$$

In equation [9.4],  $\alpha_{fi}$  is related to the total external surface, but it may be related to any convenient reference area such as the inside surface of the tube  $A_i$ , or the bare external surface  $A_b$ , as though the fins did not exist, for calculating the overall heat transfer coefficient.

Hence the effective fin-side heat transfer coefficient, related to the inside surface  $\alpha_{fi}$ , is given by:

$$\alpha_{fi} = \frac{\alpha'_f (\Omega_f A_f + A_u)}{A_i} \quad [9.5]$$

$$\text{and } \frac{1}{U_i} = \frac{1}{\alpha_{fi}} + r_{ti} + r_i + \frac{1}{\alpha_i} \quad [9.6]^*$$

or, related to the bare external surface, the effective fin-side heat transfer coefficient ( $\alpha_{fo}$ ) is given by:

$$\alpha_{fo} = \frac{\alpha'_f (\Omega_f A_f + A_u)}{A_b} \quad [9.7]$$

$$\text{and } \frac{1}{U_o} = \frac{1}{\alpha_{fo}} + r_{to} + r_{io} + \frac{1}{\alpha_{io}} \quad [9.8]^*$$

where  $r_i, r_{io}$  = internal fouling resistance, referred to inside surface and bare external surface, respectively ( $\text{W/m}^2 \text{K}$ )<sup>-1</sup>

$r_{ti}, r_{to}$  = tube-wall resistance,† referred to inside surface and bare external surface, respectively ( $\text{W/m}^2 \text{K}$ )<sup>-1</sup>

$U_i, U_o$  = overall heat transfer coefficient, referred to inside surface and bare external surface, respectively ( $\text{W/m}^2 \text{K}$ )

$\alpha_i, \alpha_{io}$  = internal fluid heat transfer coefficient, referred to inside surface and bare external surface, respectively ( $\text{W/m}^2 \text{K}$ )

For manual calculations it is of great assistance to plot or tabulate  $\alpha_{fi}$  or  $\alpha_{fo}$  versus  $\alpha'_f$  for finned tubes of known geometries. Examples of this are given for longitudinally finned tubes in Table 15.1 and Fig. 15.2, and for high-finned tubes in Table 14.3.

From equation [9.4], and noting that  $A_u = A_t - A_f$ , it can be shown that

\* Assumes no bond resistance – this must be included if present.

† In the case of L-fins (Figs 3.4(a) and (b)), the resistance of the L foot should be included. In the case of integral fins (Fig. 3.4(d)), the resistances of the outer tube and liner should be included.

$$\frac{\alpha_{ft}}{\alpha'_f} = \frac{\Omega_f A_f + A_u}{A_t} = \left\{ 1 - \left( \frac{A_f}{A_t} \right) (1 - \Omega_f) \right\} = \Omega_w \quad [9.9]$$

$\Omega_w$  is termed the weighted fin efficiency. In the above equations there are  $\Omega_f$  and  $\Omega_w$ , together with  $\alpha_f$ ,  $\alpha'_f$  and  $\alpha_{ft}$  and confusion can arise if these are not clearly defined.  $\alpha_{ft}$  is the coefficient obtained as the result of tests on finned tubes and relates only to the specific tube and fin metal and geometry being tested. It therefore accounts for the effect of fin efficiency, bond resistance and manufacturing features.  $\alpha'_f$  or  $\alpha_f$  can be obtained from equation [9.9] for use with finned tubes of identical geometry but different fin metals. Values of  $\Omega_w$  versus  $\alpha'_f$  are tabulated in Table 13.4 for low-fin tubes in various metals.

### 9.2.5 Heat flow through fin edge (longitudinal fins)

In the derivation of fin efficiency leading to equations [9.2] and [9.3], it was assumed that there was negligible heat flow into the outer fin edge compared with the sides. If the heat flow into the edge is not negligible it can be accounted for by adding half the fin-tip thickness to the fin height and using this corrected fin height  $l_{fe}$ , instead of  $l_f$ , in the equations, viz.:

longitudinal fin, rectangular profile, use  $l_{fe} = l_f + t_f/2$  in equation [9.3]

longitudinal fin, trapezoidal profile, use  $l_{fe} = l_f + t_{ft}/2$  in equation [9.3]

### 9.2.6 Non-uniform heat transfer coefficient

Another assumption made in the derivation of fin efficiency is that the fin-side heat transfer coefficient is the same over the entire surface. The fin efficiency ( $\Omega_f$ ) calculated from equations [9.2] and [9.3], may be corrected for a non-uniform heat transfer coefficient, by multiplying it by  $C_f$  where

$$C_f = \{ 1 - 0.058(ml_f) \} \text{ or } \{ 1 - 0.058(m_e l_{fe}) \}$$

It should be emphasised that this approach is entirely empirical.

## 9.3 Pressure loss calculations

Chapter 6 provides correlations for longitudinally finned, low-finned and high-finned tubes. The required geometrical factors may be calculated from Table 9.2 and Fig. 9.3.

## 9.4 Space saving

The saving in space arising from the use of extended surfaces must not be overlooked. Table 13.1 provides a comparison of shell-and-tube

**Table 12.1** Shell and tube heat exchanger design. Formulae for shell-side flow areas (see Fig. 12.3)

Cross-flow area	$S_m$	$\left\{ C_1 + \frac{(D_s - C_1 - d_o)(p - d_o)}{yp} \right\} l_s$	Pitch $y$
			$\triangle 30^\circ$ 1.0
			$\triangleright 60^\circ$ 0.866
			$\square 90^\circ$ 1.0
			$\diamond 45^\circ$ 0.707
Bundle by-pass area	$S_{bp}$	$\{ C_1 l_s \}$	
Shell-baffle leakage area for one baffle	$S_{sb}$	$\left\{ \frac{\pi}{2} + \theta_1 \right\} \left\{ \frac{D_s S_s}{2} \right\}$	$\theta_1 = \sin^{-1} \left\{ 1 - \frac{2l_c}{D_s} \right\}$ rads
Fraction of total tubes ( $N_{tt}$ ) in one window	$F_w$	$\left\{ \frac{\theta_3 - \sin \theta_3}{2\pi} \right\}$	$\theta_3 = 2 \cos^{-1} \left\{ \frac{D_s}{D_s - C_1} \left( 1 - \frac{2l_c}{D_s} \right) \right\}$ rads
Tube-baffle leakage area for one baffle	$S_{tb}$	$\left\{ \frac{\pi d_o (1 - F_w) N_{tt} S_b}{2} \right\}$	
Gross window area	$S_{wg}$	$\left\{ \frac{D_s^2}{8} (\theta_2 - \sin \theta_2) \right\}$	$\theta_2 = 2 \cos^{-1} \left\{ 1 - \frac{2l_c}{D_s} \right\}$ rads
Area occupied by tubes in one window	$S_{wt}$	$\left\{ \frac{\pi}{4} (N_{tw} d_o^2) \right\}$	$N_{tw} = \{ F_w N_{tt} \}$
Free area in one window	$S_w$	$\{ S_{wg} - S_{wt} \}$	
No. rows crossed in one cross-flow space	$N_c$	$\left\{ \frac{1 - (2l_c/D_s)}{qp} D_s \right\}$	Pitch $q$
			$\triangle 30^\circ$ 0.866
			$\triangleright 60^\circ$ 0.5
			$\square$ 1.0
			$\diamond 45^\circ$ 0.707
No. effective rows crossed in one window	$N_{cw}$	$\left\{ \frac{0.8l_c}{qp} \right\}$	
Equivalent diameter of one window (Reynolds no. < 100)	$d_w$	$\left\{ \frac{4S_w}{(\pi d_o N_{tw}) + (D_s \theta_2)/2} \right\}$	

the performance of an exchanger of known size and internal geometry is checked against given process data.

Table 12.2. Shell and tube heat exchanger design – construction data relating to Tables 12.3–12.9

Constructional feature	Diametral clearance (mm)															
Tube-baffle hole	0.65 (0.0256 in)															
Baffle-shell	As tabulated in TEMA with no overtolerance															
Bundle-shell	Shell inside diameter				Fixed tubesheet and U-tube				Split backing floating head				Pull-through floating head			
	Up to 590.55 (23.25 in)				12.70 ( $\frac{1}{2}$ in)				34.93 ( $1\frac{1}{4}$ in)				101.60 (4 in)			
	635–939.8 (25–37 in)				12.70 ( $\frac{1}{2}$ in)				41.28 ( $1\frac{5}{8}$ in)				104.78 ( $4\frac{1}{8}$ in)			
	990.6–1524 (39–60 in)				12.70 ( $\frac{1}{2}$ in)				47.63 ( $1\frac{7}{8}$ in)				111.13 ( $4\frac{3}{8}$ in)			
Baffle spacing ratio (BSR)	0.20	0.25	0.30	0.35	0.40	0.45	0.50	0.55	0.60	0.70	0.80	0.90	1.00	1.10	1.20	1.40
Baffle cut ratio (BCR)	0.190	0.199	0.210	0.220	0.235	0.250	0.260	0.268	0.275	0.285	0.293	0.300	0.305	0.310	0.314	0.320
Number of shell-bundle sealing devices	One pair (one on each side of bundle) in direction of shell-side flow, at every sixth row, with a minimum of two pairs.															

$$BSR = \frac{\text{baffle spacing (mm)}}{\text{shell inside dia. (mm)}}$$

$$BCR = \frac{\text{window opening height (mm)}}{\text{shell inside dia. (mm)}}$$

### 12.5.2 Design formulae and design factors

After incorporating the modified values of  $J_1$ ,  $R_1$ ,  $J_h$  and  $f_o$  discussed in section 12.5.1, the heat transfer and pressure loss equations presented by Bell may be transformed into the following relationships: heat transfer coefficient:

$$\alpha_o = (F_F F_P)(F_M F_C)(F_E F_A)\phi_{nl} \quad [12.2]$$

cross-flow pressure loss (one cross pass):

$$\Delta P_c = (F_F F_P)(F_M F_C)/\phi_{nl} \quad [12.3]$$

window pressure loss (one window):

$$\Delta P_w = (F_F F_P)(F_M F_C) \quad [12.4]$$

cross-flow Reynolds number:

$$Re_c = \dot{m}_c d_o / \eta_b \quad [12.5]$$

where  $\dot{m}_c = \dot{M}_o / S_m$  and  $S_m = S_{mu} l_s$ .

NOTE: The units for  $S_{mu}$  given in Table 12.3 are  $m^2/m$ . When  $l_s$  is in mm,  $l_s$  should be multiplied by  $10^{-3}$  to calculate  $S_m$  and hence  $\dot{m}_c$  and  $Re_c$ .

#### Design factors $F_F$ and $F_P$

The flow-rate factor  $F_F$  and physical property factor  $F_P$ , which are functions of the flow rate, flow regime, and fluid physical properties, are given in Table 12.4. It should be noted that the product  $(F_F F_P)$  is fixed for both design and rating cases.

Table 12.3(a) Shell-tube heat exchanger design – shell-side calculations. Cross-flow area per unit baffle pitch ( $S_{mu}$ ) (m<sup>2</sup>/m) for tube arrangements (mm) below (o.d. × pitch × angle)

Type: fixed tubesheet and U-tube											
Shell i.d. (mm)	15.875 ×19.844 △(30°)	15.875 ×22.225 □(90°)	15.875 ×22.225 ◇(45°)	19.05 ×23.813 △(30°)	19.05 ×25.4 △(30°) □(90°)	19.05 ×25.4 ◇(45°)	25.4 ×31.75 △(30°) □(90°)	25.4 ×31.75 ◇(45°)	31.75 ×39.688 △(30°) □(90°)	31.75 ×39.688 ◇(45°)	Shell i.d. (in)
205	0.0480	0.0631	0.0840	0.0474	0.0560	0.0740	0.0461	0.0599	0.0448	0.0581	8.07
257	0.0585	0.0781	0.1052	0.0578	0.0691	0.0925	0.0566	0.0748	0.0553	0.0730	10.14
307	0.0684	0.0923	0.1253	0.0678	0.0815	0.1101	0.0665	0.0888	0.0652	0.0870	12.09
337	0.0743	0.1007	0.1372	0.0737	0.0889	0.1205	0.0724	0.0971	0.0711	0.0953	13.25
387	0.0845	0.1152	0.1577	0.0838	0.1016	0.1384	0.0825	0.1115	0.0813	0.1097	15.25
438	0.0946	0.1297	0.1782	0.0940	0.1143	0.1564	0.0927	0.1259	0.0914	0.1241	17.25
489	0.1048	0.1442	0.1987	0.1041	0.1270	0.1744	0.1029	0.1402	0.1016	0.1384	19.25
540	0.1149	0.1588	0.2193	0.1143	0.1397	0.1923	0.1130	0.1546	0.1118	0.1528	21.25
591	0.1251	0.1733	0.2398	0.1245	0.1524	0.2103	0.1232	0.1690	0.1219	0.1672	23.25
635	0.1340	0.1860	0.2578	0.1334	0.1635	0.2260	0.1321	0.1816	0.1308	0.1798	25
686	0.1442	0.2005	0.2783	0.1435	0.1762	0.2440	0.1422	0.1959	0.1410	0.1941	27
737	0.1543	0.2150	0.2988	0.1537	0.1889	0.2619	0.1524	0.2103	0.1510	0.2085	29
787	0.1645	0.2295	0.3194	0.1638	0.2016	0.2799	0.1626	0.2247	0.1613	0.2229	31
838	0.1746	0.2440	0.3399	0.1740	0.2143	0.2979	0.1727	0.2390	0.1715	0.2373	33
889	0.1848	0.2585	0.3604	0.1842	0.2270	0.3158	0.1829	0.2534	0.1816	0.2516	35
940	0.1950	0.2730	0.3809	0.1943	0.2397	0.3338	0.1930	0.2678	0.1918	0.2660	37
991	0.2051	0.2876	0.4015	0.2045	0.2524	0.3518	0.2032	0.2821	0.2019	0.2804	39
1067	0.2204	0.3093	0.4323	0.2197	0.2715	0.3787	0.2184	0.3037	0.2172	0.3019	42
1143	0.2356	0.3311	0.4631	0.2350	0.2905	0.4056	0.2337	0.3253	0.2324	0.3235	45
1219	0.2508	0.3529	0.4939	0.2502	0.3096	0.4326	0.2489	0.3468	0.2477	0.3450	48
1295	0.2661	0.3746	0.5247	0.2655	0.3286	0.4595	0.2642	0.3684	0.2629	0.3666	51
1372	0.2813	0.3964	0.5554	0.2807	0.3477	0.4865	0.2794	0.3899	0.2781	0.3882	54
1448	0.2966	0.4182	0.5862	0.2959	0.3667	0.5134	0.2946	0.4115	0.2934	0.4097	57
1524	0.3118	0.4400	0.6170	0.3112	0.3858	0.5404	0.3099	0.4330	0.3086	0.4313	60

Shell i.d. (mm)	△(30°)	□(90°)	◇(45°)	△(30°)	△(30°) □(90°)	◇(45°)	△(30°) □(90°)	◇(45°)	△(30°) □(90°)	◇(45°)	Shell i.d. (in)
	$\frac{5}{8} \times \frac{25}{32}$	$\frac{5}{8} \times \frac{7}{8}$	$\frac{5}{8} \times \frac{7}{8}$	$\frac{3}{4} \times \frac{15}{16}$	$\frac{3}{4} \times 1$	$\frac{3}{4} \times 1$	$1 \times 1\frac{1}{4}$	$1 \times 1\frac{1}{4}$	$1\frac{1}{4} \times 1\frac{3}{8}$	$1\frac{1}{4} \times 1\frac{3}{8}$	(in)

**Design factor  $F_E$**

At the stationary head of an E-type shell, for instance, the distance between the tubesheet and nearest baffle, or end cross pass, is often greater than the usually regular baffle spacing in the remainder, or central part, of the exchanger. If the exchanger is a fixed tubesheet or floating-head type, a similar situation may prevail at the rear-head end. This is because the end cross-pass must be large enough to accommodate the nozzle, and sometimes a reinforcing pad. When this occurs the shell-side heat transfer coefficient in the end cross-passes is lower than the value calculated for the central cross-passes.

To account for this  $\alpha_o$ , calculated for the central cross-passes, is multiplied by  $F_E$ , values of which are given in Table 12.5. The basis for  $F_E$  is identical to that described by Taborek (1983). In rating cases  $F_E$  is

**Table 12.3(b)** Shell-tube heat exchanger design – shell-side calculations. Cross-flow area per unit baffle pitch ( $S_{mu}$ ) (m<sup>2</sup>/m) for tube arrangements (mm) below (o.d. × pitch × angle)

Type: split backing ring floating head											
Shell i.d. (mm)	15.875 ×19.844 △(30°)	15.875 ×22.225 □(90°)	15.875 ×22.225 ◇(45°)	19.05 ×23.813 △(30°)	19.05 ×25.4 △(30°) □(90°)	19.05 ×25.4 ◇(45°)	25.4 ×31.75 △(30°) □(90°)	25.4 ×31.75 ◇(45°)	31.75 ×39.688 △(30°) □(90°)	31.75 ×39.688 ◇(45°)	Shell i.d. (in)
205	0.0658	0.0790	0.0972	0.0651	0.0727	0.0883	0.0639	0.0759	0.0626	0.0741	8.07
257	0.0763	0.0940	0.1184	0.0756	0.0858	0.1069	0.0744	0.0907	0.0731	0.0889	10.14
307	0.0862	0.1082	0.1385	0.0856	0.0982	0.1244	0.0843	0.1047	0.0830	0.1029	12.09
337	0.0921	0.1166	0.1504	0.0914	0.1056	0.1348	0.0902	0.1131	0.0889	0.1113	13.25
387	0.1022	0.1311	0.1709	0.1016	0.1183	0.1528	0.1003	0.1274	0.0991	0.1256	15.25
438	0.1124	0.1456	0.1915	0.1118	0.1310	0.1708	0.1105	0.1418	0.1092	0.1400	17.25
489	0.1226	0.1601	0.2120	0.1219	0.1437	0.1887	0.1207	0.1562	0.1194	0.1544	19.25
540	0.1327	0.1746	0.2325	0.1321	0.1564	0.2067	0.1308	0.1706	0.1295	0.1688	21.25
591	0.1429	0.1891	0.2531	0.1423	0.1691	0.2247	0.1410	0.1849	0.1397	0.1831	23.25
635	0.1569	0.2064	0.2748	0.1562	0.1849	0.2445	0.1549	0.2020	0.1537	0.2003	25
686	0.1670	0.2209	0.2953	0.1664	0.1976	0.2625	0.1651	0.2164	0.1638	0.2146	27
737	0.1772	0.2354	0.3159	0.1765	0.2103	0.2804	0.1753	0.2308	0.1740	0.2290	29
787	0.1873	0.2499	0.3364	0.1867	0.2230	0.2984	0.1854	0.2452	0.1842	0.2434	31
838	0.1975	0.2644	0.3569	0.1969	0.2357	0.3163	0.1956	0.2595	0.1943	0.2577	33
889	0.2077	0.2789	0.3774	0.2070	0.2484	0.3343	0.2057	0.2739	0.2045	0.2721	35
940	0.2178	0.2935	0.3980	0.2172	0.2611	0.3523	0.2159	0.2883	0.2146	0.2865	37
991	0.2331	0.3125	0.4223	0.2324	0.2786	0.3743	0.2311	0.3072	0.2299	0.3054	39
1067	0.2483	0.3343	0.4531	0.2477	0.2977	0.4013	0.2464	0.3288	0.2451	0.3270	42
1143	0.2635	0.3561	0.4839	0.2629	0.3167	0.4282	0.2616	0.3503	0.2604	0.3485	45
1219	0.2788	0.3778	0.5147	0.2782	0.3358	0.4552	0.2769	0.3719	0.2756	0.3701	48
1295	0.2940	0.3996	0.5455	0.2934	0.3548	0.4821	0.2921	0.3934	0.2908	0.3916	51
1372	0.3093	0.4214	0.5763	0.3086	0.3739	0.5091	0.3073	0.4150	0.3061	0.4132	54
1448	0.3245	0.4431	0.6071	0.3239	0.3929	0.5360	0.3226	0.4365	0.3213	0.4348	57
1524	0.3397	0.4649	0.6378	0.3391	0.4120	0.5625	0.3378	0.4581	0.3366	0.4563	60

Shell i.d. (mm)	△(30°)	□(90°)	◇(45°)	△(30°)	△(30°) □(90°)	◇(45°)	△(30°) □(90°)	◇(45°)	△(30°) □(90°)	◇(45°)	Shell i.d. (in)
	$\frac{5}{8} \times \frac{25}{32}$	$\frac{5}{8} \times \frac{7}{8}$	$\frac{5}{8} \times \frac{7}{8}$	$\frac{3}{4} \times \frac{15}{16}$	$\frac{3}{4} \times 1$	$\frac{3}{4} \times 1$	$1 \times 1\frac{1}{4}$	$1 \times 1\frac{1}{4}$	$1\frac{1}{4} \times 1\frac{1}{16}$	$1\frac{1}{4} \times 1\frac{1}{16}$	

readily determined, but in design cases it is usual to assume  $F_E = 1$  until the baffle arrangement has been settled. The method for calculating pressure loss in the inlet and outlet cross-passes is given later.

It should be emphasized that the manual methods for calculating heat transfer and pressure loss in the inlet and outlet cross-passes are simple approximations. However, the methods serve to remind the thermal design engineer that in some cases heat transfer and pressure loss in the inlet and outlet cross-passes may affect the exchanger design considerably.

The correction factors for heat transfer and pressure loss in the inlet and outlet cross-passes are sometimes described as 'end zone correction factors', but they are applicable to the inlet and outlet nozzles wherever they are situated along the exchanger shell.



**Table 12.3(c) Shell-tube heat exchanger design – shell-side calculations.** Cross-flow area per unit baffle pitch ( $S_{mu}$ ) (m<sup>2</sup>/m) for tube arrangements (mm) below (o.d. × pitch × angle)

Type: pull through floating head											
Shell i.d. (mm)	15.875 ×19.844 Δ(30°)	15.875 ×22.225 □(90°)	15.875 ×22.225 ◇(45°)	19.05 ×23.813 Δ(30°)	19.05 ×25.4 Δ(30°) □(90°)	19.05 ×25.4 ◇(45°)	25.4 ×31.75 Δ(30°) □(90°)	25.4 ×31.75 ◇(45°)	31.75 ×39.688 Δ(30°) □(90°)	31.75 ×39.688 ◇(45°)	Shell i.d. (in)
387	0.1556	0.1787	0.2107	0.1549	0.1683	0.1959	0.1537	0.1752	0.1524	0.1735	15.25
438	0.1657	0.1932	0.2312	0.1651	0.1810	0.2139	0.1638	0.1896	0.1626	0.1878	17.25
489	0.1759	0.2077	0.2517	0.1753	0.1937	0.2318	0.1740	0.2040	0.1727	0.2022	19.25
540	0.1861	0.2223	0.2723	0.1854	0.2064	0.2498	0.1841	0.2184	0.1829	0.2166	21.25
591	0.1962	0.2368	0.2928	0.1956	0.2191	0.2678	0.1943	0.2327	0.1930	0.2309	23.25
635	0.2077	0.2517	0.3126	0.2070	0.2326	0.2855	0.2057	0.2476	0.2045	0.2458	25
686	0.2178	0.2663	0.3332	0.2172	0.2453	0.3035	0.2159	0.2620	0.2146	0.2602	27
737	0.2280	0.2808	0.3537	0.2273	0.2580	0.3215	0.2261	0.2763	0.2248	0.2745	29
787	0.2381	0.2953	0.3742	0.2375	0.2707	0.3394	0.2362	0.2907	0.2350	0.2889	31
838	0.2483	0.3098	0.3948	0.2477	0.2834	0.3574	0.2464	0.3051	0.2451	0.3033	33
889	0.2585	0.3243	0.4153	0.2578	0.2961	0.3753	0.2565	0.3194	0.2553	0.3177	35
940	0.2686	0.3388	0.4358	0.2680	0.3088	0.3933	0.2667	0.3338	0.2654	0.3320	37
991	0.2839	0.3579	0.4601	0.2832	0.3262	0.4154	0.2819	0.3527	0.2807	0.3509	39
1067	0.2991	0.3796	0.4909	0.2985	0.3453	0.4423	0.2972	0.3743	0.2959	0.3725	42
1143	0.3143	0.4014	0.5217	0.3137	0.3643	0.4693	0.3124	0.3958	0.3112	0.3941	45
1219	0.3296	0.4232	0.5525	0.3290	0.3834	0.4962	0.3277	0.4174	0.3264	0.4156	48
1295	0.3448	0.4450	0.5833	0.3442	0.4024	0.5232	0.3429	0.4390	0.3416	0.4372	51
1372	0.3601	0.4667	0.6141	0.3594	0.4215	0.5501	0.3581	0.4605	0.3569	0.4587	54
1448	0.3753	0.4885	0.6449	0.3747	0.4405	0.5770	0.3734	0.4821	0.3721	0.4803	57
1524	0.3905	0.5103	0.6757	0.3899	0.4596	0.6040	0.3886	0.5036	0.3874	0.5018	60

Shell i.d. (mm)	Δ(30°)	□(90°)	◇(45°)	Δ(30°)	Δ(30°) □(90°)	◇(45°)	Δ(30°) □(90°)	◇(45°)	Δ(30°) □(90°)	◇(45°)	Shell i.d. (in)
	$\frac{5}{8} \times \frac{25}{32}$	$\frac{5}{8} \times \frac{7}{8}$	$\frac{5}{8} \times \frac{7}{8}$	$\frac{3}{4} \times \frac{15}{16}$	$\frac{3}{4} \times 1$	$\frac{3}{4} \times 1$	$1 \times \frac{1}{4}$	$1 \times 1\frac{1}{4}$	$1\frac{1}{4} \times 1\frac{1}{2}$	$1\frac{1}{4} \times 1\frac{1}{2}$	

**Design factor  $F_A$**

This is applicable only to laminar flow and is termed the heat transfer correction factor for adverse temperature gradient. At Reynolds numbers below about 20, a large decrease in heat transfer is found to occur due to a build-up of the laminar layer. This effect decreases with increasing Reynolds number and disappears at a Reynolds number of about 100. When Reynolds number is greater than 100,  $F_A = 1$ .

Values of  $F_A$  are given in Table 12.6.

**Design factor  $\phi$**

This is the viscosity, or physical property, correction factor arising from a large temperature difference between the heat transfer surface and the bulk of the fluid, as described in section 6.8. In many applications  $\phi = 1$ , but usually becomes significant when dealing with viscous liquids.  $\phi$  is determined by trial and error, having first calculated  $(\alpha_o)_m$ , as described in section 12.5.5.

**Table 12.4(a)** Shell-and-tube heat exchanger design – shell-side calculations. Flow rate factor ( $F_F$ ) and physical property factor ( $F_p$ ) – turbulent flow

Item	Tube arrangement		Reynolds number range	Flow-rate factor ( $F_F$ )	Physical property factor ( $F_p$ )
	Angle	Pitch diameter ratio			
Heat transfer coefficient ( $\alpha_o$ )	30°, 45°	1.25, 1.33, 1.4	$3 \times 10^2 - 2 \times 10^5$	$\dot{M}_o^{0.635}$	$\frac{C_p^{0.333} \lambda^{0.667}}{\eta_b^{0.302}}$
	90°				$\frac{C_p^{0.333} \lambda^{0.667}}{\eta_b^{0.318}}$
Cross-flow pressure loss ( $\Delta P_c$ ) (one central cross-pass)	30°	1.25	$(2 \times 10^2) - (1 \times 10^5)$	$\dot{M}_o^{1.75}$	$\frac{\eta_b^{0.25}}{\rho}$
		1.33	$(1.5 \times 10^2) - (1 \times 10^5)$		
	45°	1.25	$(2.5 \times 10^2) - (1 \times 10^5)$		
		1.33	$(1.5 \times 10^2) - (1 \times 10^5)$		
		1.4	$(1 \times 10^2) - (1 \times 10^5)$		
	90° * ( $f_o = 0.1$ )	1.25	$(2.5 \times 10^2) - (1 \times 10^5)$	$\dot{M}_o^2$	$\frac{1}{\rho}$
		1.33	$(1.5 \times 10^2) - (1 \times 10^5)$		
		1.4	$(1 \times 10^2) - (1 \times 10^5)$		
Window pressure loss ( $\Delta P_w$ ) (one window)	30°, 45°, 90°	1.25, 1.33, 1.4	$\geq 100$	$\dot{M}_o^2$	$\frac{1}{\rho}$

\*Use to obtain approximate cross-flow pressure loss ( $\Delta P_c'$ ); calculate true cross-flow pressure loss ( $\Delta P_c$ ) from  $\Delta P_c = \Delta P_c' \{ \text{true } f_o / 0.1 \} = (\Delta P_c') F_s$ , where  $F_s$  is given below:

(tube pitch) (tube o.d.)	Cross-flow Reynolds number ( $Re_c$ )															
	$1 \times 10^5$	$8 \times 10^4$	$6 \times 10^4$	$4 \times 10^4$	$2 \times 10^4$	$1 \times 10^4$	$8 \times 10^3$	$6 \times 10^3$	$4 \times 10^3$	$2 \times 10^3$	$1 \times 10^3$	$8 \times 10^2$	$6 \times 10^2$	$4 \times 10^2$	$2 \times 10^2$	$1 \times 10^2$
1.25	0.82	0.88	0.95	1.07	1.30	1.40	1.40	1.38	1.34	1.20	1.14	1.18	1.30	1.60	3.00	-
1.33	0.70	0.74	0.79	0.90	1.07	1.17	1.17	1.16	1.13	1.05	0.98	0.99	1.01	1.12	2.00	-
1.40	0.64	0.67	0.70	0.79	0.94	1.03	1.04	1.04	1.02	0.94	0.84	0.80	0.82	0.95	1.47	3.00

For the complex flow in the shell of shell-and-tube exchangers, the viscosity correction factor  $\phi_o = (\eta_b/\eta_s)^{0.14}$  for both heat transfer and pressure loss, which is in accordance with the Bell (1963) method. This differs from equation [6.25] and [6.26] derived for ideal banks.

#### Design factors $F_M$ and $F_C$

These are mechanical design factors reflecting the exchanger geometry, i.e. type, size, tube arrangement, baffle arrangement and construction clearances. Both  $F_M$  and  $F_C$  are known for a rating case, but must be determined by trial and error for a design case.

Table 12.4(b) Shell-and-tube heat exchanger design – shell-side calculations. Flow-rate factor ( $F_F$ ) and physical property factor ( $F_P$ ) – laminar flow

Item	Tube arrangement		Reynolds number range	Flow rate factor ( $F_F$ )	Physical property factor ( $F_P$ )	
	Angle	Pitch/diameter ratio				
Heat transfer coefficient ( $\alpha_o$ )	30°, 45°	1.25, 1.33, 1.4	< 300	$M_o^{0.36}$	$\frac{C_p^{0.333} \lambda^{0.667}}{\eta_b^{0.027}}$	
	90°				$\frac{C_p^{0.333} \lambda^{0.667}}{\eta_b^{0.028}}$	
Cross-flow pressure loss ( $\Delta P_C$ ) (one central cross-pass)	30°	1.25	< 200	$M_o$	$\frac{\eta_b}{\rho}$	
		1.33	< 150			
	45°, 90°	1.25	< 250			
		1.33	< 150			
		1.4	< 100			
Window pressure loss ( $\Delta P_w$ ) (one window)	Friction loss ( $\Delta P_f$ ) (cross and long flow)	30°, 45°, 90°	1.25, 1.33, 1.4	< 100	$M_o$	$\frac{\eta_b}{\rho}$
		From [12.4], $\Delta P_f = (F_F F_P)(F_M F_C)$ , where ( $F_F$ ) and ( $F_P$ ) are calculated from above and $F_M$ and $F_C$ are taken from appropriate laminar flow factors for windows in Tables 12.7 and 12.8.				
$\Delta P_w = \Delta P_f + \Delta P_{ta}$	Turn-around loss ( $\Delta P_{ta}$ )	30°, 45°, 90°	1.25, 1.33, 1.4	$\geq 100$	$M_o^2$	$\frac{1}{\rho}$
		From [12.4], $\Delta P_{ta} = (F_F F_P)(F_M F_C)(F_W)$ , where $F_F$ and $F_P$ are calculated from above and $F_M$ and $F_C$ are taken from appropriate turbulent flow factors for windows in Table 12.7 and 12.8.				
		$F_W = \left\{ \frac{1}{1 + f_w D_s} \right\}$ where $f_w$ is given in Table 12.4(c).				

Table 12.4(c) Values of  $f_w$

Tube o.d. (mm)	Tube pitch (mm)	Pitch angle	Baffle spacing ratio (BSR)											Pitch angle	Tube pitch (in)	Tube o.d. (in)
			0.20	0.25	0.30	0.35	0.40	0.50	0.60	0.80	1.00	1.40				
15.875	19.844	$\Delta$ (30°)	2.65	2.78	2.93	3.07	3.28	3.63	3.84	4.09	4.26	4.47	$\Delta$ (30°)	$\frac{25}{32}$	$\frac{5}{8}$	
15.875	22.225	$\square$ (90°)	2.05	2.15	2.27	2.38	2.54	2.81	2.97	3.17	3.29	3.46	$\square$ (90°)	$\frac{7}{8}$	$\frac{5}{8}$	
15.875	22.225	$\diamond$ (45°)	2.90	3.04	3.21	3.36	3.59	3.97	4.20	4.47	4.66	4.89	$\diamond$ (45°)	$\frac{7}{8}$	$\frac{5}{8}$	
19.05	23.813	$\Delta$ (30°)	2.21	2.32	2.44	2.56	2.74	3.03	3.20	3.41	3.55	3.72	$\Delta$ (30°)	$\frac{15}{16}$	$\frac{3}{4}$	
19.05	25.4	$\Delta$ (30°)	2.07	2.17	2.29	2.40	2.56	2.84	3.00	3.20	3.33	3.49	$\Delta$ (30°)	1	$\frac{3}{4}$	
19.05	25.4	$\square$ (90°)	1.79	1.88	1.98	2.08	2.22	2.46	2.60	2.77	2.88	3.02	$\square$ (90°)	1	$\frac{3}{4}$	
19.05	25.4	$\diamond$ (45°)	2.54	2.66	2.81	2.94	3.14	3.48	3.68	3.92	4.08	4.28	$\diamond$ (45°)	1	$\frac{3}{4}$	
25.4	31.75	$\Delta$ (30°)	1.66	1.74	1.83	1.92	2.05	2.27	2.40	2.56	2.66	2.79	$\Delta$ (30°)	$1\frac{1}{4}$	1	
25.4	31.75	$\square$ (90°)	1.44	1.50	1.59	1.66	1.78	1.96	2.08	2.22	2.31	2.42	$\square$ (90°)	$1\frac{1}{4}$	1	
25.4	31.75	$\diamond$ (45°)	2.03	2.13	2.25	2.35	2.51	2.78	2.94	3.13	3.26	3.42	$\diamond$ (45°)	$1\frac{1}{4}$	1	
31.75	39.688	$\Delta$ (30°)	1.33	1.39	1.47	1.54	1.64	1.82	1.92	2.05	2.13	2.23	$\Delta$ (30°)	$1\frac{9}{16}$	$1\frac{1}{4}$	
31.75	39.688	$\square$ (90°)	1.15	1.20	1.27	1.33	1.42	1.57	1.66	1.77	1.84	1.93	$\square$ (90°)	$1\frac{9}{16}$	$1\frac{1}{4}$	
31.75	39.688	$\diamond$ (45°)	1.63	1.70	1.80	1.88	2.01	2.23	2.35	2.50	2.61	2.74	$\diamond$ (45°)	$1\frac{9}{16}$	$1\frac{1}{4}$	

**Table 12.5** Shell-and-tube heat exchanger design – shell-side calculations. Heat transfer correction factor ( $F_E$ ) when inlet and outlet baffle spaces are greater than central space

Number of baffles in exchanger ( $N_b$ )	$l_r = \frac{\text{inlet or outlet baffle space}}{\text{central baffle space}}$							
	1.25	1.50	1.75	2.00	2.25	2.50	2.75	3.00
4	0.943	0.892	0.846	0.806	0.769	0.736	0.706	0.678
5	0.952	0.907	0.867	0.830	0.796	0.765	0.737	0.710
6	0.958	0.919	0.883	0.849	0.818	0.789	0.762	0.737
7	0.963	0.928	0.895	0.864	0.835	0.808	0.782	0.759
8	0.967	0.935	0.905	0.876	0.849	0.824	0.800	0.777
9	0.970	0.941	0.913	0.887	0.861	0.837	0.815	0.793
10	0.973	0.946	0.920	0.895	0.872	0.849	0.827	0.807
11	0.975	0.950	0.926	0.903	0.880	0.859	0.839	0.819
12	0.977	0.954	0.931	0.909	0.888	0.868	0.848	0.830
13	0.978	0.957	0.936	0.915	0.895	0.876	0.857	0.839
14	0.980	0.960	0.940	0.920	0.901	0.883	0.865	0.848
15	0.981	0.962	0.943	0.924	0.906	0.889	0.872	0.855
16	0.982	0.964	0.946	0.928	0.911	0.894	0.878	0.862
17	0.983	0.966	0.949	0.932	0.915	0.899	0.884	0.868
18	0.984	0.968	0.951	0.935	0.919	0.904	0.889	0.874
19	0.985	0.969	0.954	0.938	0.923	0.908	0.894	0.879
20	0.985	0.971	0.956	0.941	0.926	0.912	0.898	0.884
21	0.986	0.972	0.958	0.943	0.929	0.915	0.902	0.889
22	0.987	0.973	0.959	0.946	0.932	0.919	0.906	0.893
23	0.987	0.974	0.961	0.948	0.935	0.922	0.909	0.897
24	0.988	0.975	0.962	0.950	0.937	0.924	0.912	0.900
25	0.988	0.976	0.964	0.951	0.939	0.927	0.915	0.903
26	0.989	0.977	0.965	0.953	0.941	0.930	0.918	0.907
27	0.989	0.978	0.966	0.955	0.943	0.932	0.920	0.909
28	0.989	0.978	0.967	0.956	0.945	0.934	0.923	0.912
29	0.990	0.979	0.968	0.957	0.947	0.936	0.925	0.915
20	0.990	0.980	0.969	0.959	0.948	0.938	0.927	0.917
31	0.990	0.980	0.970	0.960	0.950	0.940	0.930	0.920

*Notes:*

- (1) Inlet and outlet baffle space must be identical.
- (2) If only one end space is greater than central space, read off  $F_E$  for  $N_b = 2 \times (\text{actual number of baffles in exchanger}) + 0.5$ , for appropriate value of  $N_b$  and  $l_r$ .
- (3) Values of  $F_E$  above apply to turbulent flow in central space; for laminar flow,  $F_E = \{(F_E \text{ for turbulent flow} + 1)/2\}$ , for appropriate values of  $N_b$  and  $l_r$ .

$F_M$  is the base mechanical design factor. Values are given in Table 12.7 and relate to the following:

$$\text{Baffle space ratio (BSR)} = 0.2$$

$$30^\circ \triangle \text{ pitch} = 15.875 \text{ mm o.d.} \times 19.844 \text{ mm pitch}$$

$$90^\circ \square \text{ pitch} = 15.875 \text{ mm o.d.} \times 22.225 \text{ mm pitch}$$

$$45^\circ \diamond \text{ pitch} = 15.875 \text{ mm o.d.} \times 22.225 \text{ mm pitch}$$

In order to apply the method to other tube configurations and baffle space ratios (BSR),  $F_M$  must be multiplied by a correction factor  $F_C$  as given in Table 12.8. It will be seen that  $F_C$  is given in terms of a constant

**Table 12.6** Shell-and-tube heat exchanger design – shell-side calculations. Heat transfer correction factor ( $F_A$ ) for adverse temperature gradient in laminar flow

Shell i.d. (mm)	$j_1$ tabulated for tube o/dias. listed below		Total no. cross-passes in exchanger	$j_2$	Total no. cross-passes in exchanger	$j_2$	Shell i.d. (in)
	15.875 and 19.05 mm	25.4 and 31.75 mm					
205	1.059	1.135	3	0.821	27	0.553	8.07
257	1.016	1.090	4	0.779	28	0.549	10.14
307	0.984	1.056	5	0.748	29	0.545	12.09
337	0.968	1.039	6	0.724	30	0.542	13.25
387	0.944	1.013	7	0.705	31	0.539	15.25
438	0.923	0.990	8	0.688	32	0.536	17.25
489	0.906	0.971	9	0.673	33	0.533	19.25
540	0.889	0.954	10	0.661	34	0.530	21.25
591	0.875	0.938	11	0.649	35	0.527	23.25
635	0.864	0.926	12	0.639	36	0.525	25
686	0.852	0.914	13	0.630	37	0.522	27
737	0.841	0.902	14	0.622	38	0.520	29
787	0.831	0.891	15	0.614	39	0.517	31
838	0.822	0.881	16	0.607	40	0.515	33
889	0.813	0.872	17	0.600	45	0.504	35
940	0.805	0.863	18	0.594	50	0.495	37
991	0.797	0.855	19	0.589	55	0.486	39
1067	0.787	0.844	20	0.583	60	0.479	42
1143	0.777	0.833	21	0.578	65	0.472	45
1219	0.768	0.824	22	0.573	70	0.465	48
1295	0.760	0.815	23	0.569	75	0.460	51
1372	0.752	0.807	24	0.564	80	0.454	54
1448	0.745	0.799	25	0.560	85	0.449	57
1524	0.738	0.791	26	0.556	90	0.445	60

Shell i.d. (mm)	$j_1$ tabulated for tube o/dias. listed above		Total no. cross-passes in exchanger	$j_2$	Total no. cross-passes in exchanger	$j_2$	Shell i.d. (in)
	$\frac{5}{8}$ and $\frac{3}{4}$ in	1 and $1\frac{1}{4}$ in					
$F_A$ applies only when $Re_c < 100$	$20 < Re_c < 100: F_A = j + \{(1 - j)(Re_c - 20)\}/80$				$j = (j_1)(j_2)$ $F_A \neq 1.0, \neq 0.4$		
	$Re_c < 20: F_A = j$						

$X_C$  and an exponent  $m$  such that:

$$F_C = \left\{ \frac{X_C}{BSR^m} \right\} \tag{12.6}$$

$X_C$  and  $m$  depend on whether  $BSR$  lies between 0.2 and  $BSR_n$ , or  $BSR_n$  and 1.4,  $BSR_n$  being approximately 0.35.

### 12.5.3 Pressure loss in inlet and outlet cross-passes

In the inlet and outlet cross-passes allowance must be made for the fact that (a) the number of tube rows crossed is greater than that provided by

equation [12.3], which is based on the number of rows between baffle edges, (b) the leakage streams (baffle-shell, bundle-shell, tube-baffle) may not be fully developed in the inlet cross-pass, and are joining the main flow stream in the outlet cross-pass, and (c) the inlet and outlet spacings may be greater than the central baffle spacing, for the reasons described under Design factor  $F_E$ .

The *approximate* pressure loss in one end cross-pass ( $\Delta P_e$ ), which is based on the cross-flow pressure loss in one central cross-pass ( $\Delta P_c$ ), equation [12.3], is given by:

$$\Delta P_e = \left\{ \frac{\Delta P_c (X_e)}{l_r^e} \right\} \quad [12.7]$$

$$\text{where } l_r = \left\{ \frac{\text{inlet or outlet space}}{\text{central baffle space}} \right\}$$

Values of  $X_e$  and  $e$  are given in Table 12.9. The basis for  $X_e$  and  $e$  is similar to that described by Taborek (1983), except that the effective flow rate in the inlet or outlet space has been taken as:

$$\frac{\text{total flow rate} + \text{flow rate in first or last window}}{2} - \frac{(\text{E stream flow rate})}{2}$$

The window flow rate is estimated from  $\Delta P_w$  given by equation [12.4].

In rating cases  $X_e$ ,  $e$  and  $l_r$  are readily determined, but in design cases, it is usual to assume  $X_e$  and  $l_r$  as unity until the baffle arrangement has been settled. When all baffle spaces are identical  $l_r = 1$  and  $\Delta P_e = \Delta P_c (X_e)$ .

#### 12.5.4 Total pressure loss

In an E-type shell having  $N_b$  single-segmental baffles, there will be  $(N_b - 1)$  central cross-passes and  $N_b$  windows. There will also be one inlet cross-pass with a pressure loss of  $\Delta P_{ei}$ , one outlet cross-pass with a pressure loss of  $\Delta P_{eo}$ , one inlet nozzle with a pressure loss of  $\Delta P_{ni}$  and one outlet nozzle with a pressure loss of  $\Delta P_{no}$ . The total shell-side pressure loss ( $\Delta P_s$ ) is given by:

$$\Delta P_s = (N_b - 1) \Delta P_c + N_b \Delta P_w + \Delta P_{ei} + \Delta P_{eo} + \Delta P_{ni} + \Delta P_{no} \quad [12.8]$$

#### 12.5.5 Heat transfer and cross-flow pressure loss in an 'ideal' exchanger

The proposed manual method described in sections 12.5.1–12.5.4 does not determine the shell-side heat transfer coefficient  $(\alpha_o)_{nl}$ , and the cross-flow pressure loss  $(\Delta P_c)_{nl}$ , which would have been obtained had the leakage streams, described in section 12.2.2, been absent. This is referred to by Bell as an ideal tube bank. The flow pattern in the 'ideal' exchanger, without internal leakage, is shown in Fig. 12.1.

**Table 12.7(a)** Shell-and-tube heat exchanger design – shell side calculations. Base mechanical design factor ( $F_M$ ). Fixed tubesheet and U-tube types.

Shell i.d. (mm)	Heat transfer coefficient						Shell i.d. (in)
	Turbulent			Laminar			
	$\Delta$ (30°)	$\square$ (90°) ( $f_s = 0.1$ )	$\diamond$ (45°)	$\Delta$ (30°)	$\square$ (90°)	$\diamond$ (45°)	
205	25.19	21.45	26.70	68.01	50.60	84.10	8.07
257	20.75	17.39	21.36	62.99	45.20	76.19	10.14
307	17.64	14.61	17.80	58.69	40.95	69.91	12.09
337	16.15	13.29	16.14	56.38	38.77	66.68	13.25
387	13.31	10.86	13.28	50.00	33.65	59.23	15.25
438	11.80	9.56	11.63	47.32	31.23	55.53	17.35
489	10.13	8.15	9.98	43.04	27.93	50.58	19.25
540	9.18	7.35	8.97	41.13	26.28	48.00	21.25
591	8.38	6.67	8.13	39.38	24.82	45.69	23.25
635	7.52	5.97	7.31	36.76	22.90	42.75	25
686	6.95	5.50	6.71	35.41	21.81	40.98	27
737	6.46	5.08	6.20	34.16	20.81	39.37	29
787	6.02	4.72	5.76	33.01	19.91	37.90	31
838	5.63	4.41	5.36	31.94	19.08	36.55	33
889	5.28	4.12	5.02	30.94	18.32	35.30	35
940	4.97	3.87	4.71	30.00	17.63	34.15	37
991	4.69	3.65	4.43	29.14	16.98	33.08	39
1067	4.16	3.22	3.94	26.87	15.48	30.67	42
1143	3.86	2.98	3.65	25.89	14.76	29.45	45
1219	3.60	2.77	3.39	24.98	14.11	28.33	48
1295	3.36	2.58	3.16	24.15	13.52	27.31	51
1372	3.16	2.42	2.95	23.37	12.97	26.38	54
1448	2.84	2.17	2.68	21.70	11.94	24.66	57
1524	2.69	2.05	2.53	21.10	11.53	23.93	60

However,  $\phi$  is based on the heat transfer coefficient without leakage  $(\alpha_o)_{nl}$ , and not  $\alpha_o$ , and therefore  $(\alpha_o)_{nl}$  must be determined for cases when  $\phi$  is not unity.\* The calculation of  $(\alpha_o)_{nl}$  and  $(\Delta P_c)_{nl}$ , assists the thermal design engineer, even when  $\phi = 1$ , as it enables the engineer to check the reduction in heat transfer coefficient and pressure loss due to the internal leakage streams. In the procedure below, the cross-flow pressure loss without leakage  $(\Delta P_c)_{nl}$  has been added for this reason, although it is not a mandatory requirement of the method.

The heat transfer coefficient and cross-flow pressure loss in one central baffle space, when there is no leakage, is calculated as follows:

$$(\alpha_o)_{nl} \text{ and } (\Delta P_c)_{nl} = (F_F F_P) F_{NL} \quad [12.9]$$

where  $F_F$  and  $F_P$  = the same flow rate and physical property factors for heat transfer and cross-flow pressure loss, with internal leakage, given in Tables 12.4(a) and (b)

\* If  $\phi$  is based on  $\alpha_o$ , the difference is usually small. However the method of Bell, in which  $\phi$  is based on  $(\alpha_o)_{nl}$ , is retained in this chapter for exactness.

Table 12.7(a) (cont.)

Shell i.d. (mm)	Cross flow pressure loss						Shell i.d. (in)
	Turbulent			Laminar			
	$\Delta$ (30°)	$\square$ (90°) ( $f_o = 0.1$ )	$\diamond$ (45°)	$\Delta$ (30°)	$\square$ (90°)	$\diamond$ (45°)	
205	$4.246 \times 10^5$	$3.712 \times 10^4$	$2.372 \times 10^5$	$4.712 \times 10^6$	$1.754 \times 10^6$	$2.410 \times 10^6$	8.07
257	$2.907 \times 10^5$	$2.238 \times 10^4$	$1.540 \times 10^5$	$4.438 \times 10^6$	$1.644 \times 10^6$	$2.198 \times 10^6$	10.14
307	$2.121 \times 10^5$	$1.482 \times 10^4$	$1.084 \times 10^5$	$4.157 \times 10^6$	$1.534 \times 10^6$	$2.012 \times 10^6$	12.09
337	$1.788 \times 10^5$	$1.188 \times 10^4$	$8.980 \times 10^4$	$3.994 \times 10^6$	$1.471 \times 10^6$	$1.912 \times 10^6$	13.25
387	$1.243 \times 10^5$	$7.687 \times 10^3$	$6.204 \times 10^4$	$3.396 \times 10^6$	$1.253 \times 10^6$	$1.630 \times 10^6$	15.25
438	$9.821 \times 10^4$	$5.679 \times 10^3$	$4.800 \times 10^4$	$3.205 \times 10^6$	$1.179 \times 10^6$	$1.516 \times 10^6$	17.35
489	$7.349 \times 10^4$	$4.021 \times 10^3$	$3.584 \times 10^4$	$2.811 \times 10^6$	$1.036 \times 10^6$	$1.334 \times 10^6$	19.25
540	$6.059 \times 10^4$	$3.142 \times 10^3$	$2.909 \times 10^4$	$2.676 \times 10^6$	$0.984 \times 10^6$	$1.255 \times 10^6$	21.25
591	$5.063 \times 10^4$	$2.501 \times 10^3$	$2.399 \times 10^4$	$2.549 \times 10^6$	$0.935 \times 10^6$	$1.184 \times 10^6$	23.25
635	$4.124 \times 10^4$	$1.965 \times 10^3$	$1.958 \times 10^4$	$2.308 \times 10^6$	$0.848 \times 10^6$	$1.077 \times 10^6$	25
686	$3.532 \times 10^4$	$1.615 \times 10^3$	$1.660 \times 10^4$	$2.212 \times 10^6$	$0.811 \times 10^6$	$1.026 \times 10^6$	27
737	$3.052 \times 10^4$	$1.343 \times 10^3$	$1.421 \times 10^4$	$2.123 \times 10^6$	$0.777 \times 10^6$	$0.976 \times 10^6$	29
787	$2.659 \times 10^4$	$1.129 \times 10^3$	$1.228 \times 10^4$	$2.039 \times 10^6$	$0.745 \times 10^6$	$0.932 \times 10^6$	31
838	$2.333 \times 10^4$	$0.958 \times 10^3$	$1.069 \times 10^4$	$1.961 \times 10^6$	$0.716 \times 10^6$	$0.892 \times 10^6$	33
889	$2.060 \times 10^4$	$0.820 \times 10^3$	$9.381 \times 10^3$	$1.888 \times 10^6$	$0.689 \times 10^6$	$0.854 \times 10^6$	35
940	$1.830 \times 10^4$	$0.707 \times 10^3$	$8.283 \times 10^3$	$1.820 \times 10^6$	$0.663 \times 10^6$	$0.820 \times 10^6$	37
991	$1.634 \times 10^4$	$0.614 \times 10^3$	$7.357 \times 10^3$	$1.756 \times 10^6$	$0.639 \times 10^6$	$0.788 \times 10^6$	39
1067	$1.295 \times 10^4$	$0.470 \times 10^3$	$5.876 \times 10^3$	$1.552 \times 10^6$	$0.566 \times 10^6$	$0.703 \times 10^6$	42
1143	$1.118 \times 10^4$	$0.391 \times 10^3$	$5.037 \times 10^3$	$1.484 \times 10^6$	$0.541 \times 10^6$	$0.668 \times 10^6$	45
1219	$9.727 \times 10^3$	$0.329 \times 10^3$	$4.357 \times 10^3$	$1.421 \times 10^6$	$0.517 \times 10^6$	$0.637 \times 10^6$	48
1295	$8.528 \times 10^3$	$0.279 \times 10^3$	$3.799 \times 10^3$	$1.363 \times 10^6$	$0.495 \times 10^6$	$0.608 \times 10^6$	51
1372	$7.526 \times 10^3$	$0.239 \times 10^3$	$3.336 \times 10^3$	$1.309 \times 10^6$	$0.475 \times 10^6$	$0.581 \times 10^6$	54
1448	$6.169 \times 10^3$	$0.192 \times 10^3$	$2.769 \times 10^3$	$1.162 \times 10^6$	$0.424 \times 10^6$	$0.523 \times 10^6$	57
1524	$5.526 \times 10^3$	$0.167 \times 10^3$	$2.468 \times 10^3$	$1.124 \times 10^6$	$0.409 \times 10^6$	$0.504 \times 10^6$	60

$F_{NL}$  = factor for ideal exchanger having no leakage

=  $A/S_m^n$  for heat transfer coefficient

=  $BD_s \{(1 - 2(BCR))/S_m^n\}$  for cross-flow pressure loss

The heat transfer coefficient and pressure loss ratios due to leakage are given by  $\alpha_o/(\alpha_o)_{nl}$  and  $\Delta P_c/(\Delta P_c)_{nl}$  respectively. Values of  $A$ ,  $B$ ,  $m$  and  $n$  are given in Table 12.10, and values of BCR are given in Table 12.2.

As an example, consider an E-type split backing ring floating-head exchanger, 991 mm inside diameter, having tubes 25.4 mm o.d.  $\times$  31.75 mm  $\times$  30° pitch. Single-segmental baffles are spaced at 396 mm. The fluid flowing on the shell-side is water at 41.58 kg/s, having average properties of  $c_p = 4176.8$  J/kg K,  $\eta_b = 4.109 \times 10^{-4}$  N s/m<sup>2</sup>,  $\lambda = 0.65$  W/m K and  $\rho = 976.8$  kg/m<sup>3</sup>.

What is the heat transfer coefficient and cross-flow pressure loss in one central baffle space?

From Table 12.3(b):

$$S_{mu} = 0.2311 \text{ m}^2/\text{m}$$

$$S_m = (0.2311 \times 10^{-3}) \times 396 = 0.09152 \text{ m}^2$$

$$\dot{m}_c = 41.58/0.09152 = 454.33 \text{ kg/s m}^2$$



Table 12.7(a) (cont.)

Shell i.d. (mm)	Window pressure loss						Shell i.d. (in)
	Turbulent			Laminar			
	△ (30°)	□ (90°)	◇ (45°)	△ (30°)	□ (90°)	◇ (45°)	
205	5.658×10 <sup>4</sup>	4.631×10 <sup>4</sup>	4.760×10 <sup>4</sup>	1.271×10 <sup>6</sup>	0.670×10 <sup>6</sup>	0.946×10 <sup>6</sup>	8.07
257	2.956×10 <sup>4</sup>	2.336×10 <sup>4</sup>	2.403×10 <sup>4</sup>	1.188×10 <sup>6</sup>	0.611×10 <sup>6</sup>	0.851×10 <sup>6</sup>	10.14
307	1.772×10 <sup>4</sup>	1.364×10 <sup>4</sup>	1.406×10 <sup>4</sup>	1.112×10 <sup>6</sup>	0.562×10 <sup>6</sup>	0.775×10 <sup>6</sup>	12.09
337	1.354×10 <sup>4</sup>	1.029×10 <sup>4</sup>	1.063×10 <sup>4</sup>	1.071×10 <sup>6</sup>	0.535×10 <sup>6</sup>	0.734×10 <sup>6</sup>	13.25
387	8.144×10 <sup>3</sup>	6.094×10 <sup>3</sup>	6.401×10 <sup>3</sup>	0.914×10 <sup>6</sup>	0.452×10 <sup>6</sup>	0.624×10 <sup>6</sup>	15.25
438	5.696×10 <sup>3</sup>	4.187×10 <sup>3</sup>	4.411×10 <sup>3</sup>	0.867×10 <sup>6</sup>	0.423×10 <sup>6</sup>	0.580×10 <sup>6</sup>	17.35
489	3.838×10 <sup>3</sup>	2.790×10 <sup>3</sup>	2.980×10 <sup>3</sup>	0.764×10 <sup>6</sup>	0.370×10 <sup>6</sup>	0.510×10 <sup>6</sup>	19.25
540	2.887×10 <sup>3</sup>	2.070×10 <sup>3</sup>	2.216×10 <sup>3</sup>	0.731×10 <sup>6</sup>	0.350×10 <sup>6</sup>	0.480×10 <sup>6</sup>	21.25
591	2.225×10 <sup>3</sup>	1.577×10 <sup>3</sup>	1.692×10 <sup>3</sup>	0.700×10 <sup>6</sup>	0.332×10 <sup>6</sup>	0.453×10 <sup>6</sup>	23.25
635	1.700×10 <sup>3</sup>	1.197×10 <sup>3</sup>	1.298×10 <sup>3</sup>	0.636×10 <sup>6</sup>	0.300×10 <sup>6</sup>	0.412×10 <sup>6</sup>	25
686	1.363×10 <sup>3</sup>	0.950×10 <sup>3</sup>	1.032×10 <sup>3</sup>	0.612×10 <sup>6</sup>	0.287×10 <sup>6</sup>	0.392×10 <sup>6</sup>	27
737	1.110×10 <sup>3</sup>	0.767×10 <sup>3</sup>	0.834×10 <sup>3</sup>	0.590×10 <sup>6</sup>	0.275×10 <sup>6</sup>	0.373×10 <sup>6</sup>	29
787	0.914×10 <sup>3</sup>	0.627×10 <sup>3</sup>	0.684×10 <sup>3</sup>	0.569×10 <sup>6</sup>	0.263×10 <sup>6</sup>	0.356×10 <sup>6</sup>	31
838	0.762×10 <sup>3</sup>	0.519×10 <sup>3</sup>	0.567×10 <sup>3</sup>	0.549×10 <sup>6</sup>	0.253×10 <sup>6</sup>	0.341×10 <sup>6</sup>	33
889	0.642×10 <sup>3</sup>	0.435×10 <sup>3</sup>	0.475×10 <sup>3</sup>	0.530×10 <sup>6</sup>	0.243×10 <sup>6</sup>	0.327×10 <sup>6</sup>	35
940	0.546×10 <sup>3</sup>	0.367×10 <sup>3</sup>	0.402×10 <sup>3</sup>	0.512×10 <sup>6</sup>	0.234×10 <sup>6</sup>	0.314×10 <sup>6</sup>	37
991	0.468×10 <sup>3</sup>	0.313×10 <sup>3</sup>	0.344×10 <sup>3</sup>	0.496×10 <sup>6</sup>	0.225×10 <sup>6</sup>	0.301×10 <sup>6</sup>	39
1067	0.351×10 <sup>3</sup>	0.234×10 <sup>3</sup>	0.260×10 <sup>3</sup>	0.440×10 <sup>6</sup>	0.199×10 <sup>6</sup>	0.269×10 <sup>6</sup>	42
1143	0.288×10 <sup>3</sup>	0.190×10 <sup>3</sup>	0.212×10 <sup>3</sup>	0.422×10 <sup>6</sup>	0.190×10 <sup>6</sup>	0.256×10 <sup>6</sup>	45
1210	0.239×10 <sup>3</sup>	0.157×10 <sup>3</sup>	0.175×10 <sup>3</sup>	0.405×10 <sup>6</sup>	0.182×10 <sup>6</sup>	0.244×10 <sup>6</sup>	48
1295	0.200×10 <sup>3</sup>	0.131×10 <sup>3</sup>	0.146×10 <sup>3</sup>	0.389×10 <sup>6</sup>	0.174×10 <sup>6</sup>	0.233×10 <sup>6</sup>	51
1372	0.170×10 <sup>3</sup>	0.110×10 <sup>3</sup>	0.123×10 <sup>3</sup>	0.375×10 <sup>6</sup>	0.167×10 <sup>6</sup>	0.223×10 <sup>6</sup>	54
1448	0.134×10 <sup>3</sup>	0.087×10 <sup>3</sup>	0.099×10 <sup>3</sup>	0.334×10 <sup>6</sup>	0.149×10 <sup>6</sup>	0.200×10 <sup>6</sup>	57
1524	0.116×10 <sup>3</sup>	0.075×10 <sup>3</sup>	0.085×10 <sup>3</sup>	0.323×10 <sup>6</sup>	0.144×10 <sup>6</sup>	0.193×10 <sup>6</sup>	60

From equation [12.5]:

$$Re_c = (454.33 \times 0.0254)/(4.109 \times 10^{-4}) = 28085 \text{ (i.e. turbulent)}$$

$$BSR = 396/991 = 0.4$$

From Table 12.2:

$$BCR = 0.235$$

Heat transfer coefficient

From Table 12.4(a):

$$F_F = 41.58^{0.635} = 10.666$$

$$F_p = (4176.8^{0.333} \times 0.65^{0.667})/(4.109 \times 10^{-4})^{0.302} = 126.94$$

From Table 12.10:

$$A = 1.043, m = 0.635$$

From equation [12.9]:

$$F_{NL} = 1.043/0.09152^{0.635} = 4.761$$

From equation [12.9]:

$$(\alpha_o)_{al} = 10.666 \times 126.94 \times 4.761 = 6446 \text{ W/m}^2 \text{ K}$$

Table 12.7(b) Shell and tube heat exchanger design-shell side calculations. Base mechanical design factor ( $F_M$ ). Split backing ring floating-head type

Shell i.d. (mm)	Heat transfer coefficient						Shell i.d. (in)
	Turbulent			Laminar			
	$\Delta$ (30°)	$\square$ (90°)	$\diamond$ (45°)	$\Delta$ (30°)	$\square$ (90°)	$\diamond$ (45°)	
205	23.28	19.96	25.18	68.55	49.48	82.57	8.07
257	19.05	16.21	20.26	62.20	43.88	74.67	10.14
307	16.19	13.66	16.97	57.38	39.66	68.52	12.09
337	14.84	12.46	15.43	54.93	37.54	65.37	13.25
387	12.28	10.26	12.77	48.61	32.71	58.24	15.25
438	10.92	9.06	11.22	45.91	30.37	54.63	17.25
489	9.41	7.77	9.66	41.75	27.23	49.86	19.25
540	8.56	7.02	8.70	39.89	25.64	47.34	21.25
591	7.83	6.39	7.90	38.20	24.23	45.08	23.25
635	6.95	5.68	7.07	35.49	22.29	42.10	25
686	6.45	5.24	6.51	34.21	21.23	40.38	27
737	6.01	4.86	6.02	33.02	20.28	38.81	29
787	5.62	4.52	5.60	31.93	19.41	37.38	31
838	5.27	4.22	5.22	30.91	18.62	36.07	33
889	4.96	3.96	4.89	29.97	17.90	34.85	35
940	4.68	3.72	4.59	29.10	17.23	33.73	37
991	4.38	3.47	4.31	28.14	16.54	32.61	39
1067	3.89	3.09	3.84	25.98	15.12	30.28	42
1143	3.62	2.86	3.56	25.06	14.43	29.09	45
1219	3.39	2.67	3.31	24.21	13.80	28.00	48
1295	3.17	2.49	3.09	23.43	13.23	27.01	51
1372	2.99	2.34	2.89	22.70	12.71	26.09	54
1448	2.70	2.11	2.63	21.09	11.72	24.42	57
1524	2.56	1.99	2.48	20.53	11.32	23.70	60

*Cross flow pressure loss*

From Table 12.4(a):

$$F_F = 41.58^{1.75} = 680.84$$

$$F_P = (4.109 \times 10^{-4})^{0.25} / 976.8 = 1.458 \times 10^{-4}$$

From Table 12.10:

$$B = 233.2, n = 1.75$$

From equation [12.9]:

$$F_{NL} = 233.2 \times 0.991 \times \{1 - (2 \times 0.235)\} / 0.09152^{1.75} = 8043$$

From equation [12.9]:

$$(\Delta P_c)_{nl} = 680.84 \times (1.458 \times 10^{-4}) \times 8043 = 798.4 \text{ Pa}$$

This example is related to the first example of section 12.5, which deals with a 'non-ideal' heat exchanger. Inspection of that example will show that the heat transfer coefficient in the exchanger with leakage is  $4543/6446 = 0.705$  times that of the 'ideal' exchanger. The cross-flow pressure loss is  $327.5/798.4 = 0.41$  times that of the 'ideal' exchanger.

Table 12.7(b) (cont.)

Shell i.d. (mm)	Cross flow pressure loss						Shell i.d. (in)
	Turbulent			Laminar			
	$\Delta$ (30°)	$\square$ (90°) ( $f_o = 0.1$ )	$\diamond$ (45°)	$\Delta$ (30°)	$\square$ (90°)	$\diamond$ (45°)	
205	$2.475 \times 10^5$	$2.140 \times 10^4$	$1.601 \times 10^5$	$3.478 \times 10^6$	$1.266 \times 10^6$	$1.817 \times 10^6$	8.07
257	$1.814 \times 10^5$	$1.403 \times 10^4$	$1.114 \times 10^5$	$3.379 \times 10^6$	$1.240 \times 10^6$	$1.738 \times 10^6$	10.14
307	$1.392 \times 10^5$	$9.850 \times 10^3$	$8.208 \times 10^4$	$3.244 \times 10^6$	$1.195 \times 10^6$	$1.644 \times 10^6$	12.09
337	$1.203 \times 10^5$	$8.126 \times 10^3$	$6.952 \times 10^4$	$3.157 \times 10^6$	$1.165 \times 10^6$	$1.586 \times 10^6$	13.25
387	$8.735 \times 10^4$	$5.496 \times 10^3$	$4.956 \times 10^4$	$2.755 \times 10^6$	$1.019 \times 10^6$	$1.383 \times 10^6$	15.25
438	$7.111 \times 10^4$	$4.193 \times 10^3$	$3.927 \times 10^4$	$2.641 \times 10^6$	$0.977 \times 10^6$	$1.309 \times 10^6$	17.25
489	$5.479 \times 10^4$	$3.055 \times 10^3$	$2.990 \times 10^4$	$2.357 \times 10^6$	$0.874 \times 10^6$	$1.168 \times 10^6$	19.25
540	$4.612 \times 10^4$	$2.440 \times 10^3$	$2.466 \times 10^4$	$2.269 \times 10^6$	$0.840 \times 10^6$	$1.112 \times 10^6$	21.25
591	$3.925 \times 10^4$	$1.979 \times 10^3$	$2.061 \times 10^4$	$2.183 \times 10^6$	$0.808 \times 10^6$	$1.059 \times 10^6$	23.25
635	$3.057 \times 10^4$	$1.491 \times 10^3$	$1.635 \times 10^4$	$1.925 \times 10^6$	$0.714 \times 10^6$	$0.944 \times 10^6$	25
686	$2.664 \times 10^4$	$1.247 \times 10^3$	$1.403 \times 10^4$	$1.863 \times 10^6$	$0.690 \times 10^6$	$0.906 \times 10^6$	27
737	$2.338 \times 10^4$	$1.053 \times 10^3$	$1.214 \times 10^4$	$1.803 \times 10^6$	$0.667 \times 10^6$	$0.870 \times 10^6$	29
787	$2.065 \times 10^4$	$0.898 \times 10^3$	$1.059 \times 10^4$	$1.746 \times 10^6$	$0.645 \times 10^6$	$0.836 \times 10^6$	31
838	$1.834 \times 10^4$	$0.771 \times 10^3$	$9.302 \times 10^3$	$1.691 \times 10^6$	$0.624 \times 10^6$	$0.805 \times 10^6$	33
889	$1.638 \times 10^4$	$0.667 \times 10^3$	$8.223 \times 10^3$	$1.639 \times 10^6$	$0.605 \times 10^6$	$0.775 \times 10^6$	35
940	$1.470 \times 10^4$	$0.581 \times 10^3$	$7.310 \times 10^3$	$1.589 \times 10^6$	$0.586 \times 10^6$	$0.747 \times 10^6$	37
991	$1.269 \times 10^4$	$0.490 \times 10^3$	$6.368 \times 10^3$	$1.502 \times 10^6$	$0.554 \times 10^6$	$0.708 \times 10^6$	39
1067	$1.024 \times 10^4$	$0.381 \times 10^3$	$5.138 \times 10^3$	$1.343 \times 10^6$	$0.496 \times 10^6$	$0.637 \times 10^6$	42
1143	$8.958 \times 10^3$	$0.321 \times 10^3$	$4.442 \times 10^3$	$1.294 \times 10^6$	$0.477 \times 10^6$	$0.609 \times 10^6$	45
1219	$7.889 \times 10^3$	$0.273 \times 10^3$	$3.871 \times 10^3$	$1.247 \times 10^6$	$0.460 \times 10^6$	$0.584 \times 10^6$	48
1295	$6.989 \times 10^3$	$0.234 \times 10^3$	$3.398 \times 10^3$	$1.204 \times 10^6$	$0.443 \times 10^6$	$0.560 \times 10^6$	51
1372	$6.226 \times 10^3$	$0.202 \times 10^3$	$3.001 \times 10^3$	$1.163 \times 10^6$	$0.427 \times 10^6$	$0.538 \times 10^6$	54
1448	$5.162 \times 10^3$	$0.164 \times 10^3$	$2.505 \times 10^3$	$1.041 \times 10^6$	$0.383 \times 10^6$	$0.486 \times 10^6$	57
1524	$4.659 \times 10^3$	$0.144 \times 10^3$	$2.244 \times 10^3$	$1.010 \times 10^6$	$0.372 \times 10^6$	$0.470 \times 10^6$	60

### 12.5.6 Application to thermal design and rating

The simplified method does nothing to alter significantly the accuracy of calculated heat transfer and pressure loss values versus experimental values and the error ratios found by Palen and Taborek (1969) remain. Preselected design parameters mean that the method cannot be applied to design or rating problems where entirely different clearances and geometrical factors are used. However, unless the constructional features are greatly different, the proposed method will at least give the thermal design engineer a reasonable approximation to the problem. Industry applied methods for many years where the constructional clearances on which heat transfer and pressure loss were correlated were largely unknown, but assumed to be based on TEMA or 'good engineering practice'.

The advantage of the method is the elimination of tedious calculations involving exchanger geometry, design factors  $j_c$ ,  $j_b$ ,  $j_l$ ,  $R_b$  and  $R_l$  (Bell nomenclature), heat transfer factor  $J_b$  and friction factor  $f_o$ . In a rating case, where process conditions and exchanger geometry are fully defined, all factors required for equations [12.2]–[12.8] are readily determined and no trial and error is necessary. In a design case, the product ( $F_F F_P$ ) is

Table 12.7(b) (cont.)

Shell i.d. (mm)	Window pressure loss						Shell i.d. (in)
	Turbulent			Laminar			
	$\Delta$ (30°)	$\square$ (90°) ( $f_0 = 0.1$ )	$\diamond$ (45°)	$\Delta$ (30°)	$\square$ (90°)	$\diamond$ (45°)	
205	$4.442 \times 10^4$	$3.799 \times 10^4$	$3.924 \times 10^4$	$1.130 \times 10^6$	$0.585 \times 10^6$	$0.825 \times 10^6$	8.07
257	$2.357 \times 10^4$	$1.956 \times 10^4$	$2.023 \times 10^4$	$1.029 \times 10^6$	$0.533 \times 10^6$	$0.746 \times 10^6$	10.14
307	$1.435 \times 10^4$	$1.161 \times 10^4$	$1.205 \times 10^4$	$0.951 \times 10^6$	$0.491 \times 10^6$	$0.683 \times 10^6$	12.09
337	$1.106 \times 10^4$	$8.834 \times 10^3$	$9.185 \times 10^3$	$0.911 \times 10^6$	$0.470 \times 10^6$	$0.650 \times 10^6$	13.25
387	$6.786 \times 10^3$	$5.320 \times 10^3$	$5.612 \times 10^3$	$0.780 \times 10^6$	$0.401 \times 10^6$	$0.557 \times 10^6$	15.25
438	$4.800 \times 10^3$	$3.695 \times 10^3$	$3.910 \times 10^3$	$0.739 \times 10^6$	$0.377 \times 10^6$	$0.521 \times 10^6$	17.25
489	$3.280 \times 10^3$	$2.490 \times 10^3$	$2.668 \times 10^3$	$0.654 \times 10^6$	$0.332 \times 10^6$	$0.461 \times 10^6$	19.25
540	$2.489 \times 10^3$	$1.862 \times 10^3$	$1.999 \times 10^3$	$0.626 \times 10^6$	$0.316 \times 10^6$	$0.436 \times 10^6$	21.25
591	$1.933 \times 10^3$	$1.428 \times 10^3$	$1.537 \times 10^3$	$0.601 \times 10^6$	$0.301 \times 10^6$	$0.413 \times 10^6$	23.25
635	$1.440 \times 10^3$	$1.065 \times 10^3$	$1.158 \times 10^3$	$0.533 \times 10^6$	$0.268 \times 10^6$	$0.370 \times 10^6$	25
686	$1.163 \times 10^3$	$0.851 \times 10^3$	$0.927 \times 10^3$	$0.514 \times 10^6$	$0.257 \times 10^6$	$0.353 \times 10^6$	27
737	$0.953 \times 10^3$	$0.690 \times 10^3$	$0.754 \times 10^3$	$0.497 \times 10^6$	$0.247 \times 10^6$	$0.338 \times 10^6$	29
787	$0.791 \times 10^3$	$0.567 \times 10^3$	$0.621 \times 10^3$	$0.481 \times 10^6$	$0.237 \times 10^6$	$0.324 \times 10^6$	31
838	$0.664 \times 10^3$	$0.472 \times 10^3$	$0.517 \times 10^3$	$0.466 \times 10^6$	$0.229 \times 10^6$	$0.312 \times 10^6$	33
889	$0.562 \times 10^3$	$0.397 \times 10^3$	$0.436 \times 10^3$	$0.451 \times 10^6$	$0.221 \times 10^6$	$0.300 \times 10^6$	35
940	$0.480 \times 10^3$	$0.337 \times 10^3$	$0.370 \times 10^3$	$0.438 \times 10^6$	$0.213 \times 10^6$	$0.288 \times 10^6$	37
991	$0.403 \times 10^3$	$0.283 \times 10^3$	$0.312 \times 10^3$	$0.414 \times 10^6$	$0.202 \times 10^6$	$0.274 \times 10^6$	39
1067	$0.305 \times 10^3$	$0.213 \times 10^3$	$0.237 \times 10^3$	$0.371 \times 10^6$	$0.180 \times 10^6$	$0.246 \times 10^6$	42
1143	$0.252 \times 10^3$	$0.174 \times 10^3$	$0.195 \times 10^3$	$0.358 \times 10^6$	$0.173 \times 10^6$	$0.235 \times 10^6$	45
1219	$0.211 \times 10^3$	$0.144 \times 10^3$	$0.162 \times 10^3$	$0.345 \times 10^6$	$0.166 \times 10^6$	$0.225 \times 10^6$	48
1295	$0.178 \times 10^3$	$0.121 \times 10^3$	$0.136 \times 10^3$	$0.334 \times 10^6$	$0.160 \times 10^6$	$0.215 \times 10^6$	51
1372	$0.151 \times 10^3$	$0.102 \times 10^3$	$0.115 \times 10^3$	$0.323 \times 10^6$	$0.154 \times 10^6$	$0.207 \times 10^6$	54
1448	$0.120 \times 10^3$	$0.081 \times 10^3$	$0.092 \times 10^3$	$0.289 \times 10^6$	$0.137 \times 10^6$	$0.187 \times 10^6$	57
1524	$0.104 \times 10^3$	$0.070 \times 10^3$	$0.080 \times 10^3$	$0.282 \times 10^6$	$0.133 \times 10^6$	$0.180 \times 10^6$	60

immediately known, leaving  $F_M$  and  $F_C$  to be determined by trial and error, as with all manual methods. However, the method permits changes in exchanger geometry, particularly exchanger diameter and baffle spacing, to be undertaken speedily. Factors  $F_E$ ,  $F_A$  and  $\phi$ , as with all manual methods, are last-stage subsidiary calculations. In many applications all are unity, but where this is not the case, Tables 12.5 and 12.6 are given for the rapid calculation of  $F_E$  and  $F_A$ .

In both design and rating cases it is necessary to calculate the cross-flow Reynolds number ( $Re_c$ ) initially to establish the flow regime (i.e. whether turbulent or laminar) in order that the appropriate design factors may be used. Except for turbulent cross-flow pressure loss with square (90°) pitch, Reynolds number for most design cases need not be calculated again unless subsequent geometrical changes indicate that there is a change in flow regime. The calculation of Reynolds number and a knowledge of the flow regime is an essential discipline for all designs, whether manual or computer.

In design cases involving square (90°) pitch in the turbulent region, design factors  $F_M$  and  $F_C$  are based on a constant friction factor  $f_0 = 0.1$ , which is adequate to provide an approximate value for  $\Delta P_c$ . Once the design is near completion, a more exact value for  $\Delta P_c$  can be determined, as shown in Table 12.4.

Table 12.7(c) Shell-and-tube heat exchanger design-shell side calculations. Base mechanical design factor ( $F_M$ ). Pull-through floating head type.

Shell i.d. (mm)	Heat transfer coefficient						Shell i.d. (in)
	Turbulent			Laminar			
	$\Delta$ (30°)	$\square$ (90°) ( $f_s = 0.1$ )	$\diamond$ (45°)	$\Delta$ (30°)	$\square$ (90°)	$\diamond$ (45°)	
337	13.12	10.70	13.56	55.07	34.74	61.28	13.25
387	11.05	9.06	11.53	49.12	30.91	55.69	15.25
438	9.83	8.07	10.24	46.01	28.78	52.52	17.25
489	8.51	7.00	8.92	41.74	26.00	48.24	19.25
540	7.74	6.35	8.07	39.56	24.47	45.86	21.25
591	7.08	5.81	7.36	37.66	23.12	43.72	23.25
635	6.37	5.23	6.65	35.12	21.44	41.03	25
686	5.91	4.83	6.14	33.70	20.42	39.38	27
737	5.50	4.49	5.70	32.41	19.50	37.87	29
787	5.15	4.19	5.31	31.25	18.67	36.50	31
838	4.83	3.93	4.96	30.19	17.92	35.23	33
889	4.55	3.69	4.66	29.21	17.23	34.07	35
940	4.30	3.48	4.38	28.32	16.59	32.99	37
991	4.04	3.27	4.12	27.46	15.96	31.93	39
1067	3.61	2.91	3.69	25.35	14.64	29.71	42
1143	3.36	2.70	3.42	24.42	13.98	28.56	45
1219	3.15	2.52	3.19	23.57	12.58	27.51	48
1295	2.96	2.36	2.98	22.79	12.84	26.54	51
1372	2.79	2.22	2.80	22.07	12.34	25.66	54
1448	2.52	2.01	2.55	20.53	11.42	24.06	57
1524	2.39	1.90	2.41	19.97	11.03	23.36	60

## 12.5.7 Examples

- (1) An E-type split backing ring floating-head exchanger, 991 mm inside diameter, has tubes 25.4 mm o.d.  $\times$  31.75 mm  $\times$  30° pitch. Single-segmental baffles are spaced at 396 mm. The fluid flowing on the shell-side is water at 41.58 kg/s, having average properties of  $c_p = 4176.8$  J/kg K,  $\eta_b = (4.109 \times 10^{-4})$  N s/m<sup>2</sup>,  $\lambda = 0.65$  W/m K and  $\rho = 976.8$  kg/m<sup>3</sup>. (Assume  $\phi = 1$ ; hence  $(\alpha_o)_{nl}$  need not be calculated.)

- (a) What is the heat transfer coefficient and pressure loss in one cross-pass and one window?  
 (b) What is the corrected heat transfer coefficient and total shell-side pressure loss, excluding nozzles, if there are eight single-segmental baffles and two equal end spaces of 792 mm?

## Solution to 1(a)

From Table 12.3(b):

$$S_{mu} = 0.2311 \text{ m}^2/\text{m}$$

$$S_m = (0.2311 \times 10^{-3}) \times 396 = 0.09152 \text{ m}^2$$

$$\dot{m}_c = 41.58/0.09152 = 454.33 \text{ kg/s m}^2$$

Table 12.7(c) (cont.)

Shell i.d. (mm)	Cross flow pressure loss						Shell i.d. (in)
	Turbulent			Laminar			
	$\Delta$ (30°)	$\square$ (90°) ( $f_0 = 0.1$ )	$\diamond$ (45°)	$\Delta$ (30°)	$\square$ (90°)	$\diamond$ (45°)	
337	$5.461 \times 10^4$	$3.529 \times 10^3$	$3.757 \times 10^4$	$2.018 \times 10^6$	$0.713 \times 10^6$	$1.022 \times 10^6$	13.25
387	$4.221 \times 10^4$	$2.573 \times 10^3$	$2.852 \times 10^4$	$1.824 \times 10^6$	$0.651 \times 10^6$	$0.931 \times 10^6$	15.25
438	$3.593 \times 10^4$	$2.079 \times 10^3$	$2.375 \times 10^4$	$1.786 \times 10^6$	$0.643 \times 10^6$	$0.912 \times 10^6$	17.25
489	$2.900 \times 10^4$	$1.597 \times 10^3$	$1.886 \times 10^4$	$1.636 \times 10^6$	$0.593 \times 10^6$	$0.838 \times 10^6$	19.25
540	$2.525 \times 10^4$	$1.330 \times 10^3$	$1.611 \times 10^4$	$1.600 \times 10^6$	$0.583 \times 10^6$	$0.817 \times 10^6$	21.25
591	$2.215 \times 10^4$	$1.120 \times 10^3$	$1.387 \times 10^4$	$1.563 \times 10^6$	$0.572 \times 10^6$	$0.795 \times 10^6$	23.25
635	$1.849 \times 10^4$	$0.902 \times 10^3$	$1.152 \times 10^4$	$1.437 \times 10^6$	$0.527 \times 10^6$	$0.733 \times 10^6$	25
686	$1.647 \times 10^4$	$0.775 \times 10^3$	$1.010 \times 10^4$	$1.406 \times 10^6$	$0.517 \times 10^6$	$0.714 \times 10^6$	27
737	$1.475 \times 10^4$	$0.670 \times 10^3$	$8.908 \times 10^3$	$1.375 \times 10^6$	$0.506 \times 10^6$	$0.695 \times 10^6$	29
787	$1.328 \times 10^4$	$0.584 \times 10^3$	$7.902 \times 10^3$	$1.344 \times 10^6$	$0.496 \times 10^6$	$0.676 \times 10^6$	31
838	$1.120 \times 10^4$	$0.511 \times 10^3$	$7.046 \times 10^3$	$1.313 \times 10^6$	$0.485 \times 10^6$	$0.657 \times 10^6$	33
889	$1.089 \times 10^4$	$0.451 \times 10^3$	$6.313 \times 10^3$	$1.283 \times 10^6$	$0.475 \times 10^6$	$0.639 \times 10^6$	35
940	$9.914 \times 10^3$	$0.399 \times 10^3$	$5.682 \times 10^3$	$1.254 \times 10^6$	$0.464 \times 10^6$	$0.622 \times 10^6$	37
991	$8.765 \times 10^3$	$0.344 \times 10^3$	$5.021 \times 10^3$	$1.202 \times 10^6$	$0.445 \times 10^6$	$0.596 \times 10^6$	39
1067	$7.230 \times 10^3$	$0.273 \times 10^3$	$4.113 \times 10^3$	$1.090 \times 10^6$	$0.404 \times 10^6$	$0.541 \times 10^6$	42
1143	$6.426 \times 10^3$	$0.234 \times 10^3$	$3.602 \times 10^3$	$1.059 \times 10^6$	$0.393 \times 10^6$	$0.523 \times 10^6$	45
1219	$5.741 \times 10^3$	$0.202 \times 10^3$	$3.176 \times 10^3$	$1.029 \times 10^6$	$0.382 \times 10^6$	$0.505 \times 10^6$	48
1295	$5.154 \times 10^3$	$0.176 \times 10^3$	$2.816 \times 10^3$	$1.000 \times 10^6$	$0.371 \times 10^6$	$0.488 \times 10^6$	51
1372	$4.649 \times 10^3$	$0.154 \times 10^3$	$2.511 \times 10^3$	$0.973 \times 10^6$	$0.361 \times 10^6$	$0.472 \times 10^6$	54
1448	$3.913 \times 10^3$	$0.126 \times 10^3$	$2.114 \times 10^3$	$0.880 \times 10^6$	$0.326 \times 10^6$	$0.429 \times 10^6$	57
1524	$3.568 \times 10^3$	$0.112 \times 10^3$	$1.908 \times 10^3$	$0.859 \times 10^6$	$0.318 \times 10^6$	$0.417 \times 10^6$	60

From equation [12.5]:

$$Re_c = (454.33 \times 0.0254)/(4.109 \times 10^{-4}) = 28085 \text{ (i.e. turbulent)}$$

$$BSR = 396/991 = 0.4$$

#### Heat transfer

From Table 12.4(a):

$$F_F = 41.58^{0.635} = 10.666$$

$$F_P = (4176.8)^{0.333} \times 0.65^{0.667}/(4.109 \times 10^{-4})^{0.302} = 126.94$$

From Table 12.7(b):

$$F_M = 4.38$$

From Table 12.8(d):

$$X_C = 0.465, m = 0.545, (BSR > 0.35)$$

From equation [12.6]:

$$F_C = 0.465/0.4^{0.545} = 0.766$$

assume  $F_E = 1.0$  also  $F_A = 1.0$  (turbulent flow) and

$$\phi = 1.0 \text{ (specified)}$$

Table 12.7(c) (cont.)

Shell i.d. (mm)	Window pressure loss						Shell i.d. (in)
	Turbulent			Laminar			
	$\Delta$ (30°)	$\square$ (90°) ( $f_0 = 0.1$ )	$\diamond$ (45°)	$\Delta$ (30°)	$\square$ (90°)	$\diamond$ (45°)	
337	$7.426 \times 10^3$	$6.376 \times 10^3$	$6.842 \times 10^3$	$8.104 \times 10^5$	$4.050 \times 10^5$	$5.635 \times 10^5$	13.25
387	$4.654 \times 10^3$	$3.928 \times 10^3$	$4.247 \times 10^3$	$6.855 \times 10^5$	$3.449 \times 10^5$	$4.814 \times 10^5$	15.25
438	$3.335 \times 10^3$	$2.772 \times 10^3$	$3.001 \times 10^3$	$6.372 \times 10^5$	$3.226 \times 10^5$	$4.490 \times 10^5$	17.25
489	$2.326 \times 10^3$	$1.904 \times 10^3$	$2.078 \times 10^3$	$5.600 \times 10^5$	$2.846 \times 10^5$	$3.973 \times 10^5$	19.25
540	$1.787 \times 10^3$	$1.443 \times 10^3$	$1.578 \times 10^3$	$5.296 \times 10^5$	$2.700 \times 10^5$	$3.758 \times 10^5$	21.25
591	$1.405 \times 10^3$	$1.121 \times 10^3$	$1.227 \times 10^3$	$5.030 \times 10^5$	$2.571 \times 10^5$	$3.570 \times 10^5$	23.25
635	$1.087 \times 10^3$	$0.860 \times 10^3$	$0.949 \times 10^3$	$4.569 \times 10^5$	$2.336 \times 10^5$	$3.251 \times 10^5$	25
686	$0.887 \times 10^3$	$0.694 \times 10^3$	$0.766 \times 10^3$	$4.379 \times 10^5$	$2.241 \times 10^5$	$3.110 \times 10^5$	27
737	$0.733 \times 10^3$	$0.568 \times 10^3$	$0.628 \times 10^3$	$4.208 \times 10^5$	$2.154 \times 10^5$	$2.981 \times 10^5$	29
787	$0.614 \times 10^3$	$0.471 \times 10^3$	$0.521 \times 10^3$	$4.053 \times 10^5$	$2.074 \times 10^5$	$2.863 \times 10^5$	31
838	$0.519 \times 10^3$	$0.394 \times 10^3$	$0.437 \times 10^3$	$3.912 \times 10^5$	$2.000 \times 10^5$	$2.755 \times 10^5$	33
89	$0.443 \times 10^3$	$0.334 \times 10^3$	$0.371 \times 10^3$	$3.783 \times 10^5$	$1.932 \times 10^5$	$2.654 \times 10^5$	35
940	$0.381 \times 10^3$	$0.285 \times 10^3$	$0.317 \times 10^3$	$3.664 \times 10^5$	$1.868 \times 10^5$	$2.561 \times 10^5$	37
991	$0.324 \times 10^3$	$0.242 \times 10^3$	$0.270 \times 10^3$	$3.515 \times 10^5$	$1.793 \times 10^5$	$2.454 \times 10^5$	39
1067	$0.249 \times 10^3$	$0.184 \times 10^3$	$0.207 \times 10^3$	$3.154 \times 10^5$	$1.604 \times 10^5$	$2.209 \times 10^5$	42
1143	$0.207 \times 10^3$	$0.151 \times 10^3$	$0.171 \times 10^3$	$3.037 \times 10^5$	$1.541 \times 10^5$	$2.115 \times 10^5$	45
1219	$0.174 \times 10^3$	$0.126 \times 10^3$	$0.142 \times 10^3$	$2.931 \times 10^5$	$1.483 \times 10^5$	$2.029 \times 10^5$	48
1295	$0.148 \times 10^3$	$0.106 \times 10^3$	$0.120 \times 10^3$	$2.833 \times 10^5$	$1.429 \times 10^5$	$1.950 \times 10^5$	51
1372	$0.127 \times 10^3$	$0.091 \times 10^3$	$0.102 \times 10^3$	$2.742 \times 10^5$	$1.378 \times 10^5$	$1.877 \times 10^5$	54
1448	$0.102 \times 10^3$	$0.072 \times 10^3$	$0.083 \times 10^3$	$2.470 \times 10^5$	$1.239 \times 10^5$	$1.700 \times 10^5$	57
1425	$0.089 \times 10^3$	$0.063 \times 10^3$	$0.072 \times 10^3$	$2.405 \times 10^5$	$1.202 \times 10^5$	$1.645 \times 10^5$	60

From equation [12.2]:

$$\alpha_0 = 10.666 \times 126.94 \times 4.38 \times 0.766 = 4543 \text{ W/m}^2\text{K}$$

*Cross-flow pressure loss*

From Table 12.4(a):

$$F_F = 41.58^{1.75} = 680.84$$

$$F_P = (4.109 \times 10^{-4})^{0.25} / 976.8 = 1.458 \times 10^{-4}$$

From Table 12.7(b):

$$F_M = 1.269 \times 10^{-4}$$

From Table 12.8(d):

$$X_C = 0.053, m = 1.734 \text{ (BSR} > 0.34)$$

From equation [12.6]:

$$F_C = 0.053 / 0.4^{1.734} = 0.26$$

From equation [12.3]:

$$\Delta P_c = 680.84 \times (1.458 \times 10^{-4})(1.269 \times 10^4) \times 0.26 = 327.5 \text{ Pa}$$

*Window pressure loss*

From Table 12.4(a):

**Table 12.8(a)** Shell-and-tube heat exchanger design – shell-side calculations. Mechanical design correction factor ( $F_C$ ) – Fixed tubesheet and U-tube

Tube arrangement (mm)	Heat transfer coefficient										Tube arrangement (in)
	Shell dia. (mm)	Turbulent				Laminar					
		$(BSR) \leq 0.35$		$(BSR) > 0.35$		$(BSR) \leq 0.36$		$(BSR) > 0.36$			
		$X_C$	$m$	$X_C$	$m$	$X_C$	$m$	$X_C$	$m$		
15.875 × 19.844 Δ (30°)	205–257	0.794	0.144	0.600	0.423	205–257	1.236	-0.131	0.933	0.148	1/2 × 1/2 Δ (30°)
	307–1524	0.671	0.247	0.549	0.450	307–1524	1.045	-0.028	0.855	0.175	
15.875 × 22.225 □ (90°)	205–257	0.724	0.202	0.508	0.540	205–257	1.030	-0.019	0.723	0.320	1/2 × 1/2 □ (90°)
	307–1524	0.621	0.296	0.463	0.576	307–1524	0.885	0.076	0.660	0.356	
15.875 × 22.225 ◇ (45°)	205–257	0.643	0.275	0.467	0.579	205–257	1.000	0.000	0.726	0.304	1/2 × 1/2 ◇ (45°)
	307–1524	0.563	0.357	0.430	0.611	307–1524	0.877	0.082	0.669	0.336	
19.05 × 23.813 Δ (30°)	205–257	0.799	0.118	0.574	0.441	205–257	1.179	-0.157	0.848	0.166	1/2 × 1/2 Δ (30°)
	307–1524	0.677	0.227	0.527	0.474	307–1524	1.000	-0.048	0.779	0.199	
19.05 × 25.4 Δ (30°)	205–257	0.780	0.151	0.545	0.495	205–257	1.206	-0.125	0.843	0.220	1/2 × 1 Δ (30°)
	307–1524	0.651	0.250	0.486	0.531	307–1524	1.019	-0.025	0.760	0.256	
19.05 × 25.4 □ (90°)	205–257	0.730	0.170	0.505	0.523	205–257	0.974	-0.051	0.673	0.303	1/2 × 1 □ (90°)
	307–1524	0.631	0.275	0.467	0.562	307–1524	0.839	0.055	0.621	0.342	
19.05 × 25.4 ◇ (45°)	205–257	0.652	0.244	0.465	0.564	205–257	0.933	-0.031	0.665	0.289	1/2 × 1 ◇ (45°)
	307–1524	0.573	0.336	0.433	0.600	307–1524	0.819	0.061	0.619	0.325	

BSR limits 0.2–1.4

$$F_F = 41.58^2 = 1728.9$$

$$F_P = 1/976.8$$

From Table 12.7(b):

$$F_M = 0.403 \times 10^3$$

From Table 12.8(d):

$$X_C = 0.272, m = 0.825 \text{ (BSR} > 0.32)$$

From equation [12.6]:

$$F_C = 0.272/0.4^{0.825} = 0.579$$

From equation [12.4]:

$$\Delta P_w = 1728.9 \times (1/976.8)(0.403 \times 10^3) \times 0.579 = 413 \text{ Pa}$$



Table 12.8(a) (cont.)

Tube arrangement (mm)	Cross flow pressure loss										Tube arrangement (mm)
	Turbulent					Laminar					
	Shell dia. (mm)	(BSR) ≤ 0.34		(BSR) > 0.34		Shell dia. (in)	(BSR) ≤ 0.34		(BSR) > 0.34		
		X <sub>c</sub>	m	X <sub>c</sub>	m		X <sub>c</sub>	m	X <sub>c</sub>	m	
15.875 × 19.844 ° (30°)	205-257 307-838 889-1524	0.189 0.180 0.174	1.037 1.065 1.088	0.104 0.100 0.097	1.591 1.615 1.629	205-337 387-787 838-1524	0.614 0.619 0.579	0.304 0.299 0.340	0.341 0.342 0.324	0.852 0.853 0.880	1/4 × 7/8 Δ (30°)
15.875 × 22.225 □ (90°)	205-489 540-1524	0.088 0.079	1.508 1.578	0.054 0.049	1.963 2.009	205-257 307-686 737-1524	0.458 0.415 0.387	0.486 0.546 0.589	0.278 0.257 0.244	0.948 0.989 1.016	1/4 × 7/8 □ (90°)
15.875 × 22.225 ◇ (45°)	205-257 307-737 787-1524	0.115 0.104 0.097	1.343 1.408 1.450	0.073 0.068 0.064	1.763 1.800 1.827	205-257 307-737 787-1524	0.381 0.347 0.324	0.592 0.657 0.700	0.246 0.226 0.2215	1.009 1.1051 1.077	1/4 × 7/8 ◇ (45°)
19.05 × 23.813 Δ (30°)	205-257 307-737 787-1524	0.151 0.143 0.138	1.079 1.126 1.151	0.089 0.082 0.080	1.611 1.645 1.663	205-787 838-1524	0.426 0.404	0.348 0.400	0.242 0.233	0.874 0.913	1/4 × 1 1/8 Δ (30°)
19.05 × 25.4 Δ (30°)	205-257 307-838 889-1524	0.105 0.093 0.087	1.182 1.239 1.278	0.062 0.056 0.053	1.668 1.708 1.733	205-257 307-787 838-1524	0.280 0.254 0.238	0.432 0.493 0.534	0.166 0.154 0.146	0.918 0.959 0.985	1/4 × 1 Δ (30°)
19.05 × 25.4 □ (90°)	205-257 307-1524	0.098 0.090	1.452 1.533	0.059 0.055	1.928 1.982	205-257 307-1524	0.510 0.461	0.452 0.539	0.306 0.285	0.928 1.005	1/4 × 1 □ (90°)
19.05 × 25.4 ◇ (45°)	205-257 307-686 737-1524	0.121 0.144 0.105	1.311 1.366 1.427	0.076 0.073 0.069	1.740 1.776 1.814	205-337 387-1524	0.422 0.390	0.585 0.652	0.268 0.253	1.005 1.049	1/4 × 1 ◇ (45°)

**Solution to 1(b)**

*Inlet and outlet spaces – heat transfer correction*

$$l_r = 792/396 = 2$$

From Table 12.5:

$$F_E = 0.876 \text{ (for } N_b = 8)$$

corrected:

$$\alpha_o = 4543 \times 0.876 = 3980 \text{ W/m}^2 \text{ K}$$

*Inlet and outlet spaces – pressure loss*

From Table 12.9:

$$X_c = 2.0$$

$$l_r^{1.75} = 2^{1.75} = 3.364$$

From equation [12.7]:

$$\Delta P_e = (327.5 \times 2)/3.364 = 194.7 \text{ Pa}$$

Table 12.8(a) (cont.)

Tube arrangement (mm)	Window pressure loss										Tube arrangement (in)
	Shell dia. (mm)	Turbulent				Laminar					
		(BSR) ≤ 0.33		(BSR) > 0.33		(BSR) ≤ 0.36		(BSR) > 0.36			
		X <sub>c</sub>	m	X <sub>c</sub>	m	X <sub>c</sub>	m	X <sub>c</sub>	m		
15.875 × 19.844 Δ (30°)	205-438 489-1524	0.566 0.592	0.354 0.326	0.367 0.393	0.745 0.702	205-438 489-1524	2.902 3.097	-0.662 -0.702	2.245 2.382	-0.411 -0.451	1/4 × 7/8 Δ (30°)
15.875 × 22.225 □ (90°)	205-991 1067-1524	0.386 0.387	0.592 0.591	0.278 0.287	0.879 0.854	205-257 307-1524	1.952 1.762	-0.416 -0.352	1.588 1.504	-0.214 -0.199	1/4 × 7/8 □ (90°)
15.875 × 22.225 ◇ (45°)	205-991 1067-1524	0.335 0.333	0.679 0.683	0.255 0.261	0.916 0.898	205-257 307-1524	1.546 1.392	-0.271 -0.205	1.306 1.230	-0.103 -0.084	1/4 × 7/8 ◇ (45°)
19.05 × 23.813 Δ (30°)	205-438 489-1524	0.510 0.511	0.411 0.399	0.337 0.346	0.782 0.753	205-438 489-1524	1.987 2.161	-0.606 -0.653	1.567 1.693	-0.375 -0.417	1/4 × 1/2 Δ (30°)
19.05 × 25.4 Δ (30°)	205-686 737-1524	0.384 0.345	0.526 0.532	0.266 0.250	0.850 0.820	205-1524	1.183	-0.482	0.984	-0.305	1/4 × 1 Δ (30°)
19.05 × 25.4 □ (90°)	205-337 387-1524	0.422 0.415	0.562 0.574	0.294 0.306	0.876 0.846	205-1524	1.744	-0.405	1.449	-0.225	1/4 × 1 □ (90°)
19.05 × 25.4 ◇ (45°)	205-635 686-1524	0.366 0.357	0.650 0.669	0.270 0.277	0.913 0.892	205-1524	1.398	-0.268	1.198	-0.116	1/4 × 1 ◇ (45°)

**Total pressure loss**

From equation [12.8]

$$\Delta P_S = (7 \times 327.5) + (8 \times 413) + (2 \times 194.7) = 5986 \text{ Pa}$$

(excludes nozzle losses)

- (2) If the tubes in example (1) are changed to 90° pitch and all other conditions are unchanged, what is the pressure loss in one cross-pass?

**Solution to (2)**

Table 12.3(b) shows that  $S_{mu}$  is the same as example 1(a) and hence  $Re_c = 28085$  (i.e. turbulent)

From Table 12.4(a):

$$F_F = 41.58^2 = 1728.9$$

$$F_P = 1/976.8$$

From Table 12.7(b):

$$F_M = 0.49 \times 10^3$$

**Table 12.8(b)** Shell-and-tube heat exchanger design – shell side calculations. Mechanical design correction factor ( $F_C$ ) – Fixed tubesheet and U-tube (cont)

Tube arrangement (mm)	Heat transfer coefficient										Tube arrangement (in)
	Turbulent					Laminar					
	Shell dia. (mm)	(BSR) ≤ 0.35		(BSR) > 0.35		Shell dia. (mm)	(BSR) ≤ 0.36		(BSR) > 0.36		
		$X_C$	$m$	$X_C$	$m$		$X_C$	$m$	$X_C$	$m$	
25.4 × 31.75 Δ (30°)	205–257 307–1524	0.786 0.662	0.096 0.218	0.435 0.490	0.466 0.508	205–257 307–1524	1.064 0.902	–0.180 –0.057	0.725 0.668	0.191 0.233	1 × 1 1/4 Δ (30°)
25.4 × 31.75 □ (90°)	205–257 307–1524	0.745 0.650	0.110 0.238	0.500 0.475	0.493 0.539	205–257 307–1524	0.893 0.774	–0.111 0.018	0.599 0.566	0.273 0.319	1 × 1 1/4 □ (90°)
25.4 × 31.75 ◇ (45°)	205–257 307–1524	0.671 0.594	0.188 0.300	0.464 0.441	0.538 0.581	205–257 307–1524	0.836 0.738	–0.088 0.025	0.578 0.548	0.263 0.306	1 × 1 1/4 ◇ (45°)
31.75 × 39.688 Δ (30°)	205–257 307–1524	0.764 0.636	0.085 0.225	0.505 0.462	0.481 0.531	205–257 307–1524	0.967 0.814	–0.190 –0.050	0.639 0.591	0.206 0.256	1 1/4 × 1 1/8 Δ (30°)
31.75 × 39.688 □ (90°)	205–257 307–1524	0.722 0.621	0.103 0.249	0.473 0.448	0.505 0.560	205–257 307–1524	0.819 0.703	–0.117 0.029	0.537 0.508	0.285 0.340	1 1/4 × 1 1/8 □ (90°)
31.75 × 39.688 □ (90°)	205–257 307–1524	0.637 0.554	0.194 0.322	0.438 0.413	0.549 0.599	205–257 307–1524	0.741 0.646	–0.082 0.047	0.509 0.482	0.274 0.324	1 1/4 × 1 1/8 ◇ (45°)

BSR limits 0.2–1.4

From Table 12.8(d):

$$X_C = 0.053, m = 1.993 \text{ (BSR > 0.34)}$$

From equation [12.6]:

$$F_C = 0.053 / 0.4^{1.993} = 0.329$$

From equation [12.3]:

$$\Delta P_c = 1728.9 \times (1/976.8)(0.49 \times 10^3) \times 0.329 = 285.3 \text{ Pa}$$

This is a tentative value assuming  $f_o = 0.1$  (90° pitch in turbulent flow)

From Table 12.4(a):

$$f_s = 1.208 \text{ (by linear interpolation)}$$

corrected:

$$\Delta P_c = 1.208 \times 285.3 = 344.6 \text{ Pa}$$

- (3) An E-type U-tube exchanger, 737 mm inside diameter, has tubes 19.05 mm o.d × 25.4 mm × 45° pitch. Six segmental baffles are all equally spaced at 737 mm. The fluid flowing on the shell-side is heavy

Table 12.8(b) (cont.)

Tube arrangement (mm)	Cross flow pressure loss										Tube arrangement (in)
	Shell dia. (mm)	Turbulent				Laminar					
		(BSR) ≤ 0.34		(BSR) > 0.34		(BSR) ≤ 0.34		(BSR) > 0.34			
		X <sub>C</sub>	m	X <sub>C</sub>	m	X <sub>C</sub>	m	X <sub>C</sub>	m		
25.4 × 31.75 Δ (30°)	205-257 305-787 838-1524	0.108 0.101 0.098	1.127 1.193 1.231	0.063 0.060 0.059	1.634 1.679 1.705	205-489 540-1524	0.232 0.230	0.435 0.470	0.138 0.137	0.922 0.947	1 × 1/4 Δ (30°)
25.4 × 31.75 □ (90°)	205-387 438-1524	0.105 0.106	1.422 1.489	0.062 0.064	1.910 1.956	205-387 438-1524	0.492 0.484	0.422 0.489	0.291 0.293	0.910 0.956	1 × 1/4 □ (90°)
25.4 × 31.75 ◇ (45°)	205-257 305-737 787-1524	0.129 0.122 0.120	1.257 1.336 1.383	0.079 0.077 0.077	1.706 1.758 1.789	205-387 438-1524	0.431 0.414	0.533 0.609	0.268 0.264	0.973 1.023	1 × 1/4 ◇ (45°)
31.75 × 39.688 Δ (30°)	205-257 307-737 787-1524	0.083 0.077 0.074	1.151 1.232 1.281	0.049 0.047 0.046	1.643 1.698 1.731	205-387 438-1524	0.154 0.147	0.429 0.516	0.091 0.090	0.912 0.971	1 1/4 × 1 1/8 Δ (30°)
31.75 × 39.688 □ (90°)	205-257 307-635 686-1524	0.088 0.085 0.084	1.415 1.503 1.552	0.052 0.052 0.052	1.899 1.958 1.991	205-387 438-686 737-1524	0.321 0.310 0.301	0.415 0.503 0.563	0.191 0.190 0.188	0.899 0.958 0.997	1 1/4 × 1 1/8 □ (90°)
31.75 × 39.688 ◇ (45°)	205-257 307-686 737-1524	0.100 0.094 0.090	1.271 1.362 1.420	0.062 0.060 0.059	1.711 1.770 1.808	205-257 307-686 737-1524	0.283 0.268 0.258	0.521 0.612 0.670	0.176 0.172 0.170	0.961 1.020 1.058	1 1/4 × 1 1/8 ◇ (45°)

oil at 59.25 kg/s, having average properties of  $c_p = 1946.9$  J/kg K,  $\eta_b = 0.1$  N s/m<sup>2</sup>,  $\lambda = 0.121$  W/m K and  $\rho = 955.5$  kg/m<sup>3</sup>.  
What is the heat transfer coefficient and pressure loss for the shell-side if  $\phi$  is not unity? It is necessary to calculate  $(\alpha_o)_{nl}$  and  $\phi_{nl}$ .

**Solution to (3)**

From Table 12.3(a):

$$S_{mu} = 0.2619 \text{ m}^2/\text{m}$$

$$S_m = (0.2619 \times 10^{-3}) \times 737 = 0.193 \text{ m}^2$$

$$\dot{m}_c = 59.25/0.193 = 307 \text{ kg/s m}^2$$

From equation [12.5]:

$$Re_c = (307 \times 0.01905)/0.1 = 58.5 \text{ (i.e. laminar)}$$

$$BSR = 737/737 = 1.0$$

**Heat transfer**

From Table 12.4(b):

$$F_F = 59.25^{0.36} = 4.347$$

$$F_P = (1946.9^{0.333} \times 0.121^{0.667})/0.1^{0.027} = 3.24$$

Table 12.8(b) (cont.)

Tube arrangement (mm)	Window pressure loss										Tube arrangement (in)
	Shell dia. (mm)	Turbulent				Laminar					
		(BSR) ≤ 0.32		(BSR) > 0.32		(BSR) ≤ 0.36		(BSR) > 0.36			
		X <sub>C</sub>	m	X <sub>C</sub>	m	X <sub>C</sub>	m	X <sub>C</sub>	m		
25.4 × 31.75 Δ (30°)	205-737 787-1524	0.431 0.403	0.484 0.494	0.295 0.286	0.821 0.802	205-438 489-1524	1.087 1.186	-0.533 -0.574	0.876 0.957	-0.325 -0.368	1 × 1 1/4 Δ (30°)
25.4 × 31.75 Δ (30°)	205-438 489-1524	0.478 0.473	0.517 0.538	0.325 0.341	0.854 0.830	205-438 489-1524	1.547 1.650	-0.470 -0.459	1.232 1.355	-0.248 -0.270	1 × 1 1/4 □ (90°)
25.4 × 31.75 ◇ (45°)	205-438 489-1524	0.413 0.403	0.609 0.638	0.297 0.307	0.895 0.877	205-387 438-1524	1.242 1.281	-0.306 -0.292	1.044 1.102	-0.135 -0.145	1 × 1 1/4 ◇ (45°)
31.75 × 39.688 Δ (30°)	205-591 635-1524	0.391 0.344	0.525 0.548	0.267 0.249	0.858 0.838	205-438 489-991 1067-1524	0.678 0.735 0.752	-0.489 -0.513 -0.497	0.552 0.606 0.632	-0.291 -0.330 -0.334	1 1/4 × 1 9/16 Δ (30°)
31.75 × 39.688 □ (90°)	205-635 686-1524	0.434 0.407	0.552 0.585	0.298 0.297	0.879 0.863	205-387 438-737 787-1524	0.982 1.028 1.056	-0.442 -0.419 -0.400	0.785 0.852 0.894	-0.226 -0.239 -0.241	1 1/4 × 1 9/16 □ (90°)
31.75 × 39.688 ◇ (45°)	205-686 737-1524	0.361 0.341	0.653 0.677	0.269 0.263	0.909 0.904	205-387 438-737 787-1524	0.778 0.803 0.817	-0.282 -0.263 -0.241	0.653 0.695 0.722	-0.111 -0.121 -0.121	1 1/4 × 1 9/16 ◇ (45°)

From Table 12.10:

$$A = 16.512, m = 0.36$$

From equation [12.9]:

$$F_{NL} = 16.512/0.193^{0.36} = 29.85$$

From equation [12.9]:

$$(\alpha_o)_{nl} = 4.347 \times 3.24 \times 29.85 = 420 \text{ W/m}^2 \text{ K}$$

$\phi_{nl}$  is calculated by trial and error, based on  $(\alpha_o)_{nl}$ , as described in section 6.18. Calculations then continue as follows:

From Table 12.7(a):

$$F_M = 39.37$$

From Table 12.8(a):

$$X_C = 0.619, m = 0.325 \text{ (BSR} > 0.36)$$

From equation [12.6]:

$$F_C = 0.619/1^{0.325} = 0.619$$

**Table 12.8(c)** Shell-and-tube heat exchanger design – shell side calculations. Mechanical design correction factor ( $F_C$ ) – Split backing floating head

Tube arrange- ment (mm)	Heat transfer coefficient										Tube arrange- ment (in)
	Shell dia. (mm)	Turbulent				Laminar					
		$(BSR) \leq 0.35$		$(BSR) > 0.35$		$(BSR) \leq 0.36$		$(BSR) > 0.36$			
		$X_C$	$m$	$X_C$	$m$	$X_C$	$m$	$X_C$	$m$		
15.875× 19.844 Δ (30°)	205–940	0.704	0.218	0.530	0.494	205–1524	1.050	–0.030	0.819	0.214	$\frac{1}{2} \times \frac{15}{16}$ Δ (30°)
15.875× 22.225 □ (90°)	205–635 686–1524	0.630 0.585	0.287 0.333	0.456 0.441	0.594 0.602	205–787 838–1524	0.898 0.831	0.067 0.115	0.649 0.628	0.374 0.381	$\frac{1}{2} \times \frac{1}{2}$ □ (90°)
15.875× 22.225 ◇ (45°)	205–635 685–1524	0.580 0.537	0.338 0.386	0.433 0.416	0.613 0.627	205–686 737–1524	0.903 0.834	0.063 0.113	0.675 0.646	0.338 0.352	$\frac{1}{2} \times \frac{1}{2}$ ◇ (45°)
19.05× 23.813 Δ (30°)	205–737 787–1524	0.712 0.654	0.195 0.252	0.504 0.501	0.527 0.511	205–737 787–1524	1.052 0.968	–0.080 –0.023	0.744 0.741	0.252 0.236	$\frac{1}{2} \times \frac{15}{16}$ Δ (30°)
19.05× 25.4 Δ (30°)	205–686 737–1524	0.682 0.621	0.240 0.288	0.487 0.467	0.561 0.561	205–838 889–1524	1.044 0.968	–0.035 0.013	0.745 0.728	0.286 0.286	$\frac{1}{2} \times 1$ Δ (30°)
19.05× 25.4 □ (90°)	205–737 787–1524	0.622 0.587	0.268 0.318	0.444 0.440	0.586 0.591	205–940 991–1524	0.808 0.783	0.075 0.098	0.596 0.587	0.364 0.371	$\frac{1}{2} \times 1$ □ (90°)
19.05× 25.4 ◇ (45°)	205–686 737–1524	0.575 0.541	0.319 0.370	0.425 0.415	0.605 0.619	205–635 686–1524	0.828 0.781	0.044 0.089	0.611 0.597	0.330 0.342	$\frac{1}{2} \times 1$ ◇ (45°)

From Table 12.5:

$$F_E = 1 \text{ because } l_r = 737/737 = 1.0$$

From Table 12.6:

$$j_1 = 0.841, j_2 = 0.705 \text{ (7 cross-passes), } j = 0.593$$

$$F_A = 0.593 + \left[ \frac{(1 - 0.593)(58.5 - 20)}{80} \right] = 0.789$$

From equation [12.2]:

$$\alpha_o = (4.347 \times 3.24 \times 39.37 \times 0.619 \times 1 \times 0.789) \phi_{nl}$$

$$= 270.8(\phi_{nl}) \text{ W/m}^2 \text{ K}$$

*Cross-flow loss*

From Table 12.4(b):

$$F_F = 59.25$$

$$F_P = 0.1/955.5 = 1.047 \times 10^{-4}$$

Table 12.8(c) (cont.)

Cross flow pressure loss											
Tube arrangement (mm)	Shell dia. (mm)	Turbulent				Laminar				Tube arrangement (in)	
		(BSR) ≤ 0.34		(BSR) > 0.34		(BSR) ≤ 0.33		(BSR) > 0.33			
		X <sub>C</sub>	m	X <sub>C</sub>	m	X <sub>C</sub>	m	X <sub>C</sub>	m		
15.875 × 19.844 Δ (30°)	205-438 489-1524	0.143	1.210	0.086	1.684	205-438 489-1524	0.477	0.460	0.286	0.934	¾ × ¾ Δ (30)
15.875 × 22.225 □ (90°)	205-489 540-1524	0.077	1.596	0.049	2.011	205-787 838-1524	0.383	0.596	0.244	1.011	¾ × ¾ □ (90°)
15.875 × 22.225 ◇ (45°)	205-737 787-1524	0.102	1.419	0.067	1.802	205-686 737-1524	0.341	0.669	0.224	1.052	¾ × ¾ ◇ (45°)
19.05 × 23.813 Δ (30°)	205-337 387-1524	0.113	1.248	0.069	1.707	205-337 388-1524	0.327	0.498	0.199	0.957	¾ × ¾ Δ (30°)
19.01 × 23.813 Δ (30°)	205-787 838-1524	0.087	1.301	0.054	1.739	205-940 991-1524	0.225	0.563	0.141	0.997	¾ × 1 Δ (30°)
19.05 × 25.4 □ (90°)	205-387 438-1524	0.075	1.596	0.048	2.012	205-838 889-1524	0.421	0.572	0.265	1.000	¾ × 1 □ (90°)
19.05 × 25.4 ◇ (45°)	205-540 591-1524	0.099	1.420	0.065	1.804	205-889 940-1524	0.373	0.656	0.244	1.047	¾ × 1 ◇ (45°)

From Table 12.7(a):

$$F_M = 0.976 \times 10^6$$

From Table 12.8(a):

$$X_C = 0.253, m = 1.049 \text{ (BSR} > 0.34)$$

From equation [12.6]:

$$F_C = 0.253 / 1^{1.049} = 0.253$$

From equation [12.3]:

$$\Delta P_c = \{59.25 \times (1.047 \times 10^{-4})(0.976 \times 10^6) \times 0.253\} / \phi_{nl} = 1532 / \phi_{nl} \text{ Pa}$$

Window loss

Cross and long<sup>l</sup>-flow

Turn-around

From Table 12.4(b):

$$F_F = 59.25$$

$$59.25^2 = 3510.6$$

Table 12.8(c) (cont.)

Window pressure loss												
Tube arrangement (mm)	Turbulent						Laminar					
	Shell dia. (mm)	(BSR) ≤ 0.33		(BSR) > 0.33		Shell dia. (mm)	(BSR) ≤ 0.38		(BSR) > 0.38		Tube arrangement (in)	
		X <sub>C</sub>	m	X <sub>C</sub>	m		X <sub>C</sub>	m	X <sub>C</sub>	m		
15.875 × 19.844 Δ (30°)	205-337	0.457	0.487	0.321	0.804	205-257	1.870	-0.389	1.549	-0.193	¾ × ¾ Δ (30°)	
	387-991	0.515	0.414	0.354	0.754	307-337	1.965	-0.420	1.658	-0.243		
	1067-1524	0.560	0.361	0.384	0.711	387-489	2.290	-0.515	1.903	-0.325		
						540-991	2.421	-0.549	2.012	-0.362		
						1067-1524	2.651	-0.605	2.165	-0.405		
15.875 × 22.225 □ (90°)	205-438	0.356	0.641	0.261	0.910	205-337	1.492	-0.249	1.288	-0.096	¾ × ¾ □ (90°)	
	489-1524	0.370	0.618	0.281	0.863	387-1524	1.567	-0.279	1.384	-0.154	□ (90°)	
15.875 × 22.225 ◇ (45°)	205-438	0.320	0.709	0.246	0.933	205-1524	1.267	-0.147	1.145	-0.042	¾ × ¾ ◇ (45°)	
	489-1524	0.327	0.695	0.260	0.899							
19.05 × 23.813 Δ (30°)	205-438	0.429	0.509	0.305	0.816	205-257	0.298	-0.361	1.085	-0.170	¾ × ¾ Δ (30°)	
	489-1524	0.473	0.436	0.333	0.756	307-337	1.362	-0.381	1.164	-0.217		
						387-489	1.582	-0.468	1.337	-0.295		
						540-991	1.673	-0.496	1.420	-0.330		
						1067-1524	1.834	-0.546	1.538	-0.371		
19.05 × 25.4 Δ (30°)	205-540	0.337	0.610	0.247	0.884	205-337	0.870	-0.303	0.751	-0.150	¾ × 1 Δ (30°)	
	591-1524	0.336	0.569	0.248	0.839	387-991	0.985	-0.369	0.859	-0.227		
						1067-1524	1.025	-0.394	0.901	-0.264		
19.05 × 25.4 □ (90°)	205-591	0.379	0.619	0.279	0.889	205-337	1.371	-0.270	1.173	-0.110	¾ × 1 □ (90°)	
	635-1524	0.391	0.603	0.294	0.856	387-991	1.447	-0.281	1.284	-0.160		
						1067-1524	1.551	-0.321	1.358	-0.189		
19.05 × 25.4 ◇ (45°)	205-438	0.334	0.698	0.258	0.923	205-337	1.180	-0.175	1.025	-0.028	¾ × 1 ◇ (45°)	
	489-1524	0.346	0.677	0.272	0.890	387-1524	1.249	-0.201	1.100	-0.069	◇ (45°)	

From Table 12.4(b):

$$F_p \cdot 0.1/955.5 = 1.047 \times 10^{-4} \qquad 1/955.5 = 1.047 \times 10^{-3}$$

From Table 12.7(a):

$$F_M \quad 0.373 \times 10^6 \qquad 0.834 \times 10^3$$

From Table 12.8(a):

$$X_{C,m} \quad 1.198, -0.116 \text{ (BSR > 0.36)} \qquad 0.277, 0.892 \text{ (BSR > 0.33)}$$

From equation [12.6]:

$$F_C \quad 1.198/1^{-0.116} = 1.198 \qquad 0.277/1^{0.892} = 0.277$$

From Table 12.4(c) and (b):

$$f_w \cdot F_w \quad - \qquad 4.08 \cdot \{1/(1 + f_w D_s)\} = 0.25$$



**Table 12.8(d)** Shell and tube heat exchanger design – shell side calculations. Mechanical design correction factor ( $F_C$ ) – Split backing floating-head (cont)

Tube arrangement (mm)	Heat transfer coefficient										Tube arrangement (in)
	Turbulent					Laminar					
	Shell dia. (mm)	$(BSR) \leq 0.35$		$(BSR) > 0.35$		Shell dia. (mm)	$(BSR) \leq 0.36$		$(BSR) > 0.36$		
		$X_C$	m	$X_C$	m		$X_C$	m	$X_C$	m	
25.4x 31.75 $\Delta$ (30°)	205-540 591-1524	0.662 0.630	0.211 0.254	0.464 0.465	0.549 0.545	205-540 591-1524	0.883 0.860	-0.042 -0.021	0.637 0.634	0.269 0.270	1x1½ $\Delta$ (30°)
25.4x 31.75 $\square$ (90°)	205-387 438-1524	0.586 0.597	0.273 0.281	0.422 0.438	0.585 0.575	205-686 737-1524	0.730 0.713	0.039 0.070	0.525 0.529	0.352 0.356	1x1½ $\square$ (90°)
25.4x 31.75 $\diamond$ (45°)	205-540 591-1524	0.569 0.553	0.298 0.338	0.417 0.418	0.592 0.603	205-540 591-1524	0.720 0.693	0.012 0.063	0.521 0.523	0.317 0.328	1x1½ $\diamond$ (45°)
31.75x 39.688 $\Delta$ (30°)	205-540 591-1524	0.625 0.594	0.230 0.273	0.443 0.437	0.556 0.565	205-540 591-1524	0.791 0.762	-0.052 0.000	0.553 0.559	0.288 0.291	1½x1½ $\Delta$ (30°)
31.75x 39.688 $\square$ (90°)	205-387 438-1524	0.571 0.562	0.248 0.301	0.400 0.412	0.586 0.594	205-489 540-1524	0.666 0.644	0.036 0.082	0.472 0.474	0.362 0.373	1½x1½ $\square$ (90°)
31.75x 39.688 $\diamond$ (45°)	205-337 387-1524	0.529 0.516	0.300 0.352	0.384 0.390	0.602 0.616	205-540 591-1524	0.610 0.603	0.054 0.085	0.452 0.457	0.337 0.344	1½x1½ $\diamond$ (45°)

BSR limits 0.2-1.4

From Table 12.4(b):

$$\Delta P_t = 59.25 \times (1.047 \times 10^{-4})(0.373 \times 10^6) \times 1.198 = 2772 \text{ Pa}$$

From equation [12.4]:

$$\begin{aligned} \Delta P_{ta} &= 3510.6 \times (1.047 \times 10^{-3})(0.834 \times 10^3) \times 0.277 \times 0.25 = 212 \text{ Pa} \\ \Delta P_w &= 2772 + 212 = 2984 \text{ Pa} \end{aligned}$$

*Inlet and outlet spaces – pressure loss*

From Table 12.9:

$$X_c = 1.9$$

From equation [12.7]:

$$\Delta P_c = (1.9 \times 1532)/\phi_{nl} = 2911/\phi_{nl} \text{ Pa} (l_r = 1)$$

*Total pressure loss*

From equation [12.8]:

Table 12.8(d) (cont.)

Cross flow pressure loss											
Tube arrangement (mm)	Turbulent					Laminar					Tube arrangement (in)
	Shell dia. (mm)	(BSR) ≤ 0.34		(BSR) > 0.34		Shell dia. (mm)	(BSR) ≤ 0.34		(BSR) > 0.34		
		X <sub>C</sub>	m	X <sub>C</sub>	m		X <sub>C</sub>	m	X <sub>C</sub>	m	
25.4 × 31.75 Δ (30°)	205-387 438-1524	0.079 0.086	1.285 1.287	0.049 0.053	1.724 1.734	205-438 489-1524	0.183 0.200	0.550 0.537	0.114 0.123	0.986 0.984	1 × 1 1/4 Δ (30°)
25.4 × 31.75 □ (90°)	205-257 307-438 489-991 1067-1524	0.074 0.078 0.086 0.088	1.535 1.555 1.556 1.575	0.046 0.049 0.053 0.055	1.970 1.989 1.993 2.006	205-337 387-1524	0.378 0.413	0.548 0.556	0.237 0.257	0.980 0.993	1 × 1 1/4 □ (90°)
25.4 × 31.75 ◇ (45°)	205-307 337-686 737-1524	0.097 0.103 0.105	1.365 1.387 1.420	0.063 0.067 0.069	1.768 1.786 1.809	205-307 387-1524	0.351 0.372	0.615 0.640	0.227 0.241	1.018 1.039	1 × 1 1/4 ◇ (45°)
31.75 × 39.688 Δ (30°)	205-337 387-737 787-1524	0.060 0.067 0.066	1.304 1.284 1.333	0.038 0.042 0.041	1.731 1.726 1.759	205-307 337-991 1067-1524	0.116 0.129 0.129	0.554 0.550 0.590	0.073 0.081 0.081	0.981 0.987 1.014	1 1/4 × 1 1/8 Δ (30°)
31.75 × 39.688 □ (90°)	205-257 307-438 489-889 940-1524	0.060 0.065 0.069 0.071	1.548 1.562 1.579 1.614	0.038 0.041 0.044 0.045	1.973 1.989 2.000 2.026	205-307 337-686 737-1524	0.240 0.255 0.267	0.563 0.579 0.606	0.152 0.162 0.170	0.985 1.000 1.021	1 1/4 × 1 1/8 □ (90°)
31.75 × 39.688 ◇ (45°)	205-307 337-686 737-1524	0.074 0.079 0.080	1.376 1.408 1.450	0.048 0.052 0.053	1.772 1.796 1.824	205-307 337-686 737-1524	0.224 0.233 0.237	0.626 0.658 0.696	0.146 0.153 0.157	1.022 1.046 1.072	1 1/4 × 1 1/8 ◇ (45°)

$$\Delta P_s = \frac{5 \times 1532}{\phi_{nl}} + (6 \times 2984) + \frac{2 \times 2911}{\phi_{nl}}$$

i.e.

$$\Delta P_s = \left\{ \frac{13482}{\phi_{nl}} + 17904 \right\} \text{ Pa}$$

(excludes nozzle losses)

- (4) It will be seen from Chapter 17 that design involves trial and error and it is desirable to calculate revised heat transfer and pressure loss quickly to suit changes in shell diameter, baffle spacing, etc. In most cases, the product ( $F_F F_P$ ) is fixed, leaving only  $F_M$  and  $F_C$  to be calculated (if  $F_E = F_A = \phi = 1$ ). If there is no change in shell diameter, the product ( $F_M F_F F_P$ ) is fixed leaving only  $F_C$  to be calculated, arising from a change in baffle spacing.

The baffle spacing in the exchanger of example (1) is reduced to 248 mm. What is the revised heat transfer coefficient and pressure loss in one cross-pass and one window, assuming  $F_E = \phi = 1$ ?

Table 12.8(d) (cont.)

Tube arrangement (mm)	Window pressure loss										Tube arrangement (in)
	Shell dia. (mm)	Turbulent				Laminar					
		(BSR) ≤ 0.32		(BSR) > 0.32		(BSR) ≤ 0.38		(BSR) > 0.38			
		X <sub>c</sub>	m	X <sub>c</sub>	m	X <sub>c</sub>	m	X <sub>c</sub>	m		
25.4 × 31.75 Δ (30°)	205-438	0.364	0.579	0.263	0.860	205-257	0.731	-0.331	0.614	-0.152	1 × 1 1/4 Δ (30°)
	489-1524	0.375	0.537	0.272	0.825	307-337	0.764	-0.333	0.660	-0.182	
						387-489	0.880	-0.409	0.757	-0.255	
						540-991	0.931	-0.428	0.810	-0.287	
					1067-1524	1.022	-0.468	0.886	-0.325		
25.4 × 31.75 □ (90°)	205-438	0.499	0.615	0.290	0.894	205-337	1.165	-0.299	0.980	-0.122	1 × 1 1/4 □ (90°)
	489-1524	0.429	0.576	0.318	0.844	387-540	1.311	-0.350	1.115	-0.186	
						591-1067	1.359	-0.348	1.176	-0.202	
						1143-1524	1.454	-0.371	1.258	-0.227	
25.4 × 31.75 ◇ (45°)	205-438	0.353	0.684	0.268	0.923	205-387	1.039	-0.206	0.903	-0.060	1 × 1 1/4 ◇ (45°)
	489-1524	0.379	0.650	0.293	0.877	438-991	1.111	-0.233	0.970	-0.094	
						1067-1524	1.161	-0.224	1.038	-0.110	
31.75 × 39.688 Δ (30°)	205-737	0.328	0.595	0.240	0.870	205-307	0.474	-0.311	0.402	-0.144	1 1/4 × 1 3/8 Δ (30°)
	787-1524	0.318	0.578	0.236	0.845	337-387	0.512	-0.331	0.443	-0.184	
						438-635	0.575	-0.394	0.496	-0.244	
						686-1067	0.596	-0.383	0.528	-0.261	
						1143-1524	0.648	-0.419	0.572	-0.296	
31.75 × 39.688 □ (90°)	205-438	0.349	0.666	0.256	0.932	205-337	0.750	-0.286	0.632	-0.112	1 1/4 × 1 3/8 □ (90°)
	489-1524	0.371	0.622	0.274	0.886	388-540	0.836	-0.322	0.717	-0.167	
						591-1067	0.866	-0.313	0.759	-0.179	
						1143-1524	0.926	-0.329	0.815	-0.203	
31.75 × 39.688 ◇ (45°)	205-1524	0.312	0.709	0.247	0.912	205-387	0.665	-0.188	0.580	-0.047	1 1/4 × 1 3/8 ◇ (45°)
						438-991	0.707	-0.199	0.626	-0.075	
						1067-1524	0.740	-0.191	0.671	-0.091	

**Solution to (4)**

The reduction in baffle spacing from 396 mm to 248 mm increases Re so that the flow will remain turbulent. F<sub>A</sub> will again be unity. From example 1(a):

For heat transfer:

$$F_F F_P F_M = 10.666 \times 126.94 \times 4.38 = 5930.3$$

For cross loss:

$$F_F F_P F_M = 680.84 \times (1.458 \times 10^{-4})(1.269 \times 10^4) = 1259.7$$

For window loss:

$$F_F F_P F_M = 1728.9 \times (1/976.8)(0.403 \times 10^3) = 713.3$$

$$BSR = 248/991 = 0.25$$

From Table 12.8(d) and equation [12.6]:

For heat transfer:

**Table 12.8(e)** Shell and tube heat exchanger design – shell side calculations. Mechanical design correction factor ( $F_C$ ) – Pull-through floating-head

Tube arrangement (mm)	Heat transfer coefficient										Tube arrangement (in)
	Turbulent					Laminar					
	Shell dia. (mm)	(BSR) ≤ 0.35		(BSR) > 0.35		Shell dia. (mm)	(BSR) ≤ 0.35		(BSR) > 0.35		
		$X_C$	$m$	$X_C$	$m$		$X_C$	$m$	$X_C$	$m$	
15.875 × 19.844 Δ (30°)	337–591 635–1524	0.628 0.650	0.289 0.267	0.460 0.494	0.587 0.533	337–591 635–1524	0.977 1.019	0.014 –0.012	0.717 0.770	0.312 0.259	$\frac{1}{4} \times \frac{3}{8}$ Δ (30°)
15.875 × 22.225 □ (90°)	337–991 1067–1524	0.542 0.556	0.380 0.365	0.413 0.424	0.638 0.622	337–991 1067–1524	0.779 0.791	0.155 0.146	0.591 0.601	0.417 0.405	$\frac{1}{4} \times \frac{1}{2}$ □ (90°)
15.875 × 22.225 ◇ (45°)	337–1524	0.515	0.412	0.403	0.642	337–1524	0.802	0.137	0.627	0.367	$\frac{1}{4} \times \frac{1}{4}$ ◇ (45°)
19.05 × 23.813 Δ (30°)	337–591 635–1524	0.589 0.629	0.308 0.276	0.435 0.470	0.599 0.555	337–591 635–1524	0.872 0.931	0.033 0.000	0.643 0.696	0.324 0.280	$\frac{1}{4} \times \frac{15}{16}$ Δ (30°)
19.05 × 25.4 Δ (30°)	337–591 635–1524	0.569 0.594	0.342 0.325	0.427 0.448	0.617 0.592	337–591 635–1524	0.853* 0.915	0.077 0.050	0.644 0.691	0.344 0.317	$\frac{1}{4} \times 1$ Δ (30°)

BSR limits 0.2–1.4

$$X_C = 0.630, m = 0.254, F_C = 0.630/0.25^{0.254} = 0.896$$

For cross loss:

$$X_C = 0.086, m = 1.287, F_C = 0.086/0.25^{1.287} = 0.512$$

For window loss:

$$X_C = 0.375, m = 0.537, F_C = 0.375/0.25^{0.537} = 0.789$$

From equation [12.2]:

$$\alpha_o = 5930.3 \times 0.896 = 5314 \text{ W/m}^2 \text{ K}$$

From equation [12.3]:

$$\Delta P_c = 1259.7 \times 0.512 = 645 \text{ Pa}$$

From equation [12.4]:

$$\Delta P_w = 713.3 \times 0.789 = 563 \text{ Pa}$$

### 12.5.7 Method applied to other shell and baffle types

Although derived initially for E-type shells, the method may be applied

Table 12.8(e) (cont.)

Tube arrange- ment (mm)	Cross flow pressure loss										Tube arrange- ment (in)
	Shell dia. (mm)	Turbulent				Laminar					
		(BSR) ≤ 0.34		(BSR) > 0.34		(BSR) ≤ 0.34		(BSR) > 0.34			
		X <sub>C</sub>	m	X <sub>C</sub>	m	X <sub>C</sub>	m	X <sub>C</sub>	m		
15.875× 19.844 Δ (30°)	337-438 489-991 1067-1524	0.101 0.120 0.136	1.425 1.319 1.243	0.067 0.075 0.082	1.808 1.752 1.715	337-438 489-991 1067-1524	0.338 0.401 0.452	0.675 0.569 0.493	0.223 0.251 0.272	1.058 1.000 0.965	$\frac{5}{8} \times \frac{3}{4}$ Δ (30°)
15.875× 22.225 □ (90°)	337-387 438-1524	0.061 0.066	1.743 1.690	0.041 0.044	2.094 2.068	337-438 489-1524	0.303 0.336	0.743 0.678	0.207 0.221	1.094 1.063	$\frac{5}{8} \times \frac{7}{8}$ □ (90°)
15.875× 22.225 ◇ (45°)	337-1524	0.088	1.512	0.060	1.860	337-540 591-1524	0.289 0.298	0.772 0.753	0.199 0.202	1.112 1.106	$\frac{5}{8} \times \frac{7}{8}$ ◇ (45°)
19.05× 23.813 Δ (30°)	337-438 489-991 1067-1524	0.084 0.096 0.105	1.421 1.350 1.312	0.055 0.061 0.065	1.804 1.769 1.752	337-438 489-991 1067-1524	0.234 0.278 0.315	0.695 0.602 0.542	0.156 0.177 0.194	1.068 1.019 0.991	$\frac{3}{4} \times \frac{15}{16}$ Δ (30°)
19.05× 25.4 Δ (30°)	337-438 489-1524 1067-1524	0.066 0.075 0.204	1.476 1.392 0.629	0.045 0.049 0.131	1.835 1.794 1.039	337-438 489-991	0.165 0.187	0.726 0.668	0.111 0.123	1.085 1.055	$\frac{3}{4} \times 1$ Δ (30°)

to other shell types shown in Fig. 1.1, such as the J type, and with caution, to G, H and F types. Double-segmental baffle and no-tube-in-window (NTIW) design is discussed.

#### Divided-flow (J-type) shell

It is readily adapted to this shell type. All calculations are based on one-half of the total flow entering the shell-side, with cross-flow and window pressure losses being based on one-half of the total number of cross-passes in the unit.

#### Split flow (G-type) shell

Depending on tube diameter and length, some G-type shells have no cross baffles and the method is not applicable. Where G shells have cross baffles, *vertically cut*, the method will provide an *approximate* solution if the shell is treated exactly as an E type, having the same overall tube length, baffle spacing and shell-side flow rate as the G-type shell. It is assumed that there is no leakage between the longitudinal baffle and shell.

#### Double split flow (H-type) shell

The shell-side flow is equivalent to two G-type shells operating in parallel. Provided the H-type shell has cross baffles, *vertically cut*, the method will provide an *approximate* solution if the problem is treated as

Table 12.8(e) (cont.)

Tube arrangement (mm)	Heat transfer coefficient										Tube arrangement (in)
	Turbulent					Laminar					
	Shell dia. (mm)	(BSR) ≤ 0.35		(BSR) > 0.35		Shell dia. (mm)	(BSR) ≤ 0.35		(BSR) > 0.35		
		X <sub>c</sub>	m	X <sub>c</sub>	m		X <sub>c</sub>	m	X <sub>c</sub>	m	
15.875× 19.844 Δ (30°)	337-387	0.340	0.673	0.268	0.879	337-387	1.200	-0.112	1.053	0.030	
	438-591	0.384	0.596	0.295	0.834	438-489	1.352	-0.187	1.185	-0.043	
	635-991	0.444	0.504	0.330	0.779	540-686	1.511	-0.256	1.332	-0.118 $\frac{1}{4} \times \frac{1}{16}$	
	1067-1524	0.504	0.427	0.362	0.735	737-889	1.668	-0.318	1.484	-0.190 Δ (30°)	
						940-1295	1.883	-0.393	1.663	-0.260	
1372-1524	2.028	-0.439	1.774	-0.297							
15.875× 22.225 □ (90°)	337-438	0.287	0.778	0.231	0.961	337-438	1.063	-0.038	0.956	0.079	
	489-991	0.326	0.696	0.257	0.907	489-737	1.211	-0.119	1.096	0.000 $\frac{1}{4} \times \frac{1}{4}$	
	1067-1524	0.357	0.641	0.277	0.866	787-1067	1.285	-0.155	1.176	-0.058 □ (90°)	
	1143-1524	1.378	-0.199	1.252	-0.097						
15.875× 22.225 ◇ (45°)	337-438	0.280	0.793	0.230	0.958	337-387	0.992	0.006	0.894	0.120	
	489-1524	0.316	0.716	0.256	0.903	438-991	1.078	-0.047	0.980	0.060 $\frac{1}{4} \times \frac{1}{4}$	
	1067-1524	1.156	-0.090	1.067	0.000 ◇ (45°)						
19.05× 23.813 Δ (30°)	337-387	0.305	0.705	0.242	0.905	337-387	0.833	-0.091	0.738	0.039	
	438-591	0.352	0.612	0.271	0.847	438-489	0.939	-0.162	0.833	-0.029	
	635-991	0.386	0.554	0.291	0.811	540-686	1.049	-0.224	0.937	-0.100 $\frac{1}{4} \times \frac{1}{16}$	
	1067-1524	0.431	0.484	0.316	0.769	737-991	1.158	-0.277	1.048	-0.166 Δ (30°)	
						1067-1295	1.306	-0.346	1.177	-0.232	
1372-1524	1.407	-0.389	1.258	-0.269							
19.05× 25.4 Δ (30°)	337-438	0.267	0.749	0.214	0.937	336-387	0.563	-0.062	0.507	0.055	
	489-1524	0.316	0.601	0.243	0.840	438-540	0.626	-0.118	0.566	0.000	
	591-737	0.702	-0.179	0.639	-0.073 $\frac{1}{4} \times 1$						
	787-1067	0.759	-0.214	0.705	-0.130 Δ (30°)						
	1143-1524	0.861	-0.288	0.791	-0.195						

two E-type shells in parallel. In this case each E-type shell has the same baffle spacing as the H-type shell, but one-half of its overall tube length. The shell-side flow rate for each E-type shell is one-half of the total shell-side flow rate entering the H-type shell. Again it is assumed that there is no leakage between the longitudinal baffle and shell.

#### Two-pass (F-type) shell

The method may be used to obtain an *approximate* solution for an F-type shell if it is assumed that there is no leakage between the longitudinal baffle and shell, and that the cross baffles are *vertically* cut. An F-type shell may be regarded as an E-type in which the cross-flow and window areas are halved by the insertion of the longitudinal baffle. For identical baffle spacing and flow rate, the cross-flow and window velocities for the F-type are therefore twice those of the E-type. In addition, there are twice the number of cross-passes in the F-type.

If heat transfer coefficient  $\alpha_o \propto (\text{velocity})^p$ , cross-flow pressure loss  $\Delta P_c \propto (\text{velocity})^q$  and window pressure loss  $\Delta P_w \propto (\text{velocity})^r$ , then

**Table 12.8(f)** Shell and tube heat exchanger design – shell side calculations. Mechanical design correction factor ( $F_C$ ) – Pull-through floating-head (cont)

Tube arrangement (mm)	Heat transfer coefficient										Tube arrangement (in)
	Turbulent					Laminar					
	Shell dia. (mm)	(BSR) ≤ 0.35		(BSR) > 0.35		Shell dia. (mm)	(BSR) ≤ 0.35		(BSR) > 0.35		
		$X_C$	m	$X_C$	m		$X_C$	m	$X_C$	m	
19.05 × 25.4 □ (90°)	337–991 1067–1524	0.529 0.553	0.371 0.352	0.400 0.419	0.635 0.615	337–991 1067–1524	0.712 0.740	0.151 0.132	0.538 0.561	0.415 0.395	1/2 × 1 □ (90°)
19.05 × 25.4 ◇ (45°)	337–1524	0.511	0.395	0.395	0.638	337–1524	0.736	0.125	0.572	0.362	1/2 × 1 ◇ (45°)
25.4 × 31.75 △ (30°)	337–591 635–1524	0.528 0.581	0.345 0.304	0.396 0.433	0.618 0.584	337–591 635–1524	0.720 0.793	0.070 0.029	0.540 0.591	0.343 0.309	1 × 1 1/2 △ (30°)
25.4 × 31.75 □ (90°)	337–737 787–1524	0.507 0.536	0.354 0.339	0.379 0.403	0.630 0.612	337–991 1067–1524	0.623 0.678	0.139 0.096	0.467 0.505	0.410 0.377	1 × 1 1/2 □ (90°)

BSR limits 0.2–1.4

compared with an E shell, the approximate increases in  $\alpha_o$ ,  $\Delta P_c$  and  $\Delta P_w$  are  $2^p$ ,  $2^q$  and  $2^r$  respectively. In the central cross-passes of the complete F shell, the approximate increases in total cross-flow and window pressure losses are  $2(2^q)$  and  $2(2^r)$  respectively. Using this approach, the approximate heat transfer and pressure loss for an F shell may be based on an E shell of similar geometry. [Typical values of  $p$ ,  $q$  and  $r = 0.64, 1.75, 2$  for turbulent flow;  $0.36, 1, 1$  for laminar flow respectively]

If the F shell has  $N$  baffles in each shell pass, with central and return baffle spacing at the free end of the longitudinal baffle =  $l_s$ , heat transfer and pressure loss calculations are made exactly as for an E shell with  $N_b = N$  and central baffle spacing =  $l_s$ . The approximate procedure is as follows:

- (1) To check whether flow is turbulent or laminar calculate  $Re_c$  from equation [12.5] and multiply by 2, as the velocity in the F shell is twice that of the E shell, giving  $Re'_c$ .
- (2) Calculate heat transfer coefficient  $\alpha_o$  from equation [12.2] and multiply by  $F_2$  below:
  - $F_2 = 1.55$ : 30° and 45° pitch angle,  $Re'_c \geq 300$
  - $= 1.28$ : 30° and 45° pitch angle,  $Re'_c < 300$
  - $= 1.57$ : 90° pitch angle,  $Re'_c \geq 300$
  - $= 1.35$ : 90° pitch angle,  $Re'_c < 300$

If  $\phi \neq 1$ , assume, or calculate it, from section 6.8. Obtain  $F_E$  from Table 12.5 using  $2N_b$  for the number of baffles. Obtain  $F_A$  from Table 12.6 with the number of cross-passes =  $(N_b + 1)$ .

Table 12.8(f) (cont.)

Tube arrange- ment (mm)	Cross flow pressure loss										Tube arrange- ment (in)
	Turbulent					Laminar					
	Shell dia. (mm)	(BSR) ≤ 0.34		(BSR) > 0.34		Shell dia. (mm)	(BSR) ≤ 0.34		(BSR) > 0.34		
		X <sub>c</sub>	m	X <sub>c</sub>	m		X <sub>c</sub>	m	X <sub>c</sub>	m	
19.05× 25.4 □ (90°)	337-387	0.057	1.736	0.038	2.089	337-591	0.325	0.719	0.219	1.081	½×1
	438-991	0.063	1.695	0.042	2.070	635-1524	0.366	0.663	0.239	1.055	□ (90°)
	1067-1524	0.070	1.656	0.046	2.052						
19.05× 25.4 ◇ (45°)	337-591	0.082	1.511	0.056	1.855	337-438	0.300	0.770	0.207	1.109	½×1
	635-1524	0.090	1.484	0.061	1.844	489-1524	0.331	0.733	0.223	1.094	◇ (45°)
25.4× 31.75 △ (30°)	337-438	0.058	1.446	0.039	1.816	337-438	0.130	0.718	0.088	1.078	1×1½
	489-991	0.067	1.394	0.044	1.791	489-991	0.156	0.644	0.102	1.041	△ (30°)
	1067-1524	0.073	1.374	0.047	1.784	1067-1524	0.171	0.625	0.110	1.035	
25.4× 31.75 □ (90°)	337-387	0.050	1.725	0.034	2.082	337-438	0.279	0.725	0.189	1.082	1×1½
	438-635	0.057	1.674	0.038	2.054	489-991	0.324	0.661	0.212	1.050	□ (90°)
	686-1067	0.064	1.668	0.042	2.056	1067-1524	0.352	0.650	0.228	1.048	
	1143-1524	0.071	1.653	0.046	2.050						

- (3) Calculate cross-flow pressure loss ( $\Delta P_c$ ) from equation [12.3] and obtain total cross-flow pressure loss for central spacing ( $\Delta P'_c$ ) from:

$$\Delta P'_c = N_b F_2 \Delta P_c$$

where  $F_2 = 6.73$ : 30° and 45° pitch angle, turbulent flow  
 $= 8.0$ : 90° pitch angle, turbulent flow  
 $= 4.0$ : 30°, 45°, 90° pitch angle, laminar flow

turbulent flow exists when  $Re'_c \geq$  value given in column 4 of Table 12.4(b).

laminar flow exists when  $Re'_c <$  value given in column 4 of Table 12.4(b).

$\phi$  will be known from (2).

- (4) Calculate window pressure loss ( $\Delta P_w$ ) from equation [12.4] and obtain total window loss for central spacing ( $\Delta P'_w$ ) from:

$$\Delta P'_w = N_b F_2 \Delta P_w$$

where  $F_2 = 8.0$ :  $Re \geq 100$   
 $= 4.0$ :  $Re < 100$

- (5) Calculate an inlet/outlet cross-pass pressure loss ( $\Delta P_c$ ) from equation [12.7]. Obtain total loss of both inlet and outlet cross-passes ( $\Delta P''_c$ ) from:

$$\Delta P''_c = (F_2 \Delta P_c)/2$$

where  $F_2$  is given under (3).

- (6) Total pressure loss ( $\Delta P_s$ ) is given by:

$$\Delta P_s = \Delta P'_c + \Delta P'_w + \Delta P''_c + \text{nozzle losses}$$



Table 12.8(f) (cont.)

Tube arrange- ment (mm)	Window pressure loss										Tube arrange- ment (in)
	Shell dia. (mm)	Turbulent				Laminar					
		(BSR) ≤ 0.32		(BSR) > 0.32		(BSR) ≤ 0.41		(BSR) > 0.41			
		X <sub>c</sub>	m	X <sub>c</sub>	m	X <sub>c</sub>	m	X <sub>c</sub>	m		
19.05× 25.4 □ (90°)	337-438 489-91 1067-1524	0.284 0.336 0.369	0.775 0.675 0.627	0.228 0.262 0.285	0.761 0.895 0.859	337-387 438-540 591-838 889-1219 1295-1524	0.958 1.039 1.139 1.202 1.307	-0.047 -0.095 -0.148 -0.174 -0.223	0.859 0.931 1.029 1.098 1.186	0.073 0.025 -0.037 -0.075 -0.119	1/2 × 1 □ (90°)
19.05× 25.4 ◇ (45°)	337-438 489-991 1067-1524	0.277 0.307 0.334	0.788 0.732 0.688	0.228 0.248 0.268	0.957 0.918 0.887	337-438 489-737 787-1143 1219-1524	0.898 0.994 1.037 1.098	0.000 -0.063 -0.070 -0.112	0.807 0.900 0.955 1.011	0.112 0.047 0.012 -0.021	1/2 × 1 ◇ (45°)
25.4× 31.75 △ (30°)	337-438 489-991 1067-1524	0.261 0.305 0.340	0.749 0.642 0.562	0.208 0.236 0.257	0.940 0.870 0.817	337-387 438-489 540-686 737-991 1067-1295 1372-1524	0.469 0.528 0.590 0.651 0.733 0.789	-0.073 -0.132 -0.185 -0.225 -0.286 -0.325	0.448 0.474 0.535 0.601 0.677 0.724	0.049 -0.013 -0.076 -0.134 -0.197 -0.231	1 × 1 1/2 △ (30°)
25.4× 31.75 □ (90°)	337-387 438-591 635-991 1067-1524	0.279 0.318 0.347 0.373	0.774 0.697 0.663 0.627	0.222 0.248 0.269 0.287	0.964 0.914 0.888 0.862	337-387 438-540 591-737 787-991 1067-1524	0.796 0.874 0.966 1.035 1.135	-0.060 -0.111 -0.165 -0.185 -0.230	0.710 0.778 0.862 0.944 1.034	0.066 0.016 -0.041 -0.083 -0.129	1 × 1 1/2 □ (90°)

### Double-segmental baffles

Inspection of the ideal flow pattern for double-segmental baffles, shown in Fig. 1.25, indicates that the shell-side flow splits into two parallel streams and crosses only one-half the number of rows in each cross-pass. Using the typical values of  $p$ ,  $q$  and  $r$  given for F-type shells above, then compared with single-segmental baffles in turbulent flow, the heat transfer coefficient should be  $0.5^{0.64} = 0.64$  times as great, the total cross-flow loss  $0.5 \times 0.5^{1.75} = 0.15$  times as great, and the total window loss  $= 0.5 \times 0.5^2 = 0.125$  times as great. In laminar flow these values become 0.78, 0.25 and 0.25 respectively. In design cases, where shell-side pressure loss controls, a change from single- to double-segmental baffles achieves a significant reduction in pressure loss at the expense of only a modest reduction in heat transfer coefficient.

In practice, where the shell-side flow pattern is complex, the actual reductions in heat transfer and pressure loss are different. It is suggested that an *approximate* solution for double-segmental baffles is obtained by calculating heat transfer and pressure loss as for an E shell of identical geometry and multiply the results by  $F_{DS}$  below:

**Table 12.8(g)** Shell and tube heat exchanger design – shell side calculations. Mechanical design correction factor ( $F_c$ ) – Pull-through floating-head (cont)

Tube arrangement (mm)	Heat transfer coefficient										Tube arrangement (in)
	Turbulent					Laminar					
	Shell dia. (mm)	$(BSR) \leq 0.35$		$(BSR) > 0.35$		Shell dia. (mm)	$(BSR) \leq 0.35$		$(BSR) > 0.35$		
		$X_c$	m	$X_c$	m		$X_c$	m	$X_c$	m	
25.4 × 31.75 ◇ (45°)	337–838	0.486	0.389	0.373	0.637	337–991	0.628	0.107	0.480	0.360	1 × 1 $\frac{1}{2}$
	889–1524	0.505	0.385	0.389	0.629	1067–1524	0.662	0.102	0.499	0.350	◇ (45°)
31.75 × 39.688 △ (30°)	337–591	0.487	0.365	0.369	0.629	337–591	0.623	0.090	0.472	0.354	1 $\frac{1}{4}$ × 1 $\frac{5}{16}$
	635–1524	0.540	0.328	0.404	0.602	635–1524	0.693	0.053	0.518	0.327	△ (30°)
31.75 × 39.688 □ (90°)	337–635	0.472	0.366	0.354	0.639	337–991	0.549	0.160	0.415	0.423	1 $\frac{1}{4}$ × 1 $\frac{5}{16}$
	686–1524	0.500	0.359	0.376	0.628	1067–1524	0.576	0.148	0.436	0.410	□ (90°)
31.75 × 39.688 ◇ (45°)	337–787	0.449	0.401	0.347	0.645	337–991	0.540	0.133	0.419	0.372	1 $\frac{1}{4}$ × 1 $\frac{5}{16}$
	838–1524	0.466	0.410	0.363	0.644	1067–1524	0.563	0.127	0.437	0.365	◇ (45°)

BSR limits 0.2–1.4

	Values of $E_{DS}$		
	Equation	Turbulent	Laminar
Heat transfer coefficient	[12.2]	0.7	0.8
Total (cross-flow + window) loss	[12.3], [12.4]	0.5	0.7
Reynolds number	[12.5]	0.5	0.5

### No-tubes-in-window (NTIW) design

The Bell method has not been substantiated for NTIW design. As an approximation the proposed manual method may be used for cases where BSR is not greater than 1.4, but the heat transfer coefficient will be underestimated, and the pressure loss overestimated.

### Acknowledgement

The author is grateful to Dr D. S. Dean, Whessoe Technical & Computing Systems Ltd, Darlington, UK, for the development and execution of computer programs relating to Tables 12.5–12.8.

### References

A list of addresses for the service organisations is provided on p. xvi.

Table 12.8(g) (cont.)

Tube arrange- ment (mm)	Cross flow pressure loss										Tube arrange- ment (in)
	Shell dia. (mm)	Turbulent				Laminar					
		(BSR) ≤ 0.34		(BSR) > 0.34		(BSR) ≤ 0.34		(BSR) > 0.34			
		X <sub>C</sub>	m	X <sub>C</sub>	m	X <sub>C</sub>	m	X <sub>C</sub>	m		
25.4× 31.75 ◇ (45°)	337-438 489-737 787-1143 1219-1524	0.072 0.079 0.086 0.091	1.488 1.480 1.484 1.476	0.049 0.054 0.058 0.061	1.839 1.838 1.844 1.841	337-438 489-991 1067-1524	0.270 0.307 0.325	0.755 0.720 0.723	0.185 0.206 0.218	1.099 1.084 1.088	1×1 $\frac{1}{2}$ ◇ (45°)
31.75× 39.688 △ (30°)	337-438 489-787 838-1143 1219-1524	0.044 0.050 0.052 0.058	1.459 1.416 1.433 1.395	0.030 0.033 0.035 0.037	1.821 1.801 1.815 1.794	337-438 489-737 787-1067 1143-1524	0.086 0.095 0.103 0.113	0.709 0.688 0.683 0.645	0.058 0.063 0.068 0.074	1.071 1.064 1.065 1.044	1 $\frac{1}{2}$ ×1 $\frac{5}{16}$ △ (30°)
31.75× 39.688 □ (90°)	337-387 438-540 591-737 787-1219 1295-1524	0.040 0.045 0.049 0.052 0.061	1.735 1.689 1.682 1.700 1.643	0.027 0.030 0.033 0.035 0.039	2.082 2.060 2.060 2.073 2.041	337-438 489-991 1067-1524	0.177 0.208 0.225	0.734 0.687 0.684	0.121 0.138 0.148	1.085 1.063 1.065	1 $\frac{1}{2}$ ×1 $\frac{5}{16}$ □ (90°)
31.75× 39.688 ◇ (45°)	337-438 489-635 686-991 1067-1524	0.055 0.057 0.064 0.068	1.496 1.493 1.498 1.496	0.037 0.039 0.044 0.046	1.842 1.842 1.849 1.849	337-489 540-991 1067-1524	0.183 0.196 0.208	0.751 0.740 0.750	0.122 0.133 0.141	1.097 1.093 1.103	1 $\frac{1}{2}$ ×1 $\frac{5}{16}$ ◇ (45°)

- Bell, K. J. (1963) *Final Report of the Cooperative Research Program on Shell-and-Tube Heat Exchangers* University of Delaware Eng. Exp. Stat. Bulletin 5.
- Bell, K. J. (1984) 'Baffled shell-and-tube exchangers', *Perry's Chemical Engineers Handbook* (6th edn). McGraw-Hill Inc., pp. 10.26-10.31.
- Devore, A. (1962) 'Use nomograms to speed exchanger calculations', *Hydrocarbon Processing & Petroleum Refiner* 41 (No. 12), 101-6.
- Donohue, D. A. (1949) 'Heat transfer and pressure drop in heat exchangers', *Ind. Eng. Chem.* 41 (No. 11), 2499-511.
- Fraaz, A. P. and Ozisik, M. N. (1965) *Heat Exchanger Design*. Wiley & Sons Inc.
- Gilmour, C. H. (1952-1954) 'Short cut to heat exchanger design', *Chem. Eng.*, Parts I through VII.
- Kern, D. Q. (1950) *Process Heat Transfer*, McGraw-Hill Inc.
- Palen, J. W. and Taborek, J. (1969) 'Solution of shell side flow pressure drop and heat transfer by steam analysis method', *Chem. Eng. Prog. Symp. Ser.* 65 (No. 92).
- Smith, R. A. (1987) *Vaporisers - Selection, Design & Operation*. Longman.
- Taborek, J. (1983) *Heat Exchanger Design Handbook*, Vol. 3, Section 3.3. Hemisphere Publishing Corp.
- Tinker, T. (1951) 'Shell side characteristics of shell and tube heat exchangers', Parts I, II and III. General Discussion of Heat Transfer, Proc. Instn. Mech. Eng., London.

Table 12.8(g) (cont.)

Tube arrangement (mm)	Window pressure loss										Tube arrangement (in)
	Turbulent					Laminar					
	Shell dia. (mm)	(BSR) ≤ 0.35		(BSR) > 0.35		Shell dia. (mm)	(BSR) ≤ 0.35		(BSR) > 0.35		
		X <sub>C</sub>	m	X <sub>C</sub>	m		X <sub>C</sub>	m	X <sub>C</sub>	m	
25.4 × 31.75 ◇ (45°)	337-438 489-991 1067-1524	0.283 0.320 0.351	0.758 0.696 0.666	0.228 0.254 0.279	0.941 0.898 0.875	337-438 489-737 787-1143 1219-1524	0.753 0.857 0.919 0.991	-0.023 -0.086 -0.106 -0.144	0.673 0.770 0.840 0.906	0.101 0.033 0.000 -0.046	1 × 1½ ◇ (45°)
31.75 × 39.688 △ (30°)	337-438 489-991 1067-1524	0.233 0.265 0.285	0.777 0.682 0.614	0.187 0.207 0.219	0.965 0.899 0.850	337-387 438-489 540-686 737-991 1067-1295 1372-1524	0.300 0.338 0.377 0.416 0.463 0.502	-0.064 -0.117 -0.162 -0.194 -0.247 -0.285	0.271 0.306 0.345 0.388 0.433 0.469	0.053 0.000 -0.062 -0.114 -0.169 -0.207	1½ × 1⅞ △ (30°)
31.75 × 39.688 □ (90°)	337-438 489-991 1067-1524	0.253 0.298 0.326	0.798 0.701 0.653	0.202 0.232 0.253	0.986 0.918 0.880	337-387 438-540 591-787 838-1143 1219-1524	0.511 0.560 0.626 0.675 0.748	-0.054 -0.099 -0.148 -0.169 -0.221	0.458 0.502 0.566 0.621 0.685	0.067 0.022 -0.038 -0.077 -0.125	1½ × 1⅞ □ (90°)
31.75 × 39.688 ◇ (45°)	337-438 489-991 1067-1524	0.243 0.275 0.293	0.807 0.728 0.705	0.197 0.220 0.235	0.979 0.922 0.900	337-387 438-591 635-991 1067-1524	0.483 0.531 0.567 0.616	-0.017 -0.066 -0.075 -0.095	0.433 0.475 0.519 0.575	0.103 0.057 0.023 -0.016	1½ × 1⅞ ◇ (45°)

Tinker, T. (1958) 'Shell side characteristics of shell and tube heat exchangers: a simplified rating system for commercial heat exchangers', *Trans. ASME.*, Vol. 80.

## Nomenclature

Symbol	Description	Units
BSR	Baffle spacing ratio = (Baffle space/shell i.d.)	—
$c_p$	Specific heat	J/kg K
$d_i$	Inside tube diameter (plain tube)	mm
$d_o$	Outside tube diameter (plain tube)	mm
$D_s$	Shell inside diameter	mm
$f_o$	Friction factor (Fig. 6.5.)	—
$J_h$	Heat transfer factor (Fig. 6.5)	—
$l_r$	(Inlet or outlet baffle space)/(central baffle space)	—
$l_s$	Baffle space	mm
$\dot{m}_c$	Cross-flow mass velocity	kg/sm <sup>2</sup>
$M_o$	Shell-side flow rate	kg/s
$N_b$	Number of segmental baffles	—
Pr	Prandtl number = $c_p \eta_b / \lambda$	—

**Table 12.9** Shell-and-tube heat exchanger design – shell-side calculations. Factor ( $X_c$ ) for calculating pressure loss ( $\Delta P_c$ ) in inlet and outlet cross-passes

Tube arrangement (mm) o.d. × pitch × angle	Baffle space ratios (BSR)										Tube arrangement (in) o.d. × pitch × angle		
	Fixed tubesheet and U-tube		Split backing ring				Floating head		Pull through				
	0.20	0.25	0.30	0.40– 1.40	0.20	0.25	0.30	0.40– 1.40	0.20	0.25		0.30	0.40– 1.40
15.875 × 19.844 × 30° Δ	3.1	2.8	2.5	2.3	2.8	2.6	2.4	2.2	2.4	2.2	2.0	2.0	5/8 × 25/32 × 30° Δ
19.05 × 23.813 × 30° Δ	2.9	2.7	2.4	2.2	2.6	2.4	2.2	2.1	2.3	2.1	2.0	2.0	3/4 × 15/16 × 30° Δ
19.05 × 25.4 × 30° Δ													3/4 × 1 × 30° Δ
25.4 × 31.75 × 30° Δ													1 × 1.1/4 × 30° Δ
25.4 × 31.75 × 90° □	2.6	2.4	2.2	2.1	2.4	2.3	2.1	2.0	2.1	2.0	1.9	1.9	1 × 1.1/4 × 90° □
31.75 × 39.638 × 30° Δ													1.1/4 × 1.9/16 × 30° Δ
31.75 × 39.638 × 90° □													1.1/4 × 1.9/16 × 90° □
15.875 × 22.225 × 90° □	2.4	2.3	2.1	2.0	2.2	2.1	2.0	2.0	2.0	1.9	1.9	1.9	5/8 × 7/8 × 90° □
19.05 × 25.4 × 90° □													3/4 × 1 × 90° □
15.875 × 22.225 × 45° ◇													5/8 × 7/8 × 45° ◇
19.05 × 25.4 × 45° ◇	2.1	2.0	1.9	1.9	2.1	1.9	1.9	1.9	2.0	1.9	1.8	1.8	3/4 × 1 × 45° ◇
25.4 × 31.75 × 45° ◇													1 × 1.1/4 × 45° ◇
31.75 × 39.638 × 45° ◇													1.1/4 × 1.9/16 × 45° ◇

**Notes:**

- (1) Use linear interpolation for intermediate values of BSR.
- (2) Pressure loss in one inlet or outlet cross-pass  $\Delta P_c = \Delta P_c X_c / f$   
 where  $e = 1.75$  turbulent flow, Δ and ◇ pitch  
 $e = 2.00$  turbulent flow, □ pitch  
 $e = 1.00$  laminar flow, Δ, □, ◇ pitch

**Table 12.10** Shell-and-tube heat exchanger design. Factors for calculating heat transfer and cross-flow pressure loss in an 'ideal' exchanger

Tube configuration (mm)			Heat transfer				Pressure loss		Tube configuration (in)		
			A		m		B				
o.d.	Pitch	Angle	Turb.	Lam.	Turb.	Lam.	Turb.	Lam.	Angle	Pitch	o.d.
15.875	19.844	30	1.239	18.556	0.635	0.360	419.7	9384	30	25/32	5/8
15.875	22.225	90	0.896	7.838	0.651	0.431	9.000	5141	90	7/8	5/8
15.875	22.225	45	1.239	18.556	0.635	0.360	325.2	7272	45	7/8	5/8
19.05	23.813	30	1.159	16.512	0.635	0.360	334.1	6517	30	15/16	3/4
19.05	25.4	30	1.159	16.512	0.635	0.360	295.9	5771	30	1	3/4
19.05	25.4	90	0.841	7.066	0.651	0.431	7.874	3815	90	1	3/4
19.05	25.4	45	1.159	16.512	0.635	0.360	276.8	5396	45	1	3/4
25.4	31.75	30	1.043	13.736	0.635	0.360	233.2	3666	30	1.1/4	1
25.4	31.75	90	0.760	5.999	0.651	0.431	6.299	2470	90	1.1/4	1
25.4	31.75	45	1.043	13.736	0.635	0.360	222.3	3494	45	1.1/4	1
31.75	39.688	30	0.962	11.908	0.635	0.360	176.5	2346	30	1.9/16	1.1/4
31.75	39.688	90	0.703	5.283	0.651	0.431	5.039	1581	90	1.9/16	1.1/4
31.75	39.688	45	0.962	11.908	0.635	0.360	168.2	2236	45	1.9/16	1.1/4

$n = 1.75$  : turbulent flow pressure loss, pitch angle = 30° and 45°  
 $= 2.00$  : turbulent flow pressure loss, pitch angle = 90°  
 $= 1.00$  : laminar flow pressure loss, pitch angle = 30°, 45° and 90°

$Re_c$	Cross-flow Reynolds number (equation [12.5])	—
$r_i$	Internal fouling resistance	(W/m <sup>2</sup> K) <sup>-1</sup>
$r_o$	External fouling resistance	(W/m <sup>2</sup> K) <sup>-1</sup>
$r_w$	Tube wall resistance	(W/m <sup>2</sup> K) <sup>-1</sup>
$S_m$	Minimum cross-flow area	m <sup>2</sup>
$S_{mu}$	Min cross-flow area per metre of baffle space (Table 12.3)	m <sup>2</sup> /m
$U_o$	Overall heat transfer coefficient referred to outside of plain tube (equation [12.1])	W/m <sup>2</sup> K
$\alpha_i$	Heat transfer coefficient inside tube	W/m <sup>2</sup> K
$\alpha_o, (\alpha_o)_{nl}$	Heat transfer coefficient outside plain tube, with and without internal leakage respectively	W/m <sup>2</sup> K
$\Delta P_c$	Cross-flow pressure loss for one baffle space, with and without internal leakage respectively	Pa
$(\Delta P_c)_{nl}$		Pa
$\Delta P_{ci}, \Delta P_{co}$	Pressure loss due to inlet/outlet baffle space	Pa
$\Delta P_{ni}, \Delta P_{no}$	Pressure loss due to inlet/outlet nozzle	Pa
$\Delta P_s$	Total shell-side pressure loss	Pa
$\Delta P_w$	Pressure loss in one baffle window	Pa
$\eta_b$	Dynamic viscosity at bulk temperature	Ns/m <sup>2</sup>
$\eta_s$	Dynamic viscosity at surface temperature	Ns/m <sup>2</sup>
$\lambda$	Thermal conductivity	W/m K
$\rho$	Density	kg/m <sup>3</sup>
$\phi, \phi_{nl}$	Viscosity correction factor = $(\eta_b/\eta_s)^{0.14}$ based on $\alpha_o$ and $(\alpha_o)_{nl}$ respectively.	—

**324 Thermal design: shell-and-tube exchangers (plain tubes)**

**Design factors**

<i>Factor</i>	<i>Source</i>
$F_F, F_P$	Table 12.4
$F_E$	Table 12.5
$F_A$	Table 12.6
$F_M$	Table 12.7
$F_C$	Table 12.8
$X, e$	Table 12.9
$A, B, m, n$	Table 12.10

## Thermal design: shell-and-tube exchangers (low-fin tubes)

### 13.1 Description

Low-fin tubes have been discussed briefly in section 1.5.5 and illustrated by Fig. 1.20. Although they have wide application in heat transfer equipment they were developed primarily for use in shell-and-tube heat exchangers. Low-fin tubes are produced from standard heat exchanger plain tubes by a rolling process which simultaneously sinks the tube and extrudes the tube radially from the tube wall to a nominal height of 1.5 mm ( $\frac{1}{16}$  in). As fins and tube are integral with one another, the fins cannot become detached from the wall, and there can be no resistance to heat transfer at the fin/wall junction. The profile of low-fin tubes is shown in Fig. 13.1, together with the coding system which is used to define them.

The tube ends are left plain for insertion into tubesheets where they can be attached by expansion or welding as described in Chapter 2. The fin diameter is slightly less than that of the plain tube end so that the finned tube is readily passed through the holes in baffles. Plain portions or 'skips' may be provided at intervals along the tube lengths if required to provide a closer fit between baffle hole and tube. The tubes may be bent into U-tubes and most sizes can be bent to a centreline radius of twice the fin-root diameter. Plain-end diameters are in the range 12.7–25.4 mm ( $\frac{1}{2}$ –1 in) to suit most shell-and-tube heat exchangers, but other sizes are available on request.

The most common fin density is 748/m (19/in), corresponding to a gap between fins of about 1 mm (0.04 in), and these tubes are available in most of the heat exchanger tube metals including steel, aluminium, copper, admiralty brass, aluminium brass, cupro-nickel and stainless steel. The total external surface area of the low-fin tube is about 2.5 times that of the equivalent plain tube. Low-fin tubes are also available with fin densities of 1024, 1102 and 1181 fins/m (26, 28 and 30/in), depending on the metal, giving a total external surface area of about three times that of the equivalent plain tube. These tubes are supplied in titanium, high-nickel alloys and other alloys which are difficult to work.

The use of low-fin tubes is not confined to single-phase applications but may also be used for boiling and condensing applications, provided



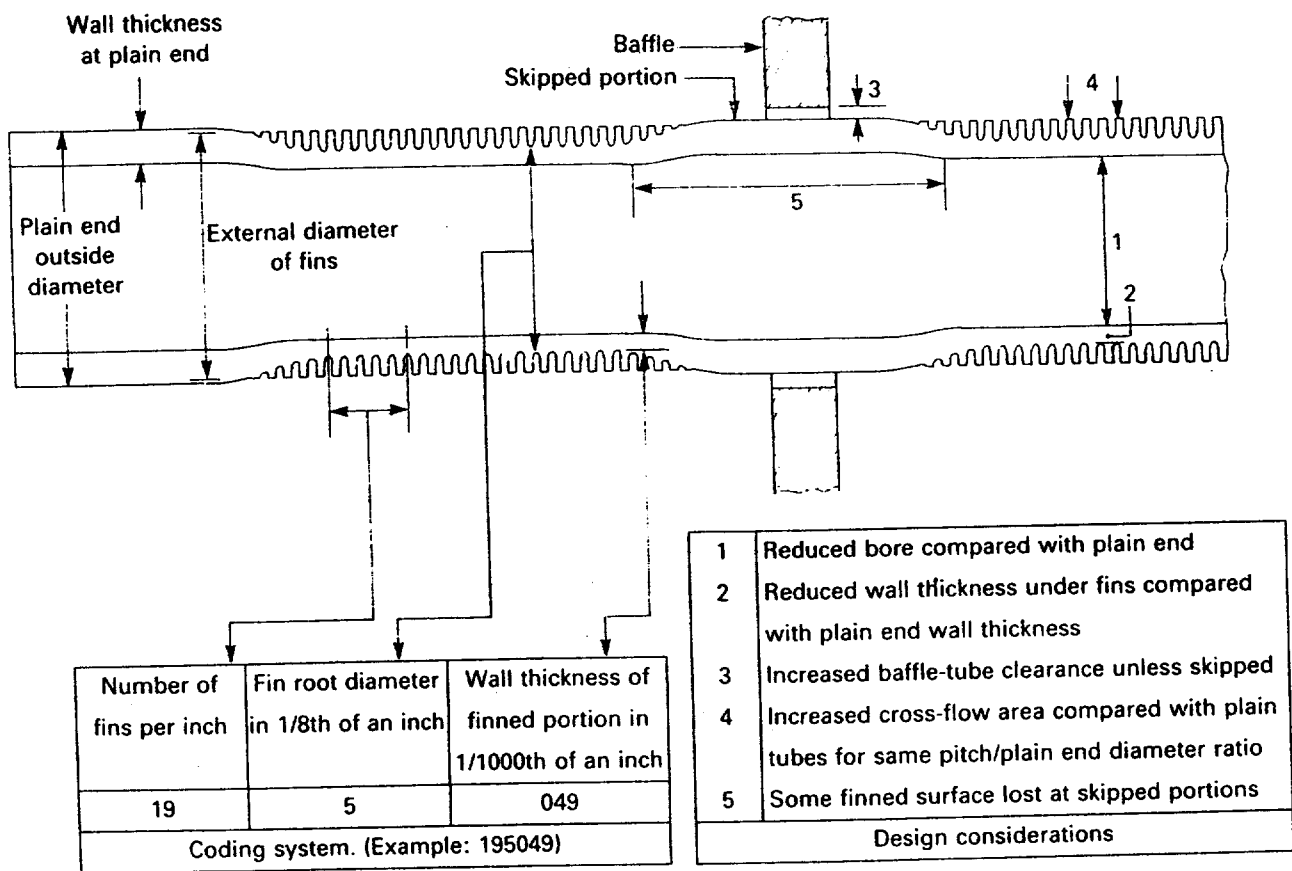


Figure 13.1 Low-fin tubes – coding system and design considerations

that the condensate surface tension is low enough to permit adequate drainage from the fins. In all applications their use may provide a shell-and-tube exchanger which is cheaper and more compact than a plain-tube unit. The substitution of low fin for plain tubes may boost performance, or change the duty, of an existing plain-tube unit, although the tube-side pressure loss of the low-fin unit should be checked carefully.

### 13.2 Cost comparison: plain versus low-fin tubes

Each case should be treated on its merits to decide whether plain or low-fin tubes should be used. In general the incentive to use low-fin tubes increases as (1) the basic tube material cost increases and (2) as the ratio ( $R$ ) of internal/external coefficient (including fouling resistances) increases. Table 13.1 provides five typical cost comparisons between plain-tube and low-fin designs for identical duties. It will be seen that low-fin tubes in aluminium, brass and stainless steel provide a significant cost reduction compared with plain tubes, despite the fact that the value of  $R$  is not large for stainless steel. In the case of carbon steel the comparison is different and in one case the use of low-fin tube provides a cost increase.

When comparing plain and low-fin tube designs, the saving in space and weight which is likely to be achieved with the latter should not be overlooked.

Table 13.1 Exchanger cost comparison – plain versus low-fin tubes<sup>(2)</sup>

Case	Tube type	Exchanger details							Cost ratio	
		No. shells	Shell diameter (mm)	Tube length (mm)	Type	Service	Tube material	$R^{(1)}$	Plain	Low fin
1	Plain	2	1626	6096	Fixed tubesheet	Cooler	Aluminium brass	17	1.0	0.77
	Low fin	1	1778	6096						
2	Plain	6	1245	7315	Fixed tubesheet	Condenser	Aluminium brass	5	1.0	0.84
	Low fin	4	1295	7315						
3	Plain	2	1346/1753	6096	U-kettle	Reboiler	Stainless steel	3	1.0	0.84
	Low fin	1	1499/1905	6096						
4	Plain	2	1168	6096	Fixed tubesheet	Condenser	Carbon steel	6	1.0	0.97
	Low fin	1	1422	6096						
5	Plain	4	1575	6096	Fixed tubesheet	Condenser	Carbon steel	5	1.0	1.21
	Low fin	3	1626	6096						

Notes:

$$(1) R = \frac{\text{(tube-side coefficient including fouling resistance for plain tube)}}{\text{(shell-side coefficient including fouling resistance for plain tube)}}$$

(2) Based on 748 fins/in (19/in).

### 13.3 Design considerations

Eight factors are listed below which should always be considered in the thermal design of shell-and-tube heat exchangers containing low-fin tubes. Some of the factors are illustrated in Fig. 13.1.

- (1) The low-fin tube geometry is such that the effective inside diameter in the finned portion is significantly less than that at the plain end. For example, code 195049 low-fin tube has a nominal bore in the finned portion of 13.4 mm (0.526 in) compared with a nominal bore at the plain end of 15.8 mm (0.620 in). If a code 195049 low-fin tube is substituted for a 19.05 mm o.d × 15.8 mm i.d. plain tube, and the same mass flow rate passed through it, the turbulent heat transfer coefficient will increase by about 1.35 times, but the frictional straight-tube pressure loss will increase by about 2.2 times. Replacing a plain-tube bundle with low-fin tubes will certainly boost performance, but the tube-side pressure loss will be doubled.
- (2) The effective tube thickness under the fins to resist corrosion will be about 0.3–0.5 mm (0.012–0.02 in) less than the thickness at the plain end. For example, code 195049 low-fin tube has a nominal thickness of 1.245 mm (0.049 in) at the fin root and a nominal thickness of

1.65 mm (0.065 in) at the plain end. This means that there is less metal under the fins to resist corrosion and pressure, but it has been found that the fins have a reinforcing effect such that the low-fin tube is stronger than the equivalent plain tube.

- (3) The fin diameter is less than the plain-end outside diameter by about 0.28 mm (0.011 in), which provides a greater baffle hole-tube clearance than that achieved with a plain tube. In order to reduce this clearance the low-fin tube may be provided with a skipped portion at each baffle, as shown in Fig. 13.1.
- (4) The cross-flow area for a low-fin bundle will be greater than that for a plain-tube bundle having the same pitch between tubes and the same plain-end diameter.
- (5) Finned surface is lost at each skip, as mentioned under (3) above, because a tube length of about 20–25 mm is required to achieve the transition from finned to plain portion. Skips are recommended if there is a possibility of flow-induced vibration.
- (6) Laminar shell-side flow develops once the Reynolds number falls below 1000. A boundary layer overlap occurs between the fin and the finned surface progressively loses its effectiveness as the Reynolds number decreases, such that heat transfer performance becomes little better than a plain tube. Factor  $J_f$  given in Table 13.2 indicates the reduction in heat transfer coefficient as Reynolds number decreases. (see Taborek 1983).

Table 13.2 Shell-and-tube heat exchanger design. Factor  $J_f$  for low-fin tubes at shell-side. Reynolds number less than 1000

Reynolds no.	Factor $J_f$	Reynolds no.	Factor $J_f$
$\geq 1000$	1.00	200	0.75
800	0.99	150	0.70
600	0.97	100	0.67
500	0.93	80	0.65
400	0.88	60	0.63
300	0.82	40	0.61
250	0.78	20	0.58

Based on Taborek (1983)

- (7) Pitch/diameter ratios exceeding 1.33 should be avoided when using square in-line pitch as there will be inadequate inter-fin penetration.
- (8) More data are required to determine the fouling characteristics of low-fin tubes under a wide range of operating conditions. It would appear that under many conditions low-fin bundles are not likely to foul more readily than plain-tube bundles and it is claimed that the fins tend to break up certain foulants. Low-fin tubes lose their effectiveness, however, with glue-like foulants which build up to block the inter-fin space.

## 13.4 Thermal design

The design of heat exchangers having low-fin tubes is similar to that used for plain tubes, except that the related plain-tube outside diameter ( $d_o$ ) is replaced by the finned tube equivalent diameter ( $d_e$ ), defined by equation [13.1]. If the Reynolds number is less than 1000, it is necessary to multiply the heat transfer coefficient for the finned tube by  $J_f$  given in Table 13.2.

In the case of baffled shell-and-tube exchangers, it must be noted that when calculating clearances, etc., the outside diameter of the finned tube is the fin outside diameter  $d_f$  and not  $d_o$ , unless the fins are skipped.

### 13.4.1 Equivalent diameter ( $d_e$ )

Low-fin tube calculations are based on an equivalent plain-tube diameter ( $d_e$ ), such that the projected area of a plain tube of diameter  $d_e$ , and bore  $d_i$  is exactly the same as that of the low-fin tube under consideration, having an identical length and bore  $d_i$ . Hence,

$$d_e = d_r + 2 (N_f t_f l_f) \times 10^{-3} \text{ (mm)} \quad [13.1]$$

where  $d_r$  = fin-root diameter (m)

$l_f$  = fin height (m)

$N_f$  = number of fins per metre length (m)<sup>-1</sup>

$t_f$  = mean fin thickness (m)

### 13.4.2 Fin-efficiency calculations

Once the heat transfer coefficient related to the external surface ( $\alpha_f$ ) is known, calculations follow the procedure described in Chapter 9.  $\alpha_f$  must first be combined with any external fouling resistance ( $r_o$ ) to provide the fouled external heat transfer coefficient  $\alpha'_f$ . Identical to equation [9.1], we obtain:

$$\frac{1}{\alpha'_f} = \frac{1}{\alpha_f} + r_o \quad [13.2]$$

After calculating the fin efficiency ( $\Omega_f$ ), from the method provided by equation [9.3] and Table 9.4, for instance,  $\alpha'_f$  must be related to a convenient reference surface in order to calculate the overall heat transfer coefficient. If the choice is the total external surface  $A_t$ , which comprises the sum of the external finned surface  $A_f$  and the external unfinned surface  $A_u$ , the following equations are obtained:

$$\alpha_{ft} = \frac{\alpha'_f (A_f \Omega_f + A_u)}{A_t} \quad [13.3]$$

$$\text{or } \alpha_{ft} = \alpha'_f \Omega_w \quad [13.4]$$

where  $\Omega_w = \{1 - (A_f/A_t)(1 - \Omega_f)\}$  = weighted fin efficiency

Table 13.3 Low-fin tubes. Dimensions for 748 fins/m (19/in)<sup>(3)</sup>

Code	Plain-end outside diameter ( $d_o$ )		Fin outside diameter		Fin root diameter ( $d_r$ )		Inside diameter in finned portion		Equivalent diameter ( $d_e$ )		External surface per unit length ( $A_e$ )		Surface area ratio external/internal
	mm	in	mm	in	mm	in	mm	in	mm	in	(m <sup>2</sup> /m)	(ft <sup>2</sup> /ft)	
193032	12.7	0.5	12.41	0.488	9.51	0.374	7.86	0.310	10.42	0.410	0.095	0.312	3.84
193049	12.7	0.5	12.41	0.488	9.51	0.374	7.01	0.276	10.42	0.410	0.095	0.312	4.32
194035 <sup>(1)</sup>	15.875	0.625	15.61	0.614	12.68	0.499	10.88	0.428	13.59	0.535	0.123	0.405	3.68
194042 <sup>(1)</sup>	15.875	0.625	15.61	0.614	12.68	0.499	10.55	0.415	13.59	0.535	0.123	0.405	3.72
194049	15.875	0.625	15.61	0.614	12.68	0.499	10.18	0.401	13.59	0.535	0.123	0.405	3.84
194065	15.875	0.625	15.61	0.614	12.68	0.499	9.36	0.368	13.59	0.535	0.123	0.405	4.19
195028 <sup>(2)</sup>	19.05	0.75	18.75	0.738	15.85	0.624	14.45	0.569	16.76	0.660	0.151	0.496	3.32
195035 <sup>(2)</sup>	19.05	0.75	18.75	0.738	15.85	0.624	14.11	0.556	16.76	0.660	0.151	0.496	3.41
195042 <sup>(1)</sup>	19.05	0.75	18.75	0.738	15.85	0.624	13.72	0.540	16.76	0.660	0.151	0.496	3.50
195049	19.05	0.75	18.75	0.738	15.85	0.624	13.35	0.526	16.76	0.660	0.151	0.496	3.59
195065	19.05	0.75	18.75	0.738	15.85	0.624	12.53	0.493	16.76	0.660	0.151	0.496	3.84
195083	19.05	0.75	18.75	0.738	15.85	0.624	11.61	0.457	16.76	0.660	0.151	0.496	4.14
196049	22.225	0.875	21.95	0.864	19.02	0.749	16.52	0.650	19.93	0.785	0.179	0.588	3.44
196065	22.225	0.875	21.95	0.864	19.02	0.749	15.70	0.618	19.93	0.785	0.179	0.588	3.63
196083	22.225	0.875	21.95	0.864	19.02	0.749	14.78	0.582	19.93	0.785	0.179	0.588	3.84
197049	25.4	1.0	25.12	0.989	22.19	0.874	19.69	0.775	23.10	0.910	0.207	0.678	3.33
197065	25.4	1.0	25.12	0.989	22.19	0.874	18.90	0.744	23.10	0.910	0.207	0.678	3.48
197083	25.4	1.0	25.12	0.989	22.19	0.874	17.98	0.708	23.10	0.910	0.207	0.678	3.66

**Notes:**

(1) Supplied in copper and 90/10 cupro-nickel only.

(2) Supplied in copper only.

Courtesy: Yorkshire Imperial Alloys.

These equations are identical to [9.4] and [9.9].

If the choice of reference surface is the internal surface of the tube  $A_i$ , the above equations become:

$$\alpha_{fi} = \frac{\alpha'_f(A_f\Omega_f + A_u)}{A_i} \quad [13.5]$$

$$\text{or } \alpha_{fi} = \alpha'_f\Omega_w \left( \frac{A_t}{A_i} \right) \quad [13.6]$$

In the case of low-fin tubes having 748 fins/m (19/in),  $A_t/A_i = 0.8$  and  $A_u/A_i = 0.2$ .

The overall heat transfer coefficient, related to the total external surface  $U_e$ , or related to the internal surface  $U_i$ , is obtained from an equation similar to [12.1], as shown in equations [13.7] and [13.8] below, where the star (\*) denotes that these resistances must be related to the chosen reference surfaces):

$$U_e = \frac{1}{(1/\alpha_e)^* + r_i^* + r_w^* + (1/\alpha_{fi})} \quad [13.7]$$

$$\text{or, } U_i = \frac{1}{(1/\alpha_i) + r_i + r_w^* + (1/\alpha_{fi})} \quad [13.8]$$

Publications issued by the makers of low-fin tubes usually provide the

Table 13.4 Weighted fin efficiencies of low-fin tubes (748 fins/m)

$\Omega_w$	$(\Omega_w)$ versus heat transfer coefficient to external surface, corrected for fouling, ( $\alpha'_f$ (W/m <sup>2</sup> K)), tabulated below, for various tube metals.							
	Copper	Aluminium	Admiralty brass	Aluminium brass	Nickel	Steel and 90/10 cupro-nickel	70/30 cupro-nickel	Stainless steel
0.99	1405	750	440	360	240	190	125	60
0.98	2835	1515	880	730	485	380	255	125
0.97	4350	2325	1355	1120	740	580	395	190
0.96	5915	3165	1840	1525	1005	795	535	260
0.95	7490	4005	2330	1925	1275	1005	675	325
0.94	9135	4885	2845	2350	1555	1225	825	400
0.93	10865	5810	3380	2795	1850	1455	980	475
0.92		6770	3940	3255	2155	1695	1145	550
0.91		7725	4495	3720	2460	1935	1305	630
0.90		8750	5090	4210	2785	2195	1480	715
0.89		9775	5690	4705	3115	2450	1650	795
0.88		10830	6305	5210	3450	2715	1830	885
0.87			6950	5745	3800	2995	2015	975
0.86			7645	6320	4185	3295	2220	1070
0.85			8355	6910	4570	3600	2425	1170
0.84			9120	7540	4990	3930	2645	1280
0.83			9850	8145	5390	4245	2860	1280
0.82			10655	8810	5830	4590	3090	1380
0.81				9460	6260	4930	3320	1495
0.80				10215	6760	5325	3585	1600
0.79					7225	5690	3835	1730
0.78					7735	6090	4100	1850
0.77					8260	6500	4380	1980
0.76					8815	6940	4675	2115
0.75					9405	7405	4990	2255
0.74					10030	7900	5320	2410
0.73						8380	5645	2570
0.72						8930	6015	2725
0.71						9485	6390	3085
0.70						10070	6785	3275

Multiply  $\alpha'_f$  in Btu/hr ft<sup>2</sup> °F by 5.678 to convert to W/m<sup>2</sup> K.

geometrical data required for equations [13.1]–[13.6] and typical values are given in Table 13.3. Values of  $\Omega_f$  or  $\Omega_w$  may also be available and typical values are given in Table 13.4.

#### 13.4.3 Modifications to the Bell method for low-fin tubes (shell-and-tube exchangers)

The Bell (1984) method, intended for plain tubes, is presented in the article by equations (10–120) to (10–138) and Figures 10–15 to 10–27. The method may be used for low-fin tubes if certain of the equations and figures are modified as follows:

- (1) Equivalent diameter ( $d_e$ ): calculate from equation [13.1] above or use makers' data.

- |                                |   |
|--------------------------------|---|
| (2) Bell equation (10-123):    | use $d_c$ instead of $D_o$ to calculate $S_m$ and use this value throughout.                      |
| (3) Bell equation (10-124):    | use $S_m$ from (2) above.   |
| (4) Bell equation (10-125):    | replace $D_o$ by $d_f$ only if fins are not skipped to calculate $S_{tb}$ .                       |
| (5) Bell Figs 10-21 and 10-26: | use $S_m$ from (2) above and $S_{tb}$ from (4) above, to obtain $j_1$ and $R_1$ .                 |
| (6) Bell equation (10-129):    | use $d_f$ instead of $D_o$ to obtain $S_{wt}$ and hence $S_w$ from equation (10-127).             |
| (7) Bell equation (10-130):    | use $S_w$ from (6) above; replace $D_o$ by $d_c$ to obtain $D_w$ .                                |
| (8) Bell equation (10-133):    | replace $D_o$ by $d_c$ and use $S_m$ from (2) above, to obtain Reynolds number.                   |
| (9) Bell Figs 10-19 and 10-25: | use Reynolds number from (8) above to obtain $j_k$ and $f_k$ .                                    |
| (10) Bell equation (10-134):   | use $S_m$ from (2) above, and $j_k$ from (9) above.   |
| (11) Bell equation (10-135):   | multiply $h_s$ by $J_f$ from Table. 13.2 if Reynolds number is less than 1000.                    |
| (12) Bell equation (10-136):   | use $f_k$ from (9) above, and $S_m$ from (2) above, to obtain $\Delta P_{bk}$ ; multiply by 1.4.  |
| (13) Bell equation (10-137):   | use $S_m$ from (2) above and $S_w$ from (6) above in equation (10-137b); replace $D_o$ by $d_c$ . |

Having obtained Bell  $h_s$ , or  $\alpha_f$  (using the nomenclature of this chapter), proceed as section 13.4.2 to obtain the overall heat transfer coefficient.

The design of shell-and-tube exchangers with low-fin tubes, using the modified Bell method, is also presented by Taborek (1983).

#### 13.4.4 Design using the manual method of Chapter 12

The manual method for plain tubes described in Chapter 12, which was based on Bell (1984), may be applied in an identical manner for low-fin tubes, using the modifications proposed in section 13.4.3. The factors are obtained as shown in Table 13.5 for shell-side Reynolds number greater than 1000 and  $\phi_o = 1$ . It will be seen that the only factor not already available is  $F_M$  given in Table 13.6.

**Table 13.5** Design factors for low-fin tubes ( $Re_c \geq 1000$ ,  $\phi_o = 1$ )

Factor	Source	Factor	Source
$F_F, F_P$	Table 12.4(a)	$\Delta P_w$	equation 12.4
$F_E$	Table 12.5	$X_c$	Table 12.9
$F_M$	Table 13.6	$\Delta P_c$	equation 12.7
$X_C, m$	Table 12.8	$\Delta P_s$	equation 12.8
$F_c$	equation 12.6	$d_c$	equation 13.1, or Table 13.3 if applicable
$\alpha_i$	equation 12.2	$S_m$	Table 12.1 using $d_c$ instead of $d_o$
$\Delta P_c$	equation 12.3 multiplied by 1.4	$Re_c$	equation 12.5 using $S_m$ and $d_c$ as above

**Table 13.6(a)** Shell-and-tube heat exchanger design – shell-side calculations. Base mechanical design factor ( $F_M$ ) for low-fin tubes<sup>(1)</sup> in turbulent flow ( $Re_c > 1000$ ). Fixed tubesheet and U-tube types (constructional data as Table 12.2)

Shell i.d. (mm)	Heat transfer coefficient			Cross-flow pressure loss			Window pressure loss			Shell i.d. (in)
	$\Delta$ (30°)	$\square$ (90°)	$\diamond$ (45°)	$\Delta$ (30°)	$\square$ (90°)	$\diamond$ (45°)	$\Delta$ (30°)	$\square$ (90°)	$\diamond$ (45°)	
	$(f_c = 0.1)$									
205	26.73	22.38	27.19	$3.516 \times 10^5$	$2.781 \times 10^4$	$1.863 \times 10^5$	$5.276 \times 10^4$	$4.225 \times 10^4$	$4.194 \times 10^4$	8.07
257	21.49	17.80	21.38	$2.306 \times 10^5$	$1.623 \times 10^4$	$1.117 \times 10^5$	$2.702 \times 10^4$	$2.096 \times 10^4$	$2.082 \times 10^4$	10.14
307	17.97	14.77	17.62	$1.633 \times 10^5$	$1.050 \times 10^4$	$8.131 \times 10^3$	$1.597 \times 10^4$	$1.209 \times 10^4$	$1.205 \times 10^4$	12.09
337	16.33	13.37	15.90	$1.357 \times 10^5$	$8.331 \times 10^3$	$6.681 \times 10^3$	$1.213 \times 10^4$	$9.068 \times 10^3$	$9.054 \times 10^3$	13.25
387	13.43	10.95	13.11	$9.406 \times 10^4$	$5.376 \times 10^3$	$4.610 \times 10^3$	$7.349 \times 10^3$	$5.392 \times 10^3$	$5.471 \times 10^3$	15.25
438	11.79	9.56	11.41	$7.301 \times 10^4$	$3.921 \times 10^3$	$3.530 \times 10^3$	$5.092 \times 10^3$	$3.678 \times 10^3$	$3.743 \times 10^3$	17.25
489	10.11	8.17	9.81	$5.462 \times 10^4$	$2.774 \times 10^3$	$2.636 \times 10^3$	$3.453 \times 10^3$	$2.459 \times 10^3$	$2.536 \times 10^3$	19.25
540	9.10	7.33	8.78	$4.444 \times 10^4$	$2.147 \times 10^3$	$2.124 \times 10^3$	$2.578 \times 10^3$	$1.815 \times 10^3$	$1.876 \times 10^3$	21.25
591	8.26	6.63	7.92	$3.672 \times 10^4$	$1.696 \times 10^3$	$1.741 \times 10^3$	$1.974 \times 10^3$	$1.375 \times 10^3$	$1.425 \times 10^3$	23.25
635	7.42	5.94	7.14	$3.000 \times 10^4$	$1.335 \times 10^3$	$1.423 \times 10^3$	$1.518 \times 10^3$	$1.048 \times 10^3$	$1.098 \times 10^3$	25
686	6.83	5.45	6.54	$2.546 \times 10^4$	$1.090 \times 10^3$	$1.200 \times 10^3$	$1.210 \times 10^3$	$0.829 \times 10^3$	$0.870 \times 10^3$	27
737	6.31	5.02	6.02	$2.182 \times 10^4$	$0.901 \times 10^3$	$1.023 \times 10^3$	$0.980 \times 10^3$	$0.666 \times 10^3$	$0.700 \times 10^3$	29
787	5.86	4.66	5.58	$1.887 \times 10^4$	$0.754 \times 10^3$	$8.803 \times 10^2$	$0.804 \times 10^3$	$0.543 \times 10^3$	$0.572 \times 10^3$	31
838	5.47	4.33	5.18	$1.645 \times 10^4$	$0.637 \times 10^3$	$7.641 \times 10^2$	$0.668 \times 10^3$	$0.448 \times 10^3$	$0.473 \times 10^3$	33
889	5.12	4.04	4.84	$1.445 \times 10^4$	$0.543 \times 10^3$	$6.682 \times 10^2$	$0.561 \times 10^3$	$0.374 \times 10^3$	$0.396 \times 10^3$	35
940	4.81	3.79	4.53	$1.276 \times 10^4$	$0.467 \times 10^3$	$5.884 \times 10^2$	$0.475 \times 10^3$	$0.315 \times 10^3$	$0.334 \times 10^3$	37
991	4.53	3.56	4.26	$1.134 \times 10^4$	$0.404 \times 10^3$	$5.213 \times 10^2$	$0.406 \times 10^3$	$0.268 \times 10^3$	$0.285 \times 10^3$	39
1067	4.02	3.16	3.81	$9.067 \times 10^3$	$0.311 \times 10^3$	$4.185 \times 10^2$	$0.307 \times 10^3$	$0.202 \times 10^3$	$0.217 \times 10^3$	42
1143	3.72	2.92	3.51	$7.779 \times 10^3$	$0.258 \times 10^3$	$3.575 \times 10^2$	$0.251 \times 10^3$	$0.164 \times 10^3$	$0.176 \times 10^3$	45
1219	3.46	2.71	3.26	$6.733 \times 10^3$	$0.216 \times 10^3$	$3.083 \times 10^2$	$0.208 \times 10^3$	$0.135 \times 10^3$	$0.145 \times 10^3$	48
1295	3.23	2.52	3.03	$5.873 \times 10^3$	$0.183 \times 10^3$	$2.681 \times 10^2$	$0.174 \times 10^3$	$0.112 \times 10^3$	$0.121 \times 10^3$	51
1372	3.02	2.35	2.83	$5.160 \times 10^3$	$0.156 \times 10^3$	$2.349 \times 10^2$	$0.147 \times 10^3$	$0.094 \times 10^3$	$0.102 \times 10^3$	54
1448	2.74	2.13	2.59	$4.284 \times 10^3$	$0.126 \times 10^3$	$1.963 \times 10^2$	$0.117 \times 10^3$	$0.075 \times 10^3$	$0.082 \times 10^3$	57
1524	2.58	2.01	2.44	$3.821 \times 10^3$	$0.109 \times 10^3$	$1.746 \times 10^2$	$0.101 \times 10^3$	$0.064 \times 10^3$	$0.071 \times 10^3$	60
Shell i.d. (mm)	$\Delta$ (30°)	$\square$ (90°)	$\diamond$ (45°)	$\Delta$ (30°)	$\square$ (90°)	$\diamond$ (45°)	$\Delta$ (30°)	$\square$ (90°)	$\diamond$ (45°)	Shell i.d. (in)
	Heat transfer coefficient			Cross-flow pressure loss			Window pressure loss			
	$(f_c = 0.1)$									

(1) Low-fin tube data as Table 13.3



**Table 13.6(b)** Shell-and-tube heat exchanger design – shell-side calculations. Base mechanical design factor ( $F_M$ ) for low-fin tubes<sup>(1)</sup> in turbulent flow ( $Re_c > 1000$ ). Split backing ring floating-head type (constructional data as Table 12.2)

Shell i.d. (mm)	Heat transfer coefficient			Cross-flow pressure loss ( $f_c = 0.1$ )			Window pressure loss			Shell i.d. (in)
	$\Delta(30^\circ)$	$\square(90^\circ)$	$\diamond(45^\circ)$	$\Delta(30^\circ)$	$\square(90^\circ)$	$\diamond(45^\circ)$	$\Delta(30^\circ)$	$\square(90^\circ)$	$\diamond(45^\circ)$	
205	25.25	21.03	26.05	$2.277 \times 10^5$	$1.791 \times 10^4$	$1.387 \times 10^5$	$4.094 \times 10^4$	$3.501 \times 10^4$	$3.524 \times 10^4$	8.07
257	20.34	16.83	20.63	$1.601 \times 10^5$	$1.128 \times 10^4$	$9.281 \times 10^4$	$2.139 \times 10^4$	$1.774 \times 10^4$	$1.785 \times 10^4$	10.14
307	17.06	14.04	17.08	$1.189 \times 10^5$	$7.681 \times 10^3$	$6.656 \times 10^4$	$1.287 \times 10^4$	$1.041 \times 10^4$	$1.050 \times 10^4$	12.09
337	15.53	12.74	15.45	$1.011 \times 10^5$	$6.243 \times 10^3$	$5.563 \times 10^4$	$9.862 \times 10^3$	$7.874 \times 10^3$	$7.953 \times 10^3$	13.25
387	12.84	10.50	12.79	$7.255 \times 10^4$	$4.172 \times 10^3$	$3.929 \times 10^4$	$6.081 \times 10^3$	$4.749 \times 10^3$	$4.862 \times 10^3$	15.25
438	11.31	9.20	11.16	$5.778 \times 10^4$	$3.124 \times 10^3$	$3.064 \times 10^4$	$4.267 \times 10^3$	$3.274 \times 10^3$	$3.361 \times 10^3$	17.25
489	9.73	7.90	9.62	$4.421 \times 10^4$	$2.260 \times 10^3$	$2.320 \times 10^4$	$2.931 \times 10^3$	$2.211 \times 10^3$	$2.296 \times 10^3$	19.25
540	8.78	7.10	8.62	$3.659 \times 10^4$	$1.781 \times 10^3$	$1.892 \times 10^4$	$2.210 \times 10^3$	$1.644 \times 10^3$	$1.711 \times 10^3$	21.25
591	7.98	6.43	7.79	$3.069 \times 10^4$	$1.427 \times 10^3$	$1.566 \times 10^4$	$1.707 \times 10^3$	$1.254 \times 10^3$	$1.308 \times 10^3$	23.25
635	7.13	5.73	7.00	$2.426 \times 10^4$	$1.088 \times 10^3$	$1.255 \times 10^4$	$1.278 \times 10^3$	$0.939 \times 10^3$	$0.991 \times 10^3$	25
686	6.57	5.27	6.42	$2.087 \times 10^4$	$0.901 \times 10^3$	$1.068 \times 10^4$	$1.027 \times 10^3$	$0.747 \times 10^3$	$0.790 \times 10^3$	27
737	6.09	4.87	5.92	$1.811 \times 10^4$	$0.754 \times 10^3$	$9.174 \times 10^3$	$0.839 \times 10^3$	$0.604 \times 10^3$	$0.640 \times 10^3$	29
787	5.67	4.52	5.48	$1.583 \times 10^4$	$0.638 \times 10^3$	$7.950 \times 10^3$	$0.693 \times 10^3$	$0.495 \times 10^3$	$0.525 \times 10^3$	31
838	5.29	4.21	5.10	$1.394 \times 10^4$	$0.544 \times 10^3$	$6.943 \times 10^3$	$0.580 \times 10^3$	$0.410 \times 10^3$	$0.436 \times 10^3$	33
889	4.96	3.93	4.77	$1.234 \times 10^4$	$0.468 \times 10^3$	$6.105 \times 10^3$	$0.489 \times 10^3$	$0.344 \times 10^3$	$0.366 \times 10^3$	35
940	4.66	3.69	4.47	$1.099 \times 10^4$	$0.405 \times 10^3$	$5.402 \times 10^3$	$0.417 \times 10^3$	$0.291 \times 10^3$	$0.311 \times 10^3$	37
991	4.37	3.45	4.19	$9.543 \times 10^3$	$0.342 \times 10^3$	$4.723 \times 10^3$	$0.349 \times 10^3$	$0.245 \times 10^3$	$0.262 \times 10^3$	39
1067	3.89	3.07	3.75	$7.722 \times 10^3$	$0.267 \times 10^3$	$3.817 \times 10^3$	$0.267 \times 10^3$	$0.185 \times 10^3$	$0.200 \times 10^3$	42
1143	3.61	2.84	3.46	$6.690 \times 10^3$	$0.223 \times 10^3$	$3.281 \times 10^3$	$0.220 \times 10^3$	$0.151 \times 10^3$	$0.163 \times 10^3$	45
1219	3.36	2.64	3.21	$5.840 \times 10^3$	$0.189 \times 10^3$	$2.844 \times 10^3$	$0.183 \times 10^3$	$0.125 \times 10^3$	$0.135 \times 10^3$	48
1295	3.14	2.46	2.99	$5.134 \times 10^3$	$0.161 \times 10^3$	$2.485 \times 10^3$	$0.154 \times 10^3$	$0.104 \times 10^3$	$0.113 \times 10^3$	51
1372	2.94	2.30	2.80	$4.542 \times 10^3$	$0.138 \times 10^3$	$2.186 \times 10^3$	$0.131 \times 10^3$	$0.088 \times 10^3$	$0.096 \times 10^3$	54
1448	2.67	2.08	2.56	$3.798 \times 10^3$	$0.112 \times 10^3$	$1.834 \times 10^3$	$0.105 \times 10^3$	$0.070 \times 10^3$	$0.077 \times 10^3$	57
1524	2.52	1.97	2.41	$3.406 \times 10^3$	$0.098 \times 10^3$	$1.637 \times 10^3$	$0.091 \times 10^3$	$0.061 \times 10^3$	$0.067 \times 10^3$	60

Shell i.d. (mm)	$\Delta(30^\circ)$	$\square(90^\circ)$	$\diamond(45^\circ)$	$\Delta(30^\circ)$	$\square(90^\circ)$	$\diamond(45^\circ)$	$\Delta(30^\circ)$	$\square(90^\circ)$	$\diamond(45^\circ)$	Shell i.d. (in)
	Heat transfer coefficient			Cross-flow pressure loss ( $f_c = 0.1$ )			Window pressure loss			

(1) Low-fin tube data as Table 13.3

As an example, consider an E-type split backing ring floating-head exchanger, 889 mm inside diameter, having code 195083 low-fin tubes at 25.4 mm  $\times$  90° pitch. Single segmental baffles are spaced at 275 mm. Flowing on the shell-side is 63.77 kg/s of crude oil having average properties of  $C_p = 2177$  J/kg K,  $\eta_b = 18.9 \times 10^{-4}$  Ns/m<sup>2</sup>,  $\lambda = 0.122$  W/m K and  $\rho = 786.4$  kg/m<sup>3</sup>. External fouling is 0.00018 (W/m<sup>2</sup> K)<sup>-1</sup>. What is the heat transfer coefficient and pressure loss in one cross pass and one window?

From Table 13.3:

$$d_c = 16.76 \text{ mm}$$

From Table 12.1:

$$S_m = [0.04128 + (0.889 - 0.04128 - 0.01676)(0.0254 - 0.01676)/0.0254] \times 0.275 = 0.0891 \text{ m}^2$$

$$\dot{m}_c = 63.77/0.0891 = 715.71 \text{ kg/s m}^2$$

**Table 13.6(c)** Shell-and-tube heat exchanger design – shell-side calculations. Base mechanical design factor ( $F_M$ ) for low-fin tubes<sup>(1)</sup> in turbulent flow ( $Re_c > 1000$ ). Pull-through floating head type (constructional data as Table 12.2)

Shell i.d. (mm)	Heat transfer coefficient			Cross-flow pressure loss			Window pressure loss			Shell i.d. (in)
	$\Delta(30^\circ)$	$\square(90^\circ)$	$\diamond(45^\circ)$	$\Delta(30^\circ)$	$\square(90^\circ)$	$\diamond(45^\circ)$	$\Delta(30^\circ)$	$\square(90^\circ)$	$\diamond(45^\circ)$	
337	13.87	11.13	13.96	$5.218 \times 10^4$	$3.130 \times 10^3$	$3.441 \times 10^4$	$6.803 \times 10^3$	$5.893 \times 10^3$	$6.186 \times 10^3$	13.25
387	11.72	9.42	11.84	$3.981 \times 10^4$	$2.242 \times 10^3$	$2.566 \times 10^4$	$4.246 \times 10^3$	$3.614 \times 10^3$	$3.819 \times 10^3$	15.25
438	10.39	8.35	10.46	$3.326 \times 10^4$	$1.774 \times 10^3$	$2.092 \times 10^4$	$3.014 \times 10^3$	$2.527 \times 10^3$	$2.672 \times 10^3$	17.25
489	9.02	7.25	9.09	$2.656 \times 10^4$	$1.346 \times 10^3$	$1.641 \times 10^4$	$2.101 \times 10^3$	$1.732 \times 10^3$	$1.845 \times 10^3$	19.25
540	8.16	6.55	8.19	$2.276 \times 10^4$	$1.102 \times 10^3$	$1.378 \times 10^4$	$1.603 \times 10^3$	$1.305 \times 10^3$	$1.390 \times 10^3$	21.25
591	7.44	5.96	7.43	$1.967 \times 10^4$	$0.913 \times 10^3$	$1.170 \times 10^4$	$1.253 \times 10^3$	$1.007 \times 10^3$	$1.074 \times 10^3$	23.25
635	6.71	5.37	6.72	$1.638 \times 10^4$	$0.733 \times 10^3$	$9.692 \times 10^3$	$0.971 \times 10^3$	$0.773 \times 10^3$	$0.831 \times 10^3$	25
686	6.20	4.95	6.18	$1.441 \times 10^4$	$0.622 \times 10^3$	$8.394 \times 10^3$	$0.788 \times 10^3$	$0.621 \times 10^3$	$0.668 \times 10^3$	27
737	5.75	4.59	5.71	$1.274 \times 10^4$	$0.532 \times 10^3$	$7.325 \times 10^3$	$0.649 \times 10^3$	$0.506 \times 10^3$	$0.545 \times 10^3$	29
787	5.36	4.26	5.30	$1.134 \times 10^4$	$0.458 \times 10^3$	$6.434 \times 10^3$	$0.541 \times 10^3$	$0.418 \times 10^3$	$0.450 \times 10^3$	31
838	5.01	3.98	4.94	$1.104 \times 10^4$	$0.397 \times 10^3$	$5.687 \times 10^3$	$0.456 \times 10^3$	$0.349 \times 10^3$	$0.376 \times 10^3$	33
889	4.70	3.73	4.62	$9.016 \times 10^3$	$0.347 \times 10^3$	$5.054 \times 10^3$	$0.388 \times 10^3$	$0.294 \times 10^3$	$0.318 \times 10^3$	35
940	4.43	3.51	4.34	$8.216 \times 10^3$	$0.304 \times 10^3$	$4.515 \times 10^3$	$0.333 \times 10^3$	$0.251 \times 10^3$	$0.271 \times 10^3$	37
991	4.16	3.29	4.07	$7.255 \times 10^3$	$0.262 \times 10^3$	$3.987 \times 10^3$	$0.283 \times 10^3$	$0.212 \times 10^3$	$0.230 \times 10^3$	39
1067	3.72	2.94	3.66	$5.971 \times 10^3$	$0.207 \times 10^3$	$3.257 \times 10^3$	$0.218 \times 10^3$	$0.162 \times 10^3$	$0.177 \times 10^3$	42
1143	3.46	2.72	3.38	$5.245 \times 10^3$	$0.176 \times 10^3$	$2.828 \times 10^3$	$0.181 \times 10^3$	$0.133 \times 10^3$	$0.146 \times 10^3$	45
1219	3.22	2.53	3.14	$4.637 \times 10^3$	$0.151 \times 10^3$	$2.474 \times 10^3$	$0.152 \times 10^3$	$0.110 \times 10^3$	$0.121 \times 10^3$	48
1295	3.01	2.36	2.93	$4.122 \times 10^3$	$0.130 \times 10^3$	$2.178 \times 10^3$	$0.129 \times 10^3$	$0.093 \times 10^3$	$0.102 \times 10^3$	51
1372	2.83	2.21	2.74	$3.684 \times 10^3$	$0.113 \times 10^3$	$1.930 \times 10^3$	$0.110 \times 10^3$	$0.079 \times 10^3$	$0.086 \times 10^3$	54
1448	2.57	2.01	2.51	$3.113 \times 10^3$	$0.093 \times 10^3$	$1.628 \times 10^3$	$0.089 \times 10^3$	$0.063 \times 10^3$	$0.070 \times 10^3$	57
1524	2.43	1.90	2.37	$2.815 \times 10^3$	$0.082 \times 10^3$	$1.461 \times 10^3$	$0.077 \times 10^3$	$0.055 \times 10^3$	$0.061 \times 10^3$	60

Shell i.d. (mm)	$\Delta(30^\circ)$	$\square(90^\circ)$	$\diamond(45^\circ)$	$\Delta(30^\circ)$	$\square(90^\circ)$	$\diamond(45^\circ)$	$\Delta(30^\circ)$	$\square(90^\circ)$	$\diamond(45^\circ)$	Shell i.d. (in)
	Heat transfer coefficient			Cross-flow pressure loss			Window pressure loss			

(1) Low-fin tube data as Table 13.3

From equation [12.5]:

$$Re_c = 715.71 \times 0.01676 / 18.9 \times 10^{-4} = 6347 \text{ (i.e. turbulent)}$$

Heat transfer

$$BSR = 0.275 / 0.889 = 0.309^*$$

From Table 12.4(a):

$$F_F = 63.77^{0.651} = 14.956^*$$

From Table 12.4(a):

$$F_P = 2177^{0.333} \times 0.122^{0.667} / (18.9 \times 10^{-4})^{0.318} = 23.34^*$$

From Table 13.6:

$$F_M = 3.93$$

From Table 12.8:

$$X_C = 0.587^*, m = 0.318^* \text{ (BSR} < 0.35)$$

From equation [12.6]:

$$F_c = 0.587/(0.309)^{0.318} = 0.853^*$$

From equation [12.2]:

$$\alpha_f = 14.956 \times 23.34 \times 3.93 \times 0.853 = 1170 \text{ W/m}^2 \text{ K}$$

*Cross-flow pressure loss*

From Table 12.4(a):

$$F_F = 63.77^2 = 4066.61^*$$

From Table 12.4(a):

$$F_p = 1/786.4 = 0.001272^*$$

From Table 13.6:

$$F_M = 468$$

From Table 12.8:

$$X_C = 0.079^*, m = 1.598^* \text{ (BSR} < 0.34)$$

From equation [12.6]:

$$F_c = 0.079/0.309^{1.598} = 0.516^*$$

From equation [12.3]:

$$\Delta P_c = 4066.61 \times 0.001272 \times 468 \times 0.516 \times 1.4 = 1749 \text{ Pa}$$

This is a tentative value, corrected for low-fin tubes, but assumes  $f_o = 0.1$

From Table 12.4(a):

$$F_s \text{ for } 90^\circ \text{ pitch, } Re_c = 6347, p/d_o = 1.333, p/d_o = 1.162$$

$$\text{corrected } \Delta P_c = 1749 \times 1.162 = 2032 \text{ Pa}$$

*Window pressure loss*

From Table 12.4(a):

$$F_F = 63.77^2 = 4066.61^*$$

From Table 12.4(a):

$$F_p = 1/786.4 = 0.001272^*$$

From Table 13.6:

$$F_M = 344$$

From Table 12.8:

$$X_c = 0.391^*, m = 0.603^* \text{ (BSR} < 0.33)$$

From equation [12.6]:

$$F_c = 0.391/0.309^{0.603} = 0.794^*$$

From equation [12.4]:

$$\Delta P_w = 4066.61 \times 0.001272 \times 344 \times 0.794 = 1413 \text{ Pa}$$

\* This example is identical to example 1, Chapter 17, except that low-fin tubes have been substituted for plain tubes. Identical results are marked with the asterisk.

$\alpha_f$  must now be combined with other conductances in the system as described in section 13.4.2 and related to the chosen reference surface. If the inside of the tube is the reference surface:

From equation [13.2]:

$$\alpha'_f = 1/\{1/1170 + 0.00018\} = 967 \text{ W/m}^2 \text{ K}$$

From Table 13.4:

$$\Omega_w = 0.952 \text{ (steel tube)}$$

From equation [13.6]

$$\alpha_{fi} = 967 \times 0.952 \times 4.14 \text{ (see Table 13.3)} = 3811 \text{ W/m}^2 \text{ K}$$

$\alpha_{fi}$  may be combined with other conductances in the system provided they are also related to the inside of the tube.

## Acknowledgement

The author is grateful to Yorkshire Imperial Alloys, Leeds, England, for the provision of technical data relating to low-fin tubes.

## References

A list of addresses for the service organisations is provided on p. xvi.

Bell, K. J. (1984) *Perry's Chemical Engineers' Handbook* (6th edn) (eds Perry, R. H. and Green, D. W.), 'Baffled shell and tube exchangers', Section 10, McGraw-Hill.

Taborek, J. (1983) *Heat exchanger Design Handbook*, Vol. 3, Section 3.3, Hemisphere Publishing Corp.

## Nomenclature (additional to Chapter 12)

<i>Symbol</i>	<i>Description</i>	<i>Units</i>
$A_f$	External finned surface per metre (low-fin tube)	$\text{m}^2/\text{m}$
$A_i$	Internal plain surface per metre (low-fin tube)	$\text{m}^2/\text{m}$
$A_t$	Total external surface per metre (low-fin tube) $= A_f + A_n$	$\text{m}^2/\text{m}$
$A_u$	External un-finned surface per metre (low-fin tube)	$\text{m}^2/\text{m}$
$d_c$	Equivalent low-fin tube diameter (equation [13.1])	mm
$d_f$	Fin outside diameter	mm

338 Thermal design: shell-and-tube exchangers (low-fin tubes)

$d_f$	Fin root diameter	mm
$J_f$	Factor for low-fin tubes when Reynolds number < 1000	—
$l_f$	Fin height	mm
$N_f$	Number of fins per metre (low-fin tubes)	(m) <sup>-1</sup>
$t_f$	Mean fin thickness (low-fin tubes)	mm
$U_i$	Overall heat transfer coefficient referred to inside of low-fin tube (equation [13.8])	W/m <sup>2</sup> K
$U_o$	Overall heat transfer coefficient, referred to total external surface of low-fin tube (equation [13.7])	W/m <sup>2</sup> K
$\alpha_f$	Heat transfer coefficient to external surface of low-fin tube	W/m <sup>2</sup> K
$\alpha'_f$	$\alpha_f$ combined with external fouling (equation [13.2])	W/m <sup>2</sup> K
$\alpha'_{fi}$	$\alpha'_f$ referred to internal surface (equations [13.5] and [13.6])	W/m <sup>2</sup> K
$\alpha'_{fo}$	$\alpha'_f$ referred to total external surface (equations [13.3] and [13.4])	W/m <sup>2</sup> K
$\Omega_f$	Fin efficiency	—
$\Omega_w$	Weighted fin efficiency	—

## Thermal design: air-cooled exchangers

### 14.1 Design variables

Modern air-cooled heat exchangers are designed thermally by computers, which are capable of examining all design variables to produce the optimum unit. It is usual for heat transfer and pressure loss calculations to be carried out on a point-to-point basis, along each row and along each pass, instead of an 'overall' basis, which is related only to the terminal conditions. However, the 'overall' basis, using manual methods, is usually satisfactory for the sensible cooling of gases and non-viscous liquids. It has been employed in this chapter and the example of Chapter 17.

Design variables include:

*base tube:* diameter, length

*fins:* height, spacing, thickness, material

*fans:* number, diameter, air-flow (velocity and temperature), power, speed, noise level

*space:* unit length, width, depth

*costs:* capital and running

In the optimisation process, whether computer or manual, it may be necessary to design many single units, each of which will meet the process requirements from which the optimum unit will be selected. The task is greatly simplified when standardised finned-tube bundles are selected in advance. The optimum unit is usually the one having the lowest overall running cost, but all the factors listed in Table 3.1 have to be considered before a decision is made.

Table 14.1 illustrates the process for a gas cooler. Here surface area, plan area, and fan power are tabulated for three outlet air temperatures, with two or three different air velocities being considered for each temperature. Eight designs, each suitable for the process conditions, are therefore established. The number of designs could be extended by

**Table 14.1** Design of gas cooler. Gas cooled from 200 °C to 80 °C using air at 25 °C

Design no.	1	2	3	4	5	6	7	8	
Exit air temp. (°C)	60		70			80			
Air velocity (face) (m/s)	2.9	3.8	1.9	3.0	4.2	1.5	3.4	4.1	
Bare external surface area (m <sup>2</sup> )	220	164	262	218	158	348	198	193	
Number of rows deep	3	3	3	4	4	4	5		
Plan area (m <sup>2</sup> )	59.5	44.6	71.4	44.6	32.7	71.4	32.7	26.8	
Fan power (kW)	24.3	40.4	8.8	25.7	46.9	6.5	32.9	54.4	
Annual costs (£)	Fan power	10 206	16 968	3 696	10 794	19 698	2 730	13 818	22 848
	Capital, maintenance, etc.	19 600	15 600	22 520	16 800	13 200	27 840	13 880	12 720
	Total operating	29 806	32 568	26 216	27 594	32 898	30 570	27 698	35 568

Basis: (a) electricity = £0.06 kWh; (b) fan loading = 7000 hours/year; (c) installed cost of cooler = (2) (ex-works cost); (d) capital, maintenance costs per year = 40% of installed cost

This gas cooler is calculated in detail in Chapter 17 and the results presented in Table 17.14.

selecting other outlet air temperatures and air velocities. After adding capital and running costs for each design to the table, the optimum unit would be selected. The fixed air inlet temperature of 25 °C in this example was chosen after careful deliberation as discussed in section 14.2.

The description below relates to a *single* manual design in the optimisation process.

## 14.2 Inlet air temperature

The selection of the inlet air temperature is of vital importance in air-cooled heat exchanger design. Sound meteorological data, related closely to the exact cooler location, must be available. If the selected inlet air temperature is too low, then the unit will not achieve design performance for a large period of the year. If the selected air temperature is too high, the capital cost will be high and the unit will run at reduced capacity for most of the year. A compromise is reached and it is typical for an inlet air temperature to be selected which will only be exceeded for about 5% of the unit's annual hours of operation. Paikert (1983) states: 'by renouncing the full cooling capacity for 4–6% of the annual operating hours, it is possible to reduce the design temperature by 12–14 °C and the investment cost by 50–60%.'

## 14.3 Preliminary sizing

Once the inlet air temperature is known, a reliable first approximation of the cooler design may be obtained from several short-cut manual methods available in the literature. One such method is that of Brown (1978) and a sample calculation is given in Chapter 17, where it is used to determine

approximate size and cost. Brown considers that his method will establish a size within 25% of optimum. Having established a preliminary design, a more rigorous computer or manual method may be applied later to establish a firm design.

#### 14.4 Outlet air temperature

The preliminary sizing method of Brown above provides an indication of the outlet air temperature required for the optimum unit. However, for a more rigorous design the optimum outlet air temperature is not known in advance and cannot be selected in the same way as the outlet water temperature in a water-cooled shell-and-tube heat exchanger. In the latter type, the outlet water temperature may be governed by the maximum cooling water quantity available, or by fouling/metallurgical considerations, which dictate a maximum outlet temperature. In an air-cooled heat exchanger the optimum outlet air temperature, being a function of the air flow rate, is finalised as a result of the optimisation process. It is necessary to produce various designs having different air outlet temperatures and velocities as shown in Table 14.1.

Fixing an outlet air temperature for any single design immediately establishes the four terminal temperatures and, from the total heat load ( $Q$ ), the air flow rate. It also enables the log MTD ( $\Delta T_{lm}$ ) to be calculated. If an overall heat transfer coefficient ( $U$ ) based on experience is assumed, an estimation of the cooler surface area may be obtained from  $A = Q/(U \Delta T_{lm})$  (The value of  $U$  must relate to the chosen reference surface  $A$ .)

#### 14.5 Air velocity

Having fixed the air flow rate, a tentative air velocity may be chosen which establishes the cooler plan (or face) area. Face velocity is that based on the gross cross-sectional area for air flow (face area), as though the tubes were absent. In air-cooled heat exchangers face velocity is usually in the range 1.5–4 m/s. Low velocities produce coolers with a low power consumption, but with shallow bundles having a large plan area and capital cost. High velocities produce coolers with deep bundles, having a small plan area and capital cost, but with high power consumption.

If standard bundles of known tube length and bundle width are to be used, the number of bundles, stacked side by side, to achieve the required face area can be determined. The surface area per tube row is also known at this stage, so that the tentative number of rows deep and total number of tubes may be estimated from the cooler surface area derived in section 14.4, from an assumed value of  $U$ .



## 14.6 Tube-side heat transfer and pressure loss calculations

Tube-side heat transfer and pressure loss calculations are similar to those for flow inside the tubes of shell-and-tube heat exchangers, as given in Chapter 12. Heat transfer and pressure loss correlations for single-phase flow are given in Chapter 6.

At this stage it is necessary either to assume the tube-side heat transfer coefficient on the basis of past experience, or to calculate a tentative value. In the latter case the tentative number of rows deep and total number of tubes established in section 14.5 are used to determine the number of tube-side passes and number of tubes per pass. If heat transfer calculations are made, it is prudent to calculate tube-side pressure loss also.

## 14.7 Air-side heat transfer and pressure loss calculations

Heat transfer and pressure loss for flow across finned-tube banks has been the subject of considerable research by manufacturers and the cooperative research organisations. Most of the experimental data have been obtained with air as the test fluid. As a result, curves relating air-side heat transfer coefficient and pressure loss per tube row, to the air-side face velocity, are usually available from manufacturers for various fin geometries and tube pitch.

The air-side heat transfer coefficients are preferably obtained from makers' test curves because they will automatically include all factors affecting fin efficiency, such as geometry, bond resistance, etc. Heat transfer and pressure loss are sensitive to small geometrical irregularities between superficially identical tubes and also to differences in manufacturing techniques. If such data are not available the correlations for finned tubes given in Chapter 6 may be used.

## 14.8 Overall heat transfer coefficient

The overall heat transfer coefficient ( $U_o$ ), referred to the bare external surface, which is the outside of the plain base tube as though the fins were absent, is given by:

$$\frac{1}{U_o} = \frac{1}{\alpha_{fo}} + r_{fo} + r_{fi} + \frac{1}{\alpha_{fi}} \quad [14.1]$$

where  $\alpha_{fo}$  = air-side heat transfer coefficient, referred to bare external surface ( $\text{W/m}^2 \text{K}$ )

$r_{to}$  = tube-wall resistance, referred to bare external surface ( $\text{W}/\text{m}^2 \text{K})^{-1}$

$r_{io}$  = internal fouling resistance, referred to bare external surface ( $\text{W}/\text{m}^2 \text{K})^{-1}$

$\alpha_{io}$  = internal heat transfer coefficient, referred to bare external surface ( $\text{W}/\text{m}^2 \text{K}$ )

This equation is identical to equation [9.8] where the external bare surface has been chosen as the reference surface for convenience. Other reference surfaces may be chosen; had the internal surface been chosen, for instance, equation [9.6] would be applicable.

As stated in section 14.7,  $\alpha_{fo}$  should be obtained from test data. If not available, the air-side heat transfer coefficient to the fins and bare surface ( $\alpha'_i$ ) should be calculated from the correlations in Chapter 6 and  $\alpha_{fo}$  calculated from equation [9.7].

## 14.9 Surface area and number of rows deep

Having established the overall heat transfer coefficient ( $U_o$ ), the bare external surface area of the cooler ( $A_o$ ) may be calculated from  $A_o = Q / (U_o \Delta T_{lm})$ . The number of rows deep may then be obtained by dividing the total surface area by the surface area per row, already determined in section 14.5. The number of tube-side passes, the tube-side heat transfer coefficient and tube-side pressure loss are recalculated and compared with the assumptions made in section 14.6. Adjustments, as necessary, are made to the number of tube-side passes and the number of rows deep.

## 14.10 Mean temperature difference

An air-cooled heat exchanger provides a cross-flow arrangement between the process fluid inside the tubes and the external coolant air. Because this flow arrangement is not strictly countercurrent, the log MTD ( $\Delta T_{lm}$ ) calculated in section 14.4 must be corrected by applying an MTD correction factor  $F$ , as explained in Chapter 7. In addition to the terminal temperatures,  $F$  depends on the number of tube rows per pass and the number of passes, and cannot be determined accurately until these parameters have been finalised in section 14.9. For given terminal temperatures  $F$  increases as the number of rows per pass and the number of passes increase, being more sensitive to the latter.

Taborek (1983) and Pignotti and Cordero (1983) present values of  $F$  for a variety of cross-flow configurations, applicable to air-cooled heat exchangers. Typical cross-flow configurations are shown in Fig. 14.1. It should be noted that the  $F$  values are applicable only to single-phase flow.

**Cross-flow, both fluids unmixed**

This basic case, shown in Fig. 7.2(b), assumes a large number of flow channels in both streams. It would only apply to an air cooler having a single tube-side pass with five or more rows deep, but provides a useful basis for comparing other cross-flow configurations. Table 14.2 shows that  $F$  values for other configurations can be predicted with reasonable accuracy from the  $F$  values obtained from the basic case.

**One tube-side pass,  $N$  rows per pass, both fluids unmixed**

A common header at one end of the tubes distributes the tube-side fluid into a single pass having  $N$  rows in parallel. A similar header at the other end collects the tube-side fluid. Values of  $F$  are shown for  $N = 1, 2, 3$  and 4 and are always less than the basic case. When  $N$  exceeds 5, the  $F$  values become identical to the basic case.

 **$N$  tube-side passes,  $N$  rows, both fluids unmixed**

This would apply to a manifold-type air cooler in which the tubes in one row are connected to the next by U-bends. Values of  $F$  are shown for  $N = 2, 3$  and 4 and are always higher than the basic case. When  $N$  becomes greater than 4,  $F$  approaches 1, i.e. pure countercurrent flow.

**2 tube-side passes, 4 rows, 2 rows per pass, tube-side fluid mixed at header**

This is a realistic air-cooler configuration in which values of  $F$  are always higher than the basic case.

## 14.11 Air-side pressure loss, fan power consumption and noise

The total air-side pressure loss is the sum of the pressure loss through the finned-tube bundle and the pressure loss due to fan and plenum. Fan losses comprise fan entry loss, plus discharge loss due to expansion into the plenum (forced draught), or to the atmosphere (induced draught). Plenum losses relate to the complex flow between bundle and fan, and depend on shape, ratio of plenum height to fan diameter and ratio of plenum cross-sectional area to fan-opening area.

### 14.11.1 Bundle pressure loss ( $\Delta P_b$ )

This is calculated from makers' test data or correlations as described in section 14.7. The air density used in the bundle pressure loss calculations is based on the average air temperature across the bundle under summer conditions and a pressure corresponding to the cooler altitude in order to determine maximum motor power requirements. The presence of fouling

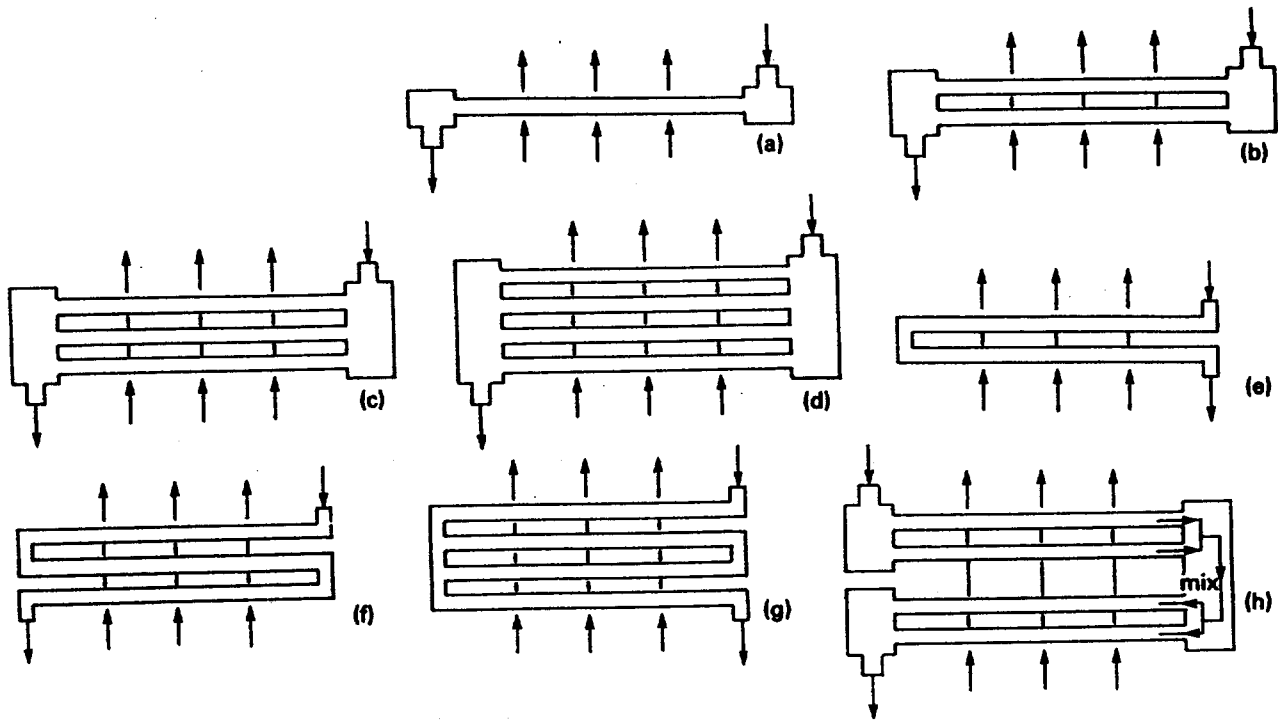


Fig.	No. of tube-side passes	No. of rows per pass	Total no. of rows
(a)	1	1	1
(b)	1	2	2
(c)	1	3	3
(d)	1	4	4
(e)	2	1	2
(f)	3	1	3
(g)	4	1	4
(h)	2	2	4

Figure 14.1 Typical cross-flow configurations

Table 14.2 Mean temperature difference correction factors ( $F$ ). Comparison for typical cross-flow arrangements (approx.)

Basic case: cross-flow, both fluids unmixed.	1 tube-side pass, $N$ rows/ pass, both fluids unmixed.				$N$ tube-side passes, $N$ rows, both fluids unmixed.				2 tube-side passes, 2 rows/ pass, 4 rows, tube-side fluid mixed at header
	1 row per pass	2 rows per pass	4 rows per pass	Above 5 rows per pass	2 rows 2 passes	3 rows 3 passes	4 rows 4 passes	Above 4 rows and 4 passes	
0.75	—	—	0.73	0.75	0.84	0.93	0.96	1.00	0.88
0.80	—	0.74	0.79	0.80	0.87	0.95	0.97	1.00	0.91
0.85	—	0.82	0.84	0.85	0.92	0.97	1.00	1.00	0.94
0.90	0.85	0.89	0.90	0.90	0.95	1.00	1.00	1.00	0.96
0.95	0.94	0.95	0.95	0.95	0.97	1.00	1.00	1.00	0.98
Not applic- able when $P$ exceeds	0.7	0.8	0.85	1.00	0.8	0.85	0.90	1.00	0.85

All units have one cross-flow pass. Overall direction of flow is countercurrent.  
Applicable only to single-phase flow. Based on curves by Taborek (1983).

on the external surface of the tubes will increase the bundle pressure loss and the fouled pressure loss may be calculated by estimating a fouling layer thickness which is assumed to be uniform over the entire external surface. The fouling layer thickness is either based on experience, or calculated from the foulant's thermal conductivity, and resistance, if known.

#### 14.11.2 Fan and plenum losses ( $\Delta P_p$ )

These are based on the air velocity head ( $u_f$ ) corresponding to the fan-opening diameter as shown below. The fan diameter is either obtained from makers' performance curves, or estimated from typical fan diameter/bundle plan area ratios described in Chapter 3.

$$\Delta P_p = K\rho_a u_f^2 \quad [14.2]$$

where  $\Delta P_p$  = fan and plenum losses (mm water)

$W_a$  = air mass flow rate (kg/s)

$D_f$  = fan-operating diameter (m)

$$u_f = \text{air velocity} = \left\{ \frac{W_a}{(\pi/4)D_f^2\rho_a} \right\} \text{ (m/s)}$$

$\rho_a$  = air density, based on a pressure corresponding to the cooler altitude, and a temperature given by the summer ambient for forced draught and the bundle outlet for induced draught ( $\text{kg/m}^3$ )

$K = 0.06$  (forced draught),  $0.075$  (induced draught)

#### 14.11.3 Fan power consumption

The total pressure loss, or fan static head ( $\Delta P_{sh}$ ), is the sum of  $\Delta P_b$  and  $\Delta P_p$ :

$$\Delta P_{sh} = \Delta P_b + \Delta P_p \quad [14.3]$$

The power absorbed at the fan shaft ( $\dot{W}_{fs}$ ), under summer conditions, is given by:

$$\dot{W}_{fs} = 9.8 (\Delta P_{sh}) V_a (10^{-3}) \quad [14.4]$$

where  $V_a$  = actual volumetric air flow through fan ( $= W_a/\rho_a$ ) ( $\text{m}^3/\text{s}$ )

The fan motor power required ( $\dot{W}_{ms}$ ), under summer conditions, is given by:

$$\dot{W}_{ms} = \dot{W}_{fs}/E_f \quad [14.5]$$

where  $E_f$  = efficiency of fan and drive system.

The fan motor power required ( $\dot{W}_{mw}$ ), under winter conditions, is given by:

$$\dot{W}_{mw} = \dot{W}_{ms} T_{sw} \quad [14.6]$$

where  $T_{sw} = \frac{\text{summer ambient design temp. (K)}}{\text{winter ambient design temp. (K)}}$  for forced draught

or  $= \frac{\text{bundle outlet temp. in summer (K)}}{\text{bundle outlet temp. in winter (K)}}$  for induced draught

#### 14.11.4 Fan noise

According to Glass (1978), the sound pressure level (SPL) (decibels) at 1m below air-cooler bundles is given by:

$$\text{SPL} = \text{const} + 30 \log(u_{ft}) + 10 \log(\dot{W}_{fs}) + 20 \log(D_f) \quad [14.7]$$

where  $u_{ft}$  = fan-tip speed (m/s)

const = 23.42 (induced draught), 26.42 (forced draught).

The simplest method of reducing noise is to reduce fan-tip speed.

#### 14.12 Fan laws

The fan laws are given below and these are useful when assessing fan parameters.

Constant fan diameter ( $D_f$ ):

$$\begin{aligned} W_a &\propto u_{ft} \\ \Delta P_{st} &\propto u_{ft}^2 \\ \dot{W}_{fs} &\propto u_{ft}^3 \\ V_a &\propto u_{ft} \end{aligned}$$

Constant tip speed ( $u_{ft}$ ):

$$\begin{aligned} W_a &\propto D_f^3 \\ \Delta P_{st} &\propto D_f^2 \\ \dot{W}_{fs} &\propto D_f^5 \\ V_a &\propto D_f^3 \end{aligned}$$

Variable tip speed ( $u_{ft}$ ) and fan diameter ( $D_f$ ):

$$\begin{aligned} W_a &\propto u_{ft} (D_f^3) \\ \Delta P_{st} &\propto u_{ft}^2 (D_f^2) \\ \dot{W}_{fs} &\propto u_{ft}^3 (D_f^2) \\ V_a &\propto u_{ft} (D_f^3) \end{aligned}$$

#### 14.13 Example of air-side calculations

The example demonstrates the step-by-step calculations required for the air-side of an air-cooled exchanger of known design. It is based on design no. 4 of Table 17.10. Inspection of the calculations indicates that they are

simplified considerably if curves relating heat transfer coefficient, referred to the bare tube, and air velocity are prepared.

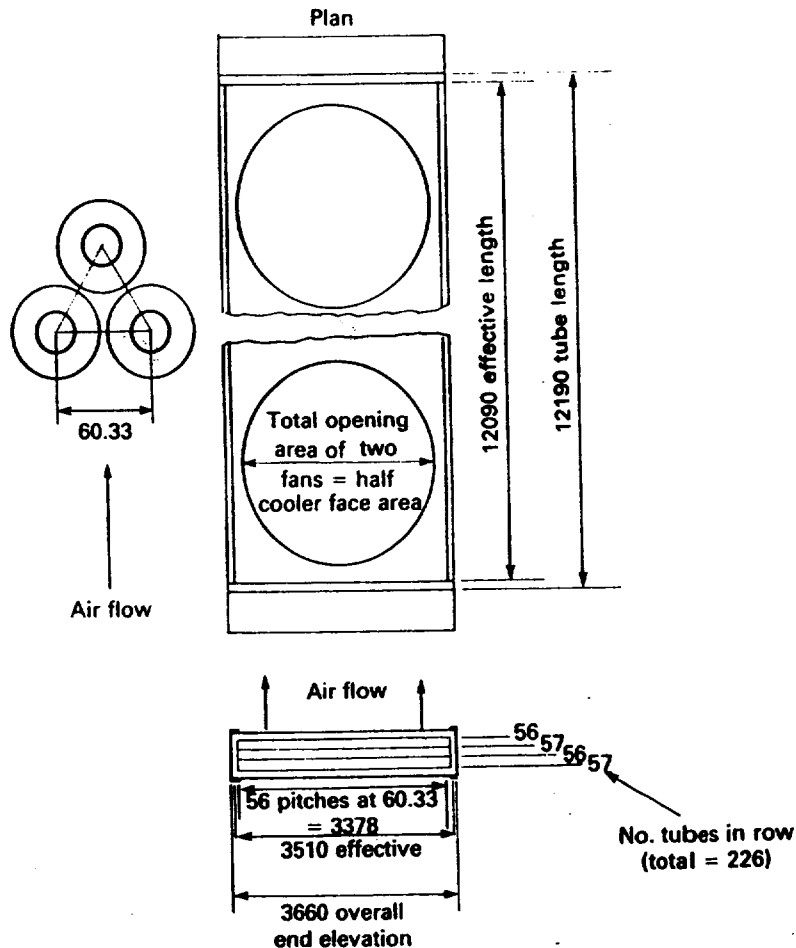
A forced-draught air cooler has one bundle, 3.66 m nominal width, 4 rows deep, and contains 226 finned tubes, 12.19 m long. The air flow rate is 151.2 kg/s, which enters the bundle at 25 °C and leaves at 70 °C. There are two fans with a total opening area of one half that of the cooler face area. Finned-tube characteristics are as follows:

- base tube material: carbon steel
- base tube: 25.4 mm o.d. × 21.18 mm i.d. × 60.33 mm × 30° pitch
- fin material and bond: aluminium, embedded
- no. of fins per metre:  $N_f = 433$
- fin o.d.:  $d_f = 57.15$  mm
- fin height:  $l_f = 15.875$  mm
- fin thickness:  $t_f = 0.4$  mm
- fin spacing:  $S_f = 1.91$  mm

The bundle arrangement is shown in Fig. 14.2.

Based on high finned-tube correlations supplied by a finned-tube maker the heat transfer coefficient to the fins ( $\alpha'_i$ ) =  $15(u_{ms}^{0.681})$  W/m<sup>2</sup> K and the pressure loss per row at the average air temperature ( $\Delta P_b$ ) =  $0.1466(u_{ms}^{1.75})$  mm water gauge.  $u_{ms}$  is the standard air velocity based on the minimum cross-sectional area between the tubes. Air densities are 1.2 kg/m<sup>3</sup> standard and 1.184 kg/m<sup>3</sup> at the fans. The thermal conductivity ( $\lambda_f$ ) of the aluminium fins from Table 9.1 is 208 W/m K.

Figure 14.2 General arrangement of air cooler



Determine the air-side heat transfer coefficient, referred to the bare external surface ( $\alpha_{fo}$ ), the pressure loss and power consumption, if the efficiency of fan and drive system ( $E_f$ ) = 0.8.

#### Geometric factors

Unfinned surface (Table 9.2):

$$A_u = \pi \times 433 \times 0.0254 \times 0.00191 = 0.0660 \text{ m}^2/\text{m}$$

Finned surface (Table 9.2):

$$A_f = \left\{ \left( \frac{\pi}{2} \right) \times 433 \times (0.05715^2 - 0.0254^2) \right\} + \left\{ \pi \times 433 \times 0.05715 \times 0.0004 \right\} = 1.8138 \text{ m}^2/\text{m}$$

Bare external surface:

$$A_b = \pi \times 0.0254 = 0.0798 \text{ m}^2/\text{m}$$

Free area ratio (Table 9.2):

$$\begin{aligned} \text{FAR} &= 1 - \left[ \left\{ (0.05715 \times 0.0004) + (0.0254 \times 0.00191) \right\} \times 433 / 0.06033 \right] \\ &= 0.488 \end{aligned}$$

Table 9.3

$$1 + \{t_{fc}/2l_f\} = 1 + \{0.0004/(2 \times 0.015875)\} = 1.0126$$

$$1 + 0.35 \ln(d_f/d_t) = 1 + 0.35 \ln(0.05715/0.0254) = 1.2838$$

( $t_{fc} = t_f$ )

$$\text{equiv. fin ht. } l_{fc} = 0.015875 \times 1.0126 \times 1.2838 = 0.02064 \text{ m}$$

Cooler face area (Fig. 14.2):

$$A_g = 3.51 \times 12.09 = 42.44 \text{ m}^2$$

Flow area between tubes:

$$A_x = 0.488 \times 42.44 = 20.71 \text{ m}^2$$

Fan-opening area:

$$0.5 \times 42.44 = 21.22 \text{ m}^2$$

#### Air velocity

Flow rate (standard):

$$151.2/1.2 = 126 \text{ m}^3/\text{s}$$

Flow rate at fans:

$$151.2/1.184 = 127.7 \text{ m}^3/\text{s}$$

Standard velocity between tubes:

$$u_{ms} = 126/20.71 = 6.08 \text{ m/s}$$

Velocity through fan opening:

$$u_f = 127.7/21.22 = 6.02 \text{ m/s}$$

#### Fin efficiency and coefficient

$$\alpha'_f = 15 \times 6.08^{0.681} = 51.3 \text{ W/m}^2 \text{ K}$$



$$m_e = \{(2 \times 51.3)/(208 \times 0.0004)\}^{0.5} = 35.12$$

$$m_e l_{fe} = 35.12 \times 0.02064 = 0.725$$

Fin efficiency (equation [9.3] or Table 9.4):

$$\Omega_f = \{\tanh(0.725)\}/0.725 = 0.855$$

$$\text{(equation [9.7]): } \alpha_{fo} = 51.3 \times \{(0.855 \times 1.8138) + 0.066\}/0.0798$$

$$= 1039 \text{ W/m}^2 \text{ K}$$

In a complete design  $\alpha_{fo}$  is combined with the tube-side coefficient, tube-wall resistance, and fouling factors in accordance with equation [14.1].

### Pressure loss and power consumption

Bundle loss (4 rows):

$$\Delta P_b = 4 \times 0.1466 \times 6.08^{1.75} = 13.8 \text{ mm w.g.}$$

Fan and plenum loss (equation [14.2]):

$$\Delta P_p = 0.06 \times 1.184 \times 6.02^2 = 2.6 \text{ mm w.g.}$$

Total loss:

$$\Delta P_{sh} = 13.8 + 2.6 = 16.4 \text{ mm w.g.}$$

Power at fan shaft (equation [14.4]):

$$\dot{W}_{fs} = (9.8 \times 16.4 \times 127.7)/1000 = 20.52 \text{ kW}$$

Fan motor power (equation [14.5]):

$$\dot{W}_{ms} = 20.52/0.8 = 25.7 \text{ kW}$$

## 14.14 Design curve for air-side heat transfer coefficients

Table 14.3 shows the calculations required to produce a curve relating  $\alpha_{fo}$  to  $u_{fs}$ , the standard air face velocity, where  $u_{fs} = \text{FAR}(u_{ms})$ . For the finned tubes and layout used in the example,  $\text{FAR} = 0.488$ , hence:

$$u_{fs} = 0.488(u_{ms}) \quad [14.8]$$

$\alpha_{fo}$  is derived from  $\alpha'_f$  in accordance with equation [9.7]. In this example:

$$\alpha'_f = 15(u_{ms}^{0.681}) \quad [14.9]$$

$$\text{and } m_e l_{fe} = \left(\frac{2\alpha'_f}{\lambda_f l_f}\right)^{0.5} l_{fe} = 0.1012(\alpha'_f)^{1/2} \quad [14.10]$$

$l_{fe}$  is derived from Table 9.3 based on  $l_f$ . The results are shown in Fig. 14.3.

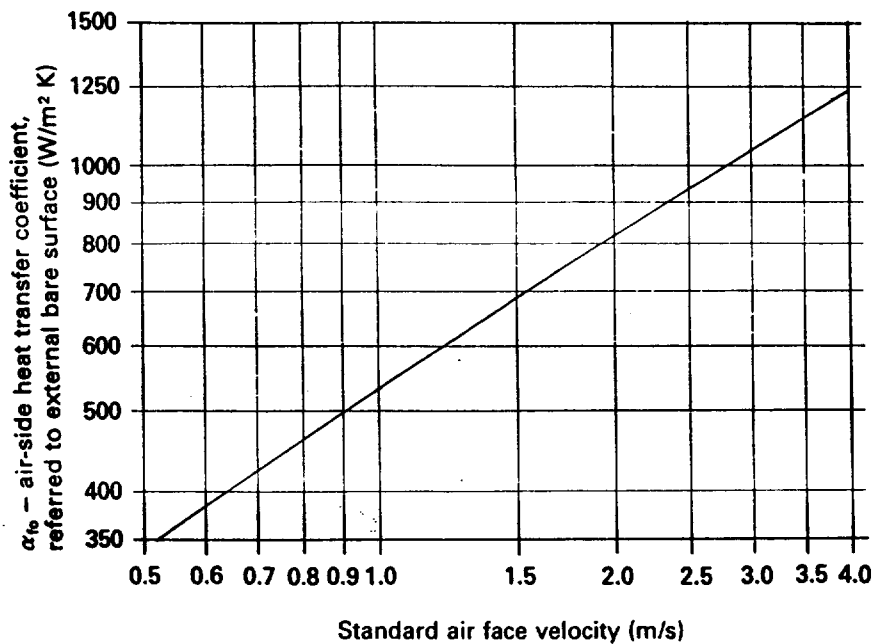
The correlations of section 6.10.5 show that the bundle pressure loss ( $\Delta P_b$ ) may be expressed as:

$$\Delta P_b = 0.5(u_{fs}^{1.75})f_m \quad [14.11]$$

Table 14.3 Air-cooled heat exchangers. Typical air-side heat transfer calculations

Air velocities (m/s)		$\alpha'_t$ (W/m <sup>2</sup> K)	$m_c l_{tc}$	Fin efficiency ( $\Omega_t$ )	$\alpha_{fo}$ (W/m <sup>2</sup> K)
Face ( $u_{fa}$ )	Between tubes ( $u_{ms}$ )				
0.223	0.456	8.79	0.3	0.971	201
0.518	1.061	15.62	0.4	0.950	350
0.998	2.044	24.41	0.5	0.924	533
1.704	3.492	35.15	0.6	0.895	744
2.680	5.491	47.84	0.7	0.863	978
3.967	8.128	62.49	0.8	0.830*	1231
[14.8]		[14.9]	[14.10]	Table 9.4 * < 0.85 but OK From Kern and Kraus (1972)	[9.7]

Figure 14.3 Air-side heat transfer coefficients for finned-tube bundles (applicable only to the finned tubes and layout listed in section 14.13)



$f_m$  is obtained from:

Average air temp. in bundle (°C)	$f_m$
0	0.851
20	0.924
40	1.000
60	1.077
80	1.154
100	1.231

The heat transfer and pressure loss data are used in the worked examples of section 17.4. It should be emphasised that the data apply only to the particular finned tubes and layout used in the example. However, the same method may be used to produce design curves for other finned tubes and layouts.

## References

A list of addresses for the service organisations is provided on p. xvi.

- Brown, R.** (1978) 'A procedure for preliminary estimates', *Chem. Eng.* (27 March) 108–11.
- Glass, J.** (1978) 'Specifying and rating fans', *Chem. Eng.* (27 March), pp. 120–4.
- Paikert, P.** (1983) *Heat Exchanger Design Handbook*, Vol. 3, Section 3.8. Hemisphere Publishing Corp.
- Pignotti, A. and Cordero, G. O.** (1983) 'Mean temperature difference charts for air coolers', *Trans. ASME, Journal of Heat Transfer* 105, 592–7.
- Taborek, J.** (1983) *Heat Exchanger Design Handbook*, Vol. 1, Section 1.5. Hemisphere Publishing Corp.

## Nomenclature

Symbol	Description	Units
$A$	Surface area, general	$m^2$
$A_o$	Bare external surface area, as though fins did not exist	$m^2$
$D_f$	Fan opening diameter	m
$E_f$	Efficiency of fan and drive system	—
$F$	MTD correction factor	—
$K$	Constant used in, and defined under, equation [14.2]	—
$Q$	Heat load	W
$r_{io}$	Internal fouling resistance, referred to bare external surface	$(W/m^2 K)^{-1}$
$r_{to}$	Tube-wall resistance, referred to bare external surface	$(W/m^2 K)^{-1}$
SPL	Sound pressure level	dB
$T_{sw}$	Temperature correction factor, used in, and defined under equation [14.6]	—
$u_f$	Air velocity, through fan opening	m/s
$u_{ft}$	Fan-tip speed	m/s
$U$	Overall heat transfer coefficient, general	$W/m^2 K$
$U_o$	Overall heat transfer coefficient, referred to bare external surface	$W/m^2 K$
$V_a$	Actual volumetric air flow through fan	$m^3/s$
$W_a$	Air mass flow rate delivered by fan	kg/s
$\dot{W}_f$	Power absorbed at fan shaft	kW
$\dot{W}_{ms}$	Fan motor power required under summer conditions	kW
$\dot{W}_{mw}$	Fan motor power required under winter conditions	kW
$\alpha_{fo}$	Air-side heat transfer coefficient, referred to bare external surface	$W/m^2 K$
$\alpha_{io}$	Internal heat transfer coefficient, referred to bare external surface	$W/m^2 K$
$\alpha'_f$	Air-side heat transfer coefficient to external surface	$W/m^2 K$

$\Delta P_b$	Bundle pressure loss	mm water
$\Delta P_p$	Fan and plenum losses	mm water
$\Delta P_{sh}$	Fan static head	mm water
$\Delta T_{lm}$	Logarithmic mean temperature difference	K
$\rho_a$	Air density	kg/m <sup>3</sup>

## Thermal design: double-pipe exchangers

The construction and application of double-pipe heat exchangers has been described in section 5.1. Chapter 19 provides typical film and overall heat transfer coefficients, together with approximate cost and size data. This chapter describes the method for thermal design.

### 15.1 Tube-side heat transfer and pressure loss calculations

Tube-side heat transfer and pressure loss calculations for flow inside the inner tube(s) are similar to those for shell-and-tube heat exchangers, as given in Chapter 12. Heat transfer and pressure loss correlations for single-phase flow inside tubes are given in Chapter 6. Heat transfer and pressure loss inside tubes for vaporising flow is given by Smith (1987).

### 15.2 Annulus heat transfer calculations

In the case of double-pipe heat exchangers the shell-side or annulus is the annular space between outer and inner tubes. As described in section 5.1, the inner tube(s) may be plain or fitted with longitudinal fins; in 1/1 units there is a single inner tube, while in multi-tube units (multis), there will be seven or more longitudinally finned tubes, depending on size.

According to Guy (1983), heat transfer calculations for the annulus may be treated as for tube-side flow, provided the annulus equivalent diameter ( $d_e$ ) is used instead of the true tube diameter. Section 6.10.3, equation [6.24], shows that:

$$d_e = \left\{ \frac{4A_x}{P_w} \right\} = 4 \left\{ \frac{\text{cross-sectional area for flow}}{\text{wetted perimeter}} \right\} \quad [15.1]$$

This value is used for the calculations of Reynolds number and the heat transfer coefficient using equations [6.16]–[6.21].

### 15.2.1 Annulus equivalent diameter

#### 1/1 double-pipe units – plain inner tube

In the case of a 1/1 double-pipe unit, where there is a single plain inner tube of outside diameter  $d_r$  and an outer tube of inside diameter  $D_i$ , section 6.10.3 shows that  $d_e$  is given by

$$d_e = D_i - d_r \quad [15.2]$$

#### 1/1 and multitube double-pipe units – finned inner tube(s)

In the case of 1/1 and multi-tube double-pipe units, having inner tube(s) finned longitudinally, the calculation of the annulus equivalent diameter ( $d_e$ ) is more lengthy. The free area for flow outside the finned tubes ( $A_x$ ), the wetted perimeter ( $P_w$ ), the total external surface per metre ( $A_t$ ), the external finned surface per metre ( $A_f$ ) and the external unfinned surface per metre ( $A_u$ ) are given by Table 9.2, namely:

Welded U-fins:

$$A_x = A_e - \left\{ \frac{\pi d_r^2}{4} + N_f t_f \left( l_f + \frac{r_f}{2} \right) \right\} N_t \quad [15.3a]$$

Extruded fins:

$$A_x = A_e - \left\{ \frac{\pi d_r^2}{4} + N_f l_f t_f \right\} N_t \quad [15.3b]$$

Welded U-fins:

$$A_t = A_f + A_u = \{ 2N_f l_f + (\pi d_r - N_f t_f) \} N_t \quad [15.4a]$$

Extruded fins:

$$A_t = A_f + A_u = \{ (2N_f l_f + N_f t_f) + (\pi d_r - N_f t_f) \} N_t \quad [15.4b]$$

$$P_w = \pi D_i + A_t \quad [15.5]$$

Calculate  $d_e = \left\{ \frac{4A_x}{P_w} \right\}$  from equation [15.1]

where  $A_e$  = total shell cross-sectional area =  $(\pi/4)D_i^2$  (m<sup>2</sup>)

$d_r$  = base tube outside diameter (m)

$l_f$  = fin height (m)

$N_f$  = number of longitudinal fins on one tube

$N_t$  = total number inner tubes

$t_f$  = fin thickness (m)

(for welded U-fins,  $r_f = 3t_f$  usually)

### 15.2.2 Fin calculations

Having calculated the clean annulus heat transfer coefficient ( $\alpha_f = \alpha_i$ ) from equations [6.16]–[6.21], using  $d_e$  from equation [15.1], it is necessary to take the fin efficiency into account as described in Chapter 9. Any annulus fouling factor ( $r_o$ ) should be combined with  $\alpha_f$  to provide the fouled annulus heat transfer coefficient  $\alpha'_f$ , as given by equation [9.1],

namely:

$$\frac{1}{\alpha'_f} = \frac{1}{\alpha_f} + r_o \quad [15.6]$$

The fin efficiency ( $\Omega_f$ ) is given by equation [9.2]:

$$\Omega_f = \left\{ \frac{\tanh(ml_f)}{ml_f} \right\} \quad [15.7]$$

where  $m = \left\{ \frac{2\alpha'_f}{\lambda_f t_f} \right\}^{1/2}$

and  $\lambda_f$  = fin thermal conductivity (W/m K)

It is then necessary to relate  $\alpha'_f$  to a selected reference surface, in order to combine it with the other heat transfer coefficients in the system. If the inside surface of the inner tube ( $A_i$ ) is selected, then equation [9.5] may be used:

$$\alpha_{fi} = \frac{\alpha'_f(\Omega_f A_f + A_u)}{A_i} \quad [15.8]$$

### 15.2.3 Overall heat transfer coefficient

Having determined  $\alpha_{fi}$ , the overall heat transfer coefficient  $U_i$  follows from equation [9.6]:

$$\frac{1}{U_i} = \frac{1}{\alpha_{fi}} + r_{ii} + r_i + \frac{1}{\alpha_i} \quad [15.9]$$

where  $r_{ii}$  = tube-wall resistance, referred to inside surface ( $\text{W/m}^2 \text{K})^{-1}$

$r_i$  = internal fouling resistance, referred to inside surface ( $\text{W/m}^2 \text{K})^{-1}$

$\alpha_i$  = internal heat transfer coefficient, referred to inside surface ( $\text{W/m}^2 \text{K}$ )

### 15.2.4 Mean temperature difference

If the double-pipe unit provides strict countercurrent or cocurrent flow, then the log mean temperature difference ( $\Delta T_{lm}$ ) is applicable. If not, an appropriate correction factor ( $F$ ) must be applied as described in Chapter 7. Figure 15.1 provides  $F$  curves for 1 series/2 parallel and 1 series/4 parallel systems. The effective temperature difference ( $\Delta T_m$ ) is then given by  $\Delta T_m = F \Delta T_{lm}$ .

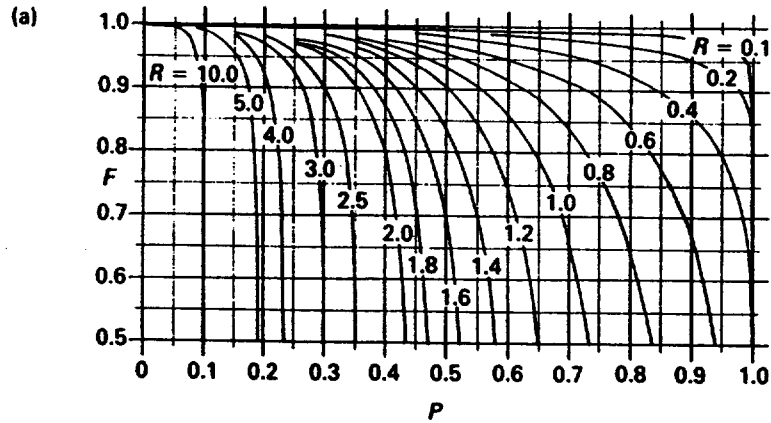
### 15.2.5 Surface area

In a design problem, the heat load ( $Q$ ) will be known and  $U_i$  and  $\Delta T$  are determined as described. The surface area, which in this case will be the internal surface area of the inner tubes ( $A_i$ ), is given by equation [6.8]:  
i.e.

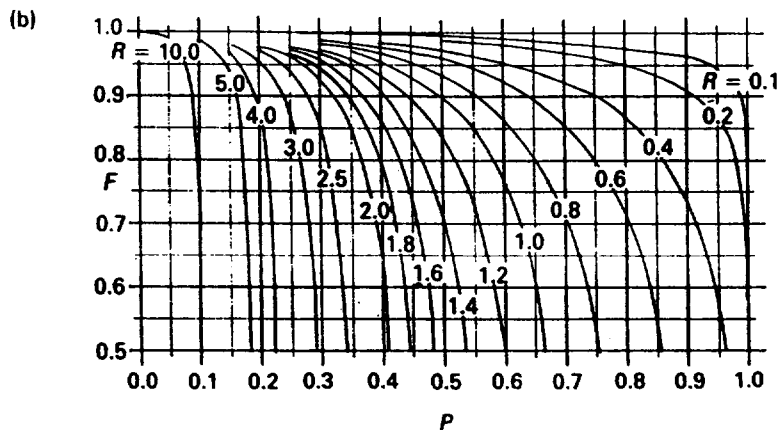
$$A_i = \frac{Q}{U_i \Delta T} \quad [15.10]$$

**Figure 15.1** *F* curves  
 (a) one-series/two-parallel system (b) one-series/four-parallel system

$T_1 = \text{hot inlet}$ $T_2 = \text{hot outlet}$ $t_1 = \text{cold inlet}$ $t_2 = \text{cold outlet}$	Cold stream in series hot stream in parallel $P = \frac{t_2 - t_1}{T_1 - t_1} \quad R = \frac{T_1 - T_2}{t_2 - t_1}$	Cold stream in parallel hot stream in series $P = \frac{T_1 - T_2}{T_1 - t_1} \quad R = \frac{t_2 - t_1}{T_1 - T_2}$
--	--	--



$T_1 = \text{hot inlet}$ $T_2 = \text{hot outlet}$ $t_1 = \text{cold inlet}$ $t_2 = \text{cold outlet}$	Cold stream in series hot stream in parallel $P = \frac{t_2 - t_1}{T_1 - t_1} \quad R = \frac{T_1 - T_2}{t_2 - t_1}$	Cold stream in parallel, hot stream in series $P = \frac{T_1 - T_2}{T_1 - t_1} \quad R = \frac{t_2 - t_1}{T_1 - T_2}$
--	--	---



### 15.3 Annulus pressure loss calculations

The external frictional pressure loss is calculated from equation [6.22] using  $d_e$  in place of  $d_i$ . The friction factor for longitudinally finned tubes is not quite the same as that for the inside of plain tubes. Based on the curves presented by Guy (1983), the friction factor ( $f_s$ ) is given by:

$$\text{Re}_s \leq 500: \quad f_s = 16/\text{Re}_s \quad [15.11a]$$

$$\text{Re}_s > 500 < 10000: \quad f_s = 0.00674 + 8.164/\text{Re}_s^{0.93} \quad [15.11b]$$

$$\text{Re}_s \geq 10000: \quad f_s = 0.0445/\text{Re}_s^{0.1865} \quad [15.11c]$$



where  $Re_s = \dot{m}_s d_e / \eta_s$

The pressure loss due to one return bend housing is 0.5 velocity heads based on the annulus velocity. Each spider tube support, for plain tube units less than 150 mm diameter, accounts for a similar pressure loss.

Hence:

$$\text{return bend loss } (\Delta P_{rb}) = \frac{\dot{m}_s^2}{4\rho_s} \quad [15.12]$$

$$\text{support loss } (\Delta P_{ts}) = \frac{\dot{m}_s^2}{4\rho_s} \quad [15.13]$$

$$\text{where } \dot{m}_s = \dot{M}_s / A_x.$$

Nozzle losses are calculated in accordance with equation [6.31].

## 15.4 Effect of cut-and-twist

When the annulus flow is in the laminar or transitional regimes, the annulus heat transfer coefficient may be enhanced by applying cut-and-twist of the fins at regular intervals as described in section 5.1.3. Inspection of equations [6.17]–[6.21], which present heat transfer coefficients for the laminar and transitional regimes inside tubes, shows that the coefficient is related to length  $L$ . This is the path length in which no internal mixing of the fluid occurs; as  $L$  decreases, the coefficient increases, so that there is an incentive to reduce  $L$ .

In the case of double-pipe exchangers fitted with return bends, mixing occurs in the bend (Guy 1983). Hence, without cut-and-twist,  $L$  = straight leg length; if cut-and-twist is used, mixing occurs at the cut-and-twist point and  $L$  = cut-and-twist pitch ( $L_{ct}$ ). The optimum value of  $L_{ct}$  is about 0.3–1 m.

The enhancement of the coefficient by cut-and-twist is accompanied by an increase in pressure loss and it is necessary to multiply  $f_s$  by a factor  $F_{ct}$ , which is given by

$$F_{ct} = 1.58 - 0.525L_{ct} \quad [15.14]$$

Note:  $F_{ct} = 1$  when  $L_{ct} > 1.0$ .

## 15.5 Example of annulus calculations

0.6 kg/s of hydrocarbon gas flows through the annulus of a multi-tube double-pipe heat exchanger having the following constructional data:

- shell nominal diameter = 100 mm (4 in)
- outside diameter = 114.3 mm (4.5 in)
- shell thickness (schedule 40) = 0.00602 m (0.237 in)
- shell inside diameter:  $D_i = 0.1023$  m (4.026 in)
- no. of finned tubes inside shell:  $N_t = 7$
- inner tube outside diameter:  $d_t = 0.01905$  m (0.75 in)

inner tube thickness = 0.00211 m (0.083 in)  
 inner tube inside diameter = 0.01483 m (0.584 in)  
 fin height:  $l_f = 0.00533$  m  
 fin thickness:  $t_f = 0.0009$  m  
 number of fins:  $N_f = 16$  (welded U)  
 material throughout = carbon steel  
 fin thermal conductivity:  $\lambda_f = 52$  W/m K  
 surface areas (one leg):  
   unfinned  $A_u = 0.319$  m<sup>2</sup>/m  
   finned  $A_f = 1.194$  m<sup>2</sup>/m  
   total external  $A_t = 1.513$  m<sup>2</sup>/m  
   internal  $A_i = 0.326$  m<sup>2</sup>/m

The average physical properties of the gas are as follows:

specific heat: (J/kg K) = 2219  
 viscosity: (Ns/m<sup>2</sup>) =  $1 \times 10^{-5}$   
 thermal conductivity: (W/m K) = 0.028  
 Prandtl number = 0.793  
 density: (kg/m<sup>3</sup>) = 4.0  
 fouling factor: (W/m<sup>2</sup> K) = 0.0003

What is the average heat transfer coefficient and pressure loss for 1m length?

**Heat transfer coefficient ( $\phi = 1$ )**

From equation [15.3a], flow area:

$$\begin{aligned}
 A_x &= (\pi/4) 0.1023^2 \\
 &\quad - \{(\pi/4) 0.01905^2 + (16 \times 0.0009 \times 0.00668)\} \times 7 = 0.00555 \text{ m}^2
 \end{aligned}$$

From equation [15.5], wetted perimeter:

$$\begin{aligned}
 P_w &= (\pi 0.1023) \\
 &\quad + \{(2 \times 16 \times 0.00533) + \pi(0.01905) - (16 \times 0.0009)\} \times 7 \\
 &= 1.833 \text{ m}
 \end{aligned}$$

From equation [15.1], equivalent diameter:

$$d_e = (4 \times 0.00555)/1.833 = 0.01211 \text{ m}$$

mass velocity:

$$\dot{m}_s = 0.6/0.00555 = 108.11 \text{ kg/s m}^2$$

Reynolds number:

$$Re_s = (108.11 \times 0.01211)/(1 \times 10^{-5}) = 130921$$

$$Re_s^{0.795} = 11695.6$$

$$\begin{aligned}
 Pr^{0.495} \exp[-0.0225\{\ln(Pr)\}^2] &= 0.793^{0.495} \exp[-0.0225\{\ln(0.793)\}^2] \\
 &= 0.8905
 \end{aligned}$$

From equation [6.16a], clean coefficient:

$$\alpha_f = 0.0225 \times (0.028/0.01211) \times 0.8905 \times 11695.6 = 541.8 \text{ W/m}^2 \text{ K}$$

From equation [15.6], fouled coefficient:

$$\alpha'_i = 1/\{(1/541.8) + 0.0003\} = 466 \text{ W/m}^2 \text{ K}$$

From equation [15.7]:

$$m = \{(2 \times 466)/(52 \times 0.0009)\}^{1/2} = 141.12$$

From equation [15.7]:

$$ml_f = 141.12 \times 0.00533 = 0.752$$

From equation [15.7], fin efficiency:

$$\Omega_f = (\tanh 0.752)/0.752 = 0.846$$

From equation [15.8]:

$$\alpha_{fi} = 466 \times \{(0.846 \times 1.194) + 0.319\}/0.326 = 1900 \text{ W/m}^2 \text{ K}$$

$\alpha_{fi}$  is combined with other coefficients, all based on tube inside diameter, to provide the overall coefficient.

**Pressure loss ( $\phi = 1$ )**

From equation [15.11c], friction factor

$$f_i = 0.0445/130921^{0.1865} = 0.00494$$

From equation [6.22], friction loss:

$$\Delta P_s = (4 \times 0.00494 \times 1 \times 108.11^2)/(2 \times 4 \times 0.01211) = 2384 \text{ Pa/m}$$

From equation [15.12], 1 bend loss:

$$\Delta P_{rb} = 108.11^2/(4 \times 4) = 730.5 \text{ Pa}$$

## 15.6 Design curve for annulus heat transfer coefficients

The example given in section 15.5 indicates that for manual calculations it is of great assistance to plot or tabulate  $\alpha_{fi}$  versus  $\alpha'_i$  for finned tubes of known geometries. As an example, a 1/1 finned-tube unit has been taken from Table 19.7 having the following characteristics:

- shell nominal diameter = 75 mm (3 in)
- outside diameter = 0.0889 m (3.5 in)
- shell thickness (schedule 40) = 0.00549 m (0.216 in)
- shell inside diameter:  $D_i = 0.07793 \text{ m}$  (3.068 in)
- inner tube outside diameter:  $d_r = 0.04826 \text{ m}$  (1.9 in)
- inner tube thickness 0.003683 m (0.145 in)
- inner tube inside diameter 0.04089 m (1.61 in)
- fin height:  $l_f = 0.0127 \text{ m}$
- fin thickness:  $t_f = 0.0009 \text{ m}$
- number of fins:  $N_f = 36$  (welded U)
- material throughout: carbon steel
- fin thermal conductivity:  $\lambda_f = 52 \text{ W/m K}$
- flow area:  $A_x = 0.002485 \text{ m}^2$
- wetted perimeter:  $P_w = 1.2784 \text{ m}$
- equivalent diameter:  $d_e = 0.00778 \text{ m}$

surface areas (one leg):

unfined:  $A_u = 0.1192 \text{ m}^2/\text{m}$

finned:  $A_f = 0.9144 \text{ m}^2/\text{m}$

total external:  $A_t = 1.0336 \text{ m}^2/\text{m}$

internal:  $A_i = 0.1285 \text{ m}^2/\text{m}$

The external coefficient  $\alpha_f$  must be combined with any external fouling ( $r_o$ ) before calculating the fin efficiency. From equation [15.6]:

$$1/\alpha'_f = 1/\alpha_f + r_o$$

From equation [15.7]:

$$m = \left\{ \frac{2\alpha'_f}{52 \times 0.0009} \right\}^{1/2} = 6.537 (\alpha'_f)^{1/2}$$

$$ml_f = (6.537 \times 0.0127)(\alpha'_f)^{1/2} = 0.083(\alpha'_f)^{1/2}$$

$$\Omega_f = \frac{\tanh\{0.083(\alpha'_f)^{1/2}\}}{0.083(\alpha'_f)^{1/2}}$$

From equation [15.8]:

$$\alpha_{fi} = \alpha'_f \{ \Omega_f(0.9144) + 0.1192 \} / 0.1285$$

Substituting into the above, the results given in Table 15.1 are obtained and plotted in Fig. 15.2. Table 9.4 is used to determine  $\Omega_f$  from  $ml_f$ . To show the effect of fin thermal conductivity, Fig. 15.1 also provides curves for copper and stainless steel. All fin thermal conductivities have been taken from Table 9.1.

**Table 15.1** Longitudinally finned double-pipe exchangers. Typical shell side calculations (carbon steel throughout)

$\alpha'_f$	$ml_f = 0.083(\alpha'_f)^{1/2}$	Table 9.4 $\Omega_f$	$\alpha_{fi}/\alpha'_f$	$\alpha_{fi}$
13.06	0.30	0.971	7.837	102.4
29.39	0.45	0.938	7.602	223.4
52.25	0.60	0.895	7.296	381.2
104.88	0.85	0.813	6.713	704.0
226.81	1.25	0.679	5.759	1306.3
496.81	1.85	0.515	4.592	2281.4
734.87	2.25	0.435	4.023	2956.4

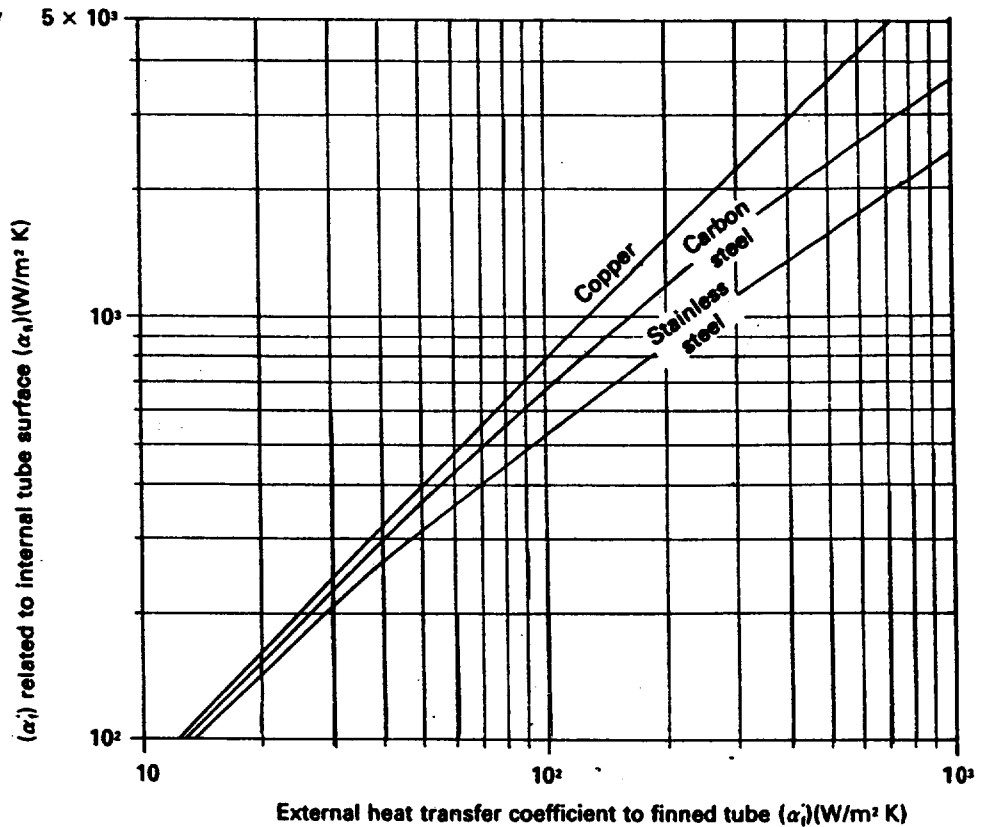
## References

A list of addresses for the service organisations is provided on p. xvi.

Guy, A. R. (1983) *Heat Exchanger Design Handbook*, Vol. 3, Section 3.2. Hemisphere Publishing Corp.

Smith, R. A. (1987) *Vaporisers - Selection, Design & Operation*. Longman.

**Figure 15.2** Longitudinally finned double-pipe exchangers. External heat transfer coefficient to finned tube ( $\alpha_f'$ ) related to internal tube surface ( $\alpha_{fi}$ ). (Tubes of section 15.6 only)



### Nomenclature

The nomenclature for this chapter is identical to that for Chapter 9, with the addition of the following:

Symbol	Description	Units
$A_i$	Total internal surface of inner tube(s)	$m^2$
$A_c$	Total outer tube, or shell, cross-sectional area (= $(\pi/4) D_o^2$ )	$m^2$
$A_x$	Free flow area for shell-side fluid (equation [15.3])	$m^2$
$d_c$	Equivalent diameter for shell-side flow (equation [15.1])	$m$
$D_i$	Outer tube, or shell, inside diameter	$m$
$f_s$	Shell-side friction factor	—
$F$	Correction factor applied to log mean temperature difference (equation [7.3])	—
$F_{ct}$	'Cut and twist' factor applied to $f_s$ , (equation [15.14])	—
$L_{ct}$	Distance between 'cut and twist' starting points	$m$
$\dot{m}_s$	Shell-side mass velocity (= $M_s/A_x$ )	$kg/s\ m^2$
$M_s$	Shell-side flow rate	$kg/s$
$N_t$	Total number of inner tubes in a single shell	—
$P_w$	Shell-side wetted perimeter	$m$
$Q$	Heat load	$W$
$r_f$	Internal distance between limbs of one U-shaped fin	$m$
$Re_s$	Shell-side Reynolds number = $\dot{m}_s d_c / \eta_s = M_s d_c / A_x \eta_s$	—
$\Delta P_{rb}$	Pressure loss due to shell-side return bends	$Pa$
$\Delta P$	Shell-side frictional pressure loss	$Pa$

$\Delta P_{ts}$	Pressure loss due to spider tube supports	Pa
$\Delta T_m$	Effective temperature difference (equation [7.3])	K
$\Delta T_{lm}$	Logarithmic mean temperature difference (equation [7.1])	K
$\eta_s$	Dynamic viscosity at bulk temperature of shell-side fluid	Ns/m <sup>2</sup>
$\rho_s$	Density of shell-side fluid	kg/m <sup>3</sup>

*Note:* 'shell-side' refers to annulus

# Thermal appraisal: gasketed-plate heat exchangers

The construction and application of gasketed-plate heat exchangers has been described in Chapter 4. Chapter 19 provides typical film and overall heat transfer coefficients together with approximate cost data. This chapter provides a thermal *appraisal* of gasketed-plate heat exchangers.

## 16.1 Plate exchanger thermal data

Chapters 12–15 have dealt with the thermal *design* of shell-and-tube (plain and low-fin tubes), air-cooled, and double-pipe heat exchangers. The thermal design methods provided by Chapters 12–15, together with the well-established heat transfer and fluid flow data of Chapters 6–11, enable the thermal design of these types of industrial units to be undertaken with confidence. As the design methods are intended for manual calculations, the units may not be of optimum design, but they can be relied upon to perform their required duties in service.

Manufacturers of gasketed-plate heat exchangers have, until recently, been criticised for not publishing their heat transfer and pressure loss correlations. Information which was published usually related to only one plate model or was of a generalised nature. As stated in section 4.2.1, the plates are mass-produced but the design of each plate pattern requires considerable research and investment, plus sound technical and commercial judgement, to achieve market success. As the market is highly competitive the manufacturer's attitude is not unreasonable. In contrast, shell-and-tube units are constructed of readily available components and this has permitted significant research to be carried out by various organisations, even before the arrival of HTFS and HTRI (see section 6.9). There is no evidence to suggest that designers and manufacturers of shell-and-tube exchangers would have been less secretive in similar circumstances.

Some secrecy was lifted when Bond (1981) and Kumar (1984), both of APV, published dimensionless correlations for chevron plates of APV manufacture. The chevron plate is the most common type in use today. If additional geometrical data are available from the makers, the

correlations enable a thermal design engineer to calculate heat transfer and pressure loss for a variety of chevron plates. Although the data have been provided by one manufacturer, and should only be applicable to his plates, it is reasonable to assume that all well-designed plates of the chevron pattern behave in a similar manner. Members of HTRI now have access to generalised heat transfer and pressure loss correlations, applicable to all plate heat exchangers of modern chevron pattern.

Whatever function is required from a gasketed-plate heat exchanger, ultimately the manufacturers must be consulted to ensure *guaranteed* performance. Only they can examine all the design parameters of their plates to achieve the optimum solution. Accordingly, this chapter provides only a thermal *appraisal* of gasketed-plate heat exchangers and is not thermal *design* as presented in Chapters 12–15.

## 16.2 Plate geometry

### 16.2.1 Chevron angle

This important factor, usually termed  $\beta$ , is shown in Fig. 16.1(a), the usual range of  $\beta$  being  $25^\circ$ – $65^\circ$ .

### 16.2.2 Effective plate length

The corrugations increase the flat or projected plate area, the extent depending on the corrugation pitch and depth. To express the increase of the developed length, in relation to the projected length (see Fig. 16.1(b)) an enlargement factor ( $\mu$ ) is used. The enlargement factor varies between 1.1 and 1.25, with 1.17 being a typical average, i.e.

$$\mu = \frac{\text{developed length}}{\text{projected length}} \quad [16.1]$$

### 16.2.3 Mean flow channel gap

Despite the complex flow area created by chevron plates, the mean flow channel gap ( $b$ ), shown in Fig. 16.1(b) by convention, is given as:

$$b = (p - t) \quad [16.2]$$

where  $p$  = plate pitch (m) and  $t$  = plate thickness (m).

### 16.2.4 Channel flow area

One channel flow area ( $A_x$ ) is given by

$$A_x = bw \quad [16.3]$$

where  $w$  = effective plate width (m).



Figure 16.1 Plate geometry (chevron plates)

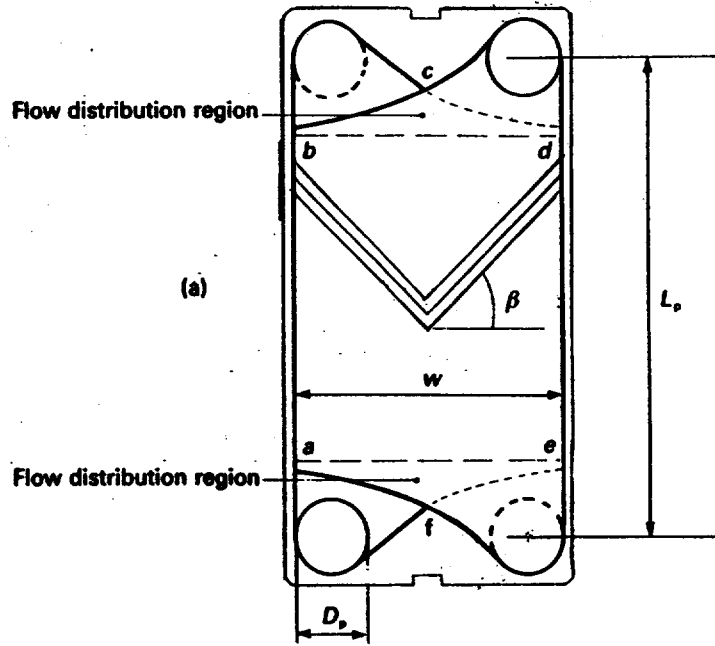
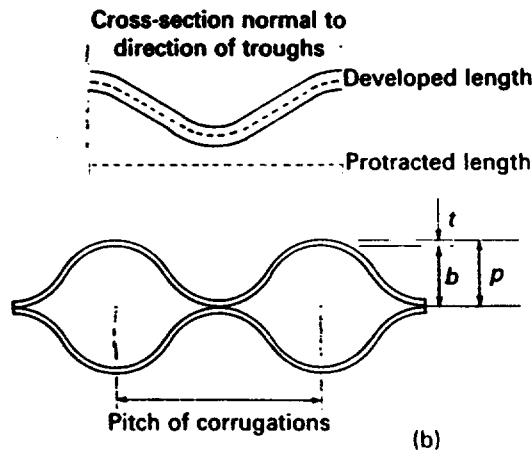


Plate surface area = within confines (abcdef)



16.2.5 Channel equivalent diameter

From equation [6.2], the channel equivalent diameter ( $d_e$ ) is given by

$$d_e = \frac{4 \text{ (channel flow area)}}{\text{(wetted surface)}} = \frac{4A_x}{P_w}$$

as  $P_w = 2(b + \mu w)$

$$d_e = \frac{4(bw)}{2(b + \mu w)}$$

In a typical plate,  $b$  is small in relation to  $w$ , hence:

$$d_e = \frac{2b}{\mu}$$

[16.4]

## 16.3 Heat transfer and pressure loss calculations

### 16.3.1 Heat transfer coefficient

The correlations presented by Kumar (1984) are in the Nusselt form similar to equations [6.11] and [6.12]. Provided the appropriate value of  $J_h$ , channel flow area, and channel equivalent diameter, are used, calculations are similar to single-phase flow inside tubes, i.e.

$$Nu = \frac{\alpha_{ch} d_c}{\lambda} = J_h Pr^{0.33} \phi \quad [16.5]$$

$$\text{or } \alpha_{ch} = \frac{J_h \lambda (Pr^{0.33}) \phi}{d_c} \quad [16.6]$$

$$\text{where } J_h = C_h Re^y \quad [16.7]$$

and Reynolds number is

$$Re = \left\{ \frac{\dot{m}_{ch} d_c}{\eta_b} \right\} = \left\{ \frac{\dot{M}_{ch} d_c}{A_x \eta_b} \right\} \quad [16.8]$$

Values of  $C_h$  and  $y$  versus  $Re$  for various chevron angles are given in Table 16.1. Nomenclature follows that of Chapters 6 and 12.

**Table 16.1** Gasketed-plate heat exchangers. Constants for single-phase heat transfer and pressure loss calculations

Chevron angle (degrees)	Heat transfer			Pressure loss		
	Reynolds number	$C_h$	$y$	Reynolds number	$K_p$	$z$
≤ 30	≤ 10	0.718	0.349	< 10	50	1
	> 10	0.348	0.663	10 – 100	19.40	0.589
				> 100	2.990	0.183
45	< 10	0.718	0.349	< 15	47	1
	10 – 100	0.400	0.598	15 – 300	18.29	0.652
	> 100	0.300	0.663	> 300	1.441	0.206
50	< 20	0.630	0.333	< 20	34	1
	20 – 300	0.291	0.591	20 – 300	11.25	0.631
	> 300	0.130	0.732	> 300	0.772	0.161
60	< 20	0.562	0.326	< 40	24	1
	20 – 400	0.306	0.529	40 – 400	3.24	0.457
	> 400	0.108	0.703	> 400	0.760	0.215
≥ 65	< 20	0.562	0.326	< 50	24	1
	20 – 500	0.331	0.503	50 – 500	2.80	0.451
	> 500	0.087	0.718	> 500	0.639	0.213

### 16.3.2 Channel pressure loss

Kumar (1984) presents 'Fanning-type' friction factors ( $f_{ch}$ ) for use in an equation similar to [6.22] which relates to single-phase frictional loss

inside tubes. Provided the appropriate value of  $f_{ch}$ , channel flow area, and channel equivalent diameter, are used, calculations are similar, i.e.

$$\Delta P_{ch} = \left\{ \frac{4f_{ch}L_{ch}\dot{m}_{ch}^2}{2\rho d_e\phi} \right\} \quad [16.9]$$

$$\text{where } f_{ch} = \frac{K_p}{Re^z} \quad [16.10]$$

If  $N_p$  = number of passes

$$L_{ch} = N_p L_p \quad [16.11]$$

Values of  $K_p$  and  $z$  versus  $Re$  for various chevron angles are given in Table 16.1.

### 16.3.3 Port pressure loss

According to Kumar, the total port loss may be taken as 1.3 velocity heads per pass based on the velocity in the port, i.e.

$$\Delta P_p = \left\{ \frac{1.3\dot{m}_p^2}{2\rho} \right\} N_p \quad [16.12]$$

$$\text{where } \dot{m}_p = \left\{ \frac{\dot{M}_t}{(\pi/4)D_p^2} \right\}$$

in which  $\dot{M}_t$  = total flow in port opening (kg/s) and  $D_p$  = port diameter (m).

## 16.4 Effective temperature difference

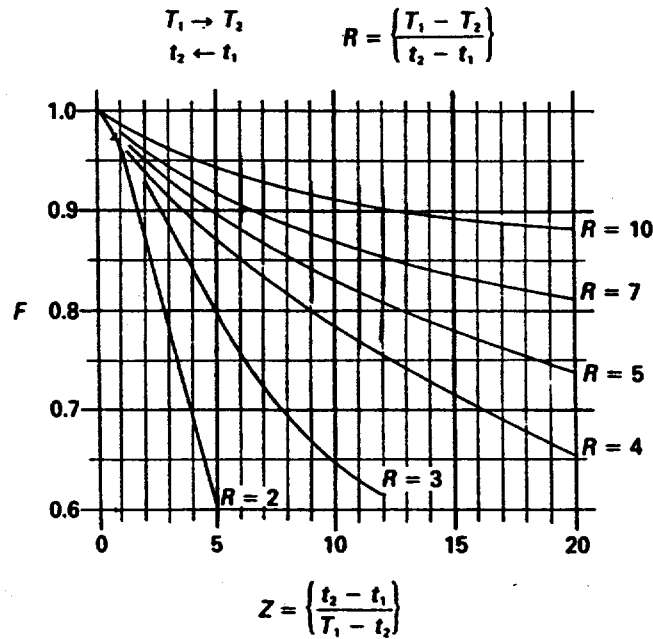
One of the features of plate-type units is that countercurrent flow is achieved (see Chapter 7). However, the logarithmic mean temperature difference ( $\Delta T_{lm}$ ) requires correction due to two factors: (a) the end plates, where heat is transferred from one side only, and (b) the central plate of two-pass/two-pass flow arrangements, where the flow is cocurrent. However, unless the number of channels per pass is less than about 20, and the number of process and service passes are not equal, the effect on temperature difference is negligible. Hence, in many applications,  $\Delta T_{lm}$  may be used.

If countercurrent flow does not apply, then a correction factor  $F$  must be applied to  $\Delta T_{lm}$  exactly as for shell-and-tube and air-cooled exchangers. Figure 16.2 provides values of  $F$  for a two-pass/one-pass system. For other systems refer to Foote (1967).

## 16.5 Overall heat transfer coefficient

Once both film heat transfer coefficients have been determined from section 16.3.1 the overall heat transfer coefficient is calculated in

**Figure 16.2** Temperature difference correction factor ( $F$ ) for gasketed-plate heat exchangers – two-pass/one-pass system (applicable to 20 or more plates) (courtesy of APV International)



accordance with equation [6.7c], assuming that pressure losses, calculated in accordance with sections 16.3.2 and 16.3.3 are satisfactory:

$$\frac{1}{U} = \frac{1}{\alpha_h} + \frac{1}{\alpha_c} + r_{fh} + r_{fc} + r_w \quad [16.13]$$

where  $U$  = overall heat transfer coefficient ( $\text{W}/\text{m}^2 \text{K}$ )

$\alpha_h, \alpha_c$  = film heat transfer coefficients of hot and cold fluids ( $\text{W}/\text{m}^2 \text{K}$ )

$r_{fh}, r_{fc}$  = fouling factors for hot and cold fluids ( $\text{W}/\text{m}^2 \text{K}$ )<sup>-1</sup>

$r_w$  = plate wall resistance ( $\text{W}/\text{m}^2 \text{K}$ )<sup>-1</sup>

Sometimes a cleanliness factor is used instead of fouling factors (see Chapter 8). In this case a 'clean' overall heat transfer ( $U_c$ ) coefficient is calculated from

$$\frac{1}{U_c} = \frac{1}{\alpha_h} + \frac{1}{\alpha_c} + r_w \quad [16.14]$$

The service or fouled overall heat transfer coefficient, when the cleanliness factor is CF, is given by:

$$U = U_c(\text{CF}) \quad [16.15]$$

## 16.6 Surface area

In a design problem, the heat load  $Q$  is known,  $\Delta T$  and  $U$  are calculated as described in sections 16.4 and 16.5 respectively, leaving the surface area ( $A$ ) to be calculated from equation [6.8]:

$$A = \frac{Q}{U \Delta T} \quad [16.16]$$

## 16.7 Exchanger arrangement

In a performance evaluation, the exchanger size and flow arrangement is known. In a design case considerable skill and experience are required to produce the optimum design involving the plate size and pattern, flow arrangement, number of passes, number of channels per pass, etc. Like shell-and-tube exchanger design, many designs may have to be produced, manually or by computer, before the optimum is found.

The heat transfer and pressure loss calculations described in sections 16.3.1, 16.3.2 and 16.3.3 assume that the plates are identical. However, at the design stage, other variations are available to the thermal design engineer as described in the following sections.

### 16.7.1 High- and low-theta plates

A plate having a low chevron angle provides high heat transfer combined with high pressure loss. A plate having a high chevron angle provides the opposite features, i.e. low heat transfer combined with low pressure loss. A low chevron angle is around 25°–30°, while a high chevron angle is around 60°–65°. These characteristics may be confirmed by inspection of  $C_h$  and  $K_p$  in Table 16.1. A log–log plot of  $J_h$  and  $f_{ch}$  versus Reynolds number with  $\beta$  as parameter, yields straight, nearly parallel lines in the fully laminar and fully turbulent regions. The values of  $C_h$  and  $K_p$  directly reflect the magnitude of heat transfer coefficients and pressure loss and it will be seen that their values increase as  $\beta$  decreases.

Manufacturers specify the plates having low values of  $\beta$  as 'high- $\theta$  plates' and plates having high values of  $\beta$  as 'low- $\theta$  plates'. Theta is used by manufacturers to denote the number of heat transfer units (NTUs) described in section 7.8. Retaining the nomenclature applicable to equations [7.8] and [7.9]:

$$\theta = \text{NTU}_c = \frac{UA}{wc} = \frac{t_2 - t_1}{\Delta T_{lm}}$$

$$\theta = \text{NTU}_h = \frac{UA}{WC} = \frac{T_1 - T_2}{\Delta T_{lm}}$$

### 16.7.2 Thermal mixing

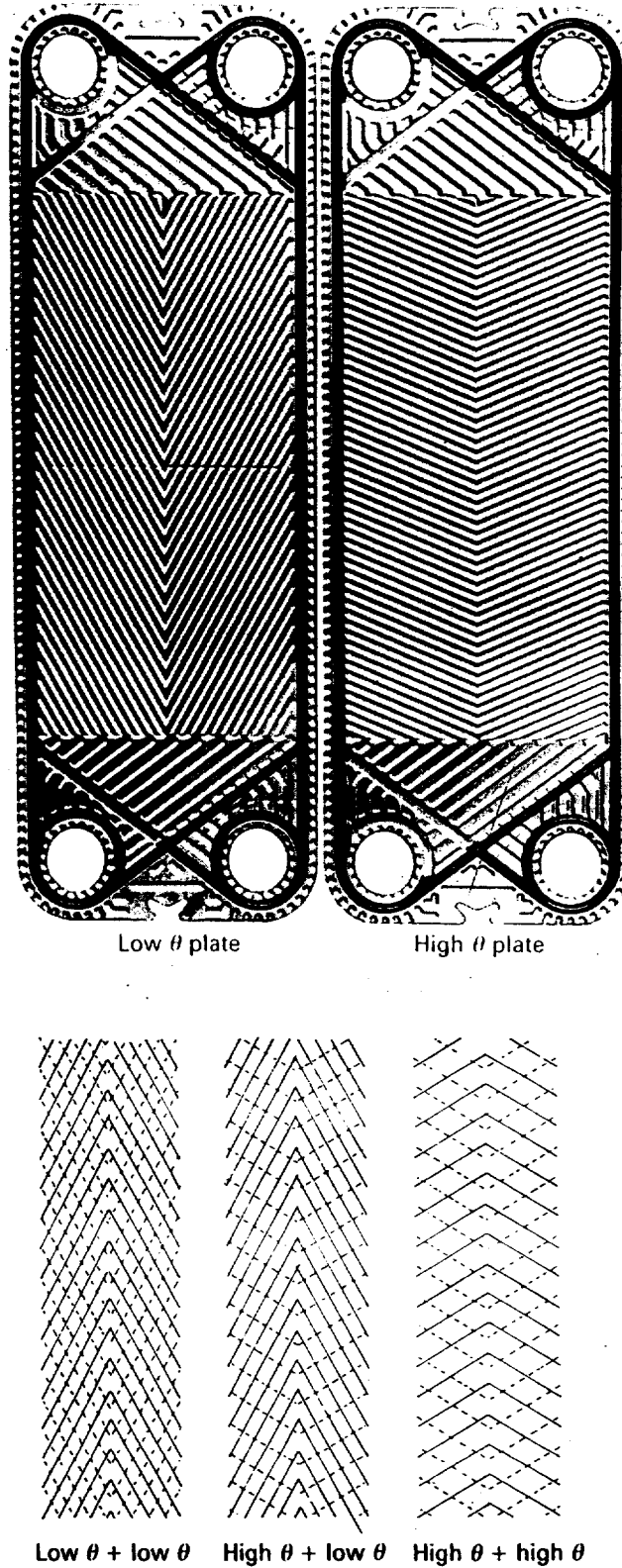
A pack of plates may be composed of all high-theta plates ( $\beta = 30^\circ$  for example), or all low-theta plates ( $\beta = 60^\circ$  for example), or high- and low-theta plates may be arranged alternately in the pack to provide an intermediate level of performance. Thus two plate configurations provide three levels of performance.

A further variation is available to the thermal design engineer. Parallel groups of two channel types, either (high + mixed) theta plates or (low + mixed) theta plates, are assembled together in the same pack in the proportions required to achieve the optimum design.

Thermal mixing provides the thermal design engineer with a better

opportunity to utilise the available pressure loss, without excessive oversurface, and with fewer standard plate patterns. Sjogren and Grueiro (1983) show how a combination of high- and low-theta plates provided the best solution to a process water/cooling water application. Figure 16.3 illustrates the effect of plate mixing.

Figure 16.3 Mixed theta concept



## Acknowledgements

The author is grateful for the assistance of the following companies: APV International Ltd, Crawley, West Sussex, UK; Alfa-Laval Co. Ltd, Great West Road, Brentford, Middlesex, UK.

## References

A list of addresses for the service organisations is provided on p. xvi.

- Bond, M. P.** (1981) 'Plate heat exchanger for effective heat transfer', *The Chemical Engineer* (April).
- Foote, M. R.** (1967) 'Effective mean temperature differences in multi-pass heat exchangers', National Engineering Laboratory (East Kilbride, Scotland), Report No. 303.
- Kumar, H.** (1984) 'The plate heat exchanger: construction and design', presented at 1st UK National Conference on Heat Transfer, University of Leeds, 3-5 July. Inst. Chem. Eng. Symp., Series No. 86, p. 1275.
- Sjogren, S. and Grueiro, W.** (1983) 'Applying plate heat exchangers in hydrocarbon processing', *Hydrocarbon Processing* (Sept.).

## Nomenclature

Symbol	Description	Units
$A$	Surface area	$m^2$
$A_x$	One channel flow area, defined by equation [16.3]	$m^2$
$b$	Mean flow channel gap, defined by equation [16.2]	$m$
CF	Cleanliness factor, defined by equation [16.15]	—
$C_b$	Constant in equation [16.7]	—
$C_p$	Fluid specific heat	$J/kg K$
$d_c$	Channel equivalent diameter	$m$
$D_p$	Port diameter	$m$
$f_{ch}$	Friction factor (see equation [6.10] and Table 16.1)	—
$J_h$	Heat transfer factor (see equation [16.7] and Table 16.1)	—
$K_p$	Constant in equation [16.10]	—
$L_{ch}$	Total channel flow length, defined by equation [16.11]	$m$
$L_p$	Flow length in one pass	$m$
$\dot{m}_{ch}$	Channel mass velocity	$kg/s m^2$
$\dot{m}_p$	Port mass velocity	$kg/s m^2$
$\dot{M}_{ch}$	Flow rate in one channel	$kg/s$
$\dot{M}_t$	Flow rate through a port	$kg/s$
$N_p$	Number of passes	—
$p$	Plate pitch	$m$
Pr	Prandtl number ( $= C_p \eta_b / \lambda$ )	—
$P_w$	Wetted perimeter	$m$
$Q$	Heat load	$W$
$r_{fc}$	Fouling factor for cold fluid	$(W/m^2 K)^{-1}$
$r_{fh}$	Fouling factor for hot fluid	$(W/m^2 K)^{-1}$
$r_w$	Plate resistance	$(W/m^2 K)^{-1}$
Re	Reynolds number, defined by equation [16.8]	—

$t$	Plate thickness	m
$U$	Overall heat transfer coefficient (service)	W/m <sup>2</sup> K
$U_c$	Overall heat transfer coefficient (clean)	W/m <sup>2</sup> K
$w$	Effective plate width	m
$y$	Exponent in equation [16.7]	—
$z$	Exponent in equation [16.10]	—
$\alpha_{ch}$	Heat transfer coefficient in channel	W/m <sup>2</sup> K
$\beta$	Chevron angle, defined in Fig. 16.1	degrees
$\eta_b$	Dynamic viscosity at bulk temperature	Ns/m <sup>2</sup>
$\eta_s$	Dynamic viscosity at surface temperature	Ns/m <sup>2</sup>
$\lambda$	Thermal conductivity of fluid	W/m K
$\mu$	Plate enlargement factor, defined by equation [16.1]	—
$\Delta P_{ch}$	Channel pressure loss	Pa
$\Delta P_p$	Port pressure loss	Pa
$\Delta T$	Temperature difference	K
$\rho$	Fluid density	kg/m <sup>3</sup>
$\phi$	Viscosity correction factor ( $= (\eta_b/\eta_s)^{0.17}$ )	—



## Worked examples for thermal design

This chapter presents step-by-step calculations for the thermal design of shell-and-tube exchangers (plain and low-fin tubes), air-cooled exchangers, and longitudinally finned double-pipe exchangers. It is significant that the thermal design calculations relate to the most widely used types of metallic tubular heat exchangers. This is because such units have always been readily available and have been the subject of considerable research for many years, even before the arrival of the cooperative research organisations, HTRI and HTFS (see section 6.9). On the other hand, non-tubular equipment such as gasketed-plate, plate-fin, lamella and spiral exchangers, etc., are highly specialised and available only from a limited number of fabricators. In general, fabricators of the non-tubular equipment have their own carefully chosen models and the associated heat transfer and pressure loss data relate only to those models.

The calculations are based on the correlations presented in Part 2 and the thermal design methods presented in Chapters 12–16. These correlations and methods are well established and may be applied with confidence to design tubular equipment which will perform their required duties. Chapter 16 presents a thermal appraisal of gasketed-plate heat exchangers, which are the most widely used non-tubular type. In order to provide an indication of the magnitude of the various design parameters given in Chapter 16, thermal calculations are presented in section 17.6. Although these calculations assist in the preliminary sizing and subsequent checking, thermal design of gasketed-plate heat exchangers must be left to the specialised fabricators.

### 17.1 Thermal design process

#### 17.1.1 Performance check and design

A thermal performance check (or rating) involves the calculation of the heat transfer coefficients and pressure losses of both fluids for a

completely defined heat exchanger, to a specified duty (i.e. both flow rates and the four terminal temperatures are known). The results show how much under- or oversurface there is in the exchanger and whether the pressure losses are within or outside the allowable values. No trial and error is involved. This type of calculation is carried out in order to determine whether an existing exchanger will be capable of performing a new duty. Alternatively, it may be necessary to determine the hot (or cold) terminal temperatures achieved in a completely defined heat exchanger, when the cold (or hot) terminal temperatures and both flow rates are known. Other calculations involving the flow rates and terminal temperatures are possible, but the exchanger is always completely defined.

Thermal design involves the determination of the heat exchanger size (and arrangement if more than one unit is required) when only the duty and allowable pressure losses are known. Whether the exchanger is designed manually or by computer, the calculation process is always the same. A tentative design of heat exchanger is assumed, based on published data or experience of a similar unit, (in the case of manual design), and a thermal performance check (or rating) is carried out, exactly as described above. If the tentative heat exchanger is greatly under- or oversized, and/or the pressure losses are well within or outside the allowable values, another tentative design of heat exchanger is assumed. A second performance check is carried out and if the results do not meet requirements, the process is repeated until they do. How quickly the final design is achieved manually depends on the knowledge, skill and judgement of the thermal design engineer, which is achieved only by experience.

### 17.1.2 Exchanger type

Part 1 Appendix provides guidance for the selection of exchanger type. If the service is highly corrosive consideration may have to be given to the use of glass, carbon or Teflon™ units. Later calculations may show that the selected unit is not the ideal choice. For instance, the duty may require a large number of long, thin shell-and-tube exchangers in series, in which case a double-pipe or plate-type exchanger may be a better choice. When handling large volumes of low-pressure gas, a non-standard box-shaped tubular exchanger, or a rotary type, may provide a cheaper design than a shell-and-tube exchanger.

### 17.1.3 Routing of fluids

Table 17.1 gives guidance for the routing of the fluids, which applies particularly to shell-and-tube exchangers. *If there are no process restrictions* switching the fluids should always be considered. If the shell-and-tube-sides require different materials, the best choice of routing can only be decided after designing both options in many cases.

For instance, if the design pressure of one fluid is much greater than the other, it is usual to route it through the tubes to avoid the expense of

**Table 17.1** Shell-and-tube heat exchangers: routing of fluids

<b>Tube-side</b>	<b>Shell-side</b>
High pressure	Small flow rate
High temperature	Viscous fluid
Corrosive	Low heat transfer coefficient
Fouling (except U-tubes)	(Consider finned tubes)

Conflicting requirements often arise and alternative designs should be investigated with fluids switched, provided there are no process restrictions.

a thick shell. In some cases, however, routing the higher pressure fluid through the shell may produce a cheaper unit, particularly if it reduces the exchanger diameter and it is made of carbon steel. It is always worthwhile examining this option in the case of fixed tubesheet exchangers, as there will be no high-pressure girth joints on the shell-side.

It is also usual to route the fluid requiring the more expensive material through the tubes. However, if this fluid is not at high pressure, and the switch reduces the shell diameter, it may provide a cheaper solution. Again this option may be particularly worthwhile in the case of a fixed tubesheet exchanger.

#### 17.1.4 Temperature cross

If the duty involves a temperature cross (section 7.2), consideration should be given to gasketed-plate and double-pipe heat exchangers. However, if the choice has to be a shell-and-tube unit, countercurrent flow designs should be investigated, if permitted by the user. These involve exchangers having one shell pass and one tube pass (1/1 units) or two shell passes and two tube passes (2/2 units), but floating-head and U-tube units have structural limitations described in sections 1.5.7 and 1.5.15. Even if there is no temperature cross, this option should be investigated and it is sometimes overlooked.

#### 17.1.5 Influence of design parameters

It is helpful to assess quickly the effect on heat transfer and pressure loss due to a change in any of the design parameters arising from a design decision or prediction in accuracy. The *approximate* relationship between heat transfer and pressure loss and all design parameters is given in Table 17.2. For instance, the turbulent heat transfer coefficient inside a tube is proportional to (thermal conductivity)<sup>2/3</sup>, (specific heat)<sup>1/3</sup> and (mass flow rate)<sup>0.8</sup>; it is inversely proportional to (viscosity)<sup>0.467</sup> and (tube inside diameter)<sup>1.8</sup>. If the thermal conductivity and specific heat are

Table 17.2 Heat transfer and pressure loss inside and outside plain tubes: influence of design parameters

	Item	Notes ( $\phi = 1$ in all cases)	Physical properties	Construction factors	Flow rate
Inside tubes	Turbulent	Heat transfer coefficient	$\frac{\lambda^{2/3} c_p^{1/3}}{\eta^{0.467}}$	$\frac{1}{d_i^{1.8}}$	$\dot{M}_i^{0.8}$
		Straight tube pressure loss	$\frac{\eta^{0.2}}{\rho}$	$\frac{L}{d_i^{4.8}}$	$\dot{M}_i^{1.8}$
	Laminar	Heat transfer coefficient	$\lambda^{2/3} c_p^{1/3}$	$\frac{1}{d_i L^{1/3}}$	$\dot{M}_i^{1/3}$
		Straight tube pressure loss	$\frac{\eta}{\rho}$	$\frac{L}{d_i^4}$	$\dot{M}_i$
Outside tubes (cross-flow)	Turbulent	Heat transfer coefficient	$\frac{\lambda^{2/3} c_p^{1/3}}{\eta^{0.267}}$	$\frac{1}{d_o^{0.4} l_i^{0.6}}$	$\dot{M}_o^{0.6}$
		Cross-flow pressure loss	$\frac{\eta^{0.2}}{\rho}$	$\frac{N_r}{d_o^{0.2} l_i^{1.8}}$	$\dot{M}_o^{1.8}$
	Laminar	Heat transfer coefficient	$\lambda^{2/3} c_p^{1/3}$	$\frac{1}{d_o^{2/3} l_i^{1/3}}$	$\dot{M}_o^{1/3}$
		Cross-flow pressure loss	(4) $\dot{M}_o$ is mass flow through flow area $A_x$	$\frac{\eta}{\rho}$	$\frac{N_r}{d_o l_s}$

overpredicted by 10%, and the viscosity is underpredicted by 10%, the heat transfer coefficient will be calculated about 15% too high. Of particular significance is the relationship between tube-side frictional loss ( $\Delta P_i$ ) and tube inside diameter ( $d_i$ ), where  $\Delta P_i \propto (1/d_i)^{4.8}$ . If the inside diameter used in design is 10% greater than the true inside diameter, straight tube frictional loss will be underpredicted by 58%.

### 17.1.6 Effect of changing number of tube passes and baffles

Consider a shell-and-tube exchanger having two tube-side passes, a fixed length and a fixed mass flow rate. The internal heat transfer coefficient is  $\alpha_i$  and the frictional pressure loss over the two passes is  $\Delta P_i$ . If the number of passes is increased to four, without altering the total number of tubes, the mass flow rate in each tube is doubled. Inspection of Table 17.2 shows that  $\alpha_i$  will be increased 2<sup>0.8</sup>-fold to become 1.74 $\alpha_i$ . With regard to pressure loss, the mass flow rate is doubled, and also the length of travel, as there are four passes instead of two. Inspection of Table 17.2 shows that  $\Delta P_i$  will be increased by 2<sup>1.8</sup>(2) to become 6.96  $\Delta P_i$ . A 1.74-fold increase in heat transfer coefficient has been achieved at the

expense of a 6.96-fold increase in pressure loss. Hence increasing the number of passes (with fixed mass flow rate, total number of tubes and tube length)  $n$ -fold increases the heat transfer coefficient  $n^{0.8}$ -fold, accompanied by a  $n^{2.8}$ -fold increase in pressure loss.

Similar considerations apply on the shell-side with fixed mass flow rate, fixed shell diameter and fixed length. Inspection of Table 17.2 shows that in a baffled shell-and-tube exchanger, reducing the baffle pitch  $n$  times increases the heat transfer coefficient  $n^{0.6}$  times, accompanied by a pressure loss increase of  $n(n^{1.8}) = n^{2.8}$  times, there being  $n$  times as many cross-flow passes. Because of internal leakage (see section 12.2), the actual increase in both heat transfer and pressure loss is less.

The effect on pressure loss is more severe for tube-side flow as the number of passes can only be changed in distinct increments, whereas small changes in baffle spacing can be achieved.

### 17.1.7 Tentative exchanger

In a design problem, the heat load ( $Q$ ) and the log mean temperature difference ( $\Delta T_{\text{lm}}$ ) must be known. The overall coefficient must be estimated from either experience or published data, such as provided by Chapter 19, for instance. A tentative surface area ( $A$ ) is obtained from  $A = Q/U \Delta T$ , after which a tentative design is established based on specified mechanical factors. Double-pipe, air-cooled and gasketed-plate type heat exchangers have the advantage of employing standardised sections, but this is seldom the case with shell-and-tube exchangers. The exception occurs when a range of standard shell-and-tube exchangers is designed to meet specific duties such as compressor aftercooling, engine oil coolers, etc. Irrespective of the exchanger type, the design is usually of a one-off nature, suited exactly to the process requirements.

### 17.1.8 Tube-side flow

If water is the coolant, the number of tubes in one pass is chosen to meet the velocity requirements given in Table 18.2. Tables 17.3(a) and 17.3(b) provide the characteristics of typical heat exchanger tubing and one column in Table 17.3(a) provides the mass flow rate (kg/s) to achieve a water velocity of 1 m/s. Typical velocities for fluids of low viscosity lie in the region of 0.5–3 m/s and the same column may be used for fluids other than water if their value is multiplied by  $\rho/998$ , where  $\rho$  is the density of the fluid ( $\text{kg/m}^3$ ) under consideration. As the fluid viscosity increases, the tube-side velocity falls and for highly viscous liquids may be as low as 0.1 m/s.

The velocity range for gases is of the order of 2–15 m/s.

Once the number of passes, and the number of tubes per pass, have been estimated, the heat transfer coefficient and pressure loss may be calculated. If the pressure loss exceeds the maximum allowable value it may be reduced by several means, such as reducing the number of passes, shortening the tube length (if permissible), increasing the shell diameter,

Table 17.3(a) Heat exchanger tubes – characteristics

Tube size (mm)			Surface area per metre length (m <sup>2</sup> )		Internal flow area (m <sup>2</sup> )	Steel tubes weight per metre length (kg) <sup>(2)</sup>	Water at 60 °F: mass flow for lm/s vel. (kg/s) <sup>(1)</sup>	Tube size (in)		
o.d.	i.d.	thk.	External	Internal				o.d.	i.d.	b.w.g.
15.875	10.335	2.77	0.0499	0.0325	$0.839 \times 10^{-4}$	0.896	0.0839	1	0.407	12
15.875	11.655	2.11	0.0499	0.0366	$1.067 \times 10^{-4}$	0.713	0.1067		0.459	14
15.875	12.575	1.65	0.0499	0.0395	$1.241 \times 10^{-4}$	0.577	0.1241		0.495	16
15.875	13.395	1.24	0.0499	0.0421	$1.407 \times 10^{-4}$	0.451	0.1407		0.527	18
15.875	14.095	0.89	0.0499	0.0443	$1.561 \times 10^{-4}$	0.329	0.1561		0.555	20
19.05	12.25	3.40	0.0598	0.0385	$1.177 \times 10^{-4}$	1.316	0.1177	1	0.482	10
19.05	13.51	2.77	0.0598	0.0424	$1.434 \times 10^{-4}$	1.113	0.1434		0.532	12
19.05	14.83	2.11	0.0598	0.0466	$1.728 \times 10^{-4}$	0.881	0.1728		0.584	14
19.05	15.75	1.65	0.0598	0.0495	$1.948 \times 10^{-4}$	0.708	0.1948		0.620	16
19.05	16.57	1.24	0.0598	0.0520	$2.154 \times 10^{-4}$	0.546	0.2154		0.652	18
19.05	17.27	0.89	0.0598	0.0543	$2.343 \times 10^{-4}$	0.400	0.2343		0.680	20
25.40	18.60	3.40	0.0798	0.0584	$2.715 \times 10^{-4}$	1.841	0.2715	1	0.732	10
25.40	19.86	2.77	0.0798	0.0624	$3.099 \times 10^{-4}$	1.543	0.3099		0.782	12
25.40	21.18	2.11	0.0798	0.0665	$3.524 \times 10^{-4}$	1.210	0.3524		0.834	14
25.40	22.10	1.65	0.0798	0.0694	$3.835 \times 10^{-4}$	0.966	0.3835		0.870	16
25.40	22.92	1.24	0.0798	0.0720	$4.123 \times 10^{-4}$	0.738	0.4123		0.902	18
25.40	23.62	0.89	0.0798	0.0742	$4.383 \times 10^{-4}$	0.536	0.4383		0.930	20
31.75	24.95	3.40	0.0997	0.0784	$4.886 \times 10^{-4}$	2.378	0.4886	1.1/4	0.982	10
31.75	26.21	2.77	0.0997	0.0823	$5.397 \times 10^{-4}$	1.978	0.5397		1.032	12
31.75	27.53	2.11	0.0997	0.0865	$5.954 \times 10^{-4}$	1.537	0.5954		1.084	14
31.75	28.45	1.65	0.0997	0.0894	$6.356 \times 10^{-4}$	1.225	0.6356		1.120	16
31.75	29.27	1.24	0.0997	0.0919	$6.723 \times 10^{-4}$	0.936	0.6723		1.152	18
31.75	29.97	0.89	0.0997	0.0942	$7.058 \times 10^{-4}$	0.679	0.7058		1.180	20

## Notes:

(1) Water density = 1000 kg/m<sup>3</sup>.(2) Steel density = 7842 kg/m<sup>3</sup>. For other metals multiply weights by the factors given in the Table 17.3(b).

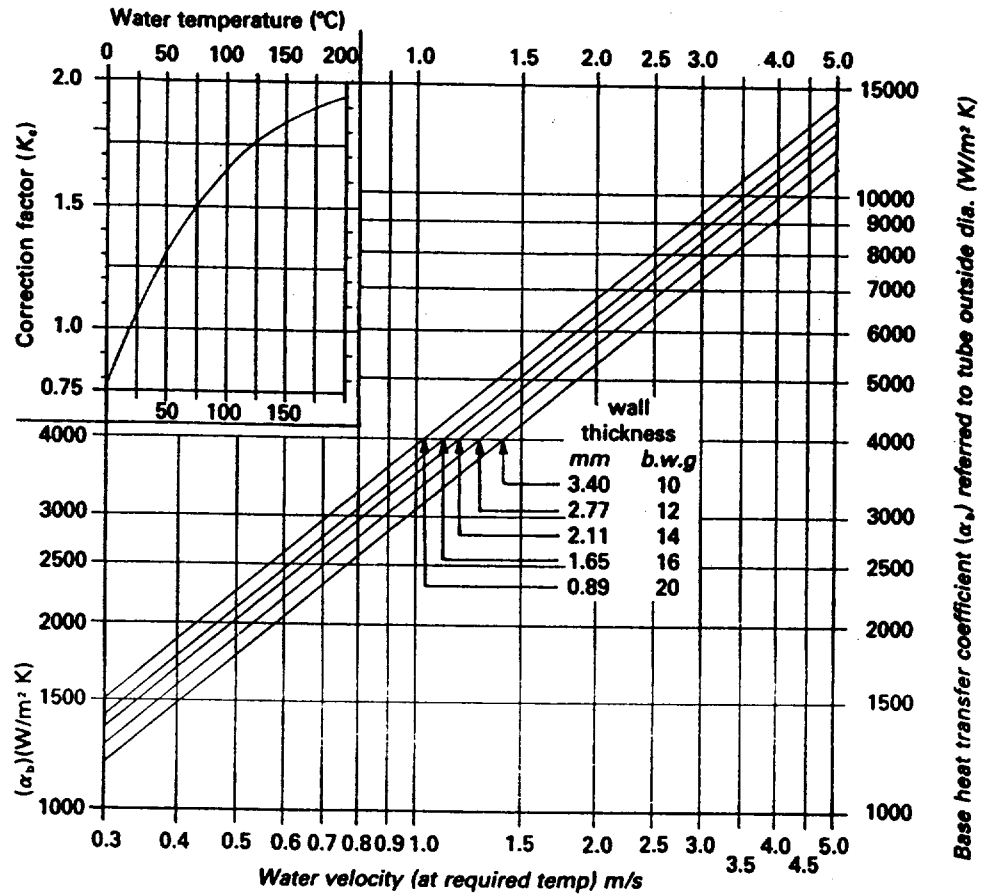
Table 17.3(b) Heat exchanger tubes – factors for weight (steel = 1.000)

Metal	Alloy type or designation	Factor	Metal	Alloy type or designation	Factor
Aluminium		0.350	Inconel™	600	1.074
Admiralty brass	443/4/5	1.088	Inconel™	625	1.078
Aluminium brass	687	1.064	Monel™	400	1.127
Aluminium bronze	608	0.968	Muntz metal	280	1.074
Carpenter 20™	20 Cb	1.032	Nickel	200, 201	1.134
Copper		1.141	Red brass	230	1.117
Cupro-nickels 70/30, 80/20, 90/10	715, 710, 706	1.141	Steel: Carbon and low alloy	Up to 9% chrome	1.000
Hastelloy™	B, B-2	1.180	austenitic stainless	300 series	1.021
Hastelloy™	C4	1.102	ferritic stainless	400 series	0.989
Hastelloy™	C276	1.134	nickel	2½%, 3½%	1.000
Hastelloy™	G, G-2, G-3	1.060	Cr–Mo alloy	XM27, 33	0.989
Hastelloy™	X	1.049	Cr–Ni alloy	XM11, 19, 29	1.021
Incoloy™	800, 800H	1.014	Titanium		0.576
Incoloy™	825	1.039	Zirconium		0.830

etc. If the pressure loss is low, it may not be essential to take remedial action unless the tube-side heat transfer coefficient is expected to be the controlling one (section 6.7).

Figure 17.1 provides heat transfer coefficients for water inside tubes for Reynolds numbers greater than 10 000.

**Figure 17.1** Heat transfer coefficients for water inside tubes (Reynolds number > 10 000)



$$\text{required heat transfer coefficient} = (\alpha_s)(K_c) \left\{ \begin{array}{l} \text{based on equation [7.14] - within } \pm 5\% \\ \text{for tube outside diameters: 15.875-31.75 mm } (\frac{5}{8}-1 \text{ in}) \end{array} \right.$$

### 17.1.9 Shell-side flow

Having temporarily settled the number of tube-side passes, a tentative baffle spacing (for instance the shell diameter) is assumed, and the shell-side heat transfer coefficient and pressure loss calculated. If the pressure loss exceeds the maximum allowable value, it may be reduced by increasing the baffle spacing, altering the shell to divided flow (J type), changing the baffles to the double- or triple-segmental type, either alone or in combination with a J shell, or altering the shell to cross-flow (X type). The maximum unsupported length must not be exceeded and flow-induced vibration must not be overlooked. If the pressure loss is low, it may not be essential to take remedial action unless the shell-side heat transfer coefficient is expected to be the controlling factor.

If it is evident that the exchanger has insufficient surface, it must be

increased in diameter or length, or both, or even additional units added. Once these changes have been made, the tube-side conditions will have to be rechecked. If the exchanger has oversurface it may be reduced in size and again the tube-side must be rechecked. Sometimes with designs having a fixed tube length, oversurface must be accepted.

#### 17.1.10 Controlling heat transfer coefficient

It will be evident that every effort must be made to maximise the controlling heat transfer coefficient, if there is one, by utilising the available pressure loss, as discussed in section 6.7. When the controlling coefficient is much lower than the other coefficients, consideration should be given to the use of low-fin tubes or internal enhancement devices, as appropriate.

#### 17.1.11 Flow-induced vibration

All shell-and-tube exchanger designs should be examined to ensure that there will be no flow-induced vibration problems. This phenomenon, and means for eliminating it, are discussed in Chapter 11.

#### 17.1.12 Physical properties

As a result of extensive research over the past twenty years, aided by computerisation, the reliability of predicting heat transfer and pressure loss has improved considerably. Accordingly, greater attention has been focused on the accuracy of the physical properties of fluids, particularly those relating to the thermal conductivity and viscosity of liquids and gaseous mixtures at all pressures and temperatures. The properties of common pure fluids are well documented, but in some cases more time is occupied in a literature search for properties, and manual calculations of mixtures, than is required to solve the design problem. The Physical Property Data Service (PPDS) was formed in 1966 to develop fluid physical property data banks for pure fluids and to develop prediction methods for mixtures. When fluid compositions can be defined completely, their computerised service may save considerable time and effort.

Physical properties should always be specified by the user. Unfortunately, even today the design engineer is faced with the task of designing an exchanger, and providing a performance guarantee, with the fluids ill-defined. Predictive methods, such as those provided by Gambill (1960) and Reid, Prausnitz and Sherwood (1977), for instance, are available for estimating physical properties from limited data. It is the responsibility of the user to ensure that any physical properties derived by the thermal design engineer meet the requirements as they form the basis of performance guarantees.



### 17.1.13 Operating and design margins

Irrespective of whether the design of heat transfer equipment is undertaken by end users, process plant contractors, design service companies or manufacturers, all will have the incentive to reduce the exchanger cost. None will wish to design an exchanger which is larger than necessary. However, thermal design is not an exact science, despite the considerable improvements in heat transfer and pressure loss predictions produced by the cooperative research organisations, HTRI and HTFS, discussed in section 6.9. In addition, it will be noted from Chapter 8 that fouling is hardly an exact science. The question arises as to what safety factors should the thermal design and process engineers allow?

In design calculations three surface areas arise: (a) the clean surface area ( $A_{cl}$ ), which is calculated from heat transfer correlations, assuming no fouling, (b) the 'service' surface area ( $A_{ser}$ ), which is derived directly from  $A_{cl}$  by the inclusion of the required fouling factors, and (c) the surface area contained in the exchanger as supplied, i.e. the installed surface area ( $A_{ins}$ ).  $A_{ins}$  must never be less than  $A_{cl}$  because the exchanger will not achieve its design performance when tested clean under *identical* process conditions. If this occurs the thermal design engineer will be responsible for taking corrective action.

#### Operating margin

The ratio  $A_{ins}/A_{cl}$  is the operating margin, usually intended to give the exchanger a 'reasonable' period of operation between shutdowns for cleaning. A high operating margin usually arises from the use of 'large' fouling factors, such that they have a significant effect on design as shown in section 8.4.1. A high margin may also arise from (a) uncertainties in the process design calculations where the process engineer may specify a larger duty for safety, (b) the user's demand for a fixed tube length, for instance, which can only be met by an unnecessary increase in  $A_{ins}$  and (c) uncertainties in the thermal design calculations, where the thermal design engineer may increase the surface area for safety.

Although a high operating margin may be regarded as a desirable objective in order to achieve a 'safe' design, capable of operating for a long period without cleaning, an excessive margin may cause operating problems in the early life of the exchanger when it is clean. Without temperature control the cold fluid may be overheated, leading to local boiling, corrosion, fouling, breakdown of the cold fluid itself and contamination of the heat transfer surface. The hot fluid may be overcooled, leading to freezing. Temperature control, which reduces the cold fluid flow in order to achieve a constant hot fluid exit temperature, may cause fouling due to its low velocity, in addition to the problems already mentioned. Temperature control itself may prove erratic.

#### Design margin

Having calculated  $A_{cl}$  and then  $A_{ser}$ , what design margin (i.e.  $A_{ins}/A_{ser}$ ) should be allowed, bearing in mind the problems which may be caused by excessive surface area? The comments below apply chiefly to single-phase applications in shell-and-tube heat exchangers, when it is assumed that

single-phase heat transfer coefficients are predicted with greater accuracy for the tube-side than for the shell-side.

There are no fixed rules regarding design margin as it will depend on (a) the reliability of the heat transfer data available to the thermal design engineer, (b) whether the shell-side coefficient is controlling (section 6.7), (c) whether the shell-side flow is laminar or turbulent, heat transfer predictions being less certain for the former, and (d) whether the fouling factors are large. A design based on HTRI or HTFS programs is more accurate than other published methods. A design in which the shell-side coefficient is controlling, the shell-side flow is laminar and the fouling factors are small, such that they have only a little effect on design – as shown in section 8.4.1 – presents more risk than one in which the tube-side coefficient is controlling, the shell-side flow is turbulent and the fouling factors are large.

In the case of HTRI and HTFS data, it is likely that the design margin will be kept to a minimum at all times and not greater than 1.1. Moreover, if the fouling factors are large, a design margin as low as 0.9 might be considered, particularly if it provided a significant cost reduction. In this event the end user should be informed. Except when the fouling factors are small, design margins between 0.9 and 1.0 should be considered when the shell-side coefficient is not controlling and the tube-side coefficient is fully turbulent.

When using heat transfer data from other sources, similar considerations apply, but the design margin must depend to a large extent on previous experience. It is prudent to examine the factors of greatest uncertainty and to check the effect on performance which would arise due to likely errors in their calculation.

## 17.2 Shell-and-tube heat exchangers: plain tubes

Nine worked examples are given to demonstrate the thermal design of shell-and-tube heat exchangers having plain tubes. Where applicable the shell-side calculations are based on the manual method described in section 12.5.1, which related to the Bell (1984) method. The examples have been chosen to deal with problems involving flow-induced tube vibration (Chapter 11), temperature cross (Chapter 7) and viscous flow (Chapter 6). An example of an X shell is also given. Although it is usually selected because of its anti-vibration characteristics, it often provides the best solution in its own right, especially when dealing with gas in the shell having a low allowable pressure loss.

Nozzle pressure losses may not be small and must always be calculated. To remind the reader of this, both shell- and tube-side nozzle losses are calculated for every example. However, in order to save space, the sum of the inlet and outlet nozzle losses on the shell-side are always based on four velocity heads, based on the velocity in the nozzle.

Where applicable a shell-side flow-induced vibration check is presented using the recommendations of Chapter 11.

As explained in section 17.1.1, thermal design, whether computer or manual, is a trial-and-error process. When using the manual method of

Chapter 12 for the thermal design of shell-and-tube exchangers, it is suggested that once a tentative shell size has been selected, the baffle spacing is initially chosen to be the same as the shell inside diameter. Hence,  $BSR = 1$ , and if  $F_E$ ,  $F_A$  and  $\phi$  are also assumed to be unity, heat transfer and pressure loss  $= (F_F F_P) F_M X_C$ . This provides a useful indication of the heat transfer coefficient and pressure loss from which subsequent design modifications may be made.

17.2.1 Example 1: Crude oil cooler (E shell)

This example demonstrates the complete thermal design of a straightforward E-shell exchanger, including the application of the manual method described in section 12.5.1. The calculations are given in Table 17.4 and the baffle arrangement in Fig. 17.2.

Figure 17.2 Baffle arrangement for example 1

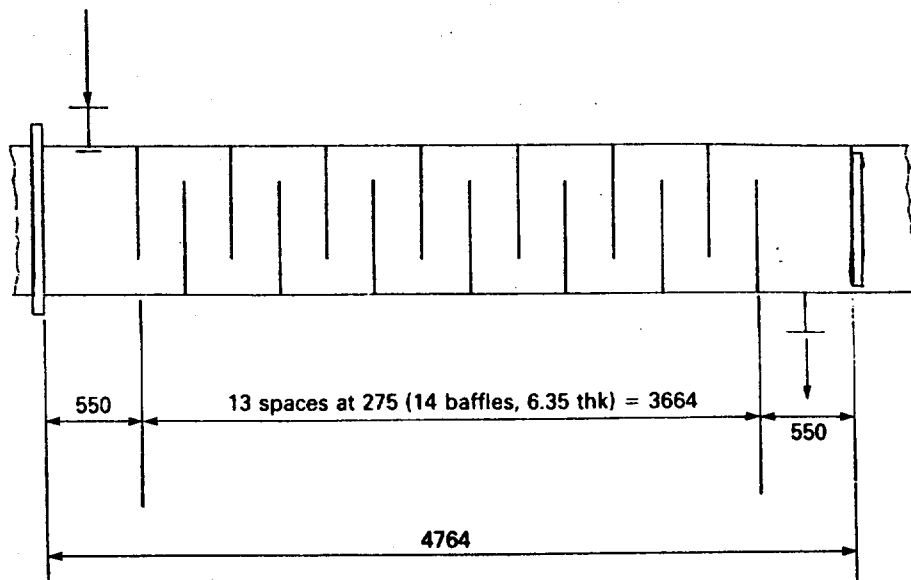


Table 17.4 Example 1: Crude oil cooler (E shell)

Process conditions			
Item	Units	Shell-side	Tube-side
Fluid name	-	Crude oil	Water
Flow rate	kg/s	63.77	45
Temperature range	°C	102 → 64	21 → 49
Specific heat <sup>(1)</sup>	J/kg K	2177	4186.8
Dynamic viscosity <sup>(1)</sup>	N s/m <sup>2</sup>	0.00189	0.00072
Thermal conductivity <sup>(1)</sup>	W/m K	0.122	-
Density <sup>(1)</sup>	kg/m <sup>3</sup>	786.4	995
Prandtl number <sup>(1)</sup>	-	33.73	-
Fouling factor <sup>(2)</sup>	(W/m <sup>2</sup> K) <sup>-1</sup>	0.000 18	0.000 26
Max. pressure loss	Pa	70 000	50 000
Tube-wall resistance <sup>(3)</sup>	(W/m <sup>2</sup> K) <sup>-1</sup>	0.000 04	

Heat load (kW)	log MTD ( $\Delta T_{lm}$ ) (eq. [7.1])
Shell-side $Q = \{63.77 \times (102 - 64) \times 2177\}/1000 = 5275.4$	$\begin{array}{ccc} 102 & \longrightarrow & 64 \\ 49 & \longleftarrow & 21 \\ \hline 53 & & 43 \end{array}$ $\Delta T_{lm} = \frac{53 - 43}{\ln \left( \frac{53}{43} \right)} = 47.8 \text{ } ^\circ\text{C}$
Tube-side $Q = \{45 \times (49 - 21) \times 4186.8\}/1000 = 5275.4$	

**Notes:**

- (1) At average bulk temperature.
- (2) Referred to its own surface.
- (3) Referred to tube o.d.

Mechanical design data				
Item		Units		
Tubes: o.d., i.d., thk., pitch, angle		mm	19.05 × 14.83 × 2.11 × 25.4 × 90°	
Tube material		–	Carbon steel	
No. of tubes per shell	No. of passes	–	744	4
Tube length: overall	effective	m	5	4.764
No. shells in unit		–	1	
Arrangement: series	parallel	–	1S	1P
Surface <sup>(1)</sup> : one shell	unit	m <sup>2</sup>	212.1	212.1
Nozzle i.d. (in/out): shell <sup>(2)</sup>	tubes	mm	254.5/254.5	202.7/202.7
Shell i.d.		mm	889	
Exchanger type		–	Split backing ring floating head	
TEMA designation		–	AES	

**Notes:**

- (1) Surface based on tube o.d.
- (2) Imping. baffle at inlet.

MTD correction factor		
Item	Ref.	
No. of shells in series	–	1
$P$	[7.5]	$\frac{102 - 64}{102 - 21} = 0.469$
$R$	[7.4]	$\frac{49 - 21}{102 - 64} = 0.737$
$F$	Fig. 7.2a	0.917
$\Delta T_m = F \Delta T_{lm}$	[7.3]	$0.917 \times 47.8 = 43.8$

Tube-side calculations ( $\phi = 1$ )		
Item	Units	Ref.
No. of tubes per pass	-	-
Int. flow area (one tube)	m <sup>2</sup>	744/4 = 186
Int. flow area (one pass)	m <sup>2</sup>	Table 17.3(a) 1.728 × 10 <sup>-4</sup>
Velocity in tubes	m/s	186 × (1.728 × 10 <sup>-4</sup> ) = 0.0321
Mass velocity in tubes	kg/s m <sup>2</sup>	45/(995 × 0.0321) = 1.41
Reynolds number (Re <sub>i</sub> )	-	45/0.0321 = 1401.9
Re <sub>i</sub> <sup>0.75</sup> Pr <sup>0.495</sup>	-	(1401.9 × 0.01483)/0.00072 = 28875
exp[-0.0225{ln(Pr)} <sup>2</sup> ]	-	av. temp = (21 + 49)/2 = 35 °C K <sub>t</sub> = 1.16
Tube-side coeff. (α <sub>io</sub> )	W/m <sup>2</sup> K	Fig. 17.1 4600 × 1.16 = 5336
Friction factor (f <sub>i</sub> )	-	[6.23c] 0.0035 + 0.264/28875 <sup>0.42</sup> = 0.007
Total travel (L)	m	4 × 5 = 20
Straight loss (ΔP <sub>f</sub> )	Pa	[6.22] (4 × 0.007 × 20 × 1401.9 <sup>2</sup> )/(2 × 995 × 0.01483) = 37293
Header loss (ΔP <sub>h</sub> )	Pa	[6.31b] (1.6 × 4 × 1401.9 <sup>2</sup> )/(2 × 995) = 6321
Nozzle flow area	m <sup>2</sup>	(π/4) × 0.2027 <sup>2</sup> = 0.0323
Nozzle mass velocity	kg/s m <sup>2</sup>	45/0.0323 = 1393.2
Nozzle loss (ΔP <sub>n</sub> )	Pa	[6.31a] (1.8 × 1393.2 <sup>2</sup> )/(2 × 995) = 1756
Total pressure loss (ΔP <sub>T</sub> )	Pa	-
		= 45370

**Shell-side calculations: baffle data and Reynolds number**

Item	Units	Ref.
Spacing: central ( $l_s$ )	mm	275
Number ( $N_b$ )	mm	14
Spacing ratios: central (BSR)	-	$275/889 = 0.309$
end ( $l_t$ )	-	$550/275 = 2$
Flow area/unit baffle pitch ( $S_{mu}$ )	m <sup>2</sup> /m	Table 12.3 0.2484
Central cross-flow area ( $S_m$ )	m <sup>2</sup>	$0.2484 \times 0.275 = 0.06831$
Mass velocity ( $\dot{m}_c$ )	kg/s m <sup>2</sup>	$63.77/0.0683 = 933.5$
Cross-flow Reynolds number ( $Re_c$ )	-	$(933.5 \times 0.01905)/0.00189 = 9409$

(i.e. turbulent)

Notes: (1) See Fig. 17.2.

**Shell-side calculations: design factors**

Design factor	Ref.	Heat transfer	Cross loss*	Window loss
Flow rate ( $F_F$ )	Table 12.4	$63.77^{0.651} = 14.956$	$63.77^2 = 4066.6$	$63.77^2 = 4066.6$
Physical property ( $F_P$ )	Table 12.4	$(2177^{0.333} \times 0.122^{0.667})/(0.00189^{0.318}) = 23.34$	$1786.4 = 0.001272$	$1786.4 = 0.001272$
Mechanical design ( $F_M$ )	Table 12.7	3.96	$0.667 \times 10^3$	$0.397 \times 10^3$
$X_c$ (BSR < 0.35)	Table 12.8	0.587	0.079	0.391
$m$ (BSR < 0.35)	Table 12.8	0.318	1.598	0.603
$F_c$	[12.6]	$0.587/0.309^{0.318} = 0.853$	$0.079/0.309^{1.598} = 0.516$	$0.391/0.309^{0.603} = 0.794$
$F_E$ (heat tr.);	Table 12.5	0.92		
$X_c, e$ (cross loss)	Table 12.9		$2.0, 1.0, X_c/l_t = 1.0$	-

\* Table 12.4(a), 90° pitch,  $Re_c = 9409, p/d_0 = 1.33, F_s = 1.17$

**Shell-side calculations: heat transfer coefficient and pressure loss ( $\phi_0 = 1$ )**

Item	Units	Ref.	
Shell-side heat trans. coeff. ( $\alpha_0$ )	W/m <sup>2</sup> K	[12.2]	$14.956 \times 23.34 \times 3.96 \times 0.853 \times 0.92 = 1085$
Central loss (one pass) ( $\Delta P_c$ )	Pa	[12.3]	$4066.6 \times 0.001272 \times 667 \times 0.516 \times 1.17 = 2083$
Window loss (one window) ( $\Delta P_w$ )	Pa	[12.4]	$4066.6 \times 0.001272 \times 397 \times 0.794 = 1630.5$
Flow area	m <sup>2</sup>		$(\pi/4) \times 0.2545^2 = 0.0509$
Mass velocity	kg/s m <sup>2</sup>		$63.77/0.0509 = 1252.8$
Loss ( $\Delta P_{ni} + \Delta P_{no}$ )	Pa		$(4 \times 1252.8^2)/(2 \times 786.4) = 3992$
Total central loss ( $\Delta P_c(N_b - 1)$ )	Pa		$2083 \times 13 = 27079$
Total window loss ( $\Delta P_w(N_b)$ )	Pa		$1630.5 \times 14 = 22827$
End space loss ( $\Delta P_e(X_e)/l_e^2$ )	Pa	[12.8]	$2 \times 2083 \times 1 = 4166$
Total loss ( $\Delta P_s$ )	Pa		$= 58064$

**Overall heat transfer coefficient**

Resistance (W/m <sup>2</sup> K) <sup>-1</sup>	(related to tube o.d.)	
Tube-side (1/ $\alpha_{to}$ )	1/5336	= 0.0001874
Shell-side (1/ $\alpha_o$ )	1/1085	= 0.0009217
Tube wall ( $r_w$ )		= 0.0000400
Fouling - tubes ( $r_{fo}$ )	$r_1 \times (\text{o.d./i.d.})$	= 0.0003340
Fouling - shell ( $r_o$ )		= 0.0001800
Overall (1/ $U_o$ )	{[6.7c]}	1/601 = 0.0016631
Surface area (m <sup>2</sup> )	Available	212.1
	Required	$5275.4 \times 1000 = 200.4$
	= $Q/(U_o \Delta T_m)$	$601 \times 43.8 = 26303.8$
		OK

Shell-side calculations: flow-induced vibration check		Units or ref.
Item		
Volume flow		63.77/786.4 = 0.0811
Correction for baffle thickness ( $B_r = 6.35$ )		[11.23] 12.7/6.35 = 2
Correction for fatigue stress ( $S_r = 8.33 \times 10^7$ )		[11.23] 1.0
Corrected baffle damage constant ( $K_{bd} = 1.603 \times 10^{-1}$ )		Table 11.6 $(1.603 \times 10^{-1}) \times 2 \times 1 = 3.206 \times 10^{-1}$
Correction for tube gap ( $C_r = 6.35$ )		[11.24] 1.0
Correction for mod. of elasticity ( $E = 2 \times 10^{11}$ )		[11.24] 1.0
Corrected collision damage constant ( $K_{cd} = 1.431 \times 10^{-4}$ )		Table 11.6 $(1.431 \times 10^{-4}) \times 1 \times 1 = 1.431 \times 10^{-4}$
Flow area $\{(S_{mu}/l_c) - (\pi/4)d_m^2\}$		$\{(0.2484 \times 0.55) - (\pi/4) \times 0.2545^2\} = 0.0857$
Inlet		
Velocity ( $\mu_r$ )		0.0811/0.0857 = 0.946
Unsupported length ( $l_c$ )		0.55
Baffle damage number		$(3.206 \times 10^{-1}) \times 786.4 \times 0.946^2 \times 0.55^2 = 0.068$
Collision damage number		$(1.431 \times 10^{-4}) \times 786.4 \times 0.946^2 \times 0.55^4 = 0.0092$
Flow area ( $S_{mu}/l_c$ )		0.2484 $\times$ 0.55 = 0.1366
Velocity ( $\mu_r$ )		0.0811/0.1366 = 0.594
Unsupported length ( $l_c + l_s$ )		0.825
Baffle damage number		$(3.206 \times 10^{-1}) \times 786.4 \times 0.594^2 \times 0.825^2 = 0.061$
Collision damage number		$(1.431 \times 10^{-4}) \times 786.4 \times 0.594^2 \times 0.825^4 = 0.0184$
Flow area ( $S_{mu}/l_c = S_m$ )		0.0683
Velocity ( $\mu_r$ )		0.0811/0.0683 = 1.187
Unsupported length ( $2l_c$ )		0.55
Baffle damage number		$(3.206 \times 10^{-1}) \times 786.4 \times 1.187^2 \times 0.55^2 = 0.107$
Collision damage number		$(1.431 \times 10^{-4}) \times 786.4 \times 1.187^2 \times 0.55^4 = 0.0145$
Flow area $\{(\pi/4)d_m^2\}$		$(\pi/4) \times 0.2545^2 = 0.0509$
Velocity ( $\mu_r$ )		0.0811/0.0509 = 1.593
Unsupported length ( $l_c$ )		0.55
Baffle damage number		$(3.206 \times 10^{-1}) \times 786.4 \times 1.593^2 \times 0.55^2 = 0.194$
Collision damage number		$(1.431 \times 10^{-4}) \times 786.4 \times 1.593^2 \times 0.55^4 = 0.026$
Max. allowable damage number		[11.15] $(0.00429 \times 786.4^{0.47})/0.00189^{0.235} = 0.43$



### 17.2.2 Example 2: Oil cooler with vibration problem

This example provides one solution for curing a suspected flow-induced vibration problem in an oil cooler having an E-type shell.

Inspection of Table 19.1 suggests a film coefficient for the oil and water of  $1850 \text{ W/m}^2 \text{ K}$  and  $8000 \text{ W/m}^2 \text{ K}$ , respectively. When combined with the specified fouling factors of  $0.000088 \text{ (W/m}^2 \text{ K)}^{-1}$  on both sides, the anticipated overall heat transfer coefficient becomes  $1163 \text{ W/m}^2 \text{ K}$ , based on the external surface area. The heat load is  $25623 \text{ kW}$ , the log MTD is  $84.6 \text{ }^\circ\text{C}$ , so that the tentative surface area is  $(25623 \times 1000)/(1163 \times 84.6) = 260 \text{ m}^2$ . For standardisation purposes, the tube length is fixed at  $7.5 \text{ m}$  and therefore the external surface for one tube is  $0.598 \text{ m}^2$ , yielding an approximate number of tubes in the exchanger of  $260/0.598 = 435$ . Inspection of Table A3.1 for a tube configuration of  $25.4 \text{ mm o.d.} \times 31.75 \text{ mm (30}^\circ\text{) pitch}$ , shows that a fixed tubesheet exchanger,  $787 \text{ mm i.d.}$  containing 469 tubes, is the nearest size. The nozzle/shell diameter ratio is  $0.43$ , compared with  $0.33$  in Table A3.1, and by following the method shown in section A3.2 the tube count is reduced to 460.

Inspection of the calculations in Table 17.5(a) shows that the tentative E-shell exchanger (design 2A) was a good estimate, but the flow-induced vibration check recommended in Chapter 11 suggests that baffle damage may occur in the end zones and collision damage may occur throughout. The baffle spacing, shown in Fig. 17.3, which is almost at its maximum, cannot be reduced without increasing the shell-side pressure loss beyond its maximum allowable value. The installation of a short intermediate support baffle at both inlet and outlet, as shown in Fig. 11.3(a), cures the problem in the end zones because the baffle and collision damage numbers are reduced to one-fourth and one-sixteenth of their original values, respectively.

This practice is not readily applicable to the remaining baffle spaces, but among several options available to the designer is the use of a divided-flow (J type) shell as shown in Fig. 1.1. In the J shell, one-half of the total shell-side fluid flows through one-half of the shell length and if the baffle spacing is one-half that of the E shell, the nominal cross-flow velocity, heat transfer coefficient and pressure loss remain unchanged. Even without reducing the baffle spacing in the J shell, the damage numbers are reduced to one-quarter of their original values. The J shell calculations (design 2B) are given in Table 17.5(b) and the baffle arrangement in Fig. 17.3.

The tube-side water velocity of  $3.04 \text{ m/s}$  is within the range recommended by Table 18.2 for 70/30 cupro-nickel.

**Table 17.5(a)** Example 2: Oil cooler with vibration problem. Design 2A. (E shell)

Process conditions			
Item	Units	Shell-side	Tube-side
Fluid name	–	Oil	Water
Flow rate	kg/s	200	244.8
Temperature range	°C	145 → 100	25 → 50
Specific heat <sup>(1)</sup>	J/kg K	2847	4186.8
Dynamic viscosity <sup>(1)</sup>	Ns/m <sup>2</sup>	$4 \times 10^{-4}$	$6.9 \times 10^{-4}$
Thermal conductivity <sup>(1)</sup>	W/m K	0.086	–
Density <sup>(1)</sup>	kg/m <sup>3</sup>	900	994
Prandtl number <sup>(1)</sup>	–	13.24	–
Fouling factor <sup>(2)</sup>	(W/m <sup>2</sup> K) <sup>-1</sup>	0.000 088	0.000 088
Max. pressure loss	Pa	135 000	100 000
Tube-wall resistance <sup>(3)</sup>	(W/m <sup>2</sup> K) <sup>-1</sup>	0.000 068	

Heat load (kW)	log MTD ( $\Delta T_{lm}$ ) ((7.1))
Shell-side $Q = \{200 \times (145 - 100) \times 2847\}/1000 = 25\ 623$	$  \begin{array}{ccc}  145 & \longrightarrow & 100 \\  50 & \longleftarrow & 25 \\  \hline  95 & & 75  \end{array}  $ $  \Delta T_{lm} = \frac{95 - 75}{\ln \left( \frac{95}{75} \right)} = 84.6 \text{ } ^\circ\text{C}  $
Tube-side $Q = \{244.8 \times (50 - 25) \times 4186.8\}/1000 = 25\ 623$	

Notes:

- (1) At average bulk temperature.  
(2) Referred to its own surface.  
(3) Referred to tube o.d.

Mechanical design data			
Item	Units		
Tubes: o.d., i.d., thk., pitch, angle	mm	$25.4 \times 21.18 \times 2.11 \times 31.75 \times 30^\circ$	
Tube material	–	70/30 cupro-nickel	
No. of tubes per shell	No. of passes	–	460      2
Tube length: overall	effective	m	7.5      7.211
No. of shells in unit	–	1	
Arrangement: series	parallel	–	1S      1P
Surface <sup>(1)</sup> : one shell	unit	m <sup>2</sup>	264.7      264.7
Nozzle i.d. (in/out): shell <sup>(2)</sup>	tubes	mm	336.6/336.6      336.6/336.6
Shell i.d.	mm	787	
Exchanger type	–	fixed tubesheet	
TEMA designation	–	BEM	

Notes: (1) Surface based on tube o.d. (2) Imping. baffle at inlet.

MTD correction factor	
Item	Ref.
No. of shells in series	1
$P$	$\frac{145 - 100}{145 - 25} = 0.375$ [7.5]
$R$	$\frac{50 - 25}{145 - 100} = 0.556$ [7.4]
$F$	0.972 Fig. 7.2(a)
$\Delta T_m = F \Delta T_m$	82.2 [7.3]

Tube-side calculations ( $\phi = 1$ )		
Item	Units	Ref.
No. of tubes per pass	-	230
Int. flow area (one tube)	$m^2$	Table 17.3(a) $3.524 \times 10^{-4}$
Int. flow area (one pass)	$m^2$	$230 \times (3.524 \times 10^{-4}) = 0.081$
Velocity in tubes	$m/s$	$244.8/(994 \times 0.081) = 3.04$
Mass velocity in tubes	$kg/s m^2$	$244.8/0.081 = 3022.2$
Reynolds number ( $Re_i$ )	-	$(3022.2 \times 0.02118)/6.9 \times 10^{-4} = 92768$
$Re_i^{0.75} Pr^{0.495}$	-	For water av. temp = $(25 + 50)/2 = 37.5^\circ C$ use $K_1 = 1.17$
$\exp[-0.0225(\ln(Pr))^2]$	-	Fig. 17.1 $1.17 \times 8300 = 9711$
Tube side coeff. ( $\alpha_{i0}$ )	$W/m^2 K$	$0.0035 + 0.264/92768^{0.42} = 0.00566$
Friction factor ( $f_i$ )	-	$2 \times 7.5 = 15$
Total travel ( $L$ )	$m$	$(4 \times 0.00566 \times 15 \times 3022.2^2)/(2 \times 0.02118 \times 994) = 73667$
Straight loss ( $\Delta P_s$ )	$Pa$	$73667$
Header loss ( $\Delta P_h$ )	$Pa$	$(2 \times 1.6 \times 3022.2^2)/(2 \times 994) = 14702$
Nozzle flow area	$m^2$	$(\pi/4) \times 0.3366^2 = 0.089$
Nozzle mass velocity	$kg/s m^2$	$244.8/0.089 = 2750.6$
Nozzle loss ( $\Delta P_n$ )	$Pa$	$(1.8 \times 2750.6^2)/(2 \times 994) = 6850$
Total pressure loss ( $\Delta P_T$ )	$Pa$	$73667 + 14702 + 6850 = 95219$

**Shell-side calculations: baffle data and Reynolds number**

Item	Units	Ref.
Baffle data <sup>(1)</sup>		
Spacing: central ( $l_s$ )	mm	787
Number ( $N_b$ )	mm	8
Spacing ratios: central (BSR)	—	787/787 = 1.0
Flow area/unit baffle pitch ( $S_{mu}$ )	m <sup>2</sup> /m	Table 12.3 0.1626
Central cross-flow area ( $S_m$ )	m <sup>2</sup>	[12.5] 0.1626 × 0.787 = 0.128
Mass velocity ( $\dot{m}_c$ )	kg/s m <sup>2</sup>	[12.5] 200/0.128 = 1562.5
Cross-flow Reynolds ( $Re_c$ )	—	[12.5] (1562.5 × 0.0254)/(4 × 10 <sup>-4</sup> ) = 99 219

(i.e. turbulent)

Notes: (1) See Fig. 17.3.

**Shell-side calculations: design factors**

Design factor	Ref.	Heat transfer	Cross loss	Window loss
Flow rate ( $F_F$ )	Table 12.4	200 <sup>0.635</sup> = 28.92	200 <sup>1.75</sup> = 10 636.6	200 <sup>2</sup> = 40 000
Physical property ( $F_P$ )	Table 12.4	(2847 <sup>0.333</sup> × 0.086 <sup>0.667</sup> )/(4 × 10 <sup>-4</sup> ) <sup>0.302</sup> = 29.23	(4 × 10 <sup>-4</sup> ) <sup>0.25</sup> /900 = 0.000157	1/900 = 0.00111
Mechanical design ( $F_M$ )	Table 12.7	6.02	2.659 × 10 <sup>4</sup>	0.914 × 10 <sup>3</sup>
$X_c$ (BSR > 0.35)	Table 12.8	0.49	0.06	0.286
$m$ (BSR > 0.35)	Table 12.8	0.508	1.679	0.802
$F_c$	[12.6]	0.49/1 <sup>0.508</sup> = 0.49	0.06/1 <sup>1.679</sup> = 0.06	0.286/1 <sup>0.802</sup> = 0.286
$F_E$ (heat tr.)	Table 12.5	1.0		
$X_{c,e}$ (cross loss)	Table 12.9		2.1, 1.75	—

**Shell-side calculations: heat transfer coefficient and pressure loss ( $\phi_0 = 1$ )**

Item	Units	Ref.	
Shell-side heat trans. coeff. ( $\alpha_0$ )	W/m <sup>2</sup> K	[12.2]	$28.92 \times 29.23 \times 6.02 \times 0.49 \times 1 = 2494$
Central loss (one pass) ( $\Delta P_c$ )	Pa	[12.3]	$10636.6 \times 0.000157 \times (2.659 \times 10^4) \times 0.06 = 2664$
Window loss (one window) ( $\Delta P_w$ )	Pa	[12.4]	$40000 \times 0.00111 \times (0.914 \times 10^4) \times 0.286 = 11606$
Nozzle loss	m <sup>2</sup>		$(\pi/4) \times 0.3366^2 = 0.089$
Mass velocity	kg/s m <sup>2</sup>		$200/0.089 = 2247.2$
Loss ( $\Delta P_{ni} + \Delta P_{no}$ )	Pa		$(4 \times 2247.2^2)/(2 \times 900) = 11222$
Total central loss ( $\Delta P_c(N_b - 1)$ )	Pa		$2664 \times 7 = 18648$
Total window loss ( $\Delta P_w(N_b)$ )	Pa		$11606 \times 8 = 92848$
End space loss ( $(\Delta P_c(X_c)/(L)^2)$ )	Pa	[12.8]	$2 \times 2664 \times 2.1 = 11189$
Total loss ( $\Delta P_s$ )	Pa		$= 133907$

**Overall heat transfer coefficient**

Resistance (W/m <sup>2</sup> K) <sup>-1</sup>	(related to tube o.d.)
Tube-side ( $1/\alpha_{io}$ )	$1/9711 = 0.000103$
Shell-side ( $1/\alpha_o$ )	$1/2494 = 0.000401$
Tube wall ( $r_w$ )	$= 0.000068$
Fouling – tubes ( $r_{fo}$ )	$r_1 \times (\text{o.d./i.d.}) = 0.000106$
Fouling – shell ( $r_o$ )	$= 0.000088$
Overall ( $1/U_o$ ) [6.7c]	$1/1305 = 0.000766$
Surface Available	264.7
Required	$25623 \times 1000 / 1305 \times 82.2 = 238.9$ o.k.

Shell-side calculations: flow-induced vibration check		Units or ref.
Item		
Volume flow		m/s
Correction for baffle thickness ( $B_1 = 16$ )		$2(0)/900 = 0.222$
Correction for fatigue stress ( $S_f = 1.27 \times 10^6$ )		$12.7/16 = 0.794$
Corrected baffle damage constant ( $K_{bd} = 1.556 \times 10^{-4}$ )		$(8.33 \times 10^7)/(1.27 \times 10^6) = 0.656$
Correction for tube gap ( $C_1 = 6.35$ )		$(1.556 \times 10^{-4}) \times 0.794 \times 0.656 = 0.81 \times 10^{-4}$
Correction for mod. of elasticity ( $E = 1.27 \times 10^{11}$ )		1.0
Corrected collision damage constant ( $K_{cd} = 0.74 \times 10^{-4}$ )		$(2 \times 10^{11})/(1.27 \times 10^{11}) = 1.575$
Inlet <sup>(1)</sup>		
Flow area ( $(S_{nu} l_c) - (\pi/4) d_m^2$ )		$(0.74 \times 10^{-4}) \times 1.0 \times 1.575 = 1.165 \times 10^{-4}$
Velocity ( $\mu_r$ )		$(0.1626 \times 0.787) - (\pi/4) \times 0.3366^2 = 0.039$
Unsupported length ( $l_c$ )		$0.222/0.039 = 5.692$
Baffle damage number		0.787
Collision damage number		$(0.81 \times 10^{-4}) \times 900 \times 5.692^2 \times 0.787^2 = 1.463^{(2)}$
Flow area ( $S_{nu} l_c$ )		$(1.165 \times 10^{-4}) \times 900 \times 5.692^2 \times 0.787^2 = 1.303^{(2)}$
Velocity ( $\mu_r$ )		$0.1626 \times 0.787 = 0.128$
Unsupported length ( $l_c + l_s$ )		$0.222/0.128 = 1.734$
Baffle damage number		$0.787 + 0.787 = 1.574$
Collision damage number		$(0.81 \times 10^{-4}) \times 900 \times 1.734^2 \times 1.574^2 = 0.543$
Flow area ( $S_{nu} l_s = S_m$ )		$(1.165 \times 10^{-4}) \times 900 \times 1.734^2 \times 1.574^2 = 1.935^{(2)}$
Velocity ( $\mu_r$ )		0.128
Unsupported length ( $2l_s$ )		$0.222/0.128 = 1.734$
Baffle damage number		$2 \times 0.787 = 1.574$
Collision damage number		$(0.81 \times 10^{-4}) \times 900 \times 1.734^2 \times 1.574^2 = 0.543$
Central space		
Flow area ( $S_{nu} l_s = S_m$ )		$(1.165 \times 10^{-4}) \times 900 \times 1.734^2 \times 1.574^2 = 1.935^{(2)}$
Velocity ( $\mu_r$ )		$(0.00429 \times 900^{0.47})/(4 \times 10^{-4})^{0.235} = 0.66$
Unsupported length ( $2l_s$ )		
Baffle damage number		
Collision damage number		
Max. allowable damage number		[11.15]

**Notes:**

- (1) Check at outlet not required as velocity (based on nozzle area) is lower.  
 (2) Vibration failure likely.

Figure 17.3 Baffle arrangements for example 2

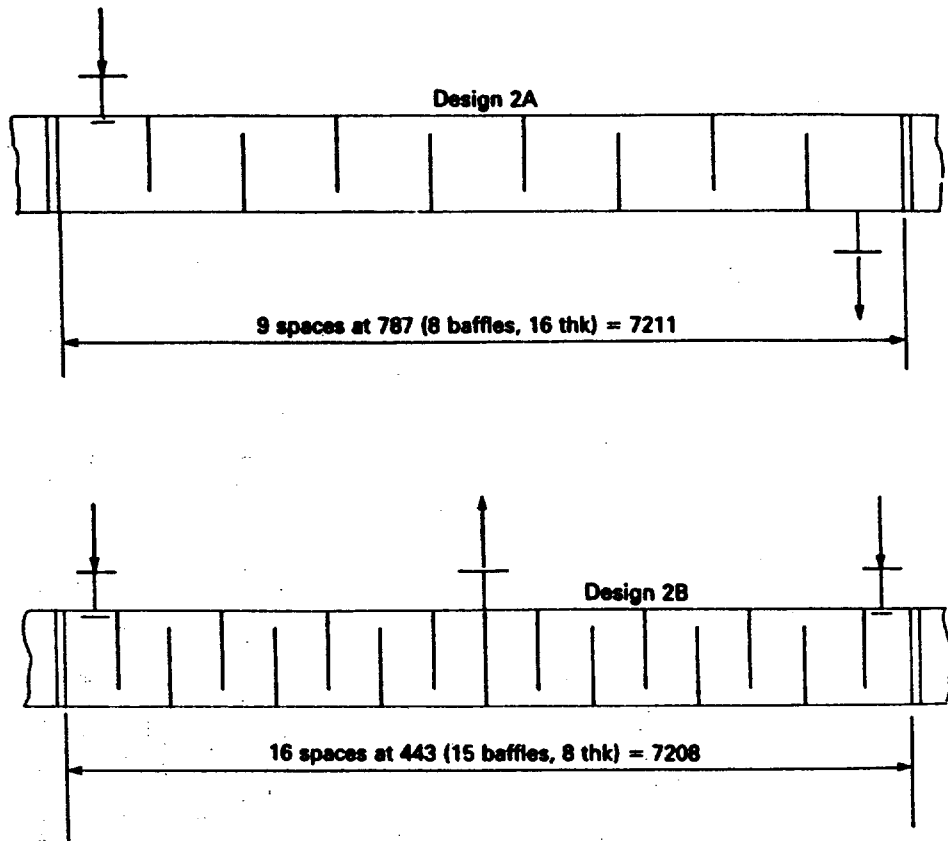


Table 17.5(b) Example 2. Design 2B (J shell)

Process conditions, heat load and  $\Delta T_{lm}$  as design 2A

Mechanical design data: as example 2A, except as shown below				
Item		Units		
Nozzle i.d. (in/out): shell	tubes	mm	(2 - 254)/(1 - 336.6)	336.6/336.6
TEMA designation		-	BJM	

M T D correction factor		
Item	Ref.	
No. of shells in series	-	1
$P$	[7.5]	$\frac{145 - 100}{145 - 25} = 0.375$
$R$	[7.4]	$\frac{50 - 25}{145 - 100} = 0.556$
$F$ (from TEMA)	Fig. T-3.2G	0.972
$\Delta T_m = F \Delta T_{lm}$	[7.3]	82.2

Tube-side calculations: exactly as example 2A

**Shell-side calculations: baffle data and Reynolds number**

Item	Units	Ref.
Baffle data <sup>(2)</sup>	Spacing: central ( $l_c$ )	443
	Number ( $N_b$ )	15
	Spacing ratios: central (BSR)	$443/787 = 0.563$
Flow area/unit baffle pitch ( $S_{mu}$ )	$m^2/m$	Table 12.3
Central cross-flow area ( $S_m$ )	$m^2$	$0.1626 \times 0.443 = 0.072$ [12.5]
Mass velocity ( $\dot{m}_c$ )	$kg/s\ m^2$	$100/0.072 = 1388.9^{(1)}$ [12.5]
Cross-flow Reynolds number ( $Re_c$ )	-	$(1388.9 \times 0.0254)/(4 \times 10^{-4}) = 88\ 195$ [12.5]

(i.e. turbulent)

Notes:  
 (1) Based on flow rate =  $0.5 \times 200 = 100\ kg/s$  for J shell  
 (2) See Fig. 17.3.

**Shell-side calculations: design factors**

Design factor	Ref.	Heat transfer	Cross loss	Window loss
Flow rate ( $F_F$ )	Table 12.4	$100^{0.635} = 18.62$	$100^{1.75} = 3162.3$	$100^2 = 10\ 000$
Physical property ( $F_P$ )	Table 12.4	$(2847^{0.333} \times 0.086^{0.667})/(4 \times 10^{-4})^{0.302} = 29.23$	$(4 \times 10^{-4})^{0.25}/900 = 0.000157$	$1/900 = 0.00111$
Mechanical design ( $F_M$ )	Table 12.7	6.02	$2.659 \times 10^4$	$0.914 \times 10^3$
$X_c$ (BSR > 0.35)	Table 12.8	0.49	0.06	0.286
$m$ (BSR > 0.35)	Table 12.8	0.508	1.679	0.802
$F_c$	[12.6]	$0.49/0.563^{0.508} = 0.656$	$0.06/0.563^{1.679} = 0.1574$	$0.286/0.563^{0.802} = 0.453$
$F_E$ (heat tr.)	Table 12.5	1.0		
$X_c, e$ (cross loss)	Table 12.9		2.1, 1.75	-



Shell-side calculations: heat transfer coefficient and pressure loss ( $\phi_b = 1$ )		
Item	Units	Ref.
Shell-side heat trans. coeff. ( $\alpha_o$ )	W/m <sup>2</sup> K	[12.2] $18.62 \times 29.23 \times 6.02 \times 0.656 \times 1 = 2149$
Central loss (one pass) ( $\Delta P_c$ )	Pa	[12.3] $3162.3 \times 0.000157 \times (2.659 \times 10^4) \times 0.1574 = 2078$
Window loss (one window) ( $\Delta P_w$ )	Pa	[12.4] $10000 \times 0.00111 \times (0.914 \times 10^3) \times 0.453 = 4596$
Nozzle loss ( $\Delta P_n$ )	Flow area	in: $(\pi/4) \times 0.254^2 = 0.0507$ out: $(\pi/4) \times 0.3366^2 = 0.089$
	mass velocity loss ( $\Delta P_{ni} + \Delta P_{no}$ )	in: $100/0.0507 = 1972.4$ out: $200/0.089 = 2247.2$
Total central loss $\{(\Delta P_c \{ (N_b - 1)/2 \} - 1)\}$	Pa	$4 \{ (1972.4 + 2247.2)/2 \}^2 / (2 \times 900) = 9892$
Total window loss $\{(\Delta P_w (N_b - 1))/2\}$	Pa	$2078 \times 6 = 12468$
End space loss $\{(\Delta P_c) X_c / r_c^2\}$	Pa	$4596 \times 7 = 32172$
Total loss ( $\Delta P_s$ )	Pa	$2 \times 2078 \times 2.1 = 8728$
		$= 63260$

Overall heat transfer coefficient	
Resistance (W/m <sup>2</sup> K) <sup>-1</sup>	(related to tube o.d.)
Tube-side ( $1/\alpha_{io}$ )	$1/9711 = 0.000103$
Shell-side ( $1/\alpha_o$ )	$1/2149 = 0.000465$
Tube wall ( $r_w$ )	$= 0.000068$
Fouling - tubes ( $r_{fo}$ )	$r_f \times (\text{o.d./i.d.}) = 0.000106$
Fouling - shell ( $r_{so}$ )	$= 0.000088$
Overall ( $1/U_o$ ) ([6.7c])	$1/1205 = 0.000830$
Surface Available	264.7
Surface Required	$25623 \times 1000 = 258.7$
$= Q/(U_o \Delta T_m)$	$1205 \times 82.2 = 258.7$ o.k.

Shell-side calculations: flow-induced vibration check		Units or ref.
Item		
Volume flow		100/900 = 0.111
Correction for baffle thickness ( $B_1 = 8$ )		[11.23] 12.7/8 = 1.588
Correction for fatigue stress ( $S_f = 1.27 \times 10^6$ )		[11.23] $(8.33 \times 10^7)/(1.27 \times 10^6) = 0.656$
Corrected baffle damage constant ( $K_{bd} = 1.556 \times 10^{-4}$ )		Table 11.6 $(1.556 \times 10^{-4}) \times 1.588 \times 0.656 = 1.621 \times 10^{-4}$
Correction for tube gap ( $C_1 = 6.35$ )		[11.24] 1.0
Correction for mod. of elasticity ( $E = 1.27 \times 10^{11}$ )		[11.24] $(2 \times 10^{11})/(1.27 \times 10^{11}) = 1.575$
Corrected collision damage constant ( $K_{cd} = 0.74 \times 10^{-4}$ )		Table 11.6 $(0.74 \times 10^{-4}) \times 1.0 \times 1.575 = 1.165 \times 10^{-4}$
Inlet <sup>(1)</sup>	Flow area ( $S_{nu} l_c - (\pi/4)d_n^2$ )	$m^2$ $(0.1626 \times 0.443) - (\pi/4) \times 0.254^2 = 0.0214$
	Velocity ( $\mu_r$ )	m/s $0.111/0.0214 = 5.187$
	Unsupported length ( $l_c$ )	m 0.443
	Baffle damage number	- $(1.621 \times 10^{-4}) \times 900 \times 5.187^2 \times 0.443^2 = 0.77^{(2)}$
	Collision damage number	- $(1.165 \times 10^{-4}) \times 900 \times 5.187^2 \times 0.443^4 = 0.109$
At first and last cross-overs	Flow area ( $S_{nu} l_c$ )	$m^2$ $0.1626 \times 0.443 = 0.072$
	Velocity ( $\mu_r$ )	m/s $0.111/0.072 = 1.542$
	Unsupported length ( $l_c + l_s$ )	m $0.443 + 0.443 = 0.886$
	Baffle damage number	- $(1.621 \times 10^{-4}) \times 900 \times 1.542^2 \times 0.886^2 = 0.272$
	Collision damage number	- $(1.165 \times 10^{-4}) \times 900 \times 1.542^2 \times 0.886^4 = 0.154$
Central space	Flow area ( $S_{nu} l_s \approx S_m$ )	$m^2$ 0.072
	Velocity ( $\mu_r$ )	m/s $0.111/0.072 = 1.542$
	Unsupported length ( $2l_s$ )	m $2 \times 0.443 = 0.886$
	Baffle damage number	- $(1.621 \times 10^{-4}) \times 900 \times 1.542^2 \times 0.886^2 = 0.272$
	Collision damage number	- $(1.165 \times 10^{-4}) \times 900 \times 1.542^2 \times 0.886^4 = 0.154$
Max. allowable damage number		[11.15] $(0.00429 \times 900^{0.47})/(4 \times 10^{-4})^{0.335} = 0.66$

**Notes:**

- (1) Check at outlet not required as velocity (based on nozzle area) is lower.
- (2) Install intermediate support baffle under impingement baffle.

### 17.2.3 Example 3: Benzene/toluene exchanger with temperature cross

In this example there is a temperature cross (section 7.2), which means that designs providing either countercurrent flow or two or more  $1/2^+$ E shells in series, must be employed. Countercurrent flow is achieved by providing either a single tube pass in an E shell, or two shell passes in an F shell (Fig. 1.1). However, the exchanger is a floating-head type and some users will not permit either a single tube pass or two shell passes because of the constructional limitations described in sections 1.5.7 and 1.5.15. The tube length is not fixed but must not exceed 7 m.

Inspection of Table 19.1, suggests film coefficients of  $1850 \text{ W/m}^2 \text{ K}$  for both fluids, and when these are combined with the specified fouling factors of  $0.000088 \text{ (W/m}^2 \text{ K)}^{-1}$  on both sides, an overall heat transfer coefficient of  $785 \text{ W/m}^2 \text{ K}$  is obtained. The heat load is  $4018.9 \text{ kW}$ , the log MTD is  $44.3 \text{ }^\circ\text{C}$ , so that the tentative surface area is  $(4018.9 \times 1000)/(785 \times 44.3) = 115.6 \text{ m}^2$ .

In the case of design 3A, inspection of Fig. 7.2(a) and TEMA Fig. (T-3.2B) shows that a minimum of two  $1/2^+$  E shells in series must be employed to achieve an MTD correction factor greater than 0.75. The tentative surface area for each shell is therefore  $115.6/2 = 57.8 \text{ m}^2$ . As there must also be a minimum of two tube-side passes in each shell, the minimum total flow path length on the tube-side is four times the tube length. By trial and error, optimum conditions are achieved on the tube-side when there are two passes in each shell, each pass containing 200–250 tubes, the tube length being 2.5–3.5 m. A greater number of tubes in each pass provides a low heat transfer coefficient, which does not utilise the available pressure loss; a smaller number increases the pressure loss beyond the allowable value.

Inspection of Table A3.3 for a tube configuration of  $15.875 \text{ mm o.d.} \times 22.225 \text{ mm (90}^\circ\text{) pitch}$ , shows that a floating-head exchanger,  $635 \text{ mm i.d.}$  and estimated to contain 500 tubes (250 per pass),  $2.75 \text{ m}$  long, is the nearest size to the optimum. The calculations are summarised in Table 17.6(a) for design 3A. Figure 17.4 shows the baffle arrangement.

In the case of the countercurrent flow design 3B, the tube-side passes of design 3A, when 'unfolded', provide a single  $1/1$  exchanger containing 250 tubes,  $11 \text{ m}$  long, and the same surface area. However, the tube length exceeds the maximum available, but the same result is achieved by having two  $1/1$  exchangers in series, each with  $5.5 \text{ m}$  long tubes.

Inspection of Table A3.3 shows that a shell,  $438 \text{ mm i.d.}$ , and containing 230 tubes, is the nearest size. Tube-side heat transfer and pressure loss is almost the same as design 3A, but on the shell-side the same flow rate as before flows through a smaller shell. Accordingly the baffle spacing must be increased to prevent the shell-side pressure loss from exceeding the maximum allowable value. This reduces the heat transfer coefficient and increases the risk of flow-induced vibration failure.

The calculations are summarised in Table 17.6(b) for design 3B, from which it will be seen that a satisfactory design is obtained when the baffle spacing is  $480 \text{ mm}$ . The maximum unsupported tube length of  $960 \text{ mm}$  is well below the maximum recommended length of  $1321 \text{ mm}$  and vibration

problems would not be expected. However, the tubes are slender and it is sound discipline to make a vibration check as shown in Table 17.6(b).

The baffle arrangement is shown in Fig. 17.4.

Table 17.6(a) Example 3: Benzene/toluene exchanger with temperature cross. Design 3A. (2 1/2 E shells in series)

Process conditions			
Item	Units	Shell-side	Tube-side
Fluid name	-	benzene	toluene
Flow rate	kg/s	33.71	49.3
Temperature range	°C	22 → 87	120 → 80
Specific heat <sup>(1)</sup>	J/kg K	1834	2038
Dynamic viscosity <sup>(1)</sup>	Ns/m <sup>2</sup>	$4 \times 10^{-4}$	$2.7 \times 10^{-4}$
Thermal conductivity <sup>(1)</sup>	W/m K	0.137	0.115
Density <sup>(1)</sup>	kg/m <sup>3</sup>	850	810
Prandtl number <sup>(1)</sup>	-	5.355	4.785
Fouling factor <sup>(2)</sup>	(W/m <sup>2</sup> K) <sup>-1</sup>	0.000088	0.000088
Max. pressure loss	Pa	37000	37000
Tube-wall resistance <sup>(3)</sup>	(W/m <sup>2</sup> K) <sup>-1</sup>	0.00003	

Heat load (kW)	log MTD ( $\Delta T_{lm}$ ) [7.1]
Shell-side $Q = \{33.71 \times (87 - 22) \times 1834\}/1000 = 4018.6$	$\begin{array}{ccc} 120 & \longrightarrow & 80 \\ 87 & \longleftarrow & 22 \\ \hline 33 & & 58 \end{array}$ $\Delta T_{lm} = \frac{58 - 33}{\ln\left(\frac{58}{33}\right)} = 44.3 \text{ } ^\circ\text{C}$
Tube-side $Q = \{49.3 \times (120 - 80) \times 2038\}/1000 = 4018.9$	

Notes:

- (1) At average bulk temperature.
- (2) Referred to its own surface.
- (3) Referred to tube o.d.

Mechanical design data			
Item		Units	
Tubes: o.d., i.d., thk., pitch, angle		mm	15.875 × 13.395 × 1.24 × 22.225 × 90°
Tube material		-	carbon steel
No. of tubes per shell	No of passes	-	500      2
Tube length: overall	effective	m	2.75      2.591
No. of shells in unit		-	2
Arrangement: series	parallel	-	2S      1P
Surface <sup>(1)</sup> : one shell	unit	m <sup>2</sup>	64.6      129.2
Nozzle i.d. (in/out): shell <sup>(2)</sup>	tubes	mm	193.7/193.7      203/203
Shell i.d.		mm	635
Exchanger type		-	Split backing ring floating head
TEMA designation		-	AES

Notes: (1) Surface based on tube o.d. (2) Imping. baffle at inlet.

M T D correction factor	
Item	Ref.
No. of Shells in series	2
$P$	$\frac{87 - 22}{120 - 22} = 0.663$ [7.5]
$R$	$\frac{120 - 80}{87 - 22} = 0.615$ [7.4]
$F$ (from TEMA)	Fig. T-3.2b
$\Delta T_m = F \Delta T_{lm}$	41.6 [7.3]

Tube-side calculations ( $\phi_s = 1$ )		
Item	Units	Ref.
No. of tubes per pass	-	500/2 = 250
Int. flow area (one tube)	m <sup>2</sup>	Table 17.3(a) 1.407 × 10 <sup>-4</sup>
Int. flow area (one pass)	m <sup>2</sup>	250 × (1.407 × 10 <sup>-4</sup> ) = 0.0352
Velocity in tubes	m/s	-
Mass velocity in tubes	kg/sm <sup>2</sup>	49.3/0.0352 = 1400.6
Reynolds (Re) <sub>i</sub>	-	(1400.6 × 0.013395)/(2.7 × 10 <sup>-4</sup> ) = 69485
$Re_i^{0.795} Pr^{0.495}$	-	69485 <sup>0.795</sup> × 4.785 <sup>0.495</sup> = 15340.7
$\exp[-0.0225 \{\ln(Pr)\}^2]$	-	$\exp[-(0.0225 \{\ln 4.785\})^2] = 0.9464$
Tube side coeff. ( $\alpha_{i0}$ )	W/m <sup>2</sup> K	0.0225 × (0.115/0.015875) × 15340.7 × 0.9464 = 2366
Friction factor ( $f_i$ )	-	0.0035 + 0.264/69485 <sup>0.42</sup> = 0.00594 [6.23c]
Total travel (L)	m	2 × 2 × 2.75 = 11
Straight loss ( $\Delta P_s$ )	Pa	(4 × 0.00594 × 11 × 1400.6 <sup>2</sup> )/(2 × 810 × 0.013395) = 23627 [6.22]
Header loss ( $\Delta P_h$ )	Pa	(2 × 2 × 1.6 × 1400.6 <sup>2</sup> )/(2 × 810) = 7750 [6.31b]
Nozzle flow area	m <sup>2</sup>	( $\pi/4$ ) × 0.203 <sup>2</sup> = 0.0324
Nozzle mass velocity	kg/s m <sup>2</sup>	49.3/0.0324 = 1521.6
Nozzle loss ( $\Delta P_n$ )	Pa	(2 × 1.8 × 1521.6 <sup>2</sup> )/(2 × 810) = 5145 [6.31a]
Total pressure loss ( $\Delta P_T$ )	Pa	= 36522

**Shell-side calculations: baffle data and Reynolds number**

Item	Units	Ref.
Spacing: central ( $l_c$ )	mm	250
end ( $l_e$ )	mm	2 at 400
Number ( $N_b$ )	mm	8
thickness ( $B_t$ )	mm	5
Spacing ratios: central (BSR)	-	250/635 = 0.394
end ( $l_e$ )	-	400/250 = 1.6
Flow area/unit baffle pitch ( $S_{mu}$ )	m <sup>2</sup> /m	Table (12.3) 0.2064
Central cross-flow area ( $S_m$ )	m <sup>2</sup>	0.2064 × 0.25 = 0.0516
Mass velocity ( $\dot{m}_c$ )	kg/s m <sup>2</sup>	33.71/0.0516 = 653.29
Cross-flow Reynolds ( $Re_c$ )	-	(653.29 × 0.015875)/(4 × 10 <sup>-4</sup> ) = 25927

(i.e. turbulent)

Notes: (1) See Fig. 17.4.

**Shell-side calculations: design factors**

Design factor	Ref.	Heat transfer	Cross loss*	Window loss
Flow rate ( $F_F$ )	Table 12.4	33.71 <sup>0.651</sup> = 9.876	33.71 <sup>2</sup> = 1136.4	33.71 <sup>2</sup> = 1136.4
Physical property ( $F_P$ )	Table 12.4	(1834 <sup>0.333</sup> × 0.137 <sup>0.667</sup> )/(4 × 10 <sup>-4</sup> ) <sup>0.333</sup> = 39.035	1/850 = 1.176 × 10 <sup>-3</sup>	1/850 = 1.176 × 10 <sup>-3</sup>
Mechanical design ( $F_M$ )	Table 12.7	5.68	1.491 × 10 <sup>3</sup>	1.065 × 10 <sup>3</sup>
$X_c$	Table 12.8	0.456	0.047	0.281
$m$	Table 12.8	0.594	2.036	0.863
$F_c$	[12.6]	0.456/0.394 <sup>0.594</sup> = 0.793	0.047/0.394 <sup>2.036</sup> = 0.313	0.281/0.394 <sup>0.863</sup> = 0.628
$F_E$ (heat tr.)	Table 12.5	0.923	-	-
$X_{c,e}$ (cross loss)	Table 12.9	-	2.0, 1.0	-

\* Table 12.4(a), 90° pitch,  $Re_c = 25927$ ,  $p/d_n = 1.4$ ,  $F_s = 0.896$

**Shell-side calculations: heat transfer coefficient and pressure loss ( $\phi_0 = 1$ )**

Item	Units	Ref.
Shell-side heat trans. coeff. ( $\alpha_0$ )	W/m <sup>2</sup> K	[12.2]
Central loss (one pass) ( $\Delta P_c$ )	Pa	[12.3]
Window loss (one window) ( $\Delta P_w$ )	Pa	[12.4]
Flow area	m <sup>2</sup>	
Nozzle loss	kg/s m <sup>2</sup>	
loss ( $\Delta P_{ni} + \Delta P_{no}$ )	Pa	
Total central loss $\{(\Delta P_c(N_b - 1))\}$	Pa	eqn.
Total window loss $\{(\Delta P_w(N_b))\}$	Pa	
End space loss $\{(\Delta P_c(X_c)/(l_c)^2)\}$	Pa	[12.8]
Total loss ( $\Delta P_s$ )	Pa	

$9.876 \times 39.035 \times 5.68 \times 0.793 \times 0.923 = 1603$   
 $1136.4 \times (1.176 \times 10^{-3})(1.491 \times 10^3) \times 0.313 \times 0.896 = 558.8$   
 $1136.4 \times (1.176 \times 10^{-3})(1.065 \times 10^3) \times 0.628 = 893.8$   
 $(\pi/4) \times 0.1937^2 = 0.0295$   
 $33.71/0.0295 = 1142.7$   
 $(2 \times 4 \times 1142.7)/(2 \times 850) = 6144$   
 $2 \times 558.8 \times 7 = 7823$   
 $2 \times 8 \times 893.8 = 14300$   
 $(2 \times 2 \times 558.8 \times 2)/1.6 = 2794$   
 $= 31061$

**Overall heat transfer coefficient**

Resistance (W/m <sup>2</sup> K) <sup>-1</sup>	(related to tube o.d.)
Tube-side (1/ $\alpha_{i0}$ )	1/2366 = 0.000423
Shell-side (1/ $\alpha_0$ )	1/1603 = 0.000624
Tube wall ( $r_w$ )	= 0.000030
Fouling-tubes ( $r_{fo}$ )	$r_1 \times (\text{o.d.}/1.\text{d.}) = 0.000104$
Fouling-shell ( $r_{fo}$ )	= 0.000088
Overall (1/ $U_o$ ) ([6.7c])	1/788 = 0.001269
Surface area (m <sup>2</sup> )	129.2
Required	$4018.9 \times 1000 = 122.6$ O.K.
	$788 \times 41.6$

Shell-side calculations: flow-induced vibration check		
Item		Units or ref.
Volume		m/s
Correction for baffle thickness ( $B_1 = 5$ )		$33.71/850 = 0.0397$
Correction for fatigue stress ( $S_f = 8.33 \times 10^7$ )		$12.7/5 = 2.54$
Corrected baffle damage constant ( $K_{bd} = 2.611 \times 10^{-4}$ )		1.0
Correction for tube gap ( $C_1 = 6.35$ )		$(2.611 \times 10^{-4}) \times 2.54 \times 1 = 6.632 \times 10^{-4}$
Correction for mod. of elasticity ( $E = 2 \times 10^{11}$ )		1.0
Corrected collision damage constant ( $K_{cd} = 3.152 \times 10^{-4}$ )		$(3.152 \times 10^{-4}) \times 1 \times 1 = 3.152 \times 10^{-4}$
Inlet	Flow area ( $(S_{mi} l_c) - (\pi/4) d_{in}^2$ )	m <sup>2</sup>
	Velocity ( $\mu_r$ )	m/s
	Unsupported length ( $l_c$ )	m
	Baffle damage number	-
	Collision damage number	-
At first and last cross-overs	Flow area ( $S_{mi} l_c$ )	m <sup>2</sup>
	Velocity ( $\mu_r$ )	m/s
	Unsupported length ( $l_c + l_s$ )	m
	Baffle damage number	-
	Collision damage number	-
Central space	Flow area ( $S_{mi} l_s = S_m$ )	m <sup>2</sup>
	Velocity ( $\mu_r$ )	m/s
	Unsupported length ( $2l_s$ )	m
	Baffle damage number	-
	Collision damage number	-
Outlet	Flow area ( $(\pi/4) d_{in}^2$ )	m <sup>2</sup>
	Velocity ( $\mu_r$ )	m/s
	Unsupported length ( $l_c$ )	m
	Baffle damage number	-
	Collision damage number	-
Max. allowable damage number		[11.15]



Design 3C deals with a third option in which countercurrent flow is achieved in a single F shell having two shell passes and two tube passes.

If the two shells of design 3B are 'merged' into a single shell it would contain 460 tubes (230 per pass), 5.5 m long. Inspection of Table A3.3 shows that the nearest size is the same as that used in design 3A, i.e. 635 mm i.d. containing 500 tubes (250 tubes per pass), each 15.875 mm o.d.  $\times$  22.225 mm (90°) pitch  $\times$  5.5 m long. Tube-side heat transfer and straight tube pressure loss are identical to design 3A, but header and nozzle losses are halved because there are only two passes instead of four, and two nozzles instead of four.

Figure 17.4 Baffle arrangements for example 3

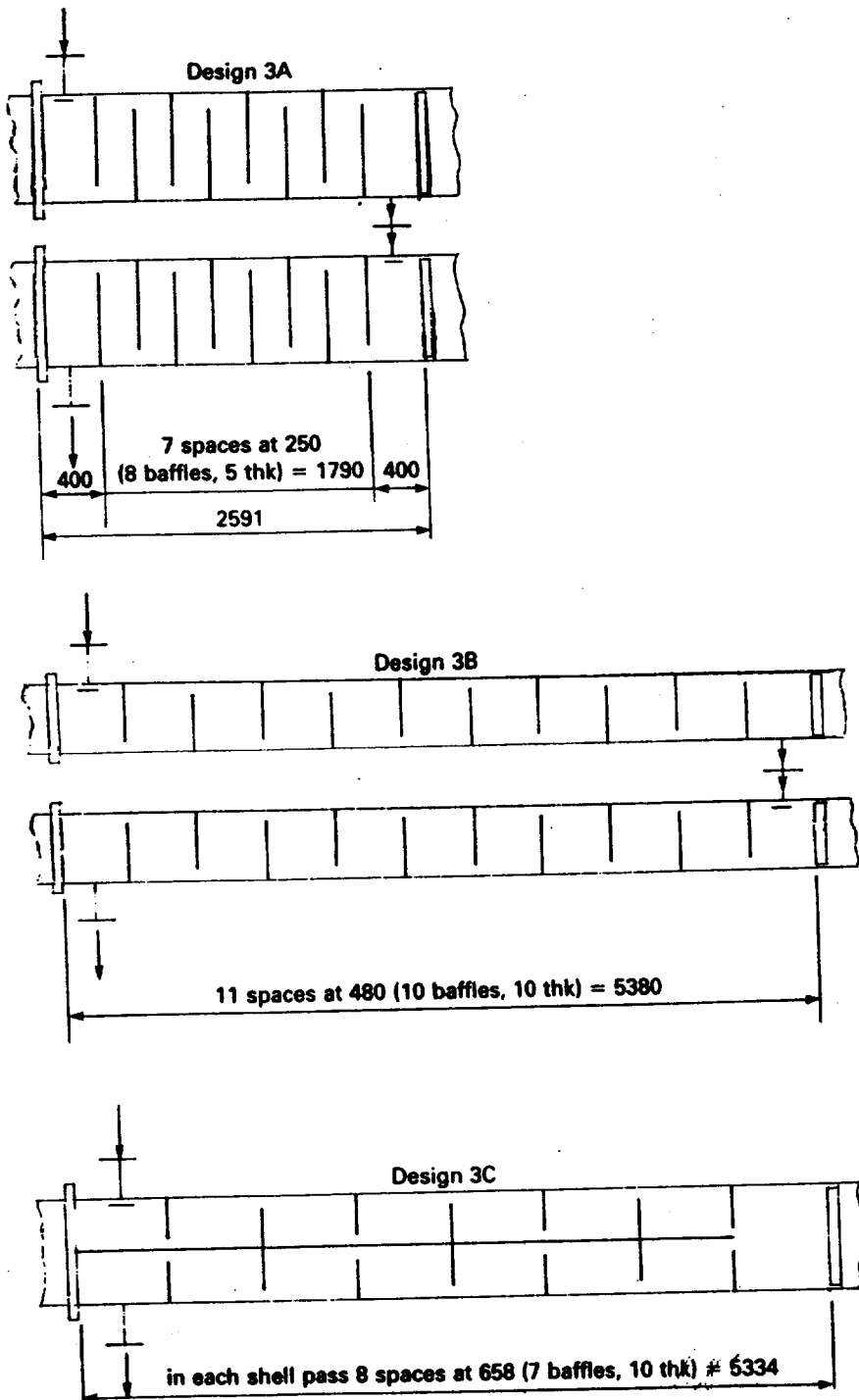


Table 17.6(b) Example 3: Design 3B (Two 1/1 E shells in series.)

Process conditions, heat load and  $\Delta T_m$  as design 3A

Mechanical design data				
Item		Units		
Tubes: o.d., i.d., thk., pitch, angle		mm		15.875 × 13.395 × 1.24 × 22.225 × 90°
Tube material		-		carbon steel
No. of tubes per shell	No. of passes	-	230	1
Tube length: overall	effective	m	5.5	5.38
No. of shells in unit		-		2
Arrangement: series	parallel	-	2S	1P
Surface <sup>(1)</sup> : one shell	unit	m <sup>2</sup>	61.7	123.4
Nozzle i.d. (in/out): shell <sup>(2)</sup>	tubes	mm	193.7/193.7	203/203
Shell i.d.		mm		438
Exchanger type		-		Split backing ring floating head
TEMA designation		-		AES

Notes: (1) Surface based on tube o.d. (2) Imping. baffle at inlet.

M T D correction factor

Countercurrent flow  $F = 1$  and  $\Delta T_m = \Delta T_{lm} = 44.3^\circ\text{C}$ 

Tube-side calculations ( $\phi_s = 1$ )				
Item	Units	Ref.		
No. of tubes per pass	-	-	230	
Int. flow area (one tube)	m <sup>2</sup>	Table 17.3(a)	$1.407 \times 10^{-4}$	
Int. flow area (one pass)	m <sup>2</sup>	-	$230 \times (1.407 \times 10^{-4}) = 0.0324$	
Velocity in tubes	m/s	-	-	
Mass velocity in tubes	kg/s m <sup>2</sup>	-	$49.3/0.0324 = 1521.6$	
Reynolds number ( $Re_i$ )	-	-	$(1521.6 \times 0.013395)/(2.7 \times 10^{-4}) = 75\,488$	
$Re_i^{0.795} Pr^{0.495}$	-	-	$75\,488^{0.795} \times 4.785^{0.495} = 16\,385.3$	
$\text{Exp}[-0.0225\{\ln(Pr)\}^2]$	-	-	$\text{exp}[-0.0225\{\ln 4.785\}^2] = 0.9464$	
Tube side coeff. ( $\alpha_{io}$ )	W/m <sup>2</sup> K	[6.16a]	$0.0225 \times (0.115/0.015\,875) \times 16\,385.3 \times 0.9464 = 2528$	
Friction factor ( $f_i$ )	-	[6.23c]	$0.0035 + 0.264/75\,488^{0.42} = 0.00586$	
Total travel ( $L$ )	m	-	$2 \times 5.5 = 11$	
Straight loss ( $\Delta P_i$ )	Pa	[6.22]	$(4 \times 0.00586 \times 11 \times 1521.6^2)/(2 \times 810 \times 0.013\,395)$	= 27 510
Header loss ( $\Delta P_h$ )	Pa	[6.31b]	$(2 \times 0.9 \times 1521.6^2)/(2 \times 810)$	= 2573
Nozzle flow area	m <sup>2</sup>	-	$(\pi/4) \times 0.203^2 = 0.0324$	
Nozzle mass velocity	kg/s m <sup>2</sup>	-	$49.3/0.0324 = 1521.6$	
Nozzle loss ( $\Delta P_n$ )	Pa	[6.31a]	$(2 \times 1.8 \times 1521.6^2)/(2 \times 810)$	= 5145
Total pressure loss ( $\Delta P_T$ )	Pa	-	= 35 228	

**Shell-side calculations: baffle data and Reynolds number**

Item	Units	Ref.
Spacing: central ( $l_c$ )	mm	480
Number ( $N_b$ )	mm	10
Thickness ( $B_c$ )	mm	10
Spacing ratios: central (BSR)	-	480/438 = 1.096
end ( $l_r$ )	-	480/480 = 1.0
Flow area/unit baffle pitch ( $S_{mu}$ )	m <sup>2</sup> /m	Table (12.3) 0.1456
Central cross-flow area ( $S_m$ )	m <sup>2</sup>	[12.5] 0.1456 × 0.48 = 0.0699
Mass velocity ( $m_c$ )	kg/s m <sup>2</sup>	[12.5] 33.71/0.0699 = 482.26
Cross-flow Reynolds number ( $Re_c$ )	-	[12.5] (482.26 × 0.015875)/(4 × 10 <sup>-4</sup> ) = 19 140

(i.e. turbulent)

Note: (1) See Fig. 17.4.

**Shell-side calculations: design factors**

Design factor	Ref.	Heat transfer	Cross loss*	Window loss
Flow rate ( $F_F$ )	Table 12.4	33.71 <sup>0.651</sup> = 9.876	33.71 <sup>2</sup> = 1136.4	33.71 <sup>2</sup> = 1136.4
Physical property ( $F_P$ )	Table 12.4	(1834 <sup>0.333</sup> × 0.137 <sup>0.667</sup> )/(4 × 10 <sup>-4</sup> ) <sup>0.318</sup> = 39.035	1/850 = 1.176 × 10 <sup>-3</sup>	1/850 = 1.176 × 10 <sup>-3</sup>
Mechanical design ( $F_M$ )	Table 12.7	9.06	4.193 × 10 <sup>3</sup>	3.695 × 10 <sup>3</sup>
$X_c$ (BSR > 0.35)	Table 12.8	0.456	0.049	0.261
$m$ (BSR > 0.35)	Table 12.8	0.594	2.011	0.910
$F_c$	[12.6]	0.456/1.096 <sup>0.594</sup> = 0.432	0.049/1.096 <sup>0.011</sup> = 0.0408	0.261/1.096 <sup>0.91</sup> = 0.24
$F_E$ (heat tr.)	Table 12.5	1.0		
$X_{c,e}$ (cross loss)	Table 12.9		2.0, 1.0	-

\* Table 12.4(a), 90° pitch,  $Re_c = 19 140$ ,  $p/d_0 = 1.4$ ,  $F_s = 0.948$



Shell-side calculations: flow-induced vibration check		Units or ref.
Item		
Volume flow		33.71/850 = 0.0397
Correction for baffle thickness ( $B_t = 10$ )		[11.23] 12.7/10 = 1.27
Correction for fatigue stress ( $S_f = 8.33 \times 10^7$ )		[11.23] 1.0
Corrected baffle damage constant ( $K_{bd} = 2.611 \times 10^{-4}$ )		Table 11.6 $(2.611 \times 10^{-4}) \times 1.27 \times 1 = 3.316 \times 10^{-4}$
Correction for tube gap ( $C_t = 6.35$ )		[11.24] 1.0
Correction for mod. of elasticity ( $E = 2 \times 10^{11}$ )		[11.24] 1.0
Corrected collision damage constant ( $K_{cd} = 3.152 \times 10^{-4}$ )		Table 11.6 $(3.152 \times 10^{-4}) \times 1 \times 1$
Inlet	Flow area $\{(S_{nu} l_c) - (\pi/4) d_{no}^2\}$	$m^2$ $(0.1456 \times 0.48) - (\pi/4) \times 0.1937^2 = 0.0404$
	Velocity ( $\mu_r$ )	$m/s$ $0.0397/0.0404 = 0.983$
	Unsupported length ( $l_c$ )	$m$ 0.48
	Baffle damage number	$-$ $(3.316 \times 10^{-4}) \times 850 \times 0.983^2 \times 0.48^2 = 0.063$
	Collision damage number	$-$ $(3.152 \times 10^{-4}) \times 850 \times 0.983^2 \times 0.48^4 = 0.014$
At first and last cross-overs	Flow area ( $S_m l_c$ )	$m^2$ $0.1456 \times 0.48 = 0.0699$
	Velocity ( $\mu_r$ )	$m/s$ $0.0397/0.0699 = 0.568$
	Unsupported length ( $l_c + l_s$ )	$m$ $0.48 + 0.48 = 0.96$
	Baffle damage number	$-$ $(3.316 \times 10^{-4}) \times 850 \times 0.568^2 \times 0.96^2 = 0.084$
	Collision damage number	$-$ $(3.152 \times 10^{-4}) \times 850 \times 0.568^2 \times 0.96^4 = 0.073$
Central space	Flow area ( $S_{nu} l_c = S_m$ )	$m^2$ $0.1456 \times 0.48 = 0.0699$
	Velocity ( $\mu_r$ )	$m/s$ $0.0397/0.0699 = 0.568$
	Unsupported length ( $2l_c$ )	$m$ $2 \times 0.48 = 0.96$
	Baffle damage number	$-$ $(3.316 \times 10^{-4}) \times 850 \times 0.568^2 \times 0.96^2 = 0.084$
	Collision damage number	$-$ $(3.152 \times 10^{-4}) \times 850 \times 0.568^2 \times 0.96^4 = 0.073$
Outlet	Flow area $\{(\pi/4) d_{no}^2\}$	$m^2$ $(\pi/4) \times 0.1937^2 = 0.0295$
	Velocity ( $\mu_r$ )	$m/s$ $0.0397/0.0295 = 1.346$
	Unsupported length ( $l_c$ )	$m$ 0.48
	Baffle damage number	$-$ $(3.316 \times 10^{-4}) \times 850 \times 1.346^2 \times 0.48^2 = 0.118$
	Collision damage number	$-$ $(3.152 \times 10^{-4}) \times 850 \times 1.346^2 \times 0.48^4 = 0.026$
	Max. allowable damage number	[11.15] $(0.00429 \times 850^{0.47}) / (4 \times 10^{-4})^{0.235} = 0.642$

On the shell-side, which is divided into two equal passes by a longitudinal baffle, the flow area is only one-half that of design 3A, but the flow rate is the same. The baffle spacing must therefore be increased to prevent excessive pressure loss. The designer's task is to check whether a sufficiently high heat transfer coefficient can be obtained to achieve the specified duty, but within the maximum allowable pressure loss. The designer must also ensure that the maximum unsupported length (1321 mm) is not exceeded and that there will be freedom from flow-induced vibration. The shell-side calculations follow the procedure of section 12.12.5.

Inspection of Table 17.6(c) shows that a satisfactory design is obtained when the baffle spacing is 658 mm, which means that the unsupported length is 1316 mm, and therefore close to the maximum value. However, the vibration check suggests that will be no problem. The shell-side pressure loss of 30086 Pa might be considered too high by some users, as it may cause leakage around the longitudinal baffle seals (see section 1.5.15 and Fig. 1.28). Figure 17.4 shows the baffle arrangement.

The Bell method, on which the shell-side thermal calculations are based, has not been substantiated for F shells and the method shown is an approximation. Both fluid and heat loss across the longitudinal baffle are assumed to be zero.

Table 17.6(c) Example 3: Design 3C (One 1/1 F shell.)

Process conditions, heat load and $\Delta T_m$ as design 3A				
Mechanical design data				
Item		Units		
Tubes: o.d., i.d., thk., pitch, angle		mm	15.875 × 13.395 × 1.24 × 22.225 × 90°	
Tube material		–	carbon steel	
No. of tubes per shell	No. passes	–	500	2
Tube length: overall	effective	m	5.5	5.334
No. of shells in unit		–	1	
Arrangement: series	parallel	–	1S	1P
Surface <sup>(1)</sup> : one shell	unit	m <sup>2</sup>	133	133
Nozzle i.d. (in/out): shell <sup>(2)</sup>	tubes	mm	193.7/193.7	203/203
Shell i.d.		mm	635	
Exchanger type		–	split backing ring floating head	
TEMA designation		–	AFS	

Notes: (1) Surface based on tube o.d. (2) Imping. baffle at inlet.

**M T D correction factor**

Countercurrent flow,  $F = 1$  and  $\Delta T_m = \Delta T_{lm} = 44.3^\circ\text{C}$

Tube-side calculations ( $\phi_1 = 1$ )		
Item	Units	Ref.
No. of tubes per pass	-	-
Int. flow area (one tube)	m <sup>2</sup>	Table 17.3(a)
Int. flow area (one pass)	m <sup>2</sup>	$250 \times (1.407 \times 10^{-4}) = 0.0352$
Velocity in tubes	m/s	-
Mass velocity in tubes	kg/s m <sup>2</sup>	$49.3/0.0352 = 1400.6$
Reynolds number ( $Re_i$ )	-	$(1400.6 \times 0.013395)/(2.7 \times 10^{-4}) = 69\,485$
$Re_i^{0.795} Pr_i^{0.495}$	-	$69\,485^{0.795} \times 4.785^{0.495} = 15\,340.7$
$\exp[-0.0225(\ln(Pr))^{-2}]$	-	$\exp[-0.0225(\ln 4.785)^{-2}] = 0.9464$
Tube-side coeff. ( $\alpha_{i0}$ )	W/m <sup>2</sup> K	$0.0225 \times (0.115/0.015\,875) \times 15\,340.7 \times 0.9464 = 2366$
Friction factor ( $f_i$ )	-	$0.0035 + 0.264/69\,485^{0.42} = 0.00594$
Total travel ( $L$ )	m	$2 \times 5.5 = 11$
Straight loss ( $\Delta P_i$ )	Pa	$(4 \times 0.00594 \times 11 \times 1400.6^2)/(2 \times 850 \times 0.013395) = 23\,627$
Header loss ( $\Delta P_h$ )	Pa	$(2 \times 1.6 \times 1400.6^2)/(2 \times 810) = 3875$
Nozzle flow area	m <sup>2</sup>	$(\pi/4) \times 0.203^2 = 0.0324$
Nozzle mass velocity	kg/s m <sup>2</sup>	$49.3/0.0324 = 1521.6$
Nozzle loss ( $\Delta P_n$ )	Pa	$(1.8 \times 1521.6^2)/(2 \times 810) = 2573$
Total pressure loss ( $\Delta P_T$ )	Pa	$= 30\,075$

**Shell-side calculations: baffle data and Reynolds number**

Item	Units	Ref.
Baffle data <sup>(1)</sup>	mm	-
Spacing: central ( $l_c$ )	mm	658
Number ( $N_b$ )	mm	7
Spacing ratios: central (BSR)	-	$658/635 = 1.036$
end ( $l_r$ )	m <sup>2</sup> /m	table (12.3)
Flow area/unit baffle pitch ( $S_{mu}$ )	m <sup>2</sup>	$0.2064 \times 0.658 = 0.1358$
Central cross-flow area ( $S_m$ )	kg/s m <sup>2</sup>	$33.71/0.1358 = 248.23$
Mass velocity ( $m_c$ )	-	$((248.23 \times 0.015875)/(4 \times 10^{-4})) \times 2 = 19704$
Cross-flow Reynolds number ( $Re_c$ )	-	(i.e. turbulent)

Note: (1) See Fig. 17.4.

**Shell-side calculations: design factors**

Design factor	Ref.	Heat transfer	Cross loss*	Window loss
Flow rate ( $F_F$ )	Table 12.4	$33.71^{0.681} = 9.876$	$33.71^2 = 1136.4$	$33.71^2 = 1136.4$
Physical property ( $F_P$ )	Table 12.4	$(1834^{0.33} \times 0.137^{0.667})/(4 \times 10^{-4})^{0.318} = 39.035$	$1/850 = 1.176 \times 10^{-3}$	$1/850 = 1.176 \times 10^{-3}$
Mechanical design ( $F_M$ )	Table 12.7	5.68	$1.491 \times 10^3$	$1.065 \times 10^3$
$X_c$ (BSR > 0.35)	Table 12.8	0.456	0.047	0.281
$m$ (BSR > 0.35)	Table 12.8	0.594	2.036	0.863
$F_c$	[12.6]	$0.456/1.036^{0.594} = 0.447$	$0.047/1.036^{0.456} = 0.0437$	$0.281/1.036^{0.863} = 0.273$
$F_E$ (heat tr.)	Table 12.5	1.0	2.0, 1.0	-
$X_c, e$ (cross loss)	Table 12.9	-	-	-

\*Table 12.4(a), 90° pitch,  $Re_c = 19704$ ,  $p/d_0 = 1.4$ ,  $F_c = 0.943$



**Shell-side calculations: heat transfer coefficient and pressure loss ( $\phi_0 = 1$ )**

Item	Units	Ref.	$F_2$ (sec 12.5.7)
Shell-side heat trans. coeff. ( $\alpha_0$ )	W/m <sup>2</sup> K	[12.2]	1.57
Central loss (one pass) ( $\Delta P_c$ )	Pa	[12.3]	8
Window loss (one window) ( $\Delta P_w$ )	Pa	[12.4]	8
Flow area	m <sup>2</sup>		$(\pi/4) \times 0.1937^2 = 0.0295$
Mass velocity	kg/s m <sup>2</sup>		$33.71/0.0295 = 1142.7$
Loss ( $\Delta P_{ni} + \Delta P_{no}$ )	Pa		$(4 \times 1142.7^2)/(2 \times 850) = 3072$
Total central loss ( $\Delta P_c(N_b - 1)$ )	Pa		$= 4598$
Total window loss ( $\Delta P_w(N_b)$ )	Pa		$= 21759$
End space loss ( $\Delta P_c(X_c)/l_c$ )	Pa	[12.8]	$= 657$
Total loss ( $\Delta P_s$ )	Pa		$= 30086$

**Overall heat transfer coefficient**

Resistance (W/m <sup>2</sup> K) <sup>-1</sup>	(related to tube o.d.)
Tube-side ( $1/\alpha_{io}$ )	$1/2366 = 0.000423$
Shell-side ( $1/\alpha_o$ )	$1/1537 = 0.000651$
Tube wall ( $r_w$ )	$= 0.000030$
Fouling - tubes ( $r_{fo}$ )	$r_i \times (\text{o.d./i.d.}) = 0.000104$
Fouling - shell ( $r_o$ )	$= 0.000088$
Overall ( $1/U_o$ ) ([6.7c])	$1/772 = 0.001296$
Surface area (m <sup>2</sup> )	133
Available	$4018.9 \times 1000$
Required	$772 \times 44.3 = 118$
	OK

Shell-side calculations: flow-induced vibration check		Units or ref.
Item		
Volume		$33.71/850 = 0.0397$
Correction for baffle thickness ( $B_t = 10$ )		$12.7/10 = 1.27$
Correction for fatigue stress ( $S_f = 8.33 \times 10^7$ )		1.0
Corrected baffle damage constant ( $K_{bd} = 2.611 \times 10^{-4}$ )		$(2.611 \times 10^{-4}) \times 1.27 \times 1 = 3.316 \times 10^{-4}$
Correction for tube gap ( $C_1 = 6.35$ )		1.0
Correction for mod. of elasticity ( $E = 2 \times 10^{11}$ )		1.0
Corrected collision damage constant ( $K_{cd} = 3.152 \times 10^{-4}$ )		$(3.152 \times 10^{-4}) \times 1 \times 1 = 3.152 \times 10^{-4}$
Inlet	Flow area $\{(S_{mu} l_e) - (\pi/4) d_{in}^2\}$	$(0.2064 \times 0.658 \times 0.5) - (\pi/4) \times 0.1937^2 = 0.0384$
	Velocity ( $\mu_r$ )	$0.0397/0.0384 = 1.034$
	Unsupported length ( $l_e$ )	0.658
	Baffle damage number	$(3.316 \times 10^{-4}) \times 850 \times 1.034^2 \times 0.658^2 = 0.130$
	Collision damage number	$(3.152 \times 10^{-4}) \times 850 \times 1.034^2 \times 0.658^4 = 0.054$
At first and last cross-overs	Flow area ( $S_{mu} l_e$ )	$0.2064 \times 0.658 \times 0.5 = 0.0679$
	Velocity ( $\mu_r$ )	$0.0397/0.0679 = 0.585$
	Unsupported length ( $l_e + l_s$ )	$0.658 + 0.658 = 1.316$
	Baffle damage number	$(3.316 \times 10^{-4}) \times 850 \times 0.585^2 \times 1.316^2 = 0.167$
	Collision damage number	$(3.152 \times 10^{-4}) \times 850 \times 0.585^2 \times 1.316^4 = 0.275$
Central space	Flow area ( $S_{mi} l_s = S_m$ )	$0.2064 \times 0.658 \times 0.5 = 0.0679$
	Velocity ( $\mu_r$ )	$0.0397/0.0679 = 0.585$
	Unsupported length ( $2l_s$ )	$2 \times 0.658 = 1.316$
	Baffle damage number	$(3.316 \times 10^{-4}) \times 850 \times 0.585^2 \times 1.316^2 = 0.167$
	Collision damage number	$(3.152 \times 10^{-4}) \times 850 \times 0.585^2 \times 1.316^4 = 0.275$
	Flow area $\{(\pi/4) d_{no}^2\}$	$(\pi/4) \times 0.1937^2 = 0.0295$
	Velocity ( $\mu_r$ )	$0.0397/0.0295 = 1.346$
Outlet	Unsupported length ( $l_e$ )	0.658
	Baffle damage number	$(3.316 \times 10^{-4}) \times 850 \times 1.346^2 \times 0.658^2 = 0.221$
	Collision damage number	$(3.152 \times 10^{-4}) \times 850 \times 1.346^4 \times 0.658^4 = 0.091$
Max. allowable damage number		$(0.00429 \times 850^{0.47}) / (4 \times 10^{-4})^{0.235} = 0.642$

### 17.2.4 Example 4: Steam/fuel oil heater

This example provides the design of a fuel oil heater in which viscous oil is heated by condensing steam. In design 4A the oil is routed through the tubes; in design 4B it is routed through the shell. Although condensing steam is not a single-phase fluid it is the most common heating medium and when used for this purpose it is customary to assume a heat transfer coefficient of 8500–10 000 W/m<sup>2</sup> K, and negligible pressure loss. Pure condensing steam would provide a heat transfer coefficient at least four times this value, but in industrial steam plant air is always present. As an air concentration as low as 1% reduces the heat transfer coefficient by 50% or more, the heat transfer coefficient is reduced to the value stated for design purposes.

The steam coefficient will be high in relation to that of the oil, and hence a significant viscosity gradient between the bulk of the oil and adjacent surface is expected. As a result, the viscosity correction factor, described in section 6.8, will not be unity. The oil viscosity decreases by ten times between inlet and outlet, and as the overall heat transfer coefficient is expected to vary considerably, it is determined at the terminal conditions, instead of the average temperature.

Usually fuel oil heating is carried-out in longitudinally finned tube equipment, either double-pipe exchangers described in section 5.1, Chapter 15 and section 17.5, or longitudinally finned shell-and-tube exchangers for large capacities. In this example a plain tube exchanger is used to demonstrate the application of laminar flow correlations given in Chapter 6. In design 4A, where oil is routed through the tubes, a fixed tubesheet exchanger having closely pitched tubes will be satisfactory. Inspection of Table 19.1 suggests an overall heat transfer coefficient of 173 W/m<sup>2</sup> K related to steam-heated heavy organics with a viscosity greater than 50 cP. In this unit the oil viscosity range is 247–2500 cP and a much lower coefficient is expected. The tube length is limited to 6 m. Table 17.7(a) summarises the calculations for the smallest unit, consistent with the maximum oil-side pressure and tube length, which is found by trial and error.

Tube-side calculations for laminar flow involve two dimensionless numbers, Graetz and Grashof, not encountered in fully turbulent applications. The Graetz number  $\{(\pi/4) \text{Re Pr} (d/L)\}$  involves  $L$ , defined as the flow path length in which no internal mixing of the fluid occurs. In a straight tube exchanger  $L$  is the length of one pass; in a U-tube exchanger it is twice the straight leg length. Unless  $L$  is fixed, it is unknown at the start of the design and a tentative value must be assumed. If  $L$  differs for the final design, the Graetz number should be corrected and the calculation reworked. However, the heat transfer coefficient is not influenced greatly by small changes in  $L$ . The Grashof number  $\{\beta g d^3 \rho^2 (\Delta T)\}/\eta^2$  involves  $\beta$ , the coefficient of expansion. This is calculated from  $\beta = \{2(\rho_1 - \rho_o)\}/\{(\rho_1 + \rho_o)(T_o - T_1)\}$  where  $\rho_1$  and  $\rho_o$  are densities at temperatures  $T_1$  and  $T_o$ , respectively. It assumes linear relationship between density and temperature. The correlation specifies that  $\Delta T$  required for the Grashof number is the logarithmic mean  $\Delta T_{\text{lm}}$ .

This is defined as the logarithmic mean of the temperature differences between the bulk and surface temperatures on the oil-side, over which heat transfer occurs without mixing. It must not be confused with  $\Delta T_{lm}$ .

Heat transfer calculations are made with  $\phi_i = 1$ , after which  $\phi_i$  is determined by trial and error, as discussed in section 6.8 and illustrated by Fig. 9.4. The surface area calculation is based on equation [7.2] which assumes that  $U$  varies linearly with temperature. The effective product  $U \Delta T_{lm}$  is obtained instead of separate values of  $U$  and  $\Delta T$ .

For laminar flow inside tubes  $f_i = 16/Re_i$  and the straight tube pressure loss from equation [6.22] may be expressed as:

$$\frac{\Delta P_i}{L} = \left\{ \frac{32\dot{m}\eta_b}{d_i^2\rho\phi_i} \right\} = \left\{ \frac{32\dot{m}}{d_i^2} \right\} \left\{ \frac{\eta_b}{\rho\phi_i} \right\} \quad [17.1]$$

The straight tube pressure loss per unit length varies appreciably through the exchanger due to the variation of viscosity, density and viscosity gradient, expressed by the factor  $\eta_b/\rho\phi_i$  in equation [17.1]. Table 17.7(a) presents the variation in pressure loss through the exchanger.

The calculations for design 4B, in which the oil is routed through the shell, follow a similar pattern to design 4A and they are summarised in Table 17.7(b). Because of fouling, cleaning lanes between the tubes are required and this is achieved by using rotated square (45°) pitch as recommended in section 1.5.4. As in design 4A, heat transfer calculations are made with  $\phi_o = 1$ , after which  $\phi_o$  is determined by trial and error. It is based on the 'ideal' exchanger as described in section 12.5.5. The shell-side pressure loss varies appreciably through the exchanger, due to the variation of viscosity, density and viscosity gradient, as shown in Table 17.7(b).

Table 17.7(a) Example 4: Steam/fuel oil heater. Design 4A (oil inside tubes)

Process conditions			
Item	Units	Shell-side	Tube-side
Fluid name	–	steam	fuel oil
Flow rate	kg/s	0.6	23.98
Temperature range	°C	111 → 111	25 → 55
Specific heat (in, out) <sup>(1)</sup>	J/kg K	–	1800                      1897
Dynamic viscosity (in, out) <sup>(1)</sup>	Ns/m <sup>2</sup>	–	2.5                              0.247
Thermal conductivity (in, out) <sup>(1)</sup>	W/m K	–	0.114                          0.116
Density (in, out) <sup>(1)</sup>	kg/m <sup>3</sup>	–	958                              939
Prandtl number (in, out) <sup>(1)</sup>	–	–	39 474                          4039
Fouling factor <sup>(2)</sup>	(W/m <sup>2</sup> K) <sup>-1</sup>	0.000 88	0.00088
Max. pressure loss	Pa	–	35 000
Tube-wall resistance <sup>(3)</sup>	(W/m <sup>2</sup> K) <sup>-1</sup>	0.000 065 5	–
Grashof number (Gr) (in, out)	–	–	0.01493 (ΔT),              1.47 (ΔT)

<b>Heat load (kW)</b>	<b>log MTD (<math>\Delta T_{lm}</math>) (<math>7.1</math>)<sup>(4)</sup></b>
<b>Shell-side <math>Q = \{0.6 \times (2.218 \times 10^6)\} / 1000 = 1330.8</math></b>	$\begin{array}{r} 111 \longrightarrow 111 \\ \underline{55} \longleftarrow \underline{25} \\ \underline{56} \end{array}$
<b>Tube-side <math>Q = (23.98 \times (55 - 25) \times 1850) / 1000 = 1330.9</math></b>	$\Delta T_{lm} = \frac{86 - 56}{\ln \frac{86}{56}} = 69.9 \text{ }^\circ\text{C}$

- Notes:
- (1) At inlet and outlet bulk temperatures.
  - (2) Referred to its own surface.
  - (3) Referred to tube o.d.
  - (4) Isothermal condensation i.e.  $F = 1$  and  $\Delta T_m = 69.9 \text{ }^\circ\text{C}$

Mechanical design data		Units
Item		
Tubes: o.d., i.d., thk., pitch, angle		31.75 × 24.95 × 3.4 × 39.688 × 30°
Tube material		carbon steel
No. of tubes per shell	No. of passes	2
Tube length: overall effective		5.35
No. of shells in unit		1
Arrangement: series	parallel	1P
Surface <sup>(1)</sup> : one shell	unit	298.8
Nozzle i.d. (in/out): shell <sup>(2)</sup>	tubes	254/52.5
Shell i.d.		1067
Exchanger type		Fixed tubesheet
TEMA designation		AEM

- Notes:
- (1) Surface based on tube o.d.
  - (2) Imping. baffle at inlet.

<b>Shell-side calculations</b>
Not required with process steam; assume $\alpha_0 = 8500 \text{ W/m}^2 \text{ K}$

Tube-side calculations: heat transfer			
Item	Units	Ref.	Outlet
No. of tubes per pass	-	-	Inlet
Int. flow area (one tube)	m <sup>2</sup>	Table 17.3(a)	560/2 = 280
Int. flow area (one pass)	m <sup>2</sup>	-	4.886 × 10 <sup>-4</sup>
Velocity in tubes	m/s	-	0.137
Mass velocity in tubes	kg/sm <sup>2</sup>	-	23.98/(0.137 × 958) = 0.18
Reynolds number (Re) <sub>i</sub>	-	-	175
Graetz number (Gz) (L = 5)	-	-	(175 × 0.02495)/2.5 = 1.75
0.0083 (GrPr) <sup>0.75</sup> (ΔT = 58.7)	-	-	{(π/4) × 1.75 × 39 474 × 0.024 95}/5 = 270.73
Tube side coeff. α' <sub>io</sub> (φ <sub>i</sub> = 1)	W/m <sup>2</sup> K	[6.18]	0.0083 × (0.014 93 × 58.7 × 39 474) <sup>0.75</sup> = 21.05
			{(1.75 × 0.114 × (270.73 + 21.05)) <sup>1/3</sup> }/0.031 75 = 41.7
			(175 × 0.02495)/0.247 = 17.68
			{(π/4) × 17.68 × 4039 × 0.024 95}/5 = 279.86
			0.0083 × (1.47 × 58.7 × 4039) <sup>0.75</sup> = 119.06
			{1.75 × 0.116 × (279.86 + 119.06) <sup>1/3</sup> }/0.031 75 = 47.1

Assume all coefficients, except oil film, are constant. Hence:  
Resistance (W/m<sup>2</sup> K)<sup>-1</sup> (related to tube o.d.)

Steam	= 1/8500	= 0.000 118
External fouling	=	= 0.000 088
Internal fouling	= r <sub>i</sub> × (o.d./i.d.)	= 0.001 120
Tube wall	=	= 0.000 066
Combined resistance between steam and interface of oil and internal fouling	= 1/1718.4	= 0.001 392

Item	Units	Ref.	Inlet	Outlet
At interface: oil and internal fouling	Assumed interface temp.		102.6	106.4
	Viscosity ( $\eta_k$ )		0.0287	0.0254
	$\phi_1 = (\eta_b/\eta_k)^{0.14}$	sec. 6.8.3	$2.5/0.0287^{0.14} = 1.87$	$0.247/0.0254^{0.14} = 1.375$
Heat flux	Interface to oil		$41.7 \times 1.87 \times (102.6 - 25) = 6051$	$47.1 \times 1.375 \times (106.4 - 55) = 3329$
	Steam to interface		$718.4 \times (111 - 102.6) = 6035$	$718.4 \times (111 - 106.4) = 3305$
Corrected tube-side coeff. ( $\alpha_{io}$ )	W/m <sup>2</sup> K	[6.18]	$41.7 \times 1.87 = 78$	$47.1 \times 1.375 = 64.8$

Overall heat transfer coefficient and surface area		Inlet	Outlet
Overall coefficient ( $U_o$ )	W/m <sup>2</sup> K [6.7c]	$(78 \times 718.4)/(78 + 718.4) = 70.4$	$(64.8 \times 718.4)/(64.8 + 718.4) = 59.4$
Terminal temp. diff	°C	$111 - 25 = 86$	$111 - 55 = 56$
$\log(U \Delta T_m)$	W/m <sup>2</sup> [7.2]	log mean $(86 \times 59.4 = 5108$ and $(70.4 \times 56) = 3942$ $= \frac{5108 - 3942}{\ln \left\{ \frac{5108}{3942} \right\}} = 4500$	
Surface area	Required	$(1330.9 \times 1000)/4500 = 295.8$	
	Available	$(5 \text{ m overall, } 4.85 \text{ m eff.}) = 560 \times \pi \times 0.03175 \times 4.85 = 270.9$	
		Inc. length to 5.5 m overall, 5.35 eff., giving 298.8 m <sup>2</sup> .	

Tube-side calculations: incremental pressure loss				
	1	2	3	4
Location number	111	111	111	111
Steam temperature	25	35	45	55
Oil temperature	86	76	66	56
Temperature difference ( $\Delta T$ )	70.4	66.7	63.1	59.4
Overall coefficient ( $U$ ) <sup>(1)</sup>				sum
Zone number				
( $U \Delta T$ ) <sub>lm</sub>	5541	4596	3724	-
Zone surface = $(1330.9 \times 1000) / \{3(U \Delta T)_{lm}\}$	80.1	96.6	119.1	295.8
Zone length ( $l$ )	2.98	3.59	4.43	11
Tube-side coefficient ( $\alpha_{io}$ ) <sup>(2)</sup>	78	73.5	69.2	64.8
$\alpha'_{io}$ for $\phi = 1$ <sup>(1)</sup>	41.7	43.5	45.3	47.1
$\phi_1$ (heat transfer) = $(\alpha_{io} / \alpha'_{io})$	1.87	1.69	1.53	1.375
( $\eta_b / \eta_s$ )	87.11	42.44	20.86	9.724
$\phi_1$ (pressure loss) = $(\eta_b / \eta_s)^{0.25}$	3.06	2.55	2.14	1.77
Oil viscosity ( $\eta_b$ )	2.5	0.935	0.445	0.247
Oil density ( $\rho$ ) <sup>(1)</sup>	958	952	946	939
$\eta_b(\rho\phi)$	$8.528 \times 10^{-4}$	$3.852 \times 10^{-4}$	$2.198 \times 10^{-4}$	$1.486 \times 10^{-4}$
Average $\eta_b / (\rho\phi)$ for zone				
Pressure loss in zone ( $\Delta P_i$ ) <sup>(3)</sup>				
	6.19	$3.025 \times 10^{-4}$	$1.842 \times 10^{-4}$	$1.842 \times 10^{-4}$
	16600	9759	7346	33705
				say 35000

**Notes:**

- (1) Assumed to vary linearly with temperature;
- (2)  $\alpha_{io} = 1 / \{ (1/U) - (1/718.4) \}$ ;
- (3)  $\Delta P_i = \{ (32 \times 175) / 0.02495^2 \} \{ \eta_b / \rho\phi \} = \{ 8.996 \times 10^4 \} \{ \eta_b / \rho\phi \}$  from equation [17.1];
- (4) header and nozzle losses negligible.



Table 17.7(b) Example 4: Steam/fuel oil heater: Design 4B (oil outside tubes)

Mechanical design data		Units
Item		
Tubes: o.d., i.d., thk., pitch, angle		31.75 × 24.95 × 3.4 × 39.688 × 45°
Tube material		carbon steel
No. of tubes per shell	No. of passes	2
Tube length <sup>(2)</sup> : overall	effective	4.9 4.714
No. of shells in unit		1
Arrangement: series	parallel	1S 1P
Surface <sup>(1)</sup> : one shell	unit	150.5
Nozzle i.d. (in/out): shell	tubes	194/194 254/52.5
Shell i.d.		889
Exchanger type		U-tube
TEMA designation		BEU

Notes: (1) Surface based on tube o.d. (2) To bend tangent.

Tube-side calculations	
Not required with process steam; assume $\alpha_{fo} = 8500 \text{ W/m}^2 \text{ K}$	

Item	Units	Ref.
Baffle data <sup>(1)</sup>	Spacing: central ( $l_c$ )	930
	end ( $l_e$ )	2 at 930
Number ( $N_b$ )	thickness ( $B_t$ )	5 <sup>(1)</sup>
		16
Spacing ratios: central (BSR)	end ( $l_r$ )	930/889 = 1.046
		930/930 = 1
Flow area/unit baffle pitch ( $S_{mu}$ )	m <sup>2</sup> /m	Table 12.3 0.2516
Central cross-flow area ( $S_m$ )	m <sup>2</sup>	[12.5] 0.2516 × 0.93 = 0.234
Mass velocity ( $\dot{m}_c$ )	kg/s m <sup>2</sup>	[12.5] 23.98/0.234 = 102.5
Cross-flow Reynolds number ( $Re_c$ ) (in/out)	-	[12.5] (102.5 × 0.03175)/2.5 = 1.3 (102.5 × 0.03175/0.247 = 13.2 (i.e. laminar)

Note:  
 (1) Baffle at bend tangent regarded as a tubesheet for heat transfer and pressure loss calculations.

**Shell-side calculations: heat transfer**

	Ref.	Inlet	Outlet
<b>Design factor</b>			
Flow rate ( $F_F$ )	Table 12.4	$23.98^{0.36} = 3.139$	
Physical property ( $F_P$ )	Table 12.4	$(1800^{0.333} \times 0.114^{0.667}) / 2.5^{0.027} = 2.781$	$1897^{0.333} \times 0.116^{0.667} / 0.247^{0.027} = 3.048$
Mechanical design ( $F_M$ )	Table 12.7	35.3	
$X_c$	Table 12.8	0.482	
$m$	Table 12.8	0.324	
$F_c$	[12.6]	$0.482 / 1.046^{0.324} = 0.475$	
$F_E$ (heat transfer)	Table 12.5	1.0	
$F_A = (j_1)(j_2)$ for $Re_c < 20$	Table 12.6	$0.872 \times 0.748 = 0.652$	
'Ideal' exchanger ( $\phi_o \neq 1$ )	Table 12.10	11.908, 0.36	
	[12.9]	$11.908 / 0.234^{0.36} = 20.087$	
	[12.9]	$3.139 \times 2.781 \times 20.087 = 175.4$	$3.139 \times 3.048 \times 20.087 = 192.2$

Assume all coefficients, except oil film, are constant. Hence:

Resistance  $(W/m^2 K)^{-1}$  (related to tube o.d.)

Stream	= 1/8500	= 0.000 118
External fouling	=	= 0.000 880
Internal fouling	= $r_i \times (\text{o.d./i.d.})$	= 0.000 112
Tube wall	=	= 0.000 066
Combined resistance between steam and interface of oil and internal fouling	= 1/850.3	= 0.001 176

Item	Units	Ref.	Inlet	Outlet
At interface: oil and inter-	°C		88.3	98.1
nal fouling	$Ns/m^2$		0.048	0.0325
Heat flux	$W/m^2$		$(2.5/0.048)^{0.14} = 1.74$	$(0.247/0.0325)^{0.14} = 1.33$
Corrected tube-side coeff. ( $\alpha_o$ )	$W/m^2 K$	[12.2]	$175.4 \times 1.74 \times (88.3 - 25) = 19319$	$192.2 \times 1.33 \times (98.1 - 55) = 11017$
			$850.3 \times (111 - 88.3) = 19302$	$850.3 \times (111 - 98.1) = 10969$
			$3.139 \times 2.781 \times 35.3 \times 0.475 \times 1 \times 0.652 \times 1.74 = 166$	$3.139 \times 3.048 \times 35.3 \times 0.475 \times 1 \times 0.652 \times 1.33 = 139.1$

Overall heat transfer coefficient and surface area		Inlet	Outlet
Overall coefficient ( $U_o$ )	W/m <sup>2</sup> K [6.7c]	$(166 \times 850.3) / (166 + 850.3) = 138.9$	$(139.1 \times 850.3) / (139.1 + 850.3) = 119.5$
Terminal temp. coeff	°C	$111 - 25 = 86$	$111 - 55 = 56$
$\log(U \Delta T_m)$	W/m <sup>2</sup>	$\log \text{mean } (119.5 \times 86) = 10277 \text{ and } (138.9 \times 56) = 7778$ $= \frac{10277 - 7778}{\ln \left( \frac{10277}{7778} \right)} = 8970$	
Surface area	Required	$Q / U_o \Delta T_m$	
	Available	$(1330.9 \times 1000) / 8970 = 148.4$ $(4.714 \text{ m to tangent of bends}) = 320 \times \pi \times 0.03175 \times 4.714 = 150.5$	

Shell-side calculations: pressure loss design factors

Design factor	Ref.	Cross-flow loss	Window loss
Flow rate ( $F_F$ )	Table 12.4	23.98	23.98
Physical property ( $F_P$ )	Table 12.4	$\eta_b / \rho$	$\eta_b / \rho$
Mechanical design ( $F_M$ )	Table 12.7	$0.854 \times 10^6$	$0.327 \times 10^6$
$X_C$	Table 12.8	0.17	0.722
$m$	Table 12.8	1.058	-0.121
$F_c$	[12.6]	$0.17 / 1.046^{1.058} = 0.162$	$0.722 / 1.046^{-0.121} = 0.726$
$X_c, e$ (cross-flow loss)	Table 12.9	1.9, 1.0	-

Shell-side calculations: incremental pressure loss						
	Units	1	2	3	4	
Location number		111	111	111	111	
Steam temperature	°C	25	35	45	55	
Oil temperature	°C	86	76	66	56	
Temperature difference ( $\Delta T$ )	W/m <sup>2</sup> K	138.9	132.4	126	119.5	
Overall coefficient ( $U$ ) <sup>(1)</sup>	Ns/m <sup>2</sup>	2.5	0.935	0.445	0.247	
Oil viscosity ( $\eta_b$ )	kg/m <sup>3</sup>	958	952	946	939	
Oil density ( $\rho$ )		$2.61 \times 10^{-3}$	$9.82 \times 10^{-4}$	$4.70 \times 10^{-4}$	$2.63 \times 10^{-4}$	
$\eta_b/\rho$	W/m <sup>2</sup> K	166	156.8	147.9	139.1	
Shell-side coefficient ( $\alpha_0$ ) <sup>(2)</sup>	W/m <sup>2</sup> K	95.4	98.5	101.6	104.6	
$\alpha'_0$ for $\phi_0 = 1$ <sup>(1)</sup>		1.74	1.59	1.46	1.33	
$\phi_0 = \alpha_0/\alpha'_0$	m <sup>2</sup> /s	$1.5 \times 10^{-3}$	$6.18 \times 10^{-4}$	$3.22 \times 10^{-4}$	$1.98 \times 10^{-4}$	
$\eta_b/(\rho\phi_0)$			1	2	3	sum
Zone number			10966	9151	7464	-
$(U\Delta T)_{im}$	m <sup>2</sup>		40.5	48.5	59.4	148.4
Zone surface = $(1330.9 \times 1000)/(3(U\Delta T)_{im})$	m		1.287	1.541	1.886	4.714
Zone length ( $l$ )		1	2	3	4	5
Cross flow	m <sup>2</sup> /s	$11.26 \times 10^{-4}$	$6.05 \times 10^{-4}$	$3.94 \times 10^{-4}$	$2.82 \times 10^{-4}$	$2.20 \times 10^{-4}$
Baffle space number	Pa	-	2007	1307	936	4250
Average $(\eta_b/(\rho\phi_0))$ <sup>(3)</sup>	Pa	$1.9 \times 3736 = 7099$	-	-	-	$730 \times 1.9 = 1387$
Central spaces ( $\Delta P_c$ ) <sup>(5)</sup>		1	2	3	4	-
End spaces ( $\Delta P_e$ ) <sup>(5)</sup>	m <sup>2</sup> /s	$12.1 \times 10^{-4}$	$7.15 \times 10^{-4}$	$4.77 \times 10^{-4}$	$3.45 \times 10^{-4}$	-
Window number	Pa	6889	4070	2716	1964	15639
Average $(\eta_b/\rho)$ <sup>(4)</sup>						Total
Window loss						28375 <sup>(6)</sup>

## Notes:

- (1) Assumed to vary linearly with temperature.
- (2)  $\alpha_0 = 1/((1/U) - (1/850.3))$ .
- (3) From plot of  $\{\eta_b/(\rho\phi_0)\}$  versus length.
- (4) From plot of  $(\eta_b/\rho)$  versus length.
- (5)  $\Delta P_c = (23.98)(0.854 \times 10^6)(0.162)\{\eta_b/(\rho\phi_0)\} = (3.318 \times 10^6)\{\eta_b/(\rho\phi_0)\}$ ;  
 $\Delta P_e = (23.98)(0.327 \times 10^6)(0.726)(\eta_b/\rho) = (5.693 \times 10^6)(\eta_b/\rho)$ .
- (6) Nozzle losses assumed negligible.

## 17.2.5 Example 5: Gas cooler (X shell)

The cross-flow (X type) shell-and-tube exchanger has increased in popularity in recent years because it may be designed to guarantee freedom from flow-induced vibration. Each baffle supports every tube and sufficient baffles may be installed to satisfy the most stringent predictive method, without affecting the heat transfer and pressure loss characteristics. However, it is necessary to provide adequate distribution spaces at inlet and outlet of the bundle and therefore a larger shell diameter is required to accommodate a given number of tubes, compared with an E shell for instance. Irrespective of vibration problems, the X shell is ideal for dealing with large volumes of low-pressure gas, particularly if the allowable gas pressure loss is low.

In the example shown, the maximum tube length was limited to 6.096 m, and the shell diameter to 1524 mm, for ease of handling. The gas pressure is 15 bar abs. and inspection of Table 19.1 suggests gas and water heat transfer coefficients of  $500 \text{ W/m}^2 \text{ K}$  and  $6000 \text{ W/m}^2 \text{ K}$ , respectively. When combined with the specified fouling factors, the anticipated overall heat transfer coefficient is  $292 \text{ W/m}^2 \text{ K}$ . The tentative surface area is therefore  $(11.441 \times 10^3)/(292 \times 37.9) = 1034 \text{ m}^2$ . At its maximum length of 6.096 m, each tube has a surface area of  $0.365 \text{ m}^2$ , and therefore the required number of tubes is  $1034/0.365 = 2833$ . Bearing in mind that inlet and outlet distribution spaces are required, this is much greater than the tube count in the largest shell of split backing ring floating-head construction shown in Table A3.3. At least two shells will be required and subsequent calculation will show whether these are arranged in series or parallel, or a combination of the two.

A summary of the calculations is shown in Table 17.8 and the baffle arrangement in Fig. 17.5. As the flow in each shell consists of a single cross-flow pass, the Bell method is not involved. The shell-side heat transfer coefficient and cross-flow pressure loss are calculated directly from equations [6.25] and [6.26], respectively, for flow across ideal plain tube banks. The calculations assume that bundle-shell leakage is prevented by the inclusion of many longitudinal sealing flats shown in Fig. 1.30.

The symmetrical horizontal bundle has inlet and outlet distribution spaces, each 384 mm deep, measured along the vertical centreline. The tube count and number of rows crossed is calculated in accordance with section A3.2 as follows:

$$\begin{aligned} \text{shell diameter:} & D_i = 1524 \text{ mm} \\ \text{inlet height:} & h = 384 \text{ mm} \\ \text{outer tube limit:} & D_1 = 1524 - 47.63 = 1476.4 \text{ mm (Table 12.2)} \\ \text{full tube count:} & N_t = 2594 \text{ (2 pass AXS type) (Table A3.3)} \end{aligned}$$

$$\text{From section A3.2:} \quad R = \frac{1 - \{(2 \times 384)/1524\}}{1476.4/1524} = 0.512$$

$$\text{From Fig. A3.2:} \quad Z = 0.19$$

$$\text{No. tubes lost at inlet:} \quad NZ = 2594 \times 0.19 = 493$$

Similarly, 493 tubes will be lost at outlet, hence

$$\text{Final count} = 2594 - (2 \times 493) = 1608$$

The depth available on the vertical centreline for tubes is  
 $1524 - (2 \times 384) = 756 \text{ mm}$

$$29 \text{ pitches} + \text{one tube dia.} = (29 \times 25.4) + 19.05 = 756 \text{ mm}$$

$$\text{Number of rows} = 29 + 1 = 30 \text{ or } 60 \text{ in two shells}$$

Figure 17.5 Baffle arrangement for example 5

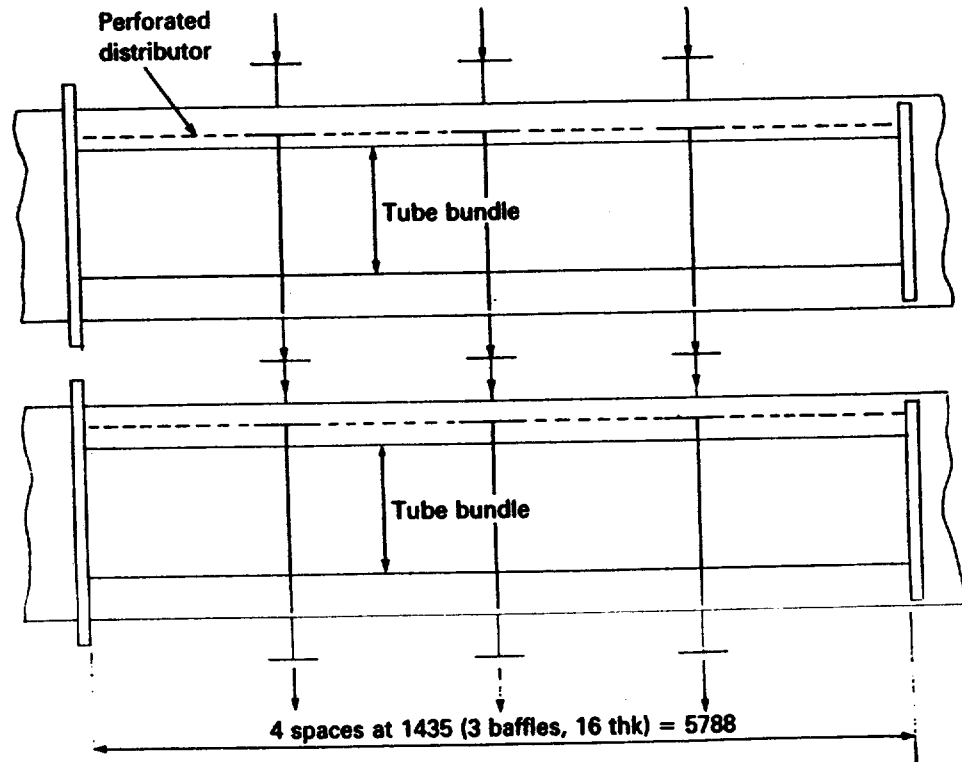


Table 17.8 Example 5: Gas cooler (X shell)

Process conditions			
Item	Units	Shell-side	Tube-side
Fluid name	-	Gas at 4.472 bar abs.	Water
Flow rate	kg/s	86.55	246.64
Temperature range	°C	103.3 → 46.1	26.7 → 37.8
Specific heat <sup>(1)</sup>	J/kg K	2311	4179
Dynamic viscosity <sup>(1)</sup>	Ns/m <sup>2</sup>	$7.577 \times 10^{-6}$	$7.647 \times 10^{-4}$
Thermal conductivity <sup>(1)</sup>	W/m K	0.03172	-
Density <sup>(1)</sup>	kg/m <sup>3</sup>	17.62	997
Prandtl number <sup>(1)</sup>	-	0.552	-
Fouling factor <sup>(2)</sup>	(W/m <sup>2</sup> K) <sup>-1</sup>	0.00035	0.00035
Max. pressure loss	Pa	3000	86000
Tube-wall resistance <sup>(3)</sup>	(W/m <sup>2</sup> K) <sup>-1</sup>	0.00004	-

<b>Heat load (kW)</b>	<b>log MTD (<math>\Delta T_m</math>) (eq. [7.1])</b>
Shell-side $Q = \{86.55 \times (103.3 - 46.1) \times 2311\} / 1000 = 11\,441$	$\frac{103.3 \rightarrow 46.1}{37.8 \leftarrow \frac{26.7}{19.4}} \quad \frac{65.5 - 19.4}{\ln \left\{ \frac{65.5}{19.4} \right\}} = 37.9^\circ\text{C}$
Tube-side $Q = \{246.64 \times (37.8 - 26.7) \times 4179\} / 1000 = 11\,441$	
<p><b>Notes:</b></p> <p>(1) At average bulk temperature.                  (2) Referred to its own surface.                  (3) Referred to tube o.d.</p>	

<b>Mechanical design data</b>	
Item	Units
Tubes: o.d., i.d., thk, pitch, angle	19.05 × 14.83 × 2.11 × 25.4 × 90°
Tube material	carbon steel
No. of tubes per shell	1608
Tube length: overall	6.096
No. of shells in unit	2
Arrangement: series	parallel
Surface <sup>(1)</sup> : one shell	unit
Nozzle i.d. (in/out): shell <sup>(2)</sup> tubes	3 at 610/3 at 610
Shell i.d.	508/508
Exchanger type	Split backing ring floating head
TEMA designation	AXS

**Notes:**

(1) Surface based on tube o.d.  
 (2) Imping. baffles and perforated distributor plate at inlet.

MTD correction factor	
Item	Ref.
No. of shells in series	2
$P$	$\frac{103.3 - 46.1}{103.3 - 26.7} = 0.747$
$R$	$\frac{37.8 - 26.7}{103.3 - 46.1} = 0.194$
$F$ 1 shell, 1 shell pass, 1 tube pass (both unmixed)	Fig. 7.2b 0.96
$F$ 2 shells 1/2* exch. in series	assume $\approx 1.0$

Tube-side calculations ( $\phi_1 = 1$ )		
Item	Units	Ref.
No. of tubes per pass	-	1608/2 = 804
Int. flow area (one tube)	m <sup>2</sup>	Table 17.3(a) $1.728 \times 10^{-4}$
Int. flow area (one pass)	m <sup>2</sup>	$804 \times (1.728 \times 10^{-4}) = 0.139$
Velocity in tubes	m/s	$246.64/(997 \times 0.139) = 1.78$
Mass velocity in tubes	kg/s m <sup>2</sup>	$246.64/0.139 = 1774.4$
Reynolds number ( $Re_i$ )	-	$(1774.4 \times 0.01483)/(7.647 \times 10^{-4}) = 34411$
$Re_i^{0.795} Pr^{0.495}$	-	For water use $K_1 = 1.13$
$\exp[-0.0225(\ln(Pr))^2]$	-	$5800 \times 1.13 = 6554$
Tube side coeff. ( $\alpha_{10}$ )	W/m <sup>2</sup> K	Fig. 17.1 $0.0035 + 0.264/34411^{0.42} = 0.00678$
Friction factor ( $f_i$ )	-	[6.23c] $2 \times 2 \times 6.096 = 24.384$
Total travel ( $L$ )	m	-
Straight loss ( $\Delta P_s$ )	Pa	[6.22] $(4 \times 0.00678 \times 24.384 \times 1774.4^2)/(2 \times 997 \times 0.01483) = 70410$
Header loss ( $\Delta P_h$ )	Pa	[6.31b] $(2 \times 2 \times 1.6 \times 1774.4^2)/(2 \times 997) = 10106$
Nozzle flow area	m <sup>2</sup>	$(\pi/4) \times 0.508^2 = 0.203$
Nozzle mass velocity	kg/s m <sup>2</sup>	$246.64/0.203 = 1215$
Nozzle loss ( $\Delta P_n$ )	Pa	[6.31a] $(2 \times 1.8 \times 1215^2)/(2 \times 997) = 2665$
Total pressure loss ( $\Delta P_T$ )	Pa	- $= 83181$



Shell-side calculations ( $\phi_s = 1$ )			
Item	Units	Ref.	
Min. no. of support baffles, spacing and thickness <sup>(2)</sup>	mm	-	3, 1435, 16
Flow area/unit baffle pitch ( $S_{mu}$ )	m <sup>2</sup> /m	Table 12.3	0.412
Central cross-flow area ( $S_m - 0.5C_1$ )/ $i_s$ <sup>(1)</sup>	m <sup>2</sup>	[12.5]	$\{(0.412 - 0.04763)/2\} \times 5.791 = 2.248$
Mass velocity ( $\dot{m}_c$ )	kg/s m <sup>2</sup>	[12.5]	$86.55/2.248 = 38.5$
Cross-flow Reynolds number ( $Re_c$ )	-	[12.5]	$(38.5 \times 0.01905)/(7.577 \times 10^{-6}) = 96796$
$J_h$ and $f_o$	-	Fig 6.5	360, 0.07
Shell-side coefficient ( $\alpha_o$ )	W/m <sup>2</sup> K	[6.25]	$(360 \times 0.03172 \times 0.552^{0.33})/0.01905 = 493$
Total no. of rows crossed (2 shells)	-	-	$2 \times 30 = 60$
Cross-flow pressure loss	Pa	[6.26]	$(2 \times 0.07 \times 38.5^2 \times 60)/17.62 = 707$
Flow area of one nozzle	m <sup>2</sup>	-	$(\pi/4) \times 0.61^2 = 0.292$
Nozzle mass velocity	kg/s m <sup>2</sup>	-	$86.55/(3 \times 0.292) = 98.8$
Nozzle pressure loss	Pa	-	$(2 \times 4 \times 98.8^2)/(2 \times 17.62) = 2216$
Total pressure loss	Pa	-	2923

Notes:

(1) From Table 12.2,  $C_1 = 47.63$  mm.

(2) See Fig. 17.5

Overall heat transfer coefficient	
Resistance (W/m <sup>2</sup> K) <sup>-1</sup>	(related to tube o.d.)
Tube-side ( $1/\alpha_{io}$ )	$1/6554 = 0.000153$
Shell-side ( $1/\alpha_o$ )	$1/493 = 0.002028$
Tube wall ( $r_w$ )	$= 0.000040$
Fouling - tubes ( $r_{fo}$ )	$r_f \times (\text{o.d./i.d.}) = 0.000450$
Fouling - shell ( $r_{fo}$ )	$= 0.000350$
Overall ( $1/U_o$ )	$1/331 = 0.003021$
Surface area (m <sup>2</sup> )	Available
	Required
$1141 \times 1000$	
$331 \times 37.9 = 912$ OK	

Shell-side calculations: flow-induced vibration check		Units or ref.
Item		
Volume flow		m/s
Correction for baffle thickness ( $B_1 = 16$ )		86.55/17.62 = 4.912
Correction for fatigue stress ( $S_f = 8.33 \times 10^7$ )		[11.23] 12.7/16 = 0.794
Corrected baffle damage constant ( $K_{bd} = 1.603 \times 10^{-4}$ )		[11.23] 1.0
Correction for tube gap ( $C_1 = 6.35$ )		Table 11.6 (1.603 $\times 10^{-4}$ )(0.794 $\times 1$ ) = 1.273 $\times 10^{-4}$
Correction for mod. of elasticity ( $E = 2 \times 10^{11}$ )		[11.24] 1.0
Corrected collision damage constant ( $K_{cd} = 1.431 \times 10^{-4}$ )		Table 11.6 (1.431 $\times 10^{-4}$ ) $\times 1 \times 1 = 1.431 \times 10^{-4}$
Flow area ( $S_m$ )		m <sup>2</sup> 2.248
Velocity ( $\mu_r$ )		m/s 4.912/2.248 = 2.19
Unsupported length		m 1.435
Baffle damage number		- (1.273 $\times 10^{-4}$ ) $\times 17.62 \times 2.19^2 \times 1.435^2 = 0.022$
Collision damage number		- (1.431 $\times 10^{-4}$ ) $\times 17.62 \times 2.19^2 \times 1.435^4 = 0.051$
Max. allowable damage number		[11.15] (0.00429 $\times 17.62^{0.47}$ )/(7.577 $\times 10^{-6}$ ) <sup>0.235</sup> = 0.264
Acoustic vibration check		
Tube equivalent mass (kg/m)		Table 11.7 (0.172 $\times 997$ )/998 = 0.172
Frequencies (Hz)		Table 11.3 Table 11.7 0.782 $\times$ (17.62/998) $\times$ (2.5/2.75) = 0.013
	Internal ( $\rho_l = 997 \text{ kg/m}^3$ )	Table 11.7 0.881
	External ( $M_a = 2.5$ ) ( $\rho_o = 17.62 \text{ kg/m}^3$ )	Table 11.7 1.066
	Tube alone ( $\rho_m = 7842 \text{ kg/m}^3$ )	[11.21] (0.881/1.066) <sup>0.5</sup> = 0.909
	Total	[11.21] 1.0
	Correction for equivalent mass	Table 11.6 (48.16 $\times 0.909 \times 1$ )/1.435 <sup>2</sup> = 21.3
	Correction for mod. of elasticity	Table 11.1 0.35
	Tube natural frequency ( $k_{nr} = 48.16$ )	[11.2] (0.35 $\times 2.19$ )/0.01905 = 40.2
	Strouhal number	[11.8] (2.19 $\times 0.01905$ )/(0.0254 $\times 0.0254$ ) = 64.67
	Vortex shedding frequency	[11.8] [3.05 {1 - (d <sub>o</sub> /P <sub>t</sub> ) <sup>2</sup> + 0.28}]
	{ $u_r d_o / (P_t P_t)$ } ( $P_t = P_t$ )	[11.8] 64.67 $\times 0.471 = 30.5$
	[3.05 {1 - (d <sub>o</sub> /P <sub>t</sub> ) <sup>2</sup> + 0.28}]	[11.17] 0.594 {(4.472 $\times 10^5$ )/17.62} <sup>0.5</sup> / 1.524 = 62.1
	Turbulent buffeting frequency	[11.18] 40.2/62.1 = 0.65
	Acoustic frequency ( $p = 4.472 \times 10^5 \text{ Pa}$ )	[11.19] 30.5/62.1 = 0.49
Frequency ratios	( $f_v/f_a$ )	[11.20] 21.3/62.1 = 0.34
	( $f_b/f_a$ )	
	( $f_n/f_a$ )	

## 17.3 Shell-and-tube heat exchangers: low-fin tubes

### 17.3.1 Example 6: Gas cooler (X shell)

In the plain tube exchanger of example 5, Table 17.8, the combined conductance of the external gas film and fouling =  $1/\{(1/493) + 0.00035\} = 420 \text{ W/m}^2 \text{ K}$ . When related to the internal surface this becomes  $(420 \times 19.05)/14.83 = 539 \text{ W/m}^2 \text{ K}$ . The combined conductance of the internal water film and fouling, related to the internal surface =  $1/\{14.83/(6554 \times 19.05) + 0.00035\} = 2133 \text{ W/m}^2 \text{ K}$ . Thus the combined internal coefficient is nearly four times the combined external coefficient and there would appear to be a case for low-fin tubes. The overall coefficient, related to the internal surface =  $(331 \times 19.05)/14.83 = 425 \text{ W/m}^2 \text{ K}$ .

If the fin efficiency is assumed to be unity, a low-fin tube unit would expect to achieve a combined external coefficient, related to the internal surface  $\approx 4.14^* \times 420 = 1739 \text{ W/m}^2 \text{ K}$ . When combined with a combined internal coefficient, assumed to be of similar magnitude to the plain tube unit above, the overall coefficient, related to the internal surface =  $1/\{(1/1739) + (1/2133)\} = 958 \text{ W/m}^2$ . The overall coefficient for the low-fin unit is double that of the plain tube unit, which would suggest that only one shell, identical to those of example 5, would suffice.

The calculations are summarised in Table 17.9, from which it will be seen that the proposed shell is undersurfaced. The baffle arrangement is identical to either shell of Fig. 17.5.

Table 17.9 Example 6: Gas cooler (X shell with low-fin tubes)

Process conditions, heat load and  $\Delta T_m$  as example 5

Mechanical design data				
Item		Units		
Low-fin tube code, <sup>(3)</sup> pitch, angle		mm	195 083 × 25.4 × 90°	
Tube material		–	carbon steel	
No. of tubes per shell	No. of passes	–	1608	2
Tube length: overall	effective	m	6.096	5.791
No. of shells in unit		–	1	
Arrangement: series	parallel	–	1S	1P
Surface <sup>(1)</sup> : one shell	unit	m <sup>2</sup>	339.9	339.9
Nozzle i.d. (in/out): shell <sup>(2)</sup>	tubes	mm	3 at 610/3 at 610	508/508
Shell i.d.		mm	1524	
Exchanger type		–	Split backing ring floating head	
TEMA designation		–	AXS	

\* From Table 13.3.

## Notes:

- (1) Surface based on tube i.d.  
 (2) Imping. baffles and perforated distributor plate at inlet.  
 (3) Tube data from Table 13.3: below:
- |   |  |
|---|--|
| Plain end o.d.                                      | = 19.05 mm                                   |
| Fin density   | = 748 per metre                              |
| Fin o.d. ( $d_f$ ), thk ( $t_f$ ), height ( $l_f$ ) | = $18.75 \times 0.42 \times 1.45$ mm         |
| Inside dia. in finned portion                       | = 11.61 mm                                   |
| Equivalent dia. ( $d_e$ )                           | = 16.76 mm                                   |
| Total external surface/metre ( $A_e$ )              | = $0.151 \text{ m}^2/\text{m}$               |
| Surface area ratio (extl: intl)                     | = 4.14                                       |
| Internal surface per metre ( $A_i$ )                | = $0.151/4.14 = 0.0365 \text{ m}^2/\text{m}$ |

**MTD correction factor**

 Take  $F \approx 0.98$ , i.e.  $\Delta T_m = 37.9 \times 0.98 = 37.1^\circ\text{C}$ 
**Tube-side calculations ( $\phi_i = 1$ )**

Item	Units	Ref.	
No. of tubes per pass	-	-	$1608/2 = 804$
Int. flow area (one tube)	$\text{m}^2$	-	$(\pi/4) \times 0.01161^2 = 1.059 \times 10^{-4}$
Int. flow area (one pass)	$\text{m}^2$	-	$804 \times (1.059 \times 10^{-4}) = 0.0851$
Velocity in tubes	$\text{m/s}$	-	$246.64/(997 \times 0.0851) = 2.907$
Mass velocity in tubes	$\text{kg/s m}^2$	-	$246.64/0.0851 = 2898.2$
Reynolds number ( $Re_i$ )	-	-	$(2898.2 \times 0.01161)/(7.647 \times 10^{-4}) = 44002$
$Re_i^{0.795} Pr^{0.495}$	-	For water use	av. temp = $(26.7 + 37.8)/2 = 32.3^\circ\text{C}$
$\exp[-0.0225\{\ln(Pr)\}^2]$	-		$K_t = 1.13$
Tube side coeff. ( $\alpha_i$ )	$\text{W/m}^2\text{K}$	Fig. 17.1	$\approx 8300 \times 1.13 = 9379$
Friction factor ( $f_i$ )	-	[6.23c]	$0.0035 + 0.264/44002^{0.42} = 0.00646$
Total travel ( $L$ )	m	-	$2 \times 6.096 = 12.192$
Straight loss ( $\Delta P_s$ )	Pa	[6.22]	$(4 \times 0.00646 \times 12.192 \times 2898.2^2)/(2 \times 997 \times 0.01161) = 114305$
Header loss ( $\Delta P_h$ )	Pa	[6.31b]	$(2 \times 1.6 \times 2898.2^2)/(2 \times 997) = 13480$
Nozzle flow area	$\text{m}^2$	-	$(\pi/4) \times 0.508^2 = 0.203$
Nozzle mass velocity	$\text{kg/s m}^2$	-	$246.64/0.203 = 1215$
Nozzle loss ( $\Delta P_n$ )	Pa	[6.31a]	$(1.8 \times 1215^2)/(2 \times 997) = 1333$
Total pressure loss ( $\Delta P_T$ )	Pa	-	$= 129118$

(high)

Shell-side calculations ( $\phi_s = 1$ )			
Item	Units	Ref.	
Min. no. of support baffles, spacing and thickness <sup>(4)</sup>	mm	-	3, 1435, 16
Cross-flow area	m <sup>2</sup>	Table [12.1]	$\left\{ 0.0238 + \frac{1.524 - 0.04763 - 0.01676}{1 \times 0.0254} (0.0254 - 0.01676) \right\} 5.791 = 3.013$
Mass velocity ( $m_e$ )	kg/s m <sup>2</sup>	-	$86.55/3.013 = 28.726$
Reynolds number ( $Re_c$ )	-	-	$(28.726 \times 0.01676)/(7.577 \times 10^{-6}) = 63541$
$J_1$ and $f_o$	-	Fig 6.5	280, 0.078
Coefficient to external surface of low fin tube ( $\alpha_f$ )	W/m <sup>2</sup> K	[6.25]	$(280 \times 0.03172 \times 0.552^{0.33})/0.01676 = 435.6$
( $\alpha_f$ ) combined with external fouling ( $\alpha_{fi}$ )	W/m <sup>2</sup> K	[13.2]	$1/(1/435.6 + 0.00035) = 378$
( $m_e$ ), ( $m_e l_e$ ) <sup>(1)</sup>	(1/m)	-	$\{(2 \times 378)/(52 \times 0.42 \times 10^{-3})\}^{0.5} = 186.05, 186.05 \times (1.45 \times 10^{-3}) = 0.27$
Fin efficiency ( $\Omega_f$ ) <sup>(2)</sup>	-	[9.3]	$\{\tanh(0.27)\}/0.27 = 0.976$
( $\alpha_f$ ) referred to internal surface ( $\alpha_{fi}$ )	W/m <sup>2</sup> K	[13.5]	$378 \times \{(0.8 \times 0.976) + 0.2\} \times 4.14 = 1535$
Cross-flow pressure loss (no. of rows = 30)	Pa	[6.26] <sup>(3)</sup>	$\{(2 \times 0.078 \times 28.726^2 \times 30)/17.62\} \times 1.4 =$
Flow area of one nozzle	m <sup>2</sup>	-	$(\pi/4) \times 0.61^2 = 0.292$
Nozzle mass velocity	kg/s m <sup>2</sup>	-	$86.55/(3 \times 0.292) = 98.8$
Nozzle pressure loss	Pa	-	$(4 \times 98.8^2)/(2 \times 17.62) =$
Total pressure loss	Pa	-	$= 1108$
			$= 1415$

Notes:

- (1)  $\lambda_f$  from Table 9.1
- (2) Also obtainable from Table 9.4.
- (3) See step (12), section 13.4.
- (4) See Fig 17.5.

Overall heat transfer coefficient	
Resistance ( $W/m^2 K$ ) <sup>-1</sup>	(related to tube o.d.)
Tube-side ( $1/\alpha_i$ )	$1/9379 = 0.000107$
Shell-side ( $1/\alpha_R$ )	$1/1535 = 0.000651$
Tube wall ( $r_w$ )	$= 0.000040$
Fouling – tubes ( $r_f$ )	$= 0.000350$
Fouling – shell ( $r_o$ )	included in ( $\alpha_R$ )
Overall ( $1/U_i$ )	$1/871.1 = 0.001148$
Surface area (m <sup>2</sup> )	
Available	339.9
Required	$\frac{11441 \times 1000}{871.1 \times 37.1} = 354$
$= Q/(U_i \Delta T_m)$	$= 354$
	OK

4% undersurfaced

Shell-side calculations: flow-induced vibration check  
 Similar to example 5

## 17.3.2 Example 7: Crude-oil cooler

This example presents a low-fin tube alternative to the plain tube design of example 1. Although the shell-side coefficient of example 1 is controlling, the ratio of internal/external coefficient, including fouling, is only about two. As the tubes are carbon steel, it is not a clear case for low-fin tubes, but serves to demonstrate the application of the manual method described in Chapter 12 and section 13.4.4.

Referring to example 1, the combined external coefficient and fouling, referred to the external surface, is  $908 \text{ W/m}^2 \text{ K}$ . The combined internal coefficient and fouling, referred to the internal surface, is  $2463 \text{ W/m}^2 \text{ K}$ . If the fin efficiency is 100%, and code 195083 low-fin tubes are used, the combined external coefficient becomes  $908 \times 4.14 = 3759 \text{ W/m}^2 \text{ K}$  when referred to the internal surface. The overall coefficient referred to the internal surface is of the order of  $1488 \text{ W/m}^2 \text{ K}$ , requiring an internal surface area of  $(5275.4 \times 1000)/(1488 \times 43.8) = 81 \text{ m}^2$ . The tentative design of example 7 has a shell of 737 mm inside diameter and an internal surface area of  $90.4 \text{ m}^2$ .

It will be seen from Table 17.10 that the tentative design was a good choice and provides 4.3% oversurface within the allowable pressure losses.

**Table 17.10** Example 7: Crude-oil cooler (E shell) (as example 1, but with low-fin tubes)

Process conditions, heat load and and log MTD as example 1

Mechanical design data				
Item		Units		
Low-fin tube code <sup>(3)</sup> , pitch, angle		mm	195 083 × 25.4 × 90°	
Tube material		–	carbon steel	
No. of tubes per shell	No. of passes	–	520	2
Tube length: overall	effective	m	5	4.764
No. of shells in unit		–	1	
Arrangement: series	parallel	–	1S	1P
Surface <sup>(1)</sup> : one shell	unit	m <sup>2</sup>	90.4	90.4
Nozzle i.d. (in/out): shell <sup>(2)</sup>	tubes	mm	254.5/254/5	202.7/202.7
Shell i.d.		mm	737	
Exchanger type		–	Split backing ring floating head	
TEMA designation		–	AES	

Notes:

- (1) Surface based on tube i.d.
- (2) Imping. baffle at inlet.
- (3) Low-fin tube data as example 6.

MTD correction factor

As example 1:  $F = 0.917$ ,  $\Delta T_{lm} = 47.8 \text{ }^\circ\text{C}$ ,  $\Delta T_m = 43.8 \text{ }^\circ\text{C}$

**Tube-side calculations ( $\phi_t = 1$ )**

Item	Units	Ref.
No. of tubes per pass	-	520/2 = 260
Int. flow area (one tube)	m <sup>2</sup>	$(\pi/4) \times 0.01161^2 = 1.059 \times 10^{-4}$
Int. flow area (one pass)	m <sup>2</sup>	$260 \times 1.059 \times 10^{-4} = 0.0275$
Velocity in tubes	m/s	$45/(995 \times 0.0275) = 1.65$
Mass velocity in tubes	kg/s m <sup>2</sup>	$45/0.0275 = 1636.36$
Reynolds number ( $Re_t$ )	-	$(1636.36 \times 0.01161)/0.00072 = 26386$
$Re_t^{0.795} Pr^{0.495}$	-	av. temp = (21 + 49)/2 = 35 °C
$\exp[-0.0225 \{\log(Pr)\}^2]$	-	$K_t = 1.16$
Tube side coeff. ( $\alpha_t$ )	W/m <sup>2</sup> K	$\approx 5100 \times 1.16 = 5916$
Friction factor ( $f_t$ )	-	$0.0035 + 0.264/26386^{0.42} = 0.00717$
Total travel (L)	m	$2 \times 5 = 10$
Straight loss ( $\Delta P_t$ )	Pa	$(4 \times 0.00717 \times 10 \times 1636.36^2)/(2 \times 995 \times 0.01161) = 33239$
Header loss ( $\Delta P_h$ )	Pa	$(1.6 \times 2 \times 1636.36^2)/(2 \times 995) = 4306$
Nozzle flow area	m <sup>2</sup>	$(\pi/4) \times 0.2027^2 = 0.0323$
Nozzle mass velocity	kg/s m <sup>2</sup>	$45/0.0323 = 1393.2$
Nozzle loss ( $\Delta P_n$ )	Pa	$(1.8 \times 1393.2^2)/(2 \times 995) = 1756$
Total pressure loss ( $\Delta P_T$ )	Pa	$= 39301$

**Shell-side calculations: baffle data and Reynolds number**

Item	Units	Ref.	
Baffle data	Spacing: central ( $l_c$ )	end ( $l_e$ )	275
	Number ( $N_b$ )	thickness ( $B_t$ )	14
	Spacing ratios: central (BSR)	end ( $l_r$ )	$275/737 = 0.373$
Central cross-flow area ( $S_m$ )	C <sub>1</sub> = 0.04128, $y = 1$ , $p = 0.0254$ $d_e = 0.01676$ , $p - d_e = 0.00864$ $D_s = 0.737$ , $D_s - C_1 - d_e = 0.679$	Tables 12.1, 12.2 and 3.5	$[0.04128 + (0.679 \times 0.00864)/(1 \times 0.0254)] \times 0.275 = 0.0749$
Mass velocity ( $m_c$ )	kg/s m <sup>2</sup>	[12.5]	$63.77/0.0749 = 851.4$
Cross-flow Reynolds number ( $Re_c$ )	-	[12.5]	$(851.4 \times 0.01676)/0.00189 = 7550$ (i.e. turbulent)

Notes:  
(1) Baffle arrangement similar to Fig. 17.2 for example 1.



**Shell-side calculations: design factors**

Design factor	Ref.	Heat transfer	Cross loss*	Window loss
Flow rate ( $F_F$ )	Table 12.4	$63.77^{0.651} = 14.956$	$63.77^2 = 4066.6$	$63.77^2 = 4066.6$
Physical property ( $F_p$ )	Table 12.4	$21770.333 \times 0.122^{20.667} = 23.34$ $0.001890.318$	$1786.4 = 0.001272$	$1786.4 = 0.001272$
Mechanical design ( $F_M$ )	Table 13.6	4.87	754	604
$X_c$ (BSR > 0.35)	Table 12.8	0.444	0.050	0.294
$m$ (BSR > 0.35)	Table 12.8	0.586	2.019	0.856
$F_c$	[12.6]	$0.444/0.373^{0.586} = 0.791$	$0.050/0.373^{2.019} = 0.366$	$0.294/0.373^{0.856} = 0.684$
$F_E$ (heat tr.); $X_c, e$ (cross loss)	Table 12.5 Table 12.9	0.92	$2.0, 1.0, X_c/l_c^* = 1.0$	-

\*Table 12.4(a), 90° pitch,  $Re_c = 7550, p/d_o = 1.33, F_c = 1.17$

**Shell-side calculations ( $\phi_b = 1$ )**

Item	Units	Ref.	
Shell-side heat trans. coeff. ( $\alpha_i$ )	W/m <sup>2</sup> K	[12.2]	$14.956 \times 23.34 \times 4.87 \times 0.791 \times 0.92 = 1237$
Central loss (one pass) ( $\Delta P_c$ )	Pa	[12.3]	$4066.6 \times 0.001272 \times 754 \times 0.366 \times 1.17 \times 1.4 = 2338$
Window loss (one window) ( $\Delta P_w$ )	Pa	[12.4]	$4066.6 \times 0.001272 \times 604 \times 0.684 = 2137$
Nozzle loss	m <sup>2</sup>		$(\pi/4) \times 0.254^2 = 0.0509$
Mass velocity loss ( $\Delta P_{ni} + \Delta P_{no}$ )	kg/s m <sup>2</sup>		$63.77/0.0509 = 1252.8$
Total central loss ( $\Delta P_c(N_b - 1)$ )	Pa		$(4 \times 1252.8^2)/(2 \times 786.4) = 3992$
Total window loss ( $\Delta P_w N_b$ )	Pa		$2338 \times 13 = 30394$
End space loss ( $(\Delta P_c X_c)/(l_c)^2$ )	Pa	[12.8]	$2137 \times 14 = 29918$
Total loss ( $\Delta P_s$ )	Pa		$2 \times 2338 \times 1 = 4676$
			$= 68980$
$\alpha_i$ combined with external fouling ( $\alpha_i'$ )	W/m <sup>2</sup> K	[13.2]	$1/(1/1237 + 0.00018) = 1011$
$m_e, m_{e,c}$ <sup>(1)</sup>	(1/m), (-)	[9.3]	$[(2 \times 1011)/(52 \times 0.42 \times 10^{-3})]^{0.5} = 304.3, 304.3 \times 1.45 \times 10^{-3} = 0.441$
Fin efficiency ( $\Omega_f$ ) <sup>(2)</sup>	-		$\tanh(0.441)/0.441 = 0.94$
$\alpha_i'$ referred to internal surface ( $\alpha_{if}$ )	W/m <sup>2</sup> K	[13.5]	$1011 \times \{(0.8 \times 0.94) + 0.2\} \times 4.14 = 3985$

**Notes:**  
 (1)  $\lambda_f$  from Table 9.1.  
 (2) Also obtainable from Table 9.4.

Overall heat transfer coefficient	
Resistance ( $\text{W/m}^2 \text{K})^{-1}$	
Tube-side ( $1/\alpha_i$ )	$1/5916 = 0.000169$
Shell-side ( $1/\alpha_n$ )	$1/3985 = 0.000251$
Tube wall ( $r_w$ )	$= 0.000040$
Fouling-tubes ( $r_f$ )	$= 0.000260$
Fouling-shell ( $r_o$ )	included in ( $\alpha_n$ )
Overall ( $1/U_1$ )	$1/1389 = 0.000720$
Surface area ( $\text{m}^2$ )	
Available	90.4
Required	$5275.4 \times 1000$
$= Q/(U_o \Delta T_m)$	$1389 \times 43.8 = 86.7$ OK

Shell-side calculations: flow-induced vibration check  
 Similar to example 1

## 17.4 Air-cooled heat exchangers

### 17.4.1 Example 8: Hydrocarbon liquid cooler

Section 19.5 provides an approximate method for the sizing of air-cooled heat exchangers, together with an example related to an oil-cooling service. The duty and constructional data for the estimated air-cooled unit are given below.

In order to demonstrate the thermal design procedure described in Chapter 14, exact heat transfer coefficients and pressure losses are calculated for the estimated unit. True and estimated performance is then compared.

#### *Duty and physical properties*

	<i>Process fluid</i> <i>Hydrocarbon liquid</i>	<i>Air</i>
Fluid flow rate (kg/s)	69.44	237.78 (198.15 m <sup>3</sup> /s*) by balance
Temperature range (°C)	150 → 100	25 → 54.2 (optimum)
Heat load (kW)	7267.4	
Log MTD (°C)	85	
Specific heat (J/kg K)	2093.4	1046.7
Viscosity (Ns/m <sup>2</sup> )	1 × 10 <sup>-3</sup>	—
Thermal cond. (W/m K)	0.1211	—
Prandtl number	17.29	—
Density (kg/m <sup>3</sup> )	800	1.2* (1.184 at fan)

(\* Based on dry air under 'standard conditions' of 21.1 °C and 760 mm Hg.

#### *Constructional data*

The constructional data for the air-cooled exchanger, generally, are based on Table 19.12, as follows:

Cooler type: forced-draught, plug-type headers  
 Number of bundles: 2 (side-by-side)  
 Plan size of one bundle (m): 3.05 wide × 9.75 long tubes  
 Number of rows deep: 4  
 Number of tubes in each bundle: 190  
 Number of fans per bundle: 2 (fan dia. = 2.75 m)  
 Total effective surface area: 295.8 m<sup>2</sup> (bare tube external)

The bundle arrangement is shown in Fig. 17.6.

The finned tubes and layout are identical to those used for the example in section 14.13, so that the heat transfer data of Fig. 14.3, and the pressure loss data given by equation [14.11], apply.

#### *Heat balance*

Air side:  $Q = 237.78 \times 1046.7 \times (54.2 - 25) = 7.267 \times 10^6$  W

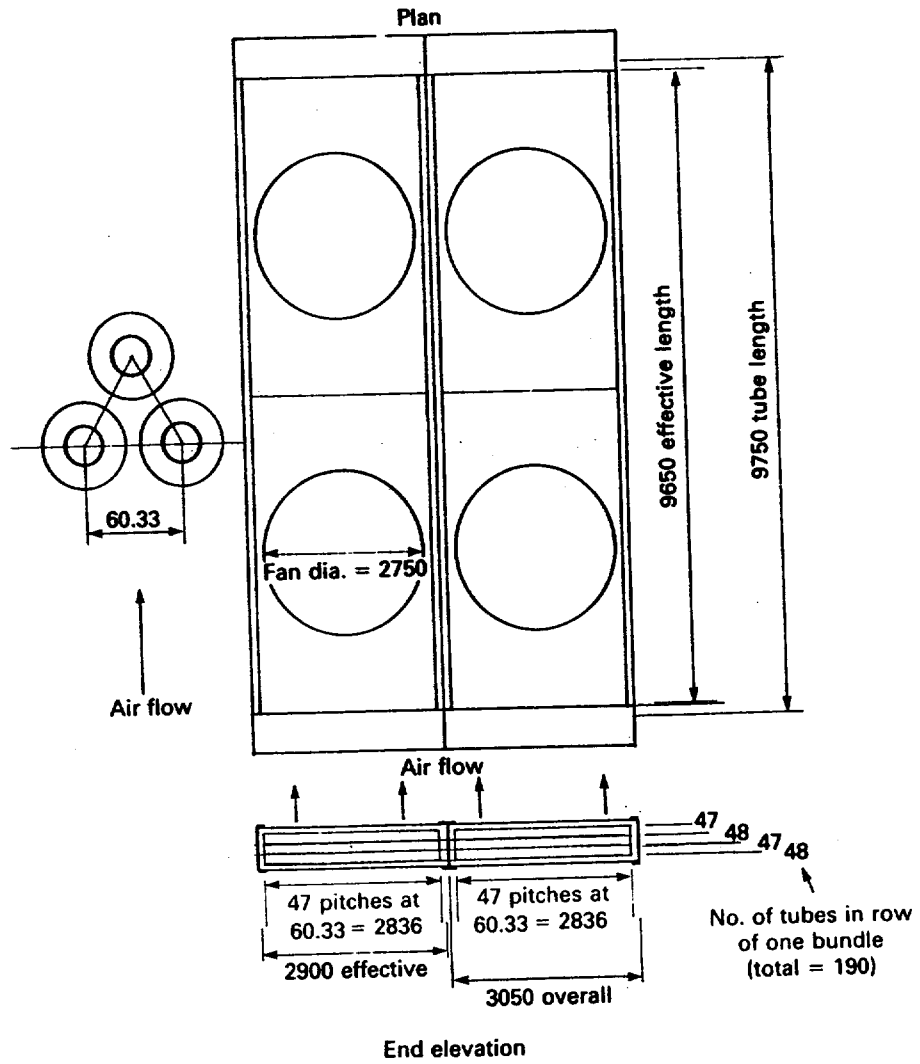
Process side:  $Q = 69.44 \times 2093.4 \times (150 - 100) = 7.268 \times 10^6$  W

#### *Air-side calculations*

Cooler face area:

$$A_g = 2 \times 2.9 \times 9.65 = 55.97 \text{ m}^2$$

Figure 17.6 General arrangement of air cooler for example 7



Std. air vel. thro' bundle:

$$u_{fs} = 198.15/55.97 = 3.54 \text{ m/s}$$

From Fig. 14.3:

$$\alpha_{fo} = 1150 \text{ W/m}^2 \text{ K}$$

Flow thro' each fan (4 fans):

$$V_a = 237.78/(4 \times 1.184) = 50.21 \text{ m}^3/\text{s}$$

Fan opening area

$$= (\pi/4) \times 2.75^2 = 5.94 \text{ m}^2$$

Velocity thro' fan opening:

$$u_f = 50.21/5.94 = 8.45 \text{ m/s}$$

Air temp. corr. (equation [14.11]):

$$f_m = 1.0$$

Bundle pressure loss (equation [14.11]):

$$\Delta P_b = 4 \times 0.5 \times 3.54^{1.75} \times 1.0 = 18.3 \text{ mm w.g.}$$

Fan and plenum pressure loss (equation [14.2]):

$$\Delta P_p = 0.06 \times 1.184 \times 8.45^2 = 5.1 \text{ mm w.g.}$$

Total loss:

$$\Delta P_{sh} = 18.3 + 5.1 = 23.4 \text{ mm w.g.}$$

Power at fan shaft (equation [14.4]):

$$\dot{W}_s = (4 \times 9.8 \times 23.4 \times 50.21)/1000 = 46.06 \text{ kW}$$

Fan motor power (equation [14.5]):

$$\dot{W}_{ms} = 46.06/0.8 (E_f = 0.8) = 58 \text{ kW}$$

#### *Process (tube-side) calculations*

From Table 19.12, the total number of tubes in one bundle is 190, and the number of tubes in each of the four horizontal rows is 48, 47, 48, 47. As there are two bundles, a total of 380 tubes is available to the tube-side fluid, but the number of passes is unknown at this stage. Unless previous calculation or experience dictates otherwise, assume two as an initial guess.

One tube, int. flow area (Table 17.3) =  $3.524 \times 10^{-4}$

2 passes, 2 bundles, no. of tubes per pass =  $2 \times (48 + 47) = 190$

Internal flow area =  $190 \times (3.524 \times 10^{-4}) = 0.067 \text{ m}^2$

Mass velocity:  $\dot{m} = 69.44/0.067 = 1036.4 \text{ kg/s m}^2$

Reynolds number:  $Re_i = (1036.4 \times 0.02118)/(1 \times 10^{-3}) = 21951$

$Re_i^{0.795} = 2827.8$

Prandtl number:  $Pr = 17.29$

$Pr^{0.495} = 4.099$

$\exp[-0.0225 \times \{\ln(Pr)\}^2] = 0.833$

Tube-side coeff. {equation [6.16a]}:

$$\begin{aligned} \alpha_i &= (0.0225 \times 0.1211)/(0.02118) \times (2827.8 \times 4.099 \times 0.833) \\ &= 1242 \text{ W/m}^2 \text{ K} \end{aligned}$$

( $\alpha_i$ ), ref. to ext. bare surface:

$$\alpha_{ib} = (1242 \times 0.02118)/0.0254 = 1036 \text{ W/m}^2 \text{ K}$$

Tube-wall resistance ( $\lambda_w = 45$ ):

$$\begin{aligned} r_w &= \{0.0254 \times \ln(0.0254/0.02118)\}/(2 \times 45) \\ &= 5.13 \times 10^{-5} \text{ (W/m}^2 \text{ K)}^{-1} \end{aligned}$$

Friction factor (equation [6.23c]):

$$f_i = 0.0035 + 0.264/21951^{0.42} = 0.00746$$

Number of passes,  $N_p = 2$ :

$$L = 2 \times 9.75 = 19.5 \text{ m}$$

Straight tube loss (equation [6.22]):

$$\begin{aligned}\Delta P_s &= (4 \times 0.00746 \times 19.5 \times 1036.4^2)/(2 \times 800 \times 0.02118) \\ &= 18443 \text{ Pa}\end{aligned}$$

Header loss (equation [6.31b]):

$$\Delta P_h = (2 \times 1.6 \times 1036.4^2)/(2 \times 800) = 2148 \text{ Pa}$$

Total loss (excluding nozzles):

$$\Delta P_T = 18443 + 2148 = 20591 \text{ Pa}$$

The initial assumption of two passes is correct as it provides a tube-side heat transfer coefficient of the same magnitude as the air-side coefficient, with acceptable pressure loss.

#### *Performance comparison*

The clean overall heat transfer coefficient ( $U_c$ ), referred to the bare external surface, is given by equation [14.1]:

$$\begin{aligned}\frac{1}{U_c} &= \frac{1}{1150} + \frac{1}{1036} + (5.13 \times 10^{-5}) \\ U_c &= 530 \text{ W/m}^2 \text{ K}\end{aligned}$$

The fouled overall heat transfer coefficient ( $U$ ), was originally estimated in Chapter 19 to be  $325 \text{ W/m}^2 \text{ K}$ , which required a surface area of  $263 \text{ m}^2$ . The internal fouling factor, referred to the bare external surface, is therefore:

$$r_f = \frac{1}{325} - \frac{1}{530} = 0.00119 \text{ (W/m}^2 \text{ K)}^{-1}$$

This is a generous fouling factor for such a service. In order to utilise standard bundles, the estimated surface area was increased by a factor of  $295.8/263 = 1.12$ , thus providing even more oversurface. The fan power consumption of  $58 \text{ kW}$  is about 1.55 times that of the estimated cooler.

The reason for the discrepancy lies in the poor estimation of the overall heat transfer coefficient for the approximate sizing method of Chapter 19. Better agreement is obtained if both sets of calculations are repeated, based on an overall heat transfer coefficient of  $450 \text{ W/m}^2 \text{ K}$ .

### 17.4.2 Example 9: Hydrocarbon gas cooler

Example 8 showed the step-by-step heat transfer and pressure loss calculations required for an air-cooled heat exchanger of known design. This example provides the step-by-step calculations for the design of an air-cooled heat exchanger where only the process conditions are known. The calculations show the relationship between exit air temperature, air velocity, plan area, capital cost and power consumption.

*Duty and physical properties*

	<i>Process side</i>	
	hydrocarbon gas	air
Fluid name		
Flow rate (kg/s)	31.5	—
Temperature range (°C)	200 → 80	inlet = 25
Heat load (kW)	7121.52	
Specific heat (J/kg K)	1884	—
Viscosity (Ns/m <sup>2</sup> )	$1.13 \times 10^{-5}$	—
Thermal conductivity (W/m K)	0.0254	—
Prandtl number	0.838	—
Density (kg/m <sup>3</sup> )	27.56	std 1.2, at fan 1.184
Fouling factor* (W/m <sup>2</sup> K) <sup>-1</sup>	0.00035	—
Max. pressure loss† (Pa)	$1 \times 10^5$	—
Operating pressure Pa(abs)	$18.25 \times 10^5$	—

\* Referred to external bare surface  
† Excluding nozzle losses

*Constructional data*

The constructional data are again based on Table 19.12 and section 14.13.

Cooler type: forced-draught, plug-type headers

Number of fins per metre: 433

Fin o.d. × thickness (mm):  $57.15 \times 0.4$

Fin material and bond: aluminium, embedded

Base tube-o.d. × i.d. × pitch × angle (mm):

$$25.4 \times 21.18 \times 60.33 \times 30^\circ$$

Base tube material: carbon steel

*Basis for calculations*

Heat transfer, pressure loss and power calculations, may be expressed by equations [17.2] – [17.11] below. Based on the proportions given in section 3.6.5 it is assumed provisionally that the total fan opening area is one-half that of the cooler face area. In addition,  $\Delta T_a$  = air temperature rise (°C) and  $n$  = number of tubes in one pass.

From section 6.10.2:

$$Re = (167.578 \times 10^6)/n \quad [17.2]$$

(Note:  $Re > 10000$ , i.e. fully turbulent, if  $n \geq 16552$ )

From equation [6.16a]:

$$\alpha_{ib} = 71150.2/n^{0.795} \quad [17.3]$$

From equation [6.23c]:

$$f_i = 0.0035 + (9.278 \times 10^{-5})(n^{0.42}) \quad [17.4]$$

From equation [6.22]:

$$\Delta P_i = (2.739 \times 10^{10})(f_i N_p L/n^2) \quad [17.5]$$

From equation [6.31b]:

$$\Delta P_h = (2.32 \times 10^8)(N_p/n^2) \quad [17.6]$$

Air mass flow rate:

$$W_a = 6803.78/\Delta T_a \quad [17.7]$$

Standard air volume flow:

$$V_s = 5669.82/\Delta T_a \quad [17.8]$$

Bundle loss/row:

$$\Delta P_b = 0.5(u_{fs})^{1.75} f_m \quad [17.9]$$

Fan and plenum loss:

$$\Delta P_p = 0.292(u_{fs})^2 \quad [17.10]$$

From equations [14.4] and [14.5]:

$$W_{ms} = 0.01035(W_a \Delta P_{sh})(\text{eff.} = 0.8) \quad [17.11]$$

### Summary of calculations

Table 17.11 provides a summary of the calculations based on various exit air temperatures and air velocities, giving a total of eight alternative designs. Further designs are possible. The operating costs are presented in Table 14.1.

## 17.5 Finned-tube double-pipe heat exchangers

### 17.5.1 Example 10: Hydrocarbon gas/hydrocarbon liquid exchanger

Chapter 15 describes a method for the thermal design of double-pipe heat exchangers. This example provides the calculations for the design of a multi-tube double-pipe gas-liquid heat exchanger having constructional data exactly as given in section 15.5.

#### Duty and physical properties

	Annulus fluid hydrocarbon gas	Tube-side fluid hydrocarbon liquid
Fluid name		
Flow rate ( $\dot{M}$ ) (kg/s)	0.6	3
Temperature range (°C)	250 → 25	20 → 62
Heat load (kW)		299.57
Specific heat (J/kg K)	2219	2377.5
Viscosity (N s/m <sup>2</sup> )	$1 \times 10^{-5}$	$5 \times 10^{-4}$
Thermal conductivity (W/m K)	0.028	0.110
Prandtl number (Pr)	0.793	10.81
Density (kg/m <sup>3</sup> )	4.0	748
Fouling factor (W/m <sup>2</sup> K) <sup>-1</sup>	0.0003	0.0002
Tube-wall resistance (W/m <sup>2</sup> K) <sup>-1</sup>		$4 \times 10^{-5}$
Max. pressure loss* (Pa)	50 000	145 000
Log mean temp. diff. ( $\Delta T_{lm}$ ) (°C)		50.4

\* Excluding nozzle losses

The annulus flow rate and average physical properties are identical to the example of section 15.5.



Table 17.11 Air-cooled heat exchangers – calculations for example 8 (Hydrocarbon gas cooler)

Item	Units	Source	Calculations (* denotes non-standard length)							
			1	2	3	4	5	6	7	8
Exit air temp.	°C	—		60		70				80
Air temperature rise ( $\Delta T$ )	°C	—		35		45				55
Average air temperature in bundle	°C	—		42.5		47.5				52.5
Air mass flow rate ( $W_a$ )	kg/s	[17.7]		194.4		151.2				123.7
Std. air volume flow ( $V_s$ )	m <sup>3</sup> /s	[17.8]	162		126		103			
No. of bundles in parallel	—	—	2	1	2	1	2	2	2	2
Nominal bundle dimensions	m x m	Table 19.12	3.05 x 9.75	3.66 x 12.19	3.66 x 9.75	3.66 x 12.19	2.44 x 6.71*	3.66 x 9.75	2.44 x 6.71*	3.66 x 3.66
Bundle face dimensions	m x m	—	2-2.9 x 9.65	1-3.51 x 12.09	2-3.51 x 9.65	1-3.51 x 12.09	2-2.29 x 6.61	2-3.51 x 9.65	2-2.29 x 6.61	2-3.51 x 3.56
Bundle face area ( $A_g$ )	m <sup>2</sup>	—	55.97	42.44	67.74	42.44	30.27	67.74	30.27	24.99
Std. air face velocity ( $u_{fs}$ )	m/s	$V_s/A_g$	2.89	3.82	1.86	2.97	4.16	1.52	3.40	4.12
Number of rows deep	—	Table 19.12	3	3	3	4	4	4	5	6
Tube arrangement in one bundle	—	Table 19.12	2 x 48, 1 x 47	2 x 57, 1 x 56	2 x 57, 1 x 56	2 x 57, 1 x 56	2 x 56, 2 x 38, 2 x 37	2 x 57, 2 x 56	3 x 38, 2 x 37	3 x 57, 3 x 56
Total number of tubes in cooler	—	Table 19.12	286	170	340	226	300	452	376	678
Number of tube side passes ( $N_p$ )	—	Table 19.12	1	1	1	1	2	1	2	4
Number of tubes in one pass ( $n$ )	—	Table 19.12	286	170	340	226	150	452	188	170
Effective surface area ( $A_o$ )	m <sup>2</sup>	Table 19.12	222.6	165.4	264.6	219.9	158.2	351.8	198.3	197.8
log MTD ( $\Delta T_{lm}$ )	°C	[7.1]	91	91	87.2	87.2	87.2	83.3	83.3	83.3
MTD correction factor ( $F$ )	—	Table 14.2	0.94	0.94	0.92	0.92	0.98	0.90	0.96	1.00

Table 17.11 (cont.)

Item	Units	Source	Calculations (* denotes non-standard length)							
			1	2	3	4	5	6	7	8
Effective temperature difference ( $\Delta T$ )	°C	$F\Delta T_{lm}$	85.5	85.5	80.2	80.2	85.5	75	80.0	83.3
Required overall coefficient ( $U_o$ )	W/m <sup>2</sup> K	$\frac{Q}{A_o\Delta T}$	374.2	503.6	335.6	403.8	526.5	269.9	448.9	432.2
Air-side coefficient ( $\alpha_{fo}$ )	W/m <sup>2</sup> K	Fig. 14.3	1020	1210	785	1030	1250	690	1130	1250
Tube-side coefficient ( $\alpha_{fb}$ )	W/m <sup>2</sup> K	[17.3]	793	1199	691	956	1325	551	1107	1199
Calculated overall coefficient ( $U$ )	W/m <sup>2</sup> K	$1/((1/\alpha_{fo}) + (1/\alpha_{fb}))$ +0.00035}	385.9	497.4	325.6	422.5	525	276.7	467.7	504.0
Over (+) or under (-) surface	(%)	$100((U/U_o) - 1)$	+3.1	-1.2	-3.0	+4.6	-0.3	+2.5	+4.2	+16.6
Tube-side Friction factor	—	[17.4]	0.0045	0.0043	0.0046	0.0044	0.0043	0.0047	0.0043	0.0043
pressure loss										
Straight friction loss ( $\Delta P_i$ )	Pa	[17.5]	14692	49678	10627	28763	70247	6144	44720	59663
Header loss ( $\Delta P_h$ )	Pa	[17.6]	2836	8028	2007	4542	20622	1136	13128	32111
Total loss ( $\Delta P_T$ )	Pa	—	17528	57706	12634	33305	90869	7280	57848	91774
Air-side pressure loss										
Bundle loss ( $\Delta P_b$ )	mm water	[17.9]	9.7	15.8	4.6	13.8	24.9	4.4	22.3	37.5
Fan and plenum loss ( $\Delta P_p$ )	mm water	[17.10]	2.4	4.3	1.0	2.6	5.1	0.7	3.4	5.0
Total loss ( $\Delta P_{sh}$ )	mm water	—	12.1	20.1	5.6	16.4	30.0	5.1	25.7	42.5
Summary										
Plan area	m <sup>2</sup>	—	59.5	44.6	71.4	44.6	32.7	71.4	32.7	26.8
Surface area	m <sup>2</sup>	—	222.6	165.4	264.6	219.9	158.2	351.8	198.2	197.8
Ex-works cost	£	Fig. 19.1	49000	39000	56300	42000	33000	59600	34700	31800
Fan power	kW	[17.11]	24.3	40.4	8.8	25.7	46.9	6.5	32.9	54.4

It is assumed that the annulus and inner tube fluids are routed through one double-pipe section in countercurrent flow. The number of lengths in series is unknown at this stage.

*Tube side-calculations ( $\phi_i = 1$ )*

Flow area (7 tubes):

$$a_i = (\pi/4)(0.01483^2 \times 7) = 0.00121 \text{ m}^2$$

Mass velocity:

$$\dot{m}_i = 3/0.00121 = 2479.3 \text{ kg/s m}^2$$

Reynolds number:

$$\text{Re}_i = (2479.3 \times 0.01483)/(5 \times 10^{-4}) = 73536$$

$$\text{Re}_i^{0.795} = 7394$$

From equation [6.16a]

$$\text{Pr}^{0.495} [\exp -0.0225\{\ln(\text{Pr})\}^2] = 10.81^{0.495} [\exp -0.0225\{\ln(10.81)\}^2] = 2.86$$

$$\alpha_i = 0.0225 \times (0.11/0.01483)(2.86 \times 7394) = 3529 \text{ W/m}^2 \text{ K}$$

From equation [6.23c], friction factor:

$$f_i = 0.0035 + 0.264/73536^{0.42} = 0.00589$$

From equation [6.22], friction loss (1 m length):

$$\Delta P_i = (4 \times 0.00589 \times 1 \times 2479.3^2)/(2 \times 748 \times 0.01483) = 6528 \text{ Pa}$$

From equation [15.12], 1 bend loss:

$$\Delta P_u = 2479.3^2/(4 \times 748) = 2054 \text{ Pa}$$

*Annulus calculations ( $\phi_o = 1$ )*

The average heat transfer coefficient, friction loss for 1 m length, and one return bend loss have already been calculated in section 15.5.

*Overall coefficient and surface area calculations*

From equation [15.9]

$$\begin{aligned} \text{overall coefficient } U_i &= \frac{1}{1/1900 + 0.00004 + 0.0002 + 1/3529} \\ &= 953 \text{ W/m}^2 \text{ K} \end{aligned}$$

From equation [15.10]

internal surface required:

$$A_i = (299.57 \times 1000)/(953 \times 50.4) = 6.24 \text{ m}^2$$

1 leg, internal surface per metre:

$$A_i = 0.326 \text{ m}^2$$

total length required:

$$L = 6.24/0.326 = 19.14 \text{ m}$$

Use 2–10 m lengths

### Pressure loss calculations

#### Annulus

$$\text{Section 15.5, friction loss: } \Delta P_s = 2 \times 10 \times 2384 = 47680 \text{ Pa}$$

$$\text{Section 15.5, 1 bend loss: } \Delta P_{\text{tb}} = 1 \times 730.5 = \underline{731 \text{ Pa}}$$

$$\text{Total (excluding nozzles)} = \underline{48411 \text{ Pa (OK)}}$$

#### Tube-side

$$\text{Friction loss: } \Delta P_i = 2 \times 10 \times 6528 = 130560 \text{ Pa}$$

$$\text{Bend loss: } \Delta P_u = 1 \times 2054 = \underline{2054 \text{ Pa}}$$

$$\text{Total (excluding nozzles)} = \underline{132614 \text{ Pa (OK)}}$$

## 17.5.2 Example 11: Lube oil heater

Example 10 showed the step-by-step calculations for the design of a longitudinally finned double-pipe heat exchanger for a gas–liquid service. This example provides the design for a finned double-pipe lube oil heater in which the oil is viscous. Its viscosity decreases almost ten-fold between the inlet and outlet temperatures. Accordingly there is a significant viscosity gradient between the bulk of the oil and adjacent surface, such that the viscosity correction factor, described in section 6.8, is not unity.

As the heat transfer coefficient for the lube oil will be considerably lower than that of the hot water, the oil is routed through the annulus. The same standard double-pipe model as section 15.6 is used, for which annulus heat transfer data are presented in Fig. 15.1. Table 17.12 provides a summary of the calculations for tubes having straight fins, but this example also examines the effect of fins having cut and twist, as discussed in section 5.13.

Table 17.12 Example 11: Lube oil heater

Process conditions				
Item	Units	Annulus	Tube-side	
Fluid name	–	lube oil	hot water	
Flow rate	kg/s	1.0	1.0658	
Temperature range	°C	50 → 150	200 → 152	
Specific heat <sup>(1)</sup>	J/kg K	1993	2416	4312
Dynamic viscosity <sup>(1)</sup>	N s/m <sup>2</sup>	0.0179	0.00186	1.488 × 10 <sup>-4</sup>
Thermal conductivity <sup>(1)</sup>	W/m K	0.1077	0.0885	0.696
Density <sup>(1)</sup>	kg/m <sup>3</sup>	849	778	888
Prandtl number <sup>(1)</sup>	–	331.24	50.78	0.922
Fouling factor <sup>(2)</sup>	(W/m <sup>2</sup> K) <sup>-1</sup>	0.00045		0.00009
Max. pressure loss <sup>(5)</sup>	Pa	56000		13000
Tube-wall resistance <sup>(3)</sup>	(W/m <sup>2</sup> K) <sup>-1</sup>	0.00007		

<b>Heat load (kW)</b>	<b>log MTD (<math>\Delta T_{lm}</math>) (7.11)<sup>(4)</sup></b>
Annulus $Q = 1 \times 2206 \times (150 - 50)/1000 = 220.6$	200 $\rightarrow$ 152
Tube-side $Q = 1.0658 \times 4312 \times (200 - 152)/1000 = 220.6$	150 $\leftarrow$ 50
	50 $\leftarrow$ 102
	$\Delta T_{lm} = \frac{102 - 50}{\ln \left\{ \frac{102}{50} \right\}} = 72.9^\circ\text{C}$

**Notes:**

- (1) At average bulk temperature.
- (2) Referred to its own surface.
- (3) Referred to tube o.d.
- (4) Countercurrent flow, i.e.  $F = 1$  and  $\Delta T_m = 72.9^\circ\text{C}$
- (5) Excluding nozzle losses.

<b>Additional oil viscosity data</b>					
Temperature ( $^\circ\text{C}$ )	75	100	125	175	200
Viscosity ( $\text{N s/m}^2$ )	0.00783	0.00425	0.00263	0.00143	0.00118

<b>Tube-side calculations (<math>\phi_1 = 1</math>)</b>		
Item	Units	Ref.
No. of tubes per pass	-	-
Tube internal diameter	m	Sec 15.6
Int. flow area (one pass)	$\text{m}^2$	$(\pi/4) \times 0.04089^2 = 0.001313$
Velocity in tubes	m/s	$1.0658/(888 \times 0.001313) = 0.91$
Mass velocity in tubes	$\text{kg/s m}^2$	$1.0658/0.001313 = 811.73$
Reynolds number ( $Re_i$ )	-	$(811.73 \times 0.04089)/(1.488 \times 10^{-4}) = 223062$
$Re_i^{0.795} Pr^{0.495}$	-	$17864.8 \times 0.9606 = 17160.9$
$\exp[-0.0225(\log(Pr))^{-2}]$	-	1
Tube side coeff. ( $\alpha_i$ )	$\text{W/m}^2 \text{K}$	[6.16a] $(0.0225 \times 0.696 \times 17160 \times 1)/(0.04089) = 6572$
Friction factor ( $f_i$ )	-	[6.23c] $0.0035 + 0.264/223062^{0.42} = 0.005$
Total travel ( $L$ ) <sup>(1)</sup>	m	$6 \times 8.125 = 48.75$
Straight loss ( $\Delta P_s$ )	Pa	[6.22] $(4 \times 0.005 \times 48.75 \times 811.73^2)/(2 \times 888 \times 0.04089) = 8846$
Bend loss ( $\Delta P_b$ )	Pa	[6.31b] $(6 \times 1.6 \times 811.73^2)/(2 \times 888) = 3562$
Total pressure loss ( $\Delta P_T$ )	Pa	12408

**Note:**

- (1) Based on final design of 6 lengths, each 8.125 m long. (Initial estimate of leg length was 9.75 m).

**Annulus calculations ( $\phi = 1$ )**

Item	Units	Ref.	Inlet	Outlet
No. of tubes in annulus	-	-	-	1
Annulus equivalent diameter	m <sup>2</sup>	sec	0.00778	
Int. flow area (one pass)	m <sup>2</sup>	15.6	0.002 485	
Velocity in annulus (inlet)	m/s	-	$1/(849 \times 0.002 485) = 0.47$	
Mass velocity in annulus	kg/s m <sup>2</sup>	-	$1/0.002 485 = 402.41$	
Reynolds number ( $Re_s$ )	-	-	$(402.41 \times 0.00778)/0.0179 = 174.9$	$(402.41 \times 0.00778)/0.00186 = 1683.2$
Graetz number ( $Gz$ ) <sup>(1)</sup>	-	-	$\{(\pi/4) \times 174.9 \times 331.24 \times 0.00778\}/9.75 = 36.3$	$\{(\pi/4) \times 1683.2 \times 50.78 \times 0.00778\}/9.75 = 53.6$
Annulus coefficient ( $\alpha'_i$ ) ( $\phi = 1$ )	W/m <sup>2</sup> K	[17.12]	$(1.75 \times 0.1077 \times 36.3^{1/3})/0.00778 = 80.2$	$(1.75 \times 0.0885 \times 53.6^{1/3})/0.00778 = 75$
Straight loss ( $\Delta P_s$ )	Pa	-	See incremental calculations	= 54 634
Bend loss ( $\Delta P_b$ )	Pa	[15.2]	$(2 \times 402.41^2)/(4 \times 814)$	= 100
Total pressure loss ( $\Delta P_T$ )	Pa	-	(excludes nozzle losses)	= 54 734

Note:

(1) Initial estimate of tube length = 9.75, final length = 8.125 m.

**Annulus calculations:  $\phi$  and heat transfer coefficient referred to tube i.d.**

At interface:						
oil and	Heat trans coeff. to fin ( $\phi_f=1$ ) ( $\alpha'_f$ )	W/m <sup>2</sup> K	calcs	80.2		75
external	Assumed interface temp	°C	-	117.6		186
fouling	Viscosity ( $\eta_s$ )	N s/m <sup>2</sup>	-	0.00306		0.00131
	$\phi_f = (\eta_b/\eta_s)^{0.14}$	-	-	$(0.0179)/0.00306^{0.14} = 1.28$		$(0.00186/0.00131)^{0.14} = 1.05$
	$\alpha'_f = \alpha'_i \phi_f$	W/m <sup>2</sup> K	sec. 9.5.2	$80.2 \times 1.28 = 102.7$		$75 \times 1.05 = 78.8$
	$\alpha'_i$	W/m <sup>2</sup> K	[15.6]	$1/((1/102.7) + 0.00045) = 98.2$		$1/((1/78.8) + 0.00045) = 76.1$
	$\alpha'_{fi}$	W/m <sup>2</sup> K	Fig. 15.1	660		530
	$\alpha'_{fi}$	W/m <sup>2</sup> K	sec. 9.5	$(98.2 \times 1.0336)/0.1285 = 790$		$(76.1 \times 1.0336)/0.1285 = 612$
	$r_m = (1/\alpha'_{fi}) - (1/\alpha'_i)$	(W/m <sup>2</sup> K) <sup>-1</sup>	[9.10]	$(1/660) - (1/790) = 0.000249$		$(1/530) - (1/612) = 0.000253$
	$\alpha'_i$ rel. tube i.d.	W/m <sup>2</sup> K	-	$(102.7 \times 1.0336)/0.1285 = 826$		$(78.8 \times 1.0336)/0.1285 = 634$
Heat flux:	Interface to oil	W/m <sup>2</sup>	-	$826 \times (117.6 - 50) = 55838$		$634 \times (186 - 150) = 22824$
	Hot water to interface	W/m <sup>2</sup>	p 452	$1621 \times (152 - 117.6) = 55762$		$1610 \times (200 - 186) = 22540$

2.3	External fouling ( $r_{fo}$ )					$(0.00045 \times 0.1285) / 1.0336 = 0.000056$	$= 0.000056$
3.4	Fin ( $r_{fm}$ )					$= 0.000249$	$= 0.000253$
4.5	Wall ( $r_w$ )			Fig. 9.4		$= 0.000070$	$= 0.000070$
5.6	Internal fouling ( $r_{fi}$ )					$= 0.000090$	$= 0.000090$
6.7	Internal coeff. ( $1/\alpha_i$ )					$1/6572$	$= 0.000152$
	Combined					$1/1621$	$= 0.000621$
						$1/1610$	total $= 0.000621$

<b>Overall heat transfer coefficient and surface area</b>			
Overall coefficient ( $U_j$ )	$W/m^2 K$ [15.9]	$(826 \times 1621) / (826 + 1621) = 547$	$(634 \times 1610) / (634 + 1610) = 455$
Terminal temp diff.	$^{\circ}C$	$152 - 50 = 102$	$200 - 150 = 50$
$\log(U\Delta T_{lm})$	$W/m^2$	$\log \text{mean } (547 \times 50) = 27350$ and $(455 \times 102) = 46410$	
		$(U\Delta T)_{lm} = \frac{46410 - 27350}{\ln \left( \frac{46410}{27350} \right)} = 36044$	
Surface area			
Required	$m^2$	$220600 / 36044 = 6.12$	
Final design	$m^2$	-	

If effective leg length = 9.75 m, 5 lengths would provide surface = 5 x 9.75 x 0.1285 = 6.26. For standard double leg units, 6 lengths (3 double legs), with effective length = 8.125 m, would provide surface = 6 x 8.125 x 0.1285 = 6.26 m. As actual leg length is less than initial estimate there is no need to recalculate annulus coefficients. Length of travel = 6 x 8.125 = 48.75 m.

Annulus calculations: incremental pressure loss					
	1	2	3	4	5
Location number	152	164	176	188	200
Water temp. °C	50	75	100	125	150
Oil temp. °C	102	89	76	63	50
Temperature difference ( $\Delta T$ )	547	525	503	481	455
Overall coefficient <sup>(1)</sup> $W/m^2 K$					
Zone number	1	2	3	4	sum
$(U\Delta T)_{in}$ $W/m^2$	51078	42287	34065	26409	-
Zone surface = $(220.6)(1000)/\{(4)(U\Delta T)_{in}\}$ $m^2$	1.08	1.30	1.62	2.09	6.09
Zone length ( $l$ ) $m$	8.64	10.41	12.97	16.73	48.75 <sup>(2)</sup>
Oil viscosity ( $\eta_b$ ) $N s/m^2$	0.0179	0.00783	0.00425	0.00263	0.00186
Oil density ( $\rho$ ) <sup>(1)</sup> $kg/m^3$	849	831	814	796	778
$\phi$ (heat transfer) = $(\eta_b/\eta_s)^{0.14}$ (1)	1.28	1.22	1.17	1.11	1.05
$(\eta_b/\eta_s)$	5.83	4.14	3.07	2.11	1.42
$\phi$ (pressure loss) = $(\eta_b/\eta_s)^{0.25}$	1.55	1.43	1.32	1.20	1.09
Reynolds number (= $md_c/\eta_b$ )	174.9	399.8	736.6	1190.4	1683.2
Friction factor ( $f_s$ ) [15.11]	0.0915	0.04	0.0243	0.018	0.0149
$f_s/\rho\phi$	$6.95 \times 10^{-5}$	$3.37 \times 10^{-5}$	$2.26 \times 10^{-5}$	$1.88 \times 10^{-5}$	$1.76 \times 10^{-5}$
Average $f_s/\rho\phi$ in zone	$5.16 \times 10^{-5}$	$2.82 \times 10^{-5}$	$2.07 \times 10^{-5}$	$1.82 \times 10^{-5}$	-
Pressure loss in zone ( $\Delta P_s$ ) <sup>(2)(3)</sup> $Pa$	18560	12221	11177	12676	54634

Notes:

- (1) Assumed to vary linearly with temperature.
- (2)  $\Delta P_s = \{(4 \times 402.41^2)/(2 \times 0.00778)\} \{f_s/\rho\phi\}$  from equations [6.22] and [15.11].
- (3) Pressure loss based on final design (i.e. 6 lengths, each 8.125 m)



As the overall heat transfer coefficient varies appreciably through the exchanger, the coefficients are determined at the terminal conditions, instead of the average temperature. As in examples 4A and 4B, the viscosity gradient ( $\phi$ ) on the oil-side is determined by trial and error. The oil-side pressure loss also varies appreciably through the exchanger, due to the variation of viscosity, density and viscosity gradient as shown in Table 17.12.

It will be noted that the lube oil is in laminar flow (Reynolds number  $< 2000$ ) and equation [6.18] for  $Gz > 9$  is applicable. The second term within the brackets represents the contribution to heat transfer of free convection, but the correlation was based on flow inside plain tubes. It is not applicable to finned annuli, which would inhibit free convection, and the second term has been omitted. Hence,

$$\alpha_i = \alpha'_i = 1.75 \left( \frac{\lambda}{d_c} \right) Gz^{1/3} \left( \frac{\eta_b}{\eta_s} \right)^{0.14} \quad [17.12]$$

where  $Gz = (\pi/4) \text{Re Pr}(d_c/L)$  (all properties based on bulk temperatures).  $L$  is the flow path length in which no internal mixing of the fluid occurs and in the case of a double-pipe exchanger, fitted with return bends, mixing occurs in the bend (Guy 1985). Hence, if cut-and-twist (section 5.1.3) is not used,  $L =$  straight leg length; if cut-and-twist is used,  $L =$  cut-and-twist pitch. As no length was specified, the initial estimate in this example is 9.75 m. The final design changed the length to 8.125 m.

#### Effect of cut-and-twist

If cut-and-twist is provided, the mixing length ( $L$ ) in  $Gz$  in equation [17.12] becomes the cut-and-twist pitch. Hence, if a cut-and-twist pitch of 0.75 m is used, for example, for the lube oil heater designed in Table 17.12,  $\alpha'_i$  is increased by  $(9.75/0.75)^{1/3} = 2.35$  times. The frictional pressure loss in the annulus is increased ( $F_{\alpha}$ )-fold, i.e.  $\{1.58 - (0.525 \times 0.75)\} = 1.186$  times from equation [15.14].

If the heater design is recalculated using the same procedure as given in Table 17.12, it will be found that the overall heat transfer coefficients at the oil inlet and outlet are 900 and 762  $\text{W/m}^2 \text{K}$ , respectively. The required internal surface area becomes 3.68  $\text{m}^2$ , which can be provided as four 7.2 m lengths, instead of six 8.125 m lengths – an appreciable saving. The pressure loss is reduced to 41 800 Pa.

## 17.6 Gasketed-plate heat exchangers

### 17.6.1 Example 12: Water/water exchanger (thermal check)

Section 19.6 provides a price comparison between shell-and-tube, plain tube double-pipe, and gasketed-plate heat exchangers for a process water/cooling water service given below. By assuming the typical overall heat transfer coefficient for such a service from Table 19.1, it was estimated that the plate unit would require a surface area of 240  $\text{m}^2$ .

In order to demonstrate the approach to thermal design described in Chapter 16, heat transfer coefficients and pressure losses are calculated for a typical gasketed-plate exchanger, having a surface area of 240 m<sup>2</sup>, and the constructional features listed below. True and estimated performance is then compared.

#### *Duty and physical properties*

	<i>Hot fluid</i>	<i>Cold fluid</i>
Fluid name	process water	cooling water
Flow rate (kg/s)	59.71	59.71
Temp. range (°C)	60 → 20	10 → 50
Heat load (kW)	10 000	
Log MTD (°C)	10	
Surface area (m <sup>2</sup> )	240	
Fouled $U$ (W/m <sup>2</sup> K)	4167	
Specific heat (J/kg K)	4187	4187
Viscosity (Ns/m <sup>2</sup> )	$0.65 \times 10^{-3}$	$0.8 \times 10^{-3}$
Thermal cond. (W/m K)	0.629	0.616
Prandtl number	4.33	5.44
Density (kg/m <sup>3</sup> )	989	994

#### *Constructional data*

The constructional data given below are not related to a particular maker's standard model, but are sufficiently realistic to demonstrate the calculations required.

- Overall plate size (mm × mm): 1740 × 550
- Effective surface area per plate (m<sup>2</sup>): 0.752
- Chevron angle (degrees): 45
- Plate pitch (m): 0.0035
- Plate thickness (m): 0.0006
- Enlargement factor ( $\mu$ ): 1.17
- Total number of plates: 321
- Total surface area (m<sup>2</sup>): 240
- Flow arrangement: two pass/two pass
- All port diameters (mm): 150
- Effective channel width (m): 0.5
- Flow length in one pass (m): 1.5

#### *Geometrical calculations*

Mean channel flow gap:

$$b = p - s = 0.0035 - 0.0006 = 0.0029 \text{ m} \quad (\text{equation [16.2]})$$

One channel flow area:

$$A_x = bw = 0.0029 \times 0.5 = 0.00145 \text{ m}^2 \quad (\text{equation [16.3]})$$

Channel equivalent diameter:

$$d_e = 2b/\mu = (2 \times 0.0029)/1.17 = 0.00496 \text{ m} \quad (\text{equation [16.4]})$$

$$\text{Number of channels per pass: } (321 - 1)/4 = 80$$

*Heat transfer calculations*

Flow per channel:

$$\dot{M}_{\text{ch}} = 59.71/80 = 0.746 \text{ kg/s}$$

Mass velocity:

$$m_{\text{ch}} = 0.746/0.00145 = 514.5 \text{ kg/s m}^2$$

Reynolds number (hot fluid):

$$(514.5 \times 0.00496)/(0.65 \times 10^{-3}) = 3926 \quad \text{(equation [16.8])}$$

Reynolds number (cold fluid):

$$(514.5 \times 0.00496)/(0.8 \times 10^{-3}) = 3190 \quad \text{(equation [16.8])}$$

Referring to Table 16.1, both fluids are in turbulent flow, hence:

$$\text{Hot fluid: } J_{\text{h}} = 0.3 \times 3926^{0.663} = 72.42 \quad \text{(equation [16.7] and Table 16.1)}$$

$$\text{Cold fluid: } J_{\text{c}} = 0.3 \times 3190^{0.663} = 63.12 \quad \text{(equation [16.7] and Table 16.1)}$$

$$\text{Hot fluid: } \alpha_{\text{ch}} = (72.42 \times 0.629 \times 4.33^{0.33})/0.00496 = 14896 \text{ W/m}^2 \text{ K} \quad \text{(equation [16.6])}$$

$$\text{Cold fluid: } \alpha_{\text{ch}} = (63.12 \times 0.616 \times 5.44^{0.33})/0.00496 = 13709 \text{ W/m}^2 \text{ K} \\ (\phi = 1 \text{ in both cases}) \quad \text{(equation [16.6])}$$

$$\text{Wall resistance: } r_{\text{w}} = 0.0006/17 = 0.000035 \text{ (W/m}^2 \text{ K)}^{-1}$$

$$\frac{1}{U_{\text{c}}} = \frac{1}{14896} + \frac{1}{13709} + 0.000035 \quad \text{(equation [16.14])}$$

$$\text{Clean overall coefficient: } U_{\text{c}} = 5712 \text{ W/m}^2 \text{ K}$$

The fouled overall coefficient ( $U$ ) is 4167 W/m<sup>2</sup> K, hence the cleanliness factor (CF) is given by equation [16.15], i.e.

$$\text{CF} = \frac{U}{U_{\text{c}}} = \frac{4167}{5712} = 0.73 \text{ (low)}$$

Alternatively, the available fouling factor from equation [16.13] is given by:

$$r_{\text{th}} + r_{\text{fc}} = \frac{1}{U} - \left\{ \frac{1}{\alpha_{\text{h}}} + \frac{1}{\alpha_{\text{c}}} + r_{\text{w}} \right\} = \frac{1}{U} - \frac{1}{U_{\text{c}}} \\ = \left( \frac{1}{4167} \right) - \left( \frac{1}{5712} \right) \\ = 0.000065 \text{ (W/m}^2 \text{ K)}^{-1}$$

This is higher than the typical fouling factors listed in Table 19.14, i.e. 0.000045.

*Pressure loss calculations*

Hot fluid:

$$f_{\text{ch}} = 1.441/3926^{0.206} = 0.262 \quad (\text{equation [16.10]})$$

Cold fluid:

$$f_{\text{ch}} = 1.441/3190^{0.206} = 0.273 \quad (\text{equation [16.10]})$$

For both hot and cold fluids  $N_p = 2$ , hence

$$L_{\text{ch}} = 2 \times 1.5 = 3 \text{ m} \quad (\text{equation [16.11]})$$

Hot fluid:

$$\begin{aligned} \Delta P_{\text{ch}} &= (4 \times 0.262 \times 3 \times 514.5^2)/(2 \times 989 \times 0.00496) \\ &= 84829 \text{ Pa} \end{aligned} \quad (\text{equation [16.9]})$$

Cold fluid:

$$\begin{aligned} \Delta P_{\text{ch}} &= (4 \times 0.273 \times 3 \times 514.5^2)/(2 \times 994 \times 0.00496) \\ &= 87946 \text{ Pa} \end{aligned} \quad (\text{equation [16.9]})$$

Port mass velocity:

$$59.71/\{(\pi/4) \times 0.15^2\} = 3378.9 \text{ kg/sm}^2$$

Hot fluid:

$$\Delta P_p = (1.3 \times 3378.9^2 \times 2)/(2 \times 989) = 15007 \text{ Pa} \quad (\text{equation [16.12]})$$

Cold fluid:

$$\Delta P_p = (1.3 \times 3378.9^2 \times 2)/(2 \times 994) = 14932 \text{ Pa} \quad (\text{equation [16.12]})$$

Hot fluid:

$$\text{total pressure loss} = 84829 + 15007 = 99836 \text{ Pa}$$

Cold fluid:

$$\text{total pressure loss} = 87946 + 14932 = 102878 \text{ Pa}$$

The calculations show that the estimated unit gave a good indication of size, but could have been smaller. If the recommended fouling factors given in Table 19.14 been used, i.e.  $1.5 \times 10^{-5}$  and  $3 \times 10^{-5} \text{ (W/m}^2 \text{ K)}^{-1}$  for treated cooling water and process water, respectively, the overall coefficient would be:

$$\frac{1}{U} = \frac{1}{5712} + (1.5 \times 10^{-5}) + (3 \times 10^{-5})$$

That is,  $U = 4544 \text{ W/m}^2 \text{ K}$ 

$$\text{and } A = \frac{10000 \times 1000}{10 \times 4544} = 220 \text{ m}^2 \text{ (i.e. about 9\% less)}$$

**Table 17.13** Comparison of shell-side heat transfer and pressure loss between manual and proprietary computer methods for identical exchanger<sup>(1)</sup>

Example no.	Design no.	Shell-side heat transfer coefficient (W/m <sup>2</sup> K)		Shell-side cross-flow and window pressure loss (Pa) <sup>(2)</sup>		Complete exchanger: % oversurface (+) or % undersurface (-)	
		Manual	Proprietary	Manual	Proprietary	Manual	Proprietary
1		1085	1369	49906	36104	+5.8	+19.2
2	A	2494	3021	111496	82388	+10.4	+21.8
	B	2149	2329	44640	33728	+2.3	+7.4
3	A	1603	2225	22123	18066	+5.4	+21.9
	B	1509	2769	27603	27243	+6.2	+38.2
	C	1537	2788	26357	28063	+12.7	+42.5
4	B	149	241	19889	11757	+1.4	+82.9
5		493	588	707	738	+22.5	+35.7
6		436	543	307	316	-4.0	+12.7
7		1237	1222	60312	51662	+4.3	+11.7

Notes (1) Heat Transfer Research Inc. (2) Excludes end zone and nozzle losses.

### 17.7 Shell-and-tube heat exchangers: comparison of manual and proprietary computer methods

Table 17.13 presents a comparison of shell-side heat transfer and pressure loss between manual and proprietary computer methods (HTRI) for examples 1–7. Example 4A has been omitted because the shell-side fluid is steam and shell-side calculations are not required.

The results for examples 1, 2A, 2B, 3A, 3C, 4B and 7 provide an approximate comparison of the Bell (1984) manual method with that of HTRI for identical conditions. An exact comparison cannot be made because of approximations made by the author in the derivation of the design factors presented in Chapter 12. If examples 3C and 4B are omitted, the remaining results show that the manual method under-predicts heat transfer coefficients by up to 45%, and over-predicts pressure loss by up to 38%, leading to over-design. The Bell method was not derived for F shells (two shell passes) as used in example 3C. In the case of example 4B, which involves the problems of deep laminar flow, the manual method under-predicts the heat transfer coefficient by 45% and over-predicts pressure loss by 69%.

Examples 5 and 6 deal with X shells (cross flow) and are not based on the Bell method. The manual method under-predicts heat transfer coefficients by up to 20%, probably due to the simplification of basing the shell-side Reynolds number on the exchanger diameter. Pressure loss agreement is good.

Although agreement between manual and proprietary methods is not good, this is hardly surprising since the proprietary method has the benefit of about 25 years exhaustive research and modern computer techniques.

## 17.8 Shell-side pressure loss due to blockage

Table 17.14 provides the shell-side pressure losses for various degrees of blockage, as calculated by a proprietary computer method (HTRI) for examples 1, 2A, 2B, 3A, 3B, 3C, 4B and 7. The problems facing the thermal design engineer, as discussed in section 8.4.2, are evident. If the baffle hole is completely blocked, but the tube surface is clean, the results show that the increase in pressure loss, compared with that of the basic design, is 10–70%, with the exception of example 4B. Here the shell-side flow is deep-laminar, whereas it is turbulent in the other examples. Different shell-side flow patterns and leakage rates occur in example 4B and the increase in pressure loss is negligible.

**Table 17.14** Shell-side pressure loss (Pa) due to blockage, as calculated by proprietary computer method<sup>(1, 2)</sup>

Example no.	Design no.	Baffle-tube diametral clearance (mm)				Pressure loss by manual method for basic design (Pa)
		0.65 <sup>(4)</sup>	0	0.65 <sup>(3)</sup>	0.65 <sup>(3)</sup>	
		External fouling layer thickness (mm)				
		0 <sup>(4)</sup>	0	0.325	0.65	
1		36104	61480	73522	86359	49906
2	A	82388	101614	124141	142422	111496
	B	33728	49148	58496	67258	44640
3	A	18066	27390	31620	36204	22123
	B	27243	30035	33365	37409	27603
	C	28063	32381	36737	42066	26357
4	B	11757	11784	13628	15822	19889
7		51662	69844	78635	87343	60312

*Notes:*

- (1) Heat Transfer Research Inc.
- (2) Excludes end zone and nozzle losses.
- (3) Fouling layer completely blocks baffle hole.
- (4) Basic design values (clean).

## References

A list of addresses for the service organisations is provided on p. xvi.

- Bell, K. J. (1984), 'Baffled shell & tube exchangers', in *Perry's Chemical Engineers Handbook*, (6th ed). McGraw-Hill Inc., pp. 10.26–10.31.
- Gambill, W. R. (1960), *Estimating Engineering Properties*, McGraw-Hill Inc.
- Reid, R. C., Prausnitz, J. M. and Sherwood, T. K. (1977) *Properties of Gases and Liquids* (3rd edn). McGraw-Hill Inc.

## Tube counts

Computer programs provide tube count data and tube layout drawings, either from stand-alone programs or as an integral part of thermal design programs. Such programs can cater for all the factors involved, including row-by-row calculations, and provide more accurate data than tables. The limitations of tables are described in section 1.5.18. Accordingly, there is less interest in tube count tables, but in the author's experience there is still a need for such tables for rapid initial sizing and costing purposes.

### A3.1 Tube count tables

Tube counts are presented in Tables A3.1–A3.3 for fixed tubesheet, U-tube and split backing ring floating-head type exchangers, having the 24 shell diameters and 13 tube configurations of Chapter 12. The tube count tables differ from those usually published, in that both a full count, and a reduced count, due to an internally fitted impingement baffle, are given for every case.

The reduced count assumes that (a) the diameters of the inlet and outlet nozzles are both equal to one-third of the shell diameter, (b) they are situated on opposite sides of the bundle, (c) the inlet nozzle has an internally fitted impingement plate, which is situated to provide an annular escape area equal to the nozzle internal flow area, (d) an escape area equal to 0.67 of the nozzle internal flow area is provided at the outlet nozzle and (e) the tube ends are expanded. The diametral clearance – shell i.d. minus outer tube limit (OTL) – is taken from Table 12.2.

### A3.2 Tube count reduction for untubed areas – procedure

A procedure is also given to enable the tube counts to be corrected for any arbitrary tube omission, which occurs in no-tube-in-window designs,

for instance. Referring to Figs A3.1 and A3.2, the approximate reduction in tube count due to untubed areas is calculated as follows:

- shell inside diameter =  $D_i$
- outer tube limit (OTL) =  $D_o$
- tube row distance =  $h_i$  inlet
- =  $h_o$  outlet
- full tube count (Tables A3) =  $N_i$

Figure A3.1 Nomenclature for tube counts

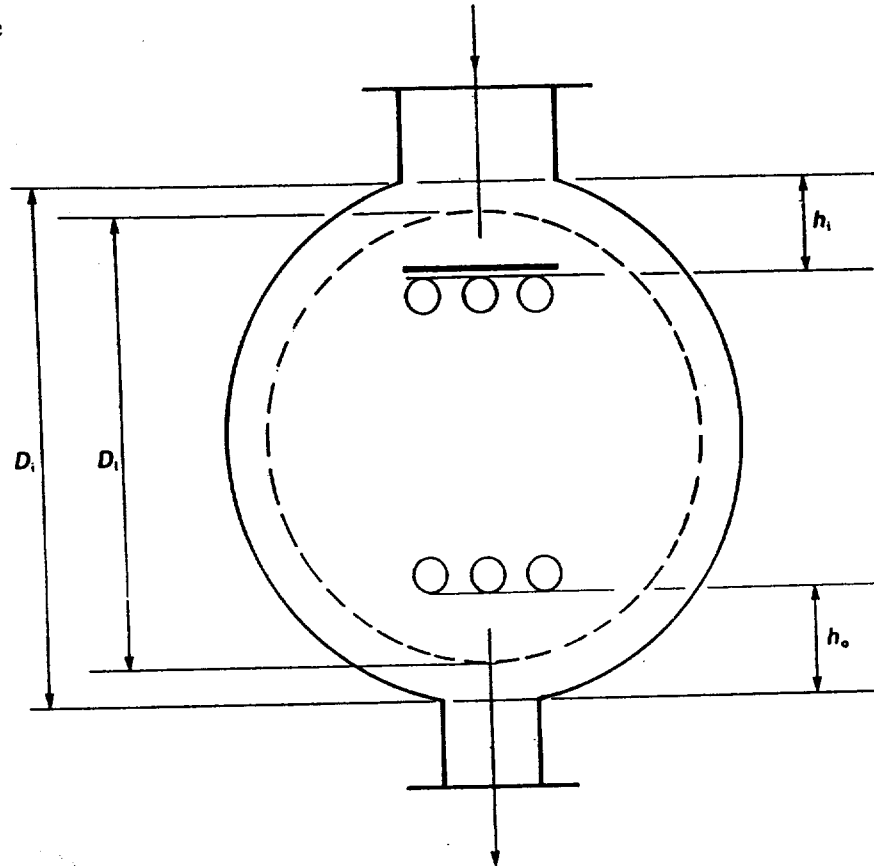


Figure A3.2 Z versus R

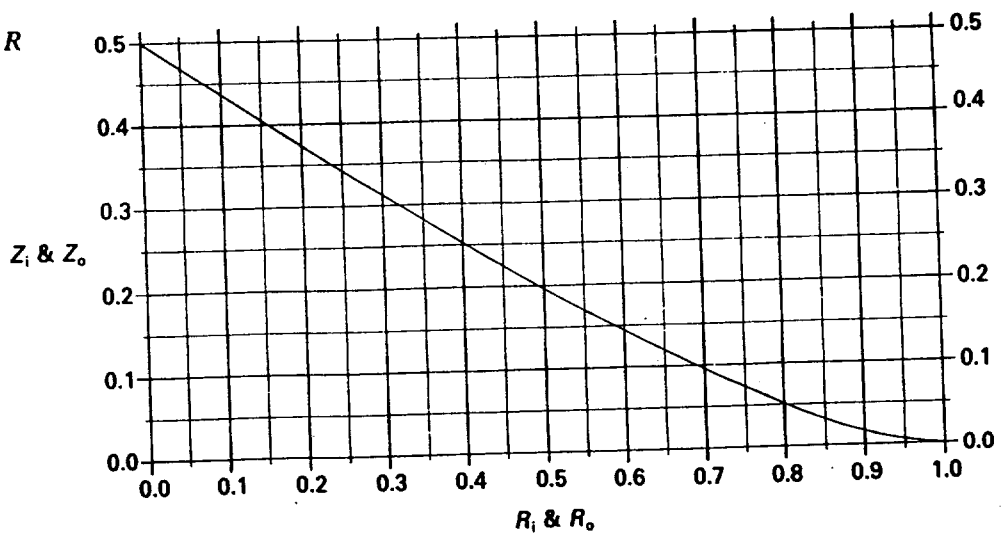




Table A3.1 Shell-and-tube heat exchanger design. Tube counts for fixed tubesheet type exchangers

Shell i.d. (mm)	15.88 mm (5/8 in) o.d. × 19.84 mm (3/4 in) pitch Δ						19.05 mm (3/4 in) o.d. × 23.81 mm (15/16 in) pitch Δ						19.05 mm (3/4 in) o.d. × 25.4 mm (1 in) pitch Δ						Shell i.d. (in)						
	1 pass		2 pass		4 pass		6 pass		1 pass		2 pass		4 pass		6 pass		1 pass			2 pass		4 pass		6 pass	
	0.0	0.33	0.0	0.33	0.0	0.33	0.0	0.33	0.0	0.33	0.0	0.33	0.0	0.33	0.0	0.33	0.0	0.33		0.0	0.33	0.0	0.33	0.0	0.33
203	77	73	66	62	49	45	39	35	52	50	45	43	32	30	26	24	46	43	40	37	29	26	23	20	8
254	125	119	112	106	90	84	78	72	85	81	76	72	60	56	52	48	75	71	67	63	53	49	46	42	10
305	186	175	170	159	143	132	129	118	127	120	116	109	98	91	88	81	112	106	102	96	86	80	77	71	12
337	230	216	212	198	193	169	167	153	158	148	146	136	125	115	105	105	138	130	127	119	110	102	100	92	13
387	310	291	290	271	256	237	238	219	213	200	199	186	175	162	163	150	187	176	175	164	154	143	143	132	15
438	401	376	378	353	340	315	319	294	276	259	260	243	234	217	220	203	243	227	229	213	206	190	193	177	17
489	505	472	480	447	437	404	414	381	348	325	330	307	301	278	285	262	306	286	290	270	264	244	250	230	19
540	621	579	593	551	546	504	521	479	428	400	408	380	376	348	359	331	376	351	359	334	330	305	315	290	21
591	748	698	717	667	666	616	638	588	516	481	495	460	459	424	440	405	454	423	435	404	404	373	387	356	23
635	869	810	836	777	780	721	751	692	600	559	577	536	539	498	518	477	527	491	507	471	473	437	455	419	25
686	1019	948	983	912	923	852	891	820	704	655	679	630	638	589	616	567	619	576	597	554	561	518	541	498	27
737	1180	1098	1142	1060	1077	995	1043	961	816	759	789	732	745	688	721	664	717	667	694	644	654	604	633	583	29
787	1354	1258	1313	1217	1244	1148	1207	1111	936	870	907	841	860	794	835	769	823	765	798	740	756	698	734	676	31
838	1539	1430	1495	1386	1422	1313	1383	1274	1064	989	1034	959	983	908	956	881	935	869	908	842	864	798	840	774	33
889	1737	1612	1691	1566	1613	1488	1572	1447	1201	1115	1169	1083	1115	1029	1087	1101	1056	980	1028	952	980	904	955	879	35
940	1946	1805	1896	1755	1815	1674	1771	1630	1346	1249	1312	1215	1255	1158	1226	1129	1183	1098	1153	1068	1103	1018	1076	991	37
991	2167	2009	2115	2097	2029	1871	1983	1825	1499	1391	1463	1355	1403	1295	1372	1264	1318	1222	1286	1190	1234	1138	1206	1110	39
1067	2520	2336	2464	2280	2371	2187	2321	2137	1745	1617	1706	1578	1642	1514	1608	1480	1533	1421	1499	1387	1442	1330	1412	1300	42
1143	2901	2688	2841	2628	2741	2528	2688	2475	2009	1861	1968	1820	1898	1750	1862	1714	1765	1635	1729	1599	1668	1538	1635	1505	45
1219	3308	3063	3244	2999	3138	2893	3081	2836	2291	2121	2247	2077	2173	2003	2134	1964	2014	1864	1975	1825	1911	1761	1875	1725	48
1295	3742	3464	3674	3396	3561	3283	3501	3223	2592	2399	2545	2352	2467	2274	2425	2232	2278	2109	2237	2068	2168	1999	2131	1962	51
1372	4203	3889	4132	3818	4011	3697	3948	3634	2912	2694	2862	2644	2779	2561	2735	2517	2559	2368	2515	2324	2443	2252	2403	2212	54
1448	4690	4338	4615	4263	4488	4136	4420	4068	3250	3006	3198	2954	3110	2866	3064	2820	2856	2641	2810	2595	2733	2518	2692	2477	57
1524	5205	4813	5126	4734	4992	4600	4921	4529	3607	3355	3552	3280	3459	3187	3411	3139	3170	2931	3121	2882	3040	2801	2997	2758	60
1600									3982	3681	3924	3623	3827	3526	3776	3475	3500	3235	3449	3184	3364	3099	3318	3053	63
1676									4376	4044	4315	3983	4214	3882	4160	3828	3846	3554	3793	3501	3704	3412	3656	3364	66
1753									4789	4424	4726	4361	4619	4254	4563	4198	4209	3888	4153	3832	4060	3739	4010	3698	69
1829									5220	4821	5154	4755	5043	4644	4984	4585	4587	4237	4529	4179	4432	4082	4379	4029	72
1981									6138	5668	6066	5595	5946	5476	5882	5412	5394	4981	5331	4918	5226	4813	5169	4756	78
2134									7130	6581	7053	6504	6923	6374	6855	6306	6266	5783	6198	5715	6085	5602	6024	5541	84
2286									8196	7563	8113	7480	7975	7342	7901	7268	7203	6646	7130	6573	7009	6452	6943	6386	90
2438									9337	8614	9249	8526	9101	8378	9022	8299	8206	7571	8128	7493	7999	7364	7929	7294	96
2591									10552	9732	10458	9638	10301	9481	10218	9398	9274	8553	9191	8470	9054	8333	8980	8259	102
2743									11842	10920	11743	10821	11576	10654	11488	10566	10407	9597	10320	9510	10174	9364	10095	9285	108
2896									13205	12176	13100	12071	12925	11896	12831	11802	11606	10701	11514	10609	11360	10455	11277	10372	114
3048									14643	13500	14533	13390	14348	13205	14250	13107	12869	11864	12772	11767	12610	11605	12522	11517	120

Table A3.1 (cont)

Shell i.d. (mm)	25.4 mm (1 in) o.d. × 31.75 mm (1 1/8 in) pitch Δ												31.75 mm (1 1/8 in) o.d. × 39.69 mm (1 5/8 in) pitch Δ												Shell i.d. (in)
	1 pass		2 pass		4 pass		6 pass		1 pass		2 pass		4 pass		6 pass										
	0.0	0.33	0.0	0.33	0.0	0.33	0.0	0.33	0.0	0.33	0.0	0.33	0.0	0.33	0.0	0.33									
203	28	27	24	23	17	16	12	12	17	16	14	13	10	9	—	—	8								
254	47	44	42	39	30	30	29	26	29	27	26	24	20	18	17	15	10								
305	70	66	64	60	54	50	48	44	43	41	39	37	33	31	29	27	12								
337	87	82	80	75	69	64	63	58	54	51	50	47	43	40	39	36	13								
387	115	110	107	102	94	89	87	82	74	69	69	64	61	56	56	51	15								
438	153	143	144	134	129	119	121	111	96	90	90	84	81	75	76	70	17								
489	193	180	183	170	167	154	158	145	122	113	116	107	105	96	100	91	19								
540	238	220	227	209	191	199	181	181	150	140	143	133	132	122	125	115	21								
591	287	267	275	252	235	244	224	224	181	169	173	161	161	149	154	142	23								
635	334	311	321	298	300	277	288	265	211	196	203	188	189	174	182	167	25								
686	392	365	378	351	355	328	342	315	248	231	239	222	224	207	216	199	27								
737	455	423	440	408	415	383	402	370	288	268	278	258	263	243	254	234	29								
787	522	485	506	469	479	442	465	428	331	307	321	297	304	280	295	271	31								
838	594	551	577	534	549	506	533	490	377	350	366	339	348	321	338	311	33								
889	671	622	653	604	623	574	607	558	426	395	414	383	395	364	385	354	35								
940	752	697	734	678	701	646	684	629	478	443	466	431	445	410	435	400	37								
991	838	776	818	756	784	722	766	704	532	493	519	480	498	459	486	447	39								
1067	975	903	953	881	917	845	897	825	620	574	606	560	583	537	571	525	42								
1143	1123	1040	1100	1017	1061	978	1040	957	715	661	700	646	675	621	662	608	45								
1219	1282	1186	1257	1161	1216	1120	1193	1097	816	755	800	739	774	713	760	699	48								
1295	1451	1342	1424	1315	1381	1272	1357	1248	924	854	907	837	879	809	864	794	51								
1372	1630	1508	1602	1480	1556	1434	1530	1408	1038	960	1020	942	990	912	975	897	54								
1448	1820	1680	1790	1652	1741	1603	1715	1577	1159	1071	1140	1052	1109	1021	1092	1004	57								
1524	2020	1867	1989	1836	1937	1784	1909	1756	1287	1189	1267	1169	1234	1136	1216	1118	60								
1600	2231	2061	2198	2028	2144	1974	2115	1945	1422	1313	1401	1292	1366	1257	1348	1239	63								
1676	2452	2265	2418	2231	2361	2174	2330	2143	1563	1443	1541	1421	1505	1385	1486	1366	66								
1753	2684	2479	2648	2443	2589	2384	2557	2351	1711	1580	1688	1557	1650	1519	1630	1499	69								
1829	2926	2701	2889	2664	2827	2602	2793	2568	1866	1722	1842	1698	1802	1658	1781	1637	72								
1981	3441	3177	3400	3136	3334	3070	3397	3033	2195	2026	2169	2000	2126	1957	2103	1934	78								
2134	3998	3689	3954	3645	3882	3573	3843	3534	2551	2353	2523	2325	2477	2279	2452	2254	84								
2286	4598	4241	4551	4194	4474	4117	4432	4075	2934	2706	2904	2676	2854	2626	2838	2600	90								
2438	5238	4832	5188	4782	5106	4700	5061	4655	3343	3083	3311	3051	3258	2998	3230	2950	96								
2591	5921	5460	5868	5407	5781	5320	5732	5271	3779	3484	3745	3450	3689	3394	3659	3364	102								
2743	6645	6127	6589	6071	6496	5798	6445	5978	4243	3911	4207	3875	4153	3815	4116	3784	108								
2896	7412	6833	7353	6774	7255	6676	7201	6622	4732	4362	4694	4324	4631	4261	4598	4228	114								
3048	8220	7576	8158	7514	8055	7411	7998	7354	5249	4837	5209	4797	5145	4733	5107	4695	120								

Table A3.2 Shell-and-tube heat exchanger design. Tube counts for U-tube type exchangers

Shell i.d. (mm)	15.88 mm (5/8 in) o.d. × 19.84 mm (3/4 in) pitch Δ				15.88 mm (5/8 in) o.d. × 22.23 mm (7/8 in) pitch □				19.05 mm (3/4 in) o.d. × 25.44 mm (1 in) pitch □				19.05 mm (3/4 in) o.d. × 23.81 mm (3/4 in) pitch Δ				19.05 mm (3/4 in) o.d. × 25.4 mm (1 in) pitch Δ				Shell i.d. (in)
	2 pass		4 pass		2 pass		4 pass		2 pass		4 pass		2 pass		4 pass		2 pass		4 pass		
	0.0	0.33	0.0	0.33	0.0	0.33	0.0	0.33	0.0	0.33	0.0	0.33	0.0	0.33	0.0	0.33	0.0	0.33	0.0	0.33	
203	58	54	46	42	40	36	32	30	28	26	22	20	36	34	28	26	32	28	26	22	8
254	100	94	88	82	70	66	60	56	50	48	44	40	64	60	56	52	58	54	50	46	10
305	158	146	140	130	108	102	96	90	78	74	70	64	104	96	92	84	90	84	80	74	12
337	200	184	180	166	138	128	124	114	100	94	90	84	132	122	120	110	114	106	104	96	13
387	274	254	252	234	190	176	174	162	140	130	128	118	182	170	168	156	160	150	148	136	15
438	360	336	336	312	248	230	232	214	184	170	172	160	242	226	226	208	212	196	198	182	17
489	460	426	434	400	318	294	300	276	236	220	222	206	310	286	292	268	272	252	256	236	19
540	570	528	542	500	394	366	374	344	294	272	280	258	386	358	366	338	338	314	322	296	21
591	694	644	662	612	478	442	456	420	358	330	342	314	470	434	448	414	414	382	394	364	23
635	810	750	776	716	560	518	536	494	420	388	402	370	550	510	528	486	484	448	462	426	25
686	956	884	918	848	660	610	634	586	496	458	476	440	650	601	626	576	572	530	550	506	27
737	1112	1030	1072	900	768	708	740	684	578	534	558	514	758	702	732	674	666	616	642	592	29
787	1280	1184	1238	1142	884	818	854	790	666	616	644	594	874	808	846	780	770	712	744	686	31
838	1460	1352	1416	1308	1008	932	978	902	760	702	738	680	1000	924	968	892	878	812	850	784	33
889	1654	1530	1606	1482	1142	1056	1108	1022	862	796	838	772	1132	1046	1098	1012	996	920	966	890	35
940	1858	1718	1808	1668	1282	1186	1248	1150	970	896	944	870	1272	1176	1238	1142	1118	1034	1088	1004	37
991	2074	1916	2022	1864	1432	1324	1394	1286	1084	1000	1056	972	1422	1314	1384	1278	1250	1154	1218	1122	39
1067	2420	2236	2366	2180	1672	1544	1632	1504	1264	1168	1236	1140	1662	1534	1622	1494	1460	1348	1426	1314	42
1143	2794	2582	2734	2522	1930	1782	1888	1740	1462	1348	1422	1318	1922	1774	1878	1730	1688	1556	1650	1520	45
1219	3194	2952	3130	2884	2206	2036	2160	1992	1672	1542	1638	1508	2206	2026	2152	1982	1932	1780	1892	1742	48
1295	3622	3344	3554	3276	2500	2308	2452	2260	1989	1750	1860	1714	2492	2300	2444	2250	2190	2020	2148	1978	51
1372	4076	3762	4002	3688	2814	2596	2764	2546	2136	1970	2098	1932	2806	2588	2756	2538	2466	2274	2420	2230	54
1448	4556	4204	4478	4126	3144	2902	3092	2848	2390	2202	2348	2162	3138	2894	3086	2842	2758	2542	2710	2496	57
1524	5064	4672	4982	4590	3494	3224	3440	3170	2656	2448	2614	2406	3488	3216	3434	3162	3066	2828	3018	2778	60

Table A3.2 (cont.)

Shell i.d. (mm)	25.4 mm (1 in) o.d. × 31.75 mm (1 1/4 in) pitch Δ						31.75 mm (1 1/4 in) o.d. × 36.69 mm (1 3/8 in) pitch Δ						31.75 mm (1 1/4 in) o.d. × 39.69 mm (1 5/8 in) pitch □						Shell i.d. (in)
	2 pass		4 pass		4 pass		2 pass		4 pass		4 pass		2 pass		4 pass				
	0.0	0.33	0.0	0.33	0.0	0.33	0.0	0.33	0.0	0.33	0.0	0.33	0.0	0.33	0.0	0.33			
203	16	14	12	10	14	12	10	8	8	16	14	12	10	12	10	8			
254	32	28	26	24	28	24	22	20	18	30	28	26	24	24	24	20			
305	52	48	46	42	46	42	38	36	30	40	38	36	32	32	28				
337	68	62	60	54	58	54	52	48	40	54	52	48	46	46	42				
387	92	88	84	80	82	76	74	68	58	72	72	66	62	62	58				
438	128	118	118	108	110	102	102	94	78	94	94	86	82	82	74				
489	164	152	154	140	142	132	134	122	102	118	118	110	102	102	96				
540	206	188	194	176	178	164	170	156	128	146	146	136	126	126	118				
591	252	232	240	220	218	200	208	190	158	170	170	162	150	150	140				
635	296	274	284	260	256	236	246	226	186	196	196	182	176	176	168				
686	352	324	338	310	304	282	292	270	220	238	238	228	224	224	214				
737	412	380	396	364	356	328	344	316	260	276	276	264	260	260	230				
787	476	438	460	422	412	380	398	366	300	316	316	306	298	298	264				
838	544	502	528	494	472	343	456	420	344	360	360	348	338	338	300				
889	618	570	600	552	536	494	520	478	390	406	406	392	382	382	340				
940	696	642	678	624	604	558	586	540	440	454	454	440	426	426	390				
991	780	718	760	698	676	622	656	604	490	506	506	490	478	478	440				
1067	912	840	890	818	792	730	770	708	578	594	594	562	550	550	500				
1143	1058	974	1032	950	916	844	896	822	670	686	686	654	640	640	580				
1219	1212	1116	1186	1090	1050	966	1028	944	768	784	784	750	736	736	664				
1295	1376	1268	1348	1240	1192	1098	1168	1072	874	890	890	854	840	840	780				
1372	1550	1428	1522	1400	1342	1236	1318	1210	984	1000	1000	964	950	950	880				
1448	1736	1598	1706	1568	1504	1384	1478	1358	1102	1118	1118	1082	1068	1068	994				
1524	1932	1780	1900	1746	1674	1542	1646	1514	1226	1242	1242	1206	1192	1192	1108				

**Table A3.3 Shell-and-tube heat exchanger design. Tube counts for split backing floating-head type exchangers**

Shell i.d. (mm)	15.88 mm ( $\frac{5}{8}$ in) o.d. $\times$ 19.84 mm ( $\frac{3}{4}$ in) pitch $\Delta$						15.88 mm ( $\frac{5}{8}$ in) 22.23 mm ( $\frac{7}{8}$ in) pitch $\square$						19.05 mm ( $\frac{3}{4}$ in) o.d. $\times$ 23.81 mm ( $1\frac{1}{2}$ in) pitch $\Delta$						Shell i.d. (in)						
	1 pass		2 pass		4 pass		6 pass		1 pass		2 pass		4 pass		6 pass		1 pass			2 pass		4 pass		6 pass	
	0.0	0.33	0.0	0.33	0.0	0.33	0.0	0.33	0.0	0.33	0.0	0.33	0.0	0.33	0.0	0.33	0.0	0.33		0.0	0.33	0.0	0.33	0.0	0.33
203	59	58	48	47	31	30	21	20	40	40	33	20	20	14	14	39	33	32	20	19	14	13	8		
254	102	100	89	87	67	65	55	53	70	69	61	46	45	37	36	69	61	60	45	44	37	36	10		
305	158	154	142	138	115	111	101	97	109	106	98	80	77	70	67	108	106	95	79	77	69	67	12		
337	198	193	180	175	151	146	135	130	137	133	125	121	105	101	94	136	133	124	103	100	93	90	13 $\frac{1}{2}$		
387	273	265	253	245	219	211	201	193	188	182	174	168	151	145	138	188	182	174	150	144	138	132	15 $\frac{1}{2}$		
438	359	347	336	324	298	286	277	263	248	239	232	223	206	197	192	247	239	231	205	205	191	183	17 $\frac{1}{2}$		
489	458	440	433	415	390	372	367	349	316	303	298	285	269	256	253	315	303	297	285	268	252	240	19 $\frac{1}{2}$		
540	568	544	540	516	493	469	468	444	392	375	372	355	340	323	323	392	375	372	355	340	323	306	21 $\frac{1}{2}$		
591	690	659	659	628	608	577	580	549	477	455	456	434	420	398	401	477	454	456	433	420	397	401	378	23 $\frac{1}{2}$	
635	790	756	757	723	701	667	672	638	545	522	522	499	484	461	463	545	522	522	499	484	461	463	440	25	
686	933	890	897	854	837	794	805	762	644	614	619	589	578	548	556	644	615	619	590	578	549	556	527	27	
737	1088	1035	1050	997	985	932	951	888	751	715	724	688	680	644	656	752	716	725	689	681	645	657	621	29	
787	1255	1192	1214	1151	1145	1082	1108	1045	866	823	837	794	790	747	765	867	824	838	795	791	748	766	723	31	
838	1433	1359	1389	1315	1316	1242	1277	1203	989	938	959	908	908	857	881	991	940	961	910	910	859	883	832	33	
889	1624	1537	1578	1491	1500	1413	1459	1372	1121	1061	1089	1029	1035	975	1007	1123	1063	1091	1031	1037	977	1009	949	35	
940	1826	1727	1776	1677	1695	1596	1651	1552	1261	1192	1227	1158	1170	1110	1141	1264	1194	1230	1160	1173	1103	1144	1074	37	
991	2034	1921	1982	1869	1869	1783	1850	1737	1404	1326	1368	1290	1308	1230	1277	1407	1330	1371	1294	1311	1234	1280	1203	39	
1067	2377	2241	2321	2185	2228	2092	2178	2042	1641	1547	1602	1508	1538	1444	1504	1645	1551	1606	1512	1542	1448	1508	1414	42	
1143	2747	2587	2687	2527	2587	2427	2534	2374	1896	1786	1855	1745	1786	1670	1751	1902	1791	1861	1750	1791	1680	1755	1644	45	
1219	3143	2955	3079	2891	2973	2785	2916	2728	2170	2040	2126	1996	2052	1922	2013	2177	2046	2133	2002	2059	1928	2020	1889	48	
1295	3567	3349	3499	3281	3386	3168	3326	3108	2463	2312	2416	2265	2338	2187	2296	2471	2320	2424	2273	2346	2195	2304	2153	51	
1372	4017	3768	3946	3697	3825	3576	3762	3513	2773	2602	2723	2552	2641	2470	2596	2783	2610	2733	2560	2650	2477	2606	2433	54	
1448	4494	4210	4419	4135	4292	4008	4224	3940	3103	2907	3051	2855	2963	2767	2917	3114	2917	3062	2865	2974	2777	2928	2731	57	
1524	4998	4678	4919	4599	4785	4465	4714	4394	3451	3230	3396	3175	3304	3083	3255	3463	3241	3408	3186	3315	3093	3267	3045	60	

Table A3.3 (cont.)

Shell i.d. (mm)	19.05 mm (3/4 in) o.d. × 25.4 mm (1 in) pitch $\Delta$												19.05 mm (3/4 in) o.d. × 25.4 mm (1 in) pitch $\square$												25.4 mm (1 in) o.d. × 31.75 mm (1 1/4 in) pitch $\Delta$												Shell i.d. (in)
	1 pass		2 pass		4 pass		6 pass		1 pass		2 pass		4 pass		6 pass		1 pass		2 pass		4 pass		6 pass														
	0.0	0.33	0.0	0.33	0.0	0.33	0.0	0.33	0.0	0.33	0.0	0.33	0.0	0.33	0.0	0.33	0.0	0.33	0.0	0.33	0.0	0.33	0.0	0.33													
203	35	35	29	29	18	18	—	—	30	24	24	15	15	—	—	21	17	17	10	10	—	—	8														
254	61	60	53	52	39	38	32	31	53	46	45	34	33	28	27	38	33	32	24	23	20	19	10														
305	95	93	85	83	69	67	60	58	82	80	74	60	58	52	50	59	58	53	43	42	37	36	12														
337	119	116	108	105	91	88	81	78	103	101	94	78	76	70	68	75	73	68	57	55	51	49	13														
387	165	160	153	148	132	127	121	116	143	138	132	114	109	105	100	103	100	95	82	79	75	72	15														
438	217	210	203	196	180	173	167	160	188	182	176	156	150	145	139	137	132	128	113	108	105	100	17														
489	277	266	261	250	235	224	221	210	240	231	227	204	195	192	183	175	168	165	149	142	140	133	19														
540	344	330	327	313	298	284	283	269	298	285	283	270	258	245	228	217	208	206	197	188	179	178	21														
591	419	399	400	380	369	349	352	332	363	346	347	319	302	305	288	265	252	253	240	233	220	222	209														
635	479	459	459	439	425	405	407	387	415	397	398	368	350	353	337	303	290	290	277	269	256	257	244														
686	566	540	544	518	508	482	488	462	490	468	471	449	439	417	401	359	342	345	328	322	305	309	292														
737	661	629	638	606	598	566	577	545	572	545	552	518	491	500	473	419	398	404	383	379	358	366	345														
787	762	724	737	699	695	657	673	635	660	627	638	605	602	569	550	483	459	467	443	440	416	426	402														
838	871	826	844	799	800	755	776	731	754	715	731	692	692	653	633	553	524	536	507	508	479	492	463														
889	987	934	959	906	911	858	886	833	855	809	831	785	789	743	722	627	593	609	575	579	545	563	529														
940	1110	1050	1080	1020	1030	970	1003	943	962	909	936	883	893	840	817	706	667	687	648	655	616	638	599														
991	1237	1168	1205	1136	1153	1084	1125	1056	1071	1012	1044	985	998	939	915	786	742	766	722	732	688	714	670														
1067	1446	1363	1412	1329	1355	1272	1325	1242	1252	1181	1223	1152	1173	1102	1076	920	867	898	845	862	809	842	789														
1143	1672	1574	1636	1538	1575	1477	1542	1444	1448	1363	1417	1332	1364	1279	1251	1064	1001	1041	978	1002	939	981	918														
1219	1913	1798	1874	1759	1810	1695	1774	1659	1657	1557	1624	1524	1567	1467	1437	1218	1144	1193	1119	1152	1078	1129	1055														
1295	2171	2039	2130	1998	2061	1929	2024	1892	1880	1766	1845	1731	1784	1670	1639	1383	1298	1356	1271	1313	1228	1289	1204														
1372	2446	2294	2402	2250	2330	2178	2290	2138	2118	1987	2080	1949	2017	1886	1852	1556	1461	1530	1433	1484	1387	1458	1361														
1448	2737	2563	2691	2517	2614	2440	2573	2399	2370	2220	2330	2180	2263	2113	2078	1744	1633	1714	1603	1665	1554	1639	1528														
1524	3044	2848	2995	2799	2914	2718	2871	2675	2636	2467	2594	2425	2523	2354	2317	1940	1815	1909	1784	1857	1732	1829	1704														

Table A.3.3 (cont.)

Shell i.d. (mm)	25.4 mm (1 in) o.d. × 31.75 mm (1¼ in) pitch □						31.75 mm (1¼ in) o.d. × 36.69 mm (1½ in) pitch △						31.75 mm (1¼ in) o.d. × 36.69 mm (1½ in) pitch □						Shell i.d. (in)							
	1 pass		2 pass		4 pass		6 pass		1 pass		2 pass		4 pass		6 pass		1 pass			2 pass		4 pass		6 pass		
	0.0	0.33	0.0	0.33	0.0	0.33	0.0	0.33	0.0	0.33	0.0	0.33	0.0	0.33	0.0	0.33	0.0	0.33		0.0	0.33	0.0	0.33	0.0	0.33	
203	18	18	14	14	8	8	—	—	—	—	—	—	—	—	—	—	—	—	—	—	—	—	—	—	8	
254	33	32	28	27	21	20	17	16	27	23	20	20	14	14	10	10	—	—	—	—	—	—	—	—	10	
305	51	50	46	45	37	36	32	31	37	36	33	32	27	26	23	22	22	22	22	22	23	22	20	19	12	
337	65	63	59	57	49	47	44	42	47	45	43	41	36	34	32	30	30	30	30	30	35	30	27	26	13½	
387	89	87	82	80	71	69	65	63	65	63	60	58	52	50	47	45	45	45	45	50	44	42	41	39	15½	
438	118	114	110	106	98	94	91	87	86	83	80	77	71	68	66	63	63	63	63	69	67	61	57	55	17½	
489	151	145	142	136	128	122	120	114	110	106	104	100	93	89	88	84	84	84	84	89	85	81	77	76	19½	
540	188	180	178	170	163	155	154	146	137	131	130	124	119	113	112	106	106	106	106	113	107	103	97	98	21½	
591	229	218	218	207	201	190	192	181	167	159	159	151	147	139	140	132	132	132	138	138	131	127	120	122	115	23½
635	263	251	252	240	233	221	223	211	192	183	184	175	170	161	163	154	154	154	159	159	152	147	140	141	134	25
686	311	296	299	284	279	264	268	253	227	216	218	207	203	192	195	184	184	184	187	189	179	176	166	170	160	27
737	363	345	332	328	310	317	299	299	265	252	255	242	240	227	231	218	218	218	218	222	210	208	196	201	189	29
787	419	397	405	383	382	360	369	347	307	291	297	281	280	264	271	255	255	255	252	256	243	241	228	234	221	31
838	479	454	464	439	437	414	426	401	351	332	340	321	322	303	312	293	293	293	304	288	295	279	263	271	255	33
889	543	513	527	497	501	471	487	457	398	376	386	364	367	345	357	335	335	335	345	326	335	316	299	320	291	35
940	611	577	594	560	567	533	552	518	448	423	436	411	415	390	405	380	380	388	366	377	355	360	338	351	329	37
991	681	643	663	625	634	596	619	581	499	471	486	458	465	437	453	425	425	432	408	421	397	402	378	393	369	39
1067	796	750	777	731	746	700	729	683	585	551	571	537	548	514	536	502	502	506	477	494	465	474	445	464	435	42
1143	921	867	901	846	867	813	849	795	676	636	661	621	636	596	623	583	583	586	551	573	538	552	517	541	506	45
1219	1054	991	1032	959	996	933	977	914	775	728	759	712	733	686	719	672	672	671	630	756	616	634	593	623	582	48
1295	1197	1124	1174	1101	1136	1063	1115	1042	880	826	863	809	835	781	820	766	766	762	715	747	700	723	676	711	664	51
1372	1349	1265	1325	1241	1284	1200	1263	1179	992	930	974	912	944	882	929	867	867	859	805	844	790	818	764	805	751	54
1448	1510	1414	1484	1388	1442	1346	1419	1323	1110	1040	1091	1021	1060	990	1043	973	973	962	900	946	884	918	856	905	843	57
1524	1680	1571	1653	1544	1608	1499	1584	1475	1236	1156	1216	1136	1183	1103	1165	1085	1085	1070	1001	1053	984	1024	955	1010	941	60

At inlet:

(a) calculate  $R_i = \left\{ \frac{1 - 2(h_i/D_i)}{D_i/D_i} \right\}$

(b) obtain  $Z_i$  from Fig. A3.2

(c) calculate number of tubes omitted from full count due to untubed area =  $Z_i N_t$

At outlet:

(a) calculate  $R_o = \left\{ \frac{1 - 2(h_o/D_i)}{D_i/D_i} \right\}$

(b) obtain  $Z_o$  from Fig. A3.2

(c) calculate number of tubes omitted from full count due to untubed area =  $Z_o N_t$

Approximate tube count:  $N_t \{1 - (Z_i + Z_o)\}$

### A3.3 Tube count reduction for untubed areas – examples

Two examples are given to demonstrate the procedure for calculating the tube count reduction for untubed areas.

#### Example 1: Fixed tubesheet exchanger

A fixed tubesheet exchanger, 889 mm inside diameter, 1 tubesheet pass, contains tubes 25.4 mm outside diameter at 31.75 mm triangular pitch.

The impingement baffle is situated such that  $h_i = 74$  mm. If the outer tube limit is 876 mm, what is the tube count?

At inlet:

$$N_t = 671 \text{ from Table A3.1}$$

$$h_i = 74$$

$$D_i = 876$$

$$D_i = 889$$

$$h_i/D_i = 74/889 = 0.0832$$

$$D_i/D_i = 876/889 = 0.985$$

$$R_i = \{1 - (2 \times 0.0832)\}/0.985 = 0.846$$

$$Z_i = 0.035 \text{ from Fig. A3.2}$$

At outlet: no calculations required.

$$\text{Approximate tube count: } 671 \{1 - 0.035\} = 647$$

#### Example 2: Split backing ring floating-head exchanger

A split backing ring floating-head exchanger, 1067 mm inside diameter, 2 tube-side passes, contains tubes 19.05 mm outside diameter at 25.4 mm square pitch. The exchanger is a no-tube-in-window design, having a



symmetrical bundle, with  $h_i = h_o = 231$  mm. If the outer tube limit is 1020 mm, what is the tube count?

At inlet:

$$\begin{aligned} N_i &= 1223 \text{ from Table A3.3} \\ h_i &= 231 \\ D_1 &= 1020 \\ D_i &= 1067 \\ h_i/D_i &= 231/1067 = 0.216 \\ D_1/D_i &= 1020/1067 = 0.956 \\ R_i &= \{1 - (2 \times 0.216)\}/0.956 = 0.594 \\ Z_i &= 0.145 \text{ from Fig. A3.2} \end{aligned}$$

At outlet: as  $h_o = h_i$ ,  $Z_o = 0.145$

$$\text{Approximate tube count: } 1223 \{1 - (0.145 + 0.145)\} = 868$$

### A3.4 Pull-through floating-head exchangers

Tube counts are not given for pull-through floating-head exchangers, because the OTL is greatly dependent on the design pressures. However, tube counts may be estimated from the tube counts for other exchanger types once the OTL is known. A quick, but rough, method is to assume that the diameter of a pull-through exchanger is 'two sizes larger' than a split backing ring exchanger to contain the same number of tubes of identical configuration. Referring to the shell diameters listed in Chapter 12, it is assumed, for example, that a 787 mm (31 in) diameter pull-through unit contains the same number of tubes as a 686 mm (27 in) diameter split backing ring unit; a 540 mm (21.25 in) diameter pull-through unit matches a 438 mm (17.25 in) diameter split backing ring unit, and so on.

A more accurate method is to attempt to match the outer tube limit for the pull-through unit with a similar outer tube limit for a full-count fixed tubesheet or split backing ring unit. As an example, consider a two-pass pull-through unit, 889 mm diameter, containing 19.05 mm outside diameter tubes at 25.4 mm triangular pitch. To estimate the tube count, proceed as follows, noting from Fig. 12.3 that

$$\begin{aligned} \text{outer tube centre limit (OTCL)} &= \text{OTL} - (\text{tube o.d.}) \\ &= D_s - C_1 - d_o \end{aligned}$$

From Table 12.2, OTCL of typical pull-through type, 889 mm dia., is  
 $889 - 104.78 - 19.05 = 765.17$  mm

From Table 12.2, OTCL of split backing ring type, 838 mm dia., is  
 $838 - 41.28 - 19.05 = 777.67$  mm

2 pass: full count = 844 (Table A3.3)

Approximate number of tubes for OTCL of 765.17 mm is

$$844 (765.17/777.67)^2 = 817$$

Alternatively, from Table 12.2, OTCL of fixed tubesheet type, 787 mm dia., is

$$787 - 12.7 - 19.05 = 755.25 \text{ mm}$$

2 pass: full count = 798 (Table A3.1)

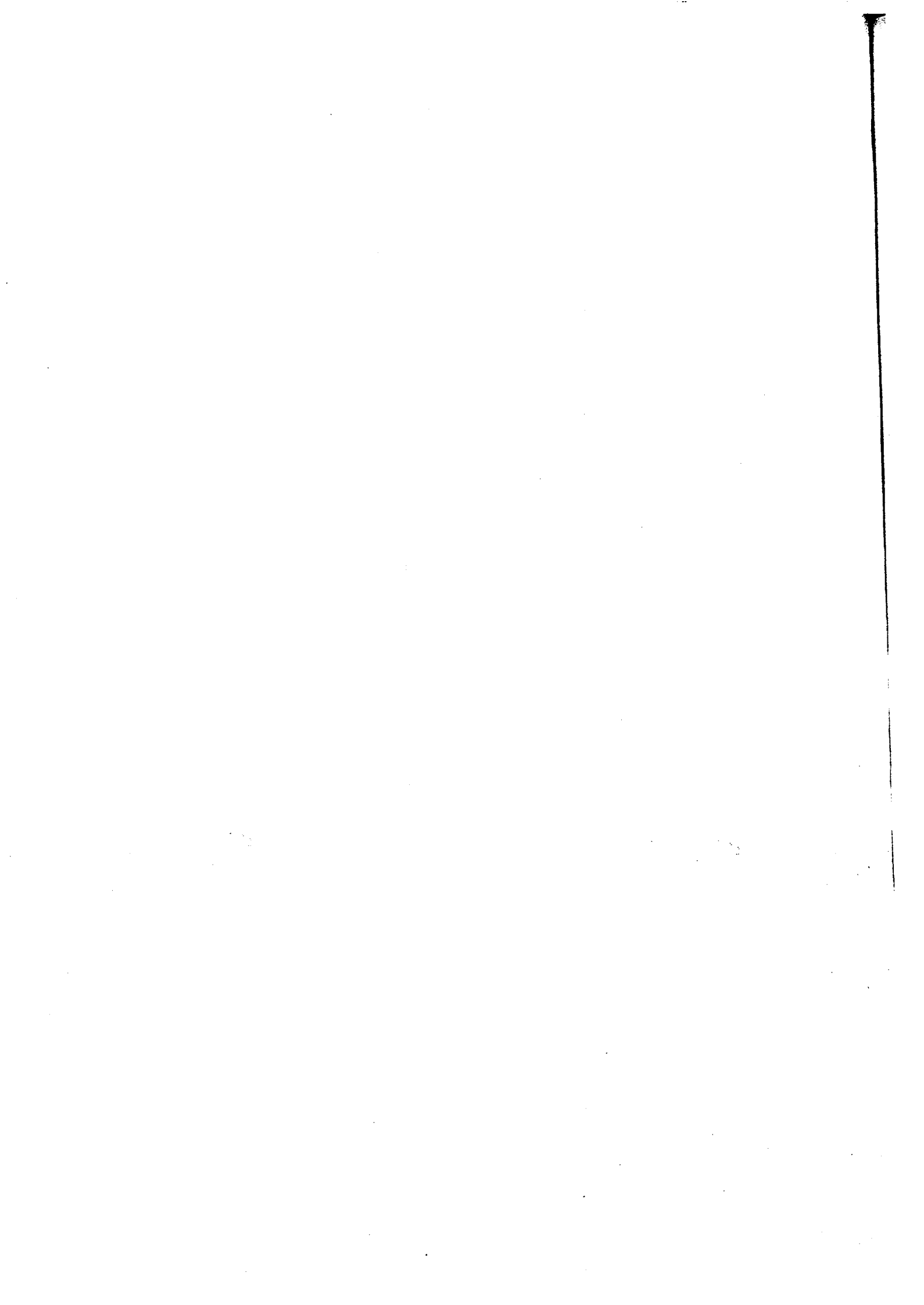
Approximate number of tubes for OTCL of 765.17 mm is

$$798(765.17/755.25)^2 = 819$$

The reduction in tube count due to any untubed area may be calculated as described in sections A3.2 and A3.3.

### Acknowledgement

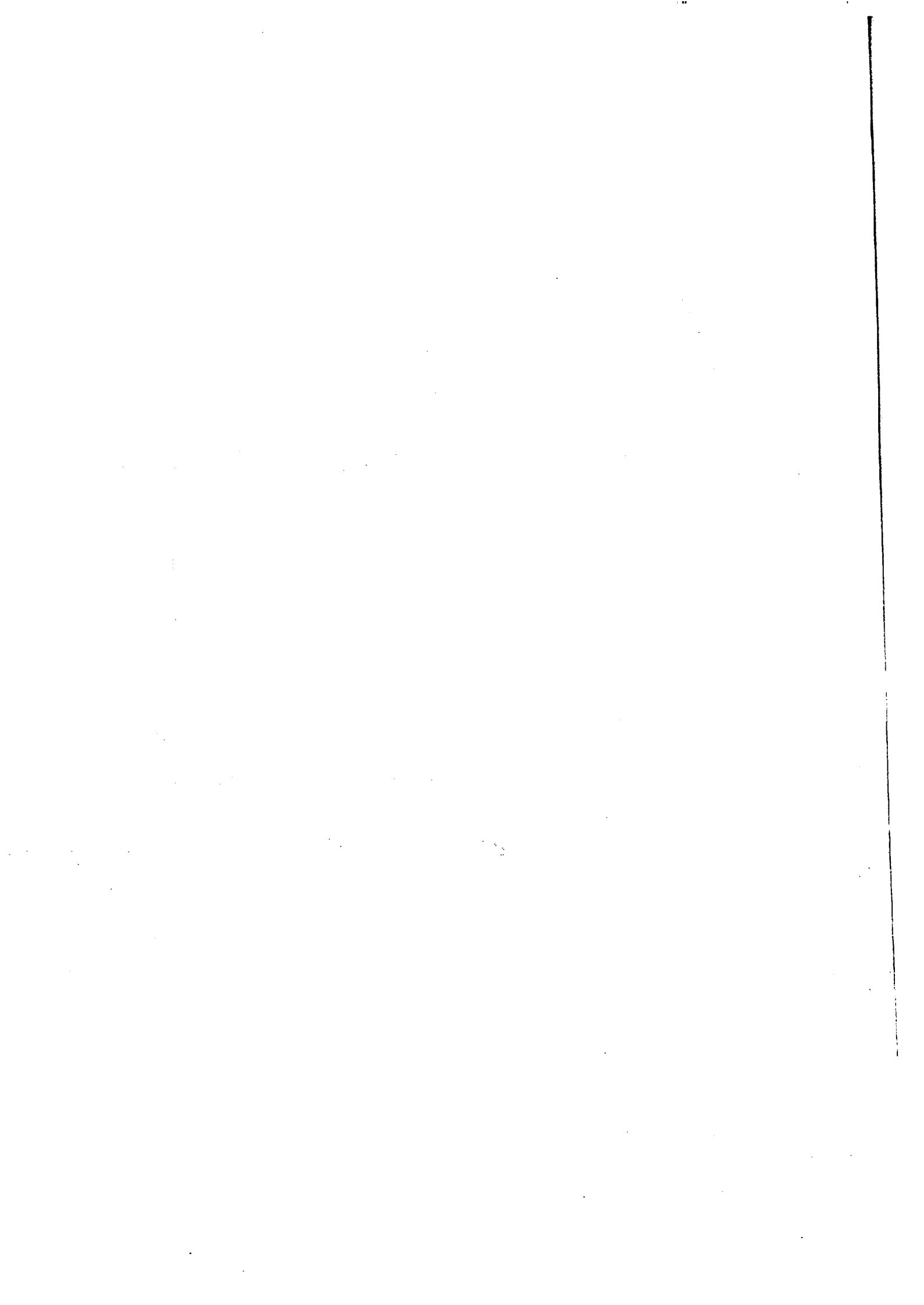
Tables A3.1–A3.3, Fig. A3.1 and Fig. A3.2 were prepared by the author for *Heat Exchanger Design Handbook* (1983), Vol. 4, Section 4.2, and are reproduced by permission of Hemisphere Publishing Corp., New York.



## Materials and cost

The choice of material for heat transfer equipment requires careful consideration. It obviously affects the capital cost and operating life of the equipment, but it may also influence the choice of exchanger type and its mechanical design features. Chapter 18 begins with a description of the various corrosion mechanisms encountered in heat transfer equipment and typical methods for eliminating them. The chapter then discusses the wide variety of materials used in heat transfer equipment, together with their principal usage, merits and limitations. The relative cost of these materials, in relation to carbon steel, is presented in the early part of Chapter 19.

Parts 2 and 3 presented correlations, methods and examples for the thermal design of some of the heat exchanger types described in Part 1. However, in the early stages of heat transfer equipment assessment an accurate thermal design is seldom required. In many cases, an approximate size and cost will suffice to decide the exchanger type and relevant economic factors. The major part of Chapter 19 presents data from which the approximate size and cost of certain heat exchanger types may be determined rapidly.



## Materials of construction

Some specialised heat exchangers are made of graphite (section 5.8), glass (section 5.9), and Teflon™ (section 5.10), for extremely high corrosion resistance, but because of their pressure and temperature limitations, the majority of heat exchangers, irrespective of type, are made of metal. The metals include a variety of steels, and alloys based on aluminium, copper, nickel and titanium. Alloying metals in varying proportions include aluminium, boron, chromium, cobalt, copper, iron, magnesium, manganese, molybdenum, nickel, niobium, palladium, tantalum, tin, tungsten, vanadium and zinc. The use of non-metals is limited to linings for metallic parts and gaskets.

The chapter begins with a brief discussion of single component corrosion data and the problems of material selection. This is followed by a description of the different forms of corrosion which the materials may have to withstand. The chapter continues by describing a numbering system, compositions, applications and limitations relating to some of the chief materials used in heat exchanger construction. The metals are usually purchased as tubes, pipes, plates, forgings and bars, and less frequently, as castings. The use of solid metal construction may become expensive as thickness increases, and the chapter is completed by describing bi-metal construction and non-metallic linings which may provide cheaper alternatives.

In 1982 the annual cost of corrosion in the UK from all causes was of the order of £10 billion, of which heat exchangers accounted for £300 million.

### 18.1 Corrosion data and material selection

Among several excellent sources of data which indicate the corrosion resistance of metals, their alloys and non-metals, are those provided by NACE - The National Association of Corrosion Engineers (1974; 1975), Perry and Green (1984), IPC Industrial Press (1983), Schweitzer (1976), Rabald (1968) and Dept of Industry publications of The National Corrosion Service, NPL, Teddington, UK.

Except for certain specific mixtures, such data usually relate to single-component fluids and it should be emphasised that the selection of materials can seldom be made with confidence from these data alone. Such data serve to narrow the choice of material.

The corrosion behaviour of a single-component fluid may be entirely different in a mixture. For instance, Kirby (1980) cites the case of 33% sulphuric acid at 90–105 °C being 6–20 times more corrosive to nickel-based alloys and stainless steel when mixed with potassium chloride and acidic sulphonated naphtha derivatives, than it is by itself. In addition, trace elements may be the cause of severe corrosion in an otherwise benign fluid. As examples, Kirby cites (a) monel, which is incompatible with brine containing trace mercury salts, (b) types 304 and 316 stainless steels which are incompatible with aqueous solutions containing trace chlorides and (c) trace amounts of water in organic chlorides which may cause hydrolysis and produce hydrochloric acid.

Corrosion data of this type, which is usually obtained under laboratory conditions, cannot be expected to take into account the design of the heat transfer equipment itself. High fluid velocity caused by an overload condition, for instance, may remove the protective film from a surface, which would be unattacked at lower velocities. There may be regions where corrosion could be caused by aeration, impingement, erosion or cavitation, etc. Conversely, stagnant regions and crevices may induce localised corrosion. The selection of two or more different metals in the same equipment needs particular care; each may be an ideal choice by itself, but in combination galvanic corrosion (see section 18.2.2) could occur.

Previous experience with plants having design and operation characteristics closely matching those of the new plant is the best approach for material selection, but this is not always possible. Field or laboratory tests, under conditions which simulate the new plant as closely as possible, is the more practical solution. When proprietary materials are involved, the makers must be consulted.

## 18.2 Forms of corrosion

The forms of corrosion described in this section are based on Fontana (1975).

### 18.2.1 Uniform attack

Corrosion occurs uniformly over the entire surface as a result of chemical or electrochemical reaction between the metal and the fluid in contact with it. It is the most common form of industrial corrosion. Unlike some of the other forms of corrosion it is usually detected visually well before failure, thus enabling remedial action to be taken, such as replacement, change of material, coatings, inhibitors, cathodic protection, etc.

### 18.2.2 Galvanic corrosion

When two dissimilar metals are in contact with one another, either physically or electrically, in a corrosive or conductive solution (electrolyte), any potential difference which exists produces a flow of electrons between them. Compared with their resistance to corrosion when not in contact with one another, there is usually an increase in corrosion of the less noble or less corrosion-resistant metal, and a reduction in the corrosion of the more noble or more corrosion-resistant metal. The more noble end is termed the cathode and the less noble end the anode. The mechanism is termed galvanic corrosion and may be illustrated by a 'dry' cell battery in which the more noble carbon electrode acts as the cathode, the less noble corroding zinc case acts as the anode, and the current which is developed passes between them via the moist conductive filler paste.

Locations in a shell-and-tube exchanger where galvanic corrosion may occur if different metals are in contact include (a) the tube-tubesheet junction at the inner face, (b) the tube-tubesheet attachment at the front face and (c) the baffle hole-tube and baffle-shell contact points.

The galvanic series for various metals and alloys given in Table 18.1 provides the order of the potential difference developed between two different metals coupled together in an electrolyte, and how galvanic corrosion is likely to arise. In a bi-metal junction, corrosion will be greatest if the two metals are far apart in the table and in order to minimise corrosion the two metals should lie close together in the table. For example, in a water system having steel pipes and copper fittings, corrosion of the steel is likely to occur, as it is anodic to the copper. Despite being made of corrosion-resistant metals, pump shafts and valve stems may fail in contact with packing material made of graphite which is well to the cathodic end of the table. Although the relative positions in the galvanic series is a valuable guide, other factors such as the relative areas of the anode and cathode, the polarisation characteristics of the metals and the flow rate, temperature and composition of the electrolyte, must be considered to determine the intensity of corrosion.

Regarding the relative areas of the anode and cathode the undesirable situation is a large cathode and a small anode. A well publicised example is a comparison of riveted copper and steel plates immersed in sea water. The copper plates (large cathode) have steel rivets (small anode) and rapid corrosion of the steel rivets occurs due to the undesirable area ratio. In the case of steel plates (large anode) and copper rivets (small cathode), the area ratio is more favourable; although the steel corrodes, a good joint is maintained as the more noble copper is resistant to sea water.

If a less noble metal, such as steel, is given a painted or similar coating to protect it from corrosion, it is essential to maintain the coating in good condition particularly if the steel is in contact with a large area of more noble metal, such as stainless steel. If the coating develops a small defect, a small anodic area will be established in the steel and local corrosion is likely to be intense due to the unfavourable large stainless-steel cathode/small steel anode situation.



**Table 18.1 Galvanic series for various metals and alloys****Anodic end (corroded end, least noble)**

Magnesium and alloys  
 Zinc  
 Aluminium and alloys  
 Cadmium  
 Steel  
 Cast iron  
 13% chrome (active)  
 Type 304 stainless (active)  
 Type 316 stainless (active)  
 Lead  
 Tin  
 Muntz metal  
 Naval brass  
 Nickel (active)  
 Inconel™ (active)  
 Admiralty brass  
 Aluminium bronze  
 Red brass  
 Copper  
 Aluminium brass  
 90/10 cupro-nickel  
 80/20 cupro-nickel  
 70/30 cupro-nickel  
 Nickel  
 Inconel™ (passive)  
 Monel™ (passive)  
 13% chrome (passive)  
 Type 304 stainless (passive)  
 Type 316 stainless (passive)  
 Silver  
 Titanium  
 Graphite  
 Gold  
 Platinum

**Cathodic end (non-corroded end, most noble)**

A heat exchanger with thin copper alloy tubes, attached to a thick steel tubesheet, would appear to be an undesirable construction should galvanic corrosion occur. In practice, the thin copper alloy tubes (small cathode) are preserved at the expense of the corroding tubesheet and in a moderately corrosive environment the large mass of the tubesheet (large anode) enables a reasonable life to be obtained.

The principles of galvanic corrosion form the basis of cathodic protection in which a metal to be protected is deliberately made the cathode of a galvanic cell. Cathodic protection may be achieved by either the use of sacrificial anodes, or by applying a current from an external d.c. power source through an inert anode (impressed current system). A familiar example of the former is galvanised steel where the zinc coating is the sacrificial anode which corrodes preferentially to protect the steel sheet. Because they lie well to the anodic end of the galvanic series, magnesium, zinc and aluminium are often used as the sacrificial anodes in

cathodic protection systems. (Figure 18.6 shows a typical heat exchanger header given cathodic protection by sacrificial zinc anodes bolted to the flat cover).

Galvanic corrosion may be prevented by insulating the metals from one another using rubber, asbestos or plastic. In a bolted flange system, it should not be assumed that the provision of a non-conductive gasket between flanges, and a non-conductive washer under each nut and bolt head, is sufficient to isolate one flange from the other and it is usually necessary to provide an insulating sleeve over the complete bolt shank itself.

### 18.2.3 Stress corrosion

An insidious form of attack is stress corrosion which results from a combination of *tensile* stress and general corrosion from a specific corrosive medium. It is often difficult to detect because there may be no apparent loss of metal due to general corrosion, but it ultimately reveals its presence, without warning, in the form of cracks – which may be intergranular or transgranular – and is commonly known as stress-corrosion cracking. Failure may occur in a few hours or many years, at any stress level, in almost all metals and alloys. It is achieved more quickly under the combined action of stress and corrosion than either by itself.

Locations in a shell-and-tube heat exchanger where stress-corrosion cracking may occur include cold-worked parts such as U-bends and roller-expanded tube ends.

An early example of stress-corrosion cracking was the 'season cracking' of brass, so called because brass cartridge cases failed due to the presence of ammonia in heavy seasonal tropical rainfall. Another early example was the 'caustic embrittlement' of steel. Explosions occurred in riveted boilers of steam locomotives and subsequent investigation of stressed areas around the rivet holes revealed cracks and the presence of sodium hydroxide (caustic).

In addition to caustic solutions, stress-corrosion cracking of carbon and low-alloy steels may occur in the presence of nitrate solutions, mixtures of sulphuric and nitric acids and calcium chloride brines.

Combinations of metals and their specific corrosive media which may exhibit stress-corrosion cracking are:

aluminium alloys: sodium chloride solutions  
 copper alloys: ammonia, amines, mercury salt solutions  
 Monel™: hydrofluoric acid  
 nickel: fused sodium hydroxide, fused potassium hydroxide  
 type 300 stainless steels: chloride and caustic solutions  
 titanium: red fuming nitric acid, methanol

It should be noted that stress-corrosion cracking can occur even with concentrations of chlorides as low as 3 p.p.m.

At the design stage, the obvious measure to avoid stress-corrosion cracking is to select the correct material, in relation to its operating

environment, based on similar service experience. If such information is not available, the likelihood of stress-corrosion cracking will be lessened if tensile stresses, stress-raising features and cold work are minimised. If the equipment is not too large and vital mechanical properties of the metal are not impaired, the most effective measure is heat treatment to relieve internal stresses. Stress relief of carbon-steel equipment is often carried out under such conditions without difficulty, but the heat-treatment temperature for austenitic stainless steels is so high that distortion of the equipment may occur.

Other methods of combating stress-corrosion cracking include (a) shot or hammer peening of the surfaces to introduce compressive stresses, (b) the introduction of inhibitors to the corrosive media and (c) the application of surface coatings and cathodic protection. However, these methods should be applied with caution. Corrosion of a surface layer, initially in compression, may induce tensile stresses, surface coatings may develop porosity and other defects, and evolved hydrogen arising from cathodic protection may increase cracking.

#### 18.2.4 Crevice corrosion

Localised corrosion, often intense, may occur in stagnant crevices, or shielded areas in contact with the corrosive media and is termed crevice corrosion. Locations in a shell-and-tube exchanger, where crevice corrosion may occur, are (a) the gap between tube and tube hole at the inner tubesheet face, (b) the tubesheet-shell attachment of fixed tubesheet exchangers (Fig. 2.15), (c) the surface beneath absorbent gaskets and (d) under bolt heads.

Deposits of dirt and corrosion products also provide shielded areas under which crevice corrosion can occur and for this reason it is sometimes termed 'deposit corrosion'.

The presence of a crevice, or shielded area, does not necessarily mean that corrosion will occur, and it depends on the particular metal/fluid combination. Prevention of corrosion consists of either changing the metal or eliminating the crevice by a change in design. Internal bore welding described in section 2.16.2 is designed to eliminate the gap between tube and tube hole. A change in gasket material to a non-absorbent metallic or plastic type prevents the capillary action associated with absorbent, fibrous gaskets.

In the case of deposit corrosion, flow passages should be designed to avoid stagnant areas and ensure complete drainage. Fluid velocities should be sufficiently high to discourage solid matter from settling, but this may only be successful if the unit is operated continuously at near-full design throughput. Deposits may settle when the throughput is reduced considerably and may still adhere to the surfaces when the throughput is later increased, in which case regular, thorough cleaning is necessary. If chemical cleaning is carried out, subsequent washing or steaming out is essential to remove all traces of the cleaning fluid from likely crevices.

### 18.2.5 Pitting corrosion

A particularly destructive form of corrosion is that due to pitting in which intense localised attack results in pits or holes in the metal, the pits having a depth about the same size as the diameter at the surface. The pits are usually small and therefore difficult to detect, particularly if they are obscured by dirt or corrosion product, and complete failure may be sudden. Although only a small quantity of metal is lost, a single small hole in the wall of a heat exchanger tube, for instance, renders it useless. Once pits begin to form, the attack usually proceeds at an accelerated rate, so that an increase in corrosion allowance of a component provides no protection.

It is not clear why pitting occurs in particular areas and leaves other identical areas unscathed, but the surface finish is regarded as an important factor. Pitting is more likely to occur where the surface has rough areas or scratches. Freedom from pitting during laboratory tests does not guarantee immunity in service.

In the design of exchangers the use of materials which are known to be immune from pitting corrosion, based on similar service experience, is the safest procedure, but pitting is likely to be minimised if the measures described earlier to resist deposit corrosion are adopted.

### 18.2.6 Erosion corrosion

Erosion is the physical deterioration of a metal surface due to the action of the fluid flowing over it, and the wear will be increased if the fluid contains solid particles in suspension. If the attack is intensified by corrosion, the process is termed erosion corrosion. It is revealed as grooves, waves or holes in a pattern related to the direction of the flowing fluid. As expected soft metals, such as copper and lead, and metals which depend on a surface film for corrosion resistance, such as aluminium and stainless steel, are particularly prone to erosion corrosion.

The location in a shell-and-tube heat exchanger which is particularly prone to erosion corrosion is the initial 100–150 mm of the internal tube surfaces at the inlet end, where high turbulence exists.

Erosion corrosion in this area may be prevented by the provision of tube-end inserts. These consist of 100–150 mm long metallic or plastic tubes, sometimes flared or collared at the inlet end, which make a tight fit inside each tube. The exit end of the insert is feathered in order to provide a gentle transition from the insert to the tube, thus preventing erosion corrosion occurring in the tube just beyond the exit of the insert. If metallic inserts are used, the metal should be chosen to avoid galvanic corrosion. In most cases, however, the problem of erosion corrosion is overcome by the correct choice of metal.

Cavitation is a special form of erosion corrosion caused by the growth and collapse of vapour bubbles in a liquid adjacent to a metal surface. The attack is caused by both chemical and mechanical action in which the collapsing bubble is capable of removing the protective film and the metal

itself from the surface. Another special form of erosion corrosion is fretting which may occur when two surfaces slide over one another with repeated oscillatory motion under load. Corrosion may occur when either frictional heat oxidises the metal, which then wears away, or when the protective layer of oxide or corrosion product is removed by mechanical means. In either case exposure of unprotected surfaces leads to continual corrosion and the parts may be damaged by seizing or galling. Flow-induced vibration may cause damage of this nature when tubes pass through the shell-side baffles of a shell-and-tube exchanger, particularly if the baffles are harder than the tubes. Table 18.2 lists desirable velocities for water flowing inside tubes of various alloys.

**Table 18.2** Desirable velocity ranges for water flowing inside tubes<sup>(1)</sup>

<b>Metal</b>	<b>Velocity range (m/s)</b>
Steel ('fresh' water)	0.8–1.5
Copper	0.9–1.2
Admiralty brass	0.9–1.8
Aluminium brass	1.2–2.4
Aluminium bronze	1.8–2.7
90/10 cupro-nickel	1.8–3.0
70/30 cupro-nickel	1.8–4.5
Monel	1.8–4.5
Stainless steel – type 316	2.4–4.5

*Notes:*

(1) Salt water unless otherwise stated.

(2) Maximum water temp. = 43 °C salt = 50 °C 'fresh'.

### 18.2.7 Selective leaching

Selective leaching, or parting, is the selective removal of one metal constituent from an alloy by corrosion. A well-known example is dezincification of 70/30 brass (70% copper, 30% zinc) where the zinc is preferentially attacked to leave a porous mass of copper which has no strength or leak-tightness. The problem is solved by the addition of inhibitors such as antimony, arsenic, phosphorus or tin to the alloy.

Another example is the graphitisation of grey cast iron in weak acid solutions, for example, where selective leaching of the ferrous matrix leaves a porous mass of graphite. White, malleable and ductile cast irons do not exhibit this feature.

### 18.2.8 Intergranular corrosion

Intergranular corrosion is preferential corrosion at or adjacent to grain boundaries, with little corrosion of the grain itself. It is also called intercrystalline corrosion. The metal may disintegrate but will certainly suffer loss of strength and ductility.

Certain austenitic stainless steels are particularly prone to intergranular corrosion when they are heated to 500–800 °C, which in the case of welding, is achieved about 3 mm or more from the weld, rather than immediately adjacent to it. This type of attack, known as weld decay, is described in section 18.7.1.

## 18.3 Materials and numbering system

A huge variety of materials is used throughout the world for heat exchanger construction and identical materials exist under a variety of numerical designations and trade names. In order to present a consistent system, all metals described in this chapter, with the exception of a small number of proprietary alloys, are listed in ASME (1986), Section VIII, Division 1, being typical metals used in heat exchanger construction. They also have an ASTM specification (American Society for Testing and Materials). Most of the technical data have been provided by material suppliers, but additional data have been taken from Gackebach (1960), Kirby (1980), Perry and Green (1984), Pickering (1979) and Sedriks (1979).

Inevitably certain alloys become well known by the trade names of their makers; some are proprietary, but many, having almost identical properties, are produced by other makers. To minimise confusion, the Unified Numbering System (UNS) was established in 1974 by ASTM and the American Society of Automotive Engineers (SAE). Every alloy is identified by a five-digit number, preceded by a code letter, which identifies the basic metal. The system related to alloys listed in Tables 18.4–18.7 is as follows:

<i>UNS number range</i>	<i>Alloy</i>
A00001–A99999	aluminium and its alloys
C00001–C99999	copper and its alloys
S00001–S99999	heat- and corrosion-resistant stainless steels
N00001–N99999	nickel and its alloys
R50001–R59999	titanium and its alloys (not numbered in ASME or ASTM at present)

Numbering systems of American organisations, such as the Aluminium Association (AA numbers), the Copper Development Association (CDA numbers) and the American Iron and Steel Institute (AISI numbers) have retained some identity. The UNS numbers incorporate these numbers by the addition of digits as necessary.

## 18.4 Carbon and low-alloy steels

The most widely used metals for construction in the process industries are iron, carbon steel, and low-alloy steel. In the case of heat transfer equipment, cast iron is sometimes used for low-pressure applications such as headers for shell-and-tube exchangers in cooling-water service, cascade coolers and components for boilers and economisers, but its usage is small in relation to carbon and low-alloy steels. 'Low-alloy' steels for heat exchangers and pressure vessels relate to steels alloyed chiefly with chromium (max. 9% with negligible nickel present), nickel (max. 9% with negligible chromium present) and molybdenum (max. 1%). Other elements which may be added intentionally in definite quantities include aluminium, boron, cobalt, tungsten and vanadium. Alloys of iron and carbon containing less than 1.7% carbon are regarded as steels, but for heat exchanger construction, which involves rolling, cutting, welding, etc., the carbon content is usually less than 0.35%.

### 18.4.1 Types of carbon steel

There are three types of steel, related to deoxidation practice, namely, rimmed, semi-killed and killed. In the steel-making process, oxygen is used to remove excess carbon from the molten metal in order to achieve the required carbon content in the finished steel. Carbon monoxide, formed by the combination of oxygen and carbon in the melt, bubbles to the surface but some oxygen may remain dissolved in the melt, which will influence the quality of the finished steel. The control of dissolved oxygen in the molten metal, before and during casting, is termed deoxidation practice.

Rimmed steel is cast into ingots with no attempt made to remove oxygen and therefore considerable reaction between carbon and oxygen occurs in the melt. The finished steel has a smooth, homogeneous surface or rim, but lacks chemical homogeneity and is used where a superior surface finish is required. The manufacture of killed steels represent the opposite procedure in that deoxidisers in the form of aluminium or silicon, or both, are added before pouring into the ingot mould. These elements combine preferentially with the oxygen in the melt so that little reaction occurs between oxygen and carbon. This steel has a homogeneous structure and may be produced with a fine or coarse grain.

Deoxidising practice for semi-killed steels falls between those for rimmed and killed steels. Semi-killed steels are only partially deoxidised and as expected properties fall between those of rimmed and killed steels. They are used for plates and bars, but unlike the killed steels are not produced to a controlled grain size.

### 18.4.2 Corrosion resistance

Because of its versatility in almost every shop operation, ready availability and low cost in relation to other metals, carbon steel is widely

used in heat transfer equipment. As it is suitable for many hydrocarbons and natural waters, it is widely used in petroleum and petrochemical applications. It is attacked by all concentrations of hydrochloric, phosphoric and nitric acids, but resists sulphuric acid at all concentrations above 70% and temperatures below 50 °C, and hydrofluoric acid at all concentrations above 80% and temperatures below 65 °C. It is resistant to alkalis such as sodium hydroxide, carbonate and phosphate. Hot concentrated alkalis are particularly aggressive and stressed parts are liable to stress-corrosion cracking. Hot dry gases such as sulphur dioxide, hydrogen chloride and chlorine do not affect steel, but if water vapour is present, severe attack may occur once condensation begins.

### 18.4.3 Hydrogen attack

Gases containing hydrogen may decarburise steel depending on temperature and hydrogen partial pressure and the hydrogen attack may occur as surface decarburisation or internal decarburisation. High temperature and low partial pressure promotes surface attack; modest temperature and high partial pressure promotes internal attack. In surface decarburisation carbon migrates to the surface where it combines with hydrogen, and oxygen if present, to form methane and carbon monoxide. The surface is depleted of carbon resulting in loss of strength and hardness, but with an increase in ductility. In the case of internal decarburisation, hydrogen permeates the steel and reacts with carbon to form methane, which cannot diffuse out. The methane accumulates in voids, many of which are at grain boundaries, to develop stresses sufficient to fissure crack or blister the steel.

To overcome this, carbide stabilizers such as chromium and molybdenum are added to steel in various proportions to produce a range of steels known as low alloys. (These are often referred to as 'carbon-molys' and 'chrome-molys'.) The low-alloy steels are considered for use when hydrogen-bearing gases are involved, termed 'hydrogen service'. The selection of the steel is based on data provided by Fig. 18.1, for example, which relate maximum operating temperature to hydrogen partial pressure for various low-alloy steels and carbon steel. The graphs in Fig. 18.1 are known as 'Nelson curves' as they were developed over many years by G. A. Nelson.

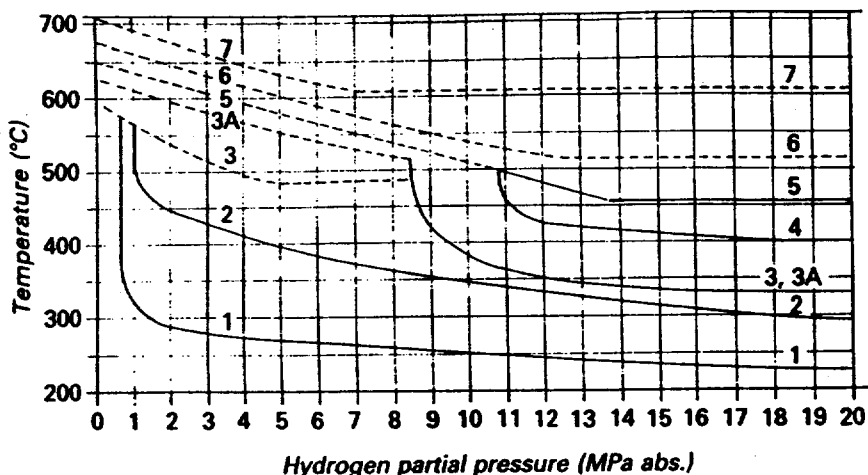
Consider a hydrogen-bearing gas at 450 °C in which the hydrogen partial pressure is 5 MPa abs. If the curves of Fig. 18.1 are entered horizontally at 450 °C and vertically at 5 MPa, the coincident point lies between alloys 2 and 3. For safety, the higher number would be selected, i.e. number 3 which is a 1% chrome-½% molybdenum low-alloy steel.

When stainless-steel clad plate is used for economy, the backing steel must still be selected from the 'Nelson curves' as hydrogen is able to migrate through the stainless-steel cladding.

Heat exchanger units in hydrogen service may have a large temperature range on each side such that several shells in series are required for the duty. Table 19.3(f) shows that the cost factor for low-alloy steel plate, in relation to carbon steel, is about 1.7–2.4. For



**Figure 18.1** Operating limits for steels in hydrogen service (based on API Publication 941 (3<sup>rd</sup> edn), 1982, Fig. 1, *Steels for hydrogen service at elevated temperatures and pressures in petroleum refineries and petrochemical plants*; by permission of American Petroleum Institute)



Key			
No.	Steel	No.	Steel
1	Carbon steel	4	2.0 Cr–0.5 Mo
2	0.5 Mo	5	2.25 Cr–1.0 Mo
3	1.0 Cr–0.5 Mo	6	3.0 Cr–0.5 Mo
3A	1.25 Cr–0.5 Mo	7	6.0 Cr–0.5 Mo
- - - Surface decarburisation			
— Internal decarburisation			

safety, every shell could be made from the particular low-alloy steel which will resist hydrogen attack at the highest temperature in the system, but there is a significant cost incentive not to select a more expensive alloy than necessary. Some purchasers will allow the designer to select the appropriate alloy from the ‘Nelson curves’ for the shell-and-tube sides independently, in each shell, according to the calculated temperature on each side. For example, a multi-shell-in-series system may have all 2¼% chrome–½% moly alloy in the hottest shells, all carbon steel in the coldest shells, with other chrome–moly or carbon–moly alloys for the various components of intermediate shells.

The strength of carbon steels falls rapidly above about 400 °C, whereas many of the low-alloy steels provide greater strengths at this temperature and maintain reasonable strength up to 540 °C. Oxidation limits for steels in air and steam are about 500 °C and 425 °C respectively; for the low-alloys the corresponding values, which increase as the chrome content increases, are about 525–650 °C and 450–600 °C.

#### 18.4.4 Low-temperature service

Unlike stainless steels and the alloys of aluminium, copper, nickel and titanium, carbon and low-alloy steels are prone to the phenomenon of brittle fracture at low temperatures. Surprisingly most failures have occurred at temperatures as high as 0 °C to +20 °C. Brittle fracture of steel has been recorded since the end of the last century, but many

failures occurred in the hulls of welded ships (Liberty ships) sailing in Arctic waters during World War Two. Brittle fracture is an insidious low-energy fracture which usually occurs without prior deformation and therefore without warning. It is the opposite of ductility which is the property of a metal to experience plastic deformation without fracture. The temperature at which the fracture characteristics of a metal changes from ductile to brittle, and vice-versa, is termed the transition temperature. In selecting a steel for low-temperature use, its transition temperature must be below the minimum operating temperature.

Toughness is the resistance of a material to fracture following plastic deformation, expressed in terms of the energy required to cause fracture. An indication of toughness is provided by Charpy impact testing. The test specimen is usually a square bar, 10 mm × 10 mm in cross-section, 55 mm long, which has a 45° V-notch, 2 mm deep, prepared in the centre of the face on one side. It is supported at each end and broken through the notch by being struck with a falling pendulum. The amount by which the pendulum rises after impact is an indication of the energy absorbed by the specimen. The required test temperature is achieved by cooling the specimen in a cold medium, such as dry ice and acetone for temperatures down to -75 °C, dry ice and pentane, for lower temperatures down to -100 °C, and liquid nitrogen for even lower temperatures.

Charpy test specimens are taken from samples of the parent metal at the steel mill. In addition, specimens are taken from production test plates, which comprise plates welded together using a welding procedure identical to that in the actual unit. All specimens are taken across the weld, some being notched in the weld metal itself and others notched in the metal adjacent to the weld (heat affected zone (HAZ)).

The design code supplemented by purchasers' own requirements will specify when impact tests are required, together with the required impact test temperatures and the corresponding impact-test values which must be achieved. Impact-test temperatures and values are related to the component material and its thickness, whether the component is welded, and whether it is post-weld heat-treated. In determining impact-test temperatures, consideration must be given to the operating temperatures, particularly winter operation, start-up, shutdown and hydraulic testing. When considering brittle fracture above 0 °C, the temperature of the water used for hydraulic testing may be a governing factor. The designer then has the choice of selecting materials to suit the test water temperature or heating the test water to a higher temperature, in order to avoid the use of impact-tested materials. If the test water is heated, the name-plate must state this so that the same or higher site water temperature is used for retests at site.

In addition to the use of impact-tested materials to increase resistance to brittle fracture, post-weld heat-treatment is one of the most important operations to achieve this. It may also eliminate the need for impact-tested materials. Other factors which increase resistance to brittle fracture are (a) increasing the manganese/carbon ratio either by increasing the former or decreasing the latter, (b) using fully killed steels having deoxidisers of silicon or aluminium, (c) adding nickel to the steel, (d) refining the grain with niobium, (e) normalising after rolling and (f)

avoiding notch-like defects, such as sharp changes in section, undercutting, excessive reinforcement, slag inclusions, etc., during fabrication.

Table 18.3 gives the selection of steels containing various quantities of nickel for use at temperatures below  $-50^{\circ}\text{C}$ . The 36% nickel steel is known as Invar<sup>TM</sup> which is noted for its low thermal expansion characteristics.

**Table 18.3** Selection of steels for service below  $-50^{\circ}\text{C}$

Service temp ( $^{\circ}\text{C}$ )	Steel	Liquefied gas	Storage temp ( $^{\circ}\text{C}$ )
-51 to -100	3½% nickel	carbon dioxide	-78
		acetylene	-84
		ethane	-88
-101 to -120	5% nickel	ethylene	-104
-121 to -196	9% nickel	methane	-162
		oxygen	-183
		argon	-186
		nitrogen	-196
-197 to -269	36% nickel or austenitic stainless	hydrogen	-253
		helium	-269

## 18.5 Aluminium and aluminium alloys

Low density is the special property of aluminium and its alloys being only one-third of that of steel. They also offer an attractive appearance, high thermal conductivity, excellent resistance against corrosion from the atmosphere, salt water and a variety of chemicals, ease of fabrication, and excellent low-temperature strength and shock-resistance properties (as low as  $-269^{\circ}\text{C}$  for liquid helium). In addition, they are non-sparking and non-toxic.

### 18.5.1 Designation system

The compositions of some aluminium alloys, which are regarded as being readily weldable and are used in pressure vessel and heat exchanger construction, are given in Table 18.4. It will be noted that wrought alloy designations are divided into groups 1000, 3000, 5000, 6000 and 7000, the

Table 18.4 Composition of some aluminium alloys<sup>(4)</sup>

Alloy	UNS number	% composition (max. except where stated) <sup>(3)</sup>							
		Mg	Mn	Zn	Si	Fe	Cu	Cr	Ti
1060	A91060	0.03	0.03	0.05	0.25	0.35	0.05	—	0.03
1100	A91100	—	0.05	0.10	(Si + Fe) = 1.0	0.05–0.2	—	—	—
3003 <sup>(1)</sup>	A93003	—	1.0–1.5	0.10	0.6	0.7	0.05–0.2	—	—
3004 <sup>(2)</sup>	A93004	0.8–1.3	1.0–1.5	0.25	0.3	0.7	0.25	—	—
5052	A95052	2.2–2.8	0.10	0.10	0.25	0.4	0.10	0.15–0.25	—
5083	A95083	4.0–4.9	0.4–1.0	0.25	0.4	0.4	0.10	0.05–0.25	0.15
5086	A95086	3.5–4.5	0.2–0.7	0.25	0.4	0.5	0.10	0.05–0.25	0.15
5154	A95154	3.1–3.9	0.10	0.20	0.25	0.4	0.10	0.15–0.35	0.20
5454	A95454	2.4–3.0	0.5–1.0	0.25	0.25	0.4	0.10	0.05–0.2	0.20
5456	A95456	4.7–5.5	0.5–1.0	0.25	0.25	0.4	0.10	0.05–0.2	0.20
6061 <sup>(2)</sup>	A96061	0.8–1.2	0.15	0.25	0.4–0.8	0.7	0.15–0.4	0.04–0.35	0.15
7072	A97072	0.10	0.10	0.8–1.3	(Si + Fe) = 0.7	0.10	—	—	—

**Notes:**

- (1) Alclad 3003. This alloy in the form of plate and tube may be clad with 7072 alloy.  
 (2) Alclad 3004 and 6061. These alloys in the form of plate may be clad with 7072 alloy.  
 (3) Balance = aluminium.  
 (4) Published by permission of ASTM, 1916 Race St, Philadelphia, Pa 19103, USA (Part 7).

first digit being the major alloying element as follows:

Group	Major alloying elements	Strength mechanism
1000	Aluminium, 99.00% and greater	SH
3000	Manganese	SH
5000	Magnesium	SH
6000	Magnesium and silicon	HT
7000	Zinc	HT
	<i>Not listed in Table 18.4</i>	
2000	Copper	HT
4000	Silicon	NHT

SH = strain hardenable; HT = heat treatable;  
 NHT = mostly non-heat treatable

In the 1000 group only, the last two digits are indicative of the aluminium content above 99.00%. These are the figures to the right of the decimal point and to cover the range 99.00–99.99% they will have a value between 00 and 99. For example, alloy 1060 in Table 18.4 has an aluminium content of 99.60%.

In the remaining groups, the last three digits are indicative of the alloy's composition.

### 18.5.2 1000 group

These are high-purity metals in which the aluminium content is not less than 99.00%. They are used extensively except where high strength is required because they offer excellent properties relating to corrosion

resistance, thermal conductivity and ease of fabrication. Alloys from the other groups are used when greater strength is required although their corrosion resistance is usually less.

### 18.5.3 3000 group

These metals, which have manganese as the main alloying element, offer similar properties as the 1000 group but with the advantage of higher strength. The alloys are widely used in heat exchangers.

### 18.5.4 5000 group

Magnesium is the main alloying element, but some of the alloys contain significant quantities of manganese. The strength of these alloys is considerably greater than the 1000 and 3000 groups. The 5000 group alloys listed in Table 18.4 with a magnesium content greater than about 3½% (i.e. alloys 5083, 5086, 5154 and 5456) are limited to an operating temperature of about 65 °C because they are susceptible to stress-corrosion cracking. The alloys are widely used in cryogenic equipment.

### 18.5.5 6000 group

Magnesium and silicon are the main alloying elements of the 6000 group which offer good corrosion resistance, ease of fabrication and medium strength.

### 18.5.6 7000 group

Several alloys are available in this group, in which zinc is the main alloying element, but only 7072 is listed. Its special significance is that it may be bonded metallurgically to aluminium alloys, such as 3003, 3004 and 6061, to act as a sacrificial anode and protect the base alloy. The process is termed Alclad and may be applied to plate and either the internal or external surface of a tube when the two alloys are drawn together during manufacture. The cladding thickness, as a percentage of the composite thickness is about 5% for plate, 10% for the inside of a tube and 7% for the outside of a tube.

Alclad provides excellent protection against pitting. The cathodic protection provided by the cladding is such that once the pit reaches the cladding/base metal interface, the pit increases in diameter but not in depth. Even after the cladding has been penetrated over a wide area, the base alloy will not be attacked until the cladding has almost disappeared. Because the cladding does not have to provide complete coverage, exposed areas due to welding or tube end expansion, are protected by the adjacent cladding. As an example, some all-aluminium exchangers having internal Alclad tubes have operated without deterioration from river water for over fifteen years.

### 18.5.7 Protection of steel with aluminium

Although they provide excellent corrosion-resistant properties, aluminium and its alloys have the disadvantage of low mechanical strength in relation to steel. In addition, the strength of aluminium and its alloys decreases sharply above 150 °C. A material which combines the corrosion resistance of aluminium with the strength of steel, particularly at high temperatures, is required.

#### Steel-aluminium alloys

It is possible to produce steel-aluminium alloys which provide the desired properties. Depending on the aluminium content (usually 6–20% by weight), such alloys exhibit equal or better resistance to high-temperature hydrogen sulphide attack, for instance, than high-chrome steels (section 18.7.3) or austenitic stainless steels (section 18.7.1). Although the addition of aluminium to the alloy increases both tensile and yield strength, the aluminium content required to ensure adequate corrosion resistance causes considerable loss of ductility and hence difficulty in fabricating equipment.

#### Aluminium clad steel

Another method of achieving the required properties is to explosively clad a backing plate of steel with a thin sheet of aluminium alloy as described in section 18.10.3. This is ideal for tubesheets, but as aluminium cannot be welded directly, or weld deposited, to steel, the fabrication of clad barrels and headers, shown in Fig. 18.3, is not possible.

Bi-metal tubes, as described in sections 1.5.5 and 18.10.1 may be used in conjunction with clad tubesheets.

#### Aluminising – spraying and dipping

Aluminium-coated steel is another method of achieving the required properties. The coating is obtained by aluminising in which the steel component is either dipped into a bath of molten aluminium, if it is not too bulky, or molten aluminium is sprayed on to the surface to be protected. Both methods may be applied to steel headers and similar components, after completion of all welding adjacent to the aluminium coating.

Great care must be taken with both dipping and spraying techniques to ensure that the coating is continuous without pin-holes, etc. Even a small imperfection may cause rapid corrosion over the whole surface. The component requires careful handling during fabrication to avoid damage to the coated surface. At high temperature such coatings are liable to melt or flake-off, unless carefully applied.

#### Aluminising – vapour diffusion

A true aluminium-iron alloy surface layer may be produced by the technique of vapour diffusion aluminisation known as calorising. Calorising is a generic term which refers to the alloying of one material into another through a high-temperature process. Alon Processing Inc. provide a proprietary vapour diffusion (or calorising) process called

Alonizing™ which provides an especially deep iron–aluminium surface layer.

The Alonizing process is performed by loading the steel in a retort and surrounding it with a mixture of blended aluminium powders. The retort is then hermetically sealed and placed in an atmosphere-controlled furnace. At elevated temperatures, the aluminium diffuses deeply into the steel to form an iron–aluminium alloy. The depth of alloy penetration can be varied by changing process times and temperatures, but the standard depths are 0.25–0.38 mm (0.010–0.015 in) for carbon steel and 0.08–0.2 mm (0.003–0.008 in) for stainless steels. The approximate aluminium content of the alloy is 50% at the surface and 20% throughout the entire diffusion zone.

It should be emphasised that Alonizing is not a coating, but a true alloy which can only be removed by machining. This means that Alonized steels have no surface flaws and do not require special handling during fabrication. Alonized steels should be treated in the same manner as non-Alonized steel. In addition, Alonized steels are readily welded without damage to areas adjacent to the weld.

An important feature is that tubes, both plain and finned, may be Alonized. Tubes 6–762 mm (0.25–30 in) in diameter and up to 17.7 m (58 ft) long may be Alonized on the inside only, or the outside only, or both surfaces. The maximum size for fabrications is about 1.8 × 1 × 6 m long (6 × 3 × 20 ft). Alonized material may be cold-formed provided the maximum metal elongation does not exceed 8%. If more severe forming is required, heating to 650 °C is recommended, where elongations greater than 25% can be accepted.

Alonized tubes are attached to the tubesheet using the same roller, rubber and hydraulic expansion techniques described in Chapter 2. If the tubes are Alonized on the outside, the tube ends are left plain on the outside for a length equal to the tubesheet thickness, less 0.8 mm (1/32 in), by masking. Because of dimensional changes which occur during Alonizing, an increase in hole diameter of about 0.25 mm (0.01 in) is required compared with plain tubes. Grooving of the tube hole and beelling or flaring of the tube ends are not recommended. Unusual tube and tubesheet material combinations may require a test block to determine the optimum expander torque, as described in Chapter 2.

The cost of Alonizing both tube surfaces is only slightly greater than Alonizing one surface. As an approximation, the plain carbon-steel tube costs given in Table 19.3(b) should be increased by a factor of 2.0–3.0 to cover for Alonizing. It should be noted that if tube length is critical, the tubes should be ordered 1% longer than the required length to allow for shrinkage which may occur during Alonizing.

Alonizing provides the required properties in that it combines the corrosion resistance of aluminium, particularly at high temperatures, with the strength of ferrous material, which is selected to suit the pressure and temperature of the process. This may be carbon steels, chrome–moly steels, ferritic and austenitic stainless steels, etc. Alonized components are widely used in the petroleum, petrochemical and chemical industries for environments involving high-temperature gaseous phase oxidation, sulphidation and/or carburisation. In these applications, Alonizing provides a cheaper, long-life, alternative to high chrome and stainless

steels.

One of its widest applications is in sulphuric acid plants and the suppliers claim that no other metal, at any price, is able to offer such effective high-temperature (230–1000 °C) corrosion resistance from hydrogen sulphide, sulphur dioxide and sulphur trioxide. The absence of corrosion is, of course, accompanied by the absence of fouling (discussed in Chapter 8), with the advantages of longer on-stream performance and reduced maintenance costs.

## 18.6 Copper and copper alloys

High-purity copper is well known for its high thermal and electrical conductivities, being second only to silver and nearly twice that of aluminium. Copper generally provides good corrosion resistance against dilute air-free acetic and sulphuric acids, caustic alkalis, sea water and the atmosphere.

In order to improve strength and corrosion resistance in certain environments, elements such as iron, zinc, tin, aluminium and nickel are added, although the resulting alloys have significantly lower thermal and electrical conductivities. Copper and its alloys have good low-temperature properties and may be used at temperatures of –200 °C.

They are noted for being attacked by moist chlorine, moist ammonia and its compounds, and minute quantities of mercury and its compounds. Moist acetylene under pressure forms an explosive compound with copper, and alloys having a copper content greater than 65% should not be used. A major industrial application for copper and its alloys is in heat transfer equipment involving a variety of cooling waters.

### 18.6.1 Designation system

The compositions of some copper alloys used in heat exchanger construction are given in Table 18.5. It will be seen that the wrought alloys are divided into groups based on their UNS number as follows:

<i>UNS number</i>	<i>Wrought products (C10000–C79999) Description</i>	<i>Major alloying elements in addition to copper</i>
C10100–C15600	Coppers	—
C16200–C19600	High coppers	Iron
C20500–C28000	Brasses	Zinc
C40400–C48500	Tin brasses	Zinc, tin
C60600–C64400	Aluminium bronzes	Aluminium
C66400–C69900	Special brasses	Zinc, aluminium
C70100–C72900	Copper nickels	Nickel, zinc
<i>Not listed in Table 18.5</i>		
C31200–C38500	Leaded brasses	Zinc, lead
C50100–C52400	Phosphor bronzes	Tin
C53200–C54800	Leaded phosphor bronzes	Tin, lead
C64700–C66100	Silicon bronzes	Silicon
C73200–C79900	Nickel silvers	Nickel, zinc



Table 18.5 Composition of some copper alloys<sup>(5)</sup>

Type	UNS number	% composition (max. except where stated)										Notes
		Cu	Al	Ni	Fe	Zn	Mn	Sn	Others			
Copper(phosphorised) low residual P high residual P	C12000	99.9 min.	—	—	—	—	—	—	—	—	{ P = 0.04-0.012 P = 0.015-0.040	(1)
	C12200	99.4 min.	—	—	—	—	—	—	—	—	{ P = 0.015-0.040 As = 0.15-0.5	—
Copper (phosphorised, arsenical)	C14200	98.7 min.	—	—	0.8-1.2	—	—	—	—	—	P = 0.01-0.04 Pb = 0.06	—
	C23000	84.0-86.0	—	—	0.05	balance	—	—	—	—	—	—
Copper-iron Red brass	C44300	70.0-73.0	—	—	0.06	balance	—	0.9-1.2	—	—	Pb = 0.07	(2)
	C44400	59.0-62.0	—	—	0.10	balance	—	0.5-1.0	—	—	Pb = 0.2	(3)
Admiralty metal C D	C44450	93.0 min.	5.0-6.5	—	0.10	—	—	—	—	—	{ Pb = 0.1 As = 0.02-0.35	—
Naval brass	C46400	88.0-92.5	6.0-8.0	—	1.5-3.5	0.2	1.0	—	—	—	{ P = 0.015 Pb = 0.10	—
Aluminium bronze	C60800	77.2-82.8	9.0-11.0	4.0-5.5	2.0-4.0	0.3	1.5	0.2	—	—	Si = 0.25	—
Aluminium bronze D	C61400	76.0-79.0	1.8-2.5	—	0.06	balance	—	—	—	—	{ Pb = 0.07 As = 0.02-0.1	—
Aluminium-nickel bronze	C63000	91.2 min.	—	4.8-6.2	1.3-1.7	1.0	0.3-0.8	—	—	—	Pb = 0.05	—
	C70400	86.5 min.	—	9.0-11.0	1.0-1.8	1.0	1.0	—	—	—	Pb = 0.05	(4)
Aluminium brass B	C70600	74.0 min.	—	19.0-23.0	0.5-1.0	1.0	1.0	—	—	—	Pb = 0.05	—
	C71000	65.0 min.	—	29.0-33.0	0.4-1.0	1.0	1.0	—	—	—	Pb = 0.05	(4)

## Notes:

(1) Copper (oxygen free, without residual deoxidants, C10200) = 99.95% min. Cu.

(2) C44300: 0.02-0.10 As; C44400: 0.02-0.10 Sb; C44500: 0.02-0.10 P.

(3) As, Pb or P may be added up to 0.10.

(4) For welding, Zn = 0.5, Pb = 0.02, S = 0.02, C = 0.05 if specified by purchaser.

(5) Published by permission of ASTM, 1916 Race St. Philadelphia, Pa 19103, USA. (Part 6)

The Copper Development Association Inc. (CDA) designates each alloy by a CDA number and the UNS number adds two zeros to it. For example, CDA 101 becomes UNS 10100.

### 18.6.2 Red brass

This alloy contains 85% copper and 15% zinc (85/15) and has good resistance to corrosion and dezincification. Because of its relatively low zinc content, however, it does not offer a high resistance to attack by sulphur-bearing products and admiralty brass is usually preferred.

### 18.6.3 Admiralty brass

Admiralty brass is nominally 71% copper, 28% zinc and 1% tin (71/28/1) and is used chiefly in the form of tubes. It is also available for clad or solid tubesheets but its strength decreases rapidly above about 175 °C. There are three alloys available differing only by the small quantity of inhibitor (0.02–0.10%) which is added as arsenic, antimony or phosphorus to prevent dezincification.

It has a low price compared with some of the other copper alloys, and offers a good corrosion resistance against most waters and sulphur-bearing products. It is also immune to pitting and crevice corrosion. However, it is prone to stress corrosion and erosion corrosion.

### 18.6.4 Naval brass

Naval brass is nominally 60% copper, 39% zinc plus 1% tin (60/39/1) which is added for greater strength and to increase its resistance against corrosion and dezincification. Its corrosion resistance is not as good as admiralty brass but it is used for clad or solid tubesheets in moderately corrosive conditions.

### 18.6.5 Muntz metal

Muntz metal (C28000 – not listed in Table 18.5) is similar to naval brass but has no tin. It is often used as a baffle material.

### 18.6.6 Aluminium brass

Aluminium brass is one of the most widely used of all the copper alloy tubes for a variety of cooling-water services. Its nominal composition is 78% copper, 20% zinc and 2% aluminium, and the small quantity of the latter element is adequate to provide a highly stable protective film on the tube surface. As a result, the alloy offers excellent resistance to corrosion and impingement attack. The inclusion of 0.02–0.1% of arsenic provides resistance to dezincification.

### 18.6.7 Aluminium bronzes

Three aluminium bronzes are listed in Table 18.5 having 5–11% aluminium with the addition in some cases of iron and nickel. The presence of aluminium in the protective surface film promotes excellent resistance to impingement attack and oxidation at high temperature. Alloy 60800 is used as tube, whereas alloys 61400 and 63000 are used as tubesheets because of their high strengths up to about 250 °C and 315 °C respectively. Stationary, rear and floating heads, as complete aluminium bronze castings, are sometimes used for low-pressure applications, particularly cooling-water services.

### 18.6.8 Cupro-nickels

Although four cupro-nickel alloys are listed in Table 18.5 having nominal percentages of copper/nickel of 95/5, 90/10, 80/20 and 70/30, the most widely used alloys are the 90/10 and 70/30. Nickel is the major alloying element, but it will be seen that all contain a small quantity of iron, without which the alloys would have less resistance to impingement attack.

Of all the copper alloys, the cupro-nickels provide the greatest resistance to the various forms of attack, especially in high-velocity sea water. In general the 70/30 alloy is slightly superior to the 90/10, but the latter alloy is used where possible due to its lower cost. Caution is required in the selection of these alloys for use in fluids containing sulphur and its compounds.

The 90/10 and 70/30 alloys are commonly used in the form of tube and solid and or clad tubesheets, while the tubes may be welded to the tubesheets if required. Although their strength is much inferior to that of steel, they have good fabrication characteristics and the complete exchanger may be manufactured from these alloys in solid form if required.

## 18.7 Stainless steels

Stainless steels are iron alloys containing at least 10% chromium, the latter element contributing to their superior corrosion resistance and staining compared with carbon and low-alloy steels. The term 'stainless' originates from the fact that steels containing more than about 10% chromium are free from corrosion under unpolluted atmospheric conditions. A thin surface film, which is self-healing in many environments, provides the resistance to corrosion. Although used primarily for their corrosion resistance, stainless-steels generally offer good mechanical properties at both elevated and low temperatures, non-contamination and ease of fabrication.

Stainless steels may be divided into five groups: austenitic, ferritic, martensitic, duplex (austenitic/ferritic) and precipitation-hardening, the grouping being related to metallurgical structure and not composition. There are numerous stainless steels available but the 'standard' types are given a three-digit type (or grade) number by the American Iron and Steel Institute (AISI), such that the 200 and 300 series relate to the austenitic group, and the 400 series to the ferritic and martensitic groups.

'Non-standard' or proprietary stainless steels are given various type or grade designations. There is a vast number of proprietary alloys available and only a small number can be discussed in this chapter. The inclusion of a particular trade name and maker for the 'non-standard' stainless steels, discussed in the chapter, does not imply that the alloy is only available from that maker, or that it is superior to other proprietary alloys not listed. *The comments regarding corrosion resistance etc., are those given in the makers' brochures and are not the author's.*

The compositions of some standard and 'non-standard' stainless steels used in heat exchanger construction are given in Tables 18.6(a)–18.6(e).

### 18.7.1 Austenitic group

#### Standard 200 series

The 200 series chromium content of 16–18% is similar to that of types 302 and 304, but about half of the 302's and 304's 8–10% nickel has been replaced by manganese and nitrogen. In the past when nickel was in short supply, the 200 series became a useful substitute for the 300 series. They also have a higher yield strength than the 300 series, but their corrosion resistance is inferior.

#### Standard 300 series

The heart of the 300 series are the types 302 and 304 containing an average of 18% chromium and 8% nickel (18/8), type 304 being the general-purpose stainless steel and produced in larger quantities than any of the others. Table 18.6(a) shows that these steels are modified by the introduction of elements such as chromium, nickel, molybdenum, titanium, niobium, tantalum and nitrogen. The 300 series cannot be hardened by heat treatment and therefore exposure at elevated temperature does not cause an appreciable change in hardness or tensile strength. Unfortunately, certain metallurgical changes occur which affect their corrosion resistance and toughness.

The general-purpose types 302 and 304, for instance, together with types 316 and 317, suffer sensitisation, or harmful carbide precipitation, when exposed to temperatures of 500–800 °C, which is likely to occur during welding, for instance. Carbon which is normally present in solution diffuses to the grain boundaries where it combines with chromium to form carbides. The zone adjacent to the grain boundaries, which is then depleted of chromium, may be preferentially attacked by certain corrosive media over a long period of time. When this type of attack occurs as a result of welding, it is referred to as the more familiar 'weld decay'.

Table 18.6(a) Composition of some austenitic type stainless steels<sup>(1)</sup>

Type	UNS number	% composition (max. except where stated) <sup>(2)</sup>										
		Cr	Ni	C	Mn	Mo	Ti	Si	P	S	N	Others
201	S20100	16.0-18.0	3.5-5.5	0.15	5.5-7.5	—	—	1.0	0.060	0.030	0.25	—
302	S30200	17.0-19.0	8.0-10.0	0.15	2.0	—	—	1.0	0.045	0.030	0.1	—
304	S30400	18.0-20.0	8.0-10.5	0.08	2.0	—	—	1.0	0.045	0.030	0.1	—
304L	S30403	18.0-20.0	8.0-12.0	0.03	2.0	—	—	1.0	0.045	0.030	0.1	—
304N	S30451	18.0-20.0	8.0-10.5	0.08	2.0	—	—	1.0	0.045	0.030	0.10-0.16	—
304H	S30409	18.0-20.0	8.0-11.0	0.04-0.10	2.0	—	—	1.0	0.040	0.030	—	—
309	S30900	22.0-24.0	12.0-15.0	0.15	2.0	—	—	0.75	0.040	0.030	—	—
309S	S30908	22.0-24.0	12.0-15.0	0.08	2.0	—	—	1.0	0.045	0.030	—	—
310	S31000	24.0-26.0	19.0-22.0	0.15	2.0	—	—	1.0	0.040	0.030	—	—
310S	S31008	24.0-26.0	19.0-22.0	0.08	2.0	—	—	1.5	0.045	0.030	—	—
316	S31600	16.0-18.0	10.0-14.0	0.08	2.0	2.0-3.0	—	1.0	0.045	0.030	0.1	—
316L	S31603	16.0-18.0	10.0-14.0	0.03	2.0	2.0-3.0	—	1.0	0.045	0.030	0.1	—
316N	S31651	16.0-18.0	10.0-14.0	0.08	2.0	2.0-3.0	—	1.0	0.045	0.030	0.10-0.16	—
316H	S31609	16.0-18.0	10.0-14.0	0.04-0.10	2.0	2.0-3.0	—	1.0	0.040	0.030	—	—
317	S31700	18.0-20.0	11.0-15.0	0.08	2.0	3.0-4.0	—	1.0	0.045	0.030	0.1	—
317L	S31703	18.0-20.0	11.0-15.0	0.03	2.0	3.0-4.0	—	1.0	0.045	0.030	0.1	—
321	S32100	17.0-19.0	9.0-12.0	0.08	2.0	—	min:5(C+N) max:0.7	1.0	0.045	0.030	0.1	—
321H	S32109	17.0 min.	9.0-12.0	0.04-0.10	2.0	—	min:4C max:0.7	1.0	0.040	0.030	—	—
330	N08330	17.0-20.0	34.0-37.0	0.08	2.0	—	—	0.75-1.5	0.030	0.030	—	Cu = 1.0, Sn = 0.025 Pb = 0.005
347	S34700	17.0-19.0	9.0-13.0	0.08	2.0	—	—	1.0	0.045	0.030	—	(Cb+Ta)=10C min., 1.1 max.
347H	S34709	17.0-20.0	9.0-13.0	0.04-0.10	2.0	—	—	1.0	0.040	0.030	—	(Cb+Ta)=8C min., 1.0 max.
348	S34800	17.0-19.0	9.0-13.0	0.08	2.0	—	—	1.0	0.045	0.030	—	(Cb+Ta)=10C min., 1.1 max. Ta = 0.1, Co = 0.2
348H	S34809	17.0-20.0	9.0-13.0	0.04-0.10	2.0	—	—	1.0	0.040	0.030	—	(Cb+Ta)=8C min., 1.0 max. Ta = 0.1, Co = 0.2
XM11	S21903	19.0-21.5	5.5-7.5	0.04	8.0-10.0	—	—	1.0	0.040	0.030	0.15-0.4	—
XM15	S38100	17.0-19.0	17.5-18.5	0.08	2.0	—	—	1.5-2.5	0.030	0.030	—	—
XM19	S20910	20.5-23.5	11.5-13.5	0.06	4.0-6.0	1.5-3.0	—	1.0	0.040	0.030	0.2-0.4	Cb=0.10-0.30 V = 0.10-0.30
XM29	S24000	17.0-19.0	2.25-3.75	0.08	11.5-14.5	—	—	1.0	0.060	0.030	0.2-0.4	—
904L	N08904	19.0-23.0	23.0-28.0	0.02	2.0	4.0-5.0	—	1.0	0.045	0.035	—	Cu = 1.0-2.0
20Cb	N08020	19.0-21.0	32.0-38.0	0.07	2.0	2.0-3.0	—	1.0	0.045	0.035	—	(Cb+Ta)=8C to 1.0
20mod	N08320	21.0-23.0	25.0-27.0	0.05	2.5	4.0-6.0	4C	1.0	0.040	0.030	—	—
28	N08028	26.0-28.0	29.5-32.5	0.03	2.5	3.0-4.0	—	1.0	0.030	0.030	—	Cu = 0.6-1.4

NB Niobium (Nb) and Columbian (Cb) are the same metal. Niobium in the UK is known as Columbian in the USA

Table 18.6(b) Composition of some ferritic type stainless steels<sup>(1)</sup>

Type	UNS number	% Composition (max. except when stated) <sup>(2)</sup>											
		Cr	Ni	C	Mn	Mo	Ti	Si	P	S	N	Others	
405	S40500	11.5-14.5	0.6	0.08	1.0	-	-	1.0	0.040	0.030	-	-	Al=0.10-0.030
409	S40900	10.5-11.75	0.5	0.08	1.0	-	min: 6C max: 0.75	1.0	0.045	0.045	-	-	-
429	S42900	14.0-16.0	0.75	0.12	1.00	-	-	1.0	0.040	0.030	-	-	-
430	S43000	16.0-18.0	0.75	0.12	1.0	-	-	1.0	0.040	0.030	-	-	-
446	S44600	23.0-30.0	0.5	0.20	1.5	-	-	0.75	0.040	0.030	0.10-0.25	-	-
XM27	S44627	25.0-27.5	0.5	0.01	0.04	0.75-1.5	-	0.4	0.020	0.020	0.15	-	Cb=0.05-0.20, Cu=0.20, (Ni+Cu)=0.5
XM33	S44626	25.0-27.0	0.5	0.06	0.75	0.75-1.5	0.20-1.00 min.: 7(C+N)	0.75	0.040	0.020	0.04	-	Cu=0.20
18 Cr-2 Mo	S44400	17.5-19.5	1.0	0.025	1.0	1.75-2.5	-	1.0	0.040	0.030	0.035	-	(Ti+Cb)=0.2+4(C+N), min. 0.80
29Cr-4 Mo	S44700	28.0-30.0	0.15	0.010	0.3	3.5-4.2	-	0.2	0.025	0.020	0.020	-	(C+N)=0.025, Cu=0.15
29 Cr-4 Mo-2Ni	S44800	28.0-30.0	2.0-2.5	0.10	0.3	3.5-4.2	-	0.2	0.025	0.020	0.020	-	C+N=0.025, Cu=0.15
25-4-4	S44635	24.5-26.0	3.5-4.5	0.025	1.0	3.5-4.5	-	0.75	0.040	0.030	0.035	-	Ti+Cb0.2+4(C+N)min., 0.8 max.

Table 18.6(c) Composition of some martensitic type stainless steels<sup>(1)</sup>

Type	UNS number	% Composition (max. except when stated) <sup>(2)</sup>											
		Cr	Ni	C	Mn	Mo	Ti	Si	P	S	N	Others	
410	S41000	11.5-13.5	0.75	0.15	1.0	-	-	1.0	0.040	0.030	0.030	-	-
410S	S41008	11.5-13.5	0.6	0.08	1.0	-	-	1.0	0.040	0.030	0.030	-	-

Table 18.6(d) Composition of some duplex type stainless steels<sup>(1)</sup>

Type	UNS number	% Composition (max. except when stated) <sup>(2)</sup>										
		Cr	Ni	C	Mn	Mo	Ti	Si	P	S	N	Others
329	S32900	23.0-28.0	2.5-5.0	0.08	1.0	1.0-2.0	-	0.75	0.040	0.030	-	-
18 Cr-5 Ni-3 Mo	S31500	18.0-19.0	4.25-5.25	0.03	1.2-2.0	2.5-3.0	-	1.4-2.0	0.030	0.030	-	-
22 Cr-6 Ni-3 Mo	S31803	21.0-23.0	4.5-6.5	0.03	2.0	2.5-3.5	-	1.0	0.030	0.02	0.08-0.2	-

Table 18.6(e) Composition of a precipitation hardening austenitic stainless steel<sup>(1)</sup>

Type	UNS number	% Composition (max. except when stated) <sup>(2)</sup>										
		Cr	Ni	C	Mn	Mo	Ti	Si	P	S	N	Others
25 Ni-15 Cr-2 Ti	K63198	13.5-16.0	24.0-27.0	0.08	2.0	1.0-1.5	1.9-2.35	1.0	0.040	0.030	-	Al=0.35, V=0.1-0.5, B=0.001-0.01

Notes:

(1) Published by permission of ASTM, 1916 Race St, Philadelphia, Pa 19103, USA.

(2) Balance = iron.

Sensitisation may be overcome by reducing the carbon content of the alloy to at least 0.03% as provided by the low-carbon versions of types 304, 316 and 317, namely, 304L, 316L and 317L. It may also be overcome by adding elements such as titanium, niobium and tantalum during steel-making, which tie-up the carbon and leaves little available to form chromium carbides during subsequent heating in the critical temperature range. These alloys are termed 'stabilised stainless steels', the stabiliser being titanium for type 321, niobium + tantalum for type 347, and niobium + restricted tantalum and cobalt for the nuclear application type 348. Matching welding electrodes or wires, containing niobium would be used. Another method of preventing sensitisation of unstabilised stainless steels is to anneal after welding at about 1050 °C, but this may be expensive and difficult to carry out, particularly with large fabrications, or site welds.

In order to improve the strength of types 304 and 316, nitrogen is added and these steels are then designated types 304N and 316N. By controlling the carbon content and grain size, better elevated temperature creep and stress-rupture properties are obtained for types 304, 316, 321, 347 and 348 and these steels are designated type 304H, 316H, 321H, 347H, and 348H.

Sigma formation, an undesirable intermetallic phase, may occur as a result of long exposure at temperatures in the range 565–925 °C. It increases hardness, but at the expense of reduced ductility, corrosion resistance and notch toughness. This problem is one encountered in service, not heat treatment, because the rate of sigma formation is slow. The greater the chromium content, the greater the possibility of sigma formation, which is accentuated by the presence of molybdenum, titanium and silicon. Increasing the nickel content reduces the possibility of sigma formation.

The chief disadvantage of the 300 series stainless steels is that the alloys are prone to stress-corrosion cracking, particularly in hot chloride solutions. High-nickel alloys or special stainless steels have been developed to overcome this problem. The chloride content of the water used for hydraulic testing of heat exchangers constructed of these steels must be considered. The maximum acceptable chloride level for testing depends on the extent to which the exchanger can be drained afterwards and the maximum metal temperature which will be experienced in service. The water temperature is usually too low to cause stress-corrosion cracking during test, but it will occur during service if the exchanger operates at a higher temperature and all chlorides have not been flushed away. Cavities holding chloride-containing water accentuate the risk of stress-corrosion cracking. Hot-air drying should be employed only after flushing-out.

If the service temperature exceeds 50 °C, a chloride content of 200 p.p.m. for instance, is acceptable for testing only if the exchanger can be drained *completely* or flushed out with condensate or demineralised water. If the service temperature never exceeds 50 °C a chloride content of 200 p.p.m. is acceptable without special provision for draining or flushing. However, caution should be exercised as a shell-and-tube exchanger is not crevice-free and bellows cannot be drained.



**Type XM-11 (Armco Nitronic™ alloy 40)**

The alloy has a nominal composition of 20% chromium, 6% nickel and 9% manganese and is available in two grades, one having a maximum carbon content of 0.08% and the other 0.04%. The latter's low carbon content makes it resistant to intergranular attack and in many cases it may be used in the as-welded condition. The room temperature yield of this nitrogen-strengthened stainless steel is nearly twice that of types 304, 321 and 347, and its corrosion resistance is between that of types 304 and 316. In addition to good elevated temperature properties it retains high strength and toughness at sub-zero temperatures.

**Type XM-19 (Armco Nitronic™ alloy 50)**

The alloy is a nitrogen-strengthened stainless steel which provides better corrosion resistance than types 316 and 316L and also has nearly twice the yield strength. Its nominal composition is 22% chromium, 13% nickel and 5% manganese. It has good mechanical properties at both elevated and sub-zero temperatures and is available as an economical replacement where the properties of types 316 and 316L are marginal.

**Type XM-29 (Armco Nitronic™ alloy 33)**

The alloy is a low-nickel, high-manganese, nitrogen-strengthened stainless steel having a nominal composition of 18% chromium, 3% nickel and 12% manganese. It is superior to type 304 in that it has nearly twice the yield strength in the annealed condition, better resistance to stress-corrosion cracking, low magnetic permeability even after severe cold work, excellent strength and ductility at cryogenic temperatures, and better resistance to wear and galling. It is available as an economical replacement where the properties of type 304 are marginal.

**Type 904L (Uddeholm alloy NU stainless 904L™)**

The alloy has a nominal composition of 25% nickel, 20% chromium, 4.5% molybdenum and 1.5% copper, with a low carbon content of 0.02% maximum, and was developed to resist corrosion in sulphuric acid. However, as it has good resistance to stress-corrosion cracking, pitting and crevice corrosion, it is used for many industrial applications including sea water cooling.

**Sandvik alloy 2RK65™**

This is a similar alloy, produced by Sandvik Steel, to type 904L and not listed in Table 18.6(a).

**Alloy 20 Cb (Carpenter alloy 20 Cb-3™)**

The original Carpenter alloy 20 was developed in 1951 to provide a metal having a corrosion resistance to sulphuric acid superior to that of the other stainless steels. This was followed by a niobium stabilised version (alloy 20 Cb) which could be used in the as-welded condition. Later, more nickel was added to provide an alloy which is virtually immune to stress-corrosion cracking (alloy 20 Cb-3), its composition being nominally 20% chromium 34% nickel, 35% iron, 3.5% copper with the addition of niobium + tantalum up to 1% maximum.

The alloy provides good resistance to sulphuric acid for concentrations up to 50% and temperatures below 80 °C, and for greater concentrations at temperatures below 65 °C. However, it also offers resistance to many other fluids, including nitric acid (at concentrations and temperatures less than 70% and 120 °C, respectively), phosphoric acid, organic acids, alkalis and most waters.

**Alloy 20 Mod (Haynes alloy No. 20 Mod™)**

This Cabot Corp. alloy has a nominal composition of 26% nickel, 22% chromium, and 5% molybdenum. It offers a resistance to corrosion and chloride pitting intermediate to that of the austenitic stainless steels and the Hastelloys™.

**Alloy Al-6X (Allegheny Ludlum Corp. alloy AL-6X™)**

The alloy, not listed in Table 18.6(a), has a basic composition of 24.5% nickel, 20.25% chromium and 6.25% molybdenum. It was developed for service in chloride environments, such as sea water, where it provides outstanding resistance to pitting, stress corrosion and crevice corrosion.

**Alloy 28 (Sandvik Sanicro™ 28)**

This is an all-purpose austenitic, low-carbon stainless steel with a nominal composition of 31% nickel, 27% chromium, 3.5% molybdenum and 1% copper, originally developed for use in the manufacture of phosphoric acid. The alloy has good resistance to sulphuric acid and also to hydrochloric, hydrofluoric and hydrofluosilicic acids when they occur as contaminants. It is completely resistant to acetic acid at all temperatures and concentrations at atmospheric pressure. It is also suitable for sea water and sodium hydroxide.

## 18.7.2 Ferritic group

### Standard 400 series

The compositions of some 400 series ferritic stainless steels, including the better known 13% and 17% chrome steels (types 405 and 430), are listed in Table 18.6(b), from which it will be seen that the chromium content lies in the range 10.5–30%. Unlike the 300 series, however, there is little nickel, being less than 0.75%. Corrosion resistance increases as the chromium content increases, but the higher chromium content may provide fabrication problems as described later. The 400 series is not used as widely as the 300 series.

Compared with the 300 series, their toughness, formability and corrosion resistance is lower, but because of their low nickel content, they are cheaper and have the added advantage that they are considered to be almost immune from chloride stress-corrosion cracking. The 400 series is similar to the 300 series in that the alloys cannot be hardened by heat treatment, but exposure at certain temperatures causes metallurgical changes which adversely affect corrosion resistance and other properties.

Ferritic stainless steels are subject to embrittlement following long exposure to temperatures of 400–550 °C, whereas austenitic stainless

steels do not experience such attack. An increase in hardness is accompanied by a reduction in ductility and toughness at and below the service temperature. Because the worst embrittlement occurs at about 475 °C, the phenomenon is termed '475 °C (or 885 °F) embrittlement' and becomes more pronounced with increasing chromium content above 13%. Significant embrittlement has been observed at temperatures of only 315 °C with a chromium content of 15% after an exposure time of about 3000 hours.

Although 475 °C embrittlement may be remedied by reheating to 600 °C, prolonged heating of these steels having a chromium content greater than 20% may cause sigma formation, as mentioned in section 18.7.1. Cold work and the presence of molybdenum assist sigma formation. Any area of the weld and heat-affected zone, which has reached a temperature of about 900 °C or greater, is prone to intergranular attack, but unlike the 300 series, the problem is not remedied by a reduction in carbon content or the addition of stabilising elements. Re-annealing the steel to about 800 °C is a remedy.

#### **Type XM-27 (Allegheny Ludlum Corp. E-Brite™)**

E-Brite is a high-purity ferritic stainless steel which has nominally 27% chromium and 1% molybdenum, with exceptionally low levels of carbon and nitrogen and controlled low levels of nickel and copper. Compared with the standard austenitic and ferritic stainless steels, its ferritic structure, combined with a low nickel and copper content, gives this alloy a superior resistance to stress-corrosion cracking. It is also superior with regard to pitting and crevice corrosion.

It has good corrosion resistance to sodium hydroxide, nitric acid, amines, ammonium carbamate and organic acids. Because of its high chromium content, substantial resistance is offered at high temperatures to oxidation and sulphidation. It has been shown to be resistant to wet air/sulphur dioxide mixtures and combustion gases at 816 °C. The alloy is subject to 475 °C embrittlement following extended exposure at 370–570 °C and its strength falls off rapidly above 540 °C.

#### **Type 29 Cr – 4 Mo – 2 Ni (Allegheny Ludlum Corp. alloys AL29-4-2™ and 29-4C™)**

Alloy AL29-4-2 is another high-purity ferritic stainless steel which has nominally 29% chromium, 4% molybdenum, 2% nickel, with exceptionally low levels of carbon and nitrogen. In general it provides an even better resistance to stress-corrosion cracking, pitting and crevice corrosion than E-Brite. It was developed to provide superior resistance to corrosion by aggressive environments and its corrosion-resistance properties are often comparable to titanium and high-nickel alloys.

AL29-4C is another alloy produced by the same company specifically for power plant surface condenser tubing. Its nominal composition is 29% chromium and 4% molybdenum which was considered to provide the best balance of corrosion resistance, ductility and cost. A small controlled amount of titanium has been added to combine with carbon and nitrogen to improve weldability, toughness and resistance to intergranular corrosion. It has excellent resistance to a wide range of corrosive media,

particularly sea water, and is also resistant to erosion attack from both impinging steam and sand or debris at the inlet to the tubes. It is also highly resistant to pitting, crevice corrosion and stress-corrosion cracking.

#### **25-4-4 alloy (Uddeholm alloy NU Monit™)**

This is a titanium stabilised ferritic steel, with extra low carbon and nitrogen contents, having a nominal composition of 25% chromium, 4% nickel and 4% molybdenum. It was developed to resist corrosion in sea water and other corrosive media containing chlorides.

#### **18 Cr - 2 Mo (Uddeholm alloy NU EL1-T18-2™)**

The composition of NU EL1-T18-2 is nominally 18% chromium, 2% molybdenum, with 0.4% titanium and low-carbon and nitrogen contents. Its general corrosion resistance is similar to type 316, but is immune to stress-corrosion cracking and intergranular corrosion. With regard to pitting and crevice corrosion, it is similar to type 316, and its thermal expansion coefficient is about 40% lower than the standard austenitics. The alloy is used widely in applications where there would be a risk of stress corrosion with the standard austenitics.

### **18.7.3 Martensitic group**

The standard 400 series martensitic stainless steels have a chromium content of 11.5–18% and the most popular of these is the 12% chrome, type 410, the composition of which is given in Table 18.6(c), together with its lower carbon version type 410S. They can be hardened by heat treatment and are selected when good mechanical properties are required in a moderately corrosive environment. The 300 series has a greatly superior corrosion resistance but like the 400 series ferritics, the martensitics are considered almost immune to chloride stress-corrosion cracking. Although cheaper than the 300 series, the 400 series are less widely used.

### **18.7.4 Duplex (austenitic/ferritic) group**

#### **Standard 300 series**

Duplex stainless steels contain both austenite and ferrite and the composition of the only standard steel, type 329, is shown in Table 18.6(d), the chromium and nickel contents being 23–28% and 2.5–5%, respectively. The amount of the austenitic and ferrite phases may be altered by the addition of austenite stabilisers (carbon, nitrogen, nickel) and ferrite formers (molybdenum, silicon, titanium, aluminium).

The duplex stainless steels are noted for their high yield strengths, being about double those of the 'standard' austenitics and ferritics listed. In the annealed condition, they offer better resistance to stress-corrosion cracking than the low-alloy austenitics. They are also more resistant to sensitisation, but less resistant to crevice corrosion and pitting.

**18 Cr – 5 Ni – 3 Mo alloy (Sandvik alloy 3RE 60™)**

This low-carbon alloy has high resistance to stress-corrosion cracking and is well suited for tubes in heat exchangers dealing with water of moderate chloride content. It has good resistance to general corrosion, pitting and corrosion fatigue and also has a yield strength nearly twice that of the austenitic types. The makers recommend their alloy 2RK65, where the chloride content is so high as to demand a metal with even greater resistance to pitting and stress corrosion.

**Sandvik alloy SAF2205**

This is a 22% chromium, 5.5% nickel, 3% molybdenum, nitrogen-alloyed low-carbon duplex alloy, not listed in Table 18.6(d), designated SAF2205. It has high resistance to stress-corrosion cracking in chloride and hydrogen sulphide-bearing media.

**22 Cr–6 Ni–3 Mo alloy (Uddeholm alloy NU stainless 744LN™)**

This is another nitrogen-alloyed low-carbon duplex alloy, with similar properties to Sandvik 3RE60.

**18.7.5 Precipitation hardening group**

The alloy listed in Table 18.6(e), with a nominal composition of 25% nickel, 15% chromium and 2% titanium, is used when bolts having high strength at elevated temperatures are required. The thermal expansion coefficients are similar to those of the austenitic stainless steels.

## **18.8 Nickel and high-nickel alloys**

There is a vast number of proprietary nickel alloys available and only a small number can be mentioned. The inclusion of a particular trade name and maker does not imply that the alloy is only available from that maker, or that it is superior to other proprietary alloys not listed. *The comments regarding corrosion resistance, etc., are those given in the makers' brochures and are not the author's.*

The compositions of some nickel alloys used in heat exchanger construction are given in Table 18.7.

**18.8.1 Nickel (alloy 200) and low-carbon nickel (alloy 201)**

Nickel alloys 200 and 201 are both commercially pure wrought nickels, nickel 201 having a controlled low-carbon content. Nickel 200 offers good mechanical properties and has excellent corrosion resistance against a variety of fluids. It is considered non-toxic which makes it especially suitable for maintaining the product purity of foods. Although most suitable for reducing conditions, it is suitable for oxidising conditions which promote the formation of a passive oxide film. Its outstanding

Table 18.7 Composition of some high nickel alloys<sup>(1)</sup>

Alloy	UNS number	% Composition (max. except where stated)										Others	
		Ni	Cr	Fe	Mo	Cu	Si	Mn	C				
200	N02200	99.0	-	0.4	-	0.25	0.35	0.35	0.15	0.15			S = 0.01
201	N02201	99.0	-	0.4	-	0.25	0.35	0.35	0.02	0.02			S = 0.01
400	N04400	63.0 min.	-	2.5	-	28.0-34.0	0.5	2.0	0.30	0.30			S = 0.024
600	N06600	72.0 min.	14.0-17.0	6.0-10.0	-	0.5	0.5	1.0	0.15	0.15			S = 0.015
625	N06625	58.0 min.	20.0-23.0	5.0	8.0-10.0	-	0.5	0.5	0.10	0.10			{(Cb + Ta) = 3.15-4.15, Co = 1.0 S = 0.015, P = 0.015, Al = 0.4, Ti = 0.4
800	N08800	30.0-35.0	19.0-22.0	39.5 min.	-	0.75	1.0	1.5	800 = 0.10	800H = 0.05-0.1			S = 0.015, Al = 0.15-0.6, Ti = 0.15-0.6
800H	N08810	38.0-46.0	19.5-23.5	22.0 min.	2.5-3.0	1.5-3.0	0.5	1.0	0.05	0.05			S = 0.03, Al = 0.2, Ti = 0.6-1.2
825	N08825	68 nom.	1.0	2.0	26.0-30.0	-	0.1	1.0	0.02	0.02			S = 0.03, P = 0.04, Co = 1.0
B-2	N10665	70 nom.	6.0-8.0	5.0	15.0-18.0	0.35	1.0	1.0	0.04-0.08	0.04-0.08			{V = 0.5, (Al + Ti) = 0.5, B = 0.01 S = 0.02, P = 0.015, Co = 0.2, W = 0.5
X	N06002	49 nom.	20.5-23.0	17.0-20.0	8.0-10.0	-	1.0	1.0	0.05-0.15	0.05-0.15			{W = 0.2-1.0 S = 0.03, P = 0.04, Co = 0.5-2.5 S = 0.03, P = 0.04, Ti = 0.07, Co = 2.0
C-4	N06445	64 nom.	14.0-18.0	3.0	14.0-17.0	-	0.08	1.0	0.015	0.015			{W = 3.0-4.5, V = 0.35 S = 0.03, P = 0.04, Co = 2.5 (Cb + Ta) = 1.75-2.5
C-276	N10276	59 nom.	14.5-16.5	4.0-7.0	15.0-17.0	-	0.08	1.0	0.02	0.02			{S = 0.03, P = 0.04, Co = 2.5 (Cb + Ta) = 1.75-2.5 S = 0.03, P = 0.04, Co = 2.5, W = 1
G	N06007	42 nom.	21.0-23.5	18.0-21.0	5.5-7.5	1.5-2.5	1.0	1.0-2.0	0.05	0.05			{S = 0.03, P = 0.04, Co = 2.5, W = 1 S = 0.03, P = 0.03, Ti = 0.7-1.5
G-2	N06975	47.0-52.0	23.0-26.0	balance	5.0-7.0	0.7-1.2	1.0	1.0	0.03	0.03			S = 0.03, P = 0.03, Ti = 0.7-1.5

Note:  
(1) Published by permission of ASTM (Part 8), 1916 Race St, Philadelphia, Pa 19103, USA.

resistance to caustics is based on the latter.

Excellent corrosion resistance against flowing sea water is provided by nickel 200, but localised attack may occur in stagnant water, particularly if fouling organisms or deposits are permitted to accumulate. Its resistance against organic acids at all concentrations is excellent, while useful resistance is offered against other acids such as de-aerated sulphuric acid solutions at room temperature, aerated or de-aerated hydrochloric acid up to 30% concentration at room temperature, quiescent hydrofluoric acid up to 600 °C, and anhydrous hydrofluoric acid at elevated temperatures. Nickel 200 may also be used for dry bromine and fluorine at room temperature, dry chlorine up to 600 °C and dry hydrogen chloride up to 700 °C. Wet chlorine and hydrogen chloride behave as hydrochloric acid.

The resistance to caustic soda and other alkalis at all concentrations up to and including the molten state, is outstanding. It is not subject to stress corrosion cracking and has excellent resistance against non-oxidising halides, most organic compounds containing chlorine, bromine and fluorine, plus many chlorides with the exception of ferric, cupric and mercuric chlorides which are highly corrosive.

Nickel 201 has similar properties and applications, but is not subject to embrittlement by the intergranular precipitation of carbon or graphite when given lengthy exposure at 300–700 °C. It is therefore preferred to nickel 200 above 300 °C for alkalis.

#### 18.8.2. Nickel–copper alloy (Monel™ 400)

Monel 400, which contains a minimum of 63% nickel and 28% copper, plus iron and manganese, was first made over seventy-five years ago and is regarded as one of the most versatile nickel alloys on the market for general engineering applications. It offers good strength, ease of fabrication and excellent corrosion resistance against a variety of fluids. Although it has a high modulus of elasticity and its thermal expansion coefficient is only slightly greater than steel, it has a low thermal conductivity, being roughly half that of steel at 100 °C.

Its resistance to sea water, particularly at velocities greater than 3 m/s, is superior to the copper alloys described in section 18.6, including 70/30 cupro-nickel. It offers good resistance against deaerated sulphuric acid at temperatures below 100 °C and 80% concentration, de-aerated hydrochloric acid below 50 °C and 20% concentration and hydrofluoric acid below 50 °C.

#### 18.8.3 Nickel–chromium–iron alloy (Inconel™ 600)

Inconel 600, which is nominally 76% nickel, 15% chromium and 8% iron, has good high-temperature strength up to 1150 °C and is resistant to high temperatures and chemical corrosion. It resists attack by nitrogen/hydrogen mixtures and gaseous ammonia at high temperatures and is a standard material for ammonia cracker systems.

As it does not suffer from nitride formation, it is used for nitriding plant. It is resistant to dry chlorine, dry hydrogen chloride, all concentrations of ammonia, hot fatty acids and hot concentrated solutions of magnesium chloride.

In the chemical and process industries, it is resistant to stress-corrosion cracking in the presence of chlorides, water and dissolved oxygen, and to general attack and stress-corrosion cracking in sea and saline waters. In nuclear engineering, it is resistant to primary and secondary water in pressurised water circuits, including ammoniated and lithium hydroxide treated primary water and is the standard material for steam generators of pressurised water reactors.

#### 18.8.4 Nickel-chromium-molybdenum alloy (Inconel™ 625)

Inconel 625 contains nominally 61% nickel, 21% chromium, 9% molybdenum plus iron, niobium and tantalum. It has excellent tensile, creep and rupture properties and is suitable for temperatures ranging from cryogenic to 1100 °C, while the various alloying elements enable it to withstand a wide range of corrosive environments. It provides bolts having high strength at elevated temperatures.

In environments, such as the atmosphere, fresh and sea water, neutral salts and alkaline media, there is almost no attack. In more severe corrosive environments, the combination of nickel and chromium provides resistance to oxidising chemicals, while the high nickel and molybdenum content provides resistance to non-oxidising environments. The high molybdenum content in particular makes Inconel 625 exceptionally resistant to pitting in chlorides, even in oxidising acid conditions, and resistant to crevice corrosion, particularly in sea water and at elevated temperatures. The high nickel content ensures virtual immunity to chloride stress-corrosion cracking and provides excellent resistance to caustic stress-corrosion cracking. Due to the high niobium content, alloy 625 shows unusual stability after being welded, or when subjected to heat treatments which might cause serious sensitisation in other nickel-chromium and nickel-iron-chromium alloys.

#### 18.8.5 Nickel-iron-chromium alloys (Incoloy™ 800 and 800H)

Incoloy 800 is a high strength, heat and corrosion resistant material containing nominally 32% nickel, 46% iron and 21% chromium. Incoloy 800H has a similar composition, but has been modified slightly to enhance creep-rupture strength. An important feature of both alloys are their relative freedom from stress-corrosion cracking.

The alloys are widely used in petrochemical processing due to their good resistance to corrosion, which includes resistance to hydrogen sulphide over a wide range of temperatures and pressures. In addition, their high-temperature strength enables them to be used for high-temperature components such as piping, manifolds and waste heat boilers of steam-hydrocarbon reforming plants, and for the convection sections,



radiant tubes and transfer-line exchangers of ethylene crackers.

Good corrosion resistance is provided against flowing sea water, steam, mixtures of steam, air and carbon dioxide, acids such as formic, acetic and propanoic (except for the most severe conditions) and salts, both oxidising and non-oxidising, except halides.

#### 18.8.6 Nickel-iron-chromium-molybdenum-copper alloy (Incoloy™ 825)

Incoloy 825 was developed to meet corrosive conditions of unusual severity and contains nominally 42% nickel, 21% chromium, 30% iron, 3% molybdenum and 2% copper. The nickel content is sufficient to make it resistant to stress-corrosion cracking in chloride environments which may attack the 300 series stainless steels. Because of this, it is often selected for thin-wall expansion joints in preference to the stainless steels. The alloy has been developed to provide optimum stabilisation against intergranular corrosion.

Many of the applications for the alloy are in sulphuric acid solutions in a variety of processes where few other materials provide adequate resistance. These include sulphuric acid (all concentrations up to 65 °C, 60% at 80 °C, 40% at boiling temperature), nitric acid at all temperatures and concentrations up to 65%, wet sulphur dioxide, phosphoric acid at all temperatures and concentrations up to 85%, sea waters, most organic acids, ammonia and ammonium hydroxide.

#### 18.8.7 Hastelloys™

A range of alloys, having a nickel content greater than 40%, with varying additions of molybdenum, chromium, iron, copper and cobalt are known as Hastelloys, and are produced by the Cabot Corp. Some of these are listed in Table 18.7 and discussed below.

##### Nickel-molybdenum alloy (Hastelloy™ B-2)

Hastelloy B-2 is a high molybdenum alloy containing nominally 68% nickel, 28% molybdenum, with small additions of cobalt, chromium and iron. It is particularly noted for its resistance to hydrochloric acid at all concentrations and temperatures, including the boiling temperature. It is also resistant to hydrogen chloride gas and sulphuric, acetic and phosphoric acids. It has excellent resistance to pitting and stress-corrosion cracking.

The alloy should not be used in a system containing hydrochloric acid and iron or copper piping. Ferric and cuprous salts, which may develop in such a system, cause rapid corrosion failure of the alloy.

A reduction in ductility occurs when the alloy is exposed to temperatures of 538–816 °C. In the presence of oxidising gas, its upper temperature limit is 538 °C, but in the presence of reducing gases, or vacuum, it may be used at higher temperatures.

Alloy B-2 is a modified version of alloy B(N10001), not tabulated in

Table 18.7, which is similar in composition, except that the iron content is 4.0–6.0%, cobalt 2.5%, carbon 0.05% with the addition of 0.2–0.4% vanadium. Resistance to corrosion is the same, but alloy B-2 has improved resistance to heat affected zone attack so that it may be used in the as-welded condition in many applications.

#### **Nickel–chromium–molybdenum–iron alloy (Hastelloy™ X)**

Hastelloy X has a nominal composition of 49% nickel, 22% chromium, 18.5% iron and 9% molybdenum and possesses exceptional strength and oxidation resistance up to 1200 °C. Because of this, it is used for high-temperature applications such as furnace components, jet engine tailpipes and afterburner components. It has been found to be exceptionally resistant to stress-corrosion cracking in petrochemical applications.

#### **Low carbon nickel–molybdenum–chromium alloys (Hastelloys™ C-4, C-276 and C-22)**

These alloys are modifications of alloy C which was developed in the 1930s. Alloy C-276, with a nominal composition of 59% nickel, 16% molybdenum, 15.5% chromium, 4% tungsten, 5.5% iron, 2.5% cobalt and only 0.02% carbon, resists the formation of grain boundary precipitates in the weld heat-affected zone. It is suitable for most chemical process applications in the as-welded condition and has excellent resistance to pitting, stress-corrosion cracking and oxidising atmospheres up to 1038 °C. It is one of the few metallic materials which will resist the corrosive effects of wet chlorine gas, hypochlorite and chlorine dioxide solutions.

Alloy C-4 has a similar composition of 64% nickel, 15.5% molybdenum, 16% chromium, 3% iron, 2% cobalt, but no tungsten and only 0.015% carbon. Its properties are similar to alloy C-276, but has outstanding high-temperature stability as evidenced by high ductility and corrosion resistance even after long time ageing in the range 649–1038 °C.

C-22, not listed in Table 18.7, is a more recent low-carbon alloy, which provides a better overall corrosion resistance than the C-4 and C-276 alloys. Its nominal composition is 55% nickel, 21% chromium, 13.5% molybdenum, 4% iron and 2.5% cobalt.

#### **Nickel–chromium–iron–molybdenum–copper alloys (Hastelloy™ G and G-3)**

Hastelloy G has a nominal composition of 42% nickel, 22% chromium, 19.5% iron, 6.5% molybdenum and 2% copper and is stabilised by the addition of 2% niobium plus tantalum. Because of its resistance to the formation of grain boundary precipitates, it may be used in the as-welded condition, for most applications, but in some cases, solution heat treatment after fabrication may be necessary to achieve optimum corrosion resistance.

Alloy G-3 is an improved version with a slightly modified composition as shown in Table 18.7.

These alloys have excellent resistance to sulphate compounds, flue gases and acids, such as hot sulphuric, hot phosphoric, contaminated nitric, fluosilicic and hydrofluoric.

## 18.9 Titanium and titanium alloys

Although titanium is the fourth most abundant structural metal in the earth's crust, and the ninth most common element, extraction from the ore initially proved difficult and it was regarded as a rare metal. Since the end of World War Two it has been used extensively in aerospace applications because of its high strength to weight ratio.

50 °C, which titanium is well able to withstand. At velocities below 1.2 m/s the water should be chlorinated. No corrosion occurs due to the biofouling.

Titanium has an affinity for hydrogen and nitrogen which may cause embrittlement, and in certain environments, such as anhydrous red fuming nitric acid, ignition may be initiated by impact or friction. The addition of about 2% water appears to eliminate this reaction. A similar reaction may occur in gaseous mixtures containing oxygen, depending on the oxygen content and the pressure of the mixture. The greater the oxygen content, the smaller the mixture pressure to initiate the reaction. Dry chlorine also attacks titanium with possible ignition hazard.

Table 18.8 provides the composition of three commercially pure grades and two alloys. The commercially pure grades contain various proportions of oxygen and nitrogen which increase strength. One alloy contains palladium (0.12–0.25%) to increase resistance to crevice corrosion; the other includes small quantities of nickel and molybdenum to provide a low-cost, higher strength substitute in certain media.

### 18.9.2 Fabrication

Fabrication of titanium should be carried out in a special area of its own and isolated from shops where other metals and gases are handled. In addition to preventing contamination by hydrogen, oxygen and nitrogen, pick-up of even minute quantities of iron leaves welds prone to preferential corrosive attack. For this reason the cleaning of titanium surfaces must never be carried out with steel-wire brushes which are likely to deposit iron-bearing particles. Titanium-wire brushes are preferred, although stainless-steel-wire brushes have been proved satisfactory.

Some welding of titanium is carried out in inert gas-filled chambers but mostly it is carried out under shielded conditions in the open. The welding must be shielded completely, but typical processes such as shielded metal arc and submerged arc welding cannot be used because titanium reacts with gases and fluxes. It also reacts readily with air, grease, dirt, moisture and most metals to form brittle compounds and therefore exceptional cleanliness is essential. Although resistance and electron beam welding is carried out, the chief methods are tungsten inert gas (TIG) or metal inert gas (MIG) using argon, helium or argon-helium mixture as the shielding gas. In addition to the primary shielding of the molten weld, a secondary or trailing shield is required in order that the completed weld and heat-affected zone are protected from contamination until their temperature has been reduced to about 425 °C. A back-up shield is also required to shield the root side of the weld and heat-affected zone. Provided both sides of the weld can be shielded and inspected, weld-joint design for welding solid titanium is similar to those used for other metals. Before welding, the joints should be covered with plastic to prevent contamination.

Weld quality may be determined by tensile, bend, impact, hardness and liquid penetrant tests together with X-ray and visual examination.

The colour of a good weld is bright silver; light straw to light blue indicates surface oxide, which may be removed by brushing; and dark blue, grey or white indicates useless welds due to contamination.

Other shop operations involving titanium present no problems provided its special characteristics are taken into account. Titanium is particularly liable to gall which necessitates sharp tools and generous lubrication. The modulus of elasticity is about half that of steel which results in considerable spring-back after forming. It has low ductility and hot forming may be required. The low thermal conductivity, already mentioned, may cause excessive heat on the edges of cutting tools. Minute pieces of titanium are capable of being ignited.

### 18.9.3 Applications

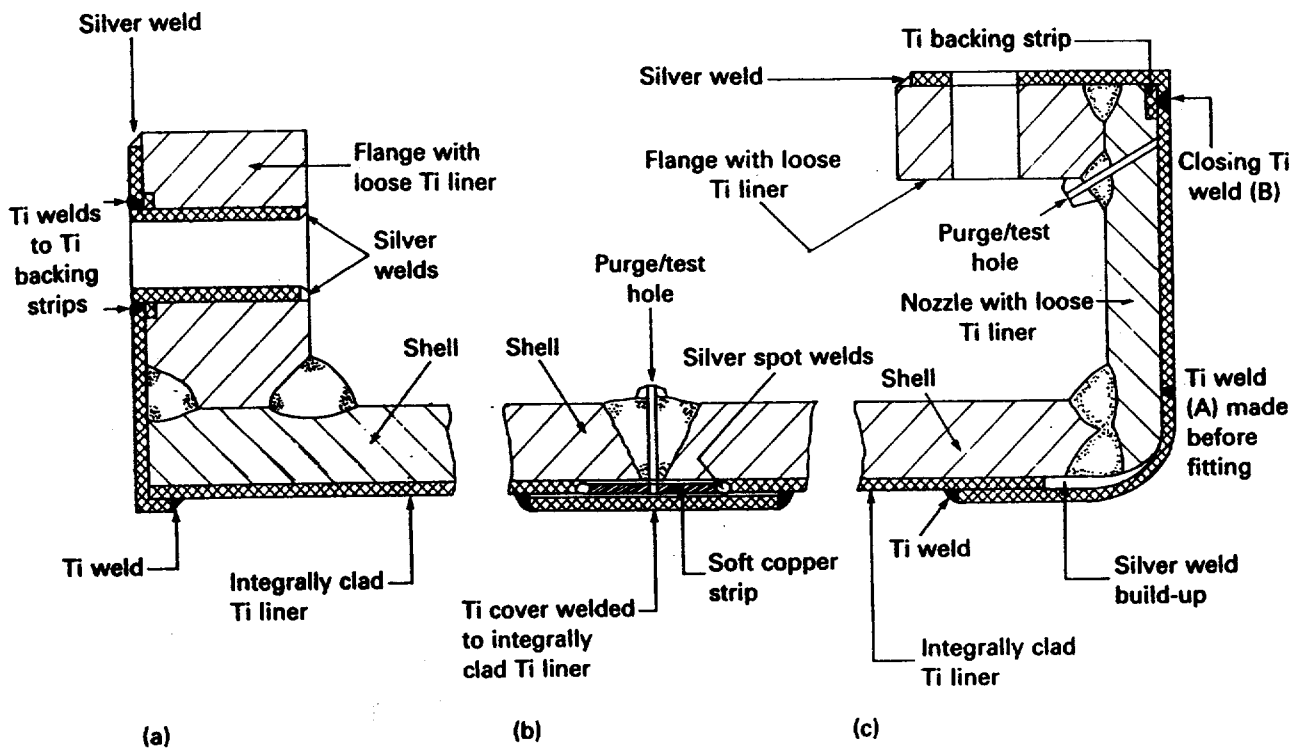
Titanium is used extensively in gasketed-plate heat exchangers where it is almost a standard material. It finds increasing usage in shell-and-tube heat exchangers, but this type cannot compete with gasketed-plate exchangers if the service is within the latter's temperature/pressure limitations, described in Chapter 4.

Because of its excellent corrosion resistance, titanium tubes thinner than normal are often employed in shell-and-tube exchangers, the chief reason being to reduce cost. Titanium has a low thermal conductivity of about 18 W/m K at 100 °C, which is only slightly above that of the austenitic stainless steels, and one-seventh of naval and admiralty brass. Hence, thinner tubes are desirable to offset the low thermal conductivity. Titanium tube thicknesses of 20 and 22 b.w.g. (0.89 and 0.71 mm) are common compared with 16 and 18 b.w.g. (1.65 and 1.24 mm) for many other metals. This may promote flow-induced vibration problems and the design should be checked thoroughly. The hard, smooth surface of titanium prevents the build-up of scale and in many cases lower fouling factors than normal are used.

Solid titanium or titanium-clad tubesheets eliminate the possibility of galvanic corrosion at the tube-tubesheet attachments, but tests have shown that 18/8 stainless steel and aluminium bronze alloy 614 tubesheets provide a reasonable life despite the latter's unfavourable position in relation to titanium in the galvanic series. Titanium tubes have been roller expanded successfully into tubesheets of 18/8 stainless steel and aluminium bronze for instance, using conventional techniques.

### 18.9.4 Titanium-clad construction

As the diameter and thickness of components increase, the use of titanium-clad construction should be investigated as an alternative to solid titanium. Figure 18.2 shows typical designs for welds in barrels, nozzles and flanges using explosion-clad titanium on steel. Compared with the welding of steel, special techniques must be employed to provide shielding gas and to avoid contamination. Other types of lining include the loose type, where the lining is formed to the required shape



**Figure 18.2** Titanium-clad construction (a) girth flange (b) seam (c) nozzle

and positioned inside the vessel, and linings which are attached to the vessel by titanium bolts. Linings are not recommended for vacuum service or for temperatures exceeding 200 °C because the thermal expansion coefficient of titanium is only 75% of that of steel.

## 18.10 Bi-metal construction

### 18.10.1 Bi-metal tubes and tubesheets

In certain applications it may be difficult or expensive to obtain a single metal tube capable of resisting the corrosive action of non-identical shell- and tube-side fluids, in which case bi-metal tubes should be considered, as described in section 1.5.5. Consider an exchanger in which ammonia on the shell-side is to be cooled using sea water as coolant on the tube-side. Carbon steel is resistant to ammonia, but not to sea water, whereas a copper alloy, which is the usual choice for sea-water applications, will be attacked by ammonia. A bi-metal tube would have a carbon-steel outer tube and a copper-alloy inner tube in this instance.

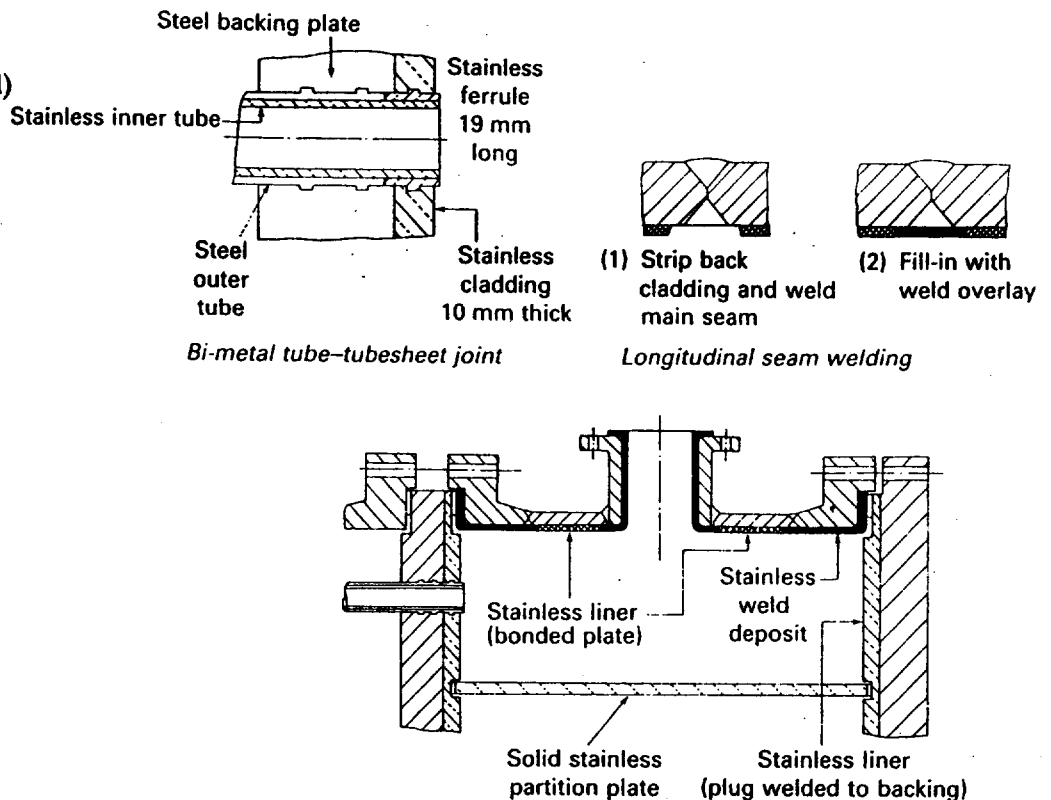
As a mechanical bond exists between inner and outer tubes, the question arises as to whether the thermal calculations should include an additional resistance to heat transfer, or bond resistance, to cater for lack of bond between the tubes. Whessoe Heavy Engineering Ltd has successfully supplied 160 bi-metal tube exchangers having steel outer tubes, copper-alloy inner tubes and cooling water inside the tubes, in which bond resistance has been ignored. However, each case must be treated individually, and as bond resistance is related to bond

temperature and the relative thermal expansion coefficients of the two metals it may be significant at higher temperatures and/or other metal combinations.

When bi-metal tubes are used, the tubesheets are invariably of bi-metal construction. In the ammonia cooler, described above, the backing plate on the shell-side would be carbon steel and its thickness would be calculated to meet the specified design temperature and pressure. The tube-side face would be clad with a 10 mm layer of the selected copper alloy. In order to prevent galvanic action at the tube ends, due to two different metals being in contact with the tube-side fluid, it is usual to remove about 19 mm of outer tube at each end and replace it with a ferrule of similar metal to the inner tube, as shown in Fig. 18.3. (The selected copper alloy would replace the stainless-steel inner tube shown.)

Consider an exchanger in which a hydrocarbon on the shell-side is to be cooled using sea water on the tube-side. The hydrocarbon does not attack either carbon steel or the copper alloy, which is necessary to resist the sea water. Single-metal construction is acceptable and the tubes and tubesheets could be made of the selected copper alloy. It may still be cheaper, however, to install bi-metal tubesheets as used in the ammonia cooler. Each case must be treated on its merits, but the incentive to use bi-metal tubesheets increases as (a) the alloy cost increases, (b) the solid alloy tubesheet thickness becomes greater than that of the steel backing plate due to a lower design stress and (c) the tubesheet diameter increases. When the single-metal tubesheet exceeds both 600 mm in diameter and 50 mm in thickness, bi-metal tubesheets merit consideration.

Figure 18.3 Bi-metal construction (parts not labelled are carbon steel)



### 18.10.2 Bi-metal barrels, heads and flanges

When an 'expensive' barrel and head material, such as monel or stainless steel, is required solely for corrosion resistance and not for strength, the use of clad plate should be considered, i.e. a backing plate, usually steel, thick enough to resist the specified design pressure and temperature, bonded to, say a 3 mm layer of the corrosion-resistant metal by weld deposition, integral rolling or explosive means.

Each case must be treated individually, but the use of clad plate for the barrels and heads may be cheaper than making them in solid corrosion-resistant material, particularly if the plate thickness is greater than, say, 12 mm. Similar considerations apply both to girth and nozzle flanges.

Figure 18.3 shows typical bi-metal construction for tubes, tubesheets and an A-type stationary head. The material combination is shown as steel-stainless steel, but if 70/30 cupro-nickel is substituted for the stainless steel, for instance, it would be suitable for the ammonia/sea-water cooler described in section 18.10.1.

It will be seen that the gasket face of both girth and nozzle flanges have weld-deposited stainless steel. Other metals, such as monel, cupro-nickel and aluminium bronze may be similarly weld-deposited, but not brass, aluminium or titanium. The weld deposit is applied in two or more layers, depending on the metal, and machined down to 3-5 mm. At this thickness the surface layer is usually free of iron contamination from the flange.

Figure 18.3 shows the inside of the nozzle pipe as weld-deposited stainless steel, as an example, but other methods are used depending on diameter and service. Small nozzles are usually solid alloy forged long-weld necks, but large nozzles may be solid alloy pipe or rolled from clad plate, or have an alloy loose liner.

Lead is sometimes used as a lining and it is especially resistant to salt water. In this case, the surface to be lead lined is 'tinned' to prevent oxidation and to bond the lead. Pure lead is applied to the surface, drop by drop, in strips about 25 mm wide from a lead stick, an oxy-acetylene torch being used. Two layers are required to achieve a final thickness of 3 mm. (This type of construction is illustrated by Fig. 18.6 - lead replacing the resin lining - and both sides of the partition plate is lead lined.)

### 18.10.3 Explosively bonded plate

The technique of explosive bonding dates from the late 1950s with the discovery in the USA of a metallurgical bond having been made by explosive means during explosive metal-forming operations. Explosively bonded plates on a commercial scale became available from DuPont in the early 1960s under the trade name Detaclad™, after which other companies throughout the world were licensed for its manufacture. In the UK it is produced by Nobel's Explosive Co. Ltd with the trade name Kelomet™.

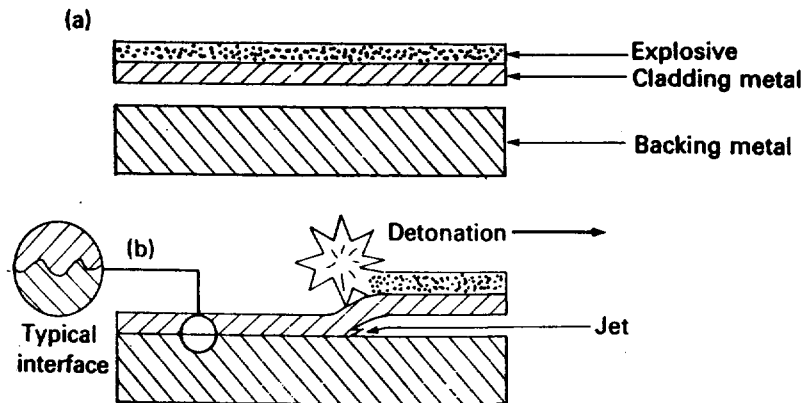


### Manufacture

A parallel 'stand-off' technique is employed in which the cladding plate is positioned at a closely controlled distance above the backing plate, the surfaces to be bonded having been machined or dressed to a smooth finish. Explosive is spread uniformly on the outer surface of the cladding plate and an initiator is placed at one edge. The function of the initiator is to detonate the explosive and also to start the bonding action by deforming the cladding plate and forcing it down across the air gap to impact the backing plate with considerable force.

The detonation, once started, progresses radially outwards from the initiation point across the cladding plate to collapse it at a controlled angle. The impact of cladding plate on backing plate creates a contact pressure of the order of 1 million bar as the metal is brought to rest. This results in a jet of surface metal being expressed from the apex of the collapse angle immediately in front of the arc of impact, thus effectively removing any residual contamination from the mating surfaces and producing a metallurgical bond. The process is shown in Fig. 18.4.

**Figure 18.4** Principle of explosive cladding  
(a) before detonation  
(b) after detonation



After firing, quality is immediately checked both visually and ultrasonically and the composite is then sent for heat treatment, flattening and cutting as required. Certain combinations such as steel-titanium or stainless steel-titanium are heat treated as a matter of course to improve bond ductility.

Additional non-destructive testing includes magnetic particle and dye penetrant for surface or peripheral cracks, and ferroxyI for non-contamination with titanium composites. Destructive testing, on request, includes shear, bend, tensile and impact testing.

### Size

There is no upper limit to the backing-plate thickness, but normally it should not be less than 13 mm and be at least twice the cladding thickness. Typical minimum and maximum thicknesses (mm) of the cladding plate are: brasses and bronze, 1.5-16; copper, 1.5-22; nickel and alloys and titanium, 1.5-20; stainless steels, 1.5-25; and aluminium, 6-50. The maximum plate size which can be clad is ultimately governed by the size of the explosion which is permitted under environmental regulations, but in practice it is usually the size of the available cladding plate which is

the governing factor. In some cases two cladding plates may be welded together to provide the required size. Clad shell plates up to 12 m<sup>2</sup> area, clad tubesheets up to 3500 mm diameter and one-piece composites up to 23 tonnes are available, for example. In addition, *small* amounts of clad plate can be produced economically, and if materials are available, the clad plate can be produced in a matter of hours.

#### **Bond integrity**

In sections cut radially relative to the initiation point, the metallurgical bond is shown as a rippled configuration. The normal bond has 100% continuity, although the guaranteed bond for tubesheets is 98%, with no individual non-bond greater than 650 mm<sup>2</sup>, while for shell plates the corresponding values are 95% and 5800 mm<sup>2</sup>. However, a guaranteed bond continuity may be obtained by special agreement. Guaranteed shear strengths (N/mm<sup>2</sup>) are: brasses, bronze, 90/10 and 70/30 cupro-nickel and titanium = 140; copper = 103; and nickel and alloys and stainless steel = 206. Typical values are 40–100% higher.

#### **Materials**

A wide range of cladding and backing-plate combinations may be bonded metallurgically by explosive means, including titanium–steel, titanium–stainless steel and steel–aluminium composites, for example, which could not be produced by other means. In addition, the backing plate may be clad on both sides with similar or different cladding plates as required. In order to ensure high bond integrity, both cladding and backing plates must be supplied to accepted material specifications with steels tested ultrasonically to ensure freedom from laminations and inclusions.

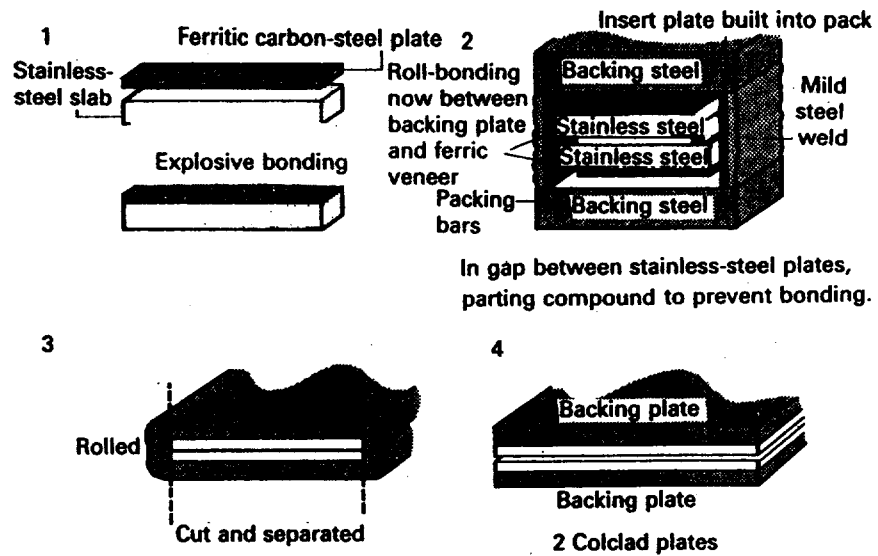
An important advantage of the explosively clad plate is that the cladding plate cannot experience contamination from the backing plate, or other problems, which may occur with weld deposition, such as inclusions, porosity, cracking and distortion.

### **18.10.4 Roll-bonded plate**

#### **Manufacture**

Roll-bonded composite plate, produced by forge-welding, has been available since the 1930s. In one method stainless-steel cladding, for example, is nickel-plated followed by hot-rolling of the carbon-steel backing plate to the plated surface. In another method, shown in Fig. 18.5, a layer of carbon steel is fusion-welded to one side of a thick stainless-steel plate, after which a thin carbon-steel plate is hot-rolled to the fusion-welded carbon-steel layer. (Step 1.) This produces a steel–stainless steel composite plate, in which the cladding plate is much thicker than the backing plate. Two such composites are then placed together such that the stainless-steel plates are face to face, with a layer of parting compound between them to prevent bonding during subsequent hot-rolling. A thick carbon-steel backing plate is placed on each side of the composites and the edges sealed by welding-in carbon-steel packing bars. (Step 2.) The complete pack is hot-rolled during which the thick

**Figure 18.5** Typical method for roll-bonded plate manufacture (courtesy of British Steel Corporation)



carbon-steel backing plates are forged-welded to the thin carbon steel plates of the composites. (Step 3.) After removing the edge welding and packing bars, two roll-bonded plates are produced. (Step 4.)

The process is shown in Fig. 18.5, but it should be noted that in recent years the traditional method has been modified to benefit from explosion bonding technique. Each steel-stainless steel composite is produced by explosively bonding the thin carbon-steel backing plate to the thick stainless-steel plate, instead of using fusion-welding. In the hot-rolling process only the backing carbon-steel surfaces contact the rolls, thus eliminating the possibility of contamination of the stainless-steel surfaces.

Ultrasonic testing of the roll-bonded plates is always carried out, and further tests include impact, tensile, bend and shear, a minimum shear strength of 137 N/mm<sup>2</sup> being readily achieved for the latter test.

**Size**

An important advantage of roll-bonded plate is that it is available in large sizes, which minimises the number of welded seams for heat exchanger shell barrels. Roll-bonded plates may be supplied with total thicknesses of 5–200 mm, and those above 30 mm thick may be supplied in sizes up to 11 m in length, 3.6 m in width, with a maximum weight of 15 tonnes. Cladding thicknesses of 1–10 mm may be supplied, depending on backing thickness, which may be 4–190 mm thick.

Typical examples of cladding and total thickness (cladding + backing) are:

<i>Cladding Thickness (mm)</i>	<i>Total thickness Range (mm)</i>
1	5–21
4	16–165
10	29–200

### Materials

Cladding plates include 13% chrome, 304L, 316L, 321 and 347 type stainless steels, nickel, monel, Inconel 600 and Incoloy 825. These may be combined with backing plates of carbon and low-alloy steels. Roll-bonded plates are also available with the backing plate clad on both sides.

## 18.11 Non-metallic coatings

Where operating conditions permit, the use of carbon-steel headers and tubesheets having corrosion-resistant organic coatings should be considered as a cheaper alternative to solid metal or metallic-clad steel construction. Although these coatings provide corrosion resistance to many fluids, they are used widely for sea and brackish cooling-water services. There is a wide variety of coatings available including rubber, polyvinylchloride, and phenolic and epoxy-based resins. Some resins are catalyst-cured and may be applied at the coating contractors' works or on site; other resins are thermally cured and are best applied at the coating contractors' works because suitable stoving facilities are required. Resin thicknesses generally lie in the range 0.175–0.3 mm, depending on type.

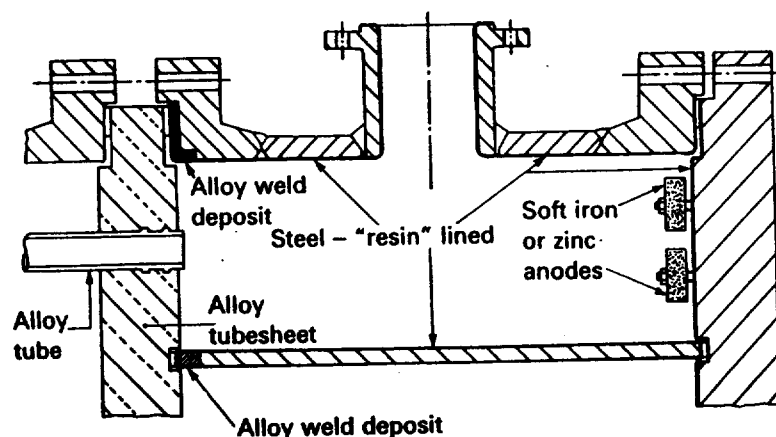
Maximum operating temperatures depend on the type of lining and whether the fluid is wet or dry. British Standards Code of Practice CP 3003: 1966 provides the following upper limits (°C).

	Dry	Wet
Epoxide resins (amine cured)	90	70
Epoxide resins (stoved)	120	80
Phenolic resins	150	80

Figure 18.6 shows a typical shell-and-tube heat exchanger header having a non-metallic coating. It will be seen that the gasket face of the flange, and the pass partition tip adjacent to the alloy tubesheet, has an alloy weld deposit to prevent galvanic corrosion.

Of particular interest are the thermally cured phenolic resins which, by a special technique, may be applied to both surfaces of shell-and-tube exchanger tubes, and the internal surfaces of air-cooler tubes, in addition

Figure 18.6 Resin-lined construction



to the headers and tubesheets. Hence, in the ammonia/sea-water exchanger discussed in section 18.10.1, bi-metal tubes and tubesheets could be eliminated and, as an alternative, the complete exchanger could be fabricated in carbon steel with phenolic resin-coating applied to the headers, tubesheet face and tube internal surfaces. If necessary, a complete carbon-steel exchanger may be coated with phenolic resin throughout and different grades selected for the shell- and tube-sides according to their respective corrosive media. However, it cannot be guaranteed that there will be 100% complete coating of the external surfaces at the baffle holes and tube-tubesheet crevice at the shell-side face. Shell-side lining is restricted to removable bundle exchangers and does not apply to the fixed tubesheet type.

This type of coating may be applied to the inside of straight and U-tubes, but seamless tubes are preferred to the electric resistance welded type. If the tubes are expanded into the tubesheets, they should be cut flush with the tubesheet face and then the inside edges of the tubes rounded off. The preferred method is to weld the tubes to the tubesheet, followed by a light expansion and rounding-off the welds. Expanded-in tubes are more likely to leak and the lining would need repair after re-expanding the leaking tubes. When the external tube surface is to be coated, all holes in both the baffles and tubesheets, at the shell-side face, must be well rounded. If the internal surface of the shell is to be coated, the shell should be provided with corrosion-resistant skid bars to enable the bundle to be inserted and withdrawn without damage to the coating.

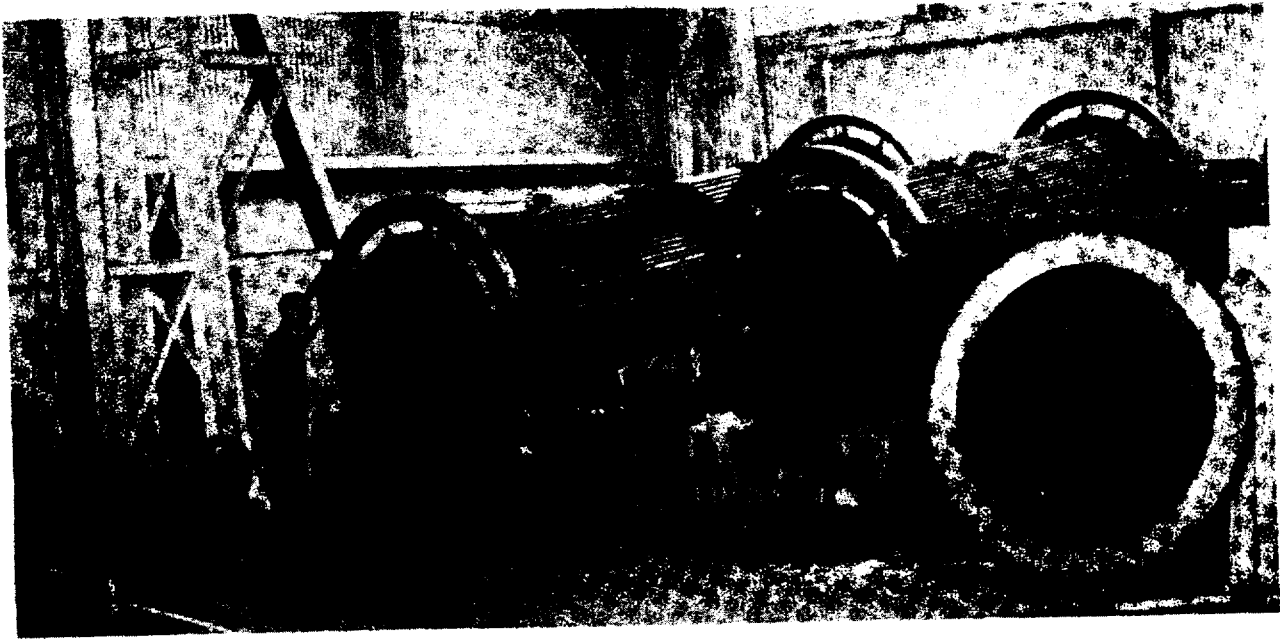
In addition to the corrosion resistant properties of the phenolic resins, their hard, hydrophobic surfaces discourage fouling and are sometimes used for this reason alone. The resistance of the finished coating on a single surface is of the order of  $(3.5 \times 10^{-4})$ – $(4.4 \times 10^{-4})$   $(\text{W/m}^2 \text{K})^{-1}$  and must be included in the calculation of the overall heat transfer coefficient. However, it is customary to ignore or substantially reduce the fouling factor on each coated side.

Irrespective of the type of coating, high integrity can only be achieved provided the exchanger manufacturer gives careful attention to the finish of structural details. In particular, sharp edges or pits where the coating is to be applied must be avoided. All welds must be continuous, free from pitting, undercutting and spatter, and ground smooth. Grease and oil must also be removed, but slight rusting is usually acceptable as the surfaces must be blast-cleaned before coating.

A quantity of phenolic resin is piped into each tube after which the tube bundle, or complete exchanger, is rotated to achieve even coverage, as shown in Fig. 18.7.

Headers and similar surfaces are sprayed.

The phenolic resins are applied in several coats and each coat is dried with air, followed by a low-temperature stoving. This process is critical to ensure that all solvents are removed and partial polymerisation of the resin occurs. After the required thickness has been achieved, a conductivity test is made to check that the lining is free from porosity. The coating is then given a high-temperature stoving at about 200 °C, during which final polymerisation occurs and the coating becomes infusible and insoluble.



**Figure 18.7** Tube bundle rotation during phenolic resin lining (courtesy of Lithgow Saekaphen Ltd)

## 18.12 National Association of Corrosion Engineers (NACE)

The text and references in this chapter show that this USA organisation is one of several which has made an appreciable contribution to our knowledge of materials and corrosion. The requirements of NACE are sometimes specified for steels to be used for 'sour service' which may be encountered in off-shore gas and oil production. 'Sour service' is related to wet hydrogen sulphide which may cause sulphide stress cracking (SCC) and hydrogen-induced cracking (HIC), sometimes termed 'step-wise' cracking, in steels.

### Acknowledgements

The author is grateful to the following companies for the provision of technical data: Allegheny Ludlum Steel Corporation, Brackenridge, Pennsylvania 15014, USA: AL-6X™, E-Brite™, AL29-4-2™ alloys. Alon Processing Inc., Tarentum, Pennsylvania 15084, USA: Alonizing™ process. American Petroleum Institute, Washington 20005, USA: API Publication 941 (Fig. 18.1). American Society for Testing and Materials, Philadelphia, Pennsylvania 19103, USA: Material compositions of Tables 18.4–18.8. Armco Inc., Stainless Steel Division, PO Box 1697, Baltimore, USA: Nitronic™ alloys. Avesta Johnson Stainless Steel Ltd, Birmingham, England: Uddeholm NU stainless 904L™, NU Monit™, NU EL1-T18-2™, NU stainless 744LN™ alloys. British Steel Corporation, Glasgow, Scotland: Colclad™ roll-bonded plate. Carpenter Technology Corporation, Reading, Pennsylvania 19603, USA: Carpenter alloy 20 Cb-3™. Lithgow Saekaphen Ltd., Buckley, Wales: Sakaphen™ epoxy resin linings. Nobels Explosives Co. Ltd, Stevenston, Scotland: Kelomet™ explosively clad plate. Sandvik Ltd, Halesowen, England: 2RK65™, 3RE60™, SAF2205™, Sanicro™ 28 alloys. Wiggins Alloys Ltd, Hereford, England: Monel™, Inconel™ and Incoloy™ alloys.

Haynes™ and Hastelloy™ are the registered trademarks of the Cabot Corporation, Kokomo, Indiana 46901, USA. Information concerning Haynes™ Alloy No. 20 Mod., and Hastelloys™ B-2, X, C-4, C-276, C-22, G and G-3 have been taken from Cabot Corp. brochures.

## References

(leading to other sources of materials and corrosion data)

A list of addresses for the service organisations is provided on p. xvi.

- Fontana, M. G. (1975) 'The eight forms of corrosion', *Process Industries Corrosion*, Chap. 1. NACE, Houston, USA.
- Gackebach, R. E. (1960) *Materials Selection for Process Plants*. Reinhold Publishing Co.
- Imperial Metal Industries (Kynoch) Ltd, *Corrosion Resistance of Titanium*. IMI, New Metals Division, Birmingham 6, England.
- IPC Industrial Press Ltd (1983) *Corrosion Chart*. IPC, Stamford Street, London.
- Kirby, G. N. (1980) 'How to select materials', *Chem. Eng.* (3 Nov.), pp. 86-131.
- The National Association of Corrosion Engineers (1974) *Corrosion Data Survey Metals Section* (5th edn). NACE, Houston, USA.
- The National Association of Corrosion Engineers (1975) *Corrosion Data Survey Non-metals Section* (5th edn). NACE, Houston, USA.
- Perry, R. H. and Green, D. (1984) *Perry's Chemical Engineers Handbook* (6th edn). McGraw-Hill.
- Pickering, F. B. (editor) (1979) *The Metallurgical Evolution of Stainless Steels*. Published by American Society for Metals and The Metals Society, London.
- Rabald, E. (1968) *Corrosion Guide* (2nd rev. edn). Elsevier.
- Schweitzer, P. A. (1976) *Corrosion Resistance Tables*. Marcel Dekker.
- Sedriks, A. John (1979) *Corrosion of Stainless Steels*. Wiley & Sons, New York.
- Titanium Metal & Alloys Ltd, *Titanium Design Handbook for Industrial Applications*. TMA, 85 London Wall, London, England (UK distributors for TIMET - Titanium Metals & Alloys Ltd).

---

## Size and cost estimation

### 19.1 Cost data

This chapter presents cost data for shell-and-tube, double-pipe, air-cooled, gasketed-plate, spiral, lamella, and rotary regenerative heat exchangers. Except for the shell-and-tube and rotary types, the cost data are presented as cost per unit surface area versus surface area for a standard set of design parameters. Cost multipliers are provided in certain cases where the design parameters differ from standard.

The data are approximate only, but serve as a guide for determining the capital cost of heat transfer equipment. When accurate costs are essential, the manufacturers must be approached. They are in a position to provide cost savings resulting from standardisation, bulk buying and modern thermal and mechanical design methods. Their experience will ensure that the equipment is economical and suited for the intended service.

Part 1 Appendix provides a guide to exchanger type selection and the cost data will assist in comparing the capital cost of the various types.

### 19.2 Surface area estimation

Before the approximate exchanger cost can be determined from the cost data, the surface area, if unknown, must be calculated from equation [19.1], which is the same as equation [6.8]:

$$A = \frac{Q}{U \Delta T} \quad [19.1]$$

In any design problem  $Q$  and the four terminal temperatures must be known. A knowledge of the terminal temperatures enables  $\Delta T$  to be calculated as described in section 19.2.1. The remaining unknown parameter for calculating  $A$  is  $U$ , which is established as described in section 19.2.2.



### 19.2.1 Mean temperature difference

Chapter 7 provides the basis for determining the mean temperature difference for heat transfer equipment in general. Chapters 14, 15 and 16 provide the basis for mean temperature difference calculations in air-cooled, double-pipe, and gasketed-plate heat exchangers, respectively.

Irrespective of the exchanger type and service, in many cases it will be sufficiently accurate as a first approximation to use the log MTD for the mean temperature difference. However, if greater precision is required, the mean temperature difference should be calculated as described in Chapters 7, 14, 15 or 16 as appropriate. This is particularly advisable if there is a temperature cross, (see section 7.2) as this may influence the number of shells required and their flow arrangement, and also if the heat release curves for condensation and boiling services are markedly non-linear.

### 19.2.2 Overall heat transfer coefficient

Unless there is previous operating experience similar to the service under consideration, the overall heat transfer coefficient can only be estimated at this stage. Tables are given in this chapter which provide typical overall heat transfer coefficients for various exchanger types and services and usually these are adequate for initial size and cost estimation.

A more precise procedure is to estimate the film heat transfer coefficient for each fluid and tables are given in this chapter which provide these for a variety of fluids and exchanger types. Once the individual film coefficients have been determined, together with the fouling factors, they may be combined to provide the overall heat transfer coefficient ( $U$ ) from equation [19.2], which is based on equation [6.7c]:

$$\frac{1}{U} = \frac{1}{\alpha_h} + \frac{1}{\alpha_c} + r_h + r_c \quad [19.2]$$

In most cases it is sufficiently accurate to omit the area correction terms and the tube-wall resistance. However, if the tubes are particularly thick, and/or their thermal conductivities are low, these factors must be considered. ( $\alpha_h$  and  $\alpha_c$ ,  $r_h$  and  $r_c$ , are the film coefficients and fouling factors for the hot and cold fluids respectively).

Fouling factors are described in Chapter 8. These are not the same for all exchanger types and their selection needs special care because they may provide the major resistance to heat transfer in the system. Tables 19.1 and 19.13 provide typical fouling factors for shell-and-tube and gasketed-plate type exchangers respectively. However, fouling factors for other than shell-and-tube exchangers are scarce.

In the case of shell-and-tube exchangers, dealing with *single-phase fluids in turbulent flow*, Smith (1981) shows how optimum fluid velocities may be calculated. The optimum fluid velocities provide the lowest annual running cost, i.e. annual pumping power cost + annual depreciation and maintenance costs. Once the optimum velocities are

known, the corresponding heat transfer coefficients can be calculated from the correlations of Chapter 6. This will lead to an optimum, rather than an estimated value of  $U$  (equation [19.2]),  $A$ , and hence capital cost.

Assuming that the various capital and operating costs are known, the method is more precise than the simple approach of using an estimated value of  $U$ , but requires more calculation. However, a plot of total running cost versus velocity yields a rather flat velocity profile, which means that the simple approach of using an estimated value of  $U$  will not lead to appreciable error.

### 19.2.3 Exchanger size

Tables are given for shell and tube, double pipe (plain and finned) and air cooled exchangers from which the physical size of the exchanger may be estimated once its surface area is known.

## 19.3 Shell-and-tube heat exchangers

Table 19.1 provides typical film and overall heat transfer coefficients, together with typical fouling factors, for various fluids in shell-and-tube heat exchangers.

Table 19.2 provides the basic cost of fixed tubesheet, U-tube, split backing ring floating-head, and pull-through floating-head shell-and-tube exchangers, in carbon steel, for a diameter range of 203–1524 mm (8–60 in), and design pressures of 10, 20, 30, 40 and 50 bar. Table 19.3 provides supporting cost factors relating to tube diameter and length, tube-end welding, and materials other than carbon steel.

The costs are based on 1984 values in the UK for AEM-, AEU-, AES- and AET-type exchangers to ASME, Section VIII, Division 1.

Purohit (1983) provides USA shell-and-tube exchanger cost data.

Table 19.4 provides data relating surface area to shell diameter for four exchanger types from which the physical size may be determined.

### 19.3.1 Method for calculating shell diameter

In order to calculate the approximate cost of a shell-and-tube heat exchanger from Tables 19.2 and 19.3, the external tube surface area, the tube configuration, the tube length and the shell inside diameter must be known. If tube-end welding is involved, the total number of ends to be welded must also be known.

Table 19.1 Shell-and-tube heat exchangers. Typical overall heat transfer coefficients ( $W/m^2 K$ )<sup>(M)</sup>

Cold side	Hot side							
	Gas at 1 bar abs. <sup>(1)</sup>	Gas at 20 bar abs. <sup>(1)</sup>	"Light" organic liquid <sup>(2)</sup>	"Heavy" organic liquid <sup>(4)</sup>	Process water	Condensing steam	Condensing "light" organics <sup>(2)</sup>	Condensing "light" organics + inerts <sup>(2)</sup>
Gas at 1 bar abs. <sup>(1)</sup>	55	93	99	63	102	107	100	86
Gas at 20 bar abs. <sup>(1)</sup>	93	300	375	120	429	530	388	240
"Light" organic liquid <sup>(2)</sup>	99	375	500	130	600	818	524	286
"Heavy" organic liquid <sup>(4)</sup>	68	138	153	82	161	173	155	124
Boiling organic liquid <sup>(2)</sup>	99	375	500	130	600	818	524	286
Treated cooling water	105	484	714	142	938	1607	764	345
Boiling water	104	467	677	140	875	1432	722	336

Table 19.1 (cont.)

The overall heat transfer coefficients above are derived from an average of the clean film coefficients  $\alpha$  ( $W/m^2 K$ ) (marked by an asterisk), and the typical fouling factors  $r_f$  ( $W/m^2 K$ )<sup>-1</sup>, given below.

Single-phase fluids	$\alpha$	$r_f \times 10^4$	Condensing fluids <sup>5</sup>	Pressure (bar abs.)	$\alpha$	$r_f \times 10^4$
Gas at 1 bar abs. <sup>(1)*</sup>	80-140	2	Organic vapours	0.1	1200-1800	2
Gas at 20 bar abs. <sup>(1)*</sup>	550-820	2	'Light', no inerts <sup>(2)*</sup>	0.1-1	1800-3500	2
Gas at 50 bar abs. <sup>(1)</sup>	700-900	2	'Light', no inerts <sup>(2)</sup>	1-10	3500-7000	2
Gas at 100 bar abs. <sup>(1)</sup>	800-1200	2	'Light', no inerts <sup>(3)</sup>	1	1200-2500	2
'Light' organic liquid <sup>(2)*</sup>	1500-1850	4	'Medium', no inerts <sup>(4)</sup>	1	500-1200	2
'Medium' organic liquid <sup>(3)</sup>	500-1200	5	'Heavy', no inerts <sup>(4)</sup>	1-10	235-635	2
'Heavy' organic liquid <sup>(4)*</sup>	190-230	8	'Light' + inerts <sup>(2)*</sup>	1	7500-12000	1
Ammonia	130-210	1	Ammonia	1	7500-12500	1
Methanol	5000-7500	1	Methanol	1	6850-9500	1
Aqueous solutions	5000-7500	1	Steam*	-	-	-
Process water*	4000-8000	5	<b>Boiling fluids</b>	$\alpha$	$K$ and $H$ <sup>(7)</sup>	$r_f \times 10^4$
Treated water*	4000-6000	2	Organic liquids		HVC <sup>(6)</sup>	
			'Light' <sup>(2)*</sup>	1800-4000	1000-1800	3
			'Medium' <sup>(3)</sup>	1500-3500	750-1500	3
			'Heavy' <sup>(4)</sup>	1000-2500	500-1000	5
			Aqueous solutions, ammonia, water*	6000-9000	3000-5000	3

**Notes:**

- (1) Gases containing a high proportion of hydrogen will have higher coefficients.
- (2) Liquid viscosity < 5cP.
- (3) Liquid viscosity 6-50 cP.
- (4) Liquid viscosity > 50 cP.
- (5) Coefficients are reduced considerably by small proportions of inerts; for high proportions use single-phase gas values.
- (6) High-velocity circulation.
- (7) Kettles and horizontal thermosyphons.
- (8) Based on data of Institution of Chemical Engineers (1982).

Table 19.2(a) Shell-and-tube heat exchangers – basic cost ( $C_b$ )(£)(1984)

Shell i.d. (mm)	Design pressure for shell- or tube-sides										Shell i.d. (in)
	Fixed tubesheet					U-tube					
	10 bar	20 bar	30 bar	40 bar	50 bar	10 bar	20 bar	30 bar	40 bar	50 bar	
203	6000	6000	6000	6000	6050	5470	5470	5500	5550	5580	8
254	6150	6150	6200	6300	6400	5700	5700	5750	5800	5850	10
305	6350	6400	6450	6700	6800	5900	5900	5950	6100	6250	12
337	6500	6550	6650	6900	7100	6000	6000	6100	6300	6450	13½
387	6750	6800	6900	7400	7650	6300	6400	6450	6700	7000	15½
438	7150	7200	7300	8000	8400	6650	6700	6750	7200	7600	17½
489	9300	9400	9500	9800	10000	8400	8700	8900	9200	9700	19½
540	9800	10000	10300	10700	11200	9100	9400	9500	10000	10500	21½
591	10400	10700	11000	11700	12400	10000	10300	10600	11000	11700	23½
635	10900	11400	11800	12600	13700	10700	11000	11400	12000	12700	25
686	11600	12200	12700	13800	15200	11500	12000	12300	13300	14000	27
737	12300	13000	13700	15000	16800	12400	12800	13400	14500	15300	29
787	13000	14000	14800	16400	18400	13400	13800	14400	15800	16800	31
838	13700	15000	15900	18000	20300	14300	14800	15500	17300	18400	33
889	14500	16100	17000	19600	22200	15300	16000	16600	18800	20300	35
940	15300	17100	18400	21200	24000	16000	17000	17800	20400	22000	37
991	16200	18700	20500	22900	26000	17000	18200	19200	22000	24000	39
1067	17500	19700	22000	26500	29400	18500	20000	21400	24500	27000	42
1143	19000	21500	24400	28500	33000	20300	22000	23800	27300	30500	45
1219	20700	23400	27000	32000	37000	22000	24000	26500	30400	34200	48
1295	23000	25400	31300	35600	41000	23700	26300	29400	33800	38500	51
1372	24200	27500	33500	39600	46000	25700	28800	32500	37500	43000	54
1448	26200	30000	37000	44200	51400	27800	31400	36000	41500	48000	57
1524	28600	32500	41200	48800	57000	30000	34300	40000	46500	53000	60

Table 19.2(b) Shell-and-tube heat exchangers – basic cost ( $C_b$ )(£)(1984)

Shell i.d. (mm)	Design pressure for shell- or tube-sides										Shell i.d. (in)
	Split backing ring floating head					Pull-through floating-head					
	10 bar	20 bar	30 bar	40 bar	50 bar	10 bar	20 bar	30 bar	40 bar	50 bar	
203	6400	6400	6400	6500	6550	–	–	–	–	–	8
254	6500	6600	6700	6900	6900	–	–	–	–	–	10
305	6800	7000	7100	7300	7400	–	–	–	–	–	12
337	7000	7200	7300	7600	7650	–	–	–	–	–	13½
387	7300	7700	7900	8100	8300	6800	6900	7250	7500	7700	15½
438	7700	8200	8500	8700	9000	7050	7100	7600	8000	8300	17½
489	9400	9500	10300	10700	11500	9200	9400	9600	10400	10700	19½
540	10100	10400	11300	11800	13000	9500	9800	10400	11200	11700	21½
591	11000	11600	12600	13200	14600	10500	10800	11500	12200	13000	23½
635	11800	12500	13600	14400	16200	11000	11500	12500	13300	14000	25
686	12700	13600	14800	15800	18200	11800	12600	13600	14500	15500	27
737	13700	14800	16000	17400	20500	12600	13700	14700	16000	17000	29
787	14600	15800	17500	19000	22700	13500	14700	16000	17400	18800	31
838	15500	17000	18800	20900	25000	14400	15800	17300	19000	20900	33
889	16500	18300	20400	22800	27500	15300	16800	18600	20600	23000	35
940	17500	19600	22000	25000	30000	16300	18000	20000	22500	25200	37

Table 19.2(b) (cont.)

Shell i.d. (mm)	Design pressure for shell- or tube-sides										Shell i.d. (in)
	Split backing ring floating-head					Pull-through floating-head					
	10 bar	20 bar	30 bar	40 bar	50 bar	10 bar	20 bar	30 bar	40 bar	50 bar	
991	18500	21000	23800	27000	32300	17400	19300	21700	24600	27600	39
1067	20200	23000	26500	30500	36400	19000	21300	24300	28000	31700	42
1143	22000	25500	29700	34500	41000	20700	23300	27000	31700	36000	45
1219	23700	28000	33000	39000	46000	22500	25500	30000	35700	41500	48
1295	25500	31000	37000	43600	52000	24300	28000	33400	40000	47000	51
1372	27700	34000	41000	49000	58500	26000	30500	37000	44500	52700	54
1448	30000	37000	45500	55000	65500	27800	33500	41000	49000	58500	57
1524	32500	40500	50400	61000	73000	29500	36500	45400	54400	64500	60

Table 19.3(a) Shell-and-tube heat exchangers. Cost factor for length ( $c_l$ )(£/m)(1984). Applicable to fixed tubesheet U-tube, split backing ring and pull-through floating-head types

Shell i.d. (mm)	Shell-side design pressure					Shell i.d. (in)
	10 bar	20 bar	30 bar	40 bar	50 bar	
203	73	73	95	98	105	8
254	90	90	121	143	166	10
305	108	108	143	174	210	12
337	120	120	156	190	230	13½
387	140	140	177	220	262	15½
438	166	166	200	243	290	17½
489	192	192	223	262	312	19½
540	218	218	244	282	328	21½
591	243	253	272	299	335	23½
635	266	276	299	328	371	25
686	292	303	331	381	449	27
737	318	338	364	476	515	29
787	341	364	400	541	550	31
838	371	397	436	591	623	33
889	400	433	476	630	666	35
940	430	472	515	666	696	37
991	459	509	558	699	732	39
1067	495	558	650	761	791	42
1143	535	600	755	823	869	45
1219	577	656	846	889	951	48
1295	627	722	919	961	1050	51
1372	682	787	997	1040	1148	54
1448	741	860	1073	1115	1247	57
1524	804	935	1148	1198	1362	60

Table 19.3(b) Shell-and-tube heat exchangers. Carbon steel tube costs (1984)

Tube o.d. (mm)	Wall thk (mm)	Seamless (C <sub>s</sub> ) Welded		Wall thk (b.w.g.)	Tube o.d. (in)
		Cost (£/m <sup>2</sup> )	Cost factor (c <sub>w</sub> )		
15.88	1.24	10.9	0.85	18	$\frac{5}{8}$
	1.65	13.3	0.86	16	
	2.11	16.2	0.86	14	
19.05	1.65	12.1	0.83	16	$\frac{3}{4}$
	2.11	14.7	0.84	14	
	2.77	17.3	0.84	12	
25.40	2.11	14.6	0.77	14	1
	2.77	17.2	0.77	12	
	3.40	20.2	0.77	10	
31.75	2.11	14.9	0.76	14	1 $\frac{1}{4}$
	2.77	17.6	0.76	12	
	3.40	20.7	0.76	10	

Table 19.3(c) Shell-and-tube heat exchangers. Cost factor (c<sub>c</sub>) for 'fixed' components (fixed tubesheet and U-tube types) (1984)

Exchanger type	Shell i.d. (mm)	Design pressure – see step (10), section 19.3.2									Shell i.d. (in)
		'Fixed' shell side components			'Fixed' channel components			Tubesheets			
		10 bar	30 bar	50 bar	10 bar	30 bar	50 bar	10 bar	30 bar	50 bar	
Fixed tubesheet	203	0.003	0.003	0.005	0.039	0.042	0.042	0.011	0.011	0.012	8
	438	0.009	0.009	0.008	0.082	0.105	0.130	0.027	0.028	0.039	17 $\frac{1}{2}$
	489	0.006	0.005	0.010	0.075	0.082	0.113	0.026	0.028	0.039	19 $\frac{1}{2}$
	686	0.007	0.007	0.011	0.081	0.094	0.125	0.029	0.034	0.045	27
	889	0.012	0.010	0.014	0.099	0.130	0.165	0.037	0.046	0.057	35
	1067	0.013	0.011	0.016	0.115	0.155	0.205	0.043	0.055	0.065	42
	1219	0.014	0.012	0.015	0.124	0.179	0.230	0.048	0.061	0.073	48
	1372	0.014	0.014	0.014	0.133	0.205	0.263	0.053	0.064	0.080	54
	1524	0.014	0.015	0.013	0.144	0.234	0.283	0.060	0.066	0.086	60
U-tube	203	0.014	0.015	0.019	0.030	0.032	0.038	0.002	0.003	0.003	8
	438	0.032	0.038	0.049	0.061	0.080	0.103	0.009	0.012	0.014	17 $\frac{1}{2}$
	489	0.022	0.027	0.040	0.051	0.064	0.088	0.010	0.013	0.016	19 $\frac{1}{2}$
	686	0.025	0.032	0.046	0.057	0.075	0.103	0.012	0.016	0.019	27
	889	0.032	0.042	0.059	0.073	0.114	0.134	0.017	0.024	0.027	35
	1067	0.036	0.051	0.070	0.085	0.123	0.165	0.022	0.032	0.033	42
	1219	0.037	0.057	0.079	0.095	0.140	0.195	0.026	0.036	0.039	48
	1372	0.038	0.064	0.087	0.103	0.157	0.213	0.030	0.040	0.043	54
	1524	0.039	0.068	0.093	0.110	0.180	0.224	0.035	0.042	0.046	60

**Table 19.3(d)** Shell-and-tube heat exchangers. Cost factor ( $c_c$ ) for 'fixed' components (floating-head types) (1984)

Exchanger type	Shell i.d. (mm)	Design pressure – see step (10), section 19.3.2												Shell i.d. (in)
		'Fixed' shell-side components			'Fixed' channel components			Tubesheets			Floating-head components			
		10 bar	30 bar	50 bar	10 bar	30 bar	50 bar	10 bar	30 bar	50 bar	10 bar	30 bar	50 bar	
Split backing ring floating head	203	0.039	0.044	0.055	0.022	0.025	0.028	0.003	0.003	0.003	0.010	0.010	0.010	8
	438	0.074	0.086	0.104	0.058	0.063	0.082	0.011	0.019	0.011	0.023	0.023	0.024	17½
	489	0.060	0.076	0.102	0.046	0.054	0.069	0.010	0.013	0.015	0.023	0.027	0.031	19½
	686	0.065	0.085	0.112	0.052	0.062	0.077	0.016	0.020	0.022	0.024	0.031	0.036	27
	889	0.079	0.105	0.137	0.067	0.081	0.099	0.025	0.030	0.029	0.029	0.042	0.048	35
	1067	0.086	0.123	0.167	0.079	0.098	0.122	0.032	0.038	0.034	0.032	0.050	0.062	42
	1219	0.091	0.138	0.190	0.087	0.114	0.142	0.038	0.043	0.041	0.035	0.056	0.075	48
	1372	0.094	0.153	0.195	0.095	0.130	0.154	0.045	0.048	0.046	0.038	0.061	0.087	54
1524	0.095	0.168	0.198	0.104	0.146	0.161	0.051	0.052	0.050	0.042	0.066	0.099	60	
Pull-through floating head	≤438	0.070	0.080	0.094	0.060	0.067	0.086	0.010	0.013	0.014	0.010	0.010	0.010	≤17½
	489	0.048	0.061	0.085	0.048	0.059	0.080	0.011	0.018	0.021	0.009	0.010	0.012	19½
	686	0.053	0.067	0.094	0.055	0.067	0.092	0.017	0.022	0.025	0.012	0.015	0.017	27
	889	0.063	0.083	0.118	0.071	0.087	0.118	0.026	0.032	0.034	0.015	0.021	0.025	35
	1067	0.070	0.100	0.138	0.084	0.106	0.138	0.034	0.042	0.041	0.017	0.026	0.030	42
	1219	0.075	0.117	0.157	0.093	0.122	0.157	0.041	0.048	0.046	0.019	0.030	0.034	48
	1372	0.079	0.133	0.175	0.104	0.138	0.175	0.048	0.053	0.051	0.022	0.034	0.039	54
	1524	0.082	0.150	0.190	0.112	0.157	0.185	0.055	0.058	0.055	0.025	0.037	0.045	60

**Table 19.3(e)** Shell-and-tube heat exchangers. Cost factor ( $c_c$ ) for 'variable' shell components (1984). Applicable to fixed tubesheet, U-tube, split backing ring and pull-through floating-head types

Shell i.d. (mm)	Shell-side design pressure					Shell i.d. (in)
	10 bar	20 bar	30 bar	40 bar	50 bar	
203	0.29	0.29	0.46	0.46	0.51	8
438	0.58	0.58	0.67	0.77	0.84	17½
489	0.21	0.24	0.29	0.32	0.34	19½
686	0.22	0.25	0.31	0.33	0.35	27
889	0.23	0.27	0.33	0.36	0.38	35
1067	0.25	0.29	0.36	0.38	0.41	42
1219	0.25	0.31	0.37	0.41	0.42	48
1372	0.24	0.31	0.37	0.41	0.43	54
1524	0.22	0.32	0.38	0.40	0.44	60



**Table 19.3(f) Shell-and-tube heat exchangers – cost factor for material ( $C_m$ ). Relative cost of heat exchanger tubes and plate (carbon steel = 1.00)**

Material		Tubes		Plate	
		Welded	Seamless		
Carbon & low-alloy steel	Carbon steel	see Table 17.2	1.00	1.00	
	Carbon- $\frac{1}{2}$ % moly.	–	1.64	1.67	
	1% chrome- $\frac{1}{2}$ % moly.	–	1.64	1.71	
	2 $\frac{1}{4}$ % chrome-0.01% moly.	–	1.87	2.37	
	5% chrome- $\frac{1}{2}$ % moly.	–4	2.13	2.20	
	3 $\frac{1}{2}$ % nickel	–	2.46	2.57	
Stainless steels	Standard	Type 304	2.55	3.72	4.48
		Type 304 L	2.61	3.83	4.89
		Type 316	3.03	4.37	6.40
		Type 316 L	3.07	4.42	6.53
		Type 321	2.72	3.88	4.89
		Type 347	–	4.28	5.17
		Type 410	–	3.84	3.87
		Type 430	–	4.18	3.27
	Sandvik/ Uddeholm	3 RE 60	–	4.73	–
		SAF 2205/744 LN	–	5.08	9.70
2 RE 10		–	5.32	–	
2 RK 65/904 L		–	6.26	18.13	
2 RE 69 SANICRO 28		–	6.38 6.62	– 18.91	
Aluminium	–	1.42	6.91		
	Gr. 2	4.34	7.40	4.69	
Titanium	Gr. 7	7.48	10.95		
Lined surfaces (SAKAPHEN)	Tube bundles	40–90 m <sup>2</sup> 100–200 m <sup>2</sup>	£33/m <sup>2</sup> £30/m <sup>2</sup>	headers 2–10 m <sup>2</sup>	£51/m <sup>2</sup>

**Table 19.3(g) Shell-and-tube heat exchangers. Additional cost per tube end for fusion welding ( $C_{te}$ )(£)(1984)**

Tube o.d. (mm)	Carbon and low-alloy steels		Stainless steel and nickel alloys		Tube o.d. (in)
	One weld pass	Two weld passes	One weld pass	Two weld passes	
15.88	0.7	1.0	1.6	2.2	$\frac{5}{8}$
19.05	1.0	1.4	2.1	2.9	$\frac{3}{4}$
25.40	1.5	2.0	3.0	4.0	1
31.75	2.2	2.8	4.0	5.3	1 $\frac{1}{4}$

Table 19.3(f) (cont.)

Material		Tubes		Plate	
		Welded	Seamless		
Copper & Copper alloys	Aluminium brass	-	2.14	-	
	Admiralty brass	-	2.15	-	
	Naval brass	-	-	10.52	
	Copper	-	2.43	9.08	
	90/10 cupro-nickel	-	3.19	10.91	
	Aluminium bronze	-	3.51	14.28	
	80/20 cupro-nickel	-	3.59	15.10	
	70/30 cupro-nickel	-	4.03	15.64	
Nickel & Nickel alloys	Incoloy 800	-	7.02	19.89	
	Incoloy 800 H	-	7.08	20.00	
	Monel 400	-	8.23	28.15	
	Incoloy 825	-	9.01	27.71	
	Inconel 600	-	9.27	29.93	
	Nickel 200	-	9.36	35.35	
	Nickel 201	-	9.55	35.35	
	Inconel 625	-	22.53	-	
Low-fin tubes	Carbon steel	195065	-	2.19	-
	Copper	195049	-	3.43	-
	Aluminium brass	195049	-	3.05	-
	90/10 cupro-nickel	195049	-	4.02	-
	70/30 cupro-nickel	195049	-	5.43	-
Bi-metal	Tubes: steel outer; alum. brass inner			6.40	-
	Expl. clad plate (>1m <sup>2</sup> )	Total plate cost + £400: stainless-steel clad (clad and backing) + £600: titanium clad			

Table 19.3(h) Shell-and-tube heat exchangers. 'Market cost factor' for size and type ( $C_z$ )(1984)

Shell i.d. (mm)	Fixed tubesheet and U-tube with tube lengths shown below			All floating-head types	Shell i.d. (in)
	2.438 m (8 ft)	3.656 m (12 ft)	6.096 m (20 ft)		
≤387	0.60	0.65	0.70	1.00	<15 $\frac{1}{4}$
438-591	0.70	0.75	0.80	1.00	17 $\frac{1}{4}$ -23 $\frac{1}{4}$
635-889	0.80	0.88	0.85	1.00	25-39
>889	1.00	1.00	1.00	1.00	>39

**Table 19.4** Shell-and-tube heat exchangers – surface area (m<sup>2</sup>) for a range of shell diameters and four exchanger types.Basis: 19.05 mm ( $\frac{3}{4}$  in) o.d.  $\times$  25.4 mm (1 in) pitch  $\times$  6.096 m (20 ft) long<sup>(1)</sup> tubes at 30° pitch angle<sup>(2)</sup>

Shell i.d.		Fixed tubesheet	U-tube	Floating-head types	
mm	in			Split backing ring	Pull through
203	8	10	9	7	–
254	10	18	17	14	–
305	12	29	27	24	16
337	13 $\frac{1}{4}$	37	35	32	22
387	15 $\frac{1}{4}$	52	50	46	34
438	17 $\frac{1}{4}$	69	66	63	49
489	19 $\frac{1}{4}$	89	86	82	67
540	21 $\frac{1}{4}$	111	108	104	87
591	23 $\frac{1}{4}$	136	133	127	110
635	25	159	155	148	131
686	27	190	186	176	158
737	29	220	216	206	189
787	31	255	250	240	221
838	33	291	286	275	255
889	35	330	325	313	292
940	37	371	366	354	332
991	39	415	409	395	369
1067	42	485	479	464	437
1143	45	561	554	539	511
1219	48	642	635	618	590
1295	51	729	722	704	676
1372	54	822	814	795	769
1448	57	919	910	890	866
1524	60	1022	1013	992	970
1600	63	1131	–	–	–
1676	66	1245	–	–	–
1753	69	1364	–	–	–
1829	72	1489	–	–	–
1981	78	1756	–	–	–
2134	84	2044	–	–	–

*Notes:*(1) For other tube lengths  $L$  (m), multiply surface areas by  $L/6.096$ .

(2) For other tube configurations, multiply surface areas by factor.

Tube o.d.		Pitch		Angle	Factor ( $f_p$ )
mm	in	mm	in		
15.88	$\frac{5}{16}$	19.84	$\frac{25}{32}$	30°, 60°	1.36
15.88	$\frac{5}{16}$	22.23	$\frac{7}{8}$	45°, 90°	0.95
19.05	$\frac{3}{4}$	23.81	$\frac{15}{16}$	30°, 60°	1.14
19.05	$\frac{3}{4}$	25.40	1	45°, 90°	0.87
25.40	1	31.75	1 $\frac{1}{4}$	30°, 60°	0.85
25.40	1	31.75	1 $\frac{1}{4}$	45°, 90°	0.74
31.75	1 $\frac{1}{4}$	36.69	1 $\frac{2}{16}$	30°, 60°	0.68
31.75	1 $\frac{1}{4}$	39.69	1 $\frac{2}{16}$	45°, 90°	0.60

In preliminary cost estimation it is usually the shell inside diameter and tube count which are unknown and these may be determined from Table 19.4. This table is based on tubes, 19.05 mm outside diameter  $\times$  25.4 mm (30°) pitch  $\times$  6.096 m long. If it is required to determine the shell diameter for a known surface area  $A$  ( $m^2$ ), but a different tube configuration and/or different length  $L$  (m),  $A$  is corrected as follows:

$$\text{corrected } A \text{ (for use in Table 19.4)} = \frac{A}{(L/6.096)(f_p \text{ from Table 19.4})} \quad [19.3]$$

$A$  is always based on the outside tube diameter  $d_o$  (m) in these calculations.

The tube count ( $N_t$ ) for a tube outside diameter  $d_o$  is given by:

$$N_t = \frac{A}{\pi d_o L} \quad [19.4]$$

Example 1 in section 19.3.3 demonstrates these calculations.

For more exact calculations, shell diameter and tube count should be determined from a computer program or from tube count tables (A3.1–A3.3) in Part 3 Appendix.

### 19.3.2 Method for calculating exchanger cost

Once surface area, tube length, shell diameter and number of tubes are known, the approximate cost of a shell-and-tube exchanger is determined as follows:

#### Exchanger cost (steel)

Step (1) From Table 19.2, depending on the shell inside diameter and exchanger type, determine the basic cost for the shell-side ( $C_{bs}$ ), corresponding to the shell-side design pressure, and the basic cost for the tube-side ( $C_{bt}$ ), corresponding to the tube-side design pressure.

Step (2) Obtain the combined basic cost ( $C_{bc}$ ) from  
 $C_{bc} = 0.65(C_{bs}) + 0.35(C_{bt})$ .

Step (3) From Table 19.3(a), determine the cost factor for length ( $c_l$ ), corresponding to the *shell-side* design pressure and shell inside diameter. Obtain the extra cost for length ( $C_L$ ) from  $C_L = c_l L$ .

Step (4) From Table 19.3(b) determine the seamless tube cost ( $C_s$ ) and obtain the tube cost ( $C_T$ ) from  $C_T = C_s A$  (seamless) =  $C_s A c_w$  (welded).

Step (5) If the tube ends are welded, obtain the welding cost per tube end ( $C_{te}$ ) from Table 19.3(g) and multiply by the number of tube ends ( $N_{te}$ ) to be welded, giving the extra cost of tube-end welding  
 $C_{TW} = C_{te} N_{te}$ .

Step (6) Total exchanger cost ( $C_E$ ) =  $C_{bc} + C_L + C_T + C_{TW}$ .

Step (7) From Table 19.3(h) determine 'market cost factor'  $c_z$ .

Step (8) Exchanger sales cost =  $C_E c_z$ .

**Extra cost for non-carbon steel components**

Steps (1)–(4) and (6) must always be carried out before the extra cost of any non-carbon steel components is determined, as described below.

The heat exchanger is divided into sections; namely, shell, channel, tubesheets, floating-head flange and cover, and tubes. The material in any one section is assumed to be the same throughout.

Step (9) From Table 19.3(f) determine the relative material cost ( $c_m$ ) for those sections of the exchanger which are not carbon steel.

Step (10) From Tables 19.3(c) or 19.3(d) obtain the cost factor ( $c_c$ ) for those sections of the exchanger which are not carbon steel.

Interpolate linearly.  $c_c$  is determined for the relevant exchanger size and type using the following design pressures and basic costs from step (1):

Exchanger section	Design pressure	Basic cost ( $C_b$ )
'Fixed' shell-side	$p_s$	$C_{bs}$
'Fixed' channel	$p_t$	$C_{bt}$
Tubesheets	greater of $p_s$ and $p_t$	greater of $C_{bs}$ and $C_{bt}$
Floating head flange and cover	$p_t \geq 0.5p_s$ , use $p_t$ $p_t < 0.5p_s$ , use $(p_t + p_s)/2$	$C_{bt}$ $(C_{bt} + C_{bs})/2$

$p_s$  = shell-side design pressure;  $p_t$  = tube-side design pressure.

In each exchanger section, the extra cost of non-carbon steel material ( $C_x$ ) is given by:

$$C_x = c_c C_b (c_m - 1)$$

Step (11) From Table 19.3(e), obtain the cost factor ( $c_v$ ) for 'variable' shell components if the shell is not carbon steel.  $c_v$  is determined according to the exchanger size and shell-side design pressure. The extra cost ( $C_x$ ) is given by:

$$C_x = c_v C_L (c_m - 1)$$

Step (12) The extra cost of non-carbon steel tubes ( $C_x$ ) is given by:

$$C_x = A C_s (c_m - c_w)$$

$c_w$  = value used in step (4).

Step (13) If the tube ends are welded, determine extra cost of tube-end welding ( $C_{TW}$ ) as shown in step (5).

Step (14) Sum all extra costs ( $C_x$ ) from steps (10), (11) and (12), plus extra cost of tube-end welding ( $C_{TW}$ ) from step (13), if appropriate, to give total extra cost ( $C_{EX}$ ).

Step (15) Total exchanger cost:  $C_E$  = cost from step (6) +  $C_{EX}$ .

Step (16) From Table 19.3(h) determine market cost factor ( $c_z$ ).

Step (17) Exchanger sales cost =  $C_E c_z$ .

The accuracy of the method for determining the extra cost of non-carbon steel components is enhanced by the fact that the actual tube cost is used. However, in the case of the other components, the reliability is reduced when their design stresses ( $f$ ) differ greatly from that of carbon steel (120 N/mm<sup>2</sup>). As an approximation, the basic costs ( $C_b$ ) in step (10) may

be multiplied by  $(120/f)^{0.5}$ , and the 'variable' shell costs in step (11) by  $(120/f)$ .

Table 19.3(h) provides arbitrary 'market size and cost factors' which attempts to allow for the fact that a manufacturer specialising in the fabrication of large units is not likely to provide competitive costs against a manufacturer specialising in the fabrication of small units, and vice-versa.

### 19.3.3 Examples of size and cost estimation

Two examples of the method for calculating the approximate exchanger cost are given below. They relate to the shell-and-tube exchangers used in the comparisons with double-pipe and gasketed-plate exchangers. (Sections 19.4 and 19.6, respectively.)

#### Example 1

Determine the cost of a fixed tubesheet exchanger, all carbon steel, surface area (based on tube o.d.)  $74.5 \text{ m}^2$ , containing seamless tubes  $19.05 \text{ mm o.d.} \times 2.11 \text{ mm thick} \times 23.81 \text{ mm (30}^\circ\text{) pitch} \times 8 \text{ m long}$ . Design pressures are 10 bar and 40 bar for the shell- and tube-sides, respectively. Tubes are welded with one weld pass to the tubesheets. The shell diameter is not known.

#### Tube count

External surface area per metre length (Table 17.3(a)):  $0.0598 \text{ m}^2/\text{m}$   
No. of tubes in exchanger:  $74.5/(8 \times 0.0598) = 156$

#### Shell diameter

Table 19.4 for determining shell diameter, when unknown, is based on tubes  $19.05 \text{ mm o.d.} \times 25.4 \text{ mm (30}^\circ\text{) pitch} \times 6.09 \text{ m long}$ . To correct required surface for use with Table 19.4.

$$\begin{aligned} \text{length correction} &= 8/6.096 = 1.312 \\ f_p = \text{tube pitch correction} &= 1.14 \\ \text{corrected surface} &= 74.5/(1.312 \times 1.14) = 49.8 \text{ m}^2 \\ \text{nearest shell diameter} &= 387 \text{ mm} \end{aligned}$$

#### Exchanger cost (steel)

Step (1) Basic cost (Table 19.2(a)), shell-side  
£6750 (10 bar)

Step (1) Basic cost (Table 19.2(a)), tube-side:  
£7400 (40 bar)

Step (2) Basic cost (Table 19.2(a)), combined:  
 $(0.65 \times 6750) + (0.35 \times 7400) = \text{£}6978$

Step (3) Cost factor for length (Table 19.3(a)):  
£140/m (10 bar)

Step (3) Extra cost for length:  
 $140 \times 8 = \text{£}1120$

Step (4) Tube cost (Table 19.3(b)):		
	£14.7/m <sup>2</sup> (seamless)	
Step (4) Extra cost of tubes:		
	14.7 × 74.5	= £1095
EXCHANGER COST WITH EXPANDED TUBES:		= £9193
Step (5) Tube-end welding cost (Table 19.3(g)):		
	£1/end	
Step (5) Extra cost of tube-end welding:		
	2 × 156 × 1	= £312
Step (6) TOTAL EXCHANGER COST:		
	9193 + 312	= £9505
Step (7) Market cost factor (Table 19.3(h)):		
	0.7	
Step (8) EXCHANGER SALES COST:		
	0.7 × 9505	= £6654

**Example 2**

Determine the cost of a carbon steel split backing ring floating-head exchanger, surface area (based on tube o.d.) 1066 m<sup>2</sup>, containing 1484 welded tubes, 25.4 mm o.d. × 2.77 mm thick × 31.75 mm (30°) pitch × 9 m long. Design pressures are 20 bar and 8 bar for the shell- and tube-sides, respectively. Tubes are expanded to the tubesheet. The shell diameter is 1448 mm.

Determine the cost of the same exchanger if the materials are changed to: shell = 1% Cr-½% Mo, channels = 5% Cr-½% Mo, tubesheets = type 321 stainless, floating-head flange and cover = 5% Cr-½% Mo, and tubes = type 321 stainless (welded).

*Tube count and shell diameter*

These are known and the use of Table 19.4 is not required.

*Exchanger cost (steel)*

Step (1) Basic cost (Table 19.2(b)), shell-side:		
	£37000 (20 bar)	
Step (1) Basic cost (Table 19.2(b)), tube-side:		
	£30000 (10 bar, nearest)	
Step (2) Basic cost (Table 19.2(b)), combined:		
	(0.65 × 37000) + (0.35 × 30000)	= £34550
Step (3) Cost factor for length (Table 19.3(a)):		
	£860/m (20 bar)	
Step (3) Extra cost for length:		
	860 × 9	= £7740
Step (4) Tube cost (Table 19.3(b)):		
	(17.2 × 0.77)(welded)	= £13.244/m <sup>2</sup>

Step (5) Extra cost of tubes:	$13.244 \times 1066$	= £14118
EXCHANGER COST WITH EXPANDED TUBES: = £56408		
<i>Extra cost for non-steel components (Steps (9) and (10))</i>		
'Fixed' shell-side (Table 19.3(d)):	0.128 (estimated for 20 bar)	
Relative material cost (Table 19.3(f)):	1.71 (1% Cr- $\frac{1}{2}$ % Mo)	
Extra cost:	$0.128 \times 37000 \times (1.71 - 1)$	= £3363
'Fixed' channel (Table 19.3(d)):	0.1 (estimated for 8 bar)	
Relative material cost (Table 19.3(f)):	2.2 (5% Cr- $\frac{1}{2}$ % Mo)	
Extra cost:	$0.1 \times 30000 \times (2.2 - 1)$	= £3600
Tubesheets:	0.049 (estimated for 20 bar)	
Relative material cost (Table 19.3(f)):	4.89 (type 321 stainless)	
Extra cost:	$0.049 \times 37000 \times (4.89 - 1)$	= £7053
Floating-head flange and cover (Table 19.3(d)):	0.045 {est. for $(20 + 8)/2 = 14$ bar}	
Relative material cost (Table 19.3(f)):	2.2 (5% Cr- $\frac{1}{2}$ % Mo)	
Extra cost:	$0.045 \times 33500 \times (2.2 - 1)$	= £1809
Step (11) 'Variable' shell-side (Table 19.3(e)):	0.315 (est. for 20 bar)	
Relative material cost (Table 19.3(f)):	1.71 (1% Cr- $\frac{1}{2}$ % Mo)	
Extra cost ( $C_L$ from step (3)):	$0.315 \times 7740 \times (1.71 - 1)$	= £1731
Step (12) Tubes - relative material cost (Table 19.3(f)):	2.72 (type 321 stainless)	
Step (13) Extra cost ( $C_s$ from step (4)):	$1066 \times 17.2 \times (2.72 - 0.77)$	= £35754
Steps (14) and (15) TOTAL EXCHANGER COST (no tube-end welding):	£109718	



Step (16) Market cost factor (Table 19.3(h)):

1.0

Step (17) EXCHANGER SALES COST:

$1 \times 109718 = \text{£}109718$

#### 19.3.4 Analysis of costs

The cost of carbon steel shell-and-tube exchangers falls approximately in the range  $\text{£}40\text{--}\text{£}300/\text{m}^2$ , and the cost/ $\text{m}^2$  varies with every design parameter. For a shell-and-tube exchanger of given type, design pressure, tube configuration and material, the cost/ $\text{m}^2$  varies considerably with surface area and the length. For the various tube configurations, which form the basis of the tube count tables (A3.1–A3.3), the variation in cost/ $\text{m}^2$  is much less.

To illustrate the effect of tube length, design pressure, and exchanger type on cost, a split backing ring floating-head exchanger, having a tube length of 6.1 m and design pressures of 20 bar on both sides, has been used to produce the cost ratios below, based on a *fixed* surface area of  $310 \text{ m}^2$ . In particular, the cost ratios emphasise that for economy the tube length should be as long as space and process constraints permit. The longer the tube length, the smaller becomes the shell diameter, with a subsequent reduction in tube-end joints and component thicknesses.

If another basis had been adopted, the cost ratios would have been different, although similar trends would have been shown.

*Effect of tube length (surface =  $310 \text{ m}^2$ )*

Tube length (m):	9.1	6.1	4.1	2.4
Cost ratio:	0.88	1.00	1.17	1.59

*Effect of design pressure (surface =  $310 \text{ m}^2$ )*

Design pressure (bars):	10	20	30	40	50	(both sides)
Cost ratio:	0.92	1.00	1.09	1.22	1.42	

*Comparison between shell-and-tube exchanger types (surface =  $310 \text{ m}^2$ )*

	Split backing ring floating-head	Fixed tubesheet	U-tube	Pull-through floating-head
cost ratio:	1.00	0.87	0.86	1.04

### 19.4 Double-pipe heat exchangers

Double-pipe heat exchangers are described in Section 5.1 and Chapter 15.

Heat transfer coefficients for plain-tube double-pipe heat exchangers are similar to those for shell-and-tube heat exchangers and may be determined directly from Table 19.1. Overall heat transfer coefficients for finned-tube double-pipe heat exchangers are given in Table 19.5. Costs per unit surface area for both plain- and finned-tube double-pipe exchangers are given in Table 19.6, and standard dimensions in Tables 19.7 and 19.8.

**Table 19.5** Finned-tube double-pipe heat exchangers. Typical overall heat transfer coefficients ( $W/m^2 K$ ) based on total external surface of longitudinally finned tube<sup>(1)</sup>

Cold side fluid	Hot side fluid							
	Gas at 1 bar abs.	Gas at 20 bar abs.	'Light' organic liquid <sup>(2)</sup>	'Heavy' organic liquid <sup>(3)</sup>	Process water	Condensing steam	Condensing 'light' organics <sup>(2)</sup>	Condensing 'light' organics + inerts <sup>(2)</sup>
Gas at 1 bar abs.	21	56	68	23	77	90	69	42
Gas at 20 bar abs.	56	97	136	70	181	301	153	91
"Light" organic liquid <sup>(2)</sup>	68	136	153	81	199	375	168	125
"Heavy" organic liquid <sup>(3)</sup>	25	68	91	25	105	134	94	51
Treated cooling water	87	239	295	108	326	534	307	205
Boiling water	84	216	170	19	284	511	267	187
Boiling organic liquid <sup>(2)</sup>	68	136	153	81	199	375	168	125

**Notes:**  
 (1) Fluid having lower film coefficient in shell-side.  
 (2) Liquid viscosity < 5 cP.  
 (3) Liquid viscosity > 50 cP.  
 Courtesy: Institution of Chemical Engineers (1982)

**Table 19.6** Carbon steel double-pipe heat exchangers – approximate cost per unit area

Plain tubes		Longitudinally finned tubes					
Surface area (m <sup>2</sup> )	Cost (£/m <sup>2</sup> )	Multi-tubular (10 and 12 in dia. shells)		Multi-tubular (4, 6 and 8 in dia. shells)		Single tube	
		Surface area (m <sup>2</sup> )	Cost (£/m <sup>2</sup> )	Surface area (m <sup>2</sup> )	Cost (£/m <sup>2</sup> )	Surface area (m <sup>2</sup> )	Cost (£/m <sup>2</sup> )
>40	130	>1000	40	5–30	80	3–8	120
3–40	175	250–1000	45				
<3	650	30–250	50				

## Cost multiplier for stainless steel

Outer pipe dia. (in)	Plain		Finned		Outer pipe dia. (in)	Plain		Finned	
	Plain	Finned	Plain	Finned		Plain	Finned		
3	2.10	1.97	10	1.74	2.61				
4	2.05	2.07	12	1.67	2.70				
6	1.89	2.30	14	1.63	2.70				
8	1.77	2.50	16	1.57	2.70				

Surface of finned tube units based on total external surface  
Adapted from Institution of Chemical Engineers (1982)

**Table 19.7** 1/1 Double-pipe units – dimensions

Shell	Thickness		Actual o.d.	Max. no of fins	Tube o.d.	Standard		High pressure			
	Nom. dia. (in)	Stand-ard				Tube thk	Fin height	Surface (m <sup>2</sup> /m)	Tube thk	Fin height	Surface (m <sup>2</sup> /m)
2	3.91	5.54	60.3	20	25.4	2.77	11.1	1.05	2.77	9.5	0.92
3	5.49	–	88.9	20	25.4	2.77	23.8	2.07	–	–	–
3	5.49	7.62	88.9	36	48.3	3.68	12.7	2.13	5.08	11.1	1.90
3½	5.74	8.08	101.6	36	48.3	3.68	19.05	3.05	5.08	15.9	2.59
3½	5.74	8.08	101.6	40	60.3	3.91	12.7	2.41	5.54	11.1	2.16
4	6.02	8.56	114.3	36	48.3	3.68	25.4	3.96	5.08	22.2	3.50
4	6.02	8.56	114.3	40	60.3	3.91	19.05	3.43	5.54	15.9	2.92
4	6.02	8.56	114.3	48	73.0	5.16	12.7	2.90	7.01	9.5	2.29

**Notes:**

- (1) Shell thickness = schedule 40 (standard), schedule 80 (high pressure).
- (2) Surface specified for two legs.
- (3) All dimensions in mm except where stated.

Courtesy: Filtration & Transfer Ltd.

It will be found that the fixed tubesheet shell-and-tube exchanger is cheaper once the surface area exceeds about 33 m<sup>2</sup>, while the floating-head type will be cheaper once the surface area exceeds about 40 m<sup>2</sup>. The comparison with finned double-pipe exchangers is influenced by the heat transfer coefficients, but a finned-tube double-pipe exchanger should be considered when its surface area is less than 100 m<sup>2</sup>.

Table 19.8 Multi-tube double-pipe units – dimensions

Shell				Standard				High pressure				
Thickness												
Nom. dia. (in)	Standard	High press.	Actual o.d.	No. tubes	No. fins	Tube o.d.	Tube thk.	Fin height	Surface (m <sup>2</sup> /m)	Tube thk.	Fin height	Surface (m <sup>2</sup> /m)
4	6.02	8.56	114.3	7	0	19.02	2.11	0	0.84	2.11	0	0.84
4	6.02	8.56	114.3	7	0	22.2	2.11	0	0.98	2.11	0	0.98
4	6.02	8.56	114.3	7	0	25.4	3.4	0	1.12	–	–	–
4	6.02	8.56	114.3	7	16	19.02	2.11	5.33	3.23	2.11	5.33	3.23
4	6.02	8.56	114.3	7	20	22.2	2.11	5.33	3.97	–	–	–
6	7.11	–	168.3	19	16	19.02	2.11	5.33	8.76	–	–	–
6	7.11	–	168.3	14	16	19.02	2.11	5.33	6.46	–	–	–
6	7.11	–	168.3	7	20	25.4	2.77	12.7	8.23	–	–	–
8	8.18	–	219.1	19	16	19.02	2.11	8.64	12.78	–	–	–
8	8.18	–	219.1	19	20	22.2	2.11	7.11	13.46	–	–	–
8	8.18	–	219.1	19	20	25.4	2.77	5.33	11.14	–	–	–
8	8.18	12.7	219.1	19	16	19.02	2.11	7.11	10.92	2.11	7.11	10.92
8	8.18	–	219.1	19	20	22.2	2.11	5.33	10.76	–	–	–

**Notes:**

(1) Shell thickness = schedule 40 (standard), schedule 80 (high pressure).

(2) Surface specified for two legs.

(3) All dimensions in mm except where stated.

Courtesy: Filtration and Transfer Ltd.

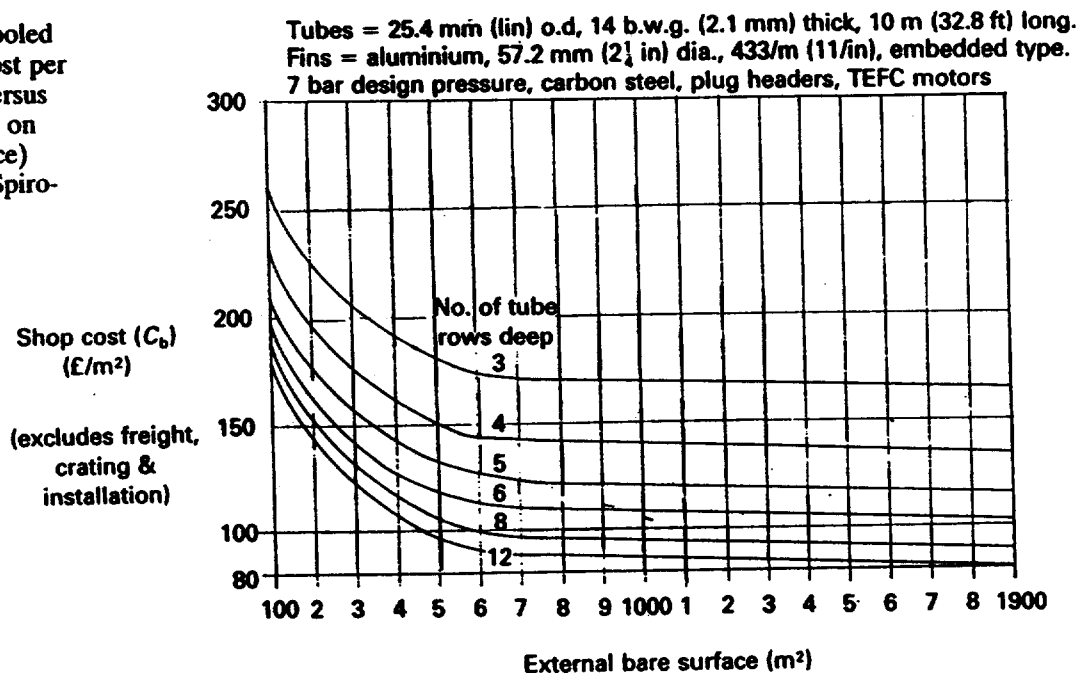
As an example, consider an oil cooler in which 2.6 kg/s of high viscosity oil at 28 bar is to be cooled from 70 °C to 35 °C, using 3.18 kg/s of cooling water entering at 20 °C and leaving at 35 °C. The specific heat of the oil is 2.2 kJ/kg K giving a heat load of 200 kW. As the operating pressure is 28 bar the plate-type exchangers cannot be considered and a comparison will be made between a shell-and-tube exchanger (one shell pass, two or more tube-side passes) and a double-pipe exchanger (countercurrent flow). The log MTD is 23.6 °C and the correction factor for the shell-and-tube exchanger is 0.8.

*Double pipe*

Exchanger type	Shell and tube	Plain	Finned
Effective $\Delta T$ (°C)	$0.8 \times 23.6 = 18.9$	23.6	23.6
$Q/\Delta T$ (W/K)	10582	8475	8475
$U$ (W/m <sup>2</sup> K)	142	142	108
Reference	(Table 19.1)	(Table 19.1)	(Table 19.5)
$A$ (m <sup>2</sup> )	74.5	59.7	78.5
Cost/m <sup>2</sup> (£)	89.3	130	50
Reference	(example 1)	(Table 19.6)	(Table 19.6)
Cost (£)	6654	7761	3925

The finned-tube double-pipe exchanger is only 59% of the shell-and-tube exchanger cost and it remains competitive up to a 2.5-fold capacity increase for this particular example. As the film coefficient for the oil is low in relation to that of the cooling water, the duty is unsuitable for a plain-tube double-pipe exchanger.

**Figure 19.1** Air-cooled heat exchangers: cost per unit surface area versus surface area (based on external bare surface) (courtesy of APV Spiro-Gills Ltd)



**Table 19.9** Air-cooled heat exchangers. Typical overall heat transfer coefficients ( $W/m^2 K$ )

Liquid cooling service		Gas cooling service			Condensing service		
		Gas	Press. (bar g.)	$\Delta P$ (bar)			
Engine jacket water	735–880				Amine reactivator	565–680	
Fuel oil	110–170				Ammonia	600–710	
Hydroformer liquids	450–510	Air or	3.5	0.07	45–70	Refrigerant 12	425–510
Platformer liquids	450–510	flue	7	0.14	90–135	Heavy naptha	400–510
Light gas oil	400–510		7	0.35	155–185	Light gasoline	510–565
Light hydrocarbons	510–680					Light hydrocarbons	540–600
Light naptha	480–540	Hydro-	1–3.5	0.07	170–225	Light naptha	450–565
Process water	680–820	carbon	3.5–17	0.21	280–340	Reactor effluents	450–565
Residium	55–110		17–103	0.35	400–510	Steam	765–1150
Tar	30–55	Ammonia reactor			510–625	(up to 1.4 bar g.)	
						Still overheads – light	
						napthas, steam and non-	
						cond. gas	425–510

Courtesy: APV Spiro-Gills Ltd.

### 19.5 Air-cooled heat exchangers

Air-cooled heat exchangers are described in Chapters 3 and 14. Figure 19.1 provides the cost per unit surface area of carbon steel air-cooled heat exchangers having an external bare surface area of 100–1900  $m^2$ , for 3, 4, 5, 6, 8 and 12 tube rows deep. The cost per unit surface area in each case becomes almost constant above a surface area of about 800  $m^2$ , and is greatly influenced by the number of tube rows. For instance, above 800  $m^2$  surface, the cost per unit surface area for three rows is about double that for twelve rows. It will be found that the cost per unit surface area of air-cooled heat exchangers is greater than that for shell-and-tube heat exchangers.

**Table 19.10** Air-cooled heat exchangers. Cost multipliers (applicable to Fig. 19.1)

Cooler type	Type	Multiplier ( $f_1$ )		
		Forced draught	1.00	
	Induced draught	0.97 (top drive)		
Length	Tube length (m)	Multiplier ( $f_2$ )		
	7.5	1.13		
	10.0	1.00		
	12.5	0.92		
	15.0	0.89		
Pressure and header type	Pressure (bar)	Multiplier ( $f_3$ )		
		Plug	Welded bonnet	Bolted cover or bonnet
	7	1.00	0.99	1.05
	20	1.01	1.00	1.08
	40	1.03	1.02	1.14
	60	1.05	1.03	—
	80	1.08	1.05	—
	100	1.12	1.09	—
Finned-tube type	Fins	Multiplier ( $f_4$ )		
	Footed L shape	0.97		
	Embedded	1.00		
	Integral	1.15		
Base tube material	Metal	Multiplier ( $f_5$ )		
	Carbon steel	1.00 (2.1 mm thick)		
	Admiralty	1.18 (1.65 mm thick)		
	Type 304 stainless	1.26 (1.65 mm thick)		

**Notes:**

- (1) Obtain basic cost ( $C_b$ ) from Fig. 17.1.
- (2) Final shop cost =  $(C_b)(f_1)(f_2)(f_3)(f_4)(f_5)$

Table 19.9 provides typical overall heat transfer coefficients for air-cooled heat exchangers. These are lower than those achieved in shell-and-tube heat exchangers, using water as coolant, for the same duty. However the comparison of cost and coefficients between air-cooled and shell-and-tube heat exchangers is of little practical interest. As discussed in Chapters 3 and 14, the comparison must be made between the overall running costs of the complete air and water systems.

Table 19.10 provides cost multipliers for various air-cooler design parameters. The procedure described in section 19.2 for the estimation of surface area is applicable to air-cooled exchangers. However, the exit air temperature must be known in order that  $\Delta T_{lm}$  may be calculated, but this is rarely the case because the designer is seeking a value which will lead to the optimum unit having the lowest overall running cost. For an exact design the optimum unit would be found by trial and error, but for

initial size and cost estimation the procedure given below, based on Brown (1978) and Glass (1978), is adequate.

Step (1) Calculate the heat load,  $Q$  (W).

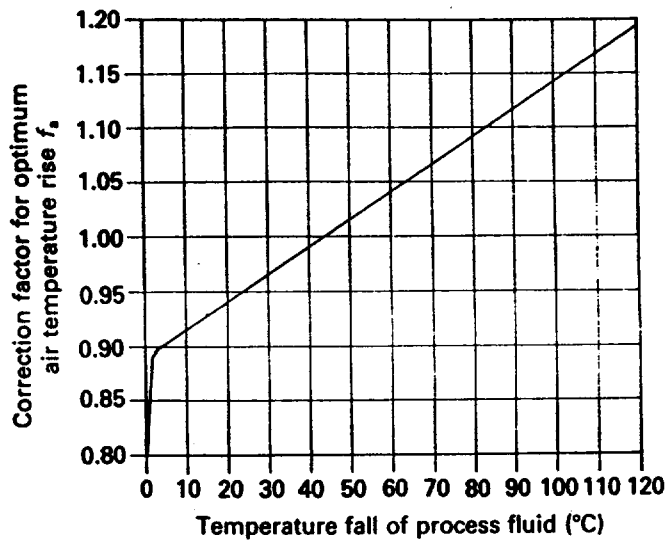
Step (2) Estimate the overall heat transfer coefficient ( $U$ ) from Table 19.9 or experience.

Step (3) Calculate the exit air temperature from the equation

$$(t_2 - t_1) = 0.00088U \left[ \frac{(T_2 + T_1)}{2} - t_1 \right] (f_a) \quad [19.5]$$

where  $t_1$  and  $t_2$  = inlet and exit air temperatures, respectively (°C);  $T_1$  and  $T_2$  = inlet and exit process fluid temperatures, respectively (°C);  $U$  = overall heat transfer coefficient, referred to external surface of bare tube (W/m<sup>2</sup> K); and  $f_a$  = correction factor for estimated air temperature rise obtained from Fig. 19.2.

**Figure 19.2** Air coolers – correction factor for estimated air temperature rise (adapted by special permission from *Chemical Engineering*, 27 March, 1978, © 1978 by McGraw-Hill, Inc., New York, NY 10020)



Step (4) Having obtained the exit air temperature, the four terminal temperatures are known. Calculate the effective temperature difference,  $\Delta T$ (°C) as described in Chapter 14. In many cases the log MTD will suffice, as described in Chapter 7.

Step (5) Calculate the duty ( $Q/\Delta T$ )(W/K).

**Table 19.11** Air-cooled heat exchangers. Approximate number of tube rows

Overall heat transfer coefficient (W/m <sup>2</sup> K)	Temperature fall of process fluid (°C)				
	Under 10	10–50	50–100	100–150	Over 150
over 350	3	4	4	5	6
225–350	3	4	5	5	6
175–225	4	4	5	6	8
Under 175	4	5	6	8	8

Based on Brown (1978)

**Table 19.12** Air-cooled heat exchangers. Approximate bare tube external surface area (m<sup>2</sup>) versus bundle size<sup>(1)</sup>

Nominal bundle width		Tube length		Number of tube rows deep <sup>(2)</sup>				No. of fans per bundle
m	ft	m	ft	3	4	5	6	
1.22	4	1.22	4	5.2	6.8	8.6	10.2	1
		1.83	6	7.7	10.2	12.8	15.3	1
		2.44	8	10.3	13.6	17.1	20.4	2
		3.05	10	12.9	17.0	21.4	25.5	2
		No. of tubes in bundle		53	70	88	105	
1.83	6	1.83	6	11.7	15.5	19.4	23.2	1
		2.44	8	15.6	20.6	25.9	30.9	1
		3.05	10	19.5	25.8	32.4	38.7	1
		3.66	12	23.3	30.9	38.8	46.4	2
		4.88	16	31.1	41.3	51.8	61.9	2
		No. of tubes in bundle		80	106	133	159	
2.44	8	2.44	8	22.0	29.2	36.6	43.8	1
		3.05	10	27.5	36.5	45.7	54.7	1
		3.66	12	33.0	43.8	54.9	65.7	1
		4.88	16	44.0	58.4	73.2	87.6	2
		6.10	20	55.0	73.0	91.5	109.5	2
		7.32	24	66.0	87.6	109.7	131.3	2
		No. of tubes in bundle		113	150	188	225	
3.05	10	3.05	10	34.8	46.2	57.9	69.3	1
		3.66	12	41.7	55.5	69.5	83.2	1
		4.88	16	55.6	73.9	92.6	110.9	1
		6.10	20	69.5	92.4	115.8	138.6	2
		7.32	24	83.4	110.9	138.9	166.4	2
		9.75	32	111.3	147.9	185.2	221.8	2
		No. of tubes in bundle		143	190	238	285	
3.66	12	3.66	12	49.6	66.0	82.6	98.9	1
		4.88	16	66.2	87.9	110.1	131.9	1
		6.10	20	82.7	109.9	137.7	164.9	1
		7.32	24	99.2	131.9	165.2	197.9	2
		9.75	32	132.3	175.9	220.2	263.8	2
		12.19	40	165.4	219.9	275.3	329.8	2
		No. of tubes in bundle		170	226	283	339	
4.88	16	4.88	16	89.5	119.1	149.0	178.6	1
		6.10	20	111.9	148.9	186.3	223.3	1
		7.32	24	134.3	178.6	223.6	267.9	1
		9.75	32	179.0	238.2	298.1	357.2	2
		12.19	40	223.8	297.7	372.6	446.6	2
		No. of tubes in bundle		230	306	383	459	

**Notes:**

- (1) Bare tube = 25.4 mm (1 in) outside diameter × 60.3 mm (2 $\frac{3}{8}$  in) triangular pitch with surface area calculated as though fins do not exist.
- (2) For number of rows deep greater than 6, add together surfaces for two smaller bundles, e.g. 8 rows, use 4 + 4 rows; 9 rows, use 4 + 5 rows, etc.



Step (6) Calculate the bare tube surface area from equation [19.1]

$$A = \frac{Q/\Delta T}{U} \text{ (m}^2\text{)}$$

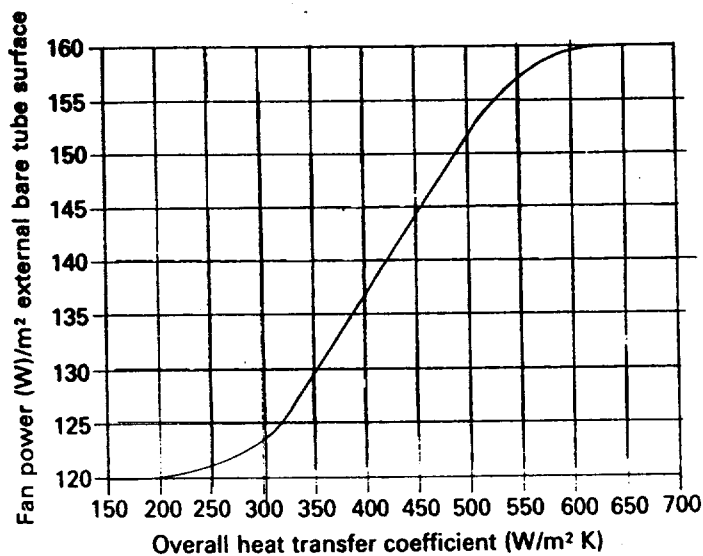
Step (7) Determine the number of rows from Table 19.11.

Step (8) Determine the air cooler size from Table 19.12.

Step (9) Determine the air cooler cost from Fig. 19.1 and Table 19.10.

Step (10) Determine the air cooler fan power requirements from Fig. 19.3.

**Figure 19.3** Air coolers – approximate fan power requirements (adapted by special permission from *Chemical Engineering*, 27 March, 1978, © 1978 by McGraw-Hill, Inc., New York, NY 10020)



### Example

A forced-draught carbon steel air-cooled exchanger, having plug-type headers designed for a pressure of 6 bar is required to cool 250 000 kg/h of process fluid from 150 °C to 100 °C with air entering at 25 °C. The specific heat is 2.093 kJ/kg.K. Fins are embedded type.

Step (1)  $Q = (250000/3600) \times 2.093 \times (150 - 100) = 7267.4 \text{ kW}$

Step (2)  $U = 325 \text{ W/m}^2 \text{ K}$  (estimated).

Step (3) From Fig. 19.2 for  $(T_1 - T_2) = 50 \text{ °C}$ ,  $f_a = 1.02$ . From equation [19.5]:

$$(t_2 - t_1) = (0.00088 \times 325) \left\{ \frac{(150 + 100)}{2} - 25 \right\} 1.02 = 29.2 \text{ °C}$$

$$t_2 = 25 + 29.2 = 54.2 \text{ °C}$$

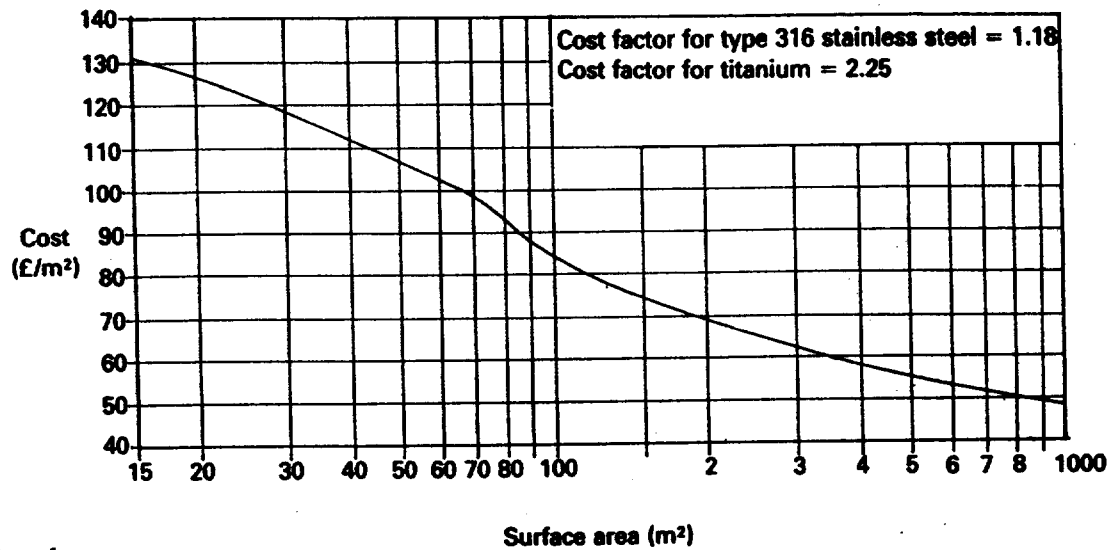
Step (4)  $\Delta T_{lm} = \log \text{ mean of } (150 - 54.2) = 95.8 \text{ and } (100 - 25) = 75$ , i.e. 85 °C.

Step (5)  $Q/\Delta T = (7267.4 \times 10^3)/85 = 85499 \text{ (W/K)}$

Step (6)  $A = 85499/325 = 263 \text{ m}^2$

Step (7) From Table 19.11; no. of rows deep = 4.

Step (8) From Table 19.12, 2 bundles, each 3.05 m wide with 9.75 m



**Figure 19.4** Gasketed-plate type heat exchangers: cost per unit surface area versus surface area for type 304 stainless steel plates (adapted from Institution of Chemical Engineers 1982)

long tubes, 4 rows deep, give a total bare surface area of  $2 \times 147.9 = 295.8 \text{ m}^2$

Step (9) From Fig. 19.1, cost = £176/m<sup>2</sup> and  $f_1 = f_2 = f_3 = f_4 = f_5 = 1.0$  i.e. basic cost =  $176 \times 295.8 = \text{£}52061$

Step (10) From Fig. 19.3, fan power = 126 W/m<sup>2</sup>, i.e. fan power =  $(126 \times 295.8)/10^3 = 37.3 \text{ kW}$

## 19.6 Gasketed-plate heat exchangers

Gasketed-plate heat exchangers are described in Chapters 4 and 16. Figure 19.4 provides the cost per unit surface area of gasketed-plate heat exchangers having type 304 stainless-steel plates and surface areas of 15–1000 m<sup>2</sup>. Cost factors for type 316 stainless steel and titanium are also given. For a surface area of 15 m<sup>2</sup>, in type 304 stainless steel, the cost is £131/m<sup>2</sup> which is almost half the cost of a carbon steel shell-and-tube heat exchanger of the same surface area. As the surface area increases, the costs become similar on a cost per unit surface area basis. However, as shown below, the true cost comparison must be made on an identical duty basis.

Table 19.13 lists typical fouling factors, and clean film and overall heat transfer coefficients for various fluids. Comparison of Table 19.13 with Table 19.1, which relates to shell-and-tube heat exchangers, shows that the gasketed-plate heat exchanger provides greater film heat transfer coefficients and requires lower fouling factors for similar fluids.

As an example consider a process water cooler in which 59.71 kg/s of process water is to be cooled from 60 °C to 20 °C using the same quantity of cooling water entering at 10 °C and leaving at 50 °C. The higher design pressure is only 20 bar and therefore shell-and-tube, double-pipe and gasketed-plate exchangers are possibilities. The large temperature cross will require countercurrent flow.

**Table 19.13** Gasketed-plate heat exchangers. Typical overall heat transfer coefficients ( $\text{W}/\text{m}^2 \text{K}$ )

Cold side	Hot side			
	'Light' organic liquid <sup>(1)</sup>	'Heavy' organic liquid <sup>(2)</sup>	Process water	Condensing low-pressure steam
'Light' organic liquid <sup>(1)</sup>	2734	322	3163	3063
'Heavy' organic liquid <sup>(2)</sup>	322	171	328	327
Treated cooling water	3457	331	4171	4000

Overall heat transfer coefficients are based on the clean film coefficients  $\alpha$  ( $\text{W}/\text{m}^2 \text{K}$ ), and fouling factors  $r_f$  ( $\text{W}/\text{m}^2 \text{K}$ )<sup>-1</sup>, given below:

Fluid	$\alpha$	$r_f \times 10^5$	Fluid	$\alpha$	$r_f \times 10^5$
'Light' organic liquid <sup>(1)</sup>	7000	2	Process water	12000	3
'Heavy' organic liquid <sup>(2)</sup>	350	4	Condensing low-pressure steam	9000	1.25
Treated cooling water	14000	1.5	Stainless-steel plates, wall resistance $\times 10^5 = 4$		

**Notes:**

(1) Viscosity &lt; 5 cP.

(2) Viscosity &gt; 50 cP.

Courtesy: Institution of Chemical Engineers (1982).

$$Q = 10,000 \text{ kW}, \quad \Delta T = 10^\circ \text{C}, \quad Q/\Delta T = 1 \times 10^6 \text{ W/K}$$

Exchanger type:	Shell and tube	Plain tube double pipe	Gasketed plate
$U$ ( $\text{W}/\text{m}^2 \text{K}$ ):	938	938	4171
Reference:	Table 19.1	Table 19.1	Table 19.13
$A$ ( $\text{m}^2$ ):	1066	1066	240
Cost/ $\text{m}^2$ (£):	52.9	130	67
Reference:	example 2	Table 19.6	Fig. 19.4
Cost (£):	56408	138580	16080

As expected, the duty was too large for the double-pipe type to be competitive and it was not a realistic exercise for it. The gasketed-plate type, with stainless-steel surfaces, was almost one quarter of the cost of the carbon steel shell-and-tube exchanger. Where the application is suitable, small gasketed-plate type exchangers with titanium plates are likely to be cheaper than carbon steel shell-and-tube exchangers.

## 19.7 Spiral and lamella heat exchangers

Spiral and lamella heat exchangers are described in sections 5.5 and 5.4 respectively. Typical overall heat transfer coefficients for various services using hot water as a heating medium are given in Table 19.14. It will be seen that coefficients for the lamella exchanger are higher by about 15–20%. Table 19.15 provides approximate costs for both types over a limited range of surface areas. A comparison between the two types for identical duties, within the surface area range specified, reveals that the lamella cost is 60–85% of the spiral cost.

When operating conditions suit a gasketed-plate type, the spiral and lamella types are not competitive with it.

## 19.8 Rotary regenerative heat exchangers

Typical ex-works costs and power consumptions of rotary regenerative heat exchangers are given in Table 19.16 for duties ( $Q/\Delta T$ ) of  $1 \times 10^3$ ,  $3 \times 10^4$  and  $1 \times 10^6$  W/K based on four rotor/heat transfer material combinations. It should be noted that installation costs, ducting and dampers are excluded, and these items may affect the total cost of the complete system appreciably.

This type of rotary regenerative heat exchanger is described in section 5.11.

**Table 19.14** Spiral and lamella heat exchangers. Typical overall heat transfer coefficients ( $W/m^2 K$ ). Hot side fluid = water

Cold side fluid	Lamella	Spiral
Gas at 1 bar abs.	275	240
Gas at 20 bar abs.	1300	1100
'Light' organic liquid <sup>(1)</sup>	1150	1000
'Heavy' organic liquid <sup>(2)</sup>	100	85
Water	3000	2500
Boiling water	3250	2700
Boiling organic liquid	1950	1700

Notes:

(1) Viscosity < 5 cP.

(2) Viscosity > 50 cP.

Courtesy: Institution of Chemical Engineers (1982).

**Table 19.15** Spiral and lamella heat exchangers. Approximate cost ( $£/m^2$ )

Spiral		Lamella	
Surface area ( $m^2$ )	Cost	Surface area ( $m^2$ )	Cost
10–75	330	3–90	290
90–125	300	100–360	215

Adapted from Institution of Chemical Engineers (1982).

**Table 19.16** Rotary regenerative heat exchangers. Ex-works cost and power consumption for various duties

Rotor material	Transfer media	Typical hot gas temp. ( $^{\circ}C$ )	Cost (£) for duty (W/K):		
			$1 \times 10^3$	$3 \times 10^4$	$1 \times 10^6$
Aluminium	Aluminium	Up to 200	$1.86 \times 10^3$	$2.4 \times 10^4$	$0.71 \times 10^6$
Steel	316 stainless	Up to 427	$2.69 \times 10^3$	$3.51 \times 10^4$	$1.03 \times 10^6$
316 stainless	316 stainless	Up to 427	$3.2 \times 10^3$	$4.2 \times 10^4$	$1.26 \times 10^6$
310 stainless	310 stainless	Up to 980	$7.11 \times 10^3$	$9.34 \times 10^4$	$2.74 \times 10^6$
Electrical power consumed by rotor (kW) 0.18				1.49	33.6

Courtesy: Institution of Chemical Engineers (1982).

## Acknowledgements

The author is grateful to the following: APV Spiro-Gills Ltd, Pulborough, West Sussex, UK, for the provision of cost data relating to air-cooled heat exchangers. Filtration & Transfer Ltd, Poole, UK, for the provision of technical data relating to double-pipe heat exchangers. Filtration & Transfer Ltd is a licensee of the Brown Fintube Co., Houston, USA. The Institution of Chemical Engineers for permission to use the cost and heat transfer data published in *User Guide on Process Integration for the Efficient Use of Energy*, 1982, Chapter 3, 'Heat transfer equipment selection'. Mr S. T. Wright, UK Division, Whessoe Heavy Engineering Ltd, Darlington, UK, for assistance with the shell-and-tube exchanger cost data.

## References

A list of addresses for the service organisations is provided on p. xvi.

- Brown, R. (1978) 'A procedure for preliminary estimates', *Chem. Eng.* (27 March), pp. 108-11.
- Glass, J. (1978) 'Specifying and Rating Fans', *Chem. Eng.* (27 March), pp. 120-4.
- Purohit, G. P. (1983) 'Estimating costs of shell-and-tube heat exchangers', *Chem. Eng.* (22 Aug.), pp. 56-67.
- Smith, R. A. (1981) 'Economic velocity in heat exchangers', *AIChE Symposium Series*, No. 208, Vol. 77, pp. 221-8.

---

# Index

- acoustic frequency – *see* acoustic vibration
- acoustic vibration, 249–50, 256–7, 264, 266
- added mass coefficient, 252
- air-cooled heat exchangers
  - air v. water-cooling, 86–7
  - API Standard 661, 88–9, 96–100, 103
  - background, 85
  - bundle framework, 96–7
  - bundle size and shape, 90
  - construction, 88–90
  - cost, 545–50
  - drivers, 99–101
  - example of air-side
    - calculations, 347–51
  - fans, 97–9, 346–7
  - forced v. induced draught, 88, 89
  - headers, 94–7
  - nomenclature, 96, 100
  - orientation of bundle, 87–8
  - plenum chamber, 97–9
  - selection criteria, 158
  - size estimation, 547–51
  - standard bundle sizes, 549
  - structure, 97–9
  - temperature control, 101–2
  - thermal design, 339–47
  - transmission, 99–100
  - tubes, 90–4
  - worked examples for thermal design, 440–7
- air test – *see* pneumatic test
- Alfa-Laval Co. Ltd, 110, 130, 156, 372
- Allegheny Ludlum alloys – *see* stainless steels
- Allegheny Ludlum Steel Corporation, 523
- Alon Processing Inc., 491, 523
- Alonizing™, 491–3
- Aluminium Association (AA), 483
- aluminium (general), 91, 135, 475, 479, 481, 484–8, 491, 493, 505, 517
  - clad steel, 491
  - in steel–aluminium alloys, 491
  - in steel manufacture, 484, 487
  - sacrificial anodes, 478
- aluminising, 491–3
- aluminium and aluminium alloys (specific)
  - 1000 group, 489
  - 3000 group, 490
  - 5000 group, 490
  - 6000 group, 490
  - 7000 group, 490
  - Alclad, 490
  - composition, 489
  - designation system, 488–9
- American Iron and Steel Institute (AISI), 483, 497
- American Petroleum Institute (API), 486, 523
  - Publication 941, 485, 486
  - Standard 660, 4
  - Standard 661, 88–9, 96–100, 103
- American Society of Mechanical Engineers (ASME), 4, 46–7, 83, 88, 103, 483, 527
- American Society for Testing and Materials (ASME), 483, 489, 494, 498–500, 507, 512, 523
- annular distributor, 33–4, 265, 269
- anode, 477–9
- antimony, 482, 495
- APV International Ltd, 104, 110, 115, 131, 156, 364, 369, 372
- APV Spiro-Gills Ltd, 103, 546, 554
- arithmetic mean temperature difference (AMTD), 191

- Armco alloys - *see* stainless steels  
 Armco Inc., 523  
 arsenic, 482, 495  
 Avesta Johnson Stainless Steel Ltd, 523
- backing ring, 9-11, 59  
 baffles, 3, 14  
   clearances, 31-2  
   cut, 30  
   double segmental, 28-30, 265, 267  
   edge orientation 30-1  
   full circle, 'holed', 266  
   impingement, 15, 33, 35, 40, 247, 265, 269  
   inlet support, 265-6  
   longitudinal, 34-7  
   maximum unsupported length, 32, 247  
   minimum spacing, 33  
   no-tubes-in-window, 30, 265, 322  
   single segmental, 28-30, 265  
   support type, 31, 41-3  
   thickness, 31  
   triple segmental, 29, 30, 265  
   window, 29, 30, 281  
 baffle cut ratio, 281, 283  
 baffle damage, 246, 255-6  
 baffle damage number, 255-6  
 baffle spacing ratio, 283  
 bank (air-cooled exchangers), 89-90  
 barrel (shell and channel)  
   fabrication, 55-6, 516-17  
 Barrington, E. A., 250, 271  
 Bavaria Anlagenbau GmbH, 129, 156  
 Bavex exchanger, 128-9, 158  
 bay (air-cooled exchangers), 89-90  
 bayonet tube exchanger, 6, 13-14  
 Bell, K. J., 275, 278, 280, 287, 291, 313, 322, 331-2, 337  
 Bergles, A. E., 232, 234, 241  
 Bergles, A. E. *et al.*, 234, 241  
 Bergman, D. J., 48, 84  
 bi-metal construction  
   barriles, 516-17  
   explosively bonded plate, 517-19  
   flanges, 516-17  
   heads, 516-17  
   nozzles, 516-17  
   roll-bonded plate, 519-21  
   tubes, 24, 515-16  
   tubesheets, 515-16  
 biological fouling, 207, 513  
 B-JAC International, 275  
 Boland, D. and Hindmarsh, E., 273  
 bolts  
   compensation devices, 48-9  
   electrical heating, 60  
   material, 48-9, 506  
   stress relaxation, 48-9  
   tensioners, 52, 60-2  
   tightening, 60-2  
 bolt extension sleeve, 48-9  
 Bond, M. P., 364, 372  
 bond resistance, 119, 221-2, 515-16  
 boron, 475, 484  
 bottom plate, 95-6  
 boundary layer, 233  
 Briggs, D. E. and Young, E. H., 179, 185  
 Briscoe, W. G., 60, 84  
 British Standards Institution (BSI), 46-7, 49  
   Code of Practice, CP3003, 1966, 521  
   BSS 5500:1985, 4, 46  
 British Steel Corporation, 520, 523  
 brittle fracture, 486-8  
 Brown Fintube, 156, 554  
 Brown, R., 341, 352, 547-8, 554  
 buffer layer, 164-5  
 bundle bypass area, 278, 281  
 bundle-in-column reboiler, 9, 15-16  
 bundle-shell clearance, 6, 38, 283  
 bypass (air-cooled exchangers)  
   at fan ring, 99  
   process fluid, 101  
   within bundle, 97
- Cabot alloys - *see* Hastelloys™ *under* nickel and high-nickel alloys;  
   Haynes™ *under* stainless steels  
 Cabot Corp., 503, 524  
 Caglayan, A. N. and Buthod, P., 201-2, 206  
 Cal Gavin Ltd, 235-6, 238, 241  
 carbon, 142, 477, 484, 497, 502, 504-6, 511  
 carbon and low-alloy steels  
   composition, 484  
   corrosion resistance, 484-5  
   hydrogen attack, 485-6  
   hydrogen service, 485-6  
   killed steel, 484, 487  
   low-temperature service, 486-8  
   'Nelson' curves, 485-6  
   rimmed steel, 484  
   semi-killed steel, 484  
 carbon monoxide, 484  
 Carnavos, T. C., 234, 241  
 Carpenter alloy - *see* stainless steels  
 Carpenter Technology corporation, 502, 523  
 castellated tube end welds, 72  
 cast iron, 482, 484  
 cathode, 477-9  
 cathodic protection, 478-9, 490  
 caustic embrittlement, 479  
 cavitation, 476

- channels, 3, 7, 10  
 bolted (A and L type), 19–20  
 bonnet (B and M type), 20–1, 56–7  
 cone (bolted), 20–1  
 high pressure, 52–3  
 modified 'C' type, 51  
 multi-head construction, 51–2  
 studded-on channel, 50–1  
 studded-on shell, 50–1  
 welded (C and N type), 20  
 characteristic length, 250, 256–7  
 charpy impact testing, 487  
 chemical reaction fouling, 207  
 Chen, Y. N., 249, 271  
 chevron plate, 106–7, 365  
 chiller, 16  
 Chisholm, D., 123, 156  
 chrome–molybdenum alloys – *see*  
 carbon and low-alloy steels  
 chromium, 475, 484, 497, 504–5, 510  
 Clark, D. F., 104, 115  
 cleaning, 6–8, 10, 13, 21, 131, 237, 267, 480  
 cleanliness factor, 210, 369, 456  
 cobalt, 475, 484, 510–11  
 co-current flow, 102, 188–90  
 coiled tube exchanger, 16–18  
 collision damage, 246, 255–6  
 collision damage number, 255–6  
 columbium – *see* niobium  
 computer programs, 47, 173, 275, 339, 460  
 concentric pipe exchanger – *see*  
 double-pipe exchangers  
 conduction, 163–5  
 Connors, H. J., 249, 254, 271  
 cooperative research  
 organisations, 173, 213, 250, 275, 342  
 copper (general), 475, 477–9, 481, 486, 489, 518–19  
 copper and copper alloys (specific)  
 admiralty brass, 495, 514  
 aluminium brass, 495  
 aluminium bronze, 496, 514, 517  
 composition, 494  
 cupro-nickels, 406, 517  
 designation system, 493, 495  
 muntz metal, 495  
 naval brass, 495, 514  
 red brass, 495  
 Copper Development Association  
 (CDA), 483, 495  
 Corning Process Systems, 147, 156  
 corrosion  
 annual cost, 475  
 crevice corrosion, 476, 480, 495, 502–5, 509  
 erosion–corrosion, 476, 481–2, 495, 505, 512  
 galvanic corrosion, 216, 476–9, 481, 514, 516  
 intergranular corrosion, 483, 502, 504–5, 508, 510, 512  
 pitting corrosion, 481, 490, 495, 502–6, 509–12  
 selective leaching, 482  
 source of data, 475–6  
 stress corrosion, 479–80, 490, 495, 501–6, 508–12  
 uniform attack, 476  
 corrosion fouling, 207  
 cost of exchangers  
 air-cooled exchangers, 545–8, 550  
 double-pipe exchangers, 542, 544–5  
 gasketed-plate exchangers, 551–2  
 lamella exchangers, 552–3  
 rotary regenerative exchangers, 553  
 shell and tube exchangers, 527, 530–42  
 spiral exchangers, 552–3  
 countercurrent flow, 117, 127–8, 138, 188–90  
 cross-flow, 138–9, 194, 196–7, 343–5  
 cross-flow area, 252–3, 281–2, 284–6, 328, 332–3  
 cross-flow velocity, 252–3  
 damping, 249, 252, 255  
 Dean, Dr D. S., 322  
 decarburisation, 485  
 design codes, 4, 46, 88, 483, 527  
 design margin, 382–3  
 Detaclad™, 517  
 detuning plates, 257, 266  
 Devore, A., 278, 322  
 dezincification, 482, 495  
 differential expansion, 8, 9, 14, 54, 118, 126  
 dimensionless numbers, 165, 166  
 dirt – *see* fouling  
 dished ends – *see* heads (dished)  
 divided flow (J shell), 41–2, 200, 265–6, 320  
 Dodd, Dr R., 196, 205, 206  
 Donohue, D. A., 278, 322  
 double-bundle exchanger, 16, 17  
 double-ended kettle reboiler, 16, 17  
 double-pipe exchangers  
 application, 117  
 construction, 118–19  
 cost, 542, 544–5  
 example of annulus calculations, 358–61  
 nomenclature, 120–2  
 selection criteria, 158, 218, 375  
 size estimation, 542–5



- standard units, 120-2, 544-5
- thermal design, 354-8
- tubes, 119-21, 544-5
- worked example for thermal design, 445, 448-54
- double-split flow (H shell), 41-4, 320
- double tubesheets, 17-19, 64
- dry cell, 477
- dry pipe, 15
- Du Pont International, 147, 149-50, 156, 517
- E shell**, 41, 265, 320
- Ecolaire Heat Transfer Co., 269-70
- Edwards, D. F. *et al.*, 113, 115
- electrically-heated exchangers
  - advantages, 152
  - construction, 153
  - control, 155-6
  - selection criteria, 159, 216
  - sheath material, 153
  - types, 153-6
- Eltron (London) Ltd, 155, 156
- embossed panel exchangers
  - application, 140
  - construction, 141
  - installation, 141
  - materials, 141
  - selection criteria, 159
  - standard units, 141
- embrittlement (475 °C) (885 °F), 503-4
- Engineering Sciences Data Unit (ESDU), 156, 175, 178, 185, 203, 206, 234, 236, 241, 244
- epoxy resin, 521
- equivalent diameter
  - axial cores, 240-1, 244
  - double-pipe exchanger annulus, 354-5
  - gasketed-plate exchanger, 366
  - low-fin tubes, 329-30
  - uniform channels, 178
- Erskine, J. B. and Waddington, W., 256, 265, 271
- Euler Number, 166
- expander torque, 67-9
- expansion grooves, 67-8, 75, 516
- expansion joints, 8, 28-9, 54, 64-6, 510
- explosively bonded plate, 517-19
- Extended surfaces
  - factors affecting fin efficiency, 220-2
  - fin efficiency calculations, 223-7
  - geometrical factors, 223-5
  - overall heat transfer coefficient, 226
  - pressure loss calculations, 227
  - space saving, 227-8
- surface temperature, 228-30
- types, 220-1
- F correction factor**
  - application to design, 197-201, 279
  - cross-flow exchangers, 196-7, 345
  - definition, 192
  - divided flow shells, 200
  - double-pipe exchangers, 356
  - examples, 198-9
  - gasketed-plate exchangers, 368
  - shell-and-tube exchangers, 195-202, 279
  - split-flow shells, 200
- F curves**
  - cross-flow exchangers, 194
  - double-pipe exchangers, 357
  - gasketed-plate exchangers, 369
  - shell-and-tube exchangers, 194
- F shell (two-pass)**, 34-7, 320-1
- Fanning equation, 176, 367
- fans**
  - blade material, 99
  - laws, 347
  - noise, 99, 347
  - power consumption, 346-7
  - pressure loss, 346
  - ring, 97-9
  - tip speed, 99
  - variable pitch, 99-102
- fatigue, 246
- feed/effluent exchangers, 127
- fillet tube-end welds, 72
- Filtration & Transfer Ltd, 121, 156, 544-5, 554
- finned tubes (refer to specific types)
- fins**
  - bond resistance, 91, 119, 221-2
  - efficiency, 220-7
  - equivalent fin height, 225
  - equivalent fin thickness, 225
  - heat transfer, 221-7
  - height, 221-2
  - surface temperature, 228-30
  - thermal conductivity, 221-2
  - thickness, 221-2
- Fitz-Hugh, J. S., 249, 271
- fixed tubesheet exchanger, 3, 6-8, 54
- flanges**
  - clad, 59, 516-17
  - floating-head cover, 9-11, 59-60
  - lap type, 59
  - manway, 52-3
  - nozzles, 57-8
  - ring type, 59
  - split backing ring, 9-11, 59
  - systems, 48-9
  - TEMA designation, 5
  - weld neck type, 59
- flexible strips, 35-6
- floating-head exchangers

- externally sealed (type W), 6, 11–12
- outside packed (type P), 6, 12–13
- pull-through (type T), 6, 10–11
- split backing ring (type S), 69–10
- flow-induced vibration – *see* vibration, flow-induced
- fluid-elastic whirling, 247, 249, 254–5
- fluid flow pattern (adjacent to surface), 164–5
- Fontana, M. G., 476, 524
- Foote M. R., 368, 372
- forced convection, 163–4
- forged long weld neck (nozzles), 57–8
- fouling, 114, 166–8
  - cost, 209
  - definition, 207, 213
  - design considerations, 209–13
  - design to minimise fouling, 216–18
  - fouling factors, 210–13, 528, 552
  - growth, 328
  - heat transfer calculations, 210–12
  - low-fin tubes, 328
  - mechanisms, 207
  - pressure-loss calculations, 212–13
  - source of fouling factors, 211
  - ratio of fouled: clean pressure loss, 214–15, 459
  - research, 213–15
  - resistance versus time, 208
- Fraaz, A. P. and Ozisik, M. N., 278, 322
- free area ratio, 223
- free convection, 163, 454
- freezing fouling, 207
- frequency constant, 251–2
- friction factor
  - double-pipe annulus, 357–8
  - gasketed-plate exchanger channels, 368
  - Heatex™ tube inserts, 238
  - inside tubes, 177–8
  - internal fins (low height), 234
  - outside high-finned tubes, 183
  - outside low-fin tubes, 183
  - outside plain banks, 179–81
  - twisted tape insert, 235
- G shell (split flow), 41, 43–4, 200, 320
- Gackenback, R. E., 483, 524
- galvanic series, 477–8
- Gambill, W. R., 381, 459
- Gardner, K. and Taborek, J., 201, 206
- gaskets, 108, 109, 111
- gasketed-plate exchangers, 111, 115
- graphite exchangers, 145
- lamella exchangers, 131
- shell-and-tube exchangers, 61–3
- gasketed-plate exchangers
  - application, 115
  - background, 104–5
  - connector plates, 111
  - construction, 105–111
  - cost, 551–2
  - features, 113–15
  - flow arrangements, 105, 111–13
  - flow distribution, 113
  - frame, 108–9
  - gaskets, 108, 109, 111
  - inspection and maintenance, 111
  - number of plates, 106, 112
  - passes, 111
  - plate corrugation, 106–7
  - plate metals, 105–6, 514
  - plate sizes, 105–6
  - plate thermal conductivities, 105–6
  - ports, 109–10
  - selection criteria, 158, 214, 217
  - thermal appraisal, 364–71
  - tie bolts, 108, 110
  - worked example for thermal design (check), 454–7
- gasketless plate exchanges, 126–8, 150
- Gentry, C. C. *et al.*, 267, 271
- Gianolo, E. and Cuti, F., 179, 185
- Gilmour, C. H., 217, 278, 322
- Glass J., 347, 352, 547, 554
- glass exchangers
  - borosilicate glass, 146
  - construction, 146–7
  - selection criteria, 159, 216
  - standard units, 147
- Govind, R., 273
- Graetz Number, 166, 175–6, 416, 454
- graphite exchanger
  - cartridge type, 146
  - cubic type, 144–5
  - multi-block type, 145–6
  - properties of impregnated graphite, 142–3
  - rectangular type, 144–5
  - selection criteria, 158, 216, 375
  - shell-and-tube type, 143
- graphitisation, 482
- Grashof Number, 166, 415–17
- Gray, R. M., 115, 116
- Grondslagen, 47
- groove and fillet tube-end welds, 72
- Guy, A. R., 354, 357, 358, 361
- H shell (double-split flow), 41, 43–4, 200, 320
- 'hairpin' exchanger – *see* double-pipe exchangers
- halogen testing, 74

- Hammond, R. H., 115, 116  
 Hampson coil exchanger - *see* coiled tube exchanger  
 Harris, D., 47, 84  
 Haskel Energy Systems Ltd., 67, 70, 83  
 Hastelloys™ - *see under* nickel and high-nickel alloys  
 Haynes™ alloy - *see under* stainless steels  
 headers (air-cooled exchangers), 94-5  
   removable cover plate, 95-6  
   removable bonnet, 95  
   plug, 95-6  
   mainfold, 95-6  
 headers (shell-and-tube exchangers) - *see* channels  
 heads (dished)  
   crown and petal, 57  
   hemispherical, 56-7  
   Korboggen, 56  
   semi-ellipsoidal, 56-7  
   torispherical, 56-7  
 heat-affected zone (HAZ), 487, 504, 511, 513  
 heat capacity ratio, 192  
*Heat Exchanger Design Handbook (HEDH)*, 49, 65, 84, 156, 249, 271, 337, 352, 361, 471  
 Heat Exchanger Institute (HEI), 4  
 Heat Exchanger Network Synthesis (HENS), 273-4  
 Heatex™ tube inserts, 235-9  
 heat-flow mechanisms, 163-5  
 heat pipes  
   application, 125-6  
   background, 122  
   container, 124  
   principle of operation, 123  
   selection criteria, 158  
   types, 123-4  
   wicks, 124-5  
   working fluid, 124  
 heat transfer augmentation - *see* internal heat transfer augmentation techniques  
 heat transfer coefficient  
   air across finned-tube bundles, 351  
   air-cooled exchangers (typical), 546  
   controlling, 168-9  
   determination, 165  
   double-pipe exchangers (typical), 362, 543  
   'film', 164-5  
   gasketed-plate exchangers (typical), 552  
   lamella exchangers (typical), 553  
   Nusselt Number relationship, 174  
   overall, 165-8  
   shell-and-tube exchangers (typical), 528  
   spiral exchangers (typical), 553  
   Stanton Number relationship, 174  
   surface temperature, 169-72  
   viscosity correction factor, 169-73  
   water inside tubes, 380  
 heat transfer correlations, 174-5  
   axial cores, 240-1  
   double-pipe annulus, 354-6  
   gasketed-plate exchangers, 367  
   Heatex™ tube inserts, 237-8  
   inside tubes, 175-6  
   inside uniform channels, 178  
   internal fins, 234  
   outside high-finned tubes, 179  
   outside low-fin tubes, 183  
   outside plain banks, 178, 180-2  
   twisted tape insert, 235  
 heat transfer enhancement - *see* internal heat transfer augmentation techniques  
 Heat Transfer and Fluid Flow Service (HTFS), 173, 250, 275, 364, 374, 382-3  
 heat transfer intensification - *see* internal heat transfer augmentation techniques  
 Heat Transfer Research Inc. (HTRI), 173, 215, 250, 275, 278, 364-5, 374, 382-3, 458-9  
 Heat Transfer Society (UK), 75  
 helium testing, 81, 83, 136  
 herringbone corrugations (plate-fin exchangers), 136-7  
 herringbone plate - *see* chevron plate  
 Hewitt, G. F., 214, 218  
 high-finned tubes  
   application, 25  
   block fin, 92-3  
   dimensions, 90-1, 94  
   embedded fin, 92-3  
   fin profiles, 221  
   footed L-shaped fin, 92  
   integral fin, 25, 92-3  
   knurled base tube, 92  
   materials, 91, 94  
   overlapped footed L-shaped fin, 92  
   plate fin, 92-3  
   temperature limits, 91  
   welded fin, 92-3  
 high-pressure closures  
   Delta ring, 54  
   double coe, 54  
   Grayloc™, 54  
   shear ring, 53-4  
   welded diaphragm, 52-4  
 Hitachi Ltd, 67, 71, 83  
 Hobart Bros., 73-4, 83

- Hydra-Tight Ltd, 62, 83  
 hydraulic expansion, 70-1  
   Hydroswaging™, 67, 70  
 hydraulic testing, 80-3, 136, 487, 501  
 hydrogen, 485-6, 513  
 hydrogen attack, 485-6  
 hydrogen-induced cracking (HIC), 523  
 hydrogen service, 485-6  
 Hydroswaging™ - *see* hydraulic expansion  
 Incoloys™ - *see* nickel and high-nickel alloys  
 Inconels™ - *see* nickel and high-nickel alloys  
 Imperial Metals Industries, 524  
 impingement attack, 33, 476, 495-6, 512  
 impingement protection criteria, 35  
 instability constant, 254-5  
 Institution of Chemical Engineers, 528, 543-4, 552-4  
 intermating plate - *see* 'washboard' plate  
 internal heat transfer augmentation techniques, 233-44  
   additional subject references, 242-4  
   axial cores, 240-1  
   background, 232  
   coiled wire inserts, 232-3, 235  
   effect on boundary layer, 233  
   electrostatic fields, 239  
   evaluation of techniques, 233  
   gas-solid suspensions, 239  
   Heatex™ tube inserts, 235-9  
   injection/suction, 240  
   internal fins, 234  
   internal scraping, 239  
   roughened surfaces, 234  
   surface rotation, 234  
   twisted tape insert, 235  
   vibration (of surface), 239  
 inter-row velocity, 252-3  
 inter-tube velocity, 252-3  
 Invar™, 488  
 IPC Industrial Press Ltd, 475, 524  
 iron, 475, 484, 493, 406, 508-11  
 J shell (divided flow), 41-2, 200, 265-6, 320  
 $J_h$  factor, 174  
 $j$  factor, 174  
 jacketed pipe exchanger - *see* double-pipe exchanger  
 jacketed U-tube exchanger - *see* double-pipe exchanger  
 Jameson, S. L., 179, 185  
 Kelomet™, 517  
 Kern, D. Q., 167, 190-1, 206, 240, 244, 278, 322  
 Kern, D. Q. and Kraus, A. D., 232, 225, 230  
 kettle reboiler, 15-17  
 killed steel, 484, 487  
 Kirby, G. N., 475, 524  
 Kumar, H., 364, 367-8, 372  
 Lamella exchangers  
   application, 128  
   construction, 129-30  
   cost, 552-3  
   material, 131  
   selection criteria, 158  
   standard units, 130-1  
 laminar flow, 163-4, 286, 328  
 laminar sub-layer, 164-5  
 lantern ring, 11-12  
 lantern ring exchanger - *see* externally sealed *under* floating-head exchangers  
 lead, 481  
 lead lining, 517  
 leakage (fluid bypassing), 35-8, 276-8, 280  
 leakage (mechanical joints), 8-13, 48, 50-2, 80, 245  
 Linde A. G., Muenchen, 18  
 Lithgow Saekaphen Ltd, 523  
 Ljungstrom exchanger, 126, 151  
 'lock-in' effect, 248, 254, 256  
 logarithmic mean temperature difference (LMTD)  
   assumptions, 189  
   definition, 190  
   example, 190-1  
 log decrement, 254-5  
 longitudinally-finned tubes  
   application, 25  
   cut and twist, 120  
   dimensions, 119-21, 544-5  
   fin shapes, 221  
   manufacture, 119-20  
   materials, 121  
   nomenclature, 120-2  
 Lopina, R. F. and Bergles, A. E., 235, 241  
 louvres, 101-2  
 low-alloy steels - *see* carbon and low-alloy steels  
 low-fin tubes  
   application, 25  
   coding system, 326  
   cost comparison with plain tubes, 326-7  
   description, 25, 325-6  
   dimensions, 330  
   manufacture, 325-6  
   materials, 325  
   skipped fins, 266-7, 326, 328

- low-temperature service, 486-8  
magnesium, 475, 478, 489-90  
manganese, 475, 489-90, 497, 502, 508  
Marston-Palmer Ltd, 136-9, 156  
materials of construction, 475  
  aluminium and aluminium alloys, 488-93  
  bi-metal construction, 515-21  
  carbon and low-alloy steels, 484-8  
  copper and copper alloys, 493-6  
  corrosion data, 475-6  
  forms of corrosion, 476-83  
  galvanic series, 477-9  
  material selection, 475-6  
  nickel and high-nickel alloys, 506-11  
  non-metallic coatings, 217, 521-3  
  numbering system, 483  
  stainless steels, 496-506  
  titanium and titanium alloys, 512-15  
McDuff, J. N. and Felgar, R. P., 251, 271  
McGraw Hill, Inc., 548, 550  
mean temperature difference (MTD)  
  arithmetic mean temperature difference (AMTD), 191  
  co-current flow, 102, 188-90  
  countercurrent flow, 117, 127-8, 132-3, 138, 188-90  
  cross-flow, 138-9, 194, 196-7, 343-5  
  *F* correction factor, 192, 196-201, 279, 345  
  *F* curves, 194, 357, 369  
  linear variation of *U*, 191  
  logarithmic mean temperature difference (LMTD), 189-91, 227, 279, 526  
  minimum number of shells in series, 197-8  
  NTU-*P*-*R* curves, 195, 203-5  
  Number of Transfer Units (NTU), 195, 201, 203-5, 370  
  pass designation system, 192-3  
  small number of baffles, 201-2  
  temperature approach, 188-9, 192  
  temperature cross, 188-9, 192  
  temperature meet, 188-9, 192  
  theta ( $\theta$ ) method, 205  
mechanical design features  
  all-welded exchanger, 52-3  
  bolted high pressure closures, 52-4  
  design codes, 4, 46, 88, 483, 527  
  fixed tubesheet exchangers, 54  
  flange systems, 48-9  
  high-pressure channels, 52-3  
  'non-bolted' high-pressure closure, 53-4  
  stationary head-shell joints, 50-2  
  metal inert gas (MIG) tube end welding, 72, 74, 513  
methane, 485  
mixed flow (cross flow), 196-7  
mixing length, 358, 416, 454  
mode number, 250  
molybdenum, 475, 484, 497, 501, 504-6, 509-11  
Monroe, R. C., 101, 103  
Moody, L. F., 176-7, 185  
Morris, M., 47, 84  
National Association of Corrosion Engineers (NACE), 475, 523, 524  
National Corrosion Service, 475  
natural convection - *see* free convection  
natural frequency (of tubes), 247-8, 251-2, 254, 257  
Nelson, G. A., 485  
NESTSTM concept, 232, 267, 269-70  
nickel (general), 475, 479, 483, 486-7, 493, 496-7, 501, 503, 505, 513, 519, 521  
nickel and high-nickel alloys (specific)  
  alloy 200, 506, 508  
  alloy 201, 506, 508  
  composition, 507  
  Hastelloy™ B-2, 510-11  
  Hastelloy™ C-4, 511  
  Hastelloy™ C-22, 511  
  Hastelloy™ C-276, 511  
  Hastelloy™ G, 511  
  Hastelloy™ G-3, 511  
  Hastelloy™ X, 511  
  Incoloy™ 800, 509-10  
  Incoloy™ 800 H, 509-510  
  Incoloy™ 825, 510, 521  
  Inconel™ 600, 508-9, 521  
  Inconel™ 625, 509  
  Monel™ 400, 508, 521  
nitrogen, 497, 501-2, 504-5, 513  
niobium, 475, 487, 497, 502, 509, 511  
Nobel's Explosive Co. Ltd, 517, 523  
noise (vibration), 245, 256-7  
non-metallic coatings, 216, 521-3  
normalising, 487  
Nouvelles Applications Technologiques, 126-7, 156  
nozzle sinkage, 56  
number of rows crossed, 281  
number of shells in series, 197-8  
number of transfer units (NTU), 195, 201, 203-5, 370  
Nusselt Number, 166, 174  
Oil Companies Materials Association (OCMA), 75, 84

- operating margin, 382  
Ormonde Ashton Ltd, 83  
outer tube limit (OTL), 6, 38, 39, 43, 268, 276, 281, 283  
overall heat transfer coefficient (typical)  
  air-cooled exchangers, 546  
  double-pipe exchangers, 543  
  gasketed-plate exchangers, 552  
  lamella exchangers, 553  
  shell and tube exchangers, 528  
  spiral exchangers, 553  
Owen, P. R., 249, 254, 271  
oxygen, 484-5, 513
- packing, 11-13  
Packinox™ exchanger, 126-7, 158  
Paikert, P., 340, 352  
Palen, J. W. and Taborek, J., 278, 297, 322  
palladium, 475, 512-13  
parallel flow eddy vibration, 247-8  
particulate fouling, 207  
passes  
  designation system, 192-3  
  single-tube side, 27-9  
  tube side, 26-8  
  two shell, 34-7, 320-1  
pass partition plates, 27-8  
Peclet Number, 166  
Perry, R. H. and Green, D., 322, 337, 474, 483, 524  
phenolic resin, 521-3  
Phillips Petroleum Co., 267, 270  
Phillips RODbaffle™ exchanger (RBE), 232, 267-9  
physical properties  
  estimation, 381  
  source of values, 381  
  temperature for calculations, 174-5  
Physical Property Data Service (PPDS), 381  
Pickering, F. B., 483, 524  
Pignotti, A. and Cordero, G. O., 344, 352  
plain (and perforated) corrugations (plate-fin exchangers), 136-7  
plate-fin exchangers  
  application, 135  
  construction, 135-6  
  corrugation types, 136-7  
  flow pattern, 138-9  
  matrix sizes, 137-8  
  multi-stream units, 139-40  
  pressure limitations, 137-8  
  selection criteria, 158  
plates - see gasketed plate exchangers  
plugging of tubes, 8, 77-8, 80  
plug sheet, 95-6  
pneumatic testing, 136  
polymerisation - see chemical reaction fouling  
Polytetrafluoroethylene (PTFE), 62, 131, 145, 146, 147, 159  
ports, 109-110  
post-weld heat treatment (PWHT), 75, 487  
Prandtl Number, 166, 174  
precipitation fouling, 207  
pressure loss correlations  
  axial cores, 240-1  
  channel nozzles, 184  
  double-pipe exchangers, 357-8  
  gasketed-plate exchangers, 367-8  
  headers (channels), 184  
  Heatex™ tube inserts, 237-8  
  inside tubes, 176-8  
  inside uniform channels, 178  
  internal fins, 234  
  outside high-finned tubes, 183  
  outside low-fin tubes, 183  
  outside plain banks, 179-82  
  shell nozzles, 184  
  twisted tape insert, 235  
Pritchard, A. M., 209, 219  
Purohit, G. P., 527, 554
- Rabald, E., 475, 524  
Rabas, T. J. *et al.*, 183, 185  
radiation, 163  
radiussed tubesheet, 40, 64  
Rayleigh Number, 166  
rear heard, 3, 5, 7; *see also* channels  
recessed tube-end welds, 72  
Reid, R. C., Prausnitz, J. M. and Sherwood, T. K., 381, 459  
reinforcing pad, 58, 246  
resin-lined construction, 521-3  
resistance, 164, 167  
resonance, 247, 249  
return bend housing, 118-19  
Reynolds Number, 163-4, 166  
Robert Jenkins Systems Ltd, 144-5, 156  
RODbaffle™ - see Phillips RODbaffle™ exchanger  
rod-like flow - see laminar flow  
roll-bonded plate, 519-21  
roller expander, 66-7, 70  
rotary regenerative exchangers  
  application, 150-1  
  construction, 151-2  
  cost, 553  
  inlet-stream leakage, 151-2  
  matrix material, 152  
  power consumption, 553  
  selection criteria, 159, 375  
rotatable bundle, 40  
roughness, 176-7

- routing of fluids, 375-6  
 rubber lining, 479, 521  
 Rubin, F. L., 101, 103  
 Ruiz, C., 47, 84
- sacrificial anodes, 478, 490  
 salt water - *see under water*  
 Sandvik alloys - *see under stainless steels*  
 Sandvik Ltd, 523  
 scaling - *see precipitation fouling*  
 Schmidt, T. E., 225, 231  
 Schweitzer, P. A., 475, 524  
 sea water - *see under water*  
 sealing devices, 35-7, 276  
 seal ring, 118-19  
 season cracking, 479  
 sedimentation fouling - *see particulate fouling*  
 Sedriks, A. John, 483, 524  
 selection criteria (exchanger type), 158-9, 214-16, 375  
 Seligman, Dr Richard, 104  
 Senior Platecoil Ltd, 140, 156  
 sensitisation, 497, 501, 505, 509  
 separate head, 118  
 serrated corrugations (plate-fin exchangers), 136-7  
 shell-and-tube exchangers  
   baffles, 3, 14, 28-38, 42-4, 246-7, 251, 255, 264-8, 276-9, 281-3, 320-2  
   basic construction, 3-4  
   channels, 3, 5, 7, 10, 19-21, 50-3, 56-7, 516, 521  
   cost, 527, 530-42  
   design codes, 4, 46, 483, 527  
   examples of shellside  
     calculations, 293-6, 314-19  
   flanges, 9-13, 48-53, 58-60, 62, 515-18, 521  
   heads (dished), 56-7  
   mechanical design features, 4, 46, 48-54  
   nomenclature (TEM), 5, 7  
   nozzles, 41-3, 56-8, 515-17  
   passes, 26-9, 34-7, 192-3, 320-1  
   selection criteria, 158, 217, 375  
   size designation, 43-4  
   summary of features, 6  
   TEM - *see Tubular Exchanger Manufacturers Association*  
   thermal design, 275-91  
   tubes, 21-6, 143, 146-8, 325-8, 330, 379, 492  
   type designation, 43-4  
   types, 5-18  
   worked examples for thermal design, 383-439, 458-9
- shell-baffle clearance, 31-2, 276-8, 281, 283  
 shell-baffle leakage area, 276-8, 281, 283  
 shell-bundle clearance, 6, 38, 39, 43, 268, 276-8, 281, 283  
 shell-bundle leakage area, 276-8, 281, 283  
 shell diameter, 44-6  
 shells (barrels), 3, 44-6, 55-6  
 shellside flow models  
   ideal, 276-7  
   Tinker, 276-8  
 shell-tubesheet connections, 64  
 shielded metal arc tube-end welding, 72-3, 513  
 shroud, 36-7  
 side frame, 96-7  
 Sieder, E. N. and Tate, G. E., 236-7, 241  
 sigma formation, 501, 504  
 silicon, 484, 487, 489-90, 501, 505  
 silver, 515  
 Singh, K. P. and Soler, A. I., 46, 84  
 size estimation  
   air-cooled exchangers, 341, 547-51  
   double-pipe exchangers, 542-5  
   shell-and-tube exchangers, 527, 536-7  
 Sjogren, S. and Grueiro, W., 371, 372  
 Smith, R. A., 184, 185, 280, 323, 526, 554  
 Society of Automotive Engineers (SAE), 483  
 Somerscales, E. F. C., 207, 219  
 spacer studs, 132-3  
 spacer tubes, 3, 36-41  
 spider tube supports, 119  
 spiral exchangers  
   application, 131-2  
   construction, 132  
   cost, 552-3  
   flow arrangements, 133-4  
   selection criteria, 158, 216, 218  
   standard units, 132-3  
 spines, 220-1  
 spring washers, 48-9  
 stabilisers, 485  
 stab-in bundle - *see bundle-in-column reboiler*  
 stainless steel (general), 481, 483, 496, 488, 496-7, 513-4, 517, 519, 521  
 stainless steels (specific)  
   Allegheny Ludlum Corp. alloy AL-6X™, 503  
   Allegheny Ludlum Corp. alloy 29-4-2™, 504  
   Allegheny Ludlum Corp. alloy 29-

- 4C™, 504  
 Allegheny Ludlum Corp. E-Brite™  
 (XM-27), 504  
 Armco Nitronic™ alloy 33  
 (XM-29), 502  
 Armco Nitronic™ alloy 40  
 (XM-19), 502  
 Armco Nitronic™ alloy 50  
 (XM-19), 502  
 austenitic group, 497–503  
 Carpenter alloy 20 Cb-3™, 502  
 compositions, 498–500  
 duplex (austenitic/ferritic)  
 group, 505–6  
 ferritic group, 503–5  
 Haynes alloy 20 Mod™, 503  
 martensitic group, 505  
 precipitation-hardening group, 506  
 Sandvik alloy 2RK 65™, 502  
 Sandvik alloy 3RK 60™, 506  
 Sandvik alloy SAF 2205, 506  
 Sandvik Sanicro™ 28, 503  
 standard 200 series, 497  
 standard 300 series, 497, 501  
 standard 400 series, 503–4  
 Uddeholm alloy NU  
 ELI-T18-2™, 505  
 Uddeholm alloy NU Monit™, 505  
 Uddeholm alloy NU stainless  
 744LN™, 506  
 Uddeholm alloy NU stainless  
 904LN™, 502  
 standing waves, 249  
 Stanton Number, 166, 174  
 stationary head, 3, 5, 7; *see also*  
 channels  
 stationary head-shell joints, 50–2  
 steam, 9, 15, 16  
 steam coils, 102  
 steam heat transfer coefficient, 416  
 steam/helium testing, 81, 83  
 steels – *see*: carbon and low alloy; and  
 stainless  
 strake, 55  
 stream analysis method, 278  
 streamline flow – *see* laminar flow  
 Strouhal Number, 248–9, 254  
 structure (air-cooled  
 exchangers), 97–9  
 sulphidation, 504  
 sulphide stress cracking (SCC), 523  
 surface area, 158–9, 168, 211–12,  
 279, 343, 356, 369, 378–9, 525–6,  
 536, 544–5, 549  
 surface temperature, 169–73  
 Taborek, J., 193, 199, 200–1, 203–6,  
 214, 219, 275, 278, 280, 284, 291,  
 323, 328, 332, 337, 344–5, 352  
 tank suction heater, 9, 25  
 tantalum, 475, 497, 502, 509, 511  
 Teflon™, 108  
 Teflon™ exchangers  
 immersion coils, 148–50  
 properties of Teflon™, 147–8  
 selection criteria, 157, 159,  
 214–16, 375  
 shell-and-tube exchangers, 148–9  
 temperature approach, 188–9, 192  
 temperature control (air-cooled  
 exchangers), 101–2  
 temperature cross, 188–9, 192  
 temperature meet, 188–9, 192  
 temperature profile, 166  
 test block, 68–9, 75  
 test flange and gland, 80–2  
 test ring, 81–2  
 test water temperature, 487  
 thermal appraisal – gasketed-plate  
 exchangers  
 channel equivalent diameter, 366  
 channel flow area, 365  
 chevron angle, 365–6  
 effective plate length, 365  
 enlargement factor, 365  
 exchanger arrangement, 370–1  
 heat transfer coefficients, 367–9  
 high theta plates, 370–1  
 low theta plates, 370–1  
 mean flow channel gap, 365  
 mean temperature difference,  
 368–9  
 pressure loss, 367–8  
 thermal mixing, 370–1  
 thermal conductivity  
 carbon, 142  
 fin metals, 222  
 glass, 146  
 graphite, 142  
 plate metals, 106  
 Teflon™, 147  
 thermal design – air-cooled exchangers  
 air-side heat transfer  
 calculations, 342, 347–9, 351  
 air-side pressure loss  
 calculations, 344, 346–7,  
 350–1  
 air velocity, 341–2  
 design variables, 339–40  
 example of air-side  
 calculations, 347–51  
 fan laws, 347  
 fan noise, 347  
 fan power consumption, 346–7  
 inlet air temperature, 340  
 mean temperature difference,  
 343–5  
 number of rows deep, 342–3  
 outlet air temperature, 341  
 preliminary sizing, 341



- surface area, 343
- thermal design - double-pipe exchangers
  - annulus equivalent diameter, 354-5
  - cut-and-twist of fins, 358
  - example of annulus calculations, 358-61
  - fin calculations, 355-6
  - mean temperature difference, 356-7
- thermal design - shell-and-tube exchangers (low-fin tubes)
  - coding systems, 325-6
  - description, 325-6
  - design considerations, 327-8
  - equivalent diameter, 329-30
  - example of proposed manual (shellside) method, 334-7
  - fin efficiency, 329-31
  - geometrical data, 330
  - modifications to Bell manual (shellside) method, 331-2
  - proposed manual (shellside) method, 332-5
- thermal design - shell-and-tube exchangers (plain tubes)
  - examples of proposed manual (shellside) method, 314-19
  - ideal shellside flow model, 276-7, 291-6
  - need for manual methods, 275-6
  - procedure for design, 279
  - proposed manual (shellside) method, 280-91
  - shellside flow problems, 276-8
  - Tinker shellside flow model, 276-8
  - tubeside calculations, 279-80
  - typical manual (shellside) methods, 278
- thermal effectiveness, 192
- Thermal Technology Ltd, 151, 156
- theta method (MTD), 205-6
- Thorngren, J. T., 255-7, 271
- tie bolts, 108
- tie rods, 3, 36-41, 277
- tin, 475, 482, 493, 495
- Tinker, T., 276-8, 323
- titanium (general), 475, 479, 486, 501, 504-6, 517, 519
- titanium and titanium alloys (specific)
  - application, 514
  - clad construction, 514-1
  - composition, 512
  - corrosion resistance, 512-13
  - fabrication, 513-14
- Titanium Metals & Alloys Ltd, 524
- top plate, 95-6
- toughness, 487, 502, 504
- transition region, 164
- transition temperature, 487
- tube-baffle clearance, 31, 276-8, 283
- tube-baffle leakage area, 281-2
- tube bundle, 3, 8-12, 36-7, 42
- tube count, 39-41, 460-71, 537, 539, 540
- tube-end ferrules, 516
- tube failures, 245-6
- tube holes
  - diameter, 62, 67-8
  - finish, 62, 67
  - grooves, 67-8, 516
- tube layout, 38-41
- tubes
  - Alonized™, 492
  - average wall, 22
  - bi-metal, 24
  - characteristics, 379
  - diameter, 21-2
  - fluted, 25-6
  - glass, 146-7
  - graphite, 143
  - high-finned (air-cooled exchangers), 25, 90-4
  - length, 23
  - longitudinally finned, 25, 119-21, 544-5
  - low-fin, 25, 266-7, 325-8, 330
  - minimum wall, 22
  - pitch, 22-4
  - pitch angle, 23-4
  - roped, 25-6
  - Teflon™, 147-8
  - thickness, 21-3
- tubesheets (shell-and-tube exchangers), 3, 62-4
  - bi-metal, 7, 515-16
  - design for fixed tubesheet exchangers, 54
  - double, 17-19, 64
  - floating, 9-13
  - radiussed, 40, 64
- tubesheet-shell connections, 7, 64
- tube spacer (air-cooled exchangers), 96
- tube-tubesheet attachment, 40, 66, 75, 96, 480
  - explosive expansion, 77-8
  - explosive plugging, 77-8
  - explosive welding, 78-9
  - fusion welding, 71-6
  - hydraulic expansion, 67, 70
  - internal bore (back-bore) welding, 76
  - roller expansion, 66-9
  - rubber expansion, 67, 71
  - tube-end inserts, 79
- tube-wall thinning, 67-9
- Tubular Exchanger Manufacturers Association (TEMA), 4-12, 15,

- 19-20, 27, 31-6, 41, 43-4, 46,  
61-2, 80, 84, 88, 103, 193, 199,  
201, 211, 219, 247, 250, 266, 271,  
277, 297
- classes, 4
- gaskets, 61-3
- impingement protection criteria, 35
- limitations, 4-5
- maximum unsupported length, 32
- nomenclature, 7
- size designation, 43-4
- type designation, 43-4
- turbulence promoters, 233
- turbulent buffeting, 249, 254
- turbulent core, 164-5
- turbulent flow, 164
- tungsten, 475, 484, 511
- tungsten inert gas (TIG) tube-end  
welding, 72-4, 513
- U arrangement, 12
- U-bend out-of-plane vibration, 252
- U-bend plane, 27-8
- U-bend support, 266
- U-bend thinning, 22-3
- U-tube exchanger, 8-9
- Uddeholm - *see* Avesta Johnson  
Stainless Steel Ltd
- Uddeholm alloys - *see under* stainless  
steels
- Unified Numbering System  
(UNS), 483
- uniform channels, 178
- unihead, 118
- unit (air-cooled exchanger), 89-90
- unmixed flow (cross-flow), 195-7,  
343-5
- Usher, J. D., 113, 116
- vanadium, 475, 484, 511
- vaporiser, 14-17
- velocity
- cross-flow, 248, 252-3
- desirable for water, 482
- face, 341
- optimum, 526
- profile, 163-4
- sound, 256
- vibration (flow-induced)
- acoustic, 249, 256, 264, 267
- background, 245
- comparison of predictive  
methods, 257-64
- cross-flow areas and  
velocities, 252-3
- design recommendations, 265-7
- Erskine and Waddington damage  
numbers, 256-7, 265
- excitation mechanisms, 247-50
- fluid-elastic whirling, 249, 254-5
- frequency match, 254
- NESTS™ concept, 267, 269-70
- noise, 256-7
- Phillips RODbaffle™  
exchanger, 267-9
- predictive methods, 250-64
- reasons for increase, 247
- Thorngren damage numbers,  
255-6
- tube failures, 245-7
- tube natural frequency, 251-2
- turbulent buffeting, 249, 254
- vortex shedding, 248-9, 254
- zones for vibration check, 253,  
264-5, 286
- viscosity, 169
- viscosity correction factor, 169-73,  
175
- viscous flow - *see* laminar flow
- Von Linde, 16
- Von Nostrand, W. L. *et al.*, 209, 219
- vortex shedding, 248-9, 254, 256-7
- wall temperature - *see* surface  
temperature
- Ward, D. J. and Young, E. H., 179,  
185
- washboard plate, 106-7
- water (general), 477, 484-5, 490,  
493, 495-6, 503, 506
- bath, 154
- desirable velocity for water, 482
- heat transfer coefficients, 380, 528,  
543, 546, 552-3
- sea (salt), 477, 488, 493, 496,  
502-3, 508-9, 512, 515, 521
- test, 487, 501
- Watkinson, A. P. and Epstein, N.,  
208, 219
- weep holes, 11-12
- weighted fin efficiency, 227
- weir plate, 15
- 'weld decay' *see* sensitisation
- Whessoe Heavy Engineering Ltd, 19,  
29, 42, 45, 55, 63, 515
- wicks (heat pipes), 124-5
- Wiggins Alloys Ltd, 523
- Wilkinson, W. L., 113, 116
- window - *see under* baffles
- worked examples for thermal design
- air-cooled exchangers, 440-5,  
446-7
- double-pipe exchangers, 445-54
- gasketed-pipe exchangers, 454-7
- shell-and-tube exchangers (low-fin  
tubes), 432-9, 458-9
- shell-and-tube exchangers (plain  
tubes), 383-431, 458-9
- working fluid (heat pipes), 124
- Wright, S. T., 554

X-ray examination, 76  
X shell, 41-2

Yorkshire Imperial Alloys, 25, 26,  
83, 330, 337

Z arrangement, 112  
zinc, 477-8, 489-90, 493, 495